THE PHYSICAL REVIEW

PUBLISHED BY THE
AMERICAN INSTITUTE OF PHYSICS
INCORPORATED

UNDER THE EDITORIAL SUPERVISION OF THE
AMERICAN PHYSICAL SOCIETY

BOARD OF EDITORS

Managing Editor, JOHN T. TATE, University of Minnesota, Minneapolis
Assistant Editor, J. W. BUCHTA, University of Minnesota, Minneapolis
K. F. HERZFELD, A. W. HULL, F. W. LOOMIS, A. J. DEMPSTER, DAVID M. DENNISON,
J. C. SLATER, R. C. GIBBS, E. O. LAWRENCE, J. H. VAN VLECK

VOLUME 41, SECOND SERIES
JULY-SEPTEMBER, 1932

THE AMERICAN INSTITUTE OF PHYSICS, INCORPORATED
11 EAST 38th STREET, NEW YORK, N. Y.

LIBRARY OF
ALLAHABAD.
Date 6.2.36
A. No. 16038
EWING CHRISTIAN COLLEGE

Composed, Printed and Bound by
The Collegiate Press
George Banta Publishing Company
Menasha, Wisconsin

CONTENTS

JULY 1, 1932

Reflecting and Resolving Power of Calcite for X-Rays – – – – SAMUEL K. ALLISON 1
Scattering of X-Rays by Gases and Crystals – – – – – – – – Y. H. WOO 21
Ionization of Air by γ-Rays as a Function of Pressure and Collecting Field – I. S. BOWEN 24
Search for Isotopes of Hydrogen and Helium – – – – – – – WALKER BLEAKNEY 32
Elastic and Inelastic Electron Scattering in Hydrogen – A. L. HUGHES AND J. H. MCMILLEN 39
Electronic Structures of Polyatomic Molecules and Valence. II. General Considerations – ROBERT S. MULLIKEN 49
Evidence of Space Quantization of Atoms upon Impact – – H. KUHN AND O. OLDENBERG 72
Equation of State of a Non-ideal Einstein-Bose or Fermi-Dirac Gas – G. E. UHLENBECK AND L. GROPPER 79
On Ferromagnetism and Related Problems of the Theory of Electrons – – PAUL S. EPSTEIN 91
Errata:
Shape of an X-Ray Line – – – – – – – – – – – – ARCHER HOYT 110
Letters to the Editor – 111
Vapour Pressure of Sulphur at 50°C – – – R. R. H. BROWN AND J. J. MUIR 111
Variation of the Cosmic Rays with Latitude – – – – – – ARTHUR H. COMPTON 111
On the Production of Ultra-short Electromagnetic Waves – – AMEDEO GIACOMINI 113
Predissociation in Nitrogen – – – – – – – – – – – – JOSEPH KAPLAN 114
Isotopic Weight of H^2 – – – – – – – – – KENNETH T. BAINBRIDGE 115
Book Reviews – 116

JULY 15, 1932

Diurnal Variation of Cosmic Rays – R. D. BENNETT, J. C. STEARNS AND A. H. COMPTON 119
Diffuse Scattering of X-Rays from Sodium Fluoride – G. E. M. JAUNCEY AND P. S. WILLIAMS 127
Very Soft X-Ray Spectra of Heavy Elements – – – – – – – – C. DEL ROSARIO 136
On the Relative Abundances of the Nitrogen and Oxygen Isotopes – GEORGE M. MURPHY AND HAROLD C. UREY 141
Mass-Spectrograph Study of the Ionization and Dissociation by Electron Impact of Benzene and Carbon Bisulfide – – – – – – – – – – – – ERNEST G. LINDER 149
Elastic Electron Scattering in Helium – A. L. HUGHES, J. H. MCMILLEN AND G. M. WEBB 154
Infrared Dispersion of Carbon Dioxide – – – – – – – HUGH M. SMALLWOOD 164
Band Spectrum of Sulphur Monoxide – – – – – – – – EMMETT V. MARTIN 167
Influence of Crystalline Fields on the Susceptibilities of Salts of Paramagnetic Ions. I. The Rare Earths, Especially Pr and Nd – – – WILLIAM G. PENNEY AND ROBERT SCHLAPP 194
Theory of the Variations in Paramagnetic Anisotropy among Different Salts of the Iron Group – J. H. VAN VLECK 208
Investigations in the Field of the Ultra-short Electromagnetic Waves. IV. On the Dependence of the Ultra-short Electromagnetic Waves upon the Heating Current and upon the Amplitude of the Oscillations – – – – – – – – – – – G. POTAPENKO 216
Hall Effect with Audiofrequency Currents – – – – – – – LAWRENCE A. WOOD 231
Some Thermo- and Galvanomagnetic Properties of a Bismuth Crystal – H. E. BANTA 239
Does Nickel Show a Positive Elongation in the Joule Magnetostrictive Effect? – – – – – – – – – – – – – – – – – – –

AUGUST 1, 1932

On the Effect of a Secondary Structure upon the Interference of X-Rays – H. M. EVJEN 265
Analysis of the (0, 0) $^2\Pi \rightarrow {}^2\Sigma$ CN Band at 9168A – – – – – ALLAN E. PARKER 274
Dirac Electron in Simple Fields – – – – – – – – – MILTON S. PLESSET 278
Infrared Absorption Spectrum of Carbon Dioxide – – P. E. MARTIN AND E. F. BARKER 291
Vibrational Levels of Linear Symmetrical Triatomic Molecules – – DAVID M. DENNISON 304
Two-Minima Problem and the Ammonia Molecule – DAVID M. DENNISON AND G. E. UHLENBECK 313
Nuclear Moment of Barium as Determined from the Hyperfine Structure of the Ba II Lines – – – – – – – – – – P. GERALD KRUGER, R. C. GIBBS AND R. C. WILLIAMS 322
Elimination of One Boundary Condition for a Sphere in Radiative Equilibrium by a Layer in Adiabatic Equilibrium – – – – – – – – – – – HERMAN ROTH 327
Magnetic Susceptibilities of Alpha- and Beta-Manganese – – – MARY A. WHEELER 331
Magnetic Susceptibility of Nitrogen Dioxide – – – – – – GLENN G. HAVENS 337
Barkhausen Effect. III. Nature of Change of Magnetization in Elementary Domains – RICHARD M. BOZORTH AND JOY F. DILLINGER 345
Variation with Temperature of the Thermoelectric Power of Nickel and Some Copper-Nickel Alloys – K. E. GREW 356
Diamond Windows for Withstanding Very High Pressures – THOS. C. POULTER AND FRANCIS BUCKLEY 364
Effect of Pressure on the Index of Refraction of Paraffin Oil and Glycerine – THOS C. POULTER, CARTER RITCHEY AND CARL A. BENZ 366
Letters to the Editor – – – – – – – – – – – – – – – – – – –

SEPTEMBER 1, 1932

Interpretation of Cosmic-Ray Phenomena – THOMAS H. JOHNSON 545
Design of a Double-Crystal X-Ray Vacuum Spectrometer – LYMAN G. PARRATT 553
X-Ray Diffraction from Calcite for Wave-Lengths 1.5 to 5 Angstroms– LYMAN G. PARRATT 561
Survey of the *K*-Satellites – O. REX FORD 577
Series and Term Values in the Arc Spectrum of Tellurium – J. E. RUEDY 588
Resonance Fluorescence of Benzene – G. B. KISTIAKOWSKY AND M. NELLES 595
Ionization of Neon and Argon by Positive Alkali Ions of Energies from 650 to 2000 Volts – J. CARLISLE MOUZON 605
Photoelectric Properties of Alkali Metal Films as a Function of their Thickness – JAMES J. BRADY 613
Optical Dissociation of Iodine and Enhancement of Predissociation by Collisions – LOUIS A. TURNER 627
Reflection of Thallium, Lead and Antimony Atoms from Sodium Chloride Crystals – J. M. B. KELLOGG 635
Electrical Resistance and the Critical Point of Mercury – FRANCIS BIRCH 641
Bearing of the Earth's Internal Magnetic Permeability upon the Self- and Mutual Inductance by Coils Wound on its Surface – W. F. G. SWANN 649
Value of the Townsend Coefficient for Ionization by Collision at Large Plate Distances and Near Atmospheric Pressure– FREDERICK H. SANDERS 667
Letters to the Editor 678

Experimental Evidence for and Determination of the Predicted $^1\Delta$ Level of the Neutral Oxygen Molecule – BERNARD LEWIS AND GUENTHER VON ELBE 678
Remark on Erikson's Measurements of the Ionization by γ-Rays at Various Pressures and Potentials – H. ZANSTRA AND J. CLAY 679
Dependence of the Ionization Produced by γ-rays upon Pressure and Temperature – NEWELL S. GINGRICH 679
Progress of Cosmic-Ray Survey – ARTHUR H. COMPTON 681
Diurnal Variation of Cosmic Rays and Terrestrial Magnetism – ROSS GUNN 683
Spin of the Neutron – R. F. BACHER AND E. U. CONDON 683
Electron Affinity of Hydrogen – GEORGE GLOCKLER 685
Equilibrium between Positive Ions and Neutral Atoms in Positive Rays of the Rare Gases – HAROLD F. BATHO 686
Radiation from Moving Helium, Neon and Argon Ions – A. I. MCPHERSON 686
Some Evidence Indicating a Removal of Positive Ions from Cold Surfaces by Electric Fields – J. W. BEAMS 687
Reflecting and Resolving Power of Calcite for X-Rays – SAMUEL K. ALLISON 688
Variation of the Cosmic-Ray Intensity with Azimuth–THOMAS H. JOHNSON AND J. C. STREET 690

Book Review 691

SEPTEMBER 15, 1932

Faraday Effect with X-Rays – DAROL K. FROMAN 693
New Measurements of the Ranges of Alpha-Particles from Polonium, Uranium I and Uranium II with the Wilson Chamber – F. N. D. KURIE 701
Relativistic Thomas-Fermi Atom – M. S. VALLARTA AND N. ROSEN 708
Wentzel-Brillouin-Kramers Method of Solving the Wave Equation – J. L. DUNHAM 713
Energy Levels of a Rotating Vibrator – J. L. DUNHAM 721
Rotational Analysis of Some CO_2 Emission Bands. Part I. – R. F. SCHMID 732
Electronic Structures of Polyatomic Molecules and Valence. III. Quantum Theory of the Double Bond – ROBERT S. MULLIKEN 751
Production of Infrared Spectra with Electric Fields – E. U. CONDON 759
Impacts of Fast Electrons and Magnetic Neutrons – J. F. CARLSON AND J. R. OPPENHEIMER 763
Photoelectric and Thermionic Emission from Composite Surfaces – WAYNE B. NOTTINGHAM 793
Relation between the Electric and Diamagnetic Susceptibilities of Monatomic Gases J. P. VINTI 813
Variation of the Principal Magnetic Susceptibilities of Certain Paramagnetic Crystals with Temperature – B. W. BARTLETT 818
Supersonic Dispersion and Absorption in CO_2 – W. H. PIELEMEIER 833
Letters to the Editor 838

Angular Distribution of Elastically Scattered Electrons in Mercury Vapour – F. L. ARNOT 838
Lower Limit for the Ground State of the Helium Atom – D. H. WEINSTEIN 839

Book Review 840
Author Index to Volume 41 841
Analytic Subject Index to Volume 41 846

Second Series *July 1, 1932* *Vol. 41, No. 1*

THE

PHYSICAL REVIEW

The Reflecting and Resolving Power of Calcite for X-rays

By SAMUEL K. ALLISON
University of Chicago

(Received May 20, 1932)

With a precision double spectrometer, the rocking curves from three pairs of calcites in the (1, −1) positive have been observed for seven wave-lengths from 0.21A, (W $K\alpha_1$) to 2.3A, (Cr $K\alpha_1$). Three quantities were observed at each wave-length, (1) the percent reflection (P_0), defined as the ratio of the maximum ionization current obtainable from crystal B to the ionization current produced by the x-rays incident on B from A, (2) the coefficient of reflection (R), defined as the ratio of the area of the rocking curve from B to the intensity incident on B from A, (3) the half width at half maximum of the rocking curve from B. One of the pairs (crystals III) was obviously more perfect than the others, and its values of P_0, R, and w are compared with theory. It is shown that none of the three quantities defined above is simply related to the analogous observations on a single crystal with monochromatic, parallel, incident x-rays, but that numerical predictions of the values of the above quantities may be obtained from somewhat laborious calculations based on Darwin's theory of diffraction by a perfect crystal as modified by Prins to take account of absorption. It is found that the predicted and observed coefficients of reflection are in good agreement in the wave-length range between 0.5 and 2.3A. On the basis of this agreement it is possible to state that calcite surfaces may be obtained for which there is no evidence of mosaic structure from measurements of the coefficient of reflection by double spectrometer methods in the wave-length region between 0.5 and 2.3A.

EXPERIMENTAL PART

Introduction

THE experiments reported here are similar to those performed on calcite in previous researches by other investigators.[1] The object of the experiments in the present case was primarily to provide a set of calibrated crystals to use in intensity measurements in this laboratory. The method consists essentially in comparing the intensity reflected from crystal B of a double spectrometer with that incident on B from crystal A, the instrument being set in a parallel position. In the present experiments only the (1, −1) position in the notation of Allison and Williams[1] was used.

[1] A. H. Compton, Phys. Rev. **10**, 95 (1917); Davis and Stempel, Phys. Rev. **17**, 608 (1921) and Phil. Mag. **45**, 463 (1923); Wagner and Kuhlenkampff, Ann. d. Physik **68**, 369 (1922); Allison and Williams, Phys. Rev. **35**, 1476 (1930); Davis and Purks, Phys. Rev. **34**, 181 (1929).

ciently high, the radiation reflected at the glancing angle for Cr $K\alpha_1$ may contain little of this wave-length and be mostly second and higher orders of the general radiation. It was shown that this effect did not invalidate the results for chromium by using the instrument as a single crystal spectrometer in the usual way and examining the spectrum, and also by the fact that the rocking curves at the two voltages indicated above for Cr were in agreement. The tungsten K spectrum was obtained from a tube operated at 110 k.v.

Adjustments

The instrument was put in adjustment by the procedure previously described by Allison and Williams[1] with some minor refinements in technique. One large improvement over the methods of Allison and Williams resulted from the fact that it was found possible to use a telescope with a Gauss eyepiece in the adjustment of the crystals. This greatly increased the accuracy with which the cleavage faces could be set parallel to the axes of rotation. With the crystal holder removed, a piece of plane parallel glass, mounted on a small block equipped with levelling screws, was placed over the axis. The plane parallel plate and the telescope were adjusted until at two positions of the plate 180° apart the reflected cross-hairs coincided with those in the telescope. The axis of the telescope was then perpendicular to that of the spectrometer. The plane parallel plate was then removed, the crystal in its mounting attached to the axis, and the crystal tilted until the reflected cross-hairs from its face coincided with those in the telescope. In this way it was found possible to set the crystals accurately enough to obtain the minimum rocking curve width in parallel positions at once, and the tilting process previously described by Allison and Williams was not necessary. The telescope was placed roughly 2 meters from the spectrometer, and the crystals could be set with their faces within ± 15 seconds of arc of the axes of rotation by this method.

In agreement with previous observers the rocking curves were found to be independent of the width of the slits used to limit the horizontal divergence of the beam of x-rays. The same slit widths, however, were not used at all wave-lengths. The inadvisability of such a procedure may be realised by considering the area on the crystal face irradiated by the x-ray beam at different glancing angles. For a constant vertical divergence of the beam this area is proportional to its horizontal extent, which to a sufficient approximation is given by

$$s = 2L_c a/L \sin\theta \tag{1}$$

where L_c is the distance from a point midway between the slits to the axis of the crystal, a is the slit width (assumed the same for both slits), L is the distance between the slits, and θ is the glancing angle. In the experiments on the tungsten K radiation, $\sin\theta = 0.034$, and the irradiated area becomes large relative to that used for softer wave-lengths. The range of wave-lengths present in the beam after reflection from crystal A can be calculated from the slit width and the distance between the slits by the formula

$$d\lambda = \lambda \cot\theta d\theta = (2a\lambda \cot\theta)/L. \tag{2}$$

The various values of $d\lambda$ used are shown in column 4 of Table I. The vertical divergence of the beam was limited by a slit over the front window of the ionization chamber, at a distance of 5.8 cm from axis B. The other limitation was the finite size of the focal spot, certainly not greater than 0.8 cm in diameter and 58 cm distant from this slit. The width of the slit in front of the ionization chamber limiting the vertical divergence of the beam in various experiments is given as h in column 5 of Table I. In column 6 of the same table is given the area irradiated on crystal B in cm², obtained roughly by multiplying the values in column 5 by the appropriate value of s obtained from Eq. (1).

TABLE I. *Adjustments.*

Radiation	Crystals	a	$d\lambda$	h	Area irradiated on crystal B.
W $K\alpha_1$	II, V	0.012 cm	6.2 X.U.	0.8 cm	1.0 cm²
"	III	0.012	6.2	0.5	0.65
Ag $K\alpha_1$	II	0.030	26	0.2	0.24
"	III	0.040	34	0.2	0.32
"	V	0.015	13	0.8	0.48
Mo $K\alpha_1$	II	0.030	25	0.2	0.19
"	III	0.040	33	0.2	0.25
"	V	0.015	12	0.8	0.42
Ir $L\beta_1$	II	0.030	25	0.2	0.12
"	III	0.040	33	0.2	0.16
"	V	0.015	12	0.8	0.23
Cu $K\alpha_1$	II	0.030	24	0.2	0.09
"	III	0.040	32	0.2	0.12
"	V	0.020	16	0.8	0.23
Fe $K\alpha_1$	II	0.030	24	0.2	0.07
"	III	0.040	32	0.2	0.09
"	V	0.020	16	0.8	0.18
Cr $K\alpha_1$	II, III, V	0.030	23	0.8	0.24

Crystals

Five pairs of split calcites were examined in this work. Two of the pairs, calcites I and IV, were examined only for a few wave-lengths and the data are not reported here. The three pairs II, III, and V had freshly cleaved surfaces. They were clear calcites, suitable for the construction of Nicol prisms, but of unknown origin. They were split by a method recommended to the author by Professor Bergen Davis. The sample to be split was mounted on the carriage of a milling machine, in such a way that the lateral motion of the carriage was accurately parallel to the cleavage direction. A very thin circular saw was then run at slow speed and a groove made across the specimen. By continued sawing in this groove a split soon started and the slight jars due to the impact of the saw teeth on the crystal spread it until fissure was complete. The two halves of the crystal were then immediately placed in a dessicator and kept until used. The crystals were parallelopipeds usually from 0.5 to 1 cm thick and some 5 cm on a side.

The ability of the crystal surfaces to give a sharp reflected image of the cross hairs of the Gauss eye-piece was different in the various specimens. It is a rather disconcerting fact that crystals III, which proved to give the high-

est resolving power for x-rays, were the poorest optical reflectors. Crystals II gave a very clear reflected image, as good as that from a polished glass plate. Crystals V were intermediate between II and III in this respect.

The most extensive investigations were carried out on crystals III, and before these crystals were finally removed from the instrument a test was performed to make sure that the resolving power had not changed during the experiments. On Nov. 19, 1931 these crystals gave a rocking curve of 2.6″ half width at half maximum for Mo $K\alpha_1(1, -1)$. After the investigation of the other wave-lengths was completed, on Jan. 2, 1932, the experiment with Mo $K\alpha_1$ was repeated and again 2.6″ obtained. There is therefore no evidence that the crystals III had changed during the period of experimentation.

Measurements

From the rocking curves for a given wave-length three quantities were determined. The half width at half maximum, w, is the angular range in seconds of arc through which crystal B must be turned to reduce the power entering the ionization chamber to one-half its maximum value. By maximum value is meant the largest ionization current observed, corrected for base-line. This base-line was taken as the ionization current observed when crystal B was rotated from its angular position for maximum reflection through an angular displacement of 6 or more times the half width at half maximum. The percent reflection, P_0, is the ratio of the maximum ionization current obtainable by reflection from crystal B to that obtainable from the beam incident on B from A. The coefficient of reflection, R, is in this paper defined as the ratio of the area under the rocking curve to the ionization current obtainable from the beam incident on crystal B from crystal A. Values of R observed and calculated in this paper are based on the radian as the unit of angle.

A regular routine was developed for the recording of rocking curves, the steps of which will now be described. A run was begun with crystal B out of the x-ray beam. The beam reflected from crystal A (which had been set at the proper angle) was allowed to enter the ionization chamber, and the current through the x-ray tube was adjusted until the rate of deflection of the electrometer was between 5 and 10 scale divisions per second. When conditions had become steady, a series of readings, usually three, were made on the beam reflected from crystal A. Between these readings the ionization chamber was shifted slightly to make perfectly sure that the entire beam was entering the window. If these three readings agreed to within 1 percent, the ionization chamber was displaced 5° and a reading taken of the diffusely scattered radiation. The difference between the average of the three readings and the base-line reading was taken as proportional to the intensity incident on B from A. Except in experiments on W $K\alpha_1$ the base-line was negligible here. Crystal B was then advanced into the beam, and the ionization chamber placed to receive the reflected beam from it. The rocking curve was then taken. Care was taken to obtain readings far enough from the maximum to supply a reliable base. Crystal B was then removed, and the power incident upon it again determined; the average of the initial and final values being used as the inten-

sity incident on B during the taking of the rocking curve. The results are given in Table II. Each value is the result of at least two independent observations.

TABLE II. *Experimental results.*
w = half width at half maximum of rocking curve (seconds).
P_0 = percent reflection.
R = coefficient of reflection, in (radians)$^{-1}$.

Line	λ (X.U.)	w II	w III	w V	$100\,P_0$ II	$100\,P_0$ III	$100\,P_0$ V	$R\times10^5$ II	$R\times10^5$ III	$R\times10^5$ V
W $K\alpha_1$	208.6	4.2	2.3	7.2	33	35	28	2.34	1.17	2.14
Ag $K\alpha_1$	558.3	3.8	2.2	7.0	48	59	34	2.15	1.53	2.38
Mo $K\alpha_1$	707.8	3.9	2.6	7.2	52	63	33	2.31	1.86	2.44
Ir $L\beta_1$	1155	4.8	4.1	8.1	59	64	37	3.49	2.95	3.24
Cu $K\alpha_1$	1537	5.6	4.9	7.8	61	62	46	3.92	3.46	3.91
Fe $K\alpha_1$	1932	6.8	6.2	9.9	54	58	42	4.45	4.18	4.45
Cr $K\alpha_1$	2285	7.7	7.1	9.3	52	55	42	4.73	4.68	4.37

If we examine the data on w in Table II, we see that the w values for crystals III are consistently lower than for crystals II or V. This is taken to indicate that crystals III approach the ideal of a perfect crystal more nearly than do the others investigated, since any mosaic structure would enlarge the angular range over which reflected can take place. The remainder of this report will be concerned with a comparison of the values of w, P_0, and R observed for crystals III with the predictions of the theory of diffraction by a perfect crystal.

THEORETICAL PART

Theory of diffraction of x-rays by an absorbing, perfect crystal

The theory of the diffraction of x-rays from the face of a perfect crystal has been developed by Darwin,[7] and later, Ewald.[8] In the discussion here we shall consider the theory as derived by Darwin. In Darwin's derivation, the absorption by incoherent processes of the x-rays as they penetrate the crystal, is neglected. The absorption due to ejection of photoelectrons or recoil electrons would be considered as an incoherent process in this sense. The result of Darwin's calculations can be expressed in the following form. The ratio of the intensity reflected from the crystal to that incident upon it is

$$\frac{I_{(\beta-\theta)}}{I_0} = \left|\frac{-q}{v+(v^2-q^2)^{1/2}}\right|^2, \tag{3}$$

where

$$v = \left\{2\pi d(\beta-\theta)\cos\theta_0\right\}/\lambda, \tag{4}$$

$$q = -\frac{2\pi d}{\lambda\sin\theta_0}\,\delta\,\frac{F(2\theta_0)}{F(0)}, \tag{5}$$

$$\theta = \theta_0 + \delta\sec\theta_0\,\mathrm{cosec}\,\theta_0, \tag{6}$$

$$\theta_0 = \sin^{-1}\frac{n\lambda}{2d}. \tag{7}$$

[7] Darwin, Phil. Mag. **27**, 325 and 675 (1914).
[8] Ewald, Phys. Zeits. **26**, 29 (1925).

In the above expressions, $(\beta-\theta)$ is the deviation of the glancing angle from the angle θ, which is the corrected Bragg angle. λ is the wave-length of the x-rays in air; d, the grating space of the crystal; n, the order of the spectrum, and δ the deviation of the index of refraction from unity. The sign to be used for the radical in the denominator of Eq. (3) is determined by the physical requirement that the ratio on the left hand side of this equation must be less

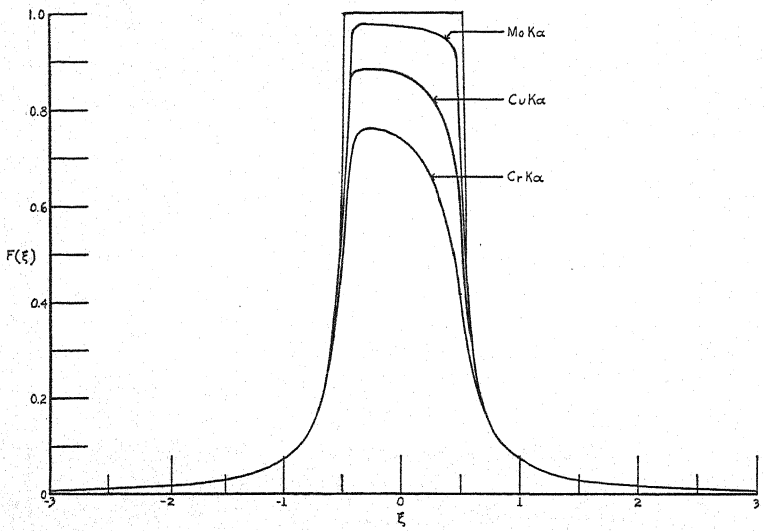


Fig. 2. Theoretical diffraction patterns from a single crystal. The outer curve is Darwin's theory, uncorrected for absorption, the inner curves illustrate Prins' absorption correction. With values of ξ plotted as abscissae, the curves apparently have about the same width at half maximum. If instead of ξ, we consider the actual angular deviations from θ, the width increases with wave-length.

than or equal to one. $F(2\theta_0)$ is the ratio of the amplitude of the wave scattered at angle $2\theta_0$ from the unit cell to the amplitude incident upon it. $F(0)$ is analogous ratio for the wave scattered in the forward direction of the incident beam. Let us first consider the simplified case in which the entire incident radiation is plane polarized in such a direction that the electric vector lies in a plane perpendicular to the plane of incidence of the radiation on the crystals. For the case,

$$F(2\theta_0)/F(0) = FZ^{-1} \tag{8}$$

where F is the structure factor and Z the number of electrons in the unit cell of the crystal. In the range $-q<v<q$, Eq. (3) gives rise to 100 percent reflection. If we call this range of angle $\Delta\theta_\sigma$ we have

$$\Delta\theta_\sigma = 4\delta FZ^{-1} \operatorname{cosec} 2\theta_0. \tag{9}$$

In this and following equations, the subscript σ indicates that the electric vector of the radiation is perpendicular to the plane of incidence. We shall use this $\Delta\theta_\sigma$ as a unit of measure of angular deviation from the corrected Bragg angle θ, and introduce the quantity ξ_σ defined by

$$\xi_\sigma = (\beta - \theta)/\Delta\theta_\sigma. \tag{10}$$

If this ξ_σ is introduced into Eq. (3) ,we obtain

$$F(\xi_\sigma) = \left| 2\xi_\sigma + (4\xi_\sigma^2 - 1)^{1/2} \right|^{-2} \tag{11}$$

A plot of $F(\xi_\sigma)$ is shown as the outer curve of Fig. 2.

Prins[9] has recently modified Darwin's theory in an attempt to take account of the absorption of the x-rays in the crystal by incoherent processes, as mentioned above. It is well known that in the classical dispersion theory, the index of refraction is the real part of a complex number, which number we may represent by $(1-\delta-i\beta)$. The real part of this number, $(1-\delta)$, is the ordinary index of refraction, i.e., the ratio of the phase velocity in vacuum to that in the medium. The imaginary part is related to the linear absorption coefficient μ_l of the radiation in the medium by

$$\beta = \lambda\mu_l/4\pi. \tag{12}$$

The essential feature of Prins' method is that he has treated the absorption in the classical manner, as if it took place by coherent processes, which in general leads to the substitution of $(\delta+i\beta)$ for δ when it appears in Darwin's treatment.

We shall take the result of Prins' calculations as it appears in Eq. (11) of his paper. This is, with a slight change of notation,

$$\frac{I_{(\beta-\theta_0)}}{I_0} \tag{13}$$

$$= \left| \frac{d + ib}{(\beta-\theta_0)\sin\theta_0\cos\theta_0 - (\delta+i\beta) + (\{(\beta-\theta_0)\sin\theta_0\cos\theta_0 - (\delta+i\beta)\}^2 - (d+ib)^2)^{1/2}} \right|^2$$

We shall first consider the application of this formula to a crystal composed of atoms of one kind only, in equally spaced planes. Under these conditions the quantity $(d+ib)$ is related to the quantity $(\delta+i\beta)$ as the amplitude of the wave scattered by an atom at angle $2\theta_0$ to the amplitude scattered in the forward direction. In order to be more specific about the relationship between the two quantities, we will adopt the simpler of Prins' two hypotheses, hypothesis *I*. This states that all electrons in the atom may be treated in the same way as regards the amplitude scattered as a function of the scattering angle, irrespective of the level to which they belong. This hypothesis leads to the relation

$$d + ib = (\delta + i\beta)f(2\theta_0)/f(0) \tag{14}$$

where $f(2\theta_0)$ is the amplitude scattered by the atom at the angle $2\theta_0$ from an incident wave of unit amplitude. A more detailed and correct procedure would be to consider the *K*, *L*, *M*, etc. electrons in the atom separately, both with respect to their contributions to δ and β, and the angular distribution of the amplitude scattered from them. In this paper, however, the simplified procedure of Eq. (14) will be adopted.

[9] Prins, Zeits. f. Physik **63**, 477 (1930).

In a crystal such as calcite, which consists of interlaced planes of different kinds of atoms; instead of $(d+ib)$ in Eq. (13), we must introduce a quantity

$$D + iB = \sum_i (\delta_i + i\beta_i) \frac{f_i(2\theta_0)}{f_i(0)} e^{2\pi n i(hx_i+ky_i+lz_i)}. \tag{15}$$

In this expression, δ_i is the contribution to δ for the medium from atom i. n is the order of the reflection; h, k, l, the Miller indices of the reflecting plane, and x_i, y_i, z_i the coordinates of the atom i in the unit cell. The summation is to be carried out over all the atoms present in the unit cell. In more common notation, for the σ type of polarization defined above,

$$f_i(2\theta_0)/f_i(0) = F_i Z_i^{-1} \tag{16}$$

where F_i is the atomic structure factor of the atom of type i, and Z_i is the number of electrons in the atom.

In calculating the values of $D+iB$ by Eq. (15), the author has made a further approximation, namely, that the contributions to δ and β from a given atom i are proportional to the fraction of the total number of electrons in the unit cell contained in the atom in question. If Z is the total number of electrons in the unit cell, this means that

$$\delta_i + i\beta_i = Z_i(\delta + i\beta)/Z. \tag{17}$$

It is clear that more accurate calculations could be made, the best method being perhaps to subdivide the electrons in the unit cell into groups according to their binding energy, but in view of the approximate nature of the graphical calculations to come later it would seem that the somewhat crude assumption of Eq. (17) is permissible.

Substitution of Eqs. (17) and (16) in Eq. (15) gives

$$D + iB = Z^{-1}(\delta + i\beta) \sum_i F_i e^{2\pi n i(hx_i+ky_i+lz_i)}. \tag{18}$$

The summation in Eq. (18) is commonly known as the structure factor F, so that finally,

$$D + iB = Z^{-1}F(\delta + i\beta). \tag{19}$$

We are now ready to adapt Eq. (13) to a crystal of more than one kind of atom, and to put it into a form similar to Eq. (11). It should be noted that in Eq. (13) the reference angle is θ_0, the uncorrected Bragg angle, whereas in Eq. (10) the reference angle is θ. In terms of θ_0, the expression for ξ_σ in Eq. (10) becomes, after making use of Eq. (6).

$$\xi_\sigma = \frac{(\beta - \theta_0)\sin\theta_0\cos\theta_0}{2\delta FZ^{-1}} - \frac{1}{2FZ^{-1}}. \tag{20}$$

Putting $D+iB$ from Eq. (19) in place of $d+ib$ in Eq. (13), and introducing ξ_σ from Eq. (20), we obtain

$$F(\xi_\sigma) = \left| \frac{FZ^{-1}(1 + i\beta/\delta)}{2\xi_\sigma FZ^{-1} - i\beta/\delta + [(2\xi_\sigma FZ^{-1} - i\beta/\delta)^2 - F^2Z^{-2}(1 + i\beta/\delta)^2]^{1/2}} \right|^2. \tag{21}$$

If the effect of absorption is neglected, that is, $\beta = 0$, this expression reduces to Eq. (11), Darwin's original form.

The calculation of the shape of the diffraction pattern to be expected from a perfect calcite crystal irradiated at the proper angles by monochromatic, plane, x-rays of wave-lengths 0.708A, (Mo $K\alpha_1$), 1.537A (Cu $K\alpha_1$), and 2.285A (Cr $K\alpha_1$) has been carried out from Eq. (21). The values of δ were obtained from Larsson.[10] The values of β may be obtained from the linear absorption coefficient by Eq. (12). The value of μ_l was calculated for Mo $K\alpha_1$ in calcite from data collected by A. H. Compton,[11] and extended to other wave-lengths by assuming the validity of the λ^3 law. The values used are shown in Table III.

TABLE III. *Values of δ and β used in Eq. (21).*

λ	δ	β	β/δ
0.708A	1.87×10^{-6}	1.31×10^{-8}	0.007
1.537	8.80	2.92×10^{-7}	0.033
2.285	19.5	1.43×10^{-6}	0.073

The value of FZ^{-1} for calcite in the first order from the cleavage faces, based on the atomic structure factors of Bragg and West[12] has been shown by Allison and Williams[1] to be 0.47. All the calculations of this paper have been based on this value, which may be somewhat low, as discussed later. Some of the values of $F(\xi_\sigma)$ for these three cases, both from Eq. (11) (Darwin) and Eq. (21) (Prins) are shown in Table IV.[13]

TABLE IV *Diffraction pattern of a perfect calcite crystal.*

Eq. (10) ξ_σ	$F(\xi_\sigma)$ Darwin	$F(\xi_\sigma)$ Prins Mo $K\alpha_1$	Cu $K\alpha_1$	Cr $K\alpha_1$
−2.13	0.014	0.014	0.014	0.014
−1.06	0.063	0.062	0.062	0.062
−0.85	0.106	0.105	0.105	0.105
−0.64	0.234	0.233	0.232	0.229
−0.43	1.000	0.959	0.874	0.709
−0.21	1.000	0.973	0.881	0.758
±0.00	1.000	0.971	0.870	0.735
+0.21	1.000	0.960	0.830	0.670
0.43	1.000	0.924	0.702	0.503
0.53	0.501	0.486	0.426	0.341
0.64	0.234	0.233	0.229	0.213
0.85	0.106	0.105	0.105	0.103
1.06	0.063	0.062	0.062	0.062
2.13	0.014	0.014	0.014	0.014

The calculated values of Table IV are shown graphically in Fig. 2. An interesting feature of the curves corrected for absorption by Prins' method is that

[10] Larsson, Diss. Upsala 1929. Reported in Siegbahn, Spektroskopie der Rontgenstrahlen, 2nd Ed., (1931) Table XIII, p. 39.

[11] A. H. Compton, X-rays and Electrons, (1926), Table VI–2 p. 182.

[12] Bragg and West, Zeits. f. Krist. **69**, 118 (1928).

[13] A large part of the calculations involved in this paper were made for me by Mrs. G. S. Monk, computer of this laboratory.

they are asymmetrical. The possibility of detecting such a lack of symmetry by double spectrometer measurements will be discussed later.

The areas under the curves of Fig. 2 are important in the theory of intensity of reflection. By integration of Eq. (11) it may be shown that

$$\int_{-\infty}^{\infty} F(\xi_\sigma) d\xi_\sigma = 4/3. \tag{22}$$

The unit of angular deviation in Eq. (22) is the angle $\Delta\theta_\sigma$, as is shown by Eq. (10). If we adopt more fundamental units, i.e., radians, the area under the diffraction pattern is $4\Delta\theta_\sigma/3$. The areas under the other curves of Fig. 2 were obtained by use of the integraph, and are shown in Table V.[14]

TABLE V. *Values of* $\int_{-\infty}^{\infty} F(\xi_\sigma) d\xi_\sigma$ *from Eqs. (11) and (21).*

Line	Darwin	Prins
Mo $K\alpha_1$	1.333	1.250
Cu $K\alpha_1$	1.333	1.122
Cr $K\alpha_1$	1.333	0.935

Calculation of the shape of the (1, −1) rocking curve for plane polarized radiation

A careful analysis of the operation of the double crystal spectrometer shows that the shape of the rocking curve obtained in parallel positions in the first order could not possibly be that of the curves in Fig. 2, even if perfect crystals were available and the instrument were in correct adjustment. Neither can be the area under a rocking curve be directly compared with the areas under the curves in Fig. 2. The fundamental physical reason for this is that all the theoretical curves previously described were calculated for parallel, monochromatic radiation. Due to the fact that the dispersion is zero in parallel positions, the spectral distribution of the radiation is not important, but, although the first crystal greatly reduces the horizontal divergence of the beam, it does not reduce it to zero, and the beam incident on crystal B is still a divergent one. The author has previously pointed out[15] that the function governing the shape of the rocking curves is

$$\Phi(\xi_{B\sigma}) = \int_{-\infty}^{\infty} F(\xi_\sigma) F(\xi_\sigma - \xi_{B\sigma}) d\xi_\sigma. \tag{23}$$

In this expression,

$$\xi_{B\sigma} = (\beta_B - \theta_B)/\Delta\theta_\sigma \tag{24}$$

[14] It is these areas which, expressed in radian measure, are usually defined as the coefficients of reflection, and it is true that the reflecting power of a single crystal is proportional to them. It is one of the principal objects of this paper to make clear that there is a discrepancy between this definition and the experimental attempts to measure this quantity by the double spectrometer. In this paper, the term coefficient of reflection refers to area under the rocking curve of crystal B. This is quite a different thing physically from the areas in Table V.

[15] S. K. Allison, Phys. Rev. **38**, 203 (1931) Eq. (8).

where $(\beta_B - \theta_B)$ is the angular deviation of crystal B from the position in which its reflecting face is parallel to that of A. $\Phi(\xi_{B\sigma})$ is the intensity of the beam entering the ionization chamber from a single position of crystal B. $F(\xi_\sigma)$ is the diffraction pattern for a single crystal as in Fig. 2. The derivation of Eq. (23) is perhaps made clearer by Fig. 3, in which the course of a ray through the instrument is shown.

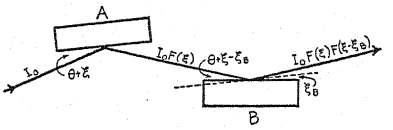


Fig. 3. Course of a ray through the double spectrometer in a parallel position, illustrating Eq. (23).

It is the custom to express the intensity reflected from B in terms of the intensity of the beam incident on B from A, which is proportional to the area under the single crystal diffraction pattern. We thus obtain the following expression

$$P_\sigma = \frac{\int_{-\infty}^{\infty} F(\xi_\sigma)F(\xi_\sigma - \xi_{B\sigma})d\xi_\sigma}{\int_{-\infty}^{\infty} F(\xi_\sigma)d\xi_\sigma} \tag{25}$$

where P_σ is the ordinate of the rocking curve from crystal B according to the convention above. The percent reflection, P_0, will be given by the value of P_σ when $\xi_{B\sigma} = 0$, or

$$P_0 = \frac{\int_{-\infty}^{\infty} [F(\xi_\sigma)]^2 d\xi_\sigma}{\int_{-\infty}^{\infty} F(\xi_\sigma)d\xi_\sigma}. \tag{26}$$

Laue[16] has discussed the possibility of solving Eq. (23), that is, of determining the shape of the single crystal diffraction pattern from the experimentally determined $\Phi(\xi_{B\sigma})$, and has come to some important conclusions. In the first place, the observed rocking curve ($\Phi(\xi_{B\sigma})$ or P_σ) will necessarily be an even function, whether or not the single crystal diffraction curves $F(\xi_\sigma)$ are asymmetrical. If we assume that the single crystal diffraction pattern is an even function, then it is possible to find its shape by solution of Eq. (23), otherwise, not. This means that by experiments of the type reported here it is impossible to discover whether the single crystal diffraction patterns are really asymmetrical as in the theory of Prins. If asymmetrical rocking curves are experimentally found, the only legitimate interpretation is that the diffraction patterns of the two crystals used are not identical. It should be remembered that the preceding statement applies only to parallel positions.

[16] Laue, Zeits. f. Physik **72**, 472 (1931).

In view of the findings of Laue, as reported above, the author has not attempted to solve the Eq. (23), using his observed $\Phi(\xi_{B\sigma})$, and discover the nature of the single crystal curve. The procedure adopted has been the reverse of this, namely to calculate $\Phi(\xi_{B\sigma})$ from Eq. (23), using theoretical $F(\xi_\sigma)$'s from Eqs. (11) and (21), and comparing the result with experiment. Calculated values of $\Phi(\xi_{B\sigma})$ are shown in Table VI. These values were obtained mainly by graphical integration.

TABLE VI. *Calculated values of* $\Phi(\xi_{B\sigma})$ *from Eq. (23). The unit of angle is* $\Delta\theta_\sigma$ *from Eq. (9).*

$\xi_{B\sigma}$	Darwin	Prins Mo $K\alpha_1$	Prins Cu $K\alpha_1$	Prins Cr $K\alpha_1$
0	1.068	0.970	0.765	0.521
±0.21	0.954	.876	.694	.475
± .43	.786	.727	.566	.401
± .64	.590	.552	.434	.308
± .85	.396	.378	.272	.212
±1.06	.209	.200	.161	.135
±1.60	.077	.070	.063	.052
±2.13	.040	.036	.033	.029
±2.66	.024	.022	.020	
±3.19	.019	.014	.013	.012

Calculation of the shape of the rocking curve with unpolarized incident radiation

Before comparing the calculations summarized in Table VI directly with experiment, we must consider the fact that after reflection from crystal A, the beam incident on crystal B is partially polarized. Since the radiation used was in each case a characteristic emission line of the target, it is known that the radiation incident on crystal A was completely unpolarized. We may then arbitrarily divide up the beam incident on A into two components of equal intensity, one polarized so that its electric vector is perpendicular to the plane of incidence (subscript σ) and one with its electric vector parallel to the plane of incidence (subscript π). We then treat each component separately in its passage through the apparatus. In Darwin's treatment, the extent of the region of 100 percent reflection with π-polarization is

$$\Delta\theta_\pi = 4\delta FZ^{-1} \operatorname{cosec} 2\theta_0 \cos 2\theta_0 = 4\delta FZ^{-1} \cot 2\theta_0 \tag{27}$$

which is to be compared with Eq. (9). We now introduce the quantities

$$\xi_\pi = (\beta - \theta)/\Delta\theta_\pi = \xi_\sigma \sec 2\theta_0 \tag{28}$$

and

$$\xi_{B\pi} = (\beta_B - \theta_B)/\Delta\theta_\pi = \xi_{B\sigma} \sec 2\theta_0. \tag{29}$$

By use of the preceding three equations, the derivation of the rocking curves for radiation polarized so that its electric vector lies in the plane of incidence (π-polarization) may be accomplished simply by changing the subscript σ to π in all the equations in which it appears up to and including Eq. (26). In adding the contributions from σ- and π-components to obtain the unpolarized values, it must be remembered that the angular unit in which σ

and π quantities are expressed is different. (Compare Eqs. (27) and (9).) We shall adopt the angular unit $\Delta\theta_\sigma$ in the following equations dealing with unpolarized radiation, and change quantities expressed in terms of $\Delta\theta_\pi$ to their values in terms of $\Delta\theta_\sigma$. We then obtain

$$P = \frac{\Phi(\xi_{B\sigma}) + \Phi(\xi_{B\pi})\cos 2\theta_0}{\int_{-\infty}^{\infty} F(\xi_\sigma)d\xi_\sigma + \int_{-\infty}^{\infty} F(\xi_\pi)d\xi_\pi} = \frac{\Phi(\xi_{B\sigma}) + (\cos 2\theta_0)\Phi(\xi_{B\sigma}\sec 2\theta_0)}{(1+\cos 2\theta_0)\int_{-\infty}^{\infty} F(\xi_\sigma)d\xi_\sigma} \tag{30}$$

where P is the ordinate of the rocking curve, that is, the ratio of the ionization current obtained from a setting of crystal B to the current obtained from the

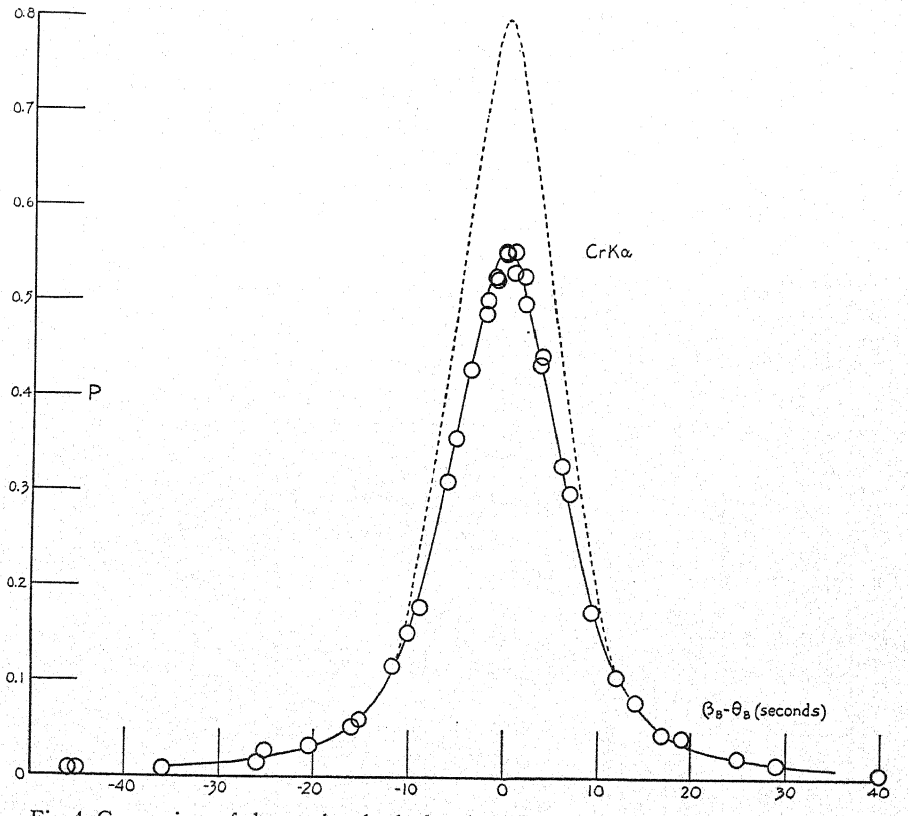


Fig. 4. Comparison of observed and calculated rocking curves for Cr $K\alpha_1$. The dotted curve is the rocking curve calculated from Darwin's theory, in which absorption in the crystal is neglected. The solid curve is the curve derived from Prins' theory. The circles represent experimental points. The points are not fitted to the curve in any way, for instance by an adjustable constant.

radiation incident on B from A. If $\xi_{B\sigma}=0$ in Eq. (30), that is, the two crystals are accurately parallel, it reduces to Eq. (26), which means that the percent reflection, P_0, is independent of the polarization. This, of course, is not true of the coefficient of reflection, R.

The use of Eq. (30) will be illustrated by a sample calculation of a point on

the rocking curve for Cr $K\alpha_1$ (1, −1) according to Prins. The denominator of Eq. (30) can be obtained from a knowledge of the Bragg angle for Cr $K\alpha_1$ on calcite, with the values in Table V. Its value is $(1+0.715)\ (0.935)=1.603$. Let us consider a setting of crystal B such that $\xi_{B\sigma}=0.64$. From Table VI we find $\Phi(\xi_{B\sigma})=0.308$. The value of $\xi_{B\sigma}\sec 2\theta_0$ is $0.64\times 1.40=0.896$. From interpolation of Table VI, we find $\Phi(0.896)=0.194$, and $\Phi(0.896)\cos 2\theta$ is 0.139. Thus P for this setting of the crystal is 0.279.

The calculated values of $\Delta\theta_\sigma$ from Eq. (9) are shown in Table VIII. They are computed for $FZ^{-1}=0.47$, using δ-values from Table III, with the exception of W $K\alpha_1$, where δ is extrapolated by assuming a variation with λ^2. The rocking curves to be expected from calcite for Cr $K\alpha_1$ (1, −1) with unpolarized radiation from Darwin's and Prins equations can be plotted from the calculated values shown in Table VII.

TABLE VII. *Theoretical form of the calcite rocking curve* Cr $K\alpha_1$ *(1, −1).*

$\xi_{B\sigma}$	$\beta_B-\theta_B$ (seconds)	P Darwin	P Prins
0.0	0	0.798	0.557
± .21	2.27	.698	.496
± .43	4.64	.540	.396
± .64	6.91	.370	.279
± .85	9.18	.229	.183
±1.06	11.4	.125	.116
±1.60	17.3	.045	.045
±2.13	23.0	.024	.025
±2.66	28.7	.015	.016
±3.19	34.5	.011	.010

TABLE VIII. *Values of* $\Delta\theta_\sigma$.

Line	λ	cosec 2θ	$\Delta\theta_\sigma$ radians	$\Delta\theta_\sigma$ seconds
W $K\alpha_1$	0.2086A	14.44	4.4×10^{-6}	0.91
Mo $K\alpha_1$	0.7078	4.31	15.2	3.14
Cu $K\alpha_1$	1.537	2.04	33.7	6.96
Cr $K\alpha_1$	2.285	1.43	52.4	10.8

The calculated rocking curves and the experimental points for Cr $K\alpha_1$ taken on crystals III are shown in Fig. 4. It is seen that the calculated rocking curve agrees within the experimental error with that obtained experimentally. The half width at half maximum of the theoretical curve is 6.9″, the observed value is 7.1″. The percent reflection P_0 is 0.557 from Table VII; the observed value is 0.554. It is of interest to note that according to the analysis of the action of the double spectrometer presented in this paper, even if the diffraction pattern from each of the two crystals could be treated by Darwin's equation, the observed percent reflection would only be 0.798 as against 1.00 which has been expected by some writers.

The shape of the rocking curve to be expected from Prins' theory has been calculated for Mo $K\alpha_1$, Cu $K\alpha_1$ and Cr $K\alpha_1$. The rocking curve to be expected from W $K\alpha_1$ has been calculated from Darwin's equation directly. The re-

sultant P_0's and half widths at half maximum, w, are compared with experiment in Fig. 5. The resolving power is calculated from a previous definition of the author,[17] which is

$$\lambda/d\lambda = D\lambda/2w. \tag{31}$$

This is to be interpreted as the resolving power which the instrument would have in the (1, 1) position with the same crystals. D is the dispersion of the instrument in the (1, 1) position.

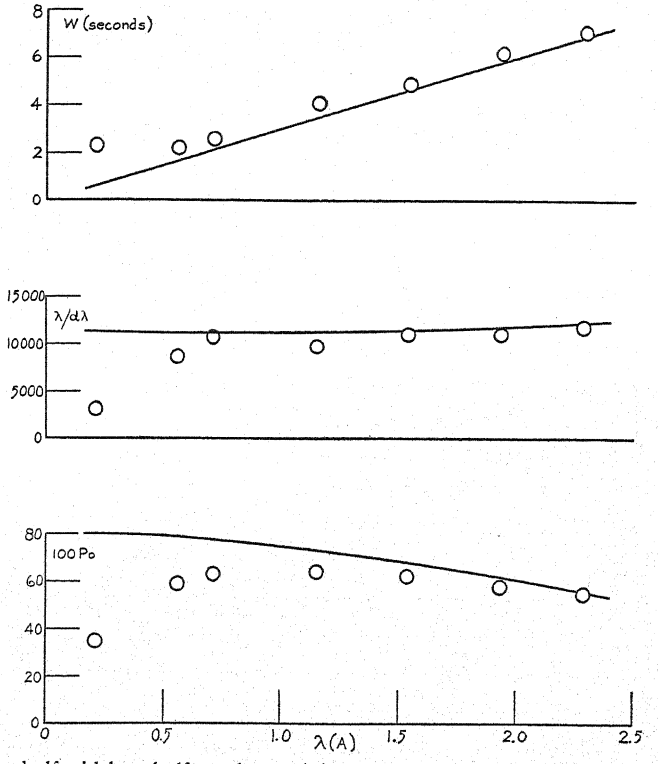


Fig. 5. The half width at half maximum (w), resolving power ($\lambda/d\lambda$), and percent reflection (P_0) of calcites III compared with theoretical values deduced from Prins. The solid curves are theoretical values, the points, experimental ones.

Calculation of the coefficient of reflection

In order to calculate the coefficient of reflection as defined in this paper we must find the area under the P curve (rocking curve) with the radian as the unit of angular measure. Thus

$$R = \Delta\theta_\sigma \frac{\int_{-\infty}^{\infty} [\Phi(\xi_{B\sigma}) + \Phi(\xi_{B\sigma} \sec 2\theta) \cos 2\theta] d\xi_{B\sigma}}{(1 + \cos 2\theta) \int_{-\infty}^{\infty} F(\xi_\sigma) d\xi_\sigma} \tag{32}$$

[17] S. K. Allison, Phys. Rev. **38**, 203 (1931), Eq. (21) 208.

or, finally,

$$R = \frac{\int_{-\infty}^{\infty} \Phi(\xi_{B\sigma}) d\xi_{B\sigma}}{\int_{-\infty}^{\infty} F(\xi_\sigma) d\xi_\sigma} \frac{1 + \cos^2 2\theta}{1 + \cos 2\theta} 4\delta FZ^{-1} \operatorname{cosec} 2\theta. \tag{33}$$

The values of the integral in the numerator of Eq. (33) have been obtained by graphical integration of curves plotted from the data of Table VI, and are shown in columns 3 and 4 of Table IX. Columns 6, 7, and 8 of Table IX show the calculated and observed coefficients of reflection.

TABLE IX. *Calculation of R from Eq. (33) and comparison with observations.*

Line	λ	$\int_{-\infty}^{\infty} \Phi(\xi_{B\sigma}) d\xi_{B\sigma}$		$\frac{1+\cos^2 2\theta}{1+\cos 2\theta}$	$R \times 10^5$		
		Darwin	Prins		Darwin	Prins	Obs.
W $K\alpha_1$	0.209A	1.631	—	0.999	0.536	—	1.17
Mo $K\alpha_1$	0.708	"	1.537	0.987	1.85	1.84	1.86
Cu $K\alpha_1$	1.54	"	1.238	0.940	3.87	3.49	3.46
Cr $K\alpha_1$	2.28	"	0.917	0.881	5.65	4.53	4.68

A graph of the information in Table IX, together with R values measured by other observers is shown in Fig. 6. Only the experimental data obtained in these experiments on crystals III are included in Fig. 6.

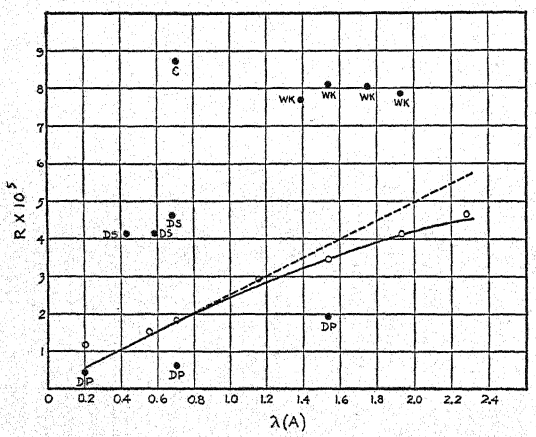


Fig. 6. Calculated and observed values of the coefficient of reflection (R). The dotted curve represents values calculated from Darwin; the solid curve, values from Prins. The open circles are experimental values of crystals III. The solid circles are points by other observers. *C*—Compton;[1] *WK*—Wagner and Kuhlenkampff;[1] *DS*—Davis and Stempel;[1] *DP*—Davis and Purks.[1]

Discussion of results

The most obvious comment to be made on the agreement of observed and calculated coefficients of reflection from 0.5 to 2.3 A as illustrated for crystals III on Fig. 6 is that the agreement is very surprising since no temperature corrections have been applied. The coefficient of reflection should decrease

with rising temperature. The calculation of the temperature correction for a complicated crystal such as calcite is difficult and has not been attempted. The value of $(\sin\theta)/\lambda$ for all the present measurements is 0.165 which is comparatively small, and the temperature correction is proportional to this. There is, however, some evidence that the value $FZ^{-1}=0.47$ used here is too small. This value was based on the structure factors of Bragg and West.[12] More recently James and Brindley[18] and Pauling and Sherman[19] have published tables of structure factors. The exact value of FZ^{-1} depends on the particular electronic structure assumed for the molecule $CaCO_3$ as it appears in the crystal. By assuming arrangements from Ca^{+2}, C^{+4}, O^{-2} to Ca^0, C^0, O^0 we get values of FZ^{-1} which in the table of James and Brindley range from 0.472 to 0.500, and from 0.496 to 0.518 in the table of Pauling and Sherman. If these newer structure factors are preferable to the older values, the value of 0.47 as used in this paper is somewhat too low.[20] It is quite possible that this choice of a low structure factor is compensated by failure to make a temperature correction, thus giving the agreement of Fig. 6. This agreement does not extend to wave-lengths as short as W $K\alpha_1$ (0.2086A), and large deviations are apparent in the quantities plotted in Fig. 5 at this wave-length also. The laws of scattering of these relatively hard wave-lengths are undoubtedly different from the laws applicable in the range 0.5 to 2.3A, a large fraction of the scattering taking place by the Compton process. It is the opinion of the author that this lack of agreement shows that the theory of diffraction by a perfect crystal should be re-investigated in this shorter wave-length region.

If the coefficients of reflection observed by Davis and Purks and entered in Fig. 6 are correct,[21] they present a very serious difficulty, since they are far below the perfect crystal values. The Davis and Purks rocking curve widths for W $K\alpha_1$ $(1, -1)$ were 2.5 seconds full widths at half maximum. The author has been unable to find any calcite specimens that even approach this small value, the values obtained ranging from 4.6 to 14.4 seconds in various specimens. The high values of the coefficient of reflection observed by other authors and entered in Fig. 6 are probably due to the use of calcite surfaces considerably less perfect than those used in the present experiments.

The general statement that these results confirm Prins' modification of Darwin's theory is incorrect in a very important aspect. The present results show that some sort of absorption correction to Darwin's results is needed, but really give no information at all as to the exact shape of the diffraction pattern from a single crystal. In particular, the present results give no information for or against the asymmetrical nature of the patterns in Prins' theory. The fact that the calculated and observed values of P_0 are appreciably dif-

[18] James and Brindley, Phil. Mag. **12**, 81 (1931).

[19] Pauling and Sherman, Zeits. f. Krist. **81**, 1 (1932).

[20] I am indebted to W. H. Zachariasen of this laboratory for stimulating discussions of these matters.

[21] Recent communications from Professor Davis state that on repeating the experiments of Davis and Purks under discussion, the rocking curves from the same sample of calcite were found to be wider than at first reported.

ferent for wave-lengths other than Cr $K\alpha_1$ (at Mo $K\alpha_1$ calculated, 0.776; observed, 0.63) may be taken as evidence that the shape of the single crystal diffraction pattern is not exactly that of Prins. The value of P_0 is quite sensitive to the shape of the pattern, and independent of the polarization. For instance, let us compare three functions all having maxima equal to unity. If the shape of the diffraction pattern for a single crystal were given by $\exp(-\xi^2)$, we should find $P_0=0.71$ from Eq. (26). In the same way if $F(\xi)=(1+\xi^2)^{-1}$, $P_0=0.500$, and if $F(\xi)=(1+\xi^2)^{-2}$, $P_0=0.625$.

A further question of interest is related to the possibility of finding other calcite surfaces as good as those of calcites III in this research. A. H. Compton[3] has reported rocking curves for Mo $K\alpha_1$ $(1, -1)$ of 5 seconds full width at half maximum which agrees with the present results. Hoyt[22] has reported rocking curves under the same conditions somewhat less than 5 seconds wide. Allison and Williams,[1] found a full width at half maximum of 6 seconds. In view of these results it does not seem that such calcite surfaces are exceedingly rare. There is no evidence from the experiments reported here that the width of the rocking curve is a constant for a given piece of calcite, that is, a large sample from a known source. In the author's experiments different splits from the same large piece showed different widths.

Darwin, and other workers following him, have interpreted high values of R, for instance, those of Wagner and Kuhlenkampff in Fig. 6, as evidence for a mosaic structure of crystals. The present research shows that it is possible to obtain calcite surfaces for which there is no evidence of mosaic structure from measurements of the coefficient of reflection by double spectrometer methods in the wave-length region from 0.5 to 2.3A. Presumably the effects of a secondary structure as postulated by Zwicky[23] would not influence the present results.

Note added in proof: Since completion of this article more accurate calculations of theoretical curves have been carried out by eliminating the assumption of Eq. (17). This assumption states that the absorption correction can be rightly applied by assuming that the absorption of an atom in the unit cell is proportional to the fraction of the total number of electrons in the unit, all contained in the atom in question. This is rather far from correct in the absorption by the calcium atoms in calcite for wave-lengths shorter than the K-absorption limit of calcium. The more rigorous calculations direct from Eq. (15) show slight changes in the theoretical values, but do not invalidate in any way the general conclusions of this article. These new calculations will appear in a paper to be submitted from this laboratory in the near future.

[22] A. Hoyt, Paper delivered at the Washington Meeting of the American Physical Society, April, 1932.

[23] Zwicky, Phys. Rev. 40, 63 (1932).

The Scattering of X-rays by Gases and Crystals

By Y. H. Woo
Department of Physics, National Tsing Hua University, Peiping, China

(Received May 6, 1932)

It is shown that, in exact agreement with the wave mechanical result worked out by Wentzel and Waller and Hartree, the Raman-Compton-Jauncey formula for the scattering of x-rays by an atom deduced on the basis of classical electrodynamics may be written

$$I_\phi = I_e\left\{F^2 + Z - \sum_{r=1}^{z} E_r^2\right\}, \qquad \text{(A)}$$

where I_ϕ is the intensity scattered in a direction ϕ with the primary beam, I_e is the scattering from a single isolated electron as calculated by Thomson, Z is the atomic number, E_r is the average amplitude of the waves scattered by the r-th electron in the atom and F is the true atomic structure factor as given by $F=\Sigma_1^z E_r$. This shows that the coherent scattering is proportional to F^2 and that the introduction of the average atomic structure factor F' by Jauncey is unnecessary. On the basis of Eq. (*A*), theoretical formulas for the scattering of x-rays by gases and crystals are redeveloped and the results turn out to explain all the disagreement between theories proposed by Jauncey and the writer.

IN DISCUSSING the scattering of x-rays by polyatomic gases, Jauncey[1] has recently pointed out that the theoretical formula deduced by the writer[2] is not exactly in agreement with that obtained by himself. Since the writer regards the atoms in a polyatomic system (a molecule or a crystal) as the scattering units, this disagreement should also occur when the scattering of x-rays by crystals is dealt with. The purpose of the present note is to discuss this matter in detail.

Taking account of the modification introduced by Jauncey,[3] the Raman-Compton[4] formula for the scattering of x-rays by an atom may be written

$$I_\phi = I_e\{F'^2 + Z - F'^2/Z\}, \qquad (1)$$

where I_ϕ is the intensity scattered at an angle ϕ to a distance R, I_e is the scattering from a single isolated electron as calculated by J. J. Thomson, Z is the atomic number and F' is the average atomic structure factor. According to Jauncey,[3] the relation between the average atomic structure factor F' and the true atomic structure factor F is expressed by

$$F'^2 = F^2 - \left(Z\sum_{r=1}^{Z} F_r^2 - F^2\right)\Big/(Z-1), \qquad (2)$$

[1] G. E. M. Jauncey, Phys. Rev. **39**, 561 (1932).
[2] Y. H. Woo, Phys. Rev. **39**, 555 (1932).
[3] G. E. M. Jauncey, Phys. Rev. **37**, 1193 (1931).
[4] C. V. Raman, Indian J. Phys. **3**, 357 (1928). A. H. Compton, Phys. Rev. **35**, 925 (1930).

where E_r is the average amplitude of the waves scattered by the r-th electron in the atom and where the true atomic structure factor F is given by

$$F = \sum_{r=1}^{Z} E_r. \tag{3}$$

In view of the similarity between Eq. (1) and the formula originally derived by Raman and Compton,[4] the part $I_e F'^2$ was taken[5] by analogy to represent the coherent scattering and the other terms to represent the incoherent scattering. However, there exists no physical or mathematical reason for justifying this separation. On substituting the value of F' given by (2) into Eq. (1), we find as a result of straightforward calculation

$$I_\phi = I_e \left\{ F^2 + Z - \sum_{r=1}^{Z} E_r^2 \right\}. \tag{4}$$

This is exactly the same expression as that obtained by Wentzel[6] and independently by Waller and Hartree[7] on the basis of wave mechanics. This shows that the coherent part of the total intensity is proportional to F^2 and that the introduction of the average atomic structure factor F' by Jauncey is unnecessary. When corrected for the change of wave-length, Eq. (4) becomes

$$I_\phi = I_e F^2 + I_e \frac{Z - \sum_{1}^{Z} E_r^2}{[1 + \gamma(1 - \cos\phi)]^3}, \tag{5}$$

where $\gamma = h/mc\lambda$ and h, m, c and λ have their usual significance.

Recently Herzog[8] has actually compared Eq. (5) with experiments reported by Wollan[9] on absolute measurements of the scattering of Mo K_α rays by helium, neon and argon gases. The agreement seems to be quite satisfactory.

On the basis of Eq. (5) and following the arguments presented by the writer in previous papers,[10] the theoretical formulas for the scattering of x-rays by gases and crystals can be easily redeveloped. For the scattering from a simple cubic crystal consisting of atoms of one kind, the diffusely scattered intensity is given by

[5] Cf. G. E. M. Jauncey, Phys. Rev. **38**, 1 (1931); **39**, 561 (1932); Y. H. Woo, Phys. Rev. **39**, 555 (1932).

[6] G. Wentzel, Zeits. f. Physik **43**, 1 and 779 (1927).

[7] I. Waller, Zeits. f. Physik **51**, 213 (1928); Waller and Hartree, Proc. Roy. Soc. **A124**, 119 (1929). The more exact formula obtained by these authors differs from Eq. (4) by including some negative terms arising from consideration of Pauli's principle, but the contribution to the total scattering due to these negative terms is negligible in comparison with that due to the terms included in Eq. (4).

[8] G. Herzog, Zeits. f. Physik **70**, 583 and 590 (1931). Cf. also Y. H. Woo, Sci. Rep. Tsing, Univ. AI, No. 4 (1932).

[9] E. O. Wollan, Phys, Rev. **37**, 862 (1931).

[10] Y. H. Woo, Proc. Nat. Acad. Sci. **17**, 467 (1931); Phys. Rev. **38**, 6 (1931), and **39**, 555 (1932).

$$I_\phi = NI_e\{(1 - e^{-2M})F^2 + \frac{Z - \sum_1^Z E_r^2}{[1 + \gamma(1 - \cos\phi)]^3}\cdot \tag{6}$$

For the intensity scattered by a gas molecule containing atoms $I, \cdots i, \cdots n$ arranged at fixed distances from each other, the formula becomes

$$I_{\phi n} = I_e \sum_1^n \sum_1^n F_i F_j \frac{\sin kS_{ij}}{kS_{ij}} + I_e \sum_1^n \frac{Z_i = \sum_1^{Z_i} E_r^2}{[1 + \gamma(1 - \cos\phi)]^3}\cdot \tag{7}$$

In Eq. (6) N is the number of atoms per unit volume of the crystal and e^{-2M} is the temperature factor as calculated by Debye[11] and Waller[12] and in Eq. (7) F_i is the true atomic structure factor for the i-th atom, $k = (4\pi/\lambda)\sin\frac{1}{2}\phi$, s_{ij} is the distance of any atom i from any other atom j. The other quantities have the same meaning as those employed in Eq. (5). When applied to the scattering by a diatomic gas consisting of two like atoms, Eq. (7) gives for the scattering per electron

$$S = \frac{I_{\phi 2}}{2ZI_e} = \left(1 + \frac{\sin kS}{kS}\right)\frac{F^2}{Z} + \frac{1 - \frac{1}{Z}\sum_1^Z E_r^2}{[1 + \gamma(1 - \cos\phi)]^3} \tag{8}$$

where s is the distance between the two atoms in the scattering molecule.

It will be noticed that Eq. (6) agrees with the formula deduced by Jauncey and Harvey[13] provided the latter is properly corrected for the change of wavelength. Also a comparison of Eqs. (7) and (8) with those recently obtained by the writer[14] and Jauncey[15] will clearly show that, if the coherent and incoherent scattering be properly separated, the disagreement pointed out by Jauncey no longer exists. Finally, referring the comparison between theory and experiment recently made by the writer,[14] it can be readily concluded that Eq. (8) is supported by Wollan's measurements[16] on the scattering of Mo K_α radiation by diatomic gases.

[11] P. Debye, Ann. d. Physik **43**, 49 (1914).
[12] I. Waller, Zeits. f. Physik **17**, 389 (1923); *Upsala Dissertation*, (1925).
[13] Jauncey and Harvey, Phys. Rev. **37**, 1203 (1931).
[14] Y. H. Woo, Phys. Rev. **39**, 555 (1932).
[15] G. E. M. Jauncey, Phys. Rev. **39**, 561 (1932).
[16] E. O. Wollan, Phys. Rev. **37**, 862 (1931); Proc. Nat. Acad. Sci. **17**, 475 (1931).

Ionization of Air by γ-Rays as a Function of Pressure and Collecting Field

By I. S. BOWEN
Norman Bridge Laboratory of Physics, California Institute of Technology

(Received May 23, 1932)

The ionization of air by γ-rays was studied for pressures from 1 to 93 atmospheres and for collecting fields from 1.55 to 1009 volts per cm. Increases in ionization current of over 40 percent were observed when the potential gradient was varied over this range, thus indicating that the lack of proportionality of ionization current with pressure obtained by previous observers was principally due to lack of saturation.

I. INTRODUCTION

THE ionization of air by γ-rays or by cosmic rays has been studied through a wide range of air pressures by Downey,[1] Fruth,[2] Broxton,[3] Swann,[4] and Millikan.[5] All of these observers agree in finding that as high pressures are reached the ionization per atmosphere decreases to a small fraction of its value at one atmosphere. In fact, the total ionization does not increase appreciably as the pressure is pushed above 100 atmospheres.

An explanation of this decrease has been proposed by Downey and elaborated by Broxton as follows. Practically all of the ionization in a gas is caused, not by the γ-rays or the cosmic rays themselves, but by the secondary β-rays ejected by them. At atmospheric pressure in any vessel of ordinary size the β-rays traversing the chamber are formed largely in the walls of the vessel. As the pressure is increased, however, the ranges of these β-particles decrease until they finally become less than the dimensions of the chamber. When this condition is reached the β-rays from the walls have produced all of the ions that they are capable of, and therefore any further increase of pressure cannot increase the total ionization caused by them. This theory appears then to predict the ionization pressure curves obtained by all observers.

However, it is a well established fact that the mass absorption coefficients of γ-rays and cosmic rays are not widely different for light substances such as air or water from their values for the metals out of which ionization chambers are usually made. Since the γ-rays or cosmic rays are absorbed in the air and since the only way in which their energy can be absorbed is by transfering it to secondary β-rays, it is obvious that the air must have approximately the same efficiency of production of β-rays as the walls. This being the case, any β-rays from the wall that are absorbed by the air are replaced by a corresponding number of β-rays ejected from the air itself. If

[1] K. M. Downey, Phys. Rev. **16**, 420 (1920); **20**, 186 (1922).
[2] H. F. Fruth, Phys. Rev. **22**, 109 (1923).
[3] J. W. Broxton, Phys. Rev. **27**, 542 (1926); **28**, 1071 (1926); **37**, 1320 (1931).
[4] W. F. G. Swann, J. Frank. Inst. **209**, 151 (1930).
[5] R. A. Millikan, Phys. Rev. **39**, 397 (1932).

this is true, the number of ions formed should be directly proportional to the pressure.

In order to reconcile this conclusion with the failure of all observers to collect this large a number of ions at the higher pressures, one is at once led to the suggestion, made independently by Millikan and Bowen[6] and by Compton, Bennett and Sterns,[7] that saturation was not attained at these high pressures, in spite of the fact that all experimenters tested for saturation in the usual way.

In all of these experiments the ionization chamber was a cylinder or sphere with a small collecting rod or fibre in the center. With this arrangement most of the potential drop is near the collecting rod while the great bulk of the chamber is subject to a potential gradient that, expressed in volts per cm, numerically amounts to only a very few percent of the total collecting potential applied. For this reason the highest potentials that these observers found it feasible to use, gave a gradient only a little above the point at which the ionization current became even approximately constant as the gradient was varied. Thus Broxton, in testing for saturation, varied his potential gradient through only 20 percent while the other experimenters carried their tests to only two or three times the gradient where the current became approximately constant. Obviously these tests would not bring to light variations of the type found in the experiments described in this paper.

II. Description of Apparatus

As no indication of a lack of saturation was found by previous observers when the collecting potential was varied through a small range, it was necessary to build an ionization chamber in which very much higher potential gradients could be applied if a satisfactory test of this lack of saturation was to be obtained. Obviously the older type of chamber was unsuited to this because of the very high total potentials necessary. Consequently a chamber was constructed in which the ions were collected between parallel plates, thus making possible a high uniform field. The ionization chamber was a steel cylinder 12.5 cm in diameter and 20 cm in length, designed to hold a pressure of 100 atmospheres. In this were placed 8 plates 10 cm in diameter which could be connected to a source of high potential. Alternating with these were 7 collecting plates 7.5 cm in diameter. These collecting plates were surrounded by grounded guard rings from which they were insulated by small amber lugs in grounded metal shields. The inside diameter of the guard rings were 7.7 cm and the outside 10 cm. The collecting plates were separated from the potential plates by 1 cm. This arrangement made possible the collection of ions from a definite known volume in which there was a uniform potential gradient which was numerically equal to the potential applied to the potential plates.

Ideally it should have been possible to measure directly the ionization by

[6] R. A. Millikan and I. S. Bowen, Nature **128**, 582 (Oct. 3, 1931), See also reference 5.

[7] A. H. Compton, R. D. Bennett and J. C. Sterns, Phys. Rev. **38**, 1565 (Oct. 15, 1931) and Phys. Rev. **39**, 873 (1932).

connecting an electrometer to the collecting plates and observing their rate of change of potential with time. Unfortunately however a change in potential of the high potential plates due to the unavoidable variation in the battery used to maintain it, produces by induction a change in potential of the collecting plates. Thus because of the large electrical capacity of the system, the ionization at the lowest pressure used, caused a change of only 0.3 volt per hour in the potential of the collecting plate. It was obviously impossible to maintain a 1000 volt battery so constant that its variation would not be an appreciable fraction of this. To compensate for this variation a second set of plates was built. This was an exact duplicate of the first set except that it was enclosed in a light brass case. The high potential plates of the ionization chamber A and the compensating chamber B were then connected to the same battery as shown in Fig. 1, while the electrometer E was arranged to measure

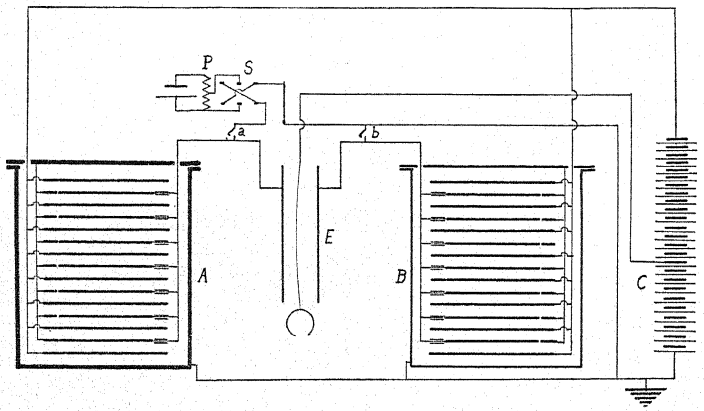


Fig. 1. Diagram of connections.

the difference in potential of the two sets of collecting plates. The electrometer used was of the single string type. The two plates of the electrometer were connected respectively to the two sets of collecting plates, while a potential of 225 volts was applied to the string. The electrometer was adjusted for a sensitivity of about 500 divisions per volt.

Because of the fact that cosmic rays at sea level cause less than $\frac{1}{4}$ of the ionization in a closed vessel, the remainder being due to γ-rays from radioactive materials in the neighborhood, and to α-rays from radioactive impurities in the walls of the ionization chamber, it was clear that more interpretable results could be obtained if the ionization of a single source such as γ-rays were studied.

For this purpose γ-rays from a small quantity of radio-thorium, filtered through 13 mm of lead were used. In order to obtain a well defined beam of γ-rays the radio-thorium and filter were placed in the center of a lead cylinder 30 cm in diameter and 30 cm long. There was a conical opening leading to one end of the cylinder which allowed a beam to pass that was somewhat larger than the ionization chamber at its position about 2 meters away. The block of lead was on a swivel so that the beam of γ-rays could be directed

either at the ionization chamber or turned to one side of it. By taking readings with the γ-rays passing through the chamber and then again with it turned to one side it was possible to determine the ionization of the γ-rays independent of the ionization of cosmic rays or α-rays.

The usual procedure in taking readings was to connect the collecting plates of the compensating chamber B to ground while the collecting plates of the ionization chamber A were held at some potential, usually 0.05 volts below ground, by means of the potentiometer P. The electrometer was then read. Next the connections a and b were broken, thus leaving both sets of collecting plates floating. The electrometer was then immediately read again, and the stop watch simultaneously started. After approximately enough time had elapsed for the collecting plates of the ionization chamber to receive enough ions to bring their potential to the same amount above that of the collecting plates of the compensating cylinder as they had started below, the electrometer position was again noted and the stop watch read. Switches a and b were now closed and this same potential above ground was then applied to the plates by means of the reversing switch S and the electrometer again read. In this way it was possible to correct for any zero drift or change in sensitivity of the electrometer.

This gave then with a considerable accuracy the rate of change of potential difference between the collecting plates. The relationship between this rate of change of potential and the ionization per cc per sec. was obtained as follows: Let C_1 be the electrical capacity between the collecting plates and the high potential plates of the ionization chamber, C_2 the capacity to ground of the collecting plates, leads and electrometer plates. By symmetry these capacities are the same for compensating chamber. Let C_3 be the capacity between the plates of the electrometer. It is then easy to show that if a charge Q is accumulated on the collecting plates of the ionization chamber and Q_2 on these plates of the compensating chamber the potential difference in volts across the electrometer is W where

$$W = (300(Q_1 - Q_2))/(C_1 + C_2 + 2C_3). \tag{1}$$

Likewise it may be shown that if the potential plates of the compensating cylinder are grounded while the potential of these plates in the ionization chamber are varied by an amount v, then the charges induced on the collecting plates (left floating) are such as to change the potential between the collecting plates of the two cylinders by an amount w, where

$$w = vC_1/(C_1 + C_2 + 2C_3). \tag{2}$$

w is obviously the change in reading of the electrometer when this variation takes place and hence can be determined directly.

From (1) it is seen that the difference of the ionization currents in the two chambers is

$$\frac{dQ_1}{dt} - \frac{dQ_2}{dt} = \frac{dW}{dt} \cdot \frac{C_1 + C_2 + 2C_3}{300} \tag{3}$$

where dW/dt is the rate of change of potential across the electrometer, in volts per sec. But substituting from (2)

$$\frac{dQ_1}{dt} - \frac{dQ_2}{dt} = \frac{dW}{dt} \cdot \frac{vC_1}{300w} . \tag{4}$$

Since, however, the distance between the potential and collecting plates is 1 cm

$$C_1 = A/4\pi$$

where A is the total effective area of the collecting plates in each cylinder

$$\frac{dQ_1}{dt} - \frac{dQ_2}{dt} = \frac{dW}{dt} \cdot \frac{v}{300w} \cdot \frac{A}{4\pi} .$$

The difference in the number of ions $(N_1 - N_2)$ collected per cc per sec. in the two chambers is then, since the volume from which ions are obtained is A cc and the charge on each ion is e,

$$N_1 - N_2 = \frac{1}{eA}\left(\frac{dQ_1}{dt} - \frac{dQ_2}{dt}\right) = \frac{dW}{dt} \cdot \frac{v}{w300 \times 4\pi e} .$$

By taking the difference of the readings with and without the γ-rays, the N_2 cancels out and the number produced by the γ-rays alone are obtained.

Since in these experiments γ-rays giving an ionization current about 20 times as large as the natural ionization current caused by cosmic rays, α-rays etc. were used, it was advisable to test whether the form of the ionization-voltage curves was dependent on the intensity of the radiation. For this purpose determinations of the ionization currents were made, at the two highest pressures, when the γ-rays were cut down to less than $\frac{1}{5}$ of their normal intensity by being passed through 5 cm of steel.

The pressures up to 25 atmospheres were measured on a pressure gauge that was calibrated, during the course of the experiments, against a gauge tester. Consequently these values should be in error by less than 0.1 atmosphere. It was not feasible to calibrate the gauge used on the highest pressure and therefore there may be a rather large error in this pressure.

In all cases a given collecting potential was maintained on the collecting plates for several hours before readings were started to allow any charges accumulated on the insulators to take up a steady value.

III. Results

The ionization currents observed in these experiments for a series of pressures and potential gradients are given in Table I. The ionization current is expressed as the number of ions per cc per sec. per atmosphere. For the two highest pressures two columns of values are given. The first column marked I_1 represents the ionization at the full intensity of the γ-rays, that is, the same intensity as that used for the lower pressures. The second column marked 5.187 I_2 is 5.187 times the number of ions obtained when the intensity of the γ-rays was reduced by passage through 5 cm of iron. Except for the two lowest gradients at the 93 atmospheres pressure, the two columns agree within the experimental error, thus indicating that with these two exceptions

TABLE I. *γ-rays. Number of ions collected per cc per second per atmosphere.*

Field in volts per cm \ Pressure in atm.	0.98	3.74	10.50	24.95 I_1	24.95 5.187 I_2	93. I_1	93. 5.187 I_2
1.55	112.5	101.6	79.8	59.8	59.8	26.2	28.4
6.2	118.4	106.9	86.2	63.9	63.7	29.7	30.3
23.0	118.7	110.1	89.5	66.5	66.5	30.6	30.5
91.5	120.0	113.9	94.5	70.2	70.4	32.1	31.9
367.	119.7	116.8	102.1	77.1	77.3	34.8	35.0
1009.	121.1	118.1	108.4	85.5	85.8	39.1	39.1

the form of the curves is independent of the intensity for intensities up to those used.

Fig. 2 displays graphically these data, the number of ions per cc per sec. per atmosphere being plotted against the log of the potential gradient of the collecting field P. It is at once seen that, in agreement with previous observers, the ionization per atmosphere falls off rapidly at the high pressures. Furthermore it agrees with their observation that when the potential gradient is of the order of 5 or 10 volts per cm, doubling this gradient produces a very small change in the current.

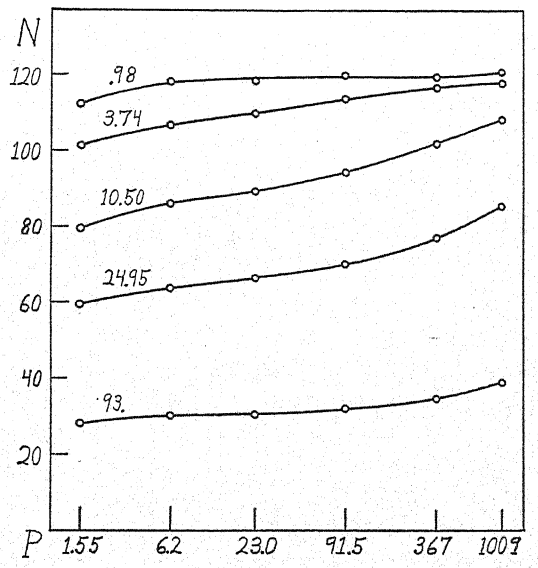


Fig. 2. The number of ions per cc per sec. per atmosphere (N) collected as a function of the potential gradient in volts per cm P for the pressures in atmospheres indicated.

However when high potential gradients are applied a very material increase of the currents is obtained thus showing that the lower gradients do not collect all of the ions formed. Thus if we assume that the number of ions per atmosphere actually formed is constant and has the value 121.1 ions per cc per sec., then the number that one fails to collect at a gradient of 6.2 volts per cm (approximately the field used by previous observers) is $(121.1 - N_{6.2})$. The fraction of these that one still fails to collect at some other higher poten-

tial P is $R=(121.1-N_P)/(121.1-N_{6.2})$. This fraction then may be taken as a measure of the success attained in pushing towards saturation by using higher fields. This fraction R as calculated from Table I is plotted against the log of P in Fig. 3.

From the figure it is seen that at 3.74 atmospheres it is possible by increasing the gradient from 6.2 to 1009 volts per cm to collect all but 21 percent of the ions that are not obtained with the lower gradient. At the higher pressures the increase of the field strength is progressively less effective.

These results provide conclusive evidence that the falling off of ionization per atmosphere at higher pressures is largely due to lack of saturation rather than to the mechanism suggested by Broxton.[8]

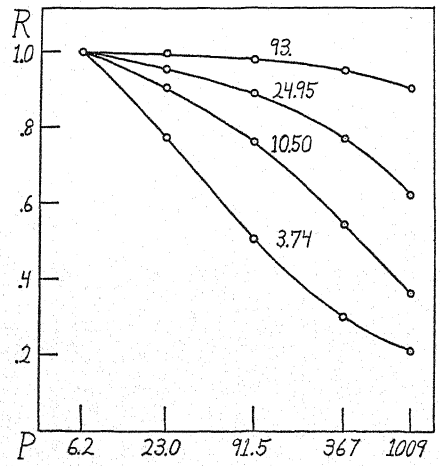


Fig. 3. $R=(121.1-N_P)/(121.1-N_{6.2})$ as a function of the potential gradient P for the pressures indicated.

Furthermore the lack of dependence of the form of the curves on the intensity of ionization, in nearly all cases, indicates that the lack of saturation is caused by recombination of the ejected electron with the parent ion rather than by random recombination between any ions formed. Presumably at the high pressures the ejected electron loses its energy before it succeeds in escaping from the region where the field of the parent ion is still very strong. This fortunately also means that this lack of saturation does not invalidate the results of many cosmic ray observers who have used high pressures, since the lack of saturation merely cuts down all currents by a constant factor and in no way effects the relative values on which absorption coefficients are based.

This increase of ionization current with potential gradient also seems to call for a modification of the theory developed by Compton, Bennett and Sterns[7] to explain this lack of saturation. According to their theory there is a

[8] There may still be a slight variation of the type suggested by Broxton due to a small difference in efficiency of production of β-rays by the air and by the steel walls of the chamber. Unpublished studies on the effect of wall materials by Workman in this laboratory indicate however that this effect of these materials is at most 30 percent and is probably in the opposite direction, i.e., it should cause the ionization per atmosphere to increase slightly with pressure.

certain critical sphere of definite radius surrounding each ion. If an oppositely charged ion finds itself inside of this sphere the force of attraction over balances the tendency to diffuse away and the two ions always recombine. On the other hand the tendency to diffuse away predominates for an ion outside of this sphere and the ion always escapes. Since at the surface of this critical sphere the field due to the ion at the center is 40,000 volts per cm any ordinary collecting field should have no effect. The question whether recombination with the parent ion takes place or not is determined, according to this theory, solely by the distance from the parent ion that the electron is ejected by the β-particle, and the factors that enter into the tendency to diffuse away such as the temperature.

Obviously this picture is much too simplified. Thus given two ions in a gas there is always a certain probability that one will diffuse close enough to the other, regardless of their original distance apart, so that recombination takes place. Of course this probability falls off rapidly as the distance increases. Furthermore this probability, particularly for an ion at a considerable distance from the parent ion, is materially changed as the strength of an external collecting field is varied. This of course changes the number that succeed in escaping from the parent ion and therefore one would expect variation in the strength of the ionization current similar to that shown in the Table I and Fig. 2.

Qualitatively this is also in agreement with the behavior indicated in Fig. 3. At the lower pressures all of the ions start at a great distance from the parent ion where its field is small and consequently the probability of recombination should be largely effected by the size of the external field, as it is found to be. On the other hand for higher pressures most of the ions start so close to the parent ion where its field is large compared to that of any feasible external field. This being the case very little effect of the strength of the external field should be expected.

TABLE II. *Residual ionization. Number of ions collected per cc per second per atmosphere.*

Field in volts per cm \ Pressure in atm.	24.95	93.
1.55	3.11	1.34
6.2	3.22	1.45
23.0	3.38	1.55
91.5	3.53	1.64
367.	4.00	1.77
1009.	4.42	1.99

The readings made when the γ-rays were turned to one side represent the difference in the residual ionization caused in the two chambers by cosmic rays and radioactivity of the chamber and room. This was large enough in the case of the upper two pressures to be read with a considerable accuracy. Also in the case of these high pressures, the ionization in the ionization chamber was large compared to that in the compensating chamber and consequently the fact that the latter is subtracted should not modify the values very greatly. These results are given in Table II. As is at once seen the effect of increase in collecting potential is essentially the same as with the γ-rays.

A Search for Isotopes of Hydrogen and Helium

By WALKER BLEAKNEY*
Palmer Physical Laboratory, Princeton University

(Received June 1, 1932)

The well-known triatomic hydrogen ion $(H^1H^1H^1)^+$ of mass 3 is formed by electron impact at a rate proportional to the square of the pressure if the pressure is very low. The isotopic molecular ion $(H^1H^2)^+$, also of mass 3, would be expected to vary linearly with pressure. These two facts constitute a method for distinguishing between the two with a mass spectrograph whose resolving power is insufficient to separate them by magnetic analysis. The method becomes successful only when the working pressures are very low. With a mass spectrograph designed for low pressure work evidence was found which amply confirms the existence of an isotope of hydrogen of mass 2 and also gives a fair estimate of the abundance. In a sample of ordinary commercial electrolytic hydrogen the data indicate an abundance ratio

$$H^2/H^1 = 1/30000 \pm 20\%.$$

The same ratio for a sample of hydrogen which had been concentrated by Urey, Brickwedde and Murphy came out to be

$$H^2/H^1 = 1/1050 \pm 5\%.$$

An effort was made to detect a difference in mass between the ions $(H^1H^1H^1)^+$ and $(H^1H^2)^+$ without success. Considering the resolving power of the apparatus this failure was interpreted as meaning that the packing fraction of H^2 is greater than 4×10^{-3} i.e., the atomic weight is greater than 2.008. A search was also made for isotopes 3 and 5 of helium but none were found. It is concluded that their abundance must be less than one part in 50,000.

INTRODUCTION

THE hydrogen and helium atoms play such fundamental roles in all physics that any new properties or characteristics of their nuclei are of wide interest. There have been indications that two or more isotopes of these elements may exist and several attempts have been made from time to time to find them experimentally. The first positive evidence for the existence of an isotope of hydrogen of mass 2 has been obtained recently by Urey, Brickwedde and Murphy[1] whose paper also gives a review of previous work and a bibliography of the subject which need not be repeated here. Their photographs of the Balmer spectrum under very high dispersion reveal weak satellite lines attributable to hydrogen atoms of mass 2. These lines were enhanced in a sample of hydrogen in which enrichment of the heavy isotope had been attempted by evaporation near the triple point. Further evidence for the existence of an isotope in hydrogen may be found in Allison's interpretation of his experiments on optical rotation[2] but his method is as yet little

* National Research Fellow.

[1] H. C. Urey, F. G. Brickwedde and G. M. Murphy, Phys. Rev. **40**, 1 (1932); also Phys. Rev. **39**, 164 (1932) and **39**, 864 (1932).

[2] F. Allison, Jour. Ind. Eng. Chem. **4**, 9 (1932).

understood. The importance of the problem seemed to warrant an independent investigation from a different angle and accordingly a careful reexamination of the hydrogen and helium ions was undertaken with a mass spectrograph.

There are many complications which arise in the magnetic analysis of hydrogen ions because of the various primary and secondary combinations involved. Let us assume that a rare isotope of mass 2 does exist and let us enumerate the possibilities when the ions are formed at a very low pressure by electron impact. It is well known[3] that under these conditions monatomic, diatomic and triatomic ions are produced. Hence we should expect the various combinations listed in Table I. The column labeled $f(p)$ gives the intensity or number of ions as a function of pressure when p is so small that

TABLE I. *Possible ions resulting from a mixture of two hydrogen isotopes in which H^1 is much more abundant than H^2.*

	Ion	m/e	$f(p)$	Intensity
1.	$(H^1)^+$	1	$a_1p+b_1p^2$	weak
2.	$(H^1H^1)^+$	2	a^2p	v. strong
3.	$(H^2)^+$	2	$a_3p+b_3p^2$	v. weak
4.	$(H^1H^1H^1)^+$	3	b_4p^2	weak
5.	$(H^1H^2)^+$	3	a_5p	weak
6.	$(H^2H^2)^+$	4	a_6p	v.v. weak
7.	$(H^1H^1H^2)^+$	4	b_5p^2	v.v. weak
8.	$(H^1H^2H^2)^+$	5	b_6p^2	v.v. weak
9.	$(H^2H^2H^2)^+$	6	b_7p^2	v.v. weak

secondary reactions are small compared with primary ones. In general the primary processes will vary linearly with pressure while secondary ones will be proportional to the square. Of the configurations listed in Table I it is to be expected that 6, 7, 8 and 9 will be too weak for observation. Number 1 is of no interest in this particular case and 3 will be completely masked by 2. Since 2 is a linear function of pressure and since it is very strong it serves as a good index of the pressure. There are left 4 and 5, two ions of comparable abundance but different functions of pressure and it is in this direction that the following studies were made. In the case of helium no such complications arise.

EXPERIMENTAL PROCEDURE

The apparatus used in this experiment has been described[4] in a previous number of this journal and some preliminary results have also been reported.[5,6] The flow method was used in every case, the gases streaming into the tube through fine capillaries or a palladium tube and out through diffusion pumps. The lighter the atom the faster will it leak through the capillary but presumably the same selective effect will occur in the diffusion pumps so that the relative concentrations of isotopes in the ionization chamber will

[3] H. D. Smyth, Rev. Mod. Phys. **3**, 347 (1931).
[4] W. Bleakney, Phys. Rev. **40**, 496 (1932).
[5] W. Bleakney, Phys. Rev. **39**, 536 (1932) (Letter).
[6] W. Bleakney, Phys. Rev. **40**. 130 (1932) (Abstract).

remain unchanged after equilibrium has once been established. No difference in the results on hydrogen were observed when the palladium tube was substituted for the fine capillary.

Through the kindness of Professor Urey and Dr. Murphy a sample of the residue of hydrogen evaporated near the triple point by Dr. Brickwedde at the Bureau of Standards was provided. The details of the preparation of this hydrogen have been described in their paper.[1] This particular sample was designated by them "Sample III." Ordinary commercial electrolytic hydrogen was used for the rest of the work.

The procedure in the case of hydrogen was to measure the total number of ions of mass 3 reaching the collector, per unit electron current, as a function

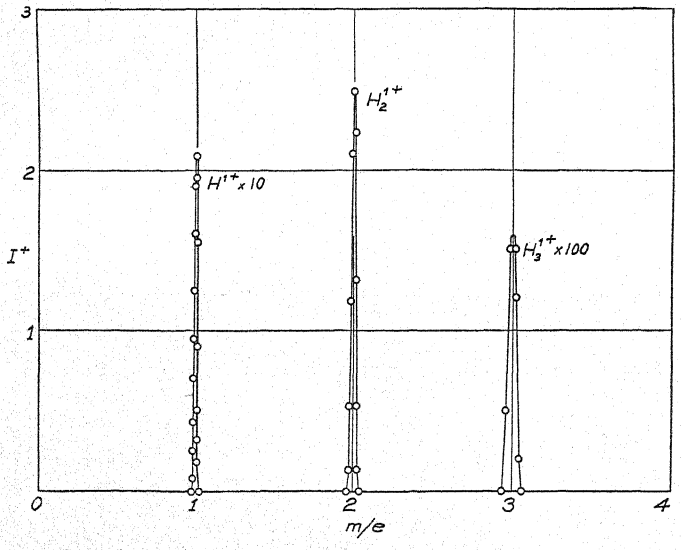


Fig. 1. A typical e/m analysis curve for ordinary hydrogen. p 10^{-5} mm Hg. H = 400 gauss. V_a = 60 volts electron velocity.

of the pressure. The pressure itself could be measured in two ways. The first method consisted in observing the intensity of the ion peak of mass 2 which is proportional to p. In the second method the tube was used as an ionization gauge by observing the total positive ion current per unit electron current. The two methods gave substantially the same results. At the low pressures used the McLeod gauge could not be read with any accuracy. After baking the tube the residual pressure of foreign gases was always in the neighborhood of 10^{-8} mm. The working pressures ranged from 10^{-4} to 10^{-6} mm.

Results for Hydrogen

Some idea of the resolving power of the apparatus may be had from Fig. 1 which shows the three typical peaks obtained in ordinary hydrogen with a magnetic field of 400 gauss and a pressure of about 10^{-5} mm. The electron velocity was 60 volts. At higher magnetic fields the peaks become somewhat sharper. Fig. 2 represents the number I of ions of mass 3 as a function of the number of ions of mass 2. Both ordinate and abscissa are plotted in the same

arbitrary units. Curve I was observed for ordinary hydrogen and curve III for Brickwedde's concentrated sample. The difference between these two curves is given by the straight line II.

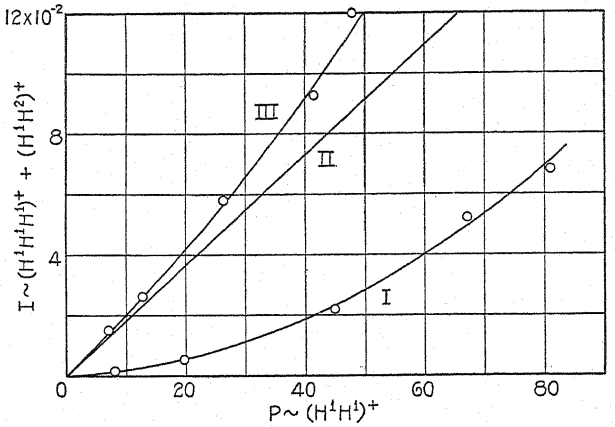


Fig. 2. Total number of ions $(H^1H^1H^1)^+ + (H^1H^2)^+$ of mass 3 as a function of the number $(H^1H^1)^+$ of mass 2. Curve I, ordinary commercial electrolytic hydrogen. Curve III Brickwedde's concentrated sample. Curve II, difference.

These data are interpreted by the author in the following manner. As indicated in Table I we should expect the number of ions of mass 3 to be given by

$$I = ap + bp^2. \tag{1}$$

Now it is significant that curves I and III may be fitted by Eq. (1) using a different value for the constant a but the same value for b in each case. The circles represent the experimental points while the curves are plotted from the following equations.

Curve I $$I_{\mathrm{I}} = (\ 6.6p - p^2) \times 10^{-5} \tag{2}$$

Curve III $$I_{\mathrm{III}} = (190.0p - p^2) \times 10^{-5} \tag{3}$$

Curve II $$I_{\mathrm{II}} = I_{\mathrm{III}} - I_{\mathrm{I}} = 183.4 \times 10^{-5}p. \tag{4}$$

The left-hand member of Eq. (4) is interpreted as the difference between the numbers of isotopic ions $(H^1H^2)^+$ in the two samples. Since p is actually measured in terms of the number of $(H^1H^1)^+$ ions it is evident that the slope of curve II gives the increase due to the concentration process.

$$H^1H^2/H^1H^1 = 1/546. \tag{5}$$

Here we assume of course that the probabilities of ionization of the two types are the same. The total concentration of the H^1H^2 molecules is given by the coefficient a of Eq. (1). For curve III this is

$$H^1H^2/H^1H^1 = 1.90 \times 10^{-3} = 1/526 \tag{6}$$

and for ordinary hydrogen

$$H^1H^2/H^1H^1 = 6.6 \times 10^{-5} = 1/15100. \quad (7)$$

The probable error in these two results is estimated to be 5 percent and 20 percent respectively. No attempt was made to treat the data by the method of least squares in detail since neither the ordinate nor the abscissa is known precisely and the probable error of each observation varies from point to point. The curves were therefore fitted in a rather arbitrary way. If we write the ratio of numbers of atoms instead of molecules we have

$$H^1/H^2 = 1050 \pm 5\% \quad (8)$$

for the concentrated sample and

$$H^1/H^2 = 30{,}000 \pm 20\% \quad (9)$$

for ordinary hydrogen. It will be noticed that there is quite a marked discrepancy between these results and those first reported by Urey, Brickwedde and Murphy,[1] but they have largely succeeded in accounting for the difference[7] by considering the relative absorption of strong and weak lines in their discharge tube.

In order to show the results in a more striking manner it is illuminating to divide Eq. (1) by the pressure and so obtain

$$I/p = a + bp \quad (10)$$

an equation of a straight line whose intercept a gives the abundance of the isotope sought. Curves I and III of Fig. 3 plotted in this manner represent the same data as are shown in Fig. 2. This method of presenting the data improves one's confidence in the evidence for the existence of the isotope in ordinary hydrogen but on the same scale the points for the concentrated sample appear scattered over a considerable range. However a little consideration will probably convince the reader that the probable error chosen is not too small. The curves I and III are plotted from Eqs. (2) and (3).

It is of importance to point out that the triatomic ion $(H^1H^1H^1)^+$ is not only a function of the pressure but also of the geometry of the apparatus and the fields applied. The coefficient b of Eq. (1) is related to the intensity of this ion and is given by the slope of the curves in Fig. 3. The relative number of isotopic molecules, however, should be independent of these conditions. Curve IV was taken with an altered set of electric and magnetic fields and it is evident that the slope b has been greatly increased while the intercept remains unchanged within the experimental error. The fact that curves I and IV have exactly the same intercept is not a coincidence. Since their probable errors overlap they were *made* to coincide by the author in fitting the curves.

Some data for another sample of hydrogen are shown by curve V in Fig. 3. This sample was prepared by Professor Urey by a diffusion method and represents a concentration of the lighter isotope. The data are admittedly rather inaccurate but the results seem to indicate less of the heavier isotope

[7] H. C. Urey, F. G. Brickwedde and G. M. Murphy, Phys. Rev. **40**, 464 (1932).

than is to be found in ordinary hydrogen. Professor Urey estimated the concentration of H^1H^2 in this sample to be about one tenth of that in ordinary hydrogen, a result which is not inconsistent with the somewhat higher one obtained here when account is taken of the rather large probable error involved in locating the intercept of curve V.

Kallmann and Lasareff[8] have attempted to verify the existence of the H^2 isotope by seeking for the $(H^1H^1H^2)^+$ ion of mass 4, but were unable to find it.

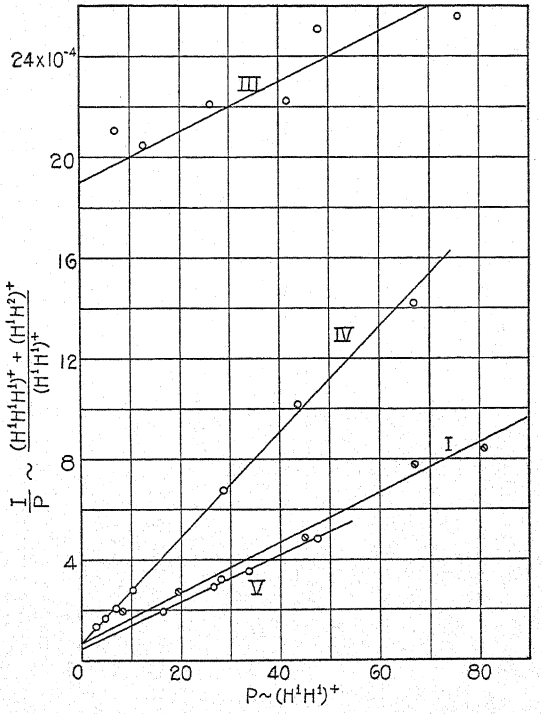


Fig. 3. I/p plotted as a function of p. Curve III, Brickwedde's concentrated sample. Curves I and IV, ordinary commercial electrolytic hydrogen each taken under a different set of fields. Curve V, sample of hydrogen enriched in H^1 by diffusion process.

Perhaps the probability for its formation is very small. They then tried the method of this experiment but at the lowest pressures possible in their apparatus (5×10^{-5}) the ratio of ions of mass 3 to those of mass 2 was 1:4000 for ordinary and concentrated samples alike. The conclusion they reach is that their concentrated sample is at most one tenth as good as the one used in this work. If this is true then there is probably no contradiction between the two experiments.

An accurate determination of the mass of the new isotope is of the greatest importance. Unfortunately the mass spectrograph employed has not a high dispersion on the mass scale. Nevertheless a trial was made to determine if possible a lower limit for the packing fraction. First ordinary hydrogen was admitted and the shape of the peak corresponding to ions of mass 3 was ex-

[8] H. Kallmann and W. Lasareff, Naturwiss. **20**, 206 (1932).

amined very carefully. The pressure was such that this peak was made up almost entirely of $(H^1H^1H^1)^+$. Then a mixture of the two samples was admitted at such a pressure that $(H^1H^1H^1)^+$ and $(H^1H^2)^+$ were present in equal numbers and again the shape of the peak was examined. If the two ions are of different weight one would expect the peak in the latter case to appear somewhat broadened. No such broadening could be detected. It is estimated from these measurements that the packing fraction of H^2 lies between 4×10^{-3} and 12×10^{-3},

$$\text{or } 2.024 > W > 2.008$$

where W represents the atomic weight.*

It may be well to point out that all the results of this paper simply point to the conclusion that a small number of normal molecules of mass 3 does exist in hydrogen. Conrad[9] has found evidence for the formation of neutral H_3 molecules in a discharge tube but it has been shown[10] on quantum mechanical grounds that three normal H atoms cannot combine to form a stable triatomic molecule. Hence if a neutral triatomic molecule exists it must be in an excited state in which case the ion would be formed as the result of a secondary or tertiary process and would not be a linear function of the pressure. Even without considering the weight of the spectroscopic evidence[11] the most reasonable assumption which accounts for the results of this experiment is the presence of H^1H^2 molecules in hydrogen.

Results for Helium

Helium purified in a misch-metal arc was admitted to the tube and a search made for isotopes 3 and 5. None were found. It is believed that a concentration of one in 50,000 or less could have been detected. This negative result agrees with that of Kallmann and Lasareff[8] but is a test not as discriminating as theirs.

The author is indebted to Professor Urey and Drs. Brickwedde and Murphy for the samples of hydrogen which made this experiment possible. He is also grateful to the members of the Palmer Laboratory staff for their kindly interest and timely suggestions.

* The author has just recently learned through private communication that Dr. K. T. Bainbridge has succeeded in measuring the atomic weight of H^2 with his mass spectrograph. His result is $W=2.0135$.

[9] R. Conrad, Zeits. f. Physik **75**, 504 (1932).

[10] W. Heitler and F. London, Zeits. f. Physik **44**, 455 (1927).

[11] The existence of the H_α^2 line has been confirmed by Shenstone and Turner using a grating in this laboratory and some of the "sample III" hydrogen.

Elastic and Inelastic Electron Scattering in Hydrogen

By A. L. HUGHES* *and* J. H. MCMILLEN
Washington University, St. Louis

(Received May 16, 1932)

A study of both the *energy distribution and the angular distribution of electrons scattered by hydrogen molecules* was made. *Elastic scattering* was investigated in the range between 40° and 165°, for collision energies between 35 and 200 volts. The number of electrons scattered at any angle was smaller the greater the energy of impact. In all the curves a minimum was found between 90° and 110°, while for the 35 and 50 volt collisions the curves rose to a definite maximum at 155° to 160°. *Inelastic scattering* was found to occur with energy losses ranging from a minimum of about 12.0 volts, through a sharply defined *most probable* loss at 12.6 volts, to a complete loss of all the energy. It was found that as the energy of collision was increased the probability of the larger energy losses increased with respect to the probability of the smaller energy losses. Angular distribution curves were steeper, the smaller the amount of energy lost at collision for a given collision energy. Also, for any particular energy loss, the steepness increased with the speed of the colliding electrons. The electrons which are torn off from atoms in ionizing collisions are termed *ejected electrons* and are presumably those which appear in our experiment with but little or no energy. The angular distribution of the ejected electrons, having various amounts of energy (1 to 8 volts), were studied for different collision energies (35 to 340 volts). In every case there was a noteworthy absence of considerable scattering at small angles, so characteristic of the scattering of faster electrons. In many cases, pronounced peaks were found in the angular distribution curves at large angles (90° to 160°). These peaks change in position and size in a regular manner with the energy of collision and the energy of the ejected electron.

THIS paper is an account of a continuation of our experimental investigations on electron scattering in gases. The results of our investigations on argon have already been published in this journal.[1] As argon is monatomic, it seemed desirable to select a diatomic gas for the second investigation; hence hydrogen was chosen for study. The method of experimentation with hydrogen was identical with that used in the work on argon.

Scattering of electrons by hydrogen has been studied by Harnwell,[2] McMillen,[3] Arnot,[4] Bullard and Massey,[5] and by Ramsauer and Kollath.[6] Harnwell and McMillen found that the number of electrons scattered elastically fell off steeply as the angle was increased (angle range 7° to 60°; energy range 40 to 180 volts). Arnot, working with electrons between 30 and

* This work was made possible by assistance to the senior author from a grant made by the Rockefeller Foundation to Washington University for research in science.

[1] A. L. Hughes and J. H. McMillen, Phys. Rev. **39**, 585 (1932). It is convenient to mention here that several paragraphs were accidentally omitted from the end of the paper referred to. The omission was rectified in a letter to the Editor of the Physical Review **40**, 469 (1932). An error in Eq. (2) of the same paper was also corrected.

[2] G. P. Harnwell, Phys. Rev. **33**, 559 (1929); **34**, 661 (1929); **35**, 285 (1930).

[3] J. H. McMillen, Phys. Rev. **36**, 1034 (1930).

[4] F. L. Arnot, Proc. Roy. Soc. **133**, 615 (1931).

[5] E. C. Bullard and H. S. W. Massey, Proc. Roy. Soc. **133**, 637 (1931).

[6] C. Ramsauer and R. Kollath, Ann. d. Physik **12**, 529 (1932).

800 volts energy, confirmed these results, but found that, at about 90°, the curve representing the number of elastically scattered electrons began to increase. (His angular range extended to 120°.) Similar results were obtained by Bullard and Massey who studied the elastic scattering of electrons having energies between 4 and 30 volts. Ramsauer and Kollath also found, for very slow electron (1.5 to 11.0 volts), a definite but rather slow increase in the elastic scattering as the angle was increased above 90° to as far as 165°. So far as we know there have been no investigations of the distributions of electrons scattered inelastically by hydrogen.

Experimental Method

The same apparatus was used in the study of electron scattering in hydrogen as in the previous work on argon.[7] The reader is therefore referred to the previous article for a description of the apparatus and method of experimentation. Hydrogen was prepared by the action of pure dilute sulphuric acid on pure zinc. The gas was dried by passing through a tube immersed in liquid air. It was then stored in a reservoir over mercury and admitted to the apparatus through a capillary tube and a liquid air trap to freeze out the mercury. A suitable constant pressure could be maintained in the apparatus by regulating the driving pressure of the hydrogen on the high pressure side of the capillary tube, the gas being pumped out of the apparatus by a condensation pump. This constant flow method provides us with pure hydrogen in the scattering experiments. In experiments on scattering in hydrogen it is particularly important to avoid impurities, as the scattering by a hydrogen molecule is small compared with the scattering by heavier molecules.

Our results on hydrogen are expressed in the same units as those used in the previous article; that is, we measure the number of electrons diverted from the main beam at an angle θ and then multiply by $\sin\theta$ to compensate for the change with angle of the effective scattering path length. The final values are therefore proportional to the scattering coefficient as defined on page 589 of our previous paper.[8]

Elastic Scattering

In view of the recent comprehensive work of Bullard and Massey and of Arnot on elastic scattering of electrons in hydrogen, we did not make an extensive study of the elastic scattering. It seemed worth while, however, to attempt to extend the studies to large angles, inasmuch as the investigators referred to did not go beyond about 120°. Our results are shown in Fig. 1. It will be seen that we confirm the discovery of Bullard and Massey and of Arnot that there is a minimum at about 90°. In addition, we find a definite maximum at large angles which is contrary to the expectations of Arnot who thought that "the curves probably continue to rise steadily as the angle is increased to 180°."

We have indicated the positions of Arnot's 29 volt curve and Bullard

[7] A. L. Hughes and J. H. McMillen, Phys. Rev. 39, 585 (1932).
[8] A. L. Hughes and J. H. McMillen, Phys. Rev. 39, 585 (1932).

and Massey's 30 volts curve in the neighborhood of our 35 volt curve. It is evident that although all three curves agree in giving a minimum at about 90°, no two curves are in satisfactory accord. We can only say, therefore, that there is qualitative agreement insofar as the curves rise and fall together.

Inelastic Scattering

The distributions of energy lost by 50 volt primary electrons, when scattered at various angles, are shown in Fig. 2. The various curves have been arbitrarily adjusted to the same height for a loss of energy amounting to 20 volts. It will be seen that the "most probable" energy loss is approximately 12.6 volts. It is evident that the larger energy losses are relatively more

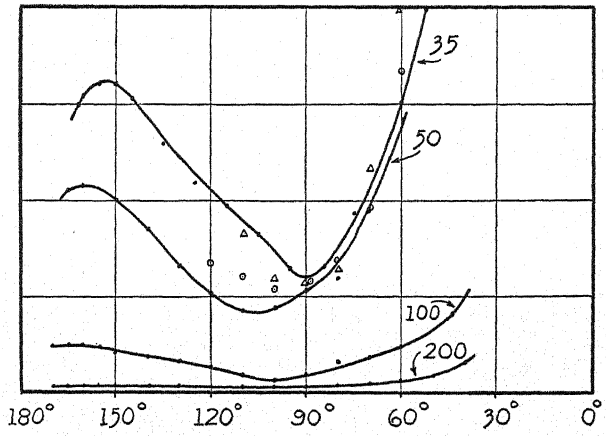


Fig. 1. Elastic scattering of electrons by hydrogen molecules. The numbers attached to the curves represent the electron energies in volts. Circles with dots, Arnot's curve for 29 volt electrons. Triangles, Bullard and Massey's curve for 30 volt electrons.

probable for the larger scattering angles. A small subsidiary maximum appears at about 16 volts in the 30° and 45° curves. In Fig. 3 we have the energy distributions of electrons, all scattered at 10°, for various primary energies between 35 and 200 volts. (The curve for 412 volt electrons, scattered at 5°, is included). As before, the curves are arbitrarily fitted together at the 20 volt loss. It is seen that, for a given scattering angle, here 10°, the 12.6 volt loss becomes relatively *more* probable the *lower* the primary electron energy. It will be noticed that there is a distinct slowing up in the rate of the fall of the curve between 15 and 20 volts, and in one curve (the 412 volt, 5° curve) there is a small subsidiary maximum at 17.5 volts.

Various energy losses, *viz.*, 12.6, 16.4, and 25.0 volts, were selected for a study of their angular distributions. The 12.6 volt loss, the most probable loss, is an excitation loss. The 16.4 loss is just above the ionization potential which is 15.9 volts. (The 15.9 volt loss was not studied, as the resolution of the apparatus was imperfect and consequently the electrons selected at a 15.9 volt setting would really include a number of electrons causing excitation). Finally the 25 volt loss was chosen because it was well above the minimum ionization loss and, at the same time, the yield was not too small to

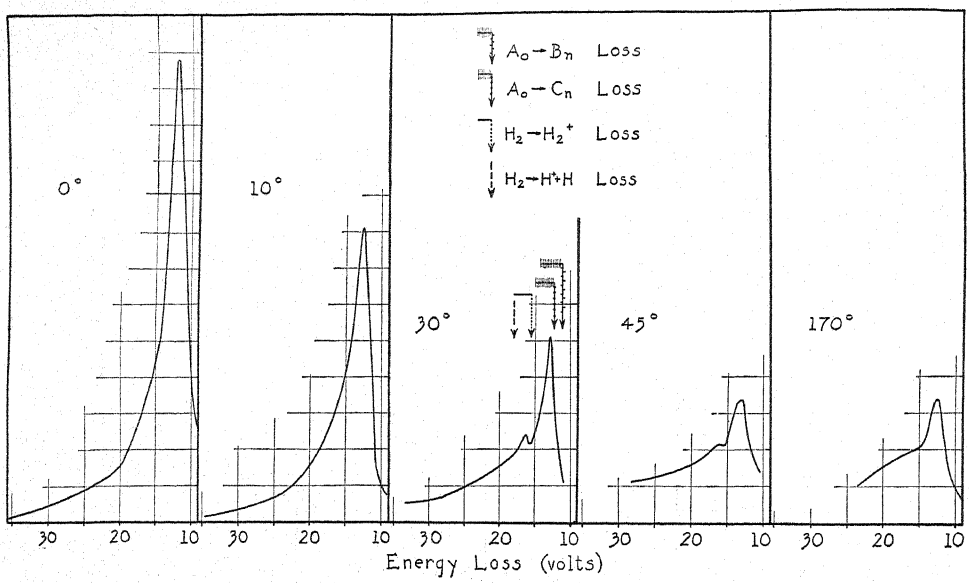


Fig. 2. Energy distribution of electrons scattered inelastically by hydrogen molecules, showing variation with *angle*. Primary energy in all cases = 50 volts. All curves are adjusted arbitrarily to the same height at the 20 volt loss. On the 30° curve, the positions of the theoretically possible types of effects are indicated by suitable vertical lines. The associated horizontal lines indicate the possible vibrational levels.

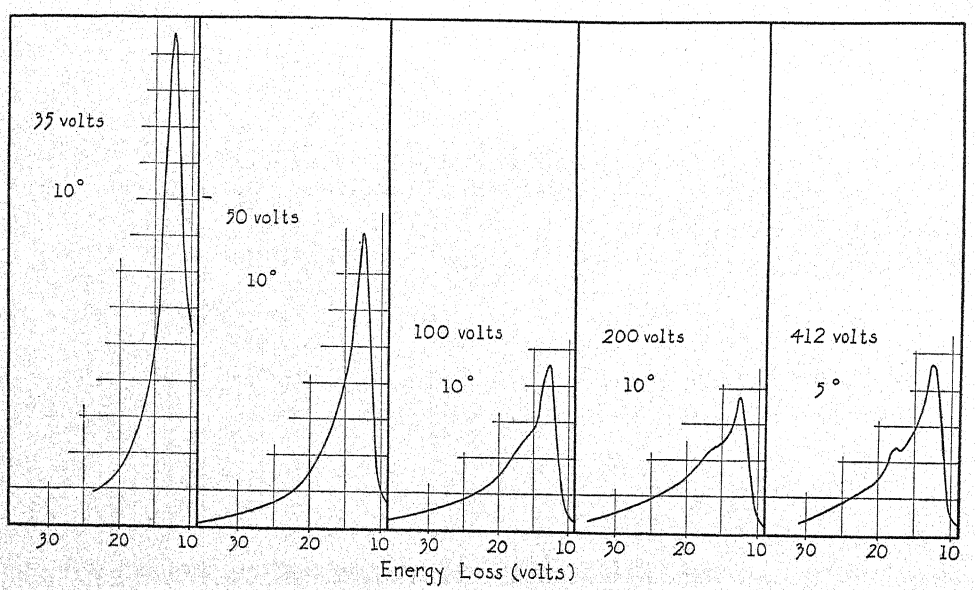


Fig. 3. Energy distributions of electrons scattered inelastically by hydrogen molecules, showing variation with *primary energy*. All curves are adjusted arbitrarily to the same height at the 20 volt loss.

16,038

make measurements unreliable. According to Fig. 4, the less the energy loss, the steeper the angular distribution curve, a result already implied in the previous paragraph. The curves are all adjusted to the same value at 10°.

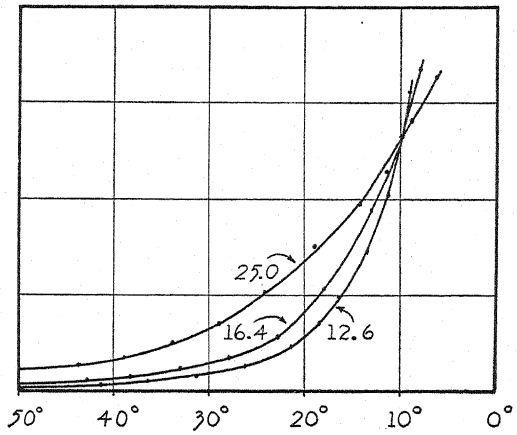


Fig. 4. Angular distribution of electrons scattered inelastically. Primary electron energy in all cases = 50 volts. Energy losses in volts are indicated on the curves. All curves are adjusted arbitrarily to the same height at 10°.

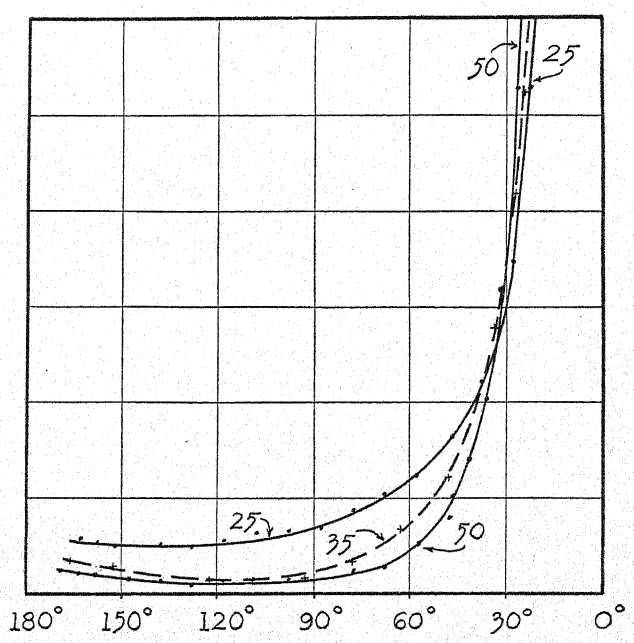


Fig. 5. Angular distribution of electrons scattered with 12.6 volts loss of energy, showing dependence on primary electron energy. The primary energy, expressed in volts, is indicated for each curve.

Finally, in Fig. 5, we show how the angular distribution curves for a constant loss, *viz.*, 12.6 volt (corresponding to excitation of the molecule), depend on the energy of the electrons before collision. Up to about 90° or so, the curves are steeper the higher the primary energy. (Too much reliance

should not be placed on the exact shape of the curves above 90°, as the readings were extremely small).

Ejected Electrons

Following the terminology used in our previous paper on argon,[9] we call those electrons which appear with very low energies the ejected electrons. When ionization takes place, an electron is detached from the atom. Consequently, after an ionizing collision we have two electrons; the faster we assume to be the colliding electron and the slower the ejected electron. (We

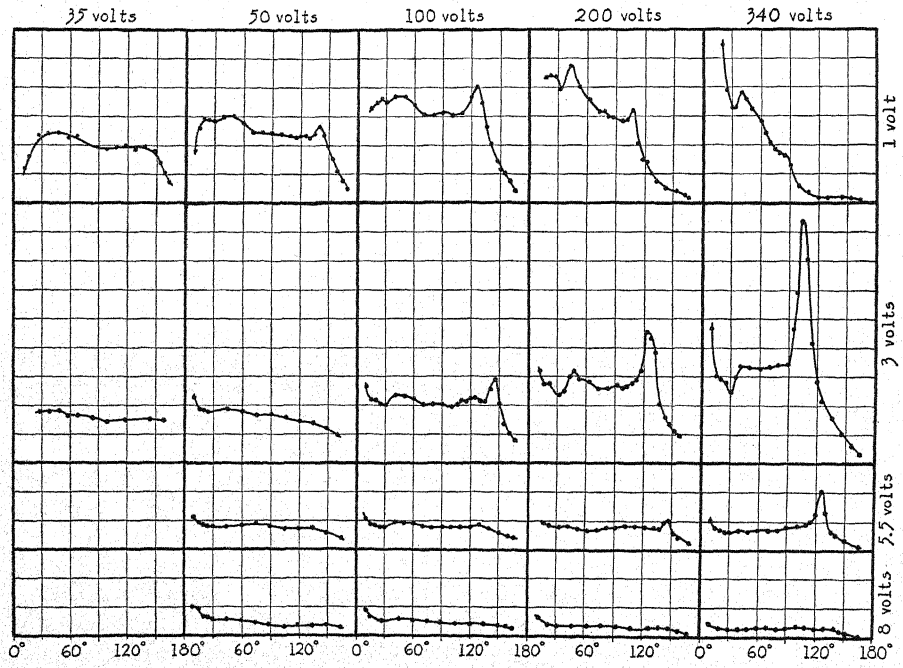


Fig. 6. Angular distributions of ejected electrons. Each row represents a single ejected electron energy which takes the values 1, 3, 5.5, and 8 volts as we go from one row to the next. Each column corresponds to a different energy of collision. All curves are to the *same* scale.

cannot, of course, demonstrate that the slower of the two electrons is the one ejected from the atom; it seems probable, however, and suggests a convenient terminology.) For a study of the angular distribution of ejected electrons we selected the 1, 3, 5.5, and 8 volt ejected electrons resulting from a collision between hydrogen molecules and primary electrons having energies ranging from 35 to 340 volts. The results are shown in Fig. 6. Perhaps the most striking feature common to all the curves is the absence of the excessively large scattering at small angles which is so characteristic of electrons scattered inelastically with considerable amounts of energy (see Fig. 4). The next feature worthy of mention is the presence, in many cases, of certain highly preferred directions for the emission of ejected electrons. A certain regularity in the way in which these peaks shift can be traced. Thus for any

[9] A. L. Hughes and J. H. McMillen, Phys. Rev. 39, 585 (1932).

one ejected electron energy, an *increase* in the energy of the primary electrons is accompanied by a progressive shift of the position of the peak to *smaller* angles. On the other hand, if we keep the primary energy fixed and study the various groups of ejected electrons, we find that the *higher* the energy of the ejected electrons the *larger* the angle at which the peak is to be found. For 8 volt ejected electrons the angular distribution curves have become practically featureless. It is to be noticed, too, that the peaks in the angular distribution curves for all the ejected electrons practically disappear when the primary energy is low (35 and 50 volts).

Discussion

Several theoretical physicists have amplified and extended the pioneer work of Born, who first applied wave mechanics to the scattering of electrons by atoms, with the result that certain features of electron scattering are now accounted for theoretically. Very little, however, has been done on the corresponding problem for molecules. Massey and Mohr[10] have carried through a calculation of the scattering of electrons by diatomic molecules. It is assumed that the diatomic molecule may be represented by a suitable potential field having axial symmetry over which passes an electron wave. The amplitude of the wave scattered in any desired direction is calculated. An average is then taken for all possible orientations of the molecular axis with respect to the direction of the primary wave. Finally it is found that the scattering by such a diatomic molecule is obtained on multiplying what is substantially the scattering by the constituent atoms by a diffraction factor $(1+\sin x/x)$, in which $x=4\pi d \sin(\theta/2)/\lambda$, where d is the distance between the atoms in the molecule and λ the electron wave-length. This diffraction factor changes sign periodically as x increases. Because of the extremely steep character of the curve for atomic scattering, however, it is not easy to detect the superposed oscillation of the diffraction pattern.[11] Thus Massey and Mohr were unable to show that Arnot's experimental curves (for 80 volts and above) for the scattering of electrons by hydrogen were in better accord with their formula for scattering by molecular hydrogen than with the formula for scattering by atomic hydrogen. Massey and Mohr state that the scattering curves obtained by McMillen[12] fall off much more rapidly with angle of scattering than the calculated values. This is incorrect, for McMillen's curves are almost superposable on Arnot's, and if anything, they are less steep. Arnot's range of angles was nearly twice as great as McMillen's, and so afforded a better test.

The rise in the scattering curves with angle as the angle is increased beyond about 90° as shown in Fig. 1 of this paper and in Arnot's work is not accounted for by Massey and Mohr's theory. This theory is probably too simplified to do more than describe the part of the scattering curves below

[10] H. S. W. Massey, Proc. Roy. Soc. **129**, 616 (1930); H. S. W. Massey and C. B. O. Mohr, Proc. Roy. Soc. **135**, 258 (1932).

[11] The oscillations of intensity superposed on rapidly falling atomic scattering curves, contributed by factors such as $(1+\sin x/x)$ have been considered by Mark and Wierl, principally in connection with their scattering of high speed electrons. (See H. Mark and R. Wierl "Die experimentellen und theoretischen Grundlagen der Electronenbeugung." Gebrüder Borntraeger, Berlin, 1931).

[12] J. H. McMillen, Phys. Rev. **36**, 1034 (1931).

about 90°. To account qualitatively for the presence of maxima and minima in the scattering of electrons by *atoms*, Bullard and Massey[13] called attention to the necessity for considering the effects of distortion of the electron wave, electron exchange and polarization. These effects have not been included in Massey and Mohr's treatment of scattering by diatomic molecules.

We are accustomed to think of a clear cut distinction between an inelastic and an elastic collision between electrons and atoms. In the latter case the electron leaves the atom unchanged, while in the former case the electron excites (or ionizes) the atom. The lowest excitation state differs in energy so

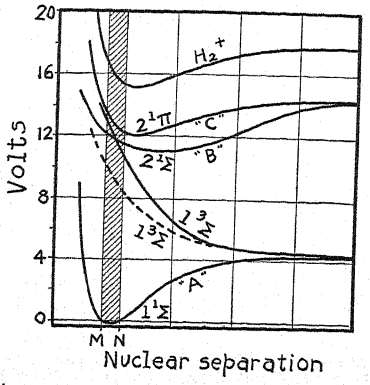


Fig. 7. Franck-Condon diagram for hydrogen. The diagrams given by Smyth and by Mulliken agree substantially in the case of all curves except the $1^3\Sigma$ curve. Mulliken's $1^3\Sigma$ curve is shown as a broken line.

considerably from the normal state that there is no difficulty in identifying an electron which has rebounded from an atom elastically and one which has rebounded inelastically. With a molecule, however, it is conceivable that an electron collision could change the vibrational state and the rotational state of the molecule without altering the electronic state. We should therefore be prepared, perhaps, to find evidences of energy losses of the order of a few tenths of a volt. Experimentally these might cause an asymmetrical broadening of the so-called elastic peak towards the low energy side. We have made as yet no special search for such an effect but it seems possible that it could be detected in view of the experimental work of Ramien[14] on the average energy lost by electrons in colliding with many hydrogen molecules, and in view of the theoretical discussion of Massey.[15]

The possible molecular changes resulting in a hydrogen molecule after an electron impact may be visualized by the help of a Franck-Condon diagram. In Fig. 7 we reproduce a somewhat simplified copy of the diagram given by Smyth[16] for hydrogen. The curve A is for the normal molecule, and the stable state is the one corresponding to a nuclear separation varying between M and N (corresponding to the lowest vibrational state). Excitation by electron impact is represented by a vertical displacement, within the shaded area, to one of the other curves. If the transition is to the $1^3\Sigma$ state, the atoms immediately fly apart and dissociation results. If, on the other hand, the transi-

[13] E. C. Bullard and H. S. W. Massey, Proc. Roy. Soc. **A133**, 637 (1931).
[14] H. Ramien, Zeits. f. Physik **70**, 353 (1931).
[15] H. S. W. Massey, Proc. Camb. Phil. Soc. **28**, 99 (1932).
[16] H. D. Smyth, Rev. Mod. Physics **3**, 347 (1931).

tion is to the B state (i.e., to the $2^1\Sigma$ state), we get an excited molecule which does not dissociate so long as it is in this state. The energy necessary to produce either state is not sharply defined because of the finite width of the shaded column resting on MN. Thus a transition to the $1^3\Sigma$ state requires anything between 10.9 volts and 13.5 volts, while a transition to the $2^1\Sigma$ state requires an amount of energy between 11.5 and 12.2 volts and a transition to the $2^1\Pi$ state calls for something between 12.2 and 13.6 volts. This overlapping makes it impossible to decide whether our most probable loss—12.6 volts—corresponds to a transition to the $1^3\Sigma$ state to the $2^1\Sigma$ state or to the $2^1\Pi$ state. It should be stated that the Franck-Condon diagram as given by Mulliken[17] differs slightly in scale from that given by Smyth, yet in such a way as to suggest a different interpretation of our results. Briefly, if the Mulliken representation is correct, we cannot regard our 12.6 volt loss as indicating transitions to either the $1^3\Sigma$ or to a low vibrational level of the $2^1\Sigma$ state; we must attribute it to a transition to the $2^1\Pi$ state, or to a high vibrational level of the $2^1\Sigma$ state. Dr. E. U. Condon informs us that, on account of the approximations made in the calculations of these curves, they cannot be regarded as exact; thus the position of the $1^3\Sigma$ curve above MN (Fig. 7) may be in error by 2 or 3 volts. In view of this situation it is evident that the identification of our 12.6 volt loss with one or other of the possible transitions cannot be made with certainty. It may well be that our 12.6 volt peak corresponds to transitions to all three states. In view of the sharpness of the energy losses to be expected in *atomic* excitation, as compared with this blurring to be expected in molecular excitation, it is possible that the most probable energy loss peak in hydrogen (e.g., in Fig. 2) would be appreciably less steep (especially on the side next to the elastic peak) than the 11.6 volt peak in argon taken under identical conditions. Tests, however, showed that if the 12.6 volt peak in hydrogen and the 11.6 volt peak in argon were superposed, then the hydrogen peak had no more *spread* toward the elastic peak than had the argon peak.

Massey and Mohr have calculated by wave mechanics the angular distribution of electrons which collide inelastically with hydrogen molecules to give rise to the $2^1\Sigma$ state. These distributions have maxima at certain angles, e.g., for 30 volt primary electrons, a sharp maximum appears at 20°. Fig. 5 gives the angular distribution of the 12.6 volt loss. Unfortunately the curve does not extend to angles smaller than 25°, but it seems obvious that there is no indication of the presence of a maximum at 20°. Massey and Mohr do not give curves for the angular distributions of electrons which have collided with hydrogen molecules and put them into the $1^3\Sigma$ state. Consequently we are unable to compare them with our experimental curves. There is one point of significance, however. By integrating over all angles Massey and Mohr have determined the probabilities of excitation of the $2^1\Sigma$ state and the $1^3\Sigma$ state of hydrogen as a function of the energy of electron impact. The scale of their curves implies that the probability of excitation of the $1^3\Sigma$ transition is about 10,000 times as large as the probability of excitation of the $2^1\Sigma$ state. If this is correct, then our 12.6 volt peak must be associated almost wholly with transitions to the $1^3\Sigma$ state and the number of transitions to the

[17] R. S. Mulliken, Rev. Mod. Phys. **4**, 1 (1932); see also W. Finkenburg and W. Weizel, Zeits. f. Physik **68**, 577 (1931).

$2^1\Sigma$ state must be neglibly small. (This ignores, of course, the possibility of transitions to the $2^1\Pi$ state).

In the case of scattering of electrons by argon atoms, we saw that if the energy lost by the colliding electrons was greater than 15.7 volts, the ionization potential of argon, then a second electron, which we termed the ejected electron, must appear. Thus the parts of the scattering curves corresponding to energy losses greater than 15.7 volts give us the distributions of the colliding, or ionizing electrons, as well as the distributions of the ejected electron. It was found convenient to assume that the ejected electron was always the slower of the two electrons moving away from the atom after an ionizing collision. The situation is still more complicated when we have a diatomic molecule like hydrogen instead of an atom like argon. When the collision is of the type which leaves a molecular ion, we have, as in the case of argon, two electrons and an ion. However, as Tate, Lozier and Bleakney[18] have shown, some types of ionization result in dissociation with the constituent atoms flying apart with considerable kinetic energy. We thus have, after collision, two ions and two electrons moving away from the place of collision, each with its own angle distribution characteristic of its energy and of the energy of the electron before collision. So far as we know, no attempt has been made to solve such a problem theoretically. It is evident, from the curves shown in Fig. 6, that, when electrons are ejected with a certain amount of energy from certain types of collisions, strongly preferred directions of emission are to be found. We can also trace certain regularities in the displacement of the peak representing preferred directions of emission as the energies concerned are progressively altered. Thus, for a given energy of ejection, the position of the peak moves to smaller angles as the energy of collision is increased. On the other hand, if we keep the energy of collision unchanged we find that, as the energy of the ejected electron is increased the position of the peak moves to larger angles. There is also a regularity in the way in which the magnitude of the peak changes as we go across a row or down a column. A comparison of these results with those for argon will show that the distributions of electrons ejected from argon atoms are similar in certain respects to the distributions for hydrogen.

The results for hydrogen were obtained with the same apparatus as that in our work on argon. In our previous article we pointed out that the method of speeding up the electrons by a suitable field into the analyser introduced a certain amount of *blurring* of the sharpness of the curves which was greater the smaller the energy of the electrons under investigation. The same comment applies also to this work on hydrogen.

So far as we know, there has been no attempt to work out a theory for the distributions of the ejected electrons. The frequent occurrence of strongly preferred directions of emission for these electrons suggests a peculiar kind of diffraction effect.

We take great pleasure in thanking Dr. E. U. Condon for his helpful comments on the situation relating to the interpretation of the Franck-Condon diagram for hydrogen.

[18] W. Bleakney, Phys. Rev. **35**, 1180 (1930); W. W. Lozier, Phys. Rev. **36**, 1285 (1930); J. T. Tate and W. W. Lozier, Phys. Rev. **39**, 254 (1932).

Electronic Structures of Polyatomic Molecules and Valence. II. General Considerations

By ROBERT S. MULLIKEN
Ryerson Physical Laboratory, University of Chicago

(Received April 23, 1932)

A description of electronic structures of polyatomic molecules in terms of atomic and molecular orbitals (one-electron orbital wave functions) is suggested, as follows. Unshared electrons are considered as occupying atomic orbitals associated with the various nuclei to which the electrons belong. Shared electrons are described from several points of view, whose simultaneous consideration should give a better understanding of their condition and functions in the molecule. In the first place, they are described, in terms of atomic orbitals, from the point of view of *each nucleus* in the molecule. In the second place, they are described from a unitary molecular point of view, in terms of molecular orbitals. It is pointed out that the chemical evidence which led Lewis to his concept of the electron-pair bond can now all be explained by the quantum theory without the necessity of using such a concept. It is noted that the Heitler-London, Pauling-Slater quantum-mechanical electron-pair bond concept differs markedly from Lewis's, also that it is of more restricted application to chemical data. It is pointed out, in agreement with Hund, that properties of the H. and L., S. and P. electron-pair bond which make it useful in dealing with chemical combination are also possessed by the concept of molecular orbitals. For example, the Pauling-Slater criterion that bonds which correspond to a maximum overlapping of atomic orbitals are the strongest is just as characteristic of bonding molecular orbitals as of electron-pair bonds. An electron-pair bond is here interpreted as being little other than two electrons occupying a bonding molecular orbital. Or in general one must say that a set of n electron-pair bonds is interpreted as a set of $2n$ electrons occupying n molecular orbitals, because molecular orbitals are not necessarily localized *between two nuclei* like electron-pair bonds. It is concluded that the essential facts of molecular electronic structure can be qualitatively understood in terms of the mode of description stated in the first paragraph above and of a semi-empirical valence rule (not essentially new) which summarizes, in the light of quantum theory, the most important regularities in regard to the types of chemical compounds which are stable.

ATOMIC AND MOLECULAR ORBITALS FOR DESCRIBING MOLECULAR ELECTRONIC STRUCTURES

1. Introduction

THE series of which the present paper is the second[1] is a development of a program initiated by Hund[2] and the writer[3] and carried forward principally by us, by Herzberg, and by Dunkel.[4,5,6,7,8,9,10,11,21] The object

[1] A brief preliminary paper outlining some of the principles used and some of the main results has already been published: R. S. Mulliken, Phys. Rev. **40**, 55 (1932). In this paper, the following changes should be made in the last paragraph on p. 58. Line 8, delete "tetrahedralized but uncombined"; lines 9 and 12, delete brackets around σ, and delete "uncombined" before $2p\sigma$; lines 10–11, delete "tetrahedralized uncombined." Also on p. 59, line 10, delete brackets. Elsewhere, do not delete brackets or "tetrahedralized."

[2] F. Hund, Zeits. f. Physik **51**, 759 (1928).

[3] R. S. Mulliken, Phys. Rev. **32**, 186, 761 (1928); **33**, 730 (1929).

of this program has been to describe and understand molecules in terms of one-electron orbital wave functions of distinctly molecular character. The first paper of the present series[1] will be referred to hereafter as I. The present paper is to a large extent a preliminary critical review rather than a presentation of new results.

2. Atomic and molecular orbitals

From here on, one-electron orbital wave functions will be referred to for brevity as *orbitals*. The method followed here will be to describe unshared electrons always in terms of *atomic orbitals* but to use *molecular orbitals* for shared electrons. This procedure was first used by Lennard-Jones[12] for diatomic molecules, and is a partial departure from the original formulation of the above program. Among the main objects of the present series are the determination of the forms of molecular orbitals and the application of a knowledge of these forms to an explanation of valence and related chemical phenomena.

Shared electrons include two types, namely *bonding* and *anti-bonding* electrons, at least in diatomic molecules; unshared electrons belong to the class of *non-bonding* electrons.[8,9,10,11] Anti-bonding electrons occur in diatomic molecules only when accompanied by a larger number of bonding electrons. Often it is hard to draw the line between shared and unshared electrons; in such cases, the electrons in question consist of bonding and anti-bonding electrons in equal numbers, at least in diatomic molecules (cf. third following paragraph and references 8, 9).

By an atomic orbital is meant an orbital corresponding to the motion of an electron in the field of a single nucleus plus other electrons, while a molecular orbital corresponds to the motion of an electron in the field of two or more nuclei plus other electrons. Both atomic and molecular orbitals may be thought of as defined in accordance with the Hartree method of the self-consistent field, in order to allow so far as possible for the effects of other electrons than the one whose orbital is under consideration.

Every non-degenerate orbital can be occupied by at most two electrons,

---

[4] F. Hund, Zeits. f. Physik **63**, 719 (1930).

[5] F. Hund, Zeits. f. Physik **73**, 1 (1931); **74**, 429 (1932).

[6] F. Hund, Zeits. f. Physik **73**, 565 (1932).

[7] F. Hund, Zeits. f. Physik **74**, 1 (1932).

[8] R. S. Mulliken, Chem. Rev. **9**, 347 (1931). On p. 351 (foot), p. 353 (middle) and p. 355 (middle), the writer gives the incorrect impression that, omitting the energy of repulsion of the nuclei, the promoted wave-function $2p\sigma$ has a *higher* energy than the original $1s$ atomic wave-function. Actually the energy is a little lower (for $R>0$) than that of $1s$ in the H atom. This, however, does not in any essential way affect the validity of the arguments given. The fact that the energy of $2p\sigma$ goes up sufficiently rapidly *with reference* to that of $1s\sigma$, in particular the fact that the energy of $2p\sigma$ plus the nuclear repulsion energy causes a net repulsion of H and H^+, is sufficient.

[9] R. S. Mulliken, Rev. Mod. Phys. **4**, 1 (1932).

[10] G. Herzberg, Zeits. f. Physik **57**, 601 (1929).

[11] G. Herzberg, "Molekülstruktur," Leipziger Vorträge, 1931, p. 167. S. Hirzel, Leipzig.

[12] J. E. Lennard-Jones, Trans. Faraday Soc. **25**, 668 (1929).

corresponding to the two possible orientations of the electron spin. Orbitals having n-fold degeneracy can be occupied by at most $2n$ electrons. Examples of non-degenerate orbitals are s orbitals in atoms, σ orbitals in diatomic or linear molecules[9,11] and most orbitals in non-linear polyatomic molecules. Examples of degenerate orbitals are p, d, . . . orbitals in atoms ($2l+1$-fold degeneracy), π, δ, . . . orbitals in diatomic or linear molecules (2-fold degeneracy), $[\pi]$ orbitals (2-fold degeneracy), in molecules like NH_3, NO_3^-, etc. (cf. I), d_γ (2-fold degeneracy) d_ϵ and p (3-fold degeneracy) in molecules having tetrahedral or octahedral symmetry (cf. I).

It should be noted that the use of atomic orbitals for describing the condition of unshared electrons in molecules often gives a false impression of the amount of degeneracy. For example if one writes $1s^2 1s^2 \sigma 2s^2$ for the electron configuration[9] of Li_2, the description suggests only one ionization energy for the $1s$ electrons, since $1s$ orbitals on two Li atoms are identical in energy. If one writes $\sigma 1s^2 \sigma^* 1s^2 \sigma 2s^2$, however, using molecular orbitals exclusively,[9] it is made explicit that there are two distinct energies corresponding to $\sigma 1s$ and $\sigma^* 1s$. In this particular example the energy difference is negligible, but in many cases, especially where there are electrons which are near the border line between unshared and shared, considerable energy-splittings may exist.

For example in O_2 one may perhaps best write $1s^2 1s^2 2s^2 2s^2$ . . . but must then grant that the $2s$ type, although essentially unshared, has a markedly double ionization energy.[9] In N_2, the sharing of the $2s$ electrons is so strong that it is best to write $1s^2 1s^2 \sigma 2s^2 \sigma^* 2s^2$, the types $\sigma 2s$ and $\sigma^* 2s$ being very different in energy.[9] In CF_4, one might write $\{1s^2 2s^2 2p[\pi]^4\}_F{}^4 \{1s^2\}_C a^2 b^6$, where a and b represent the shared electrons. In so doing, it should be recognized that four distinct energy values are to be expected for the unshared $1s$ fluorine electrons, likewise for the $2s$ and for the $2p[\pi]$,—or possibly eight values for $2p[\pi]$ because of a possible splitting up of the degeneracy implied by the symbol $[\pi]$. The four-fold splitting might be appreciable for the $2p[\pi]$ and possibly also for the $2s$, although of course negligible for the $1s$. The carbon $1s$ is of course very different in energy from the fluorine $1s$. These examples should be sufficient to show how to guard against a possible misinterpretation of the use of atomic orbitals in describing molecules.

In the present method, molecular orbitals are conceived of as entities quite independent of atomic orbitals. Nevertheless in practise molecular orbitals can usually be conveniently approximated by building up linear combinations of orbitals of the atomic type. The present method of thinking in terms of the finished molecule, used already by Lewis in his valence theory, avoids the disputes and ambiguities, or the necessity of using complicated linear combinations, which arise if one thinks of molecules as composed of definite atoms or ions.

3. One-nucleus and other viewpoints

Understanding of the electronic structure of molecules is greatly aided by introducing a set of partially overlapping descriptions whereby the electrons immediately surrounding each nucleus in a molecule are described in

terms of a set of atomic orbitals corresponding to the viewpoint of that nucleus. (Sidgwick,—reference 13, p. 98,—has used essentially this viewpoint.) Such *one-nucleus viewpoint* atomic orbitals must be taken as considerably deformed compared with ordinary atomic orbitals, the deformation being thought of as caused by the strong fields of the other nuclei. Unshared electrons, of course, are here assigned exclusively each to a particular nucleus, so that the one-nucleus viewpoints for them give the same description as that introduced in the first paragraph of section 2. Shared electrons, however, being considered as belonging to two or more nuclei, receive non-mutually-exclusive descriptions in terms of deformed atomic orbitals associated with each, or at least with several, of these nuclei (cf. descriptions of N_2^+, HCl, and $PtCl_6^=$ in section 8 below and of CF_4 and other molecules in I as examples).

An understanding of molecular electronic structures can not infrequently be advanced by using still other auxiliary viewpoints. The well-known *united-atom* viewpoint is sometimes useful (cf. reference 9, p. 19). In hydrides especially, this or, rather, a viewpoint in which each hydrogen nucleus is at first regarded as united with a neighboring nucleus of larger charge, is valuable. This amounts to saying that in hydrogen compounds, the hydrogen one-nucleus viewpoints can often appropriately be treated as unimportant compared with the viewpoints of other nuclei in the molecule or that the hydrogen nuclei can be regarded merely as perturbing force-centers. The validity of this point of view is indicated by a number of facts concerning diatomic hydride band spectra,[9] also by chemical data, notably the behavior of the boron hydrides.[8]

The familiar chemical method of regarding many molecules as built up of "radicals" suggests the usefulness of a point of view making use of shared orbitals belonging to *radicals* instead of, or in addition to, the viewpoint of molecular shared orbitals.

Quantum Theory of Valence

4. Review of theories of valence and molecular structure

A semi-historical survey of some of the theories dealing with valence and molecular structure will put the whole problem in better perspective. Incidentally, the writer hopes to show that there are no compelling reasons, either empirical or theoretical, for placing primary emphasis on electron pairs in constructing theories of valence. He hopes thereby to remove possible objections to the present method based on its lack of such emphasis.

The best chemical theory of valence covering all types of compounds is generally agreed to be that developed principally by G. N. Lewis.[13] To a rather large extent, the essential features of this theory still stand, although their meaning has been made clearer and more specific by interpreting them in the light of the quantum theory. The most important features of Lewis's theory are perhaps the following:

[13] G. N. Lewis, Valence and The Structure of Atoms and Molecules. The Chemical Catalog Co., New York, 1923. Sidgwick's excellent book should also be consulted: N. V. Sidgwick, The Electronic Theory of Valency. The Clarendon Press, Oxford, 1927.

(1)(*a*) Every atom tends so to give, take, or share electrons as to be surrounded by an outer "group of eight" electrons (reference 13, p. 79),—except that for atoms such as H, He, Li this is replaced by a group of two. (*b*) Electrons which are shared may be shared equally or unequally by atoms, so that one can readily account for all intermediate stages between homopolar molecules like H_2 or Cl_2 and polar molecules such as NaCl. (*c*) Besides the cases having a stable group of two, already mentioned, Lewis noted the existence of other probable exceptions to the "rule of eight," namely cases like those of PCl_5, SF_6, $PtCl_6^=$ where a central atom appears to share more than eight electrons with other atoms (reference 13, pp. 102, 114 *et seq.*). Lewis suggested that in such compounds, the shared electrons in excess of eight have "passed into a secondary valence shell" of higher energy.

(2)(*a*) The single bond of the old valence theory of organic chemistry is interpreted as a pair of electrons held jointly in the outer shells of two atoms, and this concept of the chemical bond is extended to inorganic compounds. This electron-pair bond may be symmetrically shared as in H_2 or Cl_2, but more often the electron-pair is nearer one atom than the other. (*b*) The valence of an atom in any molecule is defined as the number of electron pairs which it shares with other atoms (reference 13, p. 104). This is Langmuir's "covalence." Lewis's definition of valence makes the numerical valence the same as the "coordination number" of Werner (reference 13, p. 114). Using this definition, atoms which form a "group of eight" (Langmuir's "octet") by sharing have a valence of four, and "we may regard the maximum valence of four as a sort of norm," although atoms sharing more than four pairs have a higher valence, e.g., S or Pt in SF_6 or $PtCl_6^=$ has a valence of six. When there is an outer shell of eight electrons, there is a strong tendency for these to be all shared. In dealing with ionic or ionized molecules, Lewis uses the term "polar number" (reference 13, pp. 70, 104), e.g., in $Co^{++}Cl^-_2$, the Co atom is said to have a polar number $+2$, the Cl a polar number -1. This is Langmuir's "electrovalence." (*c*) Usually each atomic partner in an electron-pair bond furnishes one of the two electrons, as e.g. in H_2, CH_4, CCl_4, but very often one partner furnishes both: examples, $BR_3 \cdot NH_3$ and other ammonia complexes, where the N atom furnishes both electrons of a pair; $SO_4^=$, ClO_4^-, etc., where the central atom furnishes all the shared electrons except the ionic charges. One-sided sharing as here and in (*a*) causes polarity in the molecule, but does not require a really ionic conception of valence, such as Kossel has used,[14] except in extreme cases. (*d*) Double and triple bonds are considered to involve sharing of two and three pairs of electrons, but are considered to be something very different from merely two or three ordinary electron-pair bonds. Multiple bonds are apparently rarely formed by atoms other than C, N, and O.

The fundamental ideas of Lewis's theory are perhaps the three following: (*A*) each atom (better, each nucleus) in a molecule tends to become sur-

[14] W. Kossel, Ann. d. Physik **49**, 229 (1916); Naturwiss. **7**, 339, 360 (1919); cf. A. E. van Arkel and J. H. de Boer, Chemische Bindung als elektrostatische Erscheinung, S. Hirzel, Leipzig, 1931 (German edition).

rounded by a set of closed shells of electrons; (*B*) shared electrons, forming chemical bonds of the homopolar type, are usually localized between two atoms (or nuclei) which they link together; (*C*) a chemical bond usually consists of a pair of electrons somehow rather closely united to each other. Of these three ideas, Lewis seems to have considered (*C*) as the most fundamental (cf. reference 13, pp. 79–81). Ideas (*A*) and (*B*) were already in use before Lewis's 1916 paper, although Lewis's work greatly developed them and their application. Lewis' most important contribution to the theory consisted perhaps in his introduction of the idea of the completion of closed groups by *sharings*. Idea (*A*), limited, however, to the "group of eight," was proposed by Abegg in 1904 for polar valence and was also used in the same way by Lewis and later by Parson (1915) and Kossel (1916). Idea (*B*) was adapted by Lewis from the concepts of organic chemistry. Langmuir,[15] in further developing the subject in 1919, emphasized idea (*A*) and spoke of the "octet theory" of valence. Bury[16] in 1921 also emphasized idea (*A*).

With the development of the quantum theory, a more fundamental theoretical background has gradually been created for the originally largely empirical ideas of the Lewis theory. Bohr's theory of the periodic system, as modified by Stoner and Main Smith, shows why idea (*A*) is important in valence theory. The group of two found in H^-, He, Li^+ is $1s^2$ and presumably the shared pair of electrons in H_2 is essentially the same, while the highly stable "octet" is ns^2np^6. Bohr's theory also provides for less stable groups of 18 and 32 electrons. Sidgwick[17] showed in a general way in 1923 on the basis of the original Bohr theory how a group of 18, containing *ns*, *np* and *nd* electrons, can be used to interpret complex ions like $PtCl_6^{=}$ or $Co(NH_3)_6^{+++}$. Revised interpretations which regard the shared electrons in such compounds as belonging to *nd*, $(n+1)s$, and $(n+1)p$, have been given later (cf. Pauling,[18] also I). Knorr[19] has discussed the interpretation of Lewis's theory from the standpoint of the modified Bohr theory.

Bohr's theory was unable to give a satisfactory understanding of the sharing of electrons in molecules, but the new quantum mechanics is showing itself capable of doing this.

London and Heitler, generalizing results obtained from a quantum-theoretical study of the formation of H_2 from H+H, attempted to construct a valence theory which has often been supposed to be the quantum-mechanical equivalent of Lewis's, and which emphasizes Lewis's ideas (*B*) and especially (*C*). This so-called spin theory of valence emphasizes the pairing of electrons and their spins, but deals primarily with the interactions of atoms as wholes. It has, however, not proved very successful.[5,8,10] London made the suggestion that the shared electrons in excess of eight ($ns^2\ np^6$) in

[15] I. Langmuir, J. Am. Chem. Soc. **41**, 868 (1919); Science **53**, 290; **54**, 59 (1921).
[16] C. R. Bury, J. Am. Chem. Soc. **43**, 1602 (1921).
[17] N. V. Sidgwick, Trans. Chem. Soc. **123**, 725 (1923).
[18] L. Pauling, J. Am. Chem. Soc. **53**, 1367, 3225 (1931); **54**, 988 (1932).
[19] C. A. Knorr, Zeits. f. anorg. allgem. Chem. **129**, 109 (1923). Also W. A. Noyes (1917), and others: cf. references given by W. A. Noyes, Zeits. angew. Chem. **44**, 893 (1931).

PCl_5, SF_6 and the like are *nd* electrons; this idea is more specific than the similar idea of Lewis (cf. item 1 (*c*) above), and seems to be a good one.[18,1] One should distinguish carefully[8] between Heitler and London's valence theory and their valuable *perturbation-method for calculating energies* of molecule-formation.

Pauling[18] and Slater[20] have generalized the Heitler and London results for H_2 in a different way, considering more specifically the interactions of pairs of electrons, one electron from each of two atoms. In this way they have obtained important results on valence and valence angles in polyatomic molecules. Their work emphasizes Lewis's idea (*C*) in modified form but focuses attention more on idea (*B*). Their theory seems more limited than Lewis's in that it requires that the two electrons forming an electron-pair bond necessarily come from two different atoms. This makes it inapplicable to many chemical compounds (cf. summary of Lewis's theory, item 2*c*) unless one assumes them to be formed from ions, a procedure which in many cases seems decidedly artificial. The theories of Heitler and London, Pauling and Slater might be called *electron-pairing* theories if Lewis's is called an *electron-pair* theory. It should also be pointed out that the H.L.P.S. electron-pair differs very considerably from Lewis's conception of the electron-pair bond in that the electrons are much less closely associated (see below); in this respect it approaches the truth much more closely than does Lewis's conception.—Pauling and Slater consider a double bond to be merely two ordinary single bonds sticking out from each atom in different directions, and treat the triple bond in a similar way. In this they do not agree very well with Lewis (cf. summary, item 2*d*), nor do they agree with results obtained from the method of molecular orbitals (see below).

Dunkel[21] emphasizes Lewis's ideas (*A*) and (*B*), and describes the shared electrons in molecules in terms of the symbols $[\sigma]$ and $[\pi]$, implying orbital wave functions having properties similar to those of σ and π orbitals in diatomic molecules. The symbol $[\sigma]$, for instance, indicates a molecular orbital concentrated in the region between two nuclei and roughly symmetrical around the line joining them. This is justified by the fact that the shared electron moves in a Hartree field which is roughly symmetrical around this line. Although shared electrons of any given kind nearly always occur in pairs in stable molecules, this seems to be incidental in Dunkel's as in the present work. Unshared electrons are classified as they would be in free atoms. Dunkel's viewpoint evidently resembles that of the present paper. Hund in his recent papers[5,6] has used Dunkel's $[\sigma]$, $[\pi]$ classification, but has used the simple symbols σ, π.

Hund in his important recent papers[5,6,7] concludes that the results obtained by Slater and Pauling using the electron-pair bond method can also be obtained, sometimes more easily, by the method of molecular orbitals, and that the two methods are in many respects equivalent if one restricts the use of molecular orbitals to a type localized between two nuclei,—in agree-

[20] J. C. Slater, Phys. Rev. **37**, 481; **38**, 325, 1109 (1931).

[21] M. Dunkel, Zeits. f. phys. Chem. [B] **7**, 81; **10**, 434 (1930).

ment with Lewis's idea (*B*). Reference should be made to Hund's papers for a critical discussion of many points concerning the various quantum theories of valence.

Hund has classified valences according to a number of types, depending in part on whether they are formed by *s* or *p* electrons or involve partial hybridization of *s* and *p* (Hund's *q* type). Hund also classifies chemical bonds according to a number of types, and concludes among other things that single bonds are always of the type $[\sigma]^2$, double bonds of the type $[\sigma]^2\ [\pi]^2$, triple bonds of the type $[\sigma]^2\ [\pi]^4$. It will be noted that this description of double and triple bonds agrees better with Lewis's conclusions (cf. summary, item 2*d*) than does the description given by Slater and Pauling. The absence of free rotation about double bonds can be well accounted for[8,10] by the formulation $[\sigma]^2\ [\pi]^2$, which really goes back to Hückel,[22] while the validity of the explanation given by Pauling and Slater seems doubtful.

Hund shows[6] that the familiar rules of organic chemistry can be explained in terms of the quantum-mechanically predicted behavior of some of the possible types of valence and of bonds. He shows that not all of the theoretically possible types are found in ordinary organic compounds, and shows how this can be understood in terms of energy relations; in particular, by assuming that of the types $[\sigma]$ and $[\pi]$ corresponding to a *p* valence electron, $[\sigma]$ in practise nearly always has the lower energy.

In all this work, Hund's purpose has been to show how the ordinary rules of valence can be derived from the principles of the quantum theory. In doing this, he has found it necessary to specialize the concept of molecular orbitals to the case of *orbitals localized between two nuclei*. Such a localized molecular orbital occupied by two electrons he regards as corresponding to the valence bond of organic chemistry or to that of Lewis, and as being essentially equivalent in the case of ordinary stable molecules to the electron-pair bond of H.L.S.P.

Hund remarks incidentally that the use of localized molecular orbitals is a somewhat poorer approximation than the use of the non-localized orbitals which are advocated in the present series, and illustrates this[6] by discussion of a case which corresponds to CH_2 or H_2O. He also points out that in some cases localized orbitals cannot be used at all, and illustrates this by a consideration of crystal lattices and of the benzene molecule C_6H_6 and related molecules. In his plausible and important interpretation of C_6H_6, Hund uses the same point of view that is emphasized in the present series. His non-localized "π" type in C_6H_6 is very similar to the central-nucleus-viewpoint type $2p[\sigma]$ in $CO_3^{=}$ or NO_3^{-} if this type is assumed to be filled by two electrons shared by the O atoms in addition to their ordinarily assumed sharing of one pair each (cf. I, p. 61).

In the present series, idea (*A*) of Lewis's theory is emphasized, idea (*B*) is adopted in generalized form (non-localized molecular orbitals), while idea (*C*) is considered as corresponding more to an incidental than to a really essential characteristic of chemical combination. While the pairing of elec-

[22] E. Hückel, Zeits. f. Physik **60**, 423 (1930).

trons, which is a consequence of the Pauli principle combined with the fact that the electron spin can have two and only two orientations, is very important for the *general theory of atomic and molecular structure*, especially in connection with the formation of closed shells, the importance of the specific role of electron-pairs or of electron-pairing in the *formation of molecules* has, in the writer's opinion, been somewhat over-emphasized, first in Lewis's theory, then in the work of Heitler and London, Pauling and Slater. Reasons for this opinion have been given in a previous paper dealing mainly with diatomic molecules.[8] It seems desirable, however, to take the matter up again in some detail here, approaching it historically.

5. Analysis of the origin and development of the concept of the electron-pair bond

At the outset it is important to notice that Lewis's development of the concept of the electron-pair bond preceded our present knowledge of the electron spin and its properties and of the Pauli principle.

In developing his theory, Lewis noticed that while nearly half of the known atoms contain an odd number of electrons, very nearly all stable molecules contain an even number. This and other information on atomic structure and on molecules suggested that electrons have a tendency to form stable groups of two, held close to each other (cf. reference 13, p. 82 and Fig. 22) by strong forces of unknown character. These forces Lewis for some time considered to be magnetic, since the paramagnetism characteristic of atoms or molecules with an odd number of electrons usually disappears when they combine to give molecules with an even number. Lewis considered that in the formation of a molecule from two atoms containing unpaired electrons, the electrons attract each other in pairs, and that this attraction is, to a considerable extent at least, the cause of molecule formation (cf. e.g., reference 13, p. 149, second paragraph).

The subsequent development of the quantum theory has provided adequate explanation for the above facts concerning electron-pairs. The fact that most of the electrons in atoms as well as in molecules are paired is now well understood in terms of Pauli principle and electron spin. The fact that paramagnetism goes with unpaired electrons, diamagnetism with paired electrons, is also well understood. The fact that electrons are more often unpaired in atoms than in molecules can be understood in terms of the Pauli principle, electron spin, and orbital degeneracy (see below).

According to the quantum theory an electron-pair, in a molecule or in an atom, consists of two electrons, with spins antiparallel, occupying the same orbital and "symmetrically related" so far as their orbital motion is concerned.[8] The magnetic forces between the two electrons are very small while the electrostatic repulsion is large. It is true that the symmetrical relation keeps the electrons nearer together than they would otherwise be, and in this respect shows a similarity to Lewis's concept of a pair of electrons held together by a strong attraction. But, directly contrary to Lewis's idea, the increased nearness of the electrons usually only increases their energy of repulsion.

Thus the formation of a pair of electrons when a molecule is formed, i.e., the occupation of a shared molecular orbital by *two* electrons, far from being *per se* a *cause of combination* of two atoms initially having each an unpaired electron, should tend to prevent combination. According to the present point of view the two electrons concerned act as bonding electrons *in spite of* considerable repulsive forces acting between them. Further details will be found in a discussion of H_2^+ and H_2 in reference 8.

Why then, are unpaired electrons so very much rarer in stable chemical molecules than in atoms? The answer involves several distinct considerations. In the first place, every atom having an odd number of electrons has necessarily at least one unpaired, while as soon as the formation of molecules is permitted, this necessity disappears. This leaves three questions. (1) Why do atoms often have more unpaired electrons than the minimum possible number, which is zero for an even total number of electrons, and one for an odd total number of electrons? (2) Why do stable molecules nearly always have an even number of electrons? (3) Why do such molecules nearly always have all their electrons paired?

The answers to all these questions depend largely on the occurrence and behavior of non-degenerate and of degenerate orbitals. If every orbital in atoms and molecules were decidedly different from every other in energy, then no atom or molecule with an even number of electrons would contain unpaired electrons when in its normal state. The electrons would settle down into the orbitals of lowest energy, with two electrons in each such orbital.

But when there is orbital degeneracy, i.e., when two or more orbitals form a group whose members are equal in energy (cf. section 2 above), then the energy of the electron system as a whole is a minimum if every electron occupies a different orbital belonging to the degenerate group. For example in the nitrogen atom the energy is a minimum when we have the electron configuration $1s^2\ 2s^2\ 2p^3$ and the state ^4S. The orbitals $1s$ and $2s$ are non-degenerate and each is occupied by two electrons, but the type $2p$ has a three-fold degeneracy, being capable for example of giving rise to three distinct orbitals, $2p_{+1}$, $2p_0$, and $2p_{-1}$ in a strong magnetic field. The state ^4S corresponds to one electron, unpaired, in each of the three orbitals $2p_{+1}$, $2p_0$, and $2p_{-1}$. The energy is a minimum for this state because it permits the orbitals of the three electrons to be antisymmetrically related.[8] The resultant spin $S(S=1\frac{1}{2}$ here) is always equal, in molecules as well as in atoms, to $\frac{1}{2}$ times the number of unpaired or antisymmetrically related electrons, here three. If two electrons occupied the same orbital, e.g., $2p_{-1}$, they would necessarily be symmetrically related; but a symmetrical relation, as already noted, forces the electrons together, and would raise the energy above that of the ^4S normal state.

It remains to give reasons why stable molecules nearly always have an even number of electrons, in pairs. In the writers' opinion, this can best be explained in terms of Lewis's idea (A) according to which each nucleus in a molecule tends to become surrounded by an atomic closed shell of electrons.

Since such a closed shell, e.g., ns^2 or ns^2np^6, contains an even number of electrons,—for the reason that it is in the last analysis made up of pairs of electrons, although these often belong to degenerate groups, e.g., np^6,—every molecule which satisfies Lewis's idea *A* must automatically contain an even number of electrons, *all paired*. The quantum-mechanical background of idea *A* will be taken up below.

A further reason why molecules with an even number of electrons much more rarely contain unpaired electrons than atoms with an even number of electrons is to be found in the fact that orbital degeneracy is less usual in molecules than in atoms (cf. section 2, above). The O_2 molecule is a good example of an "exception that proves the rule." Here the electron configuration is of a type $\cdots\pi^2$, and the normal state is $^3\Sigma^-$, with $S=1$ and so two unpaired electrons. The π type of molecular orbital has a two-fold degeneracy, so that with two π electrons, one can be π^+, the other π^-, and the two can be antisymmetrically related and so give rise to the normal state with $S=1$.

From the foregoing discussion it will be seen that the empirical evidence which led Lewis to emphasize his idea (*C*), according to which the formation of electron-pairs has a peculiar importance for chemical phenomena, can now all be explained satisfactorily on the basis of general quantum-theoretical considerations without any necessity of adopting idea (*C*).

Nevertheless it must be admitted that most of the striking chemical facts are not inconsistent with an electron-pair bond theory of homopolar valence similar to Lewis's. (His idea of a special attraction between electrons as the cause of pairing must of course be dropped.) A pair of electrons occupying equivalent localized molecular orbitals appears to be on the whole the nearest quantum analogue of Lewis's bond. For the best-known stable molecules the H.L.S.P. electron-pair,—cf. Hund (section 4), and section 13,—is equally good or perhaps better, but for molecules where a pair of electrons is furnished by one atom (cf. Lewis's theory, item 2*c*, and section 6), H.L.S.P. electron-pairs are less suitable than pairs of bonding orbitals. On the other hand for describing molecules having unusually loose binding, or molecules in a high state of vibration or in process of dissociation, provided dissociation would cause the breaking up of electron-pairs into unpaired electrons, electron-pair bonds of the H.L.S.P. type should often constitute a much better approximation than bonding orbitals.

6. Advantages of the present method

The concept of the bonding molecular orbital has the following advantages over the Heitler-London, Slater-Pauling electron-pair bond. (1) It is not necessary to have two electrons to get a chemical bond; one electron occupying a bonding orbital has a bonding effect, although of course not as strong as if two were present.[8] Such "one-electron bonds" are rarely found in stable molecules, it is true, but the concept of bonding orbitals which explains them as a special case can lay claim to greater generality than the electron-pair bond concept which has to be replaced by a different special

concept in order to deal with them. The importance of one-electron bonds[18] is greatly increased if one ventures into the realm of spectroscopically observable molecular entities and of intermediate products in chemical reactions. (2) Bonding molecular orbitals can be constructed for any degree of polarity or unequalness of sharing of electrons between nuclei. H.L.S.P. electron-pair bonds, however, cannot be used for molecules of the extreme polar type, and intermediate cases can be taken care of only by forming linear combinations of wave functions of the polar and electron-pair bond types (cf. section 13). In cases like $Cu(NH_3)_4^{++}$ or CO, the H.L.P.S. method can be used only by starting with assumed states of ionization like Cu^- and NH_3^+ or C^- and O^+, while the method of molecular orbitals can start with Cu^{++} and NH_3 or C and O. For example, the pair of electrons which any N atom in NH_3 shares with the Cu or Pt atom in $Cu(NH_3)_4^{++}$ or $Pt(NH_3)_6^{++++}$ can be assigned to a symmetrically related pair of molecular orbitals which at first belong wholly to the NH_3 but take on more and more of the character of Cu or Pt atomic orbitals as the NH_3 approaches the metal atom. Here the method of molecular orbitals is superior even for loosely bound molecules. These various possibilities make the concept of molecular orbitals more generally useful than that of H.L.S.P. electron-pair bonds. (3) Bonding molecular orbitals are not restricted, like electron-pair bonds, to holding just two nuclei together, but may be distributed between several nuclei. This makes the concept a much more flexible one than that of the electron-pair bond, and makes it possible to account rather directly for a number of phenomena, many of them more or less spectroscopic but others definitely chemical in the ordinary sense, which the electron-pair bond method does not touch. In particular, molecular orbitals can be chosen in conformity to the actual symmetry of the nuclear arrangement, while the electron-pair bond method often disregards (even though it often predicts) this.

In general it may be said that there are many phenomena which can be interpreted in terms of electron-pair bonds only if after setting up these bonds, various *linear combinations* are formed, while the molecular orbital concept goes more directly at the solution, although often seemingly neglecting certain features expressed by the electron-pair concept. It appears probable that in practise one can expect most of the phenomena expressible by the special concept of electron-pair bonds to drop out of the application of the less specialized method using molecular orbitals. This should become clear in the detailed discussion of examples in later papers. It is quite possible, however, that the electron-pair bond method may for many problems be more adapted to quantitative calculations than the present method.

7. Statement and justification of a valence rule

Most of the ordinary numerical aspects of valence, alike for homopolar, heteropolar and for intermediate types of compounds, appear to be expressible by a simple *valence rule* (cf. I): *Every nucleus in a molecule tends to be surrounded, by means of sharing or transfer of electrons, by an electron distribution corresponding to some stable configuration having a total charge ap-*

proximately equal to or somewhat exceeding the charge of the nucleus. This is essentially idea (*A*) of Lewis's theory together with a generalization of his idea (*B*). This valence rule, it will be noted, is expressed in terms of one-nucleus viewpoints, according to which the state of the electrons near each nucleus is described by means of a set of electron quantum numbers or atomic orbitals associated with the viewpoint of that nucleus.

The important tendency of many atomic nuclei to have all their outer electrons shared (cf. section 4, item 2*b*), as e.g. in the formation of NH_4^+, $BR_3 \cdot NH_3$, or $Cu(NH_3)_4^{++}$ from NH_3 is not accounted for by this valence rule, but its explanation appears to follow incidentally from the application of the present method (cf. discussion of NH_3 and CH_3 in I).

By "stable configuration" in the valence rule is usually meant a set of atomic orbitals completely occupied by electrons (i.e., a set of closed shells) and of such type that further electrons could go only into orbitals of distinctly higher energy. Stable configurations are usually sharply marked off from other configurations with either more or fewer electrons, by virtue of large energy changes that go with a change in principal quantum number, or with the change from a penetrating to a non-penetrating type of orbit even without change in principal quantum number.

Stable configurations which are sharply defined in respect to energy tend to give sharply-defined valence relations. In the transition groups where a *d* shell is in the process of being built up, there is at first no limiting sharply-defined stable configuration, and highly variable valence is the result. As the *d* shell approaches completion, however, the complete group $d^{10}s^2p^6$ apparently begins to serve as a stable limit, which is approached or reached in a number of complex molecules.

A quantum-theoretical justification of the above valence rule follows in part from the fact that, for the electrons in the neighborhood of every nucleus in a molecule, the Pauli exclusion principle makes essentially the same requirements in regard to quantum numbers and closed shells as for the electrons in an isolated atom. This is obviously true for the unshared, inner electrons, and for the ionic structures in definitely heteropolar valence, while its truth for shared electrons appears plausible but requires further investigation. The best evidence for its correctness for shared electrons seems to be the empirical evidence of the success of the rule in interpreting chemical facts. Dunkel[21] has justified his (more or less tacit) use of a similar rule by similar arguments (cf. also Sidgwick, reference 13, p. 98 *et seq.*).

As a result of sharing, the numbers of electrons surrounding certain nuclei sometimes very considerably exceed the numbers in the corresponding neutral atoms. In such cases the sharing is usually relatively loose and presumably is strongly one-sided, although not necessarily ionic. Thus, for example, the electrons shared by the Pt or Cu nucleus in $Pt(NH_3)_6^{++++}$ or especially $Cu(NH_3)_4^{++}$ doubtless belong much more to the N nuclei than to the metal nucleus. The shared molecular orbitals would be approximated by linear combinations containing a relatively small proportion of an orbital,—nd, $(n+1)s$, or $(n+1)p$,—of the metal nucleus and large proportions of $2p\sigma$

orbitals of the N nucleus. Nevertheless the magnetic and other properties of such molecules[18] indicate that even such one-sided sharing is commonly (but not always) strong enough so that, as far as the Pauli principle is concerned, part or all the metal-nucleus-viewpoint orbitals nd, $(n+1)s$, $(n+1)p$ are effectively filled.

In general, the ability of a nucleus to hold more electrons, but a rather definitely limited number more, when in a molecule than in an atom, appears to be conditioned by the fact that shared electrons are, so to speak, electrostatically on a part-time basis for each nucleus while with respect to the Pauli principle they are serving full time.

Proceeding further with the quantum-mechanical justification of the valence rule, one needs next to show why an energy-decrease should occur when atoms or ions so combine that each nucleus becomes surrounded by a "stable configuration." The heteropolar case is fairly well understood. A qualitative understanding also of the energy decrease which occurs in homopolar sharing seems to be obtainable in terms of one-nucleus viewpoints.

8. Cause of homopolar valence forces

London and Heitler concluded that the previously mysterious homopolar valence forces are explained by "resonance" or "exchange" integrals,—like $\mp I_2$ in Eqs. (2), (3) below and similar integrals occurring in the electron-pair case,—which give rise to sharp attractions or repulsions. As will be seen in section 10, these energy integrals correspond to the fact that bonding molecular orbitals give a higher, anti-bonding orbitals a lower, electron density in the regions between nuclei than if they were formed by mere overlapping of the electron densities of the atomic orbitals from which they might be formed. In a certain sense the above simple explanation of the homopolar valence forces is an adequate one. But it is of interest to see if one can go farther in understanding the matter physically by seeking to find reasons *why* these changes in electron density and in energy should occur when molecular orbitals are formed.

The simple case of H_2^+ is instructive.[8] If we let $E.E.$ represent the energy of the electron, taken as zero for $R=\infty$, and $N.E.$ the energy of repulsion of the nuclei, then the energy change as the two H nuclei come together is

$$\Delta E = N.E. + E.E.$$

If $E.E.$ decreases with decreasing R considerably faster than $N.E.$ increases, until R reaches a fairly small equilibrium value, we have a stable molecule (negative ΔE). If it increases, or decreases less rapidly than $N.E.$ increases, we have repulsion. The two states $\sigma 1s$ and $\sigma^* 1s$ of H_2^+ correspond to these two cases. The exchange energies in the two cases are proportional respectively to $-I_2$ and $+I_2$.

The fact that ΔE is negative for $\sigma 1s$ and positive for $\sigma^* 1s$ corresponds to a rapid decrease of $E.E.$ with R for $\sigma 1s$ and a very much less rapid decrease for $\sigma^* 1s$. A good physical reason for this can be seen when we note that as $R \to 0$, the $1s$ atomic orbital of $H+H^+$ must shrink through $\sigma 1s$ to a much

more concentrated $1s$ orbital of the united-atom, while through σ^*1s one reaches $2p\sigma$ of the united-atom, which is of about the same degree of concentration and has the same energy as $1s$ of $H+H^+$.

These considerations suggest that the behavior of bonding molecular orbitals like $\sigma 1s$ of H_2^+ is, qualitatively at least, essentially the result of an increase in effective nuclear charge without change of quantum numbers (no promotion), as R decreases. This effect must of course be intense enough to make ΔE negative in the above equation over a considerable range of R values. The fact that it actually does so for $\sigma 1s$ of H_2^+ could hardly have been predicted from our qualitative explanation, but this does not render the latter invalid, although it does show the superiority of the Heitler-London method for quantitative prediction. With anti-bonding orbitals like σ^*1s, the changed quantum numbers (promotion) more or less neutralize the effect of the increasing effective nuclear charge, thus permitting *N.E.* always to exceed the negative of *E.E.* in the above equation.

A somewhat more complicated case than H_2^+ is that of the N_2^+ molecule (cf. also section 10). The formation of the molecule in its normal state may be expressed as follows:

$$N(1s^2 2s^2 2p^3) + N^+(1s^2 2s^2 2p^2) \rightarrow N_2^+(1s^2 1s^2 \sigma 2s^2 \sigma^* 2s^2 \pi 2p^4 \sigma 2p).$$

If we let $R=\infty \rightarrow R=R_e \rightarrow R=0$ $(N+N^+ \rightarrow N_2^+ \rightarrow Si^+)$, we should probably have[9]

$$N[2s] \rightarrow N_2^+[\sigma 2s] \rightarrow Si^+[2s],\ N[2s] \rightarrow N_2^+[\sigma^* 2s] \rightarrow Si^+[3p(\sigma)],$$
$$N[2p(\sigma)] \rightarrow N_2^+[\sigma 2p] \rightarrow Si^+[3s],\ N[2p(\pi)] \rightarrow N_2^+[\pi 2p] \rightarrow Si^+[2p(\pi)].$$

Here the bonding molecular orbitals $\sigma 2s$ and $\pi 2p$ behave like $\sigma 1s$ of H_2^+ in that they are unpromoted as $R \rightarrow 0$, while the anti-bonding orbital behaves like σ^*1s of H_2^+ in that it is promoted as $R \rightarrow 0$. But $\sigma 2p$, which is promoted as $R \rightarrow 0$, is a bonding orbital, like $\pi 2p$ which is unpromoted. These results indicate that the difference between bonding and anti-bonding orbitals is not simply a difference between an unpromoted and a promoted condition if promotion is defined according to what happens in the united-atom $(R=0)$.

If, however, we *redefine promotion* in terms of the *one-nucleus viewpoints* of the nuclei in the molecule, introducing the new word *"premotion"* in order to avoid misunderstanding, *bonding electrons* are essentially *unpremoted electrons* or (from an energy standpoint) sometimes slightly premoted electrons, while *anti-bonding electrons* are (strongly) *premoted electrons*. A few examples will make clear the exact sense in which premotion is here defined. According to the one-nucleus viewpoint of either of the two N nuclei in N_2^+ (or N_2), the seven (or eight) electrons occupying the bonding molecular orbitals $\sigma 2s$, $\sigma 2p$, and $\pi 2p$ are reckoned as $2s$, $2p\sigma$, and $2p\pi$ electrons, hence all unpremoted; in N_2 they form, from the point of view of each nucleus, a complete, although completely shared, L shell. The anti-bonding σ^*2s molecular electrons, however, must be reckoned as 3-quantum, hence premoted, electrons. In HCl, two bonding electrons may be considered as shared by the

H and Cl nuclei. From the H nucleus viewpoint, these represent $1s^2$, from the viewpoint of the Cl nucleus they are $3p\sigma^2$. But from both viewpoints they are unpremoted in the sense that their quantum numbers are the same as those of electrons already present in the H and Cl atoms. In $PtCl_6^=$ (cf. I), two bonding electrons may be considered as shared between each Cl and the Pt nucleus. From the point of view of each Cl nucleus, the electrons it shares are $3p[\sigma]^2$. From the point of view of the Pt nucleus, the twelve electrons it shares are $5d_\gamma\ {}^46s^2\ 6p^6$, while $5d_\epsilon{}^6$ is also present but unshared. The shared $5d$ and $6s$ electrons are unpremoted, the $6p$ electrons are premoted in the sense that the Pt atom alone, in its normal state, has a configuration $5d^96s$ without $6p$ electrons. But the fact that $6p$ electrons are only a little less easily ionized than $5d$ or $6s$ in the Pt atom makes it possible for the Pt nucleus in $PtCl_6^=$ to use them as bonding electrons of a slightly premoted type.

The results of the preceding paragraphs can be formulated in part as follows. *Chemical combination of the homopolar type is a result of the shrinkage and consequent energy-decrease of atomic orbitals in the fields of neighboring nuclei, when such orbitals are shared with little or no premotion.*

A condition which is necessary for successful sharing is that the binding energy shall not be too different in the atomic orbitals involved. Otherwise the sharing becomes a one-sided affair: either an electron is almost completely transferred from one nucleus to another, or else almost no sharing or transfer at all takes place (cf. Hund[5] for further discussion and details). Polar molecules like Cs^+F^- approximate the former and loosely bound molecules like $Cu(NH_3)_4^{++}$ the latter case; unstable molecules like HeH are extreme examples of the latter case.

9. Valence saturation

The important phenomenon of valence saturation can now be somewhat understood. It should first be pointed out that saturation is usually a relative rather than an absolute matter. Whether an atom or molecule acts in a saturated manner usually depends on the other atoms or molecules with which it is placed in contact, and furthermore it depends very much on circumstances such as temperature, pressure, and presence or absence of light. In practise, however, a molecule is generally considered saturated if it is stable at room temperature in the presence of others of its own kind and of air and diffused sunlight and perhaps of certain common chemicals. With this definition, a given atom can occur in many different saturated molecules.

A state of saturation usually exists when each nucleus in a molecule is surrounded by a set of closed shells which is stable with respect both to gain and to loss of electrons, including gain by sharing. A set of closed shells is stable toward loss of electrons if it has a high ionization potential; toward gain of electrons if a fairly large energy would be required to transfer an electron to an orbital outside the set. Closed shells ending with ns^2np^6, also the shell $1s^2$, usually fulfill both criteria, while closed shells ending with nd^{10}

fulfill neither since the ionization potential is relatively low and the energy of excitation required to get nd^9 $(n+1)s$ is always small, or even negative. Even "stable" closed shells do, however, often take part in further sharing, usually by allowing two of their electrons to be shared by another nucleus (cf. section 4, item 2*b* and the examples of NH_3 combinations cited in section 7). Closed shells ending with ns^2, $n>1$, are relatively stable toward gain of electrons, but not toward loss. Atoms which are surrounded by stable closed shells when alone do not form molecules, because their electrons are too strongly held for either transfer or sharing and at the same time their outer shells contain no vacant places of low energy for receiving transferred or shared electrons. From the preceding discussion it will be seen that the property of saturation is not a property of closed shells as such, but depends on the occurrence of marked energy discontinuities, which often but not always are associated with closed shells.

Electrons are not accepted beyond the point of saturation simply because the unfavorable energy effect corresponding to premotion to a vacant position is greater than the normal favorable energy effect corresponding to sharing without premotion. The quantum-mechanical forces which cause saturated molecules to repel other molecules if they come too close may be described as *premotion forces*. The action of the premotion forces in polyatomic molecules is of the same nature as the anti-bonding action [8,9] of anti-bonding electrons in diatomic molecules.

In diatomic molecules there is sometimes a forced sharing of anti-bonding electrons, incidental to the sharing of bonding electrons, which may be considered as a sort of supersaturation. That is, electrons are included in the molecule in promoted orbits which would not be expected from the valence rule. An example is the N_2 molecule with the electron-configuration $1s^2$ $1s^2$ $\sigma 2s^2$ $\sigma^* 2s^2$ $\pi 2p^4$ $\sigma 2p^2$. From the point of view of each nucleus, that nucleus is surrounded by $1s^2$ unshared, then by $2s^2$ $2p\pi^4$ $2p\sigma^2$ (shared, cf. section 8), forming a complete K and L shell, and in addition by two (partially) premoted electrons probably classifiable as 3-quantum electrons, corresponding to the shared $\sigma^* 2s^2$. The molecule NO is even more supersaturated, by the inclusion of a $\pi^* 2p$ electron in its configuration.[9] This functions very decidedly as a premoted 3-quantum electron from the point of view of one or both nuclei.

More commonly one finds an opposite condition in which nuclei in molecules are surrounded by less than a complete stable shell. This often results from a competition of different nuclei for electrons, or an inability of certain nuclei to share enough electrons to complete the shells of all the other nuclei. Probable or possible examples of nuclei with incomplete outer shells are B in BCl_3, C in $CO_3^=$, N in NO_3^-, S in SO_3 (cf. I).

Comparison of Properties of Molecular Orbitals and Electron-pair Bonds

10. Properties of molecular orbitals

It has been stated in previous sections that the concept of molecular

orbitals possesses all the important properties which make the concept of electron-pair bonds valuable in explaining and predicting molecular structures, and further, is less specialized and so adapted to explain a wider variety of phenomena. The characteristics of the two concepts can be well understood by developing them for the simple molecules H_2^+ and H_2, then generalizing.—The reader should also refer to Hund's valuable discussion[5,6] of molecular orbitals (Hund's concept *c* in reference 5) and their relation to electron-pair bonds (Hund's concept *b*).

Pauling[23] was the first to apply the Heitler-London method, developed originally for H_2 and there yielding among other things the Heitler-London electron-pair bond, to the one-electron molecule H_2^+. Applied to H_2^+, it helps one to understand molecular orbitals. One finds that when $H(1s)$ and H^+ approach, either attraction with formation of normal H_2^+, or repulsion, may occur. The two modes of interaction correspond to the two energetically distinct states one would have for $H(1s)+H^+$ if the two H nuclei were slightly different in charge.

Let the two H nuclei be designated A and B and the corresponding $1s$ atomic orbitals ϕ_A and ϕ_B. The molecular orbitals resulting when H and H^+ are brought together can be expressed in zeroth approximation as follows:

$$\phi_0 = c_0(\phi_A + \phi_B), \qquad \phi_1 = c_1(\phi_A - \phi_B), \tag{1}$$

where the normalizing factors *c* depend on the distance *R* between the nuclei. The energy changes ΔE are in first approximation as follows:[23]

$$\phi_0 : \Delta E = e^2/R + [e^2/(1+S)](-I_1 - I_2) \tag{2}$$

$$\phi_1 : \Delta E = e^2/R + [e^2/(1-S)](-I_1 + I_2). \tag{3}$$

Here

$$I_1 = \int [\phi_B^2/r_A]d\tau, \qquad S = \int \phi_A\phi_B d\tau, \qquad I_2 = \int [\phi_A\phi_B/r_A]d\tau, \tag{4}$$

where r_A is the distance of the electron from nucleus A. The "resonance" term $\mp I_2$ turns the scales in favor of attraction in the case of ϕ_0, of repulsion in that of ϕ_1.

The orbital ϕ_0, whose presence leads to formation of a stable molecule, belongs to the class of bonding orbitals and may in fact be taken as the prototype of these, at least for diatomic molecules with equal nuclei. Similarly ϕ_1 may be taken as a prototype for diatomic anti-bonding orbitals. It will be noted that ϕ_0 is symmetrical in the nuclei while ϕ_1 is antisymmetrical, and that ϕ_0 is nodeless while ϕ_1 has a nodal plane half-way between the nuclei.

The behavior of the ΔE's for ϕ_0 and ϕ_1 (Eqs. 2, 3) is easily understood when one considers the mean charge density $e^2\phi^2$ corresponding to each. One finds

$$\phi_0^2 = c_0^2(\phi_A^2 + \phi_B^2 + 2\phi_A\phi_B), \qquad \phi_1^2 = c_1^2(\phi_A^2 + \phi_B^2 - 2\phi_A\phi_B). \tag{5}$$

[23] L. Pauling, Chem. Rev. 5, 173 (1928).

This shows that $e^2\phi_0^2$ is relatively more concentrated in the region between the nuclei than if one had a mere overlapping of the densities $e^2\phi_A^2$ and $e^2\phi_B^2$, which would give $\frac{1}{2}e^2(\phi_A^2+\phi_B^2)$ for $e^2\phi^2$. On the other hand ϕ_1 is much less concentrated between the nuclei than for a mere overlapping of $e^2\phi_A^2$ and $e^2\phi_B^2$. With mere overlapping of densities, one would have a slight repulsion between H and H^+, corresponding to $e^2/R-e^2I_1$ in Eqs. (2) and (3). It is the added concentration between the nuclei or withdrawal from this region, in ϕ_0 and ϕ_1, which expresses itself in $\mp I_2$ in Eqs. (2) and (3) and is decisive in making ϕ_0 bonding and ϕ_1 anti-bonding.

The above results for molecular orbitals in H_2^+ can be generalized to other molecules. N_2^+, obtained by the union of $N^+(1s^2\ 2s^2\ 2p^2)+N(1s^2\ 2s^2\ 2p^3)$, will serve as an example. Strictly, we should use also a certain admixture of $N^{++}+N^-$, and should consider various excited states of N^++N, but it is unlikely that this would seriously affect the results. Also, it should be noted that in this discussion we are treating the group of three states of N^+ (^3P, ^1D, and ^1S) and of $N(^4S, ^2D, ^2P)$, which arise from the electron configurations mentioned, as if each group were a single state. This is, however, legitimate because of the large energy of formation of N_2^+. N_2^+ in its normal state contains one $\sigma 2p$ electron, which may be considered, approximately at least, as going over on dissociation to a $2p$ atomic orbital of the neutral N atom. This may be on either nucleus A or nucleus B, so one gets approximately

$$\phi_{\sigma 2p} = c(\phi_{A2p} + \phi_{B2p}),$$

where of course it is understood that the $2p$ atomic orbitals are based on a suitable atomic Hartree field. Instead of the bonding orbital $\sigma 2p$, one could also get the anti-bonding orbital σ^*2p, which should occur in some excited, perhaps unstable, state of N_2^+: $\phi_{\sigma^*2p}=c^*(\phi_{A2p}-\phi_{B2p})$. The bonding orbitals $\sigma 2s$ and $\pi 2p$ in N_2^+ could similarly be shown to be capable of being respectively approximated by sums $\phi_A+\phi_B$ made up of atomic $2s$ or $2p$ orbitals, and the anti-bonding orbital σ^*2s could be approximated by a difference $\phi_A-\phi_B$.

Also in *unsymmetrical diatomic molecules*, molecular orbitals can be approximated by linear combinations of atomic orbitals: bonding type, $\phi=a\phi_A+b\phi_B$. In strongly ionic molecules, $a\gg b$ or vice versa. The results stated in this and the preceding paragraph have already been given by Hund[5,6] and need not be further discussed here.

It seems clear that molecular orbitals in polyatomic molecules also can be approximated as linear combinations of atomic orbitals (cf. I for examples), and that bonding orbitals are additive linear combinations. In general, polyatomic bonding orbitals may be expected to surround several nuclei, although in special cases such orbitals may be largely confined to the neighborhood of two nuclei.

11. Maximum overlapping as a criterion of bonding power

It is now of interest to learn how the bonding power of a molecular orbital depends on its form. This can be seen from expressions like that for ϕ_0 in

Eq. (1). Since the lowered energy of bonding orbitals results from the fact that they are relatively concentrated between the nuclei, one readily sees that in order to have the bonding energy as large as possible, products such as $\phi_A\phi_B$ in Eq. (4) should be as large as possible, which is true if the atomic orbitals ϕ_A and ϕ_B overlap as much as possible. This can also be seen directly from the energy equations (cf. Eqs. 2, 4). This is Pauling's and Slater's *criterion of maximum overlapping of atomic orbitals*. The process of applying this criterion to the problem of determining the zeroth approximation atomic orbitals which give *strongest bonding* (Pauling's "best bonding eigenfunctions"), when ϕ_A and (or) ϕ_B belong originally to degenerate orbitals, seems to be the essence of the method used by Slater and Pauling (cf. reference 20, p. 1141).

Slater's and Pauling's original derivations of this criterion from the equations for electron-pair bonds (cf. Eq. (8) and related ΔE equations) give the impression that the existence of the criterion depends on the overlapping of the *orbits* of *two actual electrons*. The present approach shows, however, that the criterion for finding a *best bonding molecular orbital* for a pair of atoms depends only on the overlapping of two atomic orbitals, regardless of whether the resulting molecular orbital is occupied by two electrons, by one electron, or by none; the validity of the procedure, used in the present series, of regarding such an orbital occupied by two electrons as essentially equivalent to an electron-pair bond will be considered shortly.

Furthermore, the present approach shows that the criterion of maximum overlapping is just as applicable to molecular orbitals which are approximate linear combinations of atomic orbitals of several atoms as to those which are formed from orbitals of just two atoms. The present use of molecular orbitals which connect several nuclei is perhaps the most essential difference between the present method and that of Slater and Pauling.

12. Doubly- or multiply-occupied molecular orbitals

In nearly all chemically stable molecules, every bonding molecular orbital which is occupied at all is occupied by the full quota of electrons allowed by the Pauli principle, namely two if the orbital is non-degenerate, $2n$ if it is degenerate and n is the degree of degeneracy. The most important properties of such multiply-occupied bonding orbitals can easily be generalized from a consideration of the doubly-occupied $\sigma 1s$ orbital in normal H_2. Omitting constant factors and spins, the wave function χ for normal H_2 may be approximated by the following expression:

$$\chi = \phi_0(1)\phi_0(2) \tag{6}$$

Eq. (6) implies that the two electrons move entirely independently, in the $\sigma 1s$ orbital, here denoted by ϕ_0; the numbers 1 and 2 refer to the coördinates of the two electrons. This, however, is true only as a rough approximation. Although the agreement of Eq. (6) with the truth can be made rather good by making the best possible choice of the form of ϕ_0,—the simple form given in Eq. (1) can be greatly improved on by adjusting it to correspond

to a one-quantum orbit in a suitable Hartree field,—it can never be made exactly right without adding a correction term. This is necessary in order to take care of detailed effects of the two electrons on each other's motions. The same kind of problem is met with in atomic spectra, for example in the He atom. Eq. (5) is a fairly good approximation for this atom if ϕ_0 is taken to refer to the 1s atomic orbital in a suitable Hartree field.

Slater[24] has found, in a paper preceding the work already referred to above, that if ϕ_0 is approximated by $c_0(\phi_A+\phi_B)$ in accordance with Eq. (1), the corrected expression for χ can be closely approximated by:

$$\chi = a\phi_0(1)\phi_0(2) - b\phi_1(1)\phi_1(2), \tag{7}$$

where ϕ_1 is as given in Eq. (1). For the molecule in its equilibrium condition ($R=R_e$), Slater finds $a/b=8$, approximately; but for a molecule in the process of dissociation ($R\to\infty$), a/b approaches 1. This indicates that Eq. (6), even with ϕ_0 taken as $c_0(\phi_A+\phi_B)$, and of course all the more so if a better ϕ_0 is used, is a good approximation for H_2 in its ordinary stable state.

Reflection indicates that it is safe to generalize the type of approximation contained in Eq. (6) to unsymmetrical and to polyatomic molecules (cf. also reference 5). It even appears that the approximation may often be relatively better for polyatomic molecules than for H_2. Hence the general use of molecular orbitals in describing shared electrons in stable molecules seems to be justified as a good approximation. In the case of chemical bonds with large R and small dissociation energy, however, cases may occur where the use of molecular orbitals as in Eq. (6), although still formally possible, does not constitute a good approximation.

The nature of the correction required in Eq. (6) is somewhat different for the case of H_2 than for that of He, because of the non-centralness of the Hartree field in H_2. The nature of this difference can be seen if we consider what would happen if we increased R to a large value in H_2. One would then find that the molecule would usually be very much like two H atoms with one electron on each, which means that χ would be essentially of the form $\phi_A(1)\phi_B(2)$ or $\phi_A(2)\phi_B(1)$. There would, however, be a small possibility of finding both electrons attached to one H nucleus, in which case χ would be essentially $\phi_A(1)\phi_A(2)$ or $\phi_B(1)\phi_B(2)$, corresponding to H^-+H^+ or $H^+ +H^-$. Returning to $R=R_e$, it would seem reasonable that the true χ should be approximately a linear combination of the four expressions just given.

13. Comparison with Heitler-London electron-pair bond

Heitler and London's original approximation[25] for normal H_2, omitting constant factors, was

$$\chi = \phi_A(1)\phi_B(2) + \phi_A(2)\phi_B(1). \tag{8}$$

[24] J. C. Slater, Phys. Rev. **35**, 514–5 (1930).

[25] W. Heitler and F. London, Zeits. f. Physik **44**, 455 (1927); Y. Sugiura, Zeits. f. Physik **45**, 484 (1927).

This expresses a state of affairs in which if one electron is in ϕ_A, the other is necessarily in ϕ_B. For large R, this would keep the electrons separated, with one near each nucleus, but for $R=R_e$, where ϕ_A and ϕ_B overlap strongly, the effect is much less pronounced.

Slater[24] has found that the true state of H_2 for $R=R_0$ is better expressed by

$$\chi = \alpha[\phi_A(1)\phi_B(2) + \phi_A(2)\phi_B(1)] + \beta[\phi_A(1)\phi_A(2) + \phi_B(1)\phi_B(2)], \quad (9)$$

with α/β roughly equal to 8. [That the ratio α/β here is nearly the same as a/b in Eq. (7) is accidental.] Eq. (9) allows the two electrons to be close together near the same nucleus oftener than Eq. (8) would permit.

Eq. (9) is a step from Eq. (8) toward Eq. (6); Eq. (6) implies that the probability of any stated position for one electron is independent of the position of the other. On the other hand, Eq. (7) is a step from Eq. (6) toward Eq. (8), if ϕ_0 and ϕ_1 are as given in Eq. (1). In fact, Eqs. (7) and (9) become identical if Eq. (1) is used and if the coefficients a, b, α, β, are properly related. Slater (private communication concerning details of Ref. 25) found that for $R=R_e$ in H_2, the ratio of the coefficients c_0 and c_1 in Eq. (1) is about that given by $(c_1/c_0)^2=6.21$. Substituting this, also $a/b=8$, in Eq. (7), the latter reduces to the form of Eq. (9) with $\alpha/\beta=14.21/1.79$, which happens to be very nearly the same as a/b.

Eq. (8) is the expression, in terms of wave functions, of the Heitler-London, Pauling-Slater concept of the electron-pair bond, for the case of H_2. Eq. (6) is the expression in terms of wave functions, for H_2, of the concept of a bonding orbital occupied by two electrons. Slater's Eqs. (7) and (9), in view of his result that a/b and α/β are nearly equal, suggest that the two concepts, while departing from the truth in opposite ways, are about equally good approximations to it in their ability to describe the positions of two equivalent bonding electrons relative to each other and to two nuclei. Other considerations, pro and con, may enter besides the values of the ratios a/b and α/β, and of course such ratios would be different for other examples than H_2, but it seems fairly safe to assume that the molecular orbital concept ordinarily does not give too bad an approximation in its description of the electron positions. We have already seen that in two other important properties,—the fact of concentration between the nuclei and the existence of the criterion of maximum overlapping,—the concept of bonding molecular orbitals gives the same results as that of electron-pair bonds.

For electron-pair bonds, the first of these properties follows if one determines the electron density for a single electron; this is given by $\int\chi^2 d\tau_2$ and comes out proportional to

$$\phi_A^2 + \phi_B^2 + 2S\phi_A\phi_B, \quad (10)$$

where S is as in Eq. (4). The concentration term here is less by a factor S than in Eq. (5). When one takes $\int\chi^2 d\tau_2$ using Eq. (6), however, one gets the same result as is expressed in Eq. (5). The existence of the criterion of maximum overlapping follows in the case of the electron-pair bond by a considera-

tion of the above electron density expression, or of ΔE expressions,[25] in much the same way that it does for bonding orbitals.

It is instructive to compare the application of the method of H.L.P.S. electron-pairs and that of molecular orbitals to molecules which have unequal nuclei and are partly polar, such as LiH, HF or HCl. If one uses electron-pair bonds, one forms a linear combination of polar and electron-pair wave functions:[18]

$$\chi = \alpha[\phi_A(1)\phi_B(2) + \phi_A(2)\phi_B(1)] + \beta\phi_B(1)\phi_B(2), \qquad (11)$$

where B is the more negative atom. Using molecular orbitals, Eq. (6) applies, with

$$\phi_0 = a\phi_A + b\phi_B, \; b > a. \qquad (12)$$

Using Eq. (12), Eq. (6) becomes identical with Eq. (11) if we put $ab=\alpha$, $b^2=\beta$, except that Eq. (6) gives an extra term $a^2\phi_A(1)\phi_A(2)$. This term is relatively unimportant if the molecule is strongly polar; for example if $b=2a$, the coefficient of $\phi_A(1)\phi_A(2)$ is only one fourth that of $\phi_B(1)\phi_B(2)$. As in the case of equal nuclei discussed above, however, the truth must lie between Eq. (11) and Eqs. (6), (12). If both forms represent about equally good approximations, as seems likely, Eq. (6) may well be preferred for many purposes because of its simpler conception and formulation.

Evidence of Space Quantization of Atoms upon Impact

By H. KUHN AND O. OLDENBERG
Zweites Physikalisches Institut, Goettingen, and Physical Research Laboratory, Harvard University

(Received May 16, 1932)

The present paper offers an interpretation of certain diffuse bands observed in the spectra of metal vapors mixed with rare gases. Two separate maxima on the short wave-length side of the resonance line of the metal are not due to vibrational quanta as in the case of other similar diffuse spectra. Instead they are interpreted as separate electronic levels of the pair of colliding atoms described by space quantization taking place in the mutual approach. The diffuse structure on the long wave-length side is due to vibrational quanta of molecules.

I. EXPERIMENTAL FACTS

SEVERAL years ago, some fluorescence experiments were performed,[1] the aim of which was to investigate the interaction in a single elementary process of the three kinds of energy: light, excitation energy, and kinetic energy of atoms. It was expected that an excited atom, when colliding with a rare gas atom, might react in two ways: either it might *split up* its energy of excitation into two parts, radiation and kinetic energy of the two atoms, thus giving rise to a continuous spectrum spreading from the resonance line to the long wave-length side; or instead the kinetic energy of impact might *join* with the excitation energy thus producing radiation that belongs to a continuum on the short wave-length side of the resonance line.[2]

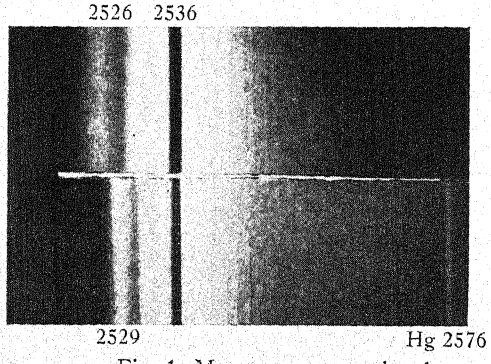


Fig. 1. Mercury—rare gas bands.

In order to check this type of interaction by experiment, the fluorescence radiation of mercury vapor with a large amount of a rare gas added has been investigated. In this experiment, the excited mercury atom has a good chance

[1] O. Oldenberg, Zeits. f. Physik **47**, 184 (1928); **51**, 605 (1928); **55**, 1 (1929).

[2] A theoretical discussion of this process has recently been given by V. Weisskopf, Zeits. f. Physik **75**, 287 (1932) and H. Margenau, Phys. Rev. **40**, 387 (1932).

to collide during its lifetime with a rare gas atom. Actually, continuous spectra have been observed on both sides of the resonance line of mercury. Under most conditions, however, instead of having a uniform distribution of intensity, they showed an unexpected diffuse structure as seen in Fig. 1. (The intense Hg line 2537 itself was taken out of the spectrum by an absorption tube with Hg vapor, in order to prevent scattering of light at the photographic plate.) When A or Kr is added to Hg vapor, two broad diffuse maxima appear at the short wave-length side of the resonance line and a finer diffuse structure on the long wave-length side. Only a trace of structure has been observed in Hg+Ne and no structure in Hg+He or Hg+Xe.

The same type of structure has recently been observed by Krefft and Rompe[3] in mixtures of thallium and other metalic vapors with rare gases. It is of interest that also with He added they obtained two well-defined separate maxima, even broader than with the other rare gases.

II. Criticism of the Interpretation as a Band Spectrum

The fine structure on the long wave-length side has been explained by the formation of molecules from mercury and rare gas atoms. In the fluorescence experiments only the mercury, not the rare gases, was excited. It must be assumed that the excited mercury atom attracts the rare gas atom by the polarization force (cf. section IV). The conspicuous broad maxima on the short wave-length side, however, which present quite a different aspect, have not been explained satisfactorily as yet. In order to interpret them in the usual

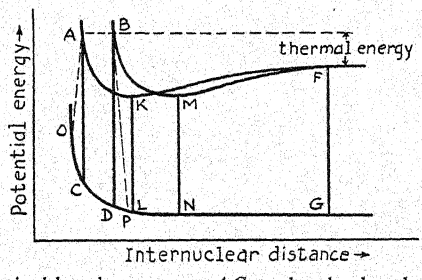


Fig. 2. Hypothetical band structure. *AC*, molecular band; *FG*, atomic line.

way as vibrational quanta of a band, potential curves must be assumed as in Fig. 2. The short wave-length position of the maxima must be represented by a longer vertical distance *AC* than *FG* representing the line emission. It must be assumed that excited molecules with strong vibration combine with normal molecules with no vibration or with just one quantum. It is not evident, however, why the vibration of the *excited* molecules is restricted to such a small range of high energy near *A* that the vibrational structure of the *normal* state comes out clearly.

It has been suggested[4] that the diagram of Fig. 2 does not apply because it fails to represent the *rotational* energy of the molecule, which can exceed

[3] H. Krefft and R. Rompe, Zeits. f. Physik **73**, 681 (1932).
[4] Oldenberg, Zeits. f. Physik **55**, 10 (1929).

considerably the dissociation energy. This argument cannot be maintained because of the selection rule. In the emission process the angular momentum of the molecule changes only by the fundamental unit $h/2\pi$. For heavy molecules as HgA or HgKr this corresponds to such a small change of rotational energy that the single band cannot spread far from its zero line. Hence the rotational energy will not affect the position of the bands to any considerable extent.

These criticisms based on a rather vague argument are strongly supported by the new observations of Krefft and Rompe, who observed the same type of structure with a particularly broad extension in the mixture of Tl vapor and He. The frequency difference between the two maxima is about 500 cm^{-1}, that is of the order of magnitude of the vibrational quantum of a regular molecule.[5] Now it cannot be assumed that the molecule TlHe exists with a considerable energy of dissociation (to be observed as a large quantum of vibration) and that it plays a part in the discharge in 800°C, for the He atom has by far the smallest polarizability[6] of all rare gases (by far the lowest condensation point, the smallest heat of vaporization, the least adsorption). Therefore the type of structure as observed in Tl+He on the short wave-length side of the Tl line must be interpreted by an entirely different process.

III. Radiation during Collision; Space Quantization

It seems that this process can be understood on the basis of the theory of band spectra without an arbitrary hypothesis. It must be assumed that the excess energy of the short wave-length diffuse structure, not explained as dissociation energy of molecules, is due to the kinetic energy of thermal impacts.[7] The mercury atom emits this radiation instead of the sharp resonance line at the moment of a collision with a rare gas atom. This is just the process mentioned above, for the study of which the experimental work was undertaken. This process has been described on the basis of potential curves by Winans and Jablonski.[8] By the same mechanism Weizel[9] recently explained the asymmetric short wave-length broadening of some helium lines discovered by Hopfield.[10] Weizel has succeeded in connecting this broadening with the

[5] The correction discussed by H. Kuhn (Zeits. f. Physik **63**, 458 (1930) and **72**, 462 (1931)) cannot change the order of magnitude of the observed difference, while still discrete maxima of intensity are observed.

[6] J. C. Slater and J. G. Kirkwood, Phys. Rev. **37**, 682 (1931); H. Margenau, Phys. Rev. **37**, 1425 (1931).

[7] From this assumption it follows that Condon's wave-mechanical interpretation of diffuse maxima (Phys. Rev. **32**, 866 (1928)) does not apply to the spectrum under discussion. Condon considered a sharply defined initial state (lowest vibrational level of the upper electronic state) and a final state which belongs to a continuous range. He concluded that diffuse maxima might appear closely connected with the waves representing the motion in the final state. This theory does not apply to the conditions described by Fig. 2, because here the initial state, too, is not sharply defined but is itself diffuse due to the velocity distribution. Moreover the obseved maxima seem to be broader than those described by Condon's theory.

[8] T. G. Winans, Phil. Mag. **7**, 558 (1929). A. Jablonski, Zeits. f. Physik **70**, 723 (1931).

[9] W. Weizel, Phys. Rev. **38**, 642 (1931).

[10] J. J. Hopfield, Astrophys. J. **72**, 133 (1930).

molecular spectrum. Discussing the broadening of the He line 585 on the basis of the theory of band spectra, he finds one potential curve that describes the interaction of two normal He atoms colliding with each other, and four separate curves for an excited 2^1P atom colliding with a normal one. Due to a selection rule only two of these four curves, both representing repulsion, combine with the normal state (Fig. 3).

It can be assumed that in the normal state the Hg atom has a smaller effective cross section than in the excited state. Hence in the diagram the potential curve of the normal state remains flat even for a small internuclear distance. Thus the kinetic energy of the collision—at the very moment in which it is turned into potential energy (*A* in Fig. 3)—takes part in radiating a larger quantum *AC* than the excited atom would radiate by itself (*FG*). The superimposed effect of the two potential curves of the upper state is observed as pressure broadening of the atomic line.

In the present problem—mercury with an added rare gas—the interaction of the two atoms is simpler because they are different from one another. In

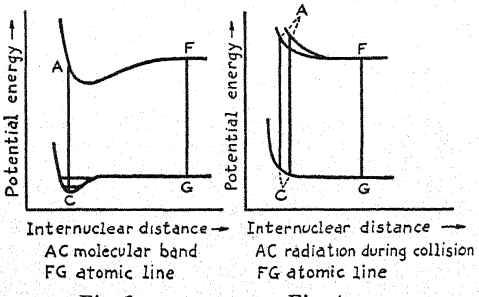


Fig. 3 Fig. 4

Fig. 3. Radiation during collision. *AC*, radiation during collision; *FG*, atomic line.

Fig. 4. Potential curves for the mercury and rare gas collision. *AC*, *BD*, diffuse maxima on the short wave-length side; *AQ*, *BP*, limits of the spectrum; *KL*, *MN* band structure on the long wave-length side; *FG*, atomic line.

the normal state of the two atoms again only one potential curve exists (representing an $^1\Sigma$ term), because both the mercury and the rare gas atom have spherical symmetry in their normal ^1S states. In the upper state (excited atom+normal rare gas atom) the method of counting the molecular electronic levels, given by Hund,[11] depends upon the coupling. In Weizel's problem (He′+He) the multiplet structure (due to the interaction between the orbital momentum and the spin) is narrow as compared with the extension of the continuous spectrum (due to the interaction between the colliding atoms); this interaction between the atoms is described as a quantized orientation of the *orbital momentum* with regard to the internuclear axis. In the present problem, however, it must be taken into account that the splitting up of the multiplet structure in the mercury or thallium atom is much larger than the extension of the diffuse molecular spectrum under consideration. Hence the interaction between the orbital momentum and the spin is large

[11] F. Hund, Zeits. f. Physik **36**, 659 (1926).

as compared with the interaction between the two colliding atoms and a quantized orientation of the *total angular momentum* of the Hg or Tl atom is to be expected with regard to the internuclear axis, just as in the case of a Stark effect in a weak electric field. The number of separate energy levels of the Hg′ or Tl′ colliding with a normal rare gas atom is given by the number of terms in the series $j, j-1 \cdots, 0$ or $\frac{1}{2}$. (Negative values of j describe another orientation but give the same energy levels as the positive values of j).[12] This argument leads to the conclusion that in the upper state $Hg'(2^3P_1)$ + rare gas (^1S) two molecular levels exist, given by $j=1$ and $j=0$, represented in the diagram by two separate potential curves. From both excited levels the transitions to the normal level are allowed. (As in general the collision will not be head on, a rotation will be superimposed with a constant angular momentum.)

Along one or the other of these curves the rare gas atoms and the mercury atoms will approach each other to a certain range of potential energy A or B determined by the thermal energy.

The effective cross section of the Hg atoms in the normal state will be supposed to be smaller than in the excited state. Hence the lowest potential curve of Fig. 4 representing the normal state will just barely begin to rise for the values of nuclear distance that belong to A and B. Therefore both transitions AC and BD, that are vertical in the diagram—following the Franck-Condon rule—represent radiations of larger energy or shorter wave-length than the atomic line FG, BD shifted by a larger amount than AC. This reasoning leads to two separate diffuse maxima on the short wave-length side of the atomic line, both of them shifted by an amount smaller than the mean kinetic energy of the collisions. This just describes the observed spectra. The two separate maxima are interpreted not by the vibration of a molecule but by two separate electronic levels of a pair of atoms to be described by two separate directions of mutual approach, both of them belonging to the same electronic levels of the atoms. Thus the separate maxima give evidence of space quantization in the collision between atoms. This interpretation is strongly supported by the fact that the two separate maxima persist at high temperature (cf. section IV).

The diffuse bands show a rather sharp limit on the short wave-length side and in some cases a much longer diffuse extension to long wave-lengths. This may be understood, too, on the basis of the potential curve diagram (Fig. 4). The dotted lines represent transitions in the case of a small change of internuclear distance during radiation. The long distance BP, representing radiation of short wave-length, cannot be much longer than BD, representing the most probable transition from B. AQ, however, representing the long wave-length extension, can be considerably shorter than AC due to the steep branch of the lower potential curve.[13]

[12] Cf. W. Pauli, Handbuch d. Physik XXIII, p. 246.

[13] The extension to long waves plays the major part in the absorption experiments. at high pressures of Füchtbauer, Joos and Dinckelacker (Ann. d. Physik **71**, 204, (1923)) and Bonhoeffer's and Reichardt's experiments with Hg dissolved in liquids (Zeits. f. Physik **67**, 780 (1931)).

The appearance of the same diffuse structure in the *absorption* spectrum will be explained by the inverse process, the absorption being produced by a mercury atom at the moment of a collision with a rare gas atom.

That these *separate* maxima were not observed by Hopfield in the spectrum of helium, was probably due to their position in the extreme ultraviolet, where the resolution of the same differences in frequency is much more difficult.

The diffuse maxima, reported by Krefft and Rompe in thallium vapor with an added rare gas near the green thallium line $2^2S_{1/2}-2^2P_{3/2}$, are explained by separate molecular levels ($j=\pm 3/2$ and $\pm 1/2$) belonging to the *lower* atomic level instead of the upper one. All other observations, too, can be interpreted on the same basis. One cannot expect, however, to observe separate maxima in every case, for which they are derived from the theory, because they may overlap too much. This is evidently the case in Hg+He, where the existence of two maxima can only be deduced by analogy with the other rare gases.

IV. Quantized Molecules Formed of Excited Mercury and Rare Gas Atoms

This explanation does not take into account the finer diffuse structure on the long wave-length side of the atomic line (Fig. 1). Its previous interpretation as oscillation quanta of a molecule will be maintained.[14] The simple structure and its position on the long wave-length side is most easily explained—contrary to the explanation published previously—by the formation of molecules of Hg atoms in their *excited* state with rare gas atoms. One expects the excited Hg atom to be able to induce an electric moment in the rare gas atom and thus by polarization form a loosely bound molecule. The normal Hg will have this power to a smaller extent because it has a high symmetry similar to that of a rare gas atom. Therefore the upper potential curves of Fig. 4 ought to show shallow minima for large values of the internuclear distance, for which the lower curve is approximately flat. This type of excited molecule would emit a diffuse band on the long wave-length side of the atomic line, in which the vibrational quanta still might be distinguished.

Hence this band system is explained by a group of vibrational levels in the *upper* electronic state combining with a lower state in which vibrational levels can not be resolved. It has been described as an apparently simple set of bands with a trace of convergence to the long wave-length side; it has been mentioned, however, that possibly the observed set of bands is due to the superposition of several sets. According to the present interpretation, two simple sets of bands (*KL* and *MN*, Fig. 4) belonging to the two upper potential curves should be superimposed. The smaller slope of the potential curve of the normal state might modify the position of the observed bands. Therefore no conclusion can be drawn concerning the convergence from the structure as shown in Fig. 1.

[14] Cf. F. London, Zeits. f. Physik **11**, 248 (1931).

This interpretation of the diffuse structure on the long wave-length side as vibrational quanta of a band system is supported by observations. This structure does not appear for the light atoms He and Ne, which—due to their smaller polarizability—might not form molecules. (It remains uncertain if this type of structure exists for Hg+X. The pictures with Xenon were taken with a quartz bulb of a few millimeter diameter, from which the scattered light was so strong that the structure might have been concealed.) At high temperature the fine structure on the long wave-length side disappears, while the broad maxima on the short wave-length side remain (observed in Hg+A). This is understood as the complete dissociation by heat; in these circumstances there will remain only the broad maxima on the short wave-length side that are explained not by vibrations of molecules but by separate electronic levels of a pair of colliding atoms.

V. Conclusion

We come to the conclusion that three different processes are to be distinguished in the collision of Hg′ with a rare gas atom. In most cases the atoms will separate without any effect, leaving the Hg′ such that it radiates its sharp atomic line (*FG* in Fig. 4). This may be the most probable process. In some other cases the radiation will take place in the moment of the collision giving rise to the broad maxima on the short wave-length side of the atomic line (*AC* and *BD* in Fig. 4). Finally in a few cases, if the temperature is not too high, some energy may be taken away in a triple collision;[15] real excited molecules with vibrational quanta will be produced emitting a band spectrum (*KL* and *MN* in Fig. 4).

The diffuse maxima in the fluorescence radiation of mercury vapor with a rare gas added are surprisingly intense. The corresponding spectra in the neighborhood of some other lines, for instance the *D* lines of Na, are much fainter or missing entirely. This leads to the question, whether in some atomic terms, but not in all of them, the collision process might produce an instantaneous increase in the probability of emission. This problem will be further investigated.

According to the present interpretation, the main conclusion is that the two separate maxima of intensity, observed in the spectra of certain metal vapors mixed with rare gases, furnish evidence that the mutual approach of these atoms can be described by space quantization.

[15] M. Born and J. Franck, Ann. d. Physik **76**, 225 (1925).

The Equation of State of a Non-ideal Einstein-Bose or Fermi-Dirac Gas

By G. E. UHLENBECK AND L. GROPPER
University of Michigan

(Received May 25, 1932)

With regard to the question if from isotherm measurements one can obtain an experimental test for the existence of Bose statistics in real gases, as is required by theory, we prove the following general theorem. The "Zustandsumme" of a non-ideal Bose or Fermi gas is given by the classical integral provided one replaces the Boltzmann $\exp(-\phi_{ij}/kT)$ factor by:

$$e^{-\phi_{ij}/kT}(1 \pm \exp\left[-4\pi^2 mkTr_{ij}^2/h^2\right] \tag{1}$$

for each pair of molecules (ij). For the second virial coefficient B, this has, i.e., in a Bose gas, as a consequence that:

$$B = B_{\text{non-ideal class}} + B_{\text{ideal Bose}} + B' \tag{2}$$

where:

$$B' = 2\pi N \int_0^\infty drr^2(1 - e^{-\phi(r)/kT}) \exp\left[-4\pi^2 mkTr^2/h^2\right]. \tag{3}$$

Only at very low temperatures do the last two terms in (2) become appreciable. They are then of the same order of magnitude, but have opposite signs. Due to this fact, due to the lack of precise knowledge of the molecular forces, and due to the absence of accurate measurements of B at very low temperatures, one can as yet not decide from isotherm measurements alone whether or not real gases obey the Bose statistics.

I. INTRODUCTION

1.

AS IS well known, it has been proved from the fact that electrons and protons obey the Fermi-Dirac (F.D.) statistics, that a gas consisting of particles of even charge obeys the Einstein-Bose (E.B.) statistics.[1] A neutral gas, for example helium, is a special case of this. The question therefore becomes very important, if one could for example verify this theoretical prediction from equation of state measurements, in particular from the experimentally determined values of the second virial coefficient B.

The theoretical expression B_{cl}, for a *non-ideal* gas, obeying *Boltzmann* statistics is, as is well known:[2]

$$B_{\text{cl}} = 2\pi N \int_0^\infty drr^2(1 - e^{-\phi(r)/kT}) \tag{1}$$

N is the number of molecules per mol. It is here assumed that the intermolecular forces are radial and have the potential $\phi(r)$.

The expression $B_{E.B.}$ or $B_{F.D.}$ for an *ideal* gas obeying Einstein-Bose or Fermi-Dirac statistics, is:

[1] E. Wigner, Sitzungsber. der Ungarischen Acad. 1928, p. 1; P. Ehrenfest and J. R. Oppenheimer, Phys. Rev. **37**, 333 (1931).

[2] See e.g., R. H. Fowler, Statistical Mechanics, Ch. VIII.

$$\left.\begin{matrix} B_{E.B.} \\ B_{F.D.} \end{matrix}\right\} = \mp \frac{1}{2^4}\left(\frac{h^2}{\pi mkT}\right)^{3/2} N \tag{2}$$

In the recent work on the quantum theory of the equation of state of real gases (London, Slater, Kirkwood, Keyes, Margenau) one has made only use of (1), introducing for $\phi(r)$ the theoretical expression obtained from a generalized Heitler-London calculation.[3] The reason that (2) was neglected is, that only at very low temperatures (say below 20°) it becomes appreciable, and *because it was always assumed that the B for a non-ideal Bose gas was the sum of* (1) *and* (2).

We wish to show in this paper that this additivity is not strictly true, but that in addition there occurs a term due to the interaction between the *Boseness* and the non-ideality of the gas. We get for a non-ideal Bose gas:

$$B = B_{\text{cl}} + B_{E.B.} + B'_{E.B.} \tag{3}$$

where:

$$B'_{E.B.} = 2\pi N \int_0^\infty drr^2(1 - e^{-\phi(r)/kT})\exp\left[-4\pi^2 mkTr^2/h^2\right] \tag{4}$$

2. The proof of (3) and (4) rests upon a kind of generalization of the exp $(-V/kT)$ theorem of Boltzmann for an E.B. or F.D. gas. Recently Slater[4] has pointed out the analogue of this fundamental theorem in the quantum theory. He remarked that quantum mechanically, due to the orthogonality and normalization of the wave functions ψ_n belonging to the energy values E_n, the *Zustandssumme* S_Q may be written:

$$S_Q = \sum_n G_n e^{-E_n/kT} = \int \cdots \int dx_1 \cdots dx_N \sum_n e^{-E_n/kT}\psi_n{}^2. \tag{5}$$

In *Boltzmann-statistics* for a given E_n *all* the G_n linearly independent wave functions ψ_n belonging to it, are allowed, and must therefore occur in the sum,[5] so that the G_n does not explicitly appear any more. In *Bose statistics* the $G_n = 1$, because only those E_n are allowed, to which belong the symmetric wave functions, and only these have therefore to occur in the sum. Similarly in the *F.D. statistics* we have the E_n to which the antisymmetric functions belong. Hereafter we will distinguish between these three cases by writing S_{QB}, $S_{QE.B.}$, $S_{QF.D.}$.

Slater compares (5) now with the classical "Zustandsintegral" after integration over the momenta:

[3] F. London, Zeits. f. Physik **63**, 245 (1930); Zeits. f. phys. Chem. B. **11**, 222 (1930). J. C. Slater, Phys. Rev. **32**, 349 (1928); J. C. Slater and J. G. Kirkwood, Phys. Rev. **37**, 682 (1931). H. Margenau, Phys. Rev. **36**, 1782 (1930); **37**, 1014, 1425 (1931); **38**, 747, 1785 (1931); Proc. Nat. Acad. **18**, 56, 230 (1932). J. G. Kirkwood and F. G. Keyes, Phys. Rev. **37**, 832; **38**, 576 (1931). J. G. Kirkwood, Phys. Zeits. **33**, 39 (1932). One has made small corrections in (1), though, to allow for the existence of discrete states (formation of polarization molecules).

[4] J. C. Slater, Phys. Rev. **38**, 237 (1931).

[5] Comp. P. Ehrenfest and G. E. Uhlenbeck, Zeits. f. Physik **41**, 24 (1927).

$$S_{\text{Cl}} = \left(\frac{2\pi mkT}{h^2}\right)^{3N/2} \int \cdots \int e^{-V/kT} dx_1 \cdots dz_N \tag{6}$$

where $V(x_1 \cdots z_N)$ is the total potential energy due to the intramolecular forces and eventually also due to external forces.

One might expect from the correspondence principle that for sufficient high temperatures where the influence of the discreteness of the translational energy levels can be neglected with respect to the influence of the intermolecular forces (which is already the case, excluding the electron gas, say for $T > 1°$ absolute)[6]

$$\sum_n {}_{B.} e^{-E_n/kT} \psi_n{}^2 \underset{(T>1°)}{\rightarrow} \left(\frac{2\pi mkT}{h^2}\right)^{3N/2} e^{-V/kT}. \tag{7}$$

Slater makes this also plausible from the meaning of $\psi_n{}^2$ as a probability density. In Chapter III we will give an analytical proof. This gives the justification even in the quantum theory for the use of (6) in the case of a Boltzmann gas.

For the case of a E.B. or F.D. gas we will prove a theorem analogous to (7):

$$\left.\begin{array}{l} \sum_n {}_{E.B.} e^{-E_n/kT} \psi_n{}^2 \\ \sum_n {}_{F.D.} e^{-E_n/kT} \psi_n{}^2 \end{array}\right\} \underset{(T>1°)}{\rightarrow} \frac{1}{N!}\left(\frac{2\pi mkT}{h^2}\right)^{3N/2} e^{-V/kT} \times \prod_{ij} (1 \pm \exp\left[-4\pi^2 mkT r_{ij}{}^2/h^2\right] \tag{8}$$

where the product has to be taken over all pairs of molecules, and r_{ij} is the distance between the (ij) pair. This again holds as indicated for temperatures so high that the influence of the discreteness of the translational energy levels is negligible, but not yet so high that the deviations due to the E.B. or F.D. statistics from the classical gas laws can be neglected. These are given by (8) in *first* approximation; in addition therefore the volume must not be too small. One sees from (8) that there is an apparent attractive force in the E.B. gas between each pair of molecules with the potential:

$$\phi' = -kT \log \left\{1 + e^{-4\pi^2 mkT/h^2 r^2}\right\} \tag{9}$$

Of course for temperatures so high that the deviations due to E.B. or F.D. statistics can be neglected compared to the non-ideality of the gas (T, say for He, $> 20°$ absolute) (8) goes over into (7).

3. Because the total potential energy V (in absence of external fields) can be written in the form:

$$V = \sum_{ij} \phi(r_{ij})$$

(8) can by using (9) be put in the form,

$$\sum {}_{E.B.} = \frac{1}{N!}\left(\frac{2\pi mkT}{h^2}\right)^{3N/2} \prod_{ij} e^{-(\phi_{ij}+(\phi_{ij}')/kT}. \tag{8a}$$

[6] We will distinguish the integrands of S_{QB}, $S_{QE.B}$ by subscripts $B, E.B.$ etc. and sometimes write for the sums simply Σ_B, $\Sigma_{E.B.}$ etc.

Exactly as (7) is carried through by way of (6) to give (1), so (8a) is carried through and will give again (1) when we replace there ϕ by $\phi+\phi'$. Introducing then the value of ϕ' we immediately obtain (3) and (4).

To obtain an idea of the contribution of $B_{E.B.}'$ to the second virial coefficient, we have made in the case of helium a graphical integration, introducing for $\phi(r)$ the theoretical expression used by Kirkwood and Keyes, and the slightly different one proposed by Margenau, as well as the half empirical one calculated by Lennard-Jones.[7] We got:

$$a. \qquad T = 20^\circ : B_{E.B.} = -0{\cdot}8 \quad B'_{E.B.} \cong +1{\cdot}2$$

$$b. \qquad T = 5^\circ : \quad B_{E.B.} = -6{\cdot}4 \quad B'_{E.B.} \cong +5.4.$$

We see therefore that $B_{E.B.}$ and $B_{E.B.}'$ are of opposite sign and of the same order of magnitude at these low temperatures. At higher temperatures of course both go to zero rapidly. It is clear therefore that because of this fact, it will be still more difficult to decide from the experimentally determined B values at low temperatures, between the classical and the E.B. statistics. In fact, with the uncertainties still existing at present, both in the theory of the intermolecular potential $\phi(r)$ and in the experimental material, in spite of the rather great accuracy and extent of the latter,[8] it seems to us rather hopeless to try to make this distinction with this method.

Quite analogous results are obtained for the F.D. statistics, the signs being merely reversed,

$$B_{F.D.} = -B_{E.B} \quad B'_{F.D.} = -B'_{E.B.}$$

so that also the existence of the F.D. statistics may not be ruled out.

II. A New Treatment of the Ideal Gas

4. In order to prove (7) and (8), it will be convenient to show it first in the case of the ideal gas, because as we will see in Chapter III, the proof for the general case can be made to rest upon the evaluation of the sum for the ideal gas. Consider first as the simplest case two atoms in a one-dimensional box of length L.

a. With Boltzmann statistics we have to take *all* linearly independent wave functions belonging to each energy value, and we get therefore for the sum:

$$\begin{aligned}\sum_B &= \frac{4}{L^2}\sum_{n_1\geqq n_2}\sum e^{-\alpha\pi^2/L^2(n_1^2+n_2^2)}\left(\tfrac{1}{2}\right)^{\delta_{n_1n_2}}\left\{\sin^2\frac{n_1\pi x_1}{L}\sin^2\frac{n_2\pi x_2}{L}\right.\\ &\left.+\sin^2\frac{n_1\pi x_2}{L}\sin^2\frac{n_2\pi x_1}{L}\right\}\\ &= \frac{4}{L^2}\sum_{n_1=0}^{\infty}\sum_{n_2=0}^{\infty}e^{-\alpha\pi^2/L^2(n_1^2+n_2^2)}\sin^2\frac{n_1\pi x_1}{L}\sin^2\frac{n_2\pi x_2}{L}\end{aligned} \tag{10}$$

[7] Comp. R. H. Fowler, Statistical Mechanics, Ch. X.
[8] Comp. G. P. Nijhoff, Dissertation Leiden, 1928.

$$= \left[\frac{2}{L}\sum_{n_1} e^{-\alpha\pi^2/L^2 n_1^2}\sin^2\frac{n_1\pi x_1}{L}\right]\cdot\left[\frac{2}{L}\sum_{n_2} e^{-\alpha\pi^2/L^2 n_2^2}\sin^2\frac{n_2\pi x_2}{L}\right]$$

where:

$$\alpha = h^2/8\pi^2 mkT$$

In the neighborhood of zero values of x_1 and x_2 we may replace the sums by integrals and obtain:

$$\sum_B \cong \frac{2\pi mkT}{h^2}(1 - e^{-x_1^2/\alpha})(1 - e^{-x_2^2/\alpha}). \tag{11}$$

From the symmetry of the problem it is clear that for x_1 and x_2 in the neighborhood of L we have an analogous expression replacing x_1 and x_2 in (11) by $L-x_1$ and $L-x_2$. We see therefore that Σ_B is zero at the boundary of the square $OABC$ and rises rapidly from all sides to the value $2\pi mkT/h^2$. In the center the wave functions in (10) will average out, because of their different

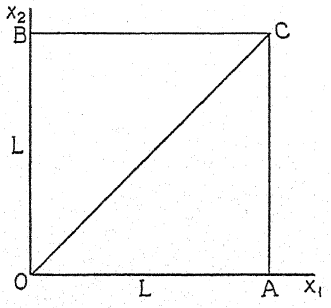


Fig. 1.

phases. Replacing them by the average value 1/4 and the rest of the sum by the integral, (10) again becomes $2\pi mkT/h^2$, so that Σ_B remains constant throughout in accordance with (7). As we will see in §5, the exponentials in (11) account for the correction due to the discreteness of the energy levels.

b. With E.B. or F.D. statistics we get:

$$\left.\begin{matrix}\sum_{E.B.}\\ \sum_{F.D.}\end{matrix}\right\} = \frac{2}{L^2}\sum_{n_1\geqq n_2}\sum e^{-\alpha\pi^2/L^2(n_1^2+n_2^2)}\left(\tfrac{1}{2}\right)^{\delta_{n_1 n_2}}\left\{\sin\frac{n_1\pi x_1}{L}\sin\frac{n_2\pi x_2}{L} \pm \sin\frac{n_1\pi x_2}{L}\sin\frac{n_2\pi x_1}{L}\right\}^2. \tag{12}$$

We see that OC is for each term of the sum a symmetry line; in the F.D. case it is a zero line, in the E.B. case a maximum line. This will therefore also be the case for the total sum. We get working the bracket out and going over from the double sum to products of single sums as in *a*:

$$\left.\begin{matrix}\sum_{E.B.}\\ \sum_{F.D.}\end{matrix}\right\} = \tfrac{1}{2}\sum_B \pm \frac{1}{2L^2}\left[\sum_{n=0}^{\infty} e^{-\alpha\pi^2/L^2 n^2}\left\{\cos\frac{n\pi}{L}(x_1 - x_2) - \cos\frac{n\pi}{L}(x_1 + x_2)\right\}\right]^2. \tag{13}$$

All the terms in the first sum of the bracket are in phase along the line $x_1 = x_2$, whereas the second sum has a value only in the corners O and C; in the rest of the square the second cos averages out to zero. Therefore we can neglect the second sum with respect to the first sum. Neglecting also the exponentials in Σ_B (this can really only be justified for N particles, see §5) and replacing the sum by an integral, we get:

$$\left.\begin{matrix}\sum_{E.B.}\\ \sum_{F.D.}\end{matrix}\right\} = \frac{1}{2}\cdot\frac{2\pi mkT}{h^2}\left\{1 \pm e^{-\frac{1}{2\alpha}(x_1-x_2)^2}\right\}. \tag{14}$$

This is in accordance with (8). We have therefore practically everywhere half the classical value; only along OC it rises in the E.B. statistics sharply to the classical value, and in the F.D. statistics it decreases equally sharp to zero.

5.

Going over now to N particles in a one-dimensional box of length L, we have:

a. for Boltzmann statistics:

$$\sum_B \cong \left(\frac{2\pi mkT}{h^2}\right)^{N/2} \prod_{i=1}^{N}(1 - e^{-x_i^2/\alpha}). \tag{15}$$

This is clearly (11) extended to N particles. From this follows the free energy ψ, according to:

$$e^{-\psi/kT} = \int_0^L \cdots \int dx_1 \cdots dx_N \sum_B. \tag{16}$$

Of course one must remember that (15) holds only for every x_i between 0 and $\frac{1}{2}L$, and that for the other half we have an analogous expression replacing x_i by $L - x_i$. Because of this symmetry we can write Eq. (16):

$$e^{-\psi/kT} = \left(\frac{2\pi mkT}{h^2}\right)^{N/2} \cdot 2^N \int_0^{L/2} \cdots \int dx_1 \cdots dx_N \prod_i (1 - e^{-x_i^2/\alpha}).$$

Of all the terms in the product we need only those which after integration give terms proportional to L^N and L^{N-1}; because we are only interested in the second virial coefficient. We then obtain:

$$e^{-\psi/kT} = \left(\frac{2\pi mkT}{h^2}\right)^{N/2} V^N \left[1 - \frac{N}{V}\left(\frac{h^2}{8\pi mkT}\right)^{1/2}\right] \tag{17}$$

writing V for L now. This gives for the pressure:

$$p = -\frac{\partial\psi}{\partial V} = \frac{NkT}{V}\left[1 + \frac{1}{V}\cdot\frac{1}{2^{3/2}}\left(\frac{h^2}{\pi mkT}\right)^{1/2}\right]. \tag{18}$$

This agrees with the result obtained by the direct calculation of the Zustandssumme.[9] The second term gives the correction due to the discreteness of the

[9] For a gas of N particles in a n-dimensional vessel this gives:

$$p = \frac{NkT}{V}\left[1 + \frac{1}{2^{3/2}}\frac{1}{V^{1/n}}\left(\frac{h^2}{\pi mkT}\right)^{1/2}\right]$$

energy levels. This correction is *independent of* N, in contrast to the correction due to the E.B. or F.D. statistics which are *proportional to* N. For this reason the above correction is completely negligible. *Because it arises from the exponentials in* (15) *we will from now on neglect these.*

b. For E.B. or F.D. statistics we get for the sum:

$$\left.\begin{matrix}\sum_{E.B.}\\ \sum_{F.D.}\end{matrix}\right\} = \frac{2^N}{L^N}\frac{1}{N!}\sum_{n_1\geqq n_2\geqq\cdots n_N}\sum\cdots\sum e^{-\alpha\pi^2/L^2(n_1^2+\cdots n_N^2)}g_{n_1\cdots n_N}$$
$$\left[\sum_P{}^{+1}_{(-1)^P}\sin\frac{n_1\pi x_1}{L}\cdots\sin\frac{n_N\pi x_N}{L}\right]^2 \tag{19}$$

where the sum goes over all permutations of the x_i keeping the quantum numbers fixed. The factor $g_{n_1\ldots n_N}$ is one, when all the n_i are different; is $\frac{1}{2!}$ when two are the same and the other different; $\frac{1}{3!}$ when three are the same, etc. When we work the square out we get first of all the square terms, which are just the Boltzmann terms evaluated in *a*. From the rest of the terms we must select only those which after integration over x_i will give terms proportional to L^{N-1}. One can easily convince oneself that these terms are of the type:

$$\sin\frac{n_1\pi x_i}{L}\sin\frac{n_1\pi x_j}{L}\sin\frac{n_2\pi x_i}{L}\sin\frac{n_2\pi x_j}{L}\cdot\begin{cases}\sin^2\frac{n_3\pi x_1}{L}\sin^2\frac{n_4\pi x_2}{L}\cdots\\ \sin^2\frac{n_3\pi x_2}{L}\sin^2\frac{n_4\pi x_1}{L}\cdots\\ \cdots\cdots\cdots\end{cases} \tag{20}$$

As in §4 we write for the first four sin:

$$\tfrac{1}{4}\left[\cos\frac{n_1\pi}{L}(x_i-x_j)-\cos\frac{n_1\pi}{L}(x_i+x_j)\right]\times$$
$$\left[\cos\frac{n_2\pi}{L}(x_i-x_j)-\cos\frac{n_2\pi}{L}(x_i+x_j)\right].$$

For the same reason as in §4 we may neglect again the cos of the sum x_i+x_j. Going over from the multiple sum to products of single sums, and replacing the sums by integrals, we get:

$$\left.\begin{matrix}\sum_{E.B.}\\ \sum_{F.D.}\end{matrix}\right\} \cong \frac{1}{N!}\left(\frac{2\pi mkT}{h^2}\right)^{N/2}\left[1\pm\frac{1}{L^2}\cdot\frac{h^2}{2\pi mkT}\times\right.$$
$$\left.\sum_{ij}\left\{\int_0^\infty e^{-\alpha\pi^2/L^2n^2}\cos\frac{n\pi}{L}(x_i-x_j)dn\right\}^2\right]$$
$$\cong\frac{1}{N!}\left(\frac{2\pi mkT}{h^2}\right)^{N/2}\left[1\pm\sum_{ij}e^{-(x_i-x_j)^2/2\alpha}\right] \tag{21}$$
$$\cong\frac{1}{N!}\left(\frac{2\pi mkT}{h^2}\right)^{N/2}\prod_{ij}\left\{1\pm e^{-(x_i-x_j)^2/2\alpha}\right\}.$$

The sum and product are to be taken over all pairs. The last two lines differ only in terms which after integration over x_i give terms proportional to powers of L lower than $N-1$, and therefore they have been neglected. Formula (21) agrees with (8), when we put there $V=0$.

To check (21) further we may calculate the free energy. One obtains:

$$e^{-\psi/kT} = \int_0^L \cdots \int dx_1 \cdots dx_N \begin{Bmatrix} \sum_{E.B.} \\ \sum_{F.D.} \end{Bmatrix}$$
$$= \frac{1}{N!}\left(\frac{2\pi mkT}{h^2}\right)^{N/2} V^N \left[1 \pm \frac{1}{V}\,\frac{N(N-1)}{2}\left(\frac{h^2}{4\pi mkT}\right)^{1/2}\right]$$

where again we write V for L. Neglecting the 1 with respect to N, we get for the pressure:

$$p = -\frac{\partial \psi}{\partial V} = \frac{NkT}{V}\left[1 \mp \frac{N}{V}\cdot\frac{1}{2^2}\left(\frac{h^2}{\pi mkT}\right)^{1/2}\right] \tag{22}$$

which agrees with well known results.[10] Comparing (15) and (21), and their consequences (18) and (22) resp. one sees that the reason why the E.B. or F.D. correction has the factor N, in contrast to the discreteness correction, is simply that the number of pairs, which one can form with N objects (x_i), is $\frac{1}{2}N(N-1)$.

These considerations can immediately be extended to a gas in a three-dimensional rectangular vessel. One obtains then instead of (21):

$$\begin{Bmatrix} \sum_{E.B.} \\ \sum_{F.D.} \end{Bmatrix} = \frac{1}{N!}\left(\frac{2\pi mkT}{h^2}\right)^{3N/2} \prod_{ij}\left(1 \pm e^{-(1/2\alpha)\{(x_i-x_j)^2+(y_i-y_j)^2+(z_i-z_j)^2\}}\right) \tag{21a}$$

so that one sees that the apparent potential due to the Bose-ness is radial (see Eq. (9)).

III. The Non-Ideal E.B. or F.D. Gas

§6.

The wave equation for the whole gas we write as:

$$(H - E)\psi = 0$$

where:

$$\left.\begin{aligned} H &= \sum_i \frac{1}{2m}(p_{xi}^2 + p_{yi}^2 + p_{zi}^2) + V(x_1 \cdots z_n) \\ V &= \sum_{ij}\phi_{ij} + \sum_i \pi_i \end{aligned}\right\} \tag{23}$$

where ϕ_{ij} is the interaction potential between the particles and π_i an eventual external potential. We shall abbreviate always all the coordinates by q and all the quantum numbers by n. We wish to show in this paragraph that:

[10] For an E.B. or F.D. gas in an n-dimensional vessel one finds according to the usual method:

$$p = \frac{NkT}{V}\left[1 \mp \frac{1}{2^{n+1}}\left(\frac{h^2}{\pi mkT}\right)^{n/2}\frac{N}{V}\right].$$

$$\sum_n e^{-E_n/kT}\psi_n^2 = \sum_n \phi_n e^{-H/kT}\phi_n. \tag{24}$$

In the right-hand side H is to be considered as an operator working on ϕ_n, which are the normalized eigenfunctions for the *ideal* gas.[11] Formula (24) is true *regardless of the statistics*, that is to say, it holds equally well when we take on both sides only the symmetric wave functions (E.B. statistics), or only the antisymmetric wave functions (F.D. statistics), or all the wave functions (Boltzmann statistics).

For the proof one remarks first that for any function (power series) $f(x)$, we have:

$$f(E_n)\psi_n = f(H)\psi_n$$

in which H again is the operator, in particular:

$$e^{-E_n/kT}\psi_n = e^{-H/kT}\psi_n. \tag{25}$$

We develop now ψ_n according to the normalized eigenfunctions of the ideal gas. In the case of a cubicle vessel this is simply a development in a multiple Fourier-series

$$\psi_n(q) = \sum_m c_{nm}\phi_m(q) \tag{26}$$

where one must then remember that $\phi_m(q)$ is an abbreviation for:[12]

$$\phi_{m_1\cdots m_{3N}}(x_1 \cdots z_N) = \left(\frac{2}{L}\right)^{3N/2} \sin\frac{m_1\pi x_1}{L}\sin\frac{m_2\pi y_1}{L}\cdots\sin\frac{m_{3N}\pi z_N}{L}.$$

Substituting (25) and (26) in the left-hand side of (24) we get:

$$\sum_n \psi_n e^{-E_n/kT}\psi_n = \sum_n \sum_i \sum_j c_{ni}c_{nj}\phi_i e^{-H/kT}\phi_j = \sum_i \phi_i e^{-H/kT}\phi_i$$

since: $\Sigma_n c_{ni}c_{nj} = \delta_{ij}$.

§7.

Introducing for simplification:

$$V' = 8\pi^2 mV/h^2 \quad E' = 8\pi^2 mE/h^2$$

the wave equation becomes:

$$d^2\psi/dq^2 + (E' - V')\psi = 0$$

and for the sum, using (24) we get:

$$\sum_n e^{-E_n/kT}\psi_n^2 = \sum_n e^{-\alpha E_n'}\psi_n^2 = \sum_n \phi_n e^{\alpha(d^2/dq^2 - V')}\phi_n$$

[11] Comp. F. Bloch, Zeits. f. Physik **74**, 295 (1932). We came to this result independently and because our point of view is somewhat different, we thought it not superfluous to repeat the proof.

[12] This is in the case of the Boltzmann statistics. For the E.B. or F.D. statistics one takes the symmetric or antisymmetric combinations, and because these form with respect to symmetric resp. antisymmetric functions a *complete* orthogonal set, the argument remains the same.

where α has again the meaning $h^2/8\pi^2mkT$ and where q abbreviates again the $3N$ coordinates of the gas.

We will prove now that *when α is very small*, we have *in first approximation*:

$$\sum_n \phi_n e^{\alpha(d^2/\alpha q^2 - V')}\phi_n \cong e^{-\alpha V'} \sum_n e^{-\alpha\epsilon_n'}\phi_n^2 \tag{27}$$

where $h^2\epsilon_n'/8\pi^2m$ are the energy values of the ideal gas. In particular for a cubicle vessel

$$\epsilon_n' = \pi^2(n_1^2 + n_2^2 + \cdots n_{3N}^2)/L^2.$$

In this way the evaluation of the sum for the *non-ideal* gas reduces to that for the *ideal* gas. Using then the results of Chapter II, we will then have proved our main theorems (7) and (8).

Formula (27) is not obvious, because d^2/dq^2 and V' are not commutable, so that in general:

$$e^{\alpha(d^2/dq^2 - V')} = e^{\alpha(-V' + d^2/dq^2)} \mp e^{-\alpha V'} \cdot e^{\alpha d^2/dq^2} \mp e^{\alpha d^2/dq^2} \cdot e^{-\alpha V'}.$$

To prove (27), write:

$$F = e^{\alpha(d^2/dq^2 - V')}\phi_n$$

then F will fulfill the differential equation:[13]

$$\partial F/\partial\alpha = (\partial^2/\partial q^2) - V')F$$

which we rewrite:

$$\partial F/\partial\alpha + (\epsilon_n' + V')F = (\partial^2/\partial q^2 + \epsilon_n')F \tag{28}$$

For $\alpha = 0$, $F = \phi_n$ and the right member is zero. In *first* approximation therefore:

$$F = \phi_n e^{-\alpha(\epsilon_n' + V')} \tag{29}$$

which gives (27). In Note I we will prove that in higher approximations:

$$\sum_n \phi_n e^{\alpha(d^2/dq^2 - V')}\phi_n = e^{-\alpha V'} \sum_n e^{-\alpha\epsilon_n'}\phi_n^2 \cdot [1 + \alpha f_1(q) + \alpha^2 f_2(q) + \cdots] \tag{30}$$

which justifies more strictly that (27) is true for small α; $f_1(q)$, $f_2(q)$ are certain functions of the coordinates, which contain V and its derivatives.

As a special example, which is of interest because the summations can be carried out exactly, we will consider in Note II the case of the harmonic oscillator.

Note I.

To find the next approximation we substitute (29) in the right-hand side of (28). Considered as a differential equation for F as a function of α, we can immediately integrate. Making use of the Schrödinger equation:

[13] Comp. F. Bloch, reference 11.

$$(d^2/dq^2 + \epsilon_n')\phi_n = 0$$

we obtain:

$$F = \left[\phi_n - \frac{\alpha^3}{2}\left\{\phi_n\frac{d^2V'}{dq^2} + 2\frac{d\phi_n}{dq}\cdot\frac{dV'}{dq}\right\} + \frac{\alpha^3}{3}\phi_n\left(\frac{dV'}{dq}\right)^2\right]e^{-\alpha(\epsilon_n' - V')} \tag{31}$$

Substituting in the left-hand side of (27) and calling the sum for the ideal gas:

$$S = \sum_n e^{-\alpha\epsilon_n}\phi_n^2$$

we get:

$$\sum_n \phi_n e^{\alpha(d^2/dq^2 - V')}\phi_n \cong e^{-\alpha V'}\left\{S - \frac{\alpha^2}{2}\left(\frac{d^2V'}{dq^2}S + \frac{dV'}{dq}\cdot\frac{dS}{dq}\right) + \frac{\alpha^3}{3}\left(\frac{dV'}{dq}\right)^2\cdot S\right\}$$

Substituting the value of S from (15) and (21), only the third term of the right-hand member will give a term proportional to α. Neglecting the terms which give α^2 and α^3, we obtain:

a. for Boltzmann statistics:

$$\sum\nolimits_{\mathrm{B}} = \left(\frac{1}{4\pi\alpha}\right)^{3N/2} e^{-\alpha V'}\prod_i(1 - e^{-x_i^2/\alpha})\cdot\left[1 - \alpha\sum_i \frac{\partial V}{\partial x_i}\frac{x_i e^{-x_i^2/\alpha}}{1 - e^{-x_i^2/\alpha}} + \cdots\right] \tag{32}$$

b. for E.B. or F.D. statistics:

$$\left.\begin{matrix}\sum\nolimits_{\mathrm{E.B}} \\ \sum\nolimits_{\mathrm{F.D}}\end{matrix}\right\} = \frac{1}{N'}\left(\frac{1}{4\pi\alpha}\right)^{3N/2} e^{-\alpha V'}\prod_{ij}(1 \pm e^{-(x_i - x_j)^2/2\alpha})$$
$$\cdot\left[1 \pm \frac{\alpha}{4}\sum_{ij}\frac{(x_i - x_j)e^{(-1/2\alpha)(x_i - x_j)^2}}{1 \pm e^{-(x_i - x_j)^2/2\alpha}}\left(\frac{\partial V'}{\partial x_i} - \frac{\partial V'}{\partial x_j}\right) + \cdots\right]. \tag{33}$$

We must remark, that the terms proportional to α in (32) and (33) contribute to the second virial coefficient, but as one easily verifies they will give corrections to (3) which are proportional to α^3 (for a gas in a three dimensional vessel), whereas (2) is only proportional to $\alpha^{3/2}$.

Further one must remark that the second term in the bracket of (32) and (33) are *not* the $f_1(g)$ of (30), for if one proceeds to the next approximation, one gets another term proportional to α, which contains $\partial^2 V'/\partial x_i^2$. One can convince oneself though that in the second virial coefficient these terms give corrections proportional to powers of α higher than α^3.

One can approach the proof of (27) from a somewhat more general standpoint. When f and g are any two non-commutable quantities, one can show that for small values of α:[14]

$$e^{\alpha(f+g)} = \{1 + (\alpha^2/2)(gf - fg) + \cdots\}e^{\alpha f}\cdot e^{\alpha g}$$

When we identify now g with d^2/dg^2 and f with V', and let $\exp[\alpha(f+g)]$ work on ϕ_n one obtains again (31).[15]

Note II.

For the harmonic oscillator it is possible to carry out the sums exactly. Introducing the abbreviations:

$$y = 2\pi x(m\nu/h)^{1/2} \qquad\qquad \theta = h\nu/kT$$

we can write:

$$(2\pi mkT)^{-1/2}\sum_n e^{-E_n/kT}\psi_n^2 = (2\theta)^{1/2}e^{-\theta/2 - y^2}\sum_n e^{-n\theta}\frac{H_n^2(y)}{2^n\cdot n!} \tag{34}$$

[14] Comp. J. E. Campbell, Theory of continuous Groups, pp. 54–57, for analogous questions.

[15] One uses here the special case $n = 2$ of a general formula for

$$f\frac{d^n}{dg^n} - \frac{d^n}{dg^n}\cdot f.$$

derived by Hylleras (Zeits. f. Physik **74**, 216 (1932)).

where ν is the frequency and H_n the nth Hermite polynomial. Introducing Weber's function $D_n(y)$:[16]

$$H_n(2^{-1/2}y) = 2^{n/2}e^{y^2/4}D_n(y)$$

the right-hand side becomes:

$$(2\theta)^{1/2}e^{-\theta/2}\sum_n e^{-n\theta}D_n{}^2(2^{1/2}y)/n!.$$

We distinguish again *two* cases;

a. Boltzmann statistics. We have to sum over *all* values of n. From the general result:[17]

$$\sum_n \frac{D_n(\xi)D_n(\eta)}{n'}e^{-nx} = (1-e^{-2x})^{-1/2}e^{(\xi^2+\eta^2))/4}\exp\left\{-\frac{\xi^2+\eta^2-2\xi\eta e^{-x}}{2(1-e^{-2x})}\right\} \tag{35}$$

putting $x=\theta$; $\xi=\eta=2^{1/2}y$, we obtain:

$$(2\pi mkT)^{-1/2}\sum_n e^{-E_n/kT}\psi_n{}^2 = \left(\frac{2\theta}{1-e^{-2\theta}}\right)^{1/2}\exp\left(-\frac{\theta}{2}-y^2\,\mathrm{tgh}\,\frac{\theta}{2}\right). \tag{36}$$

One sees that for θ very small the right-hand side goes over into:

$$e^{-\theta y^2/2} = e^{-2\pi^2 m\nu^2x^2/kT} = e^{-V/kT}.$$

b. E.B. or F.D. statistics. We must suppose then that we have to do with two particles attracting each other with a force proportional to the distance between them, moving in a one-dimensional vessel. If x stands for the distance between the particles, in E.B. statistics we must take only the eigenfunctions *even* in x, and in F.D. statistics we must take the *odd* ones. Separating into center of gravity and relative motion coordinates,[18] we have then to consider for the relative motion simply the sum (34) where in E.B. statistics we have to sum over all even values of n, and in F.D. statistics over the odd values[19] and where one must remember to replace m by $\frac{1}{2}m$. Using now the general result;[20]

$$\sum_{\substack{n\text{even}\\ n\text{odd}}}\left\{\frac{D_n(\xi)D_n(\eta)}{n'}e^{-nx} = (1-e^{-2x})^{-1/2}\exp\left(-\frac{\xi^2+\eta^2}{4}\,\mathrm{cotgh}\,x\right)\begin{matrix}\cosh\\ \sinh\end{matrix}\right\}\left\{\frac{\xi\eta e^{-x}}{1-e^{-2x}}\right\}. \tag{37}$$

From this follows then immediately:

$$\left.\begin{matrix}(\pi mkT)^{-1/2}\sum_{\text{E.B.}}\\ (\pi mkT)^{-1/2}\sum_{\text{F.D.}}\end{matrix}\right\} = \tfrac{1}{2}\left(\frac{2\theta}{1-e^{-2\theta}}\right)^{1/2}\exp\left(-\frac{\theta}{2}-y^2\,\mathrm{tgh}\,\frac{\theta}{2}\right)\cdot\left\{1\pm\exp\left(-\frac{2y^2}{\sinh\theta}\right)\right\} \tag{38}$$

For small θ the right-hand side goes over into:

$$\tfrac{1}{2}e^{-\pi^2m\nu^2x^2/kT}(1\pm e^{-4\pi^2mkTx^2/h^2})$$

in accordance with (8).

[16] Whittaker-Watson, Modern Analysis, p. 347.

[17] See G. E. Uhlenbeck and L. S. Ornstein, Phys. Rev. **36**, 823 (1930). F. Bloch reference 11 also gives the result, using a transformation function of Kennard (Zeits. f. Physik **44**, 326, 1927.)

[18] Strictly this is only possible for an infinite vessel. Because we are not interested here in the discreteness effect of the total translational motion, this is quite allowed.

[19] The center of gravity motion will simply give an extra factor $(4\pi mkT/h^2)^{1/2}$.

[20] The proof is quite analogous as given for (35) by G. E. Uhlenbeck and L. S. Ornstein, reference 17.

On Ferromagnetism and Related Problems of the Theory of Electrons*

By PAUL S. EPSTEIN
California Institute of Technology

(Received May 20, 1932)

In this paper is presented a study of those electrons which hold together a chemically elementary crystal and are responsible for the homoeopolar bonds between neighboring atoms. The starting point of the theory is Slater's form of the secular equations for first order perturbations arising from the interactions of identical atoms composing a system. A rigorous solution of these equations is given in section 4. The investigation is carried through in a unified way for magnetic and non-magnetic materials, with respect to internal energies and to magnetic properties. As anticipated by Heisenberg, the deciding factor is the sign of the Heitler and London interchange integral J_1. Substances with large negative J_1 are non-magnetic, those with large positive J_1, potentially ferromagnetic. For non-magnetic bodies, the theory gives a confirmation of Bloch's conclusions with slight differences of interpretation. On the other hand, the results for magnetic materials are new and entirely different from Bloch's. As to specific heats, it is found that at very low temperatures they have the expression $c=0.208\ sR(T/\theta)^{3/2}$, where R is the gas constant, s the number of valency electrons per atom, and θ has a close relation to the Curie point. With respect to ferromagnetism, the result is that a crystal satisfying Slater's equations is spontaneously magnetized almost to saturation but that the polarity of this magnetization changes its sense at irregular intervals. This fact suggests that ferromagnetic crystals must have a block structure and that they are coherent, in the sense of the validity of Slater s equations, only within the blocks (compare sections 10 and 11). With this hypothesis the theory accounts for the fundamental facts of ferromagnetism.

1. INTRODUCTION

THE discoveries of quantum dynamics, especially Pauli's exclusion principle and Fermi's statistics based on it, gave a new stimulus to the theory of electrons in metals. While Sommerfeld[1] treated in an exhaustive way the subject of free electrons, it was pointed out by Heisenberg[2] that the exclusion principle must exercise a powerful influence on the orientation of the spins of valency electrons and that it may play the role of the *molecular field* postulated by Weiss for ferromagnetic materials. The theory of the more tightly bound electrons was investigated by Bloch in a series of important papers. While his work is fundamental in many respects, it treats the non-magnetic properties[3] and the magnetic[4] separately and by different methods. Moreover, we believe that his results relating to ferromagnetism are open to objection.

* An abridgment of this paper was read before the *National Academy of Sciences* on April 26, 1932 at Washington, D. C.

[1] A. Sommerfeld, Zeits. f. Physik **47**, 1, 43 (1928).

[2] W. Heisenberg, Zeits. f. Physik **49**, 619 (1928).

[3] F. Bloch, Zeits. f. Physik **52**, 555 (1928); **59**, 208 (1930).

[4] F. Bloch, Zeits. f. Physik **57**, 545 (1929); **61**, 206 (1930); **74**, 295 (1932).

[5] This assumption is made for simplicity but is not necessary. We shall see in section 5 that our theory applies, almost without change, to more general cases.

2. Formulation of the Mathematical Problem

We consider with Heisenberg and Bloch a system of N electrons each pertaining, in the unperturbed state, to a different atom of a crystal.[5] Let the orbital motion of the electron be that corresponding to the lowest quantum state. Besides, with every electron there is associated a spin the projection of which on a given axis can be either positive or negative. Let r electrons have negative spins and $N-r$ positive. The projection of the total spin moment is then equal to $mh/2\pi$,where $2m=N-2r$. If all the atoms are successively labeled by the numbers 1, 2, $\cdots N$, let the positions of those containing an electron with a negative spin be $f_1, f_2, \cdots f_r$ $(f_1<f_2<\cdots<f_r)$. We denote the antisymmetric wave function for such a distribution by $\psi(f_1, f_2, \cdots f_r)$. As the magnetic interactions are neglected, all the functions with the same number r, correspond to the same energy and the total wave function pertaining to the magnetic moment m can be written as the linear expression

$$\psi(r) = \sum_{f_1,\cdots f_r} a(f_1, \cdots f_r)\psi(f_1, \cdots f_r). \tag{1}$$

The coefficients $a(f_1, \cdots f_r)$ are determined, in the usual way, by a secular system of equations when we introduce the mutual influence of the electrons and protons as a perturbation. The form of the secular equations was explicitly derived by Slater:[6]

$$\epsilon a(f_1, \cdots f_r) + \sum J_{ff'}[a(f_1', \cdots f_r') - a(f_1, \cdots f_r)] = 0. \tag{2}$$

The summation is extended over all pairs of electrons having opposite spins and $f_1', \cdots f_r'$ and $f_1, \cdots f_r$ differ only in that this pair of spins is interchanged. The coefficient $J_{ff'}$ denotes the London and Heitler interchange integral for the pair and ϵ is the energy measured from an arbitrary zero point. Usually, it is permissible to neglect the mutual influence of the more distant atoms and to take into consideration only the interactions between contiguous electrons. In this case the Eq. (2) is for most crystals reduced to

$$\epsilon a(f_1, \cdots f_r) + J_1 \sum[a(f_1', \cdots f_r') - a(f_1, \cdots f_r)] = 0. \tag{3}$$

The sum includes now all pairs of contiguous electrons having opposite spins. J_1 represents the interchange integral for two adjacent atoms.

The main problem is to find a solution of the Eqs. (2) or (3), satisfying the conditions at the surface of the crystal and other subsidiary conditions which we shall state in the next section. Bloch has given a very elegant method of transforming these equations. However, we shall not use it because the solution can be derived directly from the form given here.

3. Solution in a Special Case

In order to show how the solution is arrived at, it is best to start from an example. We take, therefore, the case of a linear chain of atoms with $r=2$. The form which Eq. (3) takes in this case is

[6] J. C. Slater, Phys. Rev. **34**, 1293 (1929); **35**, 509 (1930).

$$\epsilon a(f_1, f_2) + J_1[a(f_1 - 1, f_2) - a(f_1, f_2) + a(f_1 + 1, f_2) - a(f_1, f_2) + a(f_1, f_2 - 1) - a(f_1, f_2) + a(f_1, f_2 + 1) - a(f_1, f_2)] = 0, \tag{4a}$$

which holds for $f_2 > f_1 + 1$. In the case $f_2 = f_1 + 1$ two of the interchanges are precluded and the equation becomes

$$\epsilon a(f_1, f_2) + J_1[a(f_1 - 1, f_2) - a(f_1, f_2) + a(f_1, f_2 + 1) - a(f_1, f_2)] = 0. \tag{4b}$$

The difference equation (4a) has constant coefficients and its particular solutions can be written in the form $\exp i\alpha(k_1 f_1 + k_2 f_2)$. The corresponding energy level is

$$\epsilon_{k_1, k_2} = 4J_1(\sin^2 \tfrac{1}{2}\alpha k_1 + \sin^2 \tfrac{1}{2}\alpha k_2). \tag{5}$$

This expression is symmetrical in k_1 and k_2 so that the solution $\exp i\alpha(k_2 f_1 + k_1 f_2)$ belongs to the same energy. We can, therefore, build up the slightly more general solution $a(k_1, k_2) = c_1 \exp i\alpha(k_1 f_1 + k_2 f_2) + c_2 \exp i\alpha(k_2 f_1 + k_1 f_2)$ and try to choose the coefficients c_1 and c_2 in such a way as to satisfy the subsidiary condition (4b). It is important to note that while (4a) is supposed to apply only in the case $f_2 > f_1 + 1$, our solution is of such a type that it satisfies the Eq. (4a) for all values of f_1 and f_2, including $f_2 = f_1 + 1$. In this last case, both Eqs. (4a) and (4b) are true and we can replace the subsidiary condition by the difference

$$a(f_1 + 1, f_2) + a(f_1, f_2 - 1) - 2a(f_1, f_2) = 0, \qquad f_2 = f_1 + 1. \tag{6}$$

It is easy to see that this condition is satisfied if we put

$$c_1 : c_2 = -\exp i[\alpha(k_1 - k_2) + 2\phi(k_1, k_2)],$$

where

$$\phi(k_1, k_2) = \operatorname{arctg} \frac{\sin \alpha k_1 - \sin \alpha k_2}{2 - \cos \alpha k_1 - \cos \alpha k_2}. \tag{7}$$

The solution itself can then be written in the form

$$a(k_1, k_2) = \exp i[\alpha(k_1 f_1 + k_2 f_2) + \alpha k_1 + \phi(k_1, k_2)] - \exp i[\alpha(k_2 f_1 + k_1 f_2) + \alpha k_2 + \phi(k_2, k_1)]. \tag{8}$$

If we substitute for the surface conditions the periodicity requirement of Bloch's, all we have to do is to define k_1, k_2 as integers and $\alpha = 2\pi/N$. The Eqs. (8) and (5) will then represent a rigorous solution of the problem. It differs from Bloch's result only inasmuch as $a(k_1, k_2)$ vanishes for $k_1 = k_2$. This means that the case of two equal quantic numbers does not occur and must be excluded.

To obviate possible objections, we prefer, however, to show how a solution satisfying the actual border conditions can be found. These conditions result from the fact that when an electron is at one of the ends of the chain ($f_1 = 1$ or $f_2 = N$) a further decrease (or increase) of the number f labelling its position is no longer possible. The corresponding transitions must be, therefore, excluded from the conditions (4a) and (4b). This means

$$a(f_1 - 1, f_2) - a(f_1, f_2) = O, \qquad \text{when } f_1 = 1, \tag{9a}$$

$$a(f_1, f_2 + 1) - a(f_1, f_2) = O, \qquad \text{when } f_2 = N. \tag{9b}$$

It is easy to see that in addition to $a(k_1,k_2)$ the expressions $a(-k_1, k_2)$, $a(k_1, -k_2)$, $a(-k_1, -k_2)$ are also solutions of the system (4a), (4b) pertaining to the same energy (5), because this energy does not change if we reverse the sign of k_1 or k_2. Combining these four expressions with suitable coefficients we can build up a solution satisfying the condition (9a). In fact, the Eq. (9a) is fulfilled if the expression is arranged as a sum of terms each containing the factor $\cos\alpha k_j(f_1-\frac{1}{2})$, where j is 1 or 2. Such an arrangement is possible for any value of the parameters αk_j. On the other hand, the border condition (9b) can be satisfied by the same expression only for definite and discreet values of these parameters. It is obvious from the symmetry with respect to the two ends of the chain that α must be taken as

$$\alpha = \frac{\pi}{N}. \tag{10}$$

The condition (9b) is equivalent to the requirement that the solution can be arranged as a sum of terms each containing the factor $\cos\alpha k_j\,(f_2 - N - \frac{1}{2})$. The arguments of the cos functions can be reduced to this form only if we impose upon the numbers k_j the conditions

$$\left.\begin{aligned}(1 - 1/N)k_1 - (1/\pi)\left[\phi(k_1, k_2) + \phi(k_1, -k_2)\right] &= k_1',\\ (1 - 1/N)k_2 - (1/\pi)\left[\phi(k_2, k_1) + \phi(k_2, -k_1)\right] &= k_2'.\end{aligned}\right\} \tag{11}$$

Where the numbers k_1', k_2' are integers $(1, 2, \cdots N)$ and represent the quantic numbers of the problem. The rigorous border conditions lead, therefore, to a different result from Bloch's periodicity relation: The numbers k_j are no longer quantic numbers but non-integral auxiliary parameters.

The coefficients of the secular problem acquire in this case the simple form

$$a(f_1, f_2) = \cos\alpha k_1(f_1 - \tfrac{1}{2})\cos\alpha k_2(f_2 - N - \tfrac{1}{2}) \mp \cos\alpha k_2(f_1 - \tfrac{1}{2})\cos\alpha k_1(f_2 - N - \tfrac{1}{2}).$$

4. General Solution

The results of the preceding section apply with slight changes to the general case. For a system with $r = \frac{1}{2}N - m$ negative spins the energy expression is quite generally

$$\epsilon_m = \sum_{j=1}^{\frac{1}{2}N-|m|} \epsilon_j. \tag{12}$$

In the case of a linear chain, we have

$$\epsilon_j = 4J_1 \sin^2 \frac{\alpha k_j}{2N}, \tag{13}$$

where the parameters k_j are determined in relation to the quantic numbers $k_j'(=1, 2, \cdots N)$ by the equations

$$\left(1-\frac{1}{N}\right)k_j-\frac{1}{\pi}\sum_{i\neq j}{}_i[\phi(k_j, k_i)+\phi(k_j, -k_i)]=k_j', \qquad i, j=1, 2, \cdots, \tfrac{1}{2}N-|m|. \tag{14}$$

The expression for $a(f_1, \cdots f_r)$ becomes rather cumbersome. It is built up of terms derived from the product

$$\cos \alpha k_1(f_1-\tfrac{1}{2})\cdot\cos\left[\alpha k_2(f_2-3/2)-\phi(k_2, k_1)-\phi(k_2, -k_1)\right]$$
$$\cdot\cos\left[\alpha k_3(f_3-3/2)-\phi(k_3, k_1)-\phi(k_3, -k_1)-\phi(k_3, k_2)-\phi(k_3, -k_2)\right]\cdots$$

by all possible permutations of $k_1, k_2, \cdots k_r$.

If the number N is large, the difference between k_j and k_j' does not materially affect the energy expressions for smaller values of r, i.e., in the neighborhood of magnetic saturation. As to the opposite case $r=N/2$, $m=0$, the terms of the energy expression in which k_j is small and those in which it is large (near to N) remain practically unchanged. But the middle range of values of k_j, about $N/2$, is considerably influenced in the sense of an increase of this number. In the more important of our applications the states of small magnetic moment will play but a negligible role. Therefore, we shall be satisfied with the approximation which is obtained by identifying k with k', as it is amply sufficient for our purpose.

For a two dimensional quadratic lattice

$$\epsilon_j=4J_1\left(\sin^2\frac{\pi k_j}{2G}+\sin^2\frac{\pi l_j}{2G}\right), \qquad G^2=N. \tag{15}$$

In the case of a three-dimensional cubical crystal

$$\epsilon_j=4J_1\left(\sin^2\frac{\pi k_j}{2G}+\sin^2\frac{\pi l_j}{2G}+\sin^2\frac{\pi n_j}{2G}\right), \qquad G^3=N. \tag{16}$$

The parameters k_j, l_j, n_j are in both cases connected with a set of quantic numbers k_j', l_j', $n_j'=1, 2, \cdots G$ by the relations (14) (with G in place of N) and by two similar sets of equations which are obtained from (14) by substituting l or n instead of k.

In all cases, the Eq. (13) can be divided into a main condition, analogous to (4a), which holds when no two negative spins are in contiguous atoms, and into subsidiary conditions like (4b) which are true in the opposite case. The main condition is satisfied by an exponential function (analogous to $\exp\alpha(k_1f_1+k_2f_2)$ of the preceding section) and by a large number of other exponentials derived from this. The form of the energy terms in the sum (12) is here also completely defined by the main condition and by the exponential function satisfying it. The subsidiary conditions are satisfied by a proper combination of the exponentials and do not affect the form of the energy expressions. Finally, the border conditions serve to define the parameters entering into

the energy terms. Bloch succeeded in solving the main condition, therefore, his energy expressions are formally identical with ours, although the symbols have a somewhat different meaning. To this extent his results for other types of two and three dimensional lattices can also be used. However, if we inquire into the substance instead of the form, there is a profound difference in two other respects which are far more important than the changed definition of the parameters.

(1) In the first place, *no two terms of the energy sum* (12) *may be equal.* In the example of section (3) we see from the formula (8) that $a(f_1, f_2)$ vanishes when $k_1 = k_2$. This means that the corresponding energy level does not exist. The conditions are the same in the general case. Whenever two triples of numbers k_j, l_j, n_j are equal the function $a(f_1, \cdots f_r)$ vanishes identically. This is by no means surprising because the exclusion principle is contained in the formulation of Slater's Eqs. (2) or (3) and makes itself manifest in all the conclusions drawn from it.

(2). In the second place, the number of terms in the sum (12) depends only on the absolute value of the magnetic moment. It is equal to $\frac{1}{2}N - |m|$, and not to $\frac{1}{2}N - m$ as Bloch has it. The mathematical reason for this is that the case of no two negative spins being in contiguous atoms can be realized only as long as the number of these negative spins is smaller than (or equal to) half the number of atoms ($r = \frac{1}{2}N - m \leqq \frac{1}{2}N$, or $m \geqq 0$). If this requirement is not satisfied, we have no main condition but only subsidiary conditions, which completely changes the aspect of the problem. However, we can reduce the new problem to the old one by reversing the direction of our system of coordinates, and by counting as negative those spins which were considered as positive. *To positive and negative magnetic moments of the same absolute magnitude correspond the same energy levels.* This fact is an immediate consequence of the fundamental assumptions of this theory (section 2) which neglects magnetic interactions. Both directions in space are equivalent and the energy cannot depend on sense of the magnetic moment.

These two features of our energy expressions have an important influence on the results and lead to conclusions which are considerably different from Bloch's. Before closing this section, we should like to point out that the theory can be carried through also in the case of Slater's general Eq. (2) which takes into account interactions between non-contiguous atoms. For instance, in the case of a cubical crystal the energy expressions become

$$\epsilon_j = 4 \sum_{g_1 g_2 g_3} J_{g_1 g_2 g_3} [\sin^2 \tfrac{1}{2}\alpha g_1 k_j + \sin^2 \tfrac{1}{2}\alpha g_2 l_j + \sin^2 \tfrac{1}{2}\alpha g_3 n_j]. \qquad (18)$$

where $J_{g_1 g_2 g_3}$ is the interchange integral for two atoms with a distance between them having the projections $g_1 d$, $g_2 d$, $g_3 d$ if d denotes the lattice constant.

5. The Sum of States

To the energy expressions (12) there must be added the magnetic energy of the crystal equal to $-2\mu m H$, where μ denotes the Bohr magneton and H the strength of the magnetic field. The total energy is, therefore,

$$\epsilon = \epsilon_m - 2\mu m H. \tag{19}$$

The part ϵ_m depends only on the absolute value of the moment so that $\epsilon_{-m} = \epsilon_m$. For every energy level (19) there exists, therefore, another of the form

$$\epsilon = \epsilon_m + 2\mu m H, \tag{19'}$$

which corresponds to the magnetic moment $-\mu m$.

Accordingly, the sum of states $Q = \Sigma \exp(-\epsilon/kT)$ can be divided into two parts

$$Q = Z(H) + Z(-H), \tag{20}$$

the first containing all the terms with exponents of the type (19), the second all those of the type (19'). The two halfs $Z(H)$ and $Z(-H)$ differ only in the sign of H so that the sum of states Q is an even function of this quantity. The average magnetic moment of the system

$$M = kT \frac{d \log Q}{dH} = kT \frac{Z'(H) - Z'(-H)}{Z(H) + Z(-H)} \tag{21}$$

becomes an odd function of H which vanishes for $H=0$. This fact seems to make this theory inadequate for the explanation of permanent magnetization. We believe, however, that this average is obtained by a type of statistics which has a limited physical reality. In the case of ferromagnetic substances the averaging must be done in a different way. We shall return to this question in section 10 and shall first develop a few equations for the evaluation of the function $Z(H)$. With the help of the formula (12), we can represent each term of the sum of states as $\prod_{j=1}^{r} \exp(-\epsilon_j/kT + 2m\mu H/kT)$, where $2m = N - 2r$. But according to (13) or (16), ϵ_j is a function of the parameters k_j, l_j, n_j and, for a given m, there will be as many different terms as there are possible choices of these numbers. The totality of them is $\exp(2m\mu H/kT) Z_r$,

$$Z_r = \sum_{k_j} \prod_{j=1}^{r} \exp(-\epsilon_{k_j}/kT). \tag{22}$$

We use here the subscript k_j as an abbreviation for the triple of parameters k_j, l_j, n_j. As we found in the preceding section, all the ϵ_{k_j} in the sum (12), or all those in our product, must be different. In other words, our problem is subject to Fermi statistics. Our formula can, therefore, be treated in the usual way: If we consider the expression

$$R = \prod_{k_j} [1 + z \exp(-\epsilon_{k_j}/kT)], \tag{23}$$

then, Z_r is obviously the coefficient of the term of the degree r of the expansion of R in powers of z:

$$Z_r = \frac{1}{2\pi i} \int \frac{R}{z^{r+1}} dz, \tag{24}$$

the path of integration being a circuit round the point $z=0$.

The half $Z(H)$ of the sum of states is now

$$Z(H) = \sum_{r=0}^{N/2} \exp\,[(N - 2r)\mu H/kT]Z_r. \tag{25}$$

Strictly speaking, the expressions R are not the same in the different functions Z_r. But within the approximation of putting k_j equal to k_j', etc. (section 4) we can regard them as identical. Substituting (24) in (25) and summing under the sign of the integral, we find

$$Z(H) = \frac{1}{2\pi i}\int \frac{R}{z^{\frac{1}{2}N+1}} \cdot \frac{(ze^{\tau})^{\frac{1}{2}N+1} - 1}{ze^{\tau} - 1}\, dz, \tag{26}$$

where τ is an abbreviation for

$$\tau = 2\mu H/kT. \tag{27}$$

Although we spoke of one electron in every atom our equations apply as well to the case of several valency electrons of different energy. In fact, each of them will be in resonance only with its own kind in the other atoms and will satisfy a separate secular system. The total sum of states is then the product of the sums of state (26). If there are in an atom two or more electrons in nearly equivalent orbital states and with unlinked or weakly linked spins, the conditions are somewhat different; they are being now investigated by Mr. D. Weinstein. It is probable that our expressions will continue to be true, also in this case, with a change of the physical meaning of the symbol J_1 which will now include both the external and the inner interchange energies.

6. Partial Evaluation of the Sum of States

We consider the case that ϵ_j/kT is, in the average, large in absolute value compared with the quantity τ. In fact the characteristic feature of our theory is Heisenberg's assumption that there is a strong inner directing force due to the energies ϵ_j. The case of small ϵ_j is that when this assumption is not justified; it is, therefore, uninteresting in this connection. We have two terms under the integral (26), let us focus our attention on the second and evaluate it by the method of the steepest descents. In the usual way, we put the integrand equal to e^{ϕ} and obtain the position of the saddle point $z=A$ from the condition $d\phi/dz=0$:

$$\sum_{k_j} \frac{A \exp\,(-\epsilon_j/kT)}{1 + A \exp\,(-\epsilon_j/kT)} - (\tfrac{1}{2}N + 1) - \frac{A}{A - e^{-\tau}} = 0. \tag{28}$$

The second derivative we denote by

$$q = -\sum_{k_j}\left[\frac{\exp\,(-\epsilon_j/kT)}{1 + A \exp\,(-\epsilon_j/kT)}\right]^2 + \frac{\frac{1}{2}N + 1}{A^2} + \frac{1}{(A - e^{-\tau})^2}. \tag{29}$$

The position of the saddle point depends on the sign of the energy ϵ_j or of the interchange integral J_1. If the sign is *negative*, A is small compared

with $\exp(-\tau)$: In fact, the left side of the Eq. (28) is negative when $A=0$, but since the exponentials are large, most terms of the sum are, practically, equal to one already for moderate values of A. The sum becomes equal to N and the expression positive. There is a root in between, which does not lie close to the point $z=e^{-\tau}$. Therefore, the last term in (28) is negligible compared with the first two and must be omitted. Neglecting, at the same time, 1 beside $\frac{1}{2}N$, we write it in the form

$$\sum_{k_j} \frac{A \exp(-\epsilon_j/kT)}{1+A(-\epsilon_j/kT)} = \frac{N}{2}. \tag{28'}$$

Turning to the first term of the integrand of (26), we see that it is regular within the path of integration. It has no pole in $z=0$ and the point $z=e^{-\tau}$ lies outside the circuit of integration. The second term represents, therefore, the whole integral which takes the form

$$Z(H) = \frac{1}{(2\pi q)^{1/2}} \prod_{k_j} [1 + A \exp(-\epsilon_j/kT)] A^{-N/2} \cdot (1 - Ae^{\tau})^{-1}. \tag{30}$$

It must be noted that A does not depend on the magnetic field because the term containing τ is neglected in the Eq. (28') $Z(H)$ depends on H, only inasmuch as it enters into the last factor of the expression.

The results are quite different in the case of a *positive* energy ϵ_j. A becomes now much larger than $e^{-\tau}$. In fact, for $A=\infty$ the left side of the Eq. (28') is positive. But for comparatively large values of A the terms of the sum become negligible so that the other terms dominate and make the expression negative. The integral retains exactly the same form (30) but it does not represent now the whole function $Z(H)$. The circuit of integration is widened to pass through the distant point $z=A$ and the point $z=e^{-\tau}$ is now within this circuit. Consequently, the first term of the integrand (26) has now a pole in this point and the integral does not vanish but has the value $Z^{(1)}(H)$:

$$Z(H) = Z^{(1)}(H) + Z^{(2)}(H),$$

where

$$Z^{(1)}(H) = \exp\frac{N\tau}{2} \cdot \prod_{k_j} [1 + \exp(-\tau - \epsilon_j/kT)] \tag{31}$$

and $Z^{(2)}$ is identical with the expression (30). It is obvious , for physical and for mathematical reasons, that at low temperatures $Z^{(2)}$ is negligible compared with $Z^{(1)}$. In fact, apart from the unimportant factor $(1-Ae^{\tau})^{-1}$, $Z^{(2)}(H)$ is identical with the expression $Z_{N/e}$ of the last section which represents the totality of all terms of the sum of states corresponding to $m=0$. It follows from our expression of the energy (12) that the exponents of these terms are very large, because all the terms of the sum (12) must be different and, consequently, only few of them can have very small values. For this reason $Z_{N/2}$ is negligible, if J_1/T is sufficiently large.

7. Evaluation Continued

We now substitute into our general expressions the formula (16) for the energy term. It will be sufficient to treat the case of the three dimensional lattice as the other cases have no physical interest. We use the approximation $k_j, l_j, n_j = 1, 2, \cdots G$ which is good enough as was shown in section 4. If we define

$$\xi = \frac{\pi k_j}{2G}, \qquad \eta = \frac{\pi l_j}{2G}, \qquad \zeta = \frac{\pi n_j}{2G}, \tag{32}$$

the summation can be replaced by an integration with respect to ξ, η, ζ between the limits 0 and $\pi/2$. Moreover, we use the abbreviations

$$\beta = 2J_1/kT, \qquad \cos 2\xi + \cos 2\eta + \cos 2\zeta = \rho. \tag{33}$$

The terms of the formula (16) become then

$$\epsilon_j = 2\beta kT(\sin^2 \xi + \sin^2 \eta + \sin^2 \zeta) = \beta kT(3 - \rho). \tag{34}$$

Turning to the condition (29′) we can include the first term $3\beta kT$ into the parameter A writing $A' = A \exp(-3\beta)$. We obtain, then,

$$\frac{8}{\pi^3}\int\int_0^{\pi/2}\int \frac{A' \exp \beta\rho}{1 + A' \exp \beta\rho}\, d\xi d\eta d\zeta = \tfrac{1}{2}. \tag{35}$$

The constant A' can be determined from this relation in the following way. Let us subtract both sides of the equation from 1: The right side remains equal to $\frac{1}{2}$ while the left side has an integrand with the same denominator as (35) but with the numerator 1. The equation can, therefore, be represented as

$$\frac{8}{\pi^3}\int\int_0^{\pi/2}\int \frac{(1/A') \exp(-\beta\rho)}{1 + (1/A') \exp(-\beta\rho)}\, d\xi d\eta d\zeta = \tfrac{1}{2}.$$

We substitute now $\xi = \frac{1}{2}\pi - \xi'$ and similarly for η, ζ, so that $\rho = -(\cos 2\xi' + \cos 2\eta' + \cos 2\zeta') = -\rho'$, obtaining an equation which has quite the same form as (35) except that A' is replaced by $1/A'$. We conclude from this that $A' = 1/A'$ or

$$A' = 1, \qquad A = \exp 3\beta. \tag{36}$$

If we omit in (30) the unimportant factor $1/(2\pi q)^{\frac{1}{2}}$, $Z(H)$ takes in the case of negative interchange integrals $J_1 < \theta$ the form

$$\log Z(H) = -(3/2)\beta N + \frac{8N}{\pi^3} \int\int_0^{\pi/2}\int \log\left[1 + \exp\beta(\cos 2\xi + \cos 2\eta + \cos 2\zeta)\right] d\xi d\eta d\zeta - \log\left[1 - \exp(3\beta/2 + \tau)\right]. \tag{37}$$

Equally simple are the expressions in the case of a positive interchange integral ($J_1 > 0$). Substituting the notations (32) into the expression (31) we find

$$\log Z^{(1)}(H) = \tfrac{1}{2}N\tau + \frac{8N}{\pi^2} \cdot \int\int_0^{\pi/2} \int \log\left[1 + \exp\left(-\tau - 2\beta(\sin^2\xi + \sin^2\eta + \sin^2\zeta)\right)\right] d\xi d\eta d\zeta, \tag{38}$$

to this must be added negative term $Z^{(2)}$ of the form (37) which is negligible for low temperatures.

8. Electronic Specific Heats

If the crystal is not subject to magnetic forces ($H=\tau=0$), the two halfs of the sum of state Q become identical and $Q=2Z(0)$. As the free energy is connected with Q by the relation $\psi=-kT\log Q$, it is easy to find the expressions for the internal energy and the specific heat.

We shall see in the next section that the case $J_1<0$ is that of non-magnetic (diamagnetic) bodies. It we denote, in the usual way, $kN=R$ and, moreover,

$$\beta = -\theta/T, \qquad \theta = -2J_1/k, \tag{39}$$

and the number of valency electrons in an atom by s, we find for such materials the temperature dependent part of the internal energy

$$U = sR\theta\frac{8}{\pi^3}\int\int_0^{\pi/2}\int \frac{\rho d\xi d\eta d\zeta}{1+\exp(-\beta\rho)}. \tag{40}$$

This expression is but slightly different from Bloch's and agrees with it in every important respect giving results analogous to those obtained by Sommerfeld for free electrons. For high temperatures we can expand with respect to $\beta\rho$ taking only terms of zero and first order. This gives

$$\log Z(0) = Ns(\log 2 - 3\beta/2 + 3\beta^2/16), \tag{41}$$

the temperature dependent part of the internal energy

$$U = -3sR\theta^2/8T,$$

and the specific heat

$$c = dU/dT = 3sR(\theta/T)^2/8. \tag{42}$$

The evaluation for low temperatures can be carried out in a similar way as with the integrals of Fermi and Sommerfeld. The zero order approximation is obtained by taking the integral $\iiint\rho d\xi d\eta d\zeta$ over the part of the cube $0\leqq\xi\leqq\pi/2$, etc., limited by the surface $\rho=\theta$. This term which, in every case, constant and of little interest happens to vanish. For the next approximation it is well to remember that the normal distance between neighboring surfaces $\rho=\cos 2\xi+\cos 2\eta+\cos 2\zeta=\text{const.}$ is equal to $[(\partial\rho/\partial\xi)^2+(\partial\rho/\partial\eta)^2+(\partial\rho/\partial\zeta)^2]^{-\frac{1}{2}}\Delta\rho=\frac{1}{2}[\sin^2 2\xi+\sin^2 2\eta+\sin^2 2\zeta]^{-\frac{1}{2}}\Delta\rho$. Near $\rho=0$ it can be expressed by $\frac{1}{2}[3-2(\cos 2\eta+\cos 2\zeta)^2+2\cos 2\eta\cos 2\zeta]^{-\frac{1}{2}}\Delta\rho$. The factor of $\Delta\rho$ varies between a minimum of $1/2\cdot 3^{\frac{1}{2}}$ and a maximum of $\frac{1}{2}$. As the lower values have a larger weight, we take as a rough average $\frac{2}{3}$ of

the minimum plus $\frac{1}{3}$ of the maximum which is very close to $\frac{1}{4}$. On the other hand, we must know the area of that part of the surface $\rho=0$ which lies inside the fundamental cube. This surface goes through the middle of six edges of the cube which lie at the corners of a plane regular hexagon and also through the center of the hexagon. The surface itself is not quite plane and its area is, therefore, slightly larger than that of the hexagon. We take as its rough approximation the area of the circle circumscribed about the hexagon which is equal to $\pi^3/8$. Multiplying the area by the thickness we find that in the neighborhood of the element of volume element takes the form $d\tau=\pi^3 d\rho/32$ and the correction of the integral becomes

$$\tfrac{1}{2}\int_0^\infty \frac{\rho d\rho}{1+e^{-\beta\rho}} = \frac{\pi^2}{24\beta^2}. \tag{43}$$

The internal energy for low temperatures is, therefore,

$$U = (\pi^2/24)sRT^2/\theta, \tag{44}$$

and the specific heat

$$c = (\pi^2/12)sRT/\theta. \tag{45}$$

The expressions are different in the case of magnetic materials ($J_1>0$) and they are derived here for the first time. We have to use the expression (38) with $\tau=O$ and find

$$U = sRT\cdot\frac{8}{\pi^3}\int\int\int_0^{\pi/2}\frac{2\beta(\sin^2\xi+\sin^2\eta+\sin^2\zeta)d\xi d\eta d\zeta}{1+\exp 2\beta(\sin^2\xi+\sin^2\eta+\sin^2\zeta)}. \tag{46}$$

For high temperatures ($\beta\ll 1$) we can again expand with respect to the exponent and obtain

$$\log Z^{(1)}(0) = Ns\left(\log 2 - 3\beta/2 + \frac{21}{16}\beta^2\right), \tag{47}$$

while $-Z^{(2)}(0)$ is given by the expression (41). We see that for high temperatures $Z^{(2)}$ is not negligible compared with $Z^{(1)}$ but becomes of a similar order of magnitude, especially, as the factor $1/(2\pi q)^{\frac{1}{2}}$ is no longer small in this case. We introduce the slightly changed definitions

$$\beta = \theta/T, \qquad \theta = 2J_1/k, \tag{48}$$

If we determine U and c for $T\gg\theta$ from $Z^{(1)}$ alone,

$$U = -(21/8)sR\theta^2/T, \qquad c = (21/8)sR(\theta/T)^2, \tag{49}$$

we get the correct dependence on the temperature but coefficients which are slightly too large.

The evaluation for low temperatures $T\ll\theta$ is facilitated by the fact that the exponent retains its positive sign in the whole interval of integration. If β is large, the integrand is appreciable only for small values of the variables ξ, η, ζ. It is permissible to replace the signs by their arguments which lead to

$$U = \frac{3}{2}\frac{1}{(2\pi\beta)^{3/2}}\left[1 - \frac{1}{2^{5/2}} + \frac{1}{3^{5/2}} \cdots\right] sRT,$$

or

$$U = 0.0830 sRT^{5/2}/\theta^{3/2}, \tag{50}$$

and

$$c = 0.208 sR(T/\theta)^{3/2}. \tag{51}$$

The coefficient in this formula is rigorous and not approximate as in (45).

The measurements of Eucken and Werth[7] on the specific heats of iron and nickel show for temperatures between 16° and 22°K considerable deviations from the third power law in the sense of an increase of heat capacity. Eucken himself points out that his observations did not go to sufficiently deep temperatures to establish the law which this excess follows. All we can say is this: If the deviation is attributable to the cause discussed in the preceding paragraphs, its order of magnitude leads to a value of θ of a few hundred degrees and a value of J_1 of a few one hundredths of a volt. If the formula (51), for magnetic materials, were confirmed, it could give us very valuable information. The knowledge of the characteristic temperature θ would be very helpful in elucidating the mechanism of ferromagnetism (compare the next two sections).

It should be pointed out that our theory neglects the possible variability of J_1 and θ with temperature. This is not a rigorous procedure because J_1 must depend to some extent on the distance between the atoms. We presume, however, that this source of error is very small at low temperatures because of the insignificance of the thermal expansion in this region. Neither is the energy of magnetization contained in our expressions but this cause makes an appreciable contribution only in the vicinity of the Curie point.

9. Magnetization

We turn now to the behavior of our crystals in a magnetic field. The magnetic moment is obtained by differentiating the logarithm of the sum of states Q with respect to H

$$M = kT\frac{d \log Q}{dH}. \tag{52}$$

Let us first discuss materials with negative interchange integrals ($J_1<0$, $\beta<0$) for which we have to apply the expression (37). The dependence of $Z(H)$ on the strength of the field is all contained in the last factor $[1-\exp(-3\beta/2+\tau)]^{-1}$ which is very small compared with the other factors. In fact, it does not contain the number of atoms N and this makes its logarithm entirely negligible beside the logarithm of the rest of the expression. Substances with a negative J_1 are, therefore, magnetically inert as far as the electronic interchanges are concerned. We must remember, of course, that our formulas are valid only when β is considerably larger than τ, or $-J_1$ larger than $2\mu H$. For fields of about 10,000 gauss this would mean that $-J_1$ must

[7] A. Eucken and H. Werth, Zeits. anorg. Chemie **188**, 152 (1930).

be larger than 10^{-4} volt. We have pointed out in section 6 that the assumption of very small values for J_1 has little interest as it corresponds to the case when Heisenberg's hypothesis does not apply and the older theory of paramagnetism enters into its rights. The fact that materials with negative interchange integrals of appreciable absolute value must be nonmagnetic is evident directly from the energy expressions (12), (16). The state of vanishing magnetic moment ($m=0$) is, then, that of the lowest energy which dominates, in an overwhelming way, over all other states. We arrive, in this way to the following classification of crystals with respect to their interchange integrals J_1. Materials with large negative values of J_1 are nonmagnetic as far as electronic interchanges are concerned. Materials with small values of J_1 (negative or positive) are paramagnetic. Those with large positive values of J_1 are, potentially, ferromagnetic (compare with next section).

In the next section we shall give reasons for the view that the formula (52) should be applied with restrictions to the case of magnetic materials ($J_1>0$). Here we wish only to investigate what sort of a magnetization curve would result if this equation were always valid. We know from formula (21) that this curve is antisymmetrical of the general character of those pertaining to paramagnetic bodies. What is its slope in the point $H=0$? It is easy to see that in this point the slope is given by the expression

$$\left(\frac{dM}{dH}\right)_0 = kT\left[\frac{d^2 \log Z(H)}{dH^2} + \left(\frac{d \log Z(H)}{dH}\right)^2\right]_{H=0}.$$

We shall be satisfied with low temperatures when β becomes large. The Eq. (38) gives us then the approximation

$$\log Z(H) = \tfrac{1}{2}Ns\tau + Ns\left(\frac{T}{2\pi\theta}\right)^{3/2}\left[e^{-\tau} - \frac{e^{-2\tau}}{2^{5/2}} + \frac{e^{-3\tau}}{3^{5/2}} \cdots\right], \qquad (53)$$

$$(dM/dH)_0 = (Ns\mu)^2/kT, \qquad (54)$$

neglecting a term of the order N. If we refer M to one/cm^3 of the material, the expression must be multiplied by n/N (n being the number of atoms per/cm^3) and becomes $nNs^2\mu^2/kT$. The values of the constants are as follows $\mu=0.9\cdot10^{-20}$, r is of the order 10^{23}, kT is about $4\cdot10^{-14}$ for room temperature. $(dM/dH)_0$ is, therefore, of the order of magnitude $2s^2N\cdot10^{-4}$. This represents a steep rise of the curve even for very small crystals.

10. Explanation of Primary Ferromagnetism

We shall see in the next section that, in a sense, our Eqs. (52) and (54) describe the magnetization curve of certain systems. However, their physical reality is derived in an indirect way: We believe that the method of the sum of states is inapplicable to a coherent crystal in the conditions which prevail at low temperatures. In fact, what is the physical meaning of the sum of states $Q=\Sigma \exp(-\epsilon/kT)$? It is derived from Gibbs' concept of the ensemble of systems which is equivalent to the succession, *in time*, of the different

states of one given physical system. The mean value of any quantity derived by the use of the sum Q represents, therefore, the *time average* of this quantity. In the cases in which this method has been heretofore used this time average is what we really observe. In the theory of gases states which occur with an appreciable probability deviate but little from the mean state. The time average is very close to the most probable state of the system and very close to, or identical with, the readings of our instruments which always integrate over a finite, though sometimes small, time. The situation is entirely different in our theory of magnetization. It is true that positive and negative magnetic moments will occur equally often in the course of long periods and the time average will vanish. But this time average is not at all close to the most probable state. On the contrary, under the conditions mentioned, it coincides with one that is so improbable that it practically never occurs. To show this, let us compute the time average of the *absolute value* of the magnetic moment in the absence of a field.

$$\overline{|2\mu m|} = kT(d \log Z(H)/dH)_0 = Ns\mu[1 - 0.058(T/\theta)^{3/2}]. \qquad (55)$$

This means that, on the average, the crystal is in a state close to magnetic saturation. When we further compute the relative mean quadratic deviation from this time average

$$\overline{(|m| - \overline{|m|})^2}/\overline{|m|}^2 = (0.37/Ns)(T/\theta)^{3/2}, \qquad (56)$$

we find that the spread around the mean value is extremely small. These formulas show us that the crystal is, practically, always in a state approaching saturation. The time average zero is explained by the fact that the two senses of the magnetic moment are equally probable so that the crystal, at irregular intervals, spontaneously changes its magnetic polarity.

These results refer only to the case of low temperatures. When the temperature becomes sufficiently high, the state of vanishing magnetic moment is no longer one of low probability. This is apparent from our expression (41) valid for high temperatures. This expression is, practically, identical with the logarithm of $Z_{N/2}$ of section 6 representing the totality of all the terms of the sum of states pertaining to the magnetic moment $m=0$. The Eq. (41) shows us that this term has a negative exponent and is small as long as $3\beta/2-3\beta^2/16>\log 2$. But when the temperature rises the inequality is reversed into $3\beta/2-3\beta^2/16<\log 2$, the exponent becomes positive, and the term large. It is true that, in this form, the argument is not quite convincing: The formula is derived for small values of β and it is not certain that it still holds when $3\beta/2-3\beta^2/16$ becomes equal to log 2 or smaller. However, we get qualitatively the same result when we go back to the original definition $Z_{N/2}=\Sigma \exp(-\epsilon/kT)$ the summation being extended over all possible energy levels compatible with the condition $M=0$ or $r=N/2$. Now, let us look at our energy expressions (12) and (16). The number of terms in the sum (12) depends on the magnetic moment $2m$; it has its minimum 0 for saturation ($2m=N$) and its maximum $N/2$ for the nonmagnetic state ($2m=0$). As all the terms of the sum must be different, the mean energy also increases from

$\epsilon = 0$, for saturation, to a huge value, for the conditions of vanishing magnetic moment. It is easy to see that the energy excess of the state $2m = 0$ over the state $2m = N$ cannot be smaller than $1.45NJ_1$ (or $0.72kN\theta$) and not larger than $2.42NJ_1$ (or $1.21kN\theta$). On the other hand, the number of different energy levels pertaining to the state $2m = 0$ is $N!/(N/2)!(N/2)!$ or, within the accuracy of Stirling's formula 2^N. We find, therefore, for $Z_{N/2}$ the limits

$$N(\log 2 - 1.21\theta/T) < \log Z_{N/2} < N(\log 2 - 0.72\theta/T).$$

Owing to the large factor N, the change of $Z_{N/2}$ with T is very rapid. In the region $\log 2 > 1.21\theta/T$;(or $T > 1.8\theta$) it becomes a very large number; in the region $\log 2 < 0.72\theta/T$ (or $T < 1.04\theta$) it is a very small number. The transition from a high probability to a low probability of the unmagnetized state occurs somewhere between these two limits at a point which is roughly of the order

$$T_0 \approx 1.5\theta. \tag{57}$$

The conditions are the same for the other states of magnetization of our crystal ($2m = N - 2r$). As r increases from 0 to $N/2$ the individual terms of the groups Z_r defined by the Eq. (22) become smaller and smaller because their exponents grow in absolute value. On the other hand, the number of terms increases with r being equal to $N!/(N-r)!r!$ For high temperatures this second effect overweighs the first: The probability of a state increases with $r = \frac{1}{2}N - |m|$ and has its maximum for the unmagnetized state $m = 0$. The characteristic temperature above which such a distribution exists is, nearly, independent of r and approximately given by the Eq. (57). For temperatures $T > T_0$, the most probable state and the time average derived from the sum of states coincide and the sum of states has a good physical meaning. The crystal will be unmagnetized or very little magnetized. The opposite is true for low temperatures. The negative exponents are so large that all Z_1 are negligible but those pertaining to very small r. We have here the conditions analysed in the beginning of this section. *The point T_0 of Eq. (57) is, therefore, the primary Curie point of a coherent crystal*: Below it the crystal is a state of spontaneous magnetic saturation, above it, in a, practically, unmagnetic state.

Let us now return to the discussion of conditions below the Curie point. As we have seen, a coherent crystal is, then, in a state very near to complete magnetic alignment but its magnetic polarity spontaneously reverses itself at irregular intervals. What is the length of these intervals? Any change of magnetization is due to perturbations coming from the irregular thermokinetic state of the medium around the crystal and of the crystal itself. If there were no mutual magnetic interactions between the electronic spins, every electron would respond to these perturbations independently. In order to change its polarity, the crystal would have to pass through the extremely improbable state of vanishing magnetic moment and such an event could occur only once in an eon. In reality, there exists some measure of magnetic linking between the spins and they can turn over in groups so that the crystal

need not pass through the most improbable state. However, if the crystal is not small in size, the periods involved are still very long. The estimate can be made in a way analogous to that used by Bloch,[8] in a somewhat different case, from the magnetic linking of the spins and from the moment of momentum which the crystal has to pick up in order to reverse its magnetization. We call a crystal *coherent* if Slater's equation applies to it as to a unit, the numbers N and G determining its size. If there existed coherent crystals of a considerable size they would be always in a state of complete magnetization in some direction and a field could only change this direction but not demagnetize them. This is contrary to observation and we are compelled to conclude that the coherence extends only over microscopic elements. Even a well developed monocrystal must have a *block structure*. Slater's equation and all the consequences contained in it which we have developed in the preceding sections applies only to the separate blocks. It is unimportant for us whether these discontinuities of a crystal are irregular (in the sense of the *mosaic structure* surmized by Darwin and Smekal) or form a regular *secondary structure*, as advocated by Zwicky. The size of a few hundred atoms in each direction G, postulated by these authors, would insure a sufficiently frequent spontaneous change of magnetization.

We arrive, in this way, at the following picture of the constitution of ferromagnetic materials. They are built up of microscopical blocks which are in a state of permanent spontaneous magnetization. The polarity of this magnetization is subject to frequent spontaneous changes. As far as our simplified theory goes the electronic spins might have any direction and the magnetic axis could rotate freely within the block. In reality there must exist certain directions of preference related to the main crystallographic directions because of the interactions between spin and orbital momentum.[9] The magnetic polarity will alternate between these preferred directions. The permanent magnetization of these micro-crystalline blocks is what we designate as the *primary ferrogmagnetism*. The *secondary magnetization* of the bulk of a ferromagnetic substance is produced by the alignment of the magnetic axes of the primary elements. While this picture is, by no means, new we claim to have demonstrated, for the first time, that the permanent magnetization of the blocks is not a hypothesis but a necessary consequence of the exclusion principle.

11. Remarks on Secondary Magnetization

Already in Maxwell's *Treatise* we find the opinion that ferromagnetic materials are built up of permanently magnetized microcrystalline blocks. He believed that a magnetic field produces an alignment of the magnetic axes by rotating the whole block. Although this seemed little probable because of the enormous viscosity of these materials, I thought Maxwell's hypothesis sufficiently interesting to have it tested experimentally. A few years ago I caused Mr. Yensen[10] to look for a possible rotation using the Hull-Debye x-ray

[8] F. Bloch, Zeits. f. Physik **74**, 295 (1932).
[9] Compare F. Bloch and G. Gentile, Zeits. f. Physik **70**, 395 (1931).
[10] T. D. Yensen, Phys. Rev. **32**, 114 (1928).

method. It was not very surprising that the result was negative. According to our results of the preceding sections, Maxwell's assumption is unnecessary because the magnetic polarity of a block alternates while the block itself remains in place. In modern times the idea of permanently magnetized microcrystals was used with great success by Weiss[11] in the case of polycrystalline materials. Recently, Bitter[12] gave a considerable amount of experimental evidence which tends to show that it applies also to monocrystals.

The objective of this paper and its main result is to establish the primary ferromagnetism of the microcrystalline blocks. There exists a considerable literature about secondary magnetization and we limit ourselves, in this connection, to a few remarks. The agglomeration of blocks represents a large number of similar systems side by side. We can interpret, therefore, the statistical averages of section 9 in a new way. They represent as well the time averages for a single block as the actual mean values for the agglomerate. The simplifying assumption is implied that the blocks are all equal and that the magnetization has one of two opposite directions. It would be easy to drop these restrictions but hardly worth our while. On the contrary, we simplify still further by dropping the small second term of (53), i.e., by assuming that our blocks are completely magnetized. Eq. (52) gives then for the magnetization (per unit volume of the agglomerate)

$$M = ns\mu \operatorname{tgh} \frac{Ns\mu H}{kT} .$$

There are two effects left out of account in this formula, which can modify it sufficiently to produce a spontaneous and permanent secondary magnetization. The first is the field produced at a given point by the rest of the system. According to Lorentz,[13] this cause can be taken care of by substituting instead of the outer field H the actual strength of field $H' = H + \alpha M$. In Lorentz' cases α was of the order $\frac{1}{3}$ but it is hard to say what it is equal to in our case. The condition for secondary permanent magnetization would then be $(dM/dH)_0 < 0$ or $nNs^2\mu^2/kT > 1/\alpha$. The fact that monocrystals of iron and cobalt have little or no remanence indicates that this cause is not quite sufficient to produce permanent magnetization and points to a rather small size of the blocks or to a small value of α. The other effect which distorts the magnetization curve is the influence of mechanical stresses put forward by Akulov[14] and discussed in detail by Gans[15] and by Becker.[16] These two causes seem entirely sufficient to account for all the phenomena of secondary ferromagnetism. We wish, only, to point out that they may give rise to a secondary Curie point which would be observable by magnetic methods if it happened to be lower than the primary Curie point determined by the Eq.

[11] P. Weiss, Phys. Zeits. **9**, 361 (1908).
[12] F. Bitter, Phys. Rev. **38**, 528 (1931); **39**, 337 (1932).
[13] H. A. Lorentz, Enzyklopadie der math. Wiss. V 14, section 37.
[14] N. S. Akulov, Zeits. f. Physik **64**, 817 (1930).
[15] R. Gans, Schriften d. Königsberger gelehrten Gesellschaft **8**, 33 (1931).
[16] R. Becker, Zeits. f. Physik **62**, 256 (1930).

(57). The problem of relating these theoretical Curie points to those found by observation is not simple and we reserve it for another communication.

Note added in proof. It was overlooked by the writer that, in another paper (Leipziger Vortraege 1930, p. 67), Bloch gives the proportionality of the specific heat of ferromagnetic materials with $T^{3/2}$. However, the agreement with our results is more or less accidental, as Bloch's treatment is quite different and makes use of the two assumptions, pointed out at the end of our section 4, which we do not consider as permissible.—The experimental test of this law is complicated by the fact that the elements of the iron group contain two kinds of valency electrons, the first kind having, presumably, a negative interchange integral, the second a positive one. (Compare: Slater, note 6). The complete electronic specific heat is, then, to be represented by the sum of our formulas (45) and (51): $c=R[\alpha_1 s_1 T/\theta_1+\alpha_2 s_2(T/\theta_2)^{3/2}]$, $\alpha_1=\pi^2/12$, $\alpha_2=0.208$. Only θ_2 is related to the primary Curie point.

ERRATA

The Shape of an X-ray Line

By ARCHER HOYT
Department of Physics, Cornell University

(Phys. Rev. **40**, 477, 1932)

It has been called to the author's attention that there are two errors in Table I of the article by the above title.

Spencer[1] has been misquoted. The values published for half-maximum *half-widths* are in reality half-maximum *full-widths*. The values for Mo $K\alpha_1$ and Cu $K\alpha_1$ should be reduced by a factor $\frac{1}{2}$. The values which *should* appear in the table of half-widths at half-maximum ordinate are

for Mo $K\alpha_1$	4.8 sec.	or 0.14 X.U.
for Cu $K\alpha_1$	10.8 sec.	or 0.305 X.U.

[1] Spencer Phys. Rev. **38**, 630 (1931).

LETTERS TO THE EDITOR

Prompt publication of brief reports of important discoveries in physics may be secured by addressing them to this department. Closing dates for this department are, for the first issue of the month, the twenty-eighth of the preceding month; for the second issue, the thirteenth of the month. The Board of Editors does not hold itself responsible for the opinions expressed by the correspondents.

The Vapour Pressure of Sulphur at 50°C

Earlier workers[1] have obtained widely differing results for the vapour pressure of sulphur at 50° *viz.*, 0.00008 and 0.00036 mm of mercury. We made several determinations using a new method.

The apparatus is shown in Fig. 1. *A* is a drying tower containing soda-lime and calcium chloride. *B* is a thermostat heated and controlled electrically and maintained at 50°C. *C* is a glass spiral containing sulphur (purified by distillation in vacuo) while *D* is a Pyrex tube heated electrically to 300°C. The water jacket *E* cools the issuing gases which are then absorbed in *N*/100 iodine solution in wash bottle *F*. Bottles *G*, *G* contain potassium iodide solution to trap any iodine carried over.

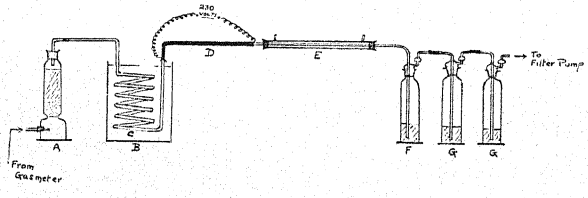


Fig. 1.

The procedure is as follows. Air is drawn through the apparatus by means of a filter pump fitted with constant leak. The air passes first through a gas meter and drying tower and then over the sulphur in the spiral which is at 50°C. The sulphur is oxidised to sulphur dioxide in the Pyrex furnace (owing to the very high partial pressure of oxygen this takes place almost quantitatively) and the issuing sulphur dioxide after cooling is absorbed in the *N*/100 iodine solution. After passing air for some time (24–48 hours) at a rate of about 10 litres/hour the wash bottles are detached and the iodine in them titrated with a sodium thiosulphate solution previously standardized against the iodine.

Thus we find the loss in iodine and hence the weight of sulphur dioxide formed. Knowing from the gas meter the volume of air which has passed and also the barometric pressure and the temperature at the meter, we can readily calculate the vapour pressure of sulphur at 50°C.

We obtained as the mean value *0.000155 mm Hg* assuming all the sulphur present as S_8.

In conclusion we wish to offer our best thanks to Mr. A. Ritchie, B.Sc for his invaluable help and advice.

R. R. H. BROWN
J. J. MUIR
Edinburgh University,
Chemistry Department,
April, 1932.

[1] Ruff and Graf, Z. Anorg. Chem. **58** 210 (1908); Greuner, J.A.C.S. 1399 (1907); West and Menzirs., J. Phys. Chem. **33**, 1887 (1929).

Variation of the Cosmic Rays with Latitude

Definite differences in the intensity of the cosmic rays at different latitudes are shown by our measurements, which have ranged from 47° north to 46° south. As far as they have gone, these measurements indicate a uniform variation with latitude, showing a

minimum at or near the equator, and increasing intensity toward the north and south poles. At sea level, the difference between the intensity at latitude 45° and 0° is roughly 16 percent, whereas at an elevation of 9000 feet the difference is about 23 percent. This would indicate that it is the least penetrating part of the cosmic rays which varies most rapidly with latitude. No significant variations with longitude have been noted.

Our present experiments are being made with a 10 cm steel sphere filled with argon at 30 atmospheres. The ionization current is measured by a Lindemann electrometer, the readings being made in such a way that the effect of any insulation leak is eliminated. To shield from the effects of the local radiation, a spherical shell of 2.5 cm copper and two spherical shells each of 2.5 cm lead, making a total of 7.5 cm of lead and copper, are used. The effect of the local gamma-rays traversing this shield is determined by comparing the ionization with and without the outer shell of 2.5 cm lead. All the readings are referred to the ionization by the gamma-rays from a capsule of 1.3 mg of radium placed at 1 meter from the center of the ionization chamber as a standard.

TABLE I. *Cosmic ray intensity at different localities*
(Ions per cc per sec. through 5 cm Pb, 2.5 cm Cu and 0.5 cm Fe)

Location	Lat.	Long.	Elev.	Barom.	I_C	I_L	Date
1 Mt. Evans	40°N	106°W	14,200ft	17.61in	6.88 ions	0.57	9/31
2 Summit Lake	40 N	106 W	12,700	18.70	5.84	0.34	9/31
3 Denver	40 N	105 W	5300	24.8	2.93	—	9/31
4 Jungfraujoch	47 N	6 E	11,400	19.70	5.08	0.51	10/31
5 Haleakala	21 N	156 W	9300	21.47	3.35±0.05	0.60	4/32
6 Idlewild	21 N	156 W	4200	25.99	2.40±0.05	0.37	4/32
7 Honolulu	21 N	158 W	70	30.09	1.89±0.02	0.11	4/32
8 S. S. Aorangi	4 S	173 W	60	29.65	1.83±0.05	0.32	4/32
9 Southern Alps	44 S	170 E	6700	23.69	3.39±0.05	0.22	4/32
10 Southern Alps	44 S	170 E	3900	26.10	2.70±0.04	0.21	4/32
11 Dunedin	46 S	170 E	80	30.08	2.16±0.03	0.11	4/32
12 Wellington	41 S	175 E	400	29.85	2.16±0.03	0.12	5/32

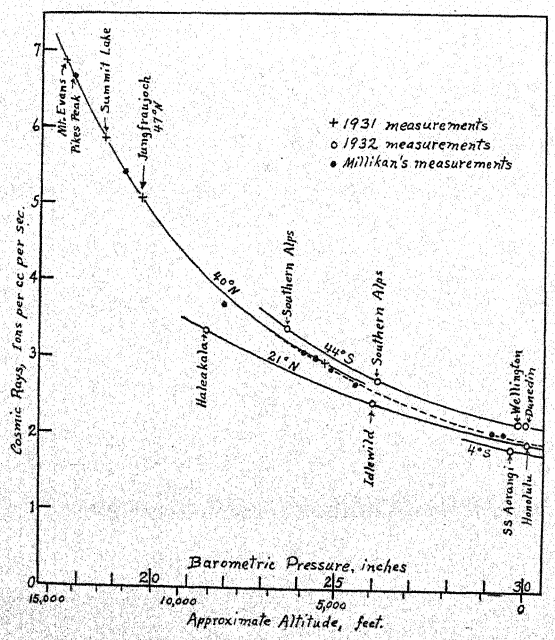


Fig. 1.

In Table I are listed the results of our various measurements. The column marked I_C represents the ionization in air at atmospheric pressure expressed in ions per cc per second due to the cosmic rays traversing our 7.5 cm filter. I_L represents the ionization due to the local rays passing through this filter expressed in the same units. Measurements 1 to 4 were made with different apparatus, using compressed air instead of compressed argon in the chamber, and lead and copper shields of different shape. These results are thus not strictly comparable with the later ones, though the difference is probably not more than 2 percent.

In Fig. 1 these results are shown graphically, and are compared with those of Millikan and his collaborators (Phys. Rev. **37**, 235 1931) as shown in the dotted line. It will be noted that for corresponding barometric pressures our measurements show consistently more intense radiation at the higher latitudes. The high altitude measurements in Hawaii are of especial interest as indicating that the difference with latitude is greater for the less penetrating rays.

Millikan's measurements were made at latitudes varying from 34°N to 59°N, most of them being at about 40°N. Our measurements near this latitude are in satisfactory agreement with his considering the slight differences in experimental arrangement. We do not however confirm the independence of the intensity of latitude which he reports.

The variation of the cosmic rays with atitude which these measurements show is of ,ust the kind to be expected if the rays consist of electrically charged particles which are deflected by the earth's magnetic field, the less penetrating rays being the more strongly affected.

This letter is the first report of an extensive program involving similar measurements by many physicists in widely distributed parts of the world. The design and construction of the instruments are due chiefly to Professor R. D. Bennett of Massachusetts Institute of Technology, with L. N. Ridenour, Dr. J. A. Hopfield and Dr. E. O. Wollan. Professor J. C. Stearns of the University of Denver with J. A. Longman, L. N. Ridenour and W. Overbeck made the measurements at Denver and Mt. Evans. Dr. Marcel Schein and Dr. Bernhard Frey of the University of Zürich cooperated in the measurements at the Jungfraujoch. Professor Harry Kirkpatrick of the University of Hawaii made the local arrangements in Hawaii, and with Professor W. H. Eller and Mr. I. Miyake assisted in the measurements. In New Zealand, Professor P. W. Burbidge of Auckland University College organized the various expeditions, and with Dr. C. M. Focken of the University of Otago helped with the observations. Valuable assistance has also been given by A. A. Compton and others. Without the cordial cooperation of the various universities where the work has taken us, the measurements would have been much more difficult.

ARTHUR H. COMPTON
University of Chicago,
The Tasman Sea,
May 7, 1932.

On the Production of Ultra-Short Electromagnetic Waves

In a note published in this journal, Mr. G. Potapenko gave an account of his interesting investigations in the field of the ultra-short electromagnetic waves.

The tubes that the author used in his experiments had pure tungsten filaments, as it was impossible to observe ultra-short waves with tubes having other kinds of filaments.[1]

As a result of some experiments I carried out recently, I found that, under particular conditions, oscillations of very high frequency may be obtained by using tubes with a heater element and a cathode coated with oxides.

Different tubes have been tested, namely, tubes of the type: −27 R.C.A. (American); E. 424 Philips (Dutch); R.E.N.S. 1104 Telefunken (German).

Although the common Barkhausen-Kurz arrangement may be used, that of Tank and Schiltneck[2] was found to be more suitable, the only modification being to connect the cathode to the negative terminal of the filament. The heating current must have a value which is only 80 percent−90 percent of its normal rated value.

Although unnecessary if the latter experimental arrangement is used, a slight positive

[1] Phys. Rev. **39**, 630 (1932).
[2] Helv. Phys. Acta. **1**, 100 (1928).

plate potential (0.5 to 2 volts) increases the amplitude of oscillations. Under these conditions a plate current is present even when the tube is not oscillating; this current being obviously increased when oscillations set up. This increase of current may vary (in accordance with the particular tube, etc.) between 10 and 200 microamperes. As the grid potential runs between 20 and 100 volts, a band of wave-lengths between 180 and 50 cm can be obtained.

AMEDEO GIACOMINI

Istituto di Fisica della Regia Università,
Milano, Italy,
June 1, 1932.

Predissociation in Nitrogen

Predissociation in nitrogen is best illustrated by the first positive bands $B_{13}\rightarrow A_9$, $B_{14}\rightarrow A_{10}$, $B_{15}\rightarrow A_{11}$ and by the bands $B_{13}\rightarrow A_8$, $B_{14}\rightarrow A_9$ and $B_{15}\rightarrow A_{10}$.[1] On small dispersion spectograms most of the bands of the first positive group possess three fairly strong heads, which correspond to transitions from the three components of the $^3\pi$ initial state of these bands to the $^3\Sigma$ state. In the above-mentioned bands however, two of the heads are almost completely missing. About a year ago, I reported the excitation of these missing heads in mixtures of nitrogen and oxygen,[2] in which the concentration of nitrogen was relatively small compared with that of the oxygen. At that time, the explanation of this effect was proposed to be the prevention of the normally occurring predissociation by electric fields, which were introduced during collisions. There is an obvious alternative explanation in which electric fields play no direct role, namely, the effect of increasing the number of molecules in the normally predissociating levels by collisions which give rise to transition from the non-predissociating component of the $^3\pi$ state to the two predissociating ones. The energy differences between the components of the $^3\pi$ state are very small and such transfers should take place without difficulty. The effect of pressure on predissociation has been discussed for AlH by Stenvinkel[3] and others, and this effect in nitrogen is in some respects, similar to the one in AlH. There is a difference, however, for in nitrogen the collision transfers are between components of an electronic state, whereas in AlH they are between rotational levels.

The occurrence of this effect in nitrogen suggests a similar explanation for the enhancement of predissociation in iodine by argon.[4] Mulliken's assignments of $^3\pi_0{}^+$ to the upper state of the visible halogen bands, makes this state a triplet state and hence provides the two other components, $^3\pi_1$ and $^3\pi_2$, which are necessary in order that the iodine problem be similar to the one in N_2. In iodine, the two levels $^3\pi_1$ and $^3\pi_2$ may themselves be unstable or they may combine with a third unstable level as in nitrogen.

Before the appearance of Van Vleck's[5] paper on the theory of the magnetic quenching of iodine fluorescence, I had proposed to myself the problem of studying the effect of magnetic fields on the predissociation in nitrogen, in order to observe the effect of magnetic fields on collisions. It was thought at the time that the magnetic field might be able to enhance collision transitions from the non-predissociating $^3\pi$ state to the two predissociating ones, and thus be able to quench the fluorescence. I am not aware of any theoretical reason for believing that this explanation has any value, but in view of the effect of collisions on predissociation both in iodine and in nitrogen, it seems worth while to suggest that the effect of magnetic fields on collisions may be of some significance.

JOSEPH KAPLAN

University of California
at Los Angeles,
June 3, 1932.

[1] J. Kaplan, Phys. Rev. **38**, 373 (1931).
[2] J. Kaplan, Phys. Rev. **38**, 1079 (1931).
[3] Stenvinkel, Zeits. f. Physik. **62**, 201 (1930).
[4] Turner, Phys. Rev. **38**, 574 (1931).
[5] Van Vleck, Phys. Rev. **40**, 544 (1932).

The Isotopic Weight of H^2

The mass of neutral H^2 has been measured as 2.01353 ± 0.000064 by comparison of the mass of $(H^1H^1H^2)^+$ with He^+ on fourteen spectra obtained with the mass-spectrograph recently described.[1] For the purpose of these measurements the mass of helium was taken as 4.00216, that of hydrogen 1.00778, and for the electron 0.00055 units on the $O^{16}=16$ scale.[2] The equivalent packing fraction of H^2 is 67.6 parts in 10,000. The energy of binding corresponds to 0.00203 mass units or approximately 2×10^6 electron-volts if the nucleus is composed of three entities, two protons and one electron. It is interesting to speculate that if the H^2 nucleus is composed of one proton and one Chadwick neurton[3] of mass 1.0067, then the binding energy would be 9.5×10^5 electron-volts and the H^2 nucleus would be loosely bound compared to He and other light nuclei. Professor Urey has pointed out to the author that for a stable configuration the mass of a free neutron must be greater than 1.00575.

The probable error of a single determination was ±0.00031. The observations were weighted from one to three depending on the definition of the lines of specific spectra and the internal consistency of the mensuration of the position of those lines. The sum of the weight factors was twenty-three.

$(3H^1)^+$ and He^+ provided the dispersion measurements for these spectra. The presence of $(H^1H^2)^+$ can only introduce a negligible correction. Earlier unreported work on the carbon and oxygen hydrides has shown that the mass scale is linear to within one part in ten thousand over the first eight centimeters of the plate, which includes the region used in this investigation.

Lines on the mass-spectrograph plates corresponding to a mass of 4.0285 were attributed to $(H^1H^1H^2)^+$ because; (1) no lines of comparable intensity appeared in this position when ordinary commercial hydrogen was used in the discharge tube; (2) the probability of the formation of $(2H^2)^+$ was much less than the probability of $(H^1H^1H^2)^+$ under the conditions existing in the discharge tube, i.e., $(3H^1)^+$ was present from 100 to 5 percent of $(2H^1)^+$; (3) the mass is less than the mass of $(4H^1)^+$ by an amount outside the limit of error.

Two samples of enriched hydrogen were used. Dr. Bleakney gave the writer a sample of the hydrogen he had examined,[4] and Dr. Brickwedde and Professor Urey[5] sent a sample of hydrogen with a slightly higher concentration of H^2.

The high value of the mass of H^2 makes it very difficult at this time to resolve the two doublets $(3H^1)^+$, $(H^1H^2)^+$, and $(2H^1)^+$, H^{2+}. It may be possible to resolve these doublets when more concentrated samples of hydrogen are available so that the lines of the respective ions can be obtained of comparable intensity. The doublet $(H^1H^1H^2)^+$, $(2H^2)^+$ will be difficult to resolve in any case as the respective masses differ by only one part in 2000.

The author is particularly indebted to Dr. Brickwedde who made this investigation possible by his preparation of the samples of enriched hydrogen at the U. S. Bureau of Standards, to Professor Urey and Dr. Murphy of Columbia University who placed a tested sample at the disposal of the author and to Dr. Bramley and Dr. Bleakney for their interest and helpful discussions.

KENNETH T. BAINBRIDGE
Bartol Research Foundation of the Franklin Institute, Swarthmore, Pa.,
June 21, 1932.

[1] K. T. Bainbridge, Phys. Rev. **40**, 130 (1932).

[2] F. W. Aston, Proc. Roy. Soc. **115**, 487 (1927).

[3] J. Chadwick, Proc. Roy. Soc. **136**, 702 (1932).

[4] W. Bleakney, Phys. Rev. **39**, 536 (1932); Phys. Rev. **41**, July 1, 1932.

[5] H. C. Urey, F. G. Brickwedde, and G. M. Murphy, Phys. Rev. **40**, 1 (1932); **39**, 164 (1932).

BOOK REVIEWS

Photoelectric Phenomena. ARTHUR LLEWELLYN HUGHES AND LEE ALVIN DUBRIDGE. Pp. 531. McGraw-Hill Book Company, Inc., New York, 1932. Price $5.00.

The preparation of an up-to-date text on "Photoelectric Phenomena" constitutes an almost hopeless undertaking. So many and varied are the researches in this field published in current technical journals that to digest, organize and include the subject matter in an orderly discussion would be next to impossible. The task is doubly difficult due to the fact that so little is known concerning the nature of the photoelectric effect and so many theories have been advanced to explain the oftimes conflicting results obtained by faulty experimental technique.

It is for these very same reasons, however, that there has been felt so keenly the need of a treatise coordinating the data so far obtained; and it is a source of considerable satisfaction to investigators in the field of photoelectricity to discover that "Electrical Phenomena" by Hughes and DuBridge so admirably meets these needs. The fact that several rather important papers published within the year seem to have been overlooked in its preparation, particularly in the field of photoconductivity, and the almost reportorial presentation of the data resorted to by the authors with little or no attempt to pass judgment on the relative merits of the research are to be expected rather than criticized in view of what has already been said.

"Photoelectric Phenomena" is a comprehensive well written, carefully edited and attractively published volume, far eclipsing any other volume on the subject published in the English language and perhaps being second to none emanating from the continent.

Defining a "photoelectric effect as one in which radiation causes a separation of electron from atoms so that an electric current may be caused to flow," the authors set out "to give a concise yet comprehensive survey of one of the many fields of physics." And within the fourteen chapters comprising the book they accomplish just that. The text, after a brief introductory chapter, consists of four chapters on the emission of electrons from metals, one chapter on the theories of photoelectric emission, a chapter each on what they have called "volume" photoelectric effects, viz., ionization of gases by light, and photoconductivity, two chapters on the photovoltaic effect and photoelectric effect in liquids and dielectrics, a chapter on the photoelectric effect of x-rays and γ-rays, a chapter each on photoelectric technique and applications and ends with a discussion of miscellaneous phenomena. The appendix includes a convenient table of physical constants, important photoelectric energy relations, a periodic table of the elements and a summary of illuminating engineering units and nomenclature. A very complete running bibliography is included in the form of footnotes with a name index and subject index at the end of the text. The book is printed in easily readable type and the sketches and diagrams are many and clear.

Unlike previous publications in English, too much valuable space is not devoted to a long historical account of the pioneering work or to the multitudinous applications of photocells. The text is essentially up-to-date and stresses important problems of the present. The order of presentation, chapter by chapter, is: first, ample citation of and reference to early related work, secondly, a complete resumé of all researches since that time, and finally a summary and discussion which generally includes a concise outline of the problems still unanswered. After presenting the researches of others with such reportorial excellence, this discussion of the outstanding problems is especially commendable. Incidentally, it reflects the thorough understanding of the field possessed by the authors.

One of the most praiseworthy features of the presentation is the differentiation between "spectral selectivity" and "polarization selectivity." Yet, after keeping these phenomena separated, as they should be, the authors, without justification perhaps, advance the doubtful suggestion that the latter is always associated with the former. Unfortunately, at the very beginning of this chapter a confusing error crept into the definition of polarization selectivity.

There are undoubtedly those who will criticize the order of presentation in the chapter on

the selective photoelectric effect and that on photoconductivity, just as they will the arbitrary classification of photoelectric phenomena as "surface photoelectric effects," "volume photoelectric effects" and "photovoltaic effects." This might follow if the reader is accustomed to the style of Gudden and Pohl in their volume bearing the same title as the one under discussion. In and of itself, however, the subject matter in "Photoelectric Phenomena," by Hughes and DuBridge will be found to be wisely classified, and coherently, competently and clearly presented. Even the chapter on "Theories of the Photoelectric Effect," though brief and undertaken apologetically by the authors, is entirely adequate for such a volume. Moreover, the discussion on photoelectric technique is pertinent and practicable, and can well be accepted as reflecting the experience of careful research workers in the field of photoelectricity.

A. R. OLPIN
Bell Telephone Laboratories, Inc.,
New York, N. Y.

Cartesian Tensors. HAROLD JEFFREYS. Pp. 93, The Macmillan Company, New York 1931. Price—$1.75.

According to the author's preface this little book is intended as a frank attempt to popularize the tensor methods for systems of rectangular axes, even to the extent of eliminating the usual extension development of vector analysis. Even within the realm of classical physics, to say nothing of relativity, one can find good reason for sympathizing with this plan. As examples, one thinks of the inertial ellipsoid of a rigid body and the polarization ellipsoid of a molecule. In these, and in other similar instances, the tensor notation seems much preferable to the Gibbsian dyadics.

The main emphasis in the book is on applications of tensors in classical physics. The fact that only twenty short pages are needed for the development of the tensor calculus itself should recommend it. The applications are made to dynamics of particles and rigid bodies, force systems, electrodynamics (potential theory), elasticity, and hydrodynamics. The discussions of the individual topics are too condensed to give more than a taste but taken together they give the student a valuable summary. The explanations are stated and easily followed.

E. L. HILL
University of Minnesota

Eenige Onderzoekingen over Paramagnetisme. E. C. WIERSMA. Pp. 122. **Paramagnetische Eigenschaften von Salzen.** C. J. GORTER. Pp. 112.

It is perhaps well to call attention in these columns to these two interesting Leiden dissertations devoted to topics in paramagnetism. Both dissertations are primarily the outgrowth of original experimental investigations, but at the same time enter into theoretical considerations with considerable detail. It is to be particularly commended that attention is focused on the newer quantum-mechanical developments rather than on obsolete classical models, as is too often done. In fact, over half of Wiersma's monograph is devoted to theory. The remainder is devoted to his experimental methods and results. The latter include the behavior of O_2 and NO at low temperatures, which is of importance in connection with theory for gases, and some interesting cryomagnetic anomalies in solid iron chloride, in which the susceptibility depends upon field strength in a peculiar way. Gorter's monograph is particularly valuable for the care with which it documents the existing determinations of susceptibilities and magneton numbers in the rare earth and iron groups. It is probably the best available compendium of such data. Gorter's own measurements have been indispensable in this field. They have corrected anomalies reported by other observers for hydrated nickel sulphate. Also his observations on Pr and Nd salts at low temperatures have enabled theoretical physists to estimate quantitatively the crystalline field.

J. H. VAN VLECK
University of Wisconsin

"Einführung in die Mechanik und Akustik" von R. W. Pohl, Zweite Auflage, Pg. 251 +viii, Figs. 440. Julius Springer, 1931. Price RM 15.80.

This volume constitutes an important contribution to the presentation and the elucidation of the introductory principles of mechanics. It is well organized and the author's style of a simple, plain unfolding of the facts of nature as revealed by experiment is a very pleasing one for the reader. The illustrations are numerous, 440 altogether, and their quality of reproduction is of a very high order. The device of silhouetting figures is frequently used and with good effect, and the experiments described exhibit methods of highly refined technique.

The first eight chapters, consisting of 115 pages, treat the mechanics of particles and of rigid bodies up to and including rotational motion and accelerated reference systems. The next two chapters of 54 pages deal with the mechanics of fluids, and these complete the mechanics division of the book. The division on acoustics consists of 75 pages and is divided into two chapters, the first of which deals with vibration theory and the second with the theory of wave motion and radiation.

As a groundwork for mechanics force is taken as a fundamental idea, and in pleasing contrast with so many texts which adopt this method the definition of force measurement is given at the outset. It is true that the author introduces the term mass simultaneously with that of force and also a convention for its measurement. Newton's second law is then an empirical relationship between force and mass as defined.

This mode of development of fundamental ideas is a possible one and is one that is very commonly used. It has certain advantages and its desirability is a matter for personal opinion. On the other hand the author expresses views to which the reviewer does not subscribe. The identity between gravitational and inertial mass is stated to be one of the curiosities of classical mechanics, a curiosity which was first made clear by Einstein's general theory of relativity. This view has also been expressed by others. However, a distinction between gravitational and inertial mass is not inherent in Newtonian mechanics although it does seem to be inherent in the mode of development which regards force as a fundamental idea. The trucks shown in Fig. 46 would afford an excellent means of introducing the mass concept without referring to forces an without introducing such vague terms as inertia or heaviness to account for it. One of the dangers in the use of force as a fundamental idea is that of attributing to it a "causal" significance rather than a "descriptive" one.

J. W. Campbell
University of Alberta

Second Series *July 15, 1932* *Vol. 41, No. 2*

THE

PHYSICAL REVIEW

Diurnal Variation of Cosmic Rays

By R. D. BENNETT, J. C. STEARNS AND A. H. COMPTON
Massachusetts Institute of Technology, University of Denver and University of Chicago

(Received April 9, 1932)

The intensity of cosmic rays at an altitude of 3900 meters was measured hourly over a consecutive period of 240 hours. The procedure eliminated the effects due to the variations of the temperature and possible variations of pressure of the gas in the chamber. The ionization was about 1.5 ± 0.25 percent more between 8 A.M. and 4 P.M. than between 8 P.M. and 4 A.M. If the variation is due to the soft component of the cosmic rays, these results are in satisfactory agreement with the results of other observers. Analysis of the data suggests that the portion of the space in the neighborhood of the sun may emit cosmic rays more copiously than the remote regions. This makes doubtful the inference that the energy in the universe in the form of cosmic rays is comparable with that in the form of light.

SOME of the earlier investigators of cosmic rays reported considerable variations in the intensity of these rays as measured at different times of day. More extensive observations have indicated that these variations were probably statistical fluctuations which did not indicate any significant changes in the intensity of the cosmic rays. There have, however, recently been found very small but consistent differences between day and night.[1] In previous papers[2] we have reported the discovery that the ionization in a pressure ionization chamber increases with increasing temperature. A review of the recent experiments showed that although in some of them the temperature of the apparatus was held constant, in others diurnal temperature changes might have affected the observed ionizations. We have therefore carried through a new series of measurements of cosmic rays over a period of 240 consecutive hours, in such a way that changes of ionization with temperature cannot influence our results. The suggestion has been made that the more absorbable portion of the cosmic rays shows the greater diurnal variation. This more absorbable component is however almost completely absent at sea level. Our work was accordingly done at a much higher altitude (3900 m) than any previous long series of observations.

[1] A good summary of this work is given by G. Hoffmann, Zeits. f. Physik **69**, 703 (1931).
[2] A. H. Compton, J. C. Stearns, and R. D. Bennett, Phys. Rev. **38**, 1565 (1931); **39**, 873 (1932).

Apparatus and Procedure

A diagram of the apparatus employed is shown partly in section, in Fig. 1. The ionization chamber is a steel sphere, approximately 10 cm internal diameter, filled with air at 30 atmospheres pressure. The ionization current is measured by a Lindemann electrometer, operating at about 50 divisions per volt. By applying an arbitrary potential to the grounding key, the sensitivity of the electrometer can be determined, and the needle can be made to move over any desired portion of the scale. The ionization current was approximately saturated when 144 volts from a dry battery were applied to the chamber. Surrounding the ionization chamber may be placed cylindrical shells of 2.5 cm of copper, and 5 successive layers of lead, each 2.5 cm thick,

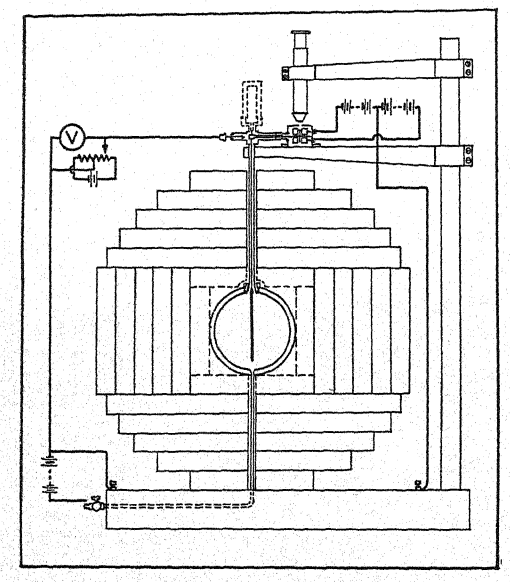


Fig. 1. Cross section of ionization chamber with shield.

a total mass of about 800 kg. The equipment was housed in a motor bus, which had a wooden roof too thin to absorb any appreciable cosmic radiation.

The readings consisted in comparing the time required for the electrometer needle to move 10 microscope scale divisions when cosmic rays alone were used with the time when a tube of 0.941 milligrams of radium enclosed in 1 cm of lead, was brought to standard position at about 22 cm from the center of the chamber. All measurements were made with 2.5 cm of copper and 5 cm of lead surrounding the chamber. Auxiliary tests showed that when the radium was removed, the ionization due to the local radiation traversing this shield was less than 3 percent of that due to the cosmic rays. Thus the ratio of the readings is a measure of the cosmic rays in terms of the gamma rays from the radium standard.

In our previous paper we showed that the ratio of gamma ray to cosmic ray ionization is independent of pressure. According to the theory of the effect of temperature on ionization developed there, the ratio of the ionizations

must thus be independent also of the temperature. Thus neither gas leaks nor temperature changes should affect our measurements of the radium equivalent of the cosmic rays.

Evidence for a Diurnal Variation

The results of the measurements are summarized in Table I and are shown in detail in Fig. 2. In Table I the values of $i_c/i_{c+\gamma}$ are the averages, over 10 days for the hours indicated, of the observed ratios of the ionization due to cosmic rays alone and due to cosmic rays plus the gamma-rays, measured as described above. The values of $I=i_c/i_\gamma$ are calculated from the observed values of $i_c/i_{c+\gamma}$ from the algebraic relation,

$$\frac{a}{b}=\frac{a}{a+b}\Big/\left(1-\frac{a}{a+b}\right).$$

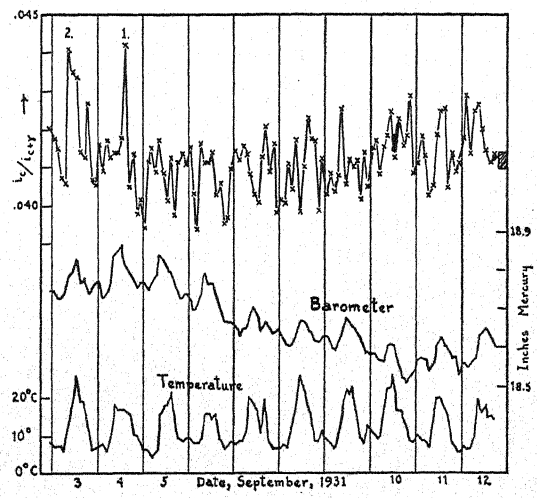


Fig. 2.

Table I. *Diurnal variation of cosmic rays at 3900 meters, 39°N 106°W, September 2–12, 1931.*

Hour	$i_c/i_{c+\gamma}$	$I=i_c/i_\gamma$	Temp. °C	Bar., inch	δI_T	δI_P	Chauvenet	I_0
6– 8A	0.04113	0.04289	9.0	18.663	−0.00002	−0.00024	—	0.04263
8–10	.04184	.04366	17.2	18.704	−.00024	+.00003	−0.00025	.04320
10–12	.04140	.04319	19.4	18.717	−.00013	+.00011	—	.04317
12– 2P	.04140	.04319	20.0	18.718	−.00010	+.00011	—	.04320
2– 4	.04179	.04361	17.7	18.687	−.00003	−.00008	−.00032	.04318
4– 6	.04106	.04282	15.4	18.673	.00000	−.00017	—	.04265
6– 8	.04119	.04296	9.8	18.657	+.00016	−.00027	—	.04285
8–10	.04092	.04267	7.8	18.651	+.00009	−.00031	—	.04245
10–12	.04082	.04256	8.4	18.663	+.00004	−.00024	—	.04236
12– 2A	.04106	.04282	8.4	18.666	+.00006	−.00022	—	.04266
2– 4	.04126	.04303	7.9	18.645	+.00007	−.00035	—	.04275
4– 6A	.04098	.04273	7.3	18.649	+.00008	−.00032	—	.04249

Probable error of bi-hourly mean value of $I=\pm 0.00019$.
Probable error of bi-hourly mean value of $I_0=\pm 0.00014$.
Mean value of $I_0=0.04280\pm 0.00005=85$ ions per cc per sec. at 30 atmospheres.

The ratio I is thus a measure of the ionization due to the cosmic rays in terms of the ionization due to the γ-rays as unity. The temperature and barometric pressure are likewise ten day averages taken over the hours indicated.

Corrections for Temperature and Pressure Variations

These values of I are subject to a small correction due to the variation of the battery voltage with the temperature; for a change of the potential applied to the ionization chamber induces a charge on the collecting electrode. It was found that a change of potential of 2.5 volts on the ionization chamber was sufficient to move the electrometer needle over the 10 scale divisions used in taking the readings. Thus if δV_T is the change in the battery potential during the reading, the correction to be applied is

$$\delta I_T = I\delta V_T/2.5.$$

The fluctuations δV_T during a single 10 minute reading were too small to be measured (of the order of 1 part in 30,000) with our field apparatus. They could be calculated, however, from the observed rate of temperature change and measurements of the electromotive force at different temperatures. These measurements were made on another dry battery of similar construction, using the Lindemann electrometer as an electrostatic voltmeter. When a battery potential of about 80 volts was applied to the plates of the electrometer, changes as small as 0.01 volt could be detected.

It was found that two types of voltage changes occur. The first is an increase of e.m.f. of about 0.015 percent per degree Centigrade, which follows closely the changes of the battery temperature. The second is a slow change, requiring more than 12 hours to come to equilibrium. This is an increase at the rate of about 0.003 percent per hour per degree change in temperature. The corrections to be applied due to these voltage changes are indicated in Table I by δI_T.

The rate at which the cosmic-ray intensity varies with the barometric pressure can be calculated from data showing the intensity at different altitudes. Using the values given by Millikan and Cameron[3] for the ionization inside lead screens, observed at different altitudes under conditions closely similar to ours, we find for barometric pressure of 18.7 inches, $(1/I)(dI/dP) = -0.147$ per inch of mercury. This enables us to standardize our intensity values by reducing them to 18.7 inches pressure. The appropriate corrections are indicated in Table I as δI_p.

The probable error of each bi-hourly value of I was calculated from the variations between the 10 daily readings which make up the average. The mean value of the 12 probable errors thus calculated is $r = \pm 0.00019$. With this probable error, it is found by applying Chauvenet's criterion that it is improbable that in 120 data there should be departures from the mean as great as those shown in Fig. 2 as points (1) and (2). By neglecting these data we thus get more reliable mean bi-hourly values, whose probable error is now reduced to $r_c = \pm 0.00018$.

[3] R. A. Millikan and G. H. Cameron, Phys. Rev. **37**, 242 (1931).

Changes in barometric pressure on successive days introduce a fluctuation in the bi-hourly values of I of $r_p = \pm 0.00011$. Similarly, due to the difference in the temperature changes on successive days, there is a fluctuation of $r_t = \pm 0.00002$. When the intensity is corrected for pressure and temperature changes, the probable error of the mean I_0 values thus becomes

$$r_0 = (r_c^2 - r_t^2 - r_p^2)^{1/2} = \pm 0.00015.$$

It will be noted from Table I and Fig. 3 that the variations in the bi-hourly values of I are hardly more than is to be expected from the probable error. On the basis of this evidence, we stated in a preliminary report of this work[4] that our readings "showed no variations in intensity greater than were to be expected from purely statistical considerations." However, when the

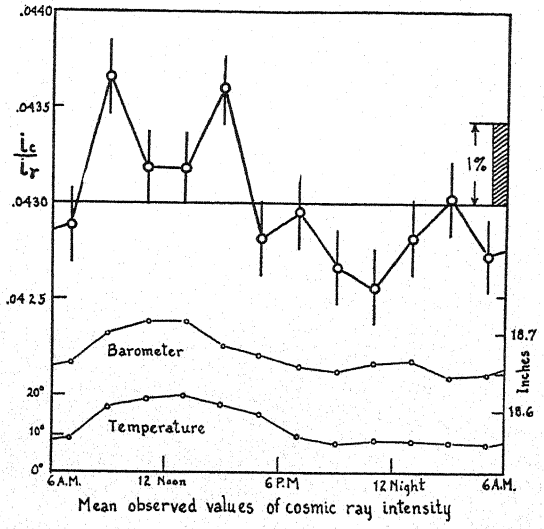


Fig. 3. Mean observed values of cosmic-ray intensity.

corrections due to the daily changes in barometric pressure are applied, there appears a marked difference between the intensity of the rays in the daytime and at night. During these experiments, the ionization was about 1.5 ± 0.25 percent more intense between 8 A.M. and 4 P.M. than between 8 P.M. and 4 A.M. There is only one chance in about 10^4 that this variation of 6 times the probable error should result from statistical fluctuations.

The existence of this diurnal variation, as well as the effect on the data of changes in the barometer, are shown graphically in Figs. 3 and 4. In Fig. 4, the dotted circles are calculated including the datum points (1) and (2) of Fig. 2 in calculating the average. In these figures the probable error of the data is represented by the length of the line drawn through each datum point. It will be noted that whereas before correction for barometric changes, 7 of the 12 points lie within the probable error of the mean position, after this correction only 3 of the 12 points lie within the probable error of the mean. In

[4] R. D. Bennett, J. C. Stearns and A. H. Compton, Phys. Rev. **38**, 1566 (1931).

Fig. 2 the "barometer effect" shows itself by the gradual rise of the mean intensity of the cosmic rays as the daily average of the barometer readings falls.

Diurnal variations similar to that here reported have been noted by other observers. Recently Lindholm[5] and Hess[6] have shown that an analysis of the data taken by Hoffmann and Lindholm[7] at 2450 m shows a diurnal change larger than the probable error, and about 0.5 percent of the whole cosmic-ray intensity. Likewise Hess and Pforte[8] from their own data at 100 m elevation find an intensity which is on the average 0.33 percent greater during the day than at night. This is precisely the magnitude of the effect reported by Millikan[9] in his most recent sea level measurements, though Millikan doubts whether the difference he observed was greater than the experimental error. Hoffmann[10] also notes an effect (at about sea level) "due to the sun" of the same order of magnitude as Millikan's, but of questionable reality.

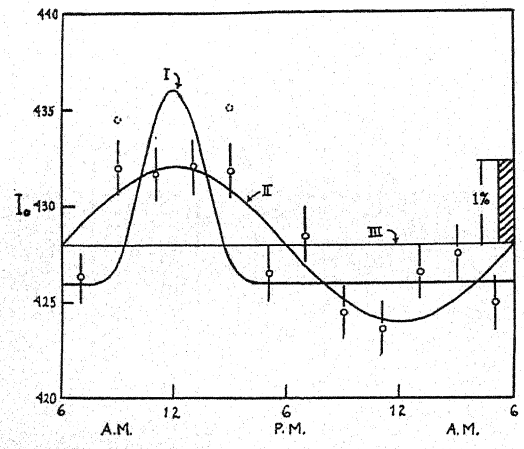


Fig. 4. Cosmic-ray ionization as function of time of day. Corrected for effects of temperature and pressure variations.

A possible explanation of the greater magnitude of the diurnal variation which we have found is that the variation occurs only in the soft component of the cosmic rays ($\mu =$ *ca.* 0.8 per meter of water). At 3900 m this constitutes about 65 percent of the whole cosmic radiation, whereas at sea level it amounts to only 8 percent. Thus our average difference of 1.0 percent between the 12 daylight hours and the 12 night hours would correspond to a difference of 0.12 percent at sea level or 0.7 per cent at 2450 meters. These values are in reasonably satisfactory agreement with those cited above.

[5] F. Lindholm, Gerlands Beitrage zur Geophysik **22**, 141 (1929).
[6] V. F. Hess, Naturwiss **18**, 1094 (1930).
[7] G. Hoffmann and F. Lindholm, Gerlands Beitrage zur Geophysik **20**, 12 (1928).
[8] V. F. Hesse and W. S. Pforte, Zeits. f. Physik **71**, 171 (1931).
[9] R. A. Millikan, Phys. Rev. **39**, 391 (1932).
[10] G. Hoffmann, reference 1.

Significance of the Diurnal Variation

Two alternative types of diurnal variations may be anticipated. The first would be due to rays coming directly from the sun. In this case the intensity of the "solar component" would be a maximum at noon, falling gradually to zero at sunset as the rays penetrate greater and greater thickness of the atmosphere. Curve I of Fig. 4 is calculated on this hypothesis, assuming that the solar component has the same absorption coefficient (*ca.* 0.8 per meter of water) as the soft component of the cosmic rays. The calculation is made for latitude 39°36′N, and sun's declination of 5°30′N.

The second alternative would be that cosmic rays are emitted more abundantly from the portions of space in the neighborhood of the sun than at remote distances. This would give rise to a gradual change, with a maximum at noon and a minimum at midnight, following approximately a sine curve, as indicated by curve II of Fig. 3.

If we represent by 1 the mean square departure of the data from the true value as calculated from the probable error, the mean square departure from curve I is found to be 1.9, from II is 0.8 and from III is 2.5. That is, curve II is much more probable than curve I or the straight line III, and agrees satisfactorily with the experimental data. It should be added that if a curve similar to I is calculated assuming the absorption of the solar component to be the same as of the total cosmic-ray beam it agrees considerably better with the experiments than does the curve I as here drawn. Such an assumption seems however to be ruled out by the fact noted above that at low altitudes the diurnal variation is much less prominent than at high altitudes.

Thus the evidence favors the view that the diurnal variation follows approximately a sine curve, with the maximum at noon and minimum at midnight. Unless this effect is due to some obscure atmospheric phenomenon, it suggests that the portion of space in the neighborhood of the sun emits cosmic rays more copiously than the more remote regions. It can be simply shown that the effective radius of the region from which the rays come should be approximately,

$$r = 2a/\delta$$

where a is the radius of the earth's orbit, and $\delta = (I \text{ noon} - I \text{ midnight})/I$. Thus if δ for the soft component of the cosmic rays is 0.02, r becomes 100 times the radius of the earth's orbit, or about twice the radius of the orbit of Pluto.

Millikan and Cameron have shown that the energy received by the earth as cosmic rays is comparable with that received as star-light. If the cosmic rays which we receive are a fair sample of those existing in interstellar space, this means that the energy in the universe in the form of cosmic rays is of the same order as that in the form of light. Curve II which these experiments confirm is however based on the assumption that the part of space near the sun emits cosmic rays more copiously than the more remote regions. That is, these experiments support the view that we do not receive a fair sample of the cosmic rays. This makes it difficult to form any reliable estimate of the energy of cosmic rays in interstellar space.

Without the cooperation of Messrs. V. J. Andrew, A. A. Compton, J. A. Longman, P. J. Mills, and L. N. Ridenour, Jr. of Chicago, and of P. Barth, C. Hedberg and W. Overbeck of Denver, the long series of readings required to obtain these results could not have been secured. We are indebted also to Mr. J. W. Ailinger, Superintendent of the Department of Mountain Parks, and to Mr. Donald Keim of the Chamber of Commerce of the City of Denver for facilitating our work on Mt. Evans in every possible way. Part of the equipment was purchased with a grant from the Rumford Committee.

Diffuse Scattering of X-Rays from Sodium Fluoride

By G. E. M. JAUNCEY* AND P. S. WILLIAMS
Washington University, St. Louis

(Received May 27, 1931)

S(class) values have been obtained for the monatomic gases argon and neon by Wollan, and for the simple cubic crystals sylvine and rocksalt by Harvey, and Jauncey and May. *F* values for the average $\frac{1}{2}(K^+ + Cl^-)$ and $\frac{1}{2}(Na^+ + Cl^-)$ atoms have been obtained by James and Brindley, and James and Firth. By means of the formulas for gases and crystals developed by Compton, and by Jauncey and Harvey, the above have yielded comparisons between *S*(class) and f' values for argon and the average sylvine atoms, and for the average $\frac{1}{2}(A+Ne)$ atoms and the average rocksalt atoms. The agreement on the whole has been excellent. The object of the present research was to make similar comparisons of the above results for neon with those for $\frac{1}{2}(Na^+ + F^-)$, by using Havighurst's *F* values for this average atom. The methods of experiment and calculation were similar to those of Jauncey and May, as modified by Harvey, except that Woo's form of the crystal formula was used to take account of the incoherent scattering. Unlike the case of argon and sylvine, we found that the f' values for the crystal of NaF are definitely lower than those for the gas neon. This implies that for weak nuclear fields the electron distribution in an atom of a crystal is perceptibly more diffuse than that in an atom of the corresponding gas. We also calculated *B* values and found that the second hump in the *B* curve which is barely indicated by Wollan's values for neon is definitely present. A Fourier analysis will therefore give a *U* curve which shows a hump for the *K* electrons of NaF.

I. INTRODUCTION

CONSIDER the case of a beam of unpolarized x-rays of intensity I_0 per unit area of the beam falling upon a speck of matter containing n molecules, where n is so small that the loss due to absorption of the x-rays in the speck may be neglected and yet so large that the intensity of the x-rays scattered by the speck per unit solid angle in a direction ϕ with the primary beam is proportional to n and to I_0, the primary intensity. We may then say that the intensity of these scattered rays is $I_{M\phi}nI_0$, where $I_{M\phi}$ is a proportionality constant for a given value of ϕ. It is possible to measure $I_{M\phi}nI_0$ experimentally, whence upon dividing by nI_0 the value of $I_{M\phi}$ may be found. We shall call $I_{M\phi}$ the scattered intensity per unit solid angle per molecule per unit primary intensity in the direction ϕ.

On the simple Thomson[1] theory of x-ray scattering, the scattered intensity from a molecule containing Z electrons is given by

$$I_{M\phi} = (Ze^4/m^2c^4)\cdot(1 + \cos^2\phi)/2 \qquad (1)$$

since each of the electrons in a molecule scatters independently. However, it is found that the experimental values of $I_{M\phi}$ are not in general given by the

* The senior author was aided in part by a grant from the Rockefeller Foundation to Washington University for research in science.

[1] J. J. Thomson, The Conduction of Electricity through Gases, 2nd Ed., p. 325.

right side of (1). Barkla and Ayers[2] found that at small angles the experimental values of $I_{M\phi}$ are greater than the right side of (1) and it has now become customary to multiply the right side of (1) by a factor S, so that

$$I_{M\phi} = (SZe^4/m^2c^4)(1 + \cos^2\phi)/2 \tag{2}$$

We shall call S the scattering factor per electron or simply the scattering factor. The value of S depends upon the electron distribution in each molecule of the speck and upon the arrangement of the molecules in the speck. The value of S may be found experimentally in all cases, but can only be calculated theoretically in particular cases. In 1930 Compton,[3] using the principles of the classical theory, showed that for the case of scattering from a monatomic gas

$$S = 1 + (Z - 1)f'^2/Z^2 \tag{3}$$

where Z is the number of electrons in an atom of the gas and f' is related to the true atomic structure factor f in a manner discussed by Jauncey[4] and Herzog.[5] In 1931 Jauncey[6] showed that for the case of scattering from a solid consisting of atoms of one kind

$$S = 1 + (Z - 1)f'^2/Z^2 + (F^2/nZ)X \tag{4}$$

where F is the atomic structure factor including the effect of thermal agitation and X is a certain double summation. Jauncey and Harvey[7] have shown that for the case of a simple cubic crystal $X = -n$, where n is the number of atoms in a speck of the crystal. Hence, for a simple cubic crystal consisting of atoms of one kind Eq. (4) becomes

$$S = 1 + (Z - 1)f'^2/Z^2 - F^2/Z. \tag{5}$$

Eqs. (3), (4) and (5) are derived from the principles of the classical theory and do not take account of the Compton effect. Wentzel[8] has applied the principles of wave mechanics to the theory of the Compton effect, and Woo[9] by extending Wentzel's arguments has arrived at a formula for S of the form

$$S = S_1 + S_2/(1 + \alpha \operatorname{vers}\phi)^3 \tag{6}$$

where $\alpha = h/mc\lambda$. For both the case of a monatomic gas and the case of a simple cubic crystal consisting of atoms of one kind, Woo gives

$$S_2 = 1 - f'^2/Z^2 \tag{7}$$

For a monatomic gas, Woo gives

$$S_1 = f'^2/Z \tag{8}$$

and, for a crystal,

$$S_1 = (f'^2 - F^2)/Z. \tag{9}$$

[2] C. G. Barkla and T. Ayers, Phil. Mag. **21**, 275 (1911).
[3] A. H. Compton, Phys. Rev. **35**, 925 (1930).
[4] G. E. M. Jauncey, Phys. Rev. **38**, 1 (1931).
[5] G. Herzog, Zeits. f. Physik **69**, 207 (1931).
[6] G. E. M. Jauncey, Phys. Rev. **37**, 1193 (1931).
[7] G. E. M. Jauncey and G. G. Harvey, Phys. Rev. **37**, 1203 (1931).
[8] G. Wentzel, Zeits. f. Physik **43**, 1 and 779 (1927).
[9] Y. H. Woo, Phys. Rev. **38**, 6 (1931).

We shall call S_1 and S_2 the coherent and incoherent scattering factors, respectively. It should be noted that from Eq. (6)

$$S = S_1 + S_2 \tag{10}$$

when $\alpha = 0$. In this case, using Eqs. (7) and (8), it is seen that the right side of Eq. (10) reduces to the right side of Eq. (3); also, using Eqs. (7) and (9), the right side of Eq. (10) reduces to the right side of Eq. (5). Since Eqs. (3) and (5) were derived by means of the classical theory, we may say that the sum of the coherent and incoherent scattering factors equals the classical scattering factor.

Jauncey and Harvey[10] have noted that, if the f' values for a monatomic gas are the same as those for a crystal consisting of the same kind of atoms as the gas, f' may be eliminated from Eqs. (3) and (5), giving

$$S_{\text{gas}} = (S + F^2/Z)_{\text{cryst}}. \tag{11}$$

This relation is also valid if Woo's Eqs. (6), (7), (8) and (9) represent the true state of affairs. Since the atoms of sylvine are argon-like, the relation expressed by Eq. (11) should hold for argon and sylvine. Using the experimental S values for argon and sylvine obtained by Wollan[11] and Harvey[12] respectively, and the F values for sylvine obtained by James and Brindley,[13] Jauncey and Harvey[10] have shown that the relation expressed by Eq. (11) holds very closely for argon and sylvine.

The purpose of the present research was to test the accuracy of the relation expressed by Eq. (11) for neon and sodium fluoride. Since S values for neon and F values for sodium fluoride have already been obtained by Wollan[11] and Havighurst[14] respectively, it remained for us to determine the S values for sodium fluoride.

II. Experimental Method

The experimental method was essentially that used by Jauncey and May[15] and modified by Harvey.[12] Unpolarized x-rays from a tungsten target tube were used. The rays were made effectively homogeneous by placing 1.65 mm of aluminum in the primary beam of x-rays. This beam was scattered by a slab of sodium fluoride crystal into an ionization chamber. With the ionization chamber placed at an angle ϕ with the primary beam, the crystal was set at various positions, so that θ, the angle between the normal to the crystal slab and the primary rays, passed through the value $\phi/2$. At $\theta = \phi/2$, which is the Crowther[16] position, a Laue spot was reflected into the chamber. Readings on both sides of the Laue spot were made and an interpolated reading at the position of the Laue spot was calculated as described in the papers of Jauncey and May[15] and Harvey.[12] The ionization chamber was filled with

[10] G. E. M. Jauncey and G. G. Harvey, Phys. Rev. **38**, 1071 (1931).
[11] E. O. Wollan, Phys. Rev. **37**, 862 (1931).
[12] G. G. Harvey, Phys. Rev. **38**, 593 (1931).
[13] R. W. James and G. W. Brindley, Proc. Roy. Soc. **A121**, 155 (1928).
[14] R. J. Havighurst, Phys. Rev. **29**, 1 (1927).
[15] G. E. M. Jauncey and H. L. May, Phys. Rev. **23**, 128 (1924).
[16] J. A. Crowther, Proc. Roy. Soc. **A86**, 478 (1912).

air saturated with ethyl bromide at a temperature of 22°C, at which temperature the vapor pressure of the bromide[17] is 415 mm of mercury. The length of the ionization chamber was 43 cm. The effective wave-length of the x-rays passing through the aluminum filter and the crystal in the Crowther position was found by observing the absorption in further sheets of aluminum. The effective wave-length was 0.39A when the x-ray tube was operated at about 65 k.v. peak and 10 m.a.

Instead of comparing the intensity of the x-rays scattered at an angle ϕ from the crystal with those of the rays scattered from the crystal at some standard angle such as 60° as in Harvey's experiment, we compared the intensity of the rays scattered from the crystal in a direction ϕ with that of the rays scattered from a slab of carbon at a constant angle of 40°. Not only were the intensity of the scattered rays compared but also the intensities of the transmitted rays. Then, later, the intensity of the rays scattered from the carbon slab were compared with that of the rays scattered from a slab of paraffin at 90°, and also the intensities of the transmitted rays were compared. We were therefore able to calculate the ratio of the intensity of the x-rays scattered by the crystal at an angle ϕ to that of the rays scattered by paraffin at 90°, and also the ratio of the intensity of the primary beam transmitted through the crystal when in the Crowther position corresponding to a scattering angle ϕ to that of the primary beam transmitted through the paraffin when in the Crowther position corresponding to a scattering angle of 90°. We shall call these two ratios the scattering ratio and the transmitted ratio, respectively.

It must be noted that the ratios actually observed are ratios of ionization currents and not ratios of intensities. This difference comes in because the length of the ionization chamber is not sufficient for the complete absorption of the x-rays entering the chamber. The values of the ratios are shown in Table I.

TABLE I. *Experimental ratios. Sodium fluoride to paraffin.*

$(\sin \frac{1}{2}\phi)/\lambda$	Scattering	Transmission
0.109	0.26	1.333
.218	2.47	1.333
.327	3.02	1.331
.434	3.16	1.327
.540	3.20	1.317
.647	3.14	1.310
.855	2.77	1.282
1.057	2.46	1.243
1.250	2.19	1.196
1.447	1.91	1.140
1.631	1.73	1.072
1.812	1.59	1.000

The surface density of the crystal was 1.443 gm/cm² while that of the paraffin was 0.701 gm/cm².

III. INTERPRETATION OF THE RESULTS

Crowther's formula[16] for the intensity of the x-rays scattered in a direction ϕ from a slab of material whose thickness is t is

[17] International Critical Tables, III, p. 217.

$$I_\phi = (AIt/R^2 \cos \tfrac{1}{2}\phi) \cdot s \tag{12}$$

where I is the intensity per unit area of the rays transmitted through the slab when held in the Crowther position, A is the area of the ionization chamber window, R is the distance of the window from the slab, and s is the linear spatial scattering coefficient per unit solid angle in a direction ϕ. At the time Eq. (2) was derived by Crowther, the Compton effect was unknown. Jauncey and Defoe[17] have considered the effect of the division of the scattered rays into coherent and incoherent rays and have shown that the simple Crowther formula must be replaced by

$$I_\phi = (AIt/R^2 \cos \tfrac{1}{2}\phi)(s_1 + s_2 T) \tag{13}$$

where s_1 and s_2 are respectively the coherent and incoherent linear spatial scattering coefficients per unit solid angle in a direction ϕ, and where T is a complicated expression involving the absorption coefficients of the coherent and incoherent scattered x-rays in the slab, in the air between the slab and in the aluminum window of the chamber. T is a function of the scattering angle ϕ. We shall write

$$I_\phi = I_{\phi 1} + I_{\phi 2} \tag{14}$$

where $I_{\phi 1}$ and $I_{\phi 2}$ are the intensities of the coherent and incoherent rays respectively. From Eq. (13),

$$I_{\phi 1} = (AIt/R^2 \cos \tfrac{1}{2}\phi) \cdot s_1 \tag{15}$$

and

$$I_{\phi 2} = \frac{AIt}{R^2 \cos \tfrac{1}{2}\phi} s_2 T. \tag{16}$$

Let the fractions of $I_{\phi 1}$ and $I_{\phi 2}$ which are absorbed in the ethyl bromide of the ionization chamber be K_0 and K_ϕ respectively. Then, if $C_{\phi 1}$ and $C_{\phi 2}$ are the respective ionization currents produced, we have

$$C_{\phi 1} = K_0 I_{\phi 1} \tag{17}$$

$$C_{\phi 2} = K_\phi I_{\phi 2}. \tag{18}$$

Also, if C is the ionization current produced by the transmitted rays,

$$C = K_0 I. \tag{19}$$

Hence, replacing the I's in Eq. (14) by the C's and taking account of Eqs. (15) and (16), we obtain, after rearranging and putting $C_\phi = C_{\phi 1} + C_{\phi 2}$,

$$C_\phi = \frac{ACt}{R^2 \cos \tfrac{1}{2}\phi} \left\{ s_1 + \frac{K_\phi T}{K_0} s_2 \right\} \tag{20}$$

C_ϕ is the actual measured ionization current. The relation between s_1 and S_1 is

$$s_1 = S_1 (NZ\rho/W) \cdot (e^4/m^2c^4) \cdot (1 + \cos^2 \phi)/2 \tag{21}$$

while that between s_2 and S_2 is

$$s_2 = S_2 \frac{(NZ\rho/W) \cdot (e^4/m^2c^4)}{(1 + \alpha \operatorname{vers} \phi)^3} \cdot \frac{(1 + \cos^2 \phi)}{2} \tag{22}$$

where ρ is the density of the slab, N is Avogadro's number, Z is the number of electrons in a molecule, and W is the molecular weight of the slab. If the scattering is from a slab of crystal, we use the values of S_1 and S_2 as given by Woo's Eqs. (7) and (9).

According to Harvey,[12] when x-rays of wave-length 0.39A are scattered at 90° from paraffin, the scattered rays are almost entirely incoherent, so that for this case, we may take $S_1=0$ and $S_2=1$. Hence, for scattering from paraffin at 90° we obtain an equation similar to Eq. (20), but with $s_1=0$ and s_2 given by Eq. (22) when $S_2=1$. In this equation for the scattering of paraffin, let us represent the ionization currents by P's. Dividing Eq. (20) by this equation for paraffin, we obtain after rearranging and taking account of Eqs. (7) and (9) for a crystal

$$K_0(f'^2-F^2)/Z_C+K_\phi T_C\cdot\frac{1-f'^2/Z_C^2}{(1+\alpha\,\mathrm{vers}\,\phi)^3}=\frac{K_{90}{}^\circ T_P}{1+\cos^2\phi}\cdot\frac{\cos\frac{1}{2}\phi}{\cos 45^\circ}\cdot\frac{\rho_P t_P}{\rho_C t_C}\cdot(W/Z)_C\cdot(Z/W)_P\cdot C_\phi/P_{90}\cdot P/C\cdot 1/(1+\alpha)^3. \tag{23}$$

Quantities with the subscript C refer to the crystal of sodium fluoride, while those with the subscript P refer to the paraffin. In the present case the changes of absorption due to change of wave-length in the air between the scattering slab and the ionization chamber and in the aluminum chamber window are negligible, so that T reduces to

$$T=(1-e^{-g})/g \tag{24}$$

where

$$g=(\mu_2-\mu_1)t/\cos\tfrac{1}{2}\phi. \tag{25}$$

The quantities μ_2 and μ_1 are the linear absorption coefficients of the incoherent and coherent scattered rays in the scattering slab.

All quantities in Eq. (23) except f' are either known, can be calculated, or can be measured. Eq. (23) therefore enables us to find f'. These values of f' are shown in Table II. Values of F^2/Z as given by Havighurst[14] are also shown in this table. Knowing f' we can find S_1 and S_2 by means of Eqs. (9) and (7) and hence also S(class), where

$$S(\text{class})=S_1+S_2. \tag{26}$$

The values of S_1, S_2 and S(class) are also shown in Table II.

TABLE II. *f' and S values for sodium fluoride.*

$(\sin\frac{1}{2}\phi)/\lambda$	F^2/Z	f'	S_1	S_2	S(class)	B
0.109	8.65	9.27	—	0.141	0.141	2.53
.218	4.95	7.20	0.240	.482	.722	3.94
.327	2.37	5.00	0.130	.750	.880	4.10
.434	.99	3.23	0.053	.895	.948	3.52
.540	.45	2.21	0.038	.951	.989	3.05
.647	.20	1.51	0.028	.977	.995	2.45
.855	.05	.74	0.005	.994	.999	1.59
1.057	.00	.17	0.003	1.000	1.003	.45
1.250	.00	.55	0.030	.997	1.027	1.72
1.447	.00	.48	0.023	.998	1.021	1.74
1.631	.00	.46	0.021	.998	1.019	1.87
1.812	.00	.00	0.000	1.000	1.000	.00

Compton has introduced a quantity B which is given by

$$BZ = 8\pi f'(\sin \phi/2)/\lambda. \tag{27}$$

The values of B are shown in the seventh column of Table II. This quantity is used in Compton's Fourier analysis method of obtaining the electron distribution within an atom.

IV. Comparison with the Scattering from Neon

Wollan's S(class) values for neon, our S(class) values for sodium fluoride and Havighurst's F^2/Z values for sodium fluoride are shown by curves I, II and III respectively, of Fig. 1. Curve IV shows the values of S(class)$+F^2/Z$ for sodium fluoride. It is seen that, unlike the case of sylvine and argon, the

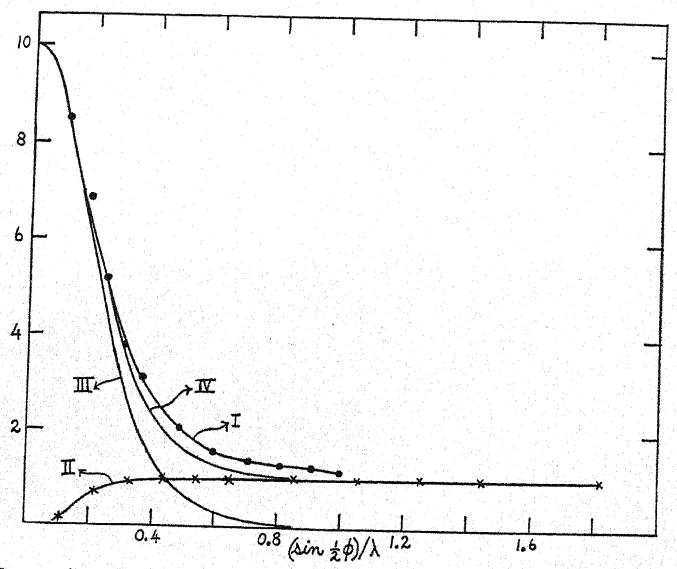


Fig. 1. Comparison of scattering from neon and NaF. Curve I—S(class) for neon (Wollan); Curve II—S(class) for NaF; Curve III—F^2/Z for NaF (Havighurst); Curve IV—S(class) $+F^2/Z$ for NaF.

(S(class)$+F^2/Z$) curve for sodium fluoride falls definitely below the S(class) curve for neon. Wollan's f' values for neon and our f' values for sodium fluoride are shown by curves I and II respectively, in Fig. 2. Comparing these curves, we note that the f' values for sodium fluoride are definitely below those for neon, so that the electron distribution for the average atom in a crystal of NaF is more diffuse than that for an atom of the gas neon. It is reasonable to expect that, when the atoms of a gas are concentrated into a crystal, there should be a distortion of the electron distribution of the atoms. This distortion explains the difference between the f' values for NaF and those for neon and it also explains the difference between the curves I and IV of Fig. 1. We might expect the distortion to be greater in the case of NaF than in the case of KCl, since the nuclear field of an atom in NaF is much weaker than that of an atom in KCl. This explains why there is such good

agreement between argon and sylvine but not such good agreement between neon and sodium fluoride.

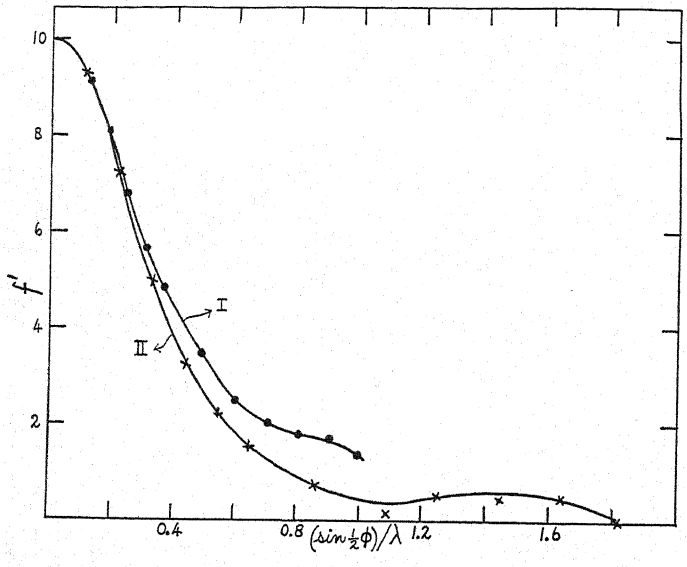


Fig. 2. Comparison of f' values. Curve I—Neon (Wollan); Curve II —NaF (Jauncey and Williams).

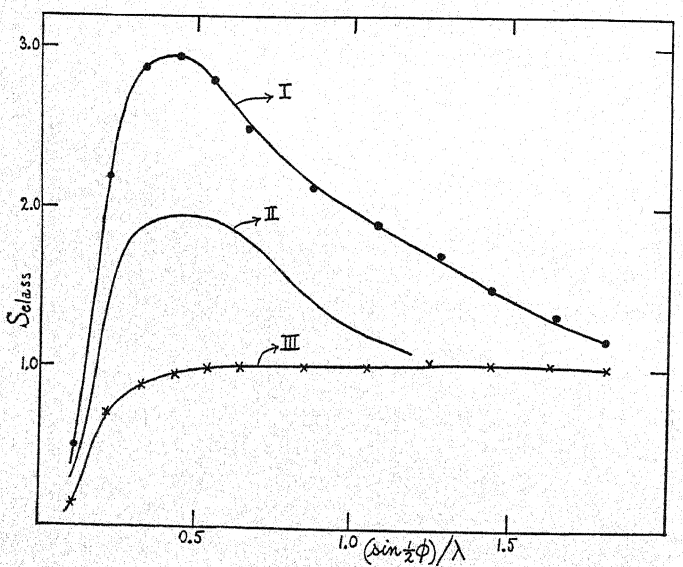


Fig. 3. Comparison of S(class) values for crystals. Curve I—sylvine (Harvey); Curve II—rock-salt (Jauncey and May); Curve III—NaF.

By referring to the seventh column of Table II, it is seen that our B values indicate two humps in the B curve in agreement with the B curve for neon which Wollan gives. It is the presence of the second hump which, according to

Wollan, causes the separation of the K electrons in the Fourier analysis of neon. We may say then that our B values support qualitatively Wollan's finding of a hump for the K electrons of neon in the U curve which he obtains by means of a Fourier analysis of his B curve for neon.

In this connection, the senior author wishes to remark that, as he[4] has already pointed out, the Compton Fourier analysis method in its present form is applicable only if $f'=f$. The senior author is not at present willing to admit that $f'=f$. Indeed, Woo has recently shown that the experimental evidence is rather in favor of $f'\neq f$. Jauncey[4] has shown that $f'<f$ if

$$\left(\sum_r E_r\right)^2 < Z\sum_r E_r^2 \tag{28}$$

which is always the case unless all the E's are equal. All the E's can be equal only if the individual electrons of an atom are indistinguishable from one another as far as the scattering of x-rays is concerned. The senior author is not at present willing to admit that the electrons in an atom are indistinguishable from one another.

V. Comparison with Sylvine and Rocksalt

An interesting comparison of the S curves for sylvine,[12] rocksalt[7] and sodium fluoride is shown by curves I, II, and III respectively of Fig. 3. It is seen that as the average atomic number decreases the hump of the S curve diminishes until in the case of NaF the presence of a hump is by no means obvious.

In conclusion it should be pointed out that we found it necessary to use Woo's formula for the diffuse scattering from crystals in preference to Jauncey and Harvey's formula. For sylvine the scattered radiation is principally coherent so that the classical formula of Jauncey and Harvey is sufficiently approximate. However, in the case of sodium fluoride it is necessary to take account of the fact that a considerable portion of the scattered radiation is incoherent. Woo's separation of the scattered radiation into coherent and incoherent radiation has enabled us to allow for the difference in the absorption of the two kinds of radiation in the ionization chamber, and also for the extra absorption of the incoherent radiation in the crystal itself.

We wish to thank Professor H. M. Randall of the University of Michigan for supplying the crystal of sodium fluoride.

Very Soft X-Ray Spectra of Heavy Elements

By C. DEL ROSARIO
University of Pennsylvania

(Received May 31, 1932)

Absolute wave-length measurements by photographic methods with plane gratings (280 and 1180 lines per mm) have been made on very soft x-ray lines of Th, Pb, Hg, Au, Ir, W and Ta. The wave-lengths range from 43.6A to 104.8A. For Hg, Au, Ir, W and Ta doublets were observed whose probable origins are transitions within the N shell, i.e., $\Delta n = 0$. These doublets fall on a smooth Moseley curve of small curvature.

INTRODUCTION

IN A recent work[1] on very soft x-rays, Thibaud measured the wave-lengths of several emission lines of the N and O series of some elements of high atomic numbers. He showed that, from the ordinary x-ray selection rules and with the energy-level values computed by Bohr and Coster, no electron transition could be selected that could predict accurately the wave-lengths of several lines he obtained by experiment. He suggested the possibility of an electron transition from one orbit to another in the same shell, and he showed a good agreement between the energy changes following such *forbidden* transitions and those experimentally observed. On account of the fundamental character of the principles and facts involved, it was thought desirable to confirm and extend Thibaud's determinations with hope of obtaining additional information on the structure of the outer part of the heavy atoms.

EXPERIMENTAL METHODS

The high absorbability of the radiation to be investigated requires the experiments to be done in vacuo. In the present work photographs of the

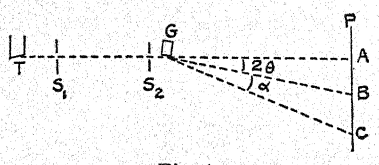


Fig. 1.

x-ray lines were taken with the aid of two vacuum spectrographs of a design resembling in general principles those used by Thibaud[2] and other investigators[3] in soft x-rays. Several variations in details were made, however, with the end in view of possible improvements or simplifications. Fig. 1 shows

[1] Thibaud, Comptes Rendus **188**, 1394 (1929).
[2] Thibaud, Jour. de Physique **8**, 447 (1927).
[3] For instance see: Hunt, Phys. Rev. **30**, 227 (1927); Weatherby, Phys. Rev. **32**, 707 (1928); Howe, Phys. Rev. **35**, 717 (1930); Soderman, Zeits. f. Physik **65**, 656 (1930).

schematically the principle involved in the wave-length measurements. X-rays from the target T pass through the limiting slits S_1 and S_2. Part of the narrow beam thus formed falls on a glass line grating G which reflects and diffracts it, while the rest passes by the grating and falls on a photographic plate P at A. The reflected and diffracted beams fall on the plate at B and C respectively.

The wave-lengths of the lines were calculated from the ordinary diffraction relation

$$n\lambda = D[\cos\theta - \cos(\theta + \alpha)]$$

using the modified form $n\lambda = 2D \sin[(2\theta+\alpha)/2] \sin \alpha/2$ where n denotes the order of the spectrum, λ, the wave-length and D the grating constant. To determine the glancing angle θ, it is necessary to know the position on the photographic plate of that part of the x-ray beam which was reflected and diffracted. This was accomplished by giving to the position of the image of the undeviated beam such correction as to make the wave-lengths of the different orders of a line—e.g., the O $K\alpha$—agree among themselves. This correction was always small. Most of the wave-length measurements were made with the nearest order of this line for comparison.

The glass gratings used in this work have spacing constants of 4.000×10^{-4} cm and 8.476×10^{-5} cm determined with the aid of the 5461A line of mercury. The grating was mounted on a carefully made holder which, by fine screws, can give it rotation about three mutually perpendicular axes besides a horizontal translation perpendicular to the x-ray beam without disturbing the orientation of the grating.

The limiting slits have beveled jaws with fine screws for width adjustment and horizontal displacement perpendicular to the x-ray beam. In addition, both slits can be rotated independently about an axis parallel to the x-ray beam to put them in the same vertical plane.

The photographic plate is held perpendicular to the x-ray beam in a light-tight box with the emulsion side pressed against a rigid metal surface in the box, obviating the necessity of measuring the thickness of the glass backing of every plate to get the grating-to-plate distance. The box is provided with a trap door in the front end which can be opened and closed at will by a magnet outside the spectrograph. One of the boxes used was so constructed that two parallel plates at different distances from the grating could be exposed at the same time. This offered a way to check up the measured distance, grating to plate, the distance between the plates being known. Five inch plates were used in the big spectrograph at about 50 cm from the grating, and lines as far as 10 cm from the undeviated line could be measured. The positions of these lines were obtained from densitometer measurements.

Fogging of the plates due to stray visible light from the hot filament, which gave trouble to some previous investigators, was effectively eliminated by three circular disks. They were bolted to the optical bench, which also carried the slits and grating holder. Two of these disks, each with an opening 1.5×0.2 cm, were placed one in front of each slit; while the third, which had a rectangular opening, part of which was covered with aluminum foils of suitable thickness to cut down the intensities of the undeviated beam and the

reflected beam, was in front of the plate box. The undesirable broadening of the images of the direct and reflected beams was prevented by the aluminum foils.

Figs. 2 and 3 show the construction of the two types of x-ray tubes employed. Copper, iron, lead, bismuth, iridium and gold targets were used, the last four in the form of buttons imbedded in copper. The electron source was a spiral filament of pure tungsten, thoriated tungsten or tantalum. It can

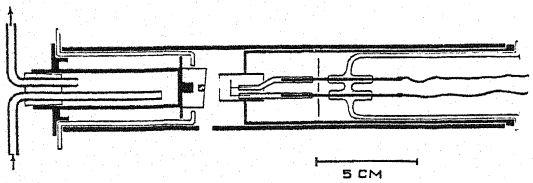


Fig. 2.

be seen that the target can easily be removed from the tube for cleaning or replacement, and put back in its original position. The filament can also be replaced readily. Its position and that of a focussing tube were adjusted by a series of trials to make the focal spot of the most satisfactory size. The wide flange at the outer end of the glass insulator for the target in the metal x-ray tube increases greatly the sparking distance, while the turned-in edges at the inside end keep the inner surface of the insulator free from sputtered metal.

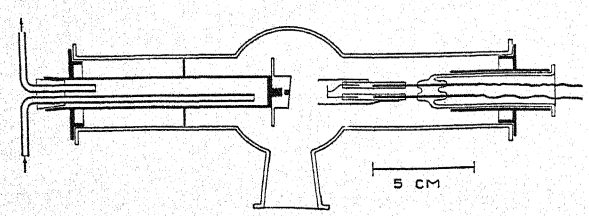


Fig. 3.

The vacuum in the spectrograph and in the x-ray tube was obtained with a Kurth two-stage mercury vapor pump backed by a Cenco Megapump. Voltages ranging from 2500 to 7500 volts were supplied to the x-ray tube by a transformer-rectifier-condenser set connected for full wave rectification. The current through the tube ranged from 30×10^{-3} to 100×10^{-3} ampere, but in no case was the power used more than 300 watts.

Experimental Results

Table I gives the wave-lengths of the observed lines, the corresponding values for ν/R and the probable transitions giving rise to these lines. For comparison, Thibaud's wave-lengths are also listed as well as computed values of ν/R based on Bohr and Coster's table of energy levels.

Discussion of Results

The agreement between the wave-lengths here obtained and those of Thibaud for the same lines is very satisfactory. The two observed lines each

of tantalum, tungsten, gold and mercury seem to form regular or relativity doublets of about 3A separation. The transitions assigned to these lines are identical for these elements but are forbidden by the selection rules, since

TABLE I. *Wave-length of observed lines.*

Element atomic number	Wave-length Present work	Wave-length Thibaud's value	Probable origin	Present work	Bohr and Coster
Tantalum 73	58.3A	58.3A	$N_{iv}-N_{vi}$	15.6	15.6
	61.3	61.4	$N_{v}-N_{vi-vii}$	14.8	14.4
Tungsten 74	56.0	56.0	$N_{iv}-N_{vi}$	16.2	15.9
	59.0	59.1	$N_{v}-N_{vi-vii}$	15.4	15.6
Iridium 77	53.0	—	$N_{v}-N_{vi-vii}$	17.2	—
Gold 79	46.2	46.8	$N_{iv}-N_{vi}$	19.7	20.0
	48.9	49.4	$N_{v}-N_{vi-vii}$	18.6	18.6
Mercury 80	43.6	—	$N_{iv}-N_{vi}$	20.8	—
	46.4	—	$N_{v}-N_{vi-vii}$	19.6	—
Lead 82	84.2	—	$N_{vi}-O_{iv}$	10.8	10.0
	102.3	—	$O_{i}-P_{ii}$	8.9	—
	104.8	—	$O_{i}-P_{iii}$	8.7	—
Thorium 90	50.4	50.3	$N_{vii}-O_{v}$	18.1	18.4
	64.5	64.5	$O_{ii}-P_{i}$	14.1	—
	68.3	68.1	$O_{iii}-P_{i}$	13.3	—

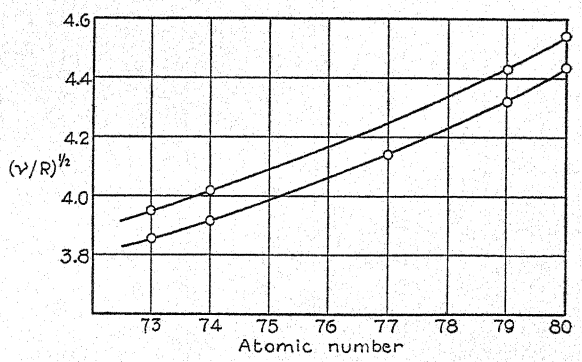


Fig. 4.

here the total quantum number does not change. The nearest values for changes in ν/R allowed by the rules are 1.9 to 2.6 or 9.5 to 17.6 percent smaller than those corresponding to the observed lines which, by the way, are the only ones found for these elements. Fig. 4 shows how closely these doublets follow Moseley's law.

No spectrum line has so far been observed characteristic of bismuth. This is not surprising since its low melting point and poor heat conductivity made it impossible to use a fair amount of power in the x-ray tube and to use a reasonably small focal spot. The lines obtained for iridium, mercury and lead

are believed to have been measured for the first time. There is some doubt about the justification of assigning to mercury the lines at 43.6A and 46.4A. The assignment was made on the basis of known facts for the doublets of tantalum, tungsten and gold. First, the two lines have about the same separation as the other doublets; second, the component of greater wave-length is of greater intensity; third, the plotted points fall close to the Moseley curve for the other elements if the atomic number for mercury is used. The line at 53.0A is probably the more intense line of the doublet for iridium. Why corresponding doublets did not appear in the spectra of lead and thorium is not yet understood; however, a further extension of this work may shed light on this question.

In conclusion I wish to express my thanks to Professor C. B. Bazzoni for his encouragement and suggestions during the progress of the work.

On the Relative Abundances of the Nitrogen and Oxygen Isotopes

By GEORGE M. MURPHY AND HAROLD C. UREY
Department of Chemistry, Columbia University

(Received June 9, 1932)

The absorption spectra of samples of nitric oxide were investigated for the purpose of obtaining the relative abundance of the nitrogen and oxygen isotopes. Nitrogen from four different sources was investigated: air nitrogen, obtained from the Haber and Birkeland-Eyde processes; nitrogen from Pennsylvania coal and from Chili saltpeter. One sample of oxygen was obtained from a Pre-Cambrian magnetite. A method has been described for converting the nitrogen and oxygen from these different sources into nitric oxide. A method of photographic photometry has been applied to the spectra obtained. The procedure for obtaining the relative abundance of the isotopes is discussed together with the possible sources of error. The average of 32 measurements gives for the ratio of $N^{15}O^{16}/N^{14}O^{18}$ the result $0.549 \pm 0.007 : 1$. This gives the value 346:1 for the ratio N^{14}/N^{15}. The isotopic composition of the four samples of nitrogen and two samples of oxygen is constant within approximately 10 percent.

THE relative abundances of isotopes that are present only in small amounts such as those of carbon, nitrogen, oxygen and hydrogen are of great importance for several reasons. Because of the fact that oxygen is chosen as the standard for atomic weight determinations, the relative abundance of its isotopes is required as precisely as possible in order to convert from the chemical scale to the mass spectrograph scale. Recent discussions[1] as to other possible standards for atomic weights, also point out that it is very important to discover whether rare isotopes such as those of oxygen are constant in abundance with respect to samples of oxygen from different sources. Although the constancy of the more common isotopes is fairly well established both for terrestrial elements and for some from meteoric sources, no experiments of this sort have been made for the rarer isotopes mentioned above.[2]

Moreover, spectroscopic determinations of King and Birge[3] on the relative abundance of C^{13} indicate an apparent dependence of this quantity on the method of excitation of the spectra. Three typical sources such as arc, furnace and *N*-type stars, the effective temperatures of which probably decrease in this order, show that the abundance of C^{13} relative to C^{12} increases in the same order.

The detection of rare isotopes in molecular emission spectra seems to be particularly difficult. King and Birge failed to find C^{13} and $C^{13}N^{14}$ in arc spec-

[1] R. T. Birge and D. H. Menzel, Phys. Rev. **37**, 1669 (1931); R. Mecke, Phys. Zeits. **33**, 49 (1932); S. Meyer, Phys. Zeits. **33**, 301 (1932).

[2] Charles A. Bradley, Jr. and Harold C. Urey have investigated the relative abundance of the H^1 and H^2 isotopes in hydrogen samples from different sources and find that any variation in relative abundances is not large. Phys. Rev. **40**, 889 (1932).

[3] A. S. King and R. T. Birge, Astrophys. J. **72**, 251 (1930).

tra. Watson and Parker[4] were not able to observe the oxygen isotopes in the BeO emission spectra and Estey[5] failed to find any indication of the O^{17}, O^{18} or C^{13} atoms in the fourth positive emission bands of CO. Almy and Rahrer[6] failed to find bands due to $O^{18}H$ in the OH spectrum. On account of these as yet unexplained difficulties, it seems that the most reliable determination of the relative abundance can be made from absorption spectra.

The discovery of an isotope of nitrogen of mass 15 and the determination of its abundance relative to N^{14} is due to Naudé[7] who investigated the γ bands of nitric oxide. He redetermined the abundance of O^{16} relative to O^{18}, obtaining $1075 \pm 110:1$. He then determined the ratio of the nitrogen isotopes from the relative intensities of the $N^{15}O^{16}\,{}^{O}P_{12}$ and the $N^{14}O^{18}\,{}^{P}Q_{12}+P_2$ branches of the $(v', v'') = (1, 0)$ band, which he states have nearly the same intensities. Our own investigation shows that this is not the case (see Fig. 1). The results of Naudé are also open to objection because even if these heads were of the same intensity, the $N^{14}O^{18}\,{}^{P}Q_{12}+P_2$ branch is superimposed on the $N^{15}O^{16}\,{}^{O}P_{12}$ branch, so that it is difficult or impossible to determine what part of the absorption is due to each molecule. The determination of Naudé has also been criticized by Mecke and Childs.[8] Using the values of Mecke and Childs for the relative abundance of O^{16}/O^{18}, Naudé's result for N^{14}/N^{15} becomes 409 ± 20 percent. Birge and Menzel have calculated from atomic weight considerations that this figure should be 320.

Because of these considerations, we have thought it worth while to redetermine the relative abundance of the nitrogen isotopes by the methods of photographic photometry. Moreover, we have worked with samples of nitrogen and oxygen from different sources as follows: Nitrogen: (1) from the air by the Haber process; (2) from the air by the Birkeland-Eyde process; (3) from Chili salt-peter; (4) from Pennsylvania coal. Oxygen: (5) from Pre-Cambrian magnetite.

The various samples of nitrogen were selected with the objects (1) of search for any variation of relative abundances of nitrogen isotopes in natural nitrogen samples, and (2) of finding whether any variation might be produced by the electric arc used in the Birkeland-Eyde process. The latter possibility seemed worth testing because of the general failure to observe these rare isotopes in emission spectra. The oxygen sample comes from the Pre-Cambrian magnetite of New York State and has not been a part of the atmosphere of the earth since the time the crust of the earth formed according to the best judgment of geologists.

Preparation of Nitric Oxide

Because of the variety of samples used, the method of preparation of the NO was different in each case. The Haber process nitrogen[9] was in the form

[4] W. W. Watson and A. E. Parker, Phys. Rev. **37**, 167 (1931).
[5] R. S. Estey, Phys. Rev. **35**, 309 (1930).
[6] G. M. Almy and G. D. Rahrer, Phys. Rev. **38**, 1816 (1931).
[7] S. M. Naudé, Phys. Rev. **34**, 1498 (1929); **35**, 130; **36**, 333 (1930).
[8] R. Mecke and W. H. J. Childs, Zeits. f. Physik **68**, 376 (1931).
[9] Kindly furnished by The Grasselli Chemical Company.

of 60 percent nitric acid and presented little difficulty. The gas generating apparatus was part of an all-glass system that also contained the absorption cell which was mounted directly in front of the slit of the spectrograph. This apparatus was first thoroughly swept out with nitrogen. The nitric acid was then allowed to drop into a solution of ferrous sulfate and concentrated sulfuric acid. By gently heating this mixture, the NO gas was evolved and after passing through several traps containing a solid CO_2-alcohol mixture was collected in a trap immersed in liquid air. After all the gas had been collected, this last container was closed from the generator by means of a stopcock and both it and the absorption cell were evacuated. Nitric oxide was admitted into the absorption cell by partially removing the liquid air and allowing it to distill slowly until the desired pressure as read on a manometer attached, was reached. Gas pressures ranging from 1 to 10 cm were used, the most convenient pressure being about 4 cm.

Sample 2 was in the form of "nitrate of lime."[10] This was dissolved in hot water, and Na_2CO_3 solution was then added to convert the calcium nitrate to sodium nitrate. The insoluble material was filtered off and the concentrated solution of sodium nitrate was added to the $FeSO_4$–H_2SO_4 mixture in the same way as described above.

Sample 3 was simply dissolved in H_2O, filtered and then added to the $FeSO_4$–H_2SO_4 mixture.

Sample 4 caused more difficulty as it was furnished to us in the form of ammonium sulfate.[11] Ammonia was liberated by adding NaOH solution. Oxygen was bubbled through this solution and then over an electrically heated platinum spiral where it was converted into oxides of nitrogen. The gases, NO and NO_2, were collected in a trap immersed in liquid air. These gases were then passed into the H_2SO_4–$FeSO_4$ solution by means of a stream of nitrogen and the NO gas collected as before in a liquid air trap.

The method for sample 5 was similar to that for sample 4. The magnetite[12] was first broken into small pieces and the oxygen was removed in the form of H_2O by passing hydrogen over the mineral at about 450°C. The H_2O was collected in a trap placed in a solid CO_2-alcohol mixture. After the addition of about 10 percent of H_2SO_4 it was electrolyzed in a small cell. The gases evolved were collected by displacement of oil from two chambers that had a volume ratio of 2:1 so that the hydrogen and oxygen gases were kept at the same pressure. After the electrolysis was finished, the oxygen was mixed with

[10] We wish to thank the Department of Chemistry of the College of the City of New York for supplying us with the sample of Birkeland-Eyde nitrogen.

[11] The ammonium sulfate was made from coal from the Pittsburgh seam mined in Washington County, Pennsylvania. The coal comes from two mines Vesta No. 4 and No. 5. These two mines are very close to one another but differ slightly in chemical analysis. It was kindly sent to us by Mr. M. W. St. John of the Jones and Laughlin Steel Corporation, Pittsburgh, Penna., whom we would like to thank in this place.

[12] The magnetite was a sample of Pre-Cambrian origin from Fort Henry, New York and came from the collection of the Geology Department of this University through the kindness of Professor Charles P. Berkey.

nitrogen and ammonia and the mixture was passed over the platinum spiral. From this point on the procedure was the same as for sample 4.[13]

Experimental Method

The absorption cell was 50 cm long and 4 cm in diameter and was fitted with two crystal-quartz windows stuck on with deKhotinsky cement.

A hydrogen discharge tube* was used as a continuous source of ultraviolet light. This tube carried about 2 amperes at 2500 volts and was constant in intensity within about 1 percent during an exposure. This was determined by means of a Moll surface thermopile placed at the back window of the tube. The deflections of a galvanometer connected to the thermopile were read continually during the time that was required to put the density marks on the plates. Two crystal-quartz lenses were used, one between the discharge tube and the absorption cell which gave a parallel beam of light through the cell and the second lens brought this light to a focus on the slit of the spectrograph. With this arrangement of lenses, a good exposure of the (1, 0) band could be obtained in one minute while the (2, 0) band at 2051A could be photographed in about five minutes. The Hilger E1 quartz spectrograph was used.

Various kinds of photographic plates were used. At first we sensitized Eastman 33 plates with vaseline or oil dissolved in petroleum ether. We then obtained an ultraviolet sensitizing solution from the Eastman Kodak Company and used this on Eastman 33 plates. These proved quite satisfactory and most of the results in this paper were obtained with them. More recently, we have secured Eastman U.V. spectroscopic plates.[13a] These have been even more convenient than the ones that we sensitized ourselves.

Calibration of Plates

We used two methods of putting density marks on our plates. At first we used a quartz wedge[14] with five steps of sputtered platinum and one clear step. It was calibrated directly on the spectrograph by means of the hydrogen tube and the method of variation of the width of the slit. Because of the irregularities on the surface of the sputtered steps and the uncertainties of the calibration of the wedge for a wave-length so far in the ultraviolet, we thought it desirable to use some other method of obtaining density marks.

We therefore made a set of neutral wire screens.[15] These screens were prepared as described by Harrison and were arranged so that they were kept in motion during use by means of a motor. Screens of this sort must be covered with CuO in order to give them a black surface. The usual method of oxidiz-

* This tube will be described in another place.

[13] We wish to thank Miss Pilar de Madariaga and Mr. S. H. Manian for their aid in working out the method and the preparation of the gas from sample 5.

[13a] C. E. K. Mees, J. Opt. Soc. Am. **21**, 753 (1931).

[14] The method of making these wedges has been investigated by Professor H. W. Webb of the Physics Department of this University. The wedge that we used was very kindly prepared for us by Professor Webb with our assistance.

[15] G. R. Harrison, J.O.S.A. and R.S.I. **18**, 492 (1929).

ing the surface by heating is not very satisfactory since the coat of CuO so formed is not adherent. We have found that the following method gives a good dull surface that is very permanent. The screens were first cleaned by dipping into a so-called mat solution which is used for producing a dull surface on articles that are to be electroplated. They were washed quickly and dipped into a boiling solution containing 1 percent potassium persulfate and 5 percent sodium hydroxide.* After the surface was black enough, they were washed and dried.

We had four screens, combinations of which would give 10 density marks. They were calibrated by means of the thermopile mentioned above and also by means of a photoelectric cell with a large tungsten lamp running on a constant source of alternating current. The results from the two methods of calibration are given in Table I.

TABLE I. *Transmission of screens.*

Screen	Photoelectric cell	Thermopile	Average
1	73.4	74.5	74.0
2	45.5	45.7	45.6
1+2	34.5	34.6	34.6
3	32.5	32.1	32.3
1+3	24.2	24.3	24.2
4	17.8	17.5	17.6
2+3	16.6	16.9	16.8
1+4	14.6	14.8	14.7
2+4	8.6	8.1	8.4
3+4	6.5	5.9	6.2

A Moll recording microphotometer was used to determine the density of the calibration marks on the plates and of the two isotopic band heads. Since the transmission of the wedge or screens was known, a curve of log i *vs.* d could be plotted by means of the relation

$$\log_{10} O = d = \log F_0/F \tag{1}$$

where O is the opacity, d is the density and F_0 and F are intensities of light transmitted by the unexposed and exposed parts of the plate respectively. Moreover

$$d = \log g_0/g \tag{2}$$

where g_0 and g are the throws of the galvanometer for an unexposed part of the plate and for one of the density marks, put on through a screen whose transmission was known.

The intensity of the isotopic bands could be determined by means of Beer's law

$$\log i_x - \log I = -kcx \tag{3}$$

where i_x and I are the intensities of the light transmitted by a layer of gas of thickness x and the incident radiation respectively; k is the molecular absorption coefficient and c is the molecular concentration.

* See: Electro-Deposition of Metals, 9th Edition, Langbein-Brannt, p. 278, 629, New York: Henry Carey Baird and Co., 1924.

The situation in the actual case is somewhat more involved because of the fact that bands are sometimes superimposed and that other absorbing molecules may be present, such as NO_2, for example. Then Eq. (3) must be replaced by

$$\log (i/I) = -(k_1c + k_2)x \tag{4}$$

where k_1 is the molecular absorption coefficient and k_2 is the absorption coefficient due to other molecules which may be present. We assume that k_1 is the same for the same branches of the different isotopic molecules. But we cannot determine the value of I, since we do not have any point on the plate, where we are certain that there is no absorption due to extraneous molecules or superimposed bands. To avoid this difficulty we extrapolate the microphotometer curves as shown by the broken lines of Fig. 1. This gives an estimate of $\log i/I$, if k_1 were zero. Then we have

$$\log (i/I) - \log (i_0/I) = -(k_1c + k_2)x + k_2x = -k_1cx \tag{5}$$

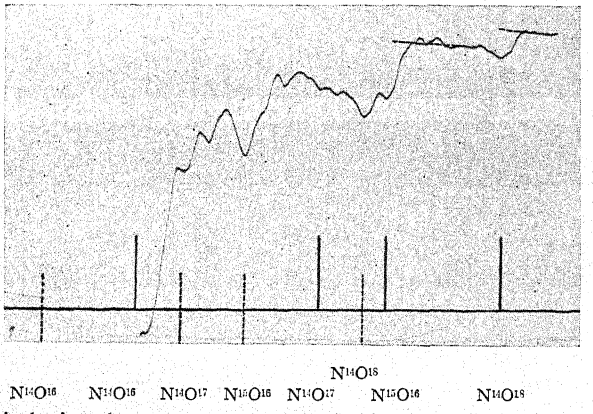


Fig. 1. A typical microphotometer curve of the (1, 0) γ-band of nitric oxide. The heads due to the different isotopic molecules are indicated. The full lines are the ${}^0P_{12}$ heads and the broken lines are the $({}^PQ_{12}+P_{12})$ heads.

where i_0 is the intensity (extrapolated) of the light which would have been transmitted if the band were not present. This equation reduces to

$$\log (i/i_0) = -k_1cx \tag{6}$$

which is identical in form with Eq. (3).

Since k_1 and x are the same for the isotopic molecules

$$\log (i'/i'_0) - \log (i''/i_0'') = c'/c'' \tag{7}$$

where the primes refer to the quantities for the first and second molecules respectively.

These quantities are related to throws of the galvanometer by the relation

$$d = \log g_0 - \log g = f(\log i) \tag{8}$$

where g_0 is again the throw at a clear part of the plate and g is now the galvanometer throw at a band head or the estimated throw if the band were not present. In all cases our densities fell on the straight line portion of the d *vs.* $\log i$ curve and for this region

$$d = \gamma \log i + a. \tag{9}$$

A typical calibration curve is shown in Fig. 2. By using Eq. (9), we have

$$\gamma \log (i'/i_0') = d' - d_0' \tag{10a}$$

and

$$\gamma \log (i''/i_0'') = d'' - d_0'' \tag{10b}$$

where d and d_0 refer respectively to the density at the band head and the extrapolated density and the primes and double primes refer to the light and heavy isotopic molecules, respectively. These four points are indicated for a typical case on Fig. 2.

Taking the ratio, we secure the ratio of concentrations

$$\frac{\log i'/i_0'}{\log i''/i_0''} = \frac{d' - d_0'}{d'' - d_0''} = c'/c''. \tag{11}$$

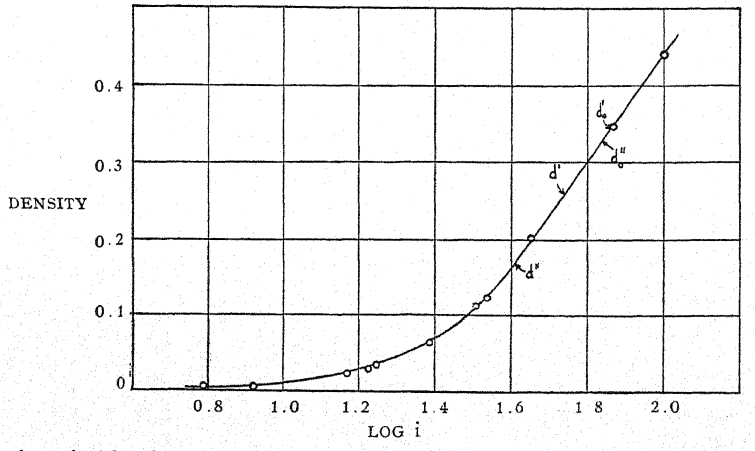


Fig. 2. A typical log i *vs.* density curve. The points indicated with arrows are those obtained from the microphotometer curves of the spectra and used for determining the ratio.

In this way we have compared the relative intensities of the ${}^0P_{12}$ branches of $N^{14}O^{18}$ and $N^{15}O^{16}$. Although the $N^{15}O^{16}$ ${}^0P_{12}$ branch is superimposed on the $N^{14}O^{18}$ ${}^0P_{12}$ branch, they are well separated by the spectrograph and it is therefore possible to estimate the contribution of each molecule to the absorption. A typical microphotometer curve is shown in Fig. 1, where the eight band heads due to the two branches and the four molecules are in-

TABLE II.

Source of sample	Number of microphotometer curves	Ratio $N^{15}O^{16}/N^{14}O^{18}$
Haber process	17(a)	0.54 ± 0.05
Coal	9(a)	0.56 ± 0.08
Birkeland-Eyde	4(b)	0.52 ± 0.08
Chili salt-peter	4(b)	0.56 ± 0.09
Haber	8(b)	0.58 ± 0.06
Pre-Cambrian	6(a)	0.54 ± 0.06

(a) Plates calibrated by means of screens.
(b) Plates calibrated by means of wedge.

dicated. The results from the four samples of nitrogen and the sample of oxygen are given in Table II.

Source of Error

The error given which is the root mean square represents only the error, if no systematic error is present. The possible errors are:

(1) The lines at the head of these bands may not give a true continuous absorption so that Beer's law may not hold. We have used gas pressures up to 10 cm of NO hoping that the lines would be somewhat broadened in this way. We have also added N_2 up to one atmosphere total pressure for the same purpose but in neither case was there any essential difference in the appearance of the microphotometer curves.

(2) It is not certain that there are no superimposed bands of $N^{14}O^{16}$. We had thought to eliminate this difficulty by working with the (2, 0) band but unfortunately a Si emission line from our hydrogen tube falls almost on top of the $N^{14}O^{18}$ $^OP_{12}$ band head. Moreover, the $^OP_{12}$ and $^PQ_{12}+P_2$ branches overlap here so we cannot allow for the continuous background.

Our most reliable determinations are those marked *a* in Table II since we have more confidence in the results from plates that were calibrated with the wire screens. The average from these thirty-two microphotometer curves is 0.549 ± 0.007 for the ratio of $N^{15}O^{16}:N^{14}O^{18}$. Because of the difficulties mentioned above, this result may be in error by more than the probable error quoted. But it seems certain that the possible source of error mentioned under 2 would be the same from sample to sample. Therefore, a change in the relative abundance of the isotopes of oxygen or nitrogen would have been detected. We feel safe in concluding that the isotopic composition of nitrogen and oxygen in the samples investigated is constant within approximately ± 10 percent.

Using Mecke and Child's[8] value for the ratio of $O^{16}:O^{18}=630:1$, we get for the ratio of N^{14} to N^{15}, the value 346:1 in satisfactory agreement with the ratio of 320:1 required by Birge and Menzel. This means that Aston's value for the atomic weight of N^{14} on the basis of $O^{16}=16.0000$ is consistent with the chemical value.

We wish to thank the Physics Department of this University and Professor H. W. Webb in particular for the use of the quartz spectrograph used in this investigation. We are also indebted to the Chemistry Department of New York University and to Mr. R. L. Garman in particular for the microphotometer curves.

Note added in proof. Herzberg (Zeits. f. physik. Chem. **B9,** 43 (1930)) has determined 800:1 for the ratio of N^{14} to N^{15} from the relative exposure times for the second positive nitrogen bands obtained in emission in an electrodeless discharge. This result differs from ours in the same direction as that of other workers for emission spectra compared with absorption spectra. Until this peculiarity is explained, relative abundances of isotopes obtained from absorption measurements seem more certain in view of the fact that the results in absorption make the values of Aston more consistent with the chemical results.

Mass-Spectrograph Study of the Ionization and Dissociation by Electron Impact of Benzene and Carbon Bisulfide

By ERNEST G. LINDER*
Cornell University, Ithaca, N. Y.
(Received June 9, 1932)

Benzene (C_6H_6) and carbon bisulfide (CS_2) have been analyzed by a mass-spectrograph designed especially for use with large molecules. In the case of benzene, ions have been found containing carbon in amounts from C_1 to C_6 with various amounts of hydrogen attached. The principal ion for electrons of 120 e-volts is $C_6H_6^+$. No negative ions and no H^+ ions were detected. Impacts of positive ions in the ionization chamber detach H atoms from the carbon ring, but the carbon content of all observed ions seems to be unaffected by such collisions. The carbon-to-carbon bonds appear to be more stable than in the straight-chain hydrocarbons. Carbon bisulfide was used principally to calibrate the mass scale, and no extensive work done on it. At a pressure of 9.7×10^{-3} mm Hg and impacts of 120 e-volts, the ions observed were CS_2^+, CS^+, S^+, and C^+.

THE only work which appears to have been done with the mass-spectrograph on large hydrocarbon molecules is that of Stewart and Olson,[1] who studied the straight-chain paraffins, propane (C_3H_8) and butane (C_4H_{10}). The present work on benzene (C_6H_6) was undertaken for the purpose of determining the behavior of a typical member of another important class of hydrocarbons, the aromatics, which are built up of rings of six carbon atoms, instead of straight chains, and therefore might be expected to exhibit a different sort of behavior in regard to dissociation by electron impact. The question was of interest to the writer in connection with studies of chemical reactions in electrical discharges, and that particular application of the data will be published in some chemical journal.

APPARATUS AND PROCEDURE

Large molecules introduce additional difficulties to mass-spectrograph technique. High resolving power at large molecular weights is necessary, which requires the use of strong electric and magnetic fields, and slits as narrow as possible. The intensity is usually low because of the narrowness of the slits, and also because the ions are spread out over a large number of peaks. Furthermore, thermal dissociation at the filament must be eliminated, this problem being more acute with large molecules since they are in general more readily decomposed by heat.

Mass-spectrographs designed to eliminate thermal effects have been described by Stewart and Olson,[1] and Smyth and Stueckelberg.[2] In both these

* Detroit Edison Research Associate. The work described in this article is a part of an investigation of the fundamentals of the disintegration of organic dielectrics. It is supported by a fund provided by the Detroit Edison Company.

[1] Stewart and Olson, J.A.C.S. **53**, 1236 (1931).

[2] Smyth and Stueckelberg, Phys. Rev. **36**, 472 (1930).

apparatuses differential pumping was employed, the gas to be analyzed being introduced into the ionization chamber through a capillary and pumped out through two narrow slits, one opening into the magnet chamber and the other into the filament chamber. High speed pumps kept the pressures in these latter two chambers extremely low. Thus high pressure gradients at the slits were maintained, against which it seems very unlikely that any dissociation products formed at the filament could diffuse back into the ionization chamber. Thermal effects were decreased also by the use of low temperature, oxide-coated filaments.

Stewart and Olson give data indicating that thermal dissociation products were thus eliminated from the ionization chamber of their apparatus. The writer's mass-spectrograph was closely modelled after theirs, and the slit dimensions and pressure ranges employed were the same. It is therefore unlikely that thermal dissociation has appreciably affected the data given here. The similarity of the two apparatuses also renders comparison between the results more reliable.

For all of the data reported here a potential of 53 volts was used for drawing the ions out of the ionization chamber, the accelerating potential was about 515 volts. The radius of the ion path in the magnet chamber was 6.95 cm. The pressure in the magnet chamber was of the order of 10^{-5} mm Hg, while that in the ionization chamber was varied over the range from 10^{-3} to 80×10^{-3} mm Hg. This latter variation was effected, sometimes by changing the size of the capillary through which the gas was admitted, and sometimes by placing cooling baths of different temperatures around the bulb of liquid from which the vapor was drawn.

The benzene was purified as follows. Kahlbaum's thiophene free benzene was shaken six times with concentrated sulfuric acid. It was then washed with concentrated sodium hydroxide, with dilute sodium hydroxide, and finally with water until the wash water was neutral to litmus. It was dried over metallic sodium for 48 hours, and then distilled from the sodium. Then it was distilled three times, the middle fraction being taken each time. After being placed in the mass-spectrograph it was distilled twice in vacuum to remove dissolved gases. The carbon bisulfide used was Eimer and Amend's C. P. It was not treated in any manner before use.

In making the runs, the magnetic field was varied rather than the accelerating potential, on account of the unusually great mass range to be explored. The procedure was followed of starting with zero magnetic field and going up to the maximum necessary without reversals. This was done in order to get a more uniform mass scale. Reversals would introduce irregularities due to hysteresis and residual magnetism. At best however, it was found extremely difficult to avoid small accidental reversals due principally to heating of the rheostats and magnet coils. The field also appeared to vary appreciably with the temperature of the magnet core. Hence in general, the mass scale is not quite uniform. However all uncertainty in regard to the masses corresponding to the great majority of the peaks is removed by the calibration of the scale by means of the carbon bisulfide peaks.

Data and Discussion

A typical curve showing the various ions found is given in Fig. 1. For this run the energy of the impacting electrons was 120 e-volts, the pressure in the ionization chamber was 3×10^{-3} mm Hg, and that in the magnet chamber, 2.7×10^{-3}. Each peak is labeled with the formula of the ion to which it corresponds. No negative ions and no H^+ ions were observed, in agreement with the results of Stewart and Olson[1] on propane and butane, and that of Hogness and Kvalnes[3] on methane.

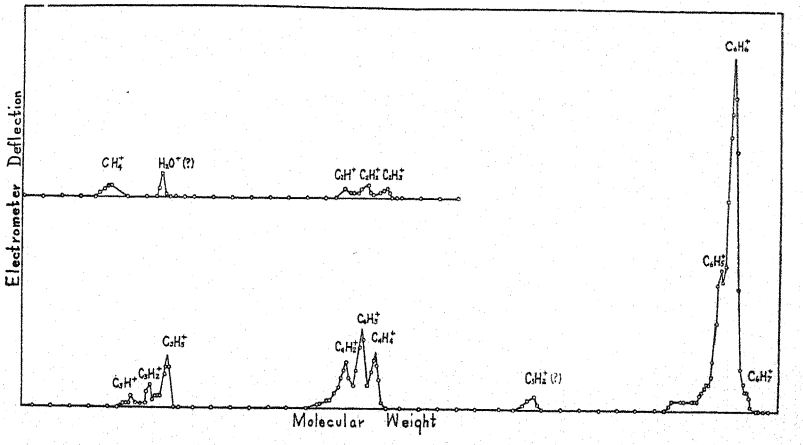


Fig. 1. Ions formed in benzene (C_6H_6) by 120 e-volt electrons.

In Table I is given the variation of ion percentage with pressure in the ionization chamber. A considerable number of runs were made in which measurements were taken only on the three largest groups of ions, i.e., the

Table I. *Percentages of ion groups formed by electron impacts in benzene at various pressures.*

Ion Group	Pressure (mm Hg$\times10^3$) 3.0	3.8	4.3	31.0
6C	71.5%	85.2%	57.0%	58.7%
5C	1.9	1.0	4.8	6.8
4C	16.1	9.9	21.6	23.7
3C	6.5	3.9	7.4	7.0
2C	3.3	0.0	4.4	1.8
1C	0.7	0.0	4.8	2.0

6C, 4C and 3C groups. The ion percentages for these three groups only (on the basis of 100 percent for the three groups only) are plotted in Fig. 2. These ion percentages were all determined by measuring the areas under the peaks with a planimeter, and correcting for the nonlinearity of the mass scale.

The scattering of the points in Fig. 2 is due principally to the difficulty of maintaining constant experimental conditions during the approximately two-hour period required to explore the large mass range. In spite of this scatter-

[3] Hogness and Kvalness, Phys. Rev. **32**, 942 (1929).

ing it is quite evident that the carbon content of these ions does not vary markedly with pressure. Likewise the hydrogen content was found not to vary, with the exception of the 6C group.

The variation of the shape of the 6C group with pressure is shown in Fig. 3. It will be observed that the structure on the left side of the peak increases with increasing pressure. This indicates that impacts made by the ions in the ionization chamber cause H atoms to be stripped from the carbon ring. The small peak corresponding to the molecular weight 79, which appeared in all the runs, is likely due to the attachment of a hydrogen atom to the $C_6H_6^+$ ion.

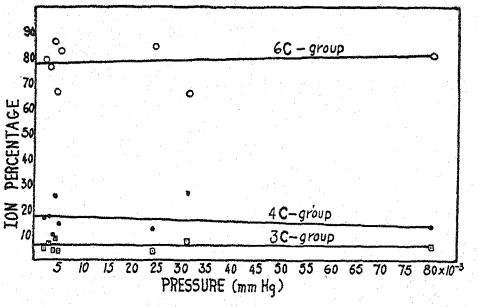


Fig. 2. Variation of ion percentage with pressure for benzene.

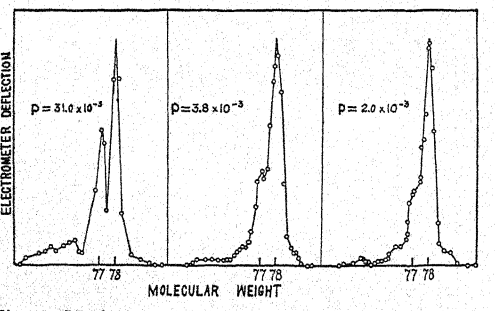


Fig. 3. Variation of 6C peak shape with pressure.

Attempts to determine critical potentials were unsuccessful due to low intensity. All that can definitely be concluded is that the appearance potential for the 6C peak is less than 40 volts.

In contradistinction to the results of Stewart and Olson[1] on normal paraffin hydrocarbons, the principal ion for benzene is a complete benzene molecule. For the paraffins, these authors found a very extensive dissociation into almost all possible lighter hydrocarbons, the ion corresponding to the entire original molecule being but a small percent of the total ions formed. Unfortunately they do not state the impacting energy of their electrons, but preliminary results of the writer's on octane, another straight-chain hydrocarbon, with 120 e-volt electrons, also show this extensive breaking up of the molecule. Thus it appears that straight carbon chains break up under electron bombardment more readily than does the six carbon ring.

This stability of the benzene ring may be partially due to the fact that in

order to divide a ring into two parts it is necessary to break it in *two* places, whereas to divide a straight chain into two portions it is necessary to break it in only *one* place. However the stability of benzene is doubtlessly due to other factors than this, since there are other six carbon ring compounds, e.g., cyclohexane, which are known from chemical evidence not to be nearly so stable as benzene.

A similar stability of the benzene ring in comparison with the paraffins has long been known in chemical reactions induced by heat,[4] and in various types of electrical discharges.[5] The reactions of benzene induced by these agents consist principally of polymerization and condensation, i.e., of the building up of more complex compounds by the adding together of benzene ring units with or without the evolution of a small amount of hydrogen. On the other hand, it is known that the normal paraffins under similar experi-

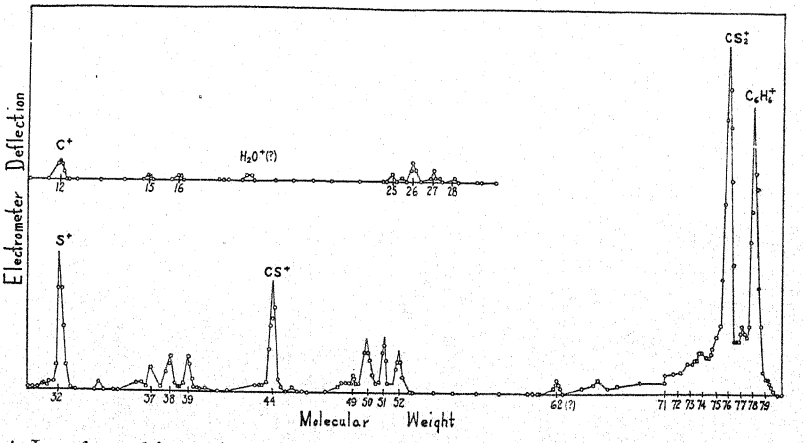


Fig. 4. Ions formed in a mixture of benzene and carbon bisulfide by 120 e-volt electrons.

mental circumstances suffer much more dissociation, and a much larger portion of the products are of a gaseous nature than in the case of benzene; see, for example, the work of Linder and Davis.[5]

The purpose of the runs with carbon bisulfide was to calibrate the mass scale and thus indentify the benzene peaks. However, since this compound seems not to have been investigated previously the data are of interest in themselves. The peaks observed are shown in Fig. 4 along with the benzene peaks. For this run the pressure was 9.7×10^{-3} mm Hg. The principal ion is CS_2^+, but peaks for S^+, CS^+, and C^+ are also present.

In conclusion the author wishes to express his thanks to the Cornell Physics Department for the laboratory facilities provided, and to Professor Vladimir Karapetoff, who is in general charge of the above-mentioned research program on dielectrics. He wishes especially to acknowledge his indebtedness to the President of the Detroit Edison Company, Mr. Alex Dow, and the Chief of Research, Mr. C. F. Hirshfeld, for the financial support of the above work and for permission to publish the results.

[4] Hurd, Pyrolysis of Carbon Compounds, Amer. Chem. Soc. Monograph No. 50.

[5] Linder and Davis, Jour. Phys. Chem. **35**, 3649 (1931).

Elastic Electron Scattering in Helium

By A. L. HUGHES,* J. H. MCMILLEN AND G. M. WEBB
Washington University, St. Louis

(Received June 4, 1932)

The scattering of electrons by helium atoms was measured experimentally over an angular range from 15° to 150° for electrons varying in speed from 25 to 700 volts. The scattering curves all fall steeply with angle, especially so for the smaller angles, provided that the speed is above 100 volts. For speeds below 100 volts, the steep fall at small angles is followed by a gentle rise beginning near 90°. Within the range cited, no maxima in the angular scattering curves were found. The theory of Mott accounted for the 700 and 500 volt curves accurately over the whole range, and for the 350 volt curve, over the range 20° to 100°. Below 20° the experimental curve was steeper than the Mott curve, and above 100° the experimental curve was flatter than the Mott curve. As we go to lower energies, the departures from the Mott curve increase progressively. For small angles the theoretical curve is not steep enough and for large angles it is too steep. The results were also compared with the theory developed by Massey and Mohr taking into account certain factors omitted by Mott. While the newer theory accounts qualitatively for the upturn in the angular scattering curve, it fails to give its correct shape. It is shown how atomic structure factors, or F values, which are employed in the theory of x-ray scattering, can be inferred from these experiments in electron scattering.

THE scattering of electrons by helium atoms has been investigated by a number of physicists. Dymond and Watson,[1] who studied the angle distribution of 210 volt electrons between 5° and 60°, established the fact that the scattering curves for elastic collisions were considerably less steep than they would have been had the scattering been due solely to the attraction of the nucleus of the atom for the electron passing by it. Results of the same general type were obtained by Harnwell,[2] who investigated the scattering of electrons at three angles, 0°, 8°, and 16°, with electron energies varying between 75 and 300 volts. McMillen[3] obtained curves for the scattering of electrons by helium atoms, the angle range being from 7° to 60° and the electron energies varied from 50 to 150 volts. According to his results, the scattering curves fall off more steeply with the angle the higher the energy of the electrons. A discussion of the results obtained by McMillen, Harnwell, and by Dymond and Watson, and their connection with the theories put forward by Sommerfeld, Mott and Mitchell, will be found on page 1043 of McMillen's paper. Investigations of the scattering of electrons at a fixed angle (90°), as the energy of the electrons was varied, have been made by Kollath[4] and by

* This work was made possible by assistance to the senior author from a grant made by the Rockefeller Foundation to Washington University for research in science.

[1] E. C. Dymond and E. E. Watson, Proc. Roy. Soc. **A22**, 571 (1929).
[2] G. P. Harnwell, Phys. Rev. **33**, 559 (1929).
[3] J. H. McMillen, Phys. Rev. **36**, 1034 (1930).
[4] R. Kollath, Ann. d. Physik **87**, 259 (1928).

Werner.[5] Kollath's measurements and Werner's measurements were for the ranges 1 to 36 volts, and 40 to 300 volts, respectively. A considerable extension in the angular range was effected by Bullard and Massey[6] who studied the elastic scattering of electrons by helium, between 20° and 140° for energies varying from 4 to 50 volts. The new features in the scattering curves found by them are that, when the electrons have energies between 20 and 50 volts, the curves become practically flat between 90° and 140°, and that, when the energies are reduced below 10 volts, there is a decided rise in the curves from about 70° to 140°. Ramsauer and Kollath[7] made very extensive measurements of the scattering over a range extending from 15° to 167° for slow electrons (1.8 to 19.2 volts). In marked contrast to the scattering for faster electrons (e.g., above 50 volts), they found but little scattering at small angles (0° to 30°), then a gradual rise to a maximum (at 90° for 19 volt-electrons, and at 110° for 1.8 volt electrons) and after that a slow decrease. The theoretical papers which we have found useful in discussing our experimental results are those of Mott[8] and of Massey and Mohr.[9]

Mott's theory leads to the result that the number of electrons scattered elastically at any angle should decrease monotonically with increasing angle. However, Arnot[10] found that in many cases this was not true; the scattering curves fall steeply as the angle is increased to somewhere between 70° and 100°, but for larger angles the curves often pass through well-marked maxima and minima. These maxima and minima fade out as the speed of the electrons is increased. Now the speed at which these maxima and minima fade out appears to be higher, the greater the atomic number of the atom under investigation. It would appear therefore that the maxima and minima should vanish at comparatively low electron energies when helium is used to scatter the electrons. As Arnot did not include helium in his comprehensive study of electron scattering in gases and as Bullard and Massey did not use electrons of energy higher than 50 volts, it appeared to be very desirable to make a study of electron scattering in helium over a wide range of energies and angles.

Experimental Method

The method of measuring the scattering of electrons by helium was very much the same as that employed by us in our studies of scattering in argon[11] and in hydrogen.[12] However, a new apparatus was constructed in which the analyzer and the collision chamber were made small enough to allow both of them to be put inside a glass tube 4.25 inches in diameter, so that they could be well outgassed if necessary. The new apparatus was designed chiefly to allow us to investigate another aspect of the general problem of scattering,

[5] S. Werner, Proc. Roy. Soc. **A134**, 202 (1931).
[6] E. C. Bullard and H. S. W. Massey, Proc. Roy. Soc. **A133**, 637 (1931).
[7] C. Ramsauer and R. Kollath, Ann. d. Physik **9**, 756 (1931); **12**, 529 (1932).
[8] N. F. Mott, Proc. Roy. Soc. **A127**, 658 (1930).
[9] H. S. W. Massey and C. B. O. Mohr, Proc. Roy. Soc. **A132**, 605 (1931); **A136**, 289 (1932).
[10] F. L. Arnot, Proc. Roy. Soc. **A133**, 615 (1931).
[11] A. L. Hughes and J. H. McMillen, Phys. Rev. **39**, 585 (1932).
[12] A. L. Hughes and J. H. McMillen, Phys. Rev. **41**, 39 (1932).

but it happened also to be very suitable for investigation of elastic scattering in helium. A detailed description of the apparatus is postponed to a later paper. Pure helium was prepared by passing helium from a tank through charcoal in liquid air into a reservoir. From the reservoir the helium passed through a fine capillary tube and then through another tube of charcoal in liquid air into the apparatus, from which it was pumped out continuously. It was possible to use pressures as high as 0.02 mm because of the two factors which worked together, (1) the small dimensions of the apparatus and (2) the long mean free path of electrons in helium.

The experimentally-measured scattering coefficients are given in Table I. By the scattering coefficient we mean, as in our previous papers, the number of electrons scattered in a direction θ from that of the original beam, through unit solid angle, per unit length of path of the original beam, per single electron in the beam, per single atom in unit volume.

TABLE I. *Scattering coefficients* $\times 10^{+20}$.

700 volts		500 volts		350 volts		200 volts	
7°	1597.0	9.5°	1195.0	11°	2088.0	11°	3192.0
9.5°	1307.0	12°	1047.0	16°	1183.0	13.5°	2367.0
12°	914.0	22°	467.0	21°	717.0	16°	1930.0
17°	541.0	27°	284.5	26°	469.0	21°	1285.0
22°	272.0	37°	148.2	31°	334.0	26°	728.0
27°	182.0	47°	60.5	41°	160.0	31°	624.0
37°	65.8	57°	30.76	51°	90.1	41°	292.3
47°	30.7	67°	15.88	61°	53.1	51°	176.6
57°	15.5	77°	11.41	71°	36.7	61°	113.9
72°	8.12	87°	6.14	81°	23.4	71°	82.0
87°	5.10	107°	5.56	91°	27.1	81°	55.85
102°	3.97	127°	4.36	106°	8.3	91°	50.4
117°	3.56	137°	2.87	136°	7.4	101°	39.45
132°	3.44	147°	1.51	151°	8.4	111°	31.65
147°	1.54					121°	29.00
						131°	28.50
						141°	27.9
						151°	25.8
100 volts		75 volts		50 volts		25 volts	
14°	3121.0	17°	3010.0	12°	3570.0	15°	2430.0
19°	2097.0	22°	2145.0	17°	2505.0	20°	1852.0
24°	1550.0	27°	1547.0	22°	1732.0	25°	1325.0
29°	1055.0	37°	844.2	27°	1320.0	35°	1012.0
39°	660.2	47°	557.0	37°	827.0	45°	791.0
49°	451.0	57°	402.0	47°	615.0	55°	693.0
59°	307.5	67°	301.0	57°	410.2	65°	588.0
69°	201.5	77°	233.0	67°	347.5	75°	560.0
74°	169.7	87°	189.0	77°	280.2	85°	513.0
79°	159.7	97°	159.2	87°	242.0	95°	513.0
89°	116.8	117°	160.5	97°	208.0	105°	523.0
99°	103.2	127°	161.0	107°	205.0	115°	545.0
109°	100.2	137°	162.0	117°	205.0	125°	576.0
119°	86.0	142°	159.5	127°	214.5	135°	609.0
129°	85.4	147°	174.0	137°	222.2		
139°	83.7			142°	210.7		
149°	74.8						

The results are also shown graphically in Figs. 1 and 2. Two diagrams are necessary to avoid undesirable crowding of the curves. The heavy black lines

are the smoothed experimental curves and the experimental points through which they were drawn are indicated in an appropriate manner. When the heavy line is continuous it means that the experimental curve coincides with Mott's theoretical curve. When the heavy line is broken, it indicates that Mott's theoretical curve and the experimental curve no longer coincide. In this case the theoretical curve is shown as a *light continuous* line. Finally, where comparison is possible with the recent theoretical curves of Massey and Mohr,[13] these theoretical curves are indicated by a *light broken* line. The Mott curves are given by the formula

$$\alpha(\theta, v) = [(e^2/2mv^2)(Z - F)\ \mathrm{cosec}^2\,\theta/2]^2$$

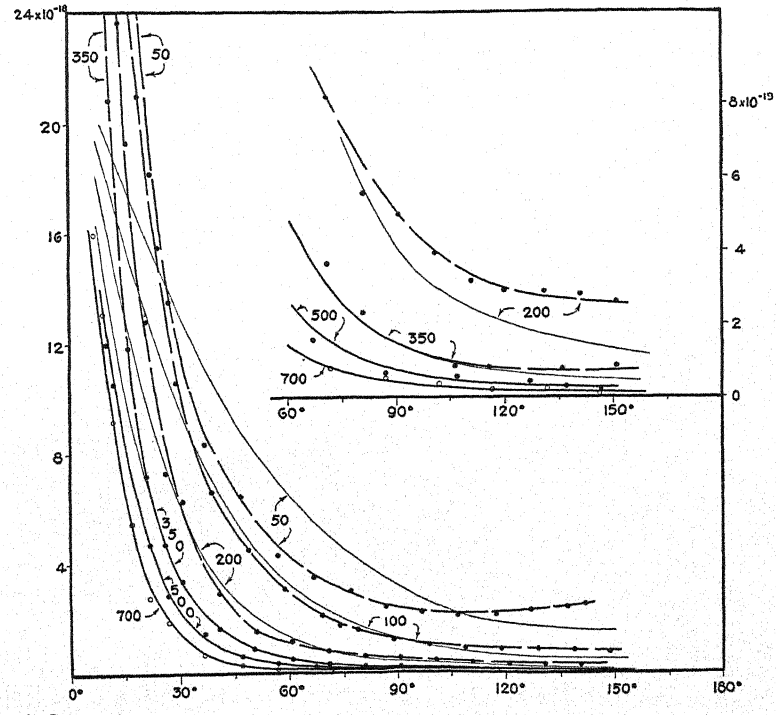


Fig. 1. Scattering of electrons by helium atoms. Angular distributions for 700 to 50 volt electrons. *Heavy continuous* lines: for experimental curves coinciding with Mott's theoretical curves. *Heavy broken* lines: for experimental curves not coinciding with Mott's theoretical curves. *Light continuous* lines: Mott's theoretical curves. *Inset:* Magnified diagram for the range 60 to 150 degrees.

where e, m, v are the charge, mass, and velocity of the electron, Z the atomic number of helium, θ the angle of scattering and F the atomic structure factor. F values for use in computing the formula were kindly supplied to us by Mr. Mott. Since then, they have been published in a paper by James and Brindley.[14] It was found that the 700 and 500 volt experimental curves fitted

[13] H. S. W. Massey and C. B. O. Mohr, Proc. Roy. Soc. **A132**, 605 (1931); **A136**, 289 (1932).

[14] R. W. James and G. W. Brindley, Phil. Mag. **12**, 81 (1931). The F values above 1.1μ were obtained by extrapolation according to the method outlined by D. K. Froman (Phys. Rev. **36**, 1339 (1930)).

Mott's formula exactly over the whole range. It will be seen that there is a slight departure from Mott's formula for the 350 volt curve at small angles and at large angles. For angles between 20° and 100° the coincidence is good. As we go to lower energies, the departure from the Mott formula becomes more and more marked. We do not show the Mott curve for the smallest electron energies, because the disagreement becomes too great to allow us to regard the theory as more than a very rough approximation to the experimental facts.

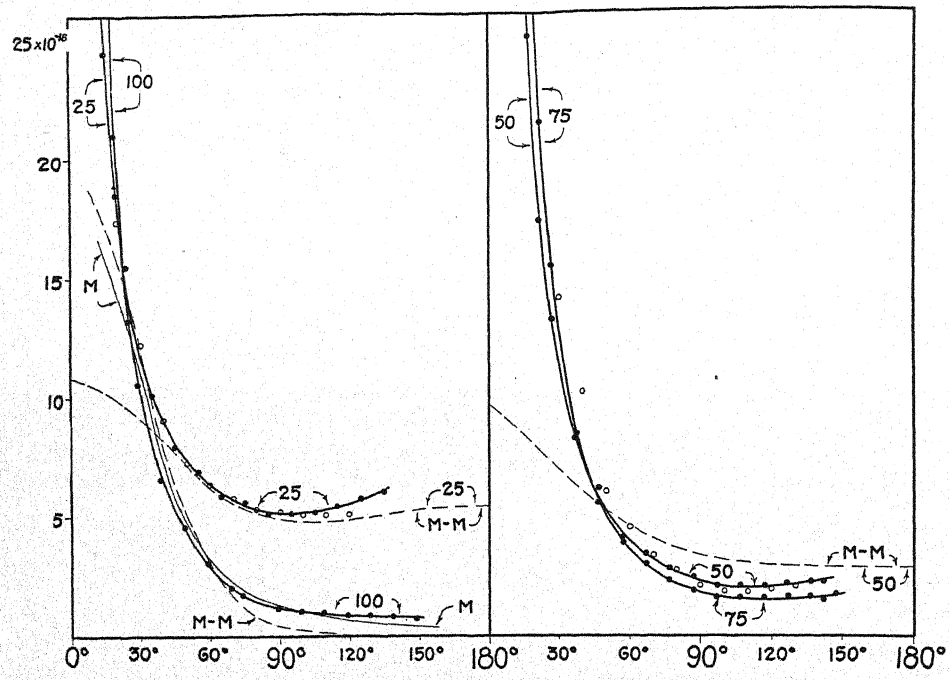


Fig. 2. Scattering of electrons by helium atoms. Angular distributions for 100 to 25 volt electrons. *Heavy continuous* lines: experimental curves. *Dots*: our experimental points. *Circles*: Bullard and Massey's experimental points (for the 50 and 25 volt curves only). *Light continuous* line: Mott's theoretical curve (for 100 volts). *Light broken* lines: Massey and Mohr's theoretical curve (for 25, 50 and 100 volts).

It should be emphasized that all the experimental curves and all the Mott curves shown in Figs. 1 and 2 are accurately drawn to the same scale. There was but one arbitrary adjustment (since our experimental arrangement did not give us accurate *absolute* values) and that was to make the 700 volt experimental curve fit the corresponding Mott curve. (The scattering coefficients, given in Table I, are obtained in this way.) When this was done it was found that the 500 volt curves fitted each other and that a departure from a perfect fit began to be discernable for 350 volts. The character of the departure of the experimental curves from the Mott curves is always of the same kind (at least down to 50 volts): the experimental curve is always steeper at small angles and always flatter at large angles. Moreover, the

experimental and theoretical curves cut each other twice as is evident from the diagrams; alternatively, at two points for each electron speed the Mott formula happens to give just the right value for the scattering.

In Fig. 1, an enlargement of the curves, for the region above 60°, is shown in the inset. In Fig. 2 we have assembled the experimental results and the theoretical curves for the lower electron energies. The 50 volt theoretical curve is taken from the more recent paper of Massey and Mohr[13] and the 25 volt theoretical curve is an interpolation between the curves they give for 20 and 30 volts. The 100 volt theoretical curve attributed to Massey and Mohr is taken from their earlier paper, as they do not give a 100 volt curve in their later paper. This procedure is of course open to question, since they believe that the method of calculation developed in the second paper is more dependable than the one used earlier.

In view of the fact that theoretical physicists are continually improving their methods of calculating electron scattering, it is therefore desirable to discuss briefly the accuracy of the experimental curves. The work of Bullard and Massey[15] overlaps our work in the region between 25 and 50 volts. We have therefore superposed their values on the corresponding curves in Fig. 2. It is clear that the agreement is very satisfactory. When one considers how different their experimental arrangements were from ours, one may now feel confident in assuming that both sets of results are free from serious error arising in some way or another from the peculiarities of the apparatus. Although we did not investigate the scattering for electrons moving with speeds less than 25 volts, it is possible to make the same sort of comparison between the results of Ramsauer and Kollath and those of Bullard and Massey in the region below 20 volts. Both investigations agree well as to the shapes of the 10 and 20 volt curves. However, there is no agreement between their 4 volt curves; all we can find in common between them is an upward trend as we go from 50° to 120°. The final conclusion to be drawn from the comparisons discussed in this paragraph is that, over the range 10 to 50 volts, the experimental angular distribution curves now available may be regarded as fairly exact, and free from systematic errors due to the particular type of apparatus used. This conclusion is based on the significant fact that there is very satisfactory agreement between the final results, where they overlap, although each investigation was carried out with an entirely different type of apparatus from that used in the other two investigations.

Our results were compared with those of Werner.[16] It will be remembered that Werner measured the scattering of electrons by helium, at a fixed angle 90°, and varied the energy of impact of the electrons. To effect a comparison, we measured the number of electrons scattered, at a fixed angle 37°, as the electron energy was varied from 25 to 700 volts. (This, incidentally, was the method whereby the relative magnitudes of the experimental curves in Figs. 1 and 2 were determined.) Then, using our experimental curves shown in Figs. 1 and 2, we calculated the relative scattering, at 90°, of electrons having

[15] E. C. Bullard and H. S. W. Massey, Proc. Roy. Soc. **A133**, 637 (1931).
[16] S. Werner, Proc. Roy. Soc. **A134**, 202 (1931).

speeds ranging from 25 to 700 volts. The results were in very satisfactory accord with those given by Werner.

Werner concluded that Mott's theory held for electron scattering by helium atoms so long as the electron energy was above 100 volts. This is true for the angle at which he worked, *viz.*, 90°, but an examination of Fig. 1 suggests that the conclusion has no particular significance, for it so happens that, at 90°, for 100 volt-electrons, the experimental curve and the Mott curve cross each other. Had any other angle been chosen the conclusion would have been such as to exclude 100 volt electrons from the generalization. From the curves shown in Fig. 1, we should be entitled to conclude that Mott's theory adequately describes the scattering of electrons at 90° so long as their energy exceeds an amount somewhere between 200 and 350 volts.

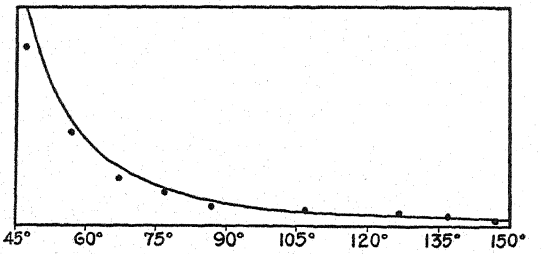


Fig. 3. Comparison of experimental scattering coefficient with values for a pure inverse square law scattering. *Continuous* line: graph of cosec $^4\theta/2$. *Dots*: experimental points for 500 volt electrons.

Mott's formula for electron scattering by atoms may be expressed in terms of μ, or in terms of v and θ, as follows,

$$\alpha(v, \theta) = [e^2/2mv^2(Z - F) \operatorname{cosec}^2 \theta/2]^2 \quad (1)$$

or,

$$\alpha(\mu) = [(e^2m/2h^2)(Z - F)(1/\mu^2)]^2 \quad (2)$$

where

$$\mu = [\sin(\theta/2)]/\lambda, \text{ and } \lambda = h/mv.$$

If the electrons within the atom contribute nothing at all to the scattering, the atomic structure factor F would be zero and the formula would then describe the scattering by a bare nucleus (Rutherford scattering, nuclear scattering, or inverse square law scattering). Now F is a function of μ which diminishes as μ increases, so that above a certain value of μ, F is negligible in comparison with Z. Evidently the larger μ is, (or, the larger θ is for a given electron speed), the more closely does the scattering approach Rutherford scattering. This is well illustrated in Fig. 3, which shows how closely the experimental points for 500 volt-electrons fit a $\operatorname{cosec}^4 \theta/2$ curve (Rutherford scattering), so long as the angles are greater than about 70°. Below this angle, it is necessary to use the Mott theory to describe the experimental results. This means that we can no longer neglect F in comparison with Z in the formula.

We may here recall the parallelism between Mott's theory of electron scattering and the theory of x-ray scattering. Eq. (2) can be resolved into two factors, $[(e^2m/2h^2)(1/\mu^2)]^2$ which measures the scattering by the nucleus per unit nuclear charge, and $(Z-F)^2$ which gives the effective nuclear charge. Here Ze is the total nuclear charge, whose full effect is diminished by the presence of the electrons within the atom by an amount which is measured by F, the atomic structure factor. F depends on the number of electrons within the atom and the way in which they are distributed. The formula for the scattering of x-rays by gaseous atoms is

$$\alpha(\theta, \lambda) = \left(F^2 + \frac{Z^2 - F^2}{Z}\right)\left(\frac{e^2}{mc^2}\right)^2\left(\frac{1 + \cos^2\theta}{2}\right). \tag{3}$$

If we retain only that part associated with coherent scattering, that is, the part most directly comparable with the elastic scattering of electrons, we have left

$$\alpha(\theta, \lambda) = (F^2)(e^2/mc^2)^2(1 + \cos^2\theta)/2. \tag{4}$$

Here the factor $(e^2/mc^2)^2(1+\cos^2\theta)/2$ denotes the Thomson scattering per single free electron, and the factor F^2 may be regarded as the effective number of electrons in the atom. Thus, in both x-ray scattering and electron scattering, the way in which the electrons are distributed in the atom leads us to the notion of an effective number of electrons which is measured by F the atomic structure factor. If all the electrons were concentrated at the nucleus, F would equal Z the total number of electrons within the atom, but because they are distributed over a finite volume the phase differences between the scattered waves for each electron lead to a value of F necessarily smaller than Z.

It is instructive to change Eq. (2) into

$$\mu^2[\alpha(\mu)]^{1/2}(2h^2/e^2m) = (Z - F). \tag{3}$$

If we replace the theoretical scattering coefficient $\alpha(\mu)$ by the experimental values I_{exp}, and then plot $\mu^2[I_{\text{exp}}]^{1/2}(2h^2/e^2m)$ against μ, we ought to get a graphical representation of $Z-F$. This is done in Fig. 4. If the F were always negligible in comparison with Z, then of course the graph would be a horizontal line parallel to the x-axis, whose height would be given by Z. The fact that it is not, indicates that F is, over a large range of μ's, of the same order of magnitude as Z. Indeed, we could say that the *points* plotted in Fig. 4 determine the atomic structure factor for helium atoms by means of electron scattering data. The *heavy continuous* line in Fig. 4 is a plot of $(Z-F)$ using the F values calculated by James and Brindley. (The *light continuous* line is a plot of F values obtained from x-ray data by Wollan[17] and Herzog[18].) The ordinates of the F curve and the $Z-F$ curve add up to Z as they should. The coincidence of the experimental points with the continuous line, over the range $\mu=0$ to $\mu=1.1$, of course shows that the Mott formula, in conjunction

[17] E. O. Wollan, Rev. Mod. Phys. 4, 205 (1932).
[18] G. Herzog, Zeits. f. Physik 70, 590 (1931).

with James and Brindley's F values, is adequate to describe electron scattering by helium atoms when the electron energy is not too low. It will be noticed that the experimental points for μ greater than about 1.1 are very irregularly distributed. This comes about from the peculiar way in which Fig. 4 involves the experimental results. Where the experimentally-measured quantities are small and difficult to measure accurately, the corresponding ordinates in the figure are large, but where they are large and easy to determine with precision the corresponding ordinates are small. Figs. 1 and 3 afford a fairer test of the relative accuracy of the results over the whole range of angle than does Fig. 4, but of course they do not bring out in so explicit a manner the shape of the curve showing the atomic structure factor as a function of μ.

The failure of Mott's theory to account for the experimental results when the electron energies are low has been attributed to the neglect of certain factors in the theory which are important only when the energies are relatively

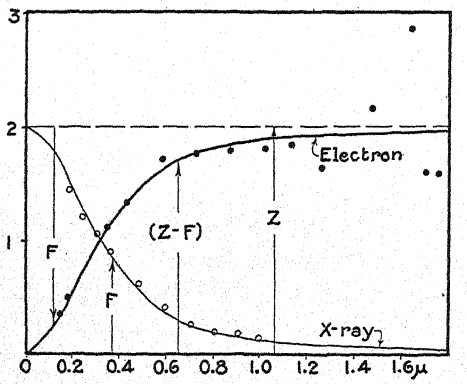


Fig. 4. Atomic structure factor for helium from electron scattering data. *Heavy continuous* line: From Mott's theory. Dots are experimental points. *Light continuous* line: F values according to Wollan.

low. Such factors are the distortion of the electron wave by the atom it passes over, electron exchange, and polarization of the atom by the electron. Massey and Mohr,[9] in the second of the papers referred to, computed the scattering when electron exchange and the distortion of the electron wave are taken into account. The calculations are difficult, and certain approximations have to be made in order to arrive at results. In Fig. 2 we show their 25 and 50 volt curves along with our experimental curves. It must be admitted that the agreement between theory and experiment is far from satisfactory. The upturn in the 25 volt curve is accounted for qualitatively by theory, but not the one in the 50 volt curve. There is also a serious difference at small angles (below about 50°) where the experimental curve is far steeper than the theoretical. In Fig. 2 we show the experimental curve for 100 volt-electrons, the Mott curve and the Massey and Mohr curve. (The Massey and Mohr curve for 100 volts is taken from their *earlier* paper in which they consider electron exchange effects, but not distortion of the electron wave. They do not give a 100 volt curve in their later paper.) It seems that, for 100 volt-electrons, the

original Mott theory gives a somewhat better agreement with experiment than does the theory of Massey and Mohr, although the latter theory takes into account the exchange effect which was supposed to be a cause of the deviation between the Mott theory and experiment.

It will be noticed that nowhere do we find a maximum in the scattering curves, although it is possible that one may be found at an angle greater than 150° for the low velocities. This is in qualitative accord with the results of Arnot, which indicate that the maxima in the scattering curves at large angles were more marked the greater the atomic number of the scattering atom.

We should like to thank Professor G. E. M. Jauncey and Dr. G. G. Harvey for information they have supplied to us in connection with the atomic structure factors.

The Infrared Dispersion of Carbon Dioxide

By HUGH M. SMALLWOOD
Mallinckrodt Chemical Laboratory, Harvard

(Received May 31, 1932)

The term in the dispersion equation of carbon dioxide corresponding to the bending vibration ($\lambda = 14.91\mu$) has been calculated from the assumption that this dispersion is due to interaction of the electric vector of the light wave and the permanent dipole moments associated with the carbon-oxygen valence bonds. The calculation indicates a magnitude of 1.17×10^{-18} e.s.u. for these dipoles, which is shown to be in agreement with the value to be expected from the measured moment of acetone.

THE experimental data on the refractive index of carbon dioxide, comprising a range from 1800A to 13μ, have been collected by Fuchs[1] and represented by a four-term dispersion equation, corresponding to the two ultraviolet and two infrared absorptions of the molecule. The term which takes account of the far infrared absorption is found by Fuchs to equal $8.1742 \times 10^{21}/(\nu_0^2 - \nu^2)$. When this empirical value is equated to the usual expression for dispersion ($Ne^2f/2\pi\bar{m}$), it is found that one must assume a value for the effective number of dispersion electrons f equal to 0.121. This result indicates the desirability of expressing the phenomenon in a somewhat different manner.

The properties of carbon dioxide have been shown to be best represented by the assumption of a symmetrical linear molecule.[2] The normal mode of vibration of this model, to which the far infrared absorption is ascribed, is a motion of the nuclei perpendicular to the line of symmetry (Fig. 1). Since this frequency is optically active, and since the resultant electric moment of the molecule is zero, it must be supposed that there is a permanent moment associated with each of the valence bonds, as shown by the heavy arrows in Fig. 1. This is, of course, also to be expected from the results of numerous

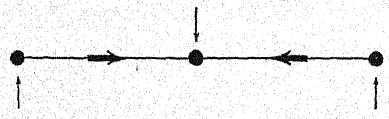


Fig. 1.

measurements of dipole moments of organic molecules. When placed in an oscillating electric field, this molecule will execute forced vibrations due to the couples exerted upon the dipoles. These forced vibrations result in a distortion of the molecule such that there is an average induced moment in the direction of the electric field. According to the present interpretation, it is this induced moment which is responsible for the infrared dispersion.

[1] O. Fuchs, Zeits. f. Physik **46**, 519 (1928).
[2] See, for example, K. W. F. Kohlrausch, *Der Smekal-Raman-Effekt*, p. 178, Berlin, 1931.

Consider a set of axes fixed in the molecule so that the carbon nucleus is stationary and at the origin, and the Y axis coincides with the line defined by the oxygen nuclei when at rest. The free vibration may then be compounded from one in the XY plane one in the YZ plane. Since the displacements are assumed to be small, the equations of motion for these component vibrations are

$$\left.\begin{aligned} \bar{m}\ddot{x} + 4\pi^2\nu_0^2\bar{m}x &= 0 \\ \bar{m}\ddot{z} + 4\pi^2\nu_0^2\bar{m}x &= 0 \end{aligned}\right\} \tag{1}$$

where $\bar{m}$ is the relative mass $(2m_om_c/2m_o+m_c)$ and ν_0 is the normal frequency of this mode of vibration. Let the molecule be subjected to the action of a beam of plane polarized light arbitrarily directed so that the direction cosines of the electric vector (at $t=0$) are α, β, γ. Then

$$\left.\begin{aligned} \mathbf{E} &= \alpha E, \beta E, \gamma E \\ E &= E_0 \exp\,[2\pi i\nu(t - r/w). \end{aligned}\right\} \tag{2}$$

The electrostatic potential energy of the molecule is

$$\epsilon = -(\mathfrak{y}_1\mathbf{E}) - (\mathfrak{y}_2\mathbf{E}). \tag{3}$$

Since it is assumed that $\mathfrak{y}_1$ and $\mathfrak{y}_2$ are directed along the lines joining the carbon nucleus with the two oxygen nuclei, and since $\mathfrak{y}_1$ and $\mathfrak{y}_2$ are assumed to have the same magnitude (μ),

$$\left.\begin{aligned} \mathfrak{y}_1 &= -\mu x/d, \; -\mu(1 - x/d - z/d), \; -\mu z/d \\ \mathfrak{y}_2 &= -\mu x/d, \quad \mu(1 - x/d - z/d), \; -\mu z/d \end{aligned}\right\} \tag{4}$$

where x and z are the displacements of the oxygen nuclei in the X and Z directions, respectively, and d is the carbon oxygen internuclear distance. Substituting Eqs. (2) and (4) in (3), it follows that

$$\epsilon = 2\mu E(\alpha x + \gamma z)/d. \tag{5}$$

From this equation may be obtained the X and Z components of the impressed force leading to the following equations for the forced vibration:

$$\left.\begin{aligned} \bar{m}\ddot{x} + 4\pi^2\nu_0^2\bar{m}x &= -2\mu E\alpha/d \\ \bar{m}\ddot{z} + 4\pi^2\nu_0^2\bar{m}z &= -2\mu E\gamma/d; \end{aligned}\right\} \tag{6}$$

$$\left.\begin{aligned} x &= -2\mu E\alpha/4\pi^2\bar{m}d(\nu_0^2 - \nu^2) \\ z &= -2\mu E\gamma/4\pi^2\bar{m}d(\nu_0^2 - \nu^2). \end{aligned}\right\} \tag{7}$$

The moment induced in the direction of the field is

$$\mu_i = \frac{1}{E}[(\mathfrak{y}_1\mathbf{E}) + (\mathfrak{y}_2\mathbf{E})]. \tag{8}$$

Upon substituting Eqs. (2), (4) and (7) in Eq. (8), it is found that

$$\mu_i = \frac{\mu^2 E}{\pi^2\bar{m}d^2(\nu_0^2 - \nu^2)}\{\alpha^2 + \gamma^2\}. \tag{9}$$

This expression must be averaged over all possible directions of $\mathbf{E}$, that is,

over all possible values of α and γ. Since the average of the square of the cosine is $\frac{1}{3}$, the polarizability per molecule is

$$\frac{\tilde{\mu}_i}{E} = \frac{2\mu^2}{3\pi^2\bar{m}d^2(\nu_0^2 - \nu^2)}. \tag{10}$$

The dispersion follows at once from the familiar expression

$$n - 1 = 2\pi N\tilde{\mu}_i/E \tag{11}$$

where n is the refractive index and N the number of molecules per cc. From Eqs. (10) and (11) it follows that the coefficient of $1/(\nu_0^2-\nu^2)$ appropriate to this type of polarization is

$$C = 4N\mu^2/3\pi\bar{m}d^2. \tag{12}$$

All of the quantities appearing in the expression for C are known with the exception of μ, the moment of the C=O bond in CO_2. Setting C equal to 8.17×10^{21} (Fuchs' value) and solving for μ, one obtains[3] 1.17×10^{-18}. This value is about what one would expect for the moment of the double bond uniting carbon and oxygen. The simplest molecule available for the measurement of the C=O moment is acetone,

$$\begin{matrix} H_3C \\ H_3C \end{matrix}\!\!\diagdown\!\!\diagup C = O,$$

the resultant moment of which is[4] 2.80×10^{-18}.

There is some uncertainty in the magnitude of the moment to be ascribed to the CH bond, but this quantity is probably not far from 0.5×10^{-18}. Since this moment is directed from carbon to hydrogen, and since the C=O moment is directed from oxygen to carbon, the latter dipole must equal 2.2×10^{-18}, if one assumes the group moments to be directed along the tetrahedral valence bonds. This value cannot, however, be compared directly with the moment in CO_2 for two reasons. In the first place, the figure 2.2×10^{-18} includes the moment induced in the two CC bonds of acetone by the CH and CO moments. This induced moment has the same direction as the CO moment so that the latter quantity must be less than 2.2×10^{-18}. Secondly, in CO_2 the two dipoles are so oriented that each lessens the other by induction. The extent of these two effects cannot be calculated for these molecules, but the results obtained for some substances that can be treated[5] indicate that the decrease due to each effect should be about $0.4-0.5\times10^{-18}$. Taking into account the induced moments, therefore, leads to the conclusion that the C=O moment calculated from the infrared dispersion is about what one would expect from the measured moment of acetone.

In conclusion, I wish to express my thanks to Professor K. F. Herzfeld for pointing out the opportunity for this calculation, and to Professor Linus Pauling for a suggestion which has proven valuable in the procedure used.

[3] d has been set equal to 1.15A, cf. W. V. Houston and C. M. Lewis, Phys. Rev. **37**, 227 (1931).

[4] C. P. Smyth, *Dielectric Constant and Molecular Structure*, p. 193, Chemical Catalog Co., 1931.

[5] H. M. Smallwood and K. F. Herzfeld, J. Am. Chem. Soc. **52**, 1919 (1930).

The Band Spectrum of Sulphur Monoxide

By EMMETT V. MARTIN
University of California, Berkeley, California

(Received May 16, 1932)

The spectrum of SO, which lies in the region 2400–4000A, has been photographed in the 2nd order of a 21-foot grating. The wave-numbers of the lines of the seven bands, (0,4), (0,5), (0,6), (0,7), (0,8), (0,9), and (1,4), are tabulated.

Rotational structure.—The analysis of the rotational structure leads to the assignment of the band system to a $^3\Sigma$, $^3\Sigma$ electronic transition, and yields the follow ing values of the constants:

$r_e' = 1.769 \times 10^{-8}$ cm	$r_e'' = 1.489 \times 10^{-8}$ cm	$D_e' = -1.280 \times 10^{-6}$ cm^{-1}
$I_e' = 55.10 \times 10^{-40}$ gr. cm^2	$I_e'' = 39.02 \times 10^{-40}$ gr. cm^2	$\beta' = -3.56 \times 10^{-9}$ cm^{-1}
$B_e' = 0.5020 \pm 0.0005$ cm^{-1}	$B_e'' = 0.70894 \pm 0.00009$ cm^{-1}	$D_e'' = -1.129 \times 10^{-6}$ cm^{-1}
$\alpha_e' = 0.0062$ cm^{-1}	$\alpha_e'' = 0.00562 \pm 0.000013$ cm^{-1}	$\beta'' = -3.20 \times 10^{-10}$ cm^{-1}

Spin fine-structure. The triplets are resolved for $K > 30$ and for $K < 13$. However, due to overlapping of the different branches, the resolution for $K < 13$ could be observed well in the (0,8) band only. It was found that, in order to represent adequately the observed separations of the triplets, it was necessary to modify somewhat the equations in Kramers' theory of spin tripling in $^3\Sigma$ states. The equations which best respresent the data are:

$$\Delta_{2-1} = A - B/(2K+3) - (\gamma' - \gamma'')(K+1)$$
$$\Delta_{2-3} = A + B/(2K-1) + (\gamma' - \gamma'')K$$

where, for the (0,8) band, $A = -2.11$, $B = -10.83$, and $(\gamma' - \gamma'') = +0.0150$. Of these three constants, A is the only one which is different for different bands; it ranges from -1.97 for the (0,4) band to -2.19 for the (0.9) band. We cannot determine which one, if either, of the two terms, A and B, represents the value of $3(\epsilon' - \epsilon'')$ in Kramers' theory. The values of $\Delta_2 F_1(K)$ and $\Delta_2 F_3(K)$ indicate that $\gamma' \sim +0.017$ and that $\gamma'' \sim -0.003$.

Predissociation and perturbations. Bands with $v' = 0$, 1, 2, and 3 are observed to break off at $K' = 66$, 53, 39, and 6, respectively. No bands with $v' > 3$ are observed. This effect is explained as predissociation, and is assumed to be caused by a $^3\Pi$ state. Not only do the rotational levels for different v' end at different values of K', but also the term value at which the break occurs decreases with increasing v'. If the potential energy curve for the $^3\Pi$ state is assumed to have a shallow minimum, a satisfactory explanation of the effect of rotation on predissociation is obtained by an application of Oldenberg's theory of dissociation by rotation. A further indication that the $^3\Pi$ potential energy curve has a shallow minimum is given by the observed perturbations of the rotational levels of the upper $^3\Sigma$ state. According to our interpretation, the term value at which the rotational levels for $v' = 3$ terminate corresponds to dissociation of the normal state of the SO molecule. The energy of dissociation of this state, measured from the $v'' = 0$ vibrational level, is calculated to be 5.053 ± 0.001 volts.

Vibrational structure. The origins of several bands of the $v' = 0$ progression are calculated, and the vibrational constants of the lower state determined from them. Since the bands with $v' > 1$ are too much perturbed to permit an analysis of their rotational structure, it was necessary to use measurements of band heads to determine the vibrational constants of the upper state. The constants obtained are: $\omega_e'' = 1123.73 \pm 0.24$ cm^{-1}, $x_e''\omega_e'' = 6.116 \pm 0.017$ cm^{-1}, $\omega_e' = 628.7$ cm^{-1}, and $x_e'\omega_e' = 5.65$ cm^{-1}.

I. Introduction

THE sulphur monoxide band spectrum, which appears in the region 4000 to 2400A, was first described in 1906 by Miss Lowater.[1] A more complete study of this spectrum was made in 1924 by Johnson and Cameron,[2] who arranged the bands in series. In 1929, Henri and Wolff[3] photographed this system with a quartz-prism Littrow spectrograph, made the vibrational analysis, and assigned the spectrum to the molecule SO. As shown below, there is good evidence that their assignment of vibrational quantum numbers is correct; hence it has been used in this work. Because of insufficient dispersion, however, they were able to make only a partial analysis of the rotational structure. From the average second differences of the frequencies of the unresolved P and R series in a number of bands with $v'=0$, they evaluated the constant α'', which is defined by the relation:[3a]

$$B_v'' = B_e'' - \alpha''(v'' + \tfrac{1}{2}). \tag{1}$$

In order to determine B_e'', they then substituted α'' into the equation:

$$\alpha''\omega_e'' = 6B_e''^2 \tag{2}$$

where ω_e'' is the frequency of vibration for infinitesimal amplitude; ω_e'' was known from the analysis of the vibrational structure of the system.

Eq. (2) results from a special form[4] of the function assumed by Kratzer[5] for the potential energy of a diatomic molecule. This function can be written:

$$U = 2k(\tfrac{1}{2} - 1/\rho + 1/2\rho^2 - c_3\xi^3 - c_4\xi^4), \tag{3}$$

where $\rho = r/r_e$, $\xi = \rho - 1$, and k, c_3, and c_4 are constants. It can be shown that[4]

$$c_3 = \tfrac{1}{2}(\alpha\omega_e/6B_e^2 - 1), \text{ and } c_4 = (x_e\omega_e/3B_e - 1) - \tfrac{1}{2}5c_3(c_3 + 2), \tag{4}$$

where $x_e\omega_e$ is the coefficient of the second degree term in the expression for the vibrational term values. If c_3 and c_4 are set equal to zero, Eq. (2) follows. Birge[6] has calculated the values of c_3 and c_4 for the electronic states of a number of different molecules, and has found that, if they are neglected as in Eq. (2), values of B_e are obtained which are in some cases in error by as much as 50 percent. Therefore, it seemed likely that the value of B_e'' given by Henri and Wolff represented only the order of magnitude of the correct value.

Henri and Wolff concluded that the band structure consisted of a Q branch only, the lines of which were narrow multiplets. This type of structure appeared to be in marked contrast with that of the known band systems

[1] Frances Lowater, Ast. Jour. **23**, 324 (1906).
[2] R. C. Johnson and W. H. B. Cameron, Proc. Roy. Soc. **A106**, 195 (1924).
[3] V. Henri and F. Wolff, Jour. Phys. Rad. **10**, 81 (1929).
[3a] The notation used in this paper is that agreed upon by leading spectroscopists, as reported by R. S. Mulliken, Phys. Rev. **36**, 611 (1930).
[4] W. Weizel, Handbuch der Experimentalphysik, Ergänzungswerk, Band I, (1931). A.E Ruark and H. C. Urey, *Atoms, Molecules, and Quanta* (1930).
[5] A. Kratzer, Zeits. f. Physik **3**, 289 (1920).
[6] R. T. Birge, Unpublished work.

of O_2[7,8] and S_2[9] which lie in the same spectral region as the SO bands. Since these systems of O_2 and S_2 are quite similar, in that both result from the same type of electronic transition, it was expected that this system of SO would also have similar characteristics. In view of these uncertainties, it was considered to be of value to obtain new spectrograms under higher dispersion in an attempt to obtain unambiguous values of the molecular constants, and to clarify the apparently anomalous rotational structure.

II. Experimental Procedure

In the investigation by Henri and Wolff, the spectrum was excited by passing a spark discharge between small aluminum rods in a quartz bulb containing SO_2 at a pressure of 30–40 mm. A quartz window was placed close to the spark to avoid the absorption by SO_2 which occurs in the same spectral region as the SO bands. This method had the disadvantages that an exposure

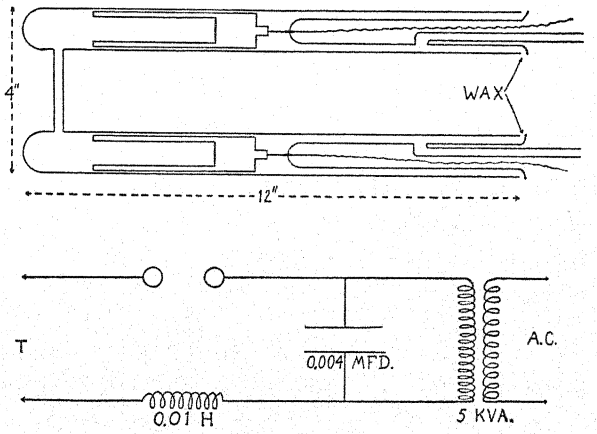


Fig. 1. Upper; diagram of the quartz discharge tube. The light was taken from the side of the constricted ($\frac{1}{4}$'' diameter) portion of the tube. Lower, schematic diagram of the electrical circuit. The leads marked *T* connect to the discharge tube.

of several hours was required even with a quartz spectrograph, and that it was necessary to interrupt exposure frequently in order to remove deposits of sulphur from the window and to allow the tube to cool.

A diagram of a discharge tube which does not have these disadvantages is shown in Fig. 1. This tube was constructed entirely of quartz, and was connected to the glass system by means of the wax seals shown. These seals were far enough removed from the discharge so that they were not overheated. The electrodes were heavy aluminum cylinders. A P_2O_5 drying tube, a liquid-air trap, and a two-liter flask comprised the remainder of the system. SO_2 was taken from a tank and frozen in the liquid-air trap; the system was then evacuated and allowed to fill with SO_2 to a pressure of about 20 mm. The two-liter flask was necessary as a reservoir, because, even with this much volume,

[7] W. Ossenbrüggen, Zeits. f. Physik **49**, 167 (1928).
[8] W. Lochte-Holtgreven and G. H. Dieke, Ann. d. Physik **3**, 937 (1929).
[9] S. M. Naude and A. Christy, Phys. Rev. **37**, 490 (1931).

the pressure in the system would fall several millimeters in an hour, due to the removal of SO_2 by the deposition of sulphur on the walls of the tube and to the oxidation of the electrodes. The SO_2 could then be replenished from the liquid-air trap supply.

If the light was taken from the side of the constricted portion ($\frac{1}{4}''$ diameter) of the tube, there was no appreciable absorption by SO_2, and the heat produced by the discharge itself prevented the deposition of sulphur on this constricted part. Previous trials had shown the impossibility of using a tube of the "end-on" type, with which these difficulties could not be avoided.

The tube adopted therefore required no interruption of exposure to be cooled or cleaned, and, when excited with a heavy current, produced a comparatively high intensity of the spectrum.

The electrical circuit also is shown in Fig. 1. The transformer was actuated by a potential of 220 volts, and had an open-circuit secondary voltage of 10 kilovolts and a capacity of 5 k.v.a. The condenser consisted of two Leyden jars in parallel, and the self-inductance coil was constructed by winding No. 24 D.C.C. copper wire in a single layer on a long paper cylinder. Henri and Wolff showed that this type of circuit was practically necessary for the production of the spectrum with any intensity. An ordinary uncondensed discharge produces the band spectrum, but most of the energy goes into the production of a continuous spectrum in the same spectral region. On the other hand, a condensed discharge produces the line spectrum only. The optimum values of capacity and inductance are indicated in Fig. 1; they could not be changed from these values by a factor of more than about five without a change in the spectrum becoming noticeable.

The intensity of the spectrum was also dependent upon the pressure in the tube; it increased with increasing pressure up to about 2 cm, but appeared to remain practically constant for pressures above this value. The power applied to the tube was controlled by regulating the primary voltage of the transformer. To obtain the maximum intensity, the power was adjusted to the maximum value at which the tube could operate continuously. This value is estimated to be about 2 k.w.

The spectrograms used for measurement were taken on Eastman Speedway plates in the first and second orders of a 21-foot grating which has a dispersion in the second order of about 1.3 A/mm. The exposure time required was six hours. The lines were measured with a Société Genévoise comparator reading to 0.001 mm. The lines of an iron arc in air were used as comparison standards. The wave-lengths used were taken from the "Transactions of the International Astronomical Union"[10] and the "Publications of the Allegheny Observatory of the University of Pittsburgh."[11] The former gives values for the arc in air, the latter for the arc in vacuum. Unfortunately, no International standard wave-lengths are available for the region below 3370A. However, the two sources agreed very closely for the wave-lengths which they both give; hence it was assumed that there was no appreciable error intro-

[10] Transactions of the International Astronomical Union, Vol. III, (1929).

[11] Publications of the Allegheny Observatory of the University of Pittsburgh, Vol. VI (1929).

duced by using for some of the standards the wave-lengths of the lines of the vacuum iron arc. The deviations of these lines from a smooth dispersion curve indicated that the SO band lines were measured with an absolute accuracy of about 0.01A, while combination relations showed for the sharper lines a relative accuracy within a band of about 0.003A.

III. Rotational Structure

The general appearance of the spectrum is shown in Fig. 2, a and b. The progression with $v'=0$ is predominant, and its most intense members, namely the (0, 4) to (0, 9) bands inclusive, are almost entirely free from overlapping by other bands of the system. These bands were therefore most suitable for the determination of the molecular constants. The constants of the lower states having $v''=4$ to 9, and of the upper state having $v'=0$, could be accurately determined from these bands, while for the upper state having $v'=1$, the (1, 4) band was found to be most suitable. No bands with $v'>1$ could be used for this purpose; those with $v'=2$ were too much perturbed to permit an analysis of their structure, while those with $v'=3$ were extremely narrow, an effect which is explained below as due to predissociation. No bands with $v'>3$ are observed, also because of predissociation.

The structure of the bands with $v'=0$ is illustrated in Fig. 2, d and f, which show enlargements of the (0, 7) and (0, 5) bands respectively. These bands show one R and one P branch, each of which consists of narrow triplets. The two high-frequency components (to left in Fig. 2) of the triplets have a frequency separation which is dependent on the value of K, while the separation of the low-frequency member from the mean of the two high-frequency members is nearly independent of K. The absence of any noticeable Q branches indicates that the transition is one for which $\Delta\Lambda=0$. Furthermore, because of the considerable intensity of the system, the possibility of an intersystem transition ($\Delta S\neq 0$) can be ruled out. Since no Λ-type doubling is observed, both states must have $\Lambda=0$. The presence of triplet R and P branches shows that the electronic states involved belong to a triplet system. These facts point quite definitely to the conclusion that this band system is produced by a $^3\Sigma$, $^3\Sigma$ transition, as is the case for the analogous systems of O_2[7,8] and S_2[9] lying in the same spectral region. Since the final $^3\Sigma$ states for these systems of O_2 and S_2 are the normal states of these molecules, the final $^3\Sigma$ state for this system of SO is probably also the normal state.

The complete resolution of the spin tripling is one of the most interesting features of the SO bands. In the corresponding bands of O_2, the tripling is much smaller, and the components arising from F_1 and F_3 terms are barely resolved at the highest observed K values. In S_2, although the triplet separations are as large as in SO, overlapping is so serious that the data are irregular and incomplete.

The rotational levels of a Σ state are given by[12]

$$F_i(K) = B_v K(K+1) + f_i(K, J-K) + D_v K^2(K+1)^2 + \cdots \qquad (5)$$

[12] For details, see R. S. Mulliken, Rev. Mod. Phys. **2**, 105 (1931). The factor $\overline{G^2}$ has been omitted from Eq. (5).

where K is the quantum number of the angular momentum exclusive of spin, J is the quantum number of the total angular momentum and takes the values $J=K+S$, $K+S-1$, $\cdots$, $K-S$, and S is the resultant spin. For a triplet state, $S=1$; hence, for this case, $J=K+1$, K, and $K-1$. Since the difference in energy for different orientations of spin is small for Σ states (Hund's case (b)), there will be, in this case, three rather closely spaced en-

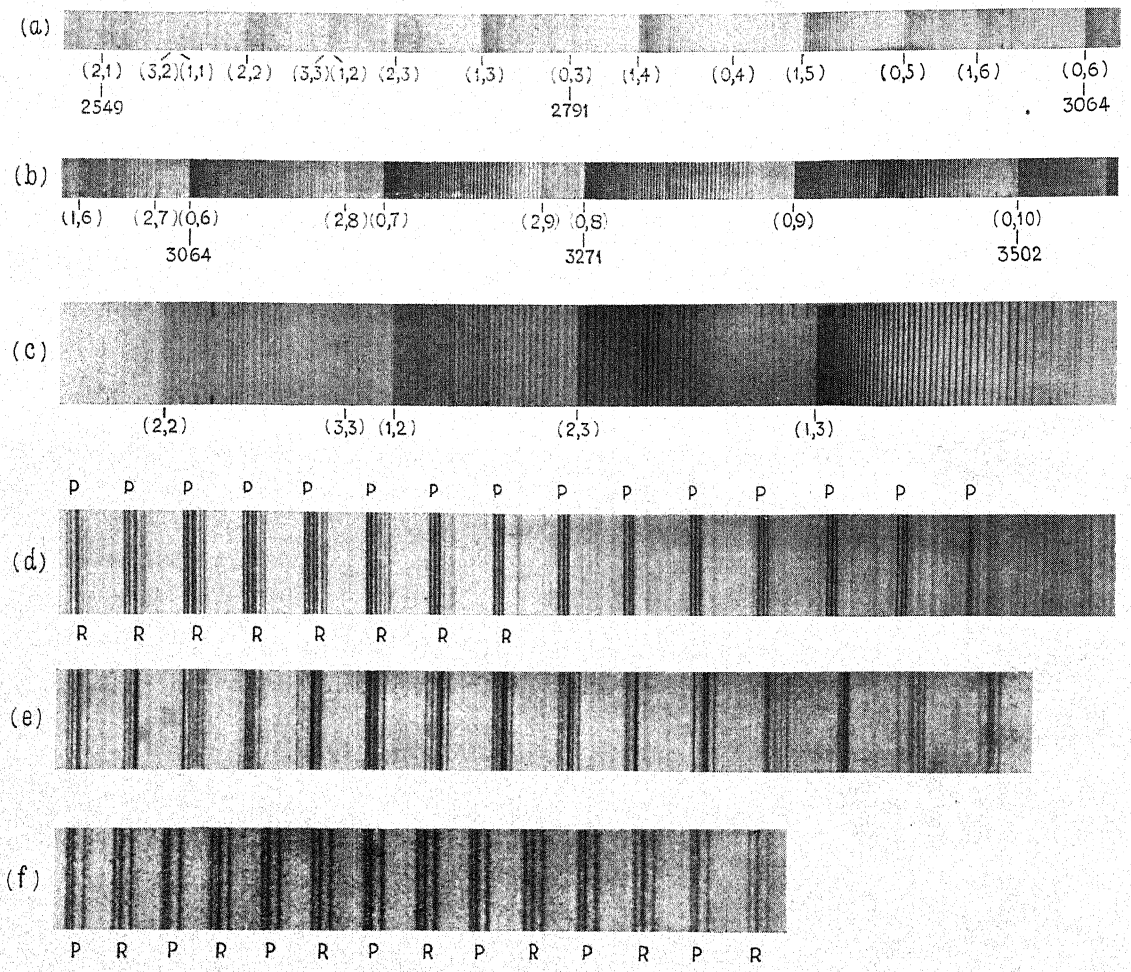


Fig. 2. Reproduction of the major parts of the SO emission spectrum, photographed with a 21-foot grating. (a) and (b). Contact prints of the region λ2500A to λ3550A, which contains most of the stronger bands. (c). Enlargement of the short wave-length end of the spectrum to show the abrupt termination of the bands with $v'=2$ and $v'=3$. This is especially well illustrated by the 2,2 band. The 3,3 band is probably too faint to show in the reproduction, but actually is only about 1 mm wide. (d). Enlargement of the end of the 0,7 band showing the abrupt ending of the R and P branches. (e). Enlargement of part of the 1,4 band illustrating the perturbations in the rotational structure. (f). Enlargement of part of the 0,5 band. The complete resolution of the triplets and their different relative spacing for adjacent lines, $R(K)$ and $P(K-6)$, are apparent.

ergy states for each value of K. These energy states are designated $F_i = F_1$, F_2, and F_3, where F_1 corresponds to $J = K+1$, F_2 to $J = K$, and F_3 to $J = K-1$.

Kramers[13] has shown that $f_i(K, J-K)$ for $^3\Sigma$ states is made up of two parts, one of which is due to the interaction of the resultant electron spin $S^*(=(S(S+1))^{\frac{1}{2}})$ and the magnetic field generated by the rotation of the nuclei, while the other is due to the interaction of the individual spins of the electrons. For the three values of J, $f_i(K, J-K)$ is given by

$$J = K+1 \qquad f_1 = -\epsilon + 3\epsilon/(2K+3) + \gamma K \tag{6}$$
$$J = K-1 \qquad f_3 = -\epsilon - 3\epsilon/(2K-1) - \gamma(K+1) \tag{7}$$
$$J = K \qquad f_2 = +2\epsilon - \gamma. \tag{8}$$

In these equations, terms containing γ arise from the interaction of the resultant spin and the magnetic field generated by the nuclear rotation, and those containing ϵ arise from the interaction of the individual spins.

The lines of the R and P branches are defined by the relations:

$$R_i(K) = \nu_0 + F_i'(K+1) - F_i''(K) \tag{9}$$
$$P_i(K) = \nu_0 + F_i'(K-1) - F_i''(K) \tag{10}$$

where ν_0 is the wave-number of the origin of the band under consideration.

In the analysis of a $^3\Sigma$, $^3\Sigma$ band system, it is impossible to determine the signs of the γ's and ϵ's. This fact prevents an unambiguous assignment of all three R (or P) branches to the series R_1, R_2, and R_3 (or P_1, P_2, and P_3). From the fact that f_2 is independent of K, we can identify the R_2 (or P_2) branch at once, but we cannot determine which of the other two R (or P) branches is R_1 (or P_1). In the present case, the low-frequency branch is R_2 (or P_2), while the high-frequency branch (for $K>18$) has been arbitrarily designated as R_1 (or P_1), by analogy with the corresponding convention used for S_2[9]. Table I gives the wave-numbers of the lines of the seven bands investigated. The lines indicated by asterisks are unresolved R_1 and R_3 (or P_1 and P_3) lines. The order in which the three branches are given in the table is, reading downward: R_1, R_3, R_2 (or P_1, P_3, P_2). This order is maintained for all of the bands with $v'=0$, and also for the (1,4) band up to $K=25$. For $K>25$, however, the (1,4) band is so much perturbed that it was impossible to arrange the R (or P) branches into three distinct series. The wave-length in I.A. of the head of each band is given at the top of the appropriate columns.

The correct designation of the lines by the values of K'' was obtained by the application of the combination principle. After a few preliminary trials, assignments were reached which yielded, for all bands with a common upper vibrational state, complete agreement in the term differences

$$\Delta_2 F_i'(K) = R_i(K) - P_i(K) = F_i'(K+1) - F_i'(K-1).$$

For the three components of the triplet, these differences should be given by:[14]

$$\Delta_2 F_1'(K) = 4B_v'(K+\tfrac{1}{2}) + 8D_v'(K+\tfrac{1}{2})^3 - 12\epsilon'/(2K+5)(2K+1) + 2\gamma' \tag{11}$$
$$\Delta_2 F_3'(K) = 4B_v'(K+\tfrac{1}{2}) + 8D_v'(K+\tfrac{1}{2})^3 + 12\epsilon'/(2K-3)(2K+1) - 2\gamma' \tag{12}$$
$$\Delta_2 F_2'(K) = 4B_v'(K+\tfrac{1}{2}) + 8D_v'(K+\tfrac{1}{2})^3. \tag{13}$$

[13] H. A. Kramers, Zeits. f. Physik 53, 422 (1929).

[14] The omission of a term $+6D_v(K+\frac{1}{2})$ from these equations introduces no appreciable error, since $6D_v$ is entirely negligible in comparison with $4B_v$.

TABLE I. *Wave numbers of the lines of the (1, 4), (0, 4), (0, 5), (0, 6), (0, 7), (0, 8), and (0, 9) bands.*

K''	(1, 4) λ2827.395		(0, 4) λ2877.643		(0, 5) λ2968.470	
	R	P	R	P	R	P
7	—	35336.56*	—	34719.20*	—	33657.37*
	—	335.55	—	—	—	—
8	—	—	—	715.47*	—	653.36*
	—	331.38	—	—	—	—
9	—	—	—	711.20*	—	649.70*
	—	326.94	—	—	—	—
10	—	323.35*	—	706.57*	—	645.18*
	—	322.05	—	—	—	—
11	—	318.10*	34724.59*	701.61*	—	640.54*
	—	316.50	722.67	—	—	637.58
12	35337.35*	312.77*	721.13*	696.25*	—	634.53*
	335.55	310.86	719.20	694.13	—	632.18
13	333.28*	306.76*	717.41*	690.48*	33655.71*	628.84*
	331.38	304.84	715.47	688.41	653.85	626.79
14	328.99*	300.40*	713.10*	684.20*	651.74*	623.07*
	326.94	298.38	711.20	682.19	649.70	620.80
15	324.27*	293.73*	708.60*	677.68*	647.39*	616.51*
	322.05	291.72	706.57	675.64	645.18	614.49
16	319.12*	286.66*	703.60*	670.78*	642.67*	609.80*
	317.12	284.64	701.61	668.71	640.54	607.79
17	313.66*	279.16*	698.32*	663.47*	637.58*	602.68*
	311.65	277.16	696.25	661.44	635.52	600.61
18	307.69*	271.33*	692.66*	655.80*	632.18*	595.25*
	305.71	269.34	690.48	653.76	630.06	593.23
19	301.46*	262.96*	686.61*	647.76*	626.32*	587.42*
	299.54	261.07	684.56	645.81	624.33	585.39
20	294.94*	253.59*	680.21*	639.41*	620.07*	579.28*
	292.86	252.50	678.22	637.42	618.08	577.25
21	287.86*	245.31*	673.42*	630.62*	613.54*	570.69*
	285.86	243.52	671.45	628.64	611.47	568.66
22	280.41*	236.28*	666.33*	621.45*	606.65*	561.84*
	278.28	234.16	664.33	619.54	604.57	559.86
23	35272.64*	35226.26*	34658.75*	34612.00*	33599.32*	33552.57*
	270.05	224.31	656.74	610.01	597.26	550.54
24	264.36*	215.97*	650.83*	602.13*	591.74*	543.01*
	262.96	214.15	648.90	600.13	589.69	541.00
25	255.48*	205.77*	642.58*	591.88*	583.81*	533.07*
	254.36	203.06	640.59	589.83	581.75	531.00
26	247.66*	194.79*	633.95*	581.30*	575.45*	522.71*
	245.31	193.14	632.11	579.32	573.52	520.71
27	238.04	185.36	625.23	570.29*	567.02	512.03*
	—	183.20	624.73		466.48	
	235.78	181.94	623.01	568.25	564.71	510.01
28	228.54	172.52	615.82	559.16	557.92	501.03*
	—	—	615.34	558.72	557.43	
	226.26	170.16	613.60	557.07	555.68	499.18
29	218.16	160.35	606.07	547.51	548.57	489.68*
	—	—	605.54	547.02	548.02	
	214.15	158.05	603.86	545.30	546.23	487.65
30	207.42	148.12	596.06	535.41	538.76	478.16
	—	—	595.38	534.87	538.23	477.69
	206.61	145.56	593.64	533.16	537.42	475.90
31	197.37	135.03	585.48	523.04	528.63	466.04
	196.66	—	584.89	522.47	528.01	465.46
	194.79	132.58	583.17	520.70	526.35	463.78
32	185.97	121.73	574.64	510.15	518.16	453.62
	185.36	—	573.99	509.54	517.54	453.04
	181.94	120.67	572.32	507.86	515.79	451.33
33	175.13	108.65	563.41	497.00	507.34	440.78
	173.08	108.06	562.72	496.36	506.75	440.22
	171.66	106.21	561.10	494.58	504.97	438.49

TABLE I. (*Cont.*).

K''	(1, 4) R	(1, 4) P	(0, 4) R	(0, 4) P	(0, 5) R	(0, 5) P
34	160.35	094.35	551.85	483.39	496.10	427.60
	—	—	551.10	482.72	495.45	427.00
	—	090.84	549.44	481.05	493.66	425.27
35	150.33	081.18	539.87	469.44	484.49	414.12
	149.74	079.14	539.08	468.70	483.76	413.45
	148.12	077.78	537.46	467.16	482.11	411.75
36	137.48	063.82	527.56	455.16	472.56	400.21
	136.84	—	526.85	454.45	471.88	399.57
	135.03	—	525.08	452.76	470.18	397.85
37	35123.69	35050.98	34514.85	34440.49	33460.32	33385.93
	—	050.34	514.03	439.76	459.48	385.34
	121.73	048.67	512.35	438.10	457.84	383.56
38	110.91	035.47	501.69	425.47	447.63	371.37
	109.96	034.81	500.86	424.78	446.80	370.63
	108.65	033.15	499.21	423.03	445.14	368.87
39	097.02	018.98	488.24	410.07	434.58	356.44
	095.82	—	487.37	409.21	433.71	355.56
	094.35	017.26	485.77	407.58	432.10	353.96
40	082.60	003.44	474.41	394.20	421.21	341.05
	—	002.58	473.43	393.44	420.26	340.21
	080.39	001.27	471.95	391.82	418.71	338.56
41	067.23	34986.83	460.12	378.00	407.39	325.41
	—	985.74	459.25	377.22	406.52	324.47
	065.26	984.32	457.70	375.59	404.93	322.86
42	050.98	969.78	445.57	361.54	393.36	309.27
	—	—	444.61	360.69	392.38	308.32
	049.31	967.56	443.13	359.10	390.80	306.77
43	037.51	951.70	430.65	344.54	378.92	292.86
	036.95	—	429.60	343.64	377.86	291.97
	036.27	949.81	428.13	342.13	376.29	290.47
44	022.67	932.77	415.28	327.45	364.06	276.11
	021.22	—	414.22	326.43	362.99	275.12
	019.85	931.14	412.75	324.87	361.45	273.52
45	005.98	916.71	399.58	309.78	348.85	258.97
	004.97	—	398.48	308.77	347.78	257.95
	003.44	915.78	397.05	307.27	346.23	256.43
46	34989.33	899.14	383.47	291.88	333.25	241.52
	988.48	897.66	382.36	290.62	332.16	240.46
	986.83	896.25	380.89	288.98	330.61	238.92
47	972.23	879.65	367.01	—	317.31	223.60
	971.44	878.76	365.90	—	316.15	222.50
	969.78	877.18	364.46	—	314.71	221.06
48	955.06	860.41	350.20	—	301.04	205.42
	—	859.53	349.01	—	299.88	204.25
	952.47	857.83	347.56	—	298.36	202.81
49	936.91	840.66	333.06	—	284.49	186.83
	936.08	839.82	331.75	—	283.14	185.67
	934.24	838.12	330.36	—	281.70	184.12
50	35917.95	34820.77	34315.41	—	33267.36	33167.87
	—	—	314.23	—	266.06	166.72
	916.71	818.20	312.72	—	264.67	165.24
51	902.81	799.92	297.47	—	249.98	148.63
	—	799.00	296.18	—	248.74	147.37
	899.98	797.32	294.71	—	247.25	145.99
52	—	778.34	—	—	232.27	—
	—	—	—	—	230.96	—
	881.98	777.30	—	—	229.38	—
53	—	760.42	—	—	214.10	—
	—	—	—	—	212.80	—
	—	757.64	—	—	211.41	—
54	—	—	—	—	195.69	—
	—	—	—	—	194.25	—
	—	—	—	—	192.85	—
55	—	—	—	—	176.78	—
	—	—	—	—	175.44	—
	—	—	—	—	174.02	—
56	—	—	—	—	157.60	—
	—	—	—	—	156.22	—
	—	—	—	—	154.62	—

TABLE I. (*Cont.*).

K''	(0, 6) λ3064.059 R	(0, 6) λ3064.059 P	(0, 7) λ3164.761 R	(0, 7) λ3164.761 P	(0, 8) λ3270.958 R	(0, 8) λ3270.958 P	(0, 9) λ3383.114 R	(0, 9) λ3383.114 P
5	—	—	—	—	30559.65	—	—	—
	—	—	—	—	560.89	—	—	—
	—	—	—	—	—	—	—	—
6	32624.35*	32611.17*	—	31572.68*	559.07	—	—	29533.82
			—		560.21	—	—	—
	—	—	—	—	—	—	—	531.72
7	622.85*	607.86*	—	569.22*	558.23	30543.42	29544.76	529.72
			—		559.65	—	546.24	—
	—	605.32	—	—	—	541.82	—	528.63
8	620.97*	604.17*	—	565.56*	556.90	540.00	543.59	526.35
			—		557.93	541.14	544.76	526.94
	—	601.71	—	563.53	555.28	538.31	541.38	524.95
9	618.45*	599.74*	—	561.51*	555.28	536.19	541.99	522.63
			—		555.93	537.08	542.73	522.91
	—	597.64	—	559.52	553.33	534.44	539.78	520.81
10	32616.05*	32595.05*	—	31557.18*	30553.07	30532.06	29539.78	29518.69*
			—		553.52	532.75	540.62	
	—	593.08	—	555.21	550.99	530.20	538.04	517.15
11	613.14*	590.20*	31575.36*	552.48*	550.42	527.53	537.40	514.36*
					550.99	528.13	538.04	
	611.17	588.20	573.57	550.52	548.54	525.60	536.23	512.70
12	610.09*	585.04*	572.68*	547.46*	547.88*	522.59	534.65	509.69*
						523.05	535.53	
	607.86	583.00	570.55	545.49	545.66	520.67	532.78	507.92
13	606.54*	579.56*	569.22*	542.01*	544.55*	517.40	531.72	504.67*
						517.77	532.11	
	604.17	577.49	567.22	540.10	542.48	515.50	529.72	502.84
14	602.63*	573.67*	565.56*	536.39*	540.92*	511.89	528.63*	499.36*
						512.21		
	600.53	571.64	563.53	534.64	538.92	509.95	526.35	497.50
15	598.39*	567.49*	561.51*	530.73*	537.08*	506.34*	524.95*	493.89*
	596.29	565.65	559.52	528.57	535.04	504.16	522.63	491.71
16	593.82*	560.92*	557.18*	524.32*	532.99*	500.06*	520.81*	487.96*
	591.82	559.02	555.21	522.18	530.83	497.96	518.69	485.80
17	588.87*	554.04*	552.48*	517.63*	528.40*	493.56*	516.47*	481.68*
	586.86	552.05	550.51	515.49	526.28	491.41	514.36	479.46
18	583.68*	546.78*	547.46*	510.54*	623.54*	486.73*	511.86*	475.07*
	581.59	544.79	545.49	508.50	621.42	484.55	509.69	472.81
19	578.09*	539.21*	542.01*	503.15*	518.36*	479.55*	506.86*	468.09*
	576.04	537.03	540.10	501.08	516.18	477.42	504.67	465.86
20	572.08*	531.29*	536.39*	495.51*	512.87*	472.09*	501.57*	460.74*
	570.04	529.02	534.19	493.48	510.72	469.96	499.36	458.51
21	565.65*	523.07*	530.24*	487.45*	507.04*	464.28*	496.04*	453.14*
	563.71	520.86	528.17	485.41	504.88	462.11	493.89	450.95
22	559.02*	514.31*	523.87*	479.09*	500.92*	456.12*	490.08*	445.23*
	557.07	512.18	521.72	477.04	498.76	453.97	487.96	443.06
23	552.05*	505.36*	517.01*	470.35*	494.39*	447.66*	483.93*	437.07*
	550.15	503.09	514.98	468.28	492.28	445.49	481.68	434.89
24	32544.79*	32496.01*	31509.89*	31461.33*	30487.60*	30438.85*	29477.32*	29428.56*
	542.72	493.69	507.87	459.21	485.48	436.69	475.07	426.37
25	537.03*	486.32*	502.53*	451.94*	480.56	429.76*	470.52*	419.76*
					480 25			
	535.00	484.25	500.44	449.84	478.33	427.57	468.09	417.52
26	529.02*	476.27*	494.85*	442.17*	473.12	420.39	463.42	410.61*
					472.83	420.18	463.12	
	527.11	474.26	492.91	440.06	470.96	418.14	461.23	408.41
27	520.40*	465.89*	487.01	432.12*	465.36	410.66	455.93	401.15*
			486.65		464.97	410.36	455.59	
	518.54	463.83	484.65	429.99	463.10	408.38	453.57	398.92
28	511.67*	455.11*	478.58	421.75*	457.30	400.60	448.18	391.52
			478.19		456.89	400.27	447.76	391.19
	509.80	453.15	476.22	419.74	454.95	398.41	445.79	389.19
29	502.59*	444.08*	469.86	411.20	448.89	390.21	440.07	381.53
			469.38	410.79	448.38	389.82	439.65	381.10
	500.70	442.05	467.45	408.79	446.55	387.89	437.72	379.06

TABLE I. (*Cont.*).

K''	(0, 6) R	(0, 6) P	(0, 7) R	(0, 7) P	(0, 8) R	(0, 8) P	(0, 9) R	(0, 9) P
30	493.17*	432.70*	460.72	400.19	440.15	379.58	431.73	371.03
			460.24	399.72	439.61	379.06	431.16	370.65
	491.22	430.64	458.34	397.77	437.74	377.16	429.26	368.72
31	483.73	420.96*	451.29	388.73	431.04	368.46	422.95	360.34
	483.27		450.77	388.27	430.52	367.98	422.40	359.89
	481.44	418.86	448.90	386.38	428.59	366.10	420.47	357.93
32	473.69	409.04	441.55	377.02	421.62	357.07	413.91	349.28
	473.11	408.54	440.98	376.51	421.04	356.57	413.32	348.83
	471.30	406.74	439.13	374.60	419.24	354.69	411.42	346.91
33	463.24	396.66	431.45	365.00	411.95	345.41	404.59	337.95
	462.62	396.04	430.83	364.38	411.31	344.85	403.94	337.45
	460.76	394.25	429.03	362.61	409.47	342.93	402.03	335.56
34	452.39	383.84	420.97	352.53	401.90	333.47	394.87	326.41
	451.68	383.25	420.34	351.96	401.22	332.81	394.20	325.82
	449.94	381.45	418.56	350.20	399.38	330.95	392.33	323.90
35	441.22	370.72	410.20	339.80	391.50	321.23	384.89	314.47
	440.43	370.10	409.54	339.18	390.80	320.47	384.20	313.82
	438.70	368.35	407.79	337.38	388.97	318.58	382.31	311.92
36	32429.69	32357.29	31399.11	31326.73	30380.77	30308.50	29374.56	29302.18
	429.19	356.59	398.50	326.02	380.11	307.74	373.93	301.53
	427.20	354.82	396.64	324.26	378.26	305.88	371.97	299.63
37	417.89	343.35	387.70	313.27	369.72	295.49	363.99	289.56
	417.05	342.73	386.83	312.57	368.95	294.74	363.21	288.91
	415.27	341.01	385.12	310.78	367.14	292.89	361.31	287.02
38	405.48	329.26	375.80	299.54	358.33	282.14	352.95	276.72
	404.72	328.55	374.97	298.83	357.52	281.48	352.22	276.02
	403.10	326.80	373.24	296.92	355.72	279.49	350.32	274.08
39	392.94	314.77	363.68	285.46	346.60	268.47	341.71	263.51
	392.09	313.96	362.85	284.63	345.79	267.71	340.92	262.76
	390.41	312.23	361.13	282.87	344.08	265.84	338.99	260.87
40	380.03	299.87	351.15	271.00	334.55	254.42	330.08	249.89
	379.09	299.03	350.20	270.20	333.62	253.69	329.25	249.16
	377.49	297.31	348.58	268.44	331.94	251.83	327.42	247.30
41	366.69	284.63	338.32	256.20	322.16	240.08	318.15	236.09
	365.81	283.80	337.38	255.33	321.23	239.35	317.34	235.33
	364.17	282.09	335.80	253.68	319.58	237.59	315.47	233.43
42	353.12	268.99	325.21	241.15	309.57	225.43	306.01	221.96
	352.14	268.15	324.26	240.25	308.50	224.61	305.10	221.12
	350.48	266.49	322.59	238.55	306.86	222.90	303.26	219.32
43	339.13	253.09	311.72	225.59	296.52	210.39	293.46	207.44
	338.11	252.22	310.78	224.77	295.49	209.65	292.52	206.62
	336.52	250.67	309.06	223.10	293.88	207.94	290.77	204.82
44	324.78	236.83	297.84	209.91	283.16	195.13	280.56	192.70
	323.72	235.91	296.92	209.02	282.14	194.36	279.60	191.77
	322.16	234.26	295.21	207.28	280.48	192.63	277.83	189.98
45	310.10	220.23	283.65	193.79	269.48	179.60	267.43	177.58
	309.01	219.23	282.66	192.79	268.47	178.68	266.39	176.59
	307.47	217.65	280.98	191.25	266.80	177.00	264.67	174.88
46	295.04	203.26	269.15	177.32	255.46	163.66	253.93	162.14
	293.96	202.20	268.10	176.30	254.42	162.68	252.86	161.11
	292.40	200.68	266.44	174.76	252.76	161.01	251.06	159.42
47	279.64	185.98	254.27	160.49	241.18	147.52	240.15	146.49
	278.49	184.87	253.18	159.48	240.08	146.42	239.04	145.41
	276.96	183.30	251.55	157.85	238.40	144.77	237.31	143.69
48	263.87	168.27	239.07	143.37	226.50	130.89	225.98	130.40
	262.72	167.13	237.93	142.34	225.43	129.80	225.41	129.33
	261.16	165.60	236.36	140.66	223.73	128.16	223.20	127.54
49	247.84	150.21	223.56	125.94	211.52	113.97	211.61	114.01
	246.57	149.07	222.33	124.79	210.39	112.86	210.39	112.91
	245.10	147.52	220.81	123.12	208.72	111.17	208.71	111.34
50	32231.35	32131.85	31207.55	31108.10	30196.15	30096.68	—	—
	230.04	130.73	206.38	106.97	195.13	095.74	—	—
	228.62	129.17	204.85	105.37	193.35	093.93	—	—
51	214.54	113.20	191.25	090.09	180.51	079.13	—	—
	213.27	111.93	190.15	088.85	179.28	078.06	—	—
	211.84	110.42	188.53	087.28	177.68	076.33	—	—

TABLE I. (*Cont.*).

K''	(0, 6) R	(0, 6) P	(0, 7) R	(0, 7) P	(0, 8) R	(0, 8) P	(0, 9) R	(0, 9) P
	197.44	094.07	174.76	071.50	164.61	061.20	—	—
52	196.01	092.76	173.54	070.32	163.27	060.10	—	—
	194.41	091.31	171.84	068.76	161.51	058.53	—	—
	179.80	074.63	157.85	052.64	148.22	043.08	—	—
53	178.51	073.40	156.55	051.42	146.92	041.83	—	—
	177.06	071.93	155.05	049.89	145.37	040.25	—	—
	161.97	054.93	140.66	033.53	131.62	024.60	—	—
54	160.61	053.60	139.26	032.24	130.26	023.14	—	—
	159.17	051.96	137.79	030.53	128.74	021.39	—	—
	143.74	034.73	123.12	013.99	114.61	005.62	—	—
55	142.40	033.43	121.69	012.70	113.26	004.23	—	—
	140.92	031.98	120.15	011.17	111.71	002.70	—	—
	125.19	014.28	105.16	30994.16	30097.25	29986.33	—	—
56	123.70	012.92	103.65	992.79	095.74	984.88	—	—
	122.34	011.50	102.19	991.26	094.35	983.39	—	—
	106.26	31993.45	086.80	974.03	079.62	966.76	—	—
57	104.76	992.04	085.35	972.64	078.06	965.31	—	—
	103.37	990.62	083.88	971.11	076.68	963.79	—	—
	086.96	972.26	068.17	953.48	061.65	946.81	—	—
58	085.43	970.85	066.70	952.08	060.10	945.38	—	—
	084.06	969.46	065.24	950.58	058.53	943.83	—	—
	067.34	950.76	049.16	932.61	043.08	926.64	—	—
59	065.86	949.27	047.71	931.14	041.83	925.26	—	—
	064.50	947.85	046.24	929.70	040.25	923.73	—	—
	047.40	928.83	029.90	911.37	024.60	906.13	—	—
60	045.63	927.34	028.20	909.91	023.14	904.69	—	—
	044.69	925.98	027.08	908.46	021.91	903.17	—	—
	027.05	906.57	010.25	889.89	005.62	885.23	—	—
61	025.38	905.13	008.62	888.36	004.23	883.82	—	—
	024.07	903.69	007.22	886.91	002.70	882.26	—	—
	006.25	884.04	30990.20	868.01	29986.33	864.10	—	—
62	004.66	882.40	988.55	866.31	984.88	862.43	—	—
	003.32	881.31	987.19	865.26	983.39	861.35	—	—
	31985.20	31861.10	30969.87	30845.81	29966.76	29842.60	—	—
63	983.61	859.54	968.19	844.22	965.31	841.00	—	—
	982.22	858.14	966.80	842.79	963.79	839.55	—	—
	963.82	837.81	949.14	823.20	946.81	820.69	—	—
64	—	836.14	947.53	821.55	945.38	819.06	—	—
	960.81	834.86	946.07	820.18	943.84	817.67	—	—
	941.95	814.11	928.08	800.27	926.29	798.54	—	—
65	—	812.49	—	798.67	924.70	796.96	—	—
	938.64	811.08	925.52	797.27	923.17	795.44	—	—
	—	790.10	—	776.95	—	776.05	—	—
66	—	788.55	—	775.40	—	774.46	—	—
	916.99	787.13	—	773.90	902.63	772.97	—	—
	—	765.72	—	753.37	—	753.14	—	—
67	—	764.27	—	—	—	—	—	—
	—	762.40	—	750.81	—	749.92	—	—
	—	—	—	—	—	—	—	—
68	—	—	—	—	—	—	—	—
	—	—	—	—	—	726.91	—	—

* These lines are made up of unresolved R_1 and R_2 (or P_1 and P_2) lines. The order in which the R branches are given is, reading downward, R_1, R_2, R_2. The same is true of the P branches.

The combination differences,

$$\Delta_2 F_i''(K) = R_i(K-1) - P_i(K+1) = F_i''(K+1) - F_i''(K-1)$$

for the lower electronic state have the same form as Eqs. (11), (12), and (13), except that the (′) is replaced by the (″). Because of lack of space, the numerical values of the combination differences are not given here. However, they can be obtained directly from the data in Table I. The values for a given

interval obtained from different bands agree, on the average, to about 0.06 cm^{-1}. The values of $\Delta_2F_2(K)$, which are not a function of ϵ or γ, were used to determine the value of B_v. Graphs of $\Delta_2F_2(K)/(K+\frac{1}{2})$ as ordinate with K as abscissa were made for all bands investigated. The ordinate at $K=-\frac{1}{2}$ is an approximate value of $4B_v$. Since

$$B_v = B_e - \alpha(v+\tfrac{1}{2}), \tag{14}$$

the difference between the values of B_v and B_{v+1} obtained from these graphs gave a preliminary value of α. The value of B_e was then calculated from Eq. (14) and substituted in the relation $D_e=-4B_e^3/\omega_e^2$ to obtain the value of D_e. D_v is given by the relation $D_v=D_e+\beta(v+\frac{1}{2})$, where $\beta=\alpha^2/6\omega_e+(20\alpha B_e^2-32x_eB_e^3)/\omega_e^2$. The value of D_v thus obtained can be used to calculate $8D_v(K+\frac{1}{2})^3$, which, when added to the observed values of $\Delta_2F_2(K)$, yields a set of values $\Delta_2F_2^*(K)$ which are practically linear in $(K+\frac{1}{2})$. $\Delta_2F_2^*(K)$ is represented by

$$\Delta_2F_2^*(K) = \Delta_2F_2(K) - 8D_v(K+\tfrac{1}{2})^3 = 4B_v(K+\tfrac{1}{2}). \tag{15}$$

The least squares solution of this equation gives an accurate value of $4B_v$. The values of $4B_v$ thus obtained were fitted to Eq. (14) by the least squares method to obtain B_e and α.

The values of the molecular constants obtained from the data given above are listed in Table II.

TABLE II. *Constants of the rotational structure.*[15]

v'	B_v'	Constants	v''	B_v''	Constants
0	0.4989	$B_e'=0.5020\pm0.0005$ cm^{-1}	4	0.68367	$B_e''=0.70894\pm0.00009$ cm^{-1}
1	0.4927	$\alpha_e'=0.0062$ cm^{-1}	5	0.67793	$\alpha_e''=0.005622\pm0.000013$ cm^{-1}
		$I_e'=55.10\times10^{-40}$ gr. cm^2	6	0.67248	$I_e''=39.02\times10^{-40}$ gr. cm^2
		$r_e'=1.769\times10^{-8}$ cm	7	0.66674	$r_e''=1.489\times10^{-8}$ cm
		$D_e'=-1.280\times10^{-6}$ cm^{-1}	8	0.66124	$D_e''=-1.129\times10^{-6}$ cm^{-1}
		$\beta'=-3.56\times10^{-9}$ cm^{-1}	9	0.65548	$\beta''=-3.20\times10^{-10}$ cm^{-1}

Band	A	B	$\gamma'-\gamma''$
(0,4)	−1.97	−10.83	+0.0150
(0,5)	−2.02	"	"
(0,6)	−2.06	"	"
(0,7)	−2.09	"	"
(0,8)	−2.11±0.01	" ±0.01	" ±0.0005
(0,9)	−2.19	"	"
	$\gamma'\backsim+0.017$	$\gamma''\backsim-0.003$	

Note: As mentioned later in the text, the signs of γ', γ'', and $(\gamma'-\gamma'')$ are somewhat arbitrarily chosen.

IV. SPIN FINE STRUCTURE OF THE ROTATIONAL LEVELS

As pointed out above, the existence of three energy levels for each value of K is to be attributed to the mutual interaction of the individual spins com-

[15] The constants A, B, and γ are discussed in the following section. The values of r_e are calculated for the molecule $S^{32}O^{16}$, since these are by far the most abundant of the isotopes of these elements.

bined with the interaction of the resultant spin S^* and the magnetic field generated by nuclear rotation. The separations of these levels from the energy given by $B_vK(K+1)+D_vK^2(K+1)^2+\cdots$ are represented by Eqs. (6), (7) and (8). The rotational term differences are expressed by Eqs. (11), (12), and (13). If the terms in ϵ in these equations are neglected, as they may be except at low K, then

$$\Delta_2F_1(K) - \Delta_2F_3(K) = 4\gamma. \tag{16}$$

The value of 4γ is, in the present case, less than the experimental error; hence, for any one value of K, Eq. (16) does not give even an approximate value of γ, and the average for a large number of K values gives only a rough approximation. The values of γ' and γ'' were determined from each of the six bands with $v'=0$ by averaging all the available differences $\Delta_2F_1(K) - \Delta_2F_3(K)$ for $K>25$. The values of γ' thus obtained ranged from $+0.025$ to $+0.011$ with an average $+0.017$. The values of γ'' ranged from -0.006 to -0.0006 with an average -0.003. No consistent variation of γ'' with v'' was observed. Although these values of γ' and γ'' represent only the order of magnitude of the correct values, they appear to be definitely of opposite sign. However, the above data alone are insufficient to determine whether γ'' is negative or positive, since we do not know which of the two high-frequency R (or P) branches is the theoretical R_1 (or P_1) branch.

It has been shown that the value of γ''[16] for the normal $^3\Sigma_g^-$ state of the O_2 molecule is negative,[13] and that the value of γ' for the excited $^3\Sigma_u^-$ state for the Schumann-Runge bands of O_2 also is negative.[8] For this reason, Naudé and Christy[9] have assumed that the values of γ for the normal $^3\Sigma_g^-$ and the excited $^3\Sigma_u^-$ states of S_2 also are both negative, since both have the same sign. A similar situation in SO, however, does not exist, since the sign of γ for the normal $^3\Sigma$ state is opposite to that for the excited $^3\Sigma$ state. If we assume that the sign of γ'' for SO is the same as that for the normal states of O_2 and S_2, then the designation of the high-frequency R (or P) branch as R_1 (or P_1) is correct.

The equations for the separations of the three components of the triplet in the R and P branches, obtained from Eqs. (9) and (10) are:

$$R_1 - R_3 = 6\epsilon'(2K+3)/(2K+5)(2K+1) - 6\epsilon''(2K+1)/(2K+3)(2K-1) + (\gamma'-\gamma'')(2K+1) + 2\gamma' \tag{17a}$$

$$R_2 - R_1 = 3(\epsilon'-\epsilon'') - 3\epsilon'/(2K+5) + 3\epsilon''/(2K+3) - (\gamma'-\gamma'')(K+1) - \gamma' \tag{18a}$$

$$R_2 - R_3 = 3(\epsilon'-\epsilon'') + 3\epsilon'/(2K+1) - 3\epsilon''/(2K-1) + (\gamma'-\gamma'')K + \gamma' \tag{19a}$$

$$P_1 - P_3 = 6\epsilon'(2K-1)/(2K+1)(2K-3) - 6\epsilon''(2K+1)/(2K+3)(2K-1) + (\gamma'-\gamma'')(2K+1) - 2\gamma' \tag{17b}$$

$$P_2 - P_1 = 3(\epsilon'-\epsilon'') - 3\epsilon'/(2K+1) + 3\epsilon''/(2K+3) - (\gamma'-\gamma'')(K+1) + \gamma' \tag{18b}$$

$$P_2 - P_3 = 3(\epsilon'-\epsilon'') + 3\epsilon'/(2K-3) - 3\epsilon''/(2K-1) + (\gamma'-\gamma'')K - \gamma' \tag{19b}$$

[16] The γ used here corresponds to $(-B)$ in Kramers' terminology (cf. reference 13) and to $(-D)$ in that of Lochte-Holtgreven and Dieke (cf. reference 8).

For $K \geqq 5$, the average of Eqs. (18a) and (18b) is:[17]

$$\Delta_{2-1} = 3(\epsilon' - \epsilon'') - 3(\epsilon' - \epsilon'')/(2K+3) - (\gamma' - \gamma'')(K+1) \quad (20)$$

and the average of Eqs. (19a) and (19b) is:[17]

$$\Delta_{2-3} = 3(\epsilon' - \epsilon'') + 3(\epsilon' - \epsilon'')/(2K-1) + (\gamma' - \gamma'')K. \quad (21)$$

The interval between R_2 and the mean of R_1 and R_3, for K greater than about 5,[17] is:

$$\Delta_{2-1,3} = 3(\epsilon' - \epsilon'') - \tfrac{1}{2}(\gamma' - \gamma''). \quad (22)$$

This interval is the same for the corresponding P branches.

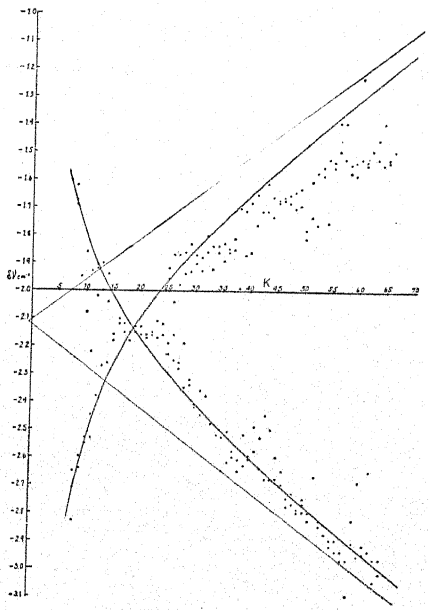


Fig. 3. Graphs showing the triplet separations in the 0,8 band. The ordinates for the circles and triangles represent, respectively, the observed separations of R_1 and R_3 from R_2, and of P_1 and P_3 from P_2. The curves are plotted according to Eqs. (23) and (24), where $A = -2.11$, $B = -10.83$, and $(\gamma' - \gamma'') = +0.0150$. These curves approach asymptotically the straight lines whose slopes are $\pm(\gamma' - \gamma'') = \pm 0.0150$.

The R_1 and R_3 (and P_1 and P_3) branches are resolved for $K > 30$, and, in some cases, for $K < 13$. The resolution for $K < 13$ was most satisfactorily observed in the (0,8) band, since this band showed very little overlapping of the different branches in the region of small K values. Accordingly, in order to determine the tripling constants as accurately as possible, the separations of the three components of the triplets of the (0,8) band were plotted on a large scale (Fig. 3). The circles and triangles represent, respectively, the wave-number separations of R_1 and R_3 from R_2, and P_1 and P_3 from P_2.

[17] These equations contain approximations of the type $(1/(2K+5))\,(1/(2K+1)) \sim (1/(2K+3))^2$, which are not very good for very low values of K.

According to Kramers' theory of spin tripling in $^3\Sigma$ states,[13] Eqs. (20) and (21) should represent the observed separations of the members of the triplets, at least for the smaller values of K. However, it was found that it was impossible to represent the data by using the same value of $3(\epsilon'-\epsilon'')$ in both of the first two terms of Eqs. (20) and (21). The equations which best represent the data for the (0,8) band, for low values of K, are:

$$\Delta_{2-1} = A - B/(2K+3) - (\gamma'-\gamma'')(K+1) \tag{23}$$

$$\Delta_{2-3} = A + B/(2K-1) + (\gamma'-\gamma'')K \tag{24}$$

where $A=-2.11$, $B=-10.83$, and $(\gamma'-\gamma'')=+0.0150$. Since there is at present no theoretical interpretation of this discrepancy, which also occurs in the $^3\Sigma_u^-$ normal state of O_2,[18] we cannot determine which one, if either, of two terms, A and B, represents the value of $3(\epsilon'-\epsilon'')$ in Kramers' theory.

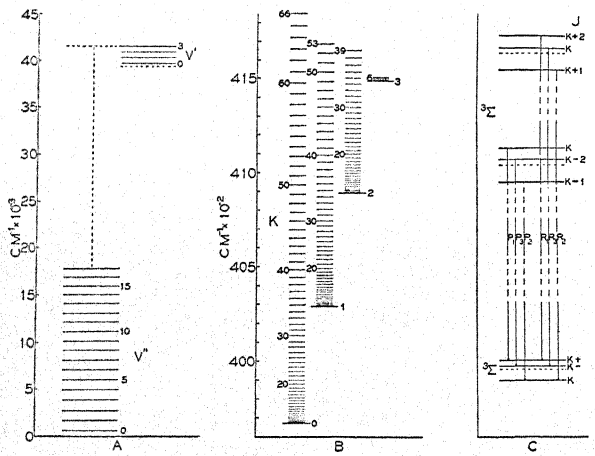


Fig. 4. Energy-level diagram. (A). The vibrational levels of the upper and lower $^3\Sigma$ states. No levels with $v'>3$ are observed. (B). The rotational levels of the upper state. This shows the values of K' at which the bands are observed to break off. (C). A schematic representation of the structure of the rotational levels of the two $^3\Sigma$ states. Only the levels associated with the lines $R(K)$ and $P(K)$ are shown. The separations of the actual levels from those which would exist if there were no spin are indicated qualitatively by the displacements of the full from the dashed lines.

The curves in Fig. 3 represent graphs of Eqs. (23) and (24) with the appropriate values of the constants A, B, and $(\gamma'-\gamma'')$. These curves approach asymptotically the straight lines whose slopes are $\pm(\gamma'-\gamma'')=\pm 0.0150$, and whose common intercept at $K=-\frac{1}{2}$ is $A-\frac{1}{2}(\gamma'-\gamma'')=-2.125$. The difference between the ordinates of the straight lines and of the corresponding curves represents the value of the terms containing K in the denominator in Eqs. (23) and (24). The data for low K values are represented well within experimental error, but for large K the data deviate considerably from sym-

[18] R. T. Birge and H. H. Nielsen, unpublished work on the atmospheric oxygen bands. The writer is indebted to Professor Birge for the methods used in the determination of the constants A, B, and $(\gamma'-\gamma'')$.

metry about the horizontal line $\delta\nu = -2.125$ cm^{-1}, due undoubtedly to the fact that the energy of interaction of S* and the magnetic field generated by the rotation of the molecule deviates appreciably from the linear form assumed in setting it equal to $\gamma(K^* \cdot S^*)$.[19]

The wave-number separations of the members of the triplets were plotted for all six bands with $v'=0$, and the constants A, B, and $(\gamma'-\gamma'')$ were determined from them as accurately as possible. On account of the fact that overlapping prevented complete resolution of the branches at low K values for bands other than the (0,8), the constants obtained from these bands are undoubtedly less accurate than those obtained from the latter.

A schematic representation of the structure of the rotational levels is shown in Fig. 4c. Only the levels associated with the lines $R(K)$ and $P(K)$ are shown. The displacement of the actual levels from those which would exist if the spin were absent is indicated qualitatively by the displacements of the full from the dotted lines.

V. Predissociation and Perturbations

An unusual feature of the bands under consideration, and one which has considerable theoretical significance, is the abrupt termination of the band system at a certain definite value of the initial vibrational quantum number, namely $v'=3$. It will be evident from the matrix diagram of Fig. 8 that no bands with $v'>3$ are observed. The phenomenon is analogous to that found in the emission bands of S_2[9] and P_2,[20] and has been shown to be the result of predissociation. Furthermore, the rotational structure of the individual bands is found in all of the SO bands to break off suddenly at a particular value of K', the rotational quantum number in the upper state. This value is large for bands with $v'=0$, but decreases with increasing v', and is very small for $v'=3$.

The abrupt termination of the rotational structure of the (0,7) band is shown in Fig. 2d, while similar effects in the (2,2), (2,3), and (3,3) bands can be seen in Fig. 2c. The (3,3) band is extremely narrow, and so faint that it is difficult to observe on the enlargement, although it was easily visible on the original plates. Two other bands with $v'=3$, which also present the same appearance, can also be seen on the original plates.

It has been shown by Bonhoeffer and Farkas,[21] and by Kronig,[22] that, if the discrete energy levels of an electronic state lie above the dissociation limit of another electronic state, there is, according to the quantum mechanics, a certain probability that a molecule in one of these levels will undergo a radiationless transition to the other electronic state, and dissociate spontaneously. This transition must obey certain selection rules derived by Kronig, and, if the conditions of the Franck-Condon principle are fulfilled, the probability

[19] R. S. Mulliken, Rev. Mod. Phys. **2**, 105 (1930) and references given there, especially J. H. Van Vleck, Phys. Rev. **33**, 467 (1929).

[20] G. Herzberg, Nature **126**, 239 (1930).

[21] K. F. Bonhoeffer and L. Farkas, Zeits. f. Physik Chem. **(A)134**, 337 (1927).

[22] R. de L. Kronig, Zeits. f. Physik **50**, 347 (1928); **62**, 300 (1930).

that such a transition will occur may be very great. In this case, the lifetime of the molecule in the discrete levels can become comparable with, or smaller than, the period of nuclear rotation. Accordingly, if these levels belong to the upper electronic state, the lines involving them will be diffuse in absorption, and either faint or absent in emission. This phenomenon is known as predissociation.[23]

Since the vibrational levels are spaced on a larger scale than the rotational levels, predissociation usually shows itself in absorption by the fact that the bands of the v' progressions become diffuse at a certain value of v', as was first observed in the S_2[24] spectrum. In emission, the same band progressions will terminate abruptly at this value of v'. The energy of this critical level represents, in some cases, the dissociation limit of the state which is causing the predissociation, and hence the phenomenon permits an evaluation of the heat of dissociation of the molecule. When the rotational structure is well resolved, as in the present case, observations on the exact value of the rotational quantum number at which the break occurs may lead to a very precise value of the heat of dissociation, and also give information of a new type concerning the mechanism of the process. The only case of this kind which has heretofore been studied is that of P_2,[20] where the resolution is less complete, and the details have not yet been published.

The K' values[25] of the last lines of the bands with $v'=0$, and $v'=1$, were found by application of the combination principle to be 66 and 53 respectively. However, the rotational levels for $v'=2$ were too much perturbed, and those for $v'=3$ too few, to permit an analysis of the rotational structure of bands involving these levels. Accordingly, the K' values of the last lines of these bands were determined from the wave-number difference between the head and last line of the band in question by means of Eq. (10), where B_v' and B_v'' were obtained from Eq. (14). These values of K' were found to be 39 for $v'=2$, and 6 for $v'=3$, but may be in error by one or two units.

The observed energy levels of the SO molecule are shown in Fig. 4; (A) shows the vibrational levels of both states, and (B) shows the rotational levels of the upper state. The rotational levels for different values of v' break off not only at different K values, but also at different energy values, and the energy at which the break occurs decreases with increasing v'. According to the interpretation of this effect given below, the term value at which the $v'=3$ levels break off (41,520 cm^{-1}) probably corresponds to dissociation of the lower electronic state. Linear extrapolation of the vibrational levels of the lower state gives 51,620 cm^{-1} as the term value corresponding to dissociation. However, it is well known that this extrapolation practically always leads to values which are considerably too large.[26]

[23] For a general discussion of predissociation, see G. Herzberg, Erg. exakt. Naturwiss. **10**, 207 (1931).

[24] V. Henri, Jour. Phys. Rad. **3**, 181 (1922); Structure of Molecules (1925).

[25] The use of K, instead of J, is justified by the fact that the three energy levels for a given K are much closer together than those with the same J.

[26] R. T. Birge, Nat'l. Research Council Bulletin on Molecular Spectra, (1926).

The oxygen atom and the sulphur atom each have a ^3P normal state and a ^1D first excited state. The energy of excitation of this ^1D state of oxygen is given by Frerichs[27] as 1.95 volts, and that of sulphur is estimated by Christy and Naudé[28] as 1.60 volts. Linear extrapolation of the vibrational levels of the excited state of SO leads to 56,840 cm^{-1} as the term value corresponding to dissociation of this state. If the convergence limit 41,520 cm^{-1} is subtracted from this limit at 56,840 cm^{-1}, we have 1.89 volts as the energy of atomic excitation. Although linear extrapolation of the levels of the excited state is especially untrustworthy in view of the fact that so few levels are observed, and that these levels may be perturbed, it seems probable that 1.89 volts is too high; therefore, we may assume that the sulphur atom is excited, and that 1.60 volts represents the energy of excitation. In this case, the dissocia-

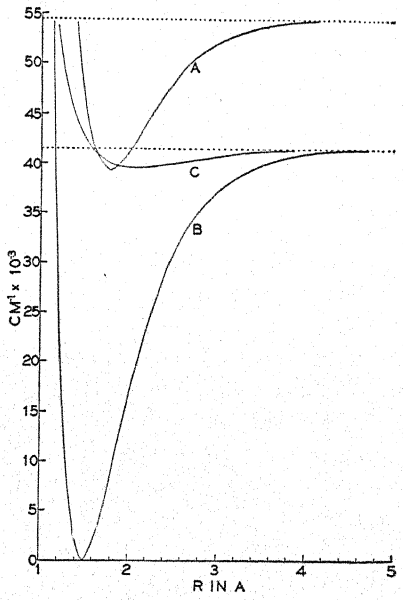


Fig. 5. Potential energy curves of the SO molecule. Curves A and B represent the two known $^3\Sigma$ states, and are plotted according to Morse's equation. Curve C ($^3\Pi$) has been assumed in order to account for predissociation.

tion limit of the excited $^3\Sigma$ state is at about 54,400 cm^{-1}, instead of 56,840 cm^{-1}, as obtained by linear extrapolation. Since this ^1D level is the first excited atomic state upon which the upper $^3\Sigma$ state of the molecule can be built, the dissociation limit at 41,520 cm^{-1} must represent dissociation into two normal ^3P atoms, and, therefore, dissociation of the normal state of the SO molecule.

Potential energy curves for the known states of the SO molecule are shown in Fig. 5; curves A and B represent the upper and lower $^3\Sigma$ states for

[27] R. Frerichs, Phys. Rev. **36**, 398 (1930).

[28] A. Christy and S. M. Naudé, Phys. Rev. **37**, 903 (1931), obtained the value for S by interpolation from the known values for O, Se, and Te atoms.

the observed bands, and are plotted according to Morse's[29] equation, while curve C must be assumed in order to account for predissocation. The electronic states represented by A and B are both $^3\Sigma$, and probably both $^3\Sigma^-$, since this is the case in O_2 and S_2. The molecule in state B is built of two ^3P atoms, and in state A of a ^3P and a ^1D atom. Since ^1D is the lowest excited atomic state, the molecule in state C, in order that C may cause predissociation, must also be built of two ^3P atoms. The possible electronic states of a molecule composed of two dissimilar ^3P atoms are:[30] two $^1\Sigma^+$, $^1\Sigma^-$, two $^1\Pi$, $^1\Delta$, two $^3\Sigma^+$, $^3\Sigma^-$, two $^3\Pi$, $^3\Delta$, two $^5\Sigma^+$, $^5\Sigma^-$, two $^5\Pi$, and $^5\Delta$. The selection rules for a radiationless transition of a molecule composed of two dissimilar atoms, as given by Kronig,[22] are: $\Delta\Lambda = 0, \pm 1$; $\Delta\Sigma$ and $\Delta S = 0$; $\Delta J = 0$; the transition can occur only between two rotational levels which are both positive or both negative. Accordingly, of the electronic states listed above, the only ones which can interact with the upper $^3\Sigma^-$ state are the $^3\Pi$ and the $^3\Sigma^-$ states. In addition to Kronig's selection rules, there is another requirement which must be fulfilled for two electronic states to be able to interact to any noticeable degree;[23] the potential energy curves of the two states must approach each other very closely. As shown in Fig. 5, the curves for the two $^3\Sigma^-$ states are everywhere well separated; hence these states cannot interact enough to cause predissociation. Therefore, the interacting state must be $^3\Pi$.

Herzberg[23] has suggested that the decrease with increasing v' of the term value at which the rotational levels break off, which was also observed in P_2,[23] is an effect of rotation of the molecule, and that an explanation is to be found by an application of the same principles which Oldenberg used to interpret the dissociation by rotation alone which occurs in the HgH bands.[31]

If we represent the potential energy of the molecule by $U(r)$, the force acting on the nuclei is given by $U'(r)$, the derivative of $U(r)$ with respect to the internuclear distance r. If the molecule is allowed to rotate, but not vibrate, it will expand to a new equilibrium position, such that the centrifugal force is equal to the attractive force; then $p^2/\mu r^3 = U'(r)$, where p is the angular momentum of the nuclei, and μ is their reduced mass. If the molecule then vibrates about this new position of equilibrium, with constant angular momentum, it will be acted upon by a restoring force $U'(r) - p^2/\mu r^3$. This force can be represented by the derivative with respect to r of the expression $U(r) + p^2/2\mu r^2$. The expression $p^2/2\mu r^2$ is equal to the kinetic energy of rotation of the molecule; or

$$T(r) = p^2/2\mu r^2 = BK(K+1) + DK^2(K+1)^2 + \cdots \qquad (25)$$

Hence, with the assumption that the angular momentum is constant, $U(r) + T(r)$ is an "effective" potential energy, and has the same meaning for

[29] P. M. Morse, Phys. Rev. **34**, 57 (1929).

[30] R. de L. Kronig, Band Spectra and Molecular Structure (Cambridge), (1930); R. S. Mulliken, Rev. Mod. Phys. **4**, 1 (1932); E. Wigner and E. E. Witmer, Zeits. f. Physik **51**, 859 (1928).

[31] O. Oldenberg, Zeits. f. Physik **56**, 563 (1929). In the case of the HgH bands, the effect was due entirely to dissociation by rotation of the molecule in the lower electronic state, while in the present case, a radiationless electronic transition is involved.

a vibrating and rotating molecule that $U(r)$ has for a molecule which is vibrating, but not rotating.

As required by the Franck-Condon principle, $T(r)$ must be added to the $U(r)$ curve of each of the interacting states, and a radiationless transition can occur between only those $U(r)+T(r)$ curves which have the same $T(r)$ (i.e., same angular momentum). Accordingly, the shape of the $^3\Pi$ curve determines the intersections of its $U(r)+T(r)$ curves with those of the upper $^3\Sigma^-$ state, and, therefore, the term values at which the rotational levels break off. If the $^3\Pi$ state is assumed to be repulsive for all values of r, as Christy and Naudé[28] assumed for S_2, the decrease with increasing v' of the term value at which the rotational levels break off would be much greater than is observed. In order to satisfactorily explain the observed facts, it was necessary to assume a shallow minimum in the $^3\Pi$ curve, as shown in Fig. 5 (curve C).

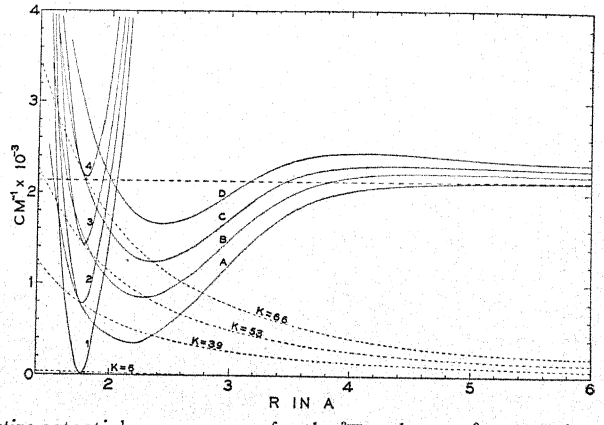


Fig. 6. *Effective* potential energy curves for the $^3\Pi$ and upper $^3\Sigma$ states for various amounts of rotation. The dashed curves represent the kinetic energy of rotation of the molecule, $T(r)=p^2/2\mu r^2$, for the K values indicated. Curves 2, 3, and 4 are obtained by adding the dashed curves to curve 1. Curves B, C, and D are obtained from A similarly. The horizontal dashed line, according to our interpretation, corresponds to the energy of dissociation of the $^3\Pi$ and lower $^3\Sigma$ states.

In Fig. 6, $U(r)+T(r)$ curves are plotted for states A (upper $^3\Sigma^-$) and $C(^3\Pi)$ of Fig. 5 for the four values of K' at which the rotational levels for the different values of v' are observed to break off. The dashed curved lines represent graphs of $T(r)=p^2/2\mu r^2$, where p, for a given K', has been evaluated from Eq. (26) by using B_e', D_e', and r_e'. Curves 1 and A of Fig. 6 correspond to curves A and C of Fig. 5 respectively, but are on a much larger scale. Curves 1 and A have also been taken to represent $U(r)+T(r)$ for $K=6$, since $T(r)$, in this case, is negligibly small for the values of r with which we are concerned here. Curves 2, 3, and 4 are obtained by adding the dashed curves ($T(r)$) to curve 1 ($U(r)$); curves B, C, and D are obtained from A similarly. The horizontal dashed line represents the term value at which the rotational levels for $v'=3$ are observed to break off.

If the molecule is in the upper $^3\Sigma^-$ state, and is rotating with $K=6$, its

potential energy is represented by curve 1, and, if in addition it is vibrating with $v'=3$, it has an energy corresponding to the horizontal dashed line. Accordingly, as the molecule vibrates along curve 1, it can undergo, at the points of intersection of 1 and A, an electronic transition, without any change of internuclear distance and momentum, from $^3\Sigma^-$ to $^3\Pi$, and begin vibrating along curve A. Since the molecule has sufficient energy, it vibrates along A to large r and dissociates. If $K'=66$, the molecule vibrates along curve 4, and can undergo a transition to curve D at the point of intersection. In this case, only the vibrational energy corresponding to $v'=0$ is required for the molecule to be able to pass the hump at large r in curve D and dissociate.

The Franck-Condon principle allows only the following transitions between the curves shown in Fig. 6: 1 to A, 2 to B, 3 to C, and 4 to D. These are the transitions which the molecule undergoes when it dissociates with $v'=3$, 2, 1, and 0, respectively. If the molecule has only the vibrational energy corresponding to $v'=0$, then, in order to dissociate, it must also have rotational energy corresponding to $K'=66$. For $K'>66$, the molecule can also dissociate, and, if the probability that this will occur is sufficiently great, spectrum lines involving these levels will not be observed in emission. A similar argument applies to the other vibrational levels.

The fact that the height of the hump at large r in the $U(r)+T(r)$ curves of the $^3\Pi$ state increases with increasing rotational energy requires the total (vibrational plus rotational) energy necessary for predissociation to increase with decreasing vibrational energy. Accordingly, the rotational levels for $v'=0$ break off at a term value greater than those for other v' levels by just the difference in the heights of the humps in the corresponding $U(r)+T(r)$ curves of the $^3\Pi$ state. If we assume that the $^3\Pi$ state has the $U(r)$ curve shown in the figures, the agreement between the heights of these humps and the term values at which the rotational levels for the various values of v' are observed to break off is quite satisfactory.

As mentioned above, the $^3\Pi$ state cannot be repulsive for all values of r, because its $U(r)+T(r)$ curves would then intersect those of the $^3\Sigma^-$ state with the same angular momentum considerably above the dissociation limit of the $^3\Pi$ state (except for small angular momentum), with the result that the decrease with increasing v' of the term value at which the rotational levels break off would be much greater than is observed. In order than an appreciable interaction between the $^3\Pi$ and upper $^3\Sigma^-$ states shall occur, the potential energy curves for these states must intersect.[23] Accordingly, the minimum in the $^3\Pi$ curve must occur at large r and be shallow, which means a low frequency of vibration. As drawn in the figures, the curve obeys the empirical rule of Morse:[29] $\omega_e r_e^3 \sim 3000\times10^{-24}$ cm^2.

A further indication that the $^3\Pi$ curve has a shallow minimum is given by the observed perturbations of the rotational levels of the upper $^3\Sigma^-$ state. Since perturbations of the type observed in the present case are the result of interaction of two electronic states which have discrete levels of nearly the same energy, they indicate, as shown below, that the $^3\Pi$ state cannot be repulsive for all values of r.

Only a few of the rotational levels for $v'=0$ are perturbed; these perturbations consist of displacements of only a single level from its expected position. The only noticeable perturbations occur at $K'=53$ and 61, where the F_2 levels only are displaced from their expected positions. The perturbation at $K'=61$ can be seen in Fig. 2d; it occurs in the P_2 branch in the sixth member from the right of the figure, and in the R_2 branch in the second member from the left. This type of perturbation indicates that the levels of the perturbing state are spaced quite differently than those of the perturbed $^3\Sigma^-$ state.

The rotational levels for $v'=1$, however, are considerably perturbed. Fig. 2e, is an enlargement of part of the (1,4) band, and shows very clearly the irregularities of the rotational structure. As can be seen in the figure, the lines occur in distinct groups, where each group is composed of the lines $P(K)$ and $R(K+5)$. The difference in appearance of successive groups is so great, however, that it is impossible to distinguish the R from the P lines by inspection. The identification and proper numbering of the lines in terms of K'' were obtained from term differences for the lower electronic state.

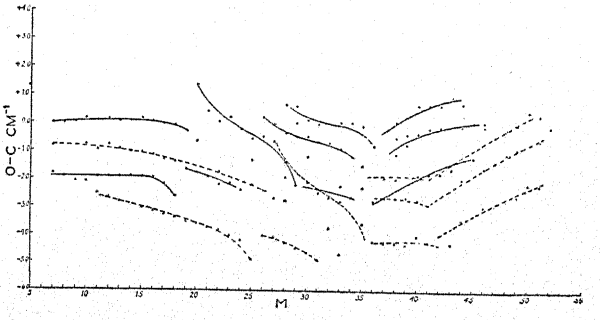


Fig. 7. Perturbations in the rotational structure of the 1,4 band. The ordinate represents the difference between the observed wave numbers of the lines and the wave numbers calculated from a formula of the type, $\nu=a+bM+cM^2+dM^3$. The circles and triangles refer to R and P lines, and the full and dashed curves represent the general course of the R and P branches, respectively. M is equal to K'' for the P branches, and to $K''-5$ for the R branches. The band is quite regular up to $K'=23$, but thereafter the perturbations are complex.

Any regularities which are present in the band can be discovered by fitting the edges of the groups to an equation of the type $\nu_M=a+bM+cM^2+dM^3$, where M is an integer. The differences between the observed wave numbers of the lines and the wave numbers calculated from this equation are shown in Fig. 7 as ordinate with M as abscissa. M is equal to K'' for the P branches (represented in the figure by dashed lines), and $K''-5$ for the R branches (solid lines). The similarity of the curves for the R and P branches is apparent. For $K''<23$, the band is fairly regular, but, for $K''>23$, the perturbations are large and complex. Because of this complexity, only the general course of the branches is represented by the curves in this region.

The rotational levels for $v'=2$ are so much perturbed that an analysis of the structure of bands involving these levels could not be made. Similarly, nothing can be said concerning perturbations of the levels for $v'=3$, since only about 6 rotational levels are present, and the bands are very weak.

Since the rules governing states which can interact to cause perturbations[22] are identical with those for predissociation, the only states which can perturb the upper $^3\Sigma^-$ state are the $^3\Pi$ and lower $^3\Sigma^-$ states, however, the potential energy curves of the $^3\Sigma^-$ states do not approach each other very closely; it therefore seems very improbable that these states could interact enough to cause perturbations of the magnitude observed. Hence the $^3\Pi$ state must be causing the perturbations. If this is the case, its potential energy curve, as stated above, must have a minimum. That the minimum is shallow is indicated by the fact that there are no perturbations of levels whose term values are less than that corresponding to $v'=1$, $K'=23$, while above this point there are many. It should be mentioned that it is possible, although it does not seem probable, that some other molecular state built on a normal and an excited atom is causing the perturbations.

Since both the perturbations and predissociation observed in the rotational structure require the $^3\Pi$ potential energy curve to have a shallow minimum, the curve must lie approximately as drawn in the figures. In this case, one would expect to observe discrete bands resulting from transitions from the $^3\Pi$ state to the lower $^3\Sigma^-$ state. However, the molecule in this $^3\Pi$ state would spend most of its time at large values of r; therefore, the most intense bands would occur at longer wave-lengths than those of the $^3\Sigma^-$, $^3\Sigma^-$ system. These bands have not been observed. Perhaps the continuum underlying the observed bands is an indication of the presence of this state.

Herzberg[23] has pointed out that the abruptness of the termination of the bands is an indication of the accuracy with which heats of dissociation can be determined by this method. If the bands terminate very abruptly, as in the present case, a very good value of the energy of dissociation can be obtained. According to the above interpretation of predissociation of the SO molecule, the term value at which the rotational levels for $v'=3$ break off corresponds to dissociation of the normal state. If the energy of dissociation is measured from the $v''=0$ vibrational level, it is calculated from the relation

$$D'' = \nu_e - G_0'' + G_0' + \Delta G_{\frac{1}{2}}' + \Delta G_{1\frac{1}{2}}' + \Delta G_{2\frac{1}{2}}' + F'_{v'=3}(6) \qquad (26)$$

to be 5.053 ± 0.001 volts. (See next section for the values of these terms, except $F_{v'=3}'$ (6), which is calculated from Eq. (5).) This result for D'' is considerably less than the value 6.42 volts obtained by Henri and Wolff by linear extrapolation of the vibrational levels. The uncertainty of 0.001 volt in our value is due principally to inaccuracy in the determination of the value of K' at which the rotational levels for $v'=3$ break off. Provided our interpretation of the phenomenon is correct, the accuracy of this value of the energy of dissociation of SO is equal to that of the most precise determination of energy of dissociation by any method, namely the spectroscopic value for I_2.[32]

If we assume that the excited $^3\Sigma^-$ state is built on a normal oxygen atom and a sulphur atom excited with 1.60 volts of energy, its energy of dissociation, measured from the $v'=0$ vibrational level, is 1.83 volts. The $^3\Pi$ state,

[32] W. G. Brown, Phys. Rev. 38, 709 (1931).

according to our interpretation, has an energy of dissociation of the order of 0.2 volt.

VI. Vibrational Structure

The wave-lengths and estimated intensities of the band heads are given in the $v'v''$ diagram in Fig. 8. These values were taken from the work of Henri and Wolff.[3] The fact that the left and upper sides of this diagram are sharply bounded by fairly intense progressions is a good indication that this assignment of vibrational quantum numbers is correct, although the assignment of v' is more certain than that of v''. The solid curve is drawn through the most intense bands of the system, and thus indicates the observed most probable changes of the vibrational quantum number. The dashed curve represents the most probable changes predicted by an application of the Franck-Condon principle, using potential energy curves plotted according to Morse's equation. The agreement between the two curves is as good as could be expected,

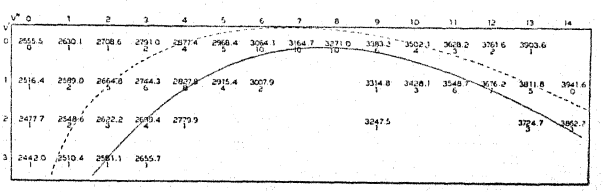


Fig. 8. This $v'v''$ matrix diagram gives the wave-lengths and estimated relative intensities of the heads of the bands of the SO spectrum. These values are taken from the work of Henri and Wolff. The solid curve is drawn through the most intense bands of the system, and thus indicates the observed most probable changes of the vibrational quantum number. The dashed curve indicates the most probable changes predicted by an application of the Franck-Condon principle, using potential energy curves plotted according to Morse's equation.

in view of the fact that the predicted values were determined from classical, instead of wave-mechanical, transition probabilities, and that the observed intensities are merely visual estimates of photographic density. The rapid decrease of plate sensitivity at the short wave-length end of the spectrum is probably responsible for the fact that, in this region, the observed curve lies below and to the right of the predicted curve.

Henri and Wolff obtained values of ω_e'', ω_e', and $x_e''\omega_e''$, but, due to inaccuracies of measurement, could not get the value of $x_e'\omega_e'$. In the present work, the origins of the six bands of the $v'=0$ progression which were measured were calculated by means of Eq. (9), using the R_2 branches. (In this calculation, the constant A of Eqs. (23) and (24) was arbitrarily taken to represent the value of $3(\epsilon'-\epsilon'')$.) From these origins, the values of ω_e'' and $x_e''\omega_e''$ were determined with much greater accuracy than is afforded by measurements of band heads only. The wave numbers of the origins and the vibrational term differences, $\Delta G_v''$, are given in Table III. The differences, $\Delta G_v''$ observed, were fitted to the equation:

$$\Delta G_v'' = \omega_e'' - 2x_e''\omega_e''(v''+\tfrac{1}{2}), \tag{26}$$

using least squares formulas. The values thus obtained are: $\omega_e''=1123.73$

± 0.24 cm^{-1}, and $2x_e''\omega_e'' = 12.232 \pm 0.034$ cm^{-1}. The values of $\Delta G_v''$ calculated from Eq. (26) are recorded in Table III as $\Delta G_v''$ calc., and the differences between the observed and calculated values are given as $O-C$.

Due to perturbations of the rotational levels, it was not possible to determine accurately the origins of bands with $v' > 1$. Therefore, in order to obthe values of ω_e' and $x_e'\omega_e'$, it was necessary to use measurements of band heads. Table III also gives the wave-lengths and wave-numbers of the heads of the bands used for this purpose, and the values of $\Delta G_v'$.

TABLE III. *Band heads, band origins, and vibrational term differences.*

Band	ν_0 cm^{-1}	$\Delta G_v''$ Obs.	$\Delta G_v''$ Calc.	$O-C$
(0, 4)	34736.31			
		1062.62	1062.57	+0.05
(0, 5)	33673.69			
		1050.20	1050.34	−0.14
(0, 6)	32623.49			
		1038.28	1038.10	+0.18
(0, 7)	31585.21			
		1025.74	1025.87	−0.13
(0, 8)	30559.47			
		1013.69	1013.64	+0.05
(0, 9)	29545.78			

Band	λ_h I.A.	ν_h cm^{-1}	$\Delta G_v'$	Band	λ_h I.A.	ν_h cm^{-1}	$\Delta G_v'$	Av. $\Delta G_v'$
(0, 3)	2791.33	35814.7		(0, 4)	2877.66	34740.4		
			617.5				617.3	617.4
(1, 3)	2744.02	36432.2		(1, 4)	2827.41	35357.7		
			606.3				605.6	606.1
(2, 3)	2699.10	37038.5		(2, 4)	2779.79	35963.3		
			606.1					
(3, 3)	2655.64	37644.6						

The fact that the values of $\Delta G_v'$ for the $v'' = 3$ progression are not linear shows that at least one of the upper state vibrational levels is perturbed. Since the $v' = 3$ level is very close to the dissociation limit of the lower state, it was considered as more likely to be perturbed than any of the others. Therefore, only the values of $\Delta G_v'$ obtained from the levels with $v' = 0$, 1, and 2 were used in the determination of the vibrational constants of the upper state. In getting the average $\Delta G_{1\frac{1}{2}}' = 606.1$, the value 606.3 was given greater weight than 605.6, since the position of the head of the (2,4) band was difficult to measure. The average $\Delta G_v'$ values thus obtained give $\omega_e' = 628.7$ cm^{-1}, and $2x_e'\omega_e' = 11.3$ cm^{-1}. Because of the fact that these were obtained from only two values of $\Delta G_v'$, no probable error for them can be given, although it seems quite likely that they may be in error by a few tenths of a wave number.

The vibrational term values of the upper state are given by:

$$G_v' = 628.7(v' + \tfrac{1}{2}) - 5.65(v' + \tfrac{1}{2})^2 \qquad (27)$$

and those of the lower state by:

$$G_v'' = 1123.73(v'' + \tfrac{1}{2}) - 6.116(v'' + \tfrac{1}{2})^2. \qquad (28)$$

The origin of the band system was calculated from the relation $\nu_e=\nu_0+G_{v''}-G_{v'}$, where ν_0 represents the origin of the (v', v'') band, and $G_{v'}$ and $G_{v''}$ are obtained from Eqs. (27) and (28). The average ν_e obtained from the seven bands investigated is 39356.3 cm^{-1}.

The writer takes this opportunity to express his sincere appreciation of the invaluable suggestions given to him by Professor F. A. Jenkins, under whose supervision this investigation has been conducted.

The Influence of Crystalline Fields on the Susceptibilities of Salts of Paramagnetic Ions. I. The Rare Earths, Especially Pr and Nd

By WILLIAM G. PENNEY* AND ROBERT SCHLAPP
Department of Physics, University of Wisconsin

(Received May 28, 1932)

The paramagnetic susceptibilities of the salts of the rare earth elements Pr and Nd are considered on the assumption that it is permissible to represent the potential of the electric field of the atoms surrounding the metallic ion by a Taylor's expansion. This amounts to applying to the whole crystal the method of the "self-consistent field," and consequently neglects exchange effects between different crystal atoms. Hund has calculated the susceptibilities on the assumption that the ion can be regarded as free and that the multiplet intervals are so large compared with kT that only the lowest level need be considered. The introduction of an electric field causes a splitting of the levels and a redistribution of magnetic moment, with a consequent change in the susceptibility. The theoretical interpretation of the Curie-Weiss law $\chi=C/(T+\Delta)$ is considered. At temperatures so high that kT is large compared with the splitting produced by the crystal field, the susceptibility can be expanded in the form of a series of inverse powers of T. It is shown that the susceptibility of a crystal powder, or the average susceptibility over all directions in a single crystal is of the form $\chi=C/T+C_2/T^3+\cdots$ the term in $1/T^2$ vanishing rigorously. Thus at sufficiently high temperatures, the susceptibility of a crystal powder obeys the simple Curie law up to and including terms in $1/T^2$. However, the curious result emerges that at ordinary temperatures kT is of the same order as the energy separations produced by the crystal field, and the behaviour of the susceptibility actually simulates the Curie-Weiss law closely over a large range of temperatures. The hydrated sulphates of Pr and Nd are considered in detail. Excellent agreement is obtained with the experimental results of Gorter and de Haas for the variation of susceptibility with temperature on the assumption that the crystal field has cubic symmetry, and can be represented by a potential $D(x^4+y^4+z^4)$. In this connection the matrix elements of the squares and fourth powers of the coordinates for a many-electron system are given. The over-all splitting produced by this field in the hydrated sulphates is 389 cm^{-1} for Pr and 834 cm^{-1} for Nd, the detailed appearance of the energy spectrum being shown in Fig. 1. A comparison of the constant D in the two cases gives a value for Nd nearly four times that for Pr.

THE theory of paramagnetic susceptibilities as developed by Van Vleck[1] and others has been applied with considerable success to the calculation of the Curie constants of salts of the rare earth group on the assumption that it is legitimate to regard the metallic ion as free. At ordinary temperatures, the theory then leads to an expression for the susceptibility of the Curie form $\chi=C/T$. Experimentally the Curie-Weiss law

$$\chi = C/(T+\Delta), \tag{1}$$

where Δ is a constant over a wide range of temperature, frequently gives a good representation of the results. It very often happens that at extremely

* Commonwealth Fund Fellow.

[1] J. H. Van Vleck, Theory of Electric and Magnetic Susceptibilities, Oxford, 1932.

low temperatures, neither law will fit the experimental measurements. It has been suggested[2] that the deviations from the simple Curie law are due to the influence of the electric fields of the surrounding ions, which remove, wholly or partially, the spatial degeneracy of the energy levels of the free ion, thereby modifying both their positions and magnetic moments. Fields of this nature have already been postulated by Becquerel[3] and by Kramers,[4] in connection with the Zeeman effect and paramagnetic rotation in crystals, while Bethe[5] has worked out by group theory the energy spectrum of ions in fields of various symmetries. In an ionic crystal, such as nickel chloride, it seems likely that the crystal field will have the same symmetry as the crystal, but in a molecular crystal, such as hydrated $Pr_2(SO_4)_3$, there is no reason why this should any longer be true. In the absence of definite knowledge of the electric field to which an ion in a given crystal is subject, the only possible procedure is to find the simplest field which will give agreement with the experimental results.

Although considerable experimental material is available, it is not as complete as could be desired; in particular, accurate measurements at different temperatures on single crystals are lacking. From the calculations given below, there seems to be no doubt that the mechanism of crystal fields is competent to account for all the observed results. A summary of the results obtained for Pr, Nd, Ni, and Cu has been given in a Letter to the Editor.[6] In the present paper an attempt is made to calculate the magnitude of the electric fields necessary to account for the experimental variation with temperature of the susceptibility of the rare earth elements Pr and Nd. In a second communication we shall present the calculations for Ni, Co and Cr while those for Cu will be given by Mr. Jordahl. We have considered only crystals of high magnetic dilution. This is necessary in order that the influence of exchange may be neglected. It has been found possible in these cases to represent the variation of susceptibility over a wide range of temperature by an equation of the form (1) although as will be discussed more fully below, this arises in a peculiar way, and also to account for the deviations from (1) which occur at very low temperatures.

The majority of measurements have been made on crystal powders, so that the observed value of Δ represents an average over all the directions in a single crystal. In such cases, the simplest assumption is that of a cubically symmetric field, and this involves only a single parameter which must be chosen to fit the experimental average Δ. With Pr and Nd it proves that a cubic field is adequate to account for all the features which have been observed up to the present. It is possible to fit the experimental curves very

[2] Reference 1, Chap. IX.

[3] J. Becquerel, Zeits. f. Physik **58**, 205 (1929).

[4] H. A. Kramers, Proc. Amst. Acad. **32**, 1176 (1929).

[5] H. Bethe, Ann. d. Physik **3**, 133, (1929); Zeits. f. Physik **60**, 218, (1930).

[6] O. M. Jordahl, W. G. Penney and R. Schlapp, Phys. Rev. **40**, 637 (1932). The affix $+++$ for Pr and Nd, and $++$ for Ni, Co, Cu, is to be understood throughout where the symbol of the element refers to the ion.

well, but owing to a discrepancy of some 16 percent in the absolute magnitude of the susceptibility as measured by different observers,[7] more refined calculations seem out of place. However, when more detailed experimental data are available it may be necessary to introduce fields of lower symmetry to obtain agreement with experiment.

One may classify crystal fields as strong or weak according as they are able or unable to break down the coupling between the total orbital and spin angular momenta. It is assumed that the fields are never strong enough to break down the coupling between the individual orbital or individual spin angular momenta. Thus the crystal field is strong or weak according as it produces a splitting of energy levels which is large or small compared with the multiplet separation. The criterion that the ion can be considered as free is that the work required to turn over the ion against the influence of the crystal field should be small compared with kT. For the rare earths, it has been shown that the magneton numbers calculated on the assumption that the ions are perfectly free agree closely with the observed values, indicating that the crystal fields are weak. For the iron group, on the other hand, the fields are so strong that the contribution of the orbital angular momentum to the susceptibility is very much less than it would be for the free ion, although the spin may still contribute its full amount. This difference in the crystal fields is in harmony with the fact that in the rare earths the $4f$ electrons causing the paramagnetism are much more completely screened from outside influences than the $3d$ electrons of the iron group. Our quantitative results are in excellent accord with the theory of Van Vleck and it was at his suggestion that the detailed calculations given in this paper were made with the object of testing numerically the general predictions of the theory.

The Constant Δ for the Rare Earths

The fundamental expression for the susceptibility is

$$\chi = -\frac{N}{H}\sum\frac{\partial W}{\partial H}e^{-W/kT}/\sum e^{-W/kT}, \tag{2}$$

the summation extending over all levels. Here H is the magnetic field, N Avogadro's number, and W the energy levels in the presence of the magnetic field. Let us assume that a certain number of the levels form a group having a range of energy much smaller than kT, while the other levels are all so far distant that on account of the Boltzmann factor, their contribution to the susceptibility can be neglected. This state of affairs would presumably be realized in the rare earths at high temperatures, the "low-frequency" group comprising the components into which the lowest multiplet level is split by the crystal field, the components of the other multiplets being much higher. Let us take as origin the center of gravity of the low frequency group. Then,

[7] The magneton numbers for the salt $Nd_2(SO_4)_3 \cdot 8H_2O$ at room temperatures according to different observers are as follows: Cabrera 18.00, Gorter and de Haas 16.68, Zernicke and James 17.50. The susceptibility is proportional to the square of the magneton number.

if we neglect saturation, i.e., retain only the part of χ independent of H, we find

$$\chi = C/T + C_1/T^2 + \cdots$$

where

$$C = N\sum \frac{\partial W^2}{\partial H}\Big/ 2kH(2J+1), \quad C_1 = -N\sum \frac{\partial W^3}{\partial H}\Big/ 6H(2J+1)$$

Thus to the approximation which neglects terms in $1/T^3$ and beyond, the constant Δ in the empirical formula (1) is given by

$$k\Delta = \tfrac{1}{3}\sum \frac{\partial W^3}{\partial H}\Big/ \sum \frac{\partial W^2}{\partial H}.$$

We shall now show that under the assumptions stated above the value of the constant C is independent of the direction of the magnetic field, and that the susceptibility averaged over three perpendicular directions follows the law $\chi = C/T + C_2/T^3 + \cdots$ the term in $1/T^2$ being absent. The Hamiltonian is of the form $\mathcal{H} = \mathcal{H}_0 + \mathcal{H}' + H\mathcal{H}_1$ where $\mathcal{H}_0$ is the Hamiltonian of the free ion, $\mathcal{H}'$ is the potential of the crystal field, and $\mathcal{H}_1$ is the component of the magnetic moment $\beta(L+2S)$ in the direction of the magnetic field. Using the property of the invariance of the spur we have

$$\sum \partial W^2/\partial H = \mathrm{Sp}(\partial/\partial H)(\mathcal{H}_0 + \mathcal{H}' + H\mathcal{H}_1)^2.$$

The spur of $(\mathcal{H}_0+\mathcal{H}')\mathcal{H}_1$ vanishes, since the terms contributing to this spur have equal and opposite values for $\pm M$, so that the above expression is equal to $2H\mathrm{Sp}\mathcal{H}_1^2$. Here Sp denotes summation over the elements diagonal in a given value of J and in all possible values of M. Since the multiplet width is large compared with kT we are concerned only with those elements of the magnetic moment $\mathcal{H}_1$ which are of the low frequency type, i.e., diagonal in J, the contribution of the off-diagonal elements to the susceptibility being independent of the temperature. Now $\mathrm{Sp}\,\mathcal{H}_1^2 = g^2\beta^2 J(J+1)(2J+1)/3$ so that the constant C has the Hund value $Ng^2\beta^2 J(J+1)/3k$ for all directions of the magnetic field.

The value of C_1 for a crystal powder is the average of the three values obtained when the magnetic field acts along the three axes x, y, z, respectively. By an argument similar to that just given, we can show that the average C_1 so defined vanishes. If we denote summation for three perpendicular directions of the magnetic field by $\sum_{xyz}$ the average is proportional to the term independent of H in $(1/H)\sum_{xyz}\sum \partial W^3/\partial H$ where the second summation extends over all the levels W in the lowest multiplet level. Using the property of the invariance of the spur, we have

$$\begin{aligned}\frac{1}{H}\sum_{xyz}\sum \frac{\partial W^3}{\partial H} &= \frac{1}{H}\sum_{xyz}\mathrm{Sp}\,\frac{\partial}{\partial H}(\mathcal{H}_0 + \mathcal{H}' + H\mathcal{H}_1)^3 \\ &= 6\sum_{xyz}\mathrm{Sp}\,(\mathcal{H}_0 + \mathcal{H}')\mathcal{H}_1^2 + \cdots \\ &= 6\,\mathrm{Sp}\left[(\mathcal{H}_0 + \mathcal{H}')\sum_{xyz}\mathcal{H}_1^2\right].\end{aligned}$$

We may replace $\sum_{xyz} \mathcal{H}_1^2$ by $(\mu_x^2+\mu_y^2+\mu_z^2)(J,\ M;\ J,\ M) = g^2\beta^2 J(J+1)(2J+1)$ where $\mu_x\mu_y\mu_z$ are the three components of the magnetic moment. Since this is independent of M, it may be taken outside the Sp sign, so that the mean value of C_1 is proportional to

$$6g^2\beta^2 J(J+1)(2J+1)\ \mathrm{Sp}\ (\mathcal{H}_0 + \mathcal{H}').$$

Since we have chosen the origin of energy at the mean centre of the unperturbed levels, Sp $(\mathcal{H}_0+\mathcal{H}')=0$, and therefore the average value of C_1 vanishes. Since we have shown that the value of C is independent of the direction of the magnetic field, and since $\Delta = -C_1/C$, this may be expressed by saying that Δ for a crystal powder vanishes, and hence, neglecting terms of order $1/T^3$, the susceptibility obeys the law $\chi = C/T$.[8] It must be borne in mind that in deducing this result we have assumed kT large compared with the splitting produced by the crystal field. However, from our calculations it appears that kT is of the same order as this splitting at ordinary temperatures. Under these conditions, it is no longer permissible to expand the exponentials as we have done, and on substituting the exact values, deviations from the law $\chi = C/T$ appear of such a kind that the susceptibility can be represented with considerable accuracy by a formula of the type $\chi = C/(T+\Delta)$, where Δ is appreciably constant over a wide range of temperature. It is to be hoped that experimenters, after having devoted so much attention to these mysterious Δ's will not be disappointed to find that in a sense they do not exist at all, at least for highly hydrated salts. At very low temperatures there are further deviations, and these will be discussed later.

The Potential of the Crystal Field

Each ion is supposed to be subject to an electric field of force represented by a potential V of the form

$$V = Ax^2 + By^2 + Cz^2 + 0(3) + 0(4) + \cdots$$

inasmuch as the first order terms vanish. If the field has cubic symmetry the first nonvanishing terms are of the fourth order; with rhombic symmetry the quadratic terms do not vanish and it is sufficient to consider these alone. The terms of any degree in the expansion of the potential V must satisfy Laplace's equation. For the quadratic terms this gives $C = -(A+B)$. For cubic symmetry, it is sufficient to write the potential

$$V = D(x^4 + y^4 + z^4)$$

since this can be made to satisfy Laplace's equation by adding a function of r^2 (*viz.* $-3Dr^4$). This corresponds to superposing a spherically symmetrical field, and merely shifts all levels equally.

[8] This point was first noticed in a particular case. We are indebted to Professor Van Vleck for the general proof. Sommerfeld, *Atombau und Spektrallinien* I (1931) p. 558, mentions that Bethe has shown in unpublished work that at all but very low temperatures the susceptibility of a crystal powder is the same as that of the free ion.

The Matrix Elements of the Crystal Field

We require the matrix elements of the squares and fourth powers of x, y and z, and shall retain only those elements which are diagonal in J. For a one-electron system they may be calculated by quadrature alone, using the usual form of the hydrogenic wave-function involving $P_J{}^M(\cos\theta)$. For our problem we shall however use the more general method given by Wigner,[9] in which the $2J+1$ wave functions $\psi_{J\,M}$, of the atom in the state J are expanded in the form $\psi_{J\,M}=\sum_\lambda D_{M\lambda}{}^J(\alpha, \beta, \gamma)\chi_\lambda{}^J(g)$, where $\chi_\lambda{}^J(g)$ depends only on the relative positions of the electrons, and $D_{M\lambda}{}^J(\alpha, \beta, \gamma)$ is the matrix element of the M-th row and λ-th column of the $(2J+1)$-dimensional representation of the rotation group. The arguments (α, β, γ) are Eulerian angles defining the spatial orientation of the atom. The coefficients $D_{M\lambda}{}^J$ satisfy certain recurrence relations,[9] by means of which it is possible, though somewhat laborious, to express the quantities $D_{M\lambda}{}^J\cos^2\beta$, $D_{M\lambda}{}^J\cos^4\beta$ etc., which occur in the integrands of the required matrix elements, as a linear combination of the quantities $D_{M\lambda}{}^{J'}$. The integration over all orientations (α, β, γ) is readily effected by means of the orthogonal relations holding between the coefficients $D_{M\lambda}{}^J$ of a representation of the rotation group; the result is to give the matrix elements in the form of a factor involving M, multiplied by a factor depending on J and the χ's, with the possible addition of a constant independent of M. We find for the elements diagonal in J of the squares and fourth powers of the coordinates of the i-th electron the following values.

$$z_i{}^4(M, M) = \gamma - \delta M^2 + \epsilon M^4$$

$$x_i{}^4(M, M+4) = y_i{}^4(M, M+4)$$
$$= \epsilon[(J-M)!(J+M+4)!/(J+M)!(J-M-4)!]^{1/2}/16$$

$$z_i{}^2(MM) = \zeta + \eta M^2, \qquad (x_i{}^4 + y_i{}^4)(M, M \pm 2) = 0,$$

$$x_i{}^2(M, M+2) = -\,y_i(M, M+2)$$
$$= \eta[(J-M-1)(J-M)(J+M+1)(J+M+2)]^{1/2}/4.$$

Here γ, ζ, ϵ, δ, η, are constants independent of M, γ and ζ being merely additive. To define the values of ϵ, δ, η, we introduce the following abbreviations

$$F = [(J-1)J(J+1)(J+2)(2J-3)(2J-1)(2J+1)(2J+3)(2J+5)]^{-1},$$

$$a = 6J(J-1)(J+1)(J+2),\ b = -\,10(6J^2+6J-5),$$

$$c = 70,\ d = a(2J^2+2J-5),$$

$$e = -\,(72J^4+144J^3-132J^2-204J+190),$$

$$f = a(2J-3)(2J+1)(2J+5)/3,\ g = -\,3f/J(J+1).$$

[9] E. Wigner, Zeits. f. Physik **43**, 624, (1927) and correction in **45**, 601, (1927).

Then in terms of these

$$\epsilon = \sum_\lambda \int F(a + b\lambda^2 + c\lambda^4)\chi^2 r_i^4 dg,$$

$$\delta = \sum_\lambda \int F(d + e\lambda^2 - b\lambda^4)\chi^2 r_i^4 dg,$$

$$\eta = \sum_\lambda \int F(f + g\lambda^2)\chi^2 r_i^2 dg$$

where we have written χ^2 for $\chi_\lambda{}^J(g)\chi_\lambda{}^{J*}(g)$ in the integrals. The matrix elements so defined suffice to determine the elements $\Delta M = 0, \pm 2$ of $x_i^2 y_i^2 z_i^2$, and the elements $\Delta M = 0, \pm 4$ of $x_i^4 y_i^4 z_i^4$, which are all that we require, since x_i^4 and y_i^4 occur only in the combination $x_i^4 + y_i^4$ which has no elements $\Delta M = \pm 2$. From these we may pass to the matrix elements of $\sum_i x_i^2$, $\sum_i x_i^4$, etc., occurring in the Hamiltonian, by using relations of the form

$$\sum_i x_i^4(J, M; J'M') = n x_i^4(J, M; J'M')$$

assuming that the n electrons are all equivalent, which is the case in our problem. In this way we find for the matrix elements of $\sum_i (x_i^4 + y_i^4 + z_i^4)$

$$\begin{aligned} &\sum (x_i^4 + y_i^4 + z_i^4)(J, M; J, M) \\ &\qquad = K + pM^2\{7M^2 + 5 - 6J(J+1)\} \\ &\sum (x_i^4 + y_i^4 + z_i^4)(J, M; J, M \pm 4) \\ &\qquad = \tfrac{1}{2}p[(J \mp M)!(J \pm M + 4)!/(J \pm M)!(J \mp M - 4)!]^{1/2} \end{aligned} \tag{3}$$

where K and p are independent of M.

In order to obtain an idea of the relative magnitude of the constant D of the crystal field in different cases, it is necessary to examine the constants p and K in greater detail. Let us consider a two electron system such as Pr: the analysis can easily be modified for systems with a greater number of electrons. We will assume that $L(=5)$ and $S(=1)$ are good quantum numbers, these two combining to give the various multiplet levels $J(=4, 5, 6)$. We have

$$x^4 + y^4 + z^4 = \tfrac{1}{4}(7\sin^4\theta - 8\sin^2\theta + 4 - \sin^4\theta\cos 4\phi).$$

The term independent of ϕ gives the matrix elements diagonal in M, while the term dependent on ϕ gives elements $\Delta M = \pm 4$.

Consider the sum S for one of the permissible J values

$$S = \sum_M (x^4 + y^4 + z^4)(J, M; J, M) \tag{4}$$

where for brevity we have written x^4 for $\sum_i x_i^4$ etc. Since all the wave functions for a given L and S have the same radial factor, the summation over M involves averaging (4) over a sphere. The result is clearly

$$\begin{aligned} S &= n(2J+1)\int_0^{\pi/2} \tfrac{1}{4}(7\sin^4\theta - 8\sin^2\theta + 4)\sin\theta d\theta \int_0^\infty r^6 R^2(r) dr \\ &= 6I(2J+1)/5 \end{aligned}$$

with $I=\int_0^\infty r^6R^2(r)dr$, n being the number of electrons, two in this case and $R(r)$ the radial wave function of one of the two equivalent electrons. The quantity I is independent of J, L, M, S but it does depend on the total quantum number and the effective nuclear charge. For elements so similar in structure as Pr and Nd a good approximation is to assume I the same for both. A better approximation is to take into account the small difference in the effective nuclear charges. From the relations (3) and (4) it is immediately possible to eliminate the constant k in the matrix elements and we obtain

$$(x^4+y^4+z^4)(J,M;J,M) = 6I/5 + p_J[7M^4+5M^2-6JM^2(J+1) + 3J(J-1)(J+1)(J+2)/5] \quad (5)$$

the subscript J on p being used to denote that p depends on J. Transforming from the J, M system to the M_L, M_S system, we have from the invariance of the spur in the two representations

$$\sum_J (x^4+y^4+z^4)(J,M;J,M) = \sum_{M_L} (x^4+y^4+z^4)(M_L,M_S;M_L,M_S), \quad (6)$$

with $M=M_L+M_S$, where the matrix elements on the right hand side of this equation can be obtained from (5) by replacing p_J by q, M by M_L and J by L. The quantity q depends on L, but since we are considering only one value of L there is no need to indicate this dependence.

If we take $M=6$, then $J=6$, $M_L=5$ and $M_S=1$; Eq. (6) then determines p_6 in terms of q. By taking in succession $M=5$, $M=4$, it is possible to find p_5 and p_4 in terms of q.

It remains now to determine q in terms of I. If we transform from the (L, S, M_L, M_S) system to the $(m_{l_1}, m_{l_2}, m_{s_1}, m_{s_2})$ system, we have another spur relation,

$$\sum_{LS}(x^4+y^4+z^4)(L,S,M_L,M_S;L,S,M_L,M_S) = \sum_{m_{l1}m_{l2}}[(x_1^4+y_1^4+z_1^4)(m_{l_1},m_{s_1};m_{l_1},m_{s_1}) + (x_2^4+y_2^4+z_2^4)(m_{l_2},m_{s_2};m_{l_2},m_{s_2})] \quad (7)$$

with $M_S=m_{s_1}+m_{s_2}$ and $M_L=m_{l_1}+m_{l_2}$. There is no need to include l_1, s_1, etc., since we are going to assume that these are always good quantum numbers. Let us take $M_S=1$; then we must have $m_{s_1}=1/2$, $m_{s_2}=1/2$. Furthermore, if we take $M_L=5$, the only possibility is $L=5$, just the value we require. Moreover, we can evaluate the matrix elements of $(x^4+y^4+z^4)(m_l;m_l)$ for a one-electron problem by quadrature alone. We find

$$(x^4+y^4+z^4)(m_l;m_l) = 3I\,\frac{7l^4+14l^3-23l^2-30l+18-6l^2m_l^2+5m_l^2-6lm_l^2+7m_l^4}{2(2l-1)(2l-3)(2l+3)(2l+5)}.$$

Using this relation and the spur relation (7) one can obtain q and hence p_4 in terms of I.

Performing the calculations, we find for Pr

$$p_6 = 14q/33, \quad p_5 = 2q/3, \quad p_4 = 21q/11, \quad q = I/10395 \tag{8}$$

and for Nd

$$p_{15/2} = 33q/91,\ p_{13/2} = 6q/13,\ p_{11/2} = 799q/1001,\ p_{9/2} = 2380q/1001,\quad q = I/32670. \tag{9}$$

These relations enable us to find the ratio of the magnitudes of the electric fields in similar salts of these two elements.

Praseodymium

The normal state of Pr is ${}^3H_4$; the multiplet separation between the levels $J=4$ and $J=5$ is about 2100 cm^{-1}, and hence in calculating the susceptibility the higher multiplet levels may be neglected. This corresponds to discarding off-diagonal elements in J in the magnetic moment and in the crystal field. Good experimental data have been given by Gorter and de Haas[10] for the variation of the susceptibility of a crystal powder of $Pr_2(SO_4)_3\ 8H_2O$.

As has already been explained, the simplest assumption is a cubically symmetrical field. The Hamiltonian is

$$D\sum_i (x_i^4 + y_i^4 + z_i^4) + H\beta\mu_z,$$

μ_z being the component of magnetic moment along the z-axis, which is also taken to be the direction of the magnetic field. The diagonal elements arising from the magnetic field are simply $g\beta HM$, where g is the Landé g-factor ($=4/5$ for Pr), M is the component of J along the axis and β is the Bohr magneton. Bethe[5] has shown that in the absence of a magnetic field the level $J=4$ splits up into a single level, a doubly degenerate level and two triply degenerate levels. In virtue of the selection rule obeyed by the Hamiltonian, the secular determinant factors into a cubic and three quadratics, two of the quadratics being identical since there is degeneracy as regards the sign of M. Hence at least one root of the cubic must be identical with one of the roots of the repeated quadratic, while another root must be the same as one of the roots of the remaining quadratic. Thus the determination of the levels in the absence of the magnetic field involves only the solution of quadratic equations. When the magnetic field is present the secular determinant still breaks up into a cubic and three quadratics, the factors being

$$\begin{vmatrix} 4G - 96a - W & s & 0 \\ s & -W & s \\ 0 & s & -4G - 96a - W \end{vmatrix}$$

$$\begin{vmatrix} \pm 3G - 936a - W & t \\ t & \pm G - 216a - W \end{vmatrix} \begin{vmatrix} 2G - 696a - W & 360a \\ 360a & -2G - 696a - W \end{vmatrix}$$

[10] C. J. Gorter and W. J. de Haas, Leiden Comm. 218b.

where

$$s = 24a(70)^{1/2},\quad t = 120a(7)^{1/2},\quad G = g\beta H$$

and $a = pD$, p being the coefficient in the matrix elements (3). Since the roots without the magnetic field are known there is no great difficulty in finding the roots in the presence of the field H as a power series in H. For convenience, we choose as origin of energy the centre of gravity of the unperturbed levels. Then the levels in the presence of the field are

$$W_1 = 672a + 5G^2/252a, \qquad W_2 = 336a + G/2 + 7G^2/3840a,$$
$$W_3 = 336a + 2G^2/105a, \qquad W_4 = 336a - G/2 + 7G^2/3840a,$$
$$W_5 = 96a + G^2/180a, \qquad W_6 = 96a - 180aG^2/,$$
$$W_7 = -624a + 5G/2 - 7G^2/3840a, \quad W_8 = -624a - G^2/180a,$$
$$W_9 = -624a - 5G/2 - 7G^2/3840a.$$

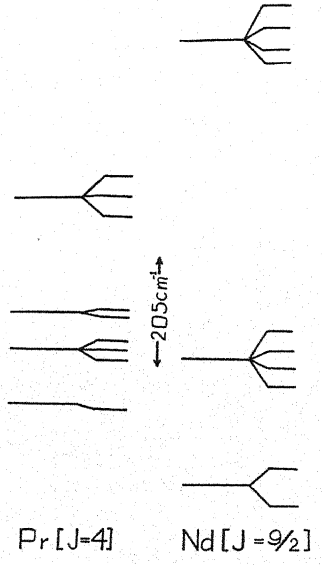


Fig. 1.

The susceptibility per gram atom is then

$$\chi = (2Ng^2\beta^2/a)\,[53e^{13\mu}/5760 + e^{-2\mu}/30 - 61e^{-7\mu}/2688 - 5e^{-14\mu}/252 + \mu(25e^{13\mu} + e^{-7\mu})/192] \div (3e^{13\mu} + 2e^{-2\mu} + 3e^{-7\mu} + e^{-14\mu}) \tag{10}$$

where $\mu = 48a/kT$. The constant a is chosen so that this formula gives the value of χ_0, the susceptibility at the absolute zero of temperature, extrapolated from the experimental data. This gives $\chi_0 = -10Ng^2\beta^2/a$, since a must be negative in order that χ_0 may be finite. From this we obtain the value $a = -0.293$ cm^{-1} which corresponds to an over-all splitting produced by the crystal field of 389 cm^{-1}. Fig. 1 gives the way in which the crystal field splits the lowest multiplet level of Pr. The same figure gives similar results for Nd, and the influence of the magnetic field in removing the degeneracy is also shown. The curve $1/\chi$ against T is given in Fig. 2 and on it are marked the ex-

perimental values for $Pr_2(SO_4)_3 \cdot 8H_2O$ as measured by Gorter and de Haas.[10] The agreement is extremely good. In order to show the sensitivity to variations in a we have plotted the curves (1) $a=-0.37$ cm^{-1} (2) $a=-0.293$ cm^{-1} (3) $a=-0.30$ cm^{-1}, while the straight line (4) through the origin gives the asymptote for all values of a at very high temperatures (but not high enough for the higher multiplet levels to count). This straight line represents the Hund formula for the susceptibility $\chi=N\beta^2g^2J(J+1)/3kT$, obtained on the assumption that the ion is perfectly free. It should be explained that the experimental values are given per gram ion. The molecular weight of $Pr_2(SO_4)_3 \cdot 8H_2O$ is 714, and since there are two Pr atoms it is necessary to divide χ as given by Eq. (10) by 357 in order to give the χ used by experimenters and employed in Fig. 2. In the temperature range 100°K to 300°K the experimental

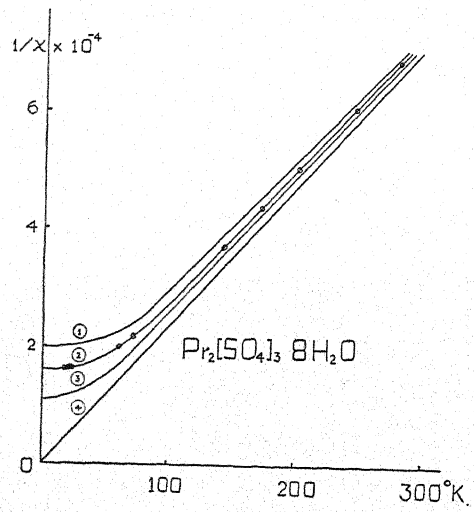


Fig. 2.

Δ is 32°, while the theoretical value is about 25°. The difference is too small to show in the figure. More will be said about the agreement with experiment when we have considered Nd.

Before it was realized that a field of cubic symmetry would give such a good account of the experimental results, a field of rhombic symmetry was tried, but with little success. A simple assumption in this case is that the potential of the field is of the form $A(x^2+y^2-2z^2)$. Since the measurements were made on crystal powders, it is necessary to average over all directions. This can be accomplished by first solving the problem where the magnetic field acts along the z-axis, the axis of symmetry, and then when it acts perpendicularly to the axis. The average susceptibility will be the average of these two, taken with the weights one and two respectively. The problem bears a formal resemblance to the problem of the symmetrical top; the group $J=4$ of energy levels are all doubly degenerate except one which is single and which must be taken as the lowest in order to fit the observed susceptibility at low temperatures. However the temperature dependence of the susceptibility calculated

on the assumption of a "symmetrical top" field bore very little resemblance to that observed and it was necessary to reject it. If data were available on single crystals one could tell immediately by comparing the three principal susceptibilities and Δ's how good an assumption a field of cubic symmetry is. If the three are equal, everything would be very satisfactory; if not, then one would have to introduce a small field of rhombic symmetry to account for the differences. The effect of introducing a field of rhombic symmetry would be to give three principal Curie constants and three principal Δ's, and the Δ's would not vanish even at high temperatures although the Curie constants would then all become equal and the mean Δ would vanish. Nothing further can be said until experiments have been made on single crystals.

NEODYMIUM

The normal state of Nd is ${}^4K_{9/2}$ (K states have $L=6$). The multiplet separation between $J=9/2$ and $J=11/2$ is about 1800 cm^{-1} and at room temperatures one ought not to neglect the higher multiplet levels. We are indebted to Miss Frank for the information that the correction for the other multiplet levels is to add about three percent to the susceptibility at room temperatures.[11] However we make no attempt to apply this correction, since the discrepancy between different observers is considerably greater than this. Since the ground state has $J=9/2$, so that J is a half integer, the electric field, as shown by Kramers,[12] will be unable to remove all the spatial degeneracy of this state; each level will be at least doubly degenerate and will have a Zeeman effect of the first as well as of the second and higher orders. It is known from the work of Bethe[5] that in the absence of the magnetic field the ten components of $J=9/2$ fall into two coincident groups of five on account of the Kramers two-fold degeneracy, and each group of five levels will split up into a single level and two doubly degenerate levels. In the presence of the magnetic field, the factoring is into a quadratic and a cubic, given by

$$\begin{vmatrix} 9G/2+5Av-W & 6A & 0 \\ 6A & G/2+5Av-W & 10A \\ 0 & 10A & -7G/2-3Av-W \end{vmatrix}$$

$$\begin{vmatrix} 5G/2+2Av-W & 5Au \\ 5Au & -3G/2-2Av-W \end{vmatrix}$$

[11] Miss Frank has shown, Phys. Rev. **39**, 119 (1932), that it is very important to take into account the off-diagonal elements in J in the magnetic moments for Eu and Sm, since for these the separation between the two lowest multiplet levels is not small compared with kT. For Eu, the lowest level has $J=0$, the next lowest $J=1$ and neither of these breaks up under the action of a crystal field of cubic symmetry nor is their relative position altered to a first approximation; and since they belong to different representations of the cubic group, the field does not introduce elements of magnetic moment between them. From analogy with the conclusions given in the present paper, one would expect the crystal fields in the rare earths to have cubic symmetry. If this is so, Miss Frank's calculations for Eu still apply. For Sm, whose two lowest levels have $J=5/2$ and $J=7/2$ as normal states, it may be necessary to amend the results given in her paper. Further calculations will be made on this point.

[12] H. A. Kramers, Proc. Amst. Acad. **33**, 959 (1930).

where $u=(6)^{1/2}$, $v=(14)^{1/2}$, $G=g\beta H$ ($g=8/11$ for Nd) and $A=12ap(14)^{1/2}$. The origin of energy has been chosen to make the spur of the quadratic zero, a device which greatly simplifies the algebra. The cubic and quadratic arising from the other quintic can be obtained from those above by changing the sign of G. The roots in the absence of the magnetic field can readily be obtained, since then the roots of the quadratic must also be roots of the cubic. Solving these equations up to terms in H^2, we find for the ten energy levels

$$W_1 = 20.95A + 1.833G + 0.3879G^2/A, \quad W_2 = 9.11A + 2.788G - 0.3411G^2/A,$$
$$W_3 = 9.11A - 0.542G + 0.1015G^2/A, \quad W_4 = -19.59A - 3.121G - .00468G^2/A$$
$$W_5 = -19.59A + 1.542G - 0.1015G^2/A.$$

and five more obtained from these by changing the sign of G.

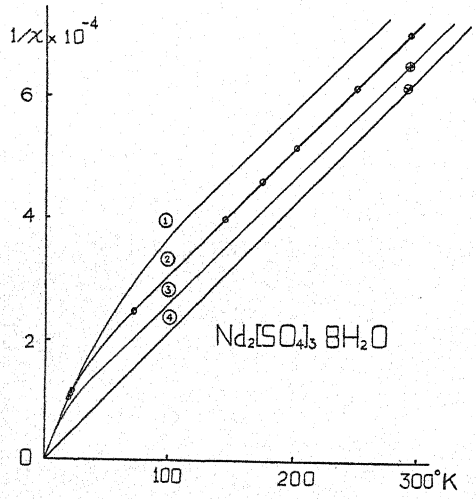


Fig. 3.

The expression for the susceptibility per gram atom is

$$\chi = (2g^2\beta^2N/A)\,[(0.1483e^{19.59\mu} + 0.2396e^{-9.11\mu} - 0.3879e^{-20.95\mu}) + \mu(6.065e^{19.59\mu} + 4.031e^{-9.11\mu} + 1.680e^{-20.95\mu})] \div [2e^{19.59\mu} + 2e^{-9.11\mu} + e^{-20.95\mu}],$$

where $\mu=A/kT$. To obtain the susceptibility per gram ion it is necessary to divide by 361. As with Pr, a is negative, and its value is about -0.458 cm^{-1} ($A=-20.6$ cm^{-1}), which gives an over-all splitting of 834 cm^{-1}. The splitting of the lowest multiplet level produced by the crystal field is shown in Fig. 1. Curve 2 in Fig. 3 gives the theoretical variation of $1/\chi$ with T, while on it are marked the experimental results of Gorter and de Haas.[10] The agreement is extremely good. Curves 1 and 2 in Fig. 3 show the sensitivity to A and are for the values $A=-36$ cm^{-1} and $A=-12$ cm^{-1} respectively, while the straight line 4 gives as before Hund's law. The measurements of Cabrera[18] at 290°K,

[18] B. Cabrera, C. R. 180, 669 (1925).

and of Zernicke and James[14] at 293°K, and of St. Meyer,[15] which agree almost exactly with Zernicke and James, are also marked and are seen to fall considerably below those of Gorter and de Haas. If, on account of some error in calibration, it should prove necessary to reduce the experimental values by a constant factor, D can still be chosen to fit the results. Exactly the same discrepancies appear with Pr. Again, the susceptibility as measured by Cabrera is 11 percent higher, and that measured by Zernicke and James and also by St. Meyer is 2 percent higher, than that obtained by Gorter and de Haas, all at room temperature. The disagreement in this case is not quite so bad as with Nd.

Using the relations (8) and (9) we can compare immediately the values of the constants D of the crystal fields in the two salts $Pr_2(SO_4)_3 \cdot 8H_2O$ and $Nd_2(SO_4)_3 \cdot 8H_2O$, on the assumption that the integral I is the same in both cases. This is not quite accurate and rather favors Pr, but it is sufficiently close for our purpose. The constant D for Nd is found to be about 3.9 times that for Pr. One would expect the electric fields in two salts so similar in every way to be of about the same magnitude. It should be remembered, however, that we determine this magnitude from the difference between the observed magneton number and the Hund value, and a small change in the observed magneton number will make a considerable difference in the calculated field. For example, the difference between the magneton number of Nd as measured by Cabrera, and the Hund value, is 0.08, while Gorter and de Haas obtain 1.24. For Pr the corresponding figures are 0.17 and 0.76 respectively. The electric fields calculated from Cabrera's values are much less than those given here. More accurate data on the susceptibilities, even at one temperature, would allow this question to be settled satisfactorily.

In conclusion we desire to express our sincere thanks to Professor J. H. Van Vleck, whose advice and criticism during the course of this work have been invaluable.

[14] J. Zernicke and C. James, Jour. Am. Chem. Soc. **48**, 2827 (1926).
[15] Stefan Meyer, Phys. Zeits. **26**, 51, 478 (1925).

Theory of the Variations in Paramagnetic Anisotropy Among Different Salts of the Iron Group

By J. H. Van Vleck
University of Wisconsin

(Received June 6, 1932)

A theoretical explanation is given of why nickel salts are nearly isotropic magnetically, while those of cobalt exhibit over 25 percent anisotropy even though the Ni^{++} and Co^{++} ions are both in F states and are adjacent in the periodic table. The cause is an inversion of the levels in the crystalline Stark effect in passing from the configuration $d^8\ ^3F$ (Ni^{++}) to $d^7\ ^4F$ (Co^{++}). If the crystalline field has only rhombic symmetry, but with the deviations from cubic symmetry comparatively small, extension of the methods in Penney and Schlapp's preceding paper shows that a nearly isotropic level will be the ground level in Ni^{++}, but an anisotropic one in Co^{++}. It is to be particularly noted that the inversion exists purely in virtue of the difference between the configurations d^7 and d^8, and does not require different crystalline fields in Ni and Co compounds. The theory predicts that hydrated Ni salts conform closer to Curie's law than those of Co, and have a Curie constant more nearly equal to the "spin only" value $4NS(S+1)(he/4\pi mc)^2/3k$. This agrees with experiment. Other pairs of ions are cited in the iron group in which the inversion phenomenon is encountered, with attendant diversity in magnetic behavior. The nearly perfect magnetic isotropy of manganous salts is trivial, as the ground state of Mn^{++} is ^6S; the slight anisotropy may be due to a small amount of incipient j-j coupling or to distortion of the constancy of orbital angular momentum by the crystalline field, so that the orbital magnetic moment does not vanish completely in S states.

NO ONE who has examined the measurements of the principal susceptibilities of salts of the iron group can fail to note how remarkably the amount of magnetic anisotropy varies with the nature of the cation. Typical determinations are, for instance, those by Rabi,[1] according to which the ammonosulphates of Mn, Co, Ni, and Cu exhibit anisotropies amounting respectively to 1, 30, $1\frac{1}{2}$, 20 percent.

The nearly perfect isotropy of the manganous salts is exactly what one expects inasmuch as the Mn^{++} ion has a ^6S ground state. Nearly complete symmetry should also be found in ferric salts, as Fe^{+++} and Mn^{++} have the same configuration, but adequate data on ferric compounds are wanting. The usual cause of magnetic anisotropy is the unsymmetrical partial freezing of orbital angular momentum by the lattice forces. The orbital magnetism is thus largely destroyed by these forces, but not completely. Particularly important is usually the coupling between the spin and the remains of the orbital angular momentum, which are not centro-symmetric and so destroy the equivalence of different spin orientations. In S states with perfect Russell-Saunders coupling there is no orbital angular momentum to congeal, and so the usual cause of anisotropy disappears in manganous salts. The ordinary explanation of the small residuum (about 1 percent) of anisotropy found in

[1] I. I. Rabi, Phys. Rev. 29, 173 (1927).

manganous compounds is the magnetic spin-spin coupling, since the electrostatic exchange coupling is well known not to cause anisotropy. However, it seems doubtful whether the magnetic spin-spin forces could be great enough to cause even the 1 percent dissymmetry in manganous salts of high "magnetic dilution," such as e.g., hydrated sulphates, where the separation of the paramagnetic ions is great. Therefore we wish to suggest the possibility of a small amount of incipient j-j coupling, not enough to distort appreciably the g-factors from their Russell-Saunders values, but enough to impart a slight amount of orbital angular momentum to S states which would then behave anisotropically. Along with this is also, perhaps more important, the angular momentum which arises because the crystalline fields do not have complete central symmetry. In quantum mechanics the orbital angular momentum cannot be constant in time in noncentral fields[2] and so cannot vanish completely in the presence of the latter.

So much for the rather straightforward case of Mn. Much more puzzling is the great difference in isotropy between nickel and cobalt salts. The ions Co^{++} and Ni^{++} are adjacent in the periodic table, and both are in F states (respectively $d^7\,{}^4F$ and $d^8\,{}^3F$). Nevertheless Ni salts are nearly as isotropic as those of Mn, while Co salts are the least symmetrical of the whole group. Closer examination reveals that precisely this behavior is to be expected if the crystalline field possesses only rhombic symmetry, but with the departures from cubic symmetry relatively small. The development of the crystalline potential then takes the form

$$V = \sum_i [f(r_i) + Ax_i^2 + By_i^2 - (A + B)z_i^2 + D(x_i^4 + y_i^4 + z_i^4)], \quad (1)$$

provided we neglect the departures from cubic symmetry in the fourth but not the second order terms. The summation need be extended for our purposes only over the electrons not in closed shells, i.e., the d electrons in the ions of the iron group, inasmuch as completed shells exhibit no orientation effect and so contribute nothing interesting to (1). The reader is referred to the preceding paper by Penney and Schlapp and to reference 3 in case he desires further general exposition of the use of crystalline potentials in connection with magnetic problems.[3] That the rhombic or second order part of (1) is subordinate to the cubic or fourth order part is evidenced by the fact that paramagnetic salts are nearly isotropic in many cases, and especially by the success which has attended Penney and Schlapp's preceding calculation of the temperature dependence of the susceptibilities of rare earth salts involving Nd and Pr under the assumption that only the cubic portion of (4) need be considered. They have also tried calculations keeping only the rhombic part of (1), but the wrong temperature dependence is then obtained in the rare earths, as well as far too much anisotropy in Ni salts.

If the "cubic" or fourth-order part of (1) is the dominant noncentral term, then from Bethe's[4] group theory of levels in crystalline fields, one finds that

[2] Cf. J. H. Van Vleck, Phys. Rev. 31, 600 (1928).
[3] J. H. Van Vleck, "The Theory of Electric and Magnetic Susceptibilities," section 73.
[4] H. Bethe, Ann. d. Physik 3, 133 (1929); especially pp. 164–167, 196–199.

the Stark splitting is arranged either as in Fig. 1, or as in this figure turned upside down. The vertical lines represent the matrix elements of magnetic moment along some one principal direction, say x. The separation of the components of Γ_4 or of Γ_5 is due only to the rhombic terms, since Γ_4, Γ_5 (in Bethe's notation) are triply degenerate "Darstellungen" in strictly cubic fields.

If Fig. 1 is right side up, the orbital magnetic moment will be largely suppressed, and its "remains" will be nearly isotropic for the following reason. By perturbation theory,[5] the magnetic moment induced in the state a by application of a magnetic field H along x is given by the expression

$$2H \sum_k |\mu_x(ak)|^2/h\nu(ka), \tag{2}$$

where the $\mu(ak)$ are the matrix elements of magnetic moment in the absence of H but in a system of representation which diagonalizes (1). The matrix μ

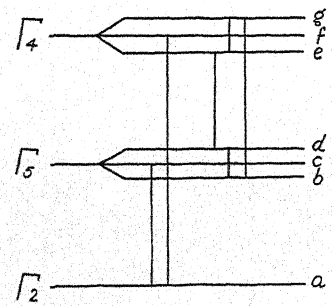


Fig. 1.
(upright in Ni^{++}, inverted in Co^{++})

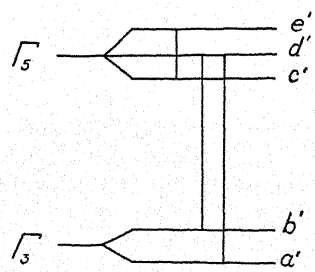


Fig. 2.
(upright in Cu^{++}, inverted in Fe^{++})

will contain no diagonal elements, because, as the writer has shown elsewhere,[3] crystalline fields of no more than rhombic symmetry suppress the diagonal elements of orbital angular momentum (neglecting perturbations by spin-orbit interaction, which restores some of the diagonal part in systems with an odd number of electrons). In the case shown in Fig. 1, the summation over k embraces only c and f, but if one changes the direction of H to another principal axis y or z, one encounters the matrix elements of μ_y, μ_z and these may join a to other components of Γ_4 and Γ_5 than c and f. One finds that the magnetic anisotropy of a exists only in virtue of the difference between the frequencies $\nu(ab)$, $\nu(ac)$, $\nu(ad)$ or between $\nu(ae)$, $\nu(af)$, $\nu(ag)$, and these percentage differences are small since the rhombic is small compared to the cubic separation.

Let us, however, turn Fig. 1 upside down, and suppose that the separations e-f-g, though small compared to a-e, etc., are nevertheless large compared to kT, making only g a normal state. The orbital magnetic moment will then be much less completely quenched than without the inversion, since

[5] See, for instance, p. 145 of reference 3.

the denominators $\nu(ge)$, $\nu(gf)$ will be involved in the formula analogous to (2). Furthermore there will be vastly more anisotropy than without the inversion. This will be true not merely because the percentage difference between $\nu(ge)$ and $\nu(gf)$ is greater than that between $\nu(ab)$ and $\nu(ac)$ or $\nu(ad)$ but also because the full symmetry of moment in the limiting case of perfectly cubic fields is achieved only with equal distribution of atoms among the three components of Γ_4 rather than concentration purely in one component g.

It is clear that one can understand the difference between Ni^{++} and Co^{++} if one can justify turning Fig. 1 upside down in passing from one of these ions to the other. Now it actually turns out that for a *fixed* sign of A, B, D in (1), precisely this behavior is to be expected theoretically. The argument is as follows. Let us consider matrix elements in the L, M_L system of representation rather than in the final system which diagonalizes (1). Then from the properties of the rotation group Penney and Schlapp find in the preceding paper that, regardless of the number n of electrons in the incomplete shell the matrix elements of $\sum(x_i^4+y_i^4+z_i^4)$ are of the form

$$\sum_i (x_i^4 + y_i^4 + z_i^4)(LM_L; LM_L) = Qf(L, M_L) + 3n\overline{r^4}/5, \tag{3}$$

where Q depends on L, S, n but not on M_L, and where

$$f(L, M_L) = M_L^2(7M_L^2 - 6L^2 - 6L + 5) + 3L(L^2 - 1)(L + 2)/5. \tag{4}$$

Besides (3) there are also elements of the form $\Delta M_L = \pm 4$ proportional to Q, as well as elements nondiagonal in L, but the explicit form of these does not concern us. Our interest is in the sign of the proportionality factor Q, which can be determined by the following adaptation of the Goudsmit-Slater method[6] of diagonal sums. For the configuration d^8, the only arrangement in m_l, m_s quantization consistent with $M_L = \sum m_l = 3$, $M_S = \sum m_s = 1$ is $m_l = 2$, $m_l = 1$, $m_l = 0$ each twice, $m_l = -1$, $m_l = -2$ each once. The spur invariant for $M_L = 3$, $M_S = 1$ thus consists of but a single term, which yields a ^3F state. Hence, since f is even in M_L,

$$Q(d^8\ {}^3F) \cdot f(3, 3) = Q(d^2D)\,[3f(2, 2) + 3f(2, 1) + 2f(2, 0)]. \tag{5}$$

Here $Q(d^8\ {}^3F)$ means the value of Q appropriate to the configuration $d^8\ {}^3F$, while $Q(d\ {}^2D)$ of course relates to a single isolated d electron. The term in $\overline{r^4}$ has been omitted since it is invariant of the vector addition involved in constructing the Russell-Saunders coupling. For the case $M_L = 3$, $M_S = 3/2$ of d^7, one has the same arrangement of m_l's as before, except that $m_l = 0$ is filled only once, and consequently

$$Q(d^7\ {}^4F)f(3, 3) = Q(d^2D)\,[3f(2, 2) + 3f(2, 1) + f(2, 0)]. \tag{6}$$

On comparing (5) and (6) and noting that

$$2f(2, 2) + 2f(2, 1) + f(2, 0) = 0, \tag{7}$$

one sees that $Q(d^8\ {}^3F)$ is the negative of $Q(d^7\ {}^4F)$. Of course the diagonal ele-

[6] S. Goudsmit, Phys. Rev. **31**, 945 (1928); J. C. Slater, *ibid.* **34**, 1293 (1929).

ments (3) are not the same as the characteristic values of $\sum(x_i^4+y_i^4+z_i^4)$, but except for the difference in Q, the matrix representing this expression in the L, M_L system is the same for $d^8\ ^3F$ as $d^7\ ^4F$ inasmuch as L is the same in both cases. Hence the characteristic values are obtained by the same canonical transformation and differ merely in the proportionality factor Q, which will thus cause inversion in the passage from Ni to Co. It is particularly gratifying that alteration of the sign of D in (1) is thus not necessary to invert the crystalline Stark effects. The crystals of Ni and Co hydrated sulphates, etc. have presumably so nearly the same structure and ionic arrangement that it would be illogical, to say the least, to postulate radically different fields in the two cases.

In the foregoing we have neglected entirely the spin in the interest of simplicity. Actually the spin is the main cause of the paramagnetism in Ni and Co, though not of its anisotropy. In point of fact, the spin-orbit interaction is comparable with the effect of the rhombic dissymmetry, but is subordinate to the "cubic" term, so that the inversion of cubic levels still comes into play. Inclusion of the spin-orbit interaction makes the remains of the orbital magnetic moment contribute to the part of the susceptibility which is inversely proportional to temperature, rather than merely a term such as (2) which is independent of temperature. When Fig. 1 is right side up, the spin interacts effectively with a smaller and more isotropic orbital moment than when Fig. 1 is inverted. The most potent elements of μ in the spin-orbit coupling, which is much looser than in the free gaseous state, can be shown[3] to be those whose associated frequencies $\nu(ij)$ are small. Hence the departures of the Curie constant C from the Stoner-Bose "spin only" value

$$C = 4NS(S+1)(he/4\pi mc)^2/3k \tag{8}$$

should be larger in Co than in Ni salts, and deviations from Curie's law in highly hydrated salts should appear at higher temperatures with a Co than with a Ni cation. (The hydration is to avoid exchange coupling between atoms.) This agrees with experiment. The deviation from (8) is about 30 percent in the nickel sulphates, as compared with 70 percent in those of cobalt. Further calculations by Schlapp and Penney, to appear shortly, predict that in hydrated nickel salts the deviations should become important only at temperatures near liquid helium. This is confirmed by Gorter, de Haas, and v. d. Handel's recent remeasurement[7] of $NiSO_4\cdot 7H_2O$ at low temperatures (down to liquid hydrogen) which has obliterated Jackson's previous large negative Δ and restored Curie's law almost perfectly. On the other hand, $CoSO_4\cdot 7H_2O$ apparently demands a Δ of about 14 in the Weiss-Curie formula $\chi = C/(T+\Delta)$, although it must be cautioned that here new measurements are not available.

By arguments very similar to the previous, one can show that the inversion phenomenon should also be found in the pair Fe^{++}, Cu^{++}, respectively $d^6\ ^5D$ and $d^9\ ^2D$, and also pairs of ions reciprocally related on the left and right sides of the group, such as (Cr^{+++}, Co^{++}) or (Ni^{++}, V^{+++}). We call ions re-

[7] C. J. Gorter, W. J. de Haas, and J. v. d. Handel, Leiden Comm. 218d.

ciprocally related if they have respectively x and $10\text{-}x$ d electrons, since then their ground states have the same L, S.

Adequate data are wanting on single crystals of Cr and V salts, but the Curie constant does have much more closely the Stoner-Bose value (8) for Cr^{+++} than for Co^{++}, as one should expect from the foregoing. In $Cr_2(SO_4)_2 K_2SO_4 \cdot 24H_2O$ the deviation from (8) is only about 2 percent.[8] The variation in the applicability of (8) is thus even more pronounced in the pair Cr^{+++}, Co^{++} (2 *vs.* 70 percent deviation) than in the pair Co^{++}, Ni^{++} (70 *vs.* 30). This is understandable on the ground that the multiplet structure and hence the spin-orbit interaction for the free ion are considerably smaller in Cr^{+++} than in Co^{++} or Ni^{++}. Of course the departures from (8) will be greater the larger this interaction, all other circumstances being equal. Consequently the alteration in free multiplet width and the inversion phenomenon reinforce each other in accentuating the deviations from (8) in Co^{++} as compared to Cr^{+++}.

The pair Fe^{++}, Cu^{++} require rather careful examination. Here we encounter D rather than F levels. Now Bethe[4] has proved that D terms split under the potential (1) in the fashion shown in Fig. 2, where the separation of the components of Γ_3 or of Γ_5 is due entirely to the deviations from cubic symmetry occasioned by the rhombic terms. The first thing to be remarked is that Fig. 2 is upright in Cu^{++} and inverted in Fe^{++} if Fig. 1 is upright in Ni^{++}. This follows from the fact that $Q(d^9\ ^2D)$ has the opposite sign from $Q(d^8\ ^3F)$ inasmuch as by the method of diagonal sums

$$Q(d^9\ ^2D)f(2,2) = Q(d^2D)[3f(2,2) + 4f(2,1) + 2f(2,0)] = -Q(d^2D)f(2,2), \quad (9)$$

and by (4) the bracketed sum in (9) has the value $-12/5$ as compared with $36/5$ for the corresponding bracketed sum in (5). Bethe[4] has shown that for a fixed sign of Q, as in a one electron system, the D level requires inversion of Fig. 2 if the F level requires an upright Fig. 1. When the sign of Q changes, there are thus two cancelling inversions which together leave Fig. 2 upright.

To be consistent with our interpretation of Ni and Co, it thus appears[9]

[8] W. J. de Haas and C. J. Gorter, Leiden Comm. 208c.

[9] At this juncture it is perhaps well to remark that the reversal of the sign of Q is perhaps a more general and certain phenomenon for the pairs Ni^{++}, Co^{++} and Fe^{++}, Cu^{++} than for the pair Ni^{++}, Cu^{++}. The reversal for the former pair is contingent only upon (7) and hence takes place for any potential whose diagonal elements vanish when summed over M_L except for an additive constant, such as $3n\overline{r^4}/5$ in (3), which is independent of the type of vector addition. That the additive constant is indeed independent of the vector compounding is shown by the theorem (cf. Niessen, Phys. Rev. **35**, 274 ff., 1929) that $\Sigma_{ML}F(n_1n_2 \cdots M_L;\ n_1n_2 \cdots M_L) = (2L+1) \times \overline{F}(n_1n_2 \cdots ;\ n_1n_2 \cdots)$ where the matrix elements relate to any function $F(r, \theta, \phi)$ of polar coordinates and $4\pi\overline{F} = \int\int F \sin\theta d\theta d\phi$. The function $\overline{F}$ is a purely radial one and consequently invariant of the vector addition involved in Russell-Saunders coupling etc. Hence the Ni^{++},Co^{++} inversion is surely found for other forms of potential besides (1), and the great diversity in anisotropy in this pair requires only that the crystal symmetry be dominantly but not completely cubic. On the other hand after Eq. (9) explicit use was made of the numerical form (4) of the matrix elements of the fourth degree part of (1) in proving the reversal in the sign of Q for the pair Ni^{++}, Cu^{++}. It is hence conceivable, though improbable, that if the cubic potential requires large sixth, eighth, etc. degree terms for its representation in addition to the fourth order terms, the reversal in the sign of Q may exist for the Ni^{++}, Co^{++} and Cu^{++}, Fe^{++} pairs, but not for Ni^{++}, Cu^{++}. Fig. 2 would then be upright in Fe^{++} and inverted in Cu^{++}.

necessary that Fig. 2 be upright in Cu^{++} and inverted in Fe^{++}. Now Bethe[4] has demonstrated that the portion Γ_3 of Fig. 2 is "nonmagnetic," and so μ consequently has no matrix elements of the form $\mu(a'b')$, whereas the elements inside Γ_5 do not all vanish. The expression analogous to (2) will consequently be much larger in Fe^{++}, where e' is a ground state, than in Cu^{++}, because of the existence of small denominators such as $\nu(e'c')$. Hence the remains of the orbital angular momentum will be larger in Fe^{++} than Cu^{++}, and, all other things being equal, the distortion from (8) with attendant magnetic anisotropy should be much more accentuated in Fe^{++} than in Cu^{++}. Actually the anisotropy of cupric salts (e.g., 26 percent in $CuK_2(SO_4)_2 \cdot (6H_2O)$ is usually greater than for ferrous ones (e.g., 16 percent in $FeK_2(SO_4)_2 \cdot 6H_2O$), while (8) holds no more closely for Cu^{++} than for Fe^{++}. About 20 percent deviations from (8) are found in both cases. Because of the somewhat greater anisotropy in the cupric case, it thus appears at first sight that the inversion of Fig. 2 comes at the wrong place. However, "all other things" are not equal. The free multiplet structure is wider for Cu than Fe, so that if there were no inversion the spin-orbit distortion would be bigger in Cu than in Fe. Also the spin quantum number has the small value 1/2 in Cu^{++}, compared with 2 in Fe^{++}, so that residual orbital angular momentum of given magnitude is relatively more important in Cu^{++} than in Fe^{++}. These two effects may more than counteract the fact that the denominators in the formula for the induced orbital moment are smaller in Fe^{++} than in Cu^{++}. One thing to be particularly emphasized in connection with the question of anisotropy is the following. The orbital moment induced in a' in Fig. 2 exists, to be sure, solely in virtue of the matrix element $\mu(a'c')$, $\mu(a'd')$, $\mu(a'e')$ rather than $\mu(a'b')$, and hence tends to be small because the frequencies $\nu(a'c')$ etc. are large. However, unlike the case of a in Fig. 1, this moment in a' does not owe its anisotropy purely to departures of the ratios $\kappa=\nu(a'c')/\nu(a'd')$ etc. from unity. Instead the full cubic isotropy of the induced moment in Γ_3 is achieved only when the two components of Γ_3 are equally populated, whereas we suppose the separation $a'-b'$ large compared to kT, so that only a' is inhabited. Consequently, the anisotropy in the induced orbital moment of a', Fig. 2 is of the order of magnitude unity, like that of g in Fig. 1 or e' in Fig. 2, whereas that in a, Fig. 1 is only of the order $\kappa-1$. By an anisotropy of the order unity we mean that the differences between the x, y, z components are comparable with the components themselves. Of course the anisotropy is in any case diminished because the residual orbital angular momentum is overshadowed by the spin, but we can say that for given deviations from (8), the anistropies should be of the same order of magnitude regardless of whether or not Fig. 2 is inverted, and inversion accentuates the anisotropy only in so far as the deviation from (8) is enhanced, whereas we have seen that in the Fe^{++}, Cu^{++} pair there are other counteracting tendencies which forestall this enhancement. The effect of inversion on anisotropy is thus a different story for Fig. 2 than Fig. 1. It must be further remembered that Fe, Cu are not adjacent in the periodic table, and their salts' crystalline fields need not resemble each other as closely as those of Co, Ni, thus obscuring the

purity of the inversion phenomenon. The inversion becomes less important the more one increases the rhombic terms at the expense of the cubic ones.

In order to make Figs. 1, 2 upright at Ni^{++}, Cu^{++} respectively rather than Co^{++}, Fe^{++}, it is necessary that the constant D in (1) be positive. This follows since the quotient of the bracketed sum in Eq. (5) and $f(3, 3)$ is positive, making Q have the same sign in Ni^{++} as for a one electron system, where Bethe[4] shows that Fig. 1 is upright if D is positive. The positive choice of D agrees with Penney and Schlapp's preceding calculations on the susceptibilities of the rare earths, but iron and rare earth salts are so widely different that it seems scarcely necessary that the sign of D be the same in both cases.

Detailed numerical calculations amplifying and testing quantitatively the foregoing ideas will be published by Schlapp and Penney and by Jordahl. The writer wishes to thank them for valuable discussions and comments.

Investigations in the Field of the Ultra-short Electromagnetic Waves. IV. On the Dependence of the Ultra-short Electromagnetic Waves upon the Heating Current and upon the Amplitude of the Oscillations*

By G. POTAPENKO**
Norman Bridge Laboratory of Physics,
California Institute of Technology

(Received May 31, 1932)

An investigation has been made of the dependence of the length of the ultra-short electromagnetic waves generated by vacuum tubes on the magnitude of the heating current. It is shown that the normal waves (i.e., waves the frequency of which corresponds to the frequency of the oscillations of the electrons about the grid of the tube) differ from the dwarf waves (i.e., waves with frequency exceeding several times the frequency of electronic oscillations) in their dependence on the heating current. The length of the normal waves increases, while the length of the dwarf waves of all orders decreases as the heating current is decreased. Therefore, as the heating current is decreased, there is a better agreement between the observed and computed values of wave-lengths of the normal and of the dwarf waves. At low heating currents the product $\lambda^2 E_g$ for dwarf waves of different orders is very close to the theoretical values

$$\lambda^2 E_g = \text{const.}_0/n^2 \qquad n=2,\ 3,\ 4,\ \cdots$$

where const.$_0$ corresponds to the value of the product $\lambda^2 E_g$ for normal waves. The results of the experiments are in agreement with the theory of P. S. Epstein, which explains the discrepancy between the calculated and the observed length of the normal and the dwarf waves being due to the influence of the alternating potentials appearing on the electrodes of the tube during oscillations. In the limit, at infinitely low amplitudes of these potentials, the ratio of the values of the products $\lambda^2 E_g$ for normal and for dwarf waves approaches the theoretical value within the limits of the experimental error. Neglecting these alternating potentials introduces the largest error in the results of the existing theories of the generation of ultra-short waves. At sufficiently intensive oscillations, this error exceeds all the others taken together, including the error introduced through the simplifying assumption of plane electrodes. The limiting value of const.$_0$ corresponding to infinitely low amplitudes of the alternating potentials, approaches very closely the value of the product $\lambda^2 E_g$ calculated from the formulas of H. Barkhausen and A. Scheibe. This shows that normal waves really do correspond to a complete period of oscillations of the electrons about the grid, i.e., to the time the electrons take to pass from the filament to the grid and back to the filament.

§1. INTRODUCTION

IN THE previous papers[1] it was shown that ultra-short waves of several kinds can be obtained when large positive potentials with respect to the filament and the plate are impressed on the grid of a vacuum tube. The wave-

* Reported at the Berkeley meeting of the American Physical Society, December 18, 1931.
** Carnegie Fellow.

[1] G. Potapenko, Phys. Rev. **39**, 625, 638, **40**, 988 (1932); these articles will be referred to as I, II and III.

length λ_0 of some of them is found to approximately correspond to the period of oscillations of the electrons about the grid of the tube, or in other words, to the time τ of the passage of the electrons from the filament of the tube to the plate and back to the filament; i.e.,

$$\lambda_0 = c_0\tau \text{ (normal waves)} \tag{1}$$

where c_0 is the velocity of light and the period τ can be approximately determined from the well-known formula:

$$\tau = d_a \times 10^{-7}/3(E_g)^{1/2} \tag{2}$$

where d_a is the diameter of the plate of the tube (in cm) and E_g is the constant positive potential (in volts) of the grid with respect to the filament and the plate. We called these waves normal or normal Barkhausen waves, since Eq. (1) is a fundamental equation of the theory proposed by Barkhausen. The lengths $\lambda_1, \lambda_2, \lambda_2, \cdots$ of the waves of the other kind are approximately 2, 3, 4, $\cdots$ times shorter than the length of the normal waves, calculated from Eq. (1), i.e.,

$$\begin{aligned} \lambda_1 &= c_0\tau/2 \text{ (dwarf waves of the 1st order)} \\ \lambda_2 &= c_0\tau/3 \text{ (“ “ “ “ 2nd “)} \\ \lambda_3 &= c_0\tau/4 \text{ (“ “ “ “ 3rd “)} \end{aligned} \tag{3}$$

We called these waves dwarf waves of the 1st, 2nd, 3rd etc. orders.

We have seen that Eqs. (3) are fairly well satisfied experimentally and that Eq. (1) gives values which differ systematically from the observed values by some 15 percent (II, §9).

While investigating the problem of the motion of the electrons within the tube, we have seen that the peculiarities of the character of this motion completely explain the causes of the generation of dwarf waves and lead us to expect waves with periods equal to integral multiples of the period of the oscillation of electrons about the grids of the tube (III, §3). In other words, the character of electronic motion permits us to expect waves satisfying Eqs. (1)–(3). These investigations gave no direct indications of the possibility of a systematic discrepancy between these equations and the observations.

Thus, so far, we do not know the causes of this discrepancy. Its systematic character shows, however, that it cannot be ascribed to experimental errors and must possess a definite physical meaning. The purpose of the present paper is to elucidate the causes of this discrepancy.

§2. The Relation between the Length of Normal and Dwarf Waves and the Magnitude of the Heating Current

All of the previously made observations refer to three tubes of the same type R5. First of all we must compare them with each other. Every one of these observations, as, for example, the measurement of the wave-length, or the determination of the amplitude of oscillations, refers to a certain length of oscillating circuits, to a certain grid voltage, etc. Therefore, unless all of

these factors are taken into account, a simple comparison of observations cannot be of any great value and will generally be avoided.

The measurements of the wave-lengths were made at such points of the working diagrams of the tubes (II, §3) which corresponded to the maximum current in the plate circuit of the generator (i.e., approximately corresponded to the maximum of the energy of oscillations). Moreover, observations were made at a constant heating current and only at such grid voltages which corresponded to the region of saturation current and were not in the neighborhood of the upper bend of the static characteristic of the tube. In this case the lengths of the normal and of the dwarf waves were satisfying Barkhausen's equation

$$\lambda^2 E_g = \text{const.} \tag{4}$$

An approximate estimate of the value of the constant could be made by means of Eqs. (1)–(3). If Eq. (4) holds true, we can compare the average values of the product $\lambda^2 E_g$ instead of comparing individual observations. This relieves us of the necessity of taking into a separate account the grid potentials as well as the lengths of the oscillating circuits. The latter follows from our having selected points of observation in such a manner that the length of the oscillating circuits already enters the value λ, in view of the definite relationship existing between these two magnitudes (II, §3).

Let us suppose that for the case of normal waves the observations give

$$\lambda_0^2 E_g = \text{const.}_0 \text{ (normal waves)} \tag{5}$$

If relations (1) and (3) hold true, we must have the following for the case of dwarf waves:

$$\begin{aligned} \lambda_1^2 E_g &= \text{const.}_1 = \text{const.}_0/4 \quad \text{(dwarf waves of the 1st order)} \\ \lambda_2^2 E_g &= \text{const.}_2 = \text{const.}_0/9 \quad (\text{ “ “ “ “ 2nd “ }) \\ \lambda_3^2 E_g &= \text{const.}_3 = \text{const.}_0/16 \ (\text{ “ “ “ “ 3rd “ }). \end{aligned} \tag{6}$$

A general form of Eqs. (5) and (6) can be written thus:

$$\lambda^2 E_g = \text{const.}_0/n^2 \tag{7}$$

where for normal waves $n=1$ and for dwarf waves of the 1st order, 2nd order, etc., we have $n=2$, $n=3$, $n=4$, etc. respectively.

If we know the average values of const._0 for the tubes investigated, then by means of Eqs. (6) we can compute the corresponding values of const._1, const._2, const._3, · · · and compare them with the observed values. Table I gives the results of these computations; the columns under the heading *Obs.* give the average values of the products $\lambda^2 E_g$ for dwarf waves of the first four orders, which we had obtained previously (II, §§10, 13). The table also gives the mean observed values of the product $\lambda^2 E_g$ for normal waves and the values of the emission current. From a comparison of the mean observed values of $\lambda^2 E_g$ it is easily seen that for the case of dwarf waves of the 1st, 2nd and 3rd orders the values of these products diminish systematically as the

heating of the filament is decreased. At the same time, for normal waves and for dwarf waves of the 4th order, the change in the value of $\lambda^2 E_g$ has no systematic character and is generally very small.

It must also be mentioned that Barkhausen's Eq. (4) was satisfied for all three tubes in spite of the fact that they were investigated at different absolute values of the heating current. Hence, it follows that under our conditions of observation the product $\lambda^2 E_g$ remains constant, regardless of the absolute value of the heating current.

TABLE I.

Tubes R5

	Tube No. 5 Const$_0$ = 5.81 × 10^5 I_e = 41 mA			Tube No. 20 Const$_0$ = 5.78 × 10^5 I_e = 19 mA			Tube No. 7 Const$_0$ = 5.85 × 10^5 I_e = 12 mA		
	Obs.	Calc.	Obs./Calc.	Obs.	Calc.	Obs./Calc.	Obs.	Calc.	Obs./Calc.
Const.$_1$	2.01 × 10^5	1.45 × 10^5	1.39	1.97 × 10^5	1.45 × 10^5	1.36	1.90 × 10^5	1.46 × 10^5	1.30
Const.$_2$	0.856 "	0.646 "	1.33	0.846 "	0.642 "	1.32	0.800 "	0.650 "	1.23
Const.$_3$	0.495 "	0.363 "	1.36	0.481 "	0.361 "	1.33	0.466 "	0.366 "	1.27
Const.$_4$	0.303 "	0.232 "	1.31	0.300 "	0.231 "	1.30	0.300 "	0.234 "	1.28
		Average	1.35		Average	1.33		Average	1.27

The ratios of the mean observed values of $\lambda^2 E_g$ to those computed from Eq. (6), which are given in Table I, indicate a systematic discrepancy between them. The mean observed values of $\lambda^2 E_g$ are systematically exceeding the calculated values by approximately 30 percent. This is as should be expected, according to what we had before. It is very significant, that the average values of these ratios Obs./Calc. decrease appreciably as we pass to tubes which worked with a lower heating of the filament. A decrease in the ratios Obs./Calc. mean, evidently, a decrease in the discrepancy between the observed wave-lengths and those computed from Eqs. (1)–(3).

§3

As there could be a difference in the vacuum of the tubes and consequently in their working regime, it is necessary to test the validity of the above relationship between the value of the ratio Obs./Calc. and the heating of the tube and to see whether it might be due to a possible difference in the vacuum of the tubes.

The simplest way of avoiding the effect of a difference in the vacuum is to make observations using only one tube at different heating currents. Such observations were made with tube No. 5. As far as could be seen, this tube possesses the greatest symmetry in the arrangement of the electrodes, its dwarf waves had a greater intensity than those generated by the two other tubes; it was therefore used for these tests. The tests were made by selecting some point on the lines of maxima of the working diagram (II, §3) and measduring the corresponding wave-length, intensity of oscillation, etc., at different heating currents I_h beginning with the largest possible values and ending with those at which the intensity of oscillations was very low and measurements were becoming uncertain. Each time the grid voltage was selected according to the maximum current I_a in the plate circuit of the generator.

The selection of the points of observations was made so as to obtain monochromatic oscillations. This circumstance was very important, since the intensity of waves of different length varies differently as the heating current is changed. Therefore, it frequently happens that waves, which at large heating currents play the role merely of an "admixture," become relatively intensive at low heating, thus completely distorting the results obtained.

As the intensity of dwarf waves of the 4th order was generally low and as the precision of the measurements of their wave-length fell off rapidly with decreasing heating current, it was decided not to include them in the tests, making observations for normal waves and dwarf waves of the first three orders only.

TABLE II. *Tube R5 (No. 5).*

I_h (Amp.)	E_g (volt)	I_a (mA)	λ (cm)	$\lambda^2 E_g$
		normal waves; $L=23$ cm		
0.701	162	4.40	60.0	5.83×10^5
0.684	161	3.75	60.6	5.91 "
0.662	160	2.90	61.0	5.95 "
0.651	161	2.25	61.3	6.05 "
0.640	162	1.75	61.6	6.15 "
0.632	165	1.30	61.8	6.30 "
0.625	167	0.90	62.0	6.42 "
0.610	169	0.30	62.4	6.58 "
		dwarf waves, 1st order; $L=13$ cm		
0.701	152	2.70	36.6	2.04×10^5
0.684	146	2.20	37.0	2.00 "
0.662	138	1.80	37.3	1.92 "
0.651	136	1.30	37.2	1.88 "
0.640	133	0.85	37.0	1.82 "
0.625	127	0.30	36.8	1.72 "
		dwarf waves, 2nd ord.; $L=6$ cm		
0.701	240	2.00	18.85	0.852×10^5
0.684	234	1.60	18.9	0.836 "
0.662	228	0.80	18.8	0.806 "
0.651	224	0.50	18.7	0.783 "
0.640	221	0.20	18.55	0.760 "
0.625	217	0.02	18.4	0.735 "
		dwarf waves, 3rd ord.; $L=8$ cm		
0.701	305	0.95	12.7	0.492×10^5
0.684	300	0.65	12.55	0.473 "
0.674	288	0.35	12.5	0.450 "
0.662	278	0.10	12.5	0.434 "

The results of the measurements[2] are presented in Table II. Figs. 1 and 2 show the relation between the wave-length and the heating current, and also the relation between the value of the grid potentials, corresponding to a maximum plate current, and the heating current. As to the normal waves, their length increases very appreciably with decreasing heating current. At

[2] In Table II the observed values are rounded off to 0.1 cm for normal waves and dwarf waves of the 1st order. They are rounded off to 0.05 cm for dwarf waves of the 2nd and 3rd orders, as the accuracy of the measurements was somewhat greater for shorter waves.

the same time, the value of the grid voltage corresponding to a maximum plate current passes through a small minimum and increases rapidly, as the heating current is further diminished. In connection with this, there is, in the

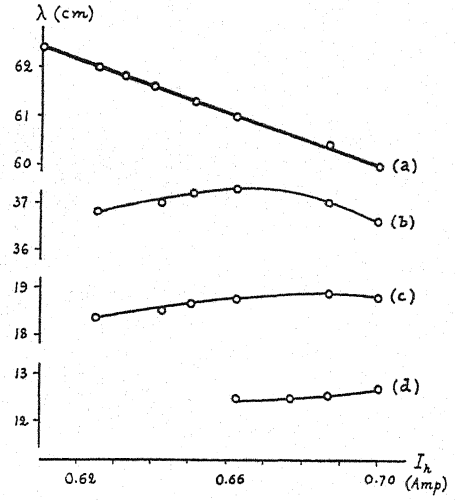


Fig. 1. Curves showing the relation between the length of the normal and dwarf waves and the heating current of the tube. Curve (a)—normal waves; curves (b), (c), (d)—dwarf waves of the 1st, 2nd and 3rd orders (E_g-variable).

case of normal waves, a rapid increase in the value of the product $\lambda^2 E_g$ as the heating current is decreased. This agrees well with the observations of W. Wechsung.[3]

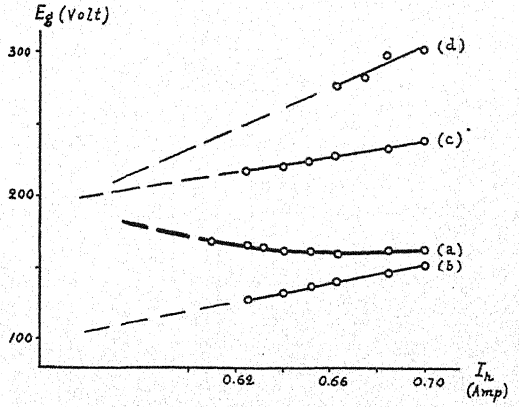


Fig. 2. Curves showing the relation between the grid voltage, corresponding to the maximum amplitude of oscillations, and the heating current. Curve (a)—normal waves; curves (b), (c), (d)—dwarf waves of the 1st, 2nd and 3rd orders.

A comparison of the results obtained for normal and for dwarf waves leads to an unexpected conclusion. It shows that *the normal waves depend on the heating current in a different way than the dwarf waves.* This is especially

[3] W. Wechsung, Zeits. f. Hochfr. **32**, 64 (1928).

clearly seen from the curves of Figs. 1 and 2 which show that the grid voltage corresponding to a maximum plate current, and also the length of the dwarf waves decrease as the heating current is decreased. As a result, in the case of dwarf waves the product $\lambda^2 E_g$ decreases as the heating current is decreased, i.e., it varies in a manner quite opposite to that of normal waves.

Table III gives a comparison of the values of const.$_1$, const.$_2$ and const.$_3$ calculated from Eq. (6) with those obtained from direct observations. For the sake of brevity the table gives the results of computation only for three values of the heating current. It is seen from Table III that the value of

TABLE III. *Tube R5 (No. 5).*

	I_h=0.701 amp. Const.$_0$=5.83×10^5 I_e=36 mA			I_h=0.684 amp. Const.$_0$=5.91×10^5 I_e=28 mA			I_h=0.662 amp. Const.$_0$=5.95×10^5 I_e=18 mA		
	Obs.	Calc.	Obs./Calc.	Obs.	Calc.	Obs./Calc.	Obs.	Calc.	Obs./Calc.
Const.$_1$	2.04×10^5	1.46×10^5	1.40	2.00×10^5	1.48×10^5	1.35	1.92×10^5	1.49×10^5	1.29
Const.$_2$	0.852 "	0.648 "	1.32	0.836 "	0.657 "	1.27	0.806 "	0.661 "	1.22
Const.$_3$	0.492 "	0.364 "	1.35	0.473 "	0.370 "	1.28	0.434 "	0.372 "	1.17
		Average	1.36		Average	1.30		Average	1.23

the ratio Obs./Calc. decreases as the heating and emission current is decreased, exactly in the same manner as we have seen from Table I. Hence it follows that *the magnitude of the discrepancy between the observed wave-lengths and those calculated from Eqs. (1)–(3) does really depend on the heating current* and that there is no reason to ascribe it to a difference in the degree of vacuum of the tubes. Of course the mere fact that the magnitude of the discrepancy depends on the heating current, is not an explanation of the cause of these discrepancies. It indicates, however, a way of discovering this explanation. This question will be treated later.

From Table III it is seen also, hat the product $\lambda^2 E_g$ varies quite uniformly as the heating current is varied. Therefore, when the heating current is still lower, the divergence between the observed and calculated values must be

TABLE IV. *Tube R5 (No. 5).*

I_h (Amp.)	Const.$_0$/Const.$_1$	Const.$_0$/Const.$_2$	Const.$_0$/Const.$_3$
0.701	2.86	6.84	11.8
0.684	2.96	7.07	12.5
0.662	3.10	7.38	13.7
0.651	3.22	7.73	—
0.640	3.32	8.09	—
0.625	3.73	8.73	—

even smaller than it is seen from Table III. Without giving any detailed computations we shall determine the values of the ratios const.$_0$/const.$_1$, const.$_0$/const.$_2$ and const.$_0$/const.$_3$. Theoretically, according to Eqs. (5) and (6) these ratios must be equal to 4, 9 and 16. Table IV gives the values of these ratios calculated from the data of Table II. It is seen from the Table IV that as the heating current is decreased these ratios increase and rather closely approach

the theoretical values. A poorer agreement is obtained for the third ratio which cannot be calculated for the low heating current in view of the low intensity of the dwarf waves of the 3rd order.

As we said before, when measuring the wave-length at different heating currents, the grid voltage was selected in such a way as to have a maximum plate current. However, a change in E_g must affect the length of the waves. Therefore, in determining the relation between the wave-length and the heating current, for the sake of greater accuracy we should have kept E_g constand and the maximum values of the plate current should have been selected by varying the length of the oscillating circuits. We have chosen the first method because of its convenience. Furthermore, the results obtained by this method permit easily to determine the results obtainable by the second method. Figs. 1 and 2 show that as the heating current is decreased the length of the normal waves increases, at the same time there is an increase in the grid voltage corresponding to the maximum plate current. Since increasing the grid voltage produces a decrease in the wave-length (see article II Tables III and VI) it is clear that, if the grid voltage had been kept constant, we would have a still more pronounced increase in the wave-length of the normal waves as the heating current was decreased. It is also easily seen that, if the grid voltage had been kept constant, decreasing the heating current would produce even a more noticeable decrease in the wave-length of the dwarf waves than it is seen from Fig. 1.

§4. On the Influence of the Amplitude of the Alternating Potentials

The data of the last three tables confirm the existence of a definite dependence of the magnitude of the discrepancy between the observed and the calculated wave-lengths (or the values of $\lambda^2 E_g$) on the heating current. The data give also a fairly complete idea as to the character of this relationship. With these data it is possible to attempt an elucidation of the causes of this relationship.

The changes in the heating current and the consequent changes in the emission current can be accompanied by the following three phenomena: (1) a change in the density of the space charges, (2) a change in the initial velocity of the electrons and (3) a change in the amplitude of the oscillations generated by the tube. We did not consider these phenomena and none of them is taken into account by formula (2).

The change in the density of the space charges is frequently used to explain the changes in the wave-lengths with changing heating current. Starting from the concept of the influence of the space charges on the motion of the electrons, H. G. Möller[4] has shown theoretically that a decrease in the emission current must produce an increase in the length of the generated waves. This does not contradict our observations on normal waves, for which the theory was devised. However, there are good reasons to maintain that in our case the change in the density of the space charges cannot have an appreciable influence on the motion of the electrons. In the first place, all of our observa-

[4] H. G. Möller, Electr. Nachr. Techn. **7**, 411–419 (1930).

tions were made at such grid voltages which lay far in the region of saturation current, even at the maximum values of the heating current used. Therefore the influence of the space charges on the motion of the electrons ought to be very small in our case. Furthermore, if the change of the space charges had any appreciable influence, its effect would be the same for all kinds of waves. Our results show, however, that with a change in the heating current the normal waves vary in a different way than the dwarf waves. For the same reason we must consider as unapplied to our case the explanation proposed by A. Rostagni[5] which is based on the possibility of the existence of a natural period of the space charges analogous to the natural period of an ionized gas, and which is dependent on the density of the space charges. There is still less ground to admit the possibility of an influence due to a change in the initial velocity of the electrons, in view of the fact that this velocity is relatively low. There remains the third factor—the effect of a change in the amplitude of the generated oscillations.

If there are oscillations in the plate and the grid currents of the tube then alternating potentials must appear on the electrodes of the tube, as on the plates of a condenser. If these potentials are not vanishingly small in comparison with the constant grid voltage, they necessarily must affect the character and the velocity of electronic motions and change the time the electrons take to pass from the filament to the grid. Thus the length of the generated waves will be changed. E. Gill and J. Morrell[6] had mentioned the possibility of an influence of the alternating potentials on the motion of electrons. H. E. Hollmann[7] was the first to make an estimate of the influence of these potentials on the time of passage of the electrons and on the length of the generated waves. The formula which he obtained shows that the wavelength must decrease as the amplitude of the oscillations is increased. The same conclusions were arrived at by N. Kapzov[8] and F. W. Sears[9] who made a graphical investigation of the electronic trajections within the tube, and also by H. G. Möller,[4] as a result of his theoretical investigations. All of these results refer to normal waves only and are in complete agreement with the results obtained for these waves, presented in Table II. From this table it is seen that the length of the normal waves decreases continuously, as the amplitude of the oscillations (or the current I_a) is increased. P. S. Epstein,[10] independently from the previous papers, made a theoretical investigation of the influence of the amplitude of the alternating potentials on the length of the normal and dwarf waves. He showed that for dwarf waves this influence must be opposite to that for normal waves.[11] To this difference he ascribed

[5] A. Rostagni, Atti della R. Acad. di Torino **66**, 123–130, 217–223, 383–395 (1931); see also Th. V. Ionescu, C. R. **193**, 575–577 (1931).

[6] E. W. B. Gill and J. H. Morrell, Phil. Mag. **44**, 161–178 (1922).

[7] H. E. Hollmann, Ann. d. Physik **86**, 129–188 (1928).

[8] N. Kapzov, Zeits. f. Physik **49**, 395–427 (1928).

[9] F. W. Sears, J. Frankl. Inst. **209**, 459–472 (1930).

[10] P. S. Epstein, Report at a Physics Research Conference, Pasadena, Mar. 5, 1931.

[11] According to his theory the above deduction is always true for dwarf waves of the 1st order. For dwarf waves of the second and higher orders this deduction depends on the dimensions of the tube.

our systematic discrepancy between the observed and the calculated wavelengths. So far we had no opportunity for a detailed verification of this theory. One of its results shows, however, that this theory not only explains the above discovered difference in the effect of the heating current on the normal and on the dwarf waves but also leads to quantitatively correct results.

We have seen above that the ratios const.$_0$/const.$_1$, const.$_0$/const.$_2$, const.$_0$/const.$_3$ must be equal to 4, 9 and 16 if Eqs. (1) and (3) are true. If the assumption of the influence of the amplitude of the alternating potentials is correct, then in comparing our observations it will be more correct to refer them to the same amplitude of oscillations and not to the same value of the

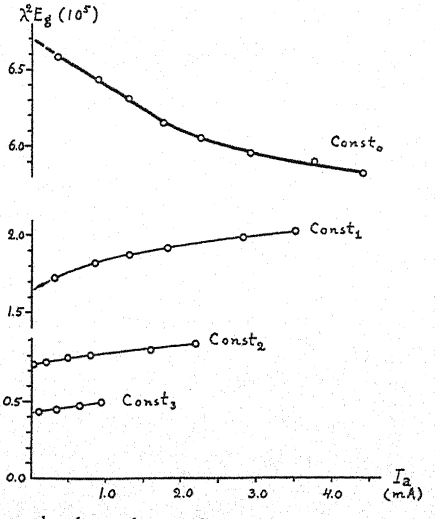


Fig. 3. Curves showing the dependence of the values of const.$_0$, const.$_1$ const.$_2$ and const.$_3$ on the amplitude of oscillations (amplitude of the alternating potentials which appear at the electrodes of the tube during oscillations).

heating current, as we have done it before. The ratios const.$_0$/const.$_1$, const.$_0$/const.$_2$, const.$_0$/const.$_3$ must be equal to 4, 9 and 16 at infinitely low amplitudes of the alternating potentials, i.e., in the limit at $I_a=0$.

The values of const.$_0$, const.$_1$, const.$_2$, and const.$_3$ at $I_a=0$ can be determined graphically from the data of Table II, by constructing curves showing the relations between these constants and the plate current which, as we have seen before (I, §6) approximately corresponds to the amplitude of oscillations and, which is more important, appears only when oscillations are present. For this last reason the condition $I_a=0$ does really correspond to the condition of infinitely small amplitudes of alternating potentials. These curves are shown on Fig. 3. We find by extrapolation

$$\left.\begin{array}{l}\text{const.}_0 = 6.70\times 10^5\\ \text{const.}_1 = 1.65\ \text{“}\\ \text{const.}_2 = 0.735\ \text{“}\\ \text{const.}_3 = 0.43\ \text{“}\end{array}\right| I_a = 0$$

where the value 0.735×10^5 is taken directly from Table II. Hence we obtain

$$\left(\frac{\text{const.}_0}{\text{const.}_1}\right)_{I_a=0} = 4.1 \quad \left(\frac{\text{const.}_0}{\text{const.}_2}\right)_{I_a=0} = 9.1 \quad \left(\frac{\text{const.}_0}{\text{const.}_3}\right)_{I_a=0} = 15.6.$$

The discrepancy between these figures and the theoretical values does not exceed the limits of the possible errors. This proves that as far as can be seen from the above investigations, the difference between the observed and calculated wave-lengths is to be completely explained by the dependence of the length of waves on the amplitude of the alternating potentials which appear on the grid and the plate of the tube during oscillations.

Evidently it does not follow that the dependence of the wave-length on the heating current can *always* be explained as being due to the influence of alternating potentials alone. When observations are made in the region $E_g<E_s$ a greater influence can be exercised by the space charges of which we have spoken previously (II, §12). On the other hand, our results permit us definitely to deny the widely spread opinion, according to which a decisive importance is attributed to the space charges in all cases when explaining the dependence of the wave-length on the emission and heating current. This opinion is usually connected with the notion that the amplitudes of the alternating potentials are vanishingly small in comparison with the constant grid potentials and that the influence of the alternating potentials on the period of electronic oscillations is insignificant. This conception is erroneous.

The dependence of the wave-length on the amplitude of oscillations and the heating current enables us to explain some of the other phenomena observed. We shall mention as an example the displacement of the regions of oscillations with a change in the heating current (II, §13). Since to each point of the diagram corresponds its own wave-length it is clear that a change in the heating current and a consequent change in the wave-length must produce a displacement of the region of oscillations. Furthermore, the regions of normal waves will be differently displaced than the regions of dwarf waves; for their wave-lengths change differently with varying heating current, as we have just seen. The fact that for normal waves of low intensity, when they are mixed with the dwarf waves (II, §13), the values of λ^2E_g are greater than usual will also be readily understood.

§5

In the previous paper we have discussed the results of a graphic integration of the equations of motion of the electrons in the tube, performed by G. Kreutzer. As we saw, the electronic trajectories showed that the alternating potentials at the electrodes of the tube must decrease the length of the dwarf waves. On the other hand, we have found above, that the length of the dwarf waves increases with an increase in the heating current and the amplitude of the alternating potentials. As a matter of fact, these two results are not contradictory. The graphic integration of the equations of the motion of the electrons was performed for the case $E_0/E_g=1/10$, E_0 being the ampli-

tude of the alternating potentials. Direct measurements of the amplitude of the alternating potentials, which we shall not discuss for the present, showed, however, that for our dwarf waves of the 2nd and 3rd order the maximum value of the ratio E_0/E_g is approximately equal to $1/30-1/45$, i.e., is considerably below the value assumed in our computations. For dwarf waves of the first order this ratio had a larger value being approximately equal to $1/14$, as a maximum. Fig. 1 shows that it is exactly for these waves that the curve showing the relation between the wave-length and the heating current has a maximum. Hence it follows that in the case of dwarf waves the alternating potentials at the electrodes of the tube have the following effect: the wave-length increases at first, reaches a maximum and decreases as the amplitude of oscillations is further increased. It is evident that no maxima are observed on the curves relating to dwarf waves of the 2nd and 3rd orders simply because the amplitudes of the alternating potentials are very small in this case. On the other hand, all the calculations were made for relatively large amplitudes of alternating potentials. This explains the apparent discrepancy mentioned above.

§6. On the Limiting Value of Const.$_0$

There are several formulas expressing the length of the waves in terms of the voltage at the electrodes and the dimensions of the tube. The simplest one is the well-known formula of H. Barkhausen

$$\lambda^2 E_g = d_a^2 \times 10^6 \tag{8}$$

which is easily obtainable from Eqs. (1) and (2). This formula claims no particular accuracy, since in deriving Eq. (2) plane electrodes were assumed for the sake of simplicity.

S. Zilitinkiewitch[12] and A. Scheibe[13] obtained more accurate formulas which take into account the cylindrical shape of the electrodes. The formula of S. Zilitinkiewitch is expressed in a function of two rather slowly converging series. It is therefore less convenient than the formula of A. Scheibe. The latter formula can be written as follows for the case when the plate potential are low or equal to zero:

$$\lambda^2 E_g = \frac{2c_0^2 d_g^2}{e/m \times 10^8}[f(\ln d_a/d_f)^{1/2} + g(\ln d_a/d_g)^{1/2}]^2 \tag{9}$$

where d_a, d_g and d_f are the diameters of the plate, grid and filament respectively, e/m is the ratio of the electronic charge to its mass[14] and the two functions in the brackets are:

[12] S. Zilitinkiewitch, Drahtl. Tel. u. Tel. (Russ) **18**, 2–22 (1923); **19**, 166–175 (1923); Arch. f. Elektrot **15**, 470–484 (1926).

[13] A. Scheibe, Ann. d. Physik **73**, 54–88 (1924).

[14] The constant coefficient $[2c_0^2/(e/m)\times 10^8] = 1.017\times 10^6$. Strictly speaking, formula (8) also ought to have this coefficient. It had been omitted, as this formula is only approximate.

$$f(\ln d_g/d_f)^{1/2} = f(x) = xe^{-x^2}\int_0^x e^{n^2}dn$$
$$g(\ln d_a/d_g)^{1/2} = g(x) = xe^{x^2}\int_0^x e^{-n^2}dn. \tag{10}$$

The numerical values of $f(x)$ and $g(x)$ can be obtained from the tables given in the paper of A. Scheibe[13] or from more detailed tables computed by N. Kapzov and S. Gwosdower.[15]

As to the accuracy of Barkhausen's formula, we have already mentioned that it gives wave-lengths which differ by approximately 15 percent from the observed values. Of course, this figure refers only to the observations described above. From what we have said, it follows that the discrepancy between the observed and the calculated lengths of normal waves must become greater at greater amplitudes of oscillations. As an example, we can mention our preliminary measurements made with two tubes working simultaneously (II, §3). During these observations the plate current was greater than the one given by a single tube, $\lambda^2 E_g$ was equal to 5.44×10^5 and the discrepancy between the observed length of normal waves and that given by formula (8) was approximately 20 percent, as could be readily shown by simple computations.

The formula of A. Scheibe has been verified experimentally several times. As could be expected, it was in better agreement with the observations than formula (8). Nevertheless, the values it gave differed by some 10 percent from the observed wave-lengths.

Approximately the same agreement with the experimental data is obtained using the formula of S. Zilitinkiewitch, judging from the data of his paper. It must be mentioned that the obtained wave-lengths (normal waves) are always shorter than those computed from formulas (8) and (9).

In deriving formula (9), as well as in deriving formula (8), the dependence of the length of waves on the amplitude of the oscillations has also not been taken into account and the electrode potentials were assumed to be constant. From the preceding it is clear that for this reason alone there could be no good agreement between these formulas and the observations.

In the limiting value of $(\text{const.}_0)I_a = 0$ the effect of the alternating potentials is eliminated. Hence, this value must be in better agreement with formulas (8) and (9) than the direct observations. We shall-verify this statement.

Let us consider formula (8). As we have seen previously (II, §4), for the tubes of the type R5 this formula gives:

$$\text{const.}_{\text{Barkh}} = 7.6\times10^5. \tag{11}$$

This value differs from our limiting value 6.70×10^5 by approximately 12 percent. This corresponds approximately to a 6 percent difference in the wave-lengths, since the constant contains the square of the wave-length.

[15] N. Kapzov u. S. Gwosdower, Zeits. f. Physik **45**, 114–134 (1927).

As previously this difference in the wave-length amounted to approximately 15 percent (the difference in the values of $\lambda^2 E_g$ being approx. 30 percent) it becomes evident that among the errors of this formula, the largest error is introduced by neglecting the effect of the alternating potentials. Of course, this statement refers only to waves of sufficient intensity, such as our normal waves. As the intensities of the waves falls off, there must be a decrease in the relative error due to the alternating potentials.

Using formula (9) we obtain:[16]

$$\text{const.}_{\text{Sch}} = 7.22 \times 10^5. \tag{12}$$

This value differs from the limiting value of $(\text{const.}_0) I_a = 0$ by approximately 7 percent, which corresponds to a difference in the wave-lengths of approximately 3.5 percent. It could be shown by computations that the difference between directly observed wave-lengths and formula (9) constitutes approximately 12 percent. By comparing this figure with the preceding one, we can see again how large is the error introduced by neglecting the influence of the alternating potentials.

Under the conditions of our experiments the possible errors in formulas (8) and (9) can roughly be estimated as thus: neglecting the alternating potentials at the electrodes introduces in the wave-lengths an error of about 9 percent; the simplification of the problem by assuming plane instead of cylindrical electrodes introduces an error of about 3 percent, finally, all the other possible causes,[17] including the effect of space charges and the initial velocity of the electrons, introduce an error of also approximately 3 percent.

Comparing the magnitudes of all these errors it can be seen that in developing a theory of the generation of ultra-short waves there is no particular need of taking into account the shape of the electrodes.

In order to simplify the problem, it is quite sufficient to assume the electrodes of the tube to be plane. At the same time, it is quite necessary to take into account the effect of the alternating potentials. This is true of all problems which aim at determining the length of the generated waves, the time it takes the electrons to pass inside the tube, etc. In other cases, for example, in deriving formulas determining the conditions of the appearance of oscillations, their energy, etc., the assumption of plane electrodes will be of greater importance.

§7.

In deriving formulas (8) and (9) the wave-lengths were determined from the time it takes the electrons to pass from the filament to the plate and back to the filament. The very small difference existing between the values of $(\text{const.}_0)_{I_a=0}$, $\text{const.}_{\text{Barkh}}$ and $\text{const.}_{\text{Sch}}$ shows that *the normal waves generated by the tubes do really correspond to the time of passage of the electrons from the*

[16] The tubes of the type R5, which we investigated, had d_a (internal) $=0.87$ cm; d_g (middle) $=0.37$ cm; $d_f=0.006$ cm.

[17] The error introduced through experimental errors is very small. For example, for observations given in Table V of article II the calculations give for normal waves $\lambda^2 E_g = 5.78 \times 10^5 \pm 0.017$.

filament to the plate[18] *and back to the filament*, in other words, they correspond to a complete period of electronic oscillations about the grid of the tube. This conclusion is of a very great importance for the theory of the generation of ultra-short waves. There exists a number of papers,[19] in which the length of waves is calculated from the time it takes the electrons to pass from the grid to the plate and back to the grid. This tendency of using a shorter path is quite understandable in view of the fact that the observed wave-lengths are always shorter than those obtained from formulas (8) and (9), as we have mentioned before. The agreement between the theory and the observations can be improved thereby. The foregoing considerations show, however, that another way must be chosen in order to obtain a better agreement between the theory and the observations. Namely, the effect of the alternating potentials on the motion of the electrons within the tube must be accurately estimated. At the same time, it is necessary to preserve the fundamental idea of H. Barkhausen's theory, according to which the length of the normal waves, generated by the tube corresponds to a complete period of electronic oscillations. This idea is unquestionably correct. The only possible exception is the case when waves are generated by a tube with a very closely wound grid (close mesh). In such a case, as it was shown by H. Hollmann,[6] it is possible to obtain, together with the usual oscillations, the so called "oscillations of a higher frequency." They will correspond to the shorter path and to a shorter time of passage of the electrons, which in this case will be easily captured by the grid on their way from the plate to the filament.

In conclusion the author wishes to express his gratitude to the Carnegie Corporation of New York for the grant of a Fellowship and to Professor R. A. Millikan for the facilities of the Norman Bridge Laboratory.

[18] Strictly speaking to the point of reversal.

[19] See, for example, E. W. Gill and J. H. Morrell, Phil. Mag. **44**, 161–178 (1922), D. Pfetscher, Phys. Zeits. **29**, 449–478 (1928); E. W. Gill, Phil. Mag. **12**, 843–853 (1931).

The Hall Effect With Audiofrequency Currents

By LAWRENCE A. WOOD
Department of Physics, Cornell University

(Received May 16, 1932)

Hall e.m.f. in tellurium for currents of frequencies up to 25,000 cycles per sec.— The Hall e.m.f. in tellurium has been investigated with currents of frequencies up to 25,000 cycles per second, with particular reference to any effect of frequency on the magnitude of the Hall coefficient R_H, and on the phase of the Hall e.m.f. relative to the longitudinal current producing it. A Hartley-circuit vacuum-tube oscillator furnishes the current for the specimen, which is placed in a constant magnetic field of about 3000 gauss. The Hall e.m.f., amplified by a resistance-coupled vacuum-tube amplifier, is observed on a cathode-ray oscillograph. A general method of procedure is indicated for use in *comparing alternating e.m.f.'s* as small as a few millivolts or less with respect to magnitude and phase. The current drawn and the power consumed are entirely inappreciable. The results of a comparison method of this sort and a null method agree in the conclusion that in the range studied, the Hall coefficient for tellurium is constant to within about 2 percent for frequencies up to 10,000 c.p.s. and to within 7 percent for the complete range. This agrees with the results of Smith on bismuth. For the specimen used the value found for the Hall coefficient is $R_H = 481$. The two methods also agree in finding the frequency, wave-form, and phase of the Hall e.m.f. the same as those of the longitudinal current producing it. The phase difference, if any, is believed to be less than 2° at frequencies below 20,000 c.p.s. and less than 4° at 25,000 c.p.s.

ALTERNATING-CURRENT HALL EFFECT

THE usual equation for the Hall e.m.f.

$$E_H = R_H H I/d \tag{1}$$

(in which R_H is the Hall coefficient, H the magnetic field, d the thickness of the plate, and I the current) shows that the e.m.f. reverses direction with reversal of the current. The Hall effect may be regarded as a rotation of the equipotential lines in the plate, and it may be readily shown[1] that

$$R_H H = \rho \tan \theta \tag{2}$$

where θ is the angle of rotation and ρ is the resistivity of the material. The angle of rotation is thus seen to be independent of the magnitude and direction of the current.

The number of workers who have investigated the Hall effect with alternating currents is surprisingly small. All investigators[2,3,4,5] agree that the

[1] Campbell, Galvanomagnetic and Thermomagnetic Effects, Longmans, Green, and Co., 1923.

[2] Des Coudres, Phys. Zeits. **2**, 586 (1901).

[3] Von Traubenberg, Ann. d. Physik **17**, 78 (1905).

[4] Zahn, Ann. d. Physik **36**, 553 (1911).

[5] Smith, Phys. Rev. **35**, 81 (1912).

magnitude of the effect is the same as with direct current, but no further observations of its character seem to have been reported.

In the work described in the present paper, alternating current, furnished by an oscillating vacuum-tube circuit was maintained in a tellurium plate. A unidirectional magnetic field produced an alternating Hall e.m.f. which was then amplified by the use of a vacuum-tube amplifier and observed on a cathode-ray oscillograph.

An arrangement of this sort has two important advantages over those previously used for studying the a.c. Hall effect. In the first place, practically no current is drawn from the circuit for the purpose of measurement (observations indicating that even the d.c. grid current is less than 10^{-9} amp.), and thus we are able to deal with an actual Hall e.m.f. rather than with a Hall current, which may disturb conditions in the plate, and which in any case necessitates corrections for the inductive effects of leads and measuring instruments. Secondly, observations can be made of the frequency, wave form, and phase of the Hall e.m.f. as well as of its magnitude.

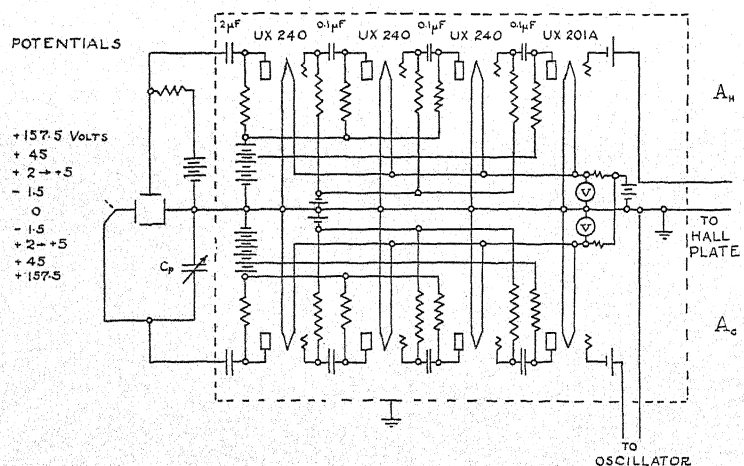


Fig. 1. Amplifier—oscillograph circuit diagram.

Tellurium was chosen because of its extremely large positive Hall coefficient. Bismuth, the material used in the high frequency work of Smith[5] (the only other observer to work at higher than commercial frequencies), has a negative coefficient of smaller magnitude.

Experimental Arrangement

Oscillator

The vacuum-tube oscillator was of the conventional Hartley circuit type, utilizing a UX 250 tube and giving a maximum power output of almost five watts. It was unshielded and was placed about twelve feet from the other apparatus, it being found by experiment that this distance was sufficient to prevent direct transfer of energy to the shielded amplifier and was more satisfactory than shielding. The inductance was a flat multilayer coil with air

core. For the purpose of electrostatic shielding a grounded strip of solid copper was placed around the coil, the lapped ends being insulated from each other in order to avoid electromagnetic shielding. Outside this, ten turns of wire formed a pick-up coil sufficient to maintain a half-ampere current in the tellurium plate.

The specimen was shielded from the oscillator and other electrical disturbances by being placed in a grounded copper box.

Hall plate and magnetic circuit

The tellurium plate itself, of dimensions $4\times2\times0.25$ cm, was cast in a rectangular hole cut in an asbestos plate and supported on a second asbestos plate rotated 45° with respect to the first, to give support to the lead wires. Platinum wires running through a groove between the asbestos plates were melted into the tellurium when the plate was cast. These made three fixed contacts with the plate—one at each end and one on one side.

A fourth contact P on the opposite side, was a movable pin which made contact with the upper surface of the plate. This pin was mounted on a carriage, similar to the tool-rest on a lathe, which gave by adjustment of micrometer screws two-dimensional motion in the plane of the specimen. The pressure of the contact at P could be adjusted by a thumbscrew.

The plate was mounted in the air gap of a magnetic circuit in which fields up to slightly more than 4000 gauss could be obtained.

Amplifiers

The two amplifiers, placed in a second large copper box, each consisted of a UX 201A tube followed by three stages of resistance-coupled amplification employing the "high-mu" UX 240 tubes. This gave a voltage amplification of 40,000 when needed. The amplification was controlled by varying the filament voltage.

One amplifier served to amplify the Hall e.m.f. or an ohmic p.d., while the other, merely in order to impress on the oscillograph a voltage of the same frequency as the first but of variable phase, amplified the voltage picked up by a single-turn coil about a foot away from the oscillator. This coil could be rotated to vary the amplitude. The variation of phase was accomplished by the use of a variable condenser C_P placed across the amplifier output. When this variation was not sufficient, a resistance was placed in series with the condenser and the potential across one or the other placed on the oscillograph.

It was not desirable to connect the oscillograph directly across the plate resistance of the last amplifier tube, because of the potential difference caused by the d.c. plate current. An output transformer did not prove satisfactory because of variations in magnitude and phase of the output with change of frequency and conditions of operation of the amplifier. Placing a two microfarad blocking condenser in the line to the oscillograph, however, accomplished the desired result without appreciable reduction of the a.c. voltage to be measured.

Oscillograph

The cathode-ray oscillograph, a Bedell-Reich Oscilloscope,[6] was used to examine the output of the first amplifier, either with the horizontal linear time axis or with the horizontal sinusoidal time axis provided by the second amplifier, or with no horizontal displacement at all. Amplified stabilization, as described by Bedell and Kuhn,[7] was employed with the linear time axis.

A method of frequency measurement[8] by means of a calibration of the current charging the condenser in the "sweep voltage" circuit of the linear time axis of the oscilloscope was employed.

In order to avoid the distortion[9] often produced in the oscillograph tube when the electric field across the vertically-deflecting plates is zero, a 45-volt B-battery in series with a resistance was placed across these plates. The spot was then brought back to the center of the screen by a permanent magnet above the tube. Experience showed that this eliminated the distortion and introduced no appreciable additional change in the beam.

Procedure

I. Comparison method

The first method consisted of the comparison of the Hall e.m.f. with an ohmic potential difference as nearly as possible in phase with the current in the tellurium plate and proportional to it. Comparison of the magnitudes of the two voltages was followed by a comparison of their phases. The magnitude comparison involved merely the measurement of the oscillograph deflections, first when the Hall e.m.f. was placed across the amplifier A_H and then when, by a switch, connections were shifted to place the ohmic potential difference across the same amplifier.

A similar plan was followed in the phase comparison, but in this case the second amplifier A_C was utilized. With the ohmic potential difference on the vertically-deflecting plates of the oscillograph, the phase of the comparison voltage E_C was varied by variation of condenser C_P until there was no phase difference. By the shift of connections already mentioned the Hall effect itself could now be amplified by the same amplifier and placed across the vertically-deflecting plates. By this means the phase of the Hall e.m.f. could be compared with that of E_C and thus with that of the ohmic potential difference. Any phase difference showed itself in an opening of the straight line into an ellipse. Measurements of the amplitude of the vertical and horizontal deflections separately and of the major and minor axes of the ellipse gave data for phase computations.

After several other methods of obtaining the ohmic potential difference had proved unreliable, it was realized that a potential difference E_B along the edge of the plate itself, obtained by displacing the movable pin contact P a fixed distance from its initial position P_1, was certain to be in phase with the

[6] Bedell and Reich, Journal Am. Inst. E. E. **46**, 563 (1927).
[7] Bedell and Kuhn, Rev. Sci. Inst. **1**, 227 (1930).
[8] Wood, Rev. Sci. Inst. **3**, 378 (1932).
[9] Bedell and Kuhn, Phys. Rev. **36**, 993 (1930).

current and proportional to it, providing only that the inductive reactance of the plate was negligible in comparison with its resistance. Calculation indicated that this was true.

II. Null method

The second or null method of observation, obviously suggested by the other method, employed the potential difference E_B along the side of the plate to balance out the Hall e.m.f. Accordingly with the amplifier A_H connected to terminals P and Q on an equipotential line as before, the magnetic field was impressed across the plate and the resulting Hall e.m.f. E_H was balanced out by a displacement of point P parallel with the edge of the tellurium plate from its former position P_1 to a new position P_2, so that P_2 and Q lay on the same new equipotential, as shown by zero vertical displacement of the oscillograph. No horizontal deflection whatever was employed. In the comparison method, E_B was made only approximately the same size as E_H; here they were made exactly equal by this adjustment for zero deflection. The amplifier and oscillograph were thus used here only as a potential-detecting instrument.

The location of P_2 should be dependent only on the angle of rotation of the equipotentials, and thus should be independent of the current and of the actual size of the Hall e.m.f. and consequently independent of the amplification. With P_2 left fixed, the frequency was varied in order to observe whether P_2 and Q still remained at the same potential.

Results

A detailed summary of some of the experimental results obtained by each method will now be given.

In the first place, the production of ellipses and straight lines on the oscillograph screen showed that the frequency of the Hall effect was the same as that of the current in the tellurium plate. There was hardly any doubt that this result was to be expected, yet apparently no direct observations of this sort had been made previously. Furthermore the fact that the ellipses and lines were undistorted showed that the wave-form of the Hall e.m.f. was essentially the same as that of the current producing it.

Values obtained in the $E_H - E_B$ comparison are given in Table I. The numerical values of the oscillograph deflections recorded are of no particular

TABLE I. *Amplitude and phase comparisons at different frequencies. $I=0.48$ amp. $H=3100$ gauss.*

f (c.p.s.)	Magnitude $2E_H$	Magnitude $2E_B$	Magnitude E_H/E_B	Phase $2E_H$	Phase $2E_c$*	Phase $2b$	Phase ϕ
750	7.63 cm	7.48 cm	1.02	7.5 cm	7.4 cm	<0.3 cm	<3° 20′
2750	7.34	7.19	1.02	7.8	7.6	<0.3	<3° 10′
5500	7.53	7.34	1.03	7.4	7.2	<0.3	<3° 20′
10000	7.27	7.25	1.00	7.2	7.2	<0.3	<3° 30′
19200	6.30	6.10	1.03	6.1	6.3	<0.3	<3° 50′
25000	2.75	2.70	1.02	2.9	3.0	<0.3	<8° 20′

* Adjusted to phase equality with E_B.

LIBRARY OF ALLAHABAD. Date ... A. ... CHRISTIAN COLLEGE

significance; it is the variation of their ratio with frequency that is of interest. The column headed ϕ gives the phase angle between E_B and E_H, as computed by the method given below from the experimental observations in the preceding three columns.

In the null method, when P was placed at the equipotential point P_2 at a given frequency by making the oscillograph deflection zero, it was observed that at each other frequency within the range studied the oscillograph deflection, if any, was too small to be measured. It could not have been greater than 0.2 cm. This held true even when the amplification (at all but the frequencies above 10,000 c.p.s.) was increased to a value which would have produced a Hall e.m.f. deflection three or four times those previously used (in the comparison method). At frequencies above 10,000 c.p.s. the full amplification obtainable was used at all times.

A similar test was also made without the magnetic field, and, to the same precision as before, the location of P_1 was also found to be unchanged with frequency.

The distance between P_1 and P_2 when a field of 2900 gauss was used was observed to be approximately 0.022 cm. This corresponds to an angle θ of rotation of the equipotentials of about 38′.

Interpretation of Results

Combining the Hall equation

$$E_H = R_H \cdot (H/d) \cdot I \tag{1}$$

with

$$E_B = IZ_B \tag{3}$$

where Z_B is the impedance between the two points P_1 and P_2 along the edge of the tellurium plate, we obtain

$$E_H/E_B = (H/d)(1/Z_B)R_H. \tag{4}$$

Thus the question of the constancy of Z_B with frequency is seen to be of importance here.

The inductance of the tellurium plate was calculated[10] to be 0.024 microhenry, corresponding to an inductive reactance of 0.0038 ohm at 25,000 c.p.s. The value of the resistance of the plate, measured directly, (2.5 ohms) is about 660 times this value, and hence Z_B should be independent of frequency within the precision of the measurements. The constancy of the E_H/E_B ratio as shown in Table I then indicates that there is no change in R_H with frequency.

The question of the determination of phase from measurements of a given ellipse has already been discussed elsewhere.[11] The formula developed there is

$$\sin \phi = ab/A_x A_y \tag{5}$$

[10] Bureau of Standards Circular No. 74 (*Radio Instruments and Measurements*), page 246.
[11] Wood, Rev. Sci. Inst. 2, 644 (1931).

where a and b are the semi-axes of the ellipse, and A_x and A_y half the horizontal and vertical deflections respectively. Measurements of all four quantities were made, and the phase angle calculated by this formula. The four quantities are also connected by the relation:

$$A_x^2 + A_y^2 = a^2 + b^2. \tag{6}$$

This relation was used as a check on the measurements.

The phase angle ϕ_{BI} between E_B and the current I should be such that

$$\tan \phi_{BI} = X_B/R_B. \tag{7}$$

The argument to show that this ratio of inductive reactance X_B to resistance R_B along the edge of the plate is negligible has already been given in the discussion of the magnitude ratio E_H/E_B.

Thus the phase of E_B is negligibly different from that of I. From Table I it may be seen that ϕ the phase angle between E_B and E_H, if different from zero, is smaller than can be detected by this method.

In the null method the simple fact that the locations of P_1 and P_2 are unchanged with frequency variation, leads to the conclusion that both magnitude and phase of the Hall effect are independent of frequency.

Since the oscillograph deflection remained zero to within 2 mm in, say, 150 mm at frequencies of 10,000 c.p.s. or below, we may say that the Hall coefficient is constant (or proportional to the impedance, if our calculations in regard to the negligibility of inductive reactance should be in error) to within 1.5 percent. At a frequency of 25,000 c.p.s. we may say that it is constant to within 2 mm in 30 mm or 7 percent. Thus this method checks with greater precision the result of the comparison method in finding no change of Hall coefficient with frequency.

The very fact that it is possible to find a point P_2 at the same potential as Q, when the magnetic field is turned on, shows that there is no phase difference between the Hall e.m.f. and the current producing it. Calculations indicate that a phase difference of 2° could have been detected at frequencies below 20,000 c.p.s. and a phase difference of 4° at 25,000 c.p.s.

Magnitude of the Hall Coefficient

Although the primary object of this work was merely to observe changes in the magnitude and phase of the Hall effect with frequency, no particular attention being paid to making a careful measurement of the actual value of the Hall coefficient R_H, it is possible to make an approximate calculation of its value, from observations made in a comparison method similar to that already described, but which involved the use of the potential across a small series resistance.

The comparison with the small series resistance proved unsatisfactory only at the higher frequencies. Therefore, since the average low-frequency value of the E_H/E_R ratio was 1.115 and $Z_R = R_R = 0.005$ ohm, we are able to utilize an equation similar to that already derived for the E_H/E_B ratio, namely,

$$E_H/E_R = (H/dZ_R)R_H \tag{8}$$

in order to calculate R_H. Other numerical values are $H=2900$ gauss, and $d=0.25$ cm, the latter dimension being somewhat uncertain. Thus we find for the Hall coefficient

$$R_H = 481$$

in reasonable agreement with values reported by other observers working exclusively with direct currents, as given in Table II (taken from Campbell's monograph[1]).

TABLE II. *Tellurium Hall coefficient.*

Temp.	H	R_H	Observer
20°C	2800	530	Ettingshausen and Nernst
27.1°	Immaterial	784	Wold
65°	4000	430	Lloyd
—	—	500	Zahn
21.8°	8800	I 536	Smith
20.3°	8800	II 621	Smith

CONCLUSIONS

It would seem manifestly desirable to continue the work to higher frequencies. In view of the radical changes in technique rendered necessary at radiofrequencies, this was not attempted in the present investigation. The null method, in particular, would seem to lend itself readily to this extension, and work upon it is now in progress.

The combination of two amplifiers and oscillograph offers, it would seem, a powerful tool for the investigation at different frequencies, of the phase and magnitude of small voltages other than the Hall e.m.f. The comparison procedure here outlined could be followed with little change.

Finally, the author desires to express heartfelt gratitude to Professor Merritt, who suggested the problem and without whose continued interest it could not have been carried to completion, as well as to many other friends whose advice and suggestions have been extremely helpful.

Some Thermo- and Galvanomagnetic Properties of a Bismuth Crystal

By H. E. BANTA
The Rice Institute

(Received June 9, 1932)

The fractional changes, due to a magnetic field, in the electrical conductivity, in the thermal conductivity, and in the thermoelectric power of a single bismuth crystal are measured in these experiments. These changes are determined as a function of the field strength, of the direction of the field, of the direction of the crystal axis, and of the direction of the heat and electric currents through the crystal. An electric current sent through the crystal cools one junction and heats the other by the Peltier effect. The temperature difference thus produced gives rise to a thermal e.m.f. in the crystal circuit. Observations of this e.m.f. allow the calculation of the fractional changes produced in the thermal conductivity and in the thermoelectric power. The change of electrical conductivity is influenced much more strongly by the crystal structure than is the change of thermal conductivity. Crystal structure and orientation of the magnetic field both affect strongly the change in the thermoelectric power. The theory of electrons in metals in its present form does not give an adequate explanation of the results. If the magnetic field changes the free electron density in bismuth some of the results may be explained in a general way.

IN 1886 Nernst and Ettingshausen[1] discovered that if a copper-bismuth thermocouple were put in a magnetic field, the e.m.f. of the couple was changed. In their experiments the magnetic field was perpendicular to the direction of heat flow. They concluded that the effect varied with the square of the magnetic field strength and with the temperature, but was independent of the dimensions of the bismuth. Other investigators[2] have found that the effect exists for other orientations of the magnetic field, but that the magnitude of the effect depends on the direction of the field; that[3] if a single crystal is used, the magnitude of the effect depends also on the orientation of the crystalline axis.

The intimate connection between the thermoelectric power, thermal conductivity, and electrical conductivity (all three being supposed to depend on free electron concentrations) suggests that a study of their changes in a magnetic field and the relation between these changes and the position of the crystalline axis might add materially to the knowledge of the nature of galvanomagnetic and thermomagnetic effects. This paper contains an account of such a study with single crystals of pure bismuth.

APPARATUS AND METHOD

The method used was in general as follows:—an electric current sent through the crystal cools one junction and heats the other by the Peltier

[1] Nernst and Ettingshausen, Wied. Ann. **29**, 343 (1886).
[2] Hall and Campbell, Proc. Am. Acad. **46**, 625 (1911); A. W. Smith, Phys. Rev. **2**, 383 (1913); Lownds, Ann. d. Physik **4**, 776 (1901).
[3] C. W. Heaps, Phys. Rev. **31**, 648 (1928).

effect. This current is broken and a very short time afterwards the crystal is connected to a potentiometer which is set to balance the thermal e.m.f. produced by the temperature difference at the junctions. This same experiment is repeated when the crystal is in a magnetic field. It is then possible to calculate the fractional change of the thermoelectric power produced in the crystal by the field. This general method was first used by la Rosa.[4] He did not, however, make a necessary correction for a possible effect of the field on the thermal conductivity.

The arrangement of the apparatus is shown in Fig. 1. A single crystal of bismuth was immersed in oil between the poles of a large Weiss water-cooled electromagnet. The electromagnet could be rotated so as to vary the direction of the magnetic field. The crystal was soldered to copper wires with Wood's metal. Two Burgess vacuum relays were connected to these wires.

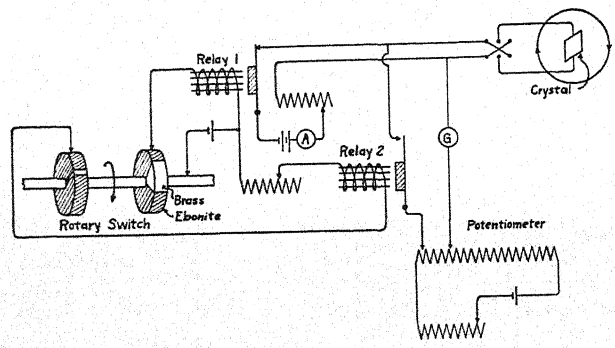


Fig. 1. Arrangement of apparatus for measuring change of thermoelectric power and thermal conductivity in a magnetic field.

The relays were operated by a rotary switch running at constant speed. They were so arranged that both were never closed at the same time. From Fig. 1 it is seen that relay 1 controlled the current through the crystal, and relay 2 connected the crystal across the potentiometer. The galvanometer used with the potentiometer, of the astatic moving magnet type, was adjusted to a sensitivity of about 300 mm per microvolt.

In the position shown the rotary switch allows a current i to pass through the crystal. This current, because of the Peltier effect, produces a temperature difference between the junctions on the crystal. Rotating the rotary switch cuts off this current by operating relay 1. At an adjustable time t later, by operating relay 2, the rotary switch connects the crystal to the potentiometer for a very short time. Farther rotation turns on the current i, and the cycle is repeated in the next revolution of the rotary switch. If the potentiometer is not adjusted to the e.m.f. of the crystal, the galvanometer will be deflected once during each cycle. By adjusting the potentiometer till the galvanometer is not deflected, the thermal e.m.f. in the crystal circuit could be measured. The rotary switch was arranged so that the e.m.f.'s E_1 and E_2

[4] La Rosa, Nuovo Cim. **18**, 26 (1919).

at two times t_1 and t_2 after the current was cut off could be determined. E_1 and E_2 were determined with and without the magnetic field. The apparatus was capable of measuring an e.m.f. to a tenth of a microvolt; but variable stray thermal and contact e.m.f.'s make the accuracy of observation somewhat less than this.

Theory of the Method

The heat generated at the hot junction, for example, raises the temperature of that junction, and is then conducted partly through the crystal to the cold junction and partly into the oil around the junction. If the electric current has been flowing long enough for the crystal junctions to reach an equilibrium temperature difference, the heat is conducted away as fast as it is liberated. If the heat conducted through the oil from one junction to the other be neglected, the heat conducted through the crystal will be equal to the Peltier heat liberated at the hot junction plus the difference between the Joule heats developed at the hot and cold junctions. Hence

$$i\pi + i^2(r_2 - r_1) = kBd\theta/dx \tag{1}$$

where i is the electric current, π the Peltier coefficient, r_1 and r_2 the resistances of the cold and hot junctions respectively, k the thermal conductivity, B a constant depending on the dimensions of the crystal, and $d\theta/dx$ the temperature gradient along the crystal. The term $i^2(r_2-r_1)$ is the difference between the Joule heats developed at the two junctions, which must be conducted through the crystal. Let $d\theta/dx=\Delta\theta/l$, l being the length of the crystal and $\Delta\theta$ the temperature difference between the junctions. In a magnetic field certain of these quantities will be changed. Denoting by a subscript H the values of these quantities in a magnetic field H, we have

$$i\pi_H + i^2(r_2 - r_1)_H = k_H B(\Delta\theta_H/l);$$

whence

$$\Delta\theta_H/\Delta\theta = k/k_H \frac{i\pi_H + i^2(r_2 - r_1)}{i\pi + i^2(r_2 - r_1)}. \tag{2}$$

When i is reversed the heat $i\pi$ is reversed in sign, but the heat $i^2(r_2-r_1)$ remains unchanged. It is thus possible by reversing i to estimate the magnitude of $i^2(r_2-r_1)/i\pi$. For example; E_1 was 76 microvolts; when the current was reversed E_1 was 84 microvolts. Thus the Joule heats developed at the two junctions contributed 4 microvolts to the observed e.m.f. In every case experiments gave $i^2(r_2-r_1)/i\pi$ less than 0.1. Thus to a good approximation

$$\Delta\theta_H/\Delta\theta = (k/k_H)(\pi_H/\pi). \tag{3}$$

Substituting $E=P\Delta\theta$ and $P=\pi/\theta$, where E is the e.m.f. of the crystal thermocouple and P its thermoelectric power, we get

$$\frac{E_H}{E} = \frac{P_H}{P}\frac{\Delta\theta_H}{\Delta\theta} = \frac{P_H}{P}\frac{k}{k_H}\frac{\pi_H}{\pi} = \frac{P_H^2}{P^2}\frac{k}{k_H}. \tag{4}$$

Putting $\Delta E = E_H - E$ and $\Delta k = k_H - k$ this relation gives

$$\Delta P/P = (1 + (\Delta E/E)_0 + \Delta k/k + (\Delta E/E)_0 \Delta k/k)^{1/2} - 1 \tag{5}$$

where $(\Delta E/E)_0$ is the value of $\Delta E/E$ at time $t=0$, immediately after the electric current is cut off, but before sufficient heat has been conducted away through the crystal to diminish $\Delta\theta$ appreciably. In order to calculate $\Delta P/P$ it is necessary to calculate $\Delta k/k$ and $(\Delta E/E)_0$.

Determination of $\Delta k/k$.

To determine $\Delta k/k$ we utilize the fact that $\Delta\theta$ is decreased after the electric current is stopped by conduction of heat through the crystal. Let $d/dt(\Delta\theta) = -Ak\Delta\theta$, A being a constant. This equation gives $\log(\Delta\theta/\Delta\theta_0) = -Akt$, where $\Delta\theta_0$ is the value of $\Delta\theta$ when $t=0$. Since $E/E_0 = \Delta\theta/\Delta\theta_0$, we have $\log(E/E_0) = -Akt$. It is impossible to observe E_0 experimentally. However, let E_1 and E_2 be the values of E at times t_1 and t_0 respectively. Then

$$\log(E_2/E_1) = -Ak(t_2 - t_1);\ \log(E_2/E_1)_H = -Ak_H(t_2 - t_1), \tag{6}$$

the H subscripts again denoting values obtained in a magnetic field. Dividing the second of these equations by the first and setting $\Delta k = k_H - k$ gives

$$\Delta k/k = \frac{\log(E_2/E_1)_H}{\log(E_2/E_1)} - 1. \tag{7}$$

Determination of $(\Delta E/E)_0$.

To determine $(\Delta E/E)_0$ we combine the two equations $\log(E_1/E_0)_H = -Ak_Ht_1$ and $\log(E_1/E_0) = -Akt_1$, getting

$$E_{0H}/E_0 = E_{1H}/E_1 e^{A(k_H - k)t_1} = E_{1H}/E_1 e^{Ak\Delta k/kt_1}. \tag{8}$$

A similar relation holds for t_2, which combined with (8) gives

$$(1/t_2 - 1/t_2)\log(E_{0H}/E_0) = 1/t_1 \log(E_{1H}/E_1) - 1/t_2 \log(E_{2H}/E_2). \tag{9}$$

This relation gives $(\Delta E/E)_0$, since $E_{0H}/E_0 = (\Delta E/E)_0 + 1$.

Thermal equilibrium must be reached in the crystal before the electric current is stopped if Eq. (1) is to apply. This condition was satisfied by increasing the time during which i flowed till further increase did not increase the values of the e.m.f.'s obtained. This made the time of one revolution of the rotary switch about 5 seconds. Then the e.m.f.'s were observed to be proportional to the current, as would be expected from equation (1) if the Joule heat be neglected. It was estimated from the magnitude of the observed e.m.f.'s that $\Delta\theta$ was about 1°C. P, π, and perhaps k are functions of the temperature, but it was assumed that the temperature changes during an experiment are so small that these quantities can be regarded as constant. A few observations were made with different currents; but within the limits of experimental error $\Delta E/E$, $\Delta k/k$, and $\Delta P/P$ were found independent of i.

With the direction of heat flow perpendicular to the crystalline axis and with a magnetic field of 8000 gauss perpendicular to both the crystalline axis and the heat flow, it was found that $E_1=85.0$ microvolts, $E_2=58.0$ microvolts, $E_{1H}=61.8$ microvolts, and $E_{2H}=45.3$ microvolts. If these values be substituted in Eq. (7), it is found that $\Delta k/k=-0.190$. From Eq. (9), with $t_1=0.129$ sec. and $t_2=0.662$ sec., it is found that $(\Delta E/E)_0=-0.285$. The variation of $\Delta E/E$ with the time is clearly seen here, since $(\Delta E/E)_{t_1}=-0.273$ and $(\Delta E/E)_{t_2}=-0.219$. If the above values be substituted in Eq. (5), $\Delta P/P=-0.245$ is obtained. These values are plotted in Figs. 4 and 6.

RESULTS

It was found much easier to determine accurately $\Delta E/E$ than $\Delta k/k$, since $\Delta k/k$ is calculated from the ratio of the logs of two quantities differing little from unity. Since the rate of cooling of the crystal couple depended on the physical dimensions of the crystal, it was found desirable for the crystal to have a cross-sectional area of about 1 mm^2; hence it was necessary to use two different specimens in order to secure all the desired orientations with

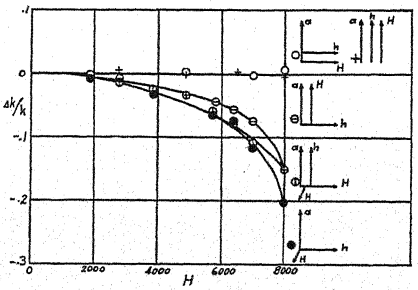


Fig. 2. Fractional change of thermal conductivity as a function of magnetic field strength.

respect to the crystalline axis. Both crystals were grown from the same very pure bismuth, supplied by Eimer and Amend. The direction of the crystalline axis was determined by observing reflections from cleavage planes by Bridgman's[5] method. The three-dimensional direction diagrams accompanying all the curves show the angles between the crystal axis a, the heat flow h, and the magnetic field H. The data for h parallel to a were obtained with one crystal, for h perpendicular to a with the other crystal.

The fractional changes in the thermal conductivity as a function of the magnetic field strength for several different orientations of the crystal axis a, heat flow h, and magnetic field H are shown in Fig. 2. It is of interest to note that the longitudinal effect, in which h is parallel to H (see the two top direction diagrams) is too small to measure.

It was found that when h was along a and H was perpendicular to both a and h, a rotation of H in this normal plane made no difference in the magnitude of the observed effects. This fact is indicated in the direction diagrams next to the bottom by showing H in two positions. The differences between

[5] Bridgman, Proc. Am. Acad. 60, 305 (1905).

the curves for the cases in which the effect is measurable are about the same as the magnitude of the errors of observation. The values at 8000 gauss, however, are averages of several sets of observations, and it is believed that they show a real effect of the orientation of a on the value of $\Delta k/k$. In general it appears that the orientation of H with respect to the heat flow is of considerably greater importance than the orientation of H with respect to the crystal axis.

So far as is known to the author $\Delta k/k$ has not been measured before for a single crystal. If a bismuth plate consists of small crystals randomly oriented, the magnitude of the transverse effect should be the same as that shown here for the transverse orientations, (H perpendicular to h) which are approximately equal. The mean of two such values obtained for polycrystalline bismuth plates by Leduc[6] and Van Everdingen[7] at 6000 gauss is -0.0575. The mean of the values shown in Fig. 2 for this field is -0.056. The agreement is very good.

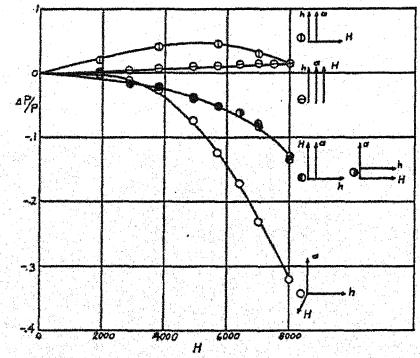


Fig. 3. Fractional change of thermoelectric power as a function of magnetic field strength.

As has been indicated, the fractional change in the thermoelectric power of the crystal couple can be calculated from the same four observations that gave $\Delta k/k$. The results obtained in this way are shown in Fig. 3. A similar set of results has been obtained by C. W. Heaps, who obtained $\Delta P/P$ by a more direct method. For h parallel to a, and H perpendicular to both a and h, his curve is almost a straight line rising to a value of 0.08 at 8000 gauss. The corresponding curve in Fig. 3 agrees with this up to about 4000 gauss. The lack of agreement between his curve and the one given here is probably due to a small angle between a and h, which would introduce components of all the negative values of $\Delta P/P$ shown in Fig. 3. A lack of uniformity in the evolution of heat over the ends of the relatively short crystals would result in a heat flow not strictly along the length of the crystal, which in this case was along a. Obviously a very small departure from parallelism of a and h would suffice to produce an appreciable decrease in the value of $\Delta P/P$. For the other curves of Fig. 3 the agreement with those of Heaps is as good as one might

[6] Leduc, Compt. Rend. 104, 783 (1887).
[7] Van Everdingen, Jour. de Physique (3) 10, 217 (1901).

expect, considering the difficulty of exact adjustment and the impossibility of securing crystals without flaws.

$\Delta P/P$ was observed to be a function of the temperature, but observations were only made between 18°C and 40°C. The results for $\Delta P/P$ are in general agreement with the experiments of A. W. Smith,[2] showing a decrease of $\Delta P/P$ with increasing temperature. The values of $\Delta P/P$, $\Delta k/k$, and the fractional changes of electrical conductivity given in this paper were all taken at 25°C.

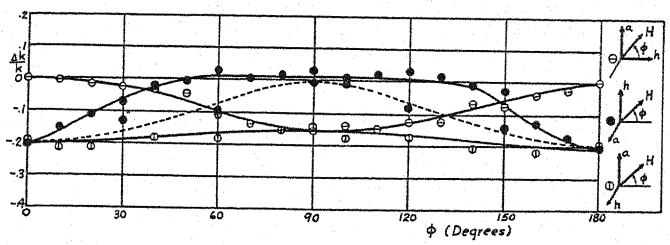


Fig. 4. Fractional change of thermal conductivity as a function of the varying angle ϕ shown in the three-dimensional direction diagrams.

Fig. 4 shows the effect on $\Delta k/k$ of rotating a constant magnetic field of 8000 gauss about h as an axis, about a as an axis, and about an axis perpendicular to both a and h. Maxima and minima are found where they would be expected from the curves of Fig. 2. The flat maximum of the curve with H perpendicular to a seemed peculiar, so the curve was repeated with another crystal and improved apparatus. All values obtained were negative; these results are shown by the dotted curve in Fig. 4. These last results are considered much more dependable than the first obtained. Hence no significance

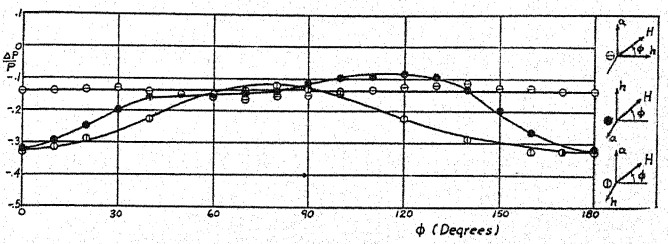


Fig. 5. Fractional changes in thermoelectric power as a function of the varying angle ϕ shown in the three-dimensional direction diagrams.

is to be attached to the small positive values of $\Delta k/k$ for the solid curve in Fig. 4, nor to the wide range through which they were obtained.

The values of $\Delta P/P$ were calculated from the data giving $\Delta k/k$ in Fig. 4. The results are shown in Fig. 5. For one direction of rotation the points fall approximately along a straight line. The outstanding feature of the other two curves is their lack of symmetry about 0° or 90°. The maxima and minima do not occur in the transverse or longitudinal positions, and one of the curves is not symmetrical about its maximum or minimum. It was found that

changing the direction of the magnetic field by 180° did not alter the magnitude of any of the effects observed, so all of these curves are repeated in the next 180°.

The curve through the black points was repeated with another crystal. The values of E_{0t_1}, E_{Ht_1}, and $\Delta P/P$ obtained are shown in the polar chart of Fig. 6. The variation in $\Delta P/P$ is not as large as that in Fig. 5, but the curve in Fig. 6 giving $\Delta P/P$ has the same general features as the corresponding one in Fig. 5.

Bismuth crystallizes in the dihexagonal alternating class of the hexagonal system. The plane of easy cleavage is parallel to the (111) planes and is per-

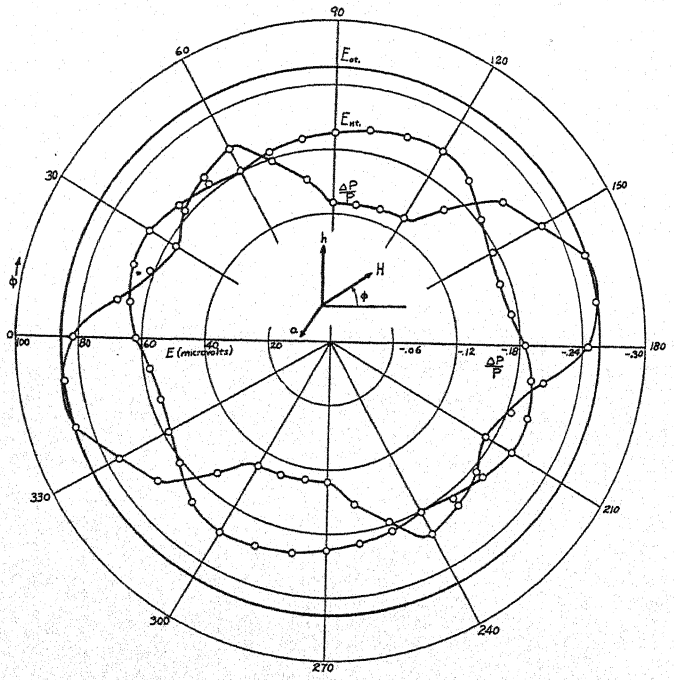


Fig. 6. Polar chart showing E_{ot_1}, E_{Ht_1}, and $\Delta P/P$ as a function of the varying angle 0 shown in the three-dimensional direction diagram.

pendicular to the trigonal axis. There is also fair cleavage parallel to the $(11\bar{1})$ planes. The crystal used to obtain Fig. 6 was found to have the magnetic field along the $(11\bar{1})$ planes as well as along the (111) planes at 165°. A maximum in $\Delta P/P$ occurs here. The $(1\bar{1}1)$ and $(\bar{1}11)$ planes intersect the (111) plane so that one is parallel to H at 105°, and the other at 45°. There is in Fig. 6 a minimum of $\Delta P/P$ at 105, but there is no similar feature at 45.

It appears from these considerations that the $\Delta P/P$ curve in Fig. 6 is not symmetrical about 0° or 90° because there are structure factors in the crystal which produce a distortion. The plane perpendicular to the crystal axis can thus not be considered as possessing circular symmetry about a. The separation in this plane of the two effects—namely, the structure effect and the

effect due to the direction of h with respect to H—appears to be impossible without a much more detailed investigation.

The fractional changes produced by the magnetic field in the electrical conductivity are shown as $\Delta c/c$ in Fig. 7. These results were obtained by soldering two more copper wires to the crystal where the current leads were soldered on, and by measuring with a potentiometer the potential drop V along the crystal. The current being held constant, the change ΔV produced in V by the field was determined, whence $\Delta c/c$ could be calculated. It was found that the temperature difference caused by the Peltier effect produced an appreciable error in these results; but since E_0 and $(\Delta E/E)_0$ could be calculated, the necessary correction could be applied.

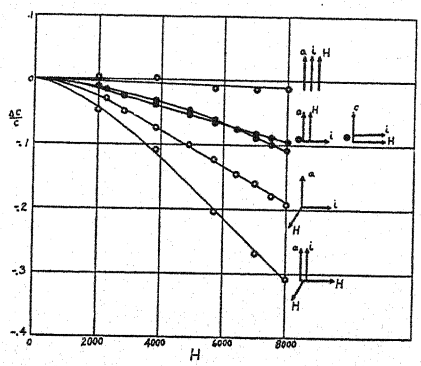


Fig. 7. Fractional changes of electrical conductivity as a function of magnetic field strength. Electric current direction is indicated by i, crystal axis by a, and magnetic field by H.

This effect is well known, and has been extensively investigated for polycrystalline bismuth. Lownds[8] gives two values of $\Delta c/c$ for a single crystal with different orientations in a magnetic field, and Borelius and Lindh[9] give several values which can be compared with the values of $\Delta c/c$ shown in Fig. 7. Their values were obtained at an average temperature of 18°C. The comparisons are made in Table I. The values given by Lownds, and by

TABLE I. *Values of $\Delta c/c$. Comparison with the results of others.*

Orientation	i ↑ a, H	a, H, i	a ↑ H, i	a, i, H	a ↑ i ↑ H	i ↑ a, H
Field H (gauss)	5000	5000	2300	2300	2300	2300
Lownds	-0.198	-0.143	----	----	----	----
Borelius & Lindh	-----	-----	-0.039	-0.053	-0.026	-0.065
Banta	-0.160	-0.103	-0.015	-0.015	-0.004	-0.055

Borelius and Lindh, are larger than the corresponding values found by the present experiments. Part of these differences can be explained as a tempera-

[8] Lownds, Ann. d. Physik (4) 9, 677 (1902).
[9] Borelius and Lindh, Ann. d. Physik (4) 53, 97 (1917).

ture difference, since Drude and Nernst[10] found that $\Delta c/c$ decreased rapidly with increasing temperature. As before, some of the differences may be due to imperfections in the crystals.

Conclusions

The results reported here are difficult to fit into any simple theory. There is at present no theory of electrons in metals which adequately accounts for all of the observed facts of thermoelectricity in crystals. Any theoretical result for $\Delta c/c$, $\Delta k/k$, or $\Delta P/P$ should be an even function of H, since the direction of H can be changed by 180° without affecting the magnitude of any of these quantities. Such a result has been obtained for $\Delta c/c$ with transverse fields by Sommerfeld[11] and Frank,[12] who get $\Delta c/c = -BH^2/(1+CH^2)$, B and C being positive constants. In obtaining this expression it is assumed that the magnetic field does not change the density of free electrons in the metal, but does disturb the distribution function. This equation has been found to fit the experimental results very well for ordinary polycrystalline metals. It is not, however, so successful in dealing with bismuth, which in many respects is abnormal; and it cannot be expected, in the form derived, to account for the important effect of crystalline structure. It might be expected that $\Delta c/c$ and $\Delta k/k$ would have their smallest values for H parallel to h and i respectively, since then the electron flow is along H. In general, this seems to be true. While the direction of the crystalline axis with respect to H or h is relatively unimportant for $\Delta k/k$, it is of decided importance for $\Delta c/c$.

Sommerfeld and Frank state that in the adiabatic case their calculations indicate that $\Delta k/k$ is only about two percent of $\Delta c/c$. Thus bismuth apparently has a much larger $\Delta k/k$ than can be accounted for by the Sommerfeld theory.

There is no satisfactory theory to account for the change in thermoelectric power in a magnetic field. If the classical result[13] $Pe = R \log (n_1/n_2)$ is assumed to hold approximately, then the only way to account for the change in P is to suppose that the density n of free electrons in bismuth is changed by the magnetic field. Possibly this change is indicated by the divergence of $\Delta c/c$ and $\Delta k/k$ from the values predicted by Sommerfeld's theory, which does not allow for a change of n. Suppose then that n_1 is the electron density in bismuth, and n_2 the electron density in copper. Then, since copper is a normal conductor and does not have its thermal e.m.f. affected by a magnetic field, $P_H e = R \log (n_{1H}/n_2)$.

Thus

$$P_H/P = \log (n_{1H}/n_2)/\log (n_1/n_2).$$

Let

$$n_{1H} = n_1 + \Delta n_1.$$

[10] Drude and Nernst, Wied. Ann. **42**, 568 (1891).
[11] Sommerfeld, Zeits. f. Physik **47**, 1 (1928).
[12] Sommerfeld and Frank, Rev. Mod. Phys. **3**, 1 (1931).
[13] O. W. Richardon, Electron Theory of Matter, p. 461.

Then

$$P_H/P = \frac{\log (1 + \Delta n_1/n_1) + \log (n_1/n_2)}{\log (n_1/n_2)}$$

$$= 1 + A \log (1 + \Delta n_1/n_1). \tag{10}$$

So $\Delta P/P = A \log (1+\Delta n_1/n_1)$, where $A = 1/\log (n_1/n_2)$.

From the curves of Fig. 3, Δn_1 is seen to be a function of both the magnetic field strength and the direction in the crystal. If we suppose that n_2 is greater than n_1 which seems a reasonable assumption in view of the relative electrical conductivities of the two metals, then A is negative. So, again from Fig. 3, Δn_1 is positive for three orientations of a, h, and H in the crystal, and negative for two orientations. The largest change in n_1 is for a, h, and H mutually perpendicular, and is an increase.

Classical electron theory[14] indicates that $k = Dn\lambda$ and $c = En\lambda$, λ being the mean free path of the electrons and D and E being constant at a given temperature.[15] It seems possible that a magnetic field, in addition to affecting n, may produce changes of molecular configuration which would alter λ. Changes of λ produced in this way would be distinct from any changes produced by such effects as curving of the free paths in the magnetic field, etc. Thus

$$\Delta c/c = \Delta n/n + \Delta\lambda/\lambda$$

and

$$\Delta k/k = \Delta n/n + \Delta\lambda/\lambda.$$

So $\Delta c/c = \Delta k/k$. According to Sommerfeld's theory, $\Delta k/k$ is only a small fraction of $\Delta c/c$. Thus the above result is more nearly in agreement with experiment than is Sommerfeld's theory. If it be assumed that the change in electrical conductivity c is due to a change in n and λ of the character indicated above, with the change predicted by Sommerfeld's theory in addition, then $\Delta c/c = \Delta n/n + \Delta\lambda/\lambda - BH^2/(1+CH^2)$. Since $\Delta k/k$ is very small according to Sommerfeld's theory, the whole effect may be given by $\Delta k/k = \Delta n/\lambda + \Delta\lambda/\lambda$.

Thus

$$\Delta c/c = \Delta k/k - BH^2/(1 + CH^2). \tag{11}$$

The experimental results indicate that this result is hardly satisfactory. According to Sommerfeld B is a positive constant; but if Eq. (11) is true, B must be negative for one orientation: namely, with H along a, and i and h respectively perpendicular to a. For these curves in Figs. 2 and 7, $\Delta k/k$ is less than $\Delta c/c$ at 8000 gauss. Another objection is based on the shape of the curves: it is hard to see how the addition of a square function of H to the curves of Fig. 2 could give the curves of Fig. 7. Also, the result of the theory of Sommerfeld and Frank is supposed to hold for transverse fields, and the quantity $BH^2/(1+CH^2)$ is thus zero for longitudinal fields—a result con-

[14] O. W. Richardson, Electron Theory of Matter, pp. 410–421.

[15] If Sommerfeld's formulae are used instead of the classical ones the results deduced are not essentially different from these above.

tradicted by these experimental results, although the longitudinal values of $\Delta k/k$ and $\Delta c/c$ are in general the smallest obtained.

Consideration of the results leads to the following conclusions: Theory indicates that $\Delta c/c$ should be negative for transverse fields. It is found negative, but the value is found to be dependent on the orientation of the crystalline axis with respect to the current and the magnetic field. The curves of Figs. 2 and 4 appear to indicate that there is some unrecognized but essential difference between the mechanisms of heat conduction and electric conduction in bismuth crystals. This conclusion is indicated by the fact that the $\Delta c/c$ curves are strongly influenced by crystal structure; the $\Delta k/k$ curves, on the other hand, appear to be roughly all the same for all cases where H is perpendicular to h. When H is parallel to h there is no measurable effect produced in $\Delta k/k$. There is some evidence that strong magnetic fields change the density of free electrons in the bismuth crystals.

The crystals used in this investigation were supplied by Professor C. W. Heaps, to whom the author is indebted for much valuable assistance and discussion. It is also a pleasure to thank Professor H. A. Wilson for generous advice on this problem.

Does Nickel Show a Positive Elongation in the Joule Magnetostrictive Effect?

By S. R. WILLIAMS
Fayerweather Laboratory of Physics, Amherst, Massachusetts

(Received June 4, 1932)

The question as to whether there is a positive Joule magnetostrictive effect in nickel has once more arisen. The following note points out that there is no positive elongation unless remanent magnetism or an extraneous field is present to give the sample of nickel a preliminary magnetization before the main field is applied. Even then, there is no positive elongation unless the preliminary magnetization is opposed to that of the main field.

THE above question seems to have cycles of recurrence. Not always does it take the form of the caption. In 1893–1904, Honda and Shimizu[1] carried on an extensive discussion with Heydweiler[2] concerning the presence or absence of a Villari reversal effect in nickel. If the Villari reversal effect occurs in nickel, then a positive elongation of nickel should also be found in the Joule magnetostrictive effect. This relation between the Villari and Joule effect seems to be very definitely established.[3]

Recently two papers[4] have appeared purporting to show a positive elongation for the Joule magnetostrictive effect in nickel and saying that it is an effect to be expected.

It is desired to point out that this may be misleading as these two papers state definitely that in the regular Joule magnetostrictive effect they did not find a positive elongation. They found a positive elongation only when the magnetizing force was reversed in observing a hysteresis curve for the Joule magnetostrictive effect. A positive elongation in nickel occurs only when there is remanent magnetism present in the specimen or an extraneous field is imposed, and then *only when the magnetizing field is opposed in direction to the remanent magnetization or the extraneous field.*

In Fig. 1 are shown continuous records of the changes in length of a nickel rod as the magnetizing force is increased from zero up to 71.2 gausses. The vertical lines in the photographs denote certain currents' strengths in the magnetizing coil. All of the photographs in Fig. 1 show six vertical lines and represent field strengths of 0, 14.2, 28.5, 42.7, 56.9, and 71.2 gausses respec-

[1] Honda and Shimizu, Ann. d. Physik **14**, 791 (1904); Phys. Zeits. **5**, 254 (1904); Ann. d. Physik **15**, 855 (1904); Phys. Zeits. **5**, 631 (1904).

[2] Heydweiler, Sitzungsber. d. Wurzb. phys. med. Ges. **11** Marz (1893); Phil. Mag. **35**, 469 (1893); Beibl. **17**, 1095 (1893); Ann. d. Physik **52**, 462 (1894); **15**, 415 (1904); Phys. Zeits. **5**, 255 (1904).

[3] Thomson, Applications of Dynamics to Physics and Chemistry, pp. 48–63, 1888. Williams, Proc. A.S.T.M. **19**, Pt. 2 (1919); School Science, and Math. **22**, 859 (1922); Phys. Rev. **10**, 129 (1917); Jour. Franklin Institute **203**, 843 (1927).

[4] Dietsch, Zeits. f. techn. Physik **12**, 380 (1931). Kersten, Zeits. f. Physik **72**, 500 (1931).

tively. In Fig. 2 the maximum field strength was carried up to 413 gausses. The constant of the magnetizing coil was 142.4 gausses per ampere.

The magnetizing coil in these experiments stood in a vertical position. In *a* the vertical rod was demagnetized by a decreasing a.c. in the presence of the vertical component of the earth's magnetic field. This shakes the rod

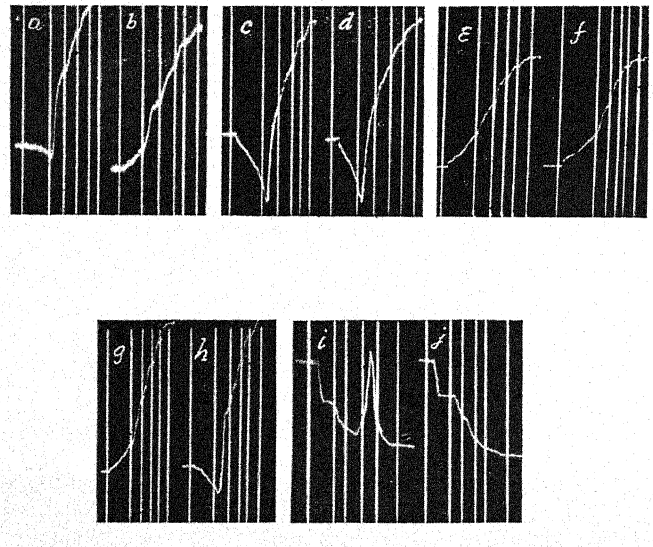


Fig. 1.

down and leaves it permanently magnetized in a direction with the north pole down. When the magnetizing field in the solenoid was applied to the rod, with the field of the solenoid directed upwards, a positive elongation occurred. In *b* the rod was again demagnetized, in the presence of the earth's magnetic field, but this time the magnetizing force in the solenoid had its

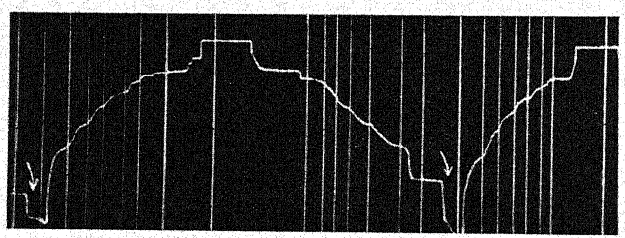


Fig. 2.

direction downwards. This time there is absolutely no positive extension of the rod.

In *c* and *d* no demagnetization occurs, but in both curves the magnetizing force is reversed to what it was in the preceding magnetization. The magnetizing force in both cases is opposed to the remanent magnetism of the nickel rod. This is the effect observed by Dietsch and theoretically discussed

by Kerstens. If no demagnetization occurs and the magnetizing force is applied each time in the same direction as the remanent magnetism of the nickel rods, then no positive elongation occurs. This is illustrated by the curves *e* and *f*, Fig. 1.

By means of a second coil surrounding the main magnetizing coil, one may apply an extraneous field and leave it on while the rod is being magnetized by the main coil. *g* and *h* show what occurs when the rod is demagnetized in the presence of this field and then the main magnetizing force is applied. This extraneous field had a value about three times as great as the vertical component of the earth's magnetic field. In *g* it will be observed that no positive elongation occurs since the main magnetizing force is in the same direction as the extraneous field. A positive elongation in the presence of this extra field occurs only when the main magnetizing force is opposed to the added field. This is shown in *h*, Fig. 1. It will be noted that the positive elongation in *h* is greater than in *a*.

One may apply any magnitude of extraneous field he chooses, and introduce it at any value of the main field desired and so get any form of curve one may select for the Joule magnetostrictive effect in nickel. In *i* and *j* are shown the queer changes in length which can be obtained for iron if one applies extraneous fields. In *i* there is an elongation then a shortening followed by a second elongation, while in *j* the change in length is wholly an elongation.

In Fig. 2 is shown a hysteresis curve of the Joule magnetostrictive effect in nickel. It is one continuous run in which the two points of positive elongation are indicated by arrows. These are the so-called positive elongations found by Dietsch and are of the same type of elongation as shown in *c* and *d*, Fig. 1. In the true sense of the word they are not positive elongations. Thus far we have no positive indications to show that either the Villari reversal effect or the Joule positive elongation occurs in nickel.

Particular attention is called to Fig. 2 to show how well the temperature changes are controlled. If temperature were affecting the length then the horizontal portions of the curve would not be parallel to the edge of the photographic film, but would be tilted up or down as the film progressed past the slit in the camera.

The inference has been made in a number of papers that the capacity-beat method is the only method by which these positive elongations may be detected. This inference is to be challenged. The mechanical-optical device with which the curves in Figs. 1 and 2 were made fifteen years ago did not begin to approach the limit to which it could have been pushed and yet it shows this positive elongation very plainly. Furthermore, since these photographs were made, a greatly improved extensometer has been constructed and will be described in a subsequent paper. The ability to secure a continuous record of the changes in length is a very desirable feature of any extensometer.

LETTERS TO THE EDITOR

Prompt publication of brief reports of important discoveries in physics may be secured by addressing them to this department. Closing dates for this department are, for the first issue of the month, the twenty-eighth of the preceding month; for the second issue, the thirteenth of the month. The Board of Editors does not hold itself responsible for the opinions expressed by the correspondents.

Electronic Structure of the a-X Band System of N_2

By using a powerful discharge in pure nitrogen it has been found possible to photograph certain bands belonging to this system[1] in the first order of a twenty-one foot Rowland grating. The nitrogen was prepared from prebaked sodium azide, and was allowed to stream through the discharge tube during the progress of a 48 hour exposure. Copper lines served as wave-length standards[2] and the very faint bands were measured using a cylindrical lens so as to eliminate the effect of plate grain. Every line was measured about twenty times in order to minimize error. The bands λλ2006.01 (3–11), 2023.48 (4–12), 2041.16 (5–13), 2059.04 (6–14), 2125.92 (5–14), 2143.95 (6–15), 2162.27 (7–16) were visible on the plates but only λ2041.16 and λ2125.92 were sufficiently developed to allow of measuring the branches.

The system is almost certainly a singlet transition to the ground state $^1\Sigma_g^+$ of nitrogen for it is the only strong system yet observed in absorption.[3] Accepting this idea, the experimental results are to be explained by the assumption that it is a $^1\Pi_u - ^1\Sigma_g^+$ transition. All the bands show in addition to the head measured by Hopfield and Birge a faint second head displaced towards longer wave-lengths by about 13 cm^{-1} though only sharp and clear in the case of λ2125.92 which is the best exposed band. In other bands it can however be made quite distinct by enlargement on contrasty film and subsequent superposition of the enlargements[4] so as to enhance the photographic contrast. It is natural to account for this as a Q head. Unfortunately, the resolving power is too small to allow one to measure the branches in the neighborhood of the head, and where the series are resolved, (at about the twentieth member of the Q branch) the R branch is so faint that it occurs only as a few stray lines very difficult to measure. A provisional analysis from the Q and P branches of (5–13) and (5–14) gives $B_5' = 1.5207 \pm 0.001\ cm^{-1}$, $B_{13}'' = 1.7625 \pm 0.001\ cm^{-1}$ and $B_{14}'' = 1.7424 \pm 0.003\ cm^{-1}$, neglecting the contribution due to Λ-doubling which must be very small, since the stray R lines lie in their predicted positions as far as the can be measured. This assignment of constants accounts for the positions of all measured lines and heads to within experimental error, and, by using an estimated effective temperature, for their intensity also. One may say therefore with some confidence that this system is indeed a $^1\Pi_u - ^1\Sigma_g^+$ transition.

To account for the existence of a $^1\Pi_u$ level in this position seems very difficult, as Mulliken,[5] has pointed out. If we assume with Hund[6] that it has the electronic structure $\sigma_u^2 2s\sigma_u^4 2p\sigma_g 2p\pi_u 3p$ then the $\pi_u 3p$ electron should be strongly bonding in character since it has descended from the high energy atomic orbit $3p$. This, experimentally, appears not to be the case.

Two other bands with heads at λ2033.6 and λ2112.1 also show on the plates. They are obscured by members of the a-X system but

[1] Birge and Hopfield, Astrophys. J. **68**, 257 (1928).

[2] Burns and Walters, Allegheny Observatory Vol. 8, No. 3. (Corrected by supplementary circular.)

[3] Hopfield (Phys. Rev. **31**, 1131, (1928)) has reported a progression of bands in absorption whose upper level lies below the 'a' level. This might be the $^3\Pi_u$ level corresponding to the $^1\Pi_u$ of this system; but the spacings of the vibrational levels appear unfavourable to this interpretation.

[4] Oldenberg, Zeits. f. Physik **58**, 722 (1929).

[5] Mulliken, Rev. Mod. Phys. **4**, 53 (1932).

[6] Hund, Zeits. f. Physik **63**, 749 (1930).

are strongly degraded to the violet; the best exposed shows strongly alternating intensities; hence it is certainly due to nitrogen or to ionized nitrogen. It has the appearance of a single branch whose spacing rapidly increases towards shorter wave-lengths. These bands appear not to have been observed before.

A more complete investigation of the a-X system is proposed in the near future using a large vacuum spectrograph.

E. T. S. APPLEYARD
Ryerson Physical Laboratory,
University of Chicago,
June 26, 1932.

Deposition of Chromium on Glass

R. Ritschl[1] has perfected a simple apparatus with which a uniform half-silvering can be done on Fabry-Perot interferometer plates. The film is put on by evaporation of silver from a hot tungsten filament in a vacuum; the silver having been tied to the tungsten with platinum.

The writer has extended this process to chromium, with an idea to its use for astronomical reflectors. As is well known, the present silver-on-glass surfaces tarnish quickly, and do not reflect a usable fraction of incident light beyond 3350A. To remedy this defect, other metals have been deposited by evaporation, but chromium seems to excel in reflectivity and permanence. The chromium was electroplated about a millimeter thick on a tungsten filament and was evaporated *in vacuo* very quickly. The resultant surface is firm, and can be dissolved only by HCl. The reflectivity of a test surface has been determined as: 60 percent at 4200A; 68 percent at 3450A; and 62 percent at 2900A. The adaptation of the process to large surfaces is now in progress.

ROBLEY C. WILLIAMS
Physical Laboratory
Cornell University,
June 27, 1932.

[1] *Half-Silvering Interferometer Plates*, Zeits. f. Physik **69**, 578–585 (1931).

Note on Molecular Structure

Hund[1] and Mulliken[2] in recent papers have considered the structure of polyatomic molecules, treating each electron as if it moved in a wave function which was a solution of a problem of many centers—a molecular orbital, as Mulliken happily names such a function. The writer[3] and Pauling[4] on the other hand have treated the same problem from a starting point in which each electron moves as in a single atom, or as Mulliken would say in an atomic orbital. It is the purpose of this note to point out the relation between the two methods. This has already been done to some extent in a paper on metallic cohesion;[5] there the method used by Hund and Mulliken has an analogue in the treatment of Sommerfeld and Bloch, whereas the other method, used by Pauling, the present writer, Heitler and London, resembles more closely Heisenberg's treatment of ferromagnetism. In that paper, the connections between the two methods were brought out, and it was shown that if treated in the proper way both methods necessarily led to the same answer, so that a choice between them must be made on the basis of convenience rather than correctness. Essentially the same situation holds in the molecular case.

A first simple calculation by either method will be incorrect, and it is necessary to go to a considerable refinement to secure good results. First we shall describe these refinements necessary in the method of Pauling and the writer. One can start by assuming covalent bonds, and taking these bonds to be located between definite pairs of atoms. Then the writer has shown how to set up wave functions, correctly taking account of antisymmetry and of spin, describing this situation. But now to improve this we must (1) take account of other possible ways of drawing the valence bonds. This can be considered in one way as the correct perturbation treatment for spin degeneracy. Or it can be considered as taking account of *shared valence*, a common phenomenon, and the one which Mulliken

[1] F. Hund, Zeits. f. Physik **73**, 1 (1931); **73**, 565; **74**, 1 (1932).
[2] R. S. Mulliken, Phys. Rev. **41**, 49 (1932). I am indebted to Professor Mulliken for sending me a copy of the latter paper before publication.
[3] J. C. Slater, Phys. Rev. **38**, 1109 (1931).
[4] Linus Pauling, Journ. Am. Chem. Soc. **53**, 1367 (1931).
[5] J. C. Slater, Phys. Rev. **35**, 509 (1930).

evidently has in mind when he does not wish his molecular orbitals to indicate bonds definitely between pairs of atoms, but to have them more diffused. In a metal, this phenomenon is of major importance, as the writer showed in the paper above quoted. It is also of major importance in the study of chemical reactions, as Eyring and others[6] have pointed out. (2) We must take into account the various possible ionic states. The importance of this step has been emphasized both by Pauling and by the writer; many structures are just intermediate between the covalent and the ionic cases, and without considering both it is not possible to get accurate results. Both these corrections (1) and (2) are to be made by setting up separate wave functions describing the various possible structures, computing the matrix of the energy with respect to them, solving the resulting secular equation, and using the resulting coefficients, making the best combination of the various wave functions to describe the resulting state.

To get a correspondingly accurate result with the method of Mulliken and Hund, we first set up the molecular orbitals, and assign electrons to the suitable orbitals. This is essentially as far as Mulliken and Hund go. But then we must set up antisymmetric combinations, taking account of spin. We must ordinarily consider several such assignments of electrons, taking into account some antibonding orbitals, and must solve the secular problem between these, finally resulting in the correct function as a linear combination. It should be pointed out that this process is particularly necessary if one is to get correct results at large distances of separation, which is very important in considering energies of dissociation of the various bonds. When this is done, as shown by an extension of the method used in the paper on metals, the results are essentially the same by either method.

There is one respect in which the method of Pauling and the writer can be made definitely better than that of Mulliken and Hund, when carried to the point described. It takes definite account of the ionic states. Hence it can use as the wave function for these states a wave function in which shielding of one electron by another is properly taken into account. The method of Mulliken and Hund, however, treats the ionic state rather as the accidental overlapping of electrons in molecular orbitals, resulting in fluctuations of electron density with an increase or decrease of the charge on an atom, with respect to the mean charge. Thus it cannot separate the ionic from the covalent cases, and cannot take account of the variation of shielding from one state to the other. On account of these ionic terms, the method of Pauling and the writer really contains, in its final wave function, a dependence of the wave function on the relative coordinates of the electrons, and it is well known that this is essential for a satisfactory representation of the correct wave functions, and is definitely lacking both in the treatment of atomic structure by the conventional method, and in the corresponding method of Mulliken and Hund as applied to molecules. This advantage of the method was not brought out in the paper on metals quoted above.

Aside from the point just mentioned, the two schemes are equivalent. We then discuss their relative merits from the standpoint of convenience. For a qualitative discussion, in which the calculations are not carried to the point just described, but are rather broken off at the earliest possible point, the writer believes the method of Mulliken and Hund to be at least as valuable as the one which he and Pauling have used. The best procedure, and one which he is accustomed to follow, seems to be to carry through a discussion of a problem qualitatively by both methods, checking them against each other to find their real relationship. For instance, in discussing a metal, even if using the method of atomic orbitals, no one would think of not comparing with the method of Sommerfeld and Bloch constantly, for better orientation and understanding of the problem if for no other reason. On the other hand, even for qualitative discussion, the method of the writer and of Pauling seems to have some advantages in that the various separate effects, as valence bonds between different pairs of atoms, states which are partly covalent and partly ionic etc., seem to have some physical significance, and it seems worth while to bring them explicitly into the picture. Further, the method of Pauling and the writer is more convenient for considering the limiting case of infinite atomic separation.

[6] Eyring and Polanyi, Zeits. f. Physik Chem. **B12**, 279 (1931); forthcoming papers by Eyring in J. Am. Chem. Soc.

When it comes to numerical application of the methods, the situation is somewhat altered. The writer has seen no general mathematical method of treating the molecular orbitals which does not rest on writing them as combinations of atomic orbitals. It goes without saying that the atomic orbitals are not to be taken as the same as electronic orbits in single atoms, but are to depend on the molecular structure. The recent calculation of Rosen[7] on H_2 is an excellent illustration of this; he allowed his atomic orbitals both to change scale, and to be polarized, in the presence of the other atom, and similar changes should surely be made in general. But when that is done, the calculation reduces to one in which atomic orbitals are used, in any case. Thus one can reduce either method, if carried through in detail, to the same integrals, and it is unimportant which scheme is used. The writer has been more inclined to use the atomic orbitals from the beginning, for the reason that it seemed an unnecessary waste to build these up into molecular orbitals, carry through a calculation in the manner of Mulliken and Hund, and eventually have to break up again into atomic orbitals for the calculation of the integrals. There are, however, important advantages which should be emphasized in the method of Mulliken and Hund, as far as numerical calculation goes. The advantage rests in the fact that the molecular orbitals are orthogonal to each other, while the atomic orbitals are not. The factors S, which come into the method of Heitler and London in the process of solving a secular equation between non-orthogonal states, come into the method of Mulliken and Hund in the process of normalization alone. For many purposes this is more convenient, and the writer is seriously of the opinion that this advantage, with complicated systems, may be a deciding factor in favor of the molecular orbital method; at least, it can well be used as a stage in the calculation.

In conclusion, it is the object of the present note to point out again that the method of Mulliken and Hund, and that of Pauling and the writer, are complementary, not antagonistic. The writer is quite sure that there are no facts explainable by the scheme of Mulliken and Hund which could not be equally well treated by his method, interpreting it in a suitable way. On the other hand, he would be the last to question the great power of the method of Mulliken and Hund, particularly for qualitative discussion, and welcomes the treatments of molecular structure which are being made by that method.

JOHN C. SLATER
Massachusetts Institute of Technology
Department of Physics,
June 28, 1932

[7] N. Rosen, Phys. Rev. **38**, 2099 (1931).

BOOK REVIEWS

Annual Tables of Constants and Numerical Data, Chemical, Physical, Biological and Technological—published under the authority of the International Research Council and the International Union of Pure and Applied Chemistry. Index for Volumes I to V (1910–1922)—Price $16.00 also Vol. VII—Years 1925–1926, inclusive; Part I, pp. i–xxxv, 1–946 (1930)—Price (including Part II); cloth $25.00—McGraw Hill Book Company, Inc. (New York).

Two extracts from Volume VII can be purchased separately: "Spectroscopy—Emission and Absorption Spectra, Electro and Magneto-Optics" (Numerical Data) by L. Bruninghaus, V. Henri and F. Wolfers. I Vol. 4-to, pp. xviii–514. Price: Cloth, Frs. 190; Paper, Frs. 170; "Electricity, Magnetism, Electrochemistry" (Numerical Data) by A. Buffat, G. Durand, G. Foex, R. L. Fortrat, N. Marinesco, N. Thon. I Vol. 4-to, pp. xviii–136. Price: Cloth, Frs. 90; Paper, Frs. 80. Publishers: Gauthier-Villars et Cie, 55, quai des Grand-Augustins, Paris 6°.

One should not attempt to use these tables without first consulting the directions given at the beginning of the volume. These are found to be very clear and explicit, so explicit that the uninitiated should have no trouble thereafter in using the tables. The newly adopted policy of stressing English so that little or no French is required will be helpful to a large group of American students.

The reviewer has found the General Index to Volumes I to V to be of considerable aid in the use of the tables. It contains three types of indexing which occupy space not in the order of their usefulness. First and most important is an Analytical Index of 38 pages in four languages. Without losing too much in conciseness it often offers somewhat more than a bare reference to volume and page. The arrangement of subjects is reasonable, the detail is sufficient, and there is some cross referencing. The wide range of subject matter covered by the Tables is brought out by a glance at this index. Then follows the Alphabetical Index of 63 pages. This gives references to those things treated in the Tables which are commonly known by name. When it is necessary, a German, English, or Italian name is listed with its French equivalent under which the references are listed. Thus—Dachshund s. Basset; Perch s. Perche; Perca v. Perche. The third index is the Formula Index—319 pages. It has an arbitrary but convenient arrangement described in the Introduction. Of course, most of this Index is devoted to organic compounds. References are given up to $C_{264}H_{176}$. At the end of each reference appropriate errata to Volume I to V are recorded. It is proposed that in addition a separate list of all errata and omissions be published. Only French is used in this part and the frequent occurrence of abbreviations makes it difficult to get along without recourse to the list of abbreviations at the beginning of the volume.

Volume VII of the Annual Tables contains the data for 1925–1926 with the exception of those data on Photography and Geophysics. Chapters on these subjects will not be published annually. The next issue to contain data on them will probably be Volume X. Two chapters appear for the first time—Explosives and Explosion in Gaseous Mixtures. The text accompanying the data is given in French and English. The English in the translation is quite satisfactory. The custom of including a bibliography of papers containing data not easily tabulated, and brief summaries of related qualitative or theoretical work is continued. These summaries often provide pleasant and sufficient substitutes for the original papers. Sometimes the assignment of space to these notices is a trifle extravagant. Thus on page 739 the same research of one author published in two places is listed under two separate headings and most of his data are given twice. Again on page 755 there are two headings for a single paper.

If the compilation is to appear four years after the data are published, the reader is entitled to a somewhat critical presentation. There is no apparent effort in this direction but on the other hand the committee promises to produce up to Volume IX (1929) (now published) and then to resume annual publication of the Tables. Such promptness should outweigh all considerations of criticism. But this is not to be taken to excuse the laxity, which, apparently

because the original author was careless, permits the recording of numerical data without indicating the units used. For example, on page 921 it is impossible to find whether Verdet's constant is given in terms of radians or degrees. While this would scarcely inconvenience a worker in the field, it is most baffling to students and most annoying to the instructor who is trying to teach them how to locate data.

Instead of attempting to describe in detail the important applications of these unique Tables or to emphasize the special features of Volume VII, Part I, which is here under review, it might be useful to remark that almost every page provides some interesting reading and as a practical primer for the study of foreign languages it is excellent. As a by-product one learns a great deal of physics and chemistry and gets a vivid panorama of the development of the exact sciences.

The importance and value of the Annual Tables becomes obvious to one who merely turns over the pages and perhaps another subscriber is made thereby. The committee in charge seems hesitant in advertising their prices. In general one has to make special inquiry by mail. The prices are, however, by no means exorbitant, although unfortunately high enough to keep the Tables out of the personal collections of the average student. Perhaps the cost in the future may be reduced as the committee has announced its intentions of lowering the price if the subscription list grows.

R. M. LANGER
University of Minnesota

The New Conceptions of Matter. By C. G. DARWIN. Pp. 224+xi. Figs. 46. The Macmillan Company, New York. 1931. Price $3.00.

Professor Darwin has undertaken, and carried out with rare skill, the difficult and oft times thankless task of expressing in non-mathematical, and indeed to an unusual degree non-technical language, the newer conceptions of modern physical theory.

Beginning with the "*building materials*"—electrons, protons, and photons,—the first lecture outlines with brief yet lucid strokes the modern ideas of the essential characteristics of these, together with a section dealing with the "*building site,*"—space and the ether. The two following lectures are devoted to the discussion of the essentials of wave propagation, and the notions of wave-velocity and group-velocity together with the diffraction of waves, leading thus naturally to the diffraction of electrons, and of atoms.

The Uncertainty-Principle is then developed in a manner which,—clear and simple as the author's style is,—still calls for close and considered concentration in its reading. Following lectures treat the wave-atom, the polarization characteristics of electrons and protons, the collisions of alpha-rays, protons, and electrons, and finally the exclusion principle of Pauli with charming simplicity of language, although simplicity of conceptions is not so readily possible.

These lectures do not,—could not reasonably be expected to,—contain adequate detail of the essential experimental bases of these newer conceptions of physics; so the volume can hardly serve as a text of modern physics, but most certainly Professor Darwin may be assured that his is a valuable contribution towards the result that "surviving readers may no longer speak of the mysteries of science" but rather "of the naturalness of Nature."

The volume contains a number of excellent illustrations of alpha-ray tracks and diffraction effects. It is regrettable that the negative of the Stern-Gerlach experiment got inverted in the plate, so that the accompanying legend will confuse the reader unacquainted with the phenomenon, (a blunder which,—curiously enough,—appears also in Gerlach's English edition of "Matter, Electricity, Energy").

JOHN E. ALMY
University of Nebraska

Hydro- und Aeromechanik nach Vorlesungen von L. Prandtl Bd. II. O. TIETJENS. Pp. 299+viii. Figs. 238, (Springer 1931). 28 tafeln. Berlin. Price RM 23.

This second volume, written as was the first by Dr. Tietjens, and based in part on Professor Prandtl's lectures, is devoted to the study of the motion of non-viscous fluids and to technical applications. The early chapters contain a summary of the theory of fluid flow, a treat-

ment of the principle of similarity, and a critical discussion of flow, both laminar and turbulent, in tubes and canals including the early work of Hagen, Poseuille, and Reynolds, together with that of more recent investigators. Formulas are given for the resistance to flow in the various turbulent regimes. Particularly interesting is the discussion of the incidence of turbulence with gradually increasing velocity of flow.

There follow three important chapters treating respectively Prandtl's boundary layer theory, the resistance encountered by a solid moving in a fluid, and the theory of lift as applied to aeroplane wings. These chapters contain a systematic presentation of the results of recent investigations. In Prandtl's boundary layer theory that has proved so valuable in the study of viscous fluid motion, the effect of viscosity is neglected except in a thin layer of fluid in contact with a solid boundary. Aside from its use in connection with turbulent flow in tubes, it plays an important rôle in the theory of the resistance suffered by a body moving through a fluid as treated in the next chapter. In addition to the purely frictional resistance encountered by such a body, there is the resistance that results from the alteration of the velocity field from that of irrotational flow and the consequent change in the pressure distribution. In a chapter that occupies about one-fourth of the book, the theory of the lift of aeroplane wings and its technical applications are fully set forth.

The last chapter is devoted to instruments and methods of experimentation including wind tunnels, devices for rendering fluid motion visible, and measurements of pressure, velocity, and resistance. At the end there are some seventy excellent photographs of fluid motion illustrating the motions of solids in water, turbulent flow in canals, and the formation of vortices.

The book is a clear and authoritative exposition of fundamental theories and experimental results in a field that has developed very rapidly in recent years.

H. W. MARCH
University of Wisconsin

PROCEEDINGS OF THE AMERICAN PHYSICAL SOCIETY

MINUTES OF THE PULLMAN MEETING

JUNE 17–18, 1932

The 178th regular meeting of the American Physical Society was held at the Washington State College, Pullman, Washington, room 110 Mechanical Arts Building, in affiliation with the Astronomical Society of the Pacific, and the Pacific Division of the A. A. A. S., on June 17th, 1932.

The sessions began at 9:30 in the morning, extended until noon, and resumed in the afternoon at 2:00 o'clock, terminating at 4:30. There were twenty-five members of the Physical Society in attendance, covering institutions from San Diego to the University of British Columbia.

It was moved, seconded, and voted to hold the 181st meeting of the American Physical Society on the Pacific Coast, on December 16–17th, 1932, at the California Institute of Technology, Pasadena. No other business was transacted.

The members of the Physical Society enjoyed a joint luncheon at noon, June 17th, and a joint dinner on the evening of June 17th, with some twenty-five members in attendance.

In spite of its small size, the meeting was highly successful in the renewal of contacts which it gave between members of the Society in the Pacific Northwest and those from other portions of the Pacific area.

LEONARD B. LOEB, *Secretary for the Pacific Coast*

ABSTRACTS

1. The energy distribution of electrons in field current emission. JOS. E. HENDERSON, R. K. DAHLSTROM, FRANK R. ABBOTT. *University of Washington.*—The energy distribution of electrons extracted from a cold tungsten filament by means of a high electrical field was obtained by using an arrangement of three cylinders with the filament as the common axis. The two inner cylinders were grids. The potential which produced the field necessary for emission also accelerated the electrons through the first grid. By connecting the second grid directly to the filament except for a small variable accelerating potential these electrons were then decelerated. With various magnitudes of field currents the current to the second grid was measured as a function of this small accelerating potential. From these data the energy distribution of the electrons was obtained. The most striking feature of the distribution was that the largest number of electrons had energies only slightly below the maximum. The relative numbers having lower energies increases with the magnitude of the field currents. The range of energies extended over approximately thirty volts. The outer cylinder provided a means of determining the effect of secondary electrons, which effect was found to be small.

2. Mobilities of sodium ions in helium measured in short time intervals. LEONARD B. LOEB. *University of California.*—Extending the mobility measurements of sodium ions in various gases (Phys. Rev. 38, 549, 1931), as a function of time to helium using an improved oscil-

lator designed for the writer by the Bell Telephone Laboratories and using a new baked-out glass chamber, the following results were obtained. In intervals of 2×10^{-5} sec. and 5×10^{-4} sec., the sodium ion has the astonishingly high mobility of about 30 cm/sec. per volt/cm. Below 5×10^{-4} sec., the mobility has a value of about 23 cm/sec. In the old metal chamber with a directly heated Kunsman source, rather uncertain values indicated the presence of ions of mobilities 30 cm/sec., 23 cm/sec., 17 cm/sec., and 13 cm/sec. on progressive aging. The latter values are somewhat in doubt and the more exact values in the new chamber are open to an uncertainty of the order of magnitude of 5 percent owing to the inadequate knowledge of the temperature correction to be applied in the new chamber.

3. Electroscope of high charge sensitivity. E. J. WORKMAN, *National Research Fellow* and H. B. DEVORE, *California Institute of Technology.*—Electroscopes for use in ionization measurements have been developed to combine a high voltage sensitivity over a limited range with a very small capacity. Bearing in mind that the character of the voltage calibration curve is determined by the rate of variation of capacity with deflection, instruments have been designed to have this vary abruptly in the voltage range in which it is desirable to work. This modification of the calibration curve has been achieved by electrically shielding the deflecting element by placing it in a small metal trough or slot. The size, shape, and position of the trough can be adjusted to give the desired sensitivity at the collecting voltage required. This principle has been applied to the deflecting fibre type in which a heavy quartz fibre, fixed at one end, is used, and to the torsion types where the deflecting element consists of a short quartz fibre fixed at the center to the torsion member. A deflecting instrument has been used which gave a full scale deflection of 100 divisions for 350 volts, but from 80 to 100 divisions the sensitivity was uniform at 10 divisions per volt. In other instruments higher sensitivities have been observed with characteristics indicating that the sensitivity may be made several times that given above. These instruments are, by nature, extremely rugged and simple of construction.

4. Photoelectric currents in gases between parallel plates as a function of the potential difference. NORRIS E. BRADBURY. *University of California.*—If one of two parallel plate electrodes in a gas emits photoelectrons, the current received at the collecting electrode is a function of the potential difference, the gas pressure, the initial velocity of the photoelectrons, and the mobility of the carrier. In the experiments reported here, a quartz mercury arc and a plane zinc electrode were used as the source of photoelectrons. Current-potential difference curves were obtained for different gas pressures in hydrogen and nitrogen, and the ratio of the current, i, to the saturation current, I_0, obtained in each case. A theoretical equation of J. J. Thomson gives the relation

$$i = [I_0(6\pi)^{1/2}kx]/[c + (6\pi)^{1/2}kx],$$

where X is the field strength, k the mobility of the carrier, and c its random velocity. Adopting the suggestion of Loeb that c is the average velocity of photoelectric emission of the electrons from the plates, the validity of this equation is established by the experimental data which permit the values of the electron mobility k to be determined as a function of X/p. Values so obtained agree well with those obtained by Loeb and by Townsend and Bailey. An equation recently given by Langmuir (Phys. Rev. **38**, 1656, (1931)), is shown to be applicable only at low pressures where it yields a satisfactory value of the mean free path of the electron.

5. On the specific heats of ferromagnetic materials. PAUL S. EPSTEIN. *California Institute of Technology.*—A theory of ferromagnetism developed by the author leads to the result that, at very low temperatures, the specific heats of ferro-magnetic substances follow the law $c=0.208sR(T/\theta)^{3/2}$, where R is the gas constant and s the number of valency electrons per atom. The constant θ is closely related to the Curie point T_0 being of the order of magnitude of $\frac{1}{2}T_0$. The available experimental data do not go to sufficiently low temperatures to permit a test of this law but they are encouraging as far as the order of magnitude is concerned.

6. Mobilities of gaseous ions in mixtures of hydrogen and nitromethane and hydrogen and methyl cyanide. ELIZABETH A. HIGLEY AND CAROLYN C. THORSEN. Introduced by L. B. LOEB. *University of California.*—In continuation of the investigations of L. B. Loeb on ionic mobilities in mixtures of various gases, it seemed worthwhile to investigate the action of nitro-bodies and cyanides. Owing to the toxic and unstable nature of these substances it was decided to study the simplest organic derivatives of the two radicals. The mobilities of the positive and negative ions in Kahlbaum's methyl cyanide were 0.237 cm/sec. and 0.234 cm/sec. respectively, and the values in Kahlbaum's nitromethane were 0.221 cm/sec. and 0.221 cm/sec. respectively. The addition of traces of both of these gases to hydrogen caused an abnormal decrease of the mobility on both ions, and cause a deviation from Blanc's law indicating the formation of a definite addition product with ions of both signs. The effect in nitromethane was distinctly greater than the effect in methyl cyanide. These measurements were made keeping the auxiliary field equal to the driving field, and therefore represent the mobilities on the new standard absolute scale.

7. Determination of the coefficient of ionization by collision using large plate distances and higher pressures. FREDERICK H. SANDERS. Introduced by L. B. LOEB. *University of California.*—The coefficient of ionization by collision, α, was measured in dry air at a pressure of 380 mm over a range of field strengths varying from $X=13{,}680$ $(X/p=36)$ to $X=7{,}600$ $(X/p=20)$. The ionization chamber used was of such dimensions as to make the investigations possible at plate distances ranging from one to five centimeters. With these large plate distances it was possible to evaulate α for values of X/p as low as 20. It was found that instead of the coefficient being equal to zero at $X/p=30.1$ as shown by Paavola (Archiv. für Elektrotechnik **443**, 22 (1929)). α actually has a measurable value at $X/p=20$. Plotting α/p as a function of X/p, the curve approaches the zero axis asymptotically. The highest value of X/p attained was 36.5, which is within two percent of the sparking potential at a plate distance of 2.5 centimeters. At this field strength no increase in current with plate distance was noted beyond that given by the simple Townsend relation $i=i_0e^{\alpha d}$. (Laboratory equipment for this research was made possible through a grant-in-aid from the National Research Council.)

8. The distribution of electrons in the photo-effect by Roentgen rays, classically treated. JAKOB KUNZ. *University of Illinois. (To be read by title.)*—Several treatments of this effect by means of wave mechanics have been given. If a beam of Roentgen rays passes through a gas, most of the electrons are not given out in the direction of the electric force E, but in a more forward direction. If the direction of observation makes an angle θ with c, the velocity of light, the component of E is $E\sin\theta$ and the intensity of light is $CE^2\sin^2\theta$ and is proportional to the number of electrons emitted in the direction θ. Moreover, I have shown in a previous article, (Phys. Rev. **6**, 413, (1915)), that in the Roentgen pulse the electric force

$$E_t = \frac{ev\sin\theta}{\delta\rho(c - v\cos\theta)}$$

where the thickness

$$\delta = l(2c - v\cos\theta)/v.$$

The intensity of the beam is again equal to

$$CE_t^2 = \frac{Ce^2v^4\sin^2\theta}{\rho^2l^2}(c - v\cos\theta)^{-2}(2c - v\cos\theta)^{-2}$$

$$= \frac{Ce^2v^4c^{-2}2}{\rho^2l^2}\left(1 + \frac{5}{2}\frac{v}{c}\cos\theta\right)\sin^2\theta$$

a formula deduced in wave mechanics with different constants.

9. A theory of the Raman rotation spectra. WILLIAM V. HOUSTON, *California Institute of Technology.*—The Raman spectrum may be treated as due to variable polarizability, as has been done by Placzek for the vibration lines. If the tensor of polarizability is transformed, by means of the Eulerian angles, to axes which are fixed with reference to the incident beam of

light, the periodic change of these angles gives the Raman lines of the rotation spectrum. It is thus possible to evaluate the relative intensities of the lines, as well as their polarization, without any knowledge of the electronic levels of the molecule. This method of treatment explains very nicely why a spherically symmetric molecule, such as methane, shows no rotation spectrum, although it does show a rotation-vibration spectrum.

10. Secondary effects in the ionization by hard gamma-rays. E. J. WORKMAN, *National Research Fellow, California Institute of Technology.*—The author has previously reported concerning the increase of the ionization in a metal electroscope, as produced by increasing the wall thickness of the chamber. Another arrangement has been used in which a canalized beam of gamma-rays from the radium, filtered by as much as 3 cm of lead, was directed along the axis of a cylindrical ionization chamber (10 cm long and 9 cm diameter) containing air at atmospheric pressure. Various thicknesses of cellophane, graphite, aluminum, iron, tin, and lead were placed on the front and then on the back of the chamber and the ionization studied. Lead, placed on the back end of the chamber, causes an increase of approximately 60 percent in the ionization when a filter of 3 cm of lead is used. For other materials the increase is nearly proportional to the atomic number. A large part of the increase is doubtless due to scattering of electrons from the back wall. Equivalent electron thicknesses of the materials on the front end of the chamber may either increase or decrease the ionization according to whether the material is of low or high atomic number. The order in which the materials arrange themselves with respect to the effect they produce on the ionization, as well as the magnitude of the effect for a given material, depends upon the thickness of the filter.

11. Absorption bands in the infrared spectrum of Venus. W. S. ADAMS AND THEODOR DUNHAM, JR. *Mt. Wilson Solar Observatory.*

12. The absolute magnitudes of the 05 to B2 stars determined from the interstellar lines. J. A. PEARCE. *Dominion Astrophysical Observatory.*

13. On the temperatures of Wolf-Rayet stars and novae. C. S. BEALS. *Dominion Astrophysical Observatory.*

14. Further details ascribable to bands of the carbon isotope C_{13} in stars of spectral classes R. and N. R. F. SANFORD. *Mt. Wilson Solar Observatory.*

15. An investigation of the hydrocarbon bands in the solar spectrum. R. S. RICHARDSON. *Mt. Wilson Solar Observatory.*

AUTHOR INDEX TO ABSTRACTS OF PULLMAN MEETING

Abbott, Frank R.—see Henderson
Adams, W. S. and Theodore Dunham, Jr.—No. 11
Beals, C. S.—No. 13
Bradbury, Norris E.—No. 4
Dahlstrom, R. K.—see Henderson
DeVore, H. B.—see Workman
Dunham, Theodore, Jr.,—see Adams
Epstein, Paul S.—No. 5
Henderson, Jos. E., R. K. Dahlstrom and Frank R. Abbott—No. 1
Higley, Elizabeth A. and Carolyn C. Thorsen—No. 6
Houston, William V.—No. 9
Kunz, Jakob—No. 8
Loeb, Leonard B.—No. 2
Pearce, J. A.—No. 12
Richardson, R. S.—No. 15
Sanders, Frederick H.—No. 7
Sanford, R. F.—No. 14
Thorsen, Carolyn C.—see Higley
Workman, E. J.—No. 10
———and H. B. DeVore—No. 3

Second Series *August 1, 1932* *Vol. 41, No. 3*

THE

PHYSICAL REVIEW

On the Effect of a Secondary Structure upon the Interference of X-rays

By H. M. EVJEN*

Norman Bridge Laboratory of Physics, California Institute of Technology

(Received June 17, 1932)

Laue's dynamic theory of x-ray interference is shown to be applicable, with only a few minor changes, to crystals having a very general type of secondary structure. It is thus applied for the purpose of obtaining a quantitative estimate of the effect of such a structure upon the nature of the x-ray interference maxima. The estimate is relative insofar as it compares the intensities of respectively the "secondarily" and the "primarily" reflected interference beams and applies only in the region where the latter have been, or can be observed. In this region the "two-dimensional lattice" type of secondary structure is found to give rise to a fine structure which, with the present insufficient resolving power, would be manifested experimentally as a weak, diffuse background. The secondary structure of this type produces *no broadening* of the primary lines. The existence of this type of structure, therefore, is not inconsistent with the sharpness of the interference maxima obtained from such crystals as calcite, and a possible objection to the existence of the secondary structure in such crystals is removed. The extinction effect is briefly considered, but absorption is not taken into account, except with a few qualitative remarks.

ARGUMENTS against the existence of a secondary structure[1] in crystals have been raised from time to time in the literature on the basis of the nature of the x-ray interference patterns. For instance,[2] it has been argued that the sharpness of the x-ray interference lines from such crystals as calcite is not consistent with the presence of a secondary structure. This argument, if theoretically tenable, would be very weighty on account of the reliability and great accuracy of the x-ray spectroscopy; and its consequences would be far reaching in the theory of the solid state.[3] For this reason, and also in view of the possibility of enlisting the aid of the x-ray spectroscopist in the detection and analysis of secondary structures, it is desirable to obtain a quan-

* National Research Fellow.

[1] Not to be confused with a "mosaic structure." For the sense in which these terms are here used, see F. Zwicky, Phys. Rev. **40**, 63 (1932).

[2] M. Siegbahn, *Spektroskopie d. Röntgenstrahlen*, 2d Ed., p. 60 (1931).

[3] As pointed out by Siegbahn, in reference 2, we would have as an immediate effect that Zwicky's explanation of the discrepancy between the values of the electronic charge obtained respectively by direct measurement and by x-ray analysis would be rendered unsatisfactory. (See F. Zwicky, Proc. Nat. Ac. **16**, 211 (1930)). There is, however, at present some controversy as to whether or not this discrepancy is significant.

titative estimate of the effect of such structures upon the interference of x-rays.[4]

Laue's dynamic theory of x-ray interference[5] is directly applicable to crystals having a very general type of secondary structure. In fact, the formulae developed by Laue remain formally the same when his theory is applied to crystals having such a structure; only the symbols involved must be given a slightly different interpretation. In order to prove this proposition we shall have to review briefly the physical background of Laue's theory.

Laue's theory in contradistinction to Ewald's[6] earlier theory and Waller's[7] modification thereof, is based on the supposition that the negative electric charges are distributed in an arbitrary manner over the entire lattice cell. It contains Ewald's theory as a special case when certain restrictions are placed on a group of symbols whereby the concentration of the said charges at the lattice points is accomplished.

His theory owes its simplicity and elegance to the following ingenious considerations.

First he shows that it is permissible to assume that for small displacements the displacement of the negative charges at any point in the lattice cell is proportional to the electric field strength at that point. The proportionality factor is calculable in principle, but since it does not enter directly into the theory, it is not necessary to go into the question as to how this factor may be calculated.

Secondly, on account of the large masses with which the positive charges are associated, these do not take any appreciable part in the scattering of the x-rays. They may therefore be distributed in any manner whatsoever over the lattice cell, provided we specify that they shall not be displaced by the electric vector. The positive charges, in fact, may be distributed in such a way that when there is no disturbing field they exactly neutralize everywhere the negative charges. A field then produces in every point of space a polarization which is proportional to the field strength at that point. The magnitude of the polarization is characterized by a proportionality factor varying from point to point within the crystal. By thus distributing the positive charges we therefore arrive at a fictitious body whose dielectric constant varies with the coordinates. In the real body, with its positive charges concentrated in the immediate neighborhood of the lattice points, the electromagnetic wave field is exactly the same. The fact that the two bodies differ electrostatically is of no consequence for our purpose.

In order to obtain the solution of the interference problem it is now only

[4] Darwin, (See reference 15), has already calculated the effect of one type of imperfections in crystals. The type of secondary structure which will be considered here, however, is essentially different from Darwin's imperfections.

[5] M. v. Laue, Erg. d. ex. Naturwiss **10**, 133 (1931).

[6] P. P. Ewald, Series of papers starting with Ann. d. Physik **54**, 519 (1917). The general method embodied in Ewald's and Laue's works is more convenient for our purpose than the method employed by Darwin in a still earlier paper, C. G. Darwin, Phil. Mag. **27**, 315, 675 (1914).

[7] J. Waller, Uppsala Universitets Aarsskrift (1925).

necessary to solve Maxwell's equations for a medium having a triply periodic dielectric constant. In the case of the ideal crystal, as treated by Laue, the periodicities of the dielectric constant, ϵ, must conform with the periodicities of the primary lattice of the crystal. In the case of the crystal having a secondary structure, on the other hand, the *periodicities of* ϵ *must conform with the periodicities of the secondary structure.* The primary structure here appears as a very prominent higher harmonic. Instead of representing ϵ itself as a triply periodic Fourier summation it is more convenient for the purpose of calculation thus to represent the factor $\psi = 1 - 1/\epsilon$ which determines the polarization, $\mathcal{D}(1 - 1/\epsilon)$, $\mathcal{D}$ being the electric displacement vector of the electromagnetic field. If we understand by, $(\boldsymbol{a}_1^0, \boldsymbol{a}_2^0, \boldsymbol{a}_3^0)$ the primitive translations of the primary lattice, and by $(\boldsymbol{b}_1^0, \boldsymbol{b}_2^0, \boldsymbol{b}_3^0)$ the corresponding elementary vectors of the reciprocal lattice, we have for the ideal crystal:

$$1 - 1/\epsilon = \psi = \sum \psi_m e^{-j(\boldsymbol{b}_m \cdot \boldsymbol{r})} \tag{1}$$

where

$$\boldsymbol{b}_m = \sum_{\alpha=1}^{3} m_\alpha \boldsymbol{b}_\alpha^0; \; j = 2\pi(-1)^{1/2}.$$

m_α is an integer, and $\boldsymbol{r}$ is the independent variable radius vector measured from an arbitrary lattice point.

From the definition,

$$\boldsymbol{b}_k^0 = [\boldsymbol{a}_i^0 \times \boldsymbol{a}_j^0]/(\boldsymbol{a}_i^0 \boldsymbol{a}_j^0 \boldsymbol{b}_k^0) \tag{1a}$$

it follows immediately that each term in the series (1) is periodic with the three periods $(\boldsymbol{a}_1^0, \boldsymbol{a}_2^0, \boldsymbol{a}_3^0)$.

This is the starting point for Laue's theory. For crystals having a secondary structure Eq. (1) must be slightly modified. Let the periodicities of the secondary structure be $(\boldsymbol{D}_1^0, \boldsymbol{D}_2^0, \boldsymbol{D}_3^0)$. Let the corresponding reciprocal lattice be defined by,

$$\boldsymbol{B}_k^0 = [\boldsymbol{D}_i^0 \times \boldsymbol{D}_j^0]/(\boldsymbol{D}_i^0 \boldsymbol{D}_j^0 \boldsymbol{D}_k^0). \tag{2}$$

The polarization factor[8] now must be represented as follows:

$$1 - 1/\epsilon' = \phi = \sum \phi_m e^{-j(\boldsymbol{B}_m \cdot \boldsymbol{r})} \tag{3}$$

where

$$\boldsymbol{B}_m = \sum_{\alpha=1}^{3} m_\alpha \boldsymbol{B}_\alpha^0.$$

By the definition (2) we are assured that each term in the series (3) is periodic with the three periods $(\boldsymbol{D}_1^0, \boldsymbol{D}_2^0, \boldsymbol{D}_3^0)$.

[8] This factor, as Laue points out, is akin to, and takes the place of the structure factor of the elementary theory; but only in so far as the polarization is proportional to the density of charge with a *constant* proportionality factor can it be said to be a measure of the distribution of charge.

Eq. (3) is formally the same as Eq. (1), the only differences being that ϕ and ϕ_m have replaced ψ and ψ_m, and $\boldsymbol{B}_m$ has replaced $\boldsymbol{b}_m$. From this it follows that any subsequent formula that may be derived on the basis of Eq. (3), in conjunction with Maxwell's questions, must be formally the same as the corresponding one derived by Laue on the basis of Eq. (1), since any subsequent development is of a purely mathematical nature. We can therefore write immediately in the place of Laue's fundamental Eqs. (I):[9]

$$\frac{K_m'^2 - k^2}{K_m'^2} \mathfrak{D}_m = \sum \phi_{m-q} \mathfrak{D}_{q[m]} \tag{I'}$$

where $\mathfrak{D}_m$ represents the electric displacement of the plane wave propagated in the direction of K_m' given by,

$$K_m' = K_0 + \boldsymbol{B}_m \tag{4}$$

and $\mathfrak{D}_{q[m]}$ represents the component of $\mathfrak{D}_q$ perpendicular to K_m'. k is the reciprocal of the vacuum wave-length.

When these conditions are fulfilled the solution of Maxwell's equations for a medium having the dielectric constant specified in Eq. (3) is given by,

$$\begin{aligned} \mathfrak{D} &= e^{i\nu t} \sum \mathfrak{D}_m e^{-i(K_m' \cdot \boldsymbol{r})} \\ \mathfrak{H} &= e^{i\nu t} \sum \mathfrak{H}_m e^{-i(K_m' \cdot \boldsymbol{r})} \end{aligned} \tag{5}$$

$\mathfrak{H}$ being the magnetic field strength.

Each member of this triple sum represents a plane wave propagated in the direction of K_m' with the phase velocity

$$v = \nu / \left| K_m' \right|$$

ν being the frequency of the wave field which is assumed to be monochromatic. The index of refraction of the plane wave therefore is given by:

$$n = c/v = c \left| K_m' \right| / \nu. \tag{6}$$

It follows moreover from Maxwell's equations that the electric vector $\mathfrak{D}_m$ is perpendicular to the vector K_m' as well as to $\mathfrak{H}_m$. Hereby the number of unknowns, (components of $\mathfrak{D}_m$ perpendicular to K_m'), as well as the number of algebraic equations in (I') is reduced to $2N$ where N is the total number of vectors $\mathfrak{D}_m$, in general infinity.

Now to solve the infinite set of linear, homogeneous Eqs. (I') in general, not only is impracticable by the methods of existing mathematics but also is useless, since as Laue points out, only a finite number of the plane waves have an appreciable intensity. If, therefore, we follow the example set by Laue and neglect all the vectors $\mathfrak{D}_m$ except those that have an appreciable absolute value, the fundamental Eqs. (I') reduce to a finite set of linear, homogeneous equations which can be solved by ordinary methods. The criterion by which this reduction is brought about is the same as that employed by Laue in the case of the ideal crystal, and for practical purposes is

[9] See reference 5, p. 139.

most easily obtained by geometrical considerations in the reciprocal space. For a detailed account of the method, however, we shall refer to Laue's admirable paper.[5] Here we shall only consider the changes brought about in the reciprocal lattice by the introduction of the secondary structure. Although the following assumption is not necessary, we shall for simplicity assume that the secondary structure belongs to the same crystallographic group as the primary structure. Then we have:

$$\boldsymbol{D}_i^0 = M_i \boldsymbol{a}_i^0; \qquad (i = 1, 2, 3) \quad (7)$$

where

$$M_1 \sim M_2 \sim M_3 \sim M \qquad (7a)$$

are integral numbers all of the same order of magnitude. From Eqs. (1a) and (2) it then follows that,

$$\boldsymbol{B}_i^0 = \boldsymbol{b}_i^0 / M_i \qquad (8)$$

By this equation the relation between respectively the primary and the secondary reciprocal lattice is determined.

Now in order to obtain a quantitative estimate of the effect of the secondary structure it is necessary first to derive the relative magnitudes of the Fourier coefficients ψ_m and ϕ_m appearing respectively in Eqs. (1) and (3). From the general theory it is known that the secondary structure must be considered as a very slight modulation of the primary structure. In other words,

$$\psi_P > \phi_\pi$$

provided the triplet $\pi = (\pi_1, \pi_2, \pi_3)$ does not represent an integral multiple of the triplet $M = (M_1, M_2, M_3)$. In the latter case, that is when $\pi = Mq = (q_1 M_1, q_2 M_2, q_3 M_3)$, the exponential function by which ϕ_π is multiplied in the summation (3) is the same as the exponential function by which ψ_q is multiplied in the summation (1), and we have,

$$\psi_q \sim \psi_P \sim \phi_{Mq}.$$

A closer estimate is possible by sacrificing some of the generality. That is, if we exclude the type of secondary structure in which the individual blocks are tilted with respect to each other, it is clear that the ratio ϕ_π / ψ_P must be of the order of magnitude of the relative amplitude of deviation in lattice constant from the primary value. This amplitude of deviation is given particularly on the basis of the one,[10] but also on the basis of the other,[11] of the two general types of secondary structure lately propounded in the literature, as follows:

$$\Delta/a \sim a/D \sim 1/M.$$

Consequently the relative order of magnitude of the two Fourier coefficients is given by,

[10] F. Zwicky, Helv. Phys. Acta **3**, 287 (1930).
[11] F. Zwicky, Phys. Rev. **38**, 1772 (1931).

$$\phi_\pi/\psi_P \sim 1/M; \qquad (\pi \neq M_q) \quad (9)$$

where M usually is of the order of 50 or larger.

Eqs. (8) and (9) in conjunction with the formulae derived by Laue enable us to arrive at the desired estimates. The constructions in the reciprocal space are the same as those employed by Laue except that a number of lattice points are added in accordance with Eq. (8) as illustrated in Fig. 1.

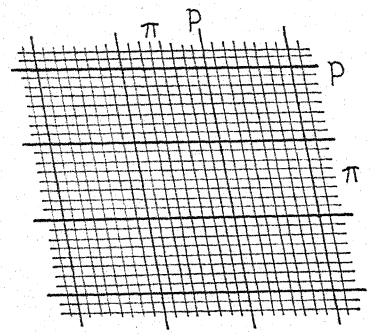


Fig. 1. Reciprocal lattice.

Associated with these additional lattice points are structure factors ϕ_π which bear the relation (9) to the factors ψ_P of the primary lattice points.

In the simplest possible case, that is when only one of the vectors $\mathcal{D}_m$, namely $\mathcal{D}_0$, has an appreciable absolute value, we obtain:

$$\mathcal{D}_\pi = (\phi_\pi/2\epsilon_\pi)\mathcal{D}_{0[\pi]}$$

$$\mathcal{D}_P = (\psi_P/2\epsilon_P)\mathcal{D}_{0[P]}.$$

Therefore, when the quantities ϵ_π and ϵ_P are roughly the same,[12] that is, when the "propagation sphere" passes at roughly the same distance from the secondary lattice point π as from the primary point p, and the geometrical status of the two points is otherwise roughly the same, our theory yields,

$$\mathcal{D}_\pi/\mathcal{D}_P \sim \phi_\pi/\psi_P$$

or by Eq. (9):

$$(\mathcal{D}_\pi/\mathcal{D}_P)^2 \sim 1/M^2. \qquad (10)$$

For the order of magnitude of M which we have indicated this ratio is very small. Nevertheless, when we consider the total or integrated energy scattered by the secondary structure we may arrive at a very sizable figure since the density of the secondary scattering centers in the reciprocal space is M^3 greater than that of the primary scattering centers. For the ordinary experimental setup, however, it is clear that this scattering from the secondary structure could be manifested only as an apparently diffuse background of radiation.

[12] See reference 5, Eq. (14a).

When more than one of the vectors $\mathfrak{D}_m$ have an appreciable absolute value we can usually write down relations similar in context to Eq. (10). Only in very particular cases do situations arise in which the plane wave created by interference from the secondary scattering centers is comparable in intensity with those produced under similar circumstances from the primary scattering centers. In these cases, however, the solid angular regions over which this intensity prevails is of the order $1/M^2$ for the secondary interference beams as compared with the primary ones. Therefore, again the experimental detection of the secondary interference beams would be very difficult.

We shall consider one such case somewhat more in detail, namely the practically very important Bragg reflection. This we shall do only in the symmetrical case, that is when the reflecting planes are parallel to the surface of the crystal. The more general case, where this condition is not fulfilled, presents no principally greater difficulties, but neither does it add any essentially novel features, so nothing is gained by its inclusion.

In the crystal of infinite thickness perpendicular to the reflecting planes the secondary as well as the primary structure will give rise to total reflection over certain angular regions. These angular regions are defined by the Eqs. IIIa and IVa derived by Laue,[13] equations which we shall reproduce here:

$$\chi_m = \chi_B + \psi_0/\sin 2\chi_B \tag{11}$$

$$\Delta\chi = 2(\psi_m\psi_{-m})^{1/2}/\sin 2\chi_B \tag{12}$$

where χ_B is the Bragg angle defined by the equation,

$$n\lambda = 2d\cos\chi_B$$

χ_m is the midpoint of the region of total reflection, and $\Delta\chi$ is the width of this region. In order to obtain the corresponding quantities for the reflection from the secondary structure it is only necessary to substitute ϕ_m for ψ_m and $D\sim Md$ for d. It follows immediately that,

$$\Delta\chi_\pi/\Delta\chi_P \sim |\phi_\pi| / |\psi_P| \sim 1/M. \tag{13}$$

For a somewhat divergent beam of incident, the apparent intensities of reflection are proportional to these widths. Again the intensity of reflection from the secondary structure is small compared with the intensity of reflection from the primary structure. Moreover, the interference maxima from the two structures ordinarily do not overlap[14] since ψ_P is of the order of magnitude 10^{-6} which hence is also the order of magnitude of the width $\Delta\chi_P$, whereas the distance between neighboring midpoints of the interference maxima is of the order $\lambda/2Md$ which is ordinarily very much larger than 10^{-6}. This type of secondary structure consequently produces no apparent widening of the primary lines, in contradistinction to the mosaic structure introduced by Darwin[15] to explain certain anomalies of x-ray reflection. Dar-

[13] See reference 5, p. 157.

[14] This is a point of considerable importance since otherwise it would be necessary to consider not only two of the rays $K_{m'}$ simultaneously but three.

[15] C. G. Darwin, Phil. Mag. **43**, 800 (1922).

win's type of mosaic structure is characterized by an angle of tilt between the elementary blocks. Such a contingency has not been taken into account in the present theory, and our results represent not a contradiction but rather a complement to those of Darwin. Whereas such an angle of tilt is apparently, in most cases, a necessary result of the energetic considerations which led to the second type of secondary structure,[11] the angle of tilt is not an adjunct of the secondary structure of the first kind.[19] In other words, our theory applies to the latter type of structure. Incidentally this was the type of structure employed by Zwicky[3] to explain the discrepancy between the values for the electronic charge obtained respectively by direct measurement and by x-ray analysis. If this discrepancy should turn out to be significant, Zwicky's explanation consequently will remain consistent with the great sharpness of the interference lines obtained from such crystals as calcite.

In spite of the weakness of the individual interference maxima arising from the secondary structure the total or integrated intensity obtained from this source when the crystal is turned through a certain finite angle may be quite appreciable, since the number of secondary interference maxima by the Bragg arrangement in general is M times greater than that of the primary maxima. Again, however, this "secondarily" reflected radiation would be manifested for experimental purposes, (with the employment of hard x-rays), as a diffuse background. This would be particularly true when the secondary structure is no longer ideal, but is degenerated into a mosaic structure, which is to be expected unless the crystal is grown under very carefully controlled conditions; for it is clear that the mosaic structure, in its effects, would bear a somewhat analogous relation to the ideal secondary structure, as the thermally agitated lattice, in its effects, bears to the ideal static one.

To complete the theory we shall consider briefly the effect of the finite thickness of the crystal. Total reflection, strictly speaking, is only obtained when the crystal is nonabsorbing and has an infinite thickness. When the crystal has a finite thickness some of the energy in the angular regions defined by Eqs. (11) and (12) is transmitted through the crystal. The energy of the transmitted beam drops off exponentially from the reflecting surface. The rapidity with which the intensity drops off depends on the coefficient in the exponent of the exponential factor. This coefficient, κ, which may be called the extinction coefficient varies from zero at one extremity of the angular region defined by Eqs. (11) and (12) through a maximum and back to zero at the other extremity. This maximum is given to a sufficiently close approximation by Laue's theory as follows:

$$\kappa_{\max} = k(\psi_m \psi_{-m})^{1/2}. \tag{14}$$

From this it is seen that the extinction coefficient is of the order M times greater for the primary interference beams than for the secondary ones. For crystals of finite thickness, therefore, the efficiency of reflection from the primary structure may be enormously greater than the efficiency of reflection from the secondary structure. Thus the relative intensity of the secondary interference beams is no longer given by the ratio $1/M$; this ratio now must

be multiplied by a factor containing exponential terms depending on the thickness of the crystal, and this factor may be very small when the crystal is thin although it reaches a value of unity asymptotically as the thickness is increased. Incidentally these considerations show that the intensity of the interference beams from the secondary structure must be reduced more by absorption than the primary beams, since the former traverse more of the crystal before they are reflected than the latter.

It should be noted that the present theory is only concerned with the *relative* intensities of the interference maxima for x-rays of the same wavelength. Nothing has been said about the absolute value of the Fourier coefficients involved, except in so far as they are known from measurements on the primary interference beams. It is therefore quite conceivable that measureable interference maxima from the secondary structure will be obtained when x-rays of sufficient softness to exclude the primary lines are employed. In this case, moreover, it is doubtful whether or not Laue's theory is applicable since the boundary solution, (i.e., the interference pattern from the cross grating forming the boundary of the crystal), might be expected to come within the region of observables.

Analysis of the (0,0) $^2\Pi \rightarrow {}^2\Sigma$ CN Band at 9168A

By ALLAN E. PARKER
Sloane Physics Laboratory, Yale University

(Received June 8, 1932)

The rotational structure of the 0,0 band of the red CN system has been analyzed by means of spectrograms taken in the first order of a 21-foot grating. The values obtained for the various constants are $B_0'' = 1.8906$ cm^{-1}, $B_0' = 1.6907$ cm^{-1}, $D_0' = -6.07 \times 10^{-6}$ cm^{-1}, $A = -53.3$ cm^{-1}, $p_0 = 0.009$ cm^{-1} and $q_0 = -0.0008$ cm^{-1}. These are in agreement with the values obtained by Jenkins, Roots and Mulliken for transitions which involve higher vibrational levels of the $^2\Pi$ state. The origin of the band is at 10905.12 cm^{-1}.

INTRODUCTION

RECENTLY Kiess[1] has reported the existance of strong carbon bands in the infrared beyond 9000A. It seemed desirable to photograph these as they might or might not be the 0, 0 and 1, 1 bands of the $^2\Pi \rightarrow {}^2\Sigma$ CN band system whose position has been determined by Asundi and Ryde.[2] Analysis of the bands shows them to be these transitions. The results obtained are in agreement with those of Jenkins, Roots and Mulliken[3] who have analyzed transitions involving higher vibrational levels of the $^2\Pi$ state.

EXPERIMENTAL PROCEDURE

The source used was a 220 volt d.c. arc drawing 9 amperes. Spectrograms were obtained upon xenocyanine plates recently developed by the Eastman Kodak Company. These plates were hypersensitized with ammonia and exposed for nine hours in order to obtain sufficiently strong spectrograms. The dispersive apparatus was a 21-foot grating mounted stigmatically. Plates were taken in the first order, the dispersion for this region being 4.78A per mm. Second and third order iron lines were used for the comparison spectrum.

ROTATIONAL ANALYSIS

The rotational analysis of the 0, 0 band yields the six main branches. The satellite, ${}^oP_{12}$ and ${}^sR_{21}$, branches are not strong enough to permit of identification. In the region to the violet of the 1, 1 band, the six principal branches of the 0, 0 band account for virtually all the lines observed. For the equations giving the term values and for the combination relations reference is made to the article of Jenkins, Roots and Mulliken. Table I gives the wave-numbers of the various branches of the 0, 0 band. The appearance of the bands is quite similar to that of the 8, 3 band of which a reproduction is shown in reference three.

[1] C. C. Kiess, Bureau of Standards, Journal of Research **8**, 393 (1932).
[2] R. K. Asundi and J. W. Ryde, Nature **124**, 57 (1929).
[3] F. A. Jenkins, Y. K. Roots and R. S. Mulliken, Phys. Rev. **39**, 16 (1932).

TABLE I.

K''	R_2	Q_2	P_2	R_1	Q_1	P_1
0	10,931.83					
1	33.62	10,929.69			10,878.25	
2	35.05	27.10			79.08	
3	36.13	24.42			79.48	
4	36.82	21.48			79.08	
5	37.27	18.26			78.05	
6	37.27	14.97		10,901.80	76.62	
7	36.82	10.89		02.90	74.65	
8	36.13	06.59		03.71	72.44	
9	35.05	02.02		04.18	69.59	
10	33.62	897.19		04.18	66.43	
11	31.83	92.02		03.71	62.65	
12	29.77	86.39		02.72	58.56	
13	27.27	80.42		01.17	53.89	
14	24.42	74.28		899.64	48.86	
15	21.23	67.66		97.77	43.37	
16	17.63	60.73		95.11	37.55	
17	13.69	53.38		92.02	31.02	
18	09.35	45.67		88.36	24.20	
19	04.66	37.55		84.60	17.01	
20	899.60	29.18	10,762.19	80.42	09.39	
21	94.08	20.35	50.06	75.49	01.20	
22	88.36	11.19	37.44	70.21	792.72	
23	82.09	01.57	24.54	64.60	83.80	10,705.83
24	75.49	791.71	11.36	58.56	74.38	693.19
25	68.48	81.37	697.39	52.05	64.62	80.09
26	61.07	70.69	83.49	45.15	54.44	66.59
27	53.38	59.62	68.99	37.55	43.87	52.63
28	45.15	48.16	54.20	30.15	32.86	38.17
29	36.63	36.30	38.94	21.98	21.44	23.46
30	27.68	24.01	23.46	13.40	09.64	08.35
31	18.31	11.36	07.43	04.45	697.39	592.74
32	08.66	698.33	591.11	795.07	84.78	76.78
33	798.50	84.78	74.37	85.32	71.65	60.52
34	88.00	77.16	57.36	75.04	58.13	43.72
35	77.11	56.95	39.69	64.62	44.27	26.46
36	65.76	42.41		53.33	29.97	08.89
37		27.41		41.93	15.28	490.72
38		12.13		30.03	00.25	71.89
39		596.31		17.60	584.76	
40		80.22		05.10	68.81	
41		63.68		692.07	52.60	
42		46.68		78.62	35.86	
43		29.34		64.60	18.76	
44		11.64		50.31	01.27	
45		493.61		35.56	483.32	
46		75.08		20.50	65.03	
47		56.13		04.94	46.31	
48		36.92		589.16	27.23	
49		17.24		72.73	07.66	
50		397.09		55.98	387.78	
51		76.79		38.76	67.51	
52		55.89		21.16	46.77	
53		34.60			25.67	
54		12.98			04.17	

TABLE I. (*Cont.*)

K''	R_2	Q_2	P_2	R_1	Q_1	P_1
55		290.91			282.27	
56		68.54			60.05	
57		45.77			37.30	
58		22.51			14.27	
59		198.90			190.77	
60		74.90			66.89	
61		50.53			42.60	
62		25.76			17.95	
63		00.63			092.84	

The combination differences for the $^2\Sigma$ state have been computed from the expression

$$R_1(K-1) - P_1(K+1) = \Delta_2F_1''(K).$$

The values obtained have been compared with those for the 0, 0 transition of the violet CN band system as determined by Uhler and Patterson.[4] Unfortunately the greater portion of the $\Delta_2F_1''(K)$ values available from the $^2\Pi \rightarrow {}^2\Sigma$ transition are not obtainable from the violet band. The reason for this is that the P lines necessary for the determination of the combination differences are, for the most part, those in the immediate vicinity of the head of the band and Uhler and Patterson were unable to resolve them. There is good agreement between those values of $\Delta_2F_1''(K)$ which are available from both band systems. The value of B_0'' obtained is 1.8906 cm^{-1} which is to be compared with 1.8904 cm^{-1}, the value predicted from the B_v'' equation given by Jenkins, Roots and Mulliken.

TABLE II. *Combination differences Δ_2F_i' for the $v=0$ level of the $^2\Pi$ state.*

J	$R_2(J)-P_2(J)$	$R_1(J)-P_1(J)$
$19\frac{1}{2}$	137.41	
$20\frac{1}{2}$	144.02	
$21\frac{1}{2}$	150.92	
$22\frac{1}{2}$	157.55	
$23\frac{1}{2}$	164.13	158.77
$24\frac{1}{2}$	171.09	165.37
$25\frac{1}{2}$	177.58	171.90
$26\frac{1}{2}$	184.39	178.56
$27\frac{1}{2}$	190.95	
$28\frac{1}{2}$	197.69	191.98
$29\frac{1}{2}$	204.22	198.52
$30\frac{1}{2}$	210.88	205.05
$31\frac{1}{2}$	217.55	211.71
$32\frac{1}{2}$	224.13	218.29
$33\frac{1}{2}$	230.64	224.80
$34\frac{1}{2}$	237.42	231.32
$35\frac{1}{2}$		238.16
$36\frac{1}{2}$		244.44
$37\frac{1}{2}$		251.21
$38\frac{1}{2}$		258.14

[4] H. S. Uhler and R. A. Patterson, Astrophys. J. **42**, 434 (1915).

Table II contains the combination differences for the $^2\Pi$ state. By means of these values the various constants have been determined by the same methods as those used by the above mentioned authors. The values are

$$B_0^*{}_{,-1/2} = 1.7404 \text{ cm}^{-1}$$
$$B_0^*{}_{,1/2} = 1.6410 \text{ cm}^{-1}$$
$$B_0' = 1.6907 \text{ cm}^{-1}$$
$$D_0' = -6.07 \times 10^{-6} \text{ cm}^{-1}$$
$$A = -53.3 \text{ cm}^{-1}$$
$$p_0 = 0.009 \text{ cm}^{-1}$$
$$q_0 = -0.0008 \text{ cm}^{-1}$$
$$\nu_0 = 10905.12 \text{ cm}^{-1}.$$

The value of B_0' is in excellent agreement with the value, 1.6903 cm^{-1}, obtained by extrapolation from the results of the analysis of other bands of this system. There is considerable inaccuracy in the determination of the values of p_0 and q_0 as the P branches could not be measured in the region of low K values. Furthermore the value of A is slightly higher than that obtained from the higher vibrational levels of this electronic state.

The analysis of the 1, 1 band has not been carried out due to the fact that the lines of low K value were absent from the spectrograms obtained. The two Q branches are easily identified and may be followed to quite high K values. There is also evidence of the R branches.

The author wishes to thank Professor W. W. Watson for his generous assistance and advice.

The Dirac Electron in Simple Fields*

By MILTON S. PLESSET
Sloane Physics Laboratory, Yale University

(Received June 6, 1932)

The relativity wave equations for the Dirac electron are transformed in a simple manner into a symmetric canonical form. This canonical form makes readily possible the investigation of the characteristics of the solutions of these relativity equations for simple potential fields. If the potential is a polynomial of any degree in x, a continuous energy spectrum characterizes the solutions. If the potential is a polynomial of any degree in $1/x$, the solutions possess a continuous energy spectrum when the energy is numerically greater than the rest-energy of the electron; values of the energy numerically less than the rest-energy are barred. When the potential is a polynomial of any degree in r, all values of the energy are allowed. For potentials which are polynomials in $1/r$ of degree higher than the first, the energy spectrum is again continuous. The quantization arising for the Coulomb potential is an exceptional case.

1.

IN HIS treatment of the reflection of the relativity electron at a potential jump Klein[1] found a paradoxical behavior of the Dirac electron associated with the possibility of the existence of states of negative kinetic energy. He showed by an ingenious treatment that the reflection coefficient for electrons incident upon a discontinuous potential jump of height P varied with P from the value zero for $P=0$ to the value unity for $P=W-mc^2$ (W being the energy of the incident electrons). For this last value of P the momentum p associated with the transmitted beam had the value zero, and as P was increased beyond $W-mc^2$ this momentum became imaginary and the reflection coefficient remained unity until P attained the value $W+mc^2$. The results thus far are exactly what would be expected. If P is increased further one enters the domain of negative kinetic energy wherein the group velocity and the momentum in the transmitted beam are oppositely directed; also the reflection coefficient falls off from the value unity and approaches the value $(W-cp)/(W+cp)$ as P is indefinitely increased. Thus by a transition to a state of negative kinetic energy the Dirac electron has apparently an appreciable probability of penetrating a barrier of infinite height. Bohr suggested that this peculiar result might be due to a jump in potential of the order of mc^2 over a region of the order of the Compton wave-length h/mc. It is within a region of the order of h/mc that the internal structure of the Dirac electron and the accompanying "trembling" phenomenon[2] manifests itself. This supposition of Bohr was verified by Sauter[3] who treated the problem of the

* The results of this paper were presented at the Washington meeting of the American Physical Society (April, 1932).

[1] O. Klein, Zeits. f. Physik **53**, 157 (1929).

[2] E. Schrödinger, Preuss. Akad. Wiss. Berlin, Ber. **24**, 418 (1930).

[3] F. Sauter, Zeits. f. Physik **69**, 742 (1931).

Dirac electron passing through a potential barrier in which the rise of potential was taken to be linear. Sauter then showed that the transmission coefficient was very small for a rise in potential $P > W + mc^2$.

Here we shall discuss analytically the nature of the stationary solutions of Dirac's equations for continuous potential functions of a more general type than those heretofore considered. A simple familiar method of treating these equations will be used. The results secured are perhaps unexpected on the basis of the corresponding results for the nonrelativistic treatment.

2.

The relativistic equation of Dirac[4] for an electron of charge $-e$ is

$$\left\{\frac{W}{c}+\frac{e}{c}A_0+\alpha_x\left(p_x+\frac{e}{c}A_x\right)+\alpha_y\left(p_y+\frac{e}{c}A_y\right)+\alpha_z\left(p_z+\frac{e}{c}A_z\right)+\rho_3 mc\right\}\Psi=0. \tag{1}$$

We shall suppose that $A=0$; then Eq. (1) may be expanded as follows

$$\begin{aligned}
(W/c - V/c + mc)\Psi_1 + (p_x - ip_y)\Psi_4 + p_z\Psi_3 &= 0\\
(W/c - V/c + mc)\Psi_2 + (p_x + ip_y)\Psi_3 - p_z\Psi_4 &= 0\\
(W/c - V/c - mc)\Psi_3 + (p_x - ip_y)\Psi_2 + p_z\Psi_1 &= 0\\
(W/c - V/c - mc)\Psi_4 + (p_x + ip_y)\Psi_1 - p_z\Psi_2 &= 0
\end{aligned} \tag{2}$$

where we have put V for the potential energy $-eA_0$. The expansion of (1) into (2) corresponds to these choices of the α's and ρ_3

$$\alpha_x=\begin{pmatrix}0&0&0&1\\0&0&1&0\\0&1&0&0\\1&0&0&0\end{pmatrix},\quad \alpha_y=\begin{pmatrix}0&0&0&-i\\0&0&i&0\\0&-i&0&0\\i&0&0&0\end{pmatrix},$$

$$\alpha_z=\begin{pmatrix}0&0&1&0\\0&0&0&-1\\1&0&0&0\\0&-1&0&0\end{pmatrix},\quad \rho_3=\begin{pmatrix}1&0&0&0\\0&1&0&0\\0&0&-1&0\\0&0&0&-1\end{pmatrix}.$$

We shall consider first the case for which V is a polynomial[5] of any degree in x,

$$V=\sum_{n=0}^{q}a_n x^n, \qquad (0<q<\infty) \tag{3}$$

[4] P. A. M. Dirac, *The Principles of Quantum Mechanics*, p. 243.

[5] The case of a uniform field, $V=ax$, has been treated by Sauter, Zeits. f. Physik **69**, 742 (1931), and that of the simple harmonic oscillator, $V=ax^2$, by K. Nikolsky, Zeits. f. Physik **62**, 677 (1930); the methods used in these cases differ from that used here and are perhaps not so readily capable of generalization as the present method.

and we shall seek solutions of the form

$$\Psi = (\exp 2\pi i(p_y y + p_z z - Wt)/h)\psi(x) \tag{4}$$

so that the components of $\psi(x)$ satisfy these differential equations

$$\begin{aligned}
\frac{d\psi_1}{dx} &= -\frac{2\pi i}{h}\left\{ip_y\psi_1 - p_z\psi_2 + \left(\frac{W}{c} - \frac{V}{c} - mc\right)\psi_4\right\};\\
\frac{d\psi_2}{dx} &= -\frac{2\pi i}{h}\left\{p_z\psi_1 - ip_y\psi_2 + \left(\frac{W}{c} - \frac{V}{c} - mc\right)\psi_3\right\};\\
\frac{d\psi_3}{dx} &= -\frac{2\pi i}{h}\left\{\left(\frac{W}{c} - \frac{V}{c} + mc\right)\psi_2 + ip_y\psi_3 - p_z\psi_4\right\};\\
\frac{d\psi_4}{dx} &= -\frac{2\pi i}{h}\left\{\left(\frac{W}{c} - \frac{V}{c} + mc\right)\psi_1 + p_z\psi_3 - ip_y\psi_4\right\}.
\end{aligned} \tag{5}$$

In view of (3) it may be said that every finite value of x corresponds to an ordinary point of the system of differential equations (5); hence for all finite values of x the solutions of (5) are not only finite but analytic. The points at infinity, $x = \pm\infty$, are, however, irregular singular points of Eqs. (5) of rank $q+1$. The behavior of the solutions of (5) in the neighborhood of these singular points will now be investigated.

We consider the possibility of formally satisfying Eqs. (5) by a set of normal solutions of the type

$$\psi_i = e^{Q(x)}u_i(x), \qquad (i = 1, \cdots 4) \tag{6}$$

where $u_i(x)$ is assumed to be regular in the neighborhood of $|x| = \infty$, and

$$Q(x) = \alpha x^{q+1}/(q+1) + \beta x^q/q + \cdots + \lambda x. \tag{7}$$

The permissible values of α are determined by the characteristic equation

$$\begin{vmatrix} -\alpha & 0 & 0 & a \\ 0 & -\alpha & a & 0 \\ 0 & a & -\alpha & 0 \\ a & 0 & 0 & -\alpha \end{vmatrix} = 0; \quad a = 2\pi i a_q/hc. \tag{8}$$

The roots of this equation, which are both double, are

$$\alpha = \pm a = \pm 2\pi i \cdot a_q/hc; \tag{9}$$

the fact that there are only two distinct roots of Eq. (8) indicates that there are only two independent sets of solutions of the system of Eqs. (5). We transform Eqs. (5) into an analytically symmetrical form by the simple transformation

$$\begin{aligned}
\psi_1' &= (1/2^{1/2})(\psi_1 + \psi_4);\\
\psi_2' &= (1/2^{1/2})(\psi_2 + \psi_3);\\
\psi_3' &= (1/2^{1/2})(\psi_2 - \psi_3);\\
\psi_4' &= (1/2^{1/2})(\psi_1 - \psi_4).
\end{aligned} \tag{10}$$

The matrix of the constants in the linear transformation (10)

$$C = \begin{pmatrix} 1/2^{1/2} & 0 & 0 & 1/2^{1/2} \\ 0 & 1/2^{1/2} & 1/2^{1/2} & 0 \\ 0 & 1/2^{1/2} & -1/2^{1/2} & 0 \\ 1/2^{1/2} & 0 & 0 & -1/2^{1/2} \end{pmatrix} = C^{-1} \tag{11}$$

generates a unitary transformation of the matrix of the determinant of the characteristic equation into the diagonal form

$$\begin{pmatrix} -\alpha + a & 0 & 0 & 0 \\ 0 & -\alpha + a & 0 & 0 \\ 0 & 0 & -\alpha - a & 0 \\ 0 & 0 & 0 & -\alpha - a \end{pmatrix}. \tag{12}$$

The "canonical" form of the system of Eqs. (5) is

$$\begin{aligned} \frac{d\psi_1'}{dx} &= -\frac{2\pi i}{h}\left\{\left(\frac{W}{c} - \frac{V}{c}\right)\psi_1' - p_z\psi_3' + (mc + ip_y)\psi_4'\right\}; \\ \frac{d\psi_2'}{dx} &= -\frac{2\pi i}{h}\left\{\left(\frac{W}{c} - \frac{V}{c}\right)\psi_2' + (mc - ip_y)\psi_3' + p_z\psi_4'\right\}; \\ \frac{d\psi_3'}{dx} &= -\frac{2\pi i}{h}\left\{p_z\psi_1' - (mc + ip_y)\psi_2' - \left(\frac{W}{c} - \frac{V}{c}\right)\psi_3'\right\}; \\ \frac{d\psi_4'}{dx} &= -\frac{2\pi i}{h}\left\{(ip_y - mc)\psi_1' - p_z\psi_2' - \left(\frac{W}{c} - \frac{V}{c}\right)\psi_4'\right\}. \end{aligned} \tag{13}$$

We are assuming solutions of this system of Eqs. (13) of the form (an additional subscript s is introduced to distinguish the two sets of solutions)

$$\begin{aligned} \psi_{1s}' &= e^{Q_s(x)}x^{\mu_s}B_{1s}(x); \quad \psi_{2s}' = e^{Q_s(x)}x^{\mu_s}B_{2s}(x); \\ \psi_{3s}' &= e^{Q_s(x)}x^{\mu_s}B_{3s}(x); \quad \psi_{4s}' = e^{Q_s(x)}x^{\mu_s}B_{4s}(x); \end{aligned} \qquad (s = 1, 2) \tag{14}$$

where

$$Q_s(x) = \alpha_s x^{q+1}/(q+1) + \beta_s x^q/q + \cdots + \lambda_s x; \tag{15}$$

and

$$B_{rs}(x) = B_{rs}^{0} + B_{rs}^{(1)}x^{-1} + B_{rs}^{(2)}x^{-2} + \cdots. \tag{16}$$

The constants of the solutions (14) are evaluated by direct substitution into Eqs. (13). Of the two sets of formal solutions the first may be written as

$$\begin{aligned} \psi_{11}' &= e^{Q_1(x)}\left\{B_{11}^{0} + B_{11}^{(q-1)}/x^{q-1} + \cdots\right\} \\ \psi_{21}' &= e^{Q_1(x)}\left\{B_{21}^{0} + B_{21}^{(q-1)}/x^{q-1} + \cdots\right\} \\ \psi_{31}' &= e^{Q_1(x)}\left\{B_{31}^{(q)}/x^{q} + \cdots\right\} \\ \psi_{41}' &= e^{Q_1(x)}\left\{B_{41}^{(q)}/x^{q} + \cdots\right\} \end{aligned} \tag{17}$$

where

$$Q_1(x) = \frac{2\pi i}{hc} \sum_{n=0}^{q} \frac{a_n x^{n+1}}{n+1} - \frac{2\pi i W x}{hc}. \tag{17a}$$

It may be shown by examination of the recurrence relations which determine the B's that ψ'_{11} and ψ_{21}' are linearly dependent as are also ψ'_{31} and ψ'_{41}. The second set of solutions is

$$\begin{aligned}
\psi_{12}' &= e^{Q_2(x)}\{B_{12}^{(q)}/x^q + \cdots\} \\
\psi_{22}' &= e^{Q_2(x)}\{B_{22}^{(q)}/x^q + \cdots\} \\
\psi_{32}' &= e^{Q_2(x)}\{B_{32}^{0} + B_{32}^{(q-1)}/x^{q-1} + \cdots\} \\
\psi_{42}' &= e^{Q_2(x)}\{B_{42}^{0} + B_{42}^{(q-1)}/x^{q-1} + \cdots\}
\end{aligned} \tag{18}$$

where

$$Q_2(x) = -\frac{2\pi i}{hc} \sum_{n=0}^{q} \frac{a_n x^{n+1}}{n+1} + \frac{2\pi i W x}{hc}. \tag{18a}$$

Again ψ_{12}' and ψ_{22}' are linearly dependent as are also ψ_{32}' and ψ_{42}'. We have further that only the constants B_{11}^{0}, B_{21}^{0}, B_{32}^{0}, B_{42}^{0} are arbitrary.

We wish to use the solutions (17) and (18), which we have found to satisfy the canonical equations (13) formally, to discuss the behavior of the true solutions for values of x numerically large; this use requires a rigorous justification since it follows from the recurrence relations for the B's that the infinite series $B_{rs}(x)$ do not in general converge for finite values of x. This justification might be carried out by eliminating as follows from the canonical Eqs. (13). Put

$$\begin{aligned}
\psi_1' &= e^{Q_1(x)}u_1(x); \quad & \psi_2' &= e^{Q_1(x)}u_2(x); \\
\psi_3' &= e^{Q_1(x)}u_3(x); \quad & \psi_4' &= e^{Q_1(x)}u_4(x);
\end{aligned} \tag{19}$$

where $Q_1(x)$ is the polynomial given above in (17a). Then the simultaneous Eqs. (13) give readily

$$\frac{d^2u_3}{dx^2} + \frac{4\pi i}{hc}\{V(x) - W\}\frac{du_3}{dx} + \frac{4\pi}{hc}\left\{i\frac{dV}{dx} - \frac{\pi c}{h}(p_y^2 + p_z^2 + m^2c^2)\right\}u_3 = 0; \tag{20}$$

u_4 satisfies the same equation as u_3. We get also

$$\frac{d^2u_1}{dx^2} + \frac{4\pi i}{hc}\{V(x) - W\}\frac{du_1}{dx} - \frac{4\pi^2}{h^2}\{p_y^2 + p_z^2 + m^2c^2\}u_1 = 0; \tag{21}$$

and u_2 satisfies the same equation as u_1. The symmetry and simplicity with which elimination can be accomplished to give Eqs. (20) and (21) show the analytical advantage of working with the canonical form of Dirac's equations. If elimination were attempted directly upon Eqs. (5), the result would be an extremely unsymmetrical set of equations.[6] Eqs. (20) and (21) show that the

[6] This analytical lack of symmetry holds also for Weyl's expansion of Dirac's equation.

points $x = \pm \infty$ are irregular singular points of the functions $u_i(x)$ as well as of the functions $\psi_i'(x)$. Instead of proceeding further with Eqs. (20) and (21), it is more convenient to treat the canonical Eqs. (13) directly. These equations, now considered in the complex plane, have as solutions the generalized Laplace contour integrals

$$\psi_{rs}' = (\exp \beta_s z^q/q + \cdots + \lambda_s z) \int_{C_s} (\exp z^{q+1}) \left(\zeta - \frac{\alpha_s}{q+1}\right)^{-(\mu_s+1)/(q+1)} \sum_{k=0}^{q} z^k \phi_{rk}^{(s)}\left(\zeta - \frac{\alpha_s}{q+1}\right) d\zeta. \tag{22}$$

The contour C_s is a loop circuit about $\zeta = \alpha_s/(q+1)$ such that the real part of $[z^{q+1}\{\zeta - \alpha_s/(q+1)\}]$ is negative along its ray. The functions $\phi_{rk}^{(s)}$ are analytic functions (determined by (13)) in the neighborhood of $\zeta = \alpha_s/(q+1)$. These contour integrals (22) are precise solutions of the canonical equations; the asymptotic expansions[7] of these contour integrals, valid in certain sectors of the z-plane which may be so taken as to include the real axis, are exactly the formal solutions (17) and (18) written above.[8] Therefore these formal solutions have significance as the asymptotic solutions of Eqs. (13). Their use in discussing the behavior of the solutions of (13) for numerically large values of x is thus justified. The importance of using the canonical form of Dirac's equations is here apparent; for, if formal solutions of the type (6) were attempted with the original Eqs. (5), a divergent expansion would result which would be meaningless.

We may now say from Eqs. (17), (17a) and (18), (18a) that the components of the Dirac wave function, remain finite as x becomes infinite; further we have

$$\int_{-a}^{a} \sum_{1}^{4} \psi_i \psi_i^* dx < c(a), \tag{23}$$

where c is a finite number, since the functions ψ_i are finite and analytic for all finite values of x. And if the constant a is sufficiently large ($b > a$),

$$\int_{a}^{b} \sum_{1}^{4} \psi_i \psi_i^* dx \propto (b-a); \qquad \int_{-a}^{-b} \sum_{1}^{4} \psi_i \psi_i^* dx \propto -(b-a); \tag{24}$$

that is, the integral square becomes proportional to the domain of integration. The wave functions exhibit, therefore, quite common characteristics of the wave functions associated with a continuous energy spectrum. It is thus clear that the Dirac electron possesses a continuous spectrum with all values of W allowed for a potential field which is a polynomial of any degree in x.

3.

Let us now consider potential fields which are polynomials in $1/x$,

$$V(x) = \sum_{n=0}^{q} a_n x^{-n}. \qquad (0 < q < \infty) \tag{25}$$

[7] Asymptotic expansions in the sense of Poincaré.
[8] Cf. E. L. Ince, *Ordinary Differential Equations* p. 484.

It is evident from the discussion given above that we may make the simplifying assumption $p_y = p_z = 0$ in Eqs. (5) without affecting the generality of the results secured. Then Eqs. (5) become

$$\frac{d\psi_1}{dx} = -\frac{2\pi i}{hc}(W - mc^2 - V)\psi_4; \tag{26a}$$

$$\frac{d\psi_2}{dx} = -\frac{2\pi i}{hc}(W - mc^2 - V)\psi_3; \tag{26b}$$

$$\frac{d\psi_3}{dx} = -\frac{2\pi i}{hc}(W + mc^2 - V)\psi_2; \tag{26c}$$

$$\frac{d\psi_4}{dx} = -\frac{2\pi i}{hc}(W + mc^2 - V)\psi_1. \tag{26d}$$

The complete behavior of this system of equations may be determined by considering only Eqs. (26a) and (26d) since this pair of equations has the same form as the pair of Eqs. (26b) and (26c). For the potential function given in (25) the system of Eqs. (26) has an irregular singularity at $x = \pm\infty$ of rank unity and an irregular singularity at $x = 0$ of rank $q-1$.

To investigate the behavior of the solutions in the neighborhood of the origin we proceed by the method given in §2 above. The transformation to the canonical form of (26a) and (26d) is given by

$$\begin{aligned} \psi_1' &= (1/2^{1/2})(\psi_1 + \psi_4), \\ \psi_2' &= (1/2^{1/2})(\psi_1 - \psi_4), \end{aligned} \tag{27}$$

so that Eqs. (26a) and (26d) become

$$\begin{aligned} \frac{d\psi_1'}{dx} &= -\frac{2\pi i}{hc}\{[W - V(x)]\psi_1' + mc^2\psi_2'\}; \\ \frac{d\psi_2'}{dx} &= \frac{2\pi i}{hc}\{mc^2\psi_1' + [W - V(x)]\psi_2'\}. \end{aligned} \tag{28}$$

To make the analytical procedure of §2 completely applicable we need only put $x = 1/y$ in Eqs. (28) to get

$$\begin{aligned} \frac{d\psi_1'}{dy} &= \frac{2\pi i}{hc}\frac{1}{y^2}\left\{\left[W - V\left(\frac{1}{y}\right)\right]\psi_1' + mc^2\psi_2'\right\}; \\ \frac{d\psi_2'}{dy} &= -\frac{2\pi i}{hc}\frac{1}{y^2}\left\{mc^2\psi_1' + \left[W - V\left(\frac{1}{y}\right)\right]\psi_2'\right\}. \end{aligned} \tag{29}$$

We now consider the behavior of the solutions of Eqs. (29) for values of y numerically large. We assume, as before, formal solutions of the normal type

$$\psi_{rs}' = e^{Q_s(y)} y^{\mu_s} B_{rs}(y) \qquad (r, s = 1, 2) \tag{30}$$

where now

$$Q_s(y) = \frac{\alpha_s y^{q-1}}{q-1} + \frac{\beta_s y^{q-2}}{q-2} + \cdots + \lambda_s y$$

and as before

$$B_{rs}(y) = B_{rs}^{0} + B_{rs}^{(1)} y^{-1} + \cdots .$$

By direct substitution it is found that the asymptotic solutions have the form

$$\psi_{rs}'(y) \cong \delta_{rs} \exp\left\{(-1)^s \frac{2\pi i}{hc}\left[\frac{a_q}{q-1} y^{q-1} + \frac{a_{q-2}}{q-2} y^{q-2} + \cdots + a_1 \log y\right]\right\} \quad (31)$$

where δ_{rs} is the Kronecker delta. From Eq. (31) it is clear that the solutions of Eqs. (29) remain finite as y approaches infinity for all values of W; that is, the solutions of Eqs. (28) remain finite in the neighborhood of $x=0$. The origin, $x=0$, does not, therefore, give any limitations on possible allowed solutions of Eqs. (28) or (26).

We must now investigate the behavior of the solutions of Eqs. (26a) and (26d) near $x = \pm\infty$. The characteristic equation for (26a) and (26d) is

$$\begin{vmatrix} -\alpha & -\frac{2\pi i}{hc}(W - mc^2 - a_0) \\ -\frac{2\pi i}{hc}(W + mc^2 - a_0) & -\alpha \end{vmatrix} = 0; \quad (32)$$

so that

$$\alpha = \pm (2\pi/hc)\left\{m^2c^4 - (W - a_0)^2\right\}^{1/2}. \quad (33)$$

We may secure a canonical form of Eqs. (26a) and (26d) by putting

$$\begin{aligned} \psi_1 &= a_1^{1/2}(\psi_1' - \psi_2') \\ \psi_4 &= a_2^{1/2}(\psi_1' + \psi_2') \end{aligned} \quad (34)$$

where

$$\frac{1}{a_1} = (W + mc^2 - a_0); \quad \frac{1}{a_2} = (W - mc^2 - a_0).$$

Eqs. (26a) and (26d) then become

$$\frac{d\psi_1'}{dx} = -\frac{2\pi}{hc}\left\{\left[m^2c^4 - (W - a_0)^2\right]^{1/2} + \frac{(W - a_0)}{\left[m^2c^4 - (W - a_0)^2\right]^{1/2}}(V - a_0)\right\}\psi_1'$$
$$-\frac{2\pi}{hc}\frac{mc^2}{\left[m^2c^4 - (W - a_0)^2\right]^{1/2}}(V - a_0)\psi_2'; \quad (35a)$$

$$\frac{d\psi_2'}{dx} = \frac{2\pi}{hc}\frac{mc^2}{\left[m^2c^4 - (W - a_0)^2\right]^{1/2}}(V - a_0)\psi_1'$$
$$+\frac{2\pi}{hc}\left\{\left[m^2c^4 - (W - a_0)^2\right]^{1/2} + \frac{(W - a_0)}{\left[m^2c^4 - (W - a_0)^2\right]^{1/2}}(V - a_0)\right\}\psi_2'. \quad (35b)$$

The formal substitution into Eqs. (35) of solutions of the normal type gives the asymptotic solutions of these equations. The asymptotic solutions are readily found to be

$$\psi_{rs}' \backsimeq e^{\alpha_s x} x^{\mu_s} \delta_{rs} \qquad (r, s = 1, 2) \quad (36)$$

where

$$\alpha_1 = -\frac{2\pi}{hc}[m^2c^4 - (W - a_0)^2]^{1/2} = -\alpha_2, \quad (37)$$

and

$$\mu_1 = -\frac{2\pi}{hc}\frac{(W - a_0)a_1}{[m^2c^4 - (W - a_0)^2]^{1/2}} = -\mu_2. \quad (38)$$

If $(W-a_0)^2 > m^2c^4$, it is evident from Eq. (36) that the solutions of Eqs. (35) are all finite at infinity; all such values of W are allowed so that a continuous spectrum arises. If, however, $(W-a_0)^2 < m^2c^4$, Eq. (36) shows that it is not possible to find solutions of (35) which remain finite both at $x=+\infty$ and at $x=-\infty$. Hence there are no proper solutions in this band; these energy values are barred.

4.

We now turn to the case in which the potential function depends on r alone. To examine the characteristics of the Dirac equations for this case we may begin with the radial equations in the form in which they are given by Dirac[9]

$$\frac{dR_a}{dr} = \frac{j}{r}R_a + \left(b_2 + \frac{2\pi}{hc}V(r)\right)R_b \quad (39a)$$

$$(j = \pm 1, \pm 2, \cdots)$$

$$\frac{dR_b}{dr} = -\frac{j}{r}R_b + \left(b_1 - \frac{2\pi}{hc}V(r)\right)R_a \quad (39b)$$

where

$$b_1 = 2\pi(mc^2 + W)/hc; \; b_2 = 2\pi(mc^2 - W)/hc.$$

The type of potential to be considered first is that for which V is a polynomial of any degree in r

$$V = \sum_{n=0}^{q} a_n r^n. \qquad (0 < q < \infty) \quad (40)$$

With $V(r)$ given by (40) Eqs. (39) for R_a and R_b have an irregular singularity at $r=\infty$ of rank $q+1$; the origin, $r=0$, is a regular singular point; and all other points are ordinary points. We consider first the nature of the solutions in the neighborhood of $r=\infty$. The characteristic equation is

[9] Dirac, *The Principles of Quantum Mechanics*, p. 252.

$$\begin{vmatrix} -\alpha & 2\pi a_q/hc \\ -2\pi a_q/hc & -\alpha \end{vmatrix} = 0; \quad \alpha = \pm \frac{2\pi i}{hc} a_q. \tag{41}$$

The transformation to a canonical form is given by

$$\begin{aligned} R_a &= (1/2^{1/2})(\psi_1 - i\psi_2) \\ R_b &= (1/2^{1/2})(-i\psi_1 + \psi_2) \end{aligned} \tag{42}$$

and the canonical form of Eqs. (39) is

$$\frac{d\psi_1}{dr} = \frac{2\pi i}{hc}\{W - V\}\psi_1 + \left\{\frac{2\pi mc}{h} - i\frac{j}{r}\right\}\psi_2; \tag{43a}$$

$$\frac{d\psi_2}{dr} = \left\{\frac{2\pi mc}{h} + i\frac{j}{r}\right\}\psi_1 - \frac{2\pi i}{hc}\{W - V\}\psi_2. \tag{43b}$$

The asymptotic solutions of Eqs. (43) may be readily found to be

$$\psi_{ms} \leqq \delta_{ms} \exp\left\{(-1)^s \frac{2\pi i}{hc}\left[\sum_{n=0}^{q} \frac{a_n}{n+1} r^{n+1} - Wr\right]\right\}. \quad (m, s = 1, 2). \tag{44}$$

From (44) it is seen that the solutions of Eqs. (43) remain finite as r approaches infinity and exhibit an integral square behavior like that discussed above. The irregular singular point at infinity, therefore, does not contribute any limitation on permitted energy values.

The singularity at the origin is regular so that in the neighborhood of the origin solutions of the form

$$R_{as} = r^{\alpha_s}(B_{as}{}^0 + B_{as}{}^{(1)}r + B_{as}{}^{(2)}r^2 + \cdots) \tag{45a}$$

$$R_{bs} = r^{\alpha_s}(B_{bs}{}^0 + B_{bs}{}^{(1)}r + B_{bs}{}^{(2)}r^2 + \cdots) \tag{45b}$$

satisfy the radial Eqs. (39). From the permissible values of α_s as determined by the characteristic equation for this case, $\alpha = \pm j$, it is evident that there is always one solution finite at the origin. Combining this result with that given in (44) we may say that there is always a solution of the radial equations which for all values of W is finite everywhere and which possesses in addition a well behaved integral square for large values of r. Hence for potential functions which are polynomials of any degree in r the equations of Dirac give a continuous spectrum with all values of W allowed.

5.

Let us consider finally the case for which the potential function $V(r)$ is a polynomial in $1/r$

$$V(r) = \sum_{n=0}^{q} a_n r^{-n}. \qquad (0 < q < \infty) \tag{46}$$

With this potential function the radial Eqs. (39) have an irregular singularity at $r = \infty$ of rank unity; the roots of the characteristic equation are

$$\alpha_1 = (2\pi/hc)[m^2c^4 - (W - a_0)^2]^{1/2} = -\alpha_2. \tag{47}$$

The transformation

$$R_a = (b_2 + 2\pi a_0/hc)^{1/2}(\psi_1 - \psi_2)$$
$$R_b = (b_1 - 2\pi a_0/hc)^{1/2}(\psi_1 + \psi_2) \tag{48}$$

gives the canonical form

$$\frac{d\psi_1}{dr} = \frac{2\pi}{hc}\left\{[m^2c^4 - (W - a_0)^2]^{1/2} + \frac{(W - a_0)}{[m^2c^4 - (W - a_0)^2]^{1/2}}(V - a_0)\right\}\psi_1$$
$$+ \left\{-\frac{j}{r} + \frac{2\pi}{h}\frac{mc}{[m^2c^4 - (W - a_0)^2]^{1/2}}(V - a_0)\right\}\psi_2; \tag{49a}$$

$$\frac{d\psi_2}{dr} = -\left\{\frac{j}{r} + \frac{2\pi}{h}\frac{mc}{[m^2c^4 - (W - a_0)^2]^{1/2}}(V - a_0)\right\}\psi_1$$
$$-\frac{2\pi}{hc}\left\{[m^2c^4 - (W - a_0)^2]^{1/2} + \frac{(W - a_0)}{[m^2c^4 - (W - a_0)^2]^{1/2}}(V - a_0)\right\}\psi_2; \tag{49b}$$

and the asymptotic behavior of the solutions of Eqs. (49) is given by

$$\psi_{rs} \backsimeq e^{\alpha_s r}r^{\mu_s}\delta_{rs} \qquad (r, s = 1, 2) \tag{50}$$

where

$$\mu_1 = \frac{2\pi}{hc}\frac{(W - a_0)}{[m^2c^4 - (W - a_0)^2]^{1/2}}a_1 = -\mu_2. \tag{51}$$

It is evident from (47) and (51) that for $(W-a_0)^2 > m^2c^4$ all the solutions remain finite as r approaches infinity; and for $(W-a_0)^2 < m^2c^4$ there is one finite and one infinite solution at $r = \infty$.

To investigate the singularity at the origin, $r=0$, it is only necessary to make the transformation $r=1/y$ in the canonical Eqs. (43). If $q=1$, that is to say, if the potential is a Coulomb potential, $y=\infty$ is a regular singular point and regular solutions may be found as follows

$$\psi_{rs} = y^{\alpha_s}(B_{rs}{}^0 + B_{rs}{}^{(1)}y^{-1} + B_{rs}{}^{(2)}y^{-2} + \cdots) \tag{52}$$

where the exponent α_s is fixed by the characteristic equation

$$\begin{vmatrix} -\alpha - 2\pi i a_1/hc & -ij \\ ij & -\alpha + 2\pi i a_1/hc \end{vmatrix} = 0; \quad \alpha = \pm (j^2 - 4\pi^2 a_1{}^2/h^2c^2)^{1/2}. \tag{53}$$

These values of the exponent α are, of course, precisely those found in the treatment of the hydrogen atom.[10] From (53) it is evident that there is one finite and one infinite solution at $r=0$; also for $r=\infty$ there is one finite and one infinite solution for $(W-a_0)^2 < m^2c^4$ (by Eq. (50)). These are exactly the conditions which lead to quantization.

[10] Dirac, p. 253.

Such is not the case, however, when $q>1$. For these potential functions the origin, $r=0$, is an irregular singularity. The behavior of the solutions may be investigated by means of Eqs. (43) by the same methods as those used previously. The asymptotic solutions are readily found to be

$$\psi_{rs}(y) \cong \delta_{rs} \exp\left\{(-1)^{s+1}\frac{2\pi i}{hc}\left[\frac{a_q}{q-1}y^{q-1} + \frac{a_{q-1}}{q-2}y^{q-2} + \cdots + a_1 \log y\right]\right\}. \qquad (y = 1/r) \quad (54)$$

From (54) it is clear that when $q>1$ all the solutions of (43) remain finite in the neighborhood of $r=0$ for all values of W. From Eq. (50) it was seen that there is always one solution finite at infinity for all values of W. Combining (50) and (54), we see that a continuous energy spectrum always arises when the potential function is of the form

$$V(r) = a_0 + a_1/r + a_2/r^2 + \cdots + a_q/r^q. \qquad (q > 1)$$

We may discuss briefly the analytical source of the difference in the results found for the potentials $V=1/x$ and $V=1/r$. We note that for the potential $1/x$ Eqs. (29) retain their canonical form; that is, the highest power of y in the expression for $d\psi_i'/dy$ occurs in the coefficient of ψ_i'. The general result (31), therefore, remains applicable to this case also. For the potential $V=1/r$, however, Eqs. (43) (transformed by $r=1/y$ and considered for $y\sim\infty$) do not have the canonical form because of the presence of the terms involving j; thus, this potential must be considered apart from those which contain powers of $1/r$ beyond the first. The general result (54) is not at all applicable to the Coulomb potential.

We may note further here that, if the potential function $V(x)$ is of the form

$$V(x) = \sum_{n=-p}^{q} a_n x^n, \qquad (0 < p, q < \infty)$$

a continuous spectrum arises with no values of W barred. Similarly, if the potential $V(r)$ contains direct as well as inverse powers of r, all values of W are allowed.

6.

By writing the relativity equation of Dirac in a symmetrical canonical form it has been possible to make deductions of a quite general nature regarding the characteristics of the stationary solutions for simple potential fields. The results here presented for the potential fields which are polynomials in x or r give an analytic generalization of the Klein paradox. We may note also that these potential functions will rise by more than mc^2 over a region of the order of h/mc if sufficiently large values of x or r are taken.[11] Hence the hypothesis of Bohr advanced to explain the results of Klein is analytically verified for these general cases also.

[11] We are referring now to polynomial potentials of degree higher than the first.

Such an argument cannot perhaps be so clearly applied to explain the results here presented for potential fields which are polynomials in $1/x$ or $1/r$ since with these potentials the steep rises occur toward the origin. For the Coulomb potential by taking sufficiently small values of r a rise in potential of mc^2 in a region of the order of a Compton wave-length may be secured, and yet this potential gives eminently satisfactory agreement with experiment. If the potential contains higher powers of $1/r$ as well as $1/r$, then, as was stated above, continuous spectra result. Here there is striking disagreement with the results of the nonrelativistic Schrödinger theory; for example potentials of the type $a/r-b/r^2$ applied to oscillating rotator models have been shown[12] to give a discrete spectrum in satisfactory agreement with observed spectra.

We may observe, however, from a purely classical point of view that none of the potentials here discussed (except the Coulomb potential and the linear potential ax) satisfy Laplace's equation. Classically, then, these potentials correspond to a continuous distribution of charge. The relativity theory of the electron is not sufficiently advanced, possibly, to deal with such a complicated physical situation. It should perhaps not be held at fault for giving peculiar results for potential functions which are over-simplified and in that over-simplification correspond to an over-complicated electromagnetic mechanism.

In conclusion the writer takes pleasure in expressing his appreciation to Professor Page for his kind interest in this work.

[12] Cf. A. Sommerfeld, *Wellenmechanischer Ergänzungsband*, p. 24 ff.

The Infrared Absorption Spectrum of Carbon Dioxide

By P. E. MARTIN AND E. F. BARKER
University of Michigan

(Received June 17, 1932)

The complete infrared spectrum of CO_2 may consistently be explained in terms of a linear symmetrical model, making use of the selection rules developed by Dennison and the resonance interaction introduced by Fermi. The inactive fundamental ν_1 appears only in combination bands, but ν_2 at 15μ and ν_3 at 4.3μ absorb intensely.

Resolution of the fundamentals ν_2 and ν_3.—The 15μ band has been resolved into several constituent bands corresponding to absorption by the normal molecule, and by molecules in the first and second excited states. Each band consists of a narrow and intense zero branch, with equally spaced rotation lines on either side. The 4.3μ band has also been resolved, best results following a material reduction in the CO_2 content of the atmospheric path. The line spacing is the same as in the 15μ band, and there is no zero branch. In each case alternate rotation lines are absent, the J values for the normal state all being even. The computed moment of inertia is 70.8×10^{-40} gr cm^2.

Harmonic and combination bands.—No first harmonic bands appear, either for ν_2 or ν_3, but the second harmonic has been observed in each case. The strong pair of doublet bands at 2.7μ are interpreted as combination bands corresponding to $\nu_3+\{\nu_1,2\nu_2\}$ and the bands at 2.0μ and 1.6μ are higher members of the same sequence. The differences $\nu_3-\{\nu_1,2\nu_2\}$ explain the weak absorption maxima observed by Schaefer and Philipps at 9.4μ and 10.4μ. The difference bands $\nu_1-\nu_2$ form a part of the 15μ pattern.

Correlation with Raman spectra.—The Raman lines corresponding to the transitions $0\rightarrow\{\nu_1,2\nu_2\}$ and the weaker pair originating in the first excited state 1_1 of ν_2 fit precisely into the energy level diagram obtained from infrared measurements.

MEASUREMENTS of the absorption due to carbon dioxide were among the earliest observations in infrared spectroscopy,[1] and, as apparatus and methods have gradually improved, these bands have been repeatedly re-examined.[2] Resolution of the rotational structure has not been achieved, however, and even the character of the vibrations has been in doubt until quite recently. Three regions of fairly intense absorption are known; those at 2.7μ and 4.3μ were discovered by Langley, while the band at 14.9μ was first observed by Rubens and Aschkinass. The most complete map of the spectrum from 1μ to 15μ is given by Schaefer and Philipps, and includes many bands of low intensity. These show the curious property that none of the frequencies are either sums or differences of others in the set, which, according to Dennison,[3] indicates a linear symmetrical molecule. Other evidence also suggesting that the three atoms of CO_2 lie on a line has been presented by Eucken[4] from

[1] Langley, Phil. Mag. **15**, 153 (1883). Rubens and Aschkinass, Astrophys. J. **8**, 176 (1898).
[2] Coblentz, Carnegie Inst. Pub. **35** (1905); Burmeister, Verh. d. D. Phys. Ges. **15**, 589 (1913); E. v. Barh, Verh. d. D. Phys. Ges. **15**, 1150 (1913); Barker, Astrophys. Jour. **55**, 391 (1922); Ellis, Phys. Rev. **26**, 469 (1925); Schaefer and Philipps, Zeits. f. Physik **36**, 641 (1926).
[3] Dennison, Rev. Mod. Phys. **3**, 280 (1931).
[4] Eucken, Zeits. f. Physik **37**, 714 (1926).

a consideration of specific heats, and by Stuart[5] who found no permanent electric moment. However, not all of the experimental evidence has seemed to be consistent with this model. The lowest frequency fundamental, though unresolved, was observed as a broad doublet, instead of a triplet as would have been expected from linear molecules vibrating normally to their axes. Also the 2.7μ band appeared as a pair of doublets of almost equal intensity, the explanation for which has not been obvious.

We are now able to present observations on the two active fundamental bands at resolutions sufficient to reveal the rotational structure. These indicate that the molecule is in fact linear and symmetrical. Moreover, they may be satisfactorily correlated with the Raman lines and the whole series of combination bands, including the pair at 2.7μ, in such a manner as to leave no further doubt about the conclusion.

The mechanical problem of the vibrations and rotations of a symmetrical linear triatomic molecule has been discussed in detail by Dennison.[3] The symmetrical vibration ν_1 of the two extreme atoms along the line connecting them is optically inactive, since no change in electric moment results; it is not observed in the infrared. The symmetrical vibration ν_2 normal to the linear axis necessarily involves changes in electric moment having components along the axis of rotation, and must exhibit P, Q and R branches. It should correspond to the lowest fundamental frequency, observed at 14.9μ. Heretofore this has been reported as a broad doublet band, except in the recent observations by Sleator.[6] The third fundamental vibration ν_3 is an unsymmetrical one involving changes of electric moment normal to the axis of rotation, and giving rise to an intense absorption band at 4.3μ with P and R branches only. On the basis of these assignments the approximate numerical value of ν_1 may be computed. It should lie between ν_2 and ν_3, at a wave-length of about 8μ. The combination relations are particularly characteristic. While $\Delta\nu_1$ may be any integer, the value of $\Delta\nu_2+\Delta\nu_3$ must always be odd. Many possibilities are thus excluded, among them the first harmonic bands. Q branches occur only when $\Delta\nu_2$ is odd. The most intense of the combination bands to be expected are $\nu_3+2\nu_2$ and $\nu_3+\nu_1$, both doublets falling in the neighborhood of 2.7μ.

Most of the equipment used in this investigation has already been described. The grating spectrometer of highest resolution is the one recently used for observations on N_2O.[7] Although very effective for measurements with small absorption cells it cannot conveniently be used with long gas paths for detecting weak bands, nor is it so arranged as to be easily cleared of atmospheric components which absorb very strongly, making observations at certain wave-lengths almost impossible. Fortunately a second instrument was available which could be completely enclosed from source to thermopile. Although equipped with mirrors of shorter focus it gave a resolution sufficient to show the rotational structure of the 4.3μ band when the concentration of

[5] Stuart, Zeits. f. Physik **47**, 457 (1928).
[6] Sleator, Phys. Rev. **38**, 147 (1931).
[7] Plyler and Barker, Phys. Rev. **38**, 1827 (1931).

CO_2 was considerably reduced. This instrument could be filled with almost pure CO_2, or with air practically free of CO_2 as required, though it could not be evacuated. No absorption cells were used. The thermopile was a particularly good one, kindly supplied to us by Dr. Hardy, and, when connected with the Firestone amplifier and recording apparatus,[8] made continuous photographic records possible. We are indebted to Professor Randall for a thin KBr prism (angle 10°) made from a crystal grown under his direction and especially useful for observations beyond 15μ.

The Low-Frequency Fundamental ν_2

In determining the form of the CO_2 molecule a study of the lowest frequency fundamental band is crucial. Fig. 1 shows a series of energy curves for this region traced from the photographic records obtained with a com-

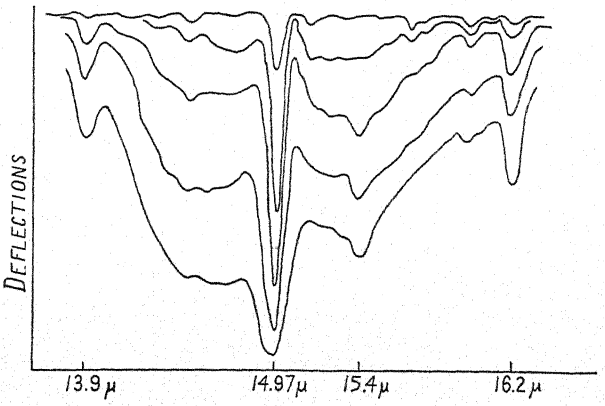


Fig. 1. Development of the 15μ band with increasing amounts of CO_2. Equivalent path lengths in cm at 76 cm pressure: 0.004, 0.05, 0.23, 0.68, 1.58.

pletely enclosed spectrometer using a coarse grating (960 lines per inch) and 1 mm slits. The narrow and intense zero branch is most striking. The whole case was washed for many hours with air from which the CO_2 had been removed, but a trace of this central maximum still persists in the upper curve. Small measured additions of gas very rapidly increase the intensity of the absorption. The estimated percentage absorbed at the peak has been plotted in Fig. 6 as a function of the equivalent length of path. The curves of Fig. 1 also show the development of the three secondary maxima described by Sleator, which lie at 13.9μ, 15.4μ and 16.2μ.

Energy curves for this same region under higher resolution are shown in Fig. 2. These were taken with a grating having 1200 lines per inch, used with a thin KBr foreprism. The slits included about 0.45 cm^{-1}. For the central portion the absorbing medium was about six meters of ordinary atmosphere, the equivalent path length in CO_2 being approximately 0.25 cm. The two lateral portions were obtained by increasing the quantity of CO_2 about one hundredfold. The structure of this absorption region is clearly revealed, and

[8] Firestone, Rev. Sci. Inst. 3, 163 (1932).

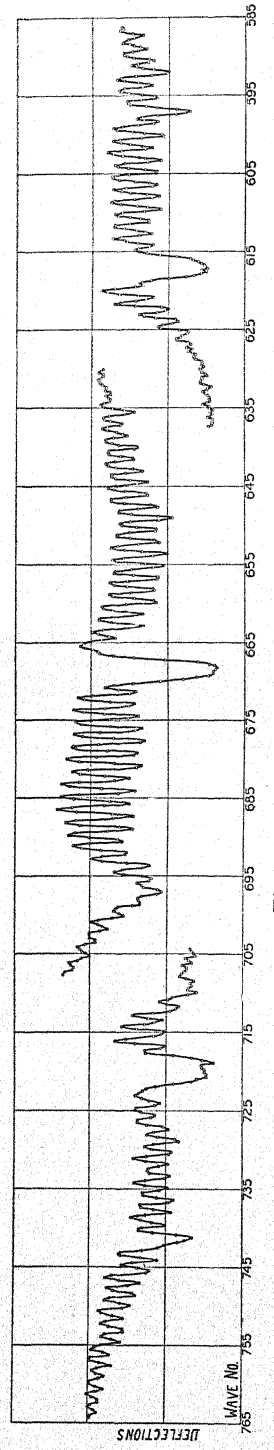


Fig. 2. Fine structure of the 15μ band.

though relatively simple, it is somewhat unusual. In addition to the strong central band with its P, Q and R branches, we find two of the secondary bands already mentioned, similar in structure and symmetrically placed at about ± 50 cm^{-1} from the center. Beyond these on either side and about 20 cm^{-1} farther out another sharp maximum of lesser intensity is found. The symmetry in arrangement and intensities is most striking, and assumes particular interest when the pattern is compared, as in Fig. 3A with the Raman spectrum observed by Dickinson, Dillon and Rasetti.[9] In fact this comparison provides an important means of checking the final interpretation. It should be remarked that the curious dip in the curve at about 697 cm^{-1} upon which the rotation lines are superposed, is not characteristic of CO_2, as it does not appear in the curves of Fig. 1.

Dennison's analysis of the motion associated with the frequency ν_2 assigns to each level two quantum numbers, of which V, the principal one, refers to the vibration state, while the subsidiary number L measures (in units

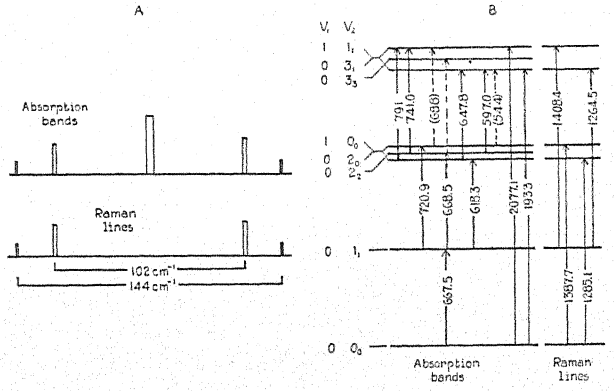


Fig. 3. Vibration levels and transitions involving ν_1 and ν_2.

of $h/2\pi$) the angular momentum about the linear axis which is introduced by the two dimensional vibration. Any transition in V is permitted, but L must change by ± 1 when ΔV is odd, and by 0 when ΔV is even. Combinations of these transitions with ν_1 are also possible, and in particular $\nu_1 - \nu_2$ may lie very close to ν_2. As has been shown[10] it is possible to interpret all of the observed CO_2 bands by this scheme, but not without certain curious intensity relations, and no explanation of the symmetry of the pattern is thus provided. Recently a modification has been introduced by Fermi[11] to take account of the interaction between the levels ν_1 and $2\nu_2$. This has been further developed by Dennison,[12] and in his notation has been introduced in the level

[9] Dickinson, Dillon and Rasetti, Phys. Rev. **34**, 582 (1929).

[10] This analysis of the absorption bands and its correlation with the observed Raman spectra, including the weaker transitions originating in the first excited state 1_1, were first reported at the Washington meeting of the Am. Physical Society in May, 1931. Phys. Rev. **37**, 1708 (1931).

[11] Fermi, Zeits. f. Physik **71**, 250 (1931).

[12] Dennison, Phys. Rev. **41**, 304 (1932).

diagram of Fig. 3B. When the carbon atom vibrates along a line normal to the molecular axis it is clear that the two oxygen atoms must swing along arcs so that the distance between them changes slightly, with two minima and two maxima per oscillation; i.e., the motion has a symmetrical component parallel to the axis, with frequency $2\nu_2$. This component alone is, of course, optically inactive. For CO_2 it happens that the frequencies ν_1 and $2\nu_2$ are almost exactly identical, so that a resonance interaction between them produces a pair of combined states (states whose wave functions are linear combinations of those appropriate to ν_1 and $2_0\nu_2$) separated rather widely and almost symmetrically with respect to their unperturbed position, which, of course, would not have been far from the level 2_2. A similar coupling occurs between succeeding pairs of states of like character, such as $3_1\nu_2$ and $\nu_1+1_1\nu_2$.[13]

The motion in the states designated 1_1, 2_2, 3_3 etc., is peculiar since it does not involve changes in the distances between atoms; the molecule is no longer linear but forms a very obtuse triangle which rotates without deformation about an axis parallel to its base. This motion is not coupled with ν_1, for no longitudinal oscillation accompanies it. Further, since there is no change in polarizability of the molecule during the motion, there can be no Raman transitions terminating at these levels.[14] Thus, none of the transitions $0_0\rightarrow1_1$, $0_0\rightarrow2_2$ or $1_1\rightarrow3_3$ is represented in the Raman spectrum.

The explanation of the patterns in Fig. 3A follows at once from this scheme of levels. The two strong Raman lines originate in the state 0_0, and the two weaker ones in the first excited state, as previously suggested.[10] The relative populations of these levels are as 13 to 1 (state 1_1 has a double weight). Infrared transitions to the same final states occur from 1_1 and 2_2 as common initial levels, the population ratio here being 26 to 1. The line $0_0\rightarrow1_1$ lies almost exactly at the midpoint, its frequency practically coinciding with that determined for $1_1\rightarrow2_2$ by subtracting 741.0 ($2_2\rightarrow3_1$) from the Raman frequency 1408.4. This indicates that for ν_2 the anharmonic term is very small, and also that ν_1 and $2\nu_2$ must coincide very exactly. It is not possible to locate the level 3_3 experimentally since the only line in which it is involved ($2_2\rightarrow3_3$) is completely masked.

The precise determination of the frequencies corresponding to the transitions indicated in Fig. 3 is rendered somewhat difficult by differences in convergence, which shift slightly the maxima of the observed zero branches, sometimes toward higher and sometimes toward lower frequencies. However, utilizing the combination principle, a consistent set of term values has been selected in which the errors probably do not exceed one half of a wave number (except for the level 3_3 which is not observed directly). These term values are listed in Table I, column 3. The positions of the vibration bands computed from them appear in column 4, while columns 5 and 6 show the observed

[13] As a result of discussions with Professor Kramers during the 1931 Summer Symposium in Ann Arbor we had already reached the conclusion before Fermi's paper appeared, that an interaction of this sort must be invoked to explain the infrared and Raman lines, but details had not been worked out.

[14] Placzek, Zeits. f. Physik **70**, 84 (1931).

wave numbers and the estimated relative intensities. A precise determination of intensities is not possible, for many of the lines are superposed upon a strong background, as in the case of 668.5 and 647.8. Furthermore, the differences in degree of convergence change the contours of the bands sufficiently so that some appear narrow and correspondingly more intense, while others are appreciably broadened. There is a tendency, also, to underestimate the absorption coefficient in regions which are almost opaque, as at the central maximum. It is somewhat surprising that the line at 688.7 has not been clearly revealed, when the corresponding one at 647.7 shows so distinctly. Both lie in regions of strong absorption due to rotation lines of the principal band. The line at 545.1 has also eluded observation although a search for it was made with the coarse grating and a path length of 200 cm of CO_2.

TABLE I. *Term values and vibrational transitions involving* ν_2.

Initial state			Vibration frequency		Relative
V_1	V_2	term value	computed	observed	intensities
			Fundamental bands		
0	0_0	0	667.5	667.5	10,000
			720.9	720.9	250
0	1_1	667.5	668.7	668.5	—
			618.3	618.3	250
			740.9	741.0	10
0	2_2	1336.2	669.5	—	—
			597.3	597.0	10
			791.3	791	1
1	0_0	1285.8	647.7	647.8	7
0	2_0	1388.4	688.7	—	—
			545.1	—	—
0	3_3	2005.7			
1	1_1	1933.5			
0	3_1	2077.1			
			Harmonic bands		
0	0_0		2077.1	2077.1	7
			1933.5	1933	1
			Raman lines		
0	0_0		1388.4	1387.7	15
			1285.8	1285.1	10
0	1_1		1409.6	1408.4	1
			1266.0	1264.5	1

The two second harmonic bands listed in Table I form a part of the absorption region near 4.9μ observed by Schaefer and Philipps. The trace of an energy curve for this region recorded automatically with a 200 cm path of CO_2 is shown in Fig. 5B. In addition to the two maxima listed, other absorption lines appear, probably due to transitions originating in excited states. A further study of this region is contemplated.

The agreement between the Raman frequencies observed by Dickinson, Dillon and Rasetti, and those computed from the term values in Table I

may be considered fairly satisfactory, though the differences are somewhat larger than our estimated errors. A better correspondence would result if our frequency scale were uniformly contracted about seven parts in ten thousand. This difference we believe to be considerably greater than our error of calibration.

Rotational Structure of the Bands at 15μ

As is well known, a necessary symmetry property of the wave function Ψ for a diatomic or a linear triatomic molecule with identical extreme atoms excludes either those alternate rotation states for which ψ_R is symmetrical, or those for which it is antisymmetrical, ψ_R being the factor of Ψ affected by an interchange of the identical atoms. It is to be expected, then, that for those vibration states of CO_2 in which $L=0$ the rotational quantum number J may assume only even or only odd values. Which of these sets is excluded depends upon the symmetry properties of the remaining factors of Ψ. When

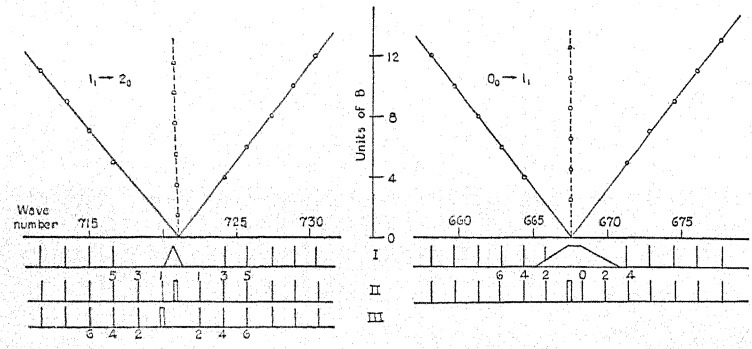


Fig. 4. Comparison of observed and predicted band patterns for $\Delta L = \pm 1$. I. Observed positions of the lines. II. Predicted positions for $\psi_R{}^0$ symmetrical. III. Predicted positions for $\psi_R{}^0$ antisymmetrical.

L is not zero the molecule is no longer precisely linear, and J may assume all integral values equal to or greater than L. In those bands involving the transitions $0 \rightarrow 1$ or $1 \rightarrow 0$ in L alternate rotation lines will be completely suppressed and the proper J transitions may be assigned only after it has been decided which are the missing levels. In the absence of zero branches this decision would not be difficult as the frequency interval between the first lines of the positive and negative series would be different for the two cases, but the zero branches are always present, and ordinarily are so broad as to obscure several of the neighboring rotation lines. If their positions could be determined precisely a criterion would be provided for assigning odd and even J values, as is indicated by the band patterns in the lower section of Fig. 4. The band centers at 13.9μ and 16.2μ are particularly favorable for observations of this sort, since, with atmosphere of normal CO_2 content, the central maxima appear weak and very narrow. The adjacent rotation lines are then too weak to be measured, but their positions can be determined, with higher concentrations of CO_2. We find the two zero branches to lie at 720.6 cm^{-1} and 617.9 cm^{-1}, with displacements toward lower frequencies as the concentrations are

increased. The rotation lines adjacent to the former, taken from Fig. 2, have been plotted in the upper section of Fig. 4 just above the characteristic band pattern for $\Delta L = -1$, and the position of the zero branch shows clearly that even numbers must be used for the J values of the upper state ($L = 0$); hence also for the normal state. This is in contrast with the molecule O_2 which, for the nonvibrating state, has only odd J values. It indicates that for CO_2 ψ_R must have the same symmetry as ψ_V. The intersection of the two straight lines falls at 720.9, which is the value given in Fig. 3 as the vertex of the zero branch, and in Table I as the band center. For the other band the coincidence is equally good, the indicated center being 618.3 cm^{-1}. Because of its great intensity we have not determined the position of the strongest zero branch at 14.9μ with equal precision, but since in the initial state (0_0) the J values are even, its frequency may be obtained graphically as on the right of Fig. 4, from the positions of the observed rotation lines. The value so obtained is 667.5 cm^{-1}.

TABLE II. *Wave numbers and wave-number differences in the band at 14.9μ.*

Initial J	Observed frequencies $\Delta J=+1$	$\Delta J=-1$	D	D'	$h/4\pi^2cI$	$h/4\pi^2cI'$	ν computed $\Delta J=0$
4	671.3	664.4	8.4	6.9	0.762	0.765	667.5
6	672.8	662.9	11.5	9.9	0.767	0.762	667.5
8	674.5	661.3	14.8	13.2	0.778	0.777	667.5
10	676.0	659.7	17.8	16.3	0.774	0.777	667.5
12	677.6	658.2	20.9	19.4	0.774	0.776	667.5
14	679.2	656.7	24.1	22.5	0.777	0.777	667.6
16	680.8	655.1	27.2	25.7	0.777	0.778	667.6
18	682.5	653.6	30.4	28.9	0.780	0.781	667.7
20	684.1	652.1	33.6	32.0	0.782	0.780	667.7
22	685.7	650.5	36.7	35.2	0.781	0.783	667.7
24	687.3	649.0	39.8	38.3	0.780	0.782	667.8
26	689.0	647.5	43.0	41.5	0.782	0.783	667.9
28	690.6	646.0	46.2	44.6	0.782	0.783	667.9
30	692.1	644.4	49.0	47.7	0.778	0.783	667.9
32	693.7	643.1	52.2	50.6	0.780	0.780	668.0
34	695.3	641.5	55.4	53.8	0.780	0.780	668.1
36	697.0	639.9	58.5	57.1	0.780	0.783	668.1
38	698.6	638.5	61.6	60.1	0.780	0.781	668.2
40	700.1	637.0	64.6	63.1	0.780	0.780	668.2
42	701.8	635.5		66.3		0.780	668.3
44	703.3						
46	705.2						
48	706.7						

The wave numbers as measured for the various rotation lines are shown in Table II with this assignment of J values. Frequency differences characteristic of the upper and lower vibration states have been obtained in the usual way, i.e.,

$$[J \rightarrow J'] - [(J+2) \rightarrow J'] = [J \rightarrow (J+2)] = (2J'+1)B$$

and

$$[J \rightarrow J'] - [J \rightarrow (J'-2)] = [J' \rightarrow (J'-2)] = (2J+1)B'.$$

These are tabulated under the headings D and D', the primes referring to the upper state. The half interval between rotation lines, $B = h/4\pi^2cI$, is obtained

by dividing these differences by the appropriate integers, the results appearing in the 6th and 7th columns. The 8th column shows the positions of the zero branch lines as determined by subtracting $h/8\pi^2cI$ from the corresponding means of columns 2 and 3. The effect of rotation upon the vibration frequency is seen to be very small. Within the limits of experimental error the positions of the zero branch lines are represented by the formula

$$\nu = 667.5 + 0.00045J^2.$$

Clearly the moment of inertia is affected very little by the change in state of vibration. The mean value of $h/4\pi cI$ is practically 0.780, and consequently $I = 70.8 \times 10^{-40}$ gr. cm^2. Here a little less weight has been assigned to the low rotation states, where larger errors are to be expected. In the same way we find the value $I' = 70.7 \times 10^{-40}$. These results agree very well with the value $I = 70.2 \times 10^{-40}$ obtained from measurements upon rotational Raman spectra by Houston and Lewis.[15] It is to be noted that these authors also reach the conclusion that the J's must be even for the nonvibrating molecule.

Since each of the bands corresponding to absorption from the first vibration state is at least partially obscured by the more intense fundamental, a similar treatment may be applied to them only for the lower rotation states, and much smaller precision is to be expected. The resulting moments of inertia, computed from the wave numbers appearing in Table III are 67.3×10^{-40} for the 13.9μ band, and 73.6×10^{-40} for the 16.4μ band.

TABLE III. *Wave numbers of rotation lines in the bands at 13.9μ and 16.2μ.*

Band at 13.9μ		Initial	Band at 16.2μ	
$\Delta J=+1$	$\Delta J=-1$	J	$\Delta J=+1$	$\Delta J=-1$
—	—	1	—	—
724.2	—	3	620.9	—
725.7	716.6	5	622.8	614.1
727.4	715.0	7	623.9	612.7
728.9	713.5	9	625.3	611.2
730.4	711.7	11		609.6
731.8		13		607.9
733.4		15		606.4
734.9		17		604.8
736.5		19		603.3
738.0		21		601.6
739.5		23		600.1
741.2		25		598.4
744.1		27		596.9
745.5		29		595.3
747.0		31		593.7
748.5		33		592.0
749.9		35		590.5
751.5		37		589.0
753.1		39		587.2
754.6		41		

THE FUNDAMENTAL BAND AT 4.3μ

The absorption associated with the other active fundamental is so intense that near the center of the band observations through ordinary atmos-

[15] Houston and Lewis, Proc. Nat. Acad. 17, 229 (1931).

phere are difficult and show very little contrast. Fig. 5C represents a typical set of absorption measurements for this region, plotted against frequencies. The rotation lines are fairly obvious on the low-frequency side of the center, but on the high-frequency side where they are closer together and the absorption is stronger, their positions can be determined only in rough approximation. Table IV shows the average values taken from this and several similar curves, and the corresponding values of $h/4\pi^2cI$ and $h/4\pi^2cI'$. The precision is much less than for the observations given in Table II, but the indicated value for the moment of inertia is practically the same. The values of ν_3 com-

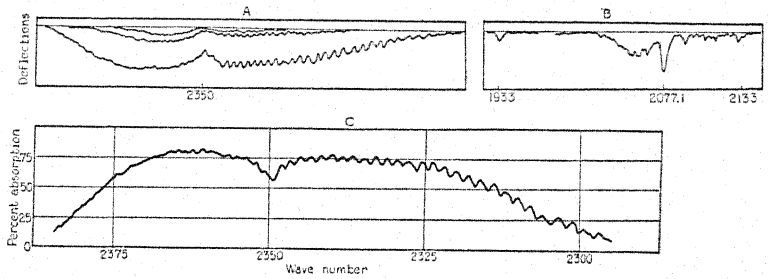


Fig. 5. *A* and *B:* Energy curves traced from automatic records for ν_3 at 4.3μ and $3\nu_2$ at 5μ; *C:* Absorption curve for ν_3 from point by point observations.

TABLE IV. *Wave numbers and wave-number differences in the band at 4.3μ.*

Initial J	Observed frequencies $\Delta J=+1$	$\Delta J=-1$	D	D'	$h/4\pi^2cI$	$h/4\pi^2cI'$	ν computed $\Delta J=0$
0	2350.9	—	2.6		0.867		
2	2352.7	2348.3	5.9	4.3	0.843	0.860	2350.1
4	2354.0	2346.8	8.7	7.2	0.791	0.800	2350.0
6	2355.5	2345.3	12.0	10.2	0.800	0.786	2350.0
8	2356.9	2343.5	15.0	13.4	0.789	0.787	2349.8
10	2358.1	2341.9	18.0	16.2	0.784	0.771	2349.6
12	2359.6	2340.1	21.2	19.5	0.785	0.780	2349.5
14	2361.0	2338.4	24.3	22.6	0.785	0.780	2349.3
16	2362.7	2336.7	27.8	26.0	0.794	0.787	2349.3
18	2364.0	2334.9	31.0	29.1	0.795	0.787	2349.1
20	2365.2	2333.0	33.8	32.2	0.786	0.785	2348.7
22	2366.4	2331.4	36.7	35.0	0.781	0.779	2348.5
24	2367.7	2329.7	40.1	38.0	0.787	0.776	2348.3
26	2369.0	2327.6	43.5	41.4	0.790	0.780	2347.9
28	2370.2	2325.5	46.7	44.7	0.790	0.784	2347.5
30	2371.2	2323.5	49.6	47.7	0.787	0.782	2347.0
32	—	2321.6					
34	—	2319.8					
36	—	2317.9					
38	2375.3	2315.7	61.5	59.6	0.780	0.776	2345.1
40	2376.3	2313.8	64.5	62.5	0.777	0.772	2344.6
42	2377.2	2311.8	67.5	65.4	0.776	0.770	2344.1
44	2378.0	2309.7	70.3	68.3	0.774	0.768	2343.5
46	2378.7	2307.7		71.0		0.765	2342.8

puted as before by averaging the numbers in columns 2 and 3 and subtracting $h/8\pi^2cI$ are shown in column 8. These may be satisfactorily represented by the equation

$$\nu_3 = 2350.1 - 0.0035J^2.$$

The convergence is larger than for the other band, but not extremely large, and hardly explains the great asymmetry of the emission band. The very strong emission observed beyond 4.4μ[16] is doubtless due in large measure to transitions between states both of which are vibrationally excited.

With the enclosed spectrometer it was possible to remove all traces of this band by washing for many hours with air from which the CO_2 had been removed. A small amount of gas was replaced, and records run with the 7200 line grating and very narrow slits. The rotation structure then showed up clearly on the low-frequency side, but on the high-frequency side was scarcely more distinct than in the plotted curve. Envelopes traced from the photographic records are shown in Fig. 5A, for quantities of CO_2 equivalent to 0.01, 0.02 and 0.11 cm path length at normal pressure. A number of such curves were obtained after adding successively measured amounts of pure CO_2, and

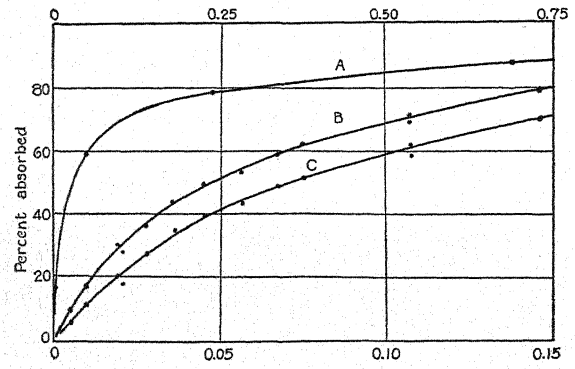


Fig. 6. Dependence of absorption upon path length. Abscissae are equivalent lengths in cm of CO_2 at one atmosphere. *A:* Zero branch of 15μ band, 668 cm^{-1} (upper scale). *B* and *C:* Maxima of 4.3μ band at 2365 and 2340 cm^{-1} (lower scale).

from each the percentage absorption at the two maxima was determined. These values are plotted in Fig. 6, curves *B* and *C*.

Harmonic and Combination Bands

The preliminary measurements upon the second harmonic of ν_2 in the region near 4.8μ have already been mentioned. These provide precise term values for the pair of interacting levels $\{(\nu_1+1_1\nu_2),3_1\nu_2\}$. With better resolution it may also be possible to identify lines originating in the level 1_2, thus determining the positions of the various compound levels involving 4_0 and 4_2. No first harmonic of ν_3 appears, but the selection rules permit the transition $\Delta V_3=3$, and a weak band has been observed in the proper position, 1.4μ, by Schaefer and Philipps.

The strong double band at 2.7μ has not yet been remeasured, but its character and position are well known. It corresponds to the allowed transitions $\nu_3+\{\nu_1,2\nu_2\}$ where the bracket represents the pair of interacting states at 1285 and 1388 cm^{-1}. Both components are doublet bands, in agreement with the

[16] Cf. Barker, reference 1.

prediction for $\Delta L = 0$. The fact that their intensities are almost equal again indicates the close resonance between ν_1 and $2\nu_2$, for both of the compound levels must partake about equally of the two component motions. A considerably weaker group of bands appears in the neighborhood of 2μ, and is doubtless to be interpreted as

$$\nu_3 + \{2\nu_1, \nu_1 + 2_0\nu_2, 4_0\nu_2\}$$

but this also remains to be examined in detail. The next member of the same sequence, obtained by adding $\{\nu_1, 2\nu_2\}$ would account for the observed bands near 1.6μ.

With very large amounts of absorbing gas Schaefer and Philipps have also located a pair of bands at 9.4μ and 10.4μ absorbed by molecules already excited to the first pair of interacting levels, and corresponding to the transitions $\nu_3 - \{\nu_1, 2_0\nu_2\}$. There remains the very weak band at 3.28μ, in a position corresponding to $\nu_2 + \nu_3$, a combination which is in apparent contradiction with the rule that $\Delta V_2 + \Delta V_3$ must be odd. If further observation definitely confirms this absorption, and if no other interpretation appears, then the question must be raised whether or not the restriction is absolute.

Thus with one possible exception every observed band is in complete accord with the vibration spectrum predicted by Dennison's rules for a linear symmetrical molecule. The fine structure of the fundamental bands leads also to the conclusion that the molecule must have the linear form O:C:O. Finally the Raman spectra, both vibrational and rotational, may be explained only in terms of the same model. All existing observational data seem now to be consistently correlated.

The Vibrational Levels of Linear Symmetrical Triatomic Molecules

By DAVID M. DENNISON
University of Michigan

(Received June 17, 1932)

The theory proposed by E. Fermi of the energy levels of molecules of the CO_2 type is discussed. It is shown that this assumes a particularly simple form when expressed in the coordinates used by Dennison for describing such molecules. When there exist no integral or nearly integral relations between the vibrational frequencies the first order energy correction λW_1 caused by the anharmonic forces vanishes leaving only the second order term $\lambda^2 W_2$. When, however, two of the fundamental frequencies are commensurable, certain of the energy levels coincide thus becoming degenerate. This degeneracy may be removed by the anharmonic forces in which case there appears a first order energy constant λW_1 different from zero. The value of λW_1 is computed explicitly for certain of the lower energy states and it appears that the only levels which interact under the influence of the resonance are those having the same value of the azimuthal quantum number l. From this it follows that the selection rules are not affected by the existence of the resonance. Finally it is shown how the first order term λW_1 goes over into the second order term $\lambda^2 W_2$ as the resonance between the frequencies becomes less and less exact. When these results are applied to the CO_2 spectrum it is found that the resonance between ν_1 and $2\nu_2$ is almost perfect and consequently the energy levels can only be ordered with the help of the first order term λW_1. For CS_2 on the other hand the difference between ν_1 and $2\nu_2$ is so large that the effect of the resonance on the positions of the energy levels may be disregarded.

WITHIN the last few months two important contributions have been made to our knowledge of the carbon dioxide molecule and its infrared spectrum. The first of these was contained in a paper by E. Fermi[1] and was intended in the first instance to explain the Raman spectrum of CO_2.The second, by P. E. Martin and E. F. Barker,[2] is reported in the foregoing paper and consists of an experimental study of the fine structure of certain of the infrared bands. It is proposed in the present paper to discuss Martin and Barker's results in the light of Fermi's theory and to relate both to the earlier work of Dennison[3] on the general properties of symmetrical molecules of the type YX_2.

It can no longer be doubted that the carbon dioxide molecule in its normal electronic state possesses a form which is both linear and symmetrical. Two sets of independent data prove this. The fact that the fine structure lines of the parallel type band at 4.3μ and of the perpendicular type band at 15μ both are linearly spaced in frequency and have the same spacing constant shows that the CO_2 molecule must be linear. The fact that alternate fine structure lines of these bands have zero intensity shows that the mole-

[1] F. Fermi, Zeits. f. Physik **71**, 250 (1931).
[2] P. Martin and E. F. Barker, Phys. Rev. **41**, 291 (1932).
[3] D. M. Dennison, Rev. Mod. Phys. **3**, 280 (1931).

cule must have the form O=C=O and not O=O=C. The second reason for believing that CO_2 is both linear and symmetrical is that it has been shown that the vibrational levels of such molecules are connected by rather unusual selection rules which permit only certain of the overtone bands to appear. A study of all the known infrared bands of CO_2 reveals that just the permitted overtones and no others are observed.

In discussing the positions of the vibrational levels of the molecule YX_2, the notation proposed by Dennison[3] will be used as well as the same coordinates. The internal or vibrational degrees of freedom are four in number since of the total $3n$ or 9 degrees of freedom, three may be associated with translation of the system as a whole and two (not three, since the molecule is linear) with rotation of the system. The coordinates of the vibrational motion are chosen as z, q, r and ϕ. z is the displacement of the Y atom along the figure axis relative to the center of gravity of the X atoms. q is the displacement of the X atoms, from their equilibrium position, relative to each other. r is the displacement of the Y atom $\perp$ to the figure axis relative to the line joining the X atoms and ϕ is the angle this latter displacement makes in a plane $\perp$ to the figure axis.

The kinetic energy of the system (internal) may be readily computed and is,

$$T = (m/4)\dot{q}^2 + (\mu/2)(\dot{z}^2 + \dot{r}^2 + r^2\dot{\phi}^2)$$

where m is the mass of an X atom and μ is the reduced mass $2mM/(M+2m)$.

We assume that the potential energy U possesses a symmetry which corresponds with the geometric symmetry of the molecule. That is, U must be an even function of z, an even function of r and independent of the angle ϕ.

We assume that the potential function may be developed after λ, a parameter of smallness so that $U = U_0 + \lambda U_1 + \lambda^2 U_2$. The function U_0 contains all the permissable terms which are quadratic in the coordinates, U_1 all the cubic terms and U_2 all the quartic terms. It is usual to let the constants of U_0 contain the normal frequencies ν_1, ν_2 and ν_3 so that it has the form,

$$U_0 = \pi^2\nu_1^2 mq^2 + 2\pi^2\nu_2^2\mu r^2 + 2\pi^2\nu_3^2\mu z^2.$$

The wave function which results from using a wave equation based on T and U_0 has been already described by Dennison.

$$\psi = \psi_{(\sigma)}{}^{V_1}\psi_{(\xi)}{}^{V_3}R_{(\rho)}{}^{V_2 l}e^{\pm il\phi}$$

where $\psi_{(\sigma)}{}^{V_1}$ and $\psi_{(\xi)}{}^{V_3}$ are the well-known Hermitian orthogonal functions.

$$R_{(\rho)}{}^{V_2 l} = \rho^l e^{-\rho^2/2}\sum_{k=0}^{V_2-l} a_k\rho^k$$

where

$$a_{k+2} = \frac{2k + 2l - 2V_2}{(k+2)(k+2+2l)}a_k.$$

The dimensionless variables σ, ξ and ρ, replace the coordinates q, z and r and are related to them by the following expressions,

$$\sigma = 2\pi[\nu_1 m/2h]^{1/2}q$$
$$\xi = 2\pi[\nu_3 \mu/h]^{1/2}z$$
$$\rho = 2\pi[\nu_2 \mu/h]^{1/2}r.$$

It will prove convenient to write the energies T and U in terms of these variables.

$$T = (h/8\pi^2)\{\dot{\sigma}^2/\nu_1 + \dot{\xi}^2/\nu_3 + (\dot{\rho}^2 + \rho^2\dot{\phi}^2)/\nu_2\}$$
$$U_0 = (h/2)\{\nu_1\sigma^2 + \nu_3\xi^2 + \nu_2\rho^2\}$$
$$\lambda U_1 = \lambda h(a\sigma^3 + b\sigma\rho^2 + c\sigma\xi^2)$$
$$\lambda^2 U_2 = \lambda^2 h(d\sigma^4 + e\rho^4 + f\xi^4 + g\sigma^2\rho^2 + i\xi^2\sigma^2 + j\rho^2\xi^2).$$

The quantities λ, $a, \cdots j$ are constants which characterize the anharmonic nature of the potential function. It will be noted that the condition that U must possess a symmetry which corresponds to the geometric symmetry of the molecule, greatly reduces the number of terms appearing in U_1 and U_2. Thus of the ten cubic terms which may be formed with three variables, only three actually appear in U_1.

The energy constant W of the system may be developed in powers of λ so that $W = W_0 + \lambda W_1 + \lambda^2 W_2$. The zeroth order term W_0 has of course the form,

$$W_0/h = \nu_1(V_1 + \tfrac{1}{2}) + \nu_2(V_2 + 1) + \nu_3(V_3 + \tfrac{1}{2})$$

where V_1, V_2, and V_3 are the quantum numbers appearing in the expression for the wave function. Since the number l does not appear in W_0, the system is in this approximation (V_2+1) fold degenerate.

The terms W_1 and W_2 which arise from the anharmonic nature of the potential function may be readily computed using perturbation theory methods. In the usual case when the frequencies ν_1, ν_2 and ν_3 are incommensurable, this leads to the following result.

$$\lambda W_1 = 0$$
$$\lambda^2 W_2/h = x_0 + x_1V_1 + x_2V_2 + x_3V_3 + x_{11}V_1^2 + x_{22}V_2^2 + x_{ll}l^2 + x_{33}V_3^2 + x_{12}V_1V_2 + x_{13}V_1V_3 + x_{23}V_2V_3$$

$x_0, \cdots x_{23}$ are a set of constants[4] which are related to the anharmonic constants $a, \cdots j$.

The important contribution of Fermi consists in an investigation of the system when two of the frequencies bear a commensurable or nearly commensurable relation to each other. He has been able to show that when $\nu_1 \cong 2\nu_2$ the first order energy constant λW_1 no longer vanishes and may exert a very considerable influence in the energy levels. We propose to make clear just how this result obtains and how it may be correlated with the observed infrared spectrum of CO_2.

[4] Dennison (reference 3) in giving the formula for $\lambda^2 W_2$ stated that the constant x_{ll} was equal to $-\frac{1}{2}x_{22}$. Unfortunately this statement is incorrect except in the special case where $\lambda U_1 = 0$. In general an independent constant x_{ll} must be introduced.

It will become evident from the analysis that when $\nu_1 \cong 2\nu_2$, λW_1 depends solely upon the anharmonic term $b\sigma\rho^2$ while if ν_1 were approximately twice ν_3, λW_1 would depend entirely upon $c\sigma\xi^2$. For CO_2 as well as CS_2 it is the former condition which holds and we may therefore confine our attention to the term $b\sigma\rho^2$.

We shall first carry out the computation, assuming first that no commensurable relation exists between ν_1 and ν_2. It is possible to ignore the existence of the vibration ν_3 since its coordinate ξ does not enter the part of U_1 we are considering. In fact we may without loss of generality confine ourselves to the case where $\lambda U_1 = \lambda h b \sigma \rho^2$ and $\lambda^2 U_2 = 0$. The usual methods of perturbation theory then give

$$\lambda W_1 = \lambda U_{1V_1V_2l}^{V_1V_2l}$$

$$\lambda^2 W_2 = \lambda^2 \sum_{V_1'V_2'} \left(U_{1V_1'V_2'l}^{V_1V_2l} \right)^2 \Big/ \left(W_0^{V_1V_2} - W_0^{V_1'V_2'} \right)$$

where $U_{1\,V_1'V_2'l}^{V_1V_2l}$ is the matrix element of U_1.

The general expression for the perturbation energy has been slightly simplified since we take only those matrix elements of U_1 which are diagonal in l and omit the corresponding integration over ϕ. This is permissible since the function U_1 is independent of ϕ and therefore all the matrix elements which are nondiagonal in l automatically vanish. It is supposed that ψ^{V_1} and $R^{V_2\,l}$ are properly normalized.

It is clear that the matrix elements of U_1 which are diagonal in V_1 must vanish since $(\psi^{V_1})^2$ is an even function of σ while the function U_1 is odd. Evidently then $\lambda W_1 = 0$. The computation of $\lambda^2 W_2$ is somewhat tedious but quite straight-forward and leads to the following result.

$$\lambda^2 W_2 = -\frac{\lambda^2 b^2 h}{8} \left\{ \frac{V_2^2 + 4V_1V_2 - l^2 + 4V_1 + 4V_2 + 4}{\nu_1 + 2\nu_2} + \frac{V_2^2 - 4V_1V_2 - l^2 - 4V_1}{\nu_1 - 2\nu_2} + \frac{4(V_2+1)^2}{\nu_1} \right\}.$$

The expression for $\lambda^2 W_2$ which has been obtained is valid except in the region where ν_1 and $2\nu_2$ are approximately equal. In this case $\lambda^2 W_2$ becomes of higher order of magnitude and the whole method of the perturbation theory which has been used breaks down. A new method must then be employed which leads to the result that when $\nu_1 \cong 2\nu_2$, a first order perturbation energy λW_1 exists.[5]

We begin by letting the unperturbed system be one where ν_1 and $2\nu_2$ are exactly equal, thus making a number of the previously distinct energy levels coincide. It is possible as before to ignore the vibration ν_3 and its coordinate ξ and to introduce the single anharmonic term $\lambda U_1 = \lambda h b \sigma \rho^2$. To this however

[5] We may remark that λW_1 and $\lambda^2 W_2$ will be given by the above expressions even when $\nu_1 \cong 2\nu_2$ for the particular states where the quantum numbers bear the relation $V_2^2 - 4V_1V_2 - l^2 - 4V_1 = 0$. This conclusion is borne out by the results of the ensuing investigation.

must be added a term involving $\Delta = \nu_1 - 2\nu_2$ to take account of the fact that in the final or perturbed system ν_1 is only of the same order but not necessarily equal to $2\nu_2$. The problem may then be treated in a manner similar to that used by Fermi, namely by the standard method of perturbations of a degenerate system.[6]

The unperturbed system may be characterized by T_0 and U_0 and the effect of the perturbation grouped into the two terms T_1 and λU_1.

$$T_0 = (h/8\pi^2\nu_2)(\dot{\sigma}^2/2 + \dot{\rho}^2 + \rho^2\dot{\phi}^2)$$
$$U_0 = (h\nu_2/2)(2\sigma^2 + \rho^2)$$
$$T_1 = (\Delta h/32\pi^2\nu_2^2)\dot{\sigma}^2 = -(\Delta h/2)(\partial^2/\partial\sigma^2)$$
$$\lambda U_1 = \lambda hb\sigma\rho^2 + \Delta h\sigma^2/2.$$

The unperturbed system having the kinetic and potential energies T_0 and U_0 respectively possesses an energy constant $W_0/h = \nu_2(2V_1 + V_2 + 2)$. The unperturbed system is thus degenerate in two ways, first because as before W_0 is independent of the quantum number l and second because the energy does not depend upon V_1 and V_2 separately but only upon the function $2V_1 + V_2$.

To find the first order perturbed energy of a degenerate system, the secular determinant must be constructed and set equal to zero.

$$\left| A_s{}^r - \lambda W_1 \delta_s{}^r \right| = 0.$$

The roots of this determinant λW_1 furnish the required perturbed energies. The quantity $A_s{}^r$ is the matrix element of the perturbing function $T_1 + \lambda U_1$.

The quantum numbers for any one secular determinant must belong to the same value of W_0, that is $2V_1 + V_2 =$ a constant. We may simplify the expression for $A_s{}^r$ by noting two properties of the system. (a) All the elements which are nondiagonal in l vanish since $T_1 + \lambda U_1$ is independent of the angle ϕ. (b) The wave function ψ^{V_1} satisfies the differential equation $(d^2\psi^{V_1}/d\sigma^2) + (2V_1 + 1 - \sigma^2)\psi^{V_1} = 0$ and therefore $(T_1 + \lambda U_1)\psi^{V_1} = \{\lambda hb\sigma\rho^2 + \Delta h(V_1 + \frac{1}{2})\}\psi^{V_1}$. Combining these properties with the other known properties of the unperturbed wave functions, we may express all the nonvanishing elements of $A_s{}^r$ as follows,

$$A^{V_1 V_2 l}_{V_1 V_2 l} = \Delta h(V_1 + \tfrac{1}{2})$$
$$A^{V_1 \quad V_2 \quad l}_{V_1 - 1 V_2 + 2 l} = -\lambda hb(V_1)^{1/2}\left[(V_2 + 2)^2 - l^2\right]^{1/2}/2^{3/2}.$$

The secular determinant may now easily be constructed for any value of $2V_1 + V_2$. The coordinate system we have used allows the determinant to be evaluated very simply since, because the elements $A_s{}^r$ which are nondiagonal in l all vanish, the determinant may be factored into a set of determinants each corresponding to a particular value of l. Thus if $2V_1 + V_2$ equals 4, the

[6] While our computation is quite equivalent to that performed by Fermi and leads to the same result we feel that a real advantage is secured by our use of the coordinates σ, ρ and ϕ. Not only is the calculation much simpler but it is found that the final results may be presented in a very natural form which allows a clear understanding of their interrelations.

original determinant is of 9th order. It can be factored into three determinants of order 3, 2, 2, 1 and 1 corresponding to $l=0$, $+2$, -2, $+4$ and -4 respectively.

The explicit solutions of the secular determinant for the smaller values of the quantum members are presented in Table I.

TABLE I.

V_1	V_2	l	$\lambda W_1/h$
0	0	0	$\Delta/2$
0	1	±1	$\Delta/2$
1	0	0	$\Delta\pm[\Delta^2/4+(\lambda b)^2/2]^{1/2}$
0	2	0	
0	2	±2	$\Delta/2$
1	1	±1	$\Delta\pm[\Delta^2/4+(\lambda b)^2]^{1/2}$
0	3	±1	
0	3	±3	$\Delta/2$
2	0	0	$(\lambda W_1)^3-(9/2)\Delta h(\lambda W_1)^2$
1	2	0	$-[3(\lambda hb)^2-(2\ 3/4)\ (\Delta h)^2]\lambda W_1$
0	4	0	$-(1\ 5/8)\ (\Delta h)^3+(1\ 1/2)\ (\lambda bh)^2\Delta h=0$
1	2	±2	$\Delta\pm[\Delta^2/4+(3/2)\ (\lambda b)^2]^{1/2}$
0	4	±2	
0	4	±4	$\Delta/2$

The degeneracy that originally existed in the unperturbed system has been to a considerable extent removed by the perturbing potential and the identities of the levels have been somewhat changed. When two or more levels are connected by lines in the above table, we mean that the original degeneracy of the levels has been removed. The wave functions which are appropriate for describing these new undegenerated levels are linear combinations of the wave functions of the degenerate levels. The coefficients in the linear combinations are given by the first minors of the secular determinant in question.

We should now like to show how the energy constant of second order $\lambda^2 W_2$ which is appropriate for the case $\nu_1 \neq 2\nu_2$ goes over into the first order constant λW_1 when $\nu_1 \cong 2\nu_2$. In order to compare these two expressions, values of $\Delta=\nu_1-2\nu_2$ must be chosen which are small compared with $\nu_1+2\nu_2$ but which are large compared with the anharmonic constant λb. The leading term of $\lambda^2 W_2$ is then $-\lambda^2 b^2 h(V_2^2-4V_1V_2-4V_1-l^2)/\Delta$ while the expressions for λW_1 may be developed. Thus the energy levels of the states (100) and (020) become $(3/2)\Delta h+\lambda^2 b^2 h/2\Delta$ and $(1/2)\Delta h-\lambda^2 b^2 h/2\Delta$. The terms $(3/2)\Delta h$ and $(1/2)\Delta h$ when added to the W_0 of the degenerate system ($\nu_1=2\nu_2$) are just equal to the W_0 of the undegenerate system and the remaining terms $\pm\lambda^2 b^2 h/2\Delta$ are just equal to $\lambda^2 W_2$ when we substitute the appropriate values of the quantum numbers. A similar agreement is found between λW_1 and $\lambda^2 W_2$ for all the other levels which have been computed.

This analysis leads to a criterion as to the method to be used in correlating the energy levels of such a system. When $|\Delta| \leq |\lambda b|$ we must treat the system as degenerate and use the first order energy constant λW_1. A second

order constant $\lambda^2 W_2$ could also be added and would probably have the usual form (i.e., a quadratic function of the quantum numbers). When $|\Delta| \gg |\lambda b|$, λW_1 becomes equal to one of the terms of $\lambda^2 W_2$ and consequently we may order the levels with the aid of the second order constant $\lambda^2 W_2$ alone. The difference between these cases will be brought out in our discussion of the CO_2 and CS_2 spectra.

Finally it will be observed that the selection rules proposed by Dennison for the symmetrical triatomic molecules apply equally well to the degenerate system and to the nondegenerate system for which they were derived. The states of the degenerate system which combine and lose their identity possess wave functions having the same quantum numbers l and V_3 and having numbers V_2 which differ by an even integer. The selection rules depend upon whether the changes ΔV_2, ΔV_3 and Δl are odd or even integers and these changes will be the same (i.e., odd or even) for all the levels of a related group. The wave functions of a related group all have the same symmetry character with regard to an interchange of the two equal atoms.

Discussion of the CO_2 Spectrum

Let us now consider the energy levels of the CO_2 molecule as determined by the observations of Martin and Barker. If the assumption is made that the system is nearly degenerate ($|\Delta| \ll |\lambda b|$), the energy may be expressed as $W_0 + \lambda W_1$ and the second order terms $\lambda^2 W_2$ may be neglected. This identification will allow us to compute from three of the levels Δ and λb (thus checking the assumption as to the degeneracy) and then to predict the positions of the remaining levels. The difference between the predicted and observed positions of these levels will be a measure of the neglected term $\lambda^2 W_2$. The results of this correlation are collected in Table II where the lowest state (000) is taken to have zero energy.

Table II.

V_1	$\nu_2 = 667.5$ cm^{-1} V_2	l	$\lambda b = \pm 72.5$ cm^{-1} Observed level	$\Delta = +4.2$ cm^{-1} Computed level
0	0	0	0	0
0	1	1	667.5 cm^{-1}	—
1	0	0	1285.8	—
0	2	0	1388.4	—
0	2	2	1336.2	1335.0
1	1	1	1933.5	1932.1
0	3	1	2077.1	2077.1
0	3	3	—	2004.6
2	0	0	—	2548.0
1	2	0	—	2675.6
0	4	0	—	2799.0

It appears that in CO_2 the resonance between ν_1 and $2\nu_2$ is almost exact so that their difference is small, $\Delta = 4.2$ cm^{-1}. The accuracy with which this constant has been determined is not great. We estimate the error to be of the order of 50 to 100 percent. The value of $|\lambda b|$ on the other hand may be fixed with considerable precision since it depends essentially on the distance

between the two strong Raman bands or between certain of the infrared bands. It is probably accurate to at least 1 percent. It will be noted that the sign of λb cannot be determined through the positions of the energy levels.

The overtone bands of CO_2 which have been observed by Barker[7] and others to lie in the region of 2.7μ must be correlated with the sum of the levels (100), (020) and the level $\nu_3 = 2350$ cm^{-1}. The computed values of these overtone frequencies are therefore 3636 and 3738 cm^{-1} while their observed positions are 3610 and 3717 cm^{-1}. The differences, 24 and 21 cm^{-1}, are due to the fact that in the computation we have neglected the second order energy constant $\lambda^2 W_2$. In a similar way the three overtone bands observed by Schaefer and Philipps[8] at about 2μ arise from a combination of the level ν_3 with the levels (200), (120), (040). The computed values of the frequencies are 4898, 5026 and 5149 cm^{-1}, while their observed positions are 4780, 4890 and 5010 cm^{-1}. The differences, which are also due to the neglected second order terms, are 118, 136 and 139 cm^{-1} respectively. We should expect these differences to be larger than those for the lower overtone bands but only by a factor of about two. The solution of this difficulty must await the results of further analysis.

Discussion of the CS_2 Spectrum

According to Krishnamurti[9] the Raman spectrum of CS_2 gas consists principally of two strong lines with an intensity ratio of about 5:1 lying at 655.5 and 795.0 cm^{-1} respectively. These may be identified with transitions from the normal state to the two combined levels (100), (020). The frequency ν_1 has been found by Dennison and Wright[10] to lie at 396.8 cm^{-1}. Combining these three data and neglecting as before the second order constant $\lambda^2 W_2$ we may compute $\lambda b = \pm 19.7$ cm^{-1} and $\Delta = -136.7$ cm^{-1}.

These results for λb and Δ show that we are in the region where the resonance between ν_1 and $2\nu_2$ is very poor and where λW_1 is equivalent to one of the terms of $\lambda^2 W_2$. (Since for these values of λb and Δ, the expression $[\Delta^2/4 + (\lambda b)^2/2]^{1/2}$ does not differ appreciably from $\Delta/2 + (\lambda b)^2/2\Delta$.) Consequently we may not neglect $\lambda^2 W_2$ in computing the energy levels. In fact we may consider that λW_1 is included among the terms of $\lambda^2 W_2$ and thus use the general expression $W_0 + \lambda^2 W_2$ alone for correlating the energy levels. This expression involves ten constants while there have been observed only eight Raman and infrared bands. Thus only certain of the anharmonic constants may be obtained and no independent relations are available with which to check the theoretical formula. (Those constants which may be computed are all small and of the correct order of magnitude). These considerations show that our initial computation of λb and Δ was somewhat meaningless. That is to say, while we can determine with accuracy the value of Δ, the difference between ν_1 and $2\nu_2$, the positions of the levels will not furnish us with any clear information as to the value of λb other than its order of magnitude.

[7] E. F. Barker, Astrophys. J. **55**, 391 (1922).
[8] Cl. Schaefer and B. Philipps, Zeits. f. Physik **36**, 641 (1926).
[9] Krishnamurti, Ind. Journ. Phys. **5**, 109 (1930).
[10] D. M. Dennison and N. Wright, Phys. Rev. **38**, 2077 (1931).

In a recent note S. Bhagavantam[11] calls attention to the fact that the Raman line at 795.0 cm^{-1} possesses properties which are characteristic of the inactive frequency ν_1 and which have nothing in common with the frequency ν_2. He therefore prefers to designate this level with the symbol ν_1' rather than with $2\nu_2$ as do Dennison and Wright. This remark by Bhagavantam illustrates very clearly the nature of the line in question. As a Raman line its existence depends wholly on the fact that the level must be described partly with the wave function (100) of the unperturbed inactive frequency ν_1. Thus its character in the Raman spectrum must be similar to ν_1 and there is some justification for calling it ν_1'. However, in ordering all the vibrational levels of the molecule, we have shown that since $|\Delta|$ is large compared with $|\lambda b|$ we may disregard the fact that $\nu_1 \cong 2\nu_2$. Therefore in speaking of the positions of the levels it is more appropriate to speak of this level as $2\nu_2$. The level possesses a wave function partly characteristic of ν_1 and partly characteristic of $2\nu_2$ and consequently its proper designation will depend upon what properties of the spectrum are being considered.

[11] S. Bhagavantam, Phys. Rev. 39, 1020 (1932).

The Two-Minima Problem and the Ammonia Molecule

By DAVID M. DENNISON AND G. E. UHLENBECK
University of Michigan

(Received June 8, 1932)

The system of a particle moving in a potential field containing two equal minima is treated by the Wentzel-Kramers-Brillouin method of approximation. The energy levels are grouped in pairs and the object of the computation is to find the separation between two levels forming a pair. This is accomplished by connecting the oscillatory and exponential approximate solutions of the wave equation by means of the Kramers connection formulae. If Δ is the separation of a pair and $h\nu$ the distance between two pairs $\Delta/h\nu = 1/\pi A^2$ where $A = \exp\left[(2\pi/h)\int_0^{x_1}[2m(V-E)]^{1/2}dx\right]$. A particular potential curve is chosen consisting of two equal parabolae connected by a straight line. The expression for Δ may then be evaluated explicitly as a function of the length of the joining line, $2(x_0-\alpha)$ and the distance between two minima, $2x_0$. These formulae may be applied to determining the form of the ammonia molecule. Substituting the experimental values for Δ_0 and Δ_1, it is found that $x_0 = 3.161$ and $\alpha = 1.916$. An exact solution for this particular potential curve may be found by joining Weber's function $D_n(x-x_0)$ and $D_n(x+x_0)$ to a hyperbolic sine or cosine. This process also leads to expressions for Δ which may be equated to the experimental values yielding $x_0 = 3.182$ and $\alpha = 1.930$, in good agreement with the earlier determination. Finally x_0 is used to compute $2q_0 = 0.760 \times 10^{-8}$ cm, the distance between the two potential minima, and the following dimensions of the ammonia molecule, $H-H = 1.64 \times 10^{-8}$, $N-H = 1.02 \times 10^{-8}$ cm.

§1.

THE one-dimensional system of a particle moving in a potential field consisting of two equal minima was first treated qualitatively by Hund[1] who showed that the vibrational energy levels which lie below the potential maximum will occur in pairs. The distance between two pairs is roughly equal to $h\nu_0$ where ν_0 is the normal frequency of oscillation, while the separation of the two levels forming a pair depends upon the height and nature of the barrier between the minima and is in general very small. We propose to compute the level separation using the Wentzel-Kramers-Brillouin method of approximation and then to compare this solution with an exact solution based on a particular potential field. Finally an application of the results will be made to the ammonia molecule.

§2.

The W. K. B. method yields an approximate solution of the wave equation whose form depends essentially upon whether the region being considered lies within or without the region in which the classical motion might take place, that is, the region where the kinetic energy is positive. In the first case the solution is oscillatory and has the form

$$\psi_{(x)} = (c/P^{1/2}) \cos\left[(2\pi/h)\int^x Pdx + \gamma\right]$$

[1] F. Hund, Zeits. f. Physik **43**, 805 (1927).

where x is the coordinate of the system, c and γ are arbitrary constants, and

$$P = + [2m | E - V |]^{1/2}.$$

In the second or non-classical region the solution consists of a linear combination of an increasing and a decreasing exponential[2] which has the form

$$\psi_{(x)} = (a/P^{1/2}) \exp \left[(2\pi/h) \int^x P dx \right]$$

$$+ (b/P^{1/2}) \exp \left[- (2\pi/h) \int^x P dx \right].$$

At each boundary or critical point there will exist two conditions upon the arbitrary constants c, γ, a and b which arise from the fact that each function must approximate the *same* exact solution of the wave equation. These relations between the constants are the so-called Kramers connection formulae.[3] The increasing exponential connects with the oscillatory solution so that $c=a$ and $\gamma=+\pi/4$ while for the decreasing exponential $c=2b$ and $\gamma=-\pi/4$.

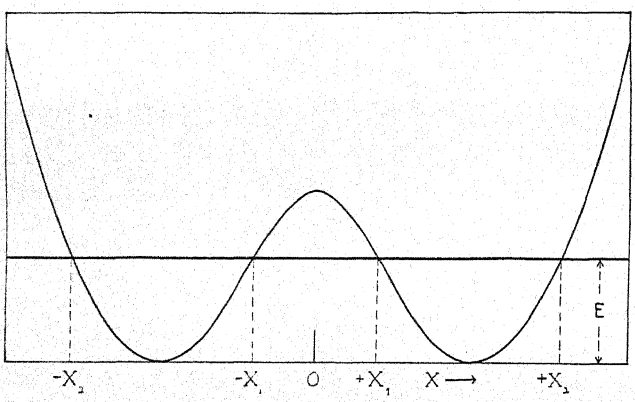


Fig. 1.

These formulae furnish a method by which we may approximate to any solution of the wave equation. When however one wishes to approximate the *eigenfunctions*, namely those functions for which $\int_{-\infty}^{+\infty} \bar{\psi}\psi dx$ is finite, one must let ψ be represented only by the *decreasing* exponential as x approaches $+$ or $-$ infinity. Thus in a region from $+\infty$ to $-\infty$ which has n critical points, there will exist $2n+2$ conditions arising from the connection formulae.

The $n+1$ regions will furnish $2n+2$ constants but one of these, the multiplicative one, must be kept arbitrary in order later to normalize the wave

[2] By increasing or decreasing exponential we will always mean increasing or decreasing when we proceed *away* from the boundary point between the classical and non-classical regions *into* the non-classical region.

[3] H. A. Kramers, Zeits. f. Physik **39**, 828 (1926), H. A. Kramers and G. P. Ittmann, Zeits. f. Physik **58**, 217 (1929), A. Zwaan, Utrecht Diss., 1929. These formulae are collected in a paper by L. A. Young and G. Uhlenbeck, Phys. Rev. **36**, 1154 (1930).

function. Thus there is one condition remaining and this just serves to fix the value of E, that is to determine the eigenvalues of the problem. When we have a system in which the potential has only a single minimum this procedure leads to the well-known half integer quantization of the phase integral.

$$\oint Pdx = (n + \tfrac{1}{2})h. \tag{1}$$

§3.

Let us now consider the case of two equal minima, (illustrated in Fig. 1) where the energy level E is assumed to lie below the potential barrier at $x=0$. Since the potential is an even function of x the wave functions will be divided into two classes, those which are even functions of x and those which are odd functions. We begin by assuming that the level in question corresponds to an even eigenfunction, ψ_+, and we denote the energy by E_+.

In the region from $-x_1$ to $+x_1$ the wave function will have the character of an hyperbolic cosine and may be written in the following manner where C is the multiplicative constant mentioned earlier.

$$\psi_+ = (C/P^{1/2}) \cosh\left[(2\pi/h)\int_0^x Pdx\right] \quad -x_1 < x < x_1.$$

It is now convenient to write $\int_0^x Pdx = \int_0^{x_1} Pdx - \int_x^{x_1} Pdx$. Further let $A = \exp[(2\pi/h)\int_0^{x_1} Pdx]$. We may then express ψ_+ as

$$\psi_+ = (C/2P^{1/2})\left\{A \exp\left[-(2\pi/h)\int_x^{x_1} Pdx\right] + (1/A)\exp\left[(2\pi/h)\int_x^{x_1} Pdx\right]\right\}$$
$$-x_1 < x < x_1.$$

Applying now the connection formulae between the regions $-x_1$ to x_1 and x_1 to x_2, we obtain the following oscillatory solution for the latter region.

$$\psi_+ = R_+ C \cos\left[(2\pi/h)\int_{x_1}^x Pdx - \theta_+\right] \tag{2}$$

where

$$\tan\theta_+ = (2A^2 - 1)/(2A^2 + 1) \tag{3}$$

and

$$R_+ = (4A^4 + 1)^{1/2}/2A.$$

Now in the region $x > x_2$ we must have the decreasing exponential, that is,

$$\psi_+ = (\alpha C/P^{1/2}) \exp\left[-(2\pi/h)\int_{x_2}^x Pdx\right]$$

where α is a new constant as yet undetermined. This connects in the region x_1 to x_2 with

$$\psi_+ = (2\alpha C/P^{1/2}) \cos\left[(2\pi/h)\int_x^{x_2} Pdx - \pi/4\right]. \tag{4}$$

Eqs. (2) and (4) must give identical values for ψ_+ as a function of x and consequently also of the first derivative of ψ_+. We may thus eliminate α by requiring that ψ_+'/ψ_+ as determined from (2) shall be the same as ψ_+'/ψ_+ determined from (4). This gives immediately

$$\tan\left[(2\pi/h)\int_{x_1}^{x} Pdx - \theta_+\right] = \tan\left[(2\pi/h)\int_{x_2}^{x} Pdx + \pi/4\right].$$

The two angles whose tangents are equal must differ by $n\pi$ where n is an integer and this leads to the result,

$$\oint Pdx = (n + \tfrac{1}{4} + \theta_+/\pi)h. \tag{5}$$

From (3) one sees that $\theta_+ < \pi/4$ and in the limit of an infinite barrier where $A \to \infty$, $\theta_+ \to \pi/4$ and (5) reduces to (1).

The foregoing calculation is appropriate for a discussion of one of the levels E_+ where ψ_+ is an even function of x. For the remaining levels E_- where ψ_- is an odd function of x we must start in the region $-x_1$ to x_1 with the hyperbolic sine. We obtain in a similar manner,

$$\oint Pdx = (n + \tfrac{1}{4} + \theta_-/\pi)h \tag{6}$$

where

$$\tan\theta_- = (2A^2 + 1)/(2A^2 - 1),$$

thus $\theta_- \geq \pi/4$.

Let us now consider a pair of levels E_+ and E_- which are defined by the same value of n. Subtracting (6) from (5) and writing out $\oint Pdx$ we find.

$$2\int_{x_1}^{x_2} \{[2m(E_- - V)]^{1/2} - [2m(E_+ - V)]^{1/2}\} dx = (\theta_- - \theta_+)h/\pi. \tag{7}$$

A is usually a large quantity and when this is the case it will be seen that θ_+ is nearly equal to θ_- and consequently we may develop both and obtain to a high degree of approximation,

$$\theta_- - \theta_+ = 1/A^2.$$

Where $\theta_- - \theta_+$ is small, both E_- and E_+ must lie very close to the energy E of a corresponding one minimum potential system. Calling the difference $E_- - E_+$ for the nth pair of levels Δ_n, we find by developing (7)

$$\Delta_n = h/2\pi m A_n^2 \int_{x_1}^{x_2} \frac{dx}{[2m(E_n - V)]^{1/2}}.$$

This expression may be somewhat simplified by remembering that

$$2m\int_{x_1}^{x_2}\frac{dx}{[2m(E-V)]^{1/2}}=\oint dt=\frac{1}{\nu}$$

where ν is the classical frequency of oscillation. When the potential V between x_2 and x_1 does not deviate too greatly from a parabolic form, $h\nu$ may be identified with the distance between neighboring pairs of levels.

$$\Delta_n/h\nu = 1/\pi A_n^2 \tag{8}$$

where

$$A_n = \exp\left[+(2\pi/h)\int_0^{x_1}[2m(V-E_n)]^{1/2}dx\right].$$

The expression (8) shows that the relative separation of a pair of levels does not depend upon the form of the curve but only upon a square root area

$$(2\pi/h)\int_0^{x_1}[2m(V-E_n)]^{1/2}dx$$

in the non-classical region. This result might have been expected from considerations analogous to the Gamow, Condon, Gurney theory of radioactive disintegration.

§4.

The infrared spectrum of the ammonia molecule exhibits features which may be directly related to the one dimensional problem of two equal minima. The parallel type vibration bands for example are observed to be composed of two nearly superimposed bands; a phenomenon whose existence depends upon the fact that there are two equivalent positions of equilibrium for the nitrogen nucleus. This problem has been treated by Dennison and Hardy,[4] who show that the normal coordinate x_3 which is to be correlated with the band at 10.5μ, may be identified with the coordinate x which we have been using. (For a more exact discussion, see the paper just cited.)

The experimental work so far done on the ammonia spectrum presents us with three data, the frequency ν_0 and the separation between the two lowest pairs of levels.

$$\nu_0 = 950\ \text{cm}^{-1},\quad \Delta_0 = 0.8\ \text{cm}^{-1},\quad \Delta_1 = 32.2\ \text{cm}^{-1}.$$

The estimated error of ν_0 and Δ_1 is less than a percent but the error in Δ_0 may be as high as 10 or 20 percent.

We should of course like to be able to reconstruct the potential V as a function of x using the known experimental data. Of the three facts we possess, ν_0 is needed to determine the curvature in the region of the minima which we designate by $x=\pm x_0$. Formula (8) now shows that if we know Δ_0 and Δ_1 we can impose two and only two conditions on the curve, namely we can de-

[4] D. M. Dennison and J. D. Hardy, Phys. Rev. 39, 938 (1932).

termine the square root area from $x=0$ to $x=(x_1)_0$ and from $x=0$ to $x=(x_1)_1$ where $(x_1)_0$ and $(x_1)_1$ are the critical points for the two states $n=0$ and 1 respectively.

We shall therefore choose a very simple curve with two parameters which will allow us to correlate the observed data. Let this curve be formed by two equal parabolae joined by a straight line as illustrated in Fig. 2. The two pairs of levels corresponding to $n=0$, 1 are shown in the figure but since the drawing is to scale the separations Δ_0 and Δ_1 are much too small to be represented. The two parameters are $(x_0-\alpha)$, half the length of the joining line and x_0, half the distance between the two minima. We do not mean that this curve represents very closely the actual potential function, but it must possess the two properties as to square root area mentioned before, and these are the only features of the potential curve which we can at present learn. The parameter x_0 is of great physical interest and it turns out that this is

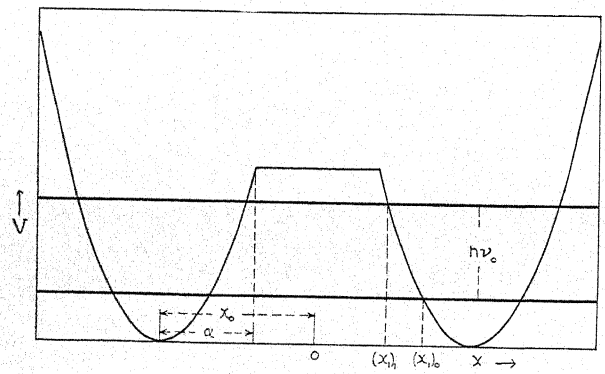


Fig. 2.

very insensitive to the exact shape of V, provided only V has the general form indicated in Figs. 1 or 2.

By use of this particular curve the quantities A and Δ may be readily computed as functions of α and x_0.

$$\frac{\Delta_n}{h\nu_0}=\left(\frac{1}{\pi}\right)\left[\frac{\alpha+[\alpha^2-2n-1]^{1/2}}{(2n+1)^{1/2}}\right]^{2n+1}\exp\left[-(2x_0-\alpha)(\alpha^2-2n-1)^{1/2}\right]. \quad (9)$$

Equating Δ_0 and Δ_1 to their observed values we obtain a transcendental equation which yields the values,

$$\alpha = 1.916$$
$$x_0 = 3.161.$$

The physical significance of these will be discussed later.

§5.

One reason for choosing the potential function illustrated in Fig. 2 is that for this particular curve we may also obtain an exact solution and thus we are able to test, for one case at least, the accuracy of the foregoing com-

putation. There are two reasons why we might doubt its validity. In the first place the W. K. B. approximation is designed to hold best for energy states where n, the quantum number is a large integer. We wish to apply the formulae however to the two lowest states where $n=0$ and 1. In the second place the W. K. B. method becomes inapplicable when the potential at the critical point is too nearly equal to the potential throughout the non-classical region. This obtains because in this case $P^{1/2}$ becomes very small and the W. K. B. expression for ψ does not satisfy the wave equation at all accurately. Fig. 2 is drawn to scale using the values for α and x_0 obtained for ammonia and it is seen that the highest critical point does not lie very far beneath the potential in the non-classical region.

The exact solution is obtained in the following manner. The wave equation may be written,

$$(d^2\psi/dx^2) + (2n + 1 - 2V/h\nu_0)\psi = 0$$

where x and $2n+1$ are proportional to the displacement coordinate q and to the energy E respectively. (n is not necessarily an integer here although it will be nearly equal to one when the potential barrier is sufficiently high.)

$$q = [h/4\pi^2\mu\nu_0]^{1/2}x, \quad E = (2n + 1)h\nu_0/2. \tag{10}$$

The potential may be expressed as follows

$$\begin{aligned} 2V/h\nu_0 &= (x - x_0)^2 \text{ from } x = (x_0 - \alpha) \text{ to } + \infty \\ &= (x + x_0)^2 \text{ from } x = (\alpha - x_0) \text{ to } - \infty \\ &= \alpha^2 \qquad \text{from } x = (x_0 - \alpha) \text{ to } (\alpha - x_0). \end{aligned}$$

In the region of the joining line, from $x=(x_0-\alpha)$ to $(\alpha-x_0)$ the differential equation is satisfied by any linear combination of a hyperbolic sine or cosine. (Assume that $2n+1<\alpha^2$.) It is known that the solutions of the total wave equation may be divided into the two classes, ψ_+ which are even functions of x and ψ_- which are odd functions. It is clear that these must just correspond to the hyperbolic cosine and sine respectively.

Thus from $x=(x_0-\alpha)$ to $(\alpha-x_0)$

$$\begin{aligned} \psi_+ &= A \cosh (\alpha^2 - 2n_+ - 1)^{1/2}x \\ \psi_- &= B \sinh (\alpha^2 - 2n_- - 1)^{1/2}x. \end{aligned}$$

Now in the region from $x=(x_0-\alpha)$ to $+\infty$, one set of solutions of the differential equation will be Weber's functions, $D_n(x-x_0)$. These functions[5] converge properly for large values of x while for small values of x (i.e., $(x-x_0)$ large and negative) we may fit them by means of the parameter n to any curve we please. Now if we join $D_{n+}(x-x_0)$ to ψ_+ or $D_{n-}(x-x_0)$ to ψ_- so that their values and first derivatives agree at the point $x=x_0-\alpha$, we shall have a complete and continuous solution to the wave equation, throughout this region. A similar process may be carried out for nega-

[5] See for example E. T. Whittaker and G. N. Watson, Modern Analysis, 4th Edition, p. 347 (1927).

tive values of x using $D_n(x+x_0)$. The conditions necessary for joining these curves will determine the n_+ or n_- and hence the energy difference Δ_n. The computation is straightforward and makes use of the asymptotic expression for $D_n(y)$ given by Whittaker and Watson, for large *negative* values of y.

$$D_{n(y)} = e^{-y^2/2}(2^{1/2}y)^n[1 - n(n-1)/4y^2 + n(n-1)(n-2)(n-3)/32y^4 \cdots] - [(2\pi)^{1/2}e^{n\pi i}e^{y^2/2}/\Gamma(-n)(2^{1/2}y)^{n+1}][1 + (n+1)(n+2)/4y^2 + (n+1)(n+2)(n+3)(n+4)/32y^4 + \cdots].$$

It does not seem possible to give Δ_n as an explicit function of n but the two quantities we need Δ_0 and Δ_1 have been computed,[6]

$$\begin{aligned} \Delta_0/h\nu_0 &= (2\alpha/\pi^{1/2}) \exp\left[-\alpha^2 - 2(x_0-\alpha)(\alpha^2-1)^{1/2}\right] \\ \Delta_1/h\nu_0 &= \left[(4\alpha^3 - 4\alpha)/\pi^{1/2}\right] \exp\left[-\alpha^2 - 2(x_0-\alpha)(\alpha^2-3)^{1/2}\right]. \end{aligned} \tag{11}$$

It is interesting to compare formulae (9) and (11). When x_0 and α are sufficiently large, the two values of Δ_0 agree to within 7 percent and the values of Δ_1 to within 3 percent. This result is in accord with the work of Young and Uhlenbeck[3] who found that the W. K. B. approximation for the hydrogenic wave functions was surprisingly good even for the low quantum states. The agreement of (9) and (11) for the particular values of x_0 and α found for ammonia is somewhat poorer, being about 10 percent for both Δ_0 and Δ_1. On the other hand we may equate (11) to the experimental data Δ_0 and Δ_1 when we find,

$$\alpha = 1.930 \quad x_0 = 3.182. \tag{12}$$

Thus the error in the determination of the constants α and x_0 is in each case about 0.7 percent.

We shall adopt the values (12) and from these may compute the actual distance between the two minima in the ammonia molecule. Substituting the appropriate values for ν_0 and μ, the reduced mass, into (10) we obtain $2q_0 = 0.760\times10^{-8}$ cm.

The moment of inertia, A, about an axis perpendicular to the symmetry axis is known from band spectrum measurements to be $A = 2.80\times10^{-40}$. Combining this datum with the value for q_0 we may find C, the moment of inertia about the figure axis and hence the normal distances between two hydrogen nuclei and between a hydrogen and nitrogen nucleus.

$$\begin{aligned} C &= 4.42 \times 10^{-40} \\ H - H &= 1.64 \times 10^{-8} \text{ cm} \\ N - H &= 1.02 \times 10^{-8} \text{ cm}. \end{aligned}$$

[6] These expressions have been calculated from the asymptotic expansion for $D_n(y)$ and are consequently only asymptotically correct. The next order term would change 2α to $2\alpha+a/\alpha^3$ and $4\alpha^3-4\alpha$ to $4\alpha^3-4\alpha+3/4\alpha+b/\alpha^3$ in the numerators of Δ_0 and Δ_1 respectively. These corrections are insignificant in the case of ammonia.

These values for C and the molecular dimensions are of considerable importance since because of the interaction between vibration and rotation it appears to be impossible to determine them from an investigation of the fine structure of the infrared bands themselves. We feel that the value of C is accurate to within 2 percent. The chief error in its determination probably lies in the uncertainty with which Δ_0 is known.

The results we have obtained may be compared with an exact solution of a two minima problem by Morse and Rosen.[7] The potential used by them has the same general form as shown in Fig. 1 in the region between the minima. For large positive and negative values of x however the potential rapidly approaches a constant asymptote in a manner which is unlikely to represent the true curve since it would predict far too low a heat of dissociation for the molecule. In spite of this difference between their potential and the one used by us, they obtain $2q_0 = 0.73 \times 10^{-8}$ cm, a value differing from ours by only 4 percent. This agreement illustrates the qualitative result of the W. K. B. approximation, namely that the magnitude of the splitting of the levels depends only upon the potential curve between the two minima. It shows also how insensitive q_0 is to the exact form of the curve in this region providing only it has the general shape of Figs. 1 or 2 and contains a sufficient number of disposable parameters which may be used to fit the observed data Δ_0 and Δ_1 with their theoretical values.

[7] P. M. Morse and N. Rosen, Phys. Rev. **40**, 1039(A) (1932).

The Nuclear Moment of Barium as Determined from the Hyperfine Structure of the Ba II Lines*

By P. GERALD KRUGER, R. C. GIBBS AND R. C. WILLIAMS**
Cornell University and the University of Illinois

(Received June 13, 1932)

The hyperfine structure of the Ba II lines λ4934A and λ4554A has been observed. The relative intensities of the observed components of λ4554A have been measured. From these data it was possible to determine the value of the nuclear moment of $Ba^{135,137}$, if it is assumed that the barium isotopes 136 and 138 have no nuclear spin. The most probable value obtained for i is 5/2. The separation of the hyperfine levels of $6s\,^2S_{1/2}$ is 0.272 cm^{-1}, of $6p\,^2P_{1/2}$ is 0.039 cm^{-1}, and of $6p\,^2P_{3/2}$ is approximately 0.033 cm^{-1}. In all other terms the hyperfine splitting is very small. There is some evidence that there is an isotopic shift of the center of gravity of the levels of the odd isotopes with respect to the even isotopes, and it has a probable value of 0.022 cm^{-1} for the $^2P_{1/2}$ state, and 0.017 cm^{-1} for the $^2P_{3/2}$ state.

INTRODUCTION

McLENNAN and Allin,[1] S. Frisch,[2] Gibbs and Kruger,[3] and Ritschl and Sawyer,[4] have previously examined the resonance lines of Ba II for hyperfine structure. The results in the first three reports were highly discordant, but the last two agreed in all essential details. However, none of the data was complete enough to determine the value of the nuclear moment for barium.

EXPERIMENTAL

The Ba II lines were strongly excited in a metal liquid air cooled Schüler lamp. The current used varied from 1 amp. to 1.4 amp. and the He gas pressure in the lamp varied from 4 mm to 10 mm. A Fabry-Perot interferometer was used in a Zeiss triple prism spectrograph to photograph the lines. Quartz etalon plates, whose silvered surfaces at various times during the work had reflection coefficients ranging from 60 percent to 94 percent, were spaced by etalon rings 1, 3, 5, 8, 10, 13, 15, 18, 20, 21, 25, and 30 mm in thickness. The times of exposure varied from thirty seconds to three hours.

Nichols and Merritt,[5] have shown that the intensity of light coming through a slit from a continuous source is proportional to the slit width, if

* The investigations upon which this article is based were supported by grants from the Heckscher Foundation for the Advancement of Research, established at Cornell University by August Heckscher. Acknowledgment is also made of the use of spectroscopic apparatus which was in part purchased by a grant from the National Research Council.

** R. C. Gibbs and R. C. Williams, Physical Laboratory, Cornell University; P. Gerald Kruger, Department of Physics, University of Illinois.

[1] McLennan and Allen, Phil. Mag. **8**, 515 (1929).
[2] S. Frisch, Zeits. f. Physik **68**, 758 (1931).
[3] Gibbs and Kruger, Phys. Rev. **38**, 1921 (1931).
[4] Ritschl and Sawyer, Zeits. f. Physik **72**, 36 (1931).
[5] Nichols and Merritt, Phys. Rev. [I] **31**, 502 (1910).

the slit is wider than 0.06 mm. This principle was used to put intensity marks on the plates so that the intensity of the components of the lines could be compared.

A dull white cardboard was placed 10 inches in front of the slit, and was uniformly illuminated by two frosted bulb lamps, which were placed two feet away, one on each side of the collimator. Slit widths of 0.8 mm, 1.0 mm, 1.2 mm, 1.4 mm, and 1.6 mm were used.

The intensity marks were photographed on the same plate as the line and its components without removing the plate from the spectrograph, so as to take account of the variation of plate sensitivity with wave-length. The time of exposure was 60 seconds. Later the plate was microphotometered and the intensity marks recorded at wave-length of the line.

Results

Table I gives the results obtained for the Ba II lines studied, and includes for the sake of comparison the data of McLennan and Allin and of Ritschl and Sawyer. Frisch found no components to these lines so his data are omitted. The intensities of the components are given in aribitrary units, and show

TABLE I. *Hyperfine structure of Ba II lines.*

λ air	Classification	Int.	Δλ of components in A	Δν of components in cm^{-1}	Total line width in cm^{-1}	Ritschl and Sawyer's data	McLennan and Allin's data
		5	+0.0279	−0.115		+0.027A	
		5	+0.0185	−0.076			+0.043A
4934.10	$6s\ ^2S_{1/2}-6p\ ^2P_{1/2}$	75	0.0000	0.0000		0.000	0.000
		5	−0.0477	+0.196		−0.045	−0.037
4899.97	$6p\ ^2P_{3/2}-7s\ ^2S_{1/2}$		sharp		0.057		0.000
							−0.060
4554.04	$6s\ ^2S_{1/2}-6p\ ^2P_{3/2}$	7	+0.0177	−0.085		+0.018	0.000
		75	0.0000	0.000		0.000	−0.051
		5	−0.0340	+0.164		−0.034	−0.085
4524.95	$6p\ ^2P_{1/2}-7s\ ^2S_{1/2}$		sharp		0.051		
4166.02	$6p\ ^2P_{3/2}-7d\ ^2D_{3/2}$		sharp		0.062		
4130.68	$6p\ ^2P_{3/2}-7d\ ^2D_{5/2}$		sharp		0.060		

the intensity ratio between components. The estimated intensity values given the strong parent line are not accurately determined with respect to those of the components, but are given merely to indicate that the parent line is very much stronger than the components.

Fig. 1 shows the hyperfine structure term schene for λ4934 $6s\ ^2S_{1/2}-6p\ ^2p_{1/2}$, and for λ4554 $6s\ ^2S_{1/2}-6p\ ^2P_{3/2}$.

Discussion

Two of the writers published a preliminary report[3] on the structure of the barium lines, and on the basis of estimated intensity ratios between the parent line and the satellites predicted a ratio of even to odd isotopes for barium of about ten to one. About the same time Aston reported isotopes 135, 136,

137 and 138, and has since then[6] reported the respective percentage ratios to be 5.9, 8.9, 11.1 and 74.2. This makes the even to odd ratio of isotopes about five to one.

At the time the preliminary report was made the two components +0.0279A and +0.0185A of λ4934 had only been suspected because of a gradual shading in intensity on the long wave-length side of the parent line. The presence of these new components increases the intensity ratio between parent line and the satellites so that it is of the right order of magnitude to agree with Aston's work.

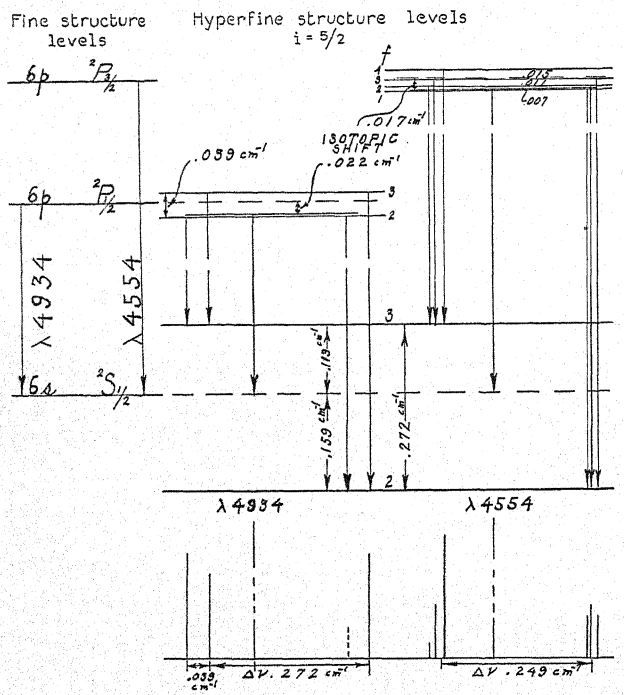


Fig. 1. Hyperfine structure energy level diagram of barium resonance lines, Ba II.

It was possible to observe these components only when using etalon spacings (25 mm), such that the −0.048A component fell on the next chief interference maximum; and (30 mm), such that −0.048A and +0.0279A fell very close to a higher order chief maximum, one on each side. This enabled accurate Δλ measurements to be made on these components, but prevented intensity measurements being made, since all the components could not be resolved on the same plate. Thus the intensities given for these components in Table I are estimated intensities. That they are all of about the same intensity can be seen from Fig. 2 which shows a microphotometer curve of λ4934. The components are unresolved, (due to the fact that the plate was taken with a 13 mm etalon separation) but are drawn in their relative positions.

Fig. 3 shows a simlar microphotometer curve for λ4554. The two com-

[6] Aston, Proc. Roy. Soc. **134**, 571 (1932).

ponents of this line are clearly resolved on the original plate but unfortunately the microphotometer does not show this. Therefore the intensity ratio of these two components was obtained in the following way. The center of the parent line was determined by bisecting the peak of the curve. Then the left side of the parent line was drawn, making it symmetrical about the center line. The right side of the -0.0340A component was projected in the same way, thus giving the shape and position of that component. The ordinates of the

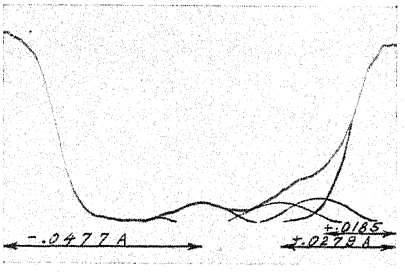


Fig. 2. Microphotometer curve of λ4934.

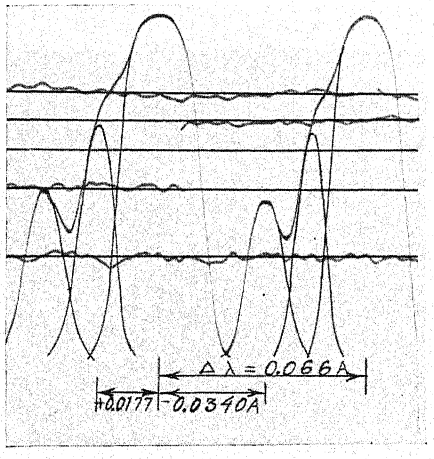


Fig. 3. Microphotometer curve of λ4554.

-0.0340A component and parent line were subtracted from the microphotometer curve to give the form and position of the $+0.0177$A component. When its position had been determined the $\Delta\lambda$ separation from the parent line was computed from measurements taken from the graph and found to agree with the measurements made on the original plate. This gives assurance that the components are correctly drawn in Fig. 3. The position of the peaks of the components may now be compared with the intensity marks (horizontal lines in Fig. 3) which were put on as described above and the intensity ratio obtained in this way. Such a calculation gives the value 1.41 to 1 for the intensity ratio of the components $+0.0177$A to -0.0340A.

A calculation of the theoretical intensities for the hyperfine components under consideration gives the following results for $i=5/2$.

	$^2P_{1/2}$		
	f	3	2
$^2S_{1/2}$	3	28	35
	2	35	10

	$^2P_{3/2}$			
f	4	3	2	1
3	81	35	10	
2		28	35	27

Thus, since the $^2P_{3/2}$ hyperfine levels separations are very small, the theoretical ratio for the components +0.0177A to −0.0340A is 1.40 to 1. This fits the above data and i has, therefore, been chosen as 5/2.

Two difficulties arise from this choice. The fourth component to λ4934A is missing. But its theoretical intensity has only a ratio of 1 to 3.5 with respect to the other components, and it is, therefore, too weak to observe. Component +0.0185A has a theoretical ratio to +0.0275A of 4 to 5, and the curves show the two about equal in intensity. This may be due to the fact that the components were unresolved on the plate from which the curve in Fig. 2 was made. It may also be added that visually, component +0.0279A appears more intense than component +0.0185 on plates taken with a 25 mm etalon separation.

If i were 7/2 the theoretical intensity ratio of components +0.0275A and +0.0185A would be about 3 to 2 and such a ratio would not fit the curve in Fig. 2. Since this ratio increases as i increases it must be concluded that i is probably less than 7/2. On the other hand, even though the experimental intensity ratio of the components of λ4554 (1:41 to 1) indicate that i is 5/2, it must be admitted that the errors involved in the method of synthesizing the curves in Fig. 3 do not eliminate entirely the possibility that i may be 2 or 3. Thus, while the data give the most probable value of i as 5/2, it may be that $3/2 \leqq i < 7/2$.

The hyperfine energy level diagram shown in Fig. 1 shows the theoretical hyperfine structure multiplets at the bottom. The observed $\Delta\nu$ separations are given. For λ4554 the two groups of three components each are unresolved and the observed $\Delta\nu$ is between the centers of gravity of the two groups. The energy level scheme has been built up from these data. The separation for the hyperfine levels of $^2S_{1/2}$ is 0.272 cm^{-1}. The unsplit $^2S_{1/2}$ level for the even isotopes, where $i=0$, has been conveniently placed at the center of gravity of the hyperfine levels. The $^2P_{1/2}$ hyperfine levels are separated by 0.039 cm^{-1}. This indicates a relative isotopic shift between the unsplit ^2P and ^2S levels for even isotopes and the center of gravity of the hyperfine levels of the odd isotopes of about 0.022 cm^{-1}.

The total widths of the hyperfine levels of $^2P_{3/2}$ is about 0.033 cm^{-1}. Here also, there is an indicated isotopic shift of about 0.017 cm^{-1}.

Other lines given in Table I were examined but no structure was found. This must mean that the hyperfine splitting in $7s^2S_{1/2}$ is very small.

All of the above mentioned etalon separations and times of exposure were used in order to make an exhaustive search for the components reported by McLennan and Allin but none were found.

The authors wish to express their appreciation for various helpful suggestions which Professor R. A. Sawyer has given them during the course of this investigation.

The Elimination of One Boundary Condition for a Sphere in Radiative Equilibrium by a Layer in Adiabatic Equilibrium

By HERMAN ROTH
Mendenhall Laboratory of Physics, Ohio State University

(Received June 21, 1932)

In a previous paper a solution of the equations for a slowly contracting or expanding fluid sphere in radiative equilibrium was obtained. In this solution, for particular values of the central pressure and temperature, a certain parameter, α, depending on the rate of contraction, determined whether or not the solution fulfilled the boundary conditions at the surface. For values of the parameter less than this critical value the solution is physically impossible. In this paper it is shown that an atmosphere in adiabatic equilibrium can be fitted to the solutions with values of α larger than the critical value. Thus the equations stating that p and T should approach zero together for some finite r and m are replaced by an inequality of which the completely radiative solution gives the limiting case. In general, the masses, radii, and luminosities, of such stars are larger, while the effective temperatures are smaller, than those of stars completely in radiative equilibrium.

I. INTRODUCTION

IN a previous paper,[1] a solution of the equations for a slowly contracting or expanding fluid sphere in radiative equilibrium with opacity given by Kramers' formula,[2] satisfying the boundary conditions at the surface, $p=0$, $T=0$, for some finite r and m, was obtained. The method used was to assume a finite pressure and temperature of stellar magnitude at the center, and then adjust a certain parameter, α, depending on the rate of contraction and the specific heat of the matter at constant volume, so that the boundary conditions at the surface were satisfied. It was found that the values of α smaller than the critical value lead to solutions which approach isothermal solutions at great distances from the center and thus have infinite mass. For values of α larger than the critical value the temperature approached zero for a finite pressure at a finite distance from the center. The suggestion was made that it might be possible to fit an atmosphere in adiabatic equilibrium to the latter case. The definite relation between the pressure and the temperature in an adiabatic atmosphere requires that the pressure and temperature approach zero at the same time. Hence the absolute value of the temperature gradient in the radiative solution with an α larger than the critical value must be larger in the outer part of the solution than the adiabatic temperature gradient. At the point where the temperature gradients are equal the entropy density determined for the radiative solution will be a maximum.[3] At points nearer the center than this point, the absolute value of the temperature gradient

[1] Herman Roth, Phys. Rev. **39**, 525 (1932). Hereafter referred to as I.

[2] Jeans, *Astronomy and Cosmogony* p. 84 (1929).

[3] This is obvious if we determine the temperature gradients from Eq. (7) and remember that the entropy is constant in an adiabatic atmosphere.

will be less than the adiabatic temperature gradient. Since the equations of adiabatic equilibrium lead to a solution fulfilling the necessary boundary conditions at the surface, the equation which states that the pressure and temperature approach zero together at the surface can be replaced by an inequality for which the completely radiative solution gives the limiting case. Thus there is the possibility of a star whose innermost portion is in radiative equilibrium and whose outer portion is in adiabatic equilibrium.[4] A large fraction of the star's mass may be contained in this outer layer as is shown by the example worked out in this paper.

II. Adiabatic Solution

The equations of radiative equilibrium for a slowly contracting or expanding fluid sphere,[1] with opacity given by Kramers' formula[2] are, with convenient units

$$dP/dm = -53.00m/r^4 \tag{1}$$

$$dT/dm = -2.793 \times 10^5 Lp/r^4T^{7.5} \tag{2}$$

$$dp/dm = -53.00m/r^4 - 1.019 \times 10^{-2}T^3dT/dm \tag{3}$$

$$dr/dm = 3.287T/r^2p \tag{4}$$

$$dL/dm = \alpha T \tag{5}$$

where

$$\begin{aligned} P &= p_r + p = (\tfrac{1}{3})aT^4 + RT/\sigma \\ \alpha &= 0.6195 \times 10^{12}f'/f, \text{ for } C_v = 3R/2. \end{aligned} \tag{6}$$

It was found[1] that the critical value[5] of α was 0.172 and that the solution for $\alpha = 0.175$ leads to the temperature approaching zero before the pressure. At the point of maximum entropy density of the radiative equilibrium solution, the temperature gradient is equal to the adiabatic temperature gradient. This is the transition point from radiative to adiabatic equilibrium. The adiabatic temperature gradient is computed as follows.[6]

The entropy per unit mass of a perfect gas with radiation is given by

$$s = 4aT^3\sigma/3 + \int C_v dT/T + R \log \sigma. \tag{7}$$

The entropy is constant in any system in adiabatic equilibrium. Therefore with C_v constant and equal to $3R/2$

$$\frac{d\sigma}{dm} = -\frac{\left(4aT^2\sigma + \frac{3}{2}\frac{R}{T}\right)\frac{dt}{dm}}{\left(\frac{4}{3}aT^3 + \frac{R}{\sigma}\right)}. \tag{8}$$

[4] The telescopic appearance of the sun's photosphere suggests that the layer just below the photosphere might be in adiabatic equilibrium.

[5] In the previous paper, this was erroneously given as 0.17.

[6] These equations are implicit in the work done by Eddington, *Internal Constitution of the Stars*, p. 190 (1928). See also L. H. Thomas, Monthly Notices of Royal Astronomical Society **91**, 123 (1930).

The total pressure is given by (6) and hence

$$\frac{dP}{dm} = \left(\frac{4}{3}aT^3 + \frac{R}{\sigma}\right)\frac{dT}{dm} - \frac{RT}{\sigma^2}\frac{d\sigma}{dm}. \tag{9}$$

Eliminating $d\sigma/dm$ between (8) and (9)

$$\frac{dT}{dm} = \frac{dP}{dm}\left\{\frac{\left(\frac{4}{3}\frac{aT^3\sigma}{R} + 1\right)}{\left(\frac{4aT^3\sigma}{3R} + 1\right)^2 + \frac{4aT^3\sigma}{R} + \frac{3}{2}}\right\}\frac{T}{p}.$$

Then substituting

$$\lambda = \frac{p_r}{p} = \frac{\frac{1}{3}aT^4}{\frac{RT}{\sigma}} = \frac{aT^3\sigma}{3R}.$$

We obtain

$$\frac{dT}{dm} = \frac{dP}{dm}\left\{\frac{(4\lambda + 1)}{(4\lambda + 1)(4\lambda + 4) - 1.5}\right\}\frac{T}{p} \tag{10}$$

in a convenient form for numerical work. Eq. (10) new replaces (2) of the radiative equations while the other equations remain the same. The transition point is found to occur at the point $m = 0.9676$ of the solution I. Starting from this point, the equations were integrated in about seventy steps. The results at a few of the steps are shown in Table I.

TABLE I. *Solution of adiabatic equilibrium equations.*

$m\times10^{-33}$ gms	$p\times10^{-12}$ dynes/cm^2	$r\times10^{-11}$ cm	$T\times10^{-6}$ degrees
0.9676	2.7278	2.2382	3.9322
1.1524	2.4042	2.4130	3.7868
1.2100	2.3206	2.4642	3.7456
1.2706	2.2356	2.5194	3.7026
1.3342	2.1496	2.5739	3.6581
. . . . .	. . . . .	. . . . .	. . . . .
2.0706	1.3329	3.1653	3.1551
2.2286	1.1931	3.2880	3.0481
2.8528	0.73745	3.7803	2.6192
3.6518	0.32035	4.4900	2.0093
4.1830	0.12884	5.1097	1.5035
4.5626	0.034324	5.8086	0.97890
4.7117	0.0086333	6.3522	0.61225
4.7566	0.0026131	6.6760	0.40614
4.7768	0.0002946	7.0164	0.19924
4.7797	0.0000033	7.2652	0.055025
4.77973	0.0000020	7.3012	0.034672

Near the surface T and p vary more rapidly compared to m than compared to r. Hence more accurate results can be obtained by changing the in-

dependent variable form m to r. Further it is easily seen that with small values of T, λ is small and hence near the boundary the equation giving the temperature gradient can be replaced by

$$\frac{dT}{dm} = f(\lambda)\frac{T}{p}\frac{dp}{dm}$$

where $f(\lambda)$ approaches the value 0.4, and dP/dm approaches dp/dm. Therefore near the boundary

$$\int_0^{T_0} \frac{1}{T}\frac{dT}{dm} = 0.4\int_0^{p_0} \frac{1}{p}\frac{dp}{dm}$$

and

$$T_0 = cp_0^{0.4}.$$

Hence near the surface a solution may be obtained in this manner. This was used to estimate the mass contained within the last few intervals of the solution.

III. Results

The mass[7] of the star completely in radiative equilibrium (for $\alpha = 0.172$) is 4.1510, while the mass of the star with an adiabatic layer (for $\alpha = 0.175$) is 4.7797, 80 percent of which is in the adiabatic layer. The luminosities are 2.3513 and 2.45 respectively and the radii are 5.3245 and 7.3012 respectively. Although the luminosity increases, r^2 has a proportionately larger increase, thus leading to a lower effective temperature. If the completely radiative solution is supposed to mark out a mass-luminosity law, then in our case we have a displacement to the side of a higher mass for the same luminosity.

The solution I represents a series of stars of the same mass but at different stages of contraction, the internal pressure, temperature and radius varying in proportions given by Lane's law. Besides these, there is a wider group with different rates of contraction which are not completely in radiative equilibrium but have an outer layer, which may contain a large fraction of the total mass of the star, in adiabatic equilibrium. In general the latter stars have more mass and also a higher luminosity.

The replacing of the equation between the parameters, stating that p and T should approach zero together at the surface in a completely radiative solution, by an inequality, for which the completely radiative solution gives the limiting case, allows a wider choice in the parameters than is possible in the completely radiative solution.

I wish to thank Dr. L. H. Thomas, for his suggestion of this problem and his assistance in its solution.

[7] In convenient units; m, 10^{33} g; r, 10^{11} cm; L, 10^{35} ergs/sec.

The Magnetic Susceptibilities of Alpha- and Beta-Manganese*

By MARY A. WHEELER
Sloane Physics Laboratory, Yale University

(Received June 6, 1932)

Pure alpha-manganese was prepared by distillation. Beta-manganese was prepared by melting a sample of the alpha-manganese in vacuum, and quenching it in water from about 1000°C. The mass susceptibilities of these two specimens were measured by a null-reading, astatic magnetometer, and found to be $9.60(10)^{-6}$ and $8.80(10)^{-6}$ respectively. These results eliminate the possibility that the ferromagnetic manganese found by some investigators is either the alpha-or the beta-crystal form.

INTRODUCTION

IN THE periodic table manganese lies in the same transition series as the ferromagnetic elements, iron, cobalt, and nickel, and adjacent to them, and also might be expected to exhibit ferromagnetism. However, although the magnetic properties of manganese have been the subject of several investigations, the results have disagreed even in such an important respect as to whether it is or is not ferromagnetic. Undoubtedly many of the discrepancies are attributable to chemical impurities, especially in the work of the early investigators. Manganese is a very active element chemically, and many of its alloys and chemical compounds are ferromagnetic. Iron as an impurity is not so important as carbon and nitrogen, as 18 percent of manganese in iron causes the iron to lose its ferromagnetism, while carbon and nitrogen, which form highly ferromagnetic compounds with manganese, are more likely than iron to be overlooked.

Honda[1] and Owen[2] found the susceptibilities of their specimens to be $10.6(10)^{-6}$ and $8.93(10)^{-6}$ respectively. Both these investigators were very careful to avoid iron. Honda and Soné,[3] and Ishiwara,[4] using similar specimens of Kahlbaum's manganese, measured susceptibilities of 9.70 and 9.66 $(10)^{-6}$. Kuh,[5] who prepared a sample electrolytically, found it to be ferromagnetic, as did Hadfield.[6] Freese[7] repeated Kuh's work, suspecting that the ferromagnetism might be due to hydrogen, since the last step in the preparation was heating a manganese amalgam in hydrogen. He also prepared specimens by sputtering in hydrogen, but found no consistent effect of the hydrogen.

* Part of a dissertation presented for the degree of Doctor of Philosophy in Yale University.

[1] K. Honda, Ann. d. Physik [4] **32**, 1027 (1910).
[2] M. Owen, Ann. d. Physik [4] **37**, 657 (1912).
[3] K. Honda and T. Soné, Sci. Rep. Tohoku Imp. Univ. [1] **2**, 27 (1913).
[4] T. Ishiwara, Sci. Rep. Tohoku Imp. Univ. [1] **5**, 53 (1916).
[5] E. Kuh, Diss. Zurich (1911).
[6] R. Hadfield, C. Chéveneau, and Ch. Géneau, Proc. Roy. Soc. [A] **94**, 65 (1917).
[7] H. Freese, Phys. Zeits. **29**, 191 (1928).

Since the magnetic susceptibilities of many substances have been found to vary in different crystal forms, the object of this research was to investigate what difference in susceptibility might exist between the alpha- and beta-crystal forms of manganese at room temperature. Manganese exists in three crystal forms, alpha, beta, and gamma. The alpha form is the low temperature modification, stable up to 742°C.[8] The beta form is stable from 742° to 1191°[9] and can be obtained in specimens quenched at room temperature from this temperature interval. Both these forms are cubic, having 58 and 20 atoms per unit cube respectively.[10] The gamma form is present in specimens prepared electrolytically, but changes back to alpha automatically in a couple of weeks. It is stable above 1191°, but has never been obtained in pure manganese by quenching.

The susceptibility of manganese as a function of the temperature was measured by Shimizu[11] who found unusually low values for his samples, which were prepared by distillation and were 99.9 percent pure. Some of his results are as follows:

Crystal form	alpha	beta	gamma
Temperature	20°C	810°C	1100°C
Susceptibility	$7.53(10)^{-6}$	$6.01(10)^{-6}$	$8.41(10)^{-6}$

None of these exhibited ferromagnetism in the temperature interval in which they were stable, but he did not investigate the high temperature forms at room temperature.

Preparation of Samples

Two samples of manganese were used for these researches, both prepared by the method of distillation, which yields manganese with a very small percentage of impurities. The first specimen was very kindly supplied by Dr. Walters of the Carnegie Institute of Technology, and was stated to have the following impurities: C, 0.009 percent; Fe, Al, Si, spectroscopic traces. Some manganese was purified similarly in an Ajax 30 KVA induction furnace. In general the method consisted in placing the crude manganese in a magnesia crucible with a second inverted crucible resting on it. The whole was placed in a silica tube which was evacuated to $(10)^{-2}$ mm. The manganese was then heated inductively to a temperature just above melting. As pure manganese is very volatile, it distilled onto the upper crucible leaving the impurities in the undistilled portion.

To obtain manganese in the beta-crystal form without impurities sufficient to vitiate magnetic measurements, it was found necessary to melt the pure distilled alpha-manganese into a lump in vacuum, then quench it in cold water, so that only the surface became impure. To do this, the manganese in a magnesia crucible was supported inside a tube of Berlin porcelain which was sufficiently nonporous at the melting point of manganese to hold

[8] M. Gayler, J. Iron and Steel Inst. **115**, 393 (1927).
[9] E. Persson and E. Öhman, Nature **124**, 333 (1929).
[10] G. D. Preston, Phil. Mag. [7] **5**, 1198 (1928).
[11] Y. Shimizu, Sci. Rep. Tohoku Imp. Univ. [1] **19**, 411 (1930).

a vacuum of $(10)^{-6}$ mm. This tube was surrounded by a carbon ring which in turn was surrounded by the coil of the induction furnace. Most of the heat was generated in the carbon ring. Ground joints between the tube and the Pyrex vacuum system were sufficiently distant from the heat to be easily water cooled. At the instant of melting the pressure rose to $(10)^{-4}$ mm, but otherwise kept down to $(10)^{-6}$ mm. When the manganese melted, argon was introduced, and then the manganese lump was quickly driven through the bottom of the tube into cold water. This lump was covered with an oxide film, which was removed by sandblasting.

No chemical analysis can as yet be obtained for this specimen. After consultation with leading authorities on the determination of gaseous impurities in metals, it appears that the errors in nitrogen determinations are as large or larger than the total amount of nitrogen probably present here. The specimen is being retained in the hope that a more precise method may soon be available. However, the susceptibility measurements are a delicate test for ferromagnetic impurities, and others cause only a small percent error. The probable impurities here would be carbon and nitrogen, both of which form ferromagnetic compounds with manganese.

X-RAY ANALYSIS

To determine the crystal structure of these samples, x-ray powder photographs were taken with Mo $K\alpha$ radiation. The value of tan 2θ for Mo $K\alpha$ was calculated from the data given in papers by Sekito[12] and Preston[10] for tan 2θ for Fe $K\alpha$, and compared with tan 2θ from these samples. (Tables I and II.)

TABLE I. *Distilled specimen compared with alpha-manganese.*

Line	Tan 2θ from Sekito	Intensity from Preston	Tan 2θ calculated from film	Estimated intensity
1	0.354	200	0.354	200
2	0.395	200	0.396	100
3	0.416	100		
4	0.435	100	0.433	75
5	0.594	40	0.593	50
6	0.624	100	0.633	50
7	0.644	200		
8	0.675	140	0.678	100
6 lines of lower intensity				
15	0.825	200	0.825	50

TABLE II. *Quenched specimen compared with beta-manganese.*

Line	Tan 2θ from Sekito	Intensity from Preston	Tan 2θ calculated from film	Estimated intensity
1	0.354	strong	0.354	very strong
2	0.374	"	0.374	strong
3	0.395	"	0.395	medium
4	0.451	"	0.454	weak
5	0.525	medium	0.541	weak
6	0.562	"		
7	0.661	very strong	0.668	fairly weak
8	0.675	medium		
9	0.712	very strong	0.710	weak

[12] R. M. Bozorth, J. Opt. Soc. Amer. **10**, 591 (1925).

In the comparison of the values for alpha-manganese with those from Sekito, it is clear that the prominent lines coincide. Preston and Sekito used cameras with circular film, and so got the lines for larger angles with relatively greater intensities. This explains the absence on our film of lines No. 9 through No. 14. The intensity maximum extending from tan 2θ 0.395 to 0.435 showed practically no structure. This was interpreted as two lines at the distances noted, but another line may have been present in the interval.

For the beta specimen, the lines coincided within the errors of measurement. The lines reflected at larger angles, No. 10 and above, were absent because of the greater distance from powder to film, as on the first film, and lines No. 5 and 6, as well as lines 7 and 8, were not resolved.

No lines which could be attributed to the gamma structure were found on either film.

Magnetometric Measurements

The magnetometer used was essentially like one described by Bozorth,[12] and was a null-reading instrument. Two small parallel magnets of equal moment were mounted horizontally, one above the other, with north poles in opposite directions, thus forming an astatic system. The specimen was placed so that each end was at the level of one of the magnets; thus each induced pole exerts the same torque on the astatic system. An equal distance from the astatic system but on the side opposite the specimen was placed a coil of proper dimensions, which, when traversed by a suitable electric current, balanced the total torque exerted on the astatic system by the specimen. The specimen was supported in a magnetizing solenoid, and the balancing coil in a similar solenoid, provided to cancel the torque on the magnets due to the magnetizing solnoid. Since the dimensions of the balancing coil and the current passing through it gave its magnetic moment, which was adjusted to be the same as that of the specimen, the magnetic moment and susceptibility of the specimen could be calculated.

The container for the specimen of powdered manganese was a glass tube cut from a 2 cm^3 hypodermic syringe of inside diameter 0.9083 cm, with ends ground flat and plugged with amber so that the inside length was 4.000 cm. The balancing coil used to counteract the torque of the specimen on the astatic system was wound on an amber spool which was so slightly paramagnetic that it deflected the magnetometer zero less than 1 mm, that being about the limit of accuracy in single readings. Two coils were wound identically, for purposes of adjustment, with two layers of 186 turns each. The winding space was 4.000 cm long, and 0.824 cm in diameter. The magnetizing solenoids were wound on brass spools 15 cm long and 1.585 cm in diameter, with 5027 turns in 20 layers. A current of air was kept constantly flowing between the specimen and the spool, and this eliminated much shifting of the wires as they heated, and also kept the specimen within a few degrees of room temperature. The adjustment was carried out as suggested by Bozorth, except that it was not found possible to hold the same adjustment for various high fields.

As the balancing coil was wound in two layers its moment was measured

magnetically by the common method of placing it in the center of a long solenoid, and measuring the charge passed through a calibrated ballistic galvanometer in series with the balancing coil and a standard mutual inductance, when a current was passed through the solenoid. From this, the magnetic moment, M, was found to be 21.62 i, with a probable error of $\frac{1}{2}$ percent, where i is the current through the balancing coil in amperes.

The average value of the field, H, in the magnetizing solenoid was calculated to be 0.982 of that of an infinite solenoid of the same number of turns per unit length. Therefore, H in gauss was found to be 413.6 I, where I is the magnetizing current in amperes; and χ, the mass susceptibility, $= M/H \cdot \text{mass}$, or $52.27(10)^{-3}\, i/I \cdot \text{mass}$.

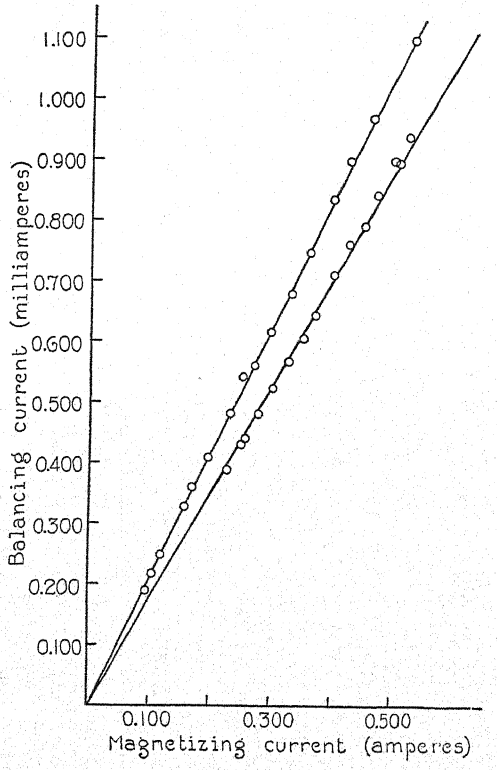


Fig. 1. Upper line, beta-manganese; lower line, alpha-manganese

The total deflection without balancing current was between 5 and 10 cm, and the limit of accuracy in each reading was about 1 mm. Since the volume susceptibility turned out to be of the order of $(10)^{-5}$, the demagnetizing effect of the poles of the specimen was neglected. With the astatic system in its zero position, the resultant field produced by its magnets on the specimen would be small. Experimentally, no change in value was noticed when the zero was changed slightly, or when the suspended system was rotated through 180°. The field on the specimen in the direction of its axis due to the second magnetizing solenoid in which the balancing coil was supported was calculated to be 1/400 that of the first magnetizing solenoid, and was neglected.

The diameter of the container was slightly larger than the average diameter of the balancing coil, but it seemed impossible that this could make a measurable change in the result, especially as the average diameter of the sample of manganese must necessarily be smaller than the container.

It is conceivable that the powdering of the manganese to place it in the container might have changed the susceptibility. Evidence would suggest that if this happened the susceptibility was increased rather than decreased by the powdering. As no change of susceptibility with field was noted, there could have been present no measurable ferromagnetic impurity, and a paramagnetic impurity would cause only a small percent error.

The results are presented in Table III and in Fig. 1 which shows the straight line relations to be expected in the absence of ferromagnetic impurities.

TABLE III. *Susceptibility measurements on alpha- and beta-manganese.*

Mass of sample, 11.307 grams			Mass of sample, 10.420 grams		
I	$i\cdot 10^3$	$(i/I)\cdot 10^3$	I	$i\cdot 10^3$	$(i/I)\cdot 10^3$
0.095	0.189	1.989	0.227	0.390	1.718
0.106	0.216	2.038	0.250	0.430	1.720
0.120	0.248	2.067	0.256	0.441	1.723
0.158	0.327	2.070	0.278	0.482	1.734
0.172	0.360	2.093	0.300	0.524	1.747
0.197	0.409	2.076	0.327	0.568	1.737
0.233	0.482	2.069	0.350	0.606	1.731
0.252	0.543	2.155	0.370	0.645	1.743
0.271	0.562	2.074	0.400	0.712	1.780
0.297	0.617	2.077	0.426	0.763	1.791
0.330	0.680	2.061	0.452	0.793	1.754
0.361	0.749	2.075	0.472	0.844	1.788
0.400	0.836	2.090	0.500	0.900	1.800
0.427	0.900	2.108	0.507	0.897	1.769
0.463	0.970	2.095	0.524	0.940	1.794
0.530	1.10	2.075			
$i/I=(2.076\pm.006)\cdot 10^{-3}$			$i/I=(1.754\pm.005)\cdot 10^{-3}$		
$\chi=(9.60\pm.03)\cdot 10^{-6}$			$\chi=(8.80\pm.02)\cdot 10^{-6}$		

CONCLUSIONS

Thus, it can be concluded that for alpha-manganese the mass susceptibility is $9.60(10)^{-6}$, and for beta-manganese, $8.80(10)^{-6}$. Considering that the specimens previously measured were probably a mixture of these two crystal structures, this result is lower than Honda's first value of $10.6(10)^{-6}$, and agrees better with his second value, $9.70(10)^{-6}$, and with that of Owen, $8.93(10)^{-6}$. The more recent work of Shimizu gave still lower values, as previously noted. For these low values no explanation can here be offered. No trace of the ferromagnetism observed in the specimens of Kuh, Hadfield, and Freese was found.

The writer wishes to extend her thanks to Dr. Walters who so kindly furnished samples of pure manganese. She also wishes to express appreciation to Professor L. W. McKeehan for suggesting the problem and for advice and criticism during its progress. The research was made possible through the grant of the Loomis Fellowship, established by Francis E. Loomis and Henry B. Loomis.

The Magnetic Susceptibility of Nitrogen Dioxide

By GLENN G. HAVENS
University of Wisconsin, Madison

(Received June 2, 1932)

A method has been developed whereby sensitivities for volume susceptibilities as high as 3×10^{-15} can be obtained. The main improvement in the method over that of other observers is in the construction of lighter test bodies and the use of smaller fibers. The method is applied to the measurement of the susceptibility of NO_2. The results agree within the limit of experimental uncertainties with Van Vleck's theoretical value for the molecular susceptibility of NO_2 namely, $\chi(NO_2)=0.375\,\chi(O_2)$. The susceptibility of N_2O_4 comes in as a second order effect and the value $\chi(N_2O_4)=-30\times10^{-6}\pm20$ percent is in fair agreement with the value $\chi(N_2O_4)=-25.8\times10^{-6}$ obtained by T. Soné.

I. INTRODUCTION

IN VIEW of the large discrepancies in the results of various observers for the magnetic susceptibilities of many gases and of the growing theoretical interest in these experimental values, it seemed advisable to carry on a series of experiments designed to increase the dependability and accuracy of the measurements. With this view the writer has designed an apparatus for the measurement of low susceptibilities for gases such as hydrogen or helium, which are fairly inert and can be readily purified.

Nitrogen dioxide is of interest both theoretically and chemically; its susceptibility should be given by the formula derived by Van Vleck,[1] namely:

$$\chi(NO_2) = 4N\beta^2S(S+1)/3kT + N\alpha$$

where $N\alpha$ is a small residual term due to high-frequency elements, β is the usual Bohr magneton, and S is the spin quantum number of the molecule and is presumably equal to $\frac{1}{2}$ for NO_2. The susceptibility of O_2 is given by the same formula. However since the ground level for this molecule is a $^3\Sigma^{-1}$ state making $S=1$, it follows that $\chi(NO_2)/\chi(O_2)=0.375$. Experimentally Soné[2] finds this ratio to be about one sixth of this value. Verhoek and Daniels[3] have worked out the dissociation constant for nitrogen tetroxide, and it is of interest to see whether the use of their value for the dissociation constant would lead to a consistent correlation of the magnetic measurements.

II. DESIGN OF THE APPARATUS

The Faraday method, whereby an oblong shaped test body is suspended in a nonhomogeneous field surrounded by the gas under investigation, was used. The method has been improved upon and used for the measurement of

[1] J. H. Van Vleck, *The Theory of Electric and Magnetic Susceptibilities*, pp. 274.
[2] Také Sóné, Sci. Rep. Toh. Imp. Univ. **11**, 139 (1922).
[3] Verhoek and Daniels, J. Am. Chem. Soc. **53**, 1250 (1931).

the susceptibility of gases by Glaser,[4] Hammar,[5] and Bitter.[6] The tube used by the writer is similar to the one used by previous workers except that the important parts of the tube were given a conducting film of gold or platinum and grounded so that there could be no electrostatic effects (Fig. 1). It was

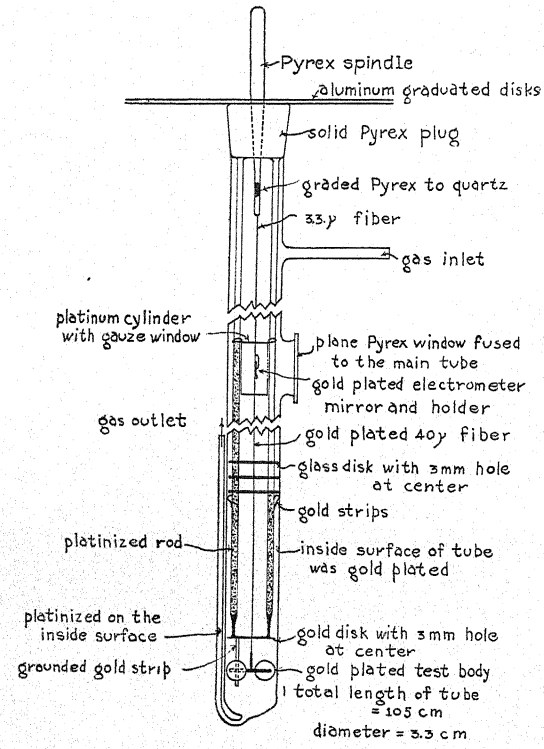


Fig. 1. Final tube.

then found that drifts of the test body and the change in total torque from day to day were, as far as could be observed, completely eliminated after the tube and moving parts were carefully grounded.

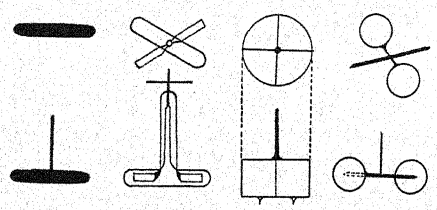


Fig. 2. Types of test bodies.

The main improvements in the method which the writer has introduced have come through the development of better test bodies and the use of smaller fibers. Four types of test bodies have been used by the writer. Fig. 2.

[4] A. Glaser, Ann. d. Physik **75**, 459 (1924).
[5] G. W. Hammar, Nat. Acad. Sci., Proc. **12**, 597 (1926).
[6] F. Bitter, Phys. Rev. **36**, 1648 (1930).

The first type is a solid ellipsoid of the type used by Hammar[5] and by Glaser.[4] The one of this form used by the writer weighs 1.8 g. The second one is a hollow quartz ellipsoid weighing less than 1 g. It has the additional advantage that the quartz compensators reduce the total torque caused by the quartz to nearly zero. The ellipsoid is evacuated and sealed off, whereas the compensators are open to the gas. These compensators not only compensate for the torque caused by the field on the material of the test body itself but also reduce the effect of temperature disturbances. The third type of test body is similar to the one designed by Bitter,[6] except that fused quartz replaced glass. It has the apparent advantage of better symmetry; but its great disadvantage is that it weighs about 7 g. The compensation resulting from symmetry is apparent rather than actual, because, even if the test body were of perfect construction, there would be total compensation for only one position in the field, and if the test body be moved even a small distance from this position, the total torque would be increased to values as great as those obtained by the use of the other types of test bodies. The test body at the right of the figure is the type finally used. It consists of two evacuated spherical bulbs attached together and compensated by a small quartz rod. The one now in use weighs less than 100 mg and has a coat of evaporated gold on the surface. By allowing the test body to rotate until the surface comes in contact with a grounded gold wire, any accumulated electrostatic charges can be removed. With this type of test body it is possible to use much smaller fibers than with the other types and it has the further advantages that the magnetic field does not have to be held so constant, and changes in temperature are not so troublesome. The following table gives approximately the sensitivity of the four different types of test bodies which were used. The volume susceptibility of hydrogen for comparison is about 2×10^{-10}.

TABLE I. *Sensitivities of test bodies.*

Type:	I	II	III	IV
Sensitivity:	4×10^{-12}	1×10^{-13}	1×10^{-12}	3×10^{-15}

The compensators of the fourth-type test body were of such diameter and length that the total torque on the test body was nearly zero when in the position indicated by Fig. 3. The angle θ was made so that one could find a position of only slightly stable equilibrium; usually θ turned out to be about 75°. The nearer θ approached the angle giving unstable equilibrium, the

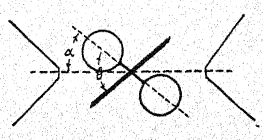


Fig. 3. Position of test body in the field.

longer would be the period of vibration and thus the higher the sensitivity, limited only for a given test body by the accuracy of the torsion head. Fig. 4 shows a typical curve of the relation of the torque to the angle α of the test

body in the magnetic field. If A and B are angles of minimum and maximum torque, the difference of the torque at A and B depends upon the angle θ, and the value of the slope of the curve in Fig. 4 indicates the degree of stability, negative slopes meaning unstable equilibrium. Thus A and B are positions of neutral equilibrium and therefore high sensitivity; A on the curve would be a better angle than B because the total torque is less and therefore the fluctuations due to changes in field strength and temperature are smaller.

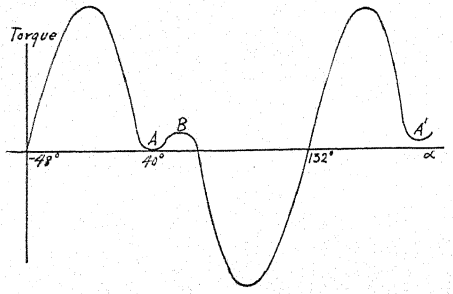


Fig. 4. Torque as a function of the angle α.

If A and B are too close together, it becomes difficult to keep the test body between these positions when the field is initially being applied; that is, while the field is rising from 0 to its final constant value. With a period of about one minute, sensitivities have been reached for which volume susceptibilities of 3×10^{-15} were observable.

The torque on a twisted fiber varies directly as the angle through which the fiber is twisted, inversely as the length, and inversely as the fourth power of the diameter. Thus for the highest sensitivities it is desirable to have a

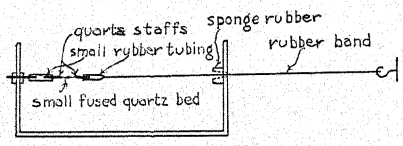


Fig. 5. Fiber drawing apparatus.

fiber of such diameter that the error in reading the torsion head will be less than that of the scale of the optical lever used to tell the position of the test body in the field. For a 3μ fiber with a 100 mg test body the torque is more than 2 revolutions of the fiber per atmosphere of hydrogen, and over 1500 revolutions per atmosphere of oxygen. The strength of this fiber is not sufficient for the heavier test bodies but is many times the strength necessary for the light test bodies.

Fibers of any diameter as low as 1μ can be readily drawn where it is not required that each end of the fiber be attached to a large staff of quartz. However, since shellac or other organic compounds could not be used in this experiment for connecting the fiber to the torsion head because of the action of NO_2, it was necessary to devise an apparatus capable of drawing a fiber of a given diameter and length from two quartz staffs without breaking the

fiber. The fiber drawing apparatus consisted merely of a stretched rubber band holding a quartz staff which would fly into a sponge rubber socket when released. (Fig. 5) At present fibers as small as 0.6μ in diameter and 50 cm long have been successfully made with this apparatus. The variation in the diameter along the entire length is less than 0.1μ, except for about 1 cm at each end. It has been found possible to draw the quartz staffs down very sharply to a 3μ to 5μ fiber. The absence of gradual tapering means that there is a definite point of contact between the staff and fiber upon which a microscope can be focused for centering purposes. The fiber is then centered very simply by heating the quartz staff in a horizontal position until its sags, due to its own weight, to the correct position. Fibers can be centered in this manner to within a radius of 5μ.

Because mercury is attacked by NO_2, a special pressure measuring device, due to Professor Daniels,[3] was used whereby the pressures of $NO_2+N_2O_4$ were measured by balancing the pressure of $NO_2+N_2O_4$ on the one side of a glass diaphragm against that of air on the other side. The pressure of air was then measured using an ordinary manometer.

TABLE II. *Taken at 20.05°C.*

Pressure of $NO_2+N_2O_4$ in cm of Hg	Torque on the fiber in revolutions	Pressure of $NO_2+N_2O_4$ in cm of Hg	Torque on the fiber in revolutions
1.94	60.752	35.58	153.558
2.99	66.000	37.69	156.727
4.18	71.995	39.55	159.998
5.28	76.087	41.66	163.079
6.28	80.991	43.51	166.254
7.49	85.925	45.89	169.988
8.67	90.080	48.20	173.728
9.89	94.182	50.00	175.675
10.92	97.082	51.52	178.165
12.64	102.429	52.64	179.648
14.42	107.522	54.23	182.272
17.03	114.623	55.91	184.382
18.43	118.358	51.09	177.673
19.87	121.720	46.72	171.678
21.21	124.827	41.53	163.694
22.68	127.988	36.55	154.603
23.94	130.814	32.25	147.338
25.36	133.585	27.89	139.090
26.91	136.580	23.52	129.947
28.10	139.135	19.28	120.088
28.72	140.170	15.56	110.64
30.55	144.195	11.76	100.05
34.01	150.414	7.85	86.791
32.25	147.659	4.54	74.148

III. RESULTS

To find the susceptibility of NO_2 it is necessary to know the dissociation constant for $N_2O_4 \rightleftarrows NO_2$ at various temperatures. The dissociation constant $k(N_2O_4)$ is given by:

$$k(N_2O_4) = p^2(NO_2)/p(N_2O_4)$$

where $p(NO_2)$ and $p(N_2O_4)$ represent the partial pressures of NO_2 and N_2O_4. Verhoek and Daniels[3] have measured this constant to about 2 percent for

the temperatures 25°C, 35°C, and 45°C. The value of $k(N_2O_4)$ can therefore be found for any other temperature from van't Hoff's equation:

$$\log \frac{k_1}{k_2} = \frac{\Delta H}{2.303R} \frac{T_2 - T_1}{T_2 T_1}$$

where ΔH is the heat of dissociation. From these equations, and a knowledge of the total pressure of the gas, the amount of NO_2 present can be readily

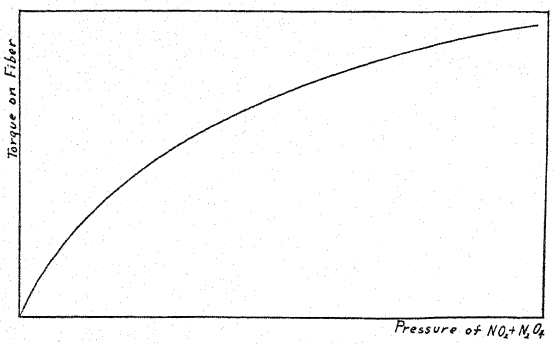


Fig. 6.

calculated. As the susceptibility of NO_2 is about 50 times that of N_2O_4, if we plot the torque on the torsion head against the partial pressure of NO_2 we

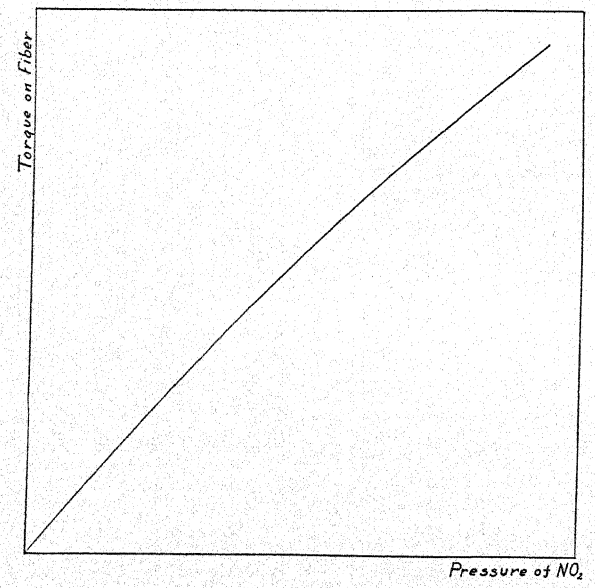


Fig. 7.

should get nearly a straight line, inasmuch as the torque due to any gas is proportional to the pressure of that gas. Fig. 6 shows a typical curve of the

observed torques plotted as ordinates and the pressures of $NO_2+N_2O_4$ as abscissas. Fig. 7 shows a typical curve of the observed torques plotted against the partial pressures of NO_2. The slight curvature is due to the fact that the

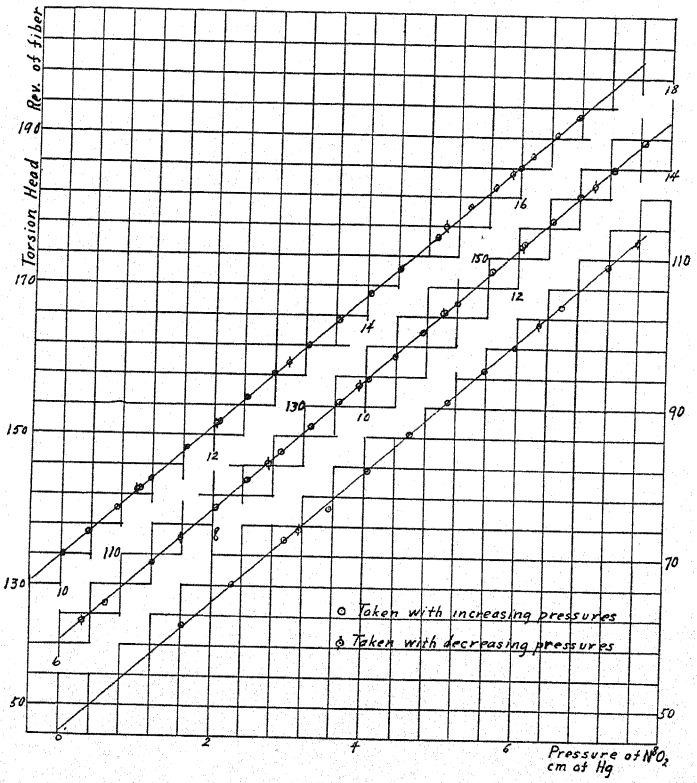


Fig. 8.

susceptibility of N_2O_4 is not zero. The curve of Fig. 8 was obtained from the data of Table III, first, by deriving from knowledge of the value of the dissociation constant, a curve of type in Fig. 7 for the susceptibility of N_2O_4 by

TABLE III. *Taken at 20.02°C.*

Pressure of Oxygen in cm of Hg	Torque on fiber in revolutions
1.63	84.34
3.75	130.66
6.73	198.70
9.62	263.51
12.25	320.50
15.08	383.63
18.30	454.65

assuming that $\chi(N_2O_4) = -2.5$ percent $\chi(NO_2)$. Fig. 8 gives the value $\chi(NO_2) = 0.390\chi(O_2)$ and is in good agreement with the theoretical value of 0.390 $\chi(O_2)$ calculated by Van Vleck,[1] which may be in error by as much as 3 percent or 4 percent because of the small neglected terms. Another factor which

might further account for the difference between this value and the theoretical value is the uncertainty in the value of $k(N_2O_4)$. The value $\chi(N_2O_4) = -30\ 10^{-6}$ agrees within the limit of error with Soné's value of -25.8×10^{-6}. Fig. 8 and three other curves at different temperatures give the values listed in Table IV. It is to be noted that the agreement with the theoretical value is

TABLE IV.

Temperature	$\chi(NO_2)/(\chi N_2O_4)$	$-\chi(N_2O_4)/\chi(NO_2)$	$\chi(N_2O_4)\times10^6$	$(\chi(O_2)=3330\times10^{-6})$
22.60°C.	0.370	2%	−25.0	
20.54	0.382	2.5%	−31.3	
20.05	0.390	2.5%	−31.3	
19.17	0.400	2.8%	−35.0	

better for the higher temperatures, which are nearer the temperatures for which $k(N_2O_4)$ was determined. Through the entire work the susceptibility of O_2 was used as a standard. Table III.

The volume susceptibility of NO_2 computed from the above relative values is $k(NO_2) = 579\times10^{-10}$. Sensitivities for k of about 10^{-12} were used, therefore the small deviations from the curves of the observed points could not be attributed to the lack of sensitivity.

An error of 0.1°C in the measurement of temperature would change the value of the dissociation constant by an amount sufficient to account for most of the deviations. However, with a thyratron tube arrangement for control, observed room temperatures was maintained constant to within 0.1°C; in addition the temperature of the tube was read to 0.01°C, on a 0.001°C thermometer, and corrections applied for each point on the curve.

IV. CONCLUSION

The results for NO_2 are entirely satisfactory and in accord with the theoretical value of Van Vleck.[1] They remove the previous very bad agreement between theory and the only existing experimental results by Soné. The results for N_2O_4, determined from the small curvature of the curves, should be correct to within 20 percent. Further work is being undertaken to determine the susceptibility of hydrogen and some other common gases.

The writer wishes to express his appreciation to Professor Mendenhall for his guidance throughout the duration of the work, to Mr. Foerst, the mechanician, for his cooperation in the construction of the apparatus, and to Mr. Verhoek and Professor Daniels for the preparation of the liquid $NO_2 + N_2O_4$.

Barkhausen Effect. III. Nature of Change of Magnetization in Elementary Domains

By Richard M. Bozorth and Joy F. Dillinger
Bell Telephone Laboratories

(Received June 24, 1932)

Transverse Barkhausen effect. It is found that the small sudden changes in magnetic moment which take place when material is magnetized, have components perpendicular as well as parallel to the direction of the magnetic field. Quantitative measurements of the transverse and longitudinal effects (changes in moment perpendicular and parallel to the direction of the field) show that the longitudinal effect is the larger when the magnetization is small and that the transverse effect is larger when the magnetization is large. Materials examined are (polycrystalline) annealed iron, hard-worked iron, and perminvar.

Domain theory of ferromagnetism. The results are interpreted in terms of the domain theory, according to which ferromagnetic materials consist of small regions or domains always magnetized to saturation. Changes in magnetization are accomplished only by changes in the *directions* of magnetization in the domains. Sudden changes from one to another of the natural directions of magnetization in the crystal give rise to the Barkhausen effect, and in general have definite transverse and longitudinal components, the former now observed for the first time. The experiments show that when the gross magnetization (that of the substance as a whole) is small, the application of an additional magnetic field causes *reversal* of the direction of magnetization in the domains for which this direction was initially nearly antiparallel to the field. Experiments on annealed iron with high gross magnetization indicate, on the contrary, that the direction of magnetization in a domain may be altered through 90°.

IN STUDYING the Barkhausen effect, experimenters have generally observed the voltage-impulses in coils encircling the material and oriented with their axes parallel to the varying magnetic field. These are ascribed to sudden changes of the magnetization of individual small domains of the metal: changes which may be either complete reversals, or rotations through angles smaller than 180°. It occurred to us that if this view is correct, voltage-impulses should appear in coils oriented with their axes at right angles to the magnetizing field; and that the study of these impulses, which we shall designate *the transverse effect*, should increase our knowledge of the elementary processes. Thus, if the transverse effect should be absent or small, it would be inferred that the magnetization in each domain affected by the field is always nearly parallel or antiparallel to the applied field. If on the other hand the transverse effect is of the same order of magnitude as the *longitudinal* effect previously observed, various other inferences can be drawn.

We have detected the transverse effect and measured it together with the longitudinal effect, on specimens of hard-worked iron, annealed iron, and perminvar. The data show that the relative importance of the two depends on the material and on the degree of magnetization of the specimen as a whole; the newly observed effect is relatively small when the magnetizing

field H is less than the coercive force, and may be equal to or greater than the longitudinal effect when the magnetization of the material approaches its saturation-value.

METHOD

The magnetic specimens examined were in the form of tubes 60 cm long and about 5 mm in diameter. For measurements of the usual (longitudinal) Barkhausen effect the tube was placed in an axial field produced by a long magnetizing solenoid as shown in Fig. 1. To measure the small changes in magnetization taking place in a direction at right angles to that of the gross magnetization (transverse effect), a current was passed through a wire coaxial with the tube, the annular field produced by it being everywhere perpendicular to the axis. The component of the change in magnetization perpendicular to the field produced an e.m.f. in the search coils placed in the same positions as they were when measuring the longitudinal effect. For both longitudinal and transverse effects the search coils were connected to the amplifier and measurements of the Barkhausen "noise" made with a thermocouple and galvanometer connected to the amplifier output.

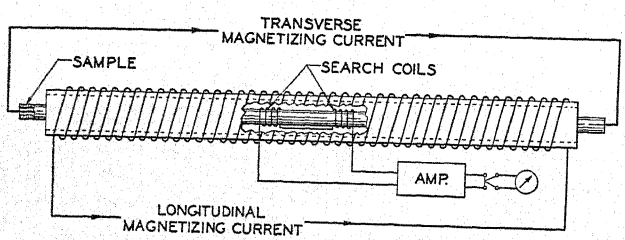


Fig. 1. Diagram of the apparatus for measuring both longitudinal and transverse effects.

As described in a previous paper,[1] the quantities measured were the slope of the B-*vs.*-H curve dB/dH, the rate at which the field was changed during measurements dH/dt, the reversible permeability μ, and the amplifier output i^2 (or the equivalent galvanometer deflection δ) which is a quantitative measure of the noise. We previously[1] derived the following expression for the average change in magnetic moment:

$$\Delta M = \frac{2(10)^{-14}\mu^{3/2}\delta}{C^2 I_s \rho^{3/2}(dB/dH)(dH/dt)} \tag{1}$$

where C is a constant of the apparatus, I_s the saturation value of the magnetization of the material under investigation, and ρ its resistivity. Since now we are dealing only with the ratio of the Barkhausen effects parallel and perpendicular to the field, it is unnecessary to determine many of the quantities in Eq. (1). The ratio of the change in magnetic moment taking place at right angles to the direction of the applied (annular) field, to the change paral-

[1] R. M. Bozorth and J. F. Dillinger, Phys. Rev. **35**, 733–752 (1930). See also the short accounts of the present work in Phys. Rev. **38**, 192–193 (1931); **39**, 353–356 (1932).

lel to the applied (axial) field, (transverse change divided by longitudinal change), is then given by

$$\frac{\Delta M_T}{\Delta M_L} = \frac{\mu_T^{3/2}\delta_T(dB/dH)_L(dH/dt)_L}{\mu_L^{3/2}\delta_L(dB/dH)_T(dH/dt)_T} \tag{2}$$

where the subscripts T and L refer to quantities measured in determining the transverse and longitudinal effects, respectively. In particular, the *transverse reversible permeability* μ_T is the ratio of the small change in induction parallel to the axis of the specimen, to the very small change in field strength applied in the same direction, when the specimen is magnetized principally annularly by the current flowing along the axis.

The rates of decay of eddy-currents caused by the discontinuities in magnetization measured, are affected by the geometry of the specimen in the same way for annular as for axial magnetization, since the search coils remain in the same position with respect to the specimen for both kinds of measurements. The eddy-currents which affect the rate of change of magnetization picked up by the search coils, are in all cases in a plane perpendicular to the axis of the specimen.

Measurements of μ, δ, dB/dH and dH/dt, were made as previously described.[1] The annular B and dB/dH were measured using an additional (third) search coil each turn of which passed inside of the tubular specimen along its length and returned on the outside. Since the cross section of magnetic material thus enclosed is relatively large, only a few turns were necessary. The axial current producing the annular magnetization was varied smoothly by means of a liquid resistance, a solution of copper sulphate into which a set of copper plates was lowered.

In a preliminary experiment the specimen was magnetized axially and the regular search coils (Fig. 1) connected to the amplifier as already described while at the same time the additional search coil wound as described above to detect the transverse change in magnetization due to an axial field, was connected to a second amplifier, the outputs of the two amplifiers being recorded simultaneously on the same moving photographic paper. It was thus observed that a single discontinuity in longitudinal magnetization was accompanied by a discontinuity in transverse magnetization. The direction of the deflection of the string recording the longitudinal effect was always the same, while the deflections of the string recording the sudden transverse changes were about half in one direction and half in the other. This showed that the average change in magnetization perpendicular to the applied field is zero, but that for any single event there was in general a change in one direction or the other. After this preliminary experiment we confined our experiments to the longitudinal effect occurring with axial field, and to the transverse effect with annular field.

Results

The materials investigated were annealed iron, hardworked iron, and annealed perminvar containing 30 percent Fe, 25 percent Co and 45 percent

Ni. No analyses of these specimens were made, but analyses of similar specimens indicate that the following impurities were present: in annealed iron, 0.1 percent C and 0.5 percent Mn; in hard iron, no impurity more than 0.02 percent; in annealed perminvar, 0.1 percent Si. The tubes were all 60 cm long. The outside diameters of the perminvar and hard iron tubes were 0.47 cm and the wall thicknesses 0.025 cm. For the annealed iron specimen the corresponding dimensions were 0.63 cm and 0.056 cm. The annealed iron was heated in vacuum for 2 hours at 1100° C and cooled 400° C per hour. The

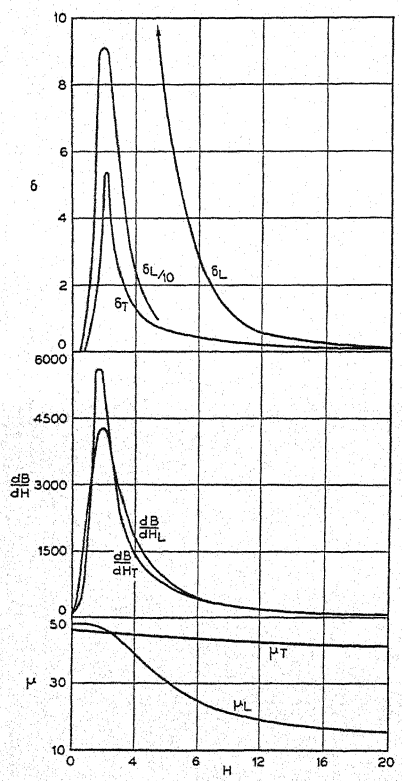


Fig. 2a

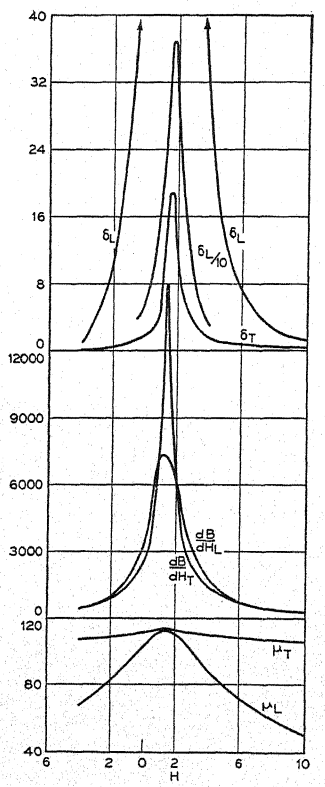


Fig. 2b

Fig. 2a. Values of δ (output power of amplifier), dB/dH and μ for the magnetization curve of annealed iron, measured with transverse and longitudinal magnetizing fields. The amplifier output δ is referred to a constant value of dH/dt.

Fig. 2b. Values of δ, dB/dH and μ for the hysteresis loop of annealed iron, measured with transverse and longitudinal magnetizing fields.

perminvar was annealed for 1 hour at 875° C and cooled at a maximum rate of about 100° C per hour.

The values of dB/dH, μ, and δ for both longitudinal and transverse effects, for the hysteresis loop and magnetization curve of *annealed iron*, are shown in Fig. 2. The two hysteresis loops for annular and axial magnetization were almost identical, differing only on the steep parts of the curves where the demagnetizing factor has the greatest influence. The galvanometer deflections were observed for various values of dH/dt and from them δ_T and

δ_L were calculated for a constant value of dH/dt, using the relation $\delta \propto dH/dt$. The relative magnitudes of the longitudinal and transverse effects for the magnetization curve as shown in Fig. 3 where the average change in moment

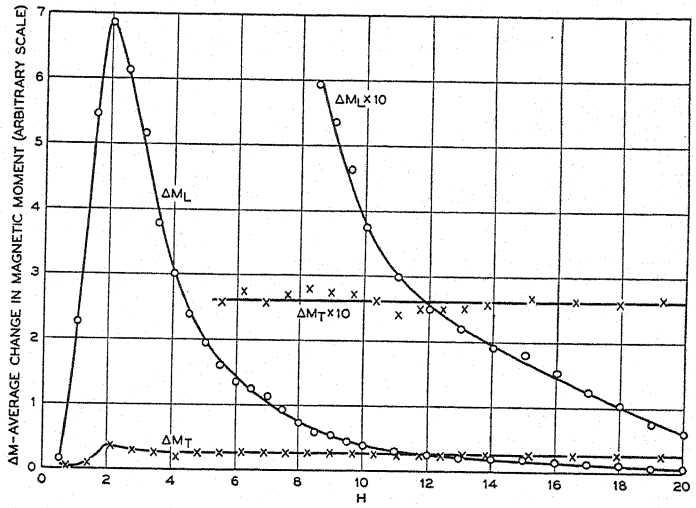


Fig. 3. Longitudinal and transverse changes in magnetic moment for the magnetization curve of annealed iron.

for each is plotted on the same scale as a function of the applied field H, and in Fig. 4 where the ratio of the effects is plotted as a function of the

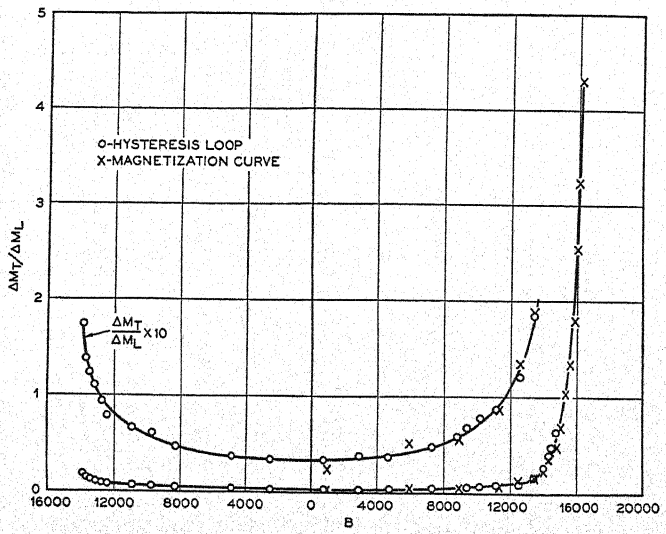


Fig. 4. Ratio of the transverse to the longitudinal change in magnetic moment in annealed iron.

induction B. Since $H \ll B$ except when B is very small, the latter is practically proportional to the magnetization. Fig. 4 shows that the change in magnetization of a domain is greater in the direction of the applied field than in direc-

tions at right angles until B is as large as 15,000. In relatively low fields, where the slope of the hysteresis loop is greatest, the direction of magnetization changes by very nearly 180°, and is antiparallel to the applied field before and parallel to it after the change. The modes of reversal of the domain will be discussed further below.

The values of dB/dH, μ, and δ for the hysteresis loop of *hard worked iron* are shown in Fig. 5. The coercive force of this material was 1.1 gauss.[2] The ratio of the transverse to the longitudinal change in magnetization in

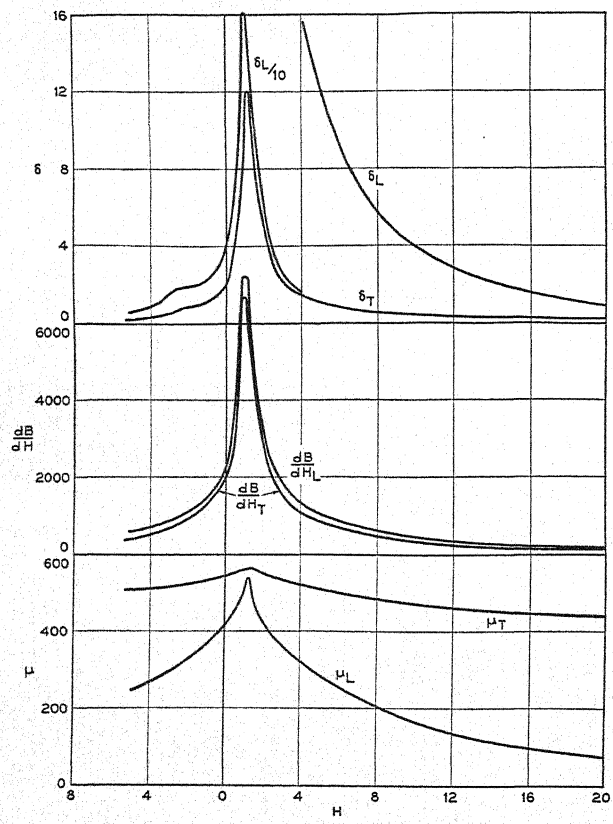


Fig. 5. Values of δ, dB/dH and μ for the hysteresis loop of hard iron, measured with transverse and longitudinal magnetizing fields.

the domains is shown in Fig. 6 as a function of B. For the same value of B, this ratio is a little larger than that for annealed iron.

The data for perminvar are shown in Fig. 7. The hysteresis loop for a maximum field strength of 4 gauss is shown in Fig. 8 because of its peculiar characteristic shape. The ratio of the transverse to the longitudinal change for this hysteresis loop is shown as a function of B in Fig. 9. No measurements were made at higher fields.

[2] Although this material is hard worked, its coercive force is about that normally found for annealed iron. This specimen was given a special treatment in hydrogen (see P. P. Cioffi, Phys. Rev. **39**, 363–367 (1932)) and if annealed would have a coercive force of about 0.1 gauss.

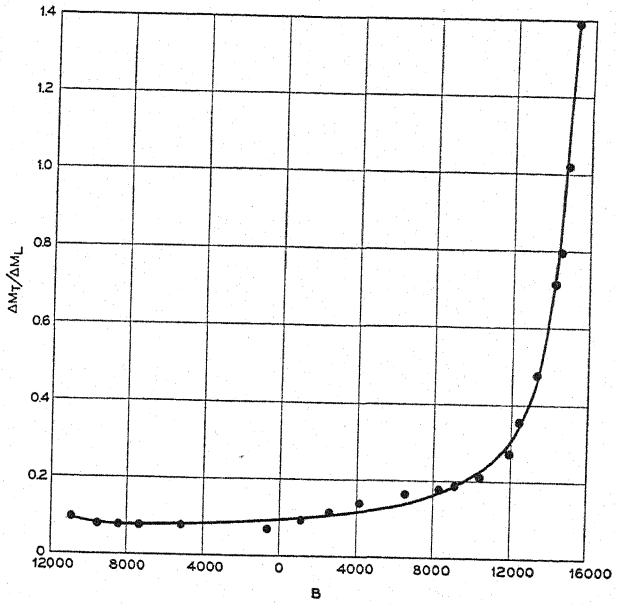


Fig. 6. Ratio of the transverse to the longitudinal change in magnetic moment in hard iron.

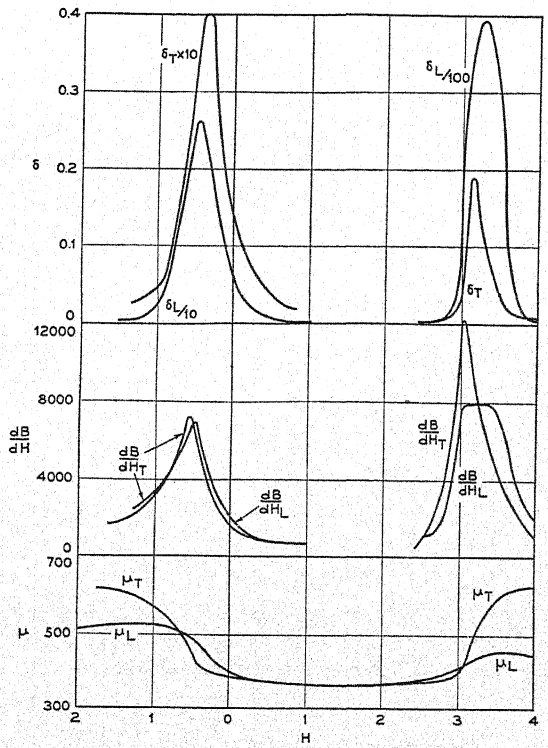


Fig. 7. Values of δ, dB/dH and μ for the hysteresis loop of perminvar, measured with transverse and longitudinal magnetizing fields.

Discussion

One of the most obvious characteristics of the curves of Figs. 4 and 6 is that when the magnetization is small the longitudinal components of the

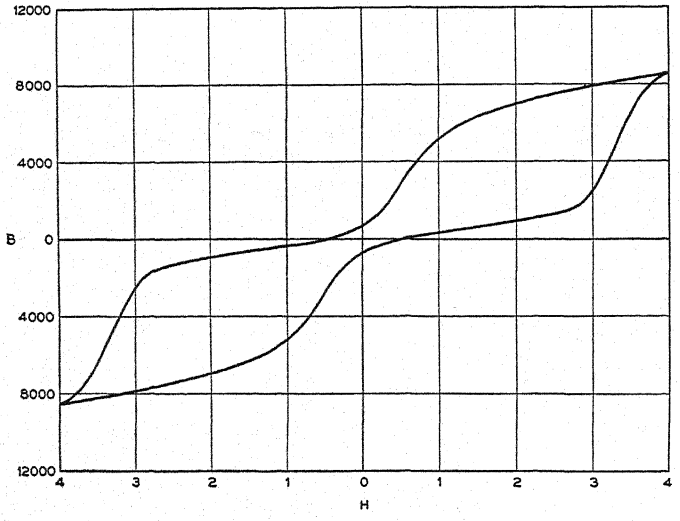


Fig. 8. Hysteresis loop for perminvar.

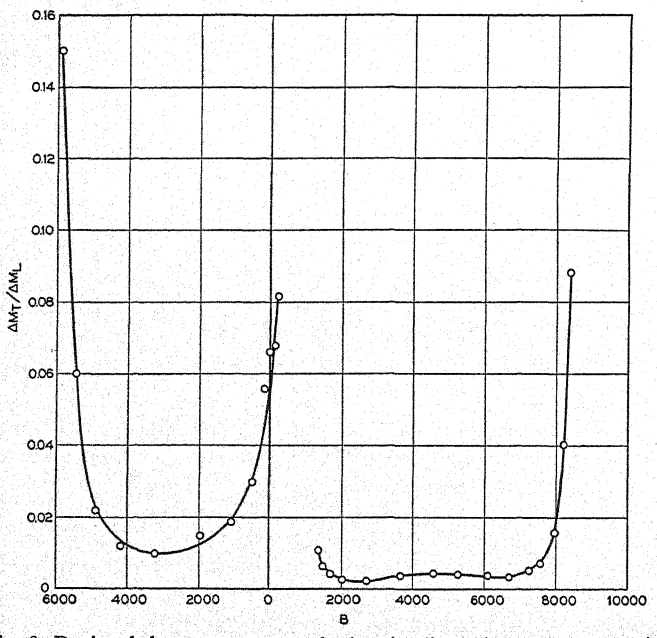


Fig. 9. Ratio of the transverse to the longitudinal change in magnetic moment in perminvar.

discontinuous changes in magnetization are larger than the transverse components, but that when the magnetization is large the transverse component is the larger. Two kinds of change of magnetization which are consistent with

this result are illustrated in two dimensions in Fig. 10. Here a shows a reversal of the magnetization-vector from the initial position (dotted line) to a final position making an angle $\theta=15°$ with the direction of the field. In this case $\Delta M_T/\Delta M_L=0.27$. If θ is 75° as in (b), this ratio is 3.7. In (c) and (d) the vectors rotate by 90° instead of 180° as in (a) and (b), and for final positions defined by $\theta=15°$, the values of $\Delta M_T/\Delta M_L$ are 0.58 and 1.73 respectively. It is evident that the ratio becomes large without limit as θ approaches 90° in (b) or 45° in (d). Since we should expect that the latter changes would occur at relatively high magnetizations, and changes of kind (a) at low magnetizations, we have here a qualitative correspondence with the data as shown in Figs. 4 and 6.

Consideration of Fig. 10 (d) also shows that as θ approaches 45° the transverse change, equal to sin $\theta+\cos\theta$, approaches asymptotically the definite limit $2^{1/2}$, taking the radius of the circle as unity. Since θ approaches 45° when

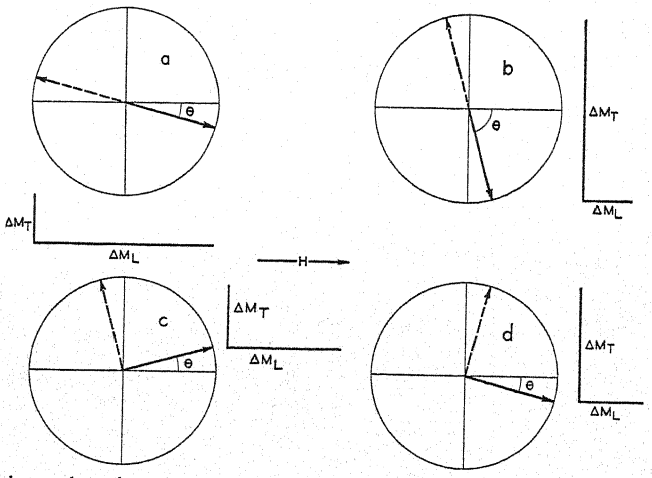


Fig. 10. Possible modes of reversal of magnetization in elementary domains, with the corresponding transverse and longitudinal components.

the magnetization is high, we should expect that then also the transverse effect should become constant. This constancy was observed as shown in Fig. 3.

The two kinds of changes shown in Fig. 10 correspond to two views of the changes which take place in ferromagnetic materials. Both are based on Weiss' idea that a ferromagnetic substance is composed of small domains, each of them initially magnetized to saturation along some direction of *natural magnetization*. According to one view (Webster's[3] and Heisenberg's[4]) which is suggested by experiments on single crystals, the directions of natural magnetization in a domain are the six <100> directions of the crystal which contains the domain; an applied field may shift the magnetization from one of these directions to another making a smaller angle with its own. According to the other view (resembling R. Becker's[5]) the directions of natural magnetization

[3] W. L. Webster, Proc. Phys. Soc. London **42**, 431–440 (1930).
[4] W. Heisenberg, Zeits. f. Physik **69**, 287–297 (1931).
[5] R. Becker, Zeits. f. Physik **62**, 253–269 (1930).

are controlled by the strains in the substance, and the only effect which an applied field can produce in a domain is a reversal of the magnetization. The changes shown in (a), (c), and (d) of Fig. 10 are compatible with the former view, (a) and (b) with the latter.

The way in which these views fit in with our results is illustrated in Fig. 11. If the directions of magnetization in the domains are controlled by the lattice of the crystal, discontinuous changes in a polycrystalline specimen can occur only until the directions of magnetization in the domains all make angles of 45° or less with the direction of the field. When this condition is attained the material is about 85 percent saturated, and the ratio $\Delta M_T/\Delta M_L$ is indefinitely large as indicated by the vertical line (a) in Fig. 11. If the control is by strain alone, the corresponding limit is designated by (b) which indicates that discontinuous processes cease when the directions of magnetization in the

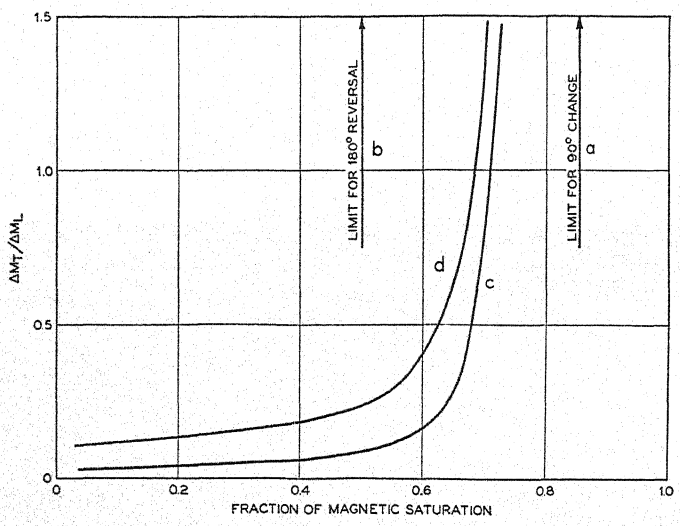


Fig. 11. Ratios of the transverse to the longitudinal change in magnetic moment in (c) annealed iron and (d) hard iron and their relation to the theoretical limits (a) for 90° changes and (b) for 180° reversals.

domains make angles of 90° or less with the direction of the field, in which case the material as a whole is only half saturated. Curves (c) and (d) represent the actual data for annealed and hard worked iron, respectively, for comparison. The curves suggest that in each material the magnetization is controlled in some of the domains by strain and in some by the lattice, the domains of the former class being increased in relative number by hard working. By interpreting the data in this way, strain has some influence even in well annealed iron, and in hard worked iron there is still a considerable amount of crystallographic control. The interpretation of the difference between the experimental curves at the lowest values of B is not yet clear; the explanation of this difference may influence the conclusions already drawn. It is intended to make a more quantitative comparison between theory and experiment in a later paper.

The curve of Fig. 9, for perminvar, is different from those for iron in that $\Delta M_T/\Delta M_L$ has relatively high values near $B=0$ as well as when B is large. This is in accord with other peculiarities of perminvar which have been regarded[6] as indicating that it is a mixture of two kinds of magnetic materials. Although the nature of the difference (if any) between these materials is yet undetermined, the data here reported are such as would be expected if about half of the material approached saturation before the other half began to change its magnetic state appreciably, and for each portion the ratio $\Delta M_T/\Delta M_L$ went through the usual changes during the cycle.

In summary, our data are in good agreement with the following conceptions: Magnetic materials are divided into small domains each of which is magnetized to saturation. In annealed materials the direction of magnetization in each domain is one of the directions of easy magnetization in the crystal which contains the domain; these, in the special case of annealed iron, are the directions of the crystal axes. With an increase in the magnetization of the material as a whole, the magnetization in each domain changes from one of these directions to another making a smaller angle with the applied field. When the net magnetization is small, most of the changes are reversals in the domains in which the initial magnetization is almost anti-parallel to the applied field. When the net magnetization is large (one half to three quarters of the saturation value), other domains are affected in which the initial magnetization is inclined at smaller angles to the field and changes of 90° occur. When saturation is almost attained a new phenomenon appears, the directions of magnetization in all of the domains cease to be controlled by the crystal lattice and approach parallelism to the applied field. This final approach to saturation is a continuous one and is not believed to be accompanied by Barkhausen effect.

[6] G. W. Elmen, J. Frank. Inst. **260**, 317–338 (1928); **207**, 583–617 (1929); U. Meyer, Phys. Zeits. **28**, 919–920 (1927); H. Kühlewein, Wiss. Veröff; Siemens-Konz. **10**, No. 2, 72–88 (1931), and Phys. Zeits. **31**, 626–640 (1930).

The Variation with Temperature of the Thermoelectric Power of Nickel and Some Copper-Nickel Alloys

By K. E. GREW
Sloane Physics Laboratory, Yale University

(Received June 9, 1932)

The thermoelectric power of pure nickel against platinum has been measured between 0°C and 500°C; similar measurements have been made on two nickel-copper alloys containing respectively 94 and 79 percent nickel. A differential method was used in which the change in thermoelectric force ΔE corresponding to a small temperature change ΔT was observed. The results are discussed in relation to Stoner's theory. Although the experimental results have the same general characteristics as those calculated, factors not considered in the simple theory are involved, even at temperatures at which the assumption that the magnetization is due to spin moments only is approximately valid.

THAT the thermoelectric properties of a ferromagnetic are in some way related to the magnetization is apparent from the sudden change in the Thomson coefficient or the "specific heat of electricity" at the Curie point.

The magnitude of this change in nickel has been deduced[1] from measurements of the thermoelectric power in the neighbourhood of the Curie point, and it is found to be approximately equal to that predicted on the quantized Weiss theory for a magnetic "carrier" for which $j=\frac{1}{2}$. This agreement in magnitude was at first regarded as implying that the carriers were free electrons, but the argument was invalidated when it was found that the specific heat of the electron increases on passing from the ferromagnetic to the paramagnetic state, whereas the "calorimetric" specific heat decreases. Stoner[2] has sought to explain this difference in sign, and on certain assumptions he has deduced an expression for the temperature variation of the thermoelectric power and the specific heat of electricity in ferromagnetics. The results of Dorfman and Jaanus[1] show considerable divergence from the theoretical values, but as they admit of a comparison over only a limited range of temperature it was thought desirable to extend the measurements.

METHOD OF EXPERIMENT

In measuring the temperature variation of the thermoelectric power it is desirable to use a direct method in which the change in thermoelectric force ΔE due to a small change in temperature ΔT is observed.

The method first adopted for the measurement of the thermoelectric power of nickel against platinum and described in a preliminary note,[3] was discarded, as it did not give consistent results at the higher temperatures; this was probably because it did not ensure that the nickel-platinum junctions were always at precisely the same temperature as the junctions of the

[1] J. Dorfman, R. Jaanus, and I. Kikoin, Zeits. f. Physik **54**, 277 (1929). J. Dorfman, R. Jaanus, K. Grigorow and M. Czernichowski, Zeits. f. Physik **70**, 796 (1931).
[2] E. C. Stoner, Proc. Leeds Phil. Soc. **2**, 149 (1931); Phil. Mag. [7] **12**, 737 (1931).
[3] K. E. Grew, Proc. Leeds Phil. Soc. **2**, 217 (1931).

couple used to measure the temperature difference. An arrangement similar to that of Dorfman and Jaanus[1] was tried, but the mica sheets used as insulation were found to become conducting at the higher temperatures.

In the method finally adopted, the nickel wire under investigation was fused to the junction of a previously calibrated platinum platinum-iridium couple, thus forming a second, nickel-platinum, couple. In series with each couple was a small resistance through which a current could be passed. The electromotive force of the couples with one junction at 0°C and the other at T°C could be almost completely counterbalanced by the potential difference across the resistances, so that the small residual potential difference could be measured on a sensitive potentiometer. The difference between this reading and a second, when the temperature had been raised to $T+\Delta T$, gave the increase in electromotive force ΔE corresponding to a change ΔT at the mean temperature $T+\frac{1}{2}\Delta T$. ΔT was calculated from the change in electromotive force of the platinum-iridium couple, and thus the thermoelectric power $\Delta E/\Delta T$ of nickel was found. This method allowed the use of a more sensitive potentiometer than would have been possible had the whole of the thermoelectric force been applied to it. It was necessary, however, in order to find the temperature T, to measure the total electromotive force of the platinum-

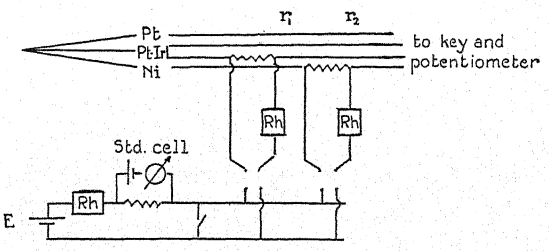


Fig. 1. The thermocouple system.

iridium couple; for this purpose the range of the potentiometer could be changed.

The circuit is shown in Fig. 1. The three wires leading to the hot junction were insulated from each other by quartz tubes. These were contained in a Pyrex tube and inserted in the furnace, which consisted of a cylindrical copper block wound with a non-inductive heating coil enclosed in a vacuum vessel; the couples passed into a hole drilled along the axis of the block. The wires emerging from the furnace were soldered to copper wires and the junctions kept in melting ice in a vacuum vessel. r_1, r_2 are the small resistances of about 1 ohm, through either of which a current from the battery E could be passed. The constancy of this current throughout a set of measurements could be checked by the standard cell and resistance; such small fluctuations as did occur were usually negligible. A key enabled (a) the platinum-iridium couple to be connected directly to the potentiometer for the measurement of the temperature T of the junction; (b) the same couple to be connected through the resistance r_1 for the measurement of the temperature difference ΔT which was usually 3 to 5 degrees; (c) the nickel-platinum couple to be connected through the resistance r_2 for the measurement of ΔE; (d) the reversal of all these connections.

To eliminate parasitic electromotive forces, it was necessary that the whole circuit with the exception of the couples themselves should be of copper. The key was constructed such that all its metal parts were of copper with no soldered connections, and as a further precaution it was enclosed in a case to avoid local heating while being operated. The small resistances were also wound from copper wire and kept at constant temperature in an ice bath on account of the large temperature coefficient of resistance of copper. Care was also taken to eliminate leakage from the heating circuit to the couple system.

The potentiometer consisted of a manganin coil wound on a marble cylinder, with a revolving contact and circular scale. By series resistances the range could be adjusted for measuring either the total electromotive force E or the small change ΔE. For the latter, 1 division on the scale corresponded to 0.075 microvolt or to a deflection of the galvanometer of 2 mm. The potentiometer was calibrated by comparison with a Wolff potentiometer. Stray electromotive forces could not be prevented in this part of the circuit, but their effect was eliminated by reversing the current and the connections to the couples.

The platinum platinum-iridium couple was calibrated between 0° and 500°C, using standard thermometers up to 200°C and the boiling points of naphthalene, benzophenone, and sulphur for the higher temperatures. The whole range was divided into 3 overlapping sections and equations of the form $T=AE+BE^2+CE^3$ were found for each. The temperatures calculated from the observed electromotive force by means of these equations should not be in error by more than 0.3°C. To calculate the change in temperature ΔT from the observed change in electromotive force ΔE it is necessary to know the temperature variation of dE/dT. This was found directly from the calibration curve.

In practice it is not possible to prevent small changes in the furnace temperature while readings are being taken. The effect of such changes, which were usually less than 0.1°C, was eliminated by taking readings at definite time intervals.

The error in individual values of the thermoelectric power is estimated at 0.7 percent.

Experimental Results

Measurements were made of the thermoelectric power of nickel and of some alloys of nickel with copper over a range from 0°C to 500°C. The nickel was drawn from rod supplied by Messrs. Hilger and was 99.97 percent pure. The copper was from the same source and of the same purity. For the preparation of the alloys and the subsequent drawing into wires I am indebted to the National Physical Laboratory, England. Melting was carried out in a crucible of china-clay and alumina, in a high frequency induction furnace using an atmosphere of hydrogen. The ingots were swaged into rods and finally drawn into wires of 0.4 mm diameter. Before measurements were made the wires were heated for some time at 800–900°C.

An obvious extension of the method allowed observations to be made on two specimens at the same time.

TABLE I. *Results for nickel and alloy A_1 (94 percent nickel).*

Temp. °C	$-\Delta_{Ni}E_{Pt}/\Delta T$	$-\Delta_{A_1}E_{Pt}/\Delta T$	Temp. °C	$-\Delta_{Ni}E_{Pt}/\Delta T$	$-\Delta_{A_1}E_{Pt}/\Delta T$
55.0	15.00	24.78	318.0	11.38	13.65
91.0	15.46	24.74	329.5	—	13.38
116.2	15.97	24.76	331.5	10.36	13.45
139.4	16.24	24.53	347.1	8.77	13.36
161.3	16.44	24.12	353.4	8.02	13.40
186.1	16.16	23.11	359.2	7.05	13.40
198.5	16.11	22.60	362.9	6.94	—
220.8	15.72	21.65	377.4	6.67	—
242.6	15.17	19.96	392.4	6.42	13.86
257.4	14.82	18.80	398.5	6.51	14.00
264.1	14.33	17.80	407.6	6.44	14.02
281.5	13.44	16.03	425.1	6.59	14.03
290.5	—	14.66	441.4	6.84	14.39
296.0	12.77	13.86	464.0	7.23	14.70
306.4	12.23	13.91	482.4	7.47	15.00

TABLE II. *Results for alloy A_2 (79 percent nickel).*

Temp. °C	$-\Delta_{A_2}E_{Pt}/\Delta T$	Temp. °C	$-\Delta_{A_2}E_{Pt}/\Delta T$
41.6	29.30	179.9	24.45
69.43	28.38	194.7	24.77
86.7	27.87	210.7	24.96
100.4	27.24	240.8	25.58
115.2	26.51	258.0	26.10
124.2	25.60	262.8	26.27
128.9	25.24	266.6	26.28
145.7	24.18	279.0	26.66
158.5	24.10	304.2	27.04
171.4	24.36		

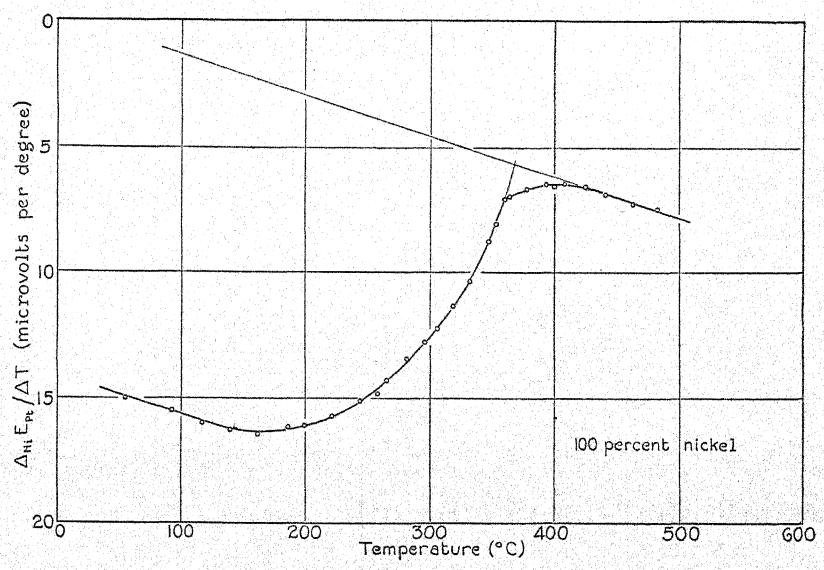


Fig. 2. The temperature variation of the thermoelectric power of nickel with respect to platinum.

The results for pure nickel and an alloy (A_1) containing 94 percent nickel are given in Table I and for a 79 percent alloy (A_2) in Table II, while they are represented graphically in Figs. 2, 3 and 4. The thermoelectric power is in microvolts per degree.

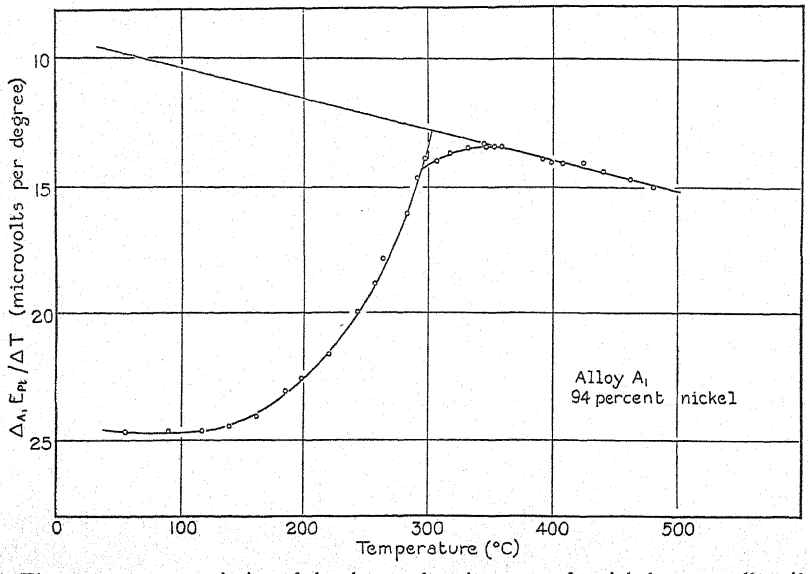


Fig. 3. The temperature variation of the thermoelectric power of a nickel copper alloy (94 percent nickel) with respect to platinum.

It will be seen that, in the case of pure nickel, the slope of the thermoelectric power curve changes abruptly at 360°C; thereafter it decreases continuously, finally assuming a constant negative value above 430°C. These changes were confirmed by the observations of the total electromotive force

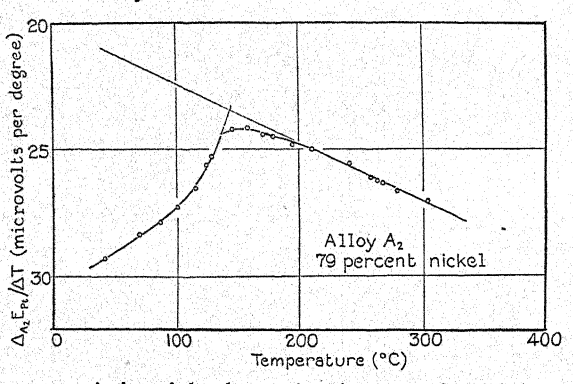


Fig. 4. The temperature variation of the thermoelectric power of a nickel copper alloy (79 percent nickel) with respect to platinum.

made concurrently, and which were in excellent agreement with those of Jordan and Swanger.[4]

The nature of the curves for the alloys is not essentially different, though the change of slope occurs at a different temperature.

[4] L. Jordan and W. H. Swanger, U. S. Bureau of Stds. Jour. of Res. **5**, 1304 (1930).

Over the limited range of temperature in which comparison is possible, the present results for pure nickel are some 4 percent greater (numerically) than those of Dorfman and Jaanus. The difference is not surprising, considering the effect of impurities and previous treatment on thermoelectric properties.

Discussion

In the papers to which reference has already been made, Stoner[2] has shown that the behavior of a ferromagnetic may be largely explained by attributing ferromagnetism to interchange interaction electrons having a spin moment $j=\frac{1}{2}$, though at temperatures approaching the Curie point it appears necessary to regard the orbital moment as being partially effective.

According to Fowler, the specific heat of electricity per electron may be defined as the increase in specific heat of the metal due to the addition of one electron. Stoner has given reasons for supposing the magnetically effective spin moments to be those of "missing" electrons, and that the addition of a free electron will neutralise one of these spins. If the contribution of each spin moment to the "magnetic" specific heat is s, and the specific heat of electricity per electron due to the magnetization is σ_e, then $\sigma_e = -s$. For the gram electron, the specific heat

$$C_E = L\sigma_e = -Ls = -S_M/q$$

where L = Avogadro's number; S_M = specific heat per gram-atom due to the magnetization; q = number of effective spin moments per atom. The thermoelectric power referred to the same units is given by

$$P_E = \int_{T/\theta}^{1} \frac{S_M/q}{T/\theta}\, d\left(\frac{T}{\theta}\right)$$

where θ is the Curie point, and P_E is the thermoelectric power of the ferromagnetic with respect to another substance without intrinsic magnetization but otherwise identical. It is zero at the Curie point, and becomes increasingly negative as the temperature decreases. Both C_E and P_E are independent of q.

These expressions refer only to the idealized ferromagnetic, in which spin moment alone is effective.

For comparison with the theoretical values, a quantity P_{obs} can be calculated from the experimental results, such that

$$P_{\text{obs}} = (\text{Ni}P_{\text{Pt}})_T - (\text{Ni}P'_{\text{Pt}})_T$$

where P' is the thermoelectric power at temperature T extrapolated from observations above the Curie point. P_{obs} should be comparable with P_E provided that the variation of the thermoelectric power can be regarded as the sum of the variation due to changing magnetization and a "normal" variation. Alternatively, the quantity C_{obs} can be calculated from the slope of the thermoelectric power curves and compared with the observed and calculated values of the specific heat S.

Values of P_E (taken from Stoner's paper) and of P_{obs} are plotted in Fig. 5 as functions of T/θ. The changing direction of the thermoelectric power curves above the Curie point makes the extrapolation involved in determining P_{obs} uncertain. The extrapolation has been made from that part of the

curve where the thermoelectric power is decreasing (algebraically) approximately uniformly with the temperature, this being the most favorable from the point of view of obtaining agreement between the theoretical and experimental values. The curve for iron is obtained from the measurements of

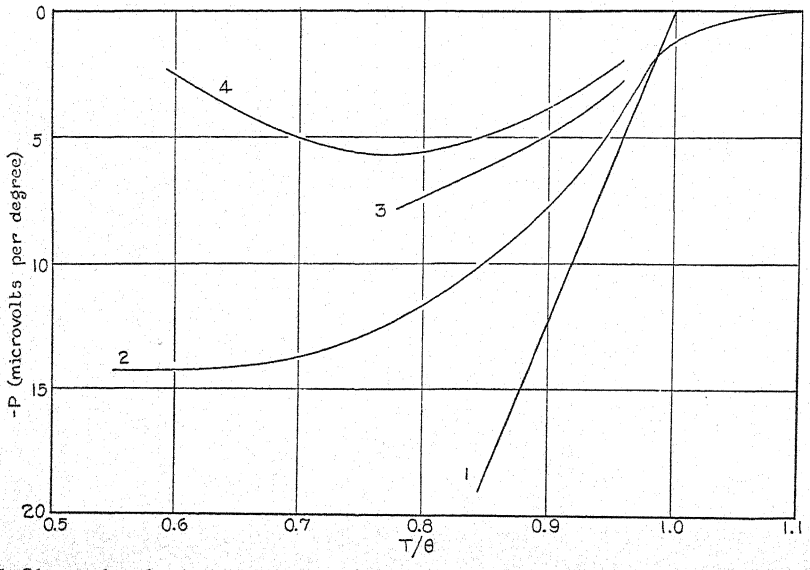


Fig. 5. Observed and calculated thermoelectric power curves. 1. P_E; 2. P_{obs} for nickel; 3. for alloy A_2; 4. for iron.

Burgess and Scott.[5] Values of P_{obs} for the alloy A_1 coincide nearly with those for pure nickel, and the curve is not shown in the figure.

In all cases, the value of P_{obs} is less (numerically) than the calculated value P_E, the divergence increasing at the lower temperatures. The ratio P_{obs}/P_E has the values found in Table III. For iron, P_{obs} actually becomes

TABLE III.

T/θ	0.9	0.8
Pure nickel	0.62	0.48
Alloy A_1	0.60	0.48
Alloy A_2	0.39	0.31
Pure iron	0.30	0.22

positive below $T/\theta = 0.5$, but the small number of observations and the probability of an effect due to the phase change near the Curie point make the justification for the extrapolation more doubtful than in the other cases.

In the case of pure nickel, it is of interest to compare the specific heat of electricity C_{obs} with the "magnetic" specific heat S given by Mme. Lapp.[6] Fig. 6 shows the variation with temperature of the observed specific heat S corrected for quantum variation, dilatation, etc.; of S_1, which Mme. Lapp calculates from the variation of the magnetization $d\sigma^2/dT$ and the molecular field constant applicable above the Curie point; and of $-C_{obs}$ derived from

[5] G. K. Burgess and H. Scott, U. S. Bureau of Stds. Bull. **14**, 15 (1917).
[6] Mme. Lapp, Ann. de Physique [10] **12**, 442 (1929).

the thermoelectric power curves. The existence of the abnormally high specific heat above the Curie point makes impossible any definite conclusion as to the relation between C_{obs} and S to be expected from Stoner's considerations. But at temperatures not too near the Curie point, where the magnetization may be attributed to spin moment alone, it would be expected that C_{obs} would be numerically greater than S or S_1, since the number of effective spin moments per atom is less than unity. This is not so, C_{obs} being less than either S or S_1 at temperatures below $T/\theta = 0.9$. Thus there is no apparent quantitative relationship between the specific heat of electricity and the "magnetic" specific heat whether one considers the values of the specific

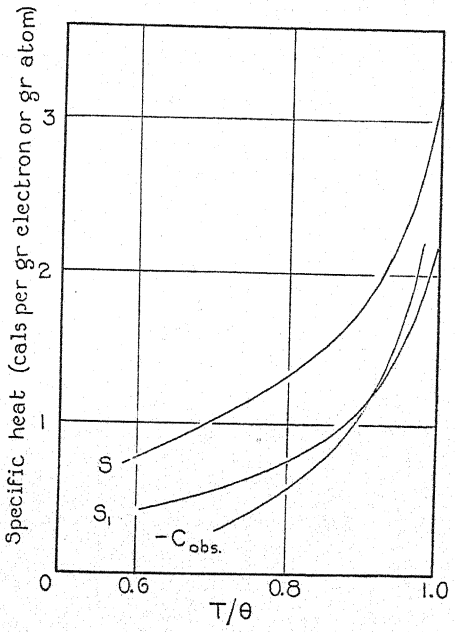


Fig. 6. Specific heat of electricity in nickel. S and S_1 after Mme. Lapp;—C_{obs} from thermoelectric power curves.

heat calculated for the idealized ferromagnetic or those experimentally determined for an actual ferromagnetic.

It appears that, although the experimental results for the temperature variation of the thermoelectric power have the same general characteristics as those calculated, factors not considered in the simple theory are involved, even at temperatures at which the assumption that the magnetization is due to spin moments only is, at least approximately, valid.

It is hoped that an investigation of other properties of the copper-nickel alloys dependent on magnetization will assist in explaining further the variation of the thermoelectric power in ferromagnetics.

This investigation was begun at the University of Leeds, England; a Commonwealth Fund Fellowship permitted of its continuation at Yale University. My thanks are due to Dr. E. C. Stoner and to Professor L. W. McKeehan for their interest and kindly criticism. I have also to acknowledge with thanks a grant from the Royal Society.

Diamond Windows for Withstanding Very High Pressures

By THOS. C. POULTER AND FRANCIS BUCKLEY
Department of Physics, Iowa Wesleyan College

(Received June 10, 1932)

Diamond windows have been tested out and found to withstand much greater pressures than glass or fused quartz windows (up to 21,500 atmospheres), particularly when water and alcohol solutions are used to transmit the pressure to the windows.

PROCEDURE AND RESULTS

NO HIGH pressure window up to the present time has been successfully constructed to withstand a pressure of more than 30,000 atmospheres, and then, only when the transmitting medium is a light paraffin oil or some similar material. If a material such as alcohol, water or ether is used to transmit the pressure the windows are usually fractured between 4000 and 8000 atmospheres.

This difficulty has in some cases been overcome by placing the above named liquids in a small collapsible or telescoping cell which is fitted at each end with a glass window through which one may make his observations.[1] The pressure is then transmitted to the cell by paraffin oil. Thus, the liquids which break the windows easily do not come in contact with those windows which support the pressure. By this method alcohol, ether, or water, and solutions in which these liquids are used as solvents can be observed up to 30,000 atmospheres.

The method of using a small cell inside the pressure cylinder is not completely satisfactory because some of the liquid in the cell may escape and come in contact with the pressure windows thus causing them to break. Another disadvantage in using such a cell is the fact that after the pressure has been built up to 10,000 atmospheres, or higher, and is then released, the inner surface of the cell windows are frequently fractured while in most cases the side of the window in contact with the oil is not injured. In some experiments carried out in this laboratory it was shown that diamonds showed no tendency to fracture when subjected to such conditions. This led us to believe that diamond windows should be very effective as pressure windows even though the medium used to transmit the pressure be one of those that readily breaks glass or fused quartz.

The diamond used in this investigation was 3 mm thick and 3.5 mm in diameter. It was mounted on a hard steel support polished to a mirror surface over a hole 1.5 mm in diameter and held in place in the usual manner by a small amount of liquid balsam.

[1] Thos. C. Poulter, Phys. Rev. **40**, 860 (1932); Thos. C. Poulter and Robert O. Wilson, Phys. Rev. **40**, 877 (1932); Thos. C. Poulter and Carl A. Benz, Phys. Rev. **40**, 872 (1932).

The diamond window was then surrounded by water and subjected to a pressure of 21,500 atmospheres. When the window was removed from the cylinder it was not damaged in any way. Since 21,500 atmospheres pressure is more than that necessary for the formation of ice VI, the diamond window was surrounded by a 50 percent solution of ethyl alcohol. A pressure of 21,500 atmospheres was applied. At this pressure the cylinder which contained the diamond window ruptured, thus releasing the pressure instantaneously but without damage to the diamond window.

Another cylinder was used in an attempt to test the diamond window to still higher pressures but this cylinder ruptured at about the same pressure. The diamond window used in these tests has been under pressure more than twenty times and in three cases the pressure has been released suddenly by the splitting of the cylinders. Since these windows show no ill effects from the tests which we have made thus far, it is the belief of the authors that such windows will prove very valuable in the field of optical studies at high pressures.

The Effect of Pressure on the Index of Refraction of Paraffin Oil and Glycerine

By THOS. C. POULTER, CARTER RITCHEY AND CARL A. BENZ
Physics Department, Iowa Wesleyan College

(Received June 10, 1932)

A refractometer for measuring the index of refraction of liquids under very high pressure is described. The values obtained for glycerine and a paraffin oil together with the constants for the Lorenz-Lorentz relation are tabulated.

PROCEDURE AND RESULTS

THERE have been relatively few studies made on the change of the refractive index with pressure and those at pressures seldom, if ever, greater than 200 atmospheres.

By making use of a liquid prism which could be subjected to high pressure, the authors have constructed a refractometer for studying the effect of very great pressure upon the index of refraction of different materials.

The windows are mounted directly in contact with the hard steel disk *R* in the figure and in such a position that the liquid in the apparatus forms a 30° prism.

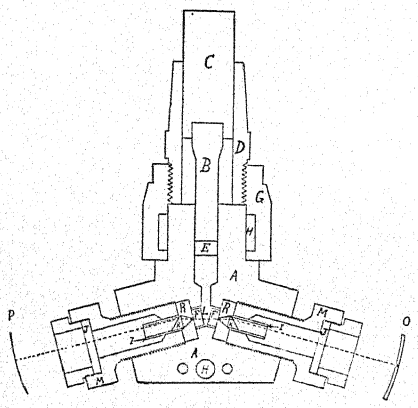


Fig. 1.

In measuring the index of refraction for different materials a much smaller opening is made in the window support than had been used in the ordinary type of pressure cylinder. This serves as a slit system to run the light through parallel to the base of the prism.

This window support is held firmly against the shoulder of the pressure cylinder by the steel plug *M* which screws down tightly against it. On the outer end of this plug is a safety window *J*, held in place by another steel plug. Because of the large shift in the light beam this safety window must be larger than the triple safety window usually used so that the light beam can be easily followed.

Since the position of the prism L formed by the liquid in the pressure cylinder would bend the light up, it is necessary to place two small correction prisms K in the cylinder to direct the beam of light from the light source O, through the liquid prism L and out onto the screen P. These two correction prisms are mounted in brass tubes which enable one to adjust their positions readily.

The space between the pressure windows and the small correction prisms is filled with a liquid of nearly the same index of refraction as the glass, so as to correct for the lens effect of the pressure windows.[1] Knowing the angle of the prism L, the pressure that is developed, and by measuring the angle of minimum deviation, it is possible to study the effect of pressure on the index of refraction of different liquids.

The liquids used were a paraffin oil, merasol, a product of the Standard Oil Company and glycerine. This oil is used for transmitting pressures in various other experiments and for this reason it was desirable that we know the effect of pressure upon its index of refraction.

The expression $n=(\sin \frac{1}{2}(R+D))/(\sin \frac{1}{2}R)$ gives the index of refraction n when the prism angle R and the angle of minimum deviation D of a transmitted beam is known. By measuring the change in deviation of the transmitted yellow light, the change in n was determined with each increase of pressure. The densities for the oil were measured by the piston travel in a cylinder designed for such measurements, while that for the glycerine was taken from data obtained by P. W. Bridgman.[2]

Tables I and II give the values for the refractive index n and density e at the pressures designated, together with the constant K for the Lorenz-Lorentz relation:

$$\frac{n^2-1}{n^2+2}\cdot\frac{1}{d}=K$$

TABLE I. *Refractive index and density of paraffin oil.*

pressure (atm.)	density (gm/cc)	n	K
1.	0.8706	1.4749	0.324
2697.	0.954	1.5340	0.325
5394.	1.006	1.5659	0.324
8091.	1.031	1.5895	0.326
10789.	1.052	1.6008	0.324
13585.	1.069	1.6039	0.324

TABLE II. *Refractive index and density of glycerine.*

pressure (atm.)	density (gm/cc)	n	K
1.	0.987	1.4722	0.282
1803.	1.025	1.4858	0.279
3703.	1.054	1.4962	0.278
4510.	1.078	1.5103	0.279
7212.	1.100	1.5210	0.279

From these values of K it can be seen that the value for the Lorenz-Lorentz relation is constant within the limits of experimental error up as far as measurements were made.

The authors wish to express their appreciation for the assistance in the form of a grant from the National Research Council.

[1] Thos. C. Poulter and Carl A. Benz, Phys. Rev. **40**, 872 (1932).

[2] P. W. Bridgman, Proc. Amer. Acad. Arts and Sci. **67**. 1–27 (1932).

LETTERS TO THE EDITOR

Prompt publication of brief reports of important discoveries in physics may be secured by addressing them to this department. Closing dates for this department are, for the first issue of the month, the twenty-eighth of the preceding month; for the second issue, the thirteenth of the month. The Board of Editors does not hold itself responsible for the opinions expressed by the correspondents.

Probable Values of e, h, e/m and α. A Reply to R. T. Birge

The Physical Review of April 15th contains a paper[1] (and a letter) by R. T. Birge on "Probable Values of $e, h, e/m$ and α." Throughout the paper Birge uses a method of estimating e and h (the electronic charge and Planck's constant) which I suggested and used.[2] Whilst adopting my method, Birge disagrees with various details of my work, and I wish to reply briefly to his criticisms.

(I) Any one of the usual methods of estimating h involves the experimental determination of a quantity A_n, which occurs in an equation of the form $h=A_n e^n$. I assumed an arbitrary value for e, plotted the values of $A_n e^n$ against n, and fitted a linear graph to the observations. From this graph estimates of e and h were deduced, which do not depend on any direct determination of e (such as Millikan's).

The probable errors may be estimated from the residuals with the help of the equation

$$r=0.6745\left(\frac{\sum(pvv)}{s-q}\right)^{1/2}$$

where r is the probable error of an observation of unit weight. I assumed, in effect, that s is the number of observations (36) and q the number of variables (2). Birge, however, (reference 1, p. 237), uses collectively all the observations of A_n for each particular value of n, obtaining three unequally weighted "points" (at $n=1$, $1\frac{1}{3}$, and $1\frac{2}{3}$). Then $s=3$, $q=2$, and his estimates of the errors are about twice my estimates (though there is no disagreement as to the line itself). Birge's explicit criticism of my method is: "That his procedure cannot be correct is immediately evident from the fact that if all observed h_n values correspond to the same value of n (giving only one point), no solution at all would be possible."

Let us suppose that the only data were 12 estimates of A_1 in the equation $h=A_1 e$. Then "no solution at all would be possible" as regards estimating e and h (and their errors); my method gives no solution. But Birge's statement needs qualifying; the slope of the line is indeterminate but its intercept on the line $n=1$ is determinate, giving an estimate of h/e. My method yields a reasonable estimate of the probable error of this value of h/e, but Birge's method gives the error in the indeterminate form $0/0(1-2)^{1/2}$. This is an absurd estimate of the probable error of the mean of 12 experimental determinations of what we designate (h/e), and I think this is sufficient to show that Birge's method of estimating the probable errors is incorrect.

(II) In the letter in the same number of the Physical Review, Birge explains that he had overlooked my statement that "By assuming a value of h, and plotting all the deduced values of e against $1/n$, the direct estimates of e could also be plotted at $1/n=0$. The increase in accuracy would, however, be negligible." This accounts for Birge referring in his paper to this method as "the essential extension of Bond's method." It also explains his statement that I had not carried my method to its logical conclusion. I deliberately did not use this second method at the start, for the same reason as Birge (reference 1, p.

[1] Birge, Phys. Rev. **40**, 228–261 and 319–320 (1932).

[2] Bond, Phil. Mag. **10**, 994 (1930) and **12**, 632 (1931). See also Proc. Phys. Soc. of London **44**, 374–382 (1932).

232), viz., I wished to show that an accurate estimate of e could be made, which was *independent* of any direct estimate, but which confirmed Millikan's value.

(III) Birge's chief disagreement with my work is in his adopting as the value for e/m (1.761 ± 0.001) or $(1.759\pm0.001)\times10^7$ e.m.u., and consequently disagreeing with both Eddington's theoretical numbers 137 and 1847.6. This estimate of e/m is the *only* experimental evidence against *either* of Eddington's theories. I would point out that, though e/m has now been measured for 35 years, it is only during the last three years that any appreciable number of physicists have accepted the value Birge advocates. Moreover, I understand from Sir Arthur Eddington that the discovery of the neutron makes it seem likely that the equations used in deducing the spectroscopic estimates of e/m are in error.

(IV) In section 4 of Birge's letter he speaks of the probable error of an estimate of e that I had given as being much larger than the error he estimates. I believe Birge's estimate must be wrong, as it would make his estimate of e ten times more accurate than the data from which it is obtained.

W. N. Bond

Department of Physics,
University of Reading, England.
May 11, 1932.

The Relation of Relative Humidity to the Absorption of Supersonic Waves in Various Mixtures of CO_2.

A sputtered quartz crystal with a frequency of 4.096×10^5 vps was used as source for supersonic waves. The absorption of these waves by a column of air mixed with different percentages of CO_2 was measured with an acoustic radiometer of the torsion vane type. A constant relative humidity of 10 percent for one set of runs was maintained with P_2O_5, 15 percent relative humidity for another set was obtained using LiCl and 35 percent for the remaining runs was obtained using CrO_3 as a dryer.

Curves plotting log of deflection (log D_x) against height (x) of radiometer from crystal face were plotted from the data and values for the absorption constant (k) were obtained by taking the slope of the straight lines thus plotted.

The following values of k were taken from these curves:

	10% R.H.	15% R.H.	35% R.H.
5% CO_2	0.053	0.09	0.11
50% CO_2	0.51	0.64	0.69
95% CO_2	0.97	1.19	1.29

These values indicate that relative humidity has a very marked and important effect upon the absorption in CO_2 or in air containing large percentages of CO_2.

Henry H. Rogers

Pennsylvania State College,
May 26, 1932.

Constants of the N_2O Molecule

In a recent paper on N_2O [1] the vibration frequencies as indicated by infrared absorption bands were correlated, and the anharmonic coefficients determined, employing an equation developed by Dennison for linear triatomic molecules. It now appears that this relation is too limited in its application, and should have been written in the more general form

$$W_l = V_1\nu_1+V_2\nu_2+V_3\nu_3+x_{11}V_1^2+x_{22}V_2^2 +x_{LL}L^2+x_{33}V_3^2+x_{12}V_1V_2+x_{13}V_1V_3 +x_{23}V_2V_3+A$$

[1] Barker, Phys. Rev. **38**, 1827 (1931).

Table I.

ν observed	transition	anharmonic coef. symbol	value	ν^0	ν computed
1285.4	$(0\rightarrow1)V_1$	x_{11}	-3.3	1288.7	1285.4
2564.2	$(0\rightarrow2)V_1$				2564.2
589.0	$(0_0\rightarrow1_1)V_2$	x_{22}	-2.2	588.3	589.1
579.5	$(1_1\rightarrow2_0)V_2$	x_{LL}	$+3.0$		578.7
590.5	$(1_1\rightarrow2_2)V_2$				590.7
1167.3	$(0_0\rightarrow2_0)V_2$				1167.8
2224.1	$(0\rightarrow1)V_3$	x_{33}	-13.8	2237.9	2224.1
4420.7	$(0\rightarrow2)V_3$				4420.6

expressing in first approximation the dependence of the vibration terms upon the various quantum numbers, A being a common constant. As a consequence it is necessary to revise the values of ν^0 and of certain of the coefficients, the results being more consistent than before. Table I supercedes parts of Tables IV and V in our report. The values of x_{13} and x_{23} remain unchanged. Those of x_{12} are somewhat modified, but as before fail to agree well among themselves.

The original report also contained a regrettable error in the value of the moment of inertia of the N_2O molecule, which should have been given as 66.0×10^{-40}.

E. F. BARKER

University of Michigan,
June 30, 1932.

Raman Effect of Methyl Acetylene

The Raman spectrum of methyl acetylene ($CH_3\cdot C\vdots CH$) has been studied and ten lines have been found as shown in Table I. A mercury light source was employed in the usual way and was used both unfiltered and with $\lambda=4358$A reduced by 2 mm of a solution of iodine in carbon tetrachloride. The photographs were taken on a Steinheil spectrograph. The expected Raman frequencies of the monosubstituted acetylene $C\vdots C\cdot$ bond (2128 cm^{-1}) and the $\vdots C\cdot H$ bond (3306 cm^{-1}) were found and are in agreement with the values of Bourguel and Daure.[1] Furthermore, lines for the aliphatic $C\cdot H$ bond (2928 cm^{-1}) and the $C\cdot C$ bond (618, 931 cm^{-1}) were found for this molecule. Some lines in Table I are not yet identified, although they also appear in other hydrocarbon molecules.[1] The ten lines mentioned are quite definite, but others are possible and it is expected to extend the work by using monochromatic excitation.

TABLE I. *Raman lines in methyl acetylene.*

Frequency cm^{-1}	Intensity	Frequency cm^{-1}	Intensity
310	weak	2871	medium
618	weak	2928	strong
931	medium	3144	medium
1384	weak	3207	weak
2128	strong	3306	weak

The methyl acetylene was made available through the kindness of Dr. G. B. Heisig of this laboratory.

GEO. GLOCKLER
H. M. DAVIS

University of Minnesota,
Minneapolis, Minn.,
July 1, 1932.

[1] Bourguel and Daure, Comptes Rendus **190**, 1298 (1930); and Bull. Soc. Chim. **47/48**, 1365 (1930).

Structure of Atomic Nuclei

For some time, there has been speculation as to whether or not the atomic nucleus can be regarded as consisting of shells of protons, just as the external structure is known to consist of shells of electrons. The writer has recently pointed out[1] that the experimental evidence seems to demand a modification of this view, in that s, p, d (etc.) shells do exist, but that a closed shell of azimuthal quantum number l consists of $2l+1$ protons and $2l+1$ neutrons. It was shown that the facts are well represented for elements of mass number (M) less than 36. It is of interest to inquire if this scheme is capable of extension to elements of higher mass number.

Detailed questions of stability must be left until later, but a qualitative analogy proves to be of help. In the outer atom, the normal state with one electron missing from a closed shell is of the same symmetry character as the normal state with just one electron in the closed shell. In the p shell, for instance, the ground states are ^2P, ^3P, ^4S, ^3P, and ^2P. There is symmetry about the middle element, which corresponds to a half-completed shell. If we make the hypothesis that such a symmetry exists for nuclei, then it is to be expected that this symmetry will be of a two-dimensional character, when the number of neutrons is plotted against the number of protons (or better, when the excess of neutrons over protons is plotted against the number of protons). For the s shell, H^3 is missing, and one cannot say very much about the symmetry. For the p and d shells, symmetries of an elementary type exist. The f shell, corresponding to the mass range 37 to 64, shows some symmetry, but so many points are missing that it is difficult to decide on the location of the center of symmetry. Either $M=50$ or $M=52$ will serve the purpose, the excess of neutrons over protons being four. The g shell corresponds

[1] J. H. Bartlett Jr., Nature (in press).

to a mass range 65 to 100 and should be symmetrical about the point of mass 82. Similarly, the h shell should be symmetrical about the point $M=122$. Barton[2] has called attention to the fact that two "clusters" of nuclei having two-dimensional symmetry do exist, the centers of symmetry being at $M=84$ and at $M=124$, respectively. An examination of the diagram leads one to conclude that the points 82 and 122 would serve equally well. In the first case, the center of symmetry is for protonic number 36.

The above evidence seems to indicate quite clearly that, for $M<144$, the picture of closed shells of protons and neutrons is in agreement with the facts. (It may be similar for heavier elements, but the information is as yet quite insufficient). Furthermore, it seems that Russell-Saunders coupling holds, and that nuclei occupying positions symmetrical about the half-completed shells will have the same resultant orbital angular momentum, but not necessarily the same total angular momentum.

Evidently, the reason why the principal quantum number does not play an important part, if any, is that the central field is a non-Coulomb one, as in molecules. No restriction is placed on the value of the azimuthal quantum number, which may increase until centrifugal force causes disruption. For the same principal quantum number, one would expect the binding energy of the protons and electrons to be approximately constant with increasing mass. The evidence indicates this to be so.[3]

The occurrence of s, p, d (etc.) symmetry is to be expected if the equations describing the system are invariant under a rotation of axes, which is so when there is no preferred direction.

While the above model probably gives many of the essential symmetry features, there remains the problem of setting up the equations of motion in order to determine the energy levels. This may require more knowledge about the law of interaction between a proton and a neutron.

JAMES H. BARTLETT, JR.

Zürich,
July 3, 1932.

[2] H. A. Barton, Phys. Rev. **35**, 408 (1930).

[3] L. Strum, Zeits. f. Physik **50**, 555 (1928).

The Becquerel Effect as a Special Case of the Barrier-layer Photoelectric Cell

The observation of E. Becquerel,[1] that illumination of one of two identical electrodes immersed in an electrolyte develops an electromotive force, marked the inception of a continuous series of investigations on this and related phenomena. The paucity of general conclusions available from these researches however,[2] furnishes a marked contrast to the rigor and elegance which have attended the development of the "Hallwachs" effect. And it is thus fortunate that a new avenue of approach to the solution of this problem has been opened by the advent of the barrier-layer cell of Lange[3] and Schottky,[4] whose formal similarities to the Becquerel cell (e.g., the circumstance that neither requires an auxilliary e.m.f. in order to operate, and a characteristic reversal of polarity with increase of wave-length[5]) almost immediately suggested their essential identity.[6,7] It is the object of this note to adduce some quantitative evidence in support of this view, which we have accumulated in an extended investigation of the subject.

The careful studies of Schottky and his coworkers[8] have established several fundamental relationships governing the behavior of the barrier-layer cell. Among others, it was demonstrated that:

a. the short-circuit current is strictly proportional to the light intensity,

b. the short-circuit current, and not the open-cuircuit e.m.f., is fundamental, and

c. the direction of electron-flow in the cell is determined by the location of the barrier-layer ("Hinterwandeffekt or Vorderwandeffekt").

[1] E. Becquerel, Comptes Rendus **9**, 144, 561 (1893).

[2] A. L. Hughes and L. A. DuBridge, "Photoelectric Phenomena" McGraw-Hill Co., New York, 1932. pp. 5–6.

[3] B. Lange, Phys. Zeits. **31**, 139, 964 (1930).

[4] W. Schottky, Phys. Zeits. **31**, 913 (1930).

[5] A. Garrison, J. Phys. Chem. **27**, 601 (1923).

[6] E. Duhme, Zeits. f. Elektrochemie **37**, 682–4 (1931).

[7] H. Simon and R. Suhrman, "Lichtelektrische Zellen und ihre Anwendung" Julius Springer, Berlin 1932, pp. 54–55.

[8] O. v. Auwers and H. Kerschbaum, Ann. d. Physik **7**, 129 (1930).

In our experiments—of which a more complete account will be published in the near future—uniform and adherent layers of cuprous oxide were formed on copper plates of approximately 40 sq. inches area by heating to about 1000°C in an electric furnace and quenching rapidly. The reverse sides of the electrodes were covered with black lacquer, followed by an insulating and water-proof coat of paraffine. Cell elements of these dimensions enable one to draw heavy photoelectric currents for low levels of illumination, and hence to minimize polarization phenomena. In this case unfiltered radiation from a small tungsten-filament lamp at a distance of five feet produced photocurrents of the order of one-half milliampere.

For constant light intensity, additions of increasing amounts of electrolyte increased the photocurrent in accord with the expression:

$$i = i_0 R_0/(R_T + R_0)$$

where i_0 is the maximum current for a given light intensity, R_T the resistance of electrolyte plus resistance of meter and leads, and R_0 the resistance of Cu-Cu_2O electrode system (assumed approximately constant for a given light intensity).

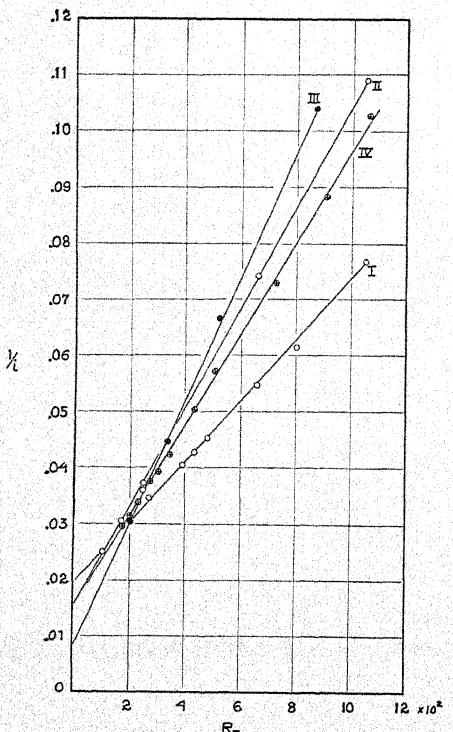


Fig. 1.

The results are exhibited in curves I, II (NaCl), and III (KCl) of Fig. 1. Since these are not superimposed it might be inferred that the electrolyte resistance is not the sole determining factor. It will be observed however that straight line functions were always obtained, although the slope and intercept varied continuously. That this must be occasioned by some secular change in the sensitive surface was demonstrated by repeating the measurements with a mixture of the two electrolytes (curve IV) a procedure which permits one to avoid the disturbing effect of progressive changes in the electrodes.

The equation predicting our results is identical with that of Auwers and Kerschbaum[8] for the network equivalent to a barrier-layer cell, save for a second term inserted by them to correct for the non-ohmic character of the internal resistance. The simplified expression, however, satisfactorily accomodates our results, and indeed, precisely accounts for the photocurrent in the barrier-layer cell as a function of external resistance, provided the resistance range is of the order encountered in the electrolytic cells.

It follows therefore that the primary function of the electrolyte is to act as conductor for the photoelectric current. That secondary chemical effects may arise is not only possible but practically inevitable. For this reason it is imperative to secure instantaneous values for the short-circuit current. Whenever such complications could be avoided the short-circuit current was found to be proportional to the light intensity. Furthermore the temperature coefficient for the Becquerel effect is accurately reproduced by combining the known thermal contributions to the barrier-layer current and the electrolyte conductivity.

If, as seems the case, the Becquerel effect arises from a Lange cell whose behavior is frequently obscured by a host of electrochemical, and possibly photochemical, complications, it seems wisest to direct more attention to the simpler phenomenon—which promises so much of practical and theoretical interest.

R. H. MÜLLER
A. SPECTOR
Washington Square College,
New York University,
July 5, 1932.

A Note on the Hyperfine Structure of Beryllium Lines

The identification of the neutron by Chadwick[1] has developed a keen interest in the value of the nuclear moment of beryllium. For this reason the beryllium lines given in Table I have been examined for structure with the aid of a Fabry-Perot interferometer. The interferometer plates were spaced 2, 3, 5, 8 and 10 mm apart. The spectrum was excited in a metal liquid air-cooled Schüler lamp so that the Doppler effect should be small.

The only line showing a definite structure was the Be II line λ4673A. $3\,^2D-4\,^2F$ transition. The wave-length separation here corresponds to a $\Delta\nu$ difference of 0.480 cm^{-1}, which is the $3\,^2D_{3/2}-3\,^2D_{5/2}$ separation.

TABLE I.

line	λ	classification	structure
Be I	8254	$2\,^1P-3\,^1S$	sharp
Be II	4673	$3\,^2D-4\,^2F$	one component at −0.105A
Be I	4572	$2\,^1P-3\,^1D$	sharp
Be II	3130	$2\,^2S-2\,^2P_{1/2,3/2}$	sharp
Be I	2348	$2\,^1S-2\,^1P$	line width about 0.030A

The term "sharp" in Table I means that no structure was found. In the case of λ3130 the two lines $^2S_{1/2}-^2P_{1/2}$ and $^2S_{1/2}-^2P_{3/2}$ are 0.648A apart and were unresolved by the prism instrument used. It was, therefore, necessary to make one line fall on the first chief maximum of the other line in the interferometer pattern so that the intervening space would be free to show any components. Even so, no components were found.

The only indication of possible structure lies in the fact that λ2348A has a line width of about 0.030A.

This negative result does not necessarily mean that $i=0$ for Be and it is hoped that an examination of the Be III and IV lines with the 21 ft. grazing incidence vacuum spectrograph which is now being set up in this laboratory will show a beryllium structure comparable with that of lithium.

P. GERALD KRUGER
R. C. WAGNER

Department of Physics,
University of Illinois,
July 5, 1932.

[1] T. Chadwick, Nature **129**, 312 (1932).

Newton's Rings in Transparent Metallic Films

In attempting to produce a film of manganese on glass by cathodic sputtering from a piece of pure manganese only 2.5×1.5 cm in area, a series of colored fringes were observed in the film by reflected light. These fringes are undoubtedly similar to those observed by Bockstahler and Overbeck[1] who reported some observations on sputtered tin. In order to make a closer study of these fringes, a mica screen having a circular opening of 1.5 cm diameter, was placed about one mm in front of the manganese cathode. Due to the intense heating, a Pyrex glass plate was used to receive the film. Manganese sputters very slowly. With a current of about 10 milliamperes, hydrogen being the residual gas, some ten hours were required to produce a film in which was visible, by reflected light, a series of brilliant Newton's rings. During the period of sputtering these rings gradually increased in size, other rings forming within, until the outermost ring had a diameter of almost 5 cm. The order of colors appearing was as follows: yellow, light brown, reddish brown, purple, blue, green, and back to yellow. This seems to be about the same as that reported by Edwards[2] who made some observations on films of copper deposited on aluminum and nickel.

The glass directly underneath the center of the circular opening in the mica, was found to be free of any metallic deposit, due doubtless to the intense heating of the glass plate produced by the cathode rays. The film was thus of variable thickness, being a maximum just under the edge of the circular opening in the mica screen, and diminishing to zero both towards the center and the edges of the glass plate. Hence a cross section of the film taken across the center of the glass plate would be like a vertical cross section of a volcanic mountain, the center of the film corresponding to the crater of the volcano.

It seems quite likely that the colored fringes are due to the interference of light between the front and rear surfaces of the transparent manganese film, confirming the

[1] L. I. Bockstahler and C. J. Overbeck, Phys. Rev. **37**, 465 (1931).

view taken by Edwards.[2] These rings enable one to test this assumption, for whatever phase differences in light that might be introduced as the result of reflection and refraction at the front and rear surfaces of the film, it must be true that adjacent rings of identical color are located at points in the film differing in thickness by one half of a wave-length as measured in the metal. This serves as a step by step method for evaluating the thickness of the film at various points. Accordingly the film was illuminated normally by monochromatic light, and the positions of the various black interference rings measured by means of a short focus cathetometer. Reflection from the rear of the glass plate was eliminated by attaching a glass prism to the rear of the plate by means of cedar oil.

There is some question as to the thickness of the film at the first or outermost black ring. Allowing for the phase differences due to reflection and refraction at the surfaces of the film, the thickness of the film at this point was estimated to be not over one tenth of a wave-length. By plotting two cross sections of the film taken at right angles to each other, the mean thickness of the film was evaluated graphically. The maximum thickness of the film was found to be 8.1×10^{-5} cm.

Assuming the film as having a circular area of 2.5 cm in diameter, the weight of the film was computed by means of the expression $\pi r^2 dN\lambda/2n$, where r is the radius of the film; d, the density of manganese; n, the refractive index of manganese as obtained previously[3] for this sample forming the cathode; λ, the wave-length in air; and N the number of black fringes which serves as a measure of the mean thickness of the film. The weight of the manganese film so computed was 0.0045 gr from measurements made on the black rings as viewed in mercury green light, and 0.0042 gr as viewed in yellow sodium light. By actual weight of the glass plate before and after sputtering, the weight of the manganese film was found to be 0.0040 gr. The results are sufficiently in agreement to justify the conclusion that the phenomenon observed is one of interference.

J. B. NATHANSON
Carnegie Institute of Technology,
Pittsburgh, Pa.,
July 8, 1932.

[2] H. W. Edwards, Phys. Rev. **38**, 166 (1931).

[3] J. B. Nathanson, J. O. S. A. **20**, 593 (1930).

Total Secondary Electron Emission from Metal Faces

It is well known that in experiments relating to the emission of secondary electrons from metal faces due to an incident beam of primary electrons, the ratio R of the total secondary to the primary current increases almost linearly with the potential from about 30 volts, attains a broad maximum (almost similar to a saturation effect) at some potential and then decreases slowly and linearly as the applied potential is increased. The energy at which the maximum occurs depends on the nature of the target and also for any particular metal, on the nature of the crystal face bombarded.[1,2] The reason why the secondary electron curve bends round and decreases at higher potentials has so far been obscure.

Copeland[3] has recently made the interesting suggestion that if the rate of fall of R with potential be divided by the actual value of R in the region, the ratio for various metals gives a fairly linear graph when plotted against the densities of the targets. The aim of this note is to draw attention to the further interesting observation that this ratio for any particular metal probably depends also on the grating constant of the crystal face presented for bombardment. Experiments on polycrystalline nickel targets[1] and on the 100[2] and 110 faces of large nickel single crystals, conducted by the writer in Prof. O. W. Richardson's laboratories in King's College, London, show that the ratio dR/RdV varies almost linearly with the grating constants of the faces.

These observations suggest that the decrease of R at higher potentials is probably due to the absorption of the primary electrons and to a much larger extent of the secondary electrons. As the potential is increased, the depth of penetration of the primary electrons within the metal increases and as a result, there is much greater absorption of the slower

[1] S. R. Rao, Proc. Roy. Soc. **A128**, 41 (1930).

[2] S. R. Rao, Proc. Roy. Soc. **A128**, 57 (1930).

[3] P. L. Copeland, Phys. Rev. **40**, 122 (1932).

secondary electrons. This absorption can itself account for the decrease in the value of R under consideration. It is also instructive to find out the variation of the ratio dR/RdV with the atomic number instead of with the density. The kind of absorption in this case may be due to the collisions of the outgoing secondary electrons with the bound orbital electrons within the atoms, while that part of the absorption depending on the grating constant may be due to the collisions of the secondary electrons with the free or valency or structure electrons.[4] The grating constant may be taken as a measure of the probability of the collisions of the secondary electrons with those mentioned above. The experiments of Davisson and Kunsman and later of Davisson and Germer[5] suggest that the largest secondary emission is in the direction of the primary beam when the incidence is normal.

These considerations indicate that the decrease of R at higher potentials is mainly due to the absorption of the secondary electrons due to their collisions with the bound or partly bound or free electrons. The efficiency of production of the secondary electrons would therefore be a constant after a certain potential is reached (this potential depending on the nature of the metal and the crystal surface) if there were no absorption of the secondary electrons.

The results mentioned above derive additional support from the fact that adsorption of gases by the crystal surface increases the ratio $dR/R\,dV$ considerably. This was found to be the case with the 110 face of a nickel crystal.

Also careful experiments by Nakaya[6] show that a similar saturation effect exists in the photoelectric efficiency curves for soft x-rays at voltages in the neighborhood of 3000 volts for ordinary metals. It is highly probable that if the potentials are carried much higher, these curves may also show a similar fall in value due to the absorption of the photoelectrons in the medium of the photoelectric target.

More accurate work on the secondary electron emission from different metals and crystal faces is necessary to settle these interesting questions.

S. RAMACHANDRA RAO

Annamalai University,
Annamalainagar, S. India,
June 8, 1932.

[4] O. W. Richardson, Proc. Roy. Soc. **A128,** 63 (1930).

[5] C. J. Davisson and L. H. Germer, Phys. Rev. **30,** 705 (1927).

[6] U. Nakaya, Proc. Roy. Soc. **A124,** 616 (1929).

A Theory of the Ozone of the Lower Atmosphere and Its Relation to the General Problem of Atmospheric Ozone

The observed failure of radiation in the region 2200–2000A to penetrate the earth's atmosphere has made it of considerable interest to identify the substances which are responsible for the stopping of this radiation lying between the ultraviolet absorption of ozone and that of oxygen. The absorption of light by the molecule O_4[1] in the earth's atmosphere can account for the removal of the greater part of this radiation. That this is the case may be shown in an approximate way by using the absorption coefficient of O_4 and its dissociation constant computed in Ref. 1, and an oxygen distribution in the atmosphere given over the heights 0 to 11 km by the expression $n=5.38\times10^{18}\ e^{-1.12\times10^{-6}z}$ molecules /cc, and above 11 km by the expression $n=1.57\times10^{18}\ e^{-1.73\times10^{-6}z}$ molecules/cc, where z, the height, is in centimeters, this distribution resembling closely that given in Table 2, p. 393, Vol. I, International Critical Tables. These quantities lead to an intensity at the earth's surface of a little less than 1 percent of the initial intensity outside the atmosphere. The absorption will, however, be greater than this, for it was shown by Warburg,[2] on whose experimental work rests the quantitative measurement of the absorption, that in air this unusual oxygen absorption was greater for the same amount of oxygen than in pure oxygen. This was briefly discussed in Ref. 1. The use of Warburg's data on air leads, in much the same way as was done for pure oxygen in Ref. 1, to an equilibrium constant of approximately $K_\rho=0.6$ gm/cc for the dissociation of O_4, if the molecular absorption coefficient is

[1] Wulf, Jour. Am. Chem. Soc. **50,** 2596 (1928); Proc. Nat. Acad. Sci. **14,** 609 (1928).

[2] Warburg, Berl. Ber., p. 230, 1915.

taken to be unchanged. The atmosphere is approximately a 79% N_2 and 21% O_2 mixture over the altitudes of appreciable O_4 absorption. Carrying out the same calculations as mentioned above, with the same distribution of oxygen but with this O_4 dissociation constant appropriate to air, one finds that radiation in the vicinity of 2100A will be reduced to roughly 10^{-5} of its original value. At a height of 4 km the intensity proves to be a few percent of the original, this being mentioned here because experiment has shown that no detectable radiation of these wavelengths occurs even at this height.[3] Qualitatively these calculations do not, of course, depend upon the interpretation of this absorption as being due to the molecule O_4, it being sufficient that there is this density-dependent absorption in oxygen, that is, this absorption which does not follow Beer's Law. The above is not intended to imply that O_4 is the only absorbing substance, but simply that its absorption cannot be entirely neglected. Ozone and the molecule O_2 undoubtedly also absorb weakly in this region.

At the same time this absorption accounts, at least in part, for the ozone in the lower atmosphere recently measured by Götz and Ladenburg.[4] For the absorption of this radiation leads to photochemical ozone formation as also has been shown by Warburg.[5] This ozone formation from O_4 occurs chiefly in the troposphere, because the greater part of the absorption lies in these relatively low altitudes. This ozone is in a singular position photochemically, being protected from radiation most active in its decomposition by the ozone formed at higher altitudes from O_2. In view of the observation that no detectable radiation in the region 2200–2000A reaches even a height of 4 km, the photochemical formation of this ozone of O_4 origin apparently occurs for the most part at moderate heights. No inconsistency enters here with the observations on the ozone content of the atmosphere close to the earth, however, since the troposphere is a stirred atmosphere, convection distributing the ozone more or less uniformly throughout it. The formation of ozone from O_4 depends evidently upon atmospheric density, not merely upon the total oxygen in the path, and hence will be related to latitude and weather conditions. The above considerations are obviously related to the general problem of atmospheric ozone, especially to its distribution, though further work is required to determine the quantitative importance of these relations.

OLIVER R. WULF
Bureau of Chemistry and Soils,
U. S. Department of Agriculture,
Washington, D. C.,
July 14, 1932.

[3] Lambert, Déjardin and Chalonge, Compt. Rend. **177,** 757 (1923).

[4] Götz and Ladenburg, Die Naturwissenschaften **19,** 373 (1931); see also Fabry and Buisson, Comp. Rend. **192,** 457 (1931).

[5] Warburg, Berl. Ber. p. 746; 1911, p. 216; 1912, p. 872; 1914; Z. Elektrochem. **26,** 54 (1920); **27,** 133 (1921).

The Raman Spectra of Two Liquid Phases of Nitrobenzene

M. Wolfke and J. Mazur have found an irregularity in the heating curve[1] and also abrupt temperature variation of the dielectric constant and density[2,3] of mononitrobenzene, at a temperature of 9.5°C, i.e., slightly above the freezing point. Their results seem to imply a definite intra-molecular energy change in the liquid state at 9.5°, and, therefore, presumably the Raman spectrum should be modified at that transition temperature. An attempt was made to find such a modification, but exposures taken above and below 9.5° failed to show any evidence of one.

[1] M. Wolfke and J. Mazur, Nature **127,** 741 (1931).

[2] J. Mazur, Nature **126,** 993 (1930).

[3] J. Mazur, Nature **127,** 893 (1931).

Three types of modification of the Raman spectrum were looked for: (1) shift of one or more of the lines, (2) intensity changes, (3) disappearance of one or more of the lines in one or the other phase.

Shifts of the order of 0.2A could have been observed in the region of the Raman lines but no shift of any line was found.

At the lower temperatures, a marked increase in the intensity of all the lines in the blue end of the spectrum was observed but, by several other experiments, this was found to be due to a large but continuous change in the absorption coefficient of nitrobenzene with temperature.

Exposures up to one and a half hours were taken at 6.0°C and room temperature but

these plates show no line appearing at one temperature and not at the other. No longer comparison exposures were made since a fourteen hour exposure at room temperature brought out only one line that the one and one half hour exposure did not show.

Our plates show a number of lines which Kohlrausch does not report[4] for nitrobenzene, but, pending further study, we cannot say whether these lines belong to nitrobenzene, nitrothiophene (which may have been present at least as a trace), or some other impurity. These unidentified lines occur at wave-number separations approximately equal to: 675, 1025, 1080, 1175, 1385, 1415, 1755, 1805, 2450, 2690, and 2830 cm^{-1}.

The sample used was C. P. mono-nitrobenzene which had been washed first with dilute Na_2CO_3 and then many times with distilled water, dried a week or more over $CaCl_2$, and triply distilled under about 1 mm of Hg pressure. The original sample had shown the presence of a trace of nitrothiophene and it may be that the distillation did not completely remove this impurity.

The spectra were taken with a Hilger constant deviation spectrograph with dispersion of about 20A/mm at 4358A. The General Electric Company Raman Outfit was used for irradiating the sample, with a 220 volt hot cathode mercury arc along one focus of the elliptical reflector and the sample tube along the other focus. Highly distilled nitrobenzene has still a slight yellow color and absorbs strongly the exciting radiation we used (4358A). Therefore the sample tube was made conical, and of such a taper as to just fill the spectrograph aperture. This arrangement greatly increased the intensity of the Raman spectrum. A glass walled cooling system was placed in contact with the whole length of the sample tube. In a final 18 hour exposure at room temperature, the cooling system contained distilled water with enough potassium chromate to absorb completely the 3650, 4046 and 4078 lines. The sample itself aided in this complete absorption. All of the lines on the final plate must have been excited by the 4358 line and its two companions or have been anti-Stokes lines due to 4916 line or those of longer wave-lengths. Computations, however, proved that none of the lines was an anti-Stokes term.

Eastman 40 and Ilford Golden Iso Zenith (H and D 700 and 1400) plates were tried but the Eastman 40 plates were selected because much less trouble was had from fogging during development with this type. The slightest fog covered up many weak lines.

A. M. THORNE
P. L. BAYLEY

Lehigh University,
Bethlehem, Pa.,
July 14, 1932.

[4] K. W. F. Kohlrausch, Der Smekal-Raman Effect. Julius Springer, Berlin, 1931.

A New Band System of Barium Hydride in the Infrared

With the aid of the new Eastman Infrared Sensitive plates the writer has discovered an intense band system of BaH in the infrared with principal heads at about 9020A and 10,000A, degraded to the red. The experimental conditions were identical with those used by Fredrickson and Watson[1] in photographing the $^2\Pi \rightarrow {}^2\Sigma$ BaH bands in the visible red region. The bands in the infrared are also $^2\Pi \rightarrow {}^2\Sigma$, the two systems having a common final $^2\Sigma$ state, but with considerably different spin multiplet spacing in the $^2\Pi$ states. For the spacing between the two groups of branches in the infrared band is about 1000 cm^{-1}, whereas $A = 462$ for the red system previously investigated.

The shorter wave-length group of branches from 8920A to about 9250A has been photographed at high dispersion with good intensity using the Infrared Sensitive plates A, but with the new Eastman Infrared Sensitive plates B only the strongest lines of the branches beyond 10,000A have been registered even with long exposure.

This is the first instance among the diatomic hydride molecules for the alkaline earths of a second $^2\Pi$ state, and the nearness of these two $^2\Pi$ levels in BaH is undoubtedly to be correlated with the fact that only for Ba is the ^3D level found below ^3P. But $A = 832$ for the lowest ^3P levels of the Ba atom, and so no definite assignment of either of the observed $^2\Pi$ levels of BaH to the ^3P level of Ba seems possible. Rather, as now seems even more evident,[1] these molecular levels must come from a forcing together of the ^3P and ^3D levels of the Ba atom. This point will be discussed and the data on this infrared BaH system presented in a later communication.

WILLIAM W. WATSON
Sloane Physics Laboratory,
Yale University,
July 15, 1932.

[1] W. R. Fredrickson and W. W. Watson, Phys. Rev. 39, 753 (1932).

Zeeman Effect and Perturbations in the CO Angstrom and the N_2^+ Bands

Rosenthal and Jenkins[1] have described an interesting example of multiple perturbations in the $^1\Sigma \rightarrow {}^1\Pi$ Angstrom CO bands, particularly in the (0, 0) band at 4511A, for which they give the undoubtedly correct quantum analysis. Spectrograms recently taken by the writer show additional faint lines which extend their "resonance" curves at several of the perturbations and which emphasize the occurrence of two lines for each J value around the perturbation points. The correctness of the quantum assignments of all these lines is attested by the $\Delta_2 F'(J)$ combination relations and by the Zeeman effect observed in the present investigation. The existence of large, irregular Zeeman effects for certain lines was first noted by Crawford[2] in his work on the regular Zeeman effect in these CO bands.

As pointed out by Rosenthal and Jenkins, the fact that these perturbations are multiple would indicate that the perturbing state is not a singlet state, and the different types of Zeeman effects observed at the several perturbations bear this out. In general, the greater the displacement of the perturbed line the larger its Zeeman effect, and the effects increase rapidly with increasing field strength. The regular Zeeman effect for lines with these intermediate and high J values for this type of electronic transition is so small as to leave the unperturbed lines totally unaffected by the magnetic field. At the first perturbation point, however, the line $P_b(8)$ for example is symmetrically broadened at low field strengths and becomes a wide asymmetrical doublet with broad components at high field strengths (30,000 gauss). The effect of the field on the Q branch lines around $J=12$ is just to increase the magnitude of the perturbation, the shift of $Q_a(14)$ at $H=26{,}000$ gauss being $+0.96$ cm^{-1}, while that of $Q_b(11)$ on the other branch of the "resonance" curve is -0.55 cm^{-1}. Those Q lines having the maximum perturbation are shifted the most, but the field lines are quite sharp, there being no indication of any shading towards the no-field position. The lines $P_a(16)$ and $R_b(16)$ near the maximum of the next perturbation, on the other hand, are merely much broadened by the magnetic field at all field strengths, the uniform broad block of radiation being not quite symmetrical about the no-field line. Some of the P, R and Q lines at the perturbation around $J=28$ in the (0, 1) band as well as in this (0, 0) band become very sharp doublets, with the two components of different intensity, for the line on the one side of the perturbation point, while a line on the other side of the perturbation is uniformly broadened.

These differences in Zeeman pattern indicate that the state perturbing this $^1\Pi$ state is multiple, in violation of one of Kronig's rules that the two perturbing states must have the same multiplicity. However, this rule need not be expected to hold strictly here, for singlet-triplet combinations do occur in CO. The $d(^3\Pi?)$ level which lies just 0.09 volts below this $^1\Pi$ state may be the level whose rotational terms are responsible for these perturbations. The differences in the spread of the magnetic sublevels in the three spin components, together with the rule that only levels of the same M value perturb each other, could account for the variations in field patterns observed for these perturbed lines. An analysis of the Merton-Johnson triplet bands in the red which arise from this d level should be made to find these corresponding perturbations.

The N_2^+ bands which are a $^2\Sigma \rightarrow {}^2\Sigma$ transition are present on some of the writer's CO spectrograms. A perturbation similar to those in the $^2\Sigma \rightarrow {}^2\Sigma$ CN tail bands occurs in this system[3] in all bands with $v'=1$ for $J=13\frac{1}{2}$. All of the lines except those displaced near the center of the perturbations are insensitive to the magnetic field, whereas these perturbed lines are either shifted or become rather sharp doublets. A more detailed description of these peculiar Zeeman effects in both of these band systems, together with the possible explanations, will be submitted in the near future for publication in this journal.

WILLIAM W. WATSON
Sloane Physics Laboratory,
Yale University,
July 15, 1932.

[1] J. E. Rosenthal and F. A. Jenkins, Proc. Nat. Acad. Sci. 15, 896 (1929).

[2] F. H. Crawford, Phys. Rev. 33, 341 (1929).

[3] M. Fassbender, Zeits. f. Physik 30, 73 (1924).

The Rôle of Gas Adsorption in Counting Chambers*

Recently in Naturwissenschaften (vol. **20**, p. 315), W. Schulze briefly outlines experiments with Geiger-Müller tube counters which indicate, according to his interpretation, that gas adsorption on metallic surfaces can have no influence on the abruptness of the interruption of the current pulse when these devices are functioning properly as counters. He is probably correct in assuming that both point counters and tube counters are dependent upon the same fundamental physical conditions, in spite of marked differences in behavior. However, the mere fact that widely different electrode treatments, in the case of tube counters, yield no noticeably different operating conditions, does not in itself justify the conclusion that gas adsorption plays no role in the operation of the counter. It is a well established fact that the surface of the point electrode in the point counter does require special and careful preparation, especially when operated at or near atmospheric pressure. It is also true that the inner surface of the tube counter can be given such treatment that it will fail to function as a counter at any pressure whatever. It is difficult to reconcile these facts with the view put forth in Schulze's communication mentioned. The adsorption of gas by solid surfaces is one of the most common occurrences with which we have to deal since gases are adsorbed under a great variety of conditions. Moreover, when, as is usual, the tube is the negative electrode, the arrangement is such that intense electric fields do not exist near the inner surface of the tube and it is not to be expected that the surface conditions would be as important as in the case of the point counter used with the point as the negative electrode.

I should like to point out that it seems questionable to try to draw any general conclusions regarding the principles underlying the operation of counters from observations only in hydrogen at reduced pressures as Schulze has done. For under such conditions adsorption of gas undoubtedly does occur and it would appear very difficult to prepare any kind of electrode surface which would not have its properties modified by such adsorption. As clearly demonstrated with a point counter, the effects of such adsorption are most evident when the kind of gas in the counter is changed while it is in operation, the pressure remaining constant. When a counter with a prepared copper point is counting with hydrogen at atmospheric pressure slowly streaming through it, the introduction of a few percent of CO into the flowing hydrogen immediately causes the counter to cease functioning. This is very difficult to explain on any basis of an effect existing only in the gas discharge in the counter but its explanation becomes relatively simple when the adsorption properties of CO on "catalytic" copper are considered.

L. F. CURTISS

National Bureau of Standards,
Washington, D. C.
July 15 1932.

* Publication Approved by the Director of the Bureau of Standards of the U. S. Department of Commerce.

BOOK REVIEWS

Graphische Darstellung in Wissenschaft und Technik, M. PIRANI. Pp. 149, figs. 71. Walter de Gruyter and Co., Berlin, 1931. Price RM 1.80.

This little booklet of the Sammlung Göschen is well up to the standard set for the series. It provides a self contained, easily understood, concise and trustworthy treatment of the matter chosen for consideration. The selection of material is good. Chapter 1, 31 pages, is an elementary and detailed discussion of the principles and methods involved in presenting graphically the information contained in a table of two variables. It is excellent reading for freshmen technical students. Chapter 2, 36 pages, presents various methods for exhibiting graphically the relationship between two variables connected by a known equation. Thus the method of reducing the graph to a straight line by constructing suitable rectangular scales is given, and with this a neat and useful central projection method of constructing scales for the linear fractional transformation. Chapter 3, 67 pages, discusses graphical representations of equations of three variables, the topographical method followed by a concise and excellent treatment of the construction of alignment charts. Throughout the text specific references to more extended treatments are made and an appendix contains a bibliography and a table of functional relationships with related suggestions as to suitable choices of graphical methods.

HENRY E. HARTIG
University of Minnesota

Vector Analysis, with Applications to Physics. RICHARD GANS. Translated from the sixth German edition by Winifred M. Deans. Pp. 163. Blackie and Son.

This is a concise and very clear introductory account of vector analysis, and of its applications to mechanics, hydrodynamics, electrodynamics, and optics, including crystal optics. Some 45 exercises are given, and the methods of solution of these are collected at the end of the book.

The treatment brings out very forcibly not only the fact that one of the reasons for the usefulness of vectorial methods in stating and solving a large class of physical problems lies in the conciseness of the notation, but also, and in the reviewer's opinion this is far more important, that vector methods allow the writing of various physical relationships in a manner which exhibits the physical content of these relationships in a most natural and lucid way.

Tensors are introduced by means of linear vector functions. The treatment is very understandable.

Incidentally, the reader must be careful to combine the remarks about vectors on page 1 with those made in Section 3 on the addition of vectors, in order to obtain a satisfactory definition of a vector.

The English translation of Professor Gans' book was made from the sixth German edition. (A Spanish translation appeared in 1926.) It should do a good service to those who wish to become acquainted with the fundamental ideas of vector analysis, and with their applications.

V. ROJANSKY
National Research Fellow
Princeton University

Ergebnisse der Exacten Naturwissenschaften, P. TEN BRUGGENCATE. Vol. X. Die Veränderlichen Sterne.

In this 80 page article ten Bruggencate gives a very useful, critical compilation of the principal contemporary knowledge of variable stars. After a brief introduction and description of a system of classification, the lion's share of the space—65 pages—is taken up by a detailed study of the cepheids and the long-period variables, both of which groups are treated ex-

haustively, especially from the more physical aspects of astronomy. Furthermore a large amount of detailed information concerning individual stars and light curves is added and discussed, which discussion becomes enhanced because of the author's extensive experience in this aspect of variable star work. Contrasted to this the treatment of the semi-regular and irregular variables appears somewhat summary, and not in proportion to their importance. As another slight criticism may be offered that no historical introduction precedes, but that the subject is considered to have begun around 1850.

W. J. LUYTEN
University of Minnesota

Interferometer Methods in Astronomy. F. G. PEASE. Vol. X.

The pamphlet begins with a short historical summary of the early attempts to apply the interferometer to astronomical measurements, then reviews Michelson's work in adapting the interferometer to the 100 inch reflector. A table is given with the measured diameters of seven stars, thus condensing into such a modest space what might well be called the most phenomenal astronomical observations of the century. A detailed description of the new and more powerful 50 foot interferometer recently constructed at Mt. Wilson, forms the closing paragraphs. The only criticism that might be offered is that instead of attributing the first calculations of stellar diameters to Eddington and Russell, Hertzsprung should have been mentioned, who predicted the diameter of Arcturus in 1905, many years before the rest of the astronomical world had become conscious of the existence of giant stars.

W. J. LUYTEN
University of Minnesota

Die dynamische Theorie der Roentgenstrahlinterferenzen in neuer Form. M. v. LAUE. Sonderabdruck aus Vol. X der Ergebnisse der exakten Naturwissenschaften, Pp. 25. Julius Springer, Berlin, 1931.

This reprint deals with a simplified presentation of the dynamic theory of x-ray interference, which is, as the author states, "one of the master works of mathematical physics of all time." However, it is incorrect to refer to this theory as Ewald's, for the results were derived several years earlier by C. G. Darwin. Darwin's work is not even mentioned in this paper. The theory as worked over by Laue presents a considerable simplification over Ewald's treatment. Nevertheless it is assumed that the reader is familiar with the wave-kinematical theory of the Laue interference as developed with the aid of the reciprocal lattice. Of course, this is usually the case. The effectiveness of the presentation is considerably marred by the several misprints in the final results.

JOSEPH VALASEK
University of Minnesota

Kerr-Effekt, Lichtzerstreuung und Molekülbau. H. A. STUART.

This is a chapter of 48 pages from Vol. X of "Ergebnisse der Exakten Naturwissenschaften." Particular attention is given to the calculation of the three principal polarizabilities of a molecule from combination of measurements on the Kerr effect and on the depolarization of light. Information obtained in this way forms an interesting supplement to the more familiar determination of dipole moments from dielectric constants. Dr. Stuart has done considerable original experimental work on depolarization and on the Kerr effect, including the difficult measurements of the latter in gases. Consequently one has the assurance that the chapter is written by an author thoroughly conversant with the field. The article properly stresses the fact that the depolarization is often difficult to measure with precision. In particular, the depolarization found by Strutt in helium seems to be in flat contradiction with quantum theory, unless imputed to experimental error.

J. H. VAN VLECK
University of Wisconsin

Die Lichtausbeute bei Stossanregung. W. HANLE AND K. LARCHÉ. Pp. 285–324, figs. 16. Ergebnisse Der Exakten Naturwissenschaften, Herausgegeben von der Schriftleitung Der "Naturwissenschaften" Vol. X Verlag von Julius Springer, Berlin, 1931.

Numerous investigators have been interested in the various processes responsible for the light emitted in a gaseous discharge. This article is a review of the literature pertaining to these processes, in particular to the intensity relations between lines and the probability of excitation of certain lines by collisions between electrons and atoms as a function of the speed of the electrons. The authors have prepared graphs of the *excitation functions* of many of the lines in the arc and spark spectra of Hg, Cd, Zn, He, and Ne, from experimental data. The positions of the maxima of the excitation functions are also given in tabular form. A brief resume of the theory of excitation by electron impact in included in the discussion.

The remainder of the article is concerned with the light yield resulting from collisions between ions and atoms, *collisions of the second kind*, and from the bombardment of solids with mass particles.

P. T. SMITH
University of Minnesota

Zur Quantenmechanik der Multipolstrahlung (Dissertation, University of Utrecht), H. C. BRINKMAN. Pp. 60. Noordhoff N. V., Groningen, 1932.

This work is divided into three chapters, of which only the last is accurately described by the title. The first chapter contains an excellent exposition of the powerful symbolic method developed by Weyl and Kramers for handling problems involving angular momentum; the second is a discussion of the classical electromagnetic radiation from a system of electrons, and its resolutions into *multipole radiations* of different orders.

The mathematical physicist will undoubtedly find the first chapter of greatest interest. Dr. Brinkman's exposition of the symbolic method of evaluating matrix elements is concise and comprehensive. The principal feature of this method is the representation of a wave function ψ_{nlm} as a symbolic product, $\xi^{l+m}\eta^{l-m}$, the factors ξ and η being treated as complex numbers and called the components of a spin vector. The coordinates, and in general the components of any vector or vector operator, are represented symbolically as

$$x = (\xi^2-\eta^2)/2,$$
$$y = (\xi^2+\eta^2)/2i,$$
$$z = -\xi\eta.$$

This notation may be heuristically derived from the fact that in certain cases the $=$ is an actual numerical equality. Its deeper significance originates in the theory of invariance under the rotation group.

The procedure is to make the required matrix elements appear as the coefficients of an invariant homogeneous polynomial in the components of one or more spin-vectors (ξ, η). Such polynomials form a very restricted class; in the case of a single vector they all have the form $c(|\xi|^2+|\eta|^2)^{2l}$. The coefficients of the polynomial are at first unknown, but simple considerations always suffice to identify it with an invariant whose coefficients are easily calculated by purely algebraic means. As only the ratios of the coefficients of an invariant are fixed, only the ratios of the matrix elements are determined in this way.

Chapter II deals with classical electromagnetic radiation, the treatment being based on the Hertzian vector. The expansion of the field in a series of spherical harmonics is discussed in a detailed manner. The terms of this series are classified as electric dipole, electric quadrupole, magnetic dipole, and in general, multipole radiation. The contribution of the magnetic properties of the electron to the magnetic dipole radiation is discussed briefly, but it is pointed out that contributions to the higher orders of radiation are also to be expected.

The last chapter is concerned with the reinterpretation of the results of Chapter II by the correspondence principle and the calculation of the matrix elements by means of the methods developed in Chapter I. From the nature of these methods, it follows that no calculations of

the absolute probability of a *forbidden* transition are attempted. The goal is a generalization of the Goudsmit-Kronig-Hönl relative intensity formulae, selection principles included.

The final results may be listed as: (1) The selection principles and intensity rules for the multipole radiation of any order emitted by an atom with Russell-Saunders coupling. (The Kronig-Hönl formulae are special cases.) (2) The Rubinowicz formulae for the relative intensties of the Zeeman components of quadrupole radiation. (3) Formulae for the relative intensities of the Zeeman components of magnetic dipole radiation, taking the magnetic moment of the electron into account.

CARL ECKART
Palo Alto

PROCEEDINGS OF THE AMERICAN PHYSICAL SOCIETY

MINUTES OF THE NEW HAVEN MEETING, JUNE 23–25, 1932

The 179th meeting of the American Physical Society was held in New Haven, Connecticut on Thursday, Friday and Saturday, June 23, 24 and 25, 1932, upon invitation from Yale University. The registration for the meeting numbered 194. The scientific sessions were held in the Sloane Physics Laboratory and in the Osborn Zoological Laboratory. The presiding officers were W. F. G. Swann, President of the Society, Paul D. Foote, Vice-president, Karl K. Darrow, Bergen Davis, Herbert E. Ives, George B. Pegram and S. R. Williams.

Thursday morning was taken up with four parallel sessions of contributed papers, abstracts of which appear in these Proceedings. Thursday afternoon there were two informal conferences, one on Definitions and Units presided over by Leigh Page, and one on The Atomic Nucleus presided over by Henry A. Barton.

Friday morning was devoted to a symposium of four invited papers on "X-rays," abstracts of which are included in these Proceedings.

Saturday morning was given over to a joint session with the Applied Mechanics Division of the American Society of Mechanical Engineers which was meeting at Yale during the same three days. This joint meeting was a symposium on "Plasticity." Abstracts of the papers appear in these Proceedings.

The local committee provided very complete arrangements for the comfort, entertainment and enjoyment of the visitors throughout the meeting. The Physical Society dinner was held at the New Haven Lawn Club on Thursday evening with 145 guests present. There were no after dinner speakers and the dinner was followed by a complimentary presentation at the University Theatre of A. A. Milne's "The Perfect Alibi" by the Yale Dramatic Association. This was thoroughly enjoyed by every one.

On Friday afternoon the members were taken to a picnic at Double Beach, a delightful place on the shore where there were sea bathing, sports and dinner. Some members, who did not attend the picnic, went to the Boat Race at New London. Throughout the three days there were special teas, trips through the museums and the Sterling Library and sightseeing trips through the city provided for the visiting ladies and any others who wished to take advantage of them.

On Saturday afternoon there was a short meeting of the Physical Society at which President Swann and others discussed for the information of the membership some of the problems relating to publications and finance to which the Council has been giving much attention.

At the close of the joint session of the two societies on Saturday morning there was a unanimous rising vote of thanks given to Yale University and the local committee and to the Yale Dramatic Association for the splendid arrangements and entertainment provided for the visiting Societies during the three days of their meetings in New Haven.

Meeting of the Council. At its meeting on Friday, June 24, 1932, the Council elected one person to fellowship. Fourteen candidates were elected to membership. *Elected to fellowship:* Harold Pender. *Elected to membership:* H. E. Banta, John E. Davis, Georges Dejardin, G. W. Heitkamp, G. B. Kistiakowsky, Shoji Makishima, Ralph E. Nusbaum, Walter J. Osterhoudt, Tokutaro Sawai, Walter Soller, S. R. Toh, C. M. Van Atta, Juanita Witters and Stephen A. Zieman.

The regular scientific program of the Society consisted of forty-three contributed and seven invited papers. Numbers 7, 8, 9, 10, 21, 23, 33 and 39 were read by title. Number 12 was withdrawn at the request of the author and therefore the abstract does not appear in the Proceedings. The abstracts of the papers are given in the following pages. An *Author Index* will be found at the end.

W. L. SEVERINGHAUS, SECRETARY

1. Theory of variation of paramagnetic anisotropy among different salts of the iron group. J. H. VAN VLECK, *University of Wisconsin.*—Experimentalists find that nickel salts are magnetically isotropic to about one percent, but that those of cobalt have anisotropy amounting to around 30 percent. A theoretical explanation is given for this difference, which at first sight is puzzling because both the Ni^{++} and Co^{++} ions have F ground terms (respectively $d^8\ ^3F$ and $d^7\ ^4F$). Suppose the crystalline potential of the form $Ax^2+By^2-(A+B)z^2+D(x^4+y^4+z^4)+f(r)$ where the rhombic or second order terms are small compared to the "cubic" or fourth order ones, as indicated by the recent investigations of Jordahl, Penney, and Schlapp (Phys. Rev. May 15, (1932)). Then by joint adaptation of the Bethe group theory of crystal Stark effect and the Goudsmit-Slater method of diagonal sums it is shown that the energy diagram connected with the splitting in the crystal field is inverted for Co^{++} as compared to Ni^{++}, so that a state which is nearly isotropic magnetically is the ground state for Ni^{++}, whereas an anisotropic one is the normal level for Co^{++}. The inversion phenomena are also discussed in connection with other ions of the iron group in which it appears. The nearly perfect isotropy of manganous salts is trivial, as Mn^{++} is in an S state.

2. Monocrystal Barkhausen effects in rotating fields. F. J. BECK AND L. W. MCKEEHAN, *Yale University.*—The directions of Barkhausen effects in a single crystal disk of silicon steel, held stationary in a magnetic field rotating slowly in the plane of the disk, have been determined. Search coils at right angles picked up impulses proportional to selected rectangular components of the changes in magnetization. Measurements on an oscillographic record were made at two values of induction: 1480 and 645. Values of the angle Φ between the change in magnetization ΔI and the corresponding variation in the applied field, $(dH/dt)\Delta t$ are determined for various positions of the applied field relative to the crystallographic axes. The normal to the disk made angles of 30°, 60°, 90° with these axes. For these low values of induction the effects are mainly transverse and are more nearly transverse for the greater value of induction. The average value of Φ is about 20° (ΔI lagging) for the lower value of B and is less than 5° for the higher value. Individual values of Φ for one setting differ by as much as 30°. The average magnetization apparently lags the applied field and makes a small angle with it. The direction and frequency of effects seemed unaffected by changing the direction of H in the plane of the disk.

3. Mechanical hardness influenced by magnetism. S. R. WILLIAMS, *Amherst College, Amherst, Mass.*—About a year ago, Herbert published a most interesting article on "magnetic hardening of metals," (American Machinist **74**, 967, 1931). Not only did he find that rotating a ferromagnetic substance in a magnetic field changes the hardness but that the same thing occurred for substances which are not ferromagnetic. This work of Herbert's confirms some observations on steel rods, made by the writer in 1924, (Williams, Trans. A. S. S. T., p. 362, 1924). The work of 1924 has been repeated and confirmed on a series of high carbon steel rods of different drawing temperatures. The study has been extended to a series of steel rods of different carbon content and hardness. The effect seems to be very clearly shown. Magnetostrictive effects have been the means for studying the changes in hardness due to magnetic fields.

4. The dielectric constant of liquid sulphur. H. J. CURTIS, *Yale University.*—The dielectric constant and power factor of liquid sulphur was measured by a bridge method at four different audiofrequencies and over the temperature range 118°C to 350°C. The dielectric constant was found to be independent of frequency and equal to 3.520 ± 0.010 at 118°C. The specific polarization is independent of temperature between 118°C and 158°C and equal to 0.2528 ± 0.0008 cm^3g^{-1}. Above 158°C the polarization decreases directly as the reciprocal of the absolute temperature, showing that molecular association occurs with very strong binding forces between the molecules. This shows that liquid sulphur is definitely nonpolar. A method was developed for differentiating between that part of the power factor which is due to conductivity and that which is due to molecular friction. The former was found to be very large, especially at high temperatures, and the latter very small at all temperatures. This is a further confirmation of the fact that sulphur is nonpolar. The infrared spectrum of liquid sulphur contains definite absorption bands, which shows that its molecules are polar. It is difficult to understand this contradiction, since both measurements seem to give conclusive results.

5. Dielectric constant and particle weight. J. W. WILLIAMS, *University of Wisconsin.*—Svedberg has been successful with the determination of the size and weight of colloidal particles by observing their linear velocities when subjected to a centrifugal field. A similar result should follow from a study of their rotational velocities in an alternating electrical field. The method, an application of the dipole theory of Debye, depends upon the fact that owing to the frictional resistance of the medium to the rotation of the suspended particles a finite time is required for their orientation in the field. If the frequency dependence of the dielectric constant is determined for a system composed of electrically dissymetrical particles supended in a liquid medium there will be found to be a region in which the dielectric constant decreases as the frequency is increased. The theory expresses the size, and therefore the weight, of the suspended particle in terms of the observed critical frequency and the "viscosity" of the medium. The available data are as yet insufficient for the exact determination of the particle size because the systems involved fail to conform to the assumptions underlying either the law of Stokes or the Clausius-Mosotti relation. Nevertheless, calculations from them indicate that once it becomes possible to evaluate the true inner friction constant of the system important results may be obtained. The method readily distinguishes monodisperse and polydisperse sols.

6. Surface charge of large particles in liquids. HAROLD A. ABRAMSON, *Columbia University, and* HANS MUELLER, *Massachusetts Institute of Technology.*—It is proposed that an advance in the study of the constitution of the solid-liquid and liquid-liquid interfaces may be made by calculation of σ, the surface density of electric charge, in addition to the analysis of the potential difference, ζ, between the movable phases. For large particles σ can be readily calculated by an extrapolation of the Debye theory. This has been done for the negatively charged surfaces of graphite, glass, cellulose, "collodion" and paraffin oil, in the case of ions (valence 1:1; 1:2; 2:1; 1:4) not producing reversal of sign of charge. Although the ζ-concentration curves are rather complex, the σ-concentration curve in every case yields a simple curve resembling typical adsorption with an initial steep slope and with saturation at salt concentrations of about 0.01 molar. Curves of this type have been predicted by Stern. The character of the curves is determined by both ions. The slope at zero concentration varies markedly, particularly with the nature and valence of the anion; e.g., for glass in the order $I > Br > Cl$, the

differences diminishing as saturation approached. The method of calculation employed here to ascertain the nature and magnitude of the forces involved in adsorption of ions by "inert" surfaces at the liquid interface is justified by previous theory and experiment of the authors.

7. Some remarks on the physical constants of cells in connection with their size and shape. N. RASHEVSKY, *Westinghouse Research Laboratories, East Pittsburgh.*—In a paper presented at the Cambridge meeting, (Physics **2**, 303, 1932) a formula was deduced, giving the size of a cell in terms of its physical constants, such as, the coefficient of diffusion for oxygen, permeability, surface tension and rate of metabolism. From values for the diffusion coefficient D as found for muscle tissue, values of the order of magnitude of 10^{-3} cm for the size were found. Bacteria, however, are much smaller, and in order to account for their size, values for D about 1000 times as small must be assumed. It is interesting, that in a recent investigation Professor R. W. Gerard arrived at a similar conclusion from an entirely different point of view; namely, from the study of oxygen consumption. He discarded, however, the assumption of such a small D, as being not supported by any other facts, and interpreted his experimental results otherwise. Questions as to the possible reason of such a small D in bacteria are discussed in the present paper. Furthermore, some applications of the author's foregoing studies to the problem of shape of certain cells are made.

8. Electric phase angle of cell membranes. KENNETH S. COLE, *Columbia University.*—From the theory of an electric network containing any combination of resistances and a single variable impedance element having a constant phase angle independent of frequency, it is shown that the graph of the terminal series reactance against the resistance is an arc of a circle with the position of the center depending upon the phase angle of the variable element. If it is assumed that biological systems are equivalent to such a network, the hypotheses are supported at low and intermediate frequencies by data on red blood cells, muscle, nerve, onion membrane and potato. For some tissues there is a marked divergence from the circle at high frequencies, which is not interpreted.

9. A theory of surface conductance at an electrolyte-solid interface. KENNETH S. COLE, *Columbia University.*—An expression has been derived on the basis of the Maxwell-Boltzmann distribution and Poisson's equation for the tangential surface conductance of an electrolyte in contact with a charged plane surface. One part of this expression is analogous to the result given by Smoluchowski for a Helmholtz double layer, while the second part arises from the movement of the ions in the diffuse ion cloud under the applied electric field. The theory shows qualitative agreement with the data of Briggs for the conductance of univalent chloride solutions at a cellulose surface. For all but the most dilute solutions, the Smoluchowski term is negligible and the surface conductance is proportional to the charge density on the surface. The theory does not agree with the data for different anions and it is suggested that the decrepancy may be due to adsorption phenomena. There may be a movement of the adsorbed ions or of a diffuse ion cloud resulting from the presence of adsorption potentials at a distance from the interface.

10. Photographic reciprocity and intermittency defects near the long wave-length limit of plate sensitivity. BRIAN O'BRIEN AND VERNON L. PARKS, *Institute of Optics, University of Rochester, N. Y.*—Previous work on compensation of reciprocity failure in photographic spectrophotometry by intermittency defect imposed on light beam of higher intensity by interrupted exposure [Phys. Rev. **33**, 640 (1929), Phys. Rev. **37**, 471 (1931)] has been extended to the long wave-length limit of plate sensitivity (λ10,000A for one emulsion) where both defects become large. The four emulsions used, Eastman Process, Process Panchromatic, Contrast Bromide, and Infrared Sensitive 3Q, all exhibit large reciprocity failure. A tungsten incandescent source was maintained constant within 1/4 percent, and mounted on a carriage with range of movement of 50 meters for varying intensity. Fixed sectors were used with aperture ratios of 1/40 to 1/1212, running 28 flashes per second. Errors in measurement of sector apertures and exposure timing were less than 1/2 percent. Although reciprocity failures were as great as 0.92 in density, the difference in density produced on adjacent areas by continuous

low intensity and interrupted high intensity exposure (for It=const.) in no case amounted to a difference in log exposure greater than 0.012, and average difference was less than 0.004. Although just within the limit of measurement this appears to be a systematic difference with reciprocity defect greater than intermittency defect, but difference, if real, is so small that it may be neglected in photographic photometry.

11. The absorption spectrum of sulfur dioxide. J. A. DUNCAN, *Columbia University (Introduced by Harold C. Urey).*—The absorption spectrum of sulfur dioxide has been photographed in the region λλ2165–2410A with a Hilger E185 quartz spectrograph having a dispersion of about 1A per mm. The bands are partially resolved into rotational band lines. In this work an effort has been made to analyze the rotational structure rather than the vibrational structure, since Chow (Bull. of the Am. Phys. Soc. Vol. 7 No. 2, 19, April 12, 1932) using lower dispersion is working on the latter problem. The more intense lines of some bands can be classified into branches having approximately constant second differences. These bands appear to fall roughly into two classifications; (1) bands consisting of only one branch resembling a Q branch; (2) bands consisting of two or more branches. It is found to be possible to include in this way nearly all the strong lines of these bands.

12. The alternation of intensities in the sodium bands. JOSEPH JOFFE, *Dept. of Chemistry, Columbia University.* Withdrawn at author's request.

13. The continuous absorption spectrum of chlorine. G. E. GIBSON AND NOEL S. BAYLISS, *The University of California, Berkeley, California.*—A photographic method was used to investigate the continuous absorption spectrum of chlorine at six different temperatures. The effect of increasing the temperature is to decrease the absorption coefficient at the maximum and to broaden the region of continuous absorption. The results were analyzed to obtain the individual contributions of the first two vibrational levels of the normal electronic state to the total absorption. Plotted against wave number, the absorption from the lowest level, ($v''=0$), has a form similar to that of a Gauss error curve, and the absorption from the next level, ($v''=1$), has two maxima. The results are in qualitative accord with a theory of continuous absorption developed by Gibson and Rice.

14. The origin of the mercury bands at 2480A. J. GIBSON WINANS, *University of Wisconsin.*—The mercury bands near 2480A were photographed under different excitation conditions with the purpose of determining their origin. A discharge through mercury vapor was produced in a quartz tube through external electrodes by a low voltage Tesla coil. A photograph of the 2476 band in the third order of a 21-ft. grating checked that of Miss Brozowska, (Zeits. f. Physik **63**, 557 (1930)). Five different tubes containing distilled mercury showed the entire group of eight bands. These bands were weakened by heat. From these observations the origin is some form of mercury molecule, the most probable being Hg_2 or Hg_2^+. Six lines of evidence favor Hg_2^+ over Hg_2: (1) observations on fluorescence, (2) comparison of intensities in mercury arc and electrodeless discharge, (3) comparison of the intensities of the 2476 and 2345 bands under strong and weak field excitation, (4) abscence of other bands of similar character in the mercury spectrum and the observation by Rayleigh that these bands do not appear in absorption, (5) classification of these bands as sequences $v'-v''=0\pm1\pm2\pm3$ which leads to a value for $D>0.5$ volts; (6) observed emission from state $v'=41$ corresponding to very high temperature molecules.

15. Observations on the fluorescence spectra of cadium vapor. W. CRAM AND J. G. WINANS, *University of Wisconsin.*—A broad band in the fluorescence of cadmium vapor has been previously observed between the limits 3050−2288A. Kapuscinski found that monochromatic light of wave-length in this band was absorbed and reemitted by the vapor. In the present experiment fluorescence was excited in cadmium vapor by light from a copper spark. The band was found to extend from 3050 to 2212A. Lines in the exciting light, of wave-length below 2288A, were reemitted by the vapor in the same manner as those observed by Kapuscinski. The spectrum of the electrodless discharge showed this same band but with different intensity distribution. These observations can be explained by the use of potential energy-

nuclear separation curves which correspond closely to those given by Winans to interpret the absorption spectra of cadmium vapor.

16. Rotational Raman effect of gases. CHARLTON M. LEWIS, *California Institute of Technology.*—The study of the Raman effect of gases has been extended to the pure rotation of the simpler hydrocarbons. Acetylene shows the same pattern of alternating intensities that was found by Hedfeld and Mecke in absorption. Ethane and ethylene, which have the form of the symmetrical and asymmetrical top, respectively, show more complicated fine structure; but in neither case is there evidence of more than one moment of inertia. The pure rotation spectrum of methane appears to be missing, or at least of a lower order of intensity than the rotation-vibration band already found by Rasetti. The P and R branches of this band are not very much weaker than the Q branch, while another mode of vibration, which yields an extremely intense Q branch, shows no P and R branches. These characteristics are largely in agreement with what is to be expected from an extension to the rotational Raman effect of Placzek's method of treating the vibration lines.

17. Raman effect in crystalline NH_4Cl. F. T. HOLMES, *Lehigh University.*—Schaefer, Matossi, and Aderhold (Zeits. f. Physik **65**, 289 (1930)) have reported two broad Raman lines for NH_4Cl at 3155 and 3035 cm^{-1}. The author has found that in addition to these lines most of the characteristic frequencies found by Reinkober (Zeits. f. Physik **5**, 192 (1921)) in the infrared appear in the Raman spectrum as rather broad lines. However the line at approximately 1700 cm^{-1} is very sharp. In addition to these, a set of four very weak lines has been observed in the region near 3155 and 3035 cm^{-1}. In consideration of the prediction by Pauling (Phys. Rev. **36**, 430 (1930)) of rotation of the ammonium ion in this substance at room temperature, it seems possible to regard the members of this set as vibrational-rotational lines. Intensity considerations indicate that they may be associated with the 3035 cm^{-1} vibrational shift. Making these assignments, and assuming $\Delta j = \pm 2$ with no "missing lines," the moment of inertia of the rotating group is calculated to be approximately 2.0×10^{-40} gm cm^2.

18. Zeeman effect in the $^2\prod$ $^2\sum$ CaH bands. W. PEYTON CUNNINGHAM, *Yale University.* (*Introduced by W. W. Watson.*)—The Zeeman effect in the λ7000, $^2\Pi$ $^2\Sigma$ CaH band has been investigated at field strengths of 10,500, 18,200 and 30,000 gauss. For the Q branches the patterns are in excellent agreement with the predictions of Hill's formulas for doublet states. In the lines of the R and P branches, however, marked departures from these predicted patterns occur in the region of intermediate and high K levels. It is shown that the inclusion of the magnetic moment due to ρ, the sizeable component of l perpendicular to the internuclear axis is the Π_d levels, gives quite closely the needed corrections for these patterns. Calculation shows that for all these lines of high K values one block of components becomes so wide and diffuse as to be unobservable. Interesting variations with ρ and H in the observed narrower block of components for the region just above the crossing of the Π_d levels are discussed.

19. Zeeman effect of Pb III. J. B. GREEN AND R. A. LORING, *Ohio State University.*—The Zeeman effect of Pb III has been studied at fields of about 40,000 gausses with the newly completed 30,000 line 21-ft. Paschen-Runge concave grating set-up at this laboratory, and the same general type of vacuum box used in our work on Sn. Of particular interest in this spectrum is the $6s6p$ configuration, which seems to violate all the rules laid down by the theory. The coupling is practically j-j in type, and accurate measurements of the four lines involved in the transition $6s6p - 6s7s\,^3S_1$ indicate that (1) the Pauli g-sum rule for the $^3P_1 + {}^1P_1$ is not accurately obeyed, the experimental value being 2.53 against the theoretical 2.50; (2) the g-value of $^3P_2$ which should be unaffected by coupling (taking into account perturbations within its own configuration) is 1.35 (exp) against 1.50 (theo.). The abnormal g-value must be attributed to perturbations by the neighboring $6p^2$ or $6s6d$ configurations.

20. Theory of quantum defect due to polarization, with application to multiplet anomalies in Al II. N. G. WHITELAW AND J. H. VAN VLECK, *University of Wisconsin.*—The formula $\Delta = (\alpha e^2 n^3 / 4chR)\overline{1/r^4}$ for the quantum defect Δ due to polarization is usually derived by introducing a model in which the atom-core is given *ad hoc* a polarizability α. Instead a derivation

is given by perturbation theory in which inter-electronic interaction is considered explicitly. The above formula for Δ is found to be valid only if exchange terms are neglected and if the absorption lines ν(A.C.) of the atom-core are large compared to those ν(V.E.) representing transitions of the valence electron. The calculation enables one to determine the "perturbations," i.e., deviations from the formula, when there is close resonance between ν(A.C.) and ν(V.E.). The theory is applied to the $3smf\,^3F$ series of Al II, which Langer, Shenstone, and Russell have noted is perturbed by a $3p3d\,^3F$ term. The widening of the multiplets in the vicinity of the perturbation is caused by a partial robbing of the intruders wide structure, and can be calculated from the observed displacement of the multiplet centroids from hydrogenic values. The calculated over-all widths for the successive members are 5.1, 10.8, 37.2, (58.2 for intruding $3p3d$), 20.8, 7.3, 3.7, . . . against observed 4.9, 12.3, 40.4, (58.1), 17.8, 5.7, 2.4. The discrepancies may be diminished by the further consideration of higher order approximations.

21. A theorem on spectroscopic stability. R. M. LANGER, *University of Minnesota.*—Recent spectroscopic observations, especially some of the rare gas spectra (e.g., E. Rasmussen, Zeits. f. Physik **75**, 695, 1932) bring out symmetries in the oscillations of the term values of similar series. They suggest a connection between the departures of related terms from Ritz formulae. In fact such a connection can be deduced theoretically. The rare gas series exemplify one of several possible types of behavior. The usual calculations of energy levels assuming separate configurations lead to multiplet separations and smooth series which often disagree with experimental data. Since these incomplete solutions for discrete spectra differ from the correct ones by a unitary transformation the sum of the energies of mutually perturbing configurations is correctly given by the incomplete solutions. This leads to the very useful theorem that the displacements of interacting levels from their expected positions on smooth series curves must add up to zero. The power of this stability theorem depends on narrowing down the set of levels under consideration. It will help in estimating certain large displacements of terms in series which are not well marked and will also help calculate constants for irregular series. Probably the most helpful application of the theorem will be the criterion it gives for deciding whether one has all of the set of levels which are affecting one another. The important but difficult case of continuous spectra has not been considered.

22. The escape of imprisoned resonance radiation from a gas. CARL KENTY, *General Electric Vapor Lamp Co. Hoboken, N. J.*—Theoretical considerations lead to the view that a large concentration of resonance quanta diffusing through a gas would, on the basis of Doppler broadening only, give rise to a distribution function for excited atoms, with respect to atomic speed, which would lie between two limiting distribution functions: (1) Maxwell's distribution function, namely

$$f_1(S)dS = [4/(\pi)^{1/2}](S^2/w^3)\exp\,-(S^2/w^2)dS$$

where S is the speed of an atom and w is the most probable speed; and (2) a distribution function expressing a lower relative excitation of the high speed atoms, namely

$$f_2(S)\,dS = 2(S/w^2)\exp\,-(S^2/w^2)dS.$$

On the basis of either (1) or (2) the diffusion coefficient as well as the average square free path are found to be infinite provided the volume of gas is infinite; otherwise, the *apparent* values of these quantities will depend on the volume, increasing therewith without limit because of the importance of extremely long free paths. Coupling or other broadening occuring at higher pressures will presumably accentuate the effect of abnormally long free paths. The results are in qualitative agreement with imprisonment experiments of Zemansky and of Webb and Messenger, in Hg, and with the experiments of Found and Langmuir and of Kenty in Ne (in print).

23. Yield of fluorescent x-rays from the K shells of various elements. DONALD K. BERKEY, *University of Cincinnati.*—The fluorescent yield w from the K shells of an aggregate of atoms is defined as the ratio of the number of characteristic K quanta emitted to the number of quanta photoelectrically absorbed in the K shells. The author has measured this ratio by comparing the total intensities of the primary and fluorescent rays from various substances, using the

ionization method devised by A. H. Compton (Phil. Mag. **7**, 961, 1929). The following results were obtained:

Element		w	Element		w
27	Cobalt	0.38	42	Molybdenum	0.78
28	Nickel	0.39	47	Silver	0.73
29	Copper	0.43	48	Cadmium	0.72
30	Zinc	0.46	50	Tin	0.67
33	Arsenic	0.53	51	Antimony	0.64
34	Selenium	0.56	52	Tellurium	0.60
38	Strontium	0.72			

These results show that the fluorescent yield increases to a maximum for elements in the neighborhood of molybdenum, beyond which it decreases. It is planned to continue this investigation for elements of higher atomic number than tellurium.

24. Fine structure in the x-ray K absorption edge of calcium in compounds. VOLA P. BARTON, *Goucher College, and* GEO. A. LINDSAY, *University of Michigan.*—The fine structure of the Ca K edge has been examined in several calcium compounds. A quartz crystal was used and the calcium compound was ground to a fine powder and suspended in a collodion film for an absorbing screen. In cases where the calcium compound could be used as reflecting crystal and at the same time as absorber, the results were found to be the same as with screens. Calcite and aragonite, the same chemically, show markedly different fine structure, thus indicating that not the chemical compound, but rather the crystal form, is the determining factor. This is in accordance with Kronig's theory. Dolomite, $Ca\,Mg(CO_3)_2$, and ankerite, $(Ca, Mg, Fe)CO_3$ have the same crystalline form as calcite, and show the same fine structure for Ca, but the appearance for Fe in ankerite is different. This is not so satisfactory for the theory, for the iron and calcium atoms are similarly placed in the same crystal, and the ejected electron in passing through the crystal should experience the same variation in potential.

25. Further experiments on x-ray reflections from quartz crystals oscillating piezoelectrically. J. M. CORK, *University of Michigan.*—By both the Bragg method and the Laue method, quartz crystals at rest and oscillating piezoelectrically have been further studied. Starting with a relatively thick crystal and using a finely collimated x-ray beam the structure of the Laue spots could be readily observed. For oscillating crystals and also for polished crystals at rest the spots are double in structure. Etching the crystal with H Fl results in single spots for the non-oscillating crystal. The perfection of the surface is revealed by observing line breadth and intensity when the crystal is employed in a Siegbahn vacuum spectrograph at a wave-length of 5.5A; and for short x-ray wave-lengths on a Bragg spectrometer of 55 cm radius. In no case was line breadth or intensity sensibly altered by piezoelectric oscillation of the crystal. Results obtained are compatible with the elastic vibrational theory already proposed, (Fox and Cork. Phys. Rev. **38**, 1420 (1931)).

26. X-ray wave-lengths by ruled grating. R. B. WITMER AND J. M. CORK, *University of Michigan.*—With a ruled glass grating, measurements have been made of the wave-lengths in the L series emission spectra for elements from Ti (22) to Zn (30); and in the K series for elements from C (6) to Si (14). The grating employed (whose constant was $d=0.00166309$ mm) was ruled by Siegbahn on his new machine and gave excellent reflections. The experimental arrangement was identical with that employed in the precision determination of the L series wave-lengths of molybdenum (Cork, Phys. Rev. **35**, 1456, (1930)). This method has the important advantage that for the complete series of plates the position of the grating is in no way altered. The results obtained for the shorter wave-length lines are greater by about 0.3 percent than the corresponding wave-length measurements obtained by the crystal method. Crystals that have been employed for the longer wave-length range are mica, sugar, and palmitic acid. The individual results obtained with these crystals are shown to be so eratic that a comparison with the results obtained with the grating method is meaningless. The change in the relative intensity and the form of the α_1 line with change in atomic number is shown. Additional data

using different incident grazing angles are being taken to observe any possible variation in wave-length with angle of incidence. (Prins and Hanawalt, Nederlandsch Tijdschrift voor Naturkunde **12**, 1 and 15, 1932).

27. Additional theory of plane gratings for x-rays. ROY C. SPENCER, *University of Nebraska.*—The positions of the diffracted virtual images of a source as seen in a plane grating placed at a distance L are given by $L' = L \sin^2\theta/\sin^2 i$ where i and θ are the grazing angles of incidence and diffraction. For use with x-rays the incident beam is confined between two equal slits of width S distant L apart with the grating close to the second slit. The diffracted beam produced backwards appears to be confined between two slits of width S' and distance L' apart where $S' = S \sin\theta/\sin i$ and L' has the value given above. The intensity of a cross section of the diffracted beam is a trapezoid, the constant part having a width S' and each side an angular width S'/L'. The former varies directly as $\sin\theta$, while the latter varies inversely. Assuming a parallel beam, the angle between the maximum and the first diffraction minimum is λ/S'. The ratio of this diffraction width to the geometrical side width is $\lambda L'/S'^2 = \lambda L/S^2$, a constant of the slit system. This should not exceed unity. The combined effect of geometric and diffraction widths may be studied using a sodium flame and two slits.

28. The gamma-ray spectrometer. M. C. HENDERSON, *Yale University.*—The method first used by Rutherford and Andrade (Phil. Mag. **27**, 854, 1914; **28**, 263 (1914)) to measure the wave-lengths of the radium gamma-rays and later adapted by Steadman (Phys. Rev. **36**, 460 (1930)) to the Geiger point counter has been improved and some preliminary results obtained. The Geiger-Müller tube counter has been adopted as the detector. It has proved easily possible to resolve and measure the 20 and 35 x.u. radium B and C gamma-rays. With 30 mg of radium, the 35 x.u. line causes 4.7 discharges per minute out of a total of 16.5. All counting is automatic and runs 24 hours a day. The resolving power is low but it will be possible to resolve lines about 5 x.u. apart without further changes in the apparatus. The lower limit of wave-length that can be measured without disturbance from the central beam is about 20 x.u. The interrelated effects of source thickness, slit width, crystal setting and slit setting upon the theoretical gamma-ray intensity transmitted through the slit can be plotted as a series of three-dimensional models, which will be shown. The method of coincidences, so successfully applied to cosmic rays, has been tried to record gamma-rays, with encouraging results and it is being further developed. Steadman's results (loc. cit.) are not confirmed.

29. The threshold counting voltage of the Geiger-Müller tube and some related phenomena. D. COOKSEY AND M. C. HENDERSON, *Yale University.*—The voltage at which a Geiger-Müller tube begins to count is determinable to 0.1 percent. The dependence of this threshold voltage upon chamber and wire dimensions, material and nature of the surfaces, temperature of the wire, and pressure and kind of gas has been investigated. It is found that the threshold voltage for proper counting is independent of the wire and wall materials. For any chosen pressure and wire size the threshold voltage so varies with the chamber diameter that the field at the surface of the wire remains constant. This threshold field depends on the gas and its pressure, passing thru a minimum at low pressures in a similar manner to the sparking potential. Knowing the threshold field, the formula: field = voltage/(a log b/a), where a and b are the radii of the wire and chamber respectively, enables the counting voltage to be calculated for any desired dimensions and gas pressure. For small wires, less than 0.075 mm diameter, the threshold field is inversely proportional to the diameter but diminishes less rapidly than this for larger wires. Raising the temperature of the wire while counting lowers the threshold voltage. One iron wire continued to count in air up to a dull red, above which temperature spurious discharges masked the proper counts.

30. New determinations of the ranges of α-particles from polonium, uranium I and uranium II. F. N. D. KURIE, *Yale University.*—The cloud chamber method described by the author in the abstracts of the New Orleans meeting (1931) has been used to determine the ranges of α-particles from polonium, uranium I and uranium II. The experiments on polonium were undertaken to test the method, but the results are in such good accord with previous values that

they may stand alone. The range of polonium α particles at 0°C and 760 mm pressure is 3.690 $\pm$0.005 cm. A graphical method has been devised for separating the number-distance curves of the two uraniums, which consists in plotting the data on probability paper. The plot then becomes three intersecting straight lines, the midpoint of the short connecting line giving the relative proportions of the two kinds of particles. The ranges of the uranium particles at 0°C and 760 mm pressure are respectively: $R_{U\,I}=2.58\pm0.015$ cm, $R_{U\,II}=3.11\pm0.01$ cm. The polonium range is derived from 335 tracks, the uranium ranges from 594 tracks. The uranium ranges are in complete agreement with the results of Laurence (Phil. Mag. 5, 1027 (1928)), got by methods more likely to be in error than those used here.

31. Generalization of wave mechanics suggested by higher order terms in the classical electrodynamic equation of motion, and its influence on β-particles ionization for velocities approaching that of light. W. F. G. SWANN AND A. BRAMLEY, *Bartol Research Foundation of The Franklin Institute.*—Classical electrodynamics gives, for small velocities, an equation of electronic motion of the form

$$\frac{e}{6\pi ac^2}\ddot{x}-\frac{e}{6\pi c^3}\dddot{x}+\text{etc.}=E+\frac{[uH]}{c} \tag{1}$$

where a is the classical electronic radius. In the present paper, the equation is solved and for the cases which are relevant gives rise to

$$\frac{e^2}{6\pi ac^2}\dddot{x}=E+\frac{[uH]}{c}+f(D)E \tag{2}$$

where $f(D)$ is a determined function of the operator d/dt. We now build a Schroedinger equation for ψ with the right-hand side of (2), replacing $E+[uH]/c$ as used in the ordinary developments, but with d/dt replaced by ∂/dt, which for the field of a high-energy β particle of velocity v becomes $-v\Delta$. The perturbation, instead of involving only the scalar and vector potentials ϕ, and U, which can be expressed in terms of it, involves also a series of spatial derivatives of ϕ. Application to the ionization of an atom gives for q the number of ions per centimeter of path, an expression which, with increasing β-particle energy, first diminishes, then increases, and finally diminishes towards zero. The first decrease followed by increase corresponds to the conclusions of Oppenheimer, as yet apparently unpublished. The final decrease comes from the new features introduced. It predicts a decrease of ionization for β-particle energies greater than about 10^{10} volts.

32. An interpretation of cosmic-ray phenomena. THOMAS H. JOHNSON, *The Bartol Research Foundation of the Franklin Institute, Swarthmore, Pa.*—Schindler's measurements form the basis for a more specific theory of the process of ionization by cosmic rays than had hitherto been possible. To explain his data the following assumptions are made. (1) The primary rays contribute nothing *per se* to the ionization but produce secondary rays such as electrons and protons from the material through which they pass, the production coefficient β_m being a characteristic of the medium. (2) The absorption of the primary rays can be represented by a single exponential function with a coefficient ν_m characteristic of the medium. (3) The absorption of the secondaries can be represented by an exponential function, with a coefficient $\mu_m{}^n$ which is characteristic of both the absorbing medium m and the medium n in which the secondary ray was produced. The ionization at distance x behind the interface nm is given by

$$I=\frac{A\beta_m}{\mu_m{}^n-\nu_m}(e^{-\nu_m x}-e^{-\overset{m}{\mu_m} x})+Be^{-\overset{n}{\mu_m} x}.$$

The constants have been determined to bring agreement with the data in the case of the air to lead, air to iron, iron to lead, and lead to iron transitions. The absorption coefficients of the secondary rays determined in this way agree with the energies measured by Millikan and Anderson. The relation of these ideas to other experiments is also discussed.

33. Study of getter action of phosphorus. HENRY J. MILLER, *Emporium, Pa.*—The clean-up of commercial 50 watt 230 volt vacuum incandescent lamps by phosphorus has been investigated and compared with the clean-up in lamps of the same type evacuated by laboratory methods by means of a third external electrode measuring the ratio of positive ions to electrons flowing to this electrode while the filament voltage is gradually raised from zero to a value somewhat above normal rating. The clean-up initiated by the thermionic current flowing between filament terminals progresses with maximum efficiency at filament potentials which, for lamps with getters, agree with the volt value of maximum ionization efficiency of 150 volts found by Mayer for air and nitrogen (Ann. d. Physik **45**, 1 (1914)). Commercial lamps without getters do not clean up. Lamps without getters evacuated by laboratory methods clean up but at higher potentials than the corresponding lamps with getters (175 to 200 volts). The clean-up curves of lamps with getters and without getters suggest the interpretation of the observed clean-up as "chain-reaction" according to Bodenstein. (*Preuss. Akad. Wiss. Phys. Math. Kl.* 1928, p. 490).

34. The Kerr electro-optical effect in carbon dioxide. C. W. BRUCE, *University of Virginia, (Introduced by J. W. Beams).*—Measurements have been made on the variation with density of the Kerr electro-optical effect in CO_2 using a method similar to that of Stevenson and Beams (Phys. Rev. **38**, 133 (1931)). The measures were taken at a constant temperature of 34.6°C. The density was varied from 0.05 to 0.288 gm/cc and was computed from pressure readings by use of Amagat's data. The results of Stevenson and Beams were confirmed for the range (0.08−0.18) over which they worked. A comparison made between the variation of the Kerr constant as determined experimentally and as computed from the relation $B \propto [(n^2+2)^2(\epsilon+2)^2]/n$, taken from the Langevin-Born theory, shows good agreement. The data for the index of refraction used in the above relation were that of Phillips (Proc. Roy. Soc. **A97**, 225 (1920)), and for the dielectric constant was that of Keyes and Kirkwood (Phys. Rev. **26**, 754 (1930)).

35. The initiation of electrical discharges in effectively ion free gases. J. W. BEAMS AND JOHN W. FLOWERS, *University of Virginia.*—A study is made of the factors that initiate the discharges described by Street and Beams (Phys. Rev. **38**, 416 (1931)). In carefully dried and filtered gases (air, hydrogen, nitrogen, helium) at atmospheric pressure, it is possible to apply 5×10^5 volts per cm between spherical brass electrodes for 10^{-6} sec. without electrical breakdown, provided the gas is kept "swept" as free as possible of ions by auxiliary fields. However, when ultraviolet light falls upon the cathode a field of 4×10^4 volts per cm starts the discharge in less than 10^{-7}sec. The maximum field depends upon the conditions of the surface of the electrodes and is of the same order of magnitude as that required to produce breakdown in a vacuum, which is known to be started by field currents from the cathode (Wood, Phys. Rev. **5**, 1 (1897); Hull and Burger, Phys. Rev. **31**, 1121 (1928); Snoddy, Phys. Rev. **37**, 1678 (1931)). When a steel point and plane were substituted for the brass spheres in the above experiment the field at the surface of the point could be made at least 10^7 volts per cm for 10^{-6} sec. without breakdown if the point was positive. However, breakdown started in less than 10^{-6} sec. if the point was made the cathode and the field raised to only 10^6 volts per cm. In a vacuum fields of 8×10^7 volts per cm were applied to the pointed steel or tungsten anode for 10^{-7} sec. without breakdown. Similar results were obtained with gaseous pressures less than 0.01 mm.

36. Ionization of helium, neon and argon under impact of their own positive ions. CHARLES J. BRASEFIELD, *Yale University.*—The number of electrons liberated from neutral rare gas atoms under impact of their own positive ions was measured as a function of the kinetic energy of the ions. It was found that helium was ionized at 100 equivalent volts; neon at 90 and 130 volts; and argon at 55 and 95 volts. It is thought that the higher ionizing potentials in the case of neon and argon are the result of impacts of doubly charged ions. The error in these measurements is hard to estimate but is thought to be within ±10 volts. If we assume (1) that half of the kinetic energy of the impacting ion is available for ionization and (2) that the energy required to liberate an electron is approximately the sum of the energies necessary to liberate it

separately from its own core and from that of the impacting ion, we might expect ionization of the rare gases under impact of their own positive ions to occur at approximately the following values: in helium at 98 volts, in neon at 86 and 125 volts and in argon at 63 and 87 volts.

37. New devices for recording Kennelly-Heaviside layer reflections. HARRY R. MIMNO AND P. H. WANG, *Harvard University.*—Two new pieces of apparatus for layer height measurement have been built and tested. The first device is merely an improved form of the "long film" type of oscillograph, ordinarily used in pulse transmission experiments. In order to increase the resolving power without wasting or tearing the photographic paper tape, the oscillograph has been constructed with a magnetic clutch, shock absorber, and magnetic brake. The second device is a high speed chronograph, designed to give an accurate record of layer heights over an extended period of time. A complete history of the reflections produced by 2000 successive pulses is recorded in compact form on a strip of photographic paper, 90 cm long and 12 cm wide. The time scale may be varied from 5 minutes to 24 hours. The received pulses modulate a glow lamp, producing a small, sharply-defined dot on the moving paper. The resolving power appears to be somewhat better than that obtained with the best galvanometer oscillographs. A cathode-ray oscillograph is used to monitor the reception. The high speed chronograph has other applications, outside of the radio transmission field.

38. A new type of vacuum or circulating pump. E. L. HARRINGTON, *University of Saskatchewan.*—A new type of vacuum or circulating pump employing a helical tube made to rotate about the axis of the helix is described. Its action depends on a pumping liquid which fills the lower bends of the helix and crowds out the gas being pumped as the helix is rotated. There is a provision for the return of the pumping liquid to the first coil of the helix as the latter continues to rotate. The liquid may be chosen to suit the work at hand. Among the advantages claimed for the pump are the following: mercury vapour is not employed, heating and cooling elements are not required, adapted equally well to corrosive and non-corrosive gases, vapors and liquids, constant personal attention is not needed, it may be started or stopped instantly without the use of stop-cocks, and its action is reversible.

39. The form of potential barrier at the surfaces of conductors. A. T. WATERMAN, *Yale University.*—The method of treatment described by the writer (Phys. Rev. **38**, 1497–1505 (1931)) has been used to investigate the form of potential barrier inside as well as outside the surface of a conductor in equilibrium with its electron atmosphere, assuming continuity of potential and electric intensity at the boundary. The results indicate that there is a sharp rise in the barrier of about 4 or 5 volts within a distance of several Angstrom units in the immediate neighborhood of the surface (assumed plane), about one fifth of the rise occurring inside the conductor. The rest of the potential curve rises more gradually. Similar treatment for the form of barrier between plane parallel electrodes shows this to consist of a potential "plateau." To be consistent with contact potential as defined by the Kelvin experiment, on bringing the electrodes together there is a flow of electrons into the less electropositive metal, the potential barrier becomes a "hill" of decreasing height, until it disappears in a point of inflection at contact. Similarly the potential "trough" within a thin conducting film flattens out and disappears as the thickness of the film approaches zero. The case of a thin film deposited on base metal is difficult to solve, but gives promise of accounting for some of the peculiarities observed in such cases.

40. The caesium-oxygen-silver photoelectric cell. C. H. PRESCOTT, JR. AND M. J. KELLY, *Bell Telephone Laboratories Inc.*—The active cathode surface of the caesium-oxygen-silver photoelectric cell appears to be a film or surface concentration of caesium of atomic dimensions adsorbed upon a matrix of caesium oxide and silver containing free caesium and a small amount of silver oxide. The spectral characteristics of the photoelectric response depend largely upon the thickness of the surface film of free caesium. This film thickness is determined by the caesium concentration in the underlying matrix and is maintained by a diffusion equilibrium. Variations in the amount of caesium upon the surface were made either by exposing the standard finished cathode to small amounts of oxygen and allowing the response to recover

by diffusion of free caesium from the underlying material, or else by allowing small amounts of additional caesium to deposit upon the standard surface. With increasing thickness of the caesium surface film the characteristics of the spectral response appear to vary continuously from a low response (with amounts of surface caesium far below the normal) which decreases with wave-length (from 6000A to 10,000A) to a high response for the normal surface with a selective maximum at 7500A–8000A, and finally to a low response with a maximum approaching 6000A.

41. Some photovoltaic properties of Cu:Cu_2O |$Pb(NO_3)_2$ solution| Cu:Cu_2O photocells. WILBUR E. MESERVE, *Cornell University* (*Introduced by Ernest Merritt*).—The light sensitive electrodes were prepared by chemical methods which produce a uniform coating of copper oxide of any desired thickness. Two identical electrodes were placed in a 1 percent solution of $Pb(NO_3)_2$, the back of the light exposed electrode being insulated from the electrolyte. Measurements were made of the photo-e.m.f. produced by the cell when illuminated by sinusoidally interrupted light of variable frequency. By impressing the output of the cell on a resistance coupled amplifier of proper design, which takes no current from the cell and thus reduces polarization and internal chemical changes to a minimum, the frequency response was determined with the use of the stabilized cathode-ray "oscilloscope." The spectral sensitivity of the cells was determined with sinusoidally interrupted light from a monochromator and checks with that which has been determined with steady illumination. The angle of phase shift of the photo-e.m.f. with respect to the interrupted light was also measured and was found to first increase and then decrease with frequency, the maximum angle occurring at about 500 cycles. The internal capacity of the cell as an electrolytic condenser was found to nearly double when one electrode was illuminated by strong sunlight.

42. The isotopic weight and packing fraction of H^2. K. T. BAINBRIDGE, *Bartol Research Foundation*.—The mass of neutral H^2 is 2.01353 ± 0.000064 obtained from comparison of the mass of $(H^1H^1H^2)^+$ with He^+ on fourteen spectra secured with the mass-spectrograph recently described. The eqivalent packing fraction of H^2 is 67.6. On the assumption that the nucleus is composed of two protons and one electron the energy of binding is approximately 2×10^6 electron-volts but if the H^2 nucleus is made up of one proton and one Chadwick neutron then the binding energy of these two particles is 9.5×10^5 electron volts. $(3H^1)^+$ and He^+ provided the dispersion measurements for these spectra and the presence of $(H^1H^2)^+$ can only introduce a negligible correction. Lines of mass 4.0285 on the spectra were attributed to $(H^1H^1H^2)$ ions because (1) no lines of comparable intensity appeared in this position when commercial hydrogen was used, (2) under the conditions existing in the discharge tube the probability of formation of $(2H^2)^+$ was much less than for $(H^1H^1H^2)^+$, (3) the mass is less than the mass of $(4H^1)^+$ by an amount outside of the limit of error. The two enriched samples of hydrogen used were prepared by Brickwedde, both had been tested spectroscopically by Urey and Murphy and one was a sample of Bleakney's.

43. The isotopes of uranium. T. B. WILKINS AND W. M. RAYTON, *University of Rochester*.—The existence of an isotope of uranium (AcU_I) of shorter life than U_I as the parent of the actinium series was predicted in 1926 (Wilkins, Nature **117**, 719 (1926)). An alpha-ray range of 3.2 cm and period 2.5×10^8 yrs., then assigned, were confirmed by Rutherford's interpretation of Aston's mass-spectrogram of lead. (Nature **313**, 1929.) A mass-spectrogram of uranium failed to reveal even U_{II}. In the present work the alpha-rays from a thin sputtered film of uranium fell on a special photographic emulsion. The number of grains in individual tracks was counted. Two main peaks are indicated in the frequency curve at 9 and 11 grains and clearly marked humps at 13 and 16. The peak at 11 is slightly higher than at 9. Polonium gave a smooth curve with peak at 13. Hence Laurence's ranges of U_I and U_{II} are confirmed (Phil. Mag. **5**, 1027 (1928)), but two and possibly three additional isotopes of a less active series are indicated. The study of the relative activities of these two series may lead to a simpler method of determining the ages of rocks.

Nos. 44 to 47 are abstracts of invited papers which made up a symposium on x-rays.

44. The spectrum of scattered radiation. J. A. GRAY, Queen's University.—It is generally assumed that, when homogeneous x-rays are scattered through an angle θ, the modified band has both an average wave-length and a wave-length of maximum intensity given by the equation

$$\lambda_m = \lambda + h/mc\,(1-\cos\theta) \quad \ldots\ldots\ldots \quad (1)$$

So that if $\lambda+\delta\lambda$ = average wave-length of scattered rays

$$\delta\lambda = (R/R+1)\cdot h/mc\,(1-\cos\theta) - (R/R+1)\times 0.0243\,(1-\cos\theta)\text{A}.$$

where R = ratio of integrated intensity of modified band to that of the unmodified line.

I have carried out experiments at different times since 1913 to obtain values of $\lambda+\delta\lambda$, but always with heterogeneous rays. A brief description of the method follows. The primary rays passed through two slits and fell on the radiator, the scattered rays passing through a second set of slits into an ionization chamber where their intensity was measured. Three readings were taken, the first with no absorber, the second with an absorber in the path of the primary rays, position A say, and the third with an absorber in the path of the scattered rays in position B say. It is essential that the ratio of the two last readings should be determined as accurately as possible. This ratio will be called A/B.

An analysis of some results obtained in 1922 is given in Table I, the average value of θ being $\pi/2$.

TABLE I.

Abs.	A/B	P	P'	μ/ρ	μ'/ρ	λ	$\delta\lambda$
0.304	1.13	0.327	0.289	3.68	4.08	0.63	0.023
0.608	1.24	0.152	0.123	3.09	3.44	0.59	0.022
0.912	1.32	0.079	0.0598	2.79	3.09	0.57	0.021
1.216	1.40	0.043	0.0307	2.59	2.86	0.56	0.020

The first column gives the mass of the aluminum absorber in g/cm². When the absorber is placed at A, the ionization is P times as great as it is with no absorber; when placed at B, P' times as great. From P and P' the values of μ/ρ and μ'/ρ are obtained. From μ/ρ, λ is obtained from tables. It is given to two figures. $\delta\lambda$ is obtained from relative values of μ/ρ and μ'/ρ' by assuming that μ/ρ varies as λ^3.

It will be seen that $\delta\lambda$ is less than 0.024A, the value it should apparently have if all the scattered radiation is modified.

The radiator was paraffin wax, 1 inch square in cross section. Assuming a value of $R=8$, $\delta\lambda$ should be of the order 0.021A, if the primary rays are homogeneous. As the table shows these rays are not homogeneous. The effect of using heterogeneous rays is shown in Table II. A primary beam has been assumed to consist of rays of wave-lengths 0.4, 0.5, 0.6, 0.7, 0.8 and 1A respectively, the scattered rays ($\theta=\pi/2$), having wave-lengths 0.424, 0.524 etc. and relative intensities 0.05, 0.20, 0.25, 0.25, 0.20,and 0.05 respectively. This assumed beam has similar properties (absorption coefficients) to the one with which the results of Table I were obtained.

TABLE II.

Abs.	A/B	P	P'	μ/ρ	λ	$\delta\lambda$
0.304	1.11	0.318	0.286	3.77	0.63	0.020
0.608	1.20	0.138	0.115	3.23	0.60	0.020
0.912	1.27	0.0693	0.0543	2.92	0.58	0.019
1.216	1.35	0.0380	0.0282	2.69	0.56	0.018

It will be noticed that $\delta\lambda$ decreases as the thickness of the absorber is increased. A comparison of the figures in the two tables indicates that $\delta\lambda$ for homogeneous rays of wave-length 0.6A is about 0.026A for the radiator used, and, if we assume $R=8$, that the average wave-length of the modified rays is 0.029A greater than λ and not 0.024A, the value given by Eq. (1).

In later experiments, I have attempted to see if $\delta\lambda$ varied with the thickness of the radiator, using heterogeneous rays. One set of results is given in Table III.

TABLE III.

Abs.	Radiator	A/B	P	P'			
0.303	1 sheet	1.20	0.220	0.183	5.00	0.7	0.028
0.303	2 sheets	1.18	0.220	0.187	5.00	0.7	0.025
0.303	12 sheets	1.16	0.220	0.190	5.00	0.7	0.023

The radiator consisted of sheets of filter paper soaked in paraffin wax, the mass of the former being 0.07 g/cm² and of the latter 0.10 g/cm². For $\theta=\pi/6$, A/B was found to be equal to 1.01.

The variation of $\delta\lambda$ with thickness of absorber is again shown in Table IV, the radiator being one sheet of waxed filter paper.

TABLE IV.

Abs.	A/B	P	P'	λ	$\delta\lambda$
0.067	1.07	0.538	0.503	0.86	0.032
0.134	1.14	0.330	0.293	0.80	0.030
0.268	1.18	0.250	0.216	0.70	0.026

It will be noted that $\delta\lambda$ decreases as the thickness of the radiator and of the absorbing material increases. It is concluded that a thorough spectroscopic examination, both photographic and electrical, must be made of the radiation scattered by thin radiators. It is recommended that all such measurements should be verified by the above absorption method, and that this method be applied to gases, particularly hydrogen, helium and other rare gases, the two former as they give us the nearest approximation to free electrons. It is also of great importance to determine the ratio R accurately.

45. X-ray evidence for high electron momenta in atoms and in solid bodies. J. W. M. DUMOND, *California Institute of Technology*.—The work of the author in collaboration with H. A. Kirkpatrick, furnishes evidence for the interpretation of the breadth and structure of the modified line in the spectrum of scattered x-rays as a Doppler broadening caused by the momenta of the electrons in the scattering body. A test of the correctness of this interpretation was made by studying the variation in the shifted line breadth at half maximum as a function of the primary wave-length and also as a function of the scattering angle. The behavior of the shifted line breadth with both these variables is shown to be entirely consistent with the doppler interpretation of its origin. Very sharply defined homogeneous scattering angles could be obtained thanks to the geometry of the multicrystal spectrograph used in this work. The wave-lengths tested covered a range from 700 x.v. to 200 x.v. The Doppler interpretation of the broadening of the shifted line is shown to be in good accord with quantum mechanics. The profile of the Compton line can be interpreted as a distribution curve expressing the relative probability of scattering by electrons of component momentum, px, resolved along on axis, x, which very nearly bisects the angle formed by the incident and scattered beams of radiation. The distribution of electrons in linear momentum has been obtained by this method for carbon and beryllium scatterers and appears to be entirely consistent with the distribution to be expected quantum-mechanically as computed from formulae of Pauling and Podolsky for hydrogenic momentum distributions. The application of these hydrogenic distributions by the introduction of screening factors gives of course only a rough approximation to the momentum distribution in the free carbon atom. It gives nevertheless a distribution curve very similar to that deduced from the experiment save that the maximum of the curve occurs at somewhat lower momenta in the theoretical curve for the free carbon atom than in the experimental curve for a solid carbon scatterer. This is exactly what is to be expected since in solid carbon the proximity of neighboring atoms requires higher momenta of the outer electrons than they would possess in a free atom.

46. Status of x-ray wave-lengths. J. A. BEARDEN, *The Johns Hopkins University.*—The determination of x-ray wave-lengths by crystal gratings requires a knowledge of the constancy of the grating constant of crystals from various sources, and as precise a determination of this constant as is possible. Recent measurements (Phys. Rev. **38**, 3089, (1931)) have shown that the grating constant of calcite crystals from various sources varies less than 1 part in 200,000. The average true value of the grating constant was found to be $d=3.02810$A at 18°C, and the effective value for the first order diffraction $d_1=3.02769$A.

The most precise methods of measuring the diffraction angles appear to be the photographic and double crystal spectrometers. For true symmetrical lines it can be shown that the two methods should give results of the same order of precision. In the case of asymmetrical lines the double crystal method has a distinct advantage in that measurements can be made on the peak of the lines, or from the shape of the lines corrections can be applied to take into account the close components. The importance of measuring x-ray wave-lengths by the double crystal method is shown by the results obtained on the K series of copper and iron where most of the lines are asymmetrical.

Since the ruled grating measurements of x-ray wave-lengths are about 0.25 percent higher than the crystal values it is important to know which value is correct. Studies of the diffraction by ruled grating when used for measuring x-ray wave-lengths have as yet given no explanation of the observed difference. However, the following facts appear to support the crystal value rather than the ruled grating results. (1) Allison (Am. Phys. Soc. Washington 1932) has examined calcite crystals which gave the theoretical rocking curve width and diffracted intensity for a perfect crystal. (2) Tu (Phys. Rev. **40**, 662 (1932)) finds no evidence for mosaic structure. (3) The agreement between Planck's constant h determined by the limit of the continuous x-ray spectrum and other methods. (4) Inconsistency of fundamental constants if the grating wave-lengths were accepted as absolute. (5) Dispersion of x-rays.

47. Fine structure in x-ray absorption spectra. J. D. HANAWALT, *The Dow Chemical Co., Midland, Mich.*—The fine structure in x-ray absorption spectra which extends over a region of several hundred volts to the short wave-length side of the principal absorption edges of many elements has been explained in terms of the simultaneous transitions of two or more electrons due to the absorption of a single quantum. However, this interpretation is not consistent with the experimental facts which are brought out by a study of the effects of the physical and chemical state of the absorbing atom on the fine structure, and by a study of the effect of temperatures changes on the fine structure. These facts are: (1). The fine structure of a polyatomic vapor and of the same material in the solid state are usually similar, though the solid exhibits an additional structure not seen in the vapor spectrum. (2) The fine structure of a polyatomic vapor may differ from that of the solid. (3) Fine structure of more than a few volts separation from the main edge is not observed for any monatomic vapor. It is important to note that the structure which is exhibited by monatomic vapors if of such small energy value as to be satisfactorily explained by the Kossel theory of the transitions of the ejected electrons to various of the virtual orbits of the atom. (4) Fine structure is not observed in the spectra of the polyatomic vapors Se_8 and AsH_3. (5) The fine structure exhibited by Hg in $HgCl_2$ in solid and in vapor forms has the same energy separations from the principal edges in both its L_{III} and its L_{II} spectra. (6) An element in different chemical compounds may show different types of fine structure. (7) In the series As, $AsCl_3$, As_2O_3, As_2O_5, AsH_3 the principal edge has the same wave-length for the vapors, while there are shifts of 5.5 ± 1.5 volts for the solids. (8) The fine structure in the K absorption spectra of Fe becomes fainter as the temperature is raised and at 800°C has almost entirely vanished. (9) There is a shift of the fine structure discontinuities in the direction of longer wave-lengths as the temperature is raised. For a change from 20°C to 800°C the magnitude of this shift is 5.0 ± 2 volts at a point 115 volts from the K edge. Statements 8 and 9 are illustrated in Fig. 1.

Kronig has shown that the principal experimental facts concerning fine structure may be understood from the theory of the quantum mechanics of electrons in crystal lattices. The theory shows that not every value of velocity is possible to the motion of electrons traveling through a crystal lattice, but rather that there exists an energy spectrum consisting of alter-

nating zones of permitted and forbidden energies. In the case of the isolated atom the electron is ejected from the atom and in addition might be given *any* value of kinetic energy. However, in a crystal lattice the x-ray quantum can only eject an electron from the atom and thereby become absorbed if it gives the electron such a value of kinetic energy as to bring it into one of the permitted energy zones. Thus one will expect variations in the absorption coefficient on the short wave-length side of the main edge related to this sequence of permitted and forbidden energy zones. Kronig shows that for a one-dimensional sequence of periodic potential barriers the forbidden levels fall together with the energy values $W_n = n^2h^2/8ma^2$, where n takes integer values, h is Planck's constant, m is the electronic mass, and a is the distance between successive potential barriers. From this equation, if the lattice constant a increases through thermal expansion the energy zones shift toward the zero level. The magnitude of this shift for Fe agrees with that experimentally observed. Also, the greater distorsion of the periodicity in the lattice at high temperature causes a smearing of the sharp boundaries between permitted and forbidden energy zones and so causes the vanishing of the fine structure.

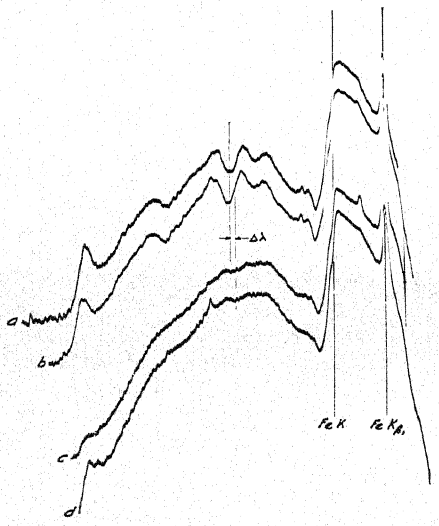


Fig. 1. Microphotometer traces of the K absorption spectra of Fe.
(a) 20°C, (b) 20°C, (c) 770°C, (d) 840°C.

The reciprocal lattice constant squared form of the energy has since been verified in other ways. Lindsay has shown that the fine structure of K in the crystals KCl, KBr, and KI has the same character for each crystal but that the energy separations from the main edge of the corresponding discontinuities in the three spectra are inversely proportional to the squares of the lattice constants. Coster and Veldkamp have demonstrated this same principle by a comparison of the F-C cubic metals Cu, Au, and Pt. They have also found by a study of a Au-Cu mixed crystal that the fine structure discontinuities of the Au L_{III} spectra have shifted to higher energies and the discontinuities of the Cu K spectra have shifted to lower energies by just such amounts that in the mixed crystal they have the same values. They have also shown many interesting facts concerning the intensity of the fine structure.

Recently Kronig has extended his theoretical considerations by investigating in how far it is possible to relate the individual minima of the fine structure, similarly as the lines of an x-ray powder diagram, to the various reflections of the electrons on the lattice planes, and has shown that a decisive agreement between theory and experiment is not obtained in this way.

Nos. 48 to 50 are abstracts of papers which made up a symposium on plasticity.

48. On the problem of the solid state. F. ZWICKY, *California Institute of Technology.*—A discussion will first be given of these particular questions which constitute the problem of the

solid state. One of the most characteristic phenomena exhibited by real crystals is a peculiar coexistence of perfection in certain respects and imperfection in others. This behavior of crystals may be traced back to the fact that the properties of crystals can roughly be divided into two groups, structure insensitive and structure sensitive, of which the latter group is responsible for hysteresis effects.

The problem of the solid state essentially consists in understanding the coexistence of structure sensitive and structure insensitive properties. After it was realized that the theory of the ideal lattices had nothing to offer in the way of a rational explanation of these phenomena, two different attempts were made in order to arrive at a solution.

The first attempt is based on the observation that in general crystals during their growth and existence are very severely affected by certain disturbing effects, such as thermal and mechanical stresses, liberation of dissolved gases, etc., which hinder the formation of ideal crystals. These facts suggest the assumption that all structure sensitive properties are due to *accidental imperfections*. Although this view has many points to recommend itself it cannot be regarded as a solution of the problem of the solid state. The main objection to the *imperfection theory* is that as we grow the crystals more and more carefully the less their structure sensitive properties conform with those which we derive from the theory of ideal crystal lattices.

The second attempt is based on the observation that the physical properties which are peculiar to the crystalline state are extending over distances far greater than the effective action radii of individual atoms and molecules. They therefore suggest the existence of certain *cooperative effects* which are exhibited only if atoms and molecules are present in very great numbers. With this observation in mind the author has undertaken a systematic study of cooperative phenomena whose physical origin is essentially related to forces depending on the distances as $1/r^2$, $1/r^3$, and $1/r^4$ and also on the exclusion principle. Mathematically speaking we are confronted with the problem of conditionally convergent series. If we consider ideal crystals only, intrinsic equations of state for crystals can not exist, as the mentioned cooperative effects introduce effects of the boundaries, no matter how large the crystals are. For this and other reasons a *secondary structure* of crystals is tentatively introduced. The conception of the secondary structure resolves many of the difficulties encountered by the older theories. It also allows us to draw many new conclusions and to predict a great number of phenomena as yet unknown. Finally theoretical and experimental work which has been done so far on the secondary structure will be discussed; special consideration will be given to the problems related to the mechanical and electrical strength of crystals. It also will be shown that the secondary structure, if its exists, will necessitate a generalization of the classical theory of elasticity inasmuch as it renders insufficient the representation of strains and stresses by tensors.

49. Magnetism and plasticity. FRANCIS BITTER, *Westinghouse Research Laboratories, East Pittsburgh, Pa.*—It is the purpose of this paper to show how the above phenomena may be used to throw light on each other. To a first approximation the magnetization of a ferromagnetic sample depends on four factors: the shape of the sample (including such geometrical details as cracks, grain boundaries, etc.), the magnitude of the applied field, its orientation with respect to the crystallographic axes, and the nature of the lattice distortions. If three of these factors are known, the fourth is calculable from the magnetization.

As an illustration the experiments of F. Schmidt (Dissertation Dresden 1931) are discussed. This author measures the induction in iron alloys in a constant field as a function of elongation up to the breaking point. He finds that the induction has a maximum during the elastic expansion, another when the material begins to flow, and a third just before rupture. These maxima indicate either a very peculiar dependence of induction on lattice distortion in iron (which is being further investigated theoretically), or an irregular dependence of lattice distortion on total elongation. Either conclusion would have interesting consequences. Once a satisfactory relationship between lattice distortion and magnetization is established, it becomes possible to make strain analyses with magnetic tools, even during the processes of flow. Becker and Kersten (Zeits. f. Physik, **71**, 553 (1931); **64**, 660, (1930)) have done important work in this direction.

The second part of the paper shows that the unsatisfactory magnetic properties of the outside layers of rolled samples results at least in part from the peculiar distribution of stresses and fibering along the surfaces just under the rolls.

50. Internal dissipational resistance to distortion in solids and its correlation with other physical properties. R. L. WEGEL AND H. WALTHER, *Bell Telephone Laboratories.*—Measurements of two internal dissipation coefficients expressed as equivalent viscosities have been made on samples of a variety of solids including glass, hard rubber, relatively pure metals and alloys. The resonant bar method was used, observing elongational and torsional vibrations within the frequency range 500 to 50,000 cycles per second, and at strain amplitudes 10^{-6} to 10^{-8} cm/cm. At these amplitudes *viscosity* is independent of strain amplitude but not of frequency. In two samples of glass viscosity is inversely proportional to frequency for both extension and torsion, which shows the energy loss per cycle to be independent of frequency and that according to current terminology the mechanism is *hysteretic.* On the assumption that the material is isotropic and that dissipation is associated only with shear, the usual expression for Young's modulus, generalized for vibrations to include viscosity, is $E+ie=9k(N+in)/(3k+N+in)$ in which the imaginary components in each case are products of viscosity and radial frequency. The imaginary components of each elastic coefficient are found experimentally to be very small compared with the real parts, from which it follows that

$$E/N = 2\,(1+\sigma); \qquad e/n = 4\,(1+\sigma)^2/3$$

in which σ is Poisson's ratio which has a negligible imaginary part. In the glass samples these ratios should be different but experimentally turn out to be equal, suggesting the likelihood that dissipation (nonthermodynamic) is associated with compression to the same extent as with shear. In high purity aluminum samples viscosity varies with frequency to the power $-4/3$ approximately and in nickel to the power $-1/2$ approximately. Other materials follow similar power laws lying between these limits in the frequency range investigated. This suggests that in all except perhaps glass there are within the samples, owing to their structure, relaxation mechanisms having relaxation times of the order of magnitude 10^{-3} to 10^{-5} seconds. The gross plastic relaxation time is usually minutes or hours or more. It is convenient to regard the internal dissipation coefficient of a solid as a complex viscosity, each component of which in general varies with frequency as it does in the case of a gas or a liquid.

Viscosity of solids at room temperature increases with extreme rapidity with temperature, a trend opposite to that in liquids. In steel alloys tested viscosity increases slowly with hardness (Rockwell) up to about the point of brittleness, after which the increase is enormous. During the aging process of lead alloys viscosity changes rapidly. In Pb-Ca (0.04 percent) the increase is over 300 percent, while the electrical conductivity changes by a matter of only 10 percent. In one sample over a year old the change is still in process. With the same heat treatment high purity lead decreases about 20 percent in a week or so, and then remains constant. A test of viscosity should be a useful guide in connection with the development of special alloys when better correlation with other physical properties is available.

AUTHOR INDEX TO ABSTRACTS OF NEW HAVEN MEETING

Abramson, Harold A. and Hans Mueller—No. 6

Bainbridge, K. T.—No. 42
Barton, Vola P. and Geo. A. Lindsay—No. 24
Bayliss, Noel S.—See Gibson
Beams, J. W. and John W. Flowers—No. 35
Bearden, J. A.—No. 46
Beck, F. J. and L. W. McKeehan—No. 2
Berkey, Donald K.—No. 23
Bitter, Francis—No. 49
Bramley, A.—see Swann
Brasefield, Charles J.—No. 36
Bruce, C. W.—No. 34

Cole, Kenneth S.—Nos. 8 and 9
Cooksey, D. and M. C. Henderson—No. 29
Cork, J. M.—No. 25
——— see R. B. Witmer
Cram, W. and J. G. Winans—No. 15
Cunningham, W. Peyton—No. 18
Curtis, H. J.—No. 4

Du Mond, J. W. M.—No. 45
Duncan, J. A.—No. 11

Flowers, John W.—see Beams

Gibson, G. E. and Noel S. Bayliss—No. 13
Gray, J. A.—No. 44
Green, J. B. and R. A. Loring—No. 19

Hanawalt, J. D.—No. 47
Harrington, E. L.—No. 38
Henderson, M. C.—No. 28
——— see Cooksey
Holmes, F. T.—No. 17

Joffe, Joseph—No. 12
Johnson, Thomas H.—No. 32

Kelly, M. J.—see Prescott
Kenty, Carl—No. 22
Kurie, F. N. D.—No. 30

Langer, R. M.—No. 21
Lewis, Charlton M.—No. 16
Lindsay, Geo. A.—see Barton
Loring, R. A.—see Green

McKeehan, L. W.—see Beck
Meserve, Wilbur E.—No. 41
Miller, Henry J.—No. 33
Mimno, Harry R. and P. H. Wang—No. 37
Mueller, Hans—see Abramson

O'Brien, Brian and Vernon L. Parks—No. 10

Parks, Vernon L.—see O'Brien
Prescott, C. H., Jr., and M. J. Kelly—No. 40

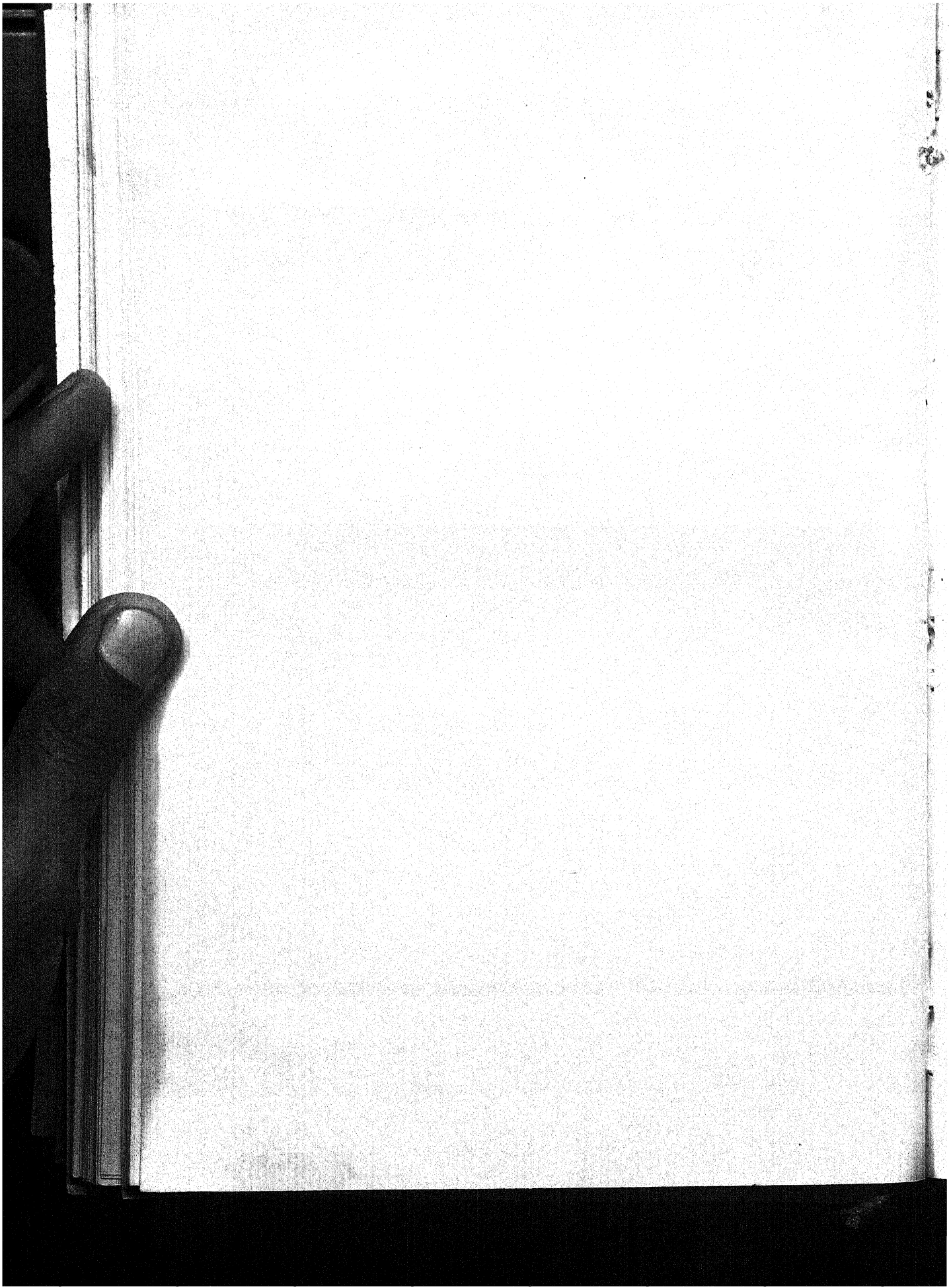
Rashevsky, N.—No. 7
Rayton, W. M.—see Wilkins

Spencer, Roy C.—No. 27
Swann, W. F. G. and A. Bramley—No. 31

Van Vleck, J. H.—No. 1
——— see Whitelaw

Walther, H.—see Wegel
Wang, P. H.—see Mimno
Waterman, A. T.—No. 39
Wegel, R. L. and H. Walther—No. 50
Whitelaw, N. G. and J. H. Van Vleck—No. 20
Wilkins, T. R. and W. M. Rayton—No. 43
Williams, J. W.—No. 5
Williams, S. R.—No. 3
Winans, J. Gibson—No. 14
——— see Cram
Witmer, R. B. and J. M. Cork—No. 26

Zwicky, F.—No. 48



Second Series *August 15, 1932* *Vol. 41, No. 4*

THE

PHYSICAL REVIEW

Energies of Cosmic-Ray Particles

By CARL D. ANDERSON
California Institute of Technology

(Received June 28, 1932)

Cloud chamber photographs of cosmic-ray tracks in a magnetic field up to 17,000 gauss are shown. On the assumption that the particles producing the tracks are travelling downward through the chamber rather than upward, particles of positive charge appear as well as electrons. From the specific ionization along the track it is concluded that the positives are protons, and are not nuclei of charge greater than unity. No evidence is uncovered demanding the introduction of a neutron for cosmic-ray phenomena. Eight examples of associated tracks are shown. Energies range from below 10^6 electron-volts to values in a few cases of the order of 10^9 electron-volts. Energy values for 70 tracks are listed. The scattering of cosmic particles in traversing a 6.0 mm lead plate is measured.

AN AUTOMATIC, vertical Wilson expansion chamber operating in a strong magnetic field up to 21,000 gauss was designed for a study of the high-energy corpuscles associated with cosmic rays. The expansion chamber itself is 15 cm in diameter and has a depth of 2 cm. The axis of the piston lies in a horizontal plane in order to effect the most favorable position for photographing the cosmic-ray tracks. The magnetic field was found by direct measurement to be homogeneous to within 10 percent throughout the volume of the chamber. Photographs are taken through a hole in the pole piece of the magnet along the lines of force, thus revealing a particle deflected by the magnetic field as an arc of a circle on the photographic film. A description of the apparatus will follow in a later publication.

A brief discussion of the results has been published jointly with Professor R. A. Millikan,[1] to whom the writer is indebted for suggesting the investigation and cooperating in planning it, and whose keen interest throughout the course of the work has been of the greatest value.

Of the 3000 photographs taken to date, 62 show cosmic-ray tracks of length sufficient for energy measurements, 19 of which are here reproduced with addition of 3 photographs taken for test purposes. The photographs are 7/10 full size. The dark back ground in several of the photographs is due to light scattered by the back wall of the expansion chamber.

[1] Millikan and Anderson, Phys. Rev. **40**, 325 (1932).

In the test photograph of Fig. 2 appear tracks in air of the secondary electrons ejected by gamma-rays from Ra. Figs. 3 and 4 show alpha-particle trajectories.

The remainder of the tracks shown, Figs. 5–23, are ascribed to cosmic rays because of their high energy. Cosmic-ray tracks are in all cases readily distinguishable from alpha-particle tracks due to the very much greater specific ionization of the latter.

Positively Charged Particles

A charged particle will be deviated by the magnetic field into an arc of a circle. The sense of rotation in the chamber as viewed in the photographs will be clockwise for a particle of negative charge, and counter-clockwise for one of positive charge. The sign of the charge can be ascertained only if the

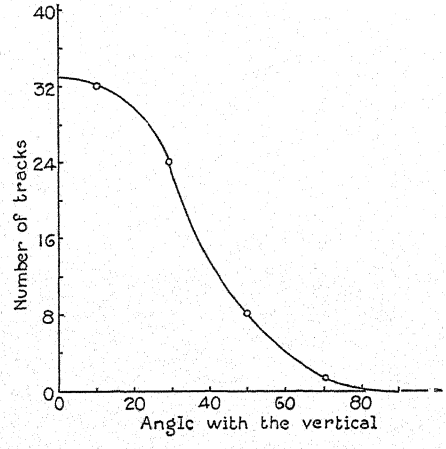


Fig. 1. The number of tracks per unit solid angle as a function of the angle with the vertical. Only those tracks are included whose curvature in the magnetic field is sufficiently small to allow a determination of the direction to be made. Therefore no electrons of energy less than 100×10^6 volts are included. This space-distribution in showing a large percentage of nearly vertical tracks differs from that reported by Skolbeltzyn.[2]

direction of motion of the particle is known. It is assumed here that the particles are traveling downward through the chamber. The small degree of scattering to be expected for high-energy particles, combined with the known fact that the rays come in from above, appears to justify this assumption. In Fig. 1 it is seen that the cosmic-ray tracks prefer the vertical direction over the horizontal indicating that backward or large angle scattering is infrequent.

In many instances on the above assumption as to the direction of motion, the tracks are deviated in a sense to indicate the presence of positively charged particles as well as electrons.

[2] Skobeltzyn, C. R. **194**, 118 (1932).

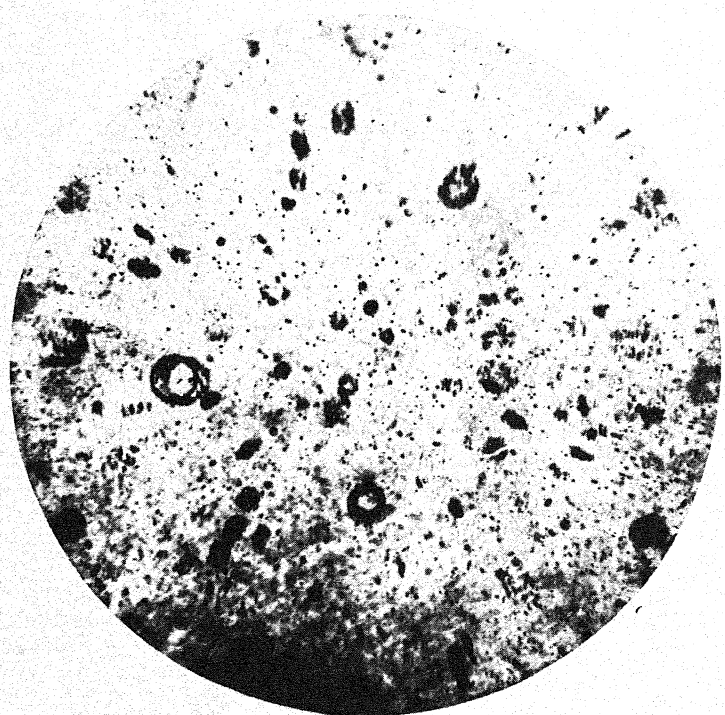


Fig. 2.

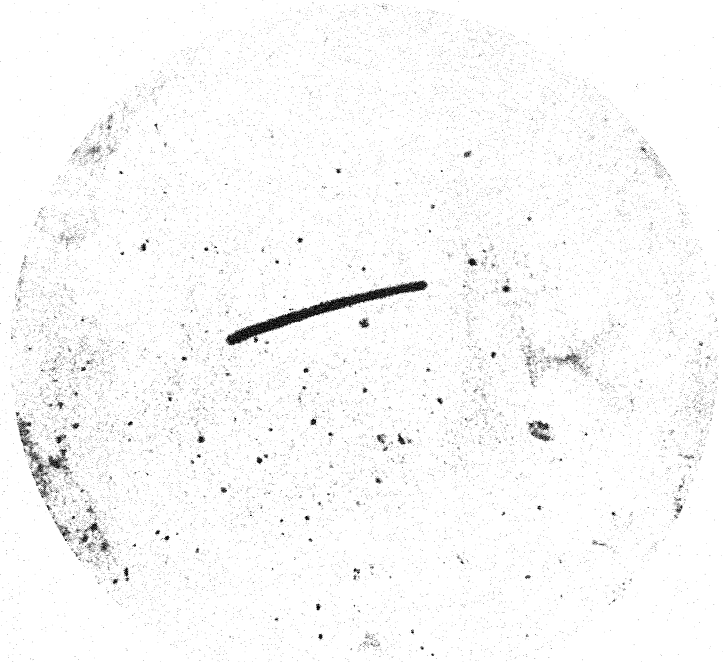


Fig. 3.

Fig. 2. 12,000 gauss. A test photograph showing tracks in air of secondary electrons ejected by gamma-rays from Ra, filtered through 2.5 cm of steel. The energies of the electrons range from 10^6 electron-volts down.

Fig. 3. 12,000 gauss. An α-particle trajectory of 3.85 cm range photographed in air.



Fig. 4.

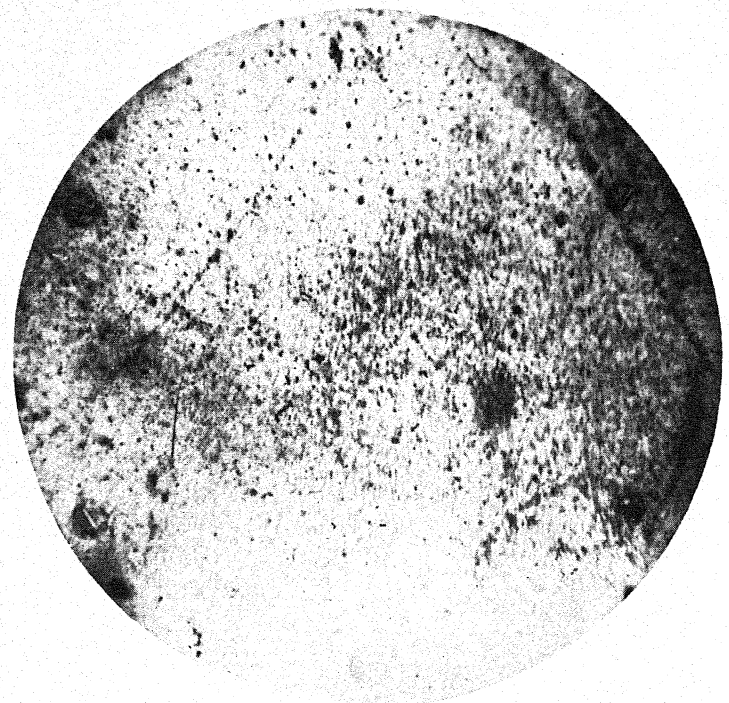


Fig. 5.

Fig. 4. 12,000 gauss. An α-particle trajectory photographed in helium, showing range of 10 cm.

Fig. 5. 17,000 gauss. A pair of associated tracks; at the left an electron of 120×10^6 volts energy, at the right a porton of 130×10^6 volts energy. Since protons and electrons, for a given velocity, have an equal specific ionization, then from the measurements of E. J. Williams and F. R. Terroux (Proc. Roy. Soc. **A126,** 300 (1929–30)) on the ionization by β-particles, the 120×10^6 volt-proton here is expected to ionize about $2\frac{1}{2}$ times as heavily as the electron.

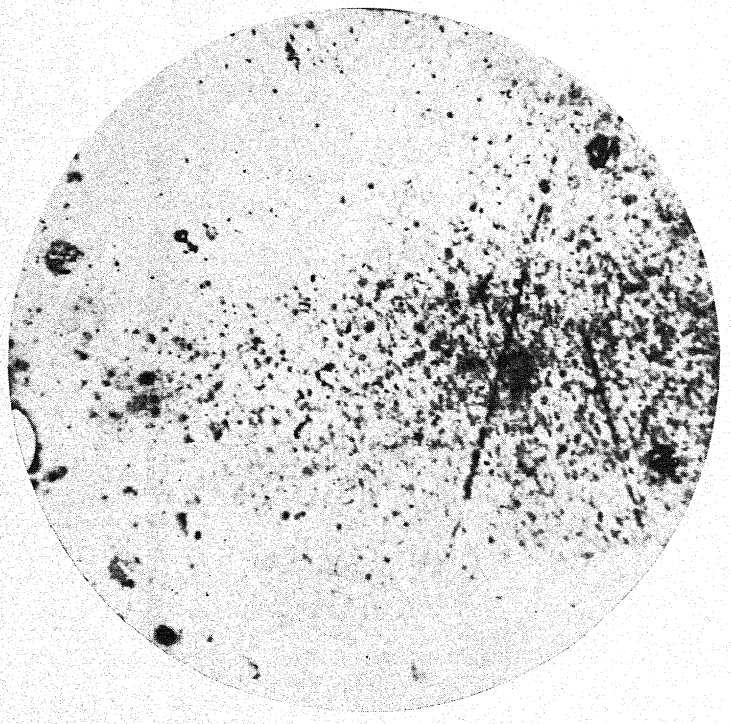


Fig. 6.



Fig. 7.

Fig. 6. 17,000 gauss. A group of three tracks; at the left an electron of 30×10^6 volts energy, at the right probably a proton of 400×10^6 volts energy. The center track, perhaps a proton of 150×10^6 volts energy, lies in a different plane from the other two, and because of its length there is a difficulty in associating it with the other two. The probability of its appearing here by chance is, however, very slight. A small scattering is noted in the center track.

Fig. 7. 12,000 gauss. A proton of 20×10^6 volts energy and an electron of about 400,000 volts energy.

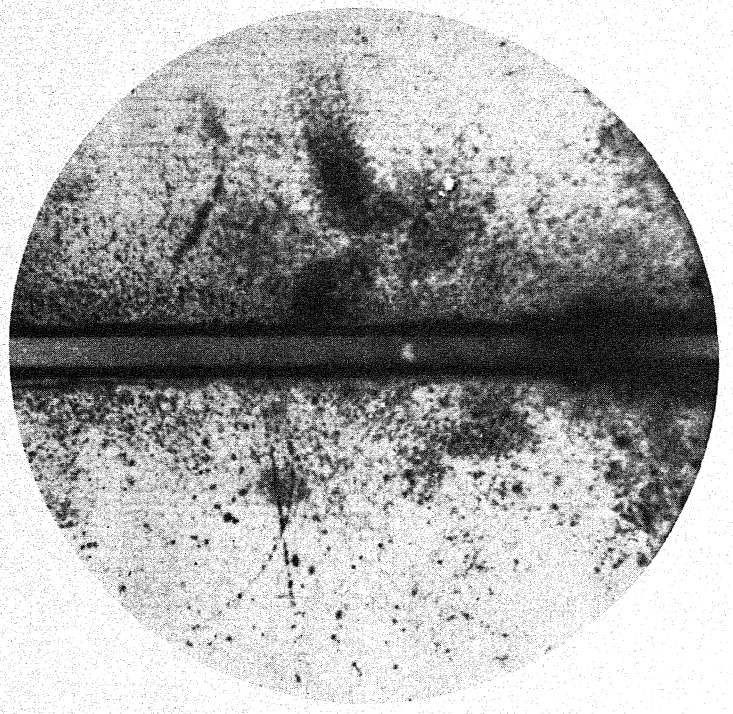


Fig. 8.

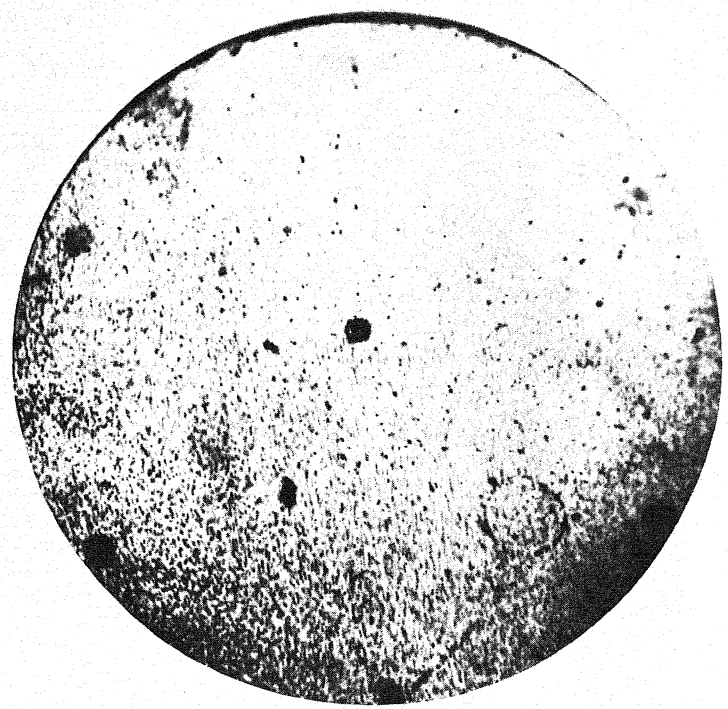


Fig. 9.

Fig. 8. 12,000 gauss. A plate of lead 6.0 mm thick extends horizontally across the chamber. Below the lead appear two tracks, one apparently a proton of about 100×10^6 volts energy, the other an electron of 11.4×10^6 volts energy which passes out through the 0.5 cm glass wall. Above the lead another electron enters through the glass wall, or perhaps the same electron after having been deflected into the chamber again by the magnetic field. It suffers a deflection of 80° upon striking the lead surface. Its energy is 8.2×10^6 volts. The assumption that the same electron re-entered the chamber above the lead is borne out by the fact that an energy loss of 3.0×10^6 volts is to be expected for an electron traversing the 0.5 cm glass wall twice as shown in the figure. The angle of divergence of the two associated tracks below the lead is 25°. (The track above the lead appears double due to a double reflection of the light before entering the camera.)

Fig. 9. 12,000 gauss. Two electrons of energy about 180×10^6 volts and 2×10^6 volts respectively.

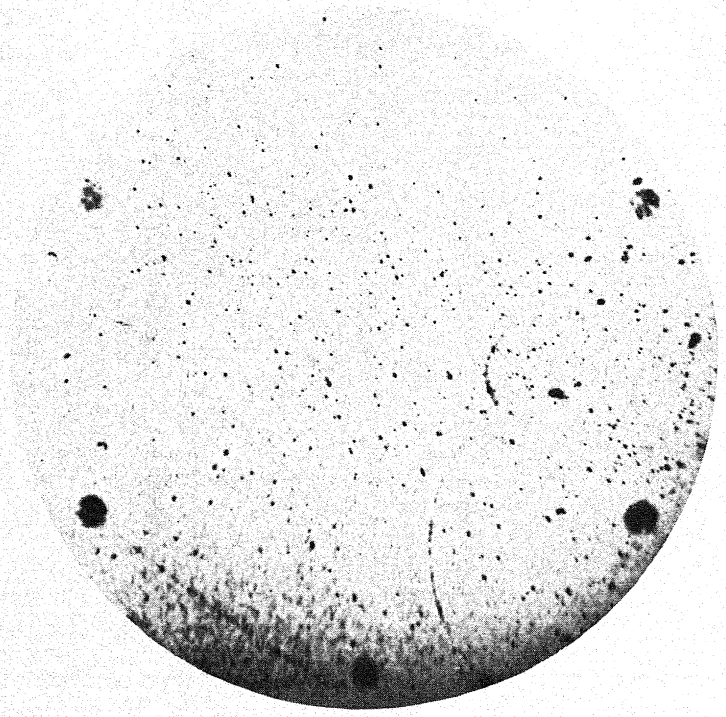


Fig. 10.

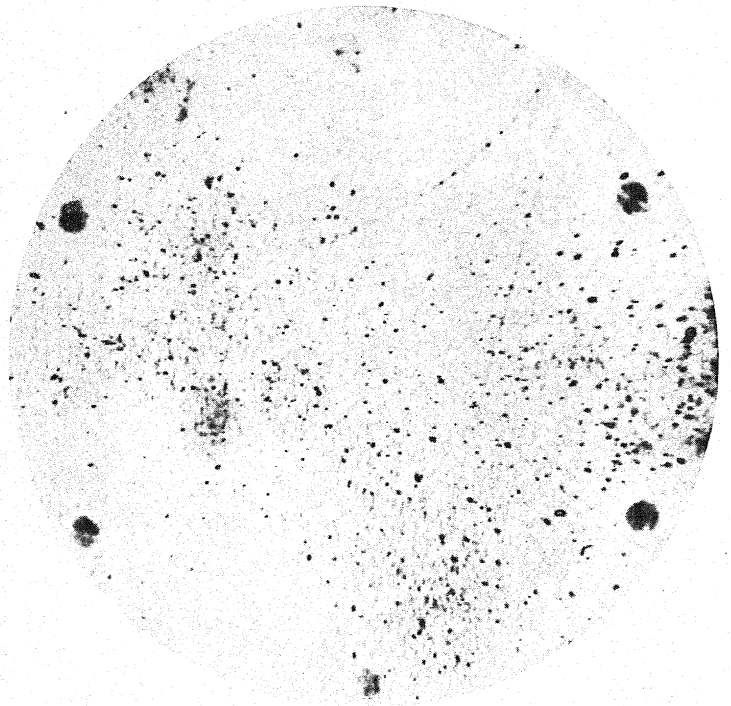


Fig. 11.

Fig. 10. 12,000 gauss. Two associated electrons moving upward through the chamber, of energy 170×10^6 volts and 11×10^6 volts respectively. A large angle scattering from the glass wall is noted.

Fig. 11. 12,000 gauss. An electron of 27×10^6 volts energy and probably a proton of 450×10^6 volts energy though the curvature here is small. A slight scattering is apparent.

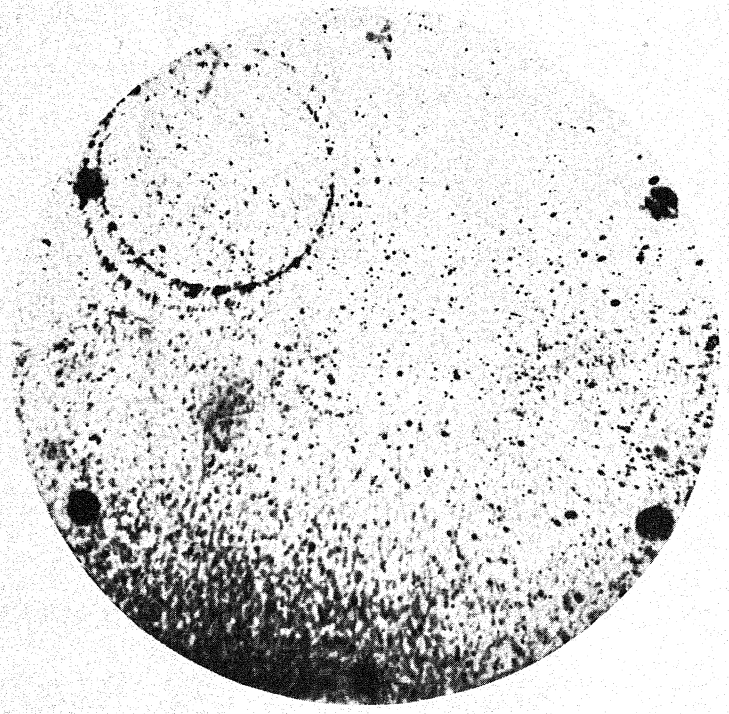


Fig. 12.

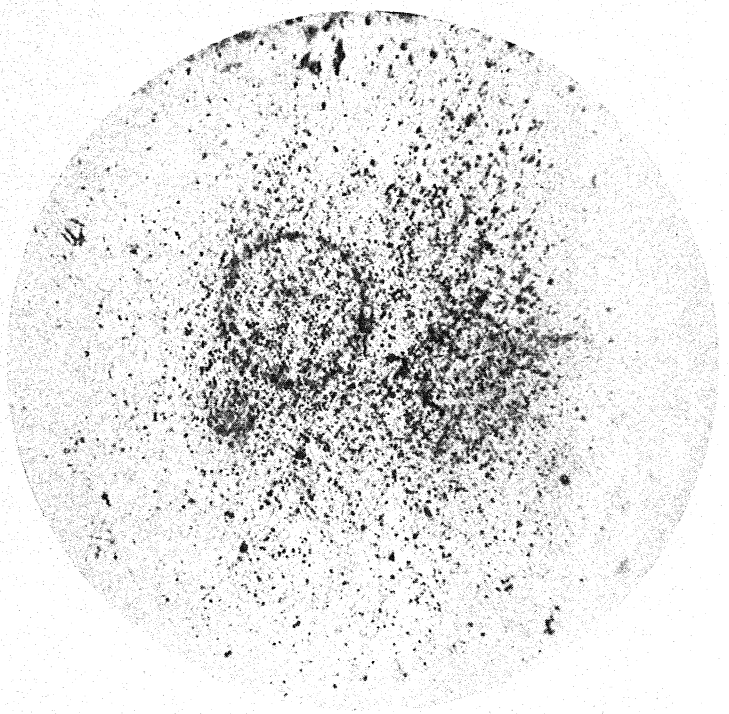


Fig. 13.

Fig. 12. 12,000 gauss. An electron of 8×10^6 volts energy. It is seen to make over $1\frac{1}{2}$ complete revolutions in the chamber. The displacement of the track from left to right is quantitatively explained by the fact that the magnetic field is 10 percent stronger at the center than at the edge of the chamber.

Fig. 13. 17,000 gauss. An electron of 7×10^6 volts energy.

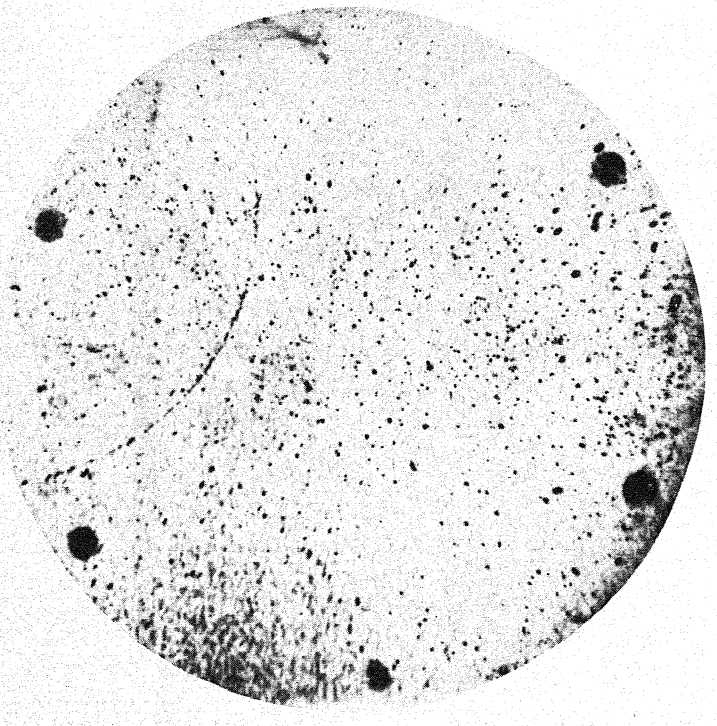


Fig. 14.

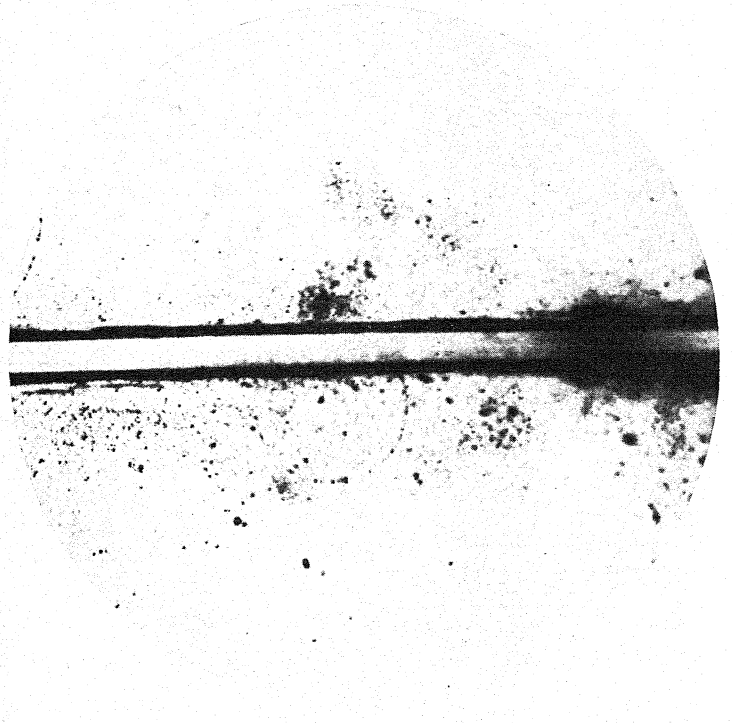


Fig. 15.

Fig. 14. 12,000 gauss. An electron of 18×10^6 volts energy.

Fig. 15. 12,000 gauss. An electron of 4.6×10^6 volts energy emerging from the lower surface of the lead. No track is seen entering the lead thus indicating a photon encounter. Above the plate to the left is another electron of 9×10^6 volts energy.

Fig. 16. 12,000 gauss. A proton of 30×10^6 volts energy.

Fig. 17. 17,000 gauss A proton of 130×10^6 volts energy, slightly scattered.

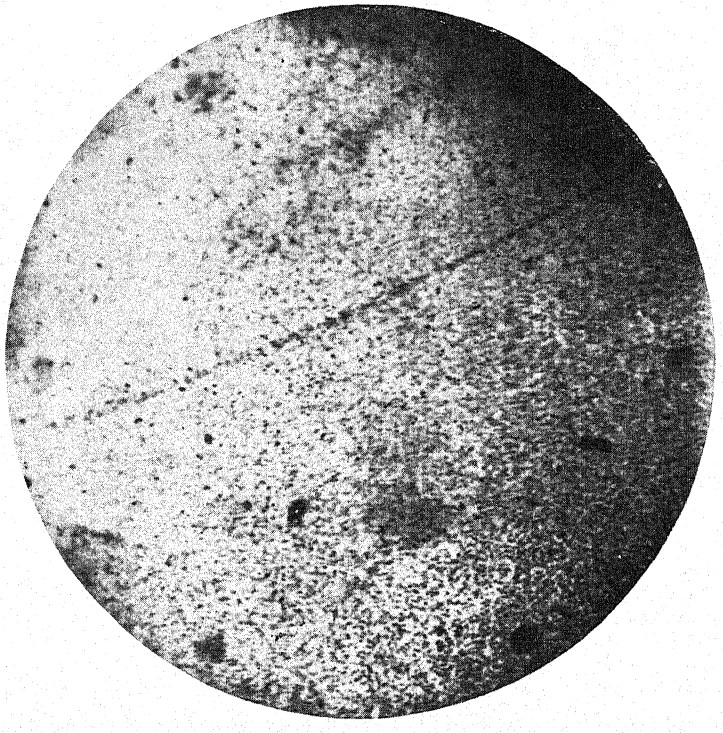


Fig. 19. 12,000 gauss. A proton of 40×10^6 volts energy.

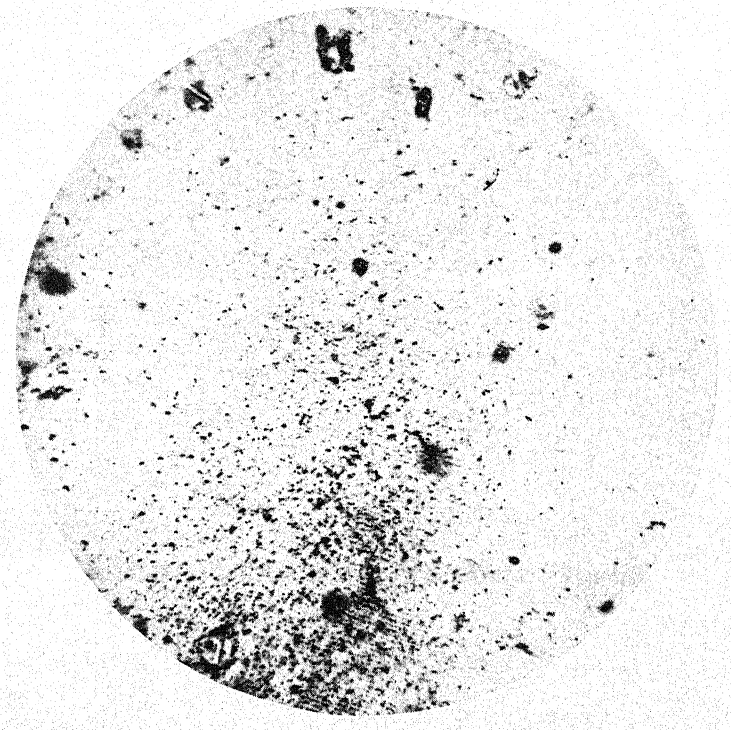


Fig. 18. 17,000 gauss. A proton of 450×10^6 volts energy.

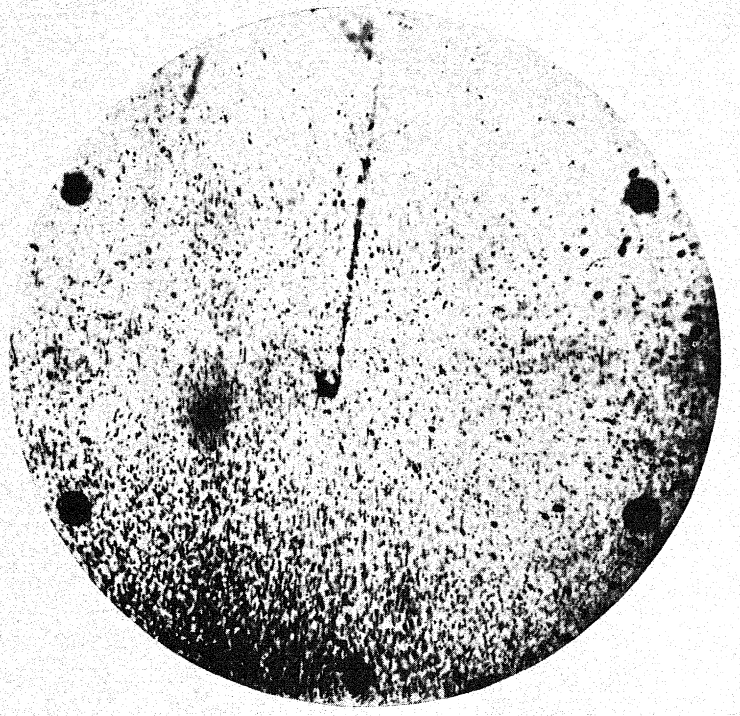


Fig. 20.

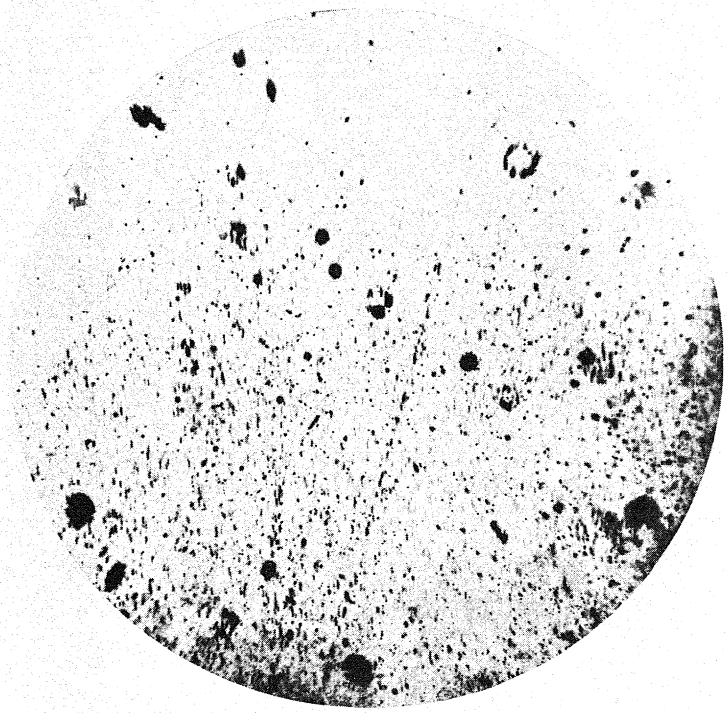


Fig. 21.

Fig. 20. 12,000 gauss. A particle of doubtful sign of charge. If an electron, the minimum energy is 600×10^6 volts, if a proton, the minimum energy is 400×10^6 volts. A close encounter with an electron takes place in the wall in which about 400,000 volts energy is transferred to the electron, shown by the small circle at the lower end of the track.

Fig. 21. 12,000 gauss. A high-energy particle of uncertain sign, photographed in helium. The energy, whether the particle is assumed to be an electron or a proton, exceeds 10^9 volts.

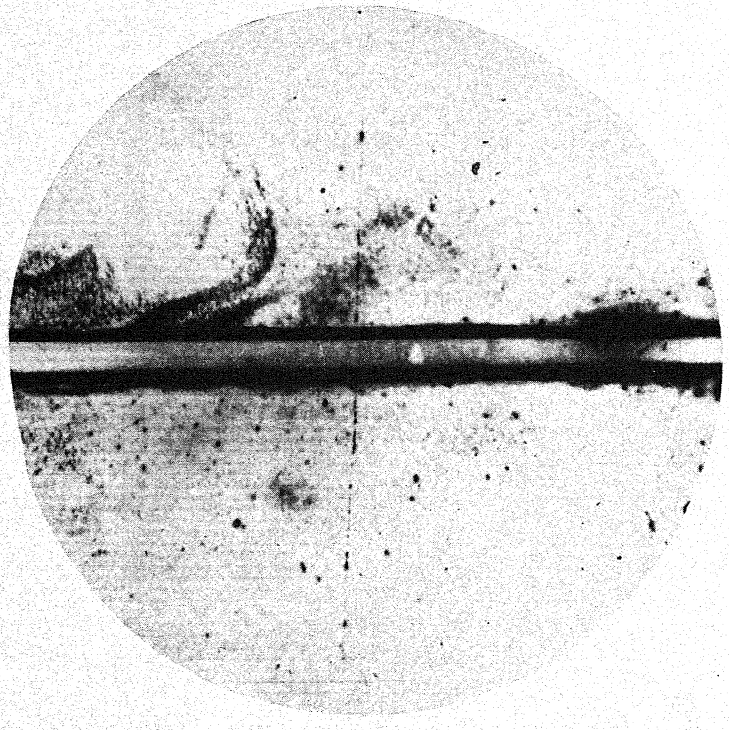


Fig. 22.

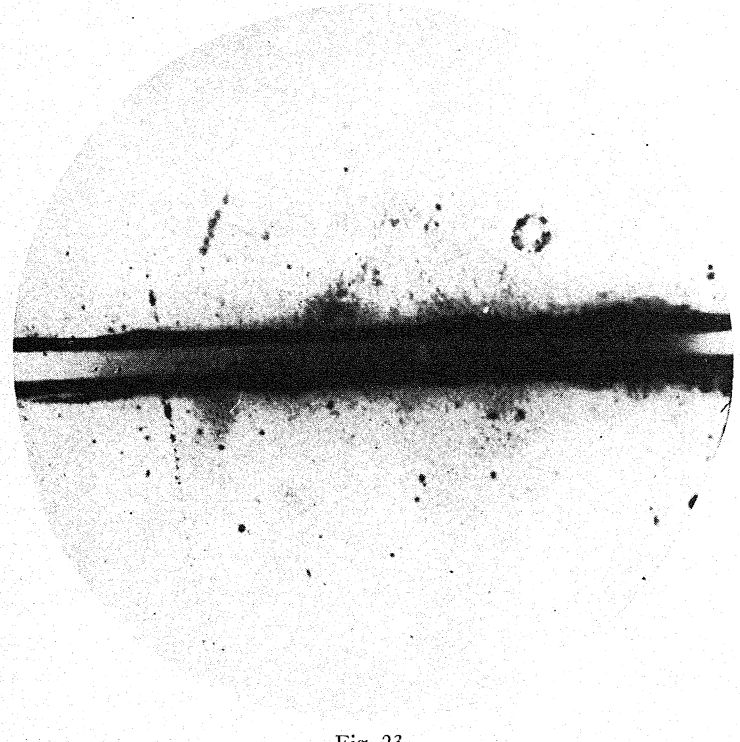


Fig. 23.

Fig. 22. 12,000 gauss. A particle of uncertain sign of charge of energy exceeding 200×10^6 volts if a proton is assumed and exceeding 600×10^6 volts if an electron is assumed. In traversing the 6.0 mm lead plate it suffers a deflection of 0.5 degrees as measured in the plane of the chamber.

Fig. 23. 12,000 gauss. A particle of uncertain sign of charge of energy exceeding 100×10^6 volts if a proton is assumed and exceeding 450×10^6 volts if an electron is assumed. The deflection in traversing the 6.0 mm lead plate is 0.8 degrees. A double scattering, however, is indicated by the sidewise displacement of the portion of the track below the lead as compared to that above the lead.

Specific Ionization

A few tracks photographed in an atmosphere of helium with 5 percent air show about 14 ion pairs per cm at standard pressure, a value close to that found for electrons of about 10^6 volts energy from Ra gamma-rays, which show about 13 ion pairs per cm in the same gas. The specific ionization for an electron remains practically independent of its energy for energies ranging from about 300,000 volts to several hundred million volts. For a given velocity, protons and electrons ionize the same, and for high energies where the velocities of both the electrons and the protons are of the order of the velocity of light it becomes impossible to distinguish electrons from protons by their ionization. Only at lower energies where the proton velocities are appreciably less than the velocity of light will protons show an appreciably greater specific ionization than electrons of the same energy. Nuclei of higher atomic charge would, for a given velocity, produce many more ions per cm, the specific ionization being to a first approximation proportional to the square of the charge on the nucleus.

The specific ionization along the tracks showing positives is in most instances not much greater than that for the electrons. It is concluded, therefor; that the positives can only be protons, and cannot themselves represent nuclei of higher atomic number than unity.

The projection of whole nuclei by the penetrating radiation produced in the bombardment of beryllium with alpha-particles has been reported in recent experiments. For the explanation of this fact, on the basis of the conservation laws, Chadwick[3] postulates a neutron. For the interpretation of the cosmic-ray effects so far observed such a neutron is not demanded on the basis of the energy-momentum arguments which apply in the experiments of Chadwick. Further work will show if the associated tracks of cosmic rays represent an effect similar, but on a higher energy scale to the disintegration tracks photographed by Feather[4] in the neutron experiments, though the frequent occurrence of electron tracks in the cosmic-ray experiments seems to indicate a different type of phenomenon.

A possibility to be borne in mind is that, in rare cases, the tracks of curvature that indicate positives might be in reality electrons scattered backwards by the material underneath the chamber and are traversing it from bottom to top. Precise data on the specific ionization of the low-energy positives will distinguish, however, between downward positives and upward negatives.

Associated Tracks

A well-known characteristic of the cosmic tracks is their tendency to occur in groups.[5,6,7] Of the 55 photographs showing cosmic tracks, 7 show double tracks and 1 shows three tracks.

[3] Chadwick, Nature **129**, 312 (1932).
[4] Feather, Proc. Roy. Soc. **A136**, 709 (1932).
[5] Skobelzyn, Zeits. f. Physik **54**, 686 (1929).
[6] Auger and Skobelzyn, C. R. **189**, 55 (1929).
[7] Locher, Phys. Rev. **39**, 883 (1932).

In general, for paired tracks, the energy of one of the associated pair is considerably less than that of the other, in some instances 10^6 volts and less. One of the associated pair is also in all cases definitely an electron.

The associated tracks have been assumed to be due to the simultaneous ejection by a photon of two particles from an atomic nucleus.[1]

Another effect which may give rise to associated tracks is a close encounter between a cosmic particle and an electron. Fig. 20 is an example of an encounter of this type, the encounter taking place in the wall. For such an encounter where an electron of high energy (energy$\gg mc^2$) produces a secondary track, giving to the secondary electron an energy E, the angle θ between the primary and secondary electron is given by $\tan\theta=(2mc^2/E)^{1/2}$. The two tracks of Fig. 10 might represent an effect of this type, the relation above being satisfied within experimental uncertainty. The possibility also exists that a proton may by direct impact give to an electron energy sufficient to produce a secondary track. It is pointed out, however, that on the basis of the conservation laws, due to the relatively large proper mass of a proton, it is difficult to explain the associated tracks as a binary collision between a proton and an electron because of the prohibitively high energy which would have to be assigned to the proton in this case to account for the electron energies observed. To produce an electron of 100×10^6 volts would require a proton energy of 10^{10} volts. In both Figs. 8 and 11 one of the associated pair has a curvature to indicate a positive, and therefore, if these curvatures are correctly measured these cases cannot represent such encounters. Even if these are incorrectly measured and are in reality electrons then for Fig. 11 the value of θ calculated for an energy of 27×10^6 volts is 11°, which would agree with the angle indicated by the photograph within experimental uncertainty. But for the case of Fig. 8, the calculated value of 17° and the measured value of 25° are in conflict. Again the associated pair of Fig. 5 can not possibly be interpreted as due to a binary collision. The hypothesis of simple binary collisions is inadequate to account for all the associated tracks. Furthermore, encounters of this type in which a large amount of energy is transferred to an electron are not to be expected frequently, and the abundance of associated tracks coupled with the fact that positives as well as electrons appear, is strong evidence that the associated tracks represent a quite different phenomenon, i.e., the ejection of two particles from a nucleus.

Scattering of the Cosmic Particles

Certain of the tracks, Figs. 11 and 17, show sudden though very small deflections identical in appearance with the deflections observed in alpha-particle tracks due to nuclear encounters, but which are to be expected in the gas only rarely on the basis of the present scattering laws for high energy electrons or protons. The deflections in some instances represent scattering from the walls of the chamber. An example of large angle scattering from a lead surface is shown in Fig. 8. In Fig. 10 another instance of large angle scattering is shown, the electron being scattered by the glass wall of the chamber.

Experiments are now in progress to study the scattering of cosmic particles in lead. Figs. 22 and 23 show particles traversing 6.0 mm of lead, the angle of scattering being in each case readily measurable.

Energies

The energies of the cosmic particles as determined from the radii of curvature of the tracks range from values below 10^6 electron-volts to, in a few cases, values of the order of 10^9 electron-volts. The greater part of them, however, have energies below 500×10^6 volts.

Precautions were taken to reduce to a minimum the effects of air movements in the expansion chamber which tend to distort the tracks. The energies of the higher energy tracks, i.e., protons of energies of the order of 500×10^6 volts and electrons of the order of 10^9 volts, can be determined only roughly due to the small curvature in the magnetic field.

Table I. *Energy distribution.*

Number of electrons	Number of protons	Energy range in electron-volts
2	0	Below 10^6
4	0	From 10^6 to 10×10^6
6	1	" 10×10^6 to 20×10^6
4	1	" 20×10^6 to 30×10^6
3	3	" 30×10^6 to 50×10^6
1	3	" 50×10^6 to 100×10^6
5	5	" 100×10^6 to 200×10^6
4	2	" 200×10^6 to 300×10^6
5	2	" 300×10^6 to 400×10^6
1	4	" 400×10^6 to 500×10^6
3	3 {	" 500×10^6 to 700×10^6
2		" 700×10^6 to 1000×10^6

Table II. *Energies of the associated tracks in electron-volts.*

Group 1	Proton	130×10^6	See Fig. 5
	Electron	120×10^6	
	Electron	30×10^6	
Group 2	Probably proton	150×10^6	See Fig. 6
	Probably proton	400×10^6	
Group 3	Probably proton	450×10^5	See Fig. 11
	Electron	27×10^6	
Group 4	Proton	20×10^6	See Fig. 7
	Electron	4×10^5	
Group 5	Probably proton	$\sim100\times10^6$	See Fig. 8
	Electron	11×10^6	
Group 6	Electron	170×10^6	See Fig. 10
	Electron	11×10^6	
Group 7	Electron	180×10^6	See Fig. 9
	Electron	2×10^6	
Group 8	Electron	4×10^5	See Fig. 20
	Electron or proton	$\sim400\times10^6$	

Table I gives the distribution in energy of the electrons and protons. The number of protons and the number of electrons in various energy ranges are listed. It is to be noted that there may be many more electrons in the energy range below 10^6 volts than those listed. Since this includes the energy region of radio-activity, it is impossible to distinguish between electrons from radio-active sources and low-energy electrons due to cosmic rays. Therefore only those very low-energy electrons which are associated with other cosmic-ray tracks, and are definitely to be attributed to cosmic rays are listed in Table I.

There are in addition 5 tracks whose sign of charge is doubtful due to the lack of an appreciable curvature in the magnetic field. For these it is possible only to assign a lower limit to the energy, i.e., 450×10^6 volts on the supposition that they are electrons and 100×10^6 volts on the supposition that they are protons. There is one track, Fig. 21 to which an energy in excess of 10^9 volts must be assigned whether it is assumed a proton or electron.

In Table II are given the energies of the 8 groups of associated tracks.

I wish to thank Mr. Seth H. Neddermeyer for assistance in the measurement of the photographs.

Scattering of X-Rays from Solids

By ALLEN W. COVEN
Ryerson Laboratory, The University of Chicago

(Received July 5, 1932)

The total scattering of the $K\alpha$ radiation of molybdenum from powdered crystals of KCl, NaF, and MgO has been observed with an ionization chamber whose window subtended several degrees of angle at the scatterers. The scattering from NaF and MgO was found to be approximately the same as that from neon. The scattering from KCl was found to be approximately the same as that from argon. The intensities of the diffracted portion of the scattered rays from the crystals have been calculated and found to be distributed along the F^2/Z curves, thus agreeing with Jauncey's relation between gas and crystal scattering, $S_g = S_c + F^2/Z$. The sums of the diffracted intensities plus diffuse intensities have been found to follow the gas scattering curves, in agreement with Compton's formula for the scattering from a monatomic gas, $S_g = (f^2/Z) + (1 - f^2/Z^2)/R^3$. The method of measurement may be used to determine values of the structure factor for the atom at rest.

I. INTRODUCTION

A. H. COMPTON[1] has shown that the intensity of x-rays scattered from a monatomic gas or vapor is given by

$$S_g = f^2/Z + (1 - f^2/Z^2)/R^3 \tag{1}$$

where S_g is the scattered intensity relative to the value given by the Thomson theory of scattering.[2] f is an average atomic structure factor for the atom at rest, Z is the number of electrons in the atom, and $1/R^3$ is the Breit-Dirac factor. R has the value $1 + (h/mc\lambda)\text{vers}\,\phi$, where ϕ is the angle of scattering. G. E. M. Jauncey[3] has developed a theory of the scattering of x-rays from solids in which Eq. (1) is included as a factor in the scattered intensity. In the special case of scattering from a simple cubic crystal consisting of atoms of one kind Jauncey's theory gives[4]

$$S_c = \frac{f^2 - F^2}{Z} + \frac{1 - f^2/z^2}{R^3} = S_g - \frac{F^2}{Z} \tag{2}$$

where F is the atomic structure factor at the temperature of the crystal. Eq. (2) connects the diffuse scattering from a crystal with the scattering from a monatomic gas of the same kind of atoms as those in the crystal. The term F^2/Z represents a correction for the effect of interference between atoms in the crystal.

The energy per second emitted in a diffraction line by one of the particles in an aggregation of powdered crystals is given by[5]

[1] A. H. Compton, Phys. Rev. **35**, 925 (1930).
[2] J. J. Thomson, *Conduction of Electricity through Gases*, 2d Ed., p. 326.
[3] G. E. M. Jauncey, Phys. Rev. **37**, 1193 (1931).
[4] G. E. M. Jauncey and G. G. Harvey, Phys. Rev. **37**, 1203 (1931).
[5] A. H. Compton, *X-Rays and Electrons*, p. 130.

$$P = \frac{In^2\lambda^3 pF'^2 e^4(1 + \cos^2 2\theta)dV}{8(\sin\theta)m^2c^4}, \tag{3}$$

where θ is the glancing angle of incidence on a crystal plane, p is the number of planes, F' is the structure factor for the crystal, n is the number of atoms per cm^3, I is the intensity of the primary beam, and dV is the volume of the particle. If the diffracted rays are measured at a distance r with an ionization chamber whose window has a length L which is short compared to $r \sin\theta$, then the energy per second entering the ionization chamber is

$$P_s = PL/2\pi r \sin 2\theta.$$

Thomson's classical theory[2] gives the intensity scattered from the $nZdV$ electrons in one of the powdered crystal particles to be

$$I_s = \frac{InZe^4(1 + \cos^2\phi)dV}{2m^2c^4r^2}, \tag{4}$$

and therefore the energy entering the ionization chamber is equal to AI_s, where A is the area of the chamber window. To get the energy per second in a diffraction line in the units corresponding to S_u and S_c of Eqs. (1) and (2) we take the ratio of P_s to AI_s. We then have

$$\frac{P_s}{AI_s} = \frac{n\lambda^3 pLrF'^2}{8\pi ZA \sin\theta \sin 2\theta}.$$

But the atomic structure factor F in Eq. (2) has a value $F'/2$ for a simple cubic crystal consisting of atoms of one kind. Substituting $2F$ for F' in the above expression, we then have for the energy in a powdered crystal line where the crystals are of the simple cubic type and contain similar atoms

$$\frac{P_s}{AI_s} = \frac{n\lambda^3 pLr}{2\pi A \sin\theta \sin 2\theta} \cdot \frac{F^2}{Z}. \tag{5}$$

If the ionization chamber window is of such width as to subtend several degrees of angle at the scatterer, there will be several diffraction lines entering the chamber at large angles of scattering where the lines are close together, and probably more than one line at each of the smaller scattering angles if the scattering crystals have a grating constant that is not too small. The total diffracted energy entering the chamber is then equal to the sum of the energies in the lines and may be expressed as

$$S_d' = \sum\left(\frac{n\lambda^3 pLr}{2\pi A \sin\theta \sin 2\theta} \cdot \frac{F^2}{Z}\right). \tag{6}$$

The total scattered intensity entering the ionization chamber is the sum of the diffuse and the diffracted intensities. Using previously measured values of F, Eq. (6) may be used to calculate the diffracted portion of the scattering and this portion may then be added to measured values of the diffuse scattering to get values of the total scattered intensitites. Values of S_d' are in terms

of energy so the corresponding quantity representing the diffuse scattering will be represented by the area under the curve of diffuse intensity between the limits of the $(\sin \phi/2)/\lambda$ ordinate corresponding to the angle subtended by the ionization chamber window. Hence we may divide each value of S_d' by a value dx, which is the length of the ordinate corresponding to the range of scattering angle subtended by the ionization chamber window and add the quotient to the intensity of diffuse scattering at the value of the ordinate corresponding to the position of the middle of the window. The total scattered intensity is thus represented by

$$S_t = S_c + S_d'/dx = S_c + S_d, \tag{7}$$

where S_d is equivalent to S_d'/dx. If the total scattering from a powdered crystal aggregation is measured with an ionization chamber whose window subtends several degrees of angle at the scatterer, a distribution of intensity equivalent to that given by Eq. (1) is observed.

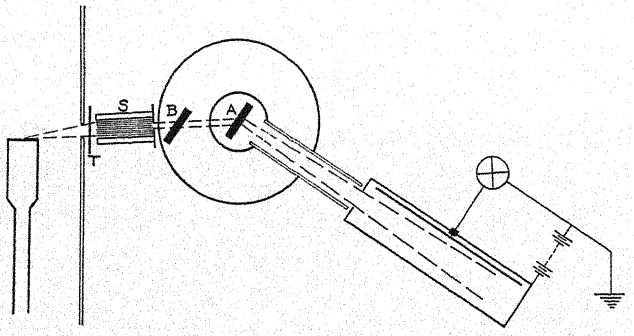


Fig. 1. Arrangement of apparatus.

The author has observed the scattered intensities from powdered crystals of KCl, NaF, and MgO, using an ionization chamber whose window subtended approximately 5 degrees of angle at the scattering plates. The observed intensities from KCl are in close agreement with the values obtained by Wollan[6] for argon and the intensities from NaF and MgO agree with Wollan's values for neon.[6] Wollan's values are in agreement with values calculated from Eq. (1), using structure factors calculated from the Hartree charge distribution.

II. Apparatus and Procedure

Fig. 1 shows the arrangement of the apparatus. A molybdenum target x-ray tube was immersed in oil in a lead box placed close to the axis of an ionization spectrometer. The scatterers were mounted directly over the axis on the spectrometer table. The x-ray tube was operated at a potential of approximately 40 k.v. and a current of 35 m.a. A Compton electrometer indicated the ionization currents. A Soller slit, S, collimated the primary beam. The use of this slit limited the divergence of the primary rays to less than a

[6] E. O. Wollan, Phys. Rev. 37, 862 (1931).

half-degree of angle. The scattered rays passed through a bronze tube 2.7 cm in diameter, 14 cm long, with 1.5 mm walls. This tube prevented stray radiation from entering the ionization chamber with the scattered rays. The window of the chamber was 1.67 cm high and 1.64 cm wide. The distance from the window to the axis of the spectrometer was 18.05 cm. The chamber contained methyl bromide vapor at atmospheric pressure.

Balanced filters of ZrO_2 and SrO were placed at T in the primary beam. These separated the $K\alpha$ lines from the general radiation as shown in Fig. 2, where the difference in the transmission by the ZrO_2 and the SrO is re-

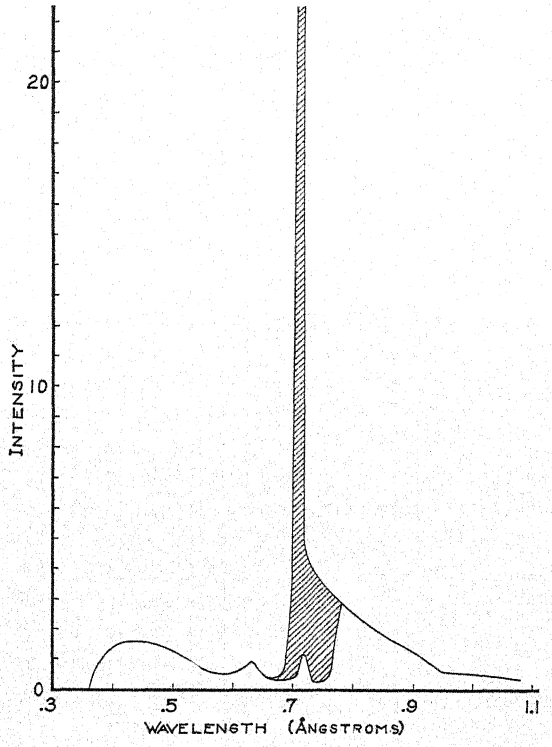


Fig. 2. Transmission through balanced filters.

presented by the shaded portion. This is the portion that was used as the primary radiation in all of the measurements of scattered intensities.

The scattering from the crystalline powders and from paraffin was observed throughout an angular range of from 20° to 100°. The scattering from each of the powdered crystal plates was compared with the scattering from a similar plate of paraffin. Since the scattering from paraffin can be calculated to a close approximation, the values of the scattered intensities for each of the other materials could be put on an absolute scale. For the $K\alpha$ radiation of molybdenum Woo[7] has found that the ratio of the incoherent to coherent radiation scattered from paraffin at 90° is 4.69. If it is assumed that for

[7] Y. H. Woo, Phys. Rev. 27, 119 (1926).

paraffin at 90° the effect of constructive interference is negligible, the total scattering can be obtained from classical theory, if the incoherent portion is corrected by the Breit-Dirac factor. Thus, at 90°, the scattering from paraffin is given by

$$S_t = 0.825(R^{-3}) + 0.175 = 0.93.$$

From this value and the experimental measurements of relative intensities at various angles, S_t for paraffin was found to be equal to unity in the range from 30° to 70°. The comparisons of the powdered crystal intensities with the paraffin intensity were all made at 60°.

The pure, finely ground, powdered crystals were pressed into brass rings which fitted into holders that could be conveniently mounted on the spectrometer table. The paraffin was melted into a similar ring so that it could be quickly substituted for any one of the powdered crystal plates.

Potassium chloride

The scattering from a thin plate of the KCl powder 2.5 cm in diameter and having a mass per unit area of 0.141 g/cm² was compared with the scattering from the paraffin which was also 2.5 cm in diameter and had a mass per unit area of 0.275 g/cm². The arrangement of the two was as shown in Fig. 1, where one scatterer is in the primary beam at A and the other in the primary beam at B, each plate being set so that the normal to its surface made an angle of 30° with the primary beam. The ionization chamber was set at the scattering angle of 60°. The intensity with the KCl at A and the paraffin at B was first observed. Then the intensity with the paraffin at A and the KCl at B was observed. The ratio of the first intensity to the second multiplied into the ratio of the masses per unit area and the ratio of the values of Z/W for the samples then gave the value of S_t for KCl at 60°. Z is atomic number and W is atomic weight. The paraffin was assumed to be equivalent to a molecule of $C_{24}H_{50}$, for which Z/W has a value of 0.5. No correction for absorption of the x-rays in the samples was necessary since by this method of comparison the portion of the primary rays transmitted by the scatterer at A does not change when the scatterers are interchanged in their positions at A and B. The intensity of the scattered rays entering the ionization chamber from each substance was of the same order of magnitude by this method, even though the absorption in the KCl was much greater than that in the paraffin.

Relative values of the scattering from KCl were observed by reflections from a plate of the powdered crystals 4.5 cm in diameter and thick enough to absorb completely the $K\alpha$-rays of molybdenum. The scatterer was always set so that the face of the crystal plate was at an angle equal to half the scattering angle. Thus the absorption of the primary and scattered rays was approximately the same in the thickness of the plate penetrated, and proportional to the reciprocal of the absorption coefficient. For the relative values, therefore, no absorption correction was necessary. The relative values of S_t were given by the relative intensities multiplied into the ratios of the values of the polarization factor, $1+\cos^2\phi$.

Sodium fluoride

The intensities from paraffin and the NaF plate, which had a mass per unit area of 0.470 g/cm^2, were of the same order of magnitude and the comparison between them at 60° was made without resorting to the method used for KCl of placing both samples in the primary beam. When a scatterer is at A and none at B (Fig. 1), S_t is proportional to $(W/mZ)(I_\phi/i_\phi)(1+\cos^2\phi)^{-1}$, where Z is atomic number, W is atomic weight, m is mass per unit area, I_ϕ is the scattered intensity, and i_ϕ is the portion of the primary rays penetrating the scatterer. i_ϕ is equal to $Ie^{-m\mu/\rho\cos(\phi/2)}$ where I is the incident ray intensity and μ/ρ is the mass absorption coefficient of the incident rays in the scatterer. The absorption of the Mo $K\alpha$ rays in the paraffin and in the NaF plate was measured with the Compton double crystal x-ray spectrometer.[8] μ/ρ for paraffin was found to have a value of 0.52 and for NaF 2.63. Relative intensities for NaF at various scattering angles were measured from the same scatterer that was compared with paraffin.

Magnesium oxide

The MgO plate that was compared with paraffin at 60° had a mass per unit area of 0.331 g/cm.^{2} The intensity comparison was made exactly as it was for NaF and paraffin. μ/ρ for MgO was calculated to be 3.18 from the values of the atomic absorption coefficients for Mg and O given on page 182 of Compton's *X-Rays and Electrons*. The relative intensities were measured from reflections from a thick plate of the powdered MgO crystals as was done for KCl.

III. Experimental Results

Froman[9] and Harvey[10] have respectively measured the intensities of the lines from powdered KCl and the diffuse scattering from a single crystal of KCl. Froman's values of F for KCl have been used to calculate values of S_d for values of ϕ between 15° and 90°, each value extending over a range of 5° and differing from adjacent values by 5°. Thus for each value of ϕ the energy in all the diffraction lines included in the 5° range made up the value of S_d. The sum of the S_d values would represent the sum of the energy in the diffraction lines between the minimum and maximum values of ϕ, 15° and 90°. At each value of ϕ the value of S_d was added to the value of S_c as shown in Fig. 3. S_g is the theoretical curve for argon as calculated by Hartree by his method of self-consistent fields. The data for the curve were taken from a paper by Herzog.[11] His values for the incoherent radiation have been reduced by the Breit-Dirac factor before being added to the values of the coherent radiation to get the values of S_g from which the curve was drawn. The F^2/Z curve was drawn from Froman's data. The circles are values of S_d and the crosses are the values of S_c+S_d. The author's experimental values of S_t, as given in column 3 of Table I, are plotted as dots.

[8] A. H. Compton, Rev. Sci. Inst. **2**, 365 (1931).
[9] D. K. Froman, Phys. Rev. **36**, 1330 (1930).
[10] G. G. Harvey, Phys. Rev. **38**, 593 (1931).
[11] G. Herzog, Zeits. f. Physik **70**, 583 (1931).

Jauncey and Williams[12] have recently measured the diffuse scattering from a single crystal of NaF. Their values were kindly sent to the author by Professor G. E. M. Jauncey and have been used together with the F values

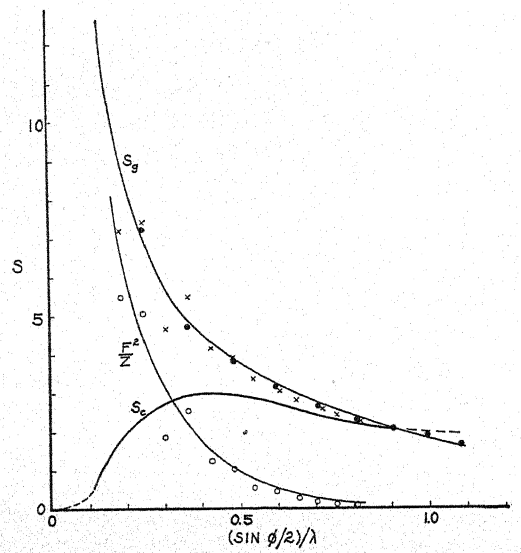


Fig. 3. Scattering from KCl. Dots S_t experimental, circles S_d, crosses S_c+S_d, S_g from argon.

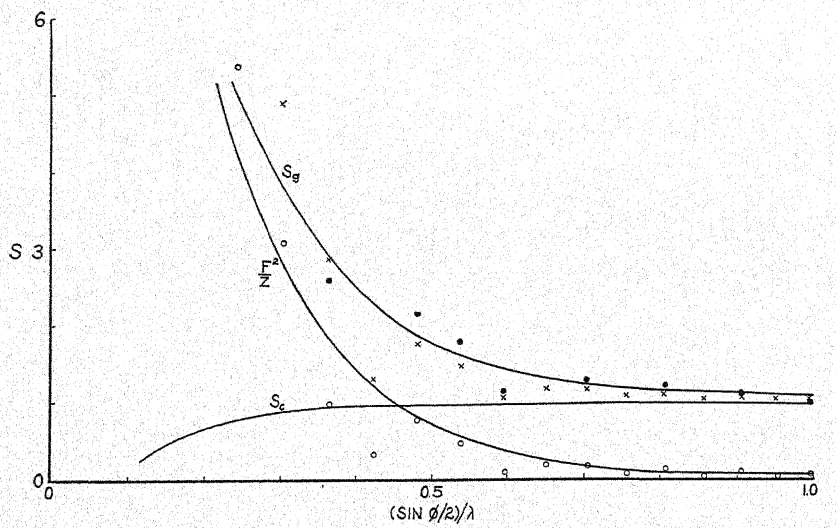


Fig. 4. Scattering from NaF. Dots S_t experimental, circles S_d, crosses S_c+S_d, S_g from neon.

of Havighurst[13] to calculate values of S_c+S_d as shown by the crosses in Fig. 4. The F^2/Z curve is also from the data of Havighurst. The S_g curve for neon is again from Herzog's values.[11] The author's experimental values of S_t for

[12] G. E. M. Jauncey and P. S. Williams, Phys. Rev. **41**, 127 (1932).
[13] R. J. Havighurst, Phys. Rev. **29**, 1 (1927).

NaF are shown by the dots. These values appear in column 4 of Table I. Values of S_d are shown by the circles.

Fig. 5 shows the results for MgO. The author is grateful to Dr. Wollan for the values of diffuse scattering from a single crystal of MgO which he has recently measured but not yet published. These have been used to draw the S_c curve. Values of S_d as shown by the circles were calculated from Wollan's[14] values of F for powdered MgO crystals. The F^2/Z curve is also drawn from Wollan's values. Values of S_c+S_d are shown by the crosses and the author's experimental values of S_t by the dots. These are the values appearing in column 5 of Table I. The S_g curve for neon is the same as the one in Fig. 4.

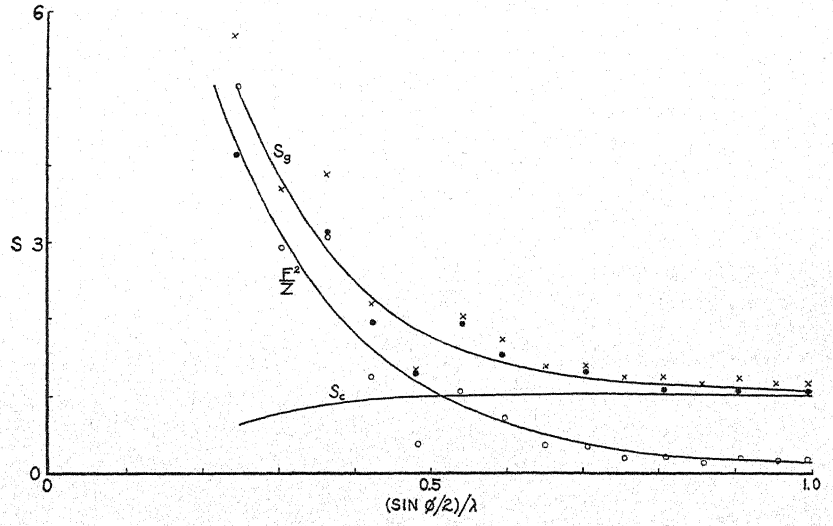


Fig. 5. Scattering from MgO. Dots S_t experimental, circles S_d, crosses S_c+S_d, S_g from neon.

The values of the total scattering, S_t, observed by the author for powdered crystals of KCl, NaF, and MgO and for paraffin are all shown in Fig. 6 together with the theoretical curves for neon and argon. The crosses indicate the values for KCl, the circles are the NaF values, the large dots are for MgO, and the small dots for paraffin.

TABLE I. *Values of S_t for paraffin and powdered crystals.*

Angle	(sin $\phi/2)/\lambda$	KCl	NaF	MgO	Paraffin
20°	0.245	7.25		4.16	1.22
30	0.365	4.77	2.59	3.13	1.00
35	0.423			1.96	
40	0.482	3.83	2.15	1.30	1.00
45	0.539		1.78	1.95	
50	0.596	3.14	1.13	1.55	1.00
60	0.705	2.65	1.28	1.31	1.00
70	0.808	2.28	1.20	1.10	1.00
80	0.906	2.01	1.10	1.09	0.93
90	0.996	1.85	1.00	1.06	0.93
100	1.082	1.80			0.89

[14] E. O. Wollan, Phys. Rev. **35**, 1019 (1930).

IV. Discussion

Fig. 6 shows that the measured values of the total scattering from KCl are in excellent agreement with the theoretical argon curve. Wollan's experimental values of the scattering from argon are slightly higher than the theoretical curve at values of $(\sin \phi/2)/\lambda$ below 0.7 and above 0.9. Hence the agreement between the author's values of the scattering from KCl and the scattering from argon is better for the theoretical values than for the experimental values. The experimental values of the total scattering from NaF and MgO are in good agreement with the theoretical neon curve for the higher values of $(\sin \phi/2)/\lambda$. At the lower values of $(\sin \phi/2)/\lambda$ the points do not lie

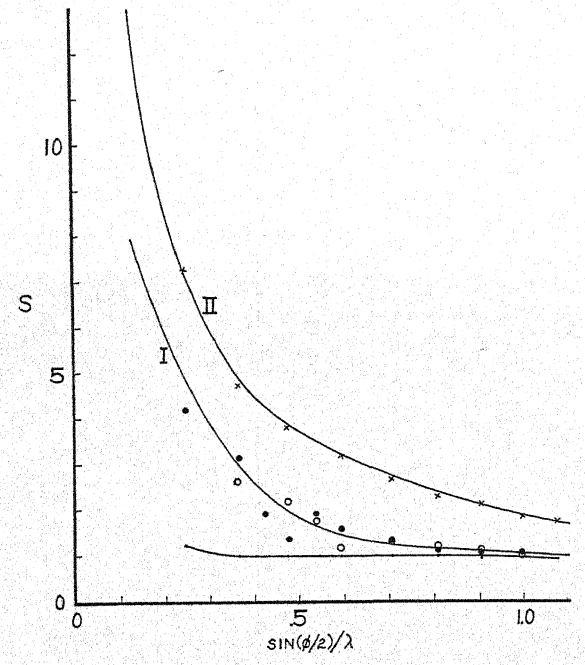


Fig. 6. Values of S_t. Crosses KCl, circles NaF, large dots MgO, small dots paraffin. Curve I neon (theoretical), curve II argon (theoretical).

on a smooth curve. This is to be expected, because crystals of NaF and MgO have a small grating constant. The diffraction lines are consequently widely separated and a good average of the diffracted energy is not obtained. However, the average distribution of the points appears to lie along the gas scattering curve. The larger grating constant of KCl insures a good average of the diffracted portion of the energy throughout the whole range of scattering angles at which observations were made. This explains the excellent agreement of the KCl values with the gas curve at all points.

Jauncey and Williams[12] have found that the values of S_c+F^2/Z for NaF are lower than the values of the scattered intensities from neon. The author's calculated values of S_c+S_d, as shown by the crosses in Fig. 4, are also lower than the gas scattering curve. The author's experimental values of the total

scattering from NaF are on the average higher than the values of S_c+S_d, but slightly less than Wollan's neon values. The values of S_c+S_d are probably more reliable than the experimental values of the total scattering because of the difficulty of averaging the diffracted energy in the ionization chamber. The values of S_c+S_d for MgO lie slightly above the theoretical curve for neon and are in good agreement with Wollan's experimental measurements of the neon intensities. The S_c+S_d values for KCl are slightly lower than the argon theoretical curve, and the author's values of the total scattering lie between the S_c+S_d values and the argon curve. The difference between the values is, however, less than the probable uncertainty in the determination of the absolute value of the total scattering by comparison with paraffin. Using the F values of Froman[9] for powdered KCl, the values of S_c+F^2/Z fall exactly on the theoretical argon curve. James and Brindley[15] have measured the F values for a single crystal of KCl and have found them to be slightly greater than Froman's values. Using these F values of James and Brindley, the S_c+F^2/Z values for KCl agree better with Wollan's values of the argon intensities than with the theoretical curve. Jauncey and Harvey[16] have used Wollan's and James and Brindley's values in testing the S_c+F^2/Z relation.

In a former paper[17] the author has published the results of measurements of the total scattering from aluminum, copper, and lead sheets. Since a sheet of metal consists of a collection of small crystals, we may consider it to be a plate of powdered crystals of the metal. The total scattering from a metal sheet measured with a wide-window ionization chamber should thus be approximately the same as the scattering from the same metal in the vapor state, for values of $(\sin\phi/2)/\lambda$ greater than 0.5. This method of measurement yields values of the atomic structure factor for the atom at rest, since from Eq. (1) we have

$$f^2=\frac{(S-R^{-3})}{(Z-R^{-3})}Z^2.$$

The author wishes to thank Professor A. H. Compton for suggesting measurements of the total scattering from powdered crystals and Dr. E. O. Wollan for his generous and helpful advice during the course of the experiment.

[15] R. W. James and G. W. Brindley, Proc. Roy. Soc. **A121**, 155 (1928).
[16] G. E. M. Jauncey and G. G. Harvey, Phys. Rev. **38**, 1071 (1931).
[17] A. W. Coven, Phys. Rev. **38**, 1424 (1931).

Sum Rules for Atomic Transition Probabilities

By J. P. VINTI
Massachusetts Institute of Technology

(Received June 27, 1932)

Some new sum rules for atomic transition probabilities are developed; they are similar to the well-known rule of Kuhn, Reiche, and Thomas. They give, if unpolarized light is incident on any gaseous element in any given discrete energy level, the total absorption, excitation plus ionization, with various types of frequency weighting. The results are similar to those of Dirac and Harding, but are more general in that they apply to any discrete state of any atom, rather than to the ground state of hydrogen only. The method differs from that of Dirac and Harding.

INTRODUCTION

THERE are well-known relations connecting the coefficients of spontaneous and induced transitions in atomic systems (the Einstein A's and B's) with the matrix components of electric moment between the initial and final states and the corresponding frequency differences. A_{0n}, the spontaneous transition probability from a state n to a lower state 0 is equal (in the dipole approximation) to a universal constant multiplied by the cube of the frequency difference and the square of the absolute value of the matrix component of electric moment, $e^2(|x_{0n}|^2+|y_{0n}|^2+|z_{0n}|^2)$, where ex, ey, ez, are the rectangular components of electric moment, so that e.g., x is equal to the sum of the x coordinates of all the electrons. B_{0n}, the induced transition probability, is proportional directly to $e^2(|x_{0n}|^2+|y_{0n}|^2+|z_{0n}|^2)$, where in this case, either 0 or n may be the lower state.

x_{0n} is given by an integral of the form $\int\bar{\psi}_0(\Sigma_{\mu=1}^{N}x_\mu)\psi_0 d\tau$, where ψ_0 and ψ_n are the wave functions of the atom for the states 0 and n, N is the number of extranuclear electrons in the atom, and the integration is extended over the coordinates of all the electrons. We see, then, that in general one must know the wave functions of the atom for the states concerned in order to calculate A_{0n} and B_{0n}. One, can, however, give some general relations satisfied by the A's or B's without knowing any wave functions, or knowing at the most the wave function of one discrete state only.

The sum rule of Kuhn, Reiche, and Thomas[1] is an example of the type of thing one can say about the matrix components, and thus about the A's and B's, without knowing any wave functions. Using atomic units, and letting x denote $\Sigma_1^N x_\mu$, the sum of the N cartesian coordinates, W_n the energy of the state n with reversed sign, this rule can be expressed in the form $\Sigma_n(W_0-W_n)|x_{0n}|^2=N$, where the state 0 denotes an arbitrary state of the discrete spectrum, and the summation is understood to include a summation over all the discrete states that have dipole combinations with the state 0, and an integral

[1] W. Kuhn, Zeits. f. Physik **33**, 408 (1925). F. Reiche and W. Thomas, Zeits. f. Physik **34**, 510 (1925).

over the continuous spectrum. (Similar relations hold for the y and z components of electric moment.) This rule is directly deducible from the commutation rules and the relation connecting the matrix components of momentum and coordinate. In terms of the A's it enables us to evaluate at once $\Sigma_n A_{0n}/\nu_{0n}^2$, where ν_{0n} is the frequency of the spectral line associated with the transition from a *running* state n to the *base* state 0. Furthermore, Wigner[2] has shown that this rule may be *sharpened* by dividing transitions into three classes: $+$, $-$, and 0, $+$ transitions being those in which the total azimuthal quantum number L increases by 1—those in which it diminishes by 1, and 0 those in which it does not change. Wigner's rule then gives the sum $g_+(L)\Sigma^+ + g_0(L)\Sigma^0$ in terms of the L-value of the state 0, where g_+ and g_0 are simple functions of L, and the summands are the f values A_{0n}/ν_{0n}^2. We wish to mention at this point that all the sum rules developed in this paper can be sharpened in a similar way.

Matrix multiplication of the simple type $xx = x^2$ furnishes another general relation connecting the matrix components:

$$\sum_n |x_{0n}|^2 = (x^2)_{00}.$$

Here, as above, 0 means a discrete state and the summation is to be extended by means of integration over the continuous spectrum. This relation can also be looked on as a sum rule, although of a less general type, since the evaluation of the sum depends on a knowledge of the wave function of the state 0. It gives directly $\Sigma_n B_{0n}$, if one knows ψ_0.

The above rules tell us how to evaluate $\Sigma_n(W_0 - W_n)^j |x_{0n}|^2$ when j has the value 1 or 0. We develop in this paper other rules of the same general type, letting j take on the values 2, 3 and 4. They constitute rules for the summation of the A's and B's (of a given base state) over all the states of the atom, with various kinds of frequency weighting.

SECTION I

We begin with the case $j=2$, and attempt to evaluate $\sum_n(W_0 - W_n)^2 (|x_{0n}|^2 + |y_{0n}|^2 + |z_{0n}|^2)$. (We abbreviate expressions of this type hereafter to $\sum_{n,xyz}(W_0 - W_n)^2 |x_{0n}|^2$). Let x_μ, y_μ, z_μ denote the coordinates of the μth electron, N the total number of extranuclear electrons in the atom, $p_{x\mu}$, $p_{y\mu}$, $p_{z\mu}$ the components of momentum of the μth electron, and $p_{x\mu}(0n)$ the matrix component of $p_{x\mu}$ between the stationary states 0 and n. Also, we shall use the contractions:

$$\sum_{\mu=1}^{N} x_\mu = x, \quad \sum_{\mu=1}^{N} p_{x\mu} = p_x, \text{ and } W_0 - W_n = W_{0n}.$$

Now

$$p_{x\mu}(0n) = (h/2\pi i)\int \bar{\psi}_0 \frac{\partial}{\partial x_\mu}\psi_n d\tau,$$

[2] E. Wigner, Phys. Zeits. 11, 450 (1931).

and it is well known that when at least one of the states 0 and n is a discrete state (to insure the vanishing of surface integrals at infinity which occur in the derivation), this can be thrown into the form $m(2\pi i/h)W_{0n}x_\mu(0n)$, where $x_\mu(0n)$ is the matrix component of x_μ between the states 0 and n, and m is the rest mass of the electron. On summing over the index μ from 1 to N, we obtain the relation:

$$p_x(0n) = m(2\pi i/h)W_{0n}x_{0n}. \tag{1}$$

Similarly

$$p_x(n0) = \bar{p}_x(0n) = m(2\pi i/h)W_{n0}x_{n0}, \tag{2}$$

(since p_x is hermitian, and $W_{n0} = -W_{0n}$). On multiplying (1) by (2) we obtain:

$$p_x(0n)p_x(n0) = m^2(2\pi/h)^2W_{0n}{}^2\,|\,x_{0n}\,|^2. \tag{3}$$

Summing (3) over all states n (complete set), and making use of the simple rule for a matrix product, *viz*:

$$\sum_n p_x(0n)p_x(n0) = (p_x{}^2)_{00},$$

we obtain the relation:

$$m^2(2\pi/h)^2\sum_n W_{0n}{}^2\,|\,x_{0n}\,|^2 = (p_x{}^2)_{00}. \tag{4}$$

Similar relations hold on replacing x by y or z. Adding,

$$m^2(2\pi/h)^2\sum_{n,\,xyz} W_{0n}{}^2\,|\,x_{0n}\,|^2 = (p_x{}^2 + p_y{}^2 + p_z{}^2)_{00}. \tag{5}$$

We next attempt to give the right hand side of (5) a physical meaning. Since

$$p_x{}^2 = \sum_\mu \sum_\nu p_{x_\mu}p_{x_\nu} = \sum_{\mu=1}^{N} p_{x_\mu}{}^2 + \sum_{\mu\neq\nu}\sum p_{x_\mu}p_{x_\nu},$$

$$(p_x{}^2)_{00} = \sum_{\mu=1}^{N}(p_{x_\mu}{}^2)_{00} + \sum_{\mu\neq\nu}\sum(p_{x\mu}p_{x\nu})_{00}.$$

The right side of (5) thus decomposes into two parts:

$$\sum_{\mu=1}^{N}(p_{x\mu}{}^2 + p_{y\mu}{}^2 + p_{z\mu}{}^2)_{00} \text{ and } \sum_{\mu\neq\nu}\sum(p_{x\mu}p_{x\nu} + p_{y\mu}p_{y\nu} + p_{z\mu}p_{z\nu})_{00}.$$

The former term is recognizable as $2mT_{00}$, where T_{00} is the diagonal component of kinetic energy in the state 0. By the virial theorem, making use of the fact that the interaction potentials in the atom are all Coulombian, we can equate T_{00} to $-W_0$. The cross-product term is expressible as

$$-(h/2\pi)^2\int \bar{\psi}_0 \nabla_\mu \cdot \nabla_\nu \psi_0 d\tau,$$

or

$$\sum_{\mu\neq\nu}\sum(\vec{p}_\mu\cdot\vec{p}_\nu)_{00}, \text{ where } \vec{p}_\mu = (p_{x\mu}, p_{y\mu}, p_{z\mu}).$$

Then

$$m^2(2\pi/h)^2 \sum_{n,xyz} W_{0n}^2 \left| x_{0n} \right|^2 = -2mW_0 + \sum_{\mu \neq \nu} \sum (\vec{p}_\mu \cdot \vec{p}_\nu)_{00} \tag{6}$$

where $|W_0|$ is the energy necessary to strip the atom of all its electrons when in the state 0.

Eq. (6), then, is the general sum rule for the case $j=2$. If the wave function of the state 0 is simple enough so that $\sum\sum_{\mu\neq\nu}(\vec{p}_\mu \cdot \vec{p}_\nu)_{00}$ can be evaluated, it is of use. For states like the ground state of helium, where one can assume separability to a good approximation,

$$(p_{x\mu} p_{x\nu})_{00} = \tilde{p}_{x\mu} \tilde{p}_{x\nu}$$

where the tilde indicates an average with respect to the wave function of that electron alone. But

$$\tilde{p}_{x\mu} = \tilde{p}_{x\nu} = 0.$$

In such a case, and for one-electron atoms, the rule becomes

$$\sum_{n,xyz} W_{0n}^2 \left| x_{0n} \right|^2 = -(h^2/2\pi^2 m) W_0. \tag{7}$$

For those cases above mentioned in which the cross term vanishes, it is of interest to express the rule in terms of the A and B coefficients:

$$\sum_n \frac{A_{0n}}{\nu_{0n}} = \frac{32\pi^2 e^2}{3mc^3 h^2} |W_0| \tag{8}$$

or

$$\sum_n \nu_{0n}^2 B_{0n} = \frac{4\pi e^2}{3mh^2} |W_0| \tag{9}$$

the Kuhn-Reiche rule ($j=1$) being expressible as

$$\sum_n \frac{A_{0n}}{\nu_{0n}^2} = \frac{8\pi^2 e^2}{mc^3} N$$

or

$$\sum_n \nu_{0n} B_{0n} = -\frac{\pi e^2}{3m} N.$$

Alternative method

The sum $\sum_n W_{0n}^2 |x_{0n}|^2$ can be expressed alternatively as $\sum_n \sum_\mu W_{0n}^2 x_\mu(0n) \sum_\nu x_\nu(n0)$. (In the rest of the paper matrix components of coordinates and momenta are understood to have time factors of the form $\exp[(2\pi i/h) W_{0n} t]$.) As before, $p_{x\mu}(0n) = m(2\pi i/h) W_{0n} x_\mu(0n)$, and making use of the above convention as to the time factor of a matrix component, we have, letting the dot denote differentiation with respect to time:

$$\dot{p}_{x\mu}(0n) = m(2\pi i/h)^2 W_{0n}^2 x_\mu(0n)$$

so that

$$W_{0n}^2 x_\mu(0n) = (1/m)(h/2\pi i)^2 \dot{p}_{x\mu}(0n).$$

The sum then becomes $(1/m)(h/2\pi i)^2 \sum_n \sum_\mu \sum_\nu \dot{p}_{x\mu}(0n)x_\nu(n0)$. We now make use of the fact that $\dot{p}_{x\mu}(0n) = -(\partial V/\partial x_\mu)_{0n}$, where V is the potential energy of the atom,[3] and of the rule for a matrix product, obtaining for the sum the expression

$$\frac{1}{m}\left(\frac{h}{2\pi}\right)^2 \sum_\mu \sum_\nu \left(\frac{\partial V}{\partial x_\mu} x_\nu\right)_{00}.$$

Summing on x, y, z, we get

$$\sum_{n,\,xyz} W_{0n}{}^2 \left| x_{0n} \right|^2 = \frac{1}{m}\left(\frac{h}{2\pi}\right)^2 \sum_\mu \sum_\nu (\nabla_\mu V \cdot R_\nu)_{00}$$

where ∇_μ is the gradient operator in the coordinates of the μth electron, and R_ν is the radius vector to the νth electron. This expression can be split into the parts

$$\frac{1}{m}\left(\frac{h}{2\pi}\right)^2 \sum_{\mu=1}^{N} (\nabla_\mu V \cdot R_\mu)_{00} \text{ and } \frac{1}{m}\left(\frac{h}{2\pi}\right)^2 \sum_{\mu \neq \nu} \sum (\nabla_\mu V \cdot R_\nu)_{00}.$$

The first part can be transformed by Euler's theorem (since V is a homogeneous function of the electron coordinates of degree -1), and becomes $(-1/m)\ (h/2\pi)^2 V_{00}$. Application of the virial theorem, according to which $V_{00} = 2W_0$, gives finally for the first part $-(h^2/2\pi^2 m)W_0$, agreeing with the non-cross term of the first method. The cross term $(1/m)(h/2\pi)^2 \sum \sum_{\mu \neq \nu}$ $(\nabla_\mu V \cdot R_\nu)_{00}$ must thus be equal to that obtained by the first method, $(1/m^2)(h/2\pi)^2 \sum \sum_{\mu \neq \nu} (\vec{p}_\mu \cdot \vec{p}_\nu)_{00}$. It does not appear that this equivalence could be shown in any other way. The new form for the cross term is more useful for calculation, since it does not require us to differentiate a wave function which may be unwieldy. For an atom of atomic number Z with N electrons it becomes:

$$\frac{e^2}{2m}\left(\frac{h}{2\pi}\right)^2 \int \bar{\psi}_0 \left[Z \sum_{\mu \neq \nu}^{N} \sum \frac{1}{r_\mu{}^3}(r_\mu{}^2 + r_\nu{}^2 - r_{\mu\nu}{}^2) + \sum_{\mu \neq \nu}^{N} \sum \sum_{j \neq \mu} \frac{1}{r_{j\mu}{}^3}(r_i{}^2 - r_\mu{}^2 + r_{\mu\nu}{}^2 - r_{j\nu}{}^2) \right] \psi_0 d\tau .$$

For the special case of a two-electron atom the cross term becomes

$$\frac{1}{m}\left(\frac{h}{2\pi}\right)^2 \int \bar{\psi}_0 \left[Ze^2 r_1 r_2 \cos\Theta_{12}\left(\frac{1}{r_1{}^3} + \frac{1}{r_2{}^3}\right) + \frac{e^2}{r_{12}} \right] \psi_0 d\tau$$

where Θ_{12} is the angle between the radius vectors. If this is calculated out with a separated wave function, the term e^2/r_{12} leads to a nonvanishing result, in contrast to the first method, which gave zero. This discrepancy is undoubtedly due to the inaccuracy of the assumption of separability.

[3] The proof is like that given by Sommerfeld, Wellenmechanischer Ergänzungsband, pp. 288, 289 for a diagonal component of momentum. The operators div, grad, and Δ, however, are now operators in 3 N-space, rather than 3-space, and with us the time component of a wave function of a stationary state k is exp $[-(2\pi i/h)W_k t]$ rather than exp $[+(2\pi i/h)W_k t]$, so that $z_{0n} = \int \bar{\psi}_0 z \psi_n d\tau$, rather than $\int \psi_0 z \bar{\psi}_n d\tau$, as with Sommerfeld.

SECTION II

We continue with the case $j=3$. The problem is to evaluate $\sum_n W_{0n}{}^3 |x_{0n}|^2$. First, $W_{0n}{}^3 |x_{0n}|^2$, because of the hermitian character of our matrices, can be expressed as $-(W_{0n}{}^2 x_{0n})(W_{n0}x_{n0})$. The factor $W_{n0}x_{n0}$ can be then placed equal, as before, to $(h/2\pi im)p_x(n0)$. Also, as before,

$$\dot{p}_x(0n) = m\left(\frac{2\pi i}{h}\right)^2 W_{0n}{}^2 x_{0n}$$

Thus

$$W_{0n}{}^2 x_{0n} = \left(\frac{h}{2\pi i}\right)^2 \frac{1}{m}\,\dot{p}_x(0n)$$

and

$$W_{0n}{}^3 |x_{0n}|^2 = \frac{h}{2\pi i}\,\frac{h^2}{4\pi^2 m^2}\,\dot{p}_x(0n)\,p_x(n0).$$

Now

$$\dot{p}_x(0n) = \sum_{\mu=1}^{N} \dot{p}_{x\mu}(0n)$$

and

$$\dot{p}_{x\mu}(0n) = -\left(\frac{\partial V}{\partial x_\mu}\right)_{0n}$$

Thus $\dot{p}_x(0n) = -\sum_\mu (\partial V/\partial x_\mu)_{0n}$, so that

$$W_{0n}{}^3 |x_{0n}|^2 = -\frac{h}{2\pi i}\,\frac{h^2}{4\pi^2 m^2} \sum_\mu \sum_\nu \left(\frac{\partial V}{\partial x_\mu}\right)_{0n} p_{x\nu}(n0).$$

Upon summing on n, making use of the rule for a matrix product, we obtain

$$\sum_n W_{0n}{}^3 |x_{0n}|^2 = -\frac{h}{2\pi i}\,\frac{h^2}{4\pi^2 m^2} \sum_\mu \sum_\nu \left(\frac{\partial V}{\partial x_\mu} p_{x\nu}\right)_{00}. \tag{10}$$

Eq. (10), then, is the rule for $j=3$ in the general case of an N-electron atom. (The i, of course, is cancelled on performing the indicated operations.) We next consider the special cases $N=1$ and $N=2$.

Case 1: $N=1$

Letting 0 denote any discrete state of an H-like atom

$$\sum_k W_{0k}{}^3 |x_{0k}|^2 = \frac{1}{m^2}\left(\frac{h}{2\pi}\right)^4 \left(\frac{\partial V}{\partial x}\,\frac{\partial}{\partial x}\right)_{00}$$

and

$$\sum_{k,\,xyz} W_{0k}{}^3 |x_{0k}|^2 = \frac{1}{m^2}\left(\frac{h}{2\pi}\right)^4 J, \text{ where } J = \int \bar{\psi}_0 \nabla V \cdot \nabla \psi_0 d\tau.$$

But $V = V$ (r only). So that

$$\nabla V \cdot \nabla \psi_0 = \frac{dV}{dr}\,\frac{\partial \psi_0}{\partial r} = \frac{Ze^2}{r}\,\frac{\partial \psi_0}{\partial r},$$

(since $V=-Ze^2/r$). Thus

$$J = Ze^2 \int \bar{\psi}_0 \frac{1}{r^2} \frac{\partial \psi_0}{\partial r} d\tau$$

and since $\psi_0 = R(r)\Theta(\theta)\Phi(\phi)$,

$$J = Ze^2 \int_0^\infty R \frac{dR}{dr} dr \int_0^\pi \Theta^2 \sin\theta d\theta \int_0^{2\pi} \bar{\Phi}\Phi d\phi.$$

Letting R, Θ, and Φ be separately normalized,

$$J = Ze^2 \int_0^\infty R \frac{dR}{dr} dr = \frac{Ze^2}{2}[R^2(\infty) - R^2(0)] = -\frac{Ze^2}{2} R^2(0),$$

since the radial wave function always vanishes at infinity. Then, making use of the properties of the Laguerre polynomials involved in the radial wave function, we find:

$$J = 0, \ l \neq 0$$
$$= -(2e^2/a_0^3)Z^4/n^3, \ l = 0$$

where a_0 is the Bohr radius, n the principal quantum number, and l the azimuthal quantum number of the state 0. Thus the cube sum vanishes for $l \neq 0$, and equals

$$-\frac{1}{m^2}\left(\frac{h}{2\pi}\right)^4 \frac{2e^2}{a_0^3} \frac{Z^4}{n^3} \text{ for } l = 0.$$

It is interesting to express these relations in terms of the A's. Since

$$A_{0k} = \frac{64\pi^4 e^2}{3c^3h^4} W_{0k}^3(|x_{0k}|^2 + |y_{0k}|^2 + |z_{0k}|^2),$$

$$\sum_k A_{0k} = 0, \ l \neq 0$$
$$= -\frac{8e^4}{3m^2c^3a_0^3} \frac{Z^4}{n^3}, \ l = 0.$$

Expressed in words, in any hydrogen-like atom, the sum of the spontaneous transition probabilities from any state not an S-state to all lower states is equal to the sum of the spontaneous transition probabilities from all higher states down to the given state. For an S-state they are unequal, the difference varying inversely with the cube of the principal quantum number and directly with the fourth power of atomic number; for S-states near the ionization limit they approach equality. (By a *state* is here meant a level with given l and m; if one wishes to treat state as meaning a given l only, that is, to average over different *orbital orientations*, one must take into account such orbital degeneracy in writing down the formulas for the A's or the B's in terms of matrix components. The necessary quantum weight factors can be found most explicitly in a paper by Y. Sugiura.[4])

[4] Y. Sugiura, Phil. Mag. [7] 4, 495 (1927).

For example, the sum of the spontaneous transition probabilities from all higher states, continuous included, to the state $2P$ (with given m) in hydrogen-like atoms is equal to the spontaneous transition probability from that state to the groundstate $1S$. (m here means magnetic quantum number.)

Applied to the case in which 0 denotes the ground state of an H-like atom, this cube rule furnishes an independent proof of a theorem familiar from direct examination of the hydrogenic functions. We have shown that this sum is of the order Z^4/n^3 for S-states of H-like atoms, and zero for other states. Since for the ground state all the A_{0k}'s have the same sign, it follows that their sum cannot vanish, so that we have: the ground state of an H-like atom must be an S-state.

Case 2: $N=2$, helium-like atoms

On writing out the double sum, we obtain:

$$\sum_n W_{0n}{}^3 \left| x_{0n} \right|^2 = -\frac{h}{2\pi i}\frac{h^2}{4\pi^2 m^2}\left(\frac{\partial V}{\partial x_1}p_{x1}+\frac{\partial V}{\partial x_2}p_{x2}+\frac{\partial V}{\partial x_1}p_{x2}+\frac{\partial V}{\partial x_2}p_{x1}\right)_{00}.$$

Using $V=-Ze^2/r_1-Ze^2/r_2+e^2/r_{12}$, and carrying through the indicated operations in a straightforward way, we obtain:

$$\sum_{n,xyz} W_{0n}{}^3 \left| x_{0n} \right|^2 = \left(\frac{h}{2\pi}\right)^4 \frac{Ze^2}{m^2}\left[\frac{1}{r_1{}^3}\sum_{xyz} x_1\frac{\partial}{\partial x_1}+\frac{1}{r_2{}^3}\sum_{xyz} x_2\frac{\partial}{\partial x_2}\right.$$
$$\left.+\frac{1}{r_1{}^3}\sum_{xyz} x_1\frac{\partial}{\partial x_2}+\frac{1}{r_2{}^3}\sum_{xyz} x_2\frac{\partial}{\partial x_1}\right]_{00}.$$

Letting 1_{r_μ}, $1_{\theta\mu}$, $1_{\phi\mu}$ be unit vectors along the radius, meridian, and parallel of latitude through the μth electron,

$$\sum_{xyz} x_\mu\frac{\partial}{\partial x_\mu} = r_\mu\frac{\partial}{\partial r_\mu}$$

Also

$$\sum_{xyz} x_\mu\frac{\partial}{\partial x_\nu} = r_\mu 1_{r\mu}\cdot\nabla_\nu,$$

where ∇_ν is the gradient in the coordinates of the νth electron. Using these abbreviations, we can write the cube sum for $N=2$ in the form:

$$\left(\frac{h}{2\pi}\right)^4\frac{Ze^2}{m^2}\int\bar{\psi}_0\left[\frac{1}{r_1{}^2}\frac{\partial}{\partial r_1}+\frac{1}{r_2{}^2}\frac{\partial}{\partial r_2}+\frac{1}{r_1{}^2}1_{r1}\cdot\nabla_2+\frac{1}{r_2{}^2}1_{r2}\cdot\nabla_1\right]\psi_0 d\tau.$$

Knowing the wave function of any discrete state of a helium-like atom, we have here a rule for the evaluation of $\sum_n A_{0n}$ for the atom. We might mention that for S-states (e.g., $(1s)^2$ or $(1s)(2s)$), an approximate function of the form $\psi_0=\psi_0(r_1, r_2)$ (no angular dependence) is often used. In such a case

$$1_{r1}\cdot\nabla_2\psi_0 = \cos\Theta_{12}\frac{\partial}{\partial r_2}\psi_0$$

$$1_{r2}\cdot\nabla_1\psi_0 = \cos\Theta_{12}\frac{\partial}{\partial r_1}\psi_0,$$

where Θ_{12} is the angle between the radius vectors $\vec{r}_1$ and $\vec{r}_2$. But $\int\cos\Theta_{12}\sin\theta_1 d\theta_1 d\phi_1\sin\theta_2 d\theta_2 d\phi_2 = 0$. Thus if $\psi_0 = \psi_0(r_1, r_2)$, the terms involving both electrons drop out of the integrand and the cube sum reduces to the integral

$$\left(\frac{h}{2\pi}\right)^4\frac{Ze^2}{m^2}\int\bar{\psi}_0\left(\frac{1}{r_1^2}\frac{\partial}{\partial r_1}+\frac{1}{r_2^2}\frac{\partial}{\partial r_2}\right)\psi_0 d\tau.$$

In applying this to the ground state of helium, it is convenient to express the cube sum in atomic units, in which case the factor in front of the integral becomes $8Z$. Using a simple screening constant wave function $\psi_0 = -(\alpha^3/\pi)^{1/2}e^{-\alpha(r_1+r_2)}$ where $\alpha = Z-5/16$, the cube sum becomes $-32Z(Z-5/16)^3$.

SECTION III $j=4$

To evaluate $\sum_{n,xyz}W_{0n}{}^4|x_{0n}|^2$. Taking the general case of an N-electron atom, we begin as before:

$$\left(\frac{\partial V}{\partial x_\mu}\right)_{0n} = -\dot{p}_{x\mu}(0n)$$

$$= m(2\pi/h)^2 W_{0n}{}^2 x_\mu(0n).$$

Thus

$$\sum_\mu\left(\frac{\partial V}{\partial x_\mu}\right)_{0n} = m(2\pi/h)^2 W_{0n}{}^2 x_{0n}$$

and

$$m^2(2\pi/h)^4 W_{0n}{}^4|x_{0n}|^2 = \sum_\mu\sum_\nu\left(\frac{\partial V}{\partial x_\mu}\right)_{0n}\left(\frac{\partial V}{\partial x_\nu}\right)_{n0}.$$

Summing over all the states n,

$$\sum_n(2\pi/h)^4 m^2 W_{0n}{}^4|x_{0n}|^2 = \sum_\mu\sum_\nu\left(\frac{\partial V}{\partial x_\mu}\frac{\partial V}{\partial x_\nu}\right)_{00}$$

$$= \left\{\left(\sum_{\mu=1}^N\frac{\partial V}{\partial x_\mu}\right)^2\right\}_{00}$$

$$= \int\bar{\psi}_0\left(\sum_{\mu=1}^N\frac{\partial V}{\partial x_\mu}\right)^2\psi_0 d\tau.$$

For a hydrogen-like atom, $N=1$, we obtain for the fourth-power sum:

$$\left(\frac{h}{2\pi}\right)^4 \frac{Z^2e^4}{m^2}\left(\frac{1}{r^4}\right)_{00}$$

where

$$\left(\frac{1}{r^4}\right)_{00} = \frac{\frac{3}{2}Z^4\left[1-\frac{l(l+1)}{3n^2}\right]}{a_0{}^4n^3(l+3/2)(l+1)(l+\frac{1}{2})l(l-\frac{1}{2})}.$$

This fourth-power rule gives a rule for summing $\sum_k \nu_{0k}A_{0k}$. The presence of l in the denominator of the above expression leads to the result that a sum of transition probabilities with this sort of frequency weighting diverges for S-states of hydrogen-like atoms.

For a helium-like atom, this rule takes a simple form. Using

$$V = -\frac{Ze^2}{r_1} - \frac{Ze^2}{r_2} + \frac{e^2}{r_{12}},$$

we find

$$\left(\sum_\mu \frac{\partial V}{\partial x_\mu}\right)^2 = Z^2e^4\left(\frac{x_1{}^2}{r_1{}^6} + \frac{x_2{}^2}{r_2{}^6} + 2\frac{x_1x_2}{r_1{}^3r_2{}^3}\right).$$

Summing over x, y, z,

$$\sum_{xyz}\left(\sum_\mu \frac{\partial V}{\partial x_\mu}\right)^2 = Z^2e^4\left(\frac{1}{r_1{}^4} + \frac{1}{r_2{}^4} + \frac{2}{r_1{}^2r_2{}^2}\cos\Theta_{12}\right)$$

where Θ_{12} is the angle between the radius vectors $\vec{r}_1$, $\vec{r}_2$, from which is obtained the fourth-power sum:

$$\left(\frac{h}{2\pi}\right)^4 \frac{Z^2e^4}{m^2}\int \bar{\psi}_0\left(\frac{1}{r_1{}^4} + \frac{1}{r_2{}^4} + \frac{2}{r_1{}^2r_2{}^2}\cos\Theta_{12}\right)\psi_0 d\tau.$$

Going back to H-like atoms, we can use the cube and fourth-power rules to deduce the asymptotic behavior of the A's between the ground state and the continuous spectrum. $\sum_k \nu_{0k}A_{0k}$ diverges for S-states, and therefore for the ground state. For this state the $\nu_{0k}A_{0k}$ all have the same sign. For the discrete spectrum (Lyman series), $\nu_{0k}A_{0k}$ is asymptotically of the order $1/n_k{}^3$, and since $\sum_1{}^\infty 1/n_k{}^3$ is known to converge, it follows that the sum $\sum_k \nu_{0k}A_{0k}$ over the discrete spectrum only must converge. Thus $\int \nu(dA_{0\nu}/d\nu)d\nu$ over the continuous spectrum must diverge. In a similar manner, using the cube rule, it follows that $\int (dA_{0\nu}/d\nu)d\nu$ over the continuous spectrum must converge. Writing $dA_{0\nu}/d\nu$ asymptotically (large ν) as const./$\nu^{1+\epsilon}$ we see that $\int_{\nu_0}{}^\infty d\nu/\nu^{1+\epsilon}$ must converge and $\int_{\nu_0}{}^\infty d\nu/\nu^\epsilon$ must diverge, (where ν_0 = frequency of Lyman series limit). The first requirement gives $\epsilon>0$, the second $\epsilon\leqq 1$, so that $0<\epsilon\leqq 1$. Thus the f-value $df_{0\nu}/d\nu\,(=\nu^{-2}\,dA_{0\nu}/d\nu)$ is of the order $1/\nu^i$, where

$3<j\leqq 4$. This example serves to illustrate how the sum rules can be used to obtain information about the intensity distribution in the continuous spectrum without knowing anything about the continuous wave functions.

It should be mentioned that Dirac and Harding[5] have already obtained the sum rules of this paper for the special case when the state 0 is the ground state of hydrogen. Besides this restriction, their method encounters an ambiguity of a peculiar sort, in that part of an operator may operate backwards and part forwards; this ambiguity has to be removed by a special investigation.

The author is indebted to Professors J. C. Slater and M. S. Vallarta, who have read the manuscript and offered suggestions, and especially to Professor P. M. Morse, who has taken a very helpful interest in the paper and offered many valuable suggestions.

[5] Dirac and Harding, Proc. Camb. Phil. Soc. 28, 209 (1932).

Multiplet Splitting and Intensities of Intercombination Lines Part I

By HUGH C. WOLFE*
Utrecht University

(Received June 13, 1932)

Kramers' symbolic representation method for the treatment of those properties of free atoms which can be derived on the basis of irreducible representations of rotations in R_3 is outlined. Wave functions and operators are represented by functions of spinor quantities (ξ, η) whose properties are known from the theory of invariants. Integrations yielding matrix elements are only symbolic and the results, being determined by the rotation invariance properties, contain therefore undetermined constant factors of the nature of radial integrals. The method is particularly adapted to the problem of multiplets (interaction between two or more "vectors"—e.g., orbital angular momenta, spins—treated as a perturbation). The method is applied to configurations involving two valence electrons of which one is in an s state. Such a configuration gives rise to a singlet and a triplet with the l value of the second electron. The deviations from the normal l to $l+1$ interval ratio in the triplet are due to a repulsion between the singlet level and the center triplet level, their j values being the same. The mixing up of the wave functions of these two levels gives rise to singlet-triplet intercombinations. The constants which represent the interaction energies (1) interchange, (2) spin-orbit, (3) spin of one electron—orbit of the other (assuming that other types of interaction may be neglected) are found in terms of the three intervals of the multiplet. Corrections to the Kronig-Hönl intensity formulas are found in terms of the intervals of the two multiplets between which the transitions occur. These formulas then give the relative intensities of combination and intercombination lines. The sum rules for intensity hold for the complete multiplet and not for the singlet and triplet separately. Part II will contain application of the theory to observed spectra.

IN HIS book, *Quantenmechanik und Gruppentheorie*, Weyl has shown that many of the properties of free atoms can be derived on the basis of irreducible representations of the rotations in three dimensional space. Kramers[1] has obtained a very elegant formulation of Weyl's methods through the use of symbolic representations of wave functions and operators with properties well known from the theory of invariants. We propose here to outline this method and to show its application to a problem in complex spectra.

THE SYMBOLIC METHOD

1.

Let ξ and η be the components of a *spinor* or *half-vector*, i.e., a two-dimensional complex vector. The transformations of the monomials $\xi^{l+m}\eta^{l-m}$ $(m=-l, -l+1, \cdots l)$, when ξ and η suffer a unitary transformation, constitute an irreducible representation of degree $2l+1 (l=1/2, 1, 3/2, \cdots)$ of the space rotation group. Except the identity, there are no other irreducible

* Fellow of the Lorentz Foundation.

[1] H. A. Kramers, Proc. Amst. Acad. **33**, 953 (1930) and **34**, 965 (1931).

representations. Then a series of $2\tau+1$ quantities G_f, which transform into each other in an irreducible way under space-rotation, may be gathered up in the one formula

$$\sum_f \binom{2\tau}{\tau-f} a^{\tau-f}(-b)^{\tau+f} G^f = (a\eta - b\xi)^{2\tau}, \tag{1}$$

where a and b are the components of an arbitrary constant spinor. The G_f can always be so chosen that they transform like $\xi^{\tau+f}\eta^{\tau-f}$. $(a\eta - b\xi)$ is invariant.

2.

In the study of multiplets, a free atom may be treated as if it consisted of two or more *vector-frames* (Vektorgerüste), to each of which belongs a quantum number of the total angular momentum and whose mutual orientation has, in first approximation, no influence on the energy of the stationary states. In the complete energy expression there appear small interaction terms which depend, in a not purely additive fashion, on the elements (Bestimmungsstücke) of a pair of vectors and which denote an energetic coupling of these vectors.[2] As a consequence of this coupling every *state*, defined by the quantum numbers of the vectors, splits up into a multiplet.

Consider the coupling of just two vectors. In analogy with the notation for Russell-Saunders coupling but without assuming anything about the physical nature of the vectors, we may designate their quantum numbers of angular momentum by l and s.

The interaction terms in the complete energy expression may be written down in the form

$$\Omega = \sum_n a_n \lambda_n \sigma_n . \tag{2}$$

Here λ_n and σ_n are functions, respectively, only of the elements of the l-frame and only of the elements of the s-frame in such fashion that λ_n and σ_n are not invariant under an arbitrary space-rotation but transform according to some linear law. The coefficients a_n may contain any combination of rotation-invariant functions of the elements of either frame. In practice, Ω is usually given immediately in this form or else, when the l-frame and the s-frame are associated with different particles, Ω contains terms involving $1/r_{12}$. The expansion

$$\frac{1}{r_{12}} = \frac{1}{r_b} \sum_m \left(\frac{r_a}{r_b}\right)^m P_m\left(\frac{(\mathbf{r}_1 \cdot \mathbf{r}_2)}{r_1 r_2}\right), \tag{3}$$

where r_a and r_b are, respectively, the smaller and the larger of the distances r_1 and r_2 (the distances of the two particles from the center of gravity), brings these terms into the required form.

In an arbitrarily rotated coordinate system K' a selected λ_n, call it $\lambda^{(1)}$, assumes the form

$$\lambda^{(1)} = \sum_{p=1}^{g} \gamma_p{}^{(1)} \lambda'^{(p)},$$

[2] There may also be energy terms involving more than two vectors. To avoid complication, we shall not discuss these for the present. They are treated by an extension of the method.

where $\lambda'^{(1)}$ is the same quantity with respect to K' as $\lambda^{(1)}$ with respect to the original coordinate system K. Thus there are $g-1$ other l-frame functions $\lambda^{(p)}$ $(p=2, \cdots, g)$ associated with $\lambda^{(1)}$ and these quantities transform in a way which gives a representation of the space-rotation group of degree g. If this representation is irreducible we shall say, for brevity: $\lambda^{(1)}$ transforms irreducibly. If it is not, one can always reduce the transformation with the result that each $\lambda^{(p)}$ is expressed by the finite sum $\sum_f \lambda_f^{(p)}$ where the $\lambda_f^{(p)}$ transform irreducibly. Thus it is always possible to express Ω in the form (2) in such a way that every λ_n and also every σ_n transforms irreducibly.

Since we are dealing with a free atomic system, the series (2) is rotation-invariant and therefore can be divided up into parts such that the λ and σ in each part transform irreducibly with the same degree g.[3] Thus we may write

$$\Omega = \sum_{g=1}^{\infty} T_g, \tag{4}$$

$$T_g = \sum a\lambda_{(g)}\sigma_{(g)}, \tag{5}$$

where the summation indices have been omitted in the last sum.

In the quantum theory, the elements which determine an atomic system are uniquely defined according to their significance; the elements of the electron spin (its angular momentum components) as well as the ordinary coordinates and momenta have this property. That we consider them as operators makes no difference. But, for even values of g, the transforming quantities are only defined up to a factor ± 1. Actually, in the series (4), only odd values of g occur and, if we set $g=2\tau+1$ and $T_g=\Omega_\tau$, (4) assumes the form

$$\Omega = \sum_{\tau=0}^{\infty} \Omega_\tau. \tag{6}$$

We are now ready to consider the symbolic representation of the energy operators. We have already remarked that $2\tau+1$ quantities which transform irreducibly under space-rotation may be represented by $\xi^{\tau+f}\eta^{\tau-f}$. If we represent the $\lambda_{(g)}$ by $x_1^{\tau+f_1}\, y_1^{\tau-f_1}$ and the $\sigma_{(g)}$ by $x_2^{\tau+f_2}\, y_2^{\tau-f_2}$, then Ω_τ must contain these quantities in the form

$$\omega_\tau = (x_2y_1 - y_2x_1)^{2\tau}. \tag{7}$$

For Ω_τ is invariant under rotation and the only simultaneous invariant that can be formed of two spinors is $(x_2y_1-y_2x_1)^n$, where n is a positive integer. In general, Ω_τ may be a sum of expressions like (7).[4]

3.

Let us now consider the symbolic representation of the wave functions. Each state of a multiplet is uniquely defined by the quantum number j of the

[3] It is well known that $\Sigma a\lambda_{(g)}\lambda_{(g')}$ is never invariant for $g \neq g'$.

[4] In case of an energy term involving three vector-frames, we shall have symbolic terms of the type

$$(x_2y_1-y_2x_1)^\alpha (x_3y_1-y_3x_1)^\beta (x_3y_2-y_3x_2)^\gamma,$$

where α, β, and γ must be all even or all odd integers.

resultant angular momentum, where

$$|l-s| \leqq j \leqq l+s.$$

Wave functions satisfying the unperturbed (i.e., interaction terms neglected) wave equation may be composed of products of two functions, one of coordinates associated only with the l-frame and one of coordinates associated only with the s-frame. There are $2l+1$ functions of the first type which transform irreducibly under space-rotation and may be represented symbolically by ${\xi_1}^{l+m_1}\ {\eta_1}^{l-m_1}$ and $2s+1$ functions of the second type, which may be represented by ${\xi_2}^{s+m_2}\ {\eta_2}^{s-m_2}$. For the state with quantum number j of the multiplet there must be $2j+1$ functions which transform irreducibly under rotation and are composed linearly of terms ${\xi_1}^{l+m_1}\ {\eta_1}^{l-m_1}\ {\xi_2}^{s+m_2}\ {\eta_2}^{s-m_2}$. We introduce a constant spinor (a, b) and form the invariants

$$P = (\xi_2\eta_1 - \eta_2\xi_1);\ Q = (a\eta_1 - b\xi_1);\ R = (a\eta_2 - b\xi_2). \tag{8}$$

Then the state with quantum number j is represented by the invariant

$$\psi_{lsj} = P^\alpha Q^\beta R^\gamma, \tag{9}$$

where

$$\alpha+\beta = 2l;\ \alpha+\gamma = 2s;\ \beta+\gamma = 2j. \tag{10}$$

The $2j+1$ functions, which would be required for the study of the Zeeman effect, are the coefficients in ψ_{lsj} of $a^{j-m'}\ b^{j+m'}$ $(m' = -j, -j+1, \cdots, j)$.[5]

4.

We now proceed to show that every term of (6) makes a contribution to the energetic splitting of the multiplet which is, up to a numerical constant C_τ which does not depend on j, a completely determined function of l, s, j, and τ.

According to the principles of the quantum mechanics, the energy splitting E_τ, due to the interaction term (7), is given by

$$E_\tau \int \psi_{lsj}{}^* \psi_{lsj} = \int \psi_{lsj}{}^* \omega_\tau \psi_{lsj}, \tag{11}$$

where $\int$ means integration and summation over all space and spin coordinates. Both integrals are invariant under rotation and every term must contain (a, b) and (a^*, b^*) each to the power $2j$. The only invariant of (a, b) and (a^*, b^*) is (a^*a+b^*b) to some integral power. Therefore, these quantities appear in both integrals only in the form of a factor $(a^*a+b^*b)^{2j}$ and E_τ does not depend on (a, b).

[5] In case there were more than two vector frames composing our atomic system, we should form our wave functions of products of all the invariants $(\xi_i\eta_k - \eta_i\xi_k)$ and $(a\eta_k - b\xi_k)$ in such a way that in every term the sum of the powers of ξ_i and η_i is $2l_i$ and the sum of the powers of a and b is $2j$. In general, it will be possible to do this in a number of linearly independent ways, say f, which means that there will be f states of the multiplet with the same j value. To find the *stabilized* linear combinations of these f functions is a perturbation problem involving the solution of an f order secular determinant.

In (11), ω_τ is an operator which works on ψ_{lsj}. ω_τ is built up by multiplication and addition of operators which involve only the coordinates of the l-frame or only those of the s-frame. Accordingly, when we have written out all the terms in (11), every term may be put in the form

$$CI_1I_2$$

where I_1 and I_2 involve, respectively, the coordinates of the l-frame and of the s-frame and are integrals of the type:

$$I_1 = \int \xi_1^{*l+m_1'} \eta_1^{*l-m_1'} x_1^{\tau+\mu_1} y_1^{\tau-\mu_1} \xi_1^{l+m_1} \eta_1^{l-m_1}, \tag{12a}$$

$$I_2 = \int \xi_2^{*s+m_2'} \eta_2^{*s-m_2'} x_2^{\tau+\mu_2} y_2^{\tau-\mu_2} \xi_2^{s+m_2} \eta_2^{s-m_2}. \tag{12b}$$

The j value appears only in the factor C which contains, in a known manner, the expansion coefficients of the various factors in (11). We will show that, on account of the irreducibility of the transformations which the factors in I_1 and in I_2 suffer under space-rotation, both integrals are completely determined in their dependence on the various m's. There remains over only a common constant C_τ, in principle undeterminable by the symbolic method, which depends in general on l, s, τ, and the particular atomic system with which we have to do and which is of the nature of a radial integral.

All integrals of the type (12a) are obtained by comparing coefficients of like powers of the components of the constant spinors on the two sides of

$$\int (a^*\eta_1^* - b^*\xi_1^*)^{2l}(A y_1 - B x_1)^{2\tau}(a\eta_1 - b\xi_1)^{2l}$$
$$= \text{const}\,(a^*a + b^*b)^{2l-\tau}(a^*A + b^*B)^{\tau}(aB - bA)^{\tau}. \tag{13}$$

The evaluation of this integral follows directly from the invariance under rotation of all the factors in the integrand and of the domain of integration. The result must be built up of the three invariants of (a^*, b^*), (a, b) and (A, B) and these quantities appear to the proper powers only in the form given in (13).

5.

Having seen that the results of the integrations in (11) are determined by the transformation properties of the factors and therefore do not depend on the special form of the operators which occur in ω_τ, we may simplify the integration in (11) by choosing special expressions for the operators $x_k^{\tau+\mu}$ $y_k^{\tau-\mu}$ which transform in the same way. We have only to take care that in so doing we do not make the integral vanish identically.

Replacing $x_k^{\tau+\mu}$ $y_k^{\tau-\mu}$ by operators acting on functions of the symbols ξ_k and η_k, we shall obtain, in place of (12a) and (12b), integrals of the type

$$\int \xi_k^{*\rho'+\nu'} \eta_k^{*\rho'-\nu'} \xi_k^{\rho+\nu} \eta_k^{\rho-\nu}. \tag{14}$$

All integrals of this type are found by comparing coefficients on the two sides of

$$\int (a^*\eta^* - b^*\xi^*)^{2\rho'}(a\eta - b\xi)^{2\rho} = \text{const. } (a^*a + b^*b)^{2\rho}\delta_{\rho'\rho}, \tag{15}$$

where the results of integration are again determined immediately by the invariance. We find for (14) the result

$$\text{const.}\begin{pmatrix} 2\rho \\ \rho + \nu \end{pmatrix}^{-1} \delta_{\rho'\rho\nu'\nu}. \tag{16}$$

Thus we find that our choice of operators to replace $x_k^{\tau+\mu}$, $y_k^{\tau-\mu}$ is limited to such as make $\psi_{lsj}^*\ \omega_\tau\ \psi_{lsj}$ homogeneous in (ξ_k^*, η_k^*) to the same degree as in (ξ_k, η_k). The most satisfactory operators fulfilling this requirement are obtained from the formula

$$(Ay_k - Bx_k)^{2\tau} = (A\eta_k - B\xi_k)^\tau\left(A\frac{\partial}{\partial\xi_k} + B\frac{\partial}{\partial\eta_k}\right)^\tau. \tag{17}$$

Both sides are rotation-invariant and the $x_k^{\tau+\mu}\ y_k^{\tau-\mu}$ are uniquely defined by comparison of terms with the same powers of A and B. We may remark that the order of the factors on the right hand side of (17) is arbitrary since we have the same thing still after exchanging them. (17) is the special case $\rho = 0$ of the more general formula

$$(Ay_k - Bx_k)^{2\tau} = (A\eta_k - Bx_k)^{\tau+\rho}\left(A\frac{\partial}{\partial\xi_n} + B\frac{\partial}{\partial\eta_k}\right)^{\tau-\rho}. \tag{18}$$

The Configuration: Two Electrons, One in an s-State

6.

We shall now see how this symbolic method works as applied to spectra involving two valence electrons, of which one is in an s-state.[6]

The two electrons have angular momentum quantum numbers respectively l for the orbit, 1/2 for the spin and 0 for the orbit, 1/2 for the spin. The $2l+1$ wave functions of the orbital coordinates of the first particle, which transform irreducibly under rotation, may be represented symbolically by the $2l+1$ monomials $\xi^{l+m}\ \eta^{l-m}$. Likewise we have two monomials S_+ and S_- (the two components of a *spinor*; hence the name) to represent the spin functions of the first particle and two monomials $\bar{S}_+$ and $\bar{S}_-$ to represent the spin functions of the second. From the spinors (ξ, η), (S_+, S_-), $(\bar{S}_+, \bar{S}_-)$, and (a, b) we form the six invariants:

$$(a\eta - b\xi), (aS_- - bS_+), (a\bar{S}_- - b\bar{S}_+), (S_+\eta - S_-\xi), (\bar{S}_+\eta - \bar{S}_-\xi), (S_+\bar{S}_- - S_-\bar{S}_+).$$

[6] Houston (Phys. Rev. **33**, 297 (1929)) has treated this case, using the explicit wave functions and energy operators. The present treatment takes account of the interaction of the spin of each electron with the orbit of the other, which Houston did not consider. As we shall see in Part II, this interaction is not negligible.

These must be multiplied together to form polynomials homogeneous in (ξ, η) to the power $2l$, in (S_+, S_-) and in $(\bar{S}_+, \bar{S}_-)$ to the power one, and in (a, b) to the power $2j$.

We find (as we should expect from the vector model) that the only possible values of j are $l+1$, l, $l-1$. The symbolic functions for $j=l+1$ and $j=l-1$ are uniquely determined but there are three functions for $j=l$, of which two are independent. Thus our multiplet will consist of four levels (a triplet and a singlet in case of pure Russell-Saunders coupling). We form the symbolic functions:

$$\begin{aligned}
j &= l+1 \quad I = A\{(a\eta - b\xi)^{2l}(S_+b - S_-a)(\bar{S}_+b - \bar{S}_-a)\} \\
j &= l \begin{cases} II_\alpha = A\{(a\eta - b\xi)^{2l-1}(\bar{S}_+\eta - \bar{S}_-\xi)(S_+b - S_-a)\} \\ II_\beta = A\{(a\eta - b\xi)^{2l-1}(S_+\eta - S_-\xi)(\bar{S}_+b - \bar{S}_-a)\} \\ II_\gamma = A\{(a\eta - b\xi)^{2l}(S_+\bar{S}_- - S_-\bar{S}_+)\} \end{cases} \qquad (19) \\
j &= l-1 \quad III = A\{(a\eta - b\xi)^{2l-2}(S_+\eta - S_-\xi)(\bar{S}_+\eta - \bar{S}_-\xi)\}.
\end{aligned}$$

The symbol A in front of a bracket means to subtract from the expression in the bracket the same expression with (S_+, S_-) and $(\bar{S}_+, \bar{S}_-)$ interchanged and (ξ, η) replaced by $(\bar{\xi}, \bar{\eta})$. Expressions in $(\bar{\xi}, \bar{\eta})$ refer to functions of the coordinates of the second particle. Thus our wave functions are made to satisfy the Pauli principle requirement of antisymmetry.

7.

Of all the terms in the interaction energy of two electrons,[7] we shall neglect, to begin with, all except Ω_1, the electrostatic interaction,[8] e^2/r_{12}; Ω_2, the leading terms,

$$\frac{Ze^2}{2m_0c^2}\left\{\frac{([\mathbf{r}_1, \mathbf{v}_1]\cdot \mathbf{s}_1)}{r_1^3} + \frac{([\mathbf{r}_2, \mathbf{v}_2]\cdot \mathbf{s}_2)}{r_2^3}\right\},$$

in the interaction of the spin of each electron with its own orbital motion; Ω_3, the leading terms,

$$\frac{e^2}{m_0c^2}\left\{\frac{([\mathbf{r}_1, \mathbf{v}_1]\cdot \mathbf{s}_2)}{r_b^3} + \frac{([\mathbf{r}_2, \mathbf{v}_2]\cdot \mathbf{s}_1)}{r_b^3}\right\},$$

in the interaction of each spin with the orbit of the other electron. In Ω_2 and Ω_3 we have neglected all terms but the first in the expansion (3) of $1/r_{12}^3$.

To find the symbolic representation of Ω_1, we must use the expansion (3). Ω_1 then assumes the form $\sum_n a_n(\mathbf{r}_1\cdot\mathbf{r}_2)^n$, where the a_n are functions of the invariants, r_1 and r_2. Then the symbolic representation is

$$\sum_n a_n(x\bar{y} - y\bar{x})^{2n}. \qquad (20)$$

[7] See, for example, Heisenberg, Zeits. f. Physik **39**, 499 (1926).

[8] Of course, the term e^2/r_{12} does not properly constitute a small perturbation, since it is of considerable importance in fixing what one should like to consider as the *unperturbed* orbit. However, the true perturbation may be considered to be the difference between some well-chosen *central field* Hamiltonian and the true Hamiltonian in which e^2/r_{12} appears. The symbolic representation of this perturbation is the same as that of e^2/r_{12}.

In the matrix integrals which we wish to calculate, the factors coming from the wave functions will give us either (ξ^*, η^*) and (ξ, η) [or $(\bar{\xi}^*, \bar{\eta}^*)$ and $(\bar{\xi}, \bar{\eta})$] to the same power $2l$ or (ξ^*, η^*) and $(\bar{\xi}, \bar{\eta})$ [or $(\bar{\xi}^*, \bar{\eta}^*)$ and (ξ, η)] to the same power $2l$. Consequently, only the terms $n=0$ and $n=l$ in (20) will yield integrals different from zero. The term from $n=l$ is the so-called resonance term. Thus, for our purpose, the operator may be represented by[9]

$$\Omega_1 = A_0 + \frac{C_1}{(2l)!}\left\{\left(\xi\frac{\partial}{\partial\bar{\xi}} + \eta\frac{\partial}{\partial\bar{\eta}}\right)^{2l} + \left(\bar{\xi}\frac{\partial}{\partial\xi} + \bar{\eta}\frac{\partial}{\partial\eta}\right)^{2l}\right\}. \tag{21}$$

The operator Ω_2 is in the form to be represented symbolically by

$$C_2\{(Xy - Yx)^2 + (\bar{X}\bar{y} - \bar{Y}\bar{x})^2\}$$

where (x, y) is associated with the orbital coordinates and (X, Y) with the spin coordinates. We find the representation of Ω_2 in terms of the spinors which occur in the wave functions by a double use of (17):

$$\begin{cases} (Xy - Yx)^2 = (X\eta - Y\xi)\left(X\dfrac{\partial}{\partial\xi} + Y\dfrac{\partial}{\partial\eta}\right) \\ x^2 = -\xi\dfrac{\partial}{\partial\eta};\ xy = \dfrac{1}{2}\left(\xi\dfrac{\partial}{\partial\xi} - \eta\dfrac{\partial}{\partial\eta}\right);\ y^2 = \eta\dfrac{\partial}{\partial\xi} \end{cases}$$

$$\begin{cases} (Xy - Yx)^2 = (xS_- - yS_+)\left(x\dfrac{\partial}{\partial S_+} + y\dfrac{\partial}{\partial S_-}\right) \\ X^2 = -S_+\dfrac{\partial}{\partial S_-};\ XY = \frac{1}{2}\left(S_+\dfrac{\partial}{\partial S_+} - S_-\dfrac{\partial}{\partial S_-}\right);\ Y^2 = S_-\dfrac{\partial}{\partial S_+}. \end{cases}$$

Substituting these expressions, we obtain

$$\begin{aligned}\Omega_2 = C_2 S\Big\{&(S_+\eta - S_-\xi)\left(\frac{\partial^2}{\partial S_+\partial\eta} - \frac{\partial^2}{\partial S_-\partial\xi}\right) \\ &- \tfrac{1}{2}\left(\xi\frac{\partial}{\partial\xi} + \eta\frac{\partial}{\partial\eta}\right)\left(S_+\frac{\partial}{\partial S_+} + S_-\frac{\partial}{\partial S_-}\right)\Big\}\end{aligned} \tag{22}$$

where the symbol S in front of the bracket means to add to the expression in the bracket the same expression with barred and unbarred symbols interchanged.

The operator Ω_3 differs from Ω_2 only in the interchange of (S_+, S_-) and $(\bar{S}_+, \bar{S}_-)$.

$$\begin{aligned}\Omega_3 = C_3 S\Big\{&(\bar{S}_+\eta - \bar{S}_-\xi)\left(\frac{\partial^2}{\partial\bar{S}_+\partial\eta} - \frac{\partial^2}{\partial\bar{S}_-\partial\xi}\right) \\ &- \tfrac{1}{2}\left(\xi\frac{\partial}{\partial\xi} + \eta\frac{\partial}{\partial\eta}\right)\left(\bar{S}_+\frac{\partial}{\partial\bar{S}} + \bar{S}_-\frac{\partial}{\partial\bar{S}_-}\right)\Big\}.\end{aligned} \tag{23}$$

[9] The term for $n=l$ comes from (18) with $\tau=l$ and $\rho=-\tau$.

Applying the operator

$$\Omega = \Omega_1 + \Omega_2 + \Omega_3 \tag{24}$$

to the wave functions (19), we find

$$\begin{aligned}
\Omega \mathrm{I} &= \{A_0 + C_1 - l(C_2 + C_3)\}\mathrm{I} \\
\Omega \mathrm{II}_\alpha &= \{A_0 - lC_2 + (l+1)C_3\}\mathrm{II}_\alpha + \{C_1 + C_2\}\mathrm{II}_\beta \\
\Omega \mathrm{II}_\beta &= \{A_0 + (l+1)C_2 - lC_3\}\mathrm{II}_\beta + \{C_1 + C_3\}\mathrm{II}_\alpha \\
\Omega \mathrm{III} &= \{A_0 + C_1 + (l+1)(C_2 + C_3)\}\mathrm{III} \ .
\end{aligned} \tag{25}$$

The multiplet energy levels ϵ_1 and ϵ_3, defined by

$$\epsilon_1 \int \mathrm{I}^*\mathrm{I} = \int \mathrm{I}^*\Omega\mathrm{I}; \ \epsilon_3 \int \mathrm{III}^*\mathrm{III} = \int \mathrm{III}^*\Omega\mathrm{III}, \tag{26}$$

are given immediately by (25) without integration:

$$\begin{aligned}
\epsilon_1 &= A_0 + C_1 - l(C_2 + C_3) \\
\epsilon_3 &= A_0 + C_1 + (l+1)(C_2 + C_3).
\end{aligned} \tag{27}$$

To find the other two energy levels and to find the linear combinations of II_α and II_β to represent the stabilized zero-approximation wave functions, we must solve the second order secular perturbation problem. The stabilized functions may be written in the form

$$\begin{aligned}
\phi_2 &= \gamma_2\mathrm{II}_\alpha + \delta_2\mathrm{II}_\beta \\
\phi_4 &= \gamma_4\mathrm{II}_\alpha + \delta_4\mathrm{II}_\beta \ .
\end{aligned} \tag{28}$$

Then our γ_2, δ_2 and γ_4, δ_4 are the two solutions of

$$\begin{aligned}
\gamma(\Omega_{\alpha\alpha} - \epsilon\Delta_{\alpha\alpha}) + \delta(\Omega_{\alpha\beta} - \epsilon\Delta_{\alpha\beta}) &= 0 \\
\gamma(\Omega_{\beta\alpha} - \epsilon\Delta_{\beta\alpha}) + \delta(\Omega_{\beta\beta} - \epsilon\Delta_{\beta\beta}) &= 0
\end{aligned} \tag{29}$$

corresponding to the two roots ϵ_2, ϵ_4 of the determinant of the coefficients in (29). Here we have defined

$$\Omega_{\alpha\beta} = \int \mathrm{II}_\alpha^*\Omega\mathrm{II}_\beta; \ \Delta_{\alpha\beta} = \int \mathrm{II}_\alpha^*\mathrm{II}_\beta; \ \text{etc.} \tag{30}$$

Making use of (15) and of the integration formula

$$\begin{aligned}
\int (a^*\eta^* - b^*\xi^*)^{q+t}(a\xi^* + b\eta^*)^{q-t}(a\eta - b\xi)^{q+t'}(a^*\xi + b^*\eta)^{q-t'} \\
= \text{const.}\ \delta_{tt'}\binom{2q}{q-t}^{-1}(a^*a + b^*b)^{2q},
\end{aligned} \tag{31}$$

which is obtained by replacing a by $a+fb^*$ and b by $b-fa^*$ in (15) and equating the coefficients of like powers of ff^* in the result, we proceed to carry out

the integrations (30). It is convenient to integrate first over the spin variables and then to make use of the relation

$$(a^*a + b^*b)(\xi^*\xi + \eta^*\eta) = (a^*\eta^* - b^*\xi^*)(a\eta - b\xi) + (a\xi^* + b\eta^*)(a^*\xi + b^*\eta), \quad (32)$$

which leaves us integrals of the type (31). We find

$$\begin{aligned} \Delta_{\alpha\alpha} &= \Delta_{\beta\beta} = \text{const.}\ (2l+1)(a^*a + b^*b)^{2l}\cdot(1/l) \\ \Delta_{\alpha\beta} &= \Delta_{\beta\alpha} = \text{const.}\ (a^*a + b^*b)^{2l}\cdot(1/l). \end{aligned} \quad (33)$$

The integrals $\Omega_{\alpha\alpha}$, etc. are given in terms of these by (25).

For the secular determinant, we find

$$\begin{vmatrix} C_1+C_2+(2l+1)\{A_0-lC_2+(l+1)C_3-\epsilon\} & (2l+1)C_1+(l+1)(C_2+C_3)+A_0-\epsilon \\ (2l+1)C_1+(l+1)(C_2+C_3)+A_0-\epsilon & C_1+C_3+(2l+1)\{A_0+(l+1)C_2-lC_3-\epsilon\} \end{vmatrix} = 0. \quad (34)$$

The solution is

$$\epsilon = A_0 + (\tfrac{1}{2})(C_2 + C_3) \pm (l(l+1)(C_2 - C_3)^2 + [C_1 + (\tfrac{1}{2})(C_2 + C_3)]^2)^{1/2}.$$

If we define the quantities ρ and θ by

$$\begin{aligned} C_1 + (\tfrac{1}{2})(C_2 + C_3) &= \rho\cos 2\theta \\ [l(l+1)]^{1/2}(C_2 - C_3) &= \rho\sin 2\theta, \end{aligned} \quad (35)$$

we have, as the roots of (33),

$$\begin{aligned} \epsilon_2 &= A_0 + (\tfrac{1}{2})(C_2 + C_3) + \rho \\ \epsilon_4 &= A_0 + (\tfrac{1}{2})(C_2 + C_3) - \rho. \end{aligned} \quad (36)$$

The complete multiplet, given by (27) and (36), is

$$\begin{aligned} \epsilon_1 &= A_0 + C_1 - l(C_2 + C_3) \\ \epsilon_2 &= A_0 + C_1 + (C_2 + C_3) + 2\rho\sin^2\theta \\ \epsilon_3 &= A_0 + C_1 + (l+1)(C_2 + C_3) \\ \epsilon_4 &= A_0 - C_1 - 2\rho\sin^2\theta. \end{aligned} \quad (37)$$

We observe that, in the limit $\theta = 0$, ϵ_1, ϵ_2, ϵ_3 form a Russell-Saunders triplet with the intervals in the ratio $l+1$ to l, while ϵ_4 appears as a singlet at a distance proportional to the resonance energy, C_1. Using these limit values of ϵ_2 and ϵ_4 in (29) and substituting in (28), we find for the *pure triplet* and *pure singlet* linear combinations of II_α and II_β

$$\begin{aligned} \phi_t &= N_t(\mathrm{II}_\alpha + \mathrm{II}_\beta) \\ \phi_s &= N_s(\mathrm{II}_\alpha - \mathrm{II}_\beta) = N_s\mathrm{II}_\gamma. \end{aligned} \quad (38)$$

From (33), we find for the normalizing constants

$$N_t = \text{const. } l^{1/2}; N_s = \text{const. } (l+1)^{1/2}. \tag{39}$$

ϕ_t, like I and III, is antisymmetric in the coordinates, symmetric in the spins; ϕ_s is symmetric in the coordinates, antisymmetric in the spins.

Now, substituting for II_α and II_β in terms of ϕ_s and ϕ_t in (28) and using the values of γ and δ obtained by putting (36) in (29), we find for our stabilized wave functions

$$\begin{aligned} \phi_2 &= -\sin\theta\,\phi_s + \cos\theta\,\phi_t \\ \phi_4 &= \cos\theta\,\phi_s + \sin\theta\,\phi_t. \end{aligned} \tag{40}$$

Here the normalizing factors have already been introduced.

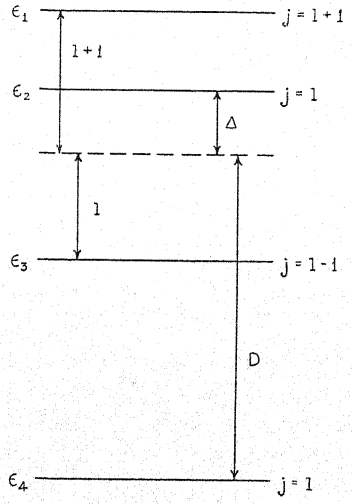


Fig. 1.

Introducing the notation $d_{12} = \epsilon_1 - \epsilon_2$, etc. and using the symbols Δ and D to represent the distances from the *normal* position of the center triplet level to ϵ_2 and ϵ_4 respectively (see Fig. 1) we find from (37)

$$\begin{aligned} \Delta &= \left| \left[(l+1)d_{23} - l d_{12}\right]/(2l+1) \right| \\ \Delta &= \left| d_{24} \right| - \Delta \\ \sin^2\theta &= \left[(l+1)d_{23} - l d_{12}\right]/\left[(2l+1)d_{24}\right] \\ C_1 &= (\tfrac{1}{2})(d_{24} + d_{12} - d_{23}) \\ C_2 + C_3 &= -(d_{12} + d_{23})/(2l+1) \\ C_2 - C_3 &= (\Delta D/l(l+1))^{1/2}. \end{aligned} \tag{41}$$

Since $\sin^2\theta$ must be positive, the sign of $(l+1)d_{23} - l d_{12}$ must be the same as the sign of d_{24}. This means that, if the singlet, ϵ_4, lies below the triplet, the

center triplet level, ϵ_2, must lie above its normal position and vice versa. A convenient way of stating this rule is that: *the center triplet level is repelled by the singlet level.*[10]

In (41), the quantities C_2 and C_3 are not completely determined since we do not know the sign of C_2-C_3. They become determined when we make the physical assumption that the interaction of the spin of each electron with its own orbital motion is larger than with that of the other electron, i.e., $|C_2|>|C_3|$. This is equivalent to making the sign of C_2-C_3 the same as the sign of C_2+C_3. This determines also the sign in (40) of the angle, θ, which was defined by (35). The sign of C_2+C_3 (and so likewise the sign of C_2-C_3) is always the same. Since we can express C_2-C_3 in the form

$$C_2 - C_3 = d_{24} \sin\theta \cos\theta/[l(l+1)]^{1/2},$$

we must change the sign of θ according as d_{24} is positive or negative, i.e., according as the singlet lies above or below the triplet.

8.

While ϵ_2 is regarded as a triplet level in spectral classification and ϵ_4 as a singlet, we observe in (40) that the wave functions for these states are partly singlet and partly triplet in character so that we may expect transitions between both of these levels and other singlet and triplet levels—i.e., we shall expect *forbidden* intercombinations between singlet and triplet systems as well as combinations within these systems—with relative intensities determined by θ.

The intensities of transitions between levels are proportional to the squared absolute values of the corresponding matrix elements of the polarization. Kramers has shown[1] how the symbolic method is adapted to calculating the matrix elements. The operators for the components of the polarization must have the transformation properties of the components of a space-vector. These operators may all be represented symbolically by the spinor invariant

$$\Omega = (AY - BX)^2, \tag{42}$$

where we make the association, according to the transformation properties,

$$P_x + iP_y \rightarrow X^2;\ -P_x + iP_y \rightarrow Y^2;\ P_z \rightarrow XY.$$

Brinkman[11] has shown in detail that calculation with the wave functions corresponding to Russell-Saunders multiplets leads to the well-known intensity rules as given by Kronig and by Hönl.[12] Hence, for our purpose, we may regard the matrix elements associated with the functions I, ϕ_t, III, ϕ_s as

[10] We must not expect this rule to hold in case of very small displacements of the center triplet from its normal position, since this may arise from cancellation of the opposite effects of the perturbations Ω_2 and Ω_3, in which case the effect of the other perturbation terms we have left out may not be negligible in comparison.

[11] Brinkman, Dissertation Utrecht 1932.

[12] Kronig, Zeits. f. Physik **31**, 885 (1925); **33**, 261 (1925). Hönl, Ann. d. Physik **79**, 273 (1926).

known. We may indicate the matrix elements for the group of transitions $l+1 \to l$ by

$$\int I\Omega\phi_t' = \Omega_{1t}, \text{ etc.} \tag{43}$$

where quantities referring to the final state are distinguished by a dash. We shall make explicit use of the fact that all matrix elements Ω_{1s}, Ω_{st}, etc., and all matrix elements for $|\Delta j| > 1$ vanish and that[13]

$$\Omega_{ss} = \frac{l+1}{[l(l+2)]^{1/2}}\,\Omega_{tt}. \tag{44}$$

Then we obtain, for the actual multiplet, the matrix elements

$$\begin{aligned}
&\int \mathrm{I}\Omega\mathrm{I}' = \Omega_{11}\\
&\int \phi_2\Omega I' = \cos\theta\,\Omega_{t1}\\
&\int \mathrm{III}\Omega\mathrm{I}' = \Omega_{31}\\
&\int \phi_4\Omega\mathrm{I}' = \sin\theta\,\Omega_{t1}\\
&\int \phi_2\Omega\phi_2' = \left\{\frac{l+1}{[l(l+2)]^{1/2}}\sin\theta\sin\theta' + \cos\theta\cos\theta'\right\}\Omega_{tt}\\
&\int \mathrm{III}\Omega\phi_2' = \cos\theta'\,\Omega_{3t}\\
&\int \phi_4\Omega\phi_2' = \left\{-\frac{l+1}{[l(l+2)]^{1/2}}\cos\theta\sin\theta' + \sin\theta\cos\theta'\right\}\Omega_{tt}\\
&\int \phi_2\Omega\phi_4' = \left\{-\frac{l+1}{[l(l+2)]^{1/2}}\sin\theta\cos\theta' + \cos\theta\sin\theta'\right\}\Omega_{tt}\\
&\int \mathrm{III}\Omega\phi_4' = \sin\theta'\,\Omega_{3t}\\
&\int \phi_4\Omega\phi_4' = \left\{\frac{l+1}{[l(l+2)]^{1/2}}\cos\theta\cos\theta' + \sin\theta\sin\theta'\right\}\Omega_{tt}\\
&\int \mathrm{III}\Omega\mathrm{III}' = \Omega_{33}.
\end{aligned} \tag{45}$$

The sum rules for intensity hold for the complete multiplet and not for the singlet and the triplet separately.[14] In applying the formulas (45), we must use the rule at the end of section 7 for determining the signs of θ and θ'.

[13] This relation is given by carrying out the symbolic integrations. Apart from the sign, it follows from the sum rules.

[14] Compare with Ornstein and Burger, Zeits. f. Physik **40**, 403 (1926).

9.

The formulas for the relative intensities of spectral lines, which are obtained by squaring the expressions in (45) and substituting in the Kronig-Hönl values for $|\Omega_{11}|^2$, $|\Omega_{t1}|^2$, etc., hold only in a sort of first approximation, i.e., with neglect of quantities of the order of magnitude $\Delta\nu/\nu$, where $\Delta\nu$ is the interval between the frequencies of the lines compared. In many cases this ratio is not small and the ambiguity may be correspondingly large. Thus we should not attempt to compare our results with experimental intensity ratios except for groups of lines of about the same frequency. The origin of this ambiguity lies in the fact that the matrix elements calculated, while assumed to be those of the polarization, might equally well be those of, say, the second time derivative of the polarization; for this quantity has the same rotation properties. But the squared matrix elements for these two quantities differ by a factor ν^4.

As remarked at the beginning of section 7, we have taken account only of certain selected terms in the interaction energy of two electrons as given by Heisenberg (reference 7). With the exception of the leading term in the spin-spin interaction, all of the neglected terms involve more than two vector-frames. To show how the method is applied in such cases, we treat now the leading term (i.e., we take only the first term in the expansion (3)) in the interaction

$$\frac{e^2}{m_0c^2}\left\{\frac{([\mathbf{r}_1, \mathbf{v}_2]\cdot \mathbf{s}_1) + ([\mathbf{r}_2, \mathbf{v}_1]\cdot \mathbf{s}_2)}{r_{12}^3}\right\}. \tag{46}$$

The expression $([\mathbf{r}_1, \mathbf{v}_2]\cdot \mathbf{s}_1)$ involves the orbital motions of both particles and the spin of one of them. To obtain a symbolic representation, we associate each of the vectors with a spinor:

$$\mathbf{r}_1 \rightarrow (x, y);\ \mathbf{v}_2 \rightarrow (X, Y);\ \mathbf{s}_1 \rightarrow (r, s).$$

We may make the association in this way. If (a, b, c) are the components of a vector and (ξ, η) are the components of a spinor, we may set[15]

$$a = \tfrac{1}{2}(\xi^2 - \eta^2);\quad b = -\frac{i}{2}(\xi^2 + \eta^2);\quad C = -\xi\eta.$$

This gives us, as the symbolic representation of $([\mathbf{r}_2, \mathbf{v}_2]\cdot \mathbf{s}_2)$,

$$(rY - sX)(ry - sx)(Xy - Yx). \tag{47}$$

We proceed to replace each of these spinors by operators involving the spinor representing the corresponding vector-frame in the wave functions. Thus we substitute

for (x, y) expressions involving $\xi, \eta, \partial/\partial\xi, \partial/\partial\eta$;
for (X, Y) expressions involving $\bar{\xi}, \eta, \partial/\partial\bar{\xi}, \partial/\partial\bar{\eta}$;
for (r, s) expressions involving $S_+, S_-, \partial\overline{S}_+, \partial/\partial\overline{S}_-$.

We observe that, in general, it will not be possible to find an operator representing this interaction term whose matrix elements do not vanish identically. Only in case $l=1$ do we get integrals different from zero. The operator may be

[15] ξ, η are the coordinates by stereographic projection of a point a, b, c on the zero sphere.

put into a form where it contains first derivatives with respect to S_+ and S_- and either second derivatives with respect to ξ and η and no derivatives with respect to $\bar{\xi}$ and $\bar{\eta}$ or second derivatives with respect to $\bar{\xi}$ and $\bar{\eta}$ and no derivatives with respect to ξ and η. We then obtain nonvanishing resonance integrals when $l=1$.

To get (47) into a form where we can use (18), we introduce a symbol T_f which means to pick out the coefficient of f in the expression following.

$$(ry - sx)(Xy - Yx) = \tfrac{1}{2}T_f\{(X + fr)y - (Y + fs)x\}^2$$

$$\rightarrow \tfrac{1}{2}T_f\left\{(X + fr)\frac{\partial}{\partial\xi} + (Y + fs)\frac{\partial}{\partial\eta}\right\}^2 = \left(r\frac{\partial}{\partial\xi} + s\frac{\partial}{\partial\eta}\right)\left(X\frac{\partial}{\partial\xi} + Y\frac{\partial}{\partial\eta}\right).$$

Applying (18) a second time[16]

$$(rY - sX)\left(r\frac{\partial}{\partial\xi} + s\frac{\partial}{\partial\eta}\right) = \tfrac{1}{2}T_f\left\{\left(Y + f\frac{\partial}{\partial\xi}\right)r - \left(X - f\frac{\partial}{\partial\eta}\right)s\right\}^2$$

$$\rightarrow \tfrac{1}{2}T_f\left\{\left(Y + f\frac{\partial}{\partial\xi}\right)S_+ - \left(X - f\frac{\partial}{\partial\eta}\right)S_-\right\}\left\{\left(X - f\frac{\partial}{\partial\eta}\right)\frac{\partial}{\partial S_+} + \left(Y + f\frac{\partial}{\partial\xi}\right)\frac{\partial}{\partial S_-}\right\}$$

$$= \tfrac{1}{2}\left\{(S_+Y - S_-X)\left(\frac{\partial^2}{\partial\xi\partial S_-} - \frac{\partial^2}{\partial\eta\partial S_+}\right) + \left(S_+\frac{\partial}{\partial\xi} + S_-\frac{\partial}{\partial\eta}\right)\left(X\frac{\partial}{\partial S_+} + Y\frac{\partial}{\partial S_-}\right)\right\}.$$

In the final step, we have simply $X\rightarrow\bar{\xi}$, $Y\rightarrow\bar{\eta}$. This gives us the symbolic operator for (47) in the form

$$\left\{(S_+\bar{\eta} - S_-\bar{\xi})\left(\frac{\partial^2}{\partial\xi\partial S_-} - \frac{\partial^2}{\partial\eta\partial S_+}\right) + \left(S_+\frac{\partial}{\partial\xi} + S_-\frac{\partial}{\partial\eta}\right)\left(\bar{\xi}\frac{\partial}{\partial S_+} + \bar{\eta}\frac{\partial}{\partial S_-}\right)\right\}\left(\bar{\xi}\frac{\partial}{\partial\xi} + \bar{\eta}\frac{\partial}{\partial\eta}\right).$$

The other usable form of the operator differs from this only in the interchange of $(\bar{\xi}, \bar{\eta})$ and (ξ, η). The term $([\boldsymbol{r}_2, \boldsymbol{v}_1]\cdot\mathbf{s}_2)$ yields operators which differ from these two by a complete interchange of barred and unbarred quantities. Obtaining symmetrical operators by lumping together those operators that differ from each other by a complete interchange and putting them in a somewhat different form, we find as the operator representing the leading term in (46),

$$\begin{aligned}\omega = {} & C_4\cdot S\left\{\left(\bar{\xi}\frac{\partial}{\partial\xi} + \bar{\eta}\frac{\partial}{\partial\eta}\right)\left[(S_+\bar{\eta} - S_-\bar{\xi})\left(\frac{\partial^2}{\partial S_+\partial\eta} - \frac{\partial^2}{\partial S_-\partial\xi}\right)\right.\right. \\ & \left.\left. - \tfrac{1}{2}\left(\bar{\xi}\frac{\partial}{\partial\xi} + \bar{\eta}\frac{\partial}{\partial\eta}\right)\left(S_+\frac{\partial}{\partial S_+} + S_-\frac{\partial}{\partial S_-}\right)\right]\right\} \\ & + C_5\cdot S\left\{\left(\xi\frac{\partial}{\partial\bar{\xi}} + \eta\frac{\partial}{\partial\bar{\eta}}\right)\left[(S_+\eta + S_-\xi)\left(\frac{\partial^2}{\partial S_+\partial\bar{\eta}} - \frac{\partial^2}{\partial S_-\partial\bar{\xi}}\right)\right.\right. \\ & \left.\left. - \tfrac{1}{2}\left(\xi\frac{\partial}{\partial\bar{\xi}} + \eta\frac{\partial}{\partial\bar{\eta}}\right)\left(S_+\frac{\partial}{\partial S_+} + S_-\frac{\partial}{\partial S_-}\right)\right]\right\}.\end{aligned} \tag{48}$$

[16] $\partial/\partial\xi$ transforms like η and $\partial/\partial\eta$ like $-\xi$.

In the special case $l=1$, we apply the operator (48) to the wave functions (19) and find

$$\begin{aligned}\omega \mathrm{I} &= (C_4 + C_5)\mathrm{I}\\ \omega \mathrm{II}_\alpha &= -C_4\mathrm{II}_\alpha + (C_4 - 2C_5)\mathrm{II}_\beta\\ \omega \mathrm{II}_\beta &= -C_5\mathrm{II}_\beta + (C_5 - 2C_4)\mathrm{II}_\alpha\\ \omega \mathrm{III} &= (C_4 + C_5)\mathrm{III}.\end{aligned}$$

In addition to neglecting what we believe to be the unimportant terms in the interaction energy, we have made another omission which may in some cases completely invalidate our results. We have assumed in our treatment of the interaction of two electrons as a perturbation that each electron configuration (defined by the n and l values for the two electrons) may be treated quite by itself. This treatment is valid only so long as there are not similar terms of nearly equal energy arising from different configurations.[17] As we follow through a series of terms from configurations differing in the n value of one of the electrons, irregularities in the values of n^* reveal the presence of perturbing terms arising from other types of configuration. Shenstone and Russell[18] have shown that perturbations of this sort are common. We cannot expect our formulas (41) for the energies of the different interaction terms as functions of the multiplet intervals to have much meaning for a configuration which is much perturbed by a neighboring one.

Part II of this paper, containing the application of the theory developed in Part I to observed spectra, will appear later. The relative energy values of the different types of interaction will be calculated for many spectra. The calculated intensities of certain multiplet lines in the spectrum of mercury will be compared with the experimental values.

The writer wishes to express his thanks to the Lorentz Foundation for the grant of a fellowship and to Professor Kramers for suggesting this problem and for many discussions while the work was in progress.

[17] This was first emphasized by Condon, Phys. Rev. **36**, 1121 (1930).
[18] Shenstone and Russell, Phys. Rev. **39**, 415 (1932).

The Isotope Shift in Hyperfine Structure

By JENNY E. ROSENTHAL AND G. BREIT
New York University, University Heights

(Received July 8, 1932)

The effect of deviations of the nuclear field from the inverse square law such as are suggested by the theory of radioactive disintegration is calculated. The isotope shift due to a change of the nuclear radius by 1 percent is found to be larger than those observed. The spectrum of Tl appears not to fit any simple modification of the theory. The isotope shifts in Pb I and Pb II can be explained roughly on the supposition that the deviations of the nuclear field from the inverse square law are local but that for the valence electrons these deviations should be taken to be smaller than is usually supposed in the theory of radioactive disintegration.

§1. INTRODUCTION

IN THE analysis of the *hfs* of Tl,[1,2] Pb[3,4,5] and Hg[6,7] there have been observed isotope shifts of the order of magnitude of 0.05 cm^{-1} in the arc spectra to 0.5 cm^{-1} in the spark spectra. It has been pointed out[1] that this displacement is greater than that to be expected on account of the mass correction to the Rydberg constant and that it might possibly be due to deviations of the nuclear electric field from the Coulomb law. The effect of such deviations has been investigated by Bartlett[8] with the apparent result that they may easily account for the observed isotope displacement. In view of the fact that Bartlett's estimate does not take into account the relativisitic nature of the electron and the screening of the nucleus by the other electrons it has been thought of interest to make a more detailed calculation. Since this work was completed there appeared a letter of Racah[9] in which the same effect is estimated for S terms of Hg with the result that it is hard to explain why the isotope shifts are as small as they are. This is in agreement with our calculations. In the course of the work the effect has been estimated for other terms as well with the same result for some and quite different results for others. Also the effect of the deviations of the nuclear field from the Coulomb law on the interaction of the electron with the nuclear spin has been estimated.

[1] H. Schuler and J. E. Keyston, Zeits. f. Physik **70**, 1 (1931).
[2] D. A. Jackson, Zeits. f. Physik **75**, 233 (1932).
[3] H. Kopfermann, Zeits. f. Physik **75**, 363 (1932); Naturwiss. **19**, 400 (1931); **19**, 675 (1931).
[4] J. L. Rose and L. P. Granath, Phys. Rev. **40**, 760 (1932).
[5] H. Schuler and E. G. Jones, Zeits. f. Physik **75**, 563 (1932).
[6] H. Schuler and J. E. Keyston, Zeits. f. Physik **72**, 423 (1931).
[7] H. Schuler and E. G. Jones, Zeits. f. Physik **74**, 631 (1932).
[8] J. H. Bartlett, Nature **128**, 408 (1931).
[9] G. Racah, Nature **129**, 723 (1932). In this letter the potential inside the nucleus is supposed to be constant and at the boundary of the nucelus it is taken to be continuous. Below the potential is taken to be discontinuous at the nuclear boundary so as to represent the potential wall of nuclear models for α-particle emission. In comparing the formulas in this paper with those of Racah one should start with (11) since in (11a) Δv is supposed to be zero. The resultant isotope shift becomes then $1/(2\rho+1)$ of (11a) with $v=0$ in the latter formula.

§2. Solutions of the Wave Equation

The central field equations for the Darwin-Gordon radial functions ϕ_1 and ϕ_2 for Dirac's equation are:

$$\begin{aligned}(d\phi_1/dy) - j'\phi_1/y &= (\tfrac{1}{2}a)[1 - (E - V)/mc^2]\phi_2 \\ (d\phi_2/dy) + j'\phi_2/y &= (\tfrac{1}{2}a)[1 + (E - V)/mc^2]\phi_1 \\ y = 8\pi^2 mZe^2 r/h^2 &= 2Zr/a_H;\ a = Z\alpha = 2\pi Ze^2/he\end{aligned} \tag{1}$$

Z is the atomic number, a_H the radius of the first Bohr orbit for hydrogen, E is the energy and V the potential energy and j' is the quantum number (analogous to Sommerfeld's k) taking the values $-1, +1, -2, +2, -3, \cdots$ for $S_{1/2}, P_{1/2}, P_{3/2}, D_{3/2}, D_{5/2} \cdots$ terms respectively.

We consider first the solutions of Eqs. (1) for $y<y_0$, where y_0 is the value of y corresponding to the nuclear radius r_0. If we assume a Gamow field inside the nucleus, V is constant for $y<y_0$. A satisfactory approximation is obtained by letting $E/mc^2=1$ which means that the term value energy is negligible in comparison with mc^2. The solutions can then be written:

$$\begin{aligned}\phi_1 &= sy^{1/2}J_{|j'-1/2|}(v^{1/2}(v-2)^{1/2}y/(2a)) \\ \phi_2 &= \mp sv^{-1/2}(v-2)^{1/2}y^{1/2}J_{|j'+1/2|}(v^{1/2}(v-2)^{1/2}y/(2a))\ \ (j' \gtrless 0).\end{aligned} \tag{2}$$

The positive index of the Bessel functions is required by the condition of integrability; $v=V/mc^2$ and s are constants, $y<y_0$ is small and if $|v|$ is not very large the Bessel functions are sufficiently accurately represented by their first term. The values of v for which this is valid may be taken to be given by $-20<v<20$. In this approximation:

$$\phi_1 = k^{(1)}y';\ \phi_2 = k^{(2)}(2-v)y^{j'+1}/[2a(2j'+1)]\ \ (j'>0) \tag{3'}$$

$$\phi_1 = k^{(2)}y^{1+|j'|}v/[2a(1+2|j'|)];\ \phi_2 = k^{(2)}y^{|j'|}\ \ (j'<0) \tag{3''}$$

and

$$\begin{aligned}\phi_1/\phi_2 &= 2a(2j'+1)/[(2-v)y]\ \ (j'>0) \\ \phi_1/\phi_2 &= vy/[2a(1+2|j'|)]\ \ (j'<0)\end{aligned}$$

$k^{(1)}$ and $k^{(2)}$ are constants which will be determined later.

In the region $y>y_0$, V is the Coulomb potential and the equations for ϕ_1 and ϕ_2 are:

$$\begin{aligned}(d\phi_1/dy) - j'\phi_1/y &= (1/2a)[1 - (E/mc^2) - 2a^2/y]\phi_2 \\ (d\phi_2/dy) + j'\phi_2/y &= (1/2a)[1 + (E/mc^2) + 2a^2/y]\phi_1.\end{aligned} \tag{5}$$

Letting as before $E/mc^2=1$, we have as the solution of Eqs. (5)

$$\begin{aligned}\phi_1/a &= CJ_{2\rho}(2y^{1/2}) + C_{-}J_{-2\rho}(2y^{1/2}) \\ \phi_2 &= CA_{2\rho}(2y^{1/2}) + C_{-}A_{-2\rho}(2y^{1/2})\end{aligned} \tag{6}$$

with the abbreviations:

$$A_{2\rho} = (j' - \rho)J_{2\rho} + y^{1/2}J_{2\rho+1}$$
$$A_{-2\rho} = (j' - \rho)J_{-2\rho} - y^{1/2}J_{-2\rho-1} \tag{7}$$

where C and C_- are constants.

The condition of continuity across the boundary is:

$$\phi_1(y_0 - \epsilon) = \phi_1(y_0 + \epsilon), \quad \phi_2(y_0 - \epsilon) = \phi_2(y_0 + \epsilon); \quad \epsilon \to 0. \tag{8}$$

Substitution of the actual solutions for ϕ_1 and ϕ_2 into (8) gives:

$$C[(\phi_1/a\phi_2)A_{2\rho} - J_{2\rho}] = C_-[J_{-2\rho} - (\phi_1/a\phi_2)A_{-2\rho}]. \tag{9}$$

The argument of the functions $J_{2\rho}$, etc. is $2y_0^{1/2}$; $\phi_1/a\phi_2$ is given by (4′) or (4″) depending on whether $j'>0$ or $j'<0$. Condition (8) also gives $k^{(1)}$ (respectively $k^{(2)}$) in terms of C and C_-.

If the field were Coulomb at the nucleus, C_- would be zero since the condition of integrability for ϕ_1 and ϕ_2 must be satisfied. The presence of the Gamow field results therefore in a modification of the eigenfunctions represented by the term in C_-. These modified or perturbed eigenfunctions will be denoted by ϕ_1 and ϕ_2; the unperturbed functions (i.e., functions with $C_-=0$) will be written as ϕ_1^0 and ϕ_2^0.

The ratio C_-/C as given by (9) was computed for a wide range of values of v in order to see to what extent the wave function is affected by deviations of the potential from the inverse square law. The results of this calculation for $j'=\pm 1$ are tabulated below. They are accurate within 5 percent for $-20<v<20$. The formulas also may be used to compute C_-/C for values of v lying outside these limits but the results will be less accurate due to the fact that for large values of $|v|$ (3′) respectively (3″) are no longer satisfactory approximations to (2). For $j'=-2$, C_-/C was estimated to be quite negligible in comparison with those for $j'=\pm 1$.

TABLE I. $Z=81$

$r_0 = 10^{-12}$ cm; $y_0 = 0.03$, $a = 0.590$, $\rho = 0.807$

$J_{2\rho} = 0.0403$, $J_{2\rho+1} = 0.0027$, $J_{-2\rho} = -4.736$, $J_{-2\rho-1} = 43.0$

$j' = 1$, $A_{2\rho} = 0.0082$, $A_{-2\rho} = -8.356$, $\phi_1/a\phi_2 = 200/(2 - v)$

$C(1.58 + 0.0403v) = C_-(4.736v + 1662)$

$j' = -1$, $A_{2\rho} = -0.0724$, $A_{-2\rho} = 1.116$, $\phi_1/a\phi_2 = v/69.6$

$C(0.0724v + 2.81) = C_-(1.116v + 330.0)$

v:	-20	-4	0	4	20
$C_-/C(j'=1)$;	0.0005	0.0009	0.0009	0.0010	0.0014
$C_-/C(j'=-1)$;	0.0044	0.0077	0.0085	0.0093	0.0120

$$Z = 91$$

$r_0 = 10^{-12}$ cm; $y_0 = 0.035$, $a = 7^{1/2}/4$, $\rho = \frac{3}{4}$

$J_{2\rho} = 0.0600$, $J_{2\rho+1} = 0.0044$, $J_{-2\rho} = -3.722$, $J_{-2\rho-1} = 28.62$

$j' = 1$, $A_{2\rho} = 0.0158$, $A_{-2\rho} = -6.286$

$C_-(5.440 + 0.1259v) = C(2245 + 7.806v)$

$j' = -1$ $A_{2\rho} = -0.1042\, A_{-2\rho} = 1.158$

$C_-(7.806 + 0.0324v) = C(0.1259 + 0.0029)$

v:	-20	-4	0	4	20
$C_-/C(j' = 1)$;	0.0014	0.0022	0.0024	0.0026	0.0033
$C_-/C(j' = -1)$;	0.0095	0.0149	0.0161	0.0173	0.0218

§3. The Isotope Displacement

Corresponding to a change δV of the potential inside the nucleus there is a change δW in the energy. The usual way of evaluating it is by means of the perturbation method using the unperturbed functions ϕ_1^0 and ϕ_2^0 corresponding to $C_- = 0$

$$\delta W = \int_0^{r_0} [V + (Ze^2/r)](\phi_1^{(0)2} + \phi_2^{(0)2})dr \tag{10}$$

where the normalization is such that

$$\int_0^{\infty} (\phi_1^{(0)2} + \phi_2^{(0)2})dr = 1.$$

To evaluate (10) $\phi_1^{(0)}$ and $\phi_2^{(0)}$ are expanded in terms of y. For small values of y such as $0 < y < y_0$ these expansions converge very rapidly, and for a first approximation it is sufficient to use only the first term of each expansion.

$$\phi_1^{(0)2} + \phi_2^{(0)2} = 2C^2j'(j' - \rho)y^{2\rho}/\Gamma^2(2\rho + 1).$$

Performing the integration we get:

$$\delta W = 2Ze^2C^2j'(j' - \rho)[(y_0^{2\rho}/2\rho) + (v/2a^2)y_0^{2\rho+1}/(2\rho + 1)]/\Gamma^2(2\rho + 1). \tag{11}$$

Supposing that y_0 changes by Δy_0 and that v remains unchanged δW changes by:

$$\Delta\delta W = 2Ze^2C^2j'(j' - \rho)[y_0^{2\rho} + (v/2a^2)y_0^{2\rho+1}](\Delta y_0/y_0)/\Gamma^2(2\rho + 1). \tag{11a}$$

For S terms the magnitude of the isotope shift can be conveniently expressed in terms of the value of $\psi^2(0)$ which the square of the nonrelativistic Schroedinger function $\overline{\psi}$ would have at $r = 0$. The normalization of the function ψ is for S terms such that

$$4\pi \int_0^{\infty} \psi^2 \cdot r^2 dr = 1.$$

The function ϕ_2 for all but very small values of r satisfies the same differential equation as $r\psi$. It may be equated to the latter provided ϕ_1 and ϕ_2 are normalized so as to have

$$4\pi \int_0^\infty (\phi_1^2 + \phi_2^2) dr = 1.$$

The expression for $\Delta\delta W$ given by (11) must then be also multiplied by 4π.

The leading term in the expression for ϕ_2 at not too small y is $Cy^{1/2} J_{2\rho+1}(2y^{1/2})$. Nonrelativistically the function $r\psi$ must have the form $-C'y^{1/2}J_1(2y^{1/2})$. The constants C and C' should be the same because the asymptotic expansions of the Bessel functions differ only by a constant phase in the trigonometric term. We have thus

$$\psi(0) = -C(y/r) = -C(2Z/a_H).$$

Substituting into (11) and noting that

$$2Ze^2C^2 = (e^2/2a_HZ)a_H{}^3\psi^2(0) = (R_\infty/Z)a_H{}^3\psi^2(0)$$

where R_∞ is the energy corresponding to the Rydberg constant we have

$$\Delta\delta W = \frac{4\pi R_\infty}{Z} a_H{}^3\psi^2(0) \frac{1+\rho}{[\Gamma(2\rho+1)]^2}\left[y_0{}^{2\rho} + \frac{v}{2a^2} y_0{}^{2\rho+1}\right]\frac{\Delta y_0}{y_0} \qquad (12)$$

which is in agreement with Racah's[9] formula.

Supposing $v=0$ and using Racah's[10] value $\psi^2(0)=0.49\times10^{26}$ cm^{-3} for the $7s$ term of Tl I we obtain for it

$$\Delta\delta W \leqq 360(\Delta y_0/y_0) \text{ cm}^{-1}.$$

If $\Delta y_0/y_0 \leqq 0.01$ the isotope shift for this term should be 3.6 cm^{-1} which is much too large according to Schüler and Keyston[1] and to Jackson.[2] This value may conceivably have to be multiplied by a factor of about 1/2 (see §4 below) in order to take into account the change in the wave functions due to the finite size of the nucleus and it may have to be multiplied by 1/3 to take into account the fact that the nuclear radius would be expected to vary with the cube root of the atomic number rather than with the first power. But even 0.6 cm^{-1} appears much too large for this term particularly when it is considered that according to Schüler and Keyston the isotope shift for it is considerably less than that for 7 $^2P_{1/2}$ which itself is about 0.05 cm^{-1}. It should be noted that the magnetic moment of the Tl nucleus as calculated[10,11] using the splitting of the 6^2S term and the value of $\psi^2(0)$ used above is smaller than that calculated using the splitting of 7 $^2P_{1/2}$ by a factor of about 4. It appears that the interaction of the $6s$ electron of Tl I with the nuclear spin as well as with the Gamow trough is smaller in reality than would be expected by comparison with other terms of the same spectrum.

[10] Racah, Il Nuovo Cimento **8**, 178 (1931); Zeits. f. Physik **71**, 431 (1931).
[11] G. Breit, Phys. Rev. **38**, 463 (1931), see p. 471.

For P, D, $\cdots$ terms of single electron spectra the magnitude of C can be obtained from the doublet splitting of these terms as has been already done in the discussion of the hyperfine structure by Racah.[10] Using Sommerfeld's doublet splitting formula one obtains for the energy difference between two parts of the doublet

$$\delta = 2l(l+1)(2l+1)Z\mu_0^2\{[(l+1)^2-a^2]^{1/2}-1-(l^2-a^2)^{1/2}\}a^{-2}\overline{(r^{-3})}_{\text{Schr}}$$
$$(\mu_0 = eh/(4\pi mc))$$

where the suffix "Schr" indicates that the average of r^{-3} is to be taken using Schroedinger's nonrelativistic wave functions. If the relativistic effects were absent we would have

$$\phi_2 = r\psi = C\lim_{a\to 0} A_{2\rho} = \pm Cy^{1/2}J_{2l+1}(2y^{1/2}) \quad (j' \gtrless 0). \tag{13}$$

For sufficiently large values of y there is no difference between the Dirac and the Schroedinger wave equations. The amplitude of the oscillations of the wave function as given by (7) is the same as that given by the nonrelativistic Eq. (13) provided the same values are given to C in the two expressions. The value of C is thus determined in terms of $\overline{(r^{-3})}$ by

$$\overline{(r^{-3})}_{\text{Schr}} = C^2(32Z^2a_H^{-2})\int_0^\infty J_{2l+1}^2(z)z^{-3}dz = 2C^2Z^2a_H^{-2}/[l(l+1)(2l+1)]$$

where a_H is the Bohr radius. Using now the relation between $(r^{-3})_{\text{Schr}}$ and δ and the expression (11) we have

$$\delta W = 2j'(j'-\rho)[\Gamma(2\rho+1)]^{-2}\{[(l+1)^2-a^2]^{1/2}-1$$
$$-(l^2-a^2)^{1/2}\}^{-1}[(y_0^{2\rho}/2\rho)+(v/2a^2)y_0^{2\rho+1}/(2\rho+1)]\delta.$$

Keeping v constant the change in δW due to a change in the nuclear radius corresponding to a change Δy_0 in y_0 is

$$\Delta\delta W = 2j'(j'-\rho)[\Gamma(2\rho+1)]^{-2}\{[(l+1)^2-a^2]^{1/2}-1$$
$$-(l^2-a^2)^{1/2}\}^{-1}[y_0^{2\rho}+(v/2a^2)y_0^{2\rho+1}](\Delta y_0/y_0)\delta. \tag{14}$$

For the $P_{1/2}$ normal level of Tl I substitution of $j'=1$, $\rho=0.807$, $y_0=0.03$, $\delta=7792$ cm^{-1} gives

$$\Delta\delta W \leqq 49(\Delta y_0/y_0)\text{ cm}^{-1}.$$

The difference in the term values of $P_{1/2}$ for the isotopes 203 and 205 would be estimated therefore to be of the order of 0.5 cm^{-1} if it is supposed that the nuclear radius differs for these two isotopes by 1 percent. The isotope shift for $P_{3/2}$ should be negligible in comparison. According to Schüler and Keyston[1] the difference in $\Delta(\delta W)$ for $P_{1/2}$ and $P_{3/2}$ is not greater than about 0.05 cm^{-1} and according to Jackson[2] it is probably of the order of 0.01 cm^{-1}. The calculated value is, therefore, considerably greater than that observed.

Essentially the same result is obtained using direct numerical calculations[11] for the wave functions ϕ_1, ϕ_2. One finds that at the nucleus $\phi_1^2+\phi_2^2 = 9.82\times10^{-4}\,y^{2\rho}/a_H$ which leads to

$$\Delta\delta W \leqq 60(\Delta y_0/y_0)\text{ cm}^{-1}.$$

§4. Validity of the Perturbation Method

Although δW is small the fields responsible for it are large so that it is not clear without an additional calculation to what extent the first order of the perturbation method is a valid approximation. It will be seen that a correction factor of the order of 1/2 must in fact be applied for the calculation of $\Delta(\delta W)$. This correction is clearly not large enough to bring about agreement with experiment for the S term of Tl.

As long as one is interested in changes of the nuclear radius the only thing which matters for $\Delta(\delta W)$ is the value of $\phi_1^2+\phi_2^2$ at $y=y_0$ because $\Delta(\delta W)$ may be considered as the change in the energy due to the perturbing potential $(Ze^2/r)+V$ applied in the region $r_0<r<r_0+\Delta r_0$. It is, furthermore, clear from the numerical calculations given above that the wave functions are practically unaffected by this perturbation. It is, therefore, sufficient to multiply the values so far obtained for $\Delta(\delta W)$ by the ratio of the (*perturbed*) value of $\phi_1^2+\phi_2^2$ at $y=y_0$ to the approximate (*unperturbed*) value which has been used so far. This ratio is found by observing that the constant C in (6) must be practically independent of y_0 and v for the range of values considered. In fact for large y the asymptotic expansions of the Bessell functions make (6) equivalent to

$$\phi_2 = y^{1/4}\pi^{-1/2}[C^2 + C_-^2 - 2CC_- \cos(2\rho+1)\pi]^{1/2} \cos(2y^{1/2} - \epsilon)$$

where ϵ is a constant phase (independent of y) which is immaterial for the present purpose. The function ϕ_2 is therefore essentially an oscillating function the amplitude of which depends on C, C_-. The dependence on C_- is seen however to be very slight in view of the small values of C_-/C. The amplitude of the oscillations for large y must be the same whether the nucleus has a finite size or not because it is determined by the continuation of the wave function from still larger values in towards the nucleus. We will thus suppose that C has the same value whether the nucleus gives a purely Coulomb field or whether it has a finite size. The factor by which the previously calculated values should be multiplied is then by (6)

$$[a^2J_{2\rho}^2 + A_{2\rho}^2 + 2(C_-/C)(a^2J_{2\rho}J_{-2\rho} + A_{2\rho}A_{-2\rho}) + (C_-/C)^2(a^2J_{-2\rho}^2 + A_{-2\rho}^2)]/(a^2J_{2\rho}^2 + A_{2\rho}^2).$$

For Tl $P_{1/2}$, $S_{1/2}$ terms this factor has the values:

$$P_{1/2}\ (j'=1): \quad 1 - 422.8(C_-/C) + 1.22\times 10^5(C_-/C)^2$$
$$S_{1/2}\ (j'=-1): 1 - 50.76(C_-/C) + 1561(C_-/C)^2.$$

Using the values of C_-/C tabulated above it is seen that the correction factor is generally greater than 1/2 and lies between 1/2 and 1. For any given v it is readily computed by the above formulas.

§5. Effect of Nuclear Field on Hyperfine Structure

The coupling of the electron to the nuclear spin axis is known to depend on the radial integrals[10,11]

$$I = \int_0^\infty \phi_1\phi_2 y^{-2} dy.$$

It has been seen in §4 that $\phi_1^2+\phi_2^2$ in the neighborhood of the nucleus is smaller than its unperturbed value $\phi_1^{(0)2}+\phi_2^{(0)2}$ corresponding to an inverse square field of force. It may be expected that $\phi_1\phi_2$ is also smaller numerically on account of the changes brought about in the functions ϕ_1, ϕ_2 by deviations of the field from the Coulomb law. The dependence of the integrand of I on y has been examined graphically for $Z=91$, 81, $v=-4$. The main modification due to the finiteness of the size of the nucleus consists in reducing $\phi_1\phi_2 y^{-2}$ to a relatively negligible amount for $y \leqq y_0$. For $y > y_0$ the integrand approaches rapidly the value which it would have if the nucleus had negligible dimensions. An inspection of the figures indicates that the area under the perturbed $\phi_1\phi_2 y^{-2}$ curve is approximately the same as the area under the unperturbed $\phi_1^{(0)}\phi_2^{(0)}y^{-2}$ curve from $y=2y_0$ to $y=\infty$. We have for the unperturbed functions

$$\int_0^\infty \phi_1^{(0)}\phi_2^{(0)}y^{-2}dy = \int_0^\infty 8aC^2[(j'-\rho)J_{2\rho}(z) + (z/2)J_{2\rho+1}(z)]J_{2\rho}(z)z^{-3}dz$$
$$= aC^2(2j'-1)/[2\rho(4\rho^2-1)]$$
$$\int_0^{py_0} \phi_1^{(0)}\phi_2^{(0)}y^{-2}dy \leqq aC^2(j'-\rho)(py_0)^{2\rho-1}/[(2\rho-1)(\Gamma(2\rho+1))^2].$$

Thus the integral over the perturbed functions is

$$I = \int_0^\infty \phi_1\phi_2 y^{-2}dy = \left\{1 - \frac{2(j'-\rho)\rho(2\rho+1)}{(2j'-1)[\Gamma(2\rho+1)]^2}(py_0)^{2\rho-1}\right\} \times$$
$$\int_0^\infty \phi_1^{(0)}\phi_2^{(0)}y^{-2}dy$$

where $p \geqq 2$. The quantity in $\{\ \}$ is a correction factor which must be applied to I as evaluated on the hypothesis of the inverse square law. It is seen that the correction factor depends in addition to y_0 also on j' and ρ. It is largest for S terms and is appreciable for $P_{1/2}$ but is negligible for $P_{3/2}$ terms. Taking $p=2$ for $Z=91$ the correction factor is 0.67 for $S_{1/2}$ and 0.86 for $P_{3/2}$ terms. Schüler and Keyston[6] and Schüler and Jones[7] find apparently that the hyperfine structure splittings of the two odd isotopes of Hg are not always proportional to each other as one would expect on a simple theory, the splitting of 199 being sometimes greater and sometimes less than that of 201. One might suppose that this is due to the difference between $\phi_1\phi_2$ and $\phi_1^{(0)}\phi_2^{(0)}$. The above estimates show however that the effect is not accounted for by the theory because the nuclear radii of the two isotopes must differ from each other by much less than 1 percent as shown by the smallness of the isotopes displacements. The resultant difference in I is then expected to be surely not greater than 0.33 percent. Nevertheless for the absolute calculation of magnetic moments the above correction factors may have to be considered.

§6. Summary and Discussion

1. The observed isotope displacements in the spectra of Hg, Tl, Pb are smaller than those calculated on the supposition that the nuclear radius changes by about 1 percent for isotopes differing from each other by 2 in their atomic number.

2. The validity of the perturbation method has been examined and it has been found that it introduces at the most a decrease in the theoretically expected value by a factor of 1/2.

3. The change in the radial functions due to deviations from the inverse square law is found to cause an appreciable effect on the coupling of the valence electron to the nuclear spin for $S_{1/2}$ and $P_{1/2}$ terms of single electron spectra. This change is not large enough however to account for the difference between the ratio of the splittings of the isotopes 199, 201 of Hg observed for different terms by Schüler and Keyston and by Schüler and Jones.

The disagreement between theory and experiment presented in §3 appears to be universal. Thus in the spectrum of Pb II Schüler and Jones[5] have found a displacement between the 206, 208 isotopes of 0.052 cm^{-1} for the lines 6660, 5609 ($7\,^2S_{1/2}-7\,^2P_{1/2}$, $7\,^2S_{1/2}-7\,^2P_{3/2}$). By formulas (13), (14) it is estimated that if this shift should be due to a change in the nuclear radius it would have to be attributed to the $7\,^2S_{1/2}$ term. The value of $\psi^2(0)$ to be used for $7S$ Hg II should be approximately the same as that for $7S$ Tl II. The latter is given by Racah[10] as 0.44×10^{26} cm^{-3}. The expected displacement is thus approximately the same as for $6S$ of Tl I and is obviously too large. All of the shifts could of course be decreased by supposing that y_0 and v change just in the correct proportion. Such an explanation appears to be a forced one at present, however.

The situation is quite different with the $6s^26d$ configuration of Pb II. The ^2D term is inverted. The *hfs* of lines terminating on it has been observed by Kopfermann,[3] Schüler and Jones,[5] and in especial detail by Rose and Granath[4] who subsequently to the publication of their results have measured the structure of the higher series members of 4245 *viz.*, λλ2948, 2526 ($6\,^2D_{5/2}-5$, 6, $7\,^2F_{7/2}$) also λλ5372, 3451, 2887 ($6s6p^2\,^2D_{5/2}-5$, 6, $7\,^2F_{7/2}$) as well as λλ3786, 2719 ($6s6p^2\,^2D_{3/2}-5$, 6, $^2F_{5/2}$), λ5367 ($6s6p^2\,^2D_{5/2}-5\,^2F_{5/2}$) and λ4242 ($6^2D_{5/2}-5\,^2F_{5/2}$). According to their data as well as that of Kopfermann and Schüler and Jones the shift between Pb^{206} and Pb^{208} is practically the same for all lines ending on the same D term so that the shifts must be attributed to the D rather than the F terms. The displacement for

$6s^26d\,^2D_{5/2}$	is 0.20 cm^{-1}	$6s6p^2\,^2D_{5/2}$	0.28 cm^{-1}
$6s^26d\,^2D_{3/2}$	0.09 cm^{-1} or (0.08)	$6s6p^2\,^2D_{3/2}$	0.43 cm^{-1}.

An application of Eq. (14) shows that for the $6s^26d\,^2D_{3/2}$ terms one expects an entirely negligible shift ($10^{-4}cm^{-1}$) as a result of a 1 percent change in the nuclear radius. Still smaller displacements are expected for $^2D_{5/2}$. The opposite is true experimentally. It is also remarkable that $6s6p^2$ gives larger isotope shifts than $6s^26d$. It may be however that the $6s^26d$ terms are per-

turbed[12] by $6s6p^2$. If this is the case the isotope displacements of all four terms could be attributed to the *lack* of one $6s$ electron in the $6s6p^2$ configuration. This view is in agreement with the fact that for the 6660, 5609 lines the Pb^{206} component is displaced towards shorter wave-lengths with respect to Pb^{208} while for 4245 and the other lines ending on the ^2D terms the Pb^{206} component lies towards longer wave-lengths. The direction of the displacement is correctly explained by an increase in the radius for the heavier isotope since the heavier isotope has the looser binding to the nucleus for the $6s$ as well as the $7s$ electron. Furthermore the sum of the isotope displacements of $6s^26d^2D_{5/2}$ and $6s6p^2\ ^2D_{5/2}$ is $0.20+0.28=0.48$ cm^{-1} while for the two $^2D_{3/2}$ the sum is 0.52 cm^{-1}. This sum may be taken to be the isotope shift of a single $6s$ electron. It is approximately 10 times as great as the shift for the $7s$ electron (0.052 cm^{-1}). It appears reasonable to suppose that the ratio of $\psi^2(0)$ for these two electrons is also approximately 10 since Racah's numerical calculations gave a ratio 6.4 for of the $6s$ and $7s$ electrons of Tl II.

Thus even though the absolute value of the isotope shift is smaller than would be expected on the hypothesis that it is due to a change of the nuclear radius by (2/3) percent (for 206 and 208) the comparison of the $6s$ and $7s$ displacements indicates that the shift is roughly proportional to the value of $\psi^2(0)$ at the nucleus that the shifts for p, d, electrons are small and that therefore the shift may be due to deviations of the field from the inverse square law.

In the *hfs* of the spectrum of Tl I as it has been analyzed by Schüler and Keyston[1] and by Jackson,[2] even this appears untrue. The main argument against such an explanation lies in the fact that according to Schüler and Keyston[1] λλ6550, 5528, 5110 ($7\ ^2S_{1/2}-8, 9, 10\ ^2P_{3/2}$) and λλ6714, 5584 ($7\ ^2S_{1/2}-8, 9\ ^2P_{1/2}$) show no isotope shift. For this reason the $7\ ^2S_{1/2}$ term is supposed to have no shift and therefore the shift of 0.05 cm^{-1} present in the 5351 line is attributed to a displacement of $^2P_{3/2}$. It should be noted, however, that while Schüler and Keyston[1] have found no isotope shift for 3776 ($6^2P_{1/2}-7\ ^2S_{1/2}$) Jackson[2] reports a displacement of roughly the same amount as for 5351. If, therefore, the experimental difficulties present in the observation of 6550, 5528, 5110, 6714, 5584 have masked the shift in these lines one could suppose that the $6\ ^2P$ terms have a negligible isotope displacement while $7\ ^2S$ of Tl^{205} has an energy higher than that of $7\ ^2S$ of Tl^{203} by 0.05 cm^{-1}. This assignment would not fit in however with the sense of the displacement in Tl II as observed by Schüler and Keyston[1] because the energy difference between the $6s7p$ and $6s7s$ configurations is higher for 205 than 203. In the Tl II spectrum the $7s$ electron appears to be more tightly bound to the nucleus in the 205 than in the 203 isotope while in Tl I even forcing the P terms to have no displacements the opposite is the case. Thus this spectrum appears not to fit in with a theory of isotopic shifts due to deviations of the nuclear field from the inverse square law even in a roughly qualitative manner.

There is another possibility for accounting for the isotope displacement

[12] Shenstone and Russell, Phys. Rev. **39**, 415 (1932). Note remark on influence of perturbations on isotope shifts in Hg.

as a direct effect of the mass.[13] It is a striking feature of the observed isotope displacements, however, that the odd isotopes of Hg and Pb fall not exactly between the even isotopes of closest atomic weight but somewhat closer to the even isotope of smaller atomic weight. This displacement cannot have anything to do with the mass and it is not due to observational error inasmuch as in the case of Pb it has been found by three independent sets of observers.[3,4,5]

The fact that the observed shifts for S terms are much smaller than those expected on the supposition of a progressive change in the nuclear radius shows that either the field used in the theory of radioactive disintegration cannot be applied in the discussion of the interaction of extranuclear electrons with the nucleus or that the change in the radius of nuclei of the same element is smaller than has been supposed. However, even with such modifications the shifts in Tl remain quite unexplained.

Note in Proof: Since the paper was written we learned of a new nuclear theory of Heisenberg according to which the nucleus is supposed to consist of protons and neutrons. The Gamow mountain may then be understood as the result of exchange forces. We have also learned of the new considerations of Bohr according to which the collision between neutrons and electrons is very improbable. According to these views the electron may be regarded as subject only to the influence of protons within the nucleus. The density of protons may be imagined either to be approximately uniform or else to vary as a simple function of the distance from the center. It is clear that the term displacement is smaller on this view than according to the model used above. A calculation for the isotope shift was made using a potential energy $V=[-(n+1)/n+(1/n)(r/r_0)^n](Ze^2/r_0)$ inside the nuclear radius r_0. The displacement of the energy for s terms is

$$\delta W = \frac{4\pi R_\infty}{Z} a_H^3 \psi^2(0) \frac{1+\rho}{\Gamma^2(2\rho+1)} \frac{(n+1)y_0^{2\rho}}{2\rho(2\rho+n+1)(2\rho+1)}$$

and for $l>0$

$$\delta W = \frac{2j'(j'-\rho)}{\Gamma^2(2\rho+1)} \frac{(n+1)y_0^{2\rho}}{2\rho(2\rho+n+1)(2\rho+1)} \left\{ [(l+1)^2-a^2]^{\frac{1}{2}} - 1 - (l^2-a^2)^{\frac{1}{2}} \right\}^{-1} \delta.$$

The expected differences in term displacements for isotopes are given therefore by the same expressions as before except for the factor

$$A(n) = (n+1)/(2\rho+1)(2\rho+n+1).$$

For $n=2$ (uniform charge density in the nucleus) and $\rho=0.81$, $A=0.25$ and for $n=1/2$, $A=0.18$. Using $A=1/5$ the isotope shift of Pb^{206} and Pb^{208} would be estimated to be 0.46 cm^{-1} for the $7s$ and 2.9 cm^{-1} for the $6s$ electrons while the observed values are 0.052 cm^{-1} and 0.50 cm^{-1} respectively. In order to bring about agreement between theory and experiment one would have to use $n \cong -0.84$, i.e., the nuclear charge would have to be concentrated practi-

[13] D. S. Hughes and C. Eckart, Phys. Rev. **36**, 694 (1930).

cally entirely at the center. It is probably incorrect however to give such a literal interpretation to the nuclear charge because forces between neutrons and electrons may not be entirely negligible and because α-particles may form groups having a volume which is affected only slightly by increasing the atomic weight. It must be recalled that in the cases considered here one isotope can be obtained from another one simply by the addition of neutrons. The small magnitude of the isotope shift suggests that the volume occupied by the positive charges is not affected greatly by the addition of neutrons to the nucleus as though the repulsive forces between the positive charges were balanced by the cementing influence of neutrons in their immediate neighborhood.

Our thanks are due to Professor W. Heisenberg for informing us of the new developments before publication and for a helpful discussion of the interaction of electrons with the nucleus.

Isotope Separations in the Infrared Absorption Spectrum of HCl and the Possible Existence of a Chlorine Isotope of Mass 39

By J. D. HARDY* AND G. B. B. M. SUTHERLAND**
Physics Department, University of Michigan

(Received June 30, 1932)

The absorption band of HCl at 1.7μ has been reëxamined under high dispersion in an attempt to verify the work of Hettner and Böhme on the existence of a third chlorine isotope, Cl^{39}. No trace of the isotope was observed although a path length of three meters, some ten times the path used by Hettner and Böhme, was used. The isotope separations due to Cl^{35} and Cl^{37} have been measured very accurately and do not agree with the separations calculated by the simple theory. When the anharmonic terms in the energy are taken into account the agreement between the calculated and observed isotope separations is within the experimental error. The isotope separation for HCl^{39} molecule has been calculated and found to be slightly different from that observed by Hettner and Böhme. Our results indicate that the relative abundance of Cl^{39} to Cl^{39} cannot be greater than 1 to 500.

RECENTLY Becker[1] has predicted the existence of a chlorine isotope, Cl^{39}, from a consideration of the form of the infrared absorption curves of HCl. This prediction was made from the curves published by Meyer and Levin[2] and by Becker[1] himself. The absorption maxima in these curves which Becker attributes to HCl^{39} are so small as to be probably within the error of the experiment. In fact, Meyer and Levin state specifically that the unevenness of their base line was due to errors in galvanometer readings, and if one examines the original curves of Meyer and Levin it is seen that the maxima mentioned by Becker do not fall at equal distances from the maxima due to Cl^{35} and in many cases do not show up at all. However, the existence of Cl^{39} was later apparently confirmed by Hettner and Böhme[3] working on the *R* branch of the HCl harmonic. In this work the maxima due to HCl^{39} stand out in all clearness with the expected constant frequency difference between these maxima and those due to Cl^{35}. The present work was undertaken with two objects in view, to verify the work of Hettner and Böhme and to measure more accurately, under high dispersion, the separation of the maxima due to HCl^{35} and HCl^{37}. The interest in the third isotope arose naturally from the apparent disagreement of observers about its existence. Aston[4] at one time considered the possibility of a Cl^{39} isotope but finally decided against its existence. Ashley and Jenkins[5] studied the absorption of AgCl in a region

* National Research Fellow.
** Commonwealth Fund Fellow.
[1] H. Becker, Zeits. f. Physik **59**, 583 and 601 (1930).
[2] C. F. Meyer and A. Levin, Phys. Rev. **34**, 44 (1929).
[3] G. Hettner and J. Böhme, Zeits. f. Physik **72**, 95 (1931).
[4] F. W. Aston, Isotopes, p. 68, 2nd ed., 1924.
[5] M. Ashley and J. A. Jenkins, Phys. Rev. **37**, 1712 (1931).

favorable for showing the isotope but found no trace of an $AgCl^{39}$ molecule. E. K. Plyler (private communication) made an attempt to find the absorption lines due to the third isotope by a close examination of the fundamental band at 3.4μ. He used the same instrument that Meyer and Levin used in their work and his results were negative within the error of his observations. The interest in the isotope separation arose from a discrepancy in the observed values and those calculated on the simple theory.

With a new type spectrometer[6] whose resolution and sensitivity are greater than any of those yet applied to the problem, the work of Hettner and Böhme, Becker, and Meyer and Levin has been repeated. That is, the short wave-length side of the harmonic band at 1.7μ has been carefully examined. A description of the spectrometer has already appeared and it need only be mentioned here that by altering the dimensions of the thermocouple a 50 percent gain in sensitivity has been realized over previous arrangements.

The region to be investigated, between 1.71μ and 1.75μ, is a particularly favorable one in which to work. It is practically free from water vapor absorption and in it lies the energy peak of the Nernst heater. Further, the impurity of the spectrum due to overlapping orders is very slight even without the use of any filtering device. The first order energy of 0.85μ is small and in the second order the energy will be only 10 percent of that in the first order. The difference between curves taken with a filter and without a filter is negligible. The filter used was opaque to visible light, transmitted 9 percent from 0.8μ to 0.9μ, and had 70 percent transmission at 1.73μ.

The grating used in this experiment was ruled by Wood with 15,000 lines to the inch and had a ruled surface of 6×3.5 inches. Previously the emission lines of helium had been examined with this grating and the definition was found to be good enough to resolve lines at 10829.1A and 10830.3A in the second order. The spectrometer was calibrated by means of the helium lines at 10830.3A and 20582.1A. The width of the slits for the most detailed examination was 0.075 mm and for the rougher curve 0.15 mm. The wave-length range across the slit in the first instance was 0.97A or 0.32 cm^{-1}, and in the rougher curve 0.64 cm^{-1}. Readings were taken one slit-width apart, and each point represents usually a single observation. The steadiness of the instrument was such that an observation could be repeated to within 2 percent in the detailed curves, where the deflections were about 30 cm between lines, and to within about 1 percent in the rougher curve where the deflections were about 60 cm. The deflections at places of maximum absorption were practically zero for the strong lines, the residual deflection probably being due to a slight impurity of the spectrum coming from overlapping orders. No radical departures from the base line were observed anywhere except in regions of the absorption lines of HCl^{35} and HCl^{37}.

The present work was done with two cell lengths. The first work, with very narrow slits, was done with a cell 31 cm long. This is the length of cell used by previous workers and it was found that the strong lines due to

[6] J. D. Hardy, Phys. Rev. **38**, 2162 (1931).

HCl^{35} gave nearly 100 percent absorption with this cell length. When this length of cell failed to show the lines due to HCl^{39} a cell of three meters length was used, and it was felt that had the isotope been present in the HCl gas which was examined, it would not have escaped detection, assuming that its relative abundance to Cl^{35} is about that shown by Hettner and Böhme's curves.

The 31 cm cell was a brass tube provided with strong windows of plate glass. The cell was evacuated and filled with HCl gas from a liquid air trap so as to ensure dryness of the gas. The HCl was prepared in the usual manner by allowing sulfuric acid to combine with pure NaCl in an evacuated Kipps apparatus. The HCl was frozen out by liquid air and then introduced into the

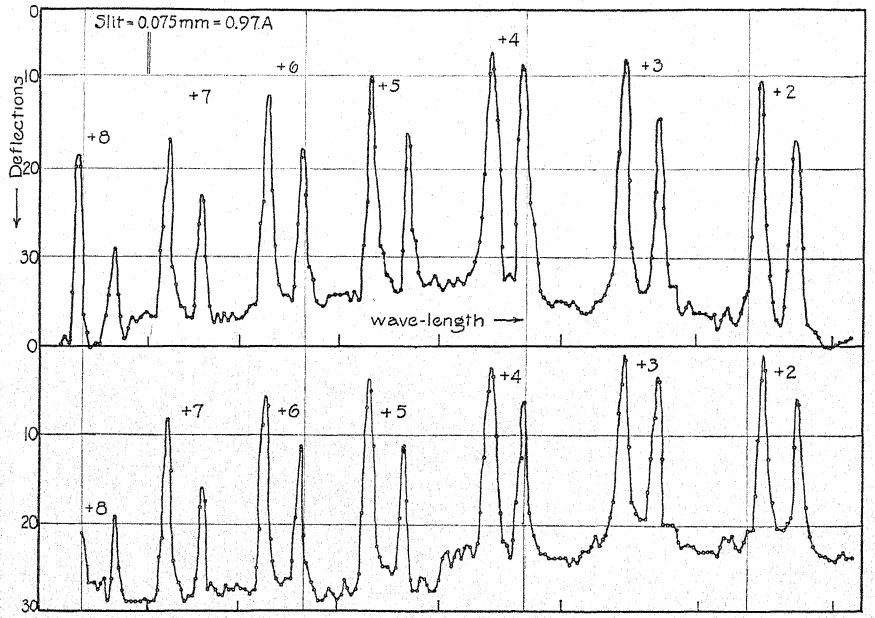


Fig. 1. Two sets of observations: *R* branch of HCl harmonic with 30 cm cell.

evacuated cell to a pressure of 90 cm of mercury. The trap from which the HCl was evaporated was never allowed to come up to the temperature of 0°C during this process. The three meter cell was of galvanized iron thickly coated inside with paraffin. The cell was eight inches in diameter and provided with stout mica windows. The HCl was introduced into the cell from a liquid air trap and the air gradually displaced by continuous flowing of the gas for several hours. Tests at the end of the filling showed that the gas inside was about 92 percent HCl.

Readings were made by taking a complete curve with the empty cell and then a run with the cell full. The background with the empty cell was found to be very smooth and since lines and line positions were desired, percentage absorption was plotted for only one curve, and deflections with the cell full for the detailed curves.

The results of observations with the 31 cm cell are shown in Fig. 1. Lines are drawn to indicate the places where the third isotope might be expected from theory, account being taken of the anharmonic terms in the energy. In Table I are given the wave-lengths and frequency separations measured in this experiment as compared with the values obtained by Meyer and Levin.

TABLE I. *Wave-length and frequency separations in absorption spectrum of HCl.*

Line	Wave-length (A) Hardy and Sutherland	Meyer and Levin	Isotope separation Hardy and Sutherland (A)	(cm^{-1})
2	17519.8	17520.2	12.3	4.04 ± 0.08
3	17467.7	17467.9	12.2	4.03
4	17418.3	17419.2	12.2	4.03
5	17373.8	17374.9	12.7	4.21
6	17334.6	17334.0	12.7	4.21
7	17298.3	17298.1	12.4	4.14
8	17266.3	17265.2	12.7	4.24
9	17238.1		12.6	4.23 ± 0.09
10	17213.3		13.0	4.34
11	17193.2		12.8	4.29
12	17176.4			
13	17163.4			

The lines 9, 10, 11, 12, and 13 were observed with the three meter cell. The isotope separation for the last two lines is not given since the convergence of the band is so strong that the HCl^{37} component of one line overlaps the HCl^{35} component of its neighbor. In Fig. 2 are shown the results obtained with the three meter cell. Again no trace of the third isotope is visible. The strong lines toward the center of the band are very wide because of the very intense absorption in this region.

Hettner and Böhme state that the theoretical separation between the lines due to HCl^{35} and HCl^{37} is $\Delta\lambda = 13.54$A, whereas the value found by Meyer and Levin is $\Delta\lambda = 12.0 \pm 1$A. Hettner and Böhme attribute the discrepancy to the lack of good separation in the curves of Meyer and Levin, and thus to a resulting "attraction" of the stronger line for the weaker. In the present experiment the lines are well resolved, not overlapping at all, and the resulting separation is in good agreement with the value found by Meyer and Levin. Upon closer examination it is found that the separation expressed in wave numbers is not constant but steadily decreases as one goes toward longer wave-lengths. This variation in isotope separation from line to line illustrates the well-known rotational isotope effect. The agreement between the accurate theory and the most precise measurements is worth examining in some detail.

We start from the Fues[7] expression for the energy of a rotating vibrating dipole.

$$E = A + h\nu_0(n + \tfrac{1}{2})[1 + B(j + \tfrac{1}{2})^2] + (h^2/8\pi^2 J)(j + \tfrac{1}{2})^2[1 - K^2(j + \tfrac{1}{2})^2] - (h^2/8\pi^2 J)(n + \tfrac{1}{2})^2 C. \quad (1)$$

[7] E. Fues, Ann. d. Physik **80**, 367 (1926).

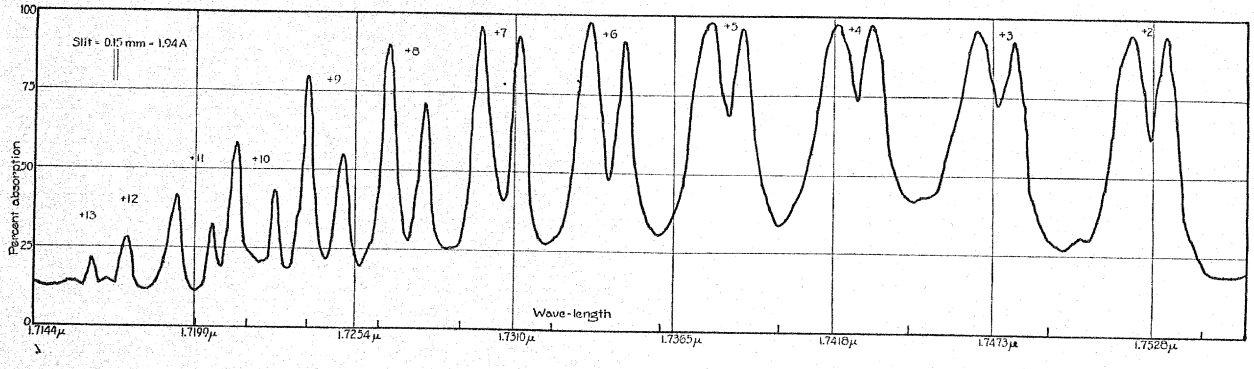


Fig. 2. Observations with three meter cell on R branch of HCl harmonic showing expected positions for HCl^{39}.

Where n is the vibrational quantum number; j is the rotational quantum number;

$$K = h/4\pi^2\nu_0 J;\ B = (3/2)K^2(1 + 2C_3);\ C = 3 + 15C_3 + (15/2)C_3^2 + 3C_4$$

and C_3 and C_4 are constants in the potential energy expression which measure the degree of anharmonicity of the motion. From this we can immediately write down the expression for the frequencies in a vibration-rotation band corresponding to the jump of n from 0 to Δn.

$$\begin{aligned} \nu = {} & \nu_0\Delta n - \tfrac{1}{4}\nu_0 B\Delta n - (h/8\pi^2 J)C(\Delta n^2 + \Delta n) \\ & + j(-\nu_0 B - \nu_0 B\Delta n + h/4\pi^2 J - hK^2/8\pi^2 J) \\ & - j^2\nu_0 B\Delta n - j^3(h/8\pi^2 J)4K^2. \end{aligned} \tag{2}$$

Here we have arranged that j is the number of the line from the center of the band, positive for the positive branch, and negative for the negative branch. Colby[8] has shown that this formula is in excellent agreement with the experimental work of Meyer and Levin on the fundamental and overtone bands of HCl.

As usual let us take ρ as the ratio of the square roots of the reduced masses of the two molecules, then

$$\begin{aligned} \nu_1 - \nu_2 = {} & \nu_0\Delta n(1-\rho) - \tfrac{1}{4}\nu_0 B\Delta n(1-\rho^3) - (h/8\pi^2 J)C(\Delta n^2 + \Delta n)(1-\rho^2) \\ & + j\{-\nu_0 B(1+\Delta n)(1-\rho^3) + h/4\pi^2 J(1-\rho^2) - (h/8\pi^2 J)K^2(1-\rho^4)\} \\ & - j^2\nu_0 B\Delta n(1-\rho^3) - j^3(h/2\pi^2 J)K^2(1-\rho^4) \end{aligned} \tag{3}$$

Where ν_1 corresponds to the HCl^{35} molecule, ν_2 corresponds to the HCl^{37} molecule,

$$\rho = [\mu(HCl^{35})/\mu(HCl^{37})]^{1/2}$$

and the dependence of the various factors on ρ can easily be verified. The values of the constants taken from Colby's analysis of the bands show that the terms with the coefficient $hk^2/\pi^2 J$ are quite negligible.

Taking out $(1-\rho)$ as a factor this may be written

$$\begin{aligned} \nu_1 - \nu_2 = {} & (1-\rho)\{\nu_0\Delta n - \tfrac{1}{4}\nu_0 B\Delta n(1+\rho+\rho^2) - (h/8\pi^2 J)C(\Delta n^2+\Delta n)(1+\rho) \\ & + j[-\nu_0 B(1+\Delta n)(1+\rho+\rho^2) + (h/4\pi^2 J)(1+\rho)] \\ & - j^2\nu_0 B\Delta n(1+\rho+\rho^2)\}. \end{aligned} \tag{4}$$

We may simplify this further by putting $\rho = 1$ everywhere except in the first factor. So the frequency separation for the general band when n changes from 0 to Δn is

$$\begin{aligned} \nu_1 - \nu_2 = {} & (1-\rho)\{\nu_a - (h/8\pi^2 J)C(\Delta n^2 + \Delta n) - \tfrac{1}{2}\nu_0 B\Delta n \\ & + j[h/2\pi^2 J - 3B\nu_0(1+\Delta n)] - 3j^2 B\nu_0\Delta n\}. \end{aligned} \tag{5}$$

[8] W. F. Colby, Phys. Rev. **34**, 53 (1929).

Where $\nu_c = \nu_0 \Delta n - \frac{1}{4}\nu_0 B \Delta n - (h/8\pi^2 J)\ C(\Delta n^2 + \Delta n)$ denotes the center of the band. The values of the constants deduced in Colby's[8] paper for the fundamental band of HCl^{35} are $C = 4.885$, $B\nu_0 = 0.303$, $h/4\pi^2 J = K\nu_0 = 21.17$. Substituting those we obtain for the separations:

Fundamental

$$\nu_1 - \nu_2 = 0.000751\{2885.88 - 103.3 + 40.5j - 0.91j^2\}. \quad (6)$$

Harmonic

$$\nu_1 - \nu_2 = 0.000751\{5667.96 - 309.9 + 39.6j - 1.82j^2\}. \quad (7)$$

Tables II and III show the agreement between the values of the separations as determined experimentally and as calculated from these expressions.

TABLE II. *Isotope separations in the fundamental band in cm^{-1}.*

j	Positive branch		Negative branch	
	Calculated value	Meyer and Levin's value	Calculated value	Meyer and Levin's value
1	2.12	2.09	2.06	2.10
2	2.14	2.09	2.03	1.97
3	2.17	2.10	1.99	1.98
4	2.20	2.16	1.96	1.90
5	2.23	2.22	1.92	2.02
6	2.25	2.12	1.88	1.72
7	2.27	2.13	1.84	1.74
8	2.29	2.27	1.80	1.77
9	2.31	2.26	1.76	1.83
10	2.33	2.23	1.72	1.61
11	2.34	2.25	1.67	1.71
12	2.36	2.34	1.63	1.57

TABLE III. *Isotope separations in the harmonic band—positive branch.*

j	Calculated		Observed				
			Hardy and Sutherland		Hettner and Böhme		Meyer and Levin
	(cm^{-1})	(A)	(cm^{-1})	(A)	(A)	(A)	(cm^{-1})
2	4.08	12.5	4.04	12.3	12.5	12.5	4.20
3	4.10	12.5	4.03	12.2	12.0	12.5	3.87
4	4.12	12.5	4.03	12.2	12.5	12.5	4.03
5	4.14	12.5	4.21	12.7	12.0	12.0	4.19
6	4.15	12.5	4.21	12.7	12.0		4.22
7	4.16	12.45	4.14	12.4	12.0		4.14
8	4.17	12.4	4.24	12.7			4.26
Mean	4.13	12.5	4.12	12.5	12.3		4.13

The discrepancies between individual line separations as computed and as observed lie in each case within the experimental error. The agreement of the various values for the mean separation in the harmonic band is very satisfactory. The variation in the separation from one end of the fundamental band to the other illustrates particularly well the rotational isotope effect. The result of considering the anharmonic terms is to reduce the value

of the separation from that calculated on the simple theory which would be given by Eq. (5) with $B=C=0$. The anharmonic term involving C is the most effective in reducing the separation. The interaction terms involving B begin to contribute appreciably only when j is very large.

If now we use the above formulae (with an appropriate value of ρ) to compute the isotope separations for an HCl^{39} molecule we obtain a set of values which disagree slightly with those found experimentally by Hettner and Böhme. The comparison is shown in Table IV.

TABLE IV. *Isotope separations in the harmonic band of HCl^{39}.*

j	Calculated value (A)	Hettner and Böhme's value (A)	
2	23.8	24.5	24.5
3	23.8	24.5	25.5
4	23.8	24.5	24.5
5	23.8	23.5	23.5
6	23.8		25.5
7	23.7		23.5
Mean	23.8	24.5	

The difference is small but the close agreement of calculated and observed separations in the case of the Cl^{37} isotope make it doubtful whether these lines are due to HCl^{39}.

To obtain an estimate of the smallest relative abundance of HCl^{39} to HCl^{35} which we could detect, we may compare the absorption coefficient of the weakest line of HCl^{35} which we could detect with that of the strongest, *viz.*, line 3. This can be done theoretically with formulae due to Dunham.[9] Now when α is the absorption coefficient so computed for a certain line it is well known that[10]

$$\alpha = KN$$

where N is the number of molecules in the initial energy level and K is an abbreviation for a number of factors which would not change appreciably for an HCl^{35} or an HCl^{39} molecule. If then we know the least ratio of α's which we can detect, we know the least ratio of N's which we can detect. We employ an equation of Dunham's, modified for use in the positive branch.

$$\frac{\alpha_3}{\alpha_m} = \frac{\bar{p}_3}{\bar{p}_m}\frac{\nu_3}{\nu_m}\{1 + 2a(\nu_m - \nu_3)\}e^{(E_{m-1}-E_2)/kT}$$

where m denotes the number of the line in the positive branch; $\bar{p}$ is the mean of the statistical weights of the initial and final states of the molecule; $2a$ is a small correction factor which we can calculate from Dunham's paper to be very close to 0.0154; E denotes the energy of the molecule in the mth rotational level of the zero vibrational level. When we apply this equation to calculate α_3/α_{13} using energy and frequency values from Colby's paper[8] we ob-

[9] J. L. Dunham, Phys. Rev. **34**, 438 (1929).
[10] D. M. Dennison, Phys. Rev. **31**, 503 (1928).

tain a ratio of 460 to 1. The calculated ratio of α_3/α_{14} was 1600 to 1. Using the three meter cell we could easily detect line 13 and there is an indication on the curve of what may be line 14. The latter is, however, uncertain, but we can safely state that had the Cl^{39} isotope been present in a ratio to Cl^{35} of 1 to 500 we could not have failed to detect it.[11]

There is still another viewpoint from which our inability to substantiate the work of Hettner and Böhme seems remarkable. The instrument we used was of considerably higher resolving power than that employed by them. Our lines are consequently deeper and have higher maxima than theirs and so our instrument is better adapted for the detection of faint companion lines. When we remember that the path length used in the present work was ten times that employed by Hettner and Böhme our failure to detect any sensible change in absorption at the expected places is quite irreconcilable with their conclusions.

It is a pleasure to express our thanks to Professor D. M. Dennison for the suggestion that the anharmonic terms might be important in the calculation of isotope separations and for his interest in the problem.

[11] *Note added in proof:* Since the above article was written the experiment has been repeated using an absorption cell seven meters long. There were still no indications of lines which might be interpreted as coming from an HCl^{39} molecule. Line 14 of the positive branch was easily detected giving quite a distinct absorption peak on the curve. This enables us to place the abundance ratio of Cl^{39} to Cl^{39} lower than 1 to 1600.

The Spectra of Na II, III, and IV in the Extreme Ultraviolet

By BRUCE B. VANCE
Ryerson Physical Laboratory, University of Chicago

(Received July 7, 1932)

New lines of Na II, III and IV have been found and classified in the region between 434,000 and 242,000 cm^{-1}.

INTRODUCTION

THE spectrum of Na II in the near ultraviolet has been classified by Frisch[1] in a recent article, who also gives a list of references to previous work on this spectrum. In the extreme ultraviolet region Bowen[2] and Edlen and Ericson[3] have observed the resonance lines 372.065A and 376.350A.[3] The spectrum of Na III (fluorine-like) has been studied by Edlen and Ericson[4] and Mack and Sawyer.[5] The lines corresponding to the $2s-2p$ transitions are the only lines recorded by these investigators for this ion. Both Edlen and Ericson[4] and Mack and Sawyer[5] predict a PP° group of Na IV in the region of 244,000 cm^{-1}. This group had been found and identified previously by Gale and Hoag of this laboratory, but had not been published. The observation of this group and of other lines in this region, which might be attributed to sodium, caused Professor Gale to suggest the present problem to the author.

GENERAL PROCEDURE

The source was a high potential vacuum spark, (*hot spark*).[6] This took place between hollow aluminum electrodes stuffed with metallic sodium which had first been rolled in nickel gauze. It was found that when the pressure in the discharge chamber was below 10^{-4} cm of Hg and the electrodes were separated about 1.5 mm, the vacuum gap (source) would not break down below 40,000 volts. The maximum voltage of the high potential source was above 100,000 volts. The primary circuit of the transformer was automatically made and broken by a very quick acting switch twenty-two times each minute, the duration of the sparks being from one-twentieth to one-tenth seconds each. The total time required for an exposure was from two to four hours.

The vacuum spectrograph used in this investigation was the one designed by Hoag,[7] with a few changes. The grating was glass, instead of speculum, with 1500 lines to the inch. The plate holder accommodated 2×18 inch plates

[1] R. Frisch, Zeits. f. Physik **70**, 498 (1931).
[2] I. S. Bowen, Phys. Rev. **23**, 1 (1924).
[3] B. Edlen and A. Ericson, Comptes Rendus **190**, 116 (1930).
[4] B. Edlen and A. Ericson, Comptes Rendus **190**, 173 (1930).
[5] J. E. Mack and R. A. Sawyer, Phys. Rev. **35**, 299 (1930).
[6] I. S. Bowen, J.O.S.A. **13**, 89 (1927).
[7] B. Hoag, Astrophys. J. **66**, 225 (1927).

and was so arranged that it could be raised to allow three exposures on one plate without removing it from the vacuum. Very thin glass Schumann plates, made by Hilger and Company, were used.

In reducing the plates a linear dispersion was assumed between the Al IV line of 160.073A[8] and the O III line at 599.598A,[9] error curves were then plotted by the aid of intermediate standards (O III 266.992,[10] Na II 372.065,[3] Na III 380.091[4] and O III 525.795A).[9] These error curves were found to be extremely smooth for all plates.

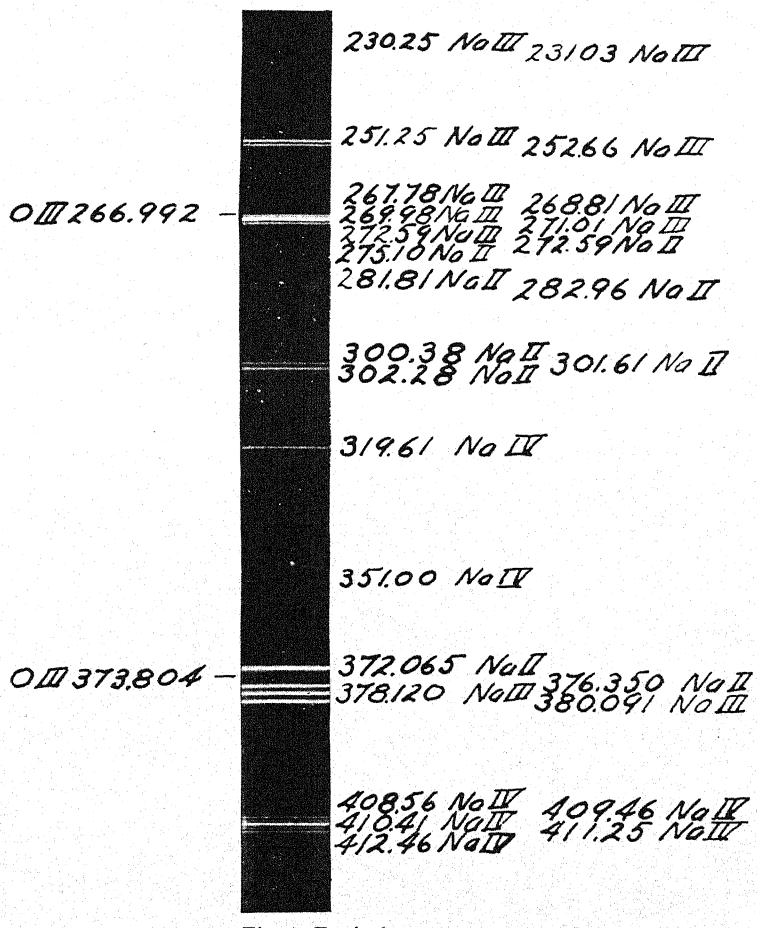


Fig. 1. Typical spectrogram.

With a very narrow slit and the pressure in the discharge chamber below 10^{-4} cm of Hg (as observed with an ionization gauge) plates were easily obtained which were free from fog and weak gas lines. Under these conditions

[8] J. Soderqvist and B. Edlen, Zeits. f. Physik **69**, 356 (1931).

[9] From a list of standard oxygen wave-lengths furnished through the courtesy of Dr. Bengt Edlen of Uppsala.

[10] A. Ericson and B. Edlen, Zeits. f. Physik **59**, 659 (1930).

only the prominent oxygen, carbon and aluminum lines appeared as impurities, which were used as standards in reducing the plates.

Na II (NEON-LIKE)

In the region investigated one would expect to find, besides the prominent resonence transitions $s^2p^6\ {}^1S_0 - s^2p^5 3s\ {}^3P_1,\ {}^1P_1$, transitions from two or three of the three $3d$ levels with $J=1$ and possibly from higher s orbits than the $3s$.

It was found possible to form two series formulas of the type

$$\nu = \nu_0 - 4R/(m+\mu+\alpha/m)^2 \text{ where } m = 1, 2, 3, \cdots$$

whose limits differed by the same amount (in cm^{-1}) as the separation of the ground terms of Na III ($s^2p^5\ {}^2P_{1/2,3/2}$). In addition to the three pairs of transitions used in forming these series formulas a fourth pair and possibly a fifth pair were found. (The latter was later found to fit better into the term scheme of Na III.) The levels thus found correspond to the ms_2 and ms_4 levels of neon as given by Paschen,[11] whose limits are ${}^2P^\circ_{1/2}$ and ${}^2P^\circ_{3/2}$, respectively. From the value of the latter limit 47.068 volts has been obtained as the ionization potential of Na II. The lines resulting from transitions from these levels to the ground term $s^2p^6\ {}^1S_0$ can be seen easily on the plates (Fig. 1 typical). They are given in Table I and II and are shown diagrammatically in Fig. 2a.

TABLE I. *Observed and calculated transitions of Na II.*

I	λ (obs.)	ν (cm^{-1})	Config. and Terms	ν (calc.†)
6	376.350[3]	265710	$s^2p^6\ {}^1S_0 - s^2p^5 3s\ {}^3P_1^\circ(s_4)$	265710
10	372.065[3]	268770	$s^2p^6\ {}^1S_0 - s^2p^5 3s\ {}^1P_1^\circ(s_2)$	268770
0	302.28	330830	$s^2p^6\ {}^1S_0 - s^2p^5 4s\ (s_4)$	330945
3	301.61	331540	$s^2p^6\ {}^1S_0 - s^2p^5 3d\ Z_{11}$	331502[1]
			$4s\ (s_2)$	332811
2	300.38	332910	$s^2p^6\ {}^1S_0 - s^2p^5$	
			$3d\ Z_2$	333050[1]
1	282.96	353260	$s^2p^6\ {}^1S_0 - s^2p^5 5s\ (s_4)$	353283
1	281.81	354850	$s^2p^6\ {}^1S_0 - s^2p^5 5s\ (s_2)$	354854
0	275.10	363500	$s^2p^6\ {}^1S_0 - s^2p^5 6s\ (s_4)$	363510
0	273.99	364960	$s^2p^6\ {}^1S_0 - s^2p^5 6s\ (s_2)$	364888
(0	271.01	369000	$s^2p^6\ {}^1S_0 - s^2p^5 7s\ (s_4)$	369028)*
(0	269.98	370400	$s^2p^6\ {}^1S_0 - s^2p^5 7s\ (s_2)$	370459)*

* Probably Na III.
† Calculated ν obtained from the following formulas:
$ms_2 \cdots \nu = 382800 - 4R/(m+0.963845-0.001872/m)^2$
$ms_4 \cdots \nu = 381430 - 4R/(m+0.949650-0.002057/m)^2$
in which $m = 1, 2, 3, \cdots$.

Of the three $3d$ levels with $J=1$ one should have the limit $s^2p^5\ {}^2P^\circ_{1/2}$ and the other two the limit $s^2p^5\ {}^2P^\circ_{3/2}$, of the latter two only the transition to the ground term from one of them is observed. This level is calculated to be 331,540 cm^{-1} above the ground term, and corresponds, within experimental error, to the Z_{11} term of Frisch.[1] The other $3d$ ($J=1$, ${}^2P^\circ_{1/2}$ limit) falls too close to the $4s(s_2)$ level to be resolved, it would correspond to the Z_2 term of Frisch.

[11] Paschen-Goetz, Seriengesetze (1922).

The transition from this level to the ground term is evident only from the fact that the line classified as the $^1S_0-4s(s_2)$ transition is unusually wide for a line of that intensity. The $4s(s_2)$ and $4s(s_4)$ levels correspond to the Z_3 and

TABLE II. *Term values of Na II.*

Config.	Term	Term Value (cm^{-1})	Limit
s^2p^6	$^1S_0$	0	
s^2p^53s	$^3P_1(s_4)$	265710	$^2P^\circ_{3/2}$
s^2p^53s	$^1P_1\ (s_2)$	268770	$^2P^\circ_{1/2}$
s^2p^54s	(s_4)	330830	$^2P^\circ_{3/2}$
s^2p^53d	Z_{11}	331540	$^2P^\circ_{3/2}$
s^2p^54s (and $3d$)	(s_2) and Z_2	332910	$^2P^\circ_{1/2}$
s^2p^55s	(s_4)	353260	$^2P^\circ_{3/2}$
s^2P^55s	(s_2)	354850	$^2P^\circ_{1/2}$
s^2p^56s	(s_4)	363500	$^2P^\circ_{3/2}$
s^2p^56s	(s_2)	364960	$^2P^\circ_{1/2}$
s^2p^57s	(s_4)	369000	$^2P^\circ_{3/2}$
s^2p^57s	(s_2)	370400	$^2P^\circ_{1/2}$

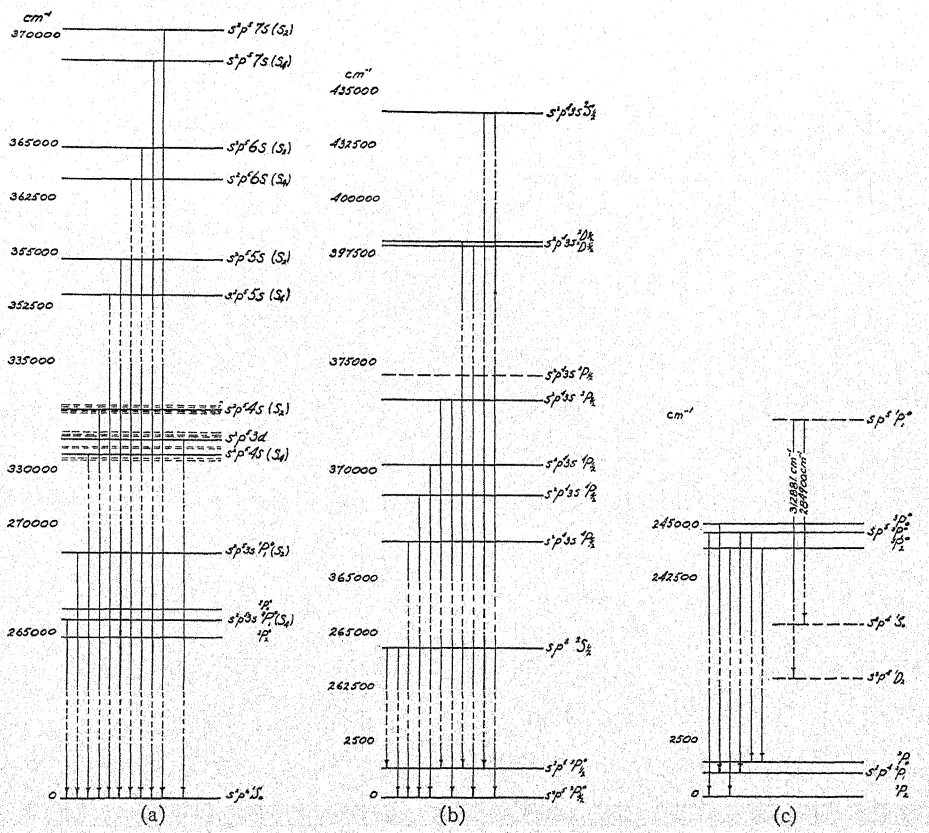


Fig. 2. Term schemes for Na II, Na III, and Na IV for transitions in the far ultraviolet.

Z_{14} levels of Frisch. The other $4s$ and $3d$ terms, which have been calculated from Frisch's values, are indicated by dotted lines in Fig. 2(a) and are given the following J values; $Z_{1,5,8,10,15}$ $J=2$, $Z_{4,9,12}$ $J=3$, Z_{13} $J=4$ and $Z_{6,7}$ $J=0$.

The levels in Fig. 2(a) between 335,000 and 330,000 cm^{-1} are Z_1 to Z_{16} reading down, $Z_{8,9}$ are indicated as one level.

Na III (FLUORINE-LIKE)

In addition to the previously observed transitions $2s-2p$ reported by Edlen and Ericson[4] and Mack and Sawyer,[5] lines have been found which can be classified as $s^2p^5-s^2p^43s$ transitions. These are given in Table III, shown diagrammatically in Fig. 2(b) and the term values are given in Table IV.

TABLE III. *Observed transitions of Na III.*

I	λ	ν (cm^{-1})	Config. and Terms
6	380.091[4]	263095	$s^2p^5\ ^2P^\circ_{1/2}-sp^6\ ^2S_{1/2}$
8	378.120[4]	264466	$s^2p^5\ ^2P^\circ_{3/2}-sp^6\ ^2S_{1/2}$
0	272.59	366840	$s^2p^5\ ^2P^\circ_{3/2}-s^2p^43s\ ^4P_{5/2}$
0*	271.01	369000	$s^2p^5\ ^2P^\circ_{3/2}-s^2p^43s\ ^4P_{3/2}$
0*	269.98	370400	$s^2p^5\ ^2P^\circ_{3/2}-s^2p^43s\ ^4P_{1/2}$
2	268.81	372060	$s^2p^5\ ^2P^\circ_{1/2}-s^2p^43s\ ^2P_{3/2}$
6	267.78	373430	$s^2p^5\ ^2P^\circ_{3/2}-s^2p^43s\ ^2P_{3/2}$
		374600[t]	$s^2p^5\ ^2P^\circ_{3/2}-s^2p^43s\ ^2P_{1/2}$
2	252.26	396410	$s^2p^5\ ^2P^\circ_{1/2}-s^2p^43s\ ^2D_{3/2}$
5	251.25	398010	$s^2p^5\ ^2P^\circ_{3/2}-s^2p^43s\ ^2D_{5/2,3/2}$
1	231.03	432840	$s^2p^5\ ^2P^\circ_{1/2}-s^2p^43s\ ^2S_{1/2}$
2	230.25	434210	$s^2p^5\ ^2P^\circ_{3/2}-s^2p^43s\ ^2S_{1/2}$

* Possibly Na II.
[t] Masked by O III line 266.992A.

The configuration s^2p^4ns theoretically yields inverted $^4P_{1/2,3/2,5/2}$, $^2P_{1/2,3/2}$ terms with limit at $s^2p^4\ ^3P$; $^2D_{3/2,5/2}$ terms with limit at $s^2p^4\ ^1D_2$; and a $^2S_{1/2}$ term with limit at $s^2p^4\ ^1S_0$. Lines are found which are considered to

TABLE IV. *Term values of Na III.*

Config.	Term	Term Value (cm^{-1})	Limit
s^2p^5	$^2P^\circ_{3/2}$	0	
s^2p^5	$^2P^\circ_{1/2}$	1370	
$s\ p^6$	$^2S_{1/2}$	264460	
s^2p^43s	$^4P_{5/2}$	366840	^3P
s^2p^43s	$^4P_{3/2}$	369000	^3P
s^2p^43s	$^4P_{1/2}$	370400	^3P
s^2p^43s	$^2P_{3/2}$	373430	^3P
s^2p^43s	$^2P_{1/2}$	[t]374600?	^3P
s^2p^43s	$^2D_{5/2}$	398010	^1D
s^2p^43s	$^2D_{3/2}$	398230	^1D
s^2p^43s	$^2S_{1/2}$	434210	^1S

[t] Masked by O III line 266.992A.

come from all these levels, for $n=3$, except from the $^2P_{1/2}$ level, and these levels fit well into a Moseley diagram with the same terms of other members of this isoelectronic sequence (F I[12] and Ne II[13]).

The transitions from the $^2P_{1/2}$ level to the $^2P^\circ_{3/2,1/2}$ levels are assumed to be masked by the prominent O III line at 266.992A and the line corresponding to the transition $^2P^\circ_{3/2}-{}^2P_{3/2}$ of Na III respectively. The relative position

[12] H. Dingle, Proc. Roy. Soc. **A117**, 411 (1927).
[13] T. L. deBruin and C. J. Bakker, Zeits. f. Physik **69**, 19 (1931).

of this $^2P_{1/2}$ level on this assumption is indicated by a dotted line in Fig. 2(b).

The lines here identified as corresponding to the transitions between the $^4P_{1/2,3/2}$ and the $^2P^\circ_{3/2}$ levels possibly may be the fifth members of the ms_2 and ms_4 series of Na II, but it seems more likely that they belong to Na III.

Na IV (Oxygen-like)

The PP° group at 244,000 cm^{-1} that had been found and identified as that of Na IV on photographs taken by Gale and Hoag,[14] during their investigation of multiply ionized lithium, was obtained on nearly all the plates taken during this investigation. The central line was not resolved, which made it difficult to determine exactly the position of the $^3P_1$ and $^3P_0{}^\circ$ levels.

In addition to the triplet levels there should be a $^1D_2$ and a $^1S_0$ level for the configuration s^2p^4, and a $^1P_1$ level for the configuration sp^5. Lines have been found which probably correspond to the allowed transitions between these levels, and these transitions fit well into a Moseley diagram with the same transitions of Ne III given by Boyce and Compton.[15] The actual position of these levels can not be given from the results obtained, but it is possible to place them roughly from the information obtained from the positions of the ^4P, ^2P, ^2D, and ^2S levels of Na III. This has been done in Fig. 2(c).

Table V. *Observed transitions of Na IV.*

I	λ	ν (cm^{-1})	Config. and Terms
3	412.46	242448	$s^2p^4\ ^3P_1-sp^5\ ^3P^\circ_2$
2	411.25	243161	$s^2p^4\ ^3P_0-sp^5\ ^3P^\circ_1$
6	410.41	243654	$s^2p^4\ ^3P_{2,1}-sp^5\ ^3P^\circ_{2,1}$
2	409.46	244224	$s^2p^4\ ^3P_1-sp^5\ ^3P^\circ_0$
3	408.56	244762	$s^2p^4\ ^3P_2-sp^5\ ^3P^\circ_1$
0	351.00	284900	$s^2p^4\ ^1S_0-sp^5\ ^1P^\circ_1$
3	319.61	312880	$s^2p^4\ ^1D_2-sp^5\ ^1P^\circ_1$

Table VI. *Term values of Na IV.*

Config.	Terms	Term Values (cm^{-1})
s^2p^4	$^3P_2$	0
s^2p^4	$^3P_1$	1110
s^2p^4	$^3P_0$	1600
s^2p^4	$^1D_2$	A
s^2p^4	$^1S_0$	$A+27980$
sp^5	$^3P^\circ_2$	244050
sp^5	$^3P^\circ_1$	244760
sp^5	$^3P^\circ_0$	245330
sp^5	$^1P^\circ_1$	$A+312880$

In conclusion the author wishes to express his appreciation to Dean Gale for suggesting the problem and for his helpful encouragement throughout the investigation, and to Professor R. S. Mulliken for his advice in the analysis.

Note added in proof: J. Soderqvest, Zeits. f. Physik **76**, 316 (1932), gives an analysis of the Na III spectrum which agrees well with the results given above.

[14] H. G. Gale and B. Hoag, Phys. Rev. **37**, 1703 (1931).

[15] J. C. Boyce and K. T. Compton, Proc. Nat. Acad. Sci. **15**, 656 (1929).

The Absorption Spectrum of Benzene in the Region of 6.75μ

By S. SILVERMAN
The Johns Hopkins University

(Received July 5, 1932)

The absorption band of benzene lying at 6.75μ has been investigated under high resolution for both liquid and gaseous states. The spectrum for the vapor shows three distinct branches with evidence of unresolved fine structure. The liquid shows a less regular spectrum with a definite shift towards longer wave-lengths. In addition, some new water vapor lines in the 6.26μ band are reported.

IN RECENT years an increasing amount of work has been done investigating the infrared absorption and Raman spectra of organic substances. The success which followed the unravelling of the fine structure of some of the more simple compounds led to attempts to resolve the spectra of molecules of increasing complexity. Among the group offering promise due to its complete symmetry is benzene, which has been investigated by a number of workers.[1,2,3,4,5,6] Particularly in the last two or three years, considerable work has been done in the near infrared in this laboratory by Barnes[6] and Leberknight.[7]* Continued improvements in apparatus and resolving power, consisting chiefly of the employment of the Pfund anastigmatic spectrometer with echelette gratings of high resolution, have led to discovery of new bands, and increased complexity in some of the older ones. These studies have thus far been restricted primarily to the region in the neighborhood of 3μ. Bands which previously were so broad as to permit, at best, mere designation as combinations of various vibrational frequencies began to show some evidence of vibration-rotation structure. As a result of several discussions with Dr. C. E. Leberknight, the writer felt that it might be profitable to examine in great detail one of the bands somewhat farther out. The band at 6.75μ, which is quite intense and hence probably represents a fundamental vibration, offered excellent possibilities.

For the purpose of this investigation, the grating spectrometer employing the resonance radiometer, which was used in a recent mapping of the absorption and reflection spectrum of calcite,[8] was found readily adaptable. The grating had 1364 lines per inch; the slit-width was 20A. As in this previous experiment, a magnesium-oxide filter was used to remove the higher

* In this work, which is soon to be published, the spectrum of benzene was investigated in solid, liquid and gaseous states in the region of 3μ under high resolution.

[1] Dougherty, Phys. Rev. **34**, 1549 (1929).
[2] J. Ellis, Phys. Rev. **27**, 298 (1926).
[3] K. W. F. Kohlrausch, Der Smekal-Raman Effekt (Springer 1931).
[4] Schaefer and Matossi, Das Ultrarote Spektrum. P. 270 ff.
[5] R. B. Barnes, Phys. Rev. **35**, 1524 (1930).
[6] R. B. Barnes, Phys. Rev. **36**, 296 (1930).
[7] C. E. Leberknight, unpublished results.
[8] S. Silverman, Phys. Rev. **39**, 72 (1932).

orders of shorter wave-lengths. The instrument was calibrated by means of visual observation of higher orders of the 5461 mercury line, and also by prominent atmospheric absorption lines.[9] The vapor cell was prepared by sealing polished rock-salt windows to the ends of a brass tube. The cement used was a clear lacquer which was found to be almost completely unattacked by the benzene. The optimum cell length was found to be about 22 mm, which length of vapor absorbed 50 percent of the incident energy in the neighborhood of the absorption maximum. A free surface of liquid benzene was kept continually in the bottom of the cell in order to maintain constantly saturation pressure. No difficulty due to condensation on the windows was experienced. A dummy cell was prepared to give a comparison set of readings, as all measurements were taken *cell-in* and *cell-out*. The liquid cell consisted of two flat plates of rock salt, separated by thin strips of silver-foil 0.01 mm thick. This thickness of liquid gives the equivalent molecular path length of 22 mm of gas; this is desirable, as it is essential for direct comparison of gas and liquid to have very much the same *molecular thickness* to traverse. The cell was made tight on 3 sides with lacquer, and the 4th, open, side was fed occasionally with liquid from a pipette; an identical dummy cell was also prepared. The cells maintained their performance unaltered throughout the duration of the experiment.

RESULTS

The absorption in the vapor cell shows the 6.75μ band to be clearly divided into three distinct bands lying at 6.683; 6.743; 6.790μ respectively; the band at 6.743 being somewhat broader and slightly more intense than

TABLE I. *Absorption maxima for benzene.*

Vapor λ	ν	Liquid λ	ν
6.683 $\pm$ 0.0015μ	1496.3 $\pm$ 0.4	6.643μ	1505.3 $\pm$ 0.4
		6.683	1496.3
6.743	1483.0	6.753	1480.8
6.790	1472.8	6.830	1468.1

its companions. All three of the branches show clear evidence of unresolved fine structure, with small but distinct maxima separated by intervals as small as 2 wave numbers. It is entirely probable, however, that the true fine structure of the band is such as to defy resolution by the instrument at our disposal; in which case these small maxima would have no meaning other than to indicate the presence of other fine structure. Inasmuch as the benzene is so complex and has such a large moment of inertia (in the neighborhood of $11 \times 10^{-39} g \times cm^2$) one would expect the structure to be very complicated and the lines to be densely packed.

The absorption of the liquid presented a less attractive map. The central band from the vapor absorption is sharpened slightly with a shift from 6.743 to 6.753μ. The band at 6.683 has been so altered as to bear little resemblence

[9] Plyler and Sleator, Phys. Rev. **37**, 1493 (1931).

to the gaseous state. It is much weaker, being nearly washed out, and shows two maxima: one at 6.643 and one at 6.683μ. The 3rd band has also changed so as to present an entirely new picture. It is much broader than its counterpart in the vapor state, and it is quite irregular in outline, with its maximum at 6.830μ. Its intensity is about that of the corresponding vapor band.

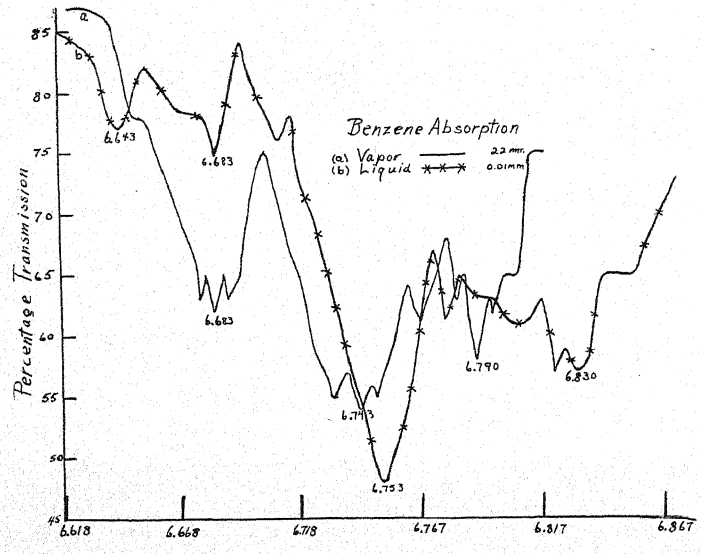


Fig. 1.

It is perhaps worthy of note that in the plotting of this spectrum many runs of the atmospheric absorption bands were obtained. An admirable check of many lines found recently by Plyler and Sleator[9] was obtained. In addition some new ones, marked by the above authors as missing, were observed. These are listed in Table II.

TABLE II. *New absorption lines in water vapor.*

λ	ν	λ	ν
$6.284 \pm 0.0015\mu$	1591.3 ± 0.4	$6.367 \pm 0.0015\mu$	1570.6 ± 0.4
6.294	1588.8	6.480	1543.2
6.299	1587.6	6.485	1542.0
6.313	1584.0	6.583	1519.1

In conclusion, it might be remarked that at present it appears impossible to derive a detailed description of the quantum states of the benzene molecule from the data at hand. The present investigation has shown the existence of hitherto undiscovered fine structure, and it is planned further to probe the spectrum with instruments of still higher resolution in an attempt to unravel the fine detail.

The writer takes great pleasure in expressing his thanks to Dr. C. E. Leberknight for many fruitful discussions concerning this experiment. He also wishes to acknowledge a Grant-in-aid of the National Research council which has helped make this investigation possible.

The Theory of the Faraday Effect in Molecules

By ROBERT SERBER
University of Wisconsin

(Received June 27, 1932)

In treating the Faraday effect two cases may be distinguished, depending upon whether the frequency of the incident light is near resonance or well removed from resonance with absorption lines of the molecule.

Frequency of incident light well removed from resonance with any absorption lines. In this case it is imperative to include the perturbation of the intensities by the magnetic field, as well as the perturbation of the energies. A general expression is obtained for the rotation by molecules (poly-, di-, or monatomic), of the form

$$V=\sum_{n'}\left\{\frac{\nu^2A(nn')}{(\nu(n'n)^2-\nu^2)^2}+\frac{\nu^2B(nn')}{\nu(n'n)^2-\nu^2}+\frac{\nu^2C(nn')}{T(\nu(n'n)^2-\nu^2)}\right\},$$

where V is the Verdet constant. This formula contains dia- and paramagnetic terms of the usual type, but augmented by terms arising from perturbation of the intensities. It contains, in addition, other diamagnetic terms which have the same frequency dependence as the paramagnetic terms. For atoms this expression reduces to that given by Rosenfeld. However for diatomic molecules our results differ from Kronig's, since we include the effects of the components of magnetic moment perpendicular to the axis of figure. The terms arising in this way were omitted by Kronig, although generally they are of the same order of magnitude as the contribution of the parallel component of the moment.

Independence of spin. When the over-all spin-multiplet width is small compared to kT/h the rotation is completely independent of spin. As a consequence the paramagnetic terms vanish for nonlinear polyatomic molecules, and for linear polyatomic and diatomic molecules in Σ states.

Magnitude of the rotation and comparison with experiment. The classical Becquerel formula for the Verdet constant is $V=\gamma(e/2mc^2)\nu\partial n/\partial\nu$, with $\gamma=1$. It is shown that the rotations, in the visible and near ultraviolet, of the gases for which data are available should be approximately representable by a formula of this form, provided γ is given the proper value. The γ value should lie between zero and one. This conclusion, in all cases but one, agrees with the known facts. The exception is oxygen, but the data are probably in error because of polymerization effects which seriously alter the absorption at high pressures.

Frequency of incident light near resonance with an absorption line. Here only the perturbation of the energies by the magnetic field need be considered. It is shown that the rotation in iodine vapour, observed by Wood, is due to rotational distortion of the excited $^3\Pi_0$ level, which partially uncouples the spin moment from the figure axis. The magnetic rotation spectrum of the alkalis, observed by Wood and Loomis, is also explained, in particular the quenching of lines of large rotational quantum number.

TWO different experimental procedures have been employed in measuring the Faraday rotation in gaseous molecules. One method uses a continuous band of incident frequencies, and a low gas pressure; rotation is then observed only in the immediate neighborhood of an absorption line. The other uses monochromatic incident radiation, and high pressures; it serves to mea-

sure the rotation in "transparent" regions of the spectrum. The first method is exemplified by Loomis's measurements of the magnetic rotation spectrum of the alkalis, the second by Siertsema's work on the rotation of hydrogen in the visible.

Correspondingly, the theory must distinguish two cases:

(I) Incident light near resonance with an absorption line of the molecule.
(II) Incident light well removed from resonance with any absorption line.

Anticipating our later results, we may remark that (I) is the simpler of the two, as here the rotation is caused by the Zeeman effect alone. In case (II) it is essential to include, in addition, the effect of the perturbation of the amplitudes (i.e., intensities) by the magnetic field.

§§1 to 5 of this paper deal with case (II). §1 discusses, in a non-mathematical way, the theoretical attack, the general conclusions, and the experimental data. §§2, 3, and 4 give the mathematical development of the theory. §5 is concerned with the magnitude of the rotation and with the application of the theory to a number of simple examples.

§6 treats case (I), in particular, the rotation of iodine as observed by Wood, and the work of Loomis mentioned above.

§1. Discussion of Theory and Experiment

The theory of the Faraday effect in atoms has been treated by Rosenfeld[1] and others. Rosenfeld found, for the case of multiplet widths small compared to kT/h, that when the frequency of the incident light is not near any absorption line the rotation can be expressed as a sum of terms of two types: the diamagnetic, characterized by independence of temperature, and the paramagnetic, proportional to $1/T$. The diamagnetic terms are given by

$$V = \frac{4\pi e N \nu^2}{3hmc^2} \sum_{n'} \frac{\nu(n'n)\,|\,P(nn')\,|^2}{(\nu(n'n)^2 - \nu^2)^2}, \tag{1}$$

where V, the Verdet constant, is the rotation per gauss per cm, the $P(nn')$ are the matrix elements of the resultant electric moment, and ν is the frequency of the incident light. Eq. (1) can also be written in the Becquerel form

$$V = \frac{e}{2mc^2} \nu \frac{\partial n}{\partial \nu},$$

in which n is the index of refraction, as given by the Kramers dispersion formula.[2] This value of V will be called the normal Verdet constant.

The purpose of the present paper will be to extend the theory to molecules. A start in this direction has already been made by Kronig,[3] who, under the same condition that ν is not too near the frequency of any line, finds a Verdet

[1] L. Rosenfeld, Zeits. f. Physik **57**, 835 (1930).

[2] See, for example, J. H. Van Vleck, *The Theory of Electric and Magnetic Susceptibilities*, p. 362.

[3] R. de L. Kronig, Zeits. f. Physik **45**, 458 and 508 (1927).

constant of only one-third the normal value.[4] This result seems unsatisfactory, for it does not agree with Rosenfeld's calculation in the limiting case of a central field. It will be shown that the error lies in Kronig's neglect of the components of magnetic moment perpendicular to the axis of figure of the diatomic molecule. Since in a central field the components of magnetic moment along any three orthogonal axes contribute equally to the rotation, neglect of two of these components will naturally lead to Kronig's result.

We shall suppose throughout that ν is well outside the Zeeman pattern of any line, i.e., that $\nu - \nu(n'n)$ is large compared to the Zeeman displacements. When only this restriction is made the rotation of any molecule[5] is found to be given by a formula of the form

$$V = B \sum_{nn'} \left\{ \frac{\nu^2 a(nn')}{(\nu(n'n)^2 - \nu^2)^2} + \frac{\nu^2 b(nn')}{\nu(n'n)^2 - \nu^2} + \frac{\nu^2 c(nn')}{T(\nu(n'n)^2 - \nu^2)} \right\} e^{-W_n/kT}, \quad (2)$$

with $B = 1/\sum_n e^{-W_n/kT}$. The three kinds of terms appearing in Eq. (2) will be called "a terms," "b terms," and "c terms," respectively. The a terms are the contributions of the Zeeman effect; the c terms are due to the altered distribution of molecules in the various normal states caused by the magnetic field. The b terms arise from the perturbation of the amplitude elements of the electric moment by the magnetic field. This perturbation is, of course, a consequence of the existence of matrix elements of the magnetic moment between the various states.

Definition of the term "magnetic interaction"

For brevity, when an element of the magnetic moment between two states exists, we shall speak of the magnetic interaction between the states.

Coalescence of *b* terms into *a* and *c* terms

The magnetic interaction between a state n' and a state n'' gives a rotation proportional to the difference quotient[6]

$$\frac{1}{\nu(n'n'')} \left\{ \frac{1}{\nu^2 - \nu(n'n)^2} - \frac{1}{\nu^2 - \nu(n''n)^2} \right\}. \quad (3)$$

If $\nu(n'n'')/(\nu - \nu(n'n))$ is small the difference quotient can be expanded in powers of this ratio (since $\nu(n'n'') = \nu(n'n) - \nu(n''n)$) giving

$$\frac{2\nu(n'n)}{(\nu^2 - \nu(n'n)^2)^2} \left\{ 1 - \frac{2\nu(n'n)\nu(n'n'')}{\nu^2 - \nu(n'n)^2} + \cdots \right\}.$$

[4] Kronig has calculated the rotation explicitly only for diatomic molecules in $^1\Sigma$ states. In comparing Kronig's result (p. 511, reference 3) with our Eq. (1), the factor 2 in his expression must be absorbed by summing over $\Lambda = \pm 1$ rather than only over $\Lambda = 1$. Making the substitution $|a_0(l_0 l_1)|^2 = 4|P_\xi(l_0 l_1)|^2$, and remembering that in a central field $|P_\xi(l_0 l_1)|^2 = \frac{1}{3}|P(l_0 l_1)|^2$, one readily verifies that the two expressions differ by a factor 1/3.

[5] Throughout this paper the term *molecule* is to be understood as including *atom*.

[6] It must be cautioned that this picture is incomplete, as not all b terms appear in the form of difference quotients (see Eq. (8)).

Neglecting terms after the first we see that the two b terms contained in Eq. (3) have reduced to a single a term. Similarly, b terms due to magnetic interactions between states with slightly different Boltzmann factors give rise to c terms when expanded in powers of $h\nu(n'n'')/kT$. Of course b terms caused by interactions between states of widely different energies cannot be simplified in this way.

The net result of the operations just described is the enrichment of a and c terms at the expense of b terms. These modified terms will be called A, B, and C terms to distinguish them from the a, b, and c terms. It should be noted that the A and C terms can not be ascribed any such simple origin as was possible for the a and c terms. Hereafter, whenever we refer to Eq. (2) we shall mean the equation modified in this way, rather than the equation as originally given.

Elimination of Boltzmann factors

The exponential factors drop out of Eq. (2) when the following conditions are satisfied:

a. The over-all spin-multiplet width is small compared to kT/h; or

a'. The separation between the two lowest spin-multiplet components is large compared to kT/h.

b. There are no electronic states with separations from the lowest state of the order of kT/h.

c. The separations between the rotational levels of the normal state are small compared to kT/h.

d. The molecule can be considered rigid (e.g., rotational distortion neglected).

e. The states of the molecule can be divided into *groups*.[7] A set of states $n_1, n_2, \cdots n_t$, will be said to constitute a group if $\nu(n_r n_s)$ is small compared to both $\nu - \nu(n_r p)$ and $\nu(n_r m)$, n_r and n_s representing any two members of the set, p one of the normal states, and m any state, normal or excited, not belonging to the set. Thus in Fig. 1 the states g form a group.

It is evident that condition (*e*) restricts us to case (II) discussed in the introduction, for if $\nu - \nu(n_r p)$ is too small (i.e., if the incident light is "near resonance with any absorption line") division of states into groups will be impossible. When ν is restricted to such a range that (*e*) is satisfied, the allowable spread of a group will be widely different in different parts of the spectrum. For example, groups lying near ν or near the normal level may consist of states differing only in their rotational quantum numbers, while groups far from ν and the normal level may include different vibrational states, or even states arising from different electronic configurations.

When either set of conditions, (*a*), (*b*), (*c*), (*d*), (*e*), or (*a'*), (*b*), (*c*), (*d*), (*e*), is met, the rotation is given by a formula of the form

$$V = \sum_{n'} \left\{ \frac{\nu^2 A(nn')}{(\nu(n'n)^2 - \nu^2)^2} + \frac{\nu^2 B(nn')}{\nu(n'n)^2 - \nu^2} + \frac{\nu^2 C(nn')}{T(\nu(n'n)^2 - \nu^2)} \right\}, \qquad (4)$$

[7] In dividing the states into groups not all states need be considered, but only those having nonvanishing terms in Eq. (8).

with $A(nn')$, $B(nn')$, $C(nn')$ constants independent of temperature. Both A and B terms are thus diamagnetic, the C terms paramagnetic. One must not be misled by the terminology into supposing that the signs of paramagnetic and diamagnetic terms are necessarily opposite, for this is not the case. The presence of diamagnetic B terms, having the same frequency dependence as the paramagnetic terms, has been generally overlooked in the previous theories (it was noted, however, by Van Vleck[8]), although, as will be shown later, the B terms are actually no less important than the more customary A terms.

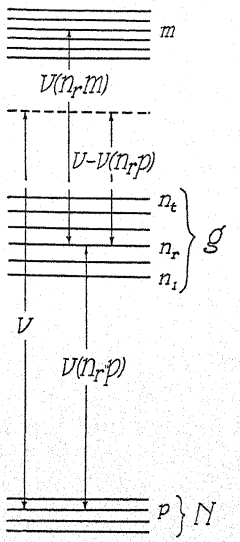


Fig. 1.

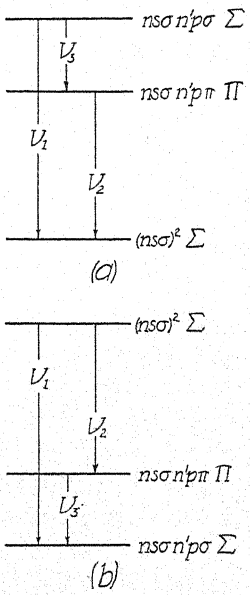


Fig. 2.

In virtue of condition (e) and in view of the discussion of Eq. (3), we can now say that the A terms are due to magnetic interactions between states lying in the same group, while B terms are due to interactions between states in different groups.

The A terms of Eq. (4) are of a more general type than the A terms obtained by Kronig and Rosenfeld, since ours include the interactions between various states in a group. These interactions were neglected by Kronig[9] and did not exist in the case considered by Rosenfeld. Rosenfeld's case of atoms with multiplet widths small compared to kT/h is simplified by the fact that M_L and M_s can be considered constants of the motion,[10] and so the z com-

[8] J. H. Van Vleck, reference 2, p. 370.

[9] Kronig, to be sure, included the elements of μ_z between states of different j, but not between states of different electronic quantum numbers. It is to the latter sort that we refer.

[10] Strictly speaking, this is true only if the magnetic field is strong enough to produce the Paschen-Back effect; however the distinction is trivial in view of the invariance of the spurs appearing in Eq. (9).

ponent of the magnetic moment has no nondiagonal elements. Thus there are no interaction terms like Eq. (3), with the consequence that the A terms reduce simply to the normal Verdet constant, while the B terms vanish entirely (see Eq. (9)).[11] Kronig's calculation of the A terms for diatomic molecules is valid in the limiting case of an axial field so far from central in character that the components of the magnetic moment perpendicular to the figure axis have elements only between states in different groups. Here obviously the A terms are due only to the parallel component of the moment, as Kronig assumed. The B terms will not vanish in this case, and, in fact, are of the same order as the A terms, although omitted by Kronig. Our A terms agree with Kronig's and Rosenfeld's in these limiting cases, but otherwise they are not the same. For example, for nonlinear polyatomic molecules the mean value of the magnetic moment along any axis is zero;[12] hence Kronig's method would give no rotation at all, although we obtain both A and B terms.

Independence of spin

An important characteristic of Eq. (2) (and consequently of Eq. (4)) is that, when (a), (c) and (e) are satisfied, it is completely independent of spin. In any calculation of the rotation, subject of course to these conditions, the spin can be regarded as completely uncoupled from the orbital angular momentum, and, in effect, forgotten completely. This result is analogous to the well-known theorem that the magnetic susceptibility is independent of the Paschen-Back effect, and like it is a consequence of the fact that we sum our expressions over all Zeeman components. In view of this property of the rotation the attempts to explain the anomalous behavior of oxygen as due to its spin are not justifiable. Another conclusion which can immediately be drawn is that the paramagnetic terms of Eq. (4) vanish for nonlinear polyatomic molecules, and for linear polyatomic molecules and diatomic molecules in Σ states. This is because the paramagnetic terms are due to the magnetic interactions between the normal states. Since spin need not be considered, these interactions are clearly zero in the cases indicated.

The absence of a spin-paramagnetic rotation is in sharp contrast to the presence of a spin term in the magnetic susceptibility under the same supposition of narrow multiplets. The difference arises because, under the circumstances, the spin and orbital moments can be regarded as completely independent systems. They thus will contribute additively to the susceptibility; on the other hand, the spin appears in the rotation only in cross terms with the orbit, and such cross terms average to zero.

Magnitude of the rotation

It frequently happens that the rotation has not been measured much beyond the visible, while all the $\nu(n'n)$ are in the far ultraviolet. The A and B

[11] Considering the phases proper to a central field, it is readily seen that, in this case, Eq. (9) is identical with Rosenfeld's expression.

[12] This statement might not hold if the molecule had a very high degree of symmetry; however, whenever we consider nonlinear polyatomic molecules we shall assume that this is not the case.

terms are then practically indistinguishable, the net result of the B terms being to change the apparent values of the $A(nn')$. Thus the diamagnetic terms of Eq. (4) will have, effectively, the frequency dependence, $\nu^2/(\nu(n'n)^2-\nu^2)^2$, of the Becquerel formula. In consequence, as will be shown more fully in §5, the rotation can often be represented fairly well by the Becquerel formula with an anomalous value of e/m.

In general our knowledge of the molecule is not sufficient to permit explicit calculation of all the terms required by Eq. (4), but simple considerations lead to the conclusion that the Verdet constant should ordinarily be less than the normal value. The experimental results in all cases confirm this. The reason is roughly as follows: The rotation is largely due to the nearest intense group of lines in the ultraviolet, which are heavily weighted compared to those further out. If all the lines lay close to this nearest group a normal Verdet constant would result, as is shown in §5. The effect of removing some of the lines further into the ultraviolet, where in fact they belong, is to diminish greatly their contribution to the rotation. If the field is not central this diminution is greater than the corresponding decrease in $\partial n/\partial\nu$, and so leads to a smaller Verdet constant.

Discussion of experiment[13]

Siertsema's measurements of the rotation in hydrogen in the visible are representable almost exactly by the normal Verdet constant. This result, remarkable in its agreement with the classical theory, will be discussed in §5. However Sirk's measurements in the ultraviolet show some evidence of the presence of a B term. The magnitude of the observed rotation in nitrogen is 63 percent of the normal Verdet constant, i.e., the Becquerel formula is valid if we insert a factor 0.63. As the measurements have not been carried beyond the visible no differentiation between A and B terms is possible. The case of N_2O is similar. Carbon dioxide has been observed in the ultraviolet, but not far enough to give any conclusive evidence as to the presence or absence of B terms (see §5).

Oxygen, on the other hand, is definitely anomalous. The measurements of Siertsema and Sirks in the visible and ultraviolet cannot be fitted by Eq. (4) using the observed absorption frequencies, and, as we have seen, this cannot be blamed on the spin. However the experimental data are open to serious objection because of the high gas pressures used: Siertsema, working in the visible, used a pressure of 100 atmospheres; Sirks, 80 atmospheres in the visible, 40 in the ultraviolet below 2800A. At these pressures a considerable amount of oxygen would be in the form of the polymer O_4.[13a] The equilibrium constant is somewhat uncertain; at 80 atmospheres the estimates of the

[13] An excellent account of the experimental data on the Faraday effect has been given by C. G. Darwin and W. H. Watson, Proc. Roy. Soc. **114A**, 474 (1927). The reader is referred to this paper for references to the literature.

[13a] The existence of this polymer was kindly called to my attention by Professor R. Ladenburg.

partial pressure of O_4 range from 1 to 10 percent of the total pressure.[14] According to Wulf,[14] O_4 shows continuous absorption below 2400A, as well as a number of bands extending towards longer wave-lengths. Moreover, the source of light used by Sirks and Siertsema was a quartz mercury arc, and Warburg[15] has shown that at high pressures the 2537A line is efficacious in producing ozone. Ozone shows strong absorption in the infrared, and in the ultraviolet beginning at about 2800A. Sirks found, in his 230 cm column of oxygen at 80 atmospheres, that absorption began at 2805A; in fact it was for this reason that he was compelled to reduce the pressure for his shorter wave-length measurements. At 40 atmospheres the absorption had moved down to 2654A. O_2 shows no absorption in this region, but both O_4 and O_3 bands have been reported at 2810A and 2654A;[16] these might readily account for Sirk's results.

In view of these facts we believe the existing measurements of the rotation entirely unreliable; solution of the problem must await more unambiguous data.

Monatomic gases should, according to Rosenfeld, have a normal Verdet constant. This has been verified for neon, although at only one wave-length, 5460A. The same result has also been found for argon.[17]

In general the rotations in the large number of liquids and solids cited by Darwin are not accurately representable by the Becquerel formula, even with an anomalous value of e/m. There are two obvious reasons for this: first, the $A(nn')$ are not proportional to the f values of the Kramers dispersion formula; second, B terms are also present.

§2. Derivation of the General Formula for the Rotation

Let the magnetic field and the light ray be directed along the z axis. The rotation of the plane of polarization per centimeter is[18]

$$\theta = CB \sum_{nn'} \tau(n'n) [P_x(nn') P_y(n'n)] e^{-W_n/kT}, \tag{5}$$

where

$$B = N/\sum_n e^{-W_n/kT}, \quad C = 4\pi^2\nu^2 i/ch,$$

and $P_x(nn')$, $P_y(nn')$ are the elements of the x and y components of the electric moment in the presence of the magnetic field. Here, and throughout this paper, the square brackets have the meaning

$$[P_x(nn')P_y(n'n)] = P_x(nn')P_y(n'n) - P_y(nn')P_x(n'n);$$

and

$$\tau(n'n) = 1/(\nu^2 - \nu(n'n)^2).$$

[14] O. R. Wulf, Proc. Nat. Acad. **14**, 356, 609, 614 (1928); Jour. Am. Chem. Soc. (II) **50**, 2596 (1928).

[15] References to Warburg's work are given by Wulf, reference 14.

[16] Wulf, reference 14; D. Chalonge and M. Lambrey, Comptes Rendus **184**, 1165 (1927).

[17] R. de Mallemann, L. Gabiano, and F. Suhner; Comptes Rendus **194**, 861 (1932).

[18] H. A. Kramers, Kon. Acad. Wet. Amsterdam **33**, 959 (1930). Kramer's Eq. (34) should be multiplied by 4π, as can be seen from his Eq. (32).

We expand P_x, P_y, $\nu(n'n)$, W_n, B in power series of the form $P_x = P_x^0 + \mathfrak{H}P_x^{(1)} + \cdots$; then, under the supposition that $\nu - \nu(n'n)$ is large compared to the Zeeman splitting, the terms of Eq. (5) linear in $\mathfrak{H}$ give

$$\begin{aligned} V = \theta/\mathfrak{H} = CB^0 \sum_{nn'} \{ & \tau^0(n'n)([P_x^0(nn')P_y^{(1)}(n'n)] + [P_x^{(1)}(nn')P_y^0(n'n)]) \\ & + 2\nu^0(n'n)\nu^{(1)}(n'n)\tau^0(n'n)^2[P_x^0(nn')P_y^0(n'n)] \\ & - (W_n^{(1)}/kT)\tau^0(n'n)[P_x^0(nn')P_y^0(n'n)]\} e^{-W_n^0/kT}. \end{aligned} \tag{6}$$

$P_x^{(1)}(nn')$ is expressed in terms of the unperturbed amplitudes by means of[19]

$$P_x^{(1)}(nn') = \frac{1}{h} \sum_{n''}{}' \left\{ \frac{H^{(1)}(nn'')P_x^0(n''n')}{\nu^0(nn'')} - \frac{P_x^0(nn'')H^{(1)}(n''n')}{\nu^0(n''n')} \right\}. \tag{7}$$

The prime on the summation sign indicates that $n'' = n$ and $n'' = n'$ are to be omitted from the summation. Denoting the z component of the magnetic moment by μ_z, we have $H^{(1)}(nn') = -\mu_z(nn')$. Using these, and a similar expression for $P_y^{(1)}(nn')$, we obtain

$$\begin{aligned} V = & - (CB^0/h) \sum_{nn'n''}{}' \nu^0(n'n'')^{-1}[P_x^0(nn')\mu_z(n'n'')P_y^0(n''n)] \\ & \{\tau^0(n'n) - \tau^0(n''n)\} e^{-W_n^0/kT} \\ & - (2CB^0/h) \sum_{nn'} \nu^0(n'n)\tau^0(n'n)^2[P_x^0(nn')\mu_z(n'n')P_y^0(n'n)]e^{-W_n^0/kT} \\ & + (CB^0/h) \sum_{nn'n''}{}' \nu^0(n''n)^{-1}\tau^0(n'n) \{[P_x^0(nn')P_y^0(n'n'')]\mu_z(n''n) \\ & + \mu_z(nn'')[P_x^0(n''n')P_y^0(n'n)]\} e^{-W_n^0/kT} \\ & + (2CB^0/h) \sum_{nn'} \nu^0(n'n)\tau^0(n'n)^2\mu_z(nn)[P_x^0(nn')P_y^0(n'n)]e^{-W_n^0/kT} \\ & + (CB^0/kT) \sum_{nn'} \tau^0(n'n)\mu_z(nn)[P_x^0(nn')P_y^0(n'n)]e^{-W_n^0/kT}. \end{aligned} \tag{8}$$

Here we have extended our definition of the square bracket to include

$$\begin{aligned} [P_x^0(nn')\mu_z(n'n'')P_y^0(n''n)] = & P_x^0(nn')\mu_z(n'n'')P_y^0(n''n) \\ & - P_y^0(nn')\mu_z(n'n'')P_x^0(n''n). \end{aligned}$$

In accordance with our division of states into groups, all matrix elements will now be written (dropping henceforth the superscript 0) in the form $P_x(nk;n'k')$, where n and n' represent the quantum numbers which are the same for all states in a group, k and k' the quantum numbers which differentiate the various states within a group.

The terms of the first sum in Eq. (8) for which $n'' = n'$ (although, of course, $k'' \neq k'$) can be simplified by expanding the factor in curly brackets in powers of $\nu(n'k';n'k'')/(\nu^2 - \nu(n'k';nk)^2)$. To simplify the terms of the third sum for which $n'' = n$ $(k'' \neq k)$ the method of pairing terms previously used by Van Vleck[20] is employed.

[19] See, for example, Born and Jordan, *Elementare Quantenmechanik*, p. 198.

[20] J. H. Van Vleck, reference 2, p. 191; Phys. Rev. **29**, 727 (1927).

The pair of terms

$$(1/h)\nu(nk''; nk)^{-1}\tau(n'k'; nk)\{[P_x(nk; n'k')P_y(n'k'; nk'')]\mu_z(nk''; nk) + \mu_z(nk; nk'')[P_x(nk''; n'k')P_y(n'k'; nk)]\}e^{-W_{nk}/kT}$$
$$+ (1/h)\nu(nk; nk'')^{-1}\tau(n'k'; nk'')\{[P_x(nk''; n'k')P_y(n'k'; nk)]\mu_z(nk; nk'') + \mu_z(nk''; nk)[P_x(nk; n'k')P_y(n'k'; nk'')]\}e^{-W_{nk''}/kT}$$

can be written

$$\{[P_x(nk; n'k')P_y(n'k'; nk'')]\mu_z(nk''; nk) + \mu_z(nk; nk'')[P_x(nk''; n'k')P_y(n'k'; nk)]\}$$
$$\frac{1}{h\nu(nk''; nk)}\left\{\frac{e^{-W_{nk}/kT}}{\nu^2 - \nu(n'k'; nk)^2} - \frac{e^{-W_{nk''}/kT}}{\nu^2 - \nu(n'k'; nk'')^2}\right\}.$$

Putting

$$W_{nk''} = W_{nk} + h\nu(nk''; nk),$$
$$\nu(n'k'; nk'') = \nu(n'k'; nk) - \nu(nk''; nk)$$

and expanding gives (the first bracket representing the first line of the above expression)

$$\{\}\left\{\frac{1}{2kT}\,\frac{e^{-W_{nk}/kT}}{\nu^2 - \nu(n'k'; nk)^2}\left[1 + \left(1 - \frac{h\nu(nk''; nk)}{kT}\right)\right]\right.$$
$$\left. + \frac{2\nu(n'k'; nk)e^{-W_{nk}/kT}}{h(\nu^2 - \nu(n'k'; nk)^2)^2}\left[1 - \frac{h\nu(nk''; nk)}{kT}\right]\right\}$$

plus higher order terms which are very small. Apart from them, this is the same as

$$\{[P_x(nk; n'k')P_y(n'k'; nk'']\mu_z(nk''; nk) + \mu_z(nk; nk'')[P_x(nk''; n'k')P_y(n'k'; nk)]\}$$
$$\{(1/h)\nu(n'k'; nk)\tau(n'k'; nk)^2 + (1/2kT)\tau(n'k'; nk)\}e^{-W_{nk}/kT}$$
$$+ \{[P_x(nk''; n'k')P_y(n'k'; nk)]\mu_z(nk; nk'') + \mu_z(nk''; nk)[P_x(nk; n'k')P_y(n'k'; nk'')]\}$$
$$\{(1/h)\nu(n'k'; nk'')\tau(n'k'; nk'')^2 + (1/2kT)\tau(n'k'; nk'')\}e^{-W_{nk''}/kT}.$$

The purpose of these manipulations is to remove all small ν's from the denominators of Eq. (8). A primed sum is no longer required for the terms written in this form, since the diagonal terms (i.e., $k''=k$) are already present in Eq. (8): namely, the fourth and fifth sums there appearing. The expansion of the first sum of Eq. (8) leads to a similar simplification, the diagonal terms being contained in the second sum.

It is now convenient to introduce the übermatrix notation used, for example, in Born and Jordan's *Elementare Quantenmechanik*. In this notation $P_x^{(nn')}$ signifies the matrix of all the elements $P_x(nk;n'k')$ having a given n and n'. Sp is an abbreviation for *spur*.

One finds, on carrying out the operations described above that Eq. (8) becomes

$$V = (CB/h)\sum_{n'}\nu(n'n)\tau(n'n)^2\,\mathrm{Sp}\{(-2[P_x^{(nn')}\mu_z^{(n'n')}P_y^{(n'n)}]$$
$$+ [P_x^{(nn')}P_y^{(n'n)}]\mu_z^{(nn)} + \mu_z^{(nn)}[P_x^{(nn')}P_y^{(n'n)}])e^{-W^{(n)}/kT}\}$$
$$+ (CB/h)\sum_{n'n''(n'\neq n'')} - \nu(n'n'')^{-1}\{\tau(n'n) - \tau(n''n)\}$$
$$\mathrm{Sp}\{[P_x^{(nn')}\mu_z^{(n'n'')}P_y^{(n''n)}]e^{-W^{(n)}/kT}\}$$
$$+ \nu(n''n)^{-1}\tau(n'n)\,\mathrm{Sp}\{([P_x^{(nn')}P_y^{(n'n'')}]\mu_z^{(n''n)}$$
$$+ \mu_z^{(nn'')}[P_x^{(n''n')}P_y^{(n'n)}])e^{-W^{(n)}/kT}\} \qquad (9)$$
$$+ (CB/2kT)\sum_{n'}\tau(n'n)\,\mathrm{Sp}\{([P_x^{(nn')}P_y^{(n'n)}]\mu_z^{(nn)}$$
$$+ \mu_z^{(nn)}[P_x^{(nn')}P_y^{(n'n)}])e^{-W^{(n)}/kT}\}.$$

As all small ν's have been removed from the denominators of Eq. (8) we have been able, in Eq. (9), to write $\nu(n'k';nk)=\nu(n'n)$. In the first sum of Eq. (9) small terms involving $\nu(nk';nk)$ have been omitted. This corresponds to neglecting the pure rotation spectrum.

§3. Independence of Spin

The spurs appearing in Eq. (9) are invariant of a transformation to a system of representation appropriate to strong fields. If the over-all spin-multiplet width is small compared to kT/h the matrix $e^{-W^{(n)}/kT}$ is independent of spin. Then the "strong field" representation the spin appears only in μ_z, which breaks up into two parts, $\mu_{lz}+\mu_{sz}$, of which only the second contains the spin. On summing over m_s this term vanishes, since μ_{sz} is a diagonal matrix with elements ranging from $-2\beta s$ to $2\beta s$. Thus, when the over-all multiplet width is small and when ν is not near resonance with any line, the rotation is independent of the spin.[21] This result, of course, is valid for all field strengths (barring saturation effects).

In §5, dealing with the magnitude of the rotation, we shall consider only narrow multiplets; μ_z may accordingly be taken as representing only that part of the magnetic moment due to the orbital angular momentum.

§4. Rotation in Rigid Molecules

We will make the approximation of supposing the molecule rigid, that is, we suppose the "internal" wave functions, which are expressed in terms of a coordinate system rotating with the molecule, independent of j. Then the summation over j, m, j', m', j'', m'' implied in Eq. (9) can be readily performed by a method given by Niessen.[22] Let x', y', z' be the rotating system of coordinates. On applying Niessen's method to Eq. (9) we find[23]

$$\begin{aligned}
V = {} & (C\,N/3hg)\sum_{x'y'z'}\sum_{n'}\nu(n'n)\tau(n'n)^2\ \mathrm{Sp}\left\{-2\left[P_{x'}^{(nn')}\mu_{z'}^{(n'n')}P_{y'}^{(n'n)}\right]\right. \\
& \left.+\left[P_{x'}^{(nn')}P_{y'}^{(n'n)}\right]\mu_{z'}^{(nn)}+\mu_{z'}^{(nn)}\left[P_{x'}^{(nn')}P_{y'}^{(n'n)}\right]\right\} \\
& +(CN/3hg)\sum_{x'y'z'}\sum_{n'n''(n''\neq n')}-\nu(n'n'')^{-1}\left\{\tau(n'n)-\tau(n''n)\right\} \\
& \mathrm{Sp}\left[P_{x'}^{(nn')}\mu_{z'}^{(n'n'')}P_{y'}^{(n''n)}\right]+\nu(n''n)^{-1}\tau(n'n) \\
& \mathrm{Sp}\left\{\left[P_{x'}^{(nn')}P_{y'}^{(n'n'')}\right]\mu_{z'}^{(n''n)}+\mu_{z'}^{(nn'')}\left[P_{x'}^{(n''n')}P_{y'}^{(n'n)}\right]\right\} \\
& +(CN/6kTg)\sum_{x'y'z'}\sum_{n'}\tau(n'n)\ \mathrm{Sp}\left\{\left[P_{x'}^{(nn')}P_{y'}^{(n'n)}\right]\mu_{z'}^{(nn)}\right. \\
& \left.+\mu_{z'}^{(nn)}\left[P_{x'}^{(nn')}P_{y'}^{(n'n)}\right]\right\}.
\end{aligned} \tag{10}$$

The symbol $\sum_{x'y'z'}$ indicates a summation of the three terms obtained by a cyclic interchange of x', y', z'. g is the statistical weight of the normal state

[21] This result has been given, for central fields, by Rosenfeld, reference 1, and in the old quantum theory, also for central fields, by Darwin, Proc. Roy. Soc. **112A**, 814 (1926).

[22] K. F. Niessen, Phys. Rev. **34**, 253 (1929). Niessen's derivation is valid only for diatomic molecules, but the proof can be given for the general case.

[23] It should be noted that Eq. (10) holds when either condition (a) or (a') is satisfied.

of the stationary molecule. The elements of matrices such as $P_{x'}{}^{(nn')}$ are, of course, independent of j, m, j', m'.

Making a simple rearrangement of the terms in the second sum of Eq. (10), we find the explicit expression for the $A(nn')$, $B(nn')$, $C(nn')$ of Eq. (4):

$$A(nn') = (CN/3hg\nu^2) \sum_{x'y'z'} \nu(n'n)$$
$$\text{Sp}\left\{ -2\left[P_{x'}{}^{(nn')}\mu_{z'}{}^{(n'n')}P_{y'}{}^{(n'n)}\right] + \left[P_{x'}{}^{(nn')}P_{y'}{}^{(n'n)}\right]\mu_{z'}{}^{(nn)} + \mu_{z'}{}^{(nn)}\left[P_{x'}{}^{(nn')}P_{y'}{}^{(n'n)}\right]\right\}$$

$$B(nn') = (CN/3hg\nu^2) \sum_{x'y'z'} \sum_{n''(n''\neq n')} - \nu(n'n'')^{-1}\,\text{Sp}\left\{\left[P_{x'}{}^{(nn')}\mu_{z'}{}^{(n'n'')}P_{y'}{}^{(n''n)} + \left[P_{x'}{}^{(nn'')}\mu_{z'}{}^{(n''n')}P_{y'}{}^{(n'n)}\right]\right\} + \nu(n''n)^{-1}\,\text{Sp}\left\{\left[P_{x'}{}^{(nn')}P_{y'}{}^{(n'n'')}\right]\mu_{z'}{}^{(n''n)} + \mu_{z'}{}^{(nn'')}\left[P_{x'}{}^{(n''n')}P_{y'}{}^{(n'n)}\right]\right\}$$

$$C(nn') = (CN/6kg\nu^2) \sum_{x'y'z'} \text{Sp}\left\{\left[P_{x'}{}^{(nn')}P_{y'}{}^{(n'n)}\right]\mu_{z'}{}^{(nn)} + \mu_{z'}{}^{(nn)}\left[P_{x'}{}^{(nn')}P_{y'}{}^{(n'n)}\right]\right\}.$$

§5. Magnitude of the Rotation

For nonlinear polyatomic molecules the matrix $\mu^{(nn)}$ will be zero, there being no "precession frequencies" which are not large compared to kT/h. Thus the $C(nn')$ will vanish. Diatomic molecules and linear polyatomic molecules in Σ states will also have no elements in $\mu^{(nn)}$ different from zero, so the $C(nn')$ again vanish. In these cases there will be no paramagnetic rotation.

The work of Rosenfeld and Kronig give limiting values for the $A(nn')$. We have shown in §1 that in a central field the $A(nn')$ have just the values which give the normal Verdet constant, and in the other limiting case (for diatomic molecules) of an extreme axial field the $A(nn')$ are reduced to one-third the previous value (the three terms of the $\sum_{x'y'z'}$ sum reducing to a single term), unless both n and n' are Σ states, in which case $A(nn')$ vanishes entirely.[24] The $A(nn')$ of polyatomic molecules similarly vanish for sufficiently asymmetrical fields.

The whole question of the magnitude of the rotation is greatly clarified by consideration of a few simple examples. The molecular wave function (in the x', y', z' system) will be supposed the product of the hydrogenic wave functions of the individual electrons. This makes Λ a constant of the motion.

Let the normal state be $(ns\sigma)^2\Sigma$, as in the hydrogen molecule. Take for excited states $ns\sigma n'p\pi\Pi$ and $ns\sigma n'p\sigma\Sigma$, and let ν_1, ν_2, ν_3 be respectively the $ns\sigma n'p\sigma\Sigma - (ns\sigma)^2\Sigma$, $ns\sigma n'p\pi\Pi - (ns\sigma)^2\Sigma$, $ns\sigma n'p\sigma\Sigma - ns\sigma n'p\pi\Pi$ separations. This situation is illustrated in Fig. 2 (*a*). No assumption will be made as to the relative magnitudes of ν_1 and ν_2, other than that condition (*e*) is satisfied; they must accordingly be considered as belonging to two different groups. This procedure, of course, is valid even when $\nu_1 - \nu_2$ (i.e., ν_3) is small. Using the well-known hydrogenic moment matrices we readily find from Eq. (10),[25]

[24] We are thinking here of the practically important case, in which the normal state is a Σ state. In general the one-third remaining after passage to the axial field limit will be divided among the states of different Λ into which the central field group breaks up.

$$V = \frac{4\pi eN\nu^2}{3hmc^2}\left\{\frac{P^2}{\nu_3(\nu_2^2-\nu^2)} - \frac{P^2}{\nu_3(\nu_1^2-\nu^2)} + \frac{\nu_2 P^2}{(\nu_2^2-\nu^2)^2}\right\}, \tag{11}$$

where $P^2 = 2\left|P_{x'}(n'p\pi, ns\sigma)\right|^2$ in the notation of footnote (25).

The normal Verdet constant is

$$V_n = \frac{4\pi eN\nu^2}{3hmc^2}\left\{\frac{\nu_1 P^2}{(\nu_1^2-\nu^2)^2} + \frac{2\nu_2 P^2}{(\nu_2^2-\nu^2)^2}\right\}. \tag{12}$$

The asymptotic properties discussed above are easily verified. If ν_3 is made small compared to $\nu_1-\nu$, Eqs. (11) and (12) both reduce to

$$V = V_n = 4\pi eN\nu^2\nu_2 P^2/hmc^2(\nu_2^2-\nu^2)^2;$$

thus V is just the normal Verdet constant. If ν_3 is very large, so that the first two terms of Eq. (11) and the first term of Eq. (12) are negligible, the rotation, as given by Eq. (11), is reduced to one-third the above value, which is Kronig's result. In this case $V=\frac{1}{2}V_n$ (the index of refraction being reduced to 2/3 its central field value, while the rotation is reduced to 1/3).

If γ is defined by $\gamma = V/V_n$, we have seen that $\gamma=1$ for a central field, and $\gamma=0.5$ for an extreme axial field.[26] In intermediate cases γ will lie between these values. For example if we take $\nu_1=2\nu_2$, $\nu=\nu_2/6$ we find $\gamma=0.817$. Taking $\nu=\nu_2/4$ gives $\gamma=0.813$. If ν_2 corresponds to a line at 1000A these two values of ν correspond to 6000A and 4000A respectively. This simple calculation strikingly illustrates the point made in §1 that A and B terms are, in such a frequency range, practically indistinguishable. Further, it shows very clearly why a Becquerel formula with an anomalous value of e/m is approximately valid for many substances. If we put $\nu=\nu_2/2.5$, corresponding to $\lambda=2500$A, we obtain $\gamma=0.79$. Thus even measurements this far in the ultraviolet would be of little value in distinguishing between Eq. (11) and the modified Becquerel formula.

Magnetic interactions between some of the excited states may be due to the "core," or part of the molecule exclusive of the excited electron, for when we remove an electron from a closed shell the residuum may have a magnetic moment. Of course states which have different core-configurations are greatly different in energy, and so the magnetic interactions of the core may easily connect widely separated levels. On the other hand, a normal Verdet constant requires narrow, rather than wide, separations. The essential difference

[25] For example, denoting the normal state by ψ_1, the Π state by ψ_2, and the wave functions of the individual electrons by $(n|x_i)$ we have

$$\psi_1 = (ns\sigma|x_1)(ns\sigma|x_2), \quad \psi_2 = (ns\sigma|x_1)(n'p\pi|x_2),$$
$$P_x(12) = -e\int\int\psi_1^*(x_1+x_2)\psi_2 d\tau_1 d\tau_2 = -e\int(ns\sigma|x_2)^* x_2(n'p\pi|x_2)d\tau_2$$
$$= P_{x_2}(ns\sigma; n'p\pi).$$

The elements such as $P_{x_2}(ns\sigma; n'p\pi)$ are given in all the standard texts, e.g., H. Weyl, *The Theory of Groups and Quantum Mechanics*, p. 200.

[26] If the Σ state is taken as the lower of the excited states γ would range from 1 to 0 (we are supposing $\nu<\nu_1, \nu_2$). For polyatomic molecules also, γ would be expected to range from 1 to 0. These figures are exclusive of negative terms, which will be discussed later.

between the rotations in atoms and molecules lies in the spread, in molecules, of levels which coincide in atoms; and the more complicated the core the larger this spread is likely to be. One would therefore expect the rough rule that molecules with complicated cores have lower values of γ than simpler molecules. The data confirm this, the γ values for H_2, N_2, CO_2, N_2O being respectively 1.00, 0.63, 0.56, 0.34.

The central field behaviour of hydrogen in the visible is now readily explained, for the core consists of a single electron in a σ state, and thus plays no part in determining the rotation. As one would anticipate, the potential energy curves[27] show that the excited $1s\sigma 2p\sigma\Sigma$ and $1s\sigma 2p\pi\Pi$ states lie quite close to each other as compared to their separation from the normal state. Since there is little possibility of exciting the core electron to obtain other states which could contribute to the rotation, the rotation is evidently due almost entirely to the two excited states mentioned above; and, as we have seen, these closely spaced levels should give a normal Verdet constant.

As an example of the case in which the core does have a magnetic moment we shall take for the normal state $(np\pi)^4(np\sigma)^2\Sigma$, the nitrogen configuration, and for excited states $(np\pi)^3(np\sigma)^2n's\sigma\Pi$ and $(np\pi)^4\, np\sigma n's\sigma\Sigma$. Magnetic interactions between these states will evidently be due to the core of the Π state. Proceeding exactly as in the previous example we again find the rotation to be given by Eq. (11). In a central field the energies of our two excited states will coincide, and a normal Verdet constant will result: in such a field no distinction need be made between the magnetic moment of the core and the magnetic moment of a valence electron. In the axial field of a diatomic molecule the energies of the excited states will be widely different, since these states have different core configurations; γ will thus be considerably less than unity. This result, as contrasted with the result obtained for the hydrogen molecule, illustrates the effect of a complex core in diminishing the Verdet constant.

When we deal with homonuclear diatomic molecules another factor may enter which we have not yet considered. For such molecules $P(nn')$ has elements only between the normal state and states of opposite symmetry with respect to reflection of the electrons in the origin. States n'' of the same symmetry as the normal state will have no effect on the refraction, but Eq. (10) shows that they will affect the magnitude of the rotation if the elements $\mu_z(nn'')$ are not negligible, although no terms containing $\tau(n''n)$ will appear.

A situation in which μ_z has elements between the normal states and an excited group of states can be obtained by inverting the energy levels of our first example, so that the $(ns\sigma)^2\Sigma$ state lies above the $ns\sigma n'p\pi\Pi$ and $ns\sigma n'p\sigma\Sigma$ states, as is shown in Fig. 2(*b*). Eq. (11) then holds only if ν_3 is small compared to kT/h, so that there is no difference in the concentrations of the molecules in the $ns\sigma n'p\pi\Pi$ and $ns\sigma n'p\sigma\Sigma$ states.[28] The second term of Eq. (11) is then due to molecules in the latter state, the first and third to those in the former.

[27] R. S. Mulliken, Rev. Mod. Phys. **4**, 1 (1932).

[28] A weight factor 1/3 should be included in Eq. (11) in this case. There will also be a paramagnetic term; however it is of no interest for our purposes.

However if the Π state is the higher of the two, that is if ν_3 is positive and large compared to kT/h, the first and third terms vanish and we are left with a negative B term. A negative B term is also obtained if the Σ state is the higher.

In our examples the effect of magnetic interactions between two excited levels is to give, when $\nu<\nu_1, \nu_2$ or $\nu>\nu_1, \nu_2$, two B terms which, although they are of opposite sign, give a net rotation which is positive; when $\nu_2<\nu<\nu_1$, two negative B terms. The effect of interaction between the normal state and an excited state of frequency ν_3 is to give a negative B term when $\nu<\nu_1$, a positive term when $\nu>\nu_1$. Negative B terms may account for the negative rotation of $TiCl_4$.

It is of some interest to calculate the rotation under the assumption that all excited levels lie in the same group. Suppose the electric moments have elements only between the normal states, n, k, and a group of states, n', k', having the same n'. Under this hypothesis the second sum of Eq. (10) vanishes, and the teilmatrices appearing in the remaining terms can be replaced by the complete matrices (the spur, of course, is still taken only over the normal states). The third sum of Eq. (10), and the second and third terms of the first sum, are zero in virtue of the commutability of the coordinates. On summing over all electrons we have

$$\begin{aligned} P_x\mu_z P_y - P_y\mu_z P_x &= -(e^3/2mc)\sum_{ijk} x_i(x_j p_{yj} - y_j p_{xj})y_k - y_k(x_j p_{yj} - y_j p_{xj})x_i \\ &= -(e^3/2mc)\sum_{ijk} x_i x_j(p_{yj}y_k - y_k p_{yj}) + y_k y_j(p_{xj}x_i - x_i p_{xj}) \\ &= -(e^3h/4\pi mci)\sum_{ij}(x_i x_j + y_i y_j) = -(eh/4\pi mci)(P_x^2 + P_y^2). \end{aligned}$$

Adding the terms obtained by cyclic interchange of x, y, z, we find

$$V = \frac{4\pi eN\nu^2}{3hmc^2}\,\frac{\nu(n'n)}{(\nu^2 - \nu(n'n)^2)^2}\,\frac{1}{g}\sum_{kk'}\left|P(nk;n'k')\right|^2,$$

which is just the normal Verdet constant.

§6. Rotation Near an Absorption Line

Going back to Eq. (6) we see that when ν is close to one of the $\nu(n'n)$ the rotation is

$$V = 2CB\sum_{m,m'}\frac{\nu(n'n)\nu^{(1)}(n'm';nm)\left[P_x(nm;n'm')P_y(n'm';nm)\right]}{(\nu^2 - \nu(n'n)^2)^2}e^{-W_n/kT}, \quad (13)$$

for, since this term contains $1/(\nu^2-\nu(n'n)^2)^2$ rather than $1/(\nu^2-\nu(n'n)^2)$, it is very much larger than all the others. The rotation thus depends only on the Zeeman effect, the perturbation of the amplitudes being negligible.

Rotation in iodine

The iodine lines observed by Wood[29] come from a $^3\Pi_0 - {}^1\Sigma$ transition, and so exhibit no Zeeman effect if we use the "rigid molecule" approximation. Actually, the Zeeman effect, and consequently the optical rotation, is due to rotational distortion, that is, to the effect of molecular rotation in uncoupling the spin from the nuclear axis of figure. The suggestion that rotational distortion is responsible for the behaviour of iodine was originally made by Kemble,[30] but an adequate mechanism was lacking, as at the time the transition was mistakenly classified as $^1\Sigma - {}^1\Sigma$. Kemble supposed that the orbital moment, rather than the spin moment, was uncoupled by the molecular rotation, but it now seems much more probable that spin uncoupling is the preponderant effect.

We shall use the rotating system of axes, x', y', z', previously employed by Van Vleck;[31] the z component of the spin in fixed axes is given in terms of this rotating system by

$$s_z = s_{y'} \sin\theta + s_{z'} \cos\theta,$$

θ denoting the angle between the axis of figure of the molecule and the fixed axis z. The term involving $s_{z'}$ gives the spin part of the ordinary rigid molecule Zeeman effect. In our case this just cancels the effect of the orbital angular momentum, since $\Omega=0$ in the $^3\Pi_0$ state; we shall not be further interested in this term. The matrix $s_{y'} \sin\theta$ can be written

$$(s_{y'} \sin\theta)(\sigma_s jm; \sigma_s' j'm') = 2s_{y'}(\sigma_s\sigma_s')L(\sigma_s jm; \sigma_s' j'm').$$

The elements $L(\sigma_s jm; \sigma_s' j'm')$ are defined and evaluated in a paper by Rademacher and Reiche.[32] As the multiplet separations of the $^3\Pi_0$ state of iodine are very wide, only the first order perturbation of s_z by the molecular rotation is required. This is given by a formula similar to Eq. (7), from which we find for the diagonal elements of $s_z^{(1)}$, when $\Omega=0$, $\sigma_l=1$,

$$\begin{aligned} s_z^{(1)}(-1jm; -1jm) &= 2H^{(1)}(-10)L(0jm; -1jm)s_{y'}(0-1)/h\nu(-10) \\ &\quad + 2L(-1jm; 0jm)s_{y'}(-10)H^{(1)}(0-1)/h\nu(-10) \\ &= 4H^{(1)}(-10)L(0jm; -1jm)s_{y'}(0-1)/h\nu(-10), \end{aligned}$$

since all the quantities involved are real.

It is convenient to write $s_z^{(1)}(\sigma_s jm; \sigma_s' j'm')$, $L(\sigma_s jm; \sigma_s' j'm')$, and $\nu(\sigma_s\sigma_s')$ in terms of Ω rather than σ_s. The elements appearing above are, in this notation, $s_z^{(1)}(0jm; 0jm)$, $L(1jm; 0jm)$ and $\nu(01)$. We then have[33]

$$s_{y'}(\sigma_s; \sigma_s \pm 1) = \tfrac{1}{2}[S(S+1) - \sigma_s(\sigma_s \pm 1)]^{1/2};$$

$$H^{(1)}(\sigma_s; \sigma_s \pm 1) = b[j(j+1) - \Omega(\Omega \pm 1)]^{1/2}[S(S+1) - \sigma_s(\sigma_s \pm 1)]^{1/2};\ b = h^2/8\pi^2 Mr^2;$$

$$L(1jm; 0jm) = -m/2[j(j+1)]^{1/2};$$

and from these

$$s_z^{(1)}(0jm; 0jm) = -2bm/h\nu(01).$$

[29] R. W. Wood and G. Ribaud, Phil. Mag. **27**, 1009 (1914).

[30] E. C. Kemble, Bull. Nat. Res. Council 57: Molecular Spectra in Gases, Chap. VII.

[31] J. H. Van Vleck, Phys. Rev. **33**, 467 (1929). The primed and unprimed systems of his Eq. (5) will be interchanged, to accord with our previous notation. We shall follow this paper in our choice of phases for $H^{(1)}$ and $s_{y'}$, and in notation: σ_l will denote the component of angular momentum along the figure axis, σ_s the component of spin along the figure axis, $\Omega=\sigma_l+\sigma_s$

[32] H. Rademacher and F. Reiche, Zeits. f. Physik **41**, 453 (1927). See Eq. (13) and the table on p. 475.

[33] Van Vleck, reference 31, Eqs. (30) and (31). From Rademacher and Reiche's table we find $L(1jm; 0jm) = |m|/2[j(j+1)]^{1/2}$. The minus sign must be taken when $m>0$ to match Van Vleck's phases for $H^{(1)}$ (see Van Vleck's footnote (25)).

Using the fact that $L(1jm;\,0jm)=L(-1jm;\,0jm)$, it is readily verified that the same result is obtained when $\sigma_l=-1$.

Thus for our $^3\Pi_0-{}^1\Sigma$ transition

$$\nu^{(1)}(j'm';jm) = -4\beta bm'/h^2\nu(01),$$

β being the Bohr magneton number.

The elements of the electric moment appearing in Eq. (13) are the familiar amplitudes of the symmetric top, given, for example, by Kronig.[34] The terms different from zero are

$$[P_x(j,m;j+1,m\pm1)P_y(j+1,m\pm1;j,m)] = \mp\frac{iP^2}{2}\frac{(j\pm m+2)(j\pm m+1)}{(2j+1)(2j+3)},$$

$$[P_x(j,m;j-1,m\pm1)P_y(j-1,m\pm1;j,m)] = \mp\frac{iP^2}{2}\frac{(j\mp m+2)(j\mp m+1)}{(2j+1)(2j+3)},$$

where $P^2=\left|P_{y'}(^1\Sigma,\,^3\Pi_0)\right|^2$.

The rotation is found by substituting these expressions in Eq. (13) and summing over all values of m, the result being multiplied by two, since the two upper states, $\sigma_l=\pm1$, contribute equally to the rotation. In this way we obtain

$$V = -\frac{8\pi eb\nu_1P^2\nu^2Be^{-W_j/kT}}{hmc^2\nu_2(\nu^2-\nu_1^2)^2}\sum_{m=-j}^{j}\frac{(m+1)(j+m+2)(j+m+1)}{(2j+1)(2j+3)} - \frac{(m-1)(j-m+2)(j-m+1)}{(2j+1)(2j+3)},$$

with $\nu_1=\nu(^3\Pi_0,\,^1\Sigma)$, $\nu_2=\nu(^3\Pi_0,\,^3\Pi_1)$ (i.e., $\nu(01)$ in our previous notation), for the R branch, and an analogous expression for the P branch. Performing the summations,

$$V = \mp\frac{16\pi eb\nu_1P^2\nu^2Be^{-W_{j\pm1}/kT}j(j+1)}{3hmc^2\nu_2(\nu^2-\nu_1^2)^2}.$$

j here is the j of the $^3\Pi_0$ level; the minus sign is to be taken for the R branch, the plus for the P. Our theory thus agrees with Wood's observations in giving positive (normal) rotations for the lines of the P branch, and negative (abnormal) rotations for the R branch.

Magnetic rotation spectra of the alkalis

The calculation of the rotations in the alkali vapours is similar. The lines observed by Wood and Loomis[35] are $^1\Pi-{}^1\Sigma$ transitions. Here the Zeeman effect is given by the well-known formula $W^{(1)}(\Lambda jm)=\beta\Lambda^2m/j(j+1)$. We have

[34] Kronig, reference 3. The phases we use are

$$P_{y'}(\Omega,j,m;\Omega',j',m\pm1) = \pm iP_{x'}(\Omega,j,m;\Omega',j',m\pm1).$$

[35] F. W. Loomis, Phys. Rev. **31**, 323 (1928); Loomis and Nusbaum, ibid. **38**, 1447 (1931); **39**, 89 (1932).

$$\nu^{(1)}(1j'm';\,0jm) = \beta m'/hj'(j'+1),$$

$$[P_x(j,m;j-1,m\mp1)P_y(j-1,m\mp1;jm)] = \pm\frac{iP^2}{2}\frac{(j-1)(j\pm m)(j\pm m-1)}{j(2j-1)(2j+1)},$$

$$[P_x(j,m;j+1,m\mp1)P_y(j+1,m\mp1;jm)] = \pm\frac{iP^2}{2}\frac{(j+2)(j\mp m+2)(j\mp m+1)}{(j+1)(2j+1)(2j+3)},$$

$$[P_x(j,m;j,m\mp1)P_y(j,m\mp1;jm)] = \pm\frac{iP^2}{2}\frac{(j\mp m+1)(j\pm m)}{j(j+1)},$$

$$P^2 = |\,P_{x'}(^1\Sigma,\,^1\Pi)\,|^2.$$

The rotations are, in terms of the j of the normal state,

$$V = \frac{4\pi e\nu_1 P^2\nu^2 Be^{-W_j/kT}f(j)}{3hmc^2(\nu^2-\nu_1^2)^2},$$

$$f(j) = (j+2)/(j+1) \quad R \text{ branch},$$

$$f(j) = -(j-1)/j \quad P \text{ branch},$$

$$f(j) = (2j+1)/j(j+1) \quad Q \text{ branch},$$

$$\nu_1 = \nu(^1\Pi,\,^1\Sigma).$$

The signs of the rotations of the R and P branches are just opposite those found for iodine. These signs are confirmed by Wood's observations of the rotation in Na_2.

It may seem a little surprising that, aside from the Boltzmann factor $e^{-W_j/kT}$, the rotations of the P and R branches are nearly independent of j when j is large. However it must be remembered that although the over-all width of the Zeeman pattern decreases as $1/j$, the number of components increases linearly with j. The angle of rotation is small, only a few degrees, hence the intensities, which are proportional to $\sin^2\theta$, vary with j approximately as $\{f(j)e^{-W_j/kT}\}^2$.[36] As the intensities in the absorption spectrum vary as $(2j+1)e^{-W_j/kT}$, the intensities of lines of large j in the P and R branches of the magnetic rotation spectrum are weighted adversely, as compared to the absorption spectrum, by a factor $e^{-W_j/kT}/(2j+1)$, and so are, comparatively, greatly reduced. It is perhaps worthy of remark that the intensity of the rotation spectrum is proportional to the square of the density, rather than the first power. The intensities of the Q branch decrease much more rapidly than those of the R and P branches, which accounts for the fact that the Q branch is not observed in the rotation spectrum. For small j the R branch is considerably more intense than the P. This, together with the piling up of the R lines at the heads of the bands, explains why sometimes the R branch alone is observed. The present theory is thus adequate to account for the principle characteristics of the magnetic rotation spectrum.

I am deeply indebted to Professor J. H. Van Vleck, under whose direction this work was done.

[36] It should be noted that, since the separations between lines increase with j, the density of lines on a photographic plate will decrease even more rapidly than the intensities.

Experiments on the Nature of Ferromagnetism

By FRANCIS BITTER
Westinghouse Research Laboratories, East Pittsburgh, Pennsylvania

(Received May 31, 1932)

Irregularities in the magnetization of ferromagnetic crystals were studied by means of magnetic Fe_2O_3 particles about 1μ in diameter suspended in ethyl acetate. On iron crystals the particles settle along parallel lines spaced about 0.1 mm apart and more or less at right angles to the applied field. On nickel crystals the pattern is similar, but the lines split up into more complicated structures as the applied field is increased. On cobalt crystals straight lines are obtained on some crystals, and spotty patterns on others. The spots arrange themselves in rows when the crystals are magnetized. The patterns can be destroyed by relatively slight surface strains. There is some evidence that in the straight line patterns the direction of the lines is related to the direction of magnetization. An explanation of these effects is not known.

THE object of the experiments described below was to find any irregularities or inhomogeneities that exist in the magnetization of ferromagnetic crystals.

APPARATUS AND MATERIALS

The method used was the old magnetic powder method. In order to reveal small details, the particles must be small and have as large a magnetic moment as possible without causing them to form chains in the direction of the magnetic field. They must further be suspended in some medium that will allow them to settle according to the pattern of the field. Particles of red Fe_2O_3 having diameters in the neighborhood of 1μ were found very satisfactory.[1] These were suspended in ethyl acetate, which, because of its low viscosity, allows the particles to settle fairly rapidly and without undue disturbance from currents in the liquid. Observations were made by magnetizing a flat sample in the direction of its length and placing a drop of the suspension on the surface of the crystal to be investigated. In order to be certain that the patterns obtained were determined by the sample investigated rather than by the interaction of the Fe_2O_3 particles, observations were made with particles of different size, and of different substances suspended in various liquids, and with no liquid at all. In all cases the same patterns were observed.

A few samples of iron were prepared by elongating small annealed slabs about 3 percent and annealing in hydrogen just below the $\alpha-\gamma$ transformation point. This material was very pure, having a total impurity before the above treatment of about 0.01 percent, chiefly Si. Some samples were ground flat and annealed. All other samples were made by melting in alundum troughs in an electrically-heated alundum tube furnace through which purified dry hydrogen flowed continuously. In order to observe the effects re-

[1] F. Bitter, Phys. Rev. **38**, 1903 (1931).

ported below, it is desirable to have a shiny, smooth, unstrained surface. Hydrogen was used to prevent surface tarnish due to oxidation. Considerable hydrogen was absorbed while the samples were molten, and given off during solidification, producing cavities in the ingots and locally imperfect surfaces. In most cases, however, at least a part of the sample was satisfactory.

I should like to express my indebtedness to various members of the Laboratories for their assistance—to Mr. L. McCulloch for preparing the Fe_2O_3 powder; to Dr. V. Hicks for making an x-ray examination of this powder; to Miss M. Ferguson for taking the best of the photographs reproduced below; to Mr. P. G. McVetty for stretching the strain-annealed samples of iron; and especially to Mr. A. A. Frey, who built the furnaces and prepared most of the samples investigated.

Results

Iron

In a sample of iron having small grains, whether annealed or not, irregular patterns are found. The deposits do not follow any obvious structural features, such as grain boundaries. If, however, the grains are somewhat larger, and unstrained, deposits like that shown in Fig. 1 are formed, which, for larger fields, degenerate into irregular patterns. In Fig. 1 some of the

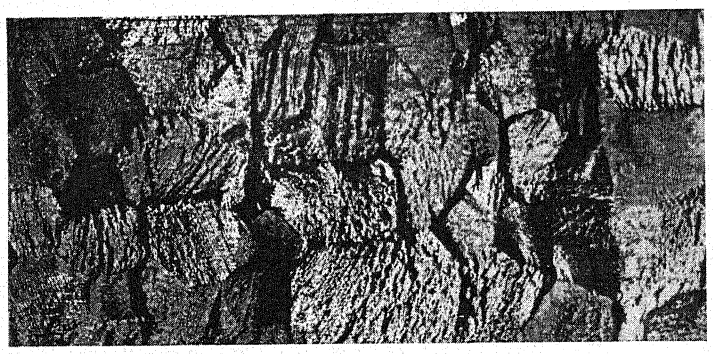


Fig. 1. Deposit on a sample of 4 percent Fe-Si with large grains. Field horizontal. Approximate magnification ×2. Deposits are black in all photographs.

grains are crossed by systems of parallel lines more or less at right angles to the direction of the applied field. The lines are not spaced perfectly evenly, but are of the order of 0.1 mm apart. Fig. 2 shows the deposit obtained near a grain boundary on an Fe-Si sample, and Fig. 3 shows the slip lines obtained on a similar sample after a slight reduction by cold rolling. The similarity is rather striking. In both cases there is a tendency for the lines to continue in a changed direction after crossing a grain boundary.

In general, the deposits on iron are indefinite, and it often occurs that no regular patterns are observed at all. Better results were obtained with an alloy containing 4 percent Si than with pure iron. An attempt was made to determine how the pattern changed as the direction of magnetization was

varied. As a rule the pattern was obscured, but on several crystals three sets of lines were observed all told. Further observation is required to establish the generality of this result.

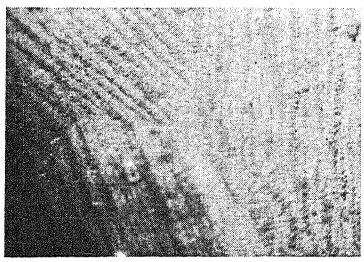


Fig. 2.

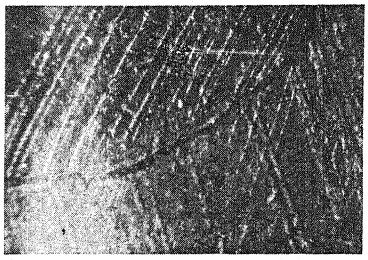


Fig. 3.

Fig. 2. Deposit on a 4 percent Fe-Si sample near a grain boundary. Field horizontal. Approximate magnification ×10.

Fig. 3. Slip lines in a 4 percent Fe-Si sample. Approximate magnification ×10.

Cobalt

Typical deposits on cobalt are shown in Figs. 4–6. These illustrate the state of affairs before a magnetic field is applied. In Fig. 4 the spots vary a good deal in size. Fig. 5 shows grain boundaries, and the tendency for the

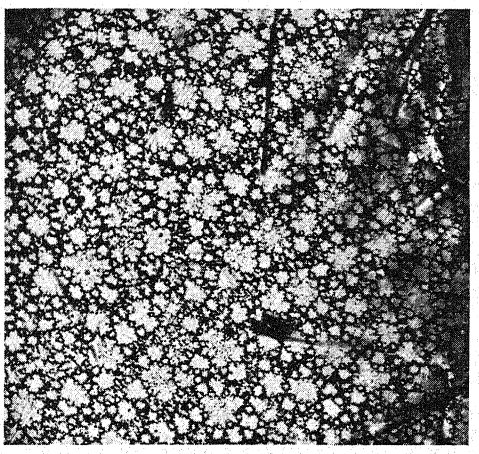


Fig. 4.

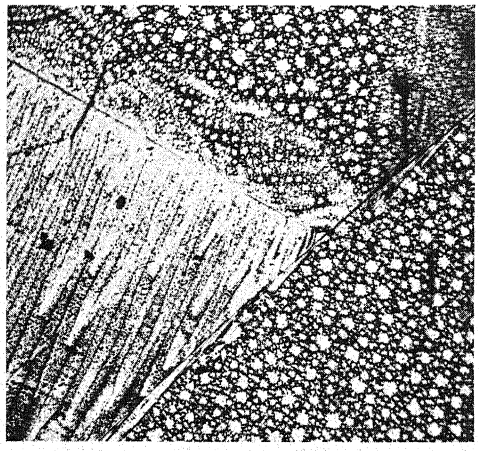


Fig. 5.

spots to form a hexagonal array. Also a grain having a straight line pattern is shown. Fig. 6 shows transition patterns between the spotty and the straight line types. Just what difference exists between samples showing different patterns is not known. One sample containing 20 percent of iron showed no pattern whatsoever. Until further evidence is obtained, we may make the reasonable assumption that the irregularities are produced by strains, impurities, or other imperfections. In Figs. 7–9 the effect of magnetization on

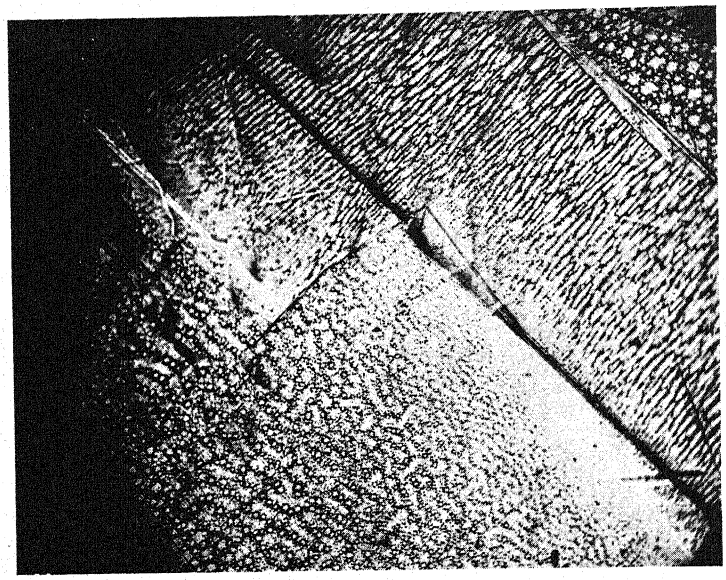


Fig. 6.

Fig. 4–6. Deposits on unmagnetized cobalt crystals. Magnification approximately ×70.

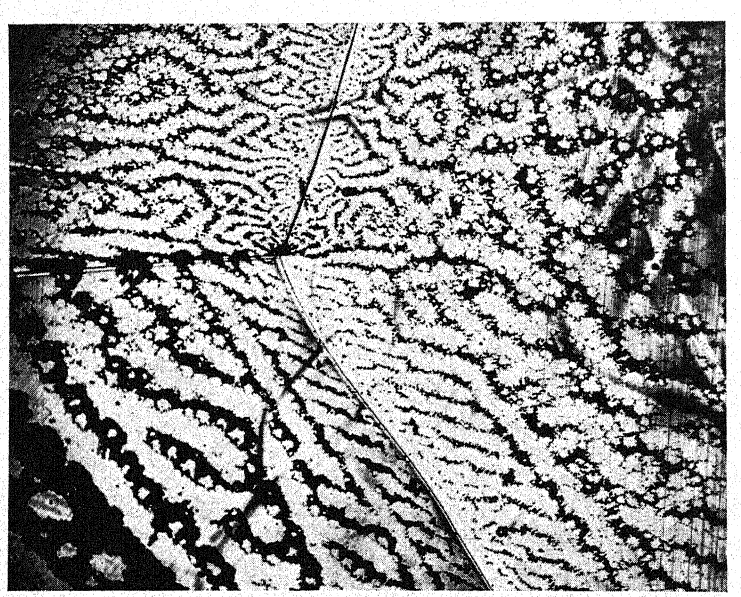


Fig. 7. Deposit on magnetized cobalt near a grain boundary. Approximate magnification ×80.

the spotty type of deposit is shown, the magnetization being stronger in Fig. 9 than in Fig. 8. Fig. 7 shows the distorting effect of the grain boundary. The line pattern illustrated in Fig. 5 is affected little if at all by magnetization, and has in no case been observed to change its direction on the crystal surface as the direction of the applied field was varied.

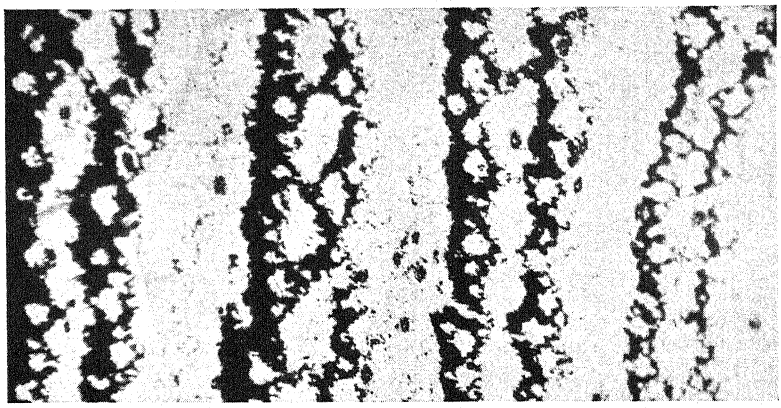


Fig. 8.

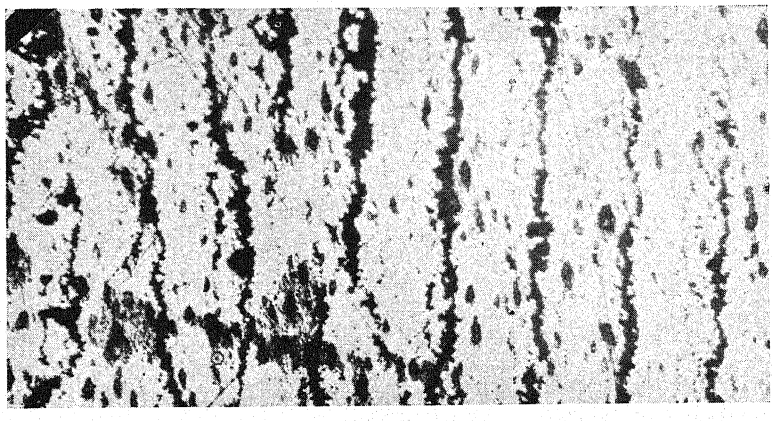


Fig. 9.

Fig. 8 and 9. Deposits on a magnetized cobalt crystal. Approximate magnification ×160.

Nickel

A typical deposit on nickel before being exposed to any magnetic field other than that of the earth is shown in Fig. 10. On magnetization the patterns become more definite, as shown in Figs. 11a and 11b. Sometimes the lines are curved, especially near grain boundaries, and sometimes they show a break as is the case for one of the lines in Fig. 10. It quite often happens that the spacing of the lines changes progressively from one side of a crystal to the other, as can be seen in Fig. 11a. These lines are not associated with

fixed places in a crystal. This is illustrated in Fig. 12 in which photographs of three different deposits on the same region are superposed. It seems quite generally true that the position of the lines changes after demagnetization.

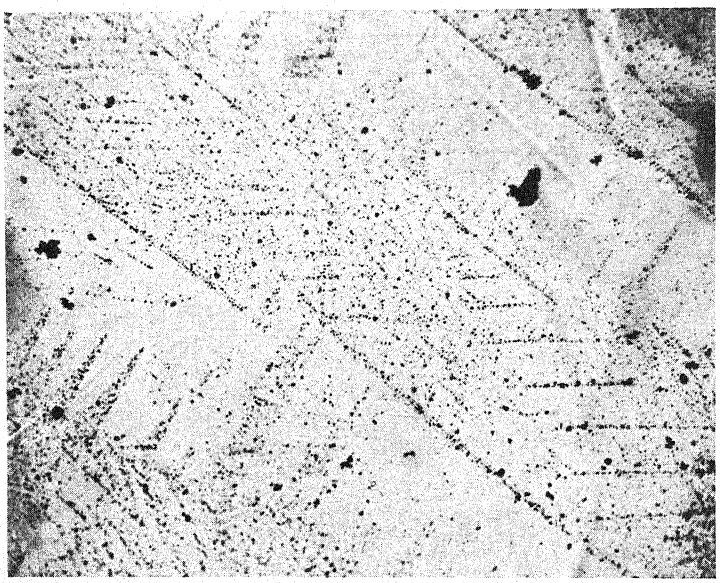
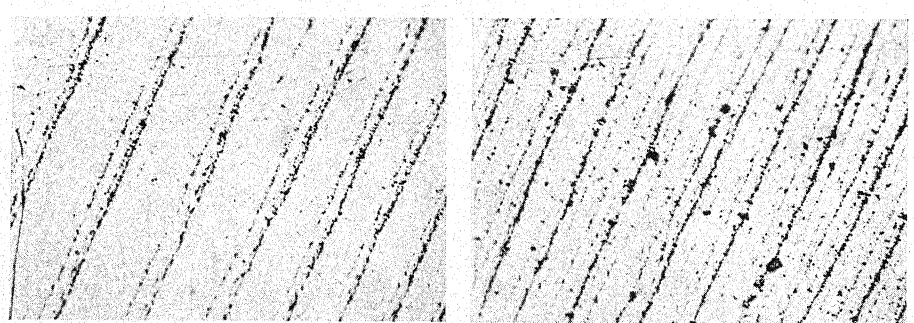


Fig. 10. Deposit on a nickel crystal before magnetization. Approximate magnification ×80.

Some samples in the shape of disks were prepared, and magnetized in eight directions at 45° intervals. The deposits were photographed and the total number of directions in which lines appeared was determined for five crystals.



a b

Figs. 11a and 11b. Typical deposits on nickel with the applied field acting in a horizontal direction. Approximate magnification ×65.

In each case the lines appeared in four directions all told. In those positions in which two such directions made nearly equal angles with the applied field chevron patterns like that shown in Fig. 13 appeared.

If successive patterns are obtained in the same region in gradually increasing fields without demagnetization between observations, the phenomenon shown in Fig. 14 is found. The wavy marks on the photographs are surface irregularities that are of no interest here except insofar as they may be used as a reference system fixed in the crystal. In the twelve photographs shown the applied field increases progressively, being smallest in 1 and largest in 12. The position of the lines as shown in the first photograph does not change radically. The lines, however, split up as the magnetizing field is increased, first into two, then four, and on the original photograph, No. 12, each of the original lines is seen to consist of eight components. In addition a new line appears between each of the main groups in photograph No. 7 and splits into two components also. The smallest splitting here shown is deter-

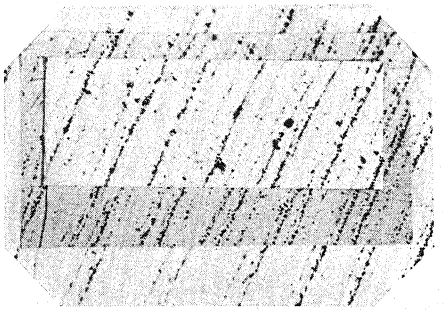


Fig. 12. Superposed photographs of deposits obtained on the same region at different times, the sample being demagnetized after each observation.

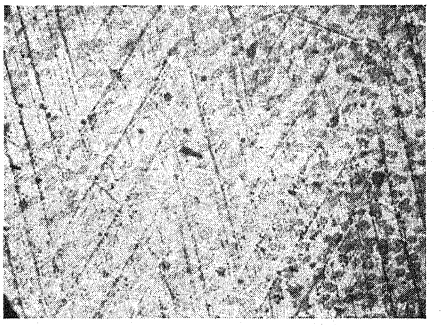


Fig. 13. Peculiar pattern obtained on a nickel crystal.

mined by the method, and it seems very probable that much more detail exists than is here indicated. To obtain these results it is essential not to demagnetize the sample between observations. The sample consisted of crystals having linear dimensions of from 1 to 4 cm imbedded in a large slab, 27 cm$\times$4 cm$\times$1 cm. It was consequently possible to measure only the intensity of magnetization of the aggregate. This was done with a fluxmeter and the value of $I=350$ or about 75 percent of saturation was obtained for the conditions under which deposit No. 12 was produced. Magnetization of this intensity is confined to the directions of easiest magnetization within the crystal.

Alloys containing 10 percent, 20 percent, and 30 percent of iron were prepared by melting and slow cooling. That containing 10 percent of iron showed patterns typical of nickel, but less distinctly than usual. No patterns whatsoever could be found on the other samples.

The effects are exceedingly sensitive to strain. Some samples that were lightly pressed by a C-clamp no longer gave any patterns, nor was anything to be found on polished samples until they had been annealed.

Discussion

If it is quite generally true, as has been found in a few cases, that the line patterns can appear in three directions in iron, in four directions in nickel, and in only one direction in cobalt, it seems reasonable to assume that they are somehow related to the three (100) axes in iron, the four (111) axes in nickel, and the single (0001) axis in cobalt. This assumption is supported by

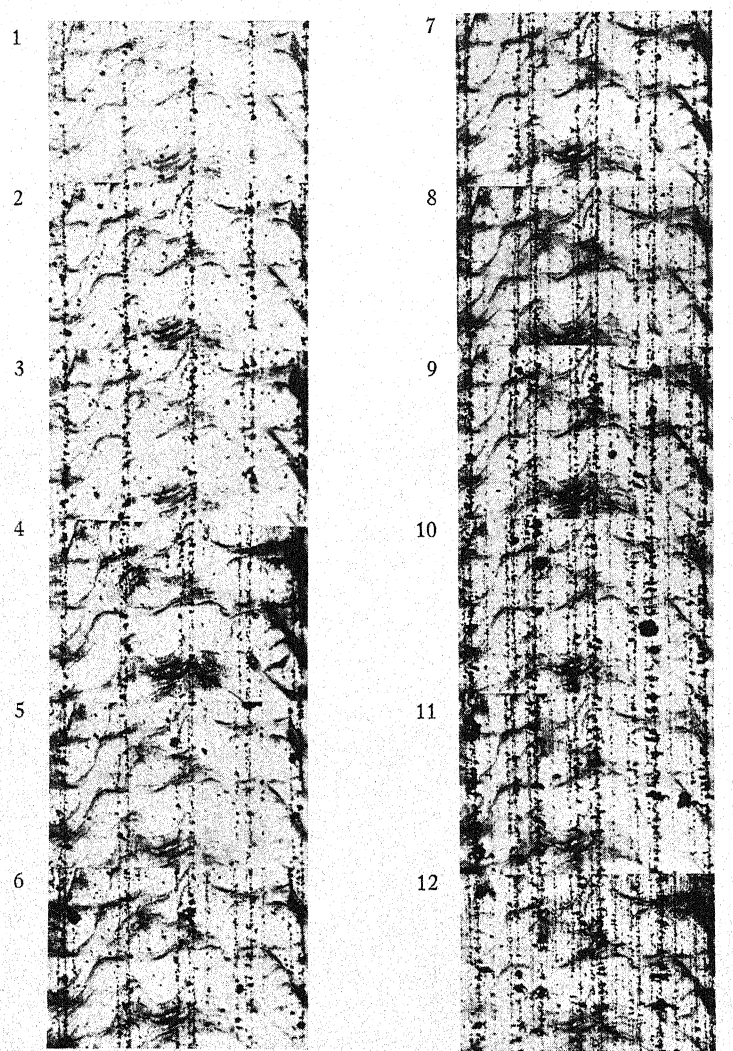


Fig. 14. Twelve photographs of the same region, the applied field being gradually increased between observations.

the fact that in each case the axis mentioned has a special significance magnetically—it is the direction of easiest magnetization within the crystal. Taking into consideration the above material, and the fact that the lines are

sometimes curved or broken, we suggest the hypothesis that inhomogeneities occur along planes perpendicular to the direction of magnetization, and that the lines observed are parallel to the intersection of such planes with the surface under observation. In the fields used the direction of magnetization probably differed in no case appreciably from the direction of easiest magnetization. The above hypothesis fits into the observation that in nickel and cobalt alloying tends to destroy the pattern, for the effect of a foreign substance must, as a rule, be to introduce local fluctuations in the direction and intensity of magnetization. This reasoning can be applied to the observations on iron if we suppose that it is exceptionally difficult to produce a satisfactorily uniform crystal of iron, and that the addition of silicon tends to remove certain imperfections. The above discussion does not take into account the spotty pattern obtained on certain cobalt crystals. It seems likely that this is more complicated in its origin, and occurs whenever the hexagonal axis is normal to the surface of the crystal.

From the observations so far made, it is not possible to determine the nature of the inhomogeneities revealed. They may be changes in direction or intensity of magnetization, or both. Bearing in mind that in this discussion a change in direction, to be detected as such, must cover a region large compared to 1μ, it is probable that we have to do with changes in direction in cases like that shown in Fig. 13, but that in patterns like that shown in Fig. 11 there is only a change in intensity. It is most important to settle definitely the nature of the inhomogeneities by further and more detailed observations.

The origin of the patterns obtained is of course even more obscure. The conception is current that ferromagnetic crystals are made up of spontaneously magnetized regions whose directions of magnetization are distributed among the various energetically possible orientations. Magnetization is then supposed to result partly from a growth of some of these regions at the expense of their neighbors,[2] partly from changes in the direction of magnetization of each region. It seems a little difficult to fit this picture into the above photographs unless the regions are smaller than 1μ. The secondary structures suggested by Zwicky[3] offer a different attack on the problem. Finally, we must remember that a crystal consists of atoms in different excited states, that the various periodic motions which its constituent atoms and electrons perform most probably are coupled together in a variety of ways, and that in addition there must be a certain amount of electromagnetic radiation present. Any of these factors may have an influence in determining the equilibrium configuration of a crystal, and it is perhaps the most important aspect of experiments such as the above to furnish evidence from which conclusions on these points may eventually be drawn.

[2] F. Bloch, Zeits. f. Physik. **74**, 295 (1932).
[3] F. Zwicky, Phys. Rev. **38**, 1772 (1932).

Thermoelectric Power of Single Crystal Bismuth Near the Melting Point

By ADOLF SOROOS
Physical Laboratory, University of Iowa

(Received June 14, 1932)

By investigating directly the thermoelectric power of bismuth single crystals near the melting point a transition region is found in which the thermoelectric power changes gradually from that characteristic of the solid to that characteristic of the *final* liquid state. The region extends from the melting point to about 8° above it. As an explanation it is supposed that a definite crystal structure persists into the liquid state.

INTRODUCTION

IN measuring the thermal e.m.f. of bismuth single crystals against constantan as a reference metal, Boydston[1] found certain irregularities in the e.m.f.-temperature curves in the region just beyond the melting point. As an explanation he says, "It appears, in fact, as if some crystalline arrangement still persists in the molten metal as shown by a transition region between the thermal e.m.f. of solid and liquid."

Goetz[2] makes use of a similar explanation for certain effects observed in his study of the factors influencing the growth and perfection of bismuth crystals. He found that if he used a seed crystal with regions of twinning to inoculate a molten rod he would invariably obtain a crystal which still showed the twin orientation unless he melted the seed back considerably beyond the region of twinning so that this region was at a much higher temperature than the melting point. He also found that a polycrystalline rod melted and raised to a temperature just slightly above the melting point, recrystallized, on cooling, into a rod which had the "same position and same orientation of the prominent crystal elements" as the original rod. If he heated the specimen considerably above the melting point, however, he found an entirely new arrangement on recrystallization.

Although Boydston observed only slight deviations of thermal e.m.f. from what is expected on the basis of an abrupt change at the melting point, it is obvious that these deviations must be accompanied by relatively large changes in the derived thermoelectric power curve. For this reason it seemed advisable to investigate directly the thermoelectric power of bismuth crystals over a temperature range extending on both sides of the melting point with the hope of definitely establishing the phenomenon foreshadowed by Boydston.

The method devised to do this consists in measuring the thermal e.m.f. over a small temperature interval at successive mean temperatures in the

[1] R. W. Boydston, Phys. Rev. **30**, 911 (1927).
[2] A. Goetz, Phys. Rev. **35**, 193 (1930).

desired region. The observed e.m.f. divided by the temperature interval gives directly the mean thermoelectric power at the mean temperature. By use of a small enough temperature interval the resolution can be made sufficiently high to justify considering this mean thermoelectric power as the actual.

Apparatus and Method

The experimental arrangement is shown in Fig. 1. The bismuth crystal, BB, has its ends fused to two copper blocks, AA. In fusing, the copper surface is cleaned with a flux ($ZnCl_2$) and then with the end of the crystal pressed lightly against the block, the latter is heated until the bismuth just begins to melt. A little added pressure with the finger tip at this point insures a good contact. The crystal structure is not altered at the junction. Two holes a, b were drilled into the ends of each copper block, with the bottoms of the holes separated from the surface onto which the bismuth was fused by a thickness of copper of about 0.5 mm. Into the holes, aa, were inserted the two junctions of a constantan—copper thermocouple which measured the difference in temperature of the two ends of the bismuth rod. These junctions were en-

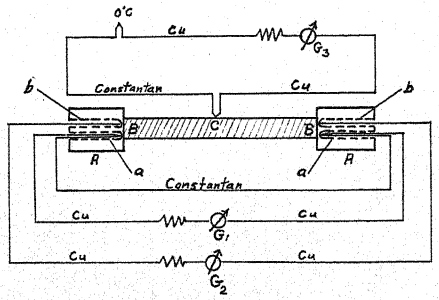


Fig. 1. Diagram of apparatus.

closed in small Pyrex glass tubes, the copper and constantan wires being separated by thin strips of mica. To the bottoms of the holes, bb, were silver soldered copper wires which completed the bismuth-copper thermal e.m.f. circuit. These wires were insulated from the side walls of the holes by small Pyrex tubes. This latter procedure was necessary in order to make sure that the effective junctions of this bismuth-copper couple should be at the surface of separation between the copper block and bismuth crystal. A second copper-constantan circuit had one junction placed at C, the other junction being maintained at zero degrees.

The electrical circuits are also pictured in Fig. 1. The reading of the galvanometer, G_1, is proportional to the temperature difference between the ends of the bismuth crystal, the reading of galvanometer, G_2, is proportional to the e.m.f. of the bismuth-copper circuit, and the reading of the galvanometer, G_3, is proportional to the mean temperature of the crystal.

The crystals were grown by a method similar to that described by Kapitza.[3] A groove[4] in an asbestos block was used for a mold. Crystals were

[3] P. Kapitza, Proc. Roy. Soc. A119, 358 (1929).

[4] The cross section was almost V-shaped, but with a rounded bottom.

grown of three brands of bismuth, Mallinckrodt C.P.,[5] a special silver-free[6] and Kahlbaum's best.

The results given below are for only the first brand, preliminary work[7] having shown no essential difference in the behavior of the others. The crystals were about 0.5 cm^2 in cross section and either 10 or 20 cm long. The longer ones were cut in half and a separate determination made on each piece.

In making a determination the crystal was put into an asbestos holder and placed in a horizontal furnace. The temperature gradient in the furnace was so controlled by auxiliary coils that the temperature difference between the ends of the crystal could be kept at about 1°C. The furnace temperature was allowed to pass slowly through the region under investigation. The time required to take the crystal through the desired temperature range (260° to 290°C) was about one hour.

Results and Discussions

Measurements were made on six single crystals ranging in orientation[8] from 29° to 69°. These results are shown in Fig. 2. All crystals at a temperature sufficiently above the melting point, (i.e., in the region 280°–290°) showed a constant thermoelectric power against copper of 4.5 microvolts per degree (within 1 microvolt per degree). This has therefore been taken as a zero point and the ordinates of the curves depict the excess values above this constant level. While the curves are plotted against mean temperature, this is not obtained directly from the readings of the thermocouple, *C*, Fig. 1. This couple could not be placed in thermal contact with the crystal, and while for any one crystal it is believed that its readings give a correct measure of the rising temperature these readings may differ from the actual temperature of the center of the crystal by a presumably constant and small but undetermined amount. The observed curves have therefore been so adjusted in plotting Fig. 2 that they agree in mean temperature at the point where the final constant value is reached. This adjustment does not amount for any crystal to more than about 2° difference between the adjusted temperature scale and the indication of thermocouple, *C*, Fig. 1. The location of the melting point (271°C) as shown on the figure actually coincides with the reading of thermocouple *C* in the case of the 40° crystal. Moreover, it occurs, for this crystal, about 0.5° above the first sharp break which is then interpreted as coinciding with the beginning of the melting process. For no other crystal is the onset of melting so sharply marked. Even without such an adjustment,

[5] This is the same grade of bismuth that Boydston used and has the same stated analysis. Other work in this laboratory has shown that the silver content may be much less than the 0.04 percent maximum limit.

[6] The writer has to thank the U.S.S. Lead Refinery for this material. The analysis given with it shows: Pb 0.005 percent, Ag 0.0006 percent, Cu, Fe 0.000 percent.

[7] In this preliminary work about fifteen crystals were investigated, the experimental set-up being improved from time to time. As soon as a reliable arrangement was obtained the set of crystals reported on herein was grown and measured. The preliminary results were all in agreement with the final ones in their general characteristics.

[8] Angle between the trigonal axis and the length of the specimen.

however, the general character of the results is unchanged. To avoid confusion, the curves in Fig. 2 are plotted with an arbitrary displacement in the scale of ordinates between successive curves. Four of the crystals were sufficiently long for two determinations to be made, the circles indicating determinations made on the half onto which the nucleus had been fused during growth and crosses indicating the second half of the same crystal.

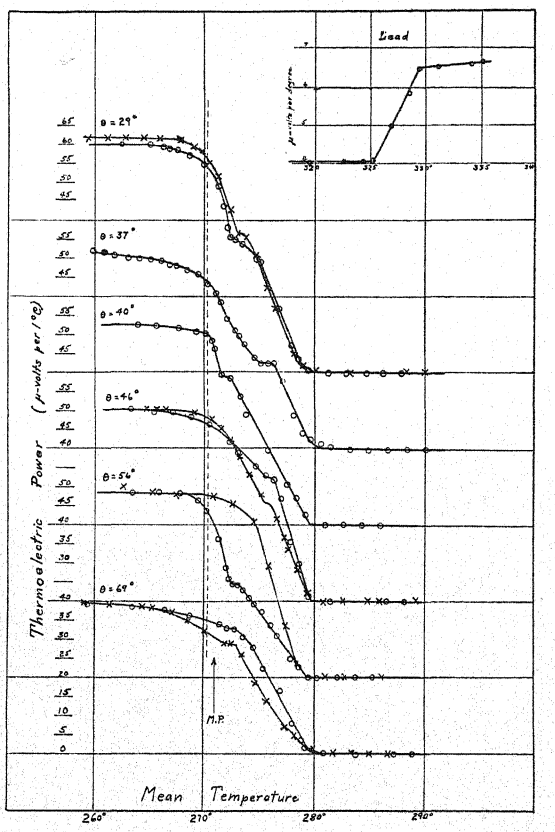


Fig. 2. Thermoelectric power as a function of temperature.

It is clear from Fig. 2 that bismuth is abnormal in its thermoelectric behavior in the region just above the melting point. For most substances which melt at a definite temperature, the thermoelectric power changes abruptly at the melting point or the thermal e.m.f. curve suffers an abrupt change in slope.[9,10] For the crystals shown here, however, the curves before settling down to a practically constant final liquid value pass through a transition region which lasts for approximately 8°C. This is exactly the effect predicted by Boydston. This transition of thermoelectric power, of course, takes place entirely in the liquid state since the crystal is completely melted when the mean temperature (temperature at center of crystal) is 0.5° above 270°, since

[9] E. G. Linder, Phys. Rev. **29**, 554 (1927).
[10] T. R. Harrison and P. D. Foote, J.O.S.A. and R.S.I., **7**, 389 (1923).

the difference in temperature between the two ends of the crystal is only one degree.

On account of the doubt of the exact indication of thermocouple *C* and from the general appearance of the curves in Fig. 2 one might be inclined to believe that the melting process was not complete until the final constant value of the thermoelectric power had been reached and that the observed effect all lies in a region below the melting point and is, therefore, characteristic of the solid and not the liquid state. That this is not the case was verified by an independent experiment. A separate determination was made on a 90° crystal and as all of the curves show a small constant portion shortly after melting, the determination was stopped when that place was reached. The holder containing the crystal was then quickly taken from the furnace, tipped on its side and jarred a little. There was only one possible place where the liquid could seep out through the holder and this was at the position where the thermocouple *C* was inserted. It was found that the liquid had indeed forced its way out and on examining the material remaining in the holder, it was found recrystallized into a changed orientation[11] from what it was at the beginning. This seems conclusive evidence that the transition region belongs to the liquid state.

It seemed desirable also to make a check on the apparatus to be sure that the results obtained were not due to some peculiarity in the apparatus itself. To check this point a determination was made on a specimen of polycrystalline lead. The results of this determination are shown in the curve in the upper right corner of Fig. 2. Since the thermoelectric power of lead against copper is small, a temperature difference between the ends of the specimen of 4°C had to be used in order to obtain a conveniently large galvanometer deflection. This made the resolution much less than that for any of the bismuth crystals. The result obtained for lead, however, is the one to be expected on the assumption of no transition region existing. The thermoelectric power passes directly from the solid value to the liquid value without a change of slope in this region and the temperature interval of this change corresponds almost exactly to the temperature difference of the ends of the lead rod. The fact that the transition is not shown by a line parallel to the ordinate axis, is, of course, due to the finite resolution.

The above results yield incidently a value of *2.6* microvolts per 1°C for the thermoelectric power of solid against liquid lead at the melting point.

As a matter of interest a plot has been made, Fig. 3 of the thermoelectric power of the solid crystals just below the melting point against the square of the cosine of the orientation angle. To do this ordinates were read from Fig. 2 for the value of temperature shown by the dotted line. This is 0.25° below the temperature at which the hotter end of the crystals start to melt. The points lie on a straight line, confirming the Voigt-Thomson relation. This is in agreement with Boydston though at variance with the slight deviation from

[11] Doubtless from tipping and jarring. From Goetz's observation it should remain the same if undisturbed.

the law later found by Bridgman[12] and Fagan and Collins.[13] It does, however, give the writer considerable confidence in the method used to adjust the mean temperature scale. A numerical comparison[14] of Boydston's and the writer's data shows that at the melting point the former obtains:

$$e_{\parallel} - e_1 = 70 \text{ microvolts/degree}^{15}$$

$$e_{\perp} - e_1 = 29 \text{ microvolts/degree}$$

while the writer obtains:

$$e_{\parallel} - e_1 = 65.5 \text{ microvolts/degree}$$

$$e_{\perp} - e_1 = 31.0 \text{ microvolts/degree.}$$

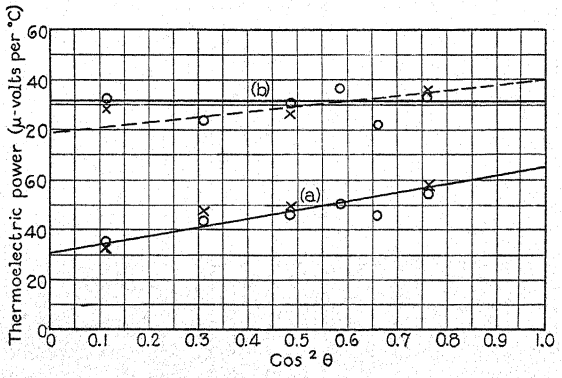


Fig. 3. Thermoelectric power as a function of $\cos^2\theta$. (a) At the melting point. (b) At the *knee* of the curves of Fig. 2.

The results then show that the thermal e.m.f. curve of bismuth does not change its shape as abruptly and in as clearly defined a fashion as in the case of zinc, tin, lead and some other substances. The thermoelectric power before settling down to a final constant value passes through a transition region lasting for a temperature interval of about 8°C above the melting point. Moreover, this settling down is gradual. The curves for differently oriented crystals preserve their individuality for several degrees above the melting point. Although it is only quite close to the final liquid stage that the curves become practically identical there is within the transition region a feature common to all but one of the curves of Fig. 2, namely a slight *knee* or practically stationary value of thermoelectric power. This seems to indicate a definite phase, or intermediate liquid state, existing for a temperature range of about one degree. If this is the case it ought to occur at the same tempera-

[12] P. W. Bridgman, Proc. Amer. Acad. of A. and S. **63**, 351 (1929).

[13] H. D. Fagan and T. R. D. Collins, Phys. Rev. **35**, 421 (1930).

[14] Boydston's values for comparison were obtained by plotting his data for $e_1 - e_s$ against $\cos^2\theta$ and then extrapolating the straight line to the ordinates of 0° and 90° crystals.

[15] $e = dE/dT$, the thermoelectric power, E being the thermal e.m.f., e_1 = thermoelectric power of liquid bismuth, e_{11} = thermoelectric power of crystal of 0° orientation, $e_{\perp}$ = thermoelectric power of 90° crystal.

ture for all the crystals. Although it obviously does not do so its significance can be tested in another fashion. This is shown in Fig. 3b in which the value of the thermoelectric power at the knee is plotted against $\cos^2\theta$. A definite intermediate liquid phase might be expected to give either (1) a straight line (dotted in the figure) with a positive slope indicating that the liquid is still very much like its *parent crystal* (2) a straight line (solid line in the figure) of zero slope, indicating that an identical state has been reached for all crystals. Unfortunately the observed data do not decide unambiguously between these two suppositions. In spite of this the existence of a knee at all strongly supports the idea of an intermediate state. It may be noted that this knee was also obtained for most of the crystals which were studied in the preliminary work previously mentioned.

The writer believes that the existence of a transition region extending from the melting point to about 8° above it, is established by the foregoing and that the explanation which has already been advanced is adequate to explain this phenomenon. Up to 8° beyond the melting point the liquid retains, but in decreasing measure, the organization of the crystal from which it is derived. Beyond that point the state of the liquid is independent of its previous history. It is practically impossible to think of any state or condition of the liquid, other than that postulated, which could give rise to such a transition region. It must be noted however, that the thermoelectric effect must be particularly well suited to observe this phenomenon as the appearance of a transition region for other properties which depend on crystal orientation has not been observed, so far as the writer knows. W. L. Webster's study[16] of the change in magnetic susceptibility in solidifying bismuth apparently shows no transition region for this quantity of the type shown here, but a sudden change occurring at the melting point. It may be, however, that a degree of organization suitable for modifying the thermoelectric effect may have little effect on susceptibility. Moreover, Webster was looking for an effect said to occur 10° below the melting point and not for one above.

It may be said finally that only x-ray diffraction can give positive and unambiguous proof of the explanation offered to explain the transition region.

The writer wishes to express his most sincere thanks to Professor E. P. T. Tyndall, who suggested the problem and under whose direction the work was carried out.

[16] W. L. Webster, Proc. Roy. Soc. **A133**, 162 (1931).

The Acoustic Resonator Interferometer: II. Ultrasonic Velocity and Absorption in Gases

By J. C. HUBBARD
The Johns Hopkins University

(Received June 13, 1932)

The derivation of the equivalent electric network of the acoustic resonator interferometer in Part I of this paper has made it possible to develop the theory for the current in a simple resonant circuit in which the electrodes of the piezoelectric plate of the interferometer are connected to the terminals of the variable condenser of the circuit. The special case of this theory in which the circuit is excited at a constant frequency determined by the crevasse frequency of the resonator plate in its given situation with respect to electrodes and associated circuit, when the acoustic path in the interferometer is *detuned* and the resonant circuit is tuned so that its resonant maximum occurs at the same frequency, takes an especially simple form and leads to a direct procedure for determination of ultrasonic velocity and absorption in a gas in terms only of current in the resonant circuit and path-length in the interferometer, all circuit and interferometer constants dropping out. The values of current as a function of path-length obtained experimentally are in complete accord with the theory and data for ultrasonic absorption in air and in CO_2 so far obtained are in agreement with the meager data available by other methods. The role of the coefficient of reflection at the fluid-reflector surface is discussed.

I. EXPERIMENTAL OBJECTIVES AND METHODS

THE vibration of a column of fluid of variable length, one end of which is bounded by a vibrating plane face of an electrical vibrator such as a piezoelectric plate, the other end being bounded by a plane reflector parallel to the vibrating face of the plate, has been considered in Part I[1] of the present paper, and the equivalent electric network of the system was there shown to be the same as that of the quartz plate alone with modified resistance and capacity coefficients. Such a system, associated with an appropriate driving circuit, may be termed an acoustic resonator interferometer, and has already been used for the measurement of compressional velocities in liquids,[2,3,4,5] and in gases,[6] of absorption coefficients in gases,[6] and of the modification of velocity in liquids due to scattering.[5] Specific consideration of some of the methods of measurement of absorption in gases and of the role of the reflection coefficient at the boundary of the fluid will be given in the

[1] J. C. Hubbard, Phys. Rev. **38**, 1011–1019 (1931). Part I will be referred to hereinafter as I.

[2] J. C. Hubbard and A. L. Loomis, Phil. Mag. **5**, 1178–1190 (1928); and A. L. Loomis and J. C. Hubbard, J.O.S.A. and R.S.I. **17**, 295–307 (1928).

[3] E. B. Freyer with J. C. Hubbard and D. H. Andrews, Jour. Am. Chem. Soc. **51**, 759–770 (1929). E. B. Freyer, *ibid.* **53**, 1313–1319 (1931).

[4] E. Klein and W. D. Hershberger, Phys. Rev. **37**, 760–774 (1931).

[5] C. R. Randall, Bur. Stand. Jour. Res. **8**, 79–99 (1932).

[6] J. C. Hubbard, Phys. Rev. **35**, 1442 (1930); **36**, 1668–1669 (1930).

present paper. Mr. W. D. Hershberger[7] has presented independently an analysis of the motion of the fluid column and of its reaction on the piezoelectric plate, his treatment being somewhat more restricted than that of the author, particularly in that he does not consider the effects of coefficients of reflection at the fluid-reflector surface of value less than unity.

Among the methods of measurement which have been used, undoubtedly the simplest is that in which the interferometer electrodes are connected to the terminals of a variable condenser which is part of a simple resonant circuit driven by an oscillation generator of suitable frequency. The measurements consist in this case of a determination of current in the resonant circuit as a function of the length r of the fluid column.[2,3,4,6] The current readings pass through sharp maxima (for gases, minima for liquids) or peaks as r is increased, these peaks having been interpreted as marking the value of r, for resonance in the fluid, successive resonant positions of the reflector being one-half wave-length apart. An analysis of this method for gases is given in the present paper.

In a second method, far more sensitive than the first, the interferometer electrodes are connected to a secondary coil coupled to the primary of an oscillation generator. As r is varied a cyclical variation of frequency of the generator takes place which is compensated by the variation of a vernier condenser in parallel with the capacity of the generator, constancy of frequency being assured by using the double heterodyne beat method.[2,3,6] From the variation of vernier condenser readings as a function of r the acoustic behavior of the medium is deduced. The theory of this method will be given in a later paper.

A third method[5] makes use of the current in the leads to the interferometer itself as a function of r, the circuits being otherwise as in the first method described above. Klein and Hershberger[4] report a variety of experiments in which a number of methods were employed, the interferometer system being treated as an impedance in alternating current measurements.

It is essential that the power dissipated in the acoustic system be so small as to produce negligible temperature effects. In practice it has been found possible to reach the limits of accuracy imposed by the sensitiveness of the thermocouple and galvanometer used in the first method with amounts of power several orders smaller than that which is capable of influencing the results. The power necessary in the second method is still much smaller.

The most important factor causing a departure of the acoustic system from that theoretically expected is to be found in the conditions at the electrodes of the piezoelectric plate. This factor need not be considered if the electrodes are of sufficiently small mass and if their attachment to the plate is of such nature as not materially to modify the crevasse. As will be seen the constants of the crystal including the effect of electrode mounting upon the position and shape of the crevasse may be eliminated from consideration in determinations of velocity and absorption.

[7] W. D. Hershberger, J. Acous. Soc. Am. **3**, 263–268 (1931).

II. Method of Forced Vibrations. Ultrasonic Velocity and Absorption in a Gas

As shown in I the acoustic interferometer may be represented by an electric network consisting of a fixed capacity K_1 shunted by a series consisting of the fictitious inductance L, capacity K' and resistance R', where

$$R' = R + AB\rho vP \tag{1}$$

$$1/K' = 1/K + AB\rho v\omega Q \tag{2}$$

R and K being the fictitious series resistance and capacity respectively of the quartz plate itself, A the cross section of the fluid column, B a constant of quartz, and ρ and v, respectively the density of the fluid and the wave velocity in it.

P and Q have the values, in general, with $x=0$ in I, Eqs. (12) and (13), respectively

$$P = \frac{1 - \gamma^3 e^{-4r\alpha} + \gamma(1-\gamma)e^{-2r\alpha}\cos(2r\omega/v)}{1 - 2\gamma^2 e^{-2r\alpha}\cos(2r\omega/v) + \gamma^4 e^{-4r\alpha}} \tag{3}$$

$$Q = \frac{\gamma(1+\gamma)\sin(2r\omega/v)}{1 - 2\gamma^2 e^{-2r\alpha}\cos(2r\omega/v) + \gamma^4 e^{-4r\alpha}} \tag{4}$$

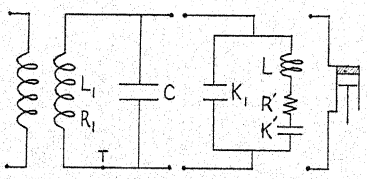


Fig. 1. Resonator circuit with interferometer replaced by its equivalent electric network.

where α is the attenuation factor of particle velocity in the fluid and is equal to one-half the coefficient of absorption, and γ is the coefficient of reflection of particle velocity between the fluid and the reflecting plate. The distance r is that between the vibrating plate and the reflector, i.e., the length of the fluid column.

Let the electrodes of the piezoelectric plate be connected to the terminals of the variable condenser C of the resonant circuit L_1, R_1, C, Fig. 1. The resistance R_1 includes the resistance of the vacuum thermocouple T which is inserted between C and L_1 on the grounded side of the interferometer. Let the inductance L_1 be loosely coupled to the output of an oscillation generator which may be kept at any desired frequency, so that in L_1 we have the induced e.m.f., $E=E_0 e^{j\omega t}$. We have for the impedances of the various branches of the circuit, putting $\theta=j\omega$: $Z=L_1\theta+R_1$; $Z_1=1/K_1\theta$; $Z_2=L\theta+R'+1/K'\theta$; $Z_3=1/C\theta$.

Solving for i_0, the amplitude of current in the L_1R_1 branch, including the thermocouple heater, we have

$$i_0^2 = \frac{E_0^2\left\{ R'^2K'^2\omega^2 + \left[1 - LK'\omega^2 + \frac{K'}{C+K_1}\right]^2\right\}\omega^2}{\left\{\left[\frac{1-(C+K_1)L_1\omega^2}{C+K_1}(1-LK'\omega^2) - \left(R_1R'K' + \frac{L_1K'}{C+K_1}\right)\omega^2\right]^2 + \left[R'K'\frac{1-(C+K_1)L_1\omega^2}{C+K_1} + R_1(1-LK'\omega^2) + \frac{R_1K'}{C+K_1}\right]^2\omega^2\right\}}. \quad (5)$$

Putting $I_0 = E_0/R_1$, the maximum value of i_0 at resonance with the interferometer disconnected, and also putting

$$p = 1 - (C+K_1)L_1\omega^2 \quad (6)$$

$$q = 1 - LK'\omega^2,\ q_0 = 1 - LK\omega^2 \quad (7)$$

$$\phi_1 = R_1(C+K_1)\omega \quad (8)$$

$$\phi_2 = R'K'\omega \quad (9)$$

and

$$\sigma = i_0/I_0$$

we have

$$\sigma^2 = \frac{\phi_1^2[\phi_2^2 + (q + K'/(C+K_1))^2]}{[pq - \phi_1\phi_2 - (1-p)K'/(C+K_1)]^2 + [\phi_2 p + \phi_1(q + K'/(C+K_1))]^2}. \quad (10)$$

Eq. (10) is an exact description of the current amplitude in the thermocouple heater relative to the current amplitude at resonance in the resonant circuit with the interferometer disconnected, as a function of the decrements of the oscillating circuit and of the interferometer system, of the departure from resonance in the two systems, of the pure capacity $C+K_1$, and of the fictitious capacity K' of the acoustic system. This equation is similar to the one deduced by D. W. Dye[8] for the piezoelectric resonator in a resonant circuit but is complicated by the inclusion of the modified R', K' and ϕ_2 terms introduced because of the interferometer system. Dye's analysis includes a capacity K_2 between the resonator and the resonant electrical circuit to account for the effect of variable electrode distance from the quartz plate. This capacity is here suppressed, the electrode conditions being maintained constant.

In view of the exhaustive study which Dye has made of his equation no extended discussion of its analogue, Eq. (10), is necessary here. It should be pointed out, however, that in general σ^2 as a function of the frequency rises to the usual resonance maximum for $p=0$, and that further, if $q+K'/(C+K_1) = 0$ in the same neighborhood there will be a sharp minimum or *crevasse* in the resonance curve. This crevasse is extraordinarily narrow because of the extremely small value of ϕ_2 as compared to ϕ_1, and at its center σ^2 falls to a small fraction of its value on either side. By repeated adjustment of C and ω it is possible to find the value of the frequency for which p and $q+K'/(C+K_1)$

[8] D. W. Dye, Proc. Phys. Soc. Lond. **38**, 399–458 (1926).

are zero simultaneously, provided the reflecting plate is set at a distance $r=(2n+1)\lambda/4$, so that P and Q are both equal to zero and $K'=K$, making $q=q_0$. In practice it is sufficient to find a crevasse for any setting of r, whereupon a rough determination of $\lambda/2$ is made. The setting of r is now made at $\lambda/4$, then by successive adjustment of C and ω the crevasse is made symmetrical. The interferometer is then disconnected and C is varied, ω being kept constant, until i_0 has the maximum value I_0, which is determined. The interferometer is then reconnected and C is adjusted to its former value for a symmetrical crevasse, which completes the adjustment necessary for a determination of σ^2 as a function of r. A series of observations of i taken under these conditions is shown in Fig. 2, curves I and II, in which only maxima

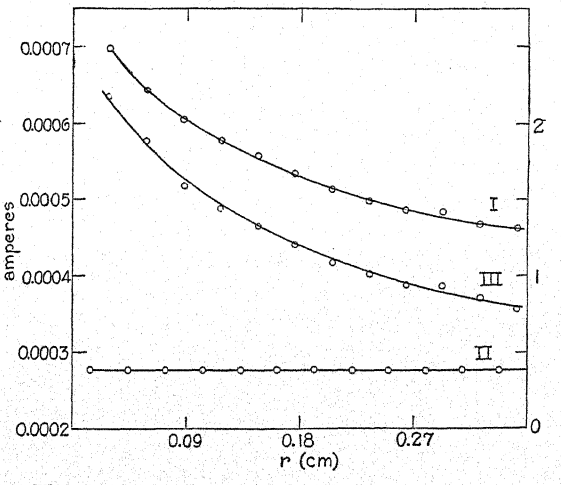


Fig. 2. Curves I and II, maximum and minimum galvanometer readings as a function of r. Curve III, representation of Eq. (17) as a function of the same observations.

and minima of current are shown. The behavior in the immediate neighborhood of a maximum for the same case is shown in Fig. 4, Insert a, the abscissa scale being magnified twentyfold. In the preliminary adjustments just described, we have made $p=0$, $q_0+K/(C+K_1)=0$, and, remembering Eqs. (1), (6) and (7), $q+K'/(C+K_1)=K'AB\rho v\omega Q$, so that

$$\sigma^2=\frac{(1+SP)^2+S^2Q^2}{[1+SP+1/R\omega\phi_1(C+K_1)]^2+S^2Q^2} \tag{11}$$

where

$$S=AB\rho v/R. \tag{12}$$

When the reflector is at a distance $r=(2n+1)\lambda/4$ from the face of the vibrating plate, if n is small, $P=$zero to a very close approximation, and $Q=0$.[9] Let σ_0 be the value of σ for this reflector position. We have then

[9] See I, Figs. 2 and 3. These figures were drawn for the case in which γ was assumed to be unity. As we shall see later the statement made above is practically always valid for gases.

$$\sigma_0 = 1/[1 + 1/R\omega\phi_1(C + K_1)]$$

or

$$R\omega\phi_1(C + K_1) = \sigma_0/(1 - \sigma_0). \tag{13}$$

The value of σ given by Eq. (11) under the prescribed conditions will have maximum values, σ_m, for values of r such that $Q=0$ and $P=P_m$ given by

$$P_m = (1 + \gamma e^{-2r\alpha})/(1 - \gamma^2 e^{-2r\alpha}). \tag{14}$$

We then have

$$\sigma_m = (1 + SP_m)/[1 + SP_m + (1 - \sigma_0)/\sigma_0], \text{ or}$$

$$S = AB\rho v/R = [\sigma_m(1 - \sigma_0)/(1 - \sigma_m)\sigma_0 - 1]/P_m = \text{constant}. \tag{15}$$

Putting $\gamma = e^{-\beta}$, Eq. (14) becomes $P_m = e^{\beta/2}\,[\cosh\,(r\alpha+\beta/2)]/\sinh\,(r\alpha+\beta)$, or, to a very close approximation, unless r is large

$$P_m = (1 + \beta/2)/(r\alpha + \beta). \tag{16}$$

This value of P_m inserted in Eq. (15) would lead at once to a determination of α and β if we had the means of accurate determination of A, assumed to be the area of the vibrating plate exposed to the fluid. As is well known, only a small portion of the surface of a piezoelectric plate as ordinarily cut is in vibration in a given mode[10,11] though by optical means it can be shown that the entire cross section of the column of a fluid in an interferometer is set into resonant vibration and presumably reacts upon the crystal over the whole of its exposed face. Hershberger[12] has recently pointed out that the assumption that A is to be taken as the area of the plate exposed to the fluid is not valid. As we shall see, however, it is sufficient to assume an effective A, which is constant. In the absence of knowledge of its magnitude we have then in Eq. (15) only a means of computing the relative effects of absorption and reflection. For, substituting P_m from Eq. (16) into (15), we have

$$[(1 - \sigma_0)/\sigma_0][\sigma_m/(1 - \sigma_m) - \sigma_0/(1 - \sigma_0)](r\alpha/\beta + 1) = S' \tag{17}$$

where

$$S' = S(1 + \beta/2)/\beta = \text{constant}. \tag{18}$$

Eq. (17) enables us at once to compute α/β from a series of observations of values of σ_m and the corresponding values of r, and the mean value of σ_0. Fig. 2, curve III, shows the observations of Fig. 2, curves I and II, in terms of Eq. (17), the smooth curve passing through the maxima being the hyperbola given by Eq. (17), where $\alpha/\beta=6.276$, and $S'=2.548$. All types of acoustic interferometers which have been used by the method described here yield results for gases in entire accord with the theory showing that within the limits of errors of observation the quantities entering into S', Eq. (18), may be considered as constant.

[10] Nat. Phys. Lab. Report for 1928.
[11] P. Vigoureux, Quartz Resonators and Oscillators, London (1931).
[12] W. D. Hershberger, Physics **2**, 269–273 (1932).

Having determined α/β from a given series of observations, it remains to be seen how α and β may separately be determined. Putting $(1-\sigma_0)/\sigma_0=a$, combining Eqs. (11) and (13), and solving for $1+SP$, we have

$$1 + SP = (a/b)\{1 + [1 + b - (QSb/a)^2]^{1/2}\} \tag{19}$$

where $b=(1-\sigma^2)/\sigma^2$. Remembering Eq. (15), it is seen that in (19) we have a relation, free of all circuit and interferometer constants, involving only galvanometer readings, values of r, and the values of α and β. Having determined the ratio α/β from a series of observations, using Eq. (17), we may assume a value of α, from which we may compute β and S'. The corresponding value of S is then found by means of Eq. (18). Choosing any value of σ on the r, σ curve, preferably at about one-half the altitude of a peak, we compute the value of b. The corresponding value of r is found from the curve for use in computing P and Q. These functions involve r both in the hyperbolic and circular functions composing them. The argument, $2r\omega/v$ of the circular functions may be found directly if the frequency is known, but may be found independently of frequency from the interferometric determination of $\lambda/2$, since $\theta=2r\omega/v=4\Delta r\pi/\lambda$, where Δr is the distance from the point for which σ is chosen to the axis of the peak, or one-half the peak width, since, owing to its extreme narrowness, the symmetry of the peak is not affected by damping to a determinate degree. It is now possible to compute the left and right hand sides of Eq. (19). If the left hand side is larger than the right, the tentative value of α which was chosen is too large, etc. Successive trials lead, usually in three or four steps, to the region of intersection of the curves of the two sides of this equation plotted as functions of α, when by interpolation the value of α satisfying the equation is found. The process may be shortened by noting that $1+SP$ must lie between the values a/b and $(a/b)[1+(1+b)^{1/2}]$ and by using the approximations $P=4(r\alpha+\beta)/[4(r\alpha+\beta)^2+\theta^2]$, and $Q=2\theta/[4(r\alpha+\beta)^2+\theta^2]$ in all but the last two steps.

Measurement of velocity

The values of r for successive values of maximum σ^2 given by Eq. (11) are, to a degree of precision beyond experimental measurement, independent of the damping,[13] except in excessively absorbing media, and are determined by the maximum values of P, which in turn occur when $\cos 2r\omega/v=1$, or when $r=n\lambda/2$. It then remains to measure the frequency in order to evaluate the velocity v.

III. Experimental Tests of the Theory

Three interferometers have been built for the purpose of testing the theory. As the results obtained from all of them differ in no important detail, no extensive description of them will be given.

Interferometer I, Fig. 3a, was designed for operation in the open air. It consists of the quartz plate Q resting upon a grounded electrode mounted at the top of a Bakelite support. This support is attached to a plate provided

[13] Cf. also C. D. Reid, Phys. Rev. **35**, 829 (1930).

with adjusting screws so that the face of the plate may be made parallel to the plate glass reflector R. This adjustment was made by viewing fringes in sodium light passed through R and falling upon Q when the two were close together and R was started in retreat from the crystal. The supports for R and Q are mounted upon the ways of a micrometer comparator of great accuracy made by the late Professor H. A. Rowland. The screw is provided with a large head divided into 100 parts, and has a fine adjustment making possible measurements to 10^{-4} mm. This interferometer was particularly useful in testing the effect of various methods of crystal mounting and types of electrodes. Its great accuracy and fine adjustment were used both with the method described in this paper, the crystal being used as a resonator, and with the crystal used as an oscillator, after the methods of Pierce[14] in order to test the effect of variation of velocity with reflector distance reported by

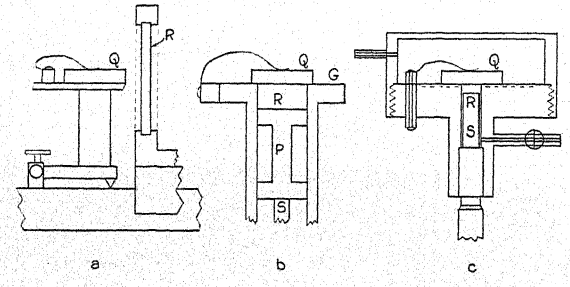


Fig. 3.

Reid.[13] The effect found by Reid was of decreasing amount with increase of frequency, being small with the highest frequencies which he employed. As the frequencies so far used in this laboratory are much higher the effect to be expected might be so small as to escape detection. So far, in the range 400 to 700 k.c. no such effect has been detected by either the resonator or oscillator method, although the interferometer distance has been varied from the face of the crystals used to a distance of 10 cm.

Interferometer II, Fig. 3b, was designed to give the largest possible reaction upon the crystal by the fluid column. It consists of a solid cylinder of brass in which a concentric hole 1″ in diameter was bored. The upper end of the cylinder was ground plane. Upon it rests the crystal Q, the lower face of which is gold sputtered providing the grounded electrode. Contact is made with the upper electrode by means of a light spring. The plunger P is close fitting, with end R ground plane and parallel to the surface G. P is displaced by the micrometer screw S.

Interferometer III, Fig. 3c, was designed to test the effect of the removal of water vapor and CO_2 from the air and to study other gases at room temperature. The end of the micrometer screw serves as the reflector, its parallelism to the surface upon which the crystal rests being tested by sodium fringes, with an optical flat in place of the sputtered crystal. The air or other gas to be tested enters a small channel at the side of the screw, passing up-

[14] G. W. Pierce, Proc. Am. Acad. **60**, 269–302 (1925).

ward and through a small slot under the crystal and into the chamber above, from which it escapes.

The constant frequency oscillator consists of a dynatron oscillator with secondary output connected to the inner grid of a UX222 tube having 45 volts applied to the outer grid. The output of this tube is amplified in two stages of resistance capacity coupling, with nonregenerative tuned output in the last stage. Loosely coupled to the output is the coil L_1 of the resonant circuit which excites the interferometer. Minute variation of the frequency of the dynatron oscillator is provided by a precision condenser of large capacity in series with the condenser of the dynatron circuit. In addition a vernier condenser of very small capacity and with a linear scale of 50 cm length is connected in parallel with the precision condenser so that rapid adjustment for symmetry of crevasse may be made. Currents are measured by a Western Electric vacuum thermocouple and a galvanometer provided with a number of shunts.

Connection to the interferometer is made through a mercury switch, which serves also at any time to connect the interferometer into a Pierce circuit so that studies by both the resonator and oscillator method may be compared, the crystal being under identical conditions. The results of these comparative studies will be presented in another paper.

The most general conclusion which can be drawn from the experiments so

TABLE I. *Galvanometer and screw readings. 597 k.c. First twelve rows give i_m with corresponding peak number m. Column (1), room air, interferometer II: (2), room air, interferometer III: (3), dry air: (4), dry, CO_2—free air: (5), CO_2.*

m	(1)	(2)	(3)	(4)	(5)
1	0.001484	0.000720	0.000698	0.000703	0.000653
2	1432	674	642	647	541
3	1383	634	603	614	484
4	1344	603	577	583	444
5	1295	582	557	557	420
6	1255	563	534	540	394
7	1211	539	513	514	386
8	1163	524	498	498	377
9	1119	508	485	486	
10	1094	504	484	483	
11	1050	492	467	470	
12	1020	483	462	456	
t°C	22.2	23.3	24.0	24.0	23.3
$\lambda/2$	0.02928	0.02944	0.02941	0.02944	0.02389
i_0	0.000235	0.000310	0.000278	0.000279	0.000304
I_0	0.002398	0.002329	0.002275	0.002293	0.002275
r cm	0.2343	0.3538	0.3529	0.3533	0.1433
$2\Delta r$	0.00322	0.00159*	0.00157	0.00156	0.00200
i	0.0006	0.000375	0.000350	0.000350	0.000350
r cm	0.3514				
$2\Delta r$	0.00325				
i	0.0006				

* Peak structure not satisfactory owing to rapid drift of frequency and necessity of repeated correction.

far carried out is that for every case investigated, in the frequency range 400–700 k.c. and with all three of the interferometers just described, the results for the maxima and minima of the σ, r curve can be expressed within experimental error by the hyperbolic relation given in Eq. (17). The value of α/β and of S' for any set of observations may be determined by the method of least squares. Table I gives the original data for five cases at the frequency 597 k.c. The computed values of α/β and S' for each of the sets are given in Table II. Fig. 2 is drawn for the results of column (3). Fig. 4, Inserts (a) and (b), show the structures respectively of the 12th peak for dry air, and the 6th peak for CO_2. From these and other similar peaks the data for $2\Delta r$ in Table I are obtained. For the purpose of comparison of different sets of results taken

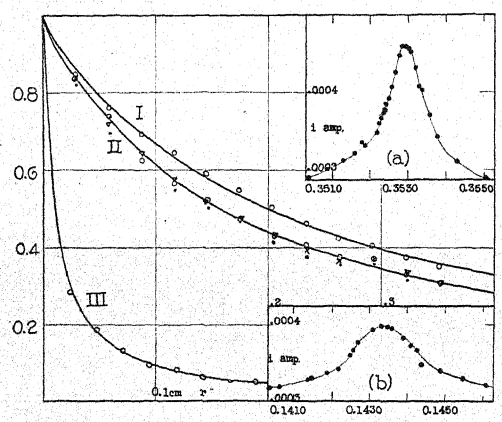


Fig. 4. Reduced observations compared with $1/(r\alpha/\beta+1)$.
Curve I, room air in interferometer II; Curve II, with circles, dry air in interferometer III; Curve III, CO_2 in interferometer III. Insert (a), twelfth current peak for dry air; Insert (b), sixth current peak for CO_2.

with different gases or under different conditions, as with different interferometers, we may plot $[(1-\sigma_0)/\sigma_0][\sigma_m/(1-\sigma_m)-\sigma_0/(1-\sigma_0)]/S'$ as a function of r. This should be compared with its theoretical equivalent, $1/(r\alpha/\beta+1)$. Fig. 4 shows as an example the first of the above functions for the observations of Table I indicated by circles, points, etc., and full curves, I, II, III, for $1/(r\alpha/\beta+1)$ for three of the sets corresponding respectively to columns (1), (3) and (5) of Table I. It is to be noted that all such curves start with ordinate unity at $r=0$.

Absorption measurements

Having determined α/β, it is possible, as has been explained, to find the separate values of α and β from some value of σ and its corresponding r by a method of graphic interpolation. The accuracy with which these quantities may be obtained is affected by the constancy with which the frequency and amplitude of the driving circuit may be maintained. In the absence of a piezo-electrically driven generator of required frequency for driving the resonant circuit containing the interferometer, it has been the practise to test the

constancy of frequency at the conclusion of readings for each peak by setting r at the nearest value of $(2n+1)\lambda/4$ and noting whether i is at the minimum value i_0. To test whether the amplitude of output has been changed, the interferometer is disconnected and a reading of I_0 is taken, corresponding to the resonance maximum of the interferometer circuit. If either i_0 or I_0 has changed the intervening observations are rejected. This practise has entailed a loss of time and labor, making it highly desirable to use crystals for driving the generator. However, since the particular crevasse of a given crystal most suitable for interferometric work is often not at one of the principal frequencies of the crystal, the process of accumulation of plates for driving purposes involves first a careful exploration of crevasses for their suitability in the interferometer, and then of preparing oscillator plates, one for each frequency which can be used.

The results given in Table I were taken with a rectangular plate. The crystal was an excellent oscillator and no other crevasses were observed in the neighborhood of its principal crevasse frequency. The peaks were symmetrical and showed no evidence at any time of having any satellites. This crystal was therefore regarded as being particularly suitable for the present purpose of illustration of the theory. The values of α/β, S', α, and γ computed from the results given in Table I are shown in Table II.

TABLE II. *Absorption and reflection coefficients. $\nu=597$ k.c.*

	Interferometer	Gas	t°C	$\lambda/2$ cm	α/β	S'	α	γ
1	II	Room air	22.2	0.02928	5.045	16.63	0.130	0.9745
2	III	Room air	23.3	0.02944	6.384	2.262	0.106*	0.9836
3	"	Dry air	24.0	0.02941	6.276	2.548	0.110	0.9827
4	"	Dry CO_2 free air	24.0	0.02944	6.312	2.561	0.108	0.9831
5	"	CO_2	23.3	0.02389	94.78	5.705	0.702	0.99261

* See remark under Table I.

Data on absorption are very meager. From Neklepajew[15] we have for dry air, $\mu=0.00073/\lambda^2$, which for $\lambda/2=0.02941$ gives $\mu=0.211$. For α this gives 0.105, in fair agreement with the value 0.110 for dry air in Table II. For CO_2, we have the calculations of Herzfeld and Rice[16] from the velocity measurements of Pierce[14] and by extrapolation from the results of Abello[17] giving respectively for μ, $3\times10^{-12}\nu^2$ and $5.6\times10^{-12}\nu^2$. We have, for $\nu=5.97\times10^5$, from the former, $\alpha=0.54$, and from the latter $\alpha=1.0$. These results may be compared with $\alpha=0.702$ for CO_2 in Table II.

The coefficient of reflection

An interesting feature of these experiments is the large departure from unity of the coefficient of reflection γ. If we take as the coefficient of reflection of air waves at a surface of brass, $\gamma=(R_1-R_2)/(R_1+R_2)$, where R_1 for brass

[15] N. Neklepajew, Ann. d. Physik **35**, 175–181 (1911).
[16] K. F. Herzfeld and F. O. Rice, Phys. Rev. **31**, 695 (1928).
[17] T. P. Abello, Proc. Nat. Acad. Sci. **13**, 699 (1927).

is $\rho v = 8.5 \times 3.65 \times 10^5 = 3.1 \times 10^6$, and for air, $R_2 = 40$, we expect γ to be $1 - 1.3 \times 10^{-5}$. The departure from unity in these experiments is actually several orders greater, as may be seen from Table II. In explanation of this we may recall that we are dealing with a resonant system, and that it is to be expected that resonance in the reflector system will result in a motion of the reflector surface depending upon the dimensions and material of the reflector. The coefficient of reflection in terms of motion of reflector surface is considered in Part I of this paper. It is to be noted in Table II that γ changes abruptly from interferometer II to III, and from air to CO_2. Similar changes are noted in passing from one frequency to another. It would be of interest in this connection to use as a reflector a second piezoelectric plate of quartz so that the amplitude of vibration of the reflecting surface could be studied directly. The equations developed for this case, where it was assumed that the reflector was rigid, I, Eqs. (17) and (18) do not apply in so far as γ is not unity. From I, Eqs. (12) and (13) we have putting $x = r$,

$$P_r = [(1+\gamma)(1-\gamma^2 e^{-2r\alpha}) e^{-r\alpha} \cos(r\omega/v)] / [1 - 2\gamma^2 e^{-2r\alpha} \cos(2r\omega/v) + \gamma^4 e^{-4r\alpha}] \quad (20)$$

$$Q_r = [(1+\gamma)(1+\gamma^2 e^{-2r\alpha}) e^{-r\alpha} \sin(r\omega/v)] / [1 - 2\gamma^2 e^{-2r\alpha} \cos(2r\omega/v) + \gamma^4 e^{-4r\alpha}]. \quad (21)$$

These equations, with Eqs. (1) and (2) applied to the reflector, considering its network in combination with a suitable thermogalvanometer connected to its electrodes, would make practicable a detailed study of reflection phenomena. Grossmann and Wien[18] have used a piezoelectric plate as reflector for the study of frequency variation of a radiating crystal oscillator as a function of reflector distance. Grossmann[19] has used an arrangement of two crystals as source and detector for the study of absorption in CO_2, but at this writing details of his method and procedure are not available.

It is of interest to compare the effect on the observations of using different cross sections of fluid column. From Eq. (12), $A = SR/B\rho v$, and from Eq. (13), $R = \sigma_0/(1-\sigma_0)\omega\phi_1(C+K_1)$. In changing under the same conditions from one interferometer to another, $B\rho v$ and $\omega\phi_1(C+K_1)$ remain practically unchanged, so that the areas of cross section of the two columns should be in proportion to the respective values of $S\sigma_0/(1-\sigma_0)$, or $S'\sigma_0\beta/(1-\sigma_0)(1+\beta/2)$. For interferometer II, room air, we have $S' = 16.63$, $\beta = 0.0258$, $\sigma_0/(1-\sigma_0) = 0.1086$, and for interferometer III these quantities have the respective values 2.262, 0.0166, 0.1537, implying a ratio of cross section of interferometer II to III of 8.03. The actual areas were 5.07 and 0.707 cm^2, having a ratio 7.18. The agreement of these figures is closer than might be expected in view of the remarks following Eq. (16). The particular crystal for which the above numbers are cited vibrates vigorously for the mode considered at two points near opposite corners of its rectangular area, little trace of motion being found over much of its surface. In using such a crystal with interferometer III it is necessary to adjust the crystal so that one of its vibrating areas is exposed to the gas. The nearness to equality of the ratios given above and

[18] E. Grossmann and M. Wien, Phys. Zeits. **32**, 377–378 (1931).
[19] E. Grossmann, Phys. Zeits. **33**, 202 (1932).

similar values in many other cases point to the conclusion that what we have called the effective value of A is nearly equal to the actual area exposed to radiation. It seems probable that this equality would be exact with crystals cut in the manner described by Straubel[20] in which case the absolute value of S in Eq. (15) could be determined and the coefficient of absorption of the gas could be evaluated directly from observations of maxima and minima of σ, using Eqs. (15) and (16), thus avoiding the laborious procedure of analysis of peak form.

A study is in progress, with the methods here outlined, of the ultrasonic absorption constants of several gases, considered as functions of frequency and temperature.

My thanks are expressed to the Rumford Committee of the American Academy of Arts and Sciences for a grant with which the quartz crystals used in this work were obtained, and to Mr. Milton Lipnick, a graduate student of the Johns Hopkins University for assistance on many occasions.

[20] H. Straubel, Phys. Zeits. **32**, 222 (1931).

Mutual Impedance of Grounded Wires above the Surface of the Earth

By RONALD M. FOSTER
American Telephone and Telegraph Company

(Received July 27, 1932)

A FORMULA already established for the mutual impedance of any grounded thin wires lying on the surface of the earth[1] has now been extended to include wires lying in horizontal planes above the surface and grounded by vertical wires at their four end-points. With the same basic assumptions and the same general method of derivation as before, the extended formula is found to be:

$$Z_{12} = \int\int \left[\frac{d^2Q(r, H, h)}{dS\, ds} + \cos\epsilon\, N(r, H, h)\right] dS\, ds,$$

where

$$Q(r, H, h) = Q_0(r) + Q_1(r, H + h) - Q_2(r, |H - h|),$$

$$N(r, H, h) = N_0(r) + N_1(r, H + h) - N_2(r, |H - h|),$$

$$Q_0(r) = \rho/2\pi r,$$

$$Q_1(r, h) = \frac{i\omega\nu}{4\pi}\int_0^\infty \left\{\frac{h}{\mu} - \frac{1 - e^{-h\mu}}{\mu^2}\left[\frac{(\mu^2 + \Gamma^2)^{1/2} - \mu}{(\mu^2 + \Gamma^2)^{1/2} + \mu}\right]\right\} J_0(r\mu)\, d\mu,$$

$$Q_2(r, h) = \frac{i\omega\nu}{4\pi}\left[h \log \frac{(r^2 + h^2)^{1/2} + h}{r} - (r^2 + h^2)^{1/2} + r\right],$$

$$N_0(r) = \frac{\rho}{2\pi r^2}[1 - (1 + \Gamma r)e^{-\Gamma r}],$$

$$N_1(r, h) = \frac{i\omega\nu}{4\pi}\int_0^\infty (1 - e^{-h\mu})\left[\frac{(\mu^2 + \Gamma^2)^{1/2} - \mu}{(\mu^2 + \Gamma^2)^{1/2} + \mu}\right] J_0(r\mu)\, d\mu,$$

$$N_2(r, h) = \frac{i\omega\nu}{4\pi}\left[\frac{1}{r} - \frac{1}{(r^2 + h^2)^{1/2}}\right].$$

The integrations in the iterated integral are extended over the two wires S and s, lying in planes at heights H and h, respectively. The elements dS and ds are separated by the horizontal distance r and include the angle ϵ between their directions The resistivity of the earth is ρ; the inductivities of the air and of the earth are each assumed to be equal to that of free space, ν. The propagation constant of plane electromagnetic waves in the earth is Γ, which

[1] R. M. Foster, Bull. Amer. Math. Soc. **36**, 367–368 (1930); Bell System Tech. J. **10**, 408–419 (1931).

equals $(i\omega\nu/\rho)^{1/2}$. All distances are measured in meters, Z_{12} in ohms, and ρ in meter-ohms; ν has the value 1.256 microhenries per meter; ω is equal to 2π times the frequency.

For zero heights, the functions Q and N reduce to Q_0 and N_0, which are the values previously obtained for wires on the surface. For any heights but with low frequencies the formula gives the direct-current mutual impedance as found by G. A. Campbell.[2] For any heights but with one wire of infinite length the formula gives the mutual impedance as published independently by F. Pollaczek,[3] J. R. Carson,[4] and G. Haberland.[5]

[2] G. A. Campbell, Bell System Tech. J. **2**, 1–30 (1923).
[3] F. Pollaczek, Elekt. Nachr. Tech. **3**, 339–359 (1926).
[4] J. R. Carson, Bell System Tech. J. **5**, 539–554 (1926).
[5] G. Haberland, Zeit. angew. Math. **6**, 366–379 (1926).

LETTERS TO THE EDITOR

Prompt publication of brief reports of important discoveries in physics may be secured by addressing them to this department. Closing dates for this department are, for the first issue of the month, the twenty-eighth of the preceding month; for the second issue, the thirteenth of the month. The Board of Editors does not hold itself responsible for the opinions expressed by the correspondents.

The Frequency of Resonance Radiation

It is of considerable importance in many astrophysical studies to know whether the atom emits as resonance radiation exactly the same frequency which it absorbs. If one supposes, following Eddington, that it does emit this precise frequency, then an atom which absorbs light of frequency slightly off "resonance" will also emit off resonance. A preliminary test was made by illuminating mercury vapor with a line (2536A) having a narrow and sharp reversal, and observing the resonance radiation. This was accomplished by using a water-cooled quartz arc shining through a quartz absorption cell onto the resonance chamber. The temperature of the absorption cell could be regulated electrically and with ice, and consequently the vapor pressure of the absorbing column of mercury vapor could be controlled. With the absorption cell cold (0°C) resonance radiation was observed; and as the temperature of the cell was raised the resonance radiation became fainter, until at 45°C the resonance could barely be detected on a long exposure photograph. This absorption cell produces a narrow and sharp reversal in the center of the emission line of the arc, the amount of the reversal being of course determined by the temperature of the cell. Yet at no time was any reversal of the line in resonance observed. Careful tests were made for stray scattered light. The spectrograph used was of the quartz Cornu prism type with a dispersion of about 3A per mm at λ2536.

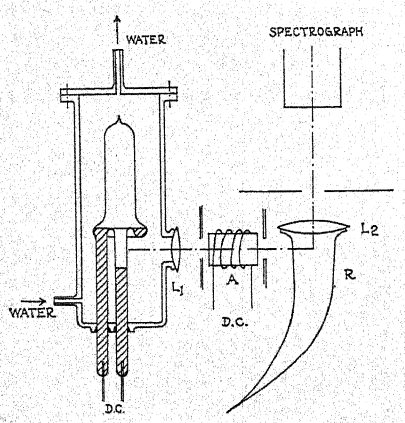


Fig. 1.

The physical interpretation of this effect is not fully understood. If one supposes a slight change in frequency to take place between the acts of absorption and emission, then energy which is absorbed in the wings would be reradiated in the center, as observed. The difference in energy between that of the absorbed and reradiated quantum presumably appears as thermal energy of motion. It will be noted that this change in energy, though apparently small, is far greater than the extremely minute Doppler width of mercury vapor at room temperature could possibly account for. If on the other hand we postulate detailed balancing and require the exact frequency absorbed to be reemitted, then the emission of a nonreversed line becomes something of a puzzle unless the upper state is more sharply quantized than the ground state—an improbable eventuality.

It is proposed to continue these experiments with a spectrograph of greater dispersion and to attempt to resolve the resonance radiated line more completely.

S. A. KORFF

Carnegie Institution of Washington,
Mt. Wilson Observatory,
July 10, 1932.

Use of Argon in the Ionization Method of Measuring Cosmic Rays

In designing apparatus for a cosmic-ray survey, we had occasion to study argon under pressure as material for the ionization chamber. The results of preliminary measurements showed that this gas was much more strongly ionized than either air or nitrogen, which have been used hitherto. A study was made of the ionization-pressure curves of argon and air. The source of ionization was about one milligram of radium at a distance of one meter. Even at the highest pressure (95 atmospheres) of argon that was used the curve was still rapidly rising.

The following current intensity ratios were obtained from our own measurements and from measurements of others on air and nitrogen, for a pressure of 95 atmospheres:

$$I_{(\text{argon})}/I_{(\text{air})}=3.22;$$
$$I_{(\text{nitrogen})}/I_{(\text{air})}=1.48$$
$$I_{(\text{argon})}/I_{(\text{nitrogen})}=2.17$$

When the ionization chamber was first filled with argon to a high pressure, the ionization current increased with time. The value on fresh filling was only about 50 percent of the final steady value; after 3 hours it was about 87 percent and the final steady value was reached in about a day. This effect depends obviously upon how much the gas is stirred in filling the bomb. In view of this effect our ionization-pressure data have been taken in the direction of decreasing pressures.

When no electric field was applied across the ionization chamber, ions produced in argon at high pressure under exposure to gamma-rays remained uncombined for many minutes. This is in accord with the small recombination coefficient that had been found for argon at low pressures. This effect was also found in air but to a less degree.

An initial recombination of ions in air and nitrogen at high pressure before they are separated by diffusion has been used to account for the fact that in these gases the effective ionization is not proportional to the pressure. It is reasonable to suppose that in argon the low recombination rate makes improbable such initial recombination, with the result that the ionization continues to increase with pressure over a much wider range.

This small speed of recombination in argon allows a relatively large concentration of ions to form under the action of an ionizing source before equilibrium is reached. If now a potential is put onto the ionization chamber, the initial current is many times the value of the steady final current, which is ordinarily used to measure the rate of formation of ions. This cumulative action suggests the properties of a photographic plate, and indicates its possible application in the measurement of weak ionization currents.

ARTHUR H. COMPTON
JOHN J. HOPFIELD
University of Chicago,
July 18, 1932.

Strain and Magnetic Orientation

Previous work[1] has shown that tension establishes the axial as the preferred direction of magnetization in a 15 Ni 85 Fe wire, but this direction is unique in other respects such as symmetry of internal strains and partial crystal orientation. More recently further experiments with large Barkhausen discontinuities have given striking and direct confirmation of the view that a large elastic strain establishes a preferred orientation independent of other factors.

The NiFe wire, lying with its axis in the OH direction, Fig. 1, was strained by twisting, with the result that, referred to the surface of the wire, the maximum elongation lay in the *OP* direction. In this state the wire exhibits self-propagating changes of magnetization under the influence of longitudinal magnetic fields as described previously, an important feature of the phenomenon being the limiting ("critical") field below which reversal cannot proceed. The critical field values for 1, 2, and 3 turns of one end of an 80 cm long, 0.019 cm radius wire are shown in Fig. 1 at H_{01}, H_{02}, H_{03}, respectively. In the present experiments, however, a transverse field was added by passing current through the wire itself. Only the value H_t of this field at the surface of the wire will be considered.

In the presence of this field a new set of critical longitudinal fields was found. For

[1] K. S. Sixtus and L. Tonks, Phys. Rev. **37**, 930 (1931).

instance, with $H_t=H_t'$, H was increased so that the terminus of the vector representing the total field traversed RQ from left to right. No jump was found for 1 turn; the jump first became possible at h_2 for 2 turns, and for 3 turns the discontinuity occurred against an opposing longitudinal field!

Confining attention to the 2-turn case, we have in OH_2 and OH_{02} two vector critical fields.

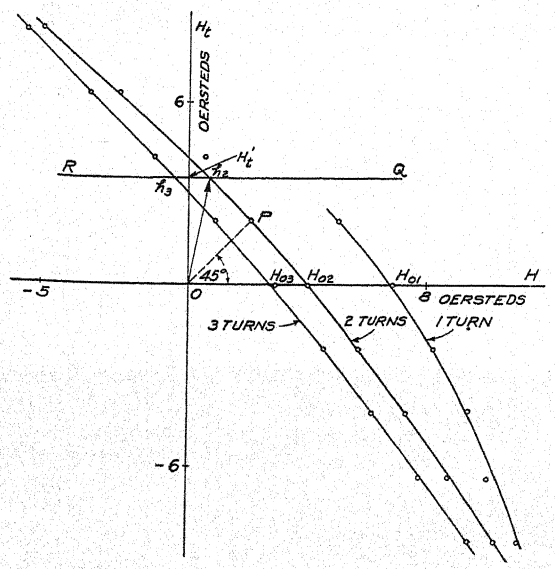


Fig. 1. Vector critical fields in twisted NiFe wire.

By using other values of H_t the curve joining h_2 and H_{02} was filled in. This curve is the same whether H_t is constant and H is increased in obtaining it, or vice versa.

The significant features of the curve are that (1) it approximates to a straight line and (2) it makes 45° with the axes. The parallelism of the 1- and 3-turn curves with the 2-turn curve shows that this is no accident. As it is a straight line, the components, taken along the direction of its normal, of all the vector critical fields are equal, and as it is at 45°, this direction coincides with OP, the direction of a principal strain. It follows that the component of the applied field in the direction of maximum elongation is solely effective in causing the large Barkhausen jump.

Characteristics were also obtained for a wire twisted while under strong tension. For zero torsion H_t was without effect, the characteristic being a straight line parallel to the H_t axis. For increasing torsion the lines inclined toward the H_t axis, the angle of inclination agreeing well with that calculated for the deviation of the principal strain from the axis.

These results lead naturally to the view that within the range of magnetic fields used and with sufficient strain applied, the magnetic intensity lies in the direction of maximum elongation, and that transverse fields are ineffective in aiding the reversal of magnetization under these conditions.

LEWI TONKS
K. J. SIXTUS

Research Laboratory,
General Electric Company,
Schenectady, New York,
July 29, 1932.

Electrons as Cosmic Rays

Professor A. H. Compton's fundamentally interesting experiments on the variation of cosmic-ray intensity with latitude raises once more, as he suggests, the possibility of cosmic rays being electrons. In addition to the bearing of such a hypothesis upon variations with altitude and with latitude, certain other matters suggest themselves as interesting for consideration.

In 1924, in connection with a theory of the

absence of ionization[1] by electrons of sufficiently high energy, the writer pointed out that an electron with velocity only 40 meters per second less than the velocity of light, i.e., with energy corresponding to 10^9 volts, could not approach the earth's surface at the equator nearer than a point at a distance of 8 earth's radii from the earth's center when projected from infinity towards the earth's surface in the magnetic equatorial plane. For the most favorable direction of projection in that plane at infinity, an electron would have to possess 10^{10} volts velocity in order to reach the surface. A. Bramley and the writer[2] having given evidence from the wave mechanics supporting the conclusion that electrons of energy comparable with this amount may be incapable of ionizing, as formerly surmised by the writer[1] for energies of the order 10^9 volts on the basis of the classical electrodynamics. Such a conclusion would render more reasonable an explanation of the maintenance of the earth's charge by the influx of such electrons, since it would relieve us of the difficulty following from the large ionization which the 1500 electrons per square centimeter per second, necessary to account for the earth's charge, would otherwise cause. Another point of interest involves the idea that for such electrons, considered as primary cosmic radiation, the action of ionization would have to occur through the intervention of secondaries shot out only occasionally by the primaries. The operation of the primaries would thus become more closely comparable with that characteristic of photons.

The actual experimental observation of secondary electrons of energies comparable with 10^9 volts, by Professor Millikan and his collaborators, raises many interesting questions. Such electrons would describe, in the earth's magnetic field, circles or helices of radius 10^7 cm; and their energy, on the basis of 16 volts per ion and 50 ions per centimeter of path at atmospheric pressure, would enable them to travel distances comparable with the whole thickness of the homogeneous atmosphere, and indeed distances forming at least appreciable fractions of the whole circumference of the circular orbits into which they are bent. The conclusions following from the foregoing considerations may best be illustrated in limited space by reference to Fig. 1, where in each case the circle represents the complete orbit of the electron if there were no absorption in earth or air (for simplicity, we consider orbits in the magnetic equatorial plane). The dotted line represents the earth's surface, and the point O, the point of emission of a secondary in the atmosphere. Even for the case of symmetrical emission of secondaries by primaries in all directions in the lower hemisphere, there will not be symmetrical emission of secondaries with respect to a plane passing through the magnetic poles. Thus, consider a case where the electron path (shown by the thick line) is one eighth of the circumference. Corresponding to an electron striking the earth at 45° from east to west as in Fig. 1*A*, there will be an electron striking at 45° from west to east as in *B*. But corresponding to an electron striking tangentially from east to west as at *C*, there will be no electron striking tangentially from west to east. Such an electron would have to have come from below the surface of the earth as at *D*, and to have been emitted partially upwards. A lack of symmetry in favor of vertical emission of secondaries would enhance still further the considerations here cited.

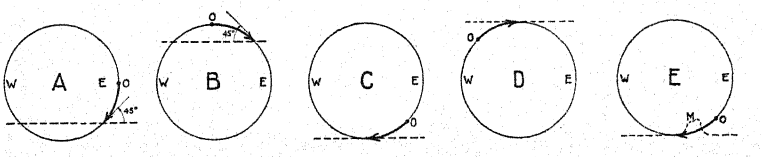


Fig. 1.

[1] W. F. G. Swann, Phil. Mag. [6] **47**, 306–319 (1924). Very exhaustive treatments of the orbits of electrons in the earth's magnetic field have been given by C. Stormer on the theoretical side and by K. Birkeland on the experimental side, in papers extending as far back as 1904. These have to do chiefly with the positions of the auroral zones.

[2] W. F. G. Swann and A. Bramley, Phys. Rev. **41**, 393 (1932). Read before the New Haven Meeting of the Am. Phys. Soc. on June 23, 1932.

Since the orbits of these high energy electrons are determined entirely by their relativistic mass, and are otherwise independent of the velocity since that velocity is practically equal to that of light, and since the mass is proportional to the energy for these electrons, the orbits will be the same for protons as for electrons of the same energy, except that they will be described in the opposite sense.

It is of interest to observe that in the case of observations on a high mountain, radiations coming from electrons which have passed their lowest point should be directed slightly upwards. It is also of interest to note the shielding effect to be expected from a mountain *M* for such conditions as are represented in Fig. 1 *E*.

W. F. G. SWANN
Bartol Research Foundation of
The Franklin Institute,
August 1, 1932.

BOOK REVIEWS

The Partial Differential Equations of Mathematical Physics. H. BATEMAN. Pp. 522+xxii. Figs. 29. Cambridge University Press, 1932. Price. $10.50.

To quote from the preface, "in this book the analysis has been developed chiefly with the aim of obtaining exact analytical expressions for the solution of the boundary value problems of mathematical physics." The volume is hence a valuable and comprehensive compendium of the mathematical technique which has been developed for solving the equations of classical physics. Professor Bateman is preeminently qualified to write a monograph of this character, since his ability is well known in finding new closed solutions of complicated equations. Among the subjects treated are Sommerfeld's method of handling diffraction problems, conformal representation, use of Green's functions, toroidal coordinates, etc. In practically all cases, physical problems are cited to which the mathematical analysis is applicable. For instance, the first section of the chapter on non-linear equations bears the caption "Riccati's equation, motion of a resisting medium, fall of an aeroplane, bimolecular chemical reactions, lines of force of a moving electric pole, examples." This is typical of the diversity of physical illustrations, although no attempt is made to draw upon the quantum mechanics of atomic structure. As the author intimates in the introduction, some of the differential equations and functions which are treated are, nevertheless, encountered in quantum mechanics; i.e., the confluent hypergeometric function. The great generality of the mathematical methods permits a high degree of comprehensiveness, but, coupled with the varied and scattered character of the physical illustrations, perhaps makes the style somewhat difficult in places. The author index of over four hundred names shows careful documentation of modern mathematical investigations on boundary value problems. The volume as a whole is focused upon exact solutions, but contains an introduction of eight pages on methods of approximation for the solution of differential equations, such as the Ritz method, least squares, etc.

J. H. VAN VLECK
University of Wisconsin

Die Relativitätstheorie. LUDWIG HOPF. (Volume XIV of **Verständliche Wissenschaft.**) Pp. 148+viii. Figs. 30. Springer, Berlin, 1931. Price RM 4.80.

This first physical volume to apear in Springer's series of semi-popular scientific expositions shows to what extent even such an abstruse discipline as the theory of relativity can be presented in a form readily understandable by the educated layman. An illuminating survey of the fundamental viewpoints of classical mechanics and electrodynamics is followed by a popular exposition of the special theory of relativity which is, in the opinion of the reviewer and within the scope of his experience in this field, the best of its kind; the only mathematics involved (elementary algebra and geometry!) is contained in several scattered paragraphs of fine print, one of which begins with the explanatory sentence "Auch hier sei eine kurze Rechnung für den Leser, der den Pythoagoräischen Lehrsatz und den Begriff der Wurzel noch Kennt, eingeschaltet." The remainder of the book is devoted to the more general theory, and although it falls somewhat behind the previous portions in clarity and fitness, is perhaps as successful an attempt as could be expected under the severe restrictions imposed.

H. P. ROBERTSON
Princeton University

Die gruppentheoretische Methode in der Quantenmechanik. B. L. VAN DER WAERDEN. (Volume XXXVI of **Die Grundlehren der mathemitschen Wissenschaften in Einzeldarstellungen.**). Pp. 157+viii. Figs. 7. Springer, Berlin. 1932. Price RM 9.–RM 9.90.

The appearance of van der Waerden's excellent exposition of the applications of group theory in quantum mechanics will be welcomed by those who wish to survey the field without subjecting themselves to the more strenuous task of digesting the more extended treatises of

Weyl or Wigner. This little book is characterized by a directness of attack which offers the interested reader a shortcut to those portions of the mathematical theory which are of immediate application in the theory of atomic and (diatomic) molecular spectra.

A short introductory account of the Schrödinger formulation of quantum mechanics is followed by a brief exposition of those theorems of the theory of groups and their representations which are to be employed in the sequel. A shortcut to the important theorems concerning the reduction of a representation into its irreducible constituents is obtained by restricting the proof of preliminary lemmas to the case of an "additive (Abelian) group with operators." These sections are followed by an explicit derivation of the complete set of irreducible representations of the rotation and Lorentz groups, and of the selection and intensity rules resulting from the former. The Lorentz group and its representations are discussed with the aid of the so-called spinor analysis, in a form immediately applicable in the following (fourth) chapter of the Pauli-Darwin and Dirac theories of the spinning electron. After a discussion of the relativistic invariance and the solution of Dirac's equations, the author drops back to the nonrelativistic Pauli-Darwin theory for a derivation of the Hund theory of atomic spectra—insofar as it does not involve the Pauli exclusion principle. This exclusion principle, which is of course bound up with the theory of the representations of the symmetric permutation group, is dealt with in Chapter V from the Dirac-Slater points of view which enable one to avoid much of the general theory of this group; the Hund vector model is then completed by the incorporation of these considerations into the scheme derived in the previous chapter. The sixth and last chapter is devoted to a brief development of the corresponding theory for the spectra of diatomic molecules.

The scope of the present book transcends that of Wigner's by the inclusion of some twenty pages on molecular spectra, and has therefore to obtain its end by the sacrifice of much of the illuminating detail contained in the latter. On the other hand, it is narrower in scope than that of Weyl—to which it bears a greater resemblance in notation, method and choice of material—but insofar as it does deal with the same topics it does so by presenting only that portion of the theory which is absolutely necessary for the applications under consideration. While it may therefore send the otherwise uninitiated reader to other treatises for a more thorough background, van der Waerden's logically self-contained and on the whole praiseworthy account of the applications of group theory to quantum mechanics should be of considerable assistance to the physicist or chemist who wishes to gain an insight into the field for himself—and who is not wholly untutored in the ways of mathematicians.

H. P. ROBERTSON
Princeton University

Second Series *September 1, 1932* *Vol. 41, No. 5*

THE

PHYSICAL REVIEW

An Interpretation of Cosmic-Ray Phenomena

By THOMAS H. JOHNSON

Bartol Research Foundation of the Franklin Institute

(Received July 9, 1932)

Schindler's data on the *transition effects* of the cosmic rays have been interpreted on the assumption that the equilibrium between the primary radiation and its secondary corpuscular rays is different in different media. The ionization behind any thickness of absorbing materials, assumed to be proportional to the flux of secondaries, is calculated in terms of the absorption coefficients, $\nu(m)$, of the primary radiation and the production and absorption coefficients, $\beta(m)$ and $\mu(m, m)$, respectively, of the secondary rays, these coefficients being characteristics of the media. A comparison with the data permits a determination of each of the absorption coefficients as well as the product of each of the production coefficients by the number of primary rays. The results are as follows, expressed in cm^{-1} lead equivalent: $\nu(Pb)=0.0064$; $\nu(Fe)=0.009$; $\mu(Pb, air)$, the absorption coefficient in lead for secondaries produced in air $=0.50$; $\mu(Pb, Pb)=0.98$; $\mu(Fe, air)=0.30$; $\mu(Fe, Fe)=0.45$; $\mu(Pb, Fe)=0.72$; $\mu(Fe, Pb)=0.48$; $\beta(Pb)/\beta(Fe)=2.0$. This determination of the absorption coefficients of the primary and secondary radiations allows the following estimates to be made. (a) The lower limit of the average energy of the secondary radiation is about 30 million volts. (b) The average number of secondaries per primary is about 100 in iron and 230 in lead. (c) The energy of a primary cosmic ray, equal to the sum of the energies of its secondaries, is about 2×10^{10} volts.

UNTIL 1929 our only knowledge of the cosmic radiation had been derived from measurements of the ionization in closed vessels at high altitudes and under various thicknesses of absorbing material. Although measurements of this type have yielded values of the absorption coefficient they have revealed little concerning the nature of this radiation or the mechanism by which the ionization is produced. The principal evidence on this point has resulted from experiments with counters and with the Wilson cloud chamber. Skobelzyn[1] first observed the tracks of high energy corpuscular rays which were believed to be associated with the cosmic radiation and Mott-Smith and Locher[2] have identified these tracks with the ionizing rays which produce the coincident discharges of Geiger-Mueller counters. From the coincidence counting rate of these counters several investigators have determined the rate of influx of these rays through our atmosphere and if a reasonable allowance is made for the probability of more than one ray passing through the

[1] Skobelzyn, Zeits. f. Physik **54**, 686 (1929); C. R. **189**, 55 (1929); **194**, 118 (1932).
[2] Mott-Smith and Locher, Phys. Rev. **38**, 1399 (1931).

counters simultaneously[1,3] these results, in conjunction with the number of ion pairs per centimeter of path as determined from the density of droplets in the cloud chamber,[1,3] give a rate of ionization in reasonable agreement with that attributed to the cosmic radiation. These corpuscular rays, however, must be regarded as a secondary effect of the primary radiation, as Skobelzyn,[1] Locher,[3] and Millikan and Anderson[4] have pointed out, for the experiments with the cloud chamber not only show that, in many instances, the rays originate within the material walls of the cloud chamber, but also the energy of these rays is low enough to rule out the possibility of an absorption coefficient comparable with that determined from the electroscope measurements. Moreover, the large number of tracks with positive curvature on Anderson's photographs, show that the secondaries are largely of nuclear origin. As Millikan and Anderson have pointed out, this fact is of the greatest interest because of its invalidation of the use of the Klein-Nishina formula for deriving the energies of the primary rays from absorption measurements even if it can be shown that the primary rays are of the gamma type, for this formula is based upon the assumption of a primary gamma-ray interacting with the extranuclear electrons alone. Although the formula itself must be in error in omitting nuclear absorption there is still the possibility that the underlying ideas are right, i.e., a material substance may be correctly represented as a cloud of free electrons and protons, if the nuclear constituents are included along with the extranuclear electrons. On the other hand the rate of absorption of the primary rays ,as well as the energies of the secondaries, may depend in a characteristic way upon the structure of the nucleus of the absorbing material.

Some recent ionization measurements made by Schindler[5] seem to reveal the first definite information on this subject. In brief, his experiments consisted of a series of measurements of the ionization in a thin-walled vessel placed behind absorbing screens of various materials and of various thicknesses. The curves obtained in the region of an interface between two different media of different nuclear type at once suggest a phenomenon analogous to the readjustment of the equilibrium between a beam of gamma-rays and its secondary beta-rays.[6] In fact, his data may be very simply and accurately interpreted on this basis. To put the matter more exactly the following postulates are required. (1) The rate of production of secondaries in any medium m is proportional to the intensity of the primary radiation, the production coefficient $\beta(m)$ being a characteristic of m. (2) The rate of absorption of the primary rays in m is proportional to their intensity, the absorption coefficient $\nu(m)$ likewise being a characteristic of m. (3) The rate of absorption in a medium m of secondaries produced in a medium n is proportional to their num-

[3] G. L. Locher, Phys. Rev. **39**, 883 (1932).

[4] Millikan and Anderson, Phys. Rev. **40**, 325 (1932).

[5] H. Schindler, Zeits. f. Physik **72**, 625 (1931); see also T. H. Johnson, Phys. Rev. **40**, 468 (1931). B. Rossi has obtained similar results with counters and has made a qualitative interpretation somewhat similar to that presented here, Rend. Lincei, **XV**, 734 (1932).

[6] K. W. F. Kohlrausch, Radioaktivität, page 139 *et seq.*

ber, the absorption coefficient $\mu(m, n)$ being a characteristic of n as well as of m. (4) Ionization is produced by the secondaries alone.[7] In accordance with these assumptions the change in the flux q_n of the secondaries produced in n while passing through the element dx of m is

$$dq_n = -\mu(m, n)q_n dx \tag{1}$$

and the corresponding change in the flux q_m of secondaries produced in m is

$$dq_m = \beta(m)Ne^{-\nu(m)x} - \mu(m, m)q_m dx \tag{2}$$

where N is the number of primary rays per square centimeter per second across the interface between media n and m. Integrals of these equations subject to the conditions at the interface, $x=0$, that $q_m=0$, and $q_n=q_{n_0}$ are

$$q_n = q_{n_0}e^{-\mu(m,n)x} \tag{3}$$

$$q_m = \beta(m)N\left[e^{-\nu(m)x} - e^{-\mu(m,m)x}\right]/\left[\mu(m, m) - \nu(m)\right]. \tag{4}$$

If I is the average number of ions per centimeter of path produced by a secondary ray in the ionization chamber, the rate of production of ions per cc in the case of the one dimensional problem considered here, is

$$J = (q_n + q_m)I. \tag{5}$$

In Schindler's experiments only the ions produced by the rays included in a cone of half angle 30° about the vertical were measured and hence the one dimensional case may be considered a fairly good approximation. In fact Eq. (5) represents the experimental data quite accurately if a suitable determination of the constants is made.

In the case of the transitions from air to lead and air to iron, respectively the first step in fitting Eq. (5) to the experimental data was the determination of $\nu(m)$. For this determination the last two points, corresponding to the greatest thicknesses of the absorbing material, were used and it was assumed that both of the μ's were large enough to make all but the term containing $e^{-\nu(m)x}$ completely negligible at these thicknesses. The fact that μ's satisfying this condition could then be determined to bring about good agreement between (5) and the data, justified this procedure although it would have been more satisfactory if more extensive data were available at the tail of the curve. These last two points also determine the multiplier $\beta(m)N/[\mu(m, m) - \nu(m)]$, and q_{n_0} is determined from the ionization with no absorbing screen ($x=0$). It remains therefore to determine two exponentials with known multiplying coefficients, the difference between which agrees with the residual of the data after the term in $e^{-\nu(m)x}$ has been subtracted. The choice of $\mu(m, n)$ and $\mu(m, m)$ is therefore very definite and a variation in one of these of the order of ten percent, from the values stated, though the other be adjusted accordingly for the best fit, is sufficient to throw the equation into serious disagreement with the data.

[7] Without seriously altering the results it is possible to assume that the primaries produce ions *per se*, but as this assumption is not required for an explanation of Schindler's results, for simplicity it is not included.

The agreement between the observed and calculated values of the ionization in the case of the air to lead, and air to iron transitions is shown in Tables I and II, the constants having the following values: $q_0(\text{air})I=0.461$ ion pairs per cc per sec.; $\beta(\text{Pb})NI/[\mu(\text{Pb, Pb})-\nu(\text{Pb})]=0.298$ ion pairs per cc per sec.; $\beta(\text{Fe})NI/[\mu(\text{Fe, Fe})-\nu(\text{Fe})]=0.0322$ ion pairs per cc per sec.; $\nu(\text{Pb})=0.0014$ cm²/g electron $=0.0064$ cm^{-1} Pb; $\nu(\text{Fe})=0.002$ cm²/g electron $=0.009$ cm^{-1} Pb; $\mu(\text{Pb, air})=0.11$ cm²/g electron $=0.50$ cm^{-1} Pb; $\mu(\text{Fe, air})=0.066$ cm²/g electron $=0.30$ cm^{-1} Pb; $\mu(\text{Pb, Pb})=0.218$ cm²/g electron $=0.98$ cm^{-1} Pb; $\mu(\text{Fe, Fe})=0.099$ cm²/g electron $=0.45$ cm^{-1} Pb.

The absorption coefficients are expressed both in terms of the units used by Schindler in which unity corresponds to $6.06\cdot 10^{23}$ extranuclear electrons per sq. cm (this unit may be conveniently named a gram electron per cm²) and in cm^{-1} lead equivalent. The multiplying constants as determined from the data have been reduced to the number of ions which would be produced under normal atmospheric conditions in one cubic centimeter by the radiation included within the 30° cone of Schindler's experiments.

TABLE I. *Air to lead transition.*

x $\left(\frac{\text{g electrons}}{\text{cm}^2}\right)$	Observed	Calculated	Ratio observed to calculated
0	0.461	0.461	1.000
2.3	.468	.471	0.995
4.1	.465	.468	0.993
9.0	.427	.424	1.005
13.1	.384	.384	1.000
18.0	.349	.349	1.000
27.0	.313	.310	1.010
45.0	.287	.284	1.010
90.0	.262	.262	1.000
135.0	.246	.246	1.000

TABLE II. *Air to iron transition.*

x $\left(\frac{\text{g electrons}}{\text{cm}^2}\right)$	Observed	Calculated	Ratio observed to calculated
0	0.461	0.461	1.000
3.5	.464	.462	1.005
7.0	.454	.453	1.001
14	.421	.422	0.998
21	.392	.392	1.000
35	.354	.345	1.000
70	.295	.302	0.976
105	.269	.269	1.000

In addition to these principal transitions Schindler also gives data for secondary transitions from lead to iron and from iron to lead, in each case starting from various thicknesses of the former substance. In calculating these transitions all but two of the necessary constants have already been determined from the data of the principal transitions, the remaining unknown constants being the absorption coefficients in the second medium of secondaries produced in the first, i.e., $\mu(\text{Fe, Pb})$ and $\mu(\text{Pb, Fe})$.

In calculating the ionization after a variable thickness x of the second substance m and a fixed thickness x_0 of the first substance n it is necessary to take account of the remaining air secondaries which have penetrated n, as well as the corresponding change in the intensity of the primary rays. The equation for the ionization as a function of x in m is therefore

$$\begin{aligned} J = {} & q_0\,(\text{air})\,I \exp\left[-\mu(n,\text{air})x_0+\mu(m,\text{air})x\right] \\ & +\beta(n)NI\left[e^{-\nu(n)x_0}-e^{-\mu(n,n)x_0}\right]e^{\mu(m,n)x}/\left[\mu(n,n)-\nu(n)\right] \\ & +\beta(m)NI\,e^{-\nu(n)x_0}\left[e^{-\nu(m)x}-e^{-\mu(m,m)x}\right]/\left[\mu(m,m)-\nu(m)\right] \end{aligned} \tag{6}$$

in which $\mu(m, n)$ is the only constant remaining to be determined from the secondary transition data. After subtracting all of the terms except that containing $\mu(m, n)$ from the experimental data of the first secondary transition the residuals were very close to pure exponentials with the absorption coefficients $\mu(\text{Pb, Fe}) = 0.159$ cm^2/g electron $= 0.751$ cm^{-1} Pb and $\mu(\text{Fe, Pb}) = 0.107$ cm^2/g electron $= 0.48$ cm^{-1} Pb. The constants thus determined could then be used in calculating the remaining secondary transitions, and the agreement in each case with the experimental data served as an additional check on the values of the constants. The results are shown in Tables III and IV.

TABLE III. *Iron to lead transitions.*

Thickness of iron g electron/cm^2	Thickness of lead g electron/cm^2	Observed	Calculated	Ratio observed to calculated
38	0	0.347	0.347	1.000
	2.3	0.349	0.351	0.995
	4.1	0.345	0.346	0.997
	18	0.295	0.382	1.048
	45	0.267	0.259	1.030
77	0	0.292	0.292	1.000
	3.2	0.286	0.304	0.940
	13.5	0.261	0.272	0.960

TABLE IV. *Lead to iron transitions.*

Thickness of lead	Thickness of iron	Observed	Calculated	Ratio observed to calculated
18	0	0.349	0.349	1.000
	3.5	.347	.341	1.018
	7.0	.336	.332	1.012
	14	.318	.321	0.991
	28	.306	.310	0.987
	42	.299	.296	1.010
	105	.265	.262	1.012
52	0	.281	.281	1.000
	14	.286	.286	1.000
	35	.279	.284	0.982
	70	.263	.268	0.980
126	0	.250	.250	1.000
	7	.254	.253	1.004
	14	.249	.258	0.965
	35	.245	.257	0.953

Schindler also gives some measurements of the absorption in aluminum and a few other substances but none of these sets of data are sufficiently extensive to make a determination of the constants with a reliability comparable with that of the foregoing data.

Table V contains the absorption coefficients $\mu(m, n)$ of the secondaries produced in medium n and absorbed in medium m and the media are arranged in the order of their atomic weights. This arrangement suggests the following laws: I. Secondaries produced by the cosmic rays in substances of lower

atomic weight are the more penetrating. II. The absorption coefficients per gram electron of the secondary cosmic rays are greater in substances of greater atomic weight. To these laws may be added two others which are suggested by the values of the other constants. III. The absorption coefficients per gram electron of the primary radiation are greater in substances of lower atomic weight. IV. The production coefficients per gram electron of the secondary radiation are greater in substances of greater atomic weight.

TABLE V. *The absorption coefficient per gram electron in medium m for secondaries produced in medium n.*

m \ n	air	iron	lead
iron	0.066	0.099	0.107
lead	0.11	0.159	0.218

The multiplying constants of Eq. (5) have the following significance. $q_{n_0}I$ is the number of ion pairs formed per cc per sec. by secondaries in equilibrium in medium n with the primaries of ground level intensity which are included within the 30° cone, and $\beta(m)NI/[\mu(m, m)-\nu(m)]$ is the corresponding number of ion pairs in equilibrium with primaries of the same intensity in medium m. If we define $j^m(\theta)$[8] by the equation

$$\beta(m)NI/[\mu(m, m) - \nu(m)] = 2\pi \int_0^{30°} j^m(\theta) \sin\theta d\theta \qquad (7)$$

and use the distribution function found by Medicus[9] for the secondary rays i.e.,

$$j^m(\theta) = j^m(0)(1 + 4\cos^2\theta)/5$$

then

$$j^m(0) = 1.4\beta(m)NI/[\mu(m, m) - \nu(m)].$$

The values for $j^m(0)$ are as follows

$$j^{\text{air}}(0) = 0.64 \text{ ion pairs per sec. per cc}$$
$$j^{\text{Fe}}(0) = 0.46 \text{ " " " " " "}$$
$$j^{\text{Pb}}(0) = 0.41 \text{ " " " " " "}.$$

THE ENERGIES OF THE SECONDARIES

Although it is impossible to make any strict correlation between the absorption coefficient of the secondary radiation and the energies of the corpuscular rays one may speculate as to the order of magnitude of one of these

[8] $J^m(\theta)$ is the number of ion pairs produced per cc per sec. at atmospheric pressure by secondaries in equilibrium with primaries of ground level intensity in medium m and reduced to unit solid angle in the direction θ with the vertical.

[9] G. Medicus, Zeits. f. Physik **74**, 350 (1932).

quantities from a knowledge of the other. For example, one may postulate that the average range is equal to the reciprocal of the absorption coefficient and that ions requiring about fifty volts per pair are formed at a rate indicated by the density of droplets in the expansion chamber, i.e., about thirty-six pairs per cm in atmospheric air.[1,3] This correlation neglects the possibility of large angle scattering of the secondary rays by nuclear collisions and it assumes that the secondaries are confined to a single direction. Hence the energies calculated in this way must be regarded as a lower limit, although perhaps not far from the right order of magnitude. Making this correlation on the basis of the absorption coefficient in lead, it is found that the air secondaries have an average energy of 30 million electron volts, that is, about one third of the most probable of the energies measured by Anderson. This agreement is perhaps as good as would have been expected from the crudity of the assumptions.

The Density of the Secondaries

The large values of the absorption coefficients of the corpuscular rays derived from Schindler's data at once given an explanation for the fact discovered by Bothe and Kolhorster[10] and by Rossi[11] that the interposition of absorbing material between two counters diminishes the coincidence counting rate in approximate agreement with the absorption coefficient of the primary radiation. An explanation first suggested by Bothe and Kolhorster[10] but rejected by them at that time as being unlikely, is that a single primary ray produces a large number of secondary rays distributed along its path so that coincident discharges of two counters separated by more than a few centimeters of lead, are caused, not by the same secondary, but by different secondaries initiated by the same primary ray. Without the absorbing material a single secondary ray having the proper direction will pass through both counters and, therefore, under this condition the counting rate is a measure of the intensity of the primary radiation N multiplied by the probability P of a primary ray being accompanied by one or more secondaries at any point along its path. With the absorbing material the counting rate is a measure of the number $Ne^{-\nu x}$ of primary rays which penetrate the material multiplied by P^2.

The ratio of counting rates with and without absorbing material is therefore, $Pe^{-\nu x}$. Since this ratio is found, in the experiments cited, to be of the order of $e^{-\nu x}$ it follows that P is of the order of unity. In other words, a primary ray is almost always accompanied by at least one of its secondaries and the coincidence counting rate is approximately a measure of the intensity of the primary radiation.

The average number of secondaries in equilibrium with one primary ray may be estimated from a comparison of the coincidence counting rate of two counters and the rate of production of ions in a closed vessel. The approximate flux of the primary radiation $N_\perp$ taking the results of the counter experi-

[10] Bothe and Kolhorster, Zeits. f. Physik **56**, 751 (1929).
[11] B. Rossi, Zeits. f. Physik **68**, 64 (1931).

ments of Street and Johnson,[12] is 0.0073 per sq. cm per sec. in unit solid angle in the vertical direction. The flux $q_\perp$ of secondaries, on the other hand, may be estimated from the ionization data of Schindler. From the relation $j^m(0) = Iq_\perp$, using the value $I=36$ obtained from the density of droplets in the cloud chamber, we have $q_\perp^{\text{air}}=0.018$; $q_\perp^{\text{Fe}}=0.013$; $q_\perp^{\text{Pb}}=0.011$. Comparing these values with the value 0.0073 for $N_\perp$ we have[13] $q_\perp^{\text{air}}/N_\perp=2.5$; $q_\perp^{\text{Fe}}/N_\perp=1.8$; $q_\perp^{\text{Pb}}/N_\perp=1.5$.

The Average Energy of the Primary Rays

It is now possible to estimate the energy of a primary ray as the sum of the energies of the secondaries produced by a single primary. Since the secondaries are produced largely from the atomic nuclei there is the *a priori* possibility that much of the secondary energy is energy of nuclear disintegration. This possibility must be rejected however because of the extremely high energies found by Anderson and because of the angular distribution of the secondaries. The conclusion is that the energy of the secondary is acquired at the expense of the primary ray. The total number of secondaries produced by a single primary of ground level energy is then approximately equal to $\mu(m, m) q_\perp^m/\nu(m)N_\perp$ which has the values: in lead, $0.218\times1.5/0.0014=233$; in iron, $0.099\times1.8/0.002=90$. With the value for iron, this being similar to the material of the cloud chamber and the average energy of a secondary ray as found by Anderson, i.e., 2.5×10^8 electron volts, the average energy of a primary ray, equal to the sum of the energies of its secondaries, is 2.2×10^{10} electron volts. Since these rays have already passed through the atmosphere and have dissipated energy by a continuous production of secondaries along their path, it is necessary to suppose the energies of these primary rays are originally greater than this figure by about a factor of two.

In conclusion it is a pleasure to acknowledge conversations with Dr. J. C. Street during which many of the ideas presented here were developed.

[12] Street and Johnson, Phys. Rev. **40**, 1048A (1932).

[13] These low values for the average number of secondaries per primary seem inconsistent with the conclusion that a primary is almost always accompanied by at least one secondary and it may be necessary to assume that the primary ray is itself an ionizing corpuscular ray. This assumption would not materially alter the interpretation of Schindler's data other than to allow a considerably greater latitude in the choice of absorption coefficients.

Design of a Double-Crystal X-Ray Vacuum Spectrometer

By LYMAN G. PARRATT
Ryerson Physical Laboratory, University of Chicago

(Received June 27, 1932)

A vacuum double-crystal x-ray ionization spectrometer has been constructed and the design of the instrument is explained in some detail. A tank, of inside diameter 50 cm, formed from sheets of rolled steel and welded together, rests on a thick steel bed-plate, the contact areas, generously wide, sealed with stop-cock grease, and the chamber evacuated with a megavac oil pump. This chamber is used as the fore-vacuum for the Hg condensation pump working on a metal x-ray tube. The slits, the first and second crystals, and the ionization chamber are contained within the tank. The axes of the two crystals are rigidly fixed with respect to each other, and, to allow change of wave-length, the x-ray tube, clamped to the side of the tank, is swung around, the tank sliding on the stop-cock grease, until the proper position is reached. Final alignment of the focal spot with the slits is effected while the tube is in operation by an adjustable target made possible by a sylphon connection in the tube. A method is explained for obtaining thermal contact with uranium for use as the target. The angular controls of the crystal *B* and the ionization chamber are made by having long, concentric, tapered bearings extend through the bed-plate of the instrument, lubricated and held air tight with stop-cock grease, and their positons read to within one minute of arc with verniers on a fixed circle. Fine motion of crystal *B* is accomplished by the usual lever arm and tangent micrometer screw. The insulated lead from a relatively small ionization chamber, 6.7 cubic inches in volume, which is constructed to function as a two-atmosphere pressure chamber, is brought out of the tank through the hollow center of the central steel shaft forming the axis of crystal *B*.

INTRODUCTION

THE development of double-crystal x-ray spectrometry[1] has provided the researcher with an invaluable tool in making more precise measurements of x-ray diffraction. The many and wide-spread applications of the two-crystal instrument in investigations of contemporary importance have been considered sufficient justification for the design and construction of a double-crystal ionization spectrometer for operation in a vacuum, which would allow this branch of study to be extended to include the soft x-rays of wave-lengths greater than two angstroms.

TYPE OF INSTRUMENT

The double-crystal spectrometer, whose assembly details are described in

[1] The double-crystal spectrometer was first used by A. H. Compton, Phys. Rev. **10**, 95 (1917). Bergen Davis and his collaborators at Columbia developed the instrument for use in the parallel positions, Phys. Rev. **17**, 608 (1921); **27**, 18 (1926); **32**, 331 (1928); and the high resolving power of the anti-parallel positions was first exploited simultaneously and independently by Davis and Purks, Proc. Nat. Acad. Sci. **13**, 419 (1927), and by Ehrenberg, Mark, and Susich, Zeits. f. Physik **42**, 807, 823 (1927). The theoretical possibilities of the two-crystal method were very thoroughly explored by M. M. Schwarzschild, Phys. Rev. **32**, 162 (1928), and the experimental side has been investigated by S. K. Allison, Phys. Rev. **34**, 176 (1929), **35**, 1476 (1930), and by others.

this article, is essentially of the usual design[2] permitting the $(n_A, \pm n_B)$, or all combinations of the parallel and antiparallel, positions, with each of the two crystals capable of rotation about a vertical axis lying in its reflecting face. The collimating slits, the two crystals, and the ionization chamber are supported on a circular steel bed-plate, and a metal cylindrical cap which can be lowered to the plate encloses them in an air-tight compartment. When this chamber is exhausted, soft x-rays, which would be absorbed in air at atmospheric pressure, can be studied. The instrument is designed to accommodate glancing angles from 0° to 57°, which, with calcite crystals, correspond to a wave-length region of 0 to 5 angstroms.

Principle of Operation

A diagrammatic sketch of the spectrometer is shown in Fig. 1. The axes of the crystals are fixed with respect to each other, the first, axis A, mounted at the center of the large bed-plate, and the second, axis B, mounted 12 cm from A. The slits rotate about axis A and the ionization chamber about B. The x-ray tube is rigidly clamped to the side of the cylindrical tank (Fig. 2) which is lowered by a large screw to its position on the bed-plate.

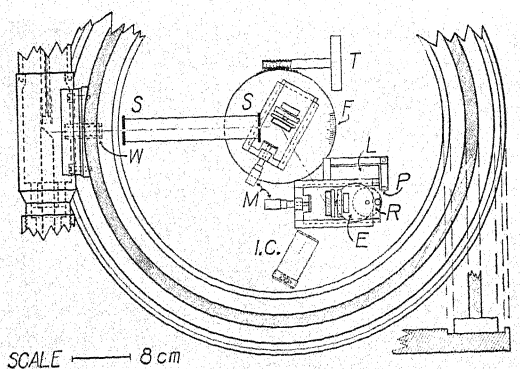


Fig. 1. Diagrammatic representation of the double-crystal spectrometer showing to scale the relative spacings of the x-ray tube, slits, first and second crystals, and the ionization chamber.

Before lowering the tank, crystal A is set for the proper glancing angle by means of the worm screw T as a vernier adjustment to 15 seconds of arc on the scale F. The proper position is determined by the condition that the reflected ray must pass directly through the axis of crystal B. The slits SS must then be placed in position as read on the same scale F and the tank lowered to the bed-plate and turned until the window W, between the tube

[2] A double-crystal spectrometer of usual design refers to one which is based upon two single-crystal spectrometers placed in proper alignment. Such an instrument can be placed alternately in the $(n_A, +n_B)$ and $(n_A, -n_B)$ positions by rotating the second crystal, B, and the ionization chamber. For descriptions of two different examples of this type of instrument see A. H. Compton, Rev. Sci. Inst. **2**, 365 (1931) and S. K. Allison, Phys. Rev. **41**, 1 (1932). Instruments of special design have been constructed by Du Mond and Hoyt, Phys. Rev. **36**, 1702 (1930), and by Spencer, Phys. Rev. **38**, 618 (1931), having certain positive advantages in treating particular problems, but which are limited in operation to the $(n, +n)$ positions.

and tank, is in line with the slits. This position has been previously allocated on a scale on the edge of the bed-plate and is now read by an indicator fastened to the tank. The tank is evacuated with a megavac oil pump and is used as the fore-vacuum for a mercury condensation pump working on the x-ray tube. This Hg pump is mounted on the top of the tank and thus is part of a rigid system.

The final adjustment of the focal spot-slits alignment is effected by a sylphon connection in the x-ray tube itself which allows independent motion of the target with respect to the tube and tank. The special features of this tube are perhaps worthy of discussion and will be briefly treated later in this paper.

The Tank

The tank itself is constructed of rolled steel $\frac{5}{8}$ of an inch thick. The curved section is shaped from a sheet bent into a cylindrical form, 50 cm inside diameter, and the ends carefully welded. The top piece is another sheet of the same material welded on to the cylinder, and a wide flange, shown in Fig. 1, furnishing large contact area with the bed-plate is similarly welded in place and turned in the lathe for a smooth surface. In the welding process

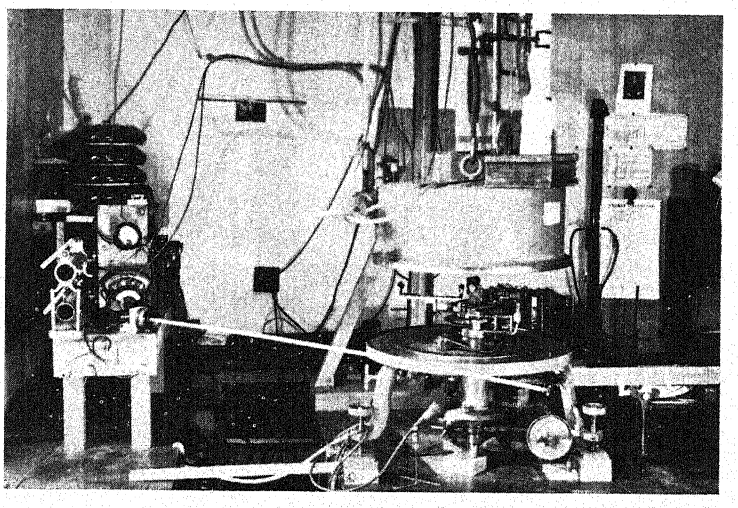


Fig. 2. Photograph of the assembly with the tank in an elevated position. On the left is seen the insulated battery stand. The electrometer is located beneath the far side of the bed-plate.

caution was taken to work the material well and to use an excess of rod to eliminate possible pin holes. The bed-plate is made of thicker steel than the tank to avoid undue warping. It was desired that the axes of the two crystals remain parallel to within one minute of arc, and calculation from structural formulae shows this condition is fulfilled by a bed-plate one inch thick. It is actually made $1\frac{5}{16}$ inches thick. An air-tight seal between the flange of the tank and the plate is made with stop-cock grease. These contact areas are of a generous width to allow a good seal and to supply additional strength.

A preliminary test for leaks was made in the following way: The tank was clamped to the bed-plate and the outside covered with soap solution. Air pressure of about 30 cm of Hg above atmospheric was maintained inside the tank and a search made for swelling soap bubbles. One small bubble was found. After a generous painting with Duco brush lacquer no bubbles were formed. The tank now holds a vacuum of less than 6 cm of Hg for about one week.

Axis of Crystal B

Following in general the design of Siegbahn's vacuum spectrograph,[3] long, concentric, tapered bearings, lubricated and held air tight by stop-cock grease are extended through the bed-plate *BP* as shown in Fig. 3. The crystal table *C* is rigidly clamped to the inner steel shaft *S*, and the support for the ioniza-

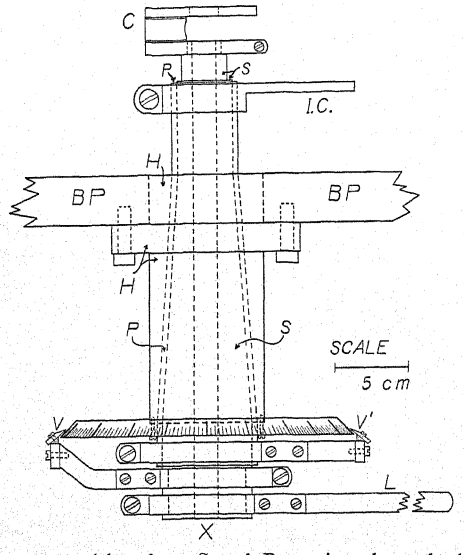


Fig. 3. Showing the tapered bearings *S* and *P* passing through the bed-plate *BP* and by means of which outside control of the second crystal and the ionization chamber is effected. Drawn to scale.

tion chamber, *IC*, is fastened to a conical shell *P* of phosphor-bronze, which in turn bears on the steel housing, *H*, screwed to the bed-plate. On the lower ends of these bearings *S* and *P* are clamped arms carrying verniers *V* and *V'*, respectively, which read the angular positions of crystal *B* and the ionization chamber to one minute of arc on the graduated circle attached to the housing *H*. Crystal *B* must be set, of course, with an accuracy much greater than one minute of arc, but this serves as a first rough adjustment. After this setting is made, fine motion of the crystal is effected by a micrometer screw, bearing, at a distance of 20.63 cm from the *B* axis, on the lever arm *L* which is clamped to the inner steel shaft *S*. Fixed to the micrometer head is a large five-inch drum with 500 graduations, so that each division on the drum corresponds to an angular motion of the crystal of one second of arc, the pitch of the micrometer screw being one-half millimeter.

[3] Siegbahn, *Spektroskopie der Roentgenstrahlen*, Second Edition, page 114, 1931.

Atmospheric pressure is sufficient to keep the bearings tight and Lubriseal between them allows fairly free motion. However if the elements have not been turned for several days the Lubriseal becomes stiff and the motion is sluggish, and a work-out is required to loosen things up. To be sure that the motion as read on the drum is accurately transmitted to the crystal, and that possible slight variations in the thickness of the stop-cock grease during an operation would not be serious, a preliminary run with Cu K_α radiation was made and the observed separation of α_1 and α_2 checked with that calculated from Siegbahn's tables of wave-lengths. The observed values were consistent among themselves and also with the calculated values to within two seconds of arc. The rocking curves obtained in the $(n,+n)$ and $(n,-n)$ positions by rotating crystal B were also consistently regular and smooth.

The center of the steel shaft S is drilled out, as indicated in Fig. 3, and through this space passes the insulated lead from the ionization chamber to

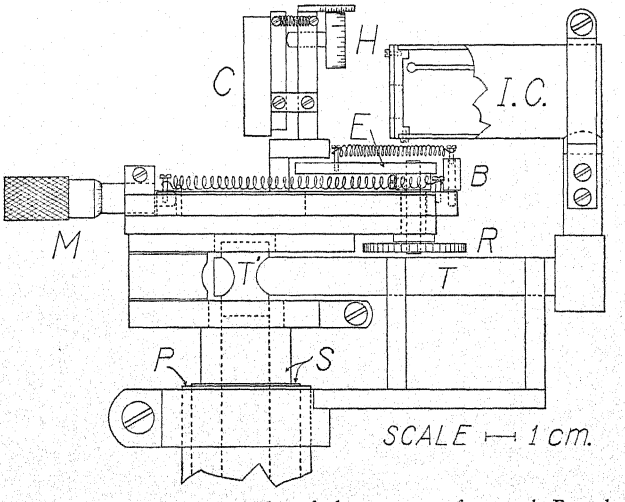


Fig. 4. Showing details, drawn to scale, of the mount of crystal B and the ionization chamber. The method of moving the crystal in and out of the x-ray beam is indicated, but the electromagnet is omitted for the sake of clarity.

the electrometer which is, of course, placed outside the tank. The air-tight seal is made at the bottom of the shaft at X where a flanged amber plug is waxed into place. The lead is unavoidably long and in consequence the capacity of the electrical system is relatively large, being 80 cm. The electrometer is of the Compton type and operates at a voltage sensitivity of 4000 mm (scale divisions) per volt per meter distance between mirror and scale.

Mounting of Crystal B

Both crystals are mounted on carefully made slides. The mount for crystal B, together with the ionization chamber, is shown in Fig. 4. The usual adjustments in aligning the crystal, labelled C, are made by the short micrometer M and the screw H. Constant pressure on the ends of these screws is maintained by springs. In many problems it is desirable to measure the in-

tensity of the x-ray beam reflected from crystal A only, and this requires that the second crystal be removed temporarily from its usual position so that it will not intercept the beam. To accomplish this purpose an electromagnet, L in Fig. 1, is clamped on the side of the crystal mount. This electromagnet, controlled by a tapping key outside the tank, activates a cog wheel R (Figs. 1 and 4) by means of a pall and ratchet arrangement (P Fig. 1). An eccentric wheel E (Figs. 1 and 4) is fastened to the axle of the cog wheel, and, as it rotates, one cog for each tap of the key, the eccentric presses against a roller bearing B (in Fig. 4) which causes the slide, carrying the crystal, to move back a maximum distance of some one and one-quarter inches, which is sufficient, for all glancing angles up to 57°, to allow the x-ray beam to pass. As the key is further tapped the eccentric moves around to its previous rest position, and the springs draw the slide after it until the motion of the slide is arrested by the micrometer screw, and the crystal is again in its usual rest position. This action is found to work very satisfactorily when a compensating spring of proper tension is attached between the eccentric and the bearing B, as in Fig. 4.

The method of alignment of the crystals and slits which was employed on this instrument has already been described by Allison[4] and by Tu.[5]

Ionization Chamber

The ionization chamber is constructed from a solid cylinder of copper $1\frac{1}{4}$ inches in diameter and $2\frac{3}{4}$ inches in length, drilled from one end to a depth of $2\frac{3}{16}$ inches, leaving the other end intact except for the introduction of the insulated electrode. The inside volume is relatively small, 6.7 cubic inches, but sufficient for the satisfactory absorption of the soft x-rays for which it is intended. The chamber is filled with one atmosphere of argon.

Because of the atmospheric pressure inside, and zero pressure outside, the chamber must actually function as a pressure chamber. A tapered amber insulator, in its grounded guard shield and Bakelite case, is carefully waxed leak-tight with a mixture of beeswax and resin and the unit firmly bound in place by two metal straps which pass over the top of the chamber (see Figs. 1 and 4). These straps are insulated from the chamber by strips of fiber since the voltage (about 70 volts) is placed on the chamber and the collecting electrode operates at earth potential, plus or minus the minute effects of the charges accumulated from the ionized gas.

The window on the ionization chamber is 3 mm by 10 mm and is cut from a piece of wrapping cellophane obtained from cigarette packages. This is the same type of window as used between the x-ray tube and tank.

The extended guard shield to which the straps are fastened, serves to support the ionization chamber as shown in Fig. 4. The chamber and the shield tube T must turn through an angle of 4 times 57° in the case of the maximum glancing angle in order to take care of both parallel and antiparallel positions. To allow this motion the table top supporting the crystal slide

[4] Allison, Phys. Rev. **41**, 1 (1932).
[5] Tu, Phys. Rev. **40**, 662 (1932).

must be hollowed out considerably. As the IC is turned the short tube T' slides inside the top of the steel shaft S supporting the crystal.

X-RAY TUBE

In constructing an adjustable target in the x-ray tube many technical difficulties in the alignment of the spectrometer were solved. Fig. 5 presents a cross-sectional view of this tube. The shell is turned from a three-inch cylinder of brass with a bearing left at B to guide and allow the target T but one degree of freedom. The sylphon S (flexible copper tubing) is soldered to this shell and also to the conical support of the target at the right end of the tube. Lubriseal makes the conical joint air tight and also allows the target to be easily removed for frequent cleaning, which is found necessary when working with soft radiation. Atmospheric pressure serves to keep a tension on the ball-bearings R, and, by screwing the cylindrical shell H in or out, the flexible sylphon contracts or expands and the target T slides on bearing B until the center of the focal spot is in line with the slits. Since the target is at earth potential this adjustment can be made while the tube is in operation.

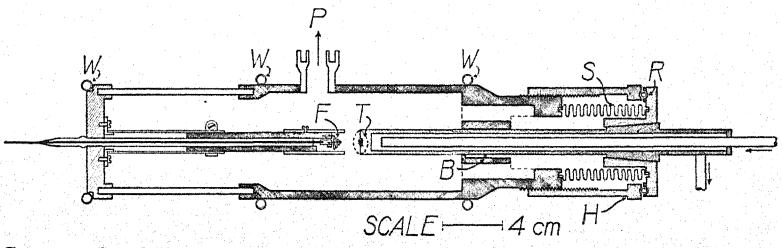


Fig. 5. Cross-sectional diagram of the x-ray tube showing the adjustable target. Drawn to scale.

Due to the drag in the ball-bearings when H is turned, a torque is transmitted to the target and an undesirable stress applied to the sylphon tube. This is eliminated by having a pin attached to the target carriage sliding in a slot in the bearing B. The pin and slot are shown in the diagram.

The filament F is easily wound by hand and is extremely simple to insert after loosening the screw and sliding back the focusing cup. The heavy nickel lead is introduced in a glass tube for mechanical support and electrical insulation and is spot-welded to tungsten to which a glass seal is made at the high-potential end of the tube. In order to keep the wax seals between the glass and metal from softening, water is circulated through the copper coils W soldered on the tube as indicated in the diagram.

The window W (see Fig. 1) to be placed between the tube and tank must be chosen to have a low absorption for wave-lengths up to 5 angstroms. The pressure differential on the two sides of the window is quite small, about 10^{-3} mm of Hg, and the mechanical strength of the window is of little importance unless it be desired to maintain a vacuum in the tube while the tank is raised for, say, a change of wave-length. Wrapping cellophane of thickness of one thousandth of an inch, similar to the window of the ionization chamber, is found to be satisfactory if the area is not too large. A window of 4 mm by 10 mm is near the limit for withholding atmospheric pressure. Such a window

ruptures frequently (about 3 hours) during operation if the tube is more than one-half kilowatt of power. This is somewhat overcome by inserting an extremely thin aluminum foil to act as an electrical conductor adjacent to and on the tube side of the window. With the tube operating at one-fifth kilowatt or less the window lasts indefinitely. However, in any case, the reduction in intensity due to absorption by the deposit of tungsten sputtered upon it may necessitate a replacement before rupture occurs.

The volume of the tube is made rather large so that the relative effect of the sudden release of gas from a gas pocket during operation would be reduced.

In a study of the reflecting powers of calcite from 2 to 5 angstroms which the author has just completed, the M series of uranium was used, and a special process of obtaining thermal contact between the uranium and the water-cooled copper part of the target was developed. The piece of uranium, whose lower surface has been freshly cleaned, is placed on a flat coil filament of 12 mil tungsten wire mounted under a bell-jar, into which are introduced two water-cooled electrodes, and the bell-jar evacuated to a pressure of approximately 10^{-4} mm of Hg. Current is passed through the filament after the desired pressure has been reached and the uranium heated. The process must be carried out in a vacuum to prevent oxidation of the uranium. Since the melting point of uranium is below that of tungsten, with a gradual increase in current, the uranium will melt at the points of contact with the filament and flow around the tungsten wire. With practice filaments can be wound so that, when heated, and the sag has taken place, they offer quite a large surface for fusion with the uranium. Repetition of the process gives a good base of tungsten on the piece of uranium to which one can either silver-solder or spot-weld without further difficulty.

Electrical Controls

The current for the filament of the x-ray tube is supplied by a series of three 6-volt A batteries, each of 150 ampere-hours capacity. A sliding contact resistance of 6 ohms is used to adjust the current through the filament, and the voltage across the tube is maintained constant during operation by a vernier control of the filament current. This vernier is another variable contact resistance of 150 ohms placed in parallel with the first, and manipulated by turning the long wooden rod extending to the observers seat from the high potential battery stand, seen at the left in the photograph, Fig. 2.

The equipment for generating the high voltage has been described by Allison and Andrew.[6] When working with low voltages, 0 to 15 k.v., a good microammeter in series with an accurately calibrated high resistance is used instead of the large electrostatic voltmeter described by them. Voltages could be read on the microammeter with an error of less than 30 volts.

The author expresses with pleasure his indebtedness to Professor S. K. Allison who proposed the construction of this spectrometer and who suggested many of the main features incorporated in its design.

[6] Allison and Andrew, Phys. Rev. **38**, 441 (1931).

X-Ray Diffraction from Calcite for Wave-Lengths 1.5 to 5 Angstroms

By LYMAN G. PARRATT
Ryerson Physical Laboratory, University of Chicago

(Received July 13, 1932)

Theoretical expressions for the coefficient of reflection, percent reflection, and width of the line to be expected from the second crystal of a double spectrometer in the (1, −1) position, based on Darwin's theory of reflection from a perfect crystal, as modified by Prins, are evaluated for calcite for six lines in the region 1.54 to 5A. This region includes, at 3.06A, the critical absorption limit of calcium. With a specially designed double-crystal spectrometer, these properties of the rocking curve from the second crystal for ten wave-lengths, copper $K\alpha$ radiation and nine spectrum lines selected from the uranium M series, are experimentally measured and these results compared with the calculated values. The agreement between the observed and calculated rocking curve widths is excellent throughout the entire region and gives no evidence of mosaic structure in the crystals. The calculated values of percent reflection are consistently above those observed by some 16 percent. Good agreement is obtained for the values of the coefficient of reflection for wave-lengths shorter than 4A including those close to and on either side of the calcium absorption limit. No correction for temperature motion of the atoms has been attempted, but it seems possible that such a correction would give very satisfactory agreement between theory and experiment, showing that calcite surfaces may be obtained for which there is no evidence of mosaic structure from the diffraction of x-rays.

INTRODUCTION

IMMEDIATELY following Bragg's interpretation of the Laue spots in 1912, Darwin attacked the problem of accounting theoretically for the intensity distribution in the diffraction pattern. The original theory developed by Darwin[1,2] is based essentially on the classical treatment of x-rays as a branch of optics and on the assumption of a perfect crystal,[3] and, while the theory is now considered a classic in x-ray reflection, the conclusions and predictions derived, with the exception of the refractive index, did not conform with experiment. Because of the great importance of this problem its solution was pursued by many investigators, mostly from the experimental approach, but the discrepancy between theory and experiment, though considerably decreased with the accumulation of more reliable data, has continued to exist. Darwin explained this discrepancy with the concept of mosaic structure present in real crystals. In 1926, the status of the problem was expressed by Professor A. H. Compton as ". . . there thus seems little hope of being able to apply the theory for a perfect crystal strictly to any real crystal."[4]

[1] Darwin, Phil. Mag. **27**, 325 and 675 (1914).
[2] Ewald, Phys. Zeits. **26**, 29 (1925).
[3] A perfect crystal is defined as one having no grating distortion, no temperature motion of the atoms, of infinite dimensions, and with the reflecting surface defining a grating plane.
[4] A. H. Compton, *X-Rays and Electrons*, D. Van Nostrand Co., page 143, 1926.

In 1930 Prins[5] offered a modification of Darwin's classical electromagnetic treatment by introducing the effects of absorption of the x-rays in the crystal, and, as has been recently pointed out by Allison,[6] the necessity of the concept of mosaic structure, at least in certain specimens of calcite crystals, is no longer acute. It is the purpose of this paper to show what agreement between the modified theory and experiment has been reached for calcite in the wavelength region of 1.5 to 5 angstroms, including at 3.06A, the critical absorption limit of calcium.

Theoretical Discussion

To facilitate an understanding of the essentials of this problem, a brief resume of Darwin's treatment is given.

Monochromatic radiation, in the form of plane waves, making a glancing angle near the Bragg angle on a perfect, non-absorbing crystal, is partially reflected and partially transmitted. The intensity of the transmitted component, in passing through the crystal, is diminished by partial reflection at every internal grating plane it encounters; and also, the inverse process is present, defeating the endeavors of the internally reflected components to emerge from the surface and contribute to the intensity of the beam reflected from the crystal as a whole. This interplay between the transmitted and reflected beams was expressed by Darwin through two simultaneous difference equations in terms of the amplitudes T_r and S_r of the transmitted and reflected rays, and the number of grating planes r, measured from the surface, involved in the process. The solution of the equations expresses directly the ratio of these amplitudes for $r=0$, at the surface of the crystal, in a complex quantity since the phase difference of the scattered rays occurs intimately throughout the analysis. The ratio of the intensities of the beams incident on and reflected from the crystal, taken as the square of the modulus of the complex expression, is given in the Darwin equation, with slight change in notation,

$$\frac{I_{\Delta\theta}}{I_0} = \left[\frac{S_0}{T_0}\right]^2 = \left[\frac{a}{\sin\theta_0\cos\theta_0\Delta\theta - \delta \pm [(\sin\theta_0\cos\theta_0\Delta\theta - \delta)^2 - a^2]^{1/2}}\right]^2 \qquad (1)$$

in which the variable, $\Delta\theta$, is the deviation of the glancing angle of the radiation on the crystal from the angle θ_0 defined by $n\lambda = 2d\sin\theta_0$; δ represents the deviation of the refractive index n from unity ($n=1-\delta$); and a is the quantity defined by $a/\delta = f(2\theta_0)/f(0)$ where $f(2\theta_0)/f(0)$ is the ratio of the amplitude of a wave scattered by the atom at an angle $2\theta_0$ to that scattered in the forward direction of the incident beam, or, in other words, at zero scattering angle. The sign of the radical is determined by the physical requirement of the conservation of energy, that $I_{\Delta\theta}/I_0$ be always less than or equal to unity.

Obviously the polarization of the incident beam will affect the quantity a and we must further qualify a by the relation $a = Q\delta(F/Z)$ in which Q is the

[5] Prins, Zeits. f. Physik **63**, 477 (1930).
[6] Allison, Phys. Rev. **41**, 1 (1932).

polarization factor, equal to $\cos 2\theta_0$ and to unity for the two polarized components π and σ, respectively, in which the directions of oscillations of the electric vectors are parallel and perpendicular to the plane of incidence of the radiation on the crystal. The term F/Z is the atomic structure factor divided by the number of electrons in the atom, and is equal to the ratio $f(2\theta_0)/f(0)$ for the σ component.

If we desire to study characteristic radiation, which we know to be completely unpolarized, Darwin's Eq. (1) is to be written in the form

$$\frac{I_{\Delta\theta}}{I_0} = \frac{1}{2}\left[\frac{(F/Z)\delta}{\sin\theta_0\cos\theta_0\Delta\theta - \delta \pm \left[(\sin\theta_0\cos\theta_0\Delta\theta - \delta)^2 - (F^2/Z^2)\delta^2\right]^{1/2}}\right]^2 + \frac{1}{2}\left[\frac{(F/Z)\delta\,|\cos 2\theta_0|}{\sin\theta_0\cos\theta_0\Delta\theta - \delta \pm \left[(\sin\theta_0\cos\theta_0\Delta\theta - \delta)^2 - (F^2/Z^2)\delta^2\cos^2 2\theta_0\right]^{1/2}}\right]^2. \quad (2)$$

Examination of this Eq. (2) shows that a region of 100 percent reflection exists for each polarized component. The angular extents of these regions are $4\delta(F/Z)\csc 2\theta_0$ and $4\delta(F/Z)\cot 2\theta_0$ for the σ and π components, respectively. The intensity distribution of each of the terms in (2) is symmetrical about the corrected Bragg angle θ ($\theta = \delta \sec\theta_0 \csc\theta_0 + \theta_0$). The refractive index is implied in the displacement of the axis of symmetry of the diffraction pattern from θ_0 to θ.

Prins' modification

Darwin considered the effect of absorption of the x-rays within the crystal upon his Eq. (1) but concluded that this introduced no essential modification. However, it should be pointed out that Darwin attempted to correct for absorption by assuming that the absorption coefficient accounted for a decrease in intensity quite independent of that due to scattering, which was already adequately treated in the difference equations. Prins reasoned that, in view of our present knowledge, the absorption coefficient includes absorption of two types: first, a coherent process or a diminution of intensity due to interference between the rays coherently scattered at zero scattering angle and the rays of the incident beam, and second, an incoherent or quantum process, such as photoeffect, recoil electrons, etc. Both types of processes must be included in a complete treatment of the problem.

The classical theory of dispersion expresses the index of refraction as a complex quantity, $n = 1 - \delta - i\beta$, of which the real part, $1-\delta$, is the ordinary refractive index. The coefficient β in the imaginary term, known as the absorptive index, is defined in the relation $\beta = \mu_l\lambda/4\pi$, in which μ_l is the linear absorption coefficient of the medium for radiation of wave-length λ. This classical expression for the index of refraction does not admit of incoherent absorption; however, Prins takes advantage of the experimental value of μ_l, which does include both types of absorption, and replaces δ in Darwin's Eq. (2) by $\delta + i\beta$, thereby incorporating in the theory a correction for incoherent absorption. When this substitution is effected, a similar replacement of a by $a + ib$ must be made because of the relation between a and δ just defined. The quantity b is considered later.

Prins' equation, or the modified Darwin Eq. (1), appears as[7]

$$\frac{I_{\Delta\theta}}{I_0} = \left[\frac{a+ib}{\sin\theta_0\cos\theta_0\Delta\theta-\delta-i\beta\pm[(\sin\theta_0\cos\theta_0\Delta\theta-\delta-i\beta)^2-(a+ib)^2]^{1/2}}\right]^2. \quad (3)$$

In accord with the previous discussion, this expression applies to the σ-component of polarization only; a similar expression in which $(a+ib)|\cos 2\theta_0|$ is written in place of $(a+ib)$ takes care of the π-component.

We are next confronted with the questions (1) of the phase relations of the scattered waves as a function of the scattering angle, (2) whether or not each electron can be treated as scattering separately, and (3) will the electronic structure factor F/Z be constant for all electrons in the atom irrespective of their various binding energies and different dimensions of the electron shells. We shall assume that the phase shift of coherently scattered radiation is the same in all directions, and that the amplitude scattered as a function of the scattering angle is the same for all electrons. This hypothesis leads to the relation[8]

$$(a+ib)/(\delta+i\beta) = f(2\theta_0)/f(0) \quad (4)$$

for the σ-component, where $f(2\theta_0)/f(0)$ is the ratio of the amplitude scattered at angle $2\theta_0$ to that scattered at zero angle.

Application to a real crystal—Calcite

It will be remembered that thus far we have dealt with reflection from that type of perfect crystal in which the atoms are of one kind only. In order for the equations to apply to a complex crystal, such as calcite, which consists of interlaced planes of different kinds of atoms, certain modifications must be made. We have written $(a+ib)$ as a summation over the various types of electrons in the atom, and we must now sum over the various types of atoms in the unit cell. In place of $(a+ib)$ we shall introduce a quantity $(A+iB)$ defined as

$$\begin{aligned} A+iB &= \sum_j (a_j+ib_j) \\ &= \sum_j (\delta_j+i\beta_j)[f_j(2\theta_0)/f_j(0)]\exp 2\pi ni(hx_j+ky_j+lz_j) \end{aligned} \quad (5)$$

in which δ_j is the contribution to δ of atom j; n the order of reflection; h, k, l the Miller indices of the reflecting plane; and x_j, y_j, z_j the coordinates of atom j in the unit cell. The summation is to be taken over all the atoms in the unit cell of the crystal.

[7] This is Eq. (11) in Prins' article, reference 5.

[8] It should be made clear that the writing of this relation (4) implies a somewhat dogmatic answer to each of the three above questions, and that a more accurate working hypothesis would be to consider each shell of electrons separately, both as regards the contributions to δ and β, and also with respect to the electronic structure factor. Then $(a+ib)$ would be written $a+ib=\sum_j (F/Z)_j(\delta_j+i\beta_j)$ where the summation extends over all the electrons of the atom in question.

Alteration of the form of the equation

Before making the numerical calculations of the various quantities for calcite, let us derive the expressions for three important characteristic properties of the theoretical diffraction pattern of the crystal: the percent reflection, the coefficient of reflection, and the width at half-maximum intensity of the reflected line.

First we shall reduce the equation to a less ponderous form. Introduce another variable, x, defined as $x \equiv \sin\theta_0 \cos\theta_0 \Delta\theta/\delta$. The old variable, $\Delta\theta$, expressing in radians the deviation of the glancing angle from the angle θ_0

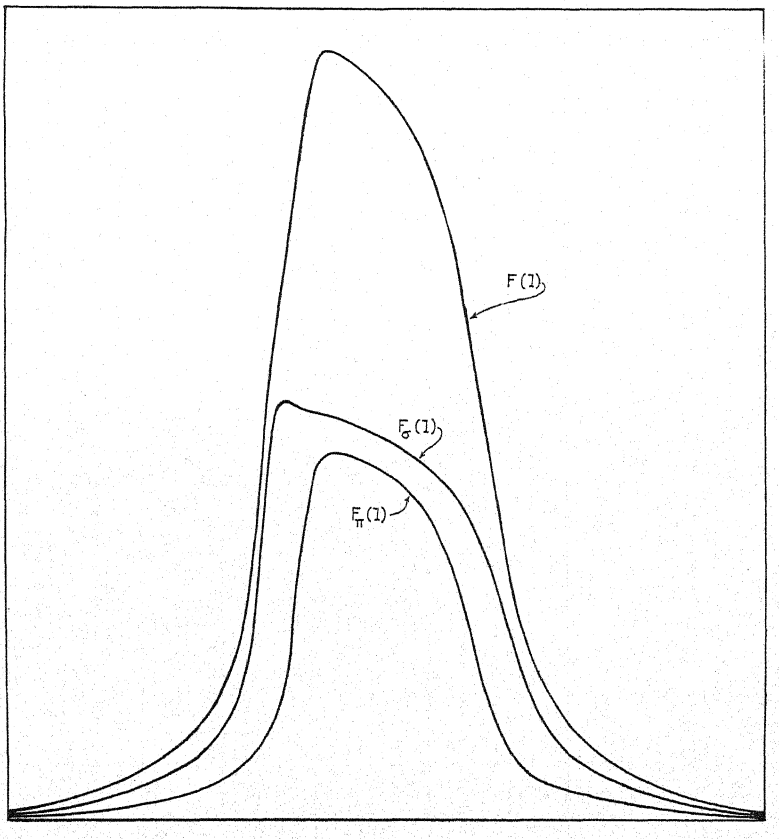


Fig. 1. Theoretical diffraction pattern from a single calcite crystal for $\lambda = 2.299$A. The outer curve, governed by the function $F(l)$, is the sum of the two polarized components, $F_\sigma(l)$ and $F_\pi(l)$. The values of the coordinates from which these curves are plotted are listed in Table I.

(given by $n\lambda = 2d \sin\theta_0$), has θ_0 as its reference origin. The variable x has the same reference origin, but represents the fractional deviation of the glancing angle, the unit of deviation being $(\delta \sec\theta_0 \csc\theta_0)$. A further change of variable to establish the position θ as the reference origin will be found convenient. We shall define a new variable, l

$$l \equiv x - 1 = \sin\theta_0 \cos\theta_0 \Delta\theta/\delta - 1. \qquad (6)$$

Then Eq. (3) reduces to the form, in l,

$$F_\sigma(l) = \left(\frac{I_l}{I_0}\right)_\sigma = \left[\frac{(A + iB)/\delta}{l - i\beta/\delta \pm \{(l - i\beta/\delta)^2 - [(A + iB)/\delta]^2\}^{1/2}}\right]^2. \quad (7)$$

Physically, $F_\sigma(l)$ is the ordinate of a point, for a given value of l, on the curve of the diffraction pattern to be expected for σ-polarized radiation reflected from a single crystal. This is the form of the equation we shall use throughout the remainder of this paper. As before, the π-component is expressed by a similar function $F_\pi(l)$ obtained by replacing $A+iB$ by $(A+iB)|\cos 2\theta_0|$ in (7). The two components and their sum are plotted for $\lambda = 2.299$A in Fig. 1, and the values of the coordinates from which these curves are drawn are given in Table I.

Percent reflection

The three properties, percent reflection, coefficient of reflection, and line width of the rocking curve, are experimentally determined with a double-crystal spectrometer, by a method to be discussed in the experimental part

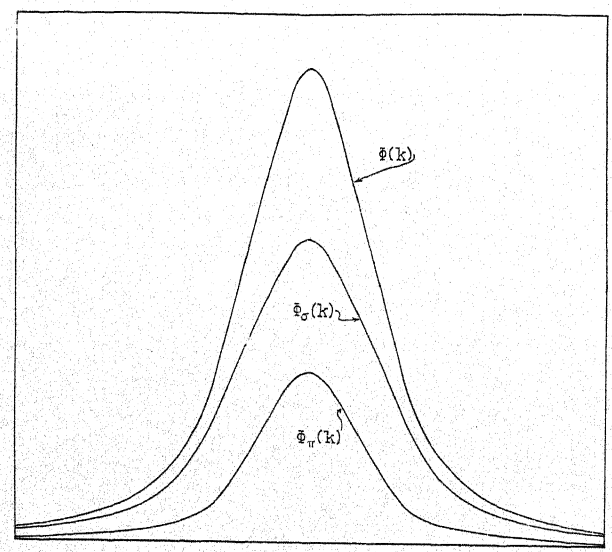


Fig. 2. Theoretical diffraction pattern from a second calcite crystal for $\lambda = 2.299$A. The polarized components represented by the function $\Phi_\sigma(k)$ and $\Phi_\pi(k)$ are added together to give the total theoretical diffraction pattern drawn as the outer curve. This pattern is to be compared with the experimental rocking curve obtained with the double-crystal spectrometer in the (1, −1) position. The coordinate values used in plotting these curves are given in Table I.

of this paper. Hence, for purposes of comparison between theory and experiment, it is desired to obtain expressions for the intensity distribution in the theoretical diffraction pattern as formed by the second crystal, or in twice-reflected radiation.

The total integrated intensity of a characteristic x-ray line reflected from the first crystal is given by

$$\int_{-\infty}^{\infty} F(l)dl = \tfrac{1}{2}\int_{-\infty}^{\infty} F_\sigma(l)dl + \tfrac{1}{2}\int_{-\infty}^{\infty} F_\pi(l)dl \quad (8)$$

assuming that each polarized component of the incident beam is of equal intensity. This expression (8) also represents the total intensity incident upon the second crystal of the spectrometer.

To treat the reflection from the second crystal, we shall introduce a new variable, k, defined as the deviation, measured in the same units as l, of the glancing angle of the radiation on the second crystal from that angle for which the two crystals are parallel. The doubly reflected intensity is given, considering both components of polarization, by

$$\Phi(k) = \tfrac{1}{2}\Phi_\sigma(k) + \tfrac{1}{2}\Phi_\pi(k) = \tfrac{1}{2}\int_{-\infty}^{\infty} F_\sigma(l)F_\sigma(l-k)dl + \tfrac{1}{2}\int_{-\infty}^{\infty} F_\pi(l)F_\pi(l-k)dl. \quad (9)$$

The function $\Phi(k)$ for a given value of k, is the ordinate of a point on the curve of the theoretical diffraction pattern from the second crystal. The two components and their sum, representing the complete theoretical diffraction pattern are plotted for the wave-length $\lambda = 2.299$A in Fig. 2, and the coordinate values used are given in Table I.

TABLE I. *Theoretical diffraction pattern formed by a single calcite crystal for $\lambda = 2.299$A.* | *Theoretical diffraction pattern formed by a second calcite crystal for $\lambda = 2.299$A.*

l	$F_\sigma(l)$	$F_\pi(l)$	$F(l)$	k	$\Phi_\sigma(k)$	$\Phi_\pi(k)$	$\Phi(k)$
2.5	0.010	0.005	0.015	0.0	0.6310	0.3565	0.9875
2.0	0.015			±0.2	0.5800	0.3185	0.8985
1.5	0.030	0.015	0.045	±0.4	0.4886	0.2335	0.7221
1.0	0.073	0.035	0.108	±0.6	0.3876	0.1510	0.5386
0.8	0.125	0.057	0.182	±0.8	0.2660	0.0815	0.3475
0.7		0.076		±1.0	0.1735	0.0480	0.2215
0.6	0.268	0.090	0.358	±1.5	0.0686	0.0220	0.0906
0.5	0.428	0.170	0.598	±2.0	0.0368	0.0120	0.0488
0.4	0.581	0.300	0.881	±2.5	0.0218	0.0050	0.0268
0.3	0.672	0.495	1.167				
0.2	0.727	0.617	1.344				
0.1	0.766	0.684	1.450				
0.0	0.795	0.725	1.520				
−0.1	0.818	0.750	1.568				
−0.2	0.839	0.766	1.605				
−0.3	0.851	0.722	1.573				
−0.4	0.871	0.370	1.241				
−0.5	0.727	0.179	0.906				
−0.6	0.299	0.111	0.410				
−0.7		0.077					
−0.8	0.126	0.057	0.183				
−1.0	0.074	0.035	0.109				
−1.5	0.030	0.015	0.045				
−2.0	0.015						
−2.5	0.010	0.005	0.015				

The percent reflection is defined as the ratio (multiplied by 100) of the maximum reflected intensity to the intensity of the beam incident upon the crystal. In the diffraction equations, the maximum intensity is reflected when $k = 0$, and the expression[9] for percent reflection P becomes

$$P = \frac{\int_{-\infty}^{\infty} F_\sigma^2(l)dl + \int_{-\infty}^{\infty} F_\pi^2(l)dl}{\int_{-\infty}^{\infty} F_\sigma(l)dl + \int_{-\infty}^{\infty} F_\pi(l)dl}. \quad (10)$$

Coefficient of reflection

The coefficient of reflection is defined as the ratio of the integrated intensity of the beam reflected from the second crystal to the intensity of the beam reflected from the first crystal only. The integrated intensity from the second crystal refers to the area under the rocking curve obtained by varying k throughout the entire region of reflection. Hence, the expression[9] for the coefficient of reflection R can be written

$$R = \delta \sec\theta_0 \csc\theta_0 \frac{\int_{-\infty}^{\infty} \Phi_\sigma(k)dk + \int_{-\infty}^{\infty} \Phi_\pi(k)dk}{\int_{-\infty}^{\infty} F_\sigma(l)dl + \int_{-\infty}^{\infty} F_\pi(l)dl}. \tag{11}$$

in which $\Phi_\sigma(k)$ and $\Phi_\pi(k)$ are defined in Eq. (9). The unit of angular measure, $\delta \sec\theta_0 \csc\theta_0$, is placed in the expression (11) in order to convert the units of the coefficient of reflection into radians.

Width of diffraction pattern

Eq. (9) when plotted for various values of k gives the contour of the theoretical diffraction pattern of an x-ray line reflected from the second crystal, Fig. 2. From this graph the width at half-maximum is obtained in terms of the variable k, and is converted into radians by multiplying by the angular unit $\delta \sec\theta_0 \csc\theta_0$. This value, $W_{1/2}$,

$$W_{1/2} = [W_k]_{1/2}\delta \sec\theta_0 \csc\theta_0 \tag{12}$$

should correspond with the width at half-maximum of the ionization rocking curve of the x-ray line measured with the double-crystal spectrometer in the $(1,-1)$ position.

Calculations

As Allison[6] points out, the shape of the rocking curve obtained experimentally with a double spectrometer in the parallel position is not to be compared with that given in Fig. 1, but rather with the shape represented in

[9] When obtaining the total reflected intensity from Darwin's Eq. (2), it is true that

$$\int_{-\infty}^{\infty} f_\pi(\Delta\Theta)d(\Delta\Theta) = |\cos 2\Theta_0| \int_{-\infty}^{\infty} f_\sigma(\Delta\Theta)d(\Delta\Theta)$$

and the integrated intensity reflected from a single crystal, assuming an unpolarized incident beam, can be written

$$J = (1 + |\cos 2\Theta_0|)/2 \int_{-\infty}^{\infty} f_\sigma(\Delta\Theta)d(\Delta\Theta).$$

However, when dealing with the complex expression of Eqs. (3), (7) or (9), this simple cos $2\theta_0$ relation between the two components is no longer true due to the fact that the integration must be performed along the real axis. Consequently, each component must be calculated separately. In Allison's recent paper,[6] the cos $2\theta_0$ relation is assumed to hold, and in consequence thereof, as Professor Allison himself points out in a letter to the editor in this issue of the Physical Review, his equations and computed values are somewhat in error.

Fig. 2 which is governed by the function $\Phi(k)$, Eq. (9). It would perhaps be a more direct comparison to determine experimentally the $\Phi(k)$ and, by means of Eq. (9), derive an experimental rocking curve from the first crystal which could then be compared with the theoretical function $F(l)$ represented in Fig. 1. However, this procedure has been shown[10] mathematically impossible unless $F(l)$ be assumed to be an even function, that is to say, symmetrical about the axis $l=0$, which assumption, of course, defeats the purpose. In this paper we shall take for granted the validity of Eq. (3) and, on this basis, calculate the $\Phi(k)$, then check the agreement between the values so computed and the experimental values. The three properties, percent reflection, coefficient of reflection, and line width, are chosen for this check because they are perhaps the most distinctive characteristics of the rocking curve that can be experimentally measured.

Evaluation of constants in $F(l)$

The values of the refractive index δ for calcite are taken directly from the experimental dispersion curve given by Larsson[11] in which values of δ/λ^2 are plotted in the region 1.5 to 4A. The δ/λ^2 values to 5A are taken from the curve plotted from classical dispersion theory.

A search through the literature for absorption coefficients of calcite in this wave-length was unsuccessful, and it was necessary to resort to an approximate method for their calculation. An extrapolation of the absorption coefficient of each element in the crystal using the λ^3 or the $\lambda^{2.8}$ law would yield values too much in error to be useful. Jönsson[12] in his investigations finds a linear relation between the product $Z\lambda$ and $(\mu_l/\rho)_K\,(W/AZ)$ where μ_l is the linear absorption coefficient, ρ the density of the element of atomic weight W and atomic number Z, and A Avogadro's number. The factor μ_l/ρ is expressed for the region between the K and L absorption limits, and if $(\mu_l/\rho)_L$ is desired $(\mu_l/\rho)_K$ must be converted to the L region by the factor E_K/E_L where E_K and E_L are the energies of the K and L levels respectively. Then, for any value of $Z\lambda$, determined by the element and wave-length in question, the corresponding value of $(\mu_l/\rho)_K$ is taken from Jönsson's tables. In this manner, the mass absorption coefficients of calcium, carbon, and oxygen are obtained for the wave-lengths selected in this study. The mass absorption coefficients are converted to atomic, and, by addition, the molecular, and, thence, the linear absorption coefficients of calcite are evaluated. This empirical method gives reasonably good values as checked (within approximately 5 percent) with Spencer's experimental measurements on oxygen and argon.[13]

The factor β, previously defined in the relation $\beta=\mu_l\lambda/4\pi$, is readily calculated as soon as μ_l is determined.

The evaluation of A and B, which have been defined in the summation (5) over the unit cell, is accomplished in the following manner.

[10] Laue, Zeits. f. Physik **72**, 472 (1931).
[11] Axel Larsson, Inaugural-Dissertation, Uppsala (1929).
[12] Edvin Jönsson, Inagurual-Dissertation, Uppsala (1928).
[13] Spencer, Phys. Rev. **38**, 1932 (1931).

The quantity δ_j may be considered as the deviation of the index of refraction from unity for a substance formed by removing all the atoms from the calcite unit cell except the atom j. The unit cell of calcite contains two molecules of $CaCO_3$. All the electrons in the oxygen and carbon atoms are so loosely bound with respect to the quantum energies of the wave-lengths employed in these experiments that their dispersion may be considered normal. This means, taking carbon as an example, that[14]

$$\delta_c = (e^2\lambda^2/2\pi mc^2)N_c \tag{13}$$

where N_c is the number of electrons per cubic centimeter in calcite due to one of the carbon atoms in the unit cell. As mentioned above, the calculations are carried out on the assumption that each atom in the crystal contains a number of electrons equal to its atomic number, that is, the calculations are made for non-ionized calcium carbonate. On this assumption

$$N_c = 6/v = 3A\rho/M \tag{14}$$

where V is the volume of the unit cell of calcite, M the molecular weight, A Avogadro's number, and ρ the density. The δ_j values for carbon and oxygen are calculated from Eqs. (13) and (14), and the value of δ_{ca} is then determined by subtracting $\delta_c+3\delta_O$ from the δ value observed by Larsson according to the formula

$$\delta_{ca} = \delta/2 - \delta_c - 3\delta_0. \tag{15}$$

The δ_j values employed here thus depend partly upon the classical dispersion theory and partly upon Larsson's experimental results.

The β_j values for each atom in the unit cell are determined from the linear absorption coefficients obtained by the method of Jönsson mentioned above.

By the factor $f_j(2\theta_0)/f_j(0)$ in Eq. (14) is meant the ratio of the amplitude scattered from the atom j at the scattering angle $2\theta_0$ to that scattered in the forward direction. This ratio is evaluated from tables of structure factors.[15,16] The recent work of Glocker and Schäfer[17] indicates that this ratio is a function of wave-length and changes near a critical absorption discontinuity of the atom. We shall not attempt to take this effect into consideration, due to the small amount of data available, and shall apply the same values to all wave-lengths in the calculations.

We have assumed the electronic structure of calcite to be $Ca^0C^0O_3^0$, and by averaging the values in the structure factor tables referred to above, we obtain

$$\frac{f_{ca}(2\theta_0)}{f_{ca}(0)} = 0.768$$

$$\frac{f_c(2\theta_0)}{f_c(0)} = 0.650 \tag{16}$$

[14] A. H. Compton, reference 4, page 210.
[15] James and Brindley, Phil. Mag. **12**, 81 (1931).
[16] Pauling and Sherman, Zeits. f. Krist. **81**, 1 (1932).
[17] Glocker and Schäfer, Zeits. f. Physik **73**, 289 (1931).

$$\frac{f_O(2\theta_0)}{f_O(0)} = 0.775.$$

The exponential term in Eq. (5) expresses the phase differences between the waves scattered from the several atoms in the unit cell. The coordinates of the atoms are

Calcium	$\frac{1}{4}$	$\frac{1}{4}$	$\frac{1}{4}$		$\frac{3}{4}$	$\frac{3}{4}$	$\frac{3}{4}$
Carbon	0	0	0		$\frac{1}{2}$	$\frac{1}{2}$	$\frac{1}{2}$
Oxygen	$\frac{1}{4}$	$\frac{\bar{1}}{4}$	0		$\frac{\bar{1}}{4}$	0	$\frac{1}{4}$
	0	$\frac{1}{4}$	$\frac{\bar{1}}{4}$		$\frac{1}{4}$	$\frac{3}{4}$	$\frac{1}{2}$
	$\frac{3}{4}$	$\frac{1}{2}$	$\frac{1}{4}$		$\frac{1}{2}$	$\frac{1}{4}$	$\frac{3}{4}$

Substituting these coordinates in the exponential term we find that the waves scattered from the two calcium atoms reinforce each other in the first order; and likewise for the two carbon atoms. The contributions of four of the six oxygens disappear by destructive interference, leaving only two oxygen atoms effectively scattering. The expansion of Eq. (12) therefore takes on the form

$$A + iB = 2\left[(\delta_{ca} + i\beta_{ca})\frac{f_{ca}(2\theta_0)}{f_{ca}(0)} + (\delta_c + i\beta_c)\frac{f_c(2\theta_0)}{f_c(0)} + (\delta_O + i\beta_O)\frac{f_O(2\theta_0)}{f_O(0)}\right] \quad (17)$$

and the summation can now be accomplished. The constants A and B are determined by equating them to the real and to the coefficient of the imaginary terms respectively.

The calculations outlined above yield the following values, presented in Table II, for the six selected wave-lengths:

TABLE II. *Evaluation of the constants in Eqs. (7) and (9) for calcite.*
λ = wave-length; θ = glancing angle; μ_l = linear absorption coefficient; δ = deviation of refractive index from unity.

λ (angstroms)	$\lvert\cos 2\theta\rvert$	δ $\times 10^6$	μ_l	β/δ (cm)	A $\times 10^6$	B $\times 10^6$
1.537	0.8712	8.753	208	0.0211	4.457	0.185
2.299	0.7120	19.21	615	0.0424	9.716	0.815
2.941	0.5286	28.32	1190	0.0710	13.50	2.010
3.114	0.4716	32.59	265	0.0106	15.78	0.345
3.902	0.1702	53.47	493	0.0149	26.54	0.795
4.937	0.3283	86.60	890	0.0207	43.20	1.792

Calculation of R, P, and $W_{1/2}$

All the constants in the functions $F(l)$ and $\Phi(k)$ are now determined and the theoretical values for the percent reflection, Eq. (10), the coefficient of reflection, Eq. (11), and the width of the diffraction pattern, Eq. (12), can be calculated. The computations were carried out by laborious graphical integration,[18] and the results are presented in Table III.

[18] The author wishes to express his indebtedness to Mrs. Ardis Monk, computor of this laboratory, for her generous cooperation in assisting with these calculations.

TABLE III. *Calculated values of R, P, and $W_{1/2}$ for calcite.*
R = coefficient of reflection (radians), *P* = percent reflection, $W_{1/2}$ = half width at half maximum intensity (seconds of arc).

λ (angstroms)	$\int_{-\infty}^{\infty} F_c(l)dl$	$\int_{-\infty}^{\infty} F_\pi(l)dl$	$\int_{-\infty}^{\infty} F_\sigma^2(l)dl$	$\int_{-\infty}^{\infty} F_\pi^2(l)dl$	$\int_{-\infty}^{\infty} \Phi_\sigma(k)dk$	$\int_{-\infty}^{\infty} \Phi_\pi(k)dk$	Angular unit $\times 10^6$ radians	$W_{1/2}$	P	R $\times 10^5$ radians
1.537	1.16	1.00	0.824	0.678	1.34	0.983	35.65	4.94	69.2	3.82
2.299	1.03	0.677	0.631	0.357	1.06	0.456	54.71	7.45	57.7	4.86
2.941	0.86	0.340	0.425	0.107	0.695	0.114	66.73	8.61	44.3	4.49
3.114	1.14	0.510	0.829	0.315	1.28	0.243	73.91	8.70	69.1	6.80
3.902	1.13	0.120	0.796	0.041	1.28	0.0144	108.52	15.05	67.0	11.2
4.937	1.09	0.268	0.707	0.115	1.15	0.0715	183.13	23.50	60.4	16.4

EXPERIMENTAL PART

As was mentioned in the introduction of th s paper, experimental work upon the problem of x-ray reflection from crystals has been undertaken by many investigators, but little agreement exists among the reported results. The experimental results for calcite are represented graphically in Fig. 6 of Allison's paper.[6] The inconsistencies of these results among themselves in all probability can be attributed to the various degrees of perfec tion in the crystals employed by the different investigators. The present experiments are an attempt to measure systematically the aforementioned three properties of reflection for one pair of calcite crystals through a comparatively large range of wave-lengths, from 1.5 to 5 angstroms. Allison has recently reported[6] a similar study for the same crystals, crystals II of his paper, in the region 0.21 to 2.28A using in his investigations a different double spectrometer. A second object of these experiments is to complete the calibration of the crystals for use in relative intensity measurements in the entire region 0.21 to 5 angstroms.

Apparatus

Air at atmospheric pressure is more or less opaque to x-rays of wave-lengths 2 to 5 angstroms and in order to perform these experiments a specially designed vacuum double-crystal ionization spectrometer was constructed. In Fig. 3 is given a photograph of this instrument. The two collimating slits, the two crystals, and the ionization chamber are supported on a heavy circular steel bed-plate, and a large metal cylindrical cap, shown in an elevated position in the photograph, can be lowered to the plate, enclosing the contents in an airtight chamber. The x-ray tube, with an uranium target whose position can be adjusted with respect to the tube itself while in operation by means of a sylphon connection, is clamped to the side of the cylindrical tank, and brought into alignment with the slits by sliding the tank on the stopcock grease which effects the seal between the tank and the bed-plate. Outside control of the second crystal and the ionization chamber is managed by having long, concentric tapered bearings, sealed

with stop-cock grease, extending through the bed-plate. Details of the design and construction of this apparatus have been reported in an earlier paper by the author.[19]

Measurements

Nine lines selected from the uranium M series[20] from 2.299 to 4.937A and the copper $K\alpha$ radiation, 1.537A were used in the measurements. The lines of wave-lengths 1.537A and 2.299A overlap the region investigated by Allison,[6] and the good agreement between the results measured with the two different spectrometers can be considered experimental evidence that the properties of the rocking curves are really characteristic of the crystals themselves and not a function of the apparatus.

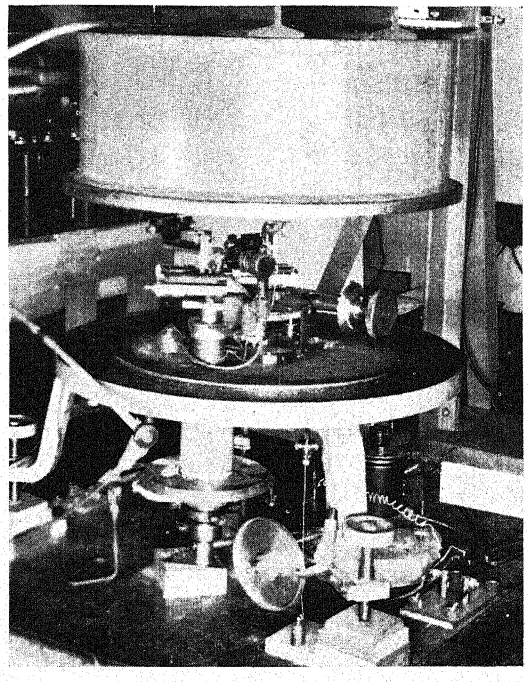


Fig. 3. Photograph of the double-crystal vacuum spectrometer.

By observing the ionization rocking curve obtained in the $(1,-1)$ position by rotating the second crystal throughout the entire range of reflection, and the intensity of the x-ray beam reflected from the first crystal only, that is, with the second crystal removed from its position so that it does not intercept the beam, one gathers all the data necessary for measurements of the percent reflection, the coefficient of reflection, and the width of the line. A regular routine, very similar to the one described by Allison,[6] was adopted in recording these data.

[19] Parratt, Phys. Rev. 41, 553 (1932).

[20] The wave-lengths of the uranium M series are taken from the tables of Siegbahn, *Spektroskopie der Roentgenstrahlen*, Julius Springer, 1931.

The accumulation of tungsten sputtered on the cellophane window between the x-ray tube and the tank, and also on the face of the target, absorbs the soft x-rays very strongly, and a correction for the exponential diminution of intensity due to this cause was found necessary. This correction was effected experimentally by taking a series of measurements with the x-ray tube operating smoothly and without change of power over a period of at least four hours and observing the intensity drop as a function of time.

In order to check the presence of any possible deterioration of the crystals, such as would affect their resolving power, measurements with the selected spectrum lines were taken in the order of increasing wave-length. About two months after the first measurements had been begun, a second series was completed, having taken the wave-lengths in the order opposite to that of the first. If the surfaces of the crystals had changed in this period of time a consistent deviation in the measured properties would have been apparent, particularly in the widths of the lines and in the percent reflection at the short wave-lengths. No such deviation was observed.

The experimental measurements are listed in Table IV. Each value is the average of at least two, usually five, independent observations. The values for the same properties computed from the theoretical equations are also included in the table for ease of comparison.

TABLE IV. *Experimental and calculated values of* $W_{1/2}$, P, *and* R.
$W_{1/2}$ = half-width at half-maximum intensity (seconds of arc), P = percent reflection, R = coefficient of reflection (in radians).

λ A	$W_{1/2}$		P		$R\times10^5$	
	obs.	calc.	obs.	calc.	obs.	calc.
1.537	5.00	4.94	60.5	69.2	3.80	3.82
2.299	7.50	7.45	50.7	57.7	4.81	4.86
2.745	9.10		43.1		4.62	
2.941	9.10	8.61	39.1	44.3	4.35	4.49
3.114	9.15	8.70	57.4	69.1	6.70	6.80
3.514	13.00		57.3		8.35	
3.708	14.20		57.7		9.30	
3.902	15.25	15.05	57.8	67.0	10.40	11.20
4.322	18.60		58.1		11.97	
4.937	23.70	23.50	51.0	60.4	14.00	16.40

DISCUSSION OF RESULTS

The experimental and calculated values of the three properties of reflection are presented graphically in Figs. 4, 5, and 6.

The agreement, close to experimental error, of the line widths throughout the entire region gives no evidence for the presence of mosaic structure in the crystals.

The calculated values of the percent reflection are consistently high, but this is not surprising when one considers that the percent reflection is particularly sensitive to the shape of the pattern, being proportional to the square of the ordinate, Eq. (10). This disagreement may be accounted for by the temperature motion of the atoms, to be discussed presently, or it may reflect an inherent inadequacy of Eq. (7) to correctly represent the diffraction pattern.

The comparison of the calculated and observed values of the coefficient of reflection should be considered in connection with the next paragraph. As seen in Fig. 6 the observed values lie below those calculated, and, in fact, another pair of calcite crystals, crystals III reported by Allison,[6] give experimental values of 3.46 and 4.68×10^{-5} radians for wave-lengths 1.537 and

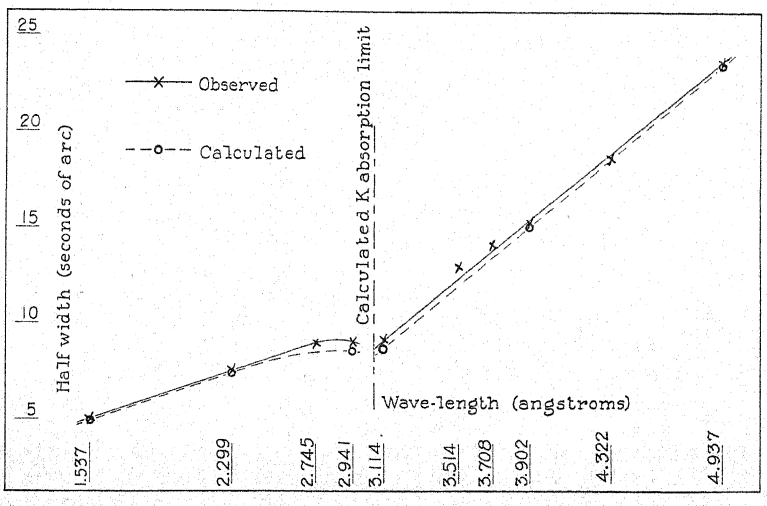


Fig. 4. Comparison of the observed and calculated half-width at half-maximum intensity ($W_{1/2}$) of the rocking curves obtained with the double-crystal spectrometer in the (1, −1) position. The differences are near the limit of experimental error. *Note added in proof:* "Calculated K absorption limit" should read "Calcium K absorption limit."

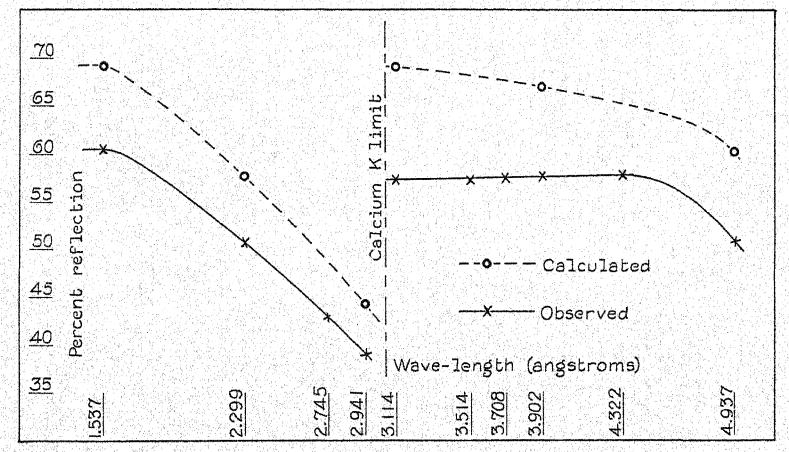


Fig. 5. Comparison of the observed and calculated percent reflection (P) of the rocking curves obtained with the double-crystal spectrometer in the (1, −1) position.

2.285A, respectively, which are even lower than those observed for crystals II given in Fig. 6. This indicates that the theoretical values uncorrected for the kinetic motion of the atoms due to temperature are somewhat too high. The deviation at $\lambda = 4.937$A between the two curves of Fig. 6 may be due to the uncertainty of the value of δ at this wave-length, the value used being taken from the theoretical dispersion curve since Larsson's work[11] did not

extend to this wave-length. Also there is reason to believe that the absorption coefficient is least reliable at this long wave-length.

In developing the equations on which the calculations are based, we considered reflection from a perfect crystal; and in the experimental measurements a real crystal is used. The differences between a real and a perfect crystal, for practical purposes, are present in the distortion of the grating

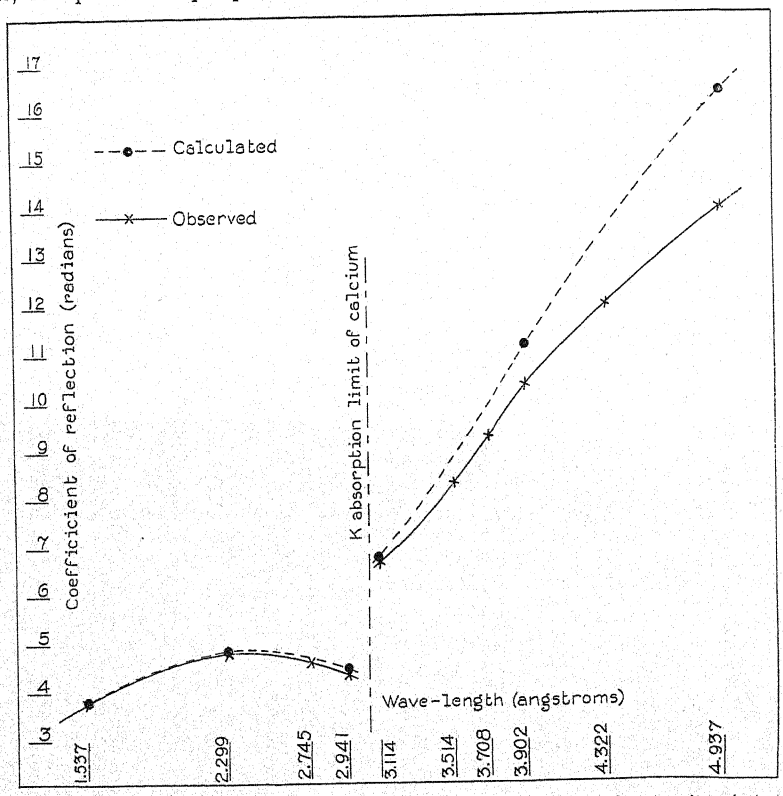


Fig. 6. Comparison of the observed and calculated coefficient of reflection (R) from the second crystal of the spectrometer. The differences for wave-lengths less than 3.902A are within experimental error.

planes, or the mosaic structure, and in the temperature motion of the atoms. In view of the excellent agreement in the width of the lines, Fig. 4, the mosaic structure in the specimens of calcite used in these experiments may be considered to be very small. A correction for temperature motion of the atoms in a calcite crystal is difficult to carry out, and has not been attempted in this paper. In general, the effect of raising the temperature of the crystal is to lower the values of percent reflection and coefficient of reflection leaving unaltered the width of the pattern, and it seems possible that such a correction for temperature would give very satisfactory agreement between theory and experiment with specimens of calcite in which the mosaic structure is a minimum.

It is a pleasure to acknowledge the many essential suggestions and the constantly helpful advice and criticism which Professor S. K. Allison has offered in the course of this work.

Survey of the *K*-Satellites

By O. Rex Ford
West Virginia University

(Received June 4, 1932)

A survey of the α-satellites from Ge (32) to Mg (12) reveals new lines in the $K\alpha'$ series, from the element Ca (20) to Va (23). The $K\alpha_{3,4}$ doublet is resolved over five additional elements, from Ca (20) to Mn (25). The $K\alpha_3$ line is shown to have two components, $K\alpha_3$ and $K\alpha_3'$, over the range of elements Al (13) to Cl (17). Microphotometer records, tracings of which are shown, reveal a significant reversal in the relative intensity of $K\alpha_3$ and $K\alpha_4$. This reversal is an atomic phenomenon and is not dependent upon chemical combination.

The survey of the β-satellites from Cu (29) to Cl (17) adds two new lines of the $K\beta''$ series in the elements Cr (24) and Cl (17), four new lines in the $K\beta\eta$ series from Va (23) to K (19), and reveals two new series, named $K\beta^{IV}$ and $K\beta^{V}$. The $K\beta^{IV}$ series was found in three elements; *viz.*, Sc (21), Ca (20) and K (19) while the $K\beta^{V}$ series, which starts at the element (20), extends downward to Cl (17) and probably farther. While none of the points in the new series was obtained from the free elements, the behavior of their semi-Moseley diagrams resembles those of the other β-satellites. To relate all the β-satellites to $K\alpha_2$ rather than $K\beta_1$, as has been customary, is shown to be of great convenience in the experimental study and classification of the β-satellites; the physical significance of this mode of representation, however, is problematic.

Introduction

As A result of some measurements on the satellites of the diagram lines $L\alpha_1$ and $L\beta_2$ over the range of elements R(37) to Sn(50), Richtmyer and Richtmyer[1] were able to show that the satellite lines were more numerous than had previously been reported and that carefully timed exposures were necessary to bring out the satellite lines. This fact alone would warrant a survey of the *K*-satellites. By making the dispersion as great as possible both by the selection of crystals, which would give large Bragg angles, and by trying exposures in high orders, it was hoped so to separate the satellites from the diagram lines as to reduce the error in the wave-length determinations. However, after several unsuccessful attempts in higher orders the survey was limited to first order spectrograms.

Microphotometer records of all spectrograms gave some notion of the relative intensities of the satellites among themselves, but, due to the very great over-exposure of the diagram lines, no idea of the intensity of the satellites in comparison with the diagram lines.

Apparatus and Procedure

All spectrograms were taken on a Siegbahn vacuum spectrograph of the relative wave-length type. The slit width, in nearly all exposures, was 0.08 cm and the distance from the slit to the photographic plate was 36.728 cm. The source of electrons was a heated tungsten spiral. The high potential across the x-ray tube was obtained from full wave rectification of the second-

[1] Richtmyer and Richtmyer, Phys. Rev. **34**, 574 (1929).

ary voltage of a transformer, with suitable condensers to reduce the voltage fluctuations to a ripple of about 5 percent. To prevent the visible light from reaching the photographic plate, the slit was covered with carbon paper, which works very satisfactorily down to and including Mg (12).

A calcite crystal was used for all spectrograms in the range of elements from Ge (32) to S (16); a quartz crystal on the elements P (15), Si (14) and Al (13); a gypsum crystal on the elements Al (13) and Mg (12). Pure elements were employed for target materials, whenever possible, to avoid the effect of chemical combination. Materials, other than pure elements, are listed in Table I.

TABLE I. *Spectrograms of elements in chemical combination.*

Element	Material used for spectrogram
Va 23	$H_4V_2O_7$ on copper target
Sc 21	Sc_2O_3 on copper target
Ca 20	CaO on copper target
K 19	K_2SO_4 on copper target
Cl 17	NaCl on aluminum target
S 16	Al_2S_3 on aluminum target
P 15	(Fe-Phos.) alloy on copper target

The procedure followed in taking each spectrogram consisted in making enough preliminary runs to find a method by which the material could be kept upon the focal spot and to obtain the exposure necessary to bring out all the known satellites. A second spectrogram was then taken, with conditions constant, using double the above exposure.

MEASUREMENT OF THE SPECTROGRAMS

All spectrograms were measured in two different ways: (1) by means of a comparator with low magnification, approximately five; (2) from microphotometer records with a magnification of ten. All values reported in the tables represent a weighted mean of the two methods. Measurements were made to the center of the lines. Since the error of superposition[1] can be estimated on the microphotometer records, it is possible to give some weight to the psychological error of contrast, inherent in the comparator readings, by comparing the separation of two lines measured by both methods. Comparison showed that the average separation of two lines, obtained from comparator readings, differed from the separation of the same two lines, determined from microphotometer records, by a value which was less than the probable error in a series of comparator readings. Hence, the probable error, in a set of comparator readings, seems to be a fair criterion of the experimental error. The probable error will vary from 0.25 percent, for a satellite well separated from the reference line, to 2.00 percent for diffuse satellites close the reference line.

Since values of $(\Delta\nu/R)^{1/2}$ are more significant in the theory of the satellites than wave-length values, it is desirable to record values of $(\Delta\nu/R)^{1/2}$ which are determined directly from the *measured* separation of the lines by the formula,

$$(\Delta\nu/R)^{1/2} = (\Delta\lambda/\lambda^2 R)^{1/2}. \qquad (1)$$

TABLES AND RESULTS

Tables II to VII give the results on the β-satellites, studied over the range of elements Cu (29) to Cl (17). The results on the α-satellites, surveyed from Ge (32) to Mg (12), are recorded in Tables VIII to XIII.

Column one gives the elements in which the satellite was measured, column two the wave-length values of the reference line taken from the tables in Vol. XXIV of the Handbuch der Experimentalphysik. The separation of the satellite from the reference line, measured on the photographic plate, is recorded in column three. Column four contains the calculated wave-length values of the satellite, while columns five and six give the values of $\Delta\nu/R$ and $(\Delta\nu/R)^{1/2}$, calculated by formula (1).

β-Satellites Referred to $K\beta$

TABLE II.

Elem.	β_1	cm $\Delta(\beta_1-\beta_\eta)$	β_η	$\Delta\nu/R$	$(\Delta\nu/R)^{1/2}$
19	3446.80	0.264	3488.67*	3.17	1.78
20	3083.43	0.301	3126.06*	4.08	2.02
21	2773.94	0.268	2813.16*	4.58	2.14
22	2508.98	0.240	2545.86*	5.34	2.31
23	2279.72	0.237	2315.25	6.25	2.50
24	2080.59	0.213	2113.54	6.98	2.64

TABLE III.

Elem.	β_1	cm $\Delta(\beta_1-\beta')$	β'	$\Delta\nu/R$	$(\Delta\nu/R)^{1/2}$
20	3083.43	0.0810	3094.92	1.102	1.050
21	2773.94	0.0632	2783.20	1.096	1.047
22	2508.98	0.0555	2517.31	1.208	1.099
23	2279.72	0.0399	2285.85	1.105	1.051
24	2080.59	0.0331	2085.78	1.092	1.045
25	1906.19	0.0286	1910.68	1.132	1.064
26	1753.01	0.0216	1756.48	1.020	1.010
27	1617.44	0.0190	1620.46	1.051	1.025
28	1497.05	0.0152	1499.48	0.988	0.994

TABLE IV.

Elem.	β_1	cm $\Delta(\beta_1-\beta'')$	β''	$\Delta\nu/R$	$(\Delta\nu/R)^{1/2}$
17	4394.60	0.0546	4385.49*	0.52	0.72
19	3446.80	0.0635	3434.15	0.98	0.99
20	3083.43	0.0610	3075.84	0.824	0.908
21	2773.94	0.0482	2765.88	0.835	0.914
22	2508.98	0.0511	2501.32	1.109	1.053
23	2279.72	0.0484	2272.28	1.272	1.179
24	2080.59	0.0460	2073.46*	1.441	1.225

TABLE V.

Elem.	β_1	cm $\Delta(\beta_1-\beta^{IV})$	β^{IV}	$\Delta\nu/R$	$(\Delta\nu/R)^{1/2}$
19	3446.80	0.249	3397.07*	3.870	1.967
20	3083.43	0.295	3041.45*	4.012	2.006
21	2773.94	0.244	2738.10*	4.264	2.065

* Indicates new lines discovered in this research.

TABLE VI.

Elem.	β_1	cm $\Delta(\beta_1-\beta''')$	β'''	$\Delta\nu/R$	$(\Delta\nu/R)^{1/2}$
19	3446.80	0.211	3404.69	3.27	1.80
20	3083.43	0.2520	3047.58	3.445	1.854
21	2773.94	0.2077	2743.44	3.617	1.901
22	2508.98	0.1692	2483.55	3.688	1.920
23	2279.72	0.1433	2257.69	4.120	2.029
24	2080.59	0.1239	2061.38	4.032	2.008
25	1906.19	0.1040	1889.90	4.088	2.022
26	1753.01	0.0990	1737.39	4.630	2.152
27	1617.44	0.0920	1602.97	5.012	2.245

TABLE VII.

Elem.	β_1	cm $\Delta(\beta_1-\beta^{V})$	β^{V}	$\Delta\nu/R$	$(\Delta\nu/R)^{1/2}$
17	4394.60	0.0228	4390.8*	0.18	0.42
19	3446.80	0.0230	3442.2*	0.36	0.60
20	3083.43	0.0227	3080.20*	0.34	0.58

α-Satellites referred to $K\alpha_2$

TABLE VIII.

Elem.	α_2	cm $\Delta(\alpha_2-\alpha')$	α'	$\Delta\nu/R$	$(\Delta\nu/R)^{1/2}$
12	9867.75	0.1194	9830.31	0.3503	0.5919
13	8319.40	0.0917	8287.75	0.4168	0.6456
14	7109.17	0.2295	7079.99	0.5261	0.7253
15	6141.71	0.1593	6116.21	0.6161	0.7849
16	5363.75	0.2856	5341.69	0.6988	0.8359
17	4721.36	0.1853	4702.15	0.7853	0.8862
19	3737.06	0.1242	3710.89	1.054	1.026
20	3354.95	0.1085	3340.04*	1.208	1.099
21	3028.40	0.0945	3004.89*	1.342	1.159
22	2746.81	0.0805	2724.97*	1.430	1.196
23	2502.13	0.0731	2491.88*	1.590	1.265

TABLE IX.

Elem.	α_2	cm $\Delta(\alpha_2-\alpha_3)$	α_3	$\Delta\nu/R$	$(\Delta\nu/R)^{1/2}$
12	9867.75	0.208	9802.46	0.611	0.782
13	8319.40	0.1561	8265.48	0.743	0.862
14	7109.17	0.366	7062.51	0.841	0.917
15	6141.71	0.240	6103.25	0.931	0.965
16	5363.75	0.433	5330.18	1.063	1.031
17	4721.36	0.279	4692.39	1.184	1.088
19	3737.06	0.1816	3713.43	1.542	1.241
20	3354.95	0.1581	3333.21	1.760	1.327
21	3028.40	0.1362	3008.92	1.935	1.391
22	2746.81	0.1196	2729.21	2.125	1.458
23	2502.13	0.1059	2486.21	2.317	1.522
24	2288.91	0.0952	2274.36	2.530	1.591
25	2101.49	0.0861	2088.16	2.750	1.658
26	1936.01	0.0841	1922.86	3.197	1.788
27	1789.19	0.0764	1777.15	3.428	1.852
28	1658.35	0.0688	1647.43	3.618	1.902
29	1541.16	0.0667	1530.52	4.083	2.021
30	1435.87	0.0615	1426.01	4.357	2.087
31	1340.87	0.0560	1331.86	4.565	2.137
32	1255.21	0.0530	1246.66	4.947	2.224

TABLE X.

Elem.	α_2	cm $\Delta(\alpha_2-\alpha_4)$	α_4	$\Delta\nu/R$	$(\Delta\nu/R)^{1/2}$
12	9867.75	0.253	9788.30	0.743	0.862
13	8319.40	0.190	8253.75	0.859	0.951
14	7109.17	0.445	7052.34	1.023	1.012
15	6141.71	0.296	6094.23	1.149	1.071
16	5363.75	0.521	5323.26	1.283	1.132
17	4721.36	0.336	4686.23	1.428	1.198
19	3737.06	0.214	3709.22	1.824	1.350
20	3354.95	0.185	3329.50	2.061	1.436
21	3028.40	0.159	3005.66	2.260	1.503
22	2746.81	0.138	2726.46	2.458	1.568
23	2502.13	0.1219	2483.80	2.667	1.633
24	2288.91	0.1084	2272.35	2.881	1.697
25	2101.49	0.0978	2086.35	3.123	1.767

TABLE XI.

Elem.	α_2	cm $\Delta(\alpha_2-\alpha_5)$	α_5	$\Delta\nu/R$	$(\Delta\nu/R)^{1/2}$
12	9867.75	0.426	9742.65	1.255	1.120
13	8319.40	0.314	8210.80	1.429	1.195
14	7109.17	0.730	7015.40	1.690	1.300

TABLE XII.

Elem.	α_2	cm $(\alpha_2-\alpha_6)$	α_6	$\Delta\nu/R$	$(\Delta\nu/R)^{1/2}$
12	9867.75	0.503	9718.35	1.483	1.218
13	8319.40	0.377	8189.90	1.717	1.310
14	7109.17	0.804	7005.77	1.822	1.366

TABLE XIII.

Elem.	α_2	cm $\Delta(\alpha_2-\alpha_3')$	α_3'	$\Delta\nu/R$	$(\Delta\nu/R)^{1/2}$
14	7109.17	0.388	7058.77	0.892	0.945
15	6141.71	0.257	6100.51*	0.995	0.997
16	5363.75	0.462	5327.90	1.135	1.066
17	4721.36	0.300	4690.20*	1.274	1.129

THE $K\alpha'$-SATELLITE

Four new lines were found in the $K\alpha'$ series, extending the series from K (19) to Va (23). However, there is a possibility of finding this satellite in a few more elements above V a(23) with very long exposures, since this line presents the behavior of gradually fading out in the elements of higher atomic number. Deodhar[2] reports, for Si (14), two components of $K\alpha'$. However, the doublet character of $K\alpha'$ is very problematic since this structure was noted in only one element and since Deodhar's careful reexamination of Bäcklin's[3]

[2] Deodhar, Proc. Roy. Soc. **A131**, 633 (1931).
[3] Bäcklin, Zeits. f. Physik **33**, 547 (1925).

original plate on silicon failed to show any trace of structure in the $K\alpha'$ line. Moreover, no trace of the doublet nature of $K\alpha'$ was found on any spectrogram of this survey although the dispersion of the author's spectrograph was greater than Deodhar's. Since quartz crystals were used in both spectrographs, the dispersion ratio of the two spectrographs is the ratio of the distances from slit to photographic plate, namely, 36.728/27.596. Intensity considerations can scarcely be urged for the failure of other observers to find the structure of $K\alpha'$ since silicon is one of the very convenient elements to handle on the focal spot.

The $K\alpha_{3,4}$ Doublet

The $K\alpha_{3,4}$ doublet was measured over the range of elements from Mg(12) to Ge(32). The extension of this doublet from Zn(30) to Ge(32) confirms the findings of Richtmyer and Ramburg[4] who first detected and measured the line in any element above Zn(30).

Resolution of $K\alpha_{3,4}$ has been reported in the literature from Na(11) to Ca(20). However, the plates obtained on this spectrograph, with the rather large dispersion noted above, show distinctly the components of the doublet from Ca(20) to Mn(25). Resolution of $K\alpha_{3,4}$ above the element Mn (25) was attempted with second order exposures, but a 22 hour exposure on Co(27) with 15 k.v. and 20 m.a. did not yield the resolution expected. The two values of $K\alpha_3$ and $K\alpha_4$ for Cu(29), Fig. 2, were taken from data obtained by Richtmyer and Taylor[5] on a double crystal x-ray spectrometer. It is seen that the two points thus determined fit the semi-Moseley diagrams plotted from the data of this survey.

That the $K\alpha_3$ line consists of two components was first observed by Bäcklin[3] in the case of Si(14). Deodhar[2] confirms the doublet nature of $K\alpha_3$ for Si (16). However, the doublet structure of $K\alpha_3$ extends over more elements than reported by Bäcklin and Deodhar. During this work, the complete resolution of $K\alpha_3$ into its components has been observed in five elements, from Al(13) to Cl(17). To show the components of $K\alpha_3$ for Al(13) it was necessary to take a spectrogram with a quartz crystal, for which the Bragg angle was $78°{-}22'$. Although the value of $K\alpha_3$, reported in Table IX, was obtained from a spectrogram of Al, with a gypsum crystal, on which $K\alpha_3$ was not resolved into its components, the two points on the semi-Moseley diagram, Fig. 2, were calculated from the separation of $K\alpha_3$ and $K\alpha_3'$ on the Al-quartz plate. The components of $K\alpha_3$ for the elements Si(14), P(15) and S(16), are shown on the tracings of the microphotometer records of these plates, Fig. 1.

Contrary to the observation of Deodhar,[2] on the $K\alpha_4$ line of Si(14), no indication of structure in this line was found on any spectrogram. Surely the aluminum spectrogram, with the quartz crystal, on which the $K\alpha'$, $K\alpha_3'$ $K\alpha_3$ and $K\alpha_4$ lines were widely separated, should have put in evidence the components of $K\alpha_4$ if they could be resolved. However, no trace of structure was noted.

[4] Richtmyer and Ramburg, Phys. Rev. **35**, 661 (1930).
[5] Richtmyer and Taylor, Phys. Rev. **36**, 1044 (1930).

Microphotometer records, tracings of which are shown in Fig. 1, show a reversal in the relative intensities of $K\alpha_3$ and $K\alpha_4$ between the elements P(15) and S(16). For the elements Mg(12), Al(13), Si(4)1 and P(15) $K\alpha_3$ is definitely more intense than $K\alpha_4$, although the difference decreases as the atomic number of the element increases. From S(16) to Mn(25), the range of elements for which $K\alpha_3$ and $K\alpha_4$ are resolved, $K\alpha_4$ is the more intense line. While it is known that chemical combination can produce changes in the relative intensity[6] of some lines, the reversal in the relative intensity of $K\alpha_3$ and $K\alpha_4$ is an atomic phenomenon; the reversal still exists if the spectrograms of elements, to be had only in the form of chemical compounds, are disregarded. While the spectrograms of P(15) and S(16) were obtained from compounds of the elements, an examination of the calcium spectrogram, the next

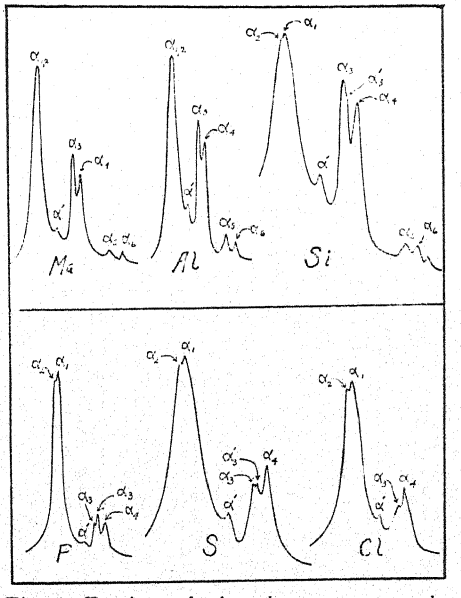


Fig. 1. Tracings of microphotometer records.

element after Si(14) to be had in the pure state, shows the greater intensity of the $K\alpha_4$ line.

The reversal in the relative intensity of the components of the $K\alpha_{3,4}$ doublet is all the more significant when compared to the behavior of the components of the diagram doublet $K\alpha_{1,2}$ in which the intensity ratio of the $K\alpha_1$ line to the $K\alpha_2$ line is 2:1 for the whole range of elements over which measurements have been made.

THE $K\alpha_5$ AND $K\alpha_6$ SATELLITES

The $K\alpha_5$ and $K\alpha_6$ satellites were detected and measured for only three elements Mg(12), Al(13) and Si(14). Hjalmar[7] reports a measurement on

[6] Handbuch der Experimental Physik, p. 45.
[7] Hjalmar, Zeits. f. Physik, 1–2, 439 (1920).

original plate on silicon failed to show any trace of structure in the $K\alpha'$ line. Moreover, no trace of the doublet nature of $K\alpha'$ was found on any spectrogram of this survey although the dispersion of the author's spectrograph was greater than Deodhar's. Since quartz crystals were used in both spectrographs, the dispersion ratio of the two spectrographs is the ratio of the distances from slit to photographic plate, namely, 36.728/27.596. Intensity considerations can scarcely be urged for the failure of other observers to find the structure of $K\alpha'$ since silicon is one of the very convenient elements to handle on the focal spot.

The $K\alpha_{3,4}$ Doublet

The $K\alpha_{3,4}$ doublet was measured over the range of elements from Mg(12) to Ge(32). The extension of this doublet from Zn(30) to Ge(32) confirms the findings of Richtmyer and Ramburg[4] who first detected and measured the line in any element above Zn(30).

Resolution of $K\alpha_{3,4}$ has been reported in the literature from Na(11) to Ca(20). However, the plates obtained on this spectrograph, with the rather large dispersion noted above, show distinctly the components of the doublet from Ca(20) to Mn(25). Resolution of $K\alpha_{3,4}$ above the element Mn (25) was attempted with second order exposures, but a 22 hour exposure on Co(27) with 15 k.v. and 20 m.a. did not yield the resolution expected. The two values of $K\alpha_3$ and $K\alpha_4$ for Cu(29), Fig. 2, were taken from data obtained by Richtmyer and Taylor[5] on a double crystal x-ray spectrometer. It is seen that the two points thus determined fit the semi-Moseley diagrams plotted from the data of this survey.

That the $K\alpha_3$ line consists of two components was first observed by Bäcklin[3] in the case of Si(14). Deodhar[2] confirms the doublet nature of $K\alpha_3$ for Si (16). However, the doublet structure of $K\alpha_3$ extends over more elements than reported by Bäcklin and Deodhar. During this work, the complete resolution of $K\alpha_3$ into its components has been observed in five elements, from Al(13) to Cl(17). To show the components of $K\alpha_3$ for Al(13) it was necessary to take a spectrogram with a quartz crystal, for which the Bragg angle was $78°-22'$. Although the value of $K\alpha_3$, reported in Table IX, was obtained from a spectrogram of Al, with a gypsum crystal, on which $K\alpha_3$ was not resolved into its components, the two points on the semi-Moseley diagram, Fig. 2, were calculated from the separation of $K\alpha_3$ and $K\alpha_3'$ on the Al-quartz plate. The components of $K\alpha_3$ for the elements Si(14), P(15) and S(16), are shown on the tracings of the microphotometer records of these plates, Fig. 1.

Contrary to the observation of Deodhar,[2] on the $K\alpha_4$ line of Si(14), no indication of structure in this line was found on any spectrogram. Surely the aluminum spectrogram, with the quartz crystal, on which the $K\alpha'$, $K\alpha_3'$ $K\alpha_3$ and $K\alpha_4$ lines were widely separated, should have put in evidence the components of $K\alpha_4$ if they could be resolved. However, no trace of structure was noted.

[4] Richtmyer and Ramburg, Phys. Rev. **35**, 661 (1930).
[5] Richtmyer and Taylor, Phys. Rev. **36**, 1044 (1930).

Microphotometer records, tracings of which are shown in Fig. 1, show a reversal in the relative intensities of $K\alpha_3$ and $K\alpha_4$ between the elements P(15) and S(16). For the elements Mg(12), Al(13), Si(4)1 and P(15) $K\alpha_3$ is definitely more intense than $K\alpha_4$, although the difference decreases as the atomic number of the element increases. From S(16) to Mn(25), the range of elements for which $K\alpha_3$ and $K\alpha_4$ are resolved, $K\alpha_4$ is the more intense line. While it is known that chemical combination can produce changes in the relative intensity[6] of some lines, the reversal in the relative intensity of $K\alpha_3$ and $K\alpha_4$ is an atomic phenomenon; the reversal still exists if the spectrograms of elements, to be had only in the form of chemical compounds, are disregarded. While the spectrograms of P(15) and S(16) were obtained from compounds of the elements, an examination of the calcium spectrogram, the next

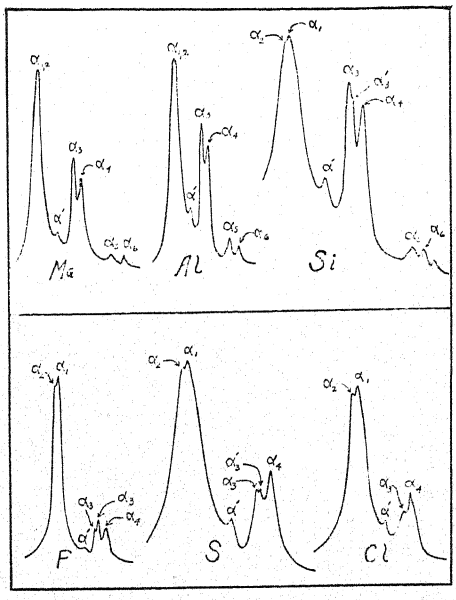


Fig. 1. Tracings of microphotometer records.

element after Si(14) to be had in the pure state, shows the greater intensity of the $K\alpha_4$ line.

The reversal in the relative intensity of the components of the $K\alpha_{3,4}$ doublet is all the more significant when compared to the behavior of the components of the diagram doublet $K\alpha_{1,2}$ in which the intensity ratio of the $K\alpha_1$ line to the $K\alpha_2$ line is 2:1 for the whole range of elements over which measurements have been made.

THE $K\alpha_5$ AND $K\alpha_6$ SATELLITES

The $K\alpha_5$ and $K\alpha_6$ satellites were detected and measured for only three elements Mg(12), Al(13) and Si(14). Hjalmar[7] reports a measurement on

[6] Handbuch der Experimental Physik, p. 45.
[7] Hjalmar, Zeits. f. Physik, **1-2**, 439 (1920).

$K\alpha_5$ for S(16) and, recently Deodhar[2] reports measurements on $K\alpha_5$ and $K\alpha_6$ for P(15), S(16) and Cl(17).

The $K\beta_\eta$ Satellite

The β_η satellite, a very faint diffuse line, probably complex in structure, at least in the lower elements for which it can be found, was detected and measured in six elements, K(19) to Cr(24). This satellite is situated upon the long wave-length side of $K\beta_1$ and, because of its faint diffuse character measurements are difficult. The accuracy with which its wave-length can be determined compares unfavorably with that of the other lines, probably reaching an error of three percent of the measured wave-length difference between $K\beta_1$ and $K\beta_\eta$. Beuthe[8] has measured this line from Va(23) to Ge(32). The combined results of the two experiments give this satellite a range from K(19) to Ge(32).

The $K\beta'$ Satellite

The β'-satellite, upon the long wave-length side and close to $K\beta_1$ was detected and measured over the range of elements from Ca(20) to Ni(28). The present work adds no element to this series, values of which are reported for the elements as low as Si (14), although no difficulty was experienced in verifying it. Dolejsek and Felcakova[9] present data to show that the $K\beta'$ line is a complex line. For elements below Mn (25) these authors claim to have found that $K\beta'$ consists of two unresolved doublets which in the case of the higher elements are superimposed. The appearance of the $K\beta'$ line on the spectrograms obtained in the course of this work does not warrant agreement with this conclusion. However, densitometer records show that the intensity ratio $K\beta_1{:}K\beta'$ becomes greater for oxides than for free elements; hence, as oxides were used in the spectrograms of the elements Ca (20) and Se (21) and Ti (22), where the dispersion was greatest, it may be that the $K\beta'$ lines were not heavy enough to bring out the structure.

The β''-Satellite

The β''-satellite between $K\beta_1$ and $K\beta_2$ was measured from Cl (17) to Cr (24). These data add two more elements to the series as found by Druyvesteyn,[10] *viz.*, the elements Cr(24) and Cl(17). Kawata,[11] however, obtained this satellite on spectrograms from Fe(26) to Zn(30). Hjalmar[12] reports a wave-length value of 4390.8 (x.u.) for the $K\beta''$ line of Cl(17), while the chlorine spectrogram obtained during this work showed two lines of wave-length values 4390.8 and 4385.5 (x.u.). When the $(\Delta\nu/R)^{1/2}$ values corresponding to these wave-lengths are added to the semi-Moseley diagrams it is the 4385.5 value which falls on the graph of the $K\beta''$ series. The 4390.8 line belongs to a

[8] Beuthe, Zeits. f. Physik, **60**, 603 (1929).
[9] Dolejsek and Felcakova, Nature **123**, 412 (1929).
[10] Druyvesteyn, Zeits. f. Physik **43**, 707 (1927).
[11] Kawata, Mem. Kyoto Imp. Univ. **A13**, No. 6, 1930.
[12] Hjalmar, Zeits. f. Physik **7**, 341 (1921).

series, here called $K\beta^{V}$, which apparently starts at Ca(20) and extends downward. The combined results of all measurements on the $K\beta''$ lines give it a range from Cl(17) to Zn(30), with the exception of Mn(25).

The β'''-Satellite

The β'''-satellite upon the short wave-length side and close to $K\beta_1$ was measured over the elements Cl(17) to Co(27). Kawata[11] measured this line for the element Ni(28). Beuthe[9] measured a line which he called $K\beta_y$ for several of the elements from Va(23) to Y(39). The values which he reports for $K\beta_y$ from Va(23) to Ni(28) coincide with other reported values of $K\beta'''$ so it has been assumed that $K\beta'''$ extends to Y(39). However, the points above

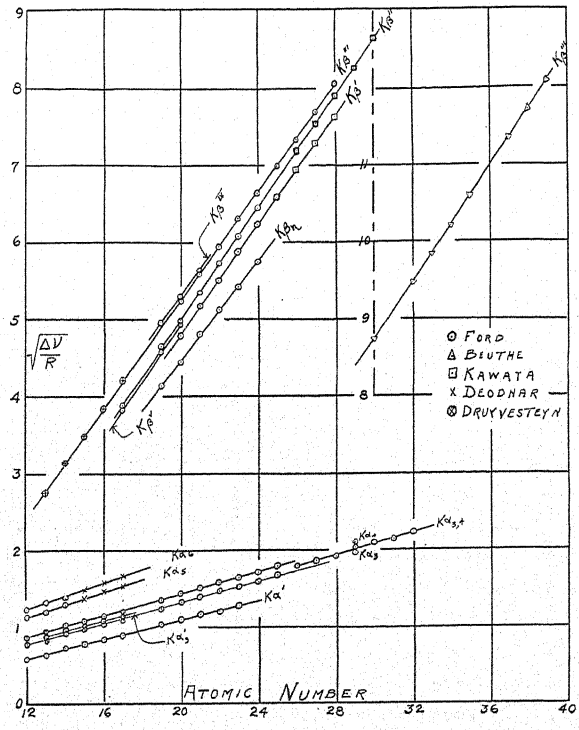


Fig. 2. The semi-Moseley diagrams of all the K-satellites referred to $K\alpha_2$.

Cu(29) may constituted a new series since the line in this range of elements appears on the long wave-length side of $K\beta_2$. Moreover, the semi-Moseley diagram of the points above Cu(29) has a different slope from the semi-Moseley graph of the points below Cu(29).

The β^{IV}-Satellite

This new line was found on the spectrograms of Ca(20), Sc(21) and K(19), all of which were run with compounds of the elements on the focal spot. Although chemical combination throws some doubt upon the validity of this series it presents the same behavior as all the β-satellites. See Fig. 2.

THE β^{V}-SATELLITE

While this satellite has been measured on only three spectrograms, its semi-Moseley diagram gives it the behavior of the other β-satellites. Again, the factor of chemical combination may be argued against its validity, but a recent spectrogram of pure Si(14), not included in the present work, shows both $K\beta''$ and $K\beta^{V}$. The fact that $K\beta^{V}$, when it first appears in calcium, is more intense than $K\beta''$ is against the view that it should be regarded as a component of $K\beta''$.

DISCUSSION OF RESULTS

In an experimental survey, it would take us too far afield to analyze the various theories which have been proposed for the origin of the satellite lines. However, the following references[13] to some of the principal papers will furnish

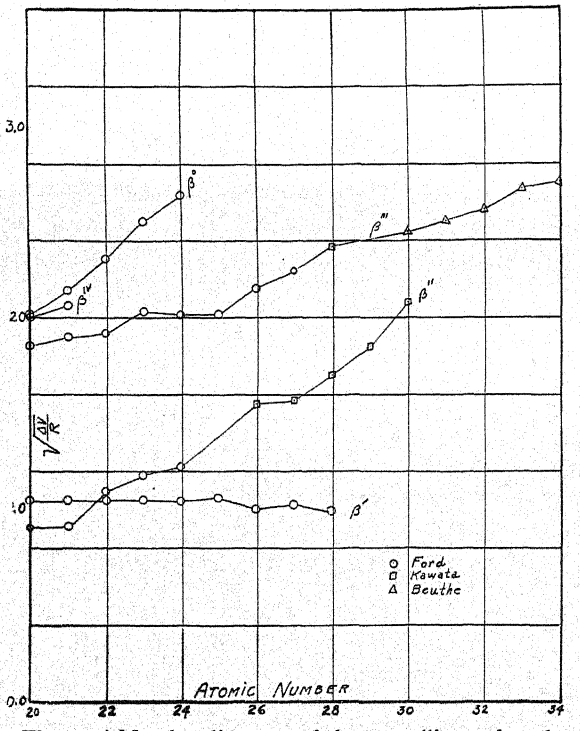


Fig. 3. The semi-Moseley diagrams of the β-satellites referred to $K\beta_1$.

a guide to the literature. The relation which, perhaps, correlates more experimental data than any other is that of the linearality[13] of the semi-Moseley diagrams. All the α-satellites, at least qualitatively, obey this law if $K\alpha_1$ or $K\alpha_2$ is taken to be the parent line. It makes little difference whether $K\alpha_1$ or

[13] Wentzel, Ann d. Physik **66**, 437 (1921); Coster, Phil. Mag. **43**, 1088 (1922); Coster, Phil. Mag. **43**, 1105 (1922); Coster and Druyvesteyn, Zeits. f. Physik **40**, 765 (1927); Druyvesteyn, Zeits. f. Physik **43**, 707 (1927); Druyvesteyn, Dissertation, Groningen; Richtmyer, J. F. Inst., **208**, 325 (1929); Beuthe, Zeits. f. Physik **60**, 603 (1930); Deodhar, Proc. Roy. Soc. **A131**, 476 (1931).

$K\alpha_2$ is chosen for the reference line; from the experimental standpoint, the probable error in the comparator reading between the satellites and $K\alpha_2$ seem a little less than the p.e. when $K\alpha_1$ is made the reference line. On the other hand the β-satellites, when referred to $K\beta_1$, about which they cluster, present poor agreement with the linear relation. Fig. 3 shows the appearance of the semi-Moseley diagrams of the β-satellites when referred to $K\beta_1$.

Deodhar,[13] seeking for a reference line which would give a better linear relation, found the desired improvement in the semi-Moseley diagrams of the $K\beta'''$, $K\beta_3$ and $K\beta_\eta$ lines by referring them to the $K\beta_1$ line. A theoretical basis for thls mode of representation can be found in an extension of the double electron transition hypothesis, which, as first proposed by Richtmyer,[13] was limited to the simultaneous transitions of two electrons, one between inner levels, and the other between peripheral levels, to include the possibility of both transitions among the inner levels. Beuthe's[13] suggestion, which is qualitatively correct, that the frequency of $K\beta'''$ derives from the addition of the frequencies of $K\alpha_1$ and $L\alpha_1$, is a specific statement of this extension.

The fact that $K\alpha_2$ serves for a reference line for the β-satellites, as well if not better than $K\alpha_1$, throws doubt upon the physical significance of this mode of representation. A recent paper by Hirsh[14] shows that the improved linearality in the semi-Moseley diagrams of $K\beta'''$, $K\beta_3$ and $K\beta_\eta$ may result from the fact that the $(\Delta\nu/R)^{1/2}$, with $K\alpha_1$ as the reference line, are larger than the $(\Delta\nu/R)^{1/2}$ values with $K\beta_1$ as the parent line. However, the improvement in the semi-Moseley diagrams of the β-satellites is not limited to the lines selected by Deodhar, but extends to all the β-satellites.

Regardless of the physical significance which may be attached to the various modes of representation, the semi-Moseley diagrams referred to $K\alpha_2$ are of great value in the experimental study and classification of the satellite lines. Two points, already mentioned, serve to illustrate this advantage. (1) Since each satellite series is characterized by a definite slope, the break which occurs in the $K\beta'''$ series at the element Ni(28) is indicative of two separate series. This observation is also confirmed by the fact that $K\beta'''$, from Ni(28) to Mg(12), appears on the long wave-length side of $K\beta_2$ while the $K\beta_y$ line, measured by Beuthe[13] from Zn(30) to Y(39), appears on the short wave-length side of $K\beta_2$. The assumption that the $K\beta_y$ line of Beuthe is an extension of $K\beta'''$ into the higher elements may be wrong, and any critical examination of the origin of the $K\beta'''$ line should be limited to the points below Cu(29). (2) The two lines, 4390.8 and 4385.5 (x.u.) of Cl(17) are definitely classified by the two semi-Moseley diagrams to which they belong.

[14] Hirsh, Phys. Rev. **40**, 151 (1932).

Series and Term Values in the Arc Spectrum of Tellurium

By J. E. RUEDY
Cornell University

(Received July 21, 1932)

Tellurium was excited in an electrodeless discharge tube in such a manner that the arc lines could be distinguished from the spark. The spectrum was photographed in the visible and infrared, and series were found corresponding to those given in Fowler's *Report on Series in Line Spectra* for the first three elements of the oxygen group. From the limit thus established, which is the lowest level of Te II ($5p^3:{}^4S_{3/2}$), term values are given down to the lowest level of Te I ($5p^4:{}^3P_2$). The ionizing potential is found to be 72,667 cm^{-1} or 8.96 volts. A list of the wave-lengths of all the stronger lines, in addition to those classified, is given.

WHILE continuing the work on selenium,[1] using an electrodeless discharge tube, it was found that conditions could be obtained which gave an apparently perfect differentiation between arc and spark lines, and there seemed to be no reason why the method could not be applied with equal success to the study of the tellurium arc spectrum, for which no analysis had ever been made in the long wave-length region.

Such was found to be the case.

Apparatus and Procedure

A cylindrical fused quartz tube 8″×1-3/4″, with plane windows on the ends, was pumped to as low a pressure as possible (about 10^{-5} mm Hg) and baked at 550°C for two hours. Some tellurium was then slid in from the side tube, through which the exhaustion was taking place, which had been outside the oven during the baking process, and was vaporized with a bunsen flame, being allowed to recondense on cool parts of the tube. This was done several times and the tube sealed off.

A silver ribbon (it must be a material which will stand a temperature of 500°) was wound around the tube and the whole mounted in an electric oven, with windows opposite the ends of the tube. The terminals of the silver coil were connected to a condenser through a spark gap. A 5 k.v.a., 100 k.v. transformer supplied the power. A thermometer was placed in the oven with its bulb touching the tube in its cooler region (as shown by condensation of tellurium).

When at room temperature, the tube might be made to flash a few times by turning on the power, but it was generally black. As the temperature was raised, a steady discharge would begin at about 340° and continue as a bright ring type to about 470°, where there was a sudden change to a dull bluish glow throughout the whole tube, sometimes with bright scintillations scattered through it with more or less axial symmetry.

Numerous photographs were taken under various conditions of temperature and electrical circuit, and widely varying types of spectra were produced.

[1] R. C. Gibbs and J. E. Ruedy, Phys. Rev. **40**, 204 (1932).

Spark lines were the easiest to obtain and were always present, except perhaps in the high temperature stage, where nothing but more or less continuous band structure could be made out. Some beautiful bands were obtained once in the region λ5500. In general, as the temperature was being raised from 340° to 470°, the arc lines would increase and the spark lines decrease in intensity.

The circuit finally adopted was an oil condenser of 0.003 mf. capacity, a spark gap of 3/8″ between brass rods mounted in a glass tube through which air was blown transversely, and 15 turns of 1/4″×1/32″ ribbon, spaced

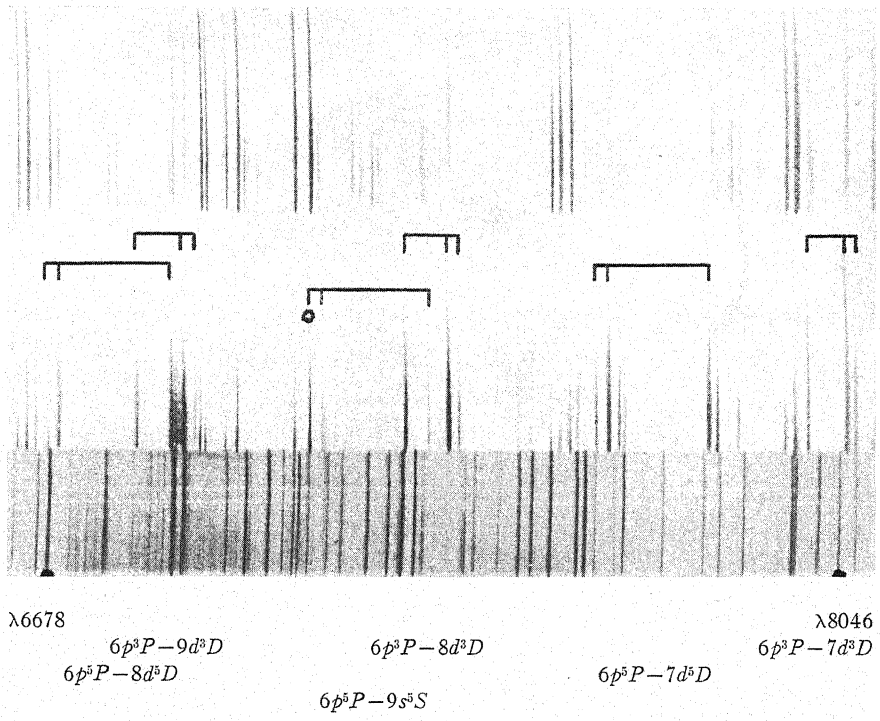


Fig. 1.

1/8″, around the tube. The procedure was to take one exposure at about 370° and another beside it on the plate, of equal length, at about 470°, with the iron comparison spectrum next to it. A Zeiss 3-prism spectrograph was used for all pictures, and an image of the bright ring in the discharge tube was focused on the slit in such a manner that the outer edge just overlapped the comparison prism. The different parts of the length of a spectrum line on the plate show the radiation coming from regions of different distance from the axis of the tube. The photographic plate was so diaphragmed that the length of a line would just cover the region from the center of the tube to one edge. Fig. 1 is an enlargement of such a plate. Due to the curvature of the lines and the shifting of the plate holder, the tops of the 470° lines do not match up with the bottoms of the 370° lines, but under a comparator this causes no

difficulty. Most of the stronger lines, of whose which are intensified at the higher temperature, have been classified and definitely belong to the tellurium arc spectrum. The first members of the triplet and quintet series of *OI*, and also *Hα* are present and behave similarly to the tellurium arc lines. Mercury is also weakly present as an impurity, but the intensity of its lines is somewhat diminished at the higher temperature.

The spectrum was photographed from λ3750 to λ11,287, but very few arc lines were found below λ5000, and careful measurement was not made in that region. Four types of Eastman plates were used. They were: hypersensitive panchromatic, λ5000—λ6680; infrared sensitive N, λ6680—8050; infrared sensitive A, λ8050—λ9080; infrared sensitive B, λ9080—λ11,287. The maximum length of exposure was seven hours in the longest wave-length region, though the crucial lines at λ9700 and λ10,000 were obtained in a few minutes. The new region opened to photography by the recent infrared B plates was lacking in standards, but Dr. Meggers of the Bureau of Standards, kindly supplied a list of iron wave-lengths up to λ10,500, and the mercury line at λ11,287 was used beyond that.

The dispersion varied from 12A per mm at λ5000 to 135A per mm at λ11,000. Wave-lengths were calculated using the Hartman formula, the entire region of sensitivity of each plate being covered at once, and a correction curve of intermediate iron standards plotted. No deviation greater than 1A was found, except for the range λ9000 to λ11,287, where it was as large as 4A. The calculations thus could be corrected to at least the accuracy of the settings on the lines. Throughout the entire region the accuracy of the measurements should be about one frequency number.

Results

The lines of tellurium, analogous to those in oxygen, sulfur, and selenium, observed and classified by Runge and Paschen[2] in 1897, and listed in Fowler's *Report* have never been observed. By extrapolation from this known group, the positions of the tellurium lines can be roughly predicted. The only wave-lengths published for that region[3] are almost meaningless. The present work indicates about 180 lines as belonging to the arc spectrum of tellurium between λ5000 and λ11,100. Some 60 of these have been classified and are shown in Table I, the arrangement of which has been made similar to the tabulations in Fowler. In both the triplet and quintet diffuse series the lines are generally obviously multiple and the wave-lengths hence inexact. Within the limits of this inexactness, both series are nearly Rydbergian, but the limits thus determined are necessarily uncertain. In the case of the quintet sharp series, the lines are sharp and the separations consistent. (The absence of one of the lines in the second member is due to a strong spark line falling exactly where it should be.) A Hicks formula was adjusted to fit the $^5P_2 - {}^5S_2$ frequencies for $n = 9$, 10, and 11,

[2] C. Runge and F. Paschen, Astrophys. J. **8**, 70 (1898).
[3] J. C. McLennan, H. G. Smith, and C. S. Peters, Trans. Roy. Soc. Canada **19**, 39 (1925).

$$\nu = 18{,}475.9 - \frac{109{,}737}{(n - 4 + 0.0232 + 0.1057/(n-4))^2},$$

TABLE I.

$6s^5S_2 - np^5P_{123}$

Int.	λ (air)	ν (vac.)	Δν	n
30	10089.0	9909.1		
40	10049.3	9948.1	39.2	
50	9721.2	10284.0	335.7	6
4	5178.9	19303.7		
7	5148.7	19417.0	113.3	
8	5083.0	19667.9	250.9	7

$6p^5P_{123} - nd^5D_{(01234)}$

Int.	λ (air)	ν (vac.)	Δν	n
15	7759.1	12884.6		
6	7754.4	12892.4	337.0	7
10	7556.8	13229.4		
6b	7552.8	13236.4	37.5	
5	7531.5	13273.9		
4	6843.9	14607.5		
20b	6837.6	14621.0	336.2	
8b	6690.0	14943.7		8
4b	6686.7	14951.0	43.3	
4	6670.6	14987.0		
3	6409.4	15597.8		
8	6405.9	15606.3	337.9	9
8bs	6273.5	15935.7	44.8	
6	6255.9	15980.5		
2b	6162.4	16223.0		
6b	6160.2	16228.8	336.9	10
3	6034.9	16565.7	38.8	
4b	6020.8	16604.5		
3b	6005.0	16648.2	334.9	
1bs	5886.5	16983.3		11
3bs	5874.6	17017.7	34.4	

b—broad
bl—broadened toward longer λ
bs—broadened toward shorter λ

$6p^5P_{123} - ns^5S_2$

Int.	λ (air)	ν (vac.)	Δν	n
8	8771.2	11397.8	335.8	
12	8521.4	11732.0	40.3	8
8	8492.2	11772.3		
4	7230.3	13826.9	336.4	9
4	7058.6	14163.3		
4	6606.3	15132.9	335.8	
4	6462.9	15468.7	38.8	10
3	6446.7	15507.5		
2	6277.7	15925.0	335.7	
1	6148.1	16260.7	39.2	11
1	6133.3	16299.9		

$6s^3S_1 - np^3P_{120}$

Int.	λ (air)	ν (vac.)	Δν	n
1	11084.5	9019.2	140.8	
1	10914.0	9160.0	30.5	6
0	10877.8	9190.5		
8	5789.1	17269.1	59.8	
6	5769.1	17328.9	107.6	7
7	5733.5	17436.5		

$6p^3P_{120} - nd^3D_{(123)}$

Int.	λ (air)	ν (vac.)	Δν	n
8	10149.2	9850.4	31.1	
8	10117.2	9881.5	138.2	6
15	9977.6	10019.7		
10bs	8082.5	12369.0	32.4	
30bs	8061.4	12401.4	137.6	7
20	7972.9	12539.0		
8	7280.9	13730.8	32.9	
20bl	7263.5	13763.7	138.5	8
15bl	7191.1	13902.2		
3b	6870.3	14551.4	33.1	
20bl	6854.7	14584.5	138.9	9
10b	6790.0	14723.4		
3b	6628.7	15081.8	34.8	
8bl	6613.4	15116.6	138.2	10
6bl	6553.3	15254.8		
1b	6469.5	15452.8	30.7	11
7b	6456.7	15483.5		
8b	6349.7	15744.4		12
8bs	6273.5	15935.7		13

in which the number 18,475.9 is the limit. For $n=8$, the frequency calculated was 52.2 larger than the observed value. Doing precisely the same for the corresponding lines of selenium, the limit obtained was 10 greater than that established by more accurate means, and the frequency calculated for the transition from the next lower term was 51.2 larger than the observed value. From this similarity it seems that the limit of the tellurium series should be 18,466, which is not at variance with the roughly obtained limit of the quintet diffuse series. McLennan, McLay, and McLeod[4] have established the separation of the $6s^5S_2$ and the $6s^3S_1$ terms through observations in the ultraviolet, and it is by this means that the triplet principle and diffuse series are brought into the term scheme, rather than by the use of a limit of uncertain accuracy, which, however, agrees well enough with the limit thus indirectly set. Table II gives the terms so far identified, including those of McLennan,[4] and also indicates those to be expected, which go to the ^2D and ^2P limits. Doubtless some of the 120 remaining unclassified lines are transitions involving these terms, but none of them has been identified in sulfur or selenium, and it is a long way to extrapolate from oxygen. The ultraviolet wave-lengths given by McLennan,[4] and by LaCroute[6] might be expected to be of assistance here, but nothing conclusive has been found, and another investigation of this region is proposed before further analysis is attempted. Table III gives the wave-lengths, in order, of all the classified lines, and the stronger of the unclassified ones which are thought to belong to the tellurium arc spectrum. All the terms listed under "Transition" are built on the ^4S limit. Intensities are comparable only over short wave-length ranges.

The separations of the $6p^5P_{123}$ levels show considerable departure from LS coupling, while those of the $6p^3P_{012}$ are extremely irregular. The partially resolved ^5D terms seem to show little uniformity as they approach their limit, which was likewise the case in selenium. It would be interesting to examine these more closely, but no instrument of sufficient resolving power was available at the time this research was in progress, to make the attempt worth while.

The absence of any triplet series in Runge and Paschen's[2] observations on sulfur and selenium (the terms listed as triplets in Fowler's *Report* are the quintets) would lead one to expect them to be weak in tellurium, whereas they are nearly as strong as the quintets. The possibility that the series here listed as $^3P-{}^3D$ going to the ^4S limit, is a series going to one of the doublet limits, seems to be ruled out by the narrowness of the separation of the terms, if for no other reason.

The second members of both the triplet and quintet principal series were chosen because they were the only lines on the plate in the expected regions.

With the quite complete analysis of the oxygen spectrum[7] as a starting

[4] J. C. McLennan, A. B. McLay, and J. H. McLeod, Phil. Mag. **4**, 486 (1927).
[5] J. C. McLennan and M. F. Crawford, Nature **124**, 874 (1929).
[6] M. P. LaCroute, Jour. Phys. Rad. **9**, 182 (1928).
[7] R. Frerichs, Phys. Rev. **34**, 1239 (1929); and Phys. Rev. **36**, 398 (1930). J. J. Hopfield, Phys. Rev. **37**, 160 (1931).

TABLE II.

$5s^24d^{10}5p^3$	$5p$	$^3P_2$:72667 $^3P_0$:67960 $^3P_1$:67916	$^1D_2$:62108	$^1S_0$:23199 (McLennan[5])
		$4s^24d^{10}5p^3:{}^4S$	$4s^24d^{10}5p^3:{}^2D$	$4s^24d^{10}5p^3:{}^2P$
	$6s$	$^5S_2$:28414 $^3S_1$:26014	^3D ^1D	^3P ^1P
	$6p$	$^5P_1$:18505 $^5P_2$:18466 $^5P_3$:18130 $^3P_1$:16992 $^3P_2$:16854 $^3P_0$:16821	$^3(PDF)$ $^1(PDF)$	$^3(SPD)$ $^1(SPD)$
	$5d$	^5D ^3D	$^3(SPDFG)$ $^1(SPDFG)$	$^3(PDF)$ $^1(PDF)$
	$7p$	$^5P_1$:9110 $^5P_2$:8997 $^5P_3$:8746 ^3P :8745 ^3P :8685 ^3P :8578		
	$6d$	^5D $^3D_{123}$:6972		
	$8s$	$^5S_2$:6734 ^3S		
	$7d$	$^5D_2$:5230 $^3D_{123}$:4453		
	$9s$	$^5S_2$:4303 ^3S		
	$8d$	$^5D_2$:3522 $^3D_{123}$:3090		
	$10s$	$^5S_2$:2997 ^3S		
	$9d$	$^5D_2$:2530 $^3D_{123}$:2269		
	$11s$	$^5S_2$:2205 ^3S		
	$10d$	$^5D_2$:1900 $^3D_{123}$:1737		
	$11d$	$^5D_2$:1483 $^3D_{123}$:1370		

TABLE III.

Int.	λ (air)	ν (vac.)	Transition	Int.	λ (air)	ν (vac.)	Transition
1	11084.5	9019.2	$6s^3S_1-6p^3P_1$	8	7280.9	13730.8	$6p^3P_0-8d^3D$
1	10914.0	9160.0	$6s^3S_1-6p^3P_2$	20bl	7263.5	13763.7	$^3P_2-8d^3D$
0	10877.8	9190.5	$6s^3S_1-6p^3P_0$	4	7230.3	13826.9	$^5P_3-9s^5S_2$
8	10149.2	9850.4	$6p^3P_0-6d^3D$	15bl	7191.1	13902.2	$^3P_1-8d^3D$
8	10117.2	9881.5	$6p^3P_2-6d^3D$	4	7058.6	14163.3	$^5P_2-9s^5S_2$
30	10089.0	9909.1	$6s^5S_2-6p^5P_1$	3b	6870.3	14551.4	$^3P_0-9d^3D$
40	10049.3	9948.1	$6s^5S_2-6p^5P_2$	20bl	6854.7	14584.5	$^3P_2-9d^3D$
15	9977.6	10019.7	$6p^3P_1-6d^3D$	5	6843.9	14607.5	$^5P_3-8d^5D$
14	9955.5	10042.0		20b	6837.6	14621.0	
7	9900.9	10097.3		10b	6790.0	14723.4	$^3P_1-9d^3D$
10	9867.0	10132.0		8b	6690.0	14943.7	$^5P_2-8d^5D$
7bl	9840.5	10159.2		4b	6686.7	14951.0	
8	9783.6	10218.5		4	6670.6	14987.0	$^5P_1-8d^5D$
50	9721.2	10284.0	$6s^5S_2-6p^5P_3$	8	6660.2	15010.4	
5bl	9206.3	10859.1		3b	6628.7	15081.8	$^3P_0-10d^3D$
6	9071.3	11020.7		8bl	6613.4	15116.6	$^3P_2-10d^3D$
8	9042.2	11056.3		4	6606.3	15132.9	$^5P_3-10s^5S_2$
30	9003.7	11103.6		6bl	6553.5	15254.8	$^3P_1-10d^3D$
15	8850.3	11296.0		1b	6469.5	15452.8	$^3P_0-11d^3D$
15	8830.4	11321.4		4	6462.9	15468.7	$^5P_2-10s^5S_2$
6	8789.1	11374.6		7b	6456.7	15483.5	$^3P_1-11d^3D$
8	8771.2	11397.8	$6p^5P_3-8s^5S_2$	3	6446.7	15507.5	$^5P_1-10s^5S_2$
50	8757.8	11415.3		3	6409.4	15597.8	$^5P_3-9d^5D$
20	8700.6	11490.3		8	6405.9	15606.3	
7bl	8632.1	11581.4		8b	6349.7	15744.4	$^3P_2-12d^3D$
5	8599.5	11625.3		2	6277.7	15925.0	$^5P_3-11s^5S_2$
12	8521.4	11732.0	$6p^5P_1-8s^5S_2$	8bs	6273.5	15935.7	$^5P_2-9d^5D$, $^3P_2-13d^3D$
8	8500.8	11760.4		6	6255.9	15980.5	$^5P_1-9d^5D$
8	8492.2	11772.3	$6p^5P_1-8s^5S_2$	2b	6162.4	16223.0	$^5P_3-10d^5D$
7	8469.8	11803.4		6b	6160.2	16228.8	
15	8355.8	11964.2		1	6148.1	16260.7	$^5P_2-11s^5S_2$
10	8291.1	12059.2		1	6133.3	16299.9	$^5P_1-11s^5S_2$
10	8276.6	12078.9		3	6034.9	16565.7	$^5P_2-10d^5D$
10	8251.5	12115.6		4b	6020.8	16604.5	$^5P_1-10d^5D$
10bs	8082.5	12369.0	$6p^3P_0-7d^3D$	3b	6005.0	16648.2	$^5P_3-11d^5D$
30bs	8061.4	12401.4	$6p^3P_2-7d^3D$	1bs	5886.5	16983.3	$^5P_2-11d^5D$
20	7972.9	12539.0	$6p^3P_1-7d^3D$	3bs	5874.6	17017.7	$^5P_1-11d^5D$
5	7819.5	12784.9		8	5789.1	17269.1	$6s^3S_1-7p^3P$
15	7759.1	12884.6	$6p^5P_3-7d^5D$	6	5769.1	17328.9	$6s^3S_1-7p^3P$
6	7754.4	12892.4		7	5733.5	17436.5	$6s^3S_1-7p^3P$
6	7575.7	13196.4		4	5178.9	19303.7	$6s^5S_2-7p^5P_1$
10	7556.8	13229.4	$6p^5P_2-7d^5D$	7	5148.7	19417.0	$6s^5S_2-7p^5P_2$
6b	7552.8	13236.4		8	5083.0	19667.9	$6s^5S_2-7p^5P_3$
5	7531.5	13273.9	$6p^5P_1-7d^5D$				

point, it should be possible to carry on a simultaneous investigation of the other three elements of the group with a much increased effectiveness over an attack on one alone, and such a procedure is now contemplated.

Valuable advice and assistance were rendered during the course of this investigation by Professor R. C. Gibbs and Dr. C. W. Gartlein, for which the author wishes to express his thanks.

The Resonance Fluorescence of Benzene

By G. B. KISTIAKOWSKY AND M. NELLES[1]
Department of Chemistry, Harvard University

(Received July 18, 1932)

The fluorescence of benzene vapor has been studied at pressures varying from 25 to 0.01 mm mercury using, as a monochromatic excitation source, the 2536A mercury line. At the lowest investigated pressures the emission spectrum consists of several narrow line groups. Their spacing shows that emission occurs in transitions from a definite vibrational level of the excited state to various vibrational levels of the normal state. The following vibrational frequencies of the normal benzene molecule have been identified: 160, 793 (uncertain), 988, 1200, 1354, 1663 and 3139 cm^{-1}. The fine structure of the line groups has not been fully resolved. They appear to consist each of two strong lines with several weaker ones grouped around them. The ordinary, high pressure, fluorescence of benzene vapor is interpreted as being due to transitions from the lowest vibrational level of the excited state (or states). This level is reached by molecules as the result of inelastic collisions upon excitation. An apparently continuous emission present at the long wave-length end of the fluorescence spectrum at higher vapor pressures is attributed to two causes, decreased intensity of bands heads owing to an increased moment of inertia of the molecule in higher vibrational levels of the normal state, and a crowding of vibrational levels when the total vibrational energy is large. This conclusion is supported by observations of the fluorescence of toluene, which appears to be almost wholly continuous.

THE ultraviolet spectrum of benzene has attracted the attention of many investigators. Among the more recent studies should be mentioned those of Henri,[2] Pringsheim,[3] Shapiro, Gibbs and Johnson[4] on the absorption of the vapor, of Kronenberger[5] on the absorption and fluorescence of the solid at low temperatures, of Pringsheim and Reiman[6] on the fluorescence of the vapor and of McVicker, Marsh and Stewart[7] and of Austin and Black[8] on the high-frequency emission spectrum of benzene. Although notable success has been achieved by these workers in the interpretation of the ultraviolet bands of benzene, the analysis is still far from complete and certain.

The first absorption bands of the vapor set in at about 2742A and extend into the ultraviolet with increasing intensity. The beginning of the spectrum, at least, consists of clearly distinguishable band groups about 920 cm^{-1} apart. The closely spaced bands within each group are shaded to the red. The intensity within each group also falls off to the red. Below 2200A the bands become diffuse, predissociation setting in.[2]

[1] M. Nelles, Charles A. Coffin Fellow.
[2] Henri, Structure des Molecules, Herman, Paris (1925).
[3] Pringsheim, Fluoreszenz und Phosphoreszenz, Springer, Berlin (1928).
[4] Shapiro, Gibbs, and Johnson, Phys. Rev. **38**, 1170 (1931).
[5] Kronenberger, Zeits. f. Physik **40**, 75 (1927); **63**, 494 (1930).
[6] Pringsheim and Reimann, Zeits. f. Physik **29**, 115 (1924); Ann. d. Physik **80**, 43 (1926).
[7] McVicker, Marsh and Stewart, J. Chem. Soc. **123**, 642 (1923).
[8] Austin and Black, Phys. Rev. **35**, 452 (1930).

It seems to be the consensus of opinion now that the major part of the spectrum can be represented by equations involving two upper electronic levels and several vibrational frequencies, of which one is about 920 cm^{-1}, and the other, 160 cm^{-1}. Although the equations proposed are essentially similar, they differ in many details. Shapiro and co-workers brought forward strong evidence that the 160 cm^{-1} frequency belongs to the normal state. This will probably necessitate some revision of earlier interpretations because Kronenberger finds a 160 cm^{-1} frequency to be present in absorption of the solid at 14°K. If his data can be applied to the vapor, it follows that both the normal and the excited electronic levels possess nearly the same vibrational frequency, a circumstance not considered in the above-mentioned eqations.

The fluorescence spectrum of benzene extends from about 2600A to the red. It is quite similar to the absorption spectrum, consisting also of band groups, but separated now by 980 cm^{-1}. Pringsheim and Reimann[6] describe the bands within each group by means of two progressions, each involving the 160 cm^{-1} frequency and being displaced one against the other by 83 cm^{-1}. Austin and Black[8] require six separate equations involving altogether five vibrational frequencies, a number so large as to be meaningless, to describe some hundred band heads found in emission in high-frequency discharge, a spectrum very similar to fluorescence.

Most of the work on the fluorescence of benzene has been done at relatively high pressures. Under these conditions the spectrum emitted is quite independent of the source of excitation. Pringsheim and Reimann[6] reported, however, that at 0.3 mm vapor pressure with illumination by the 2536A mercury line, a fluorescence spectrum is obtained which differs somewhat from that at higher pressures and polychromatic illumination. On the basis of this work, it seemed likely that, by using a monochromatic source of excitation and vapor pressures so low as to minimize the effect of inelastic collisions, one might obtain considerably simplified emission spectrum which would throw further light on the structure of benzene.

Experimental Details

For these experiments a very intense source of monochromatic illumination was needed, the fluorescence of benzene being not strong even at high pressures. Use was made of the strong emission of the 2536A line by the low pressure mercury arcs. Fig. 1 shows the arrangement adopted, which is merely a suitable modification of variously described[9] controlled-vapor-pressure mercury arcs. The lower vertical part of the lamp is immersed in cold running water (15°C) and the arc is struck, by the application of a spark coil, between the mercury electrode A and a molybdenum electrode B. A metal disk C deflects mercury vapor to the cooled glass walls. The lamp is continuously evacuated by a fast diffusion pump. The current was usually kept at 25 amp., the potential drop being about 30 volts. The lamp ran very steadily on 110 volts d.c. Two quartz tubes, D and E, are mounted coaxically

[9]Taylor and Bates, Proc. Nat. Acad. Sci. **12**, 692 (1926).

in the lamp. The De Khotinsky seals are indicated in Fig. 1 by the letter K while P is a somewhat flexible joint made of asbestos rope soaked in picein cement, the whole being covered by rubber. Benzene vapor flows very rapidly through the inner tube E. It is generated in a flask in which solid benzene is maintained at a constant temperature and is condensed, after passing E, in a liquid air trap followed by a pump. Through the annular space between the quartz tubings is passed either water or a 5 molal solution of acetic acid. The latter acts not only as a cooling agent but also as a light filter, the 2 mm layer of its absorbing all wave-lengths transmitted by quartz but shorter than 2400A. The 2536A line is absorbed by this solution only very slightly. Longer wave-lengths than this, besides being weak in a lamp of the present

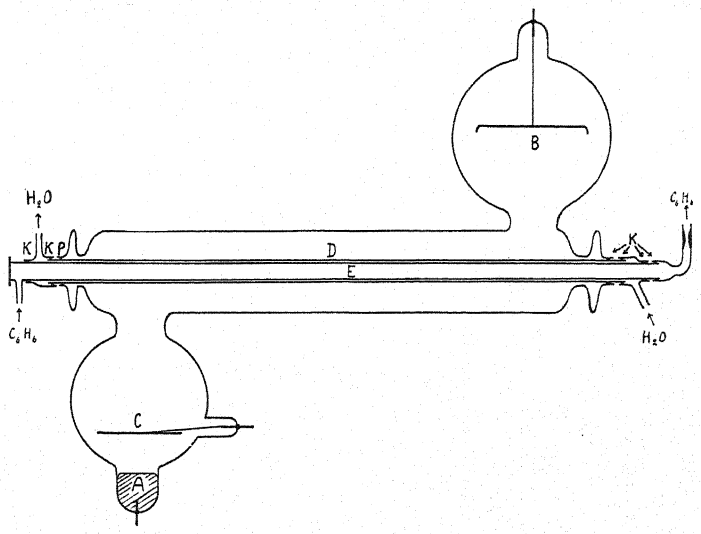


Fig. 1. The light source.

type are too feebly absorbed by dilute benzene vapor to contribute materially to excitation. Thus an almost monochromatic source of excitation is obtained, of intensity sufficient to produce a strong image of the fluorescence of benzene vapor at 25 mm pressure in one minute. With benzene at 0.01 mm pressure, exposures of ten hours' duration were required to obtain workable plates. A quartz Hilger E1 (Littrow) spectrograph was used throughout this work. The wave-length determinations were made in the usual way with an iron arc for the comparison spectrum.

Some decomposition of benzene occurred on illumination, particularly when water and not acetic acid was used as the cooling agent. The decomposition products settled on the walls of tube E and made them opaque to mercury radiation. It was necessary, therefore, during protracted runs, to remove and clean this tube occasionally.

RESULTS

Benzene fluorescence was studied at vapor pressures varying from 25 to 0.01 mm mercury. In this range no difference could be noticed between the

photographs obtained with water as the cooling agent and those for which the acetic acid light filter was used. This shows that in a lamp of the described type only the 2536A line contributes materially to fluorescence. The spectrum emitted at pressures above about 1 mm is practically independent of pressure and, as our measurements indicate, is identical with that described by other workers. Fig. 2, curve 2, reproduces a microphotometer record of the short wave-length half of it. Two complete band groups and the beginning of a third can be seen on the figure. One progression in each group is marked by

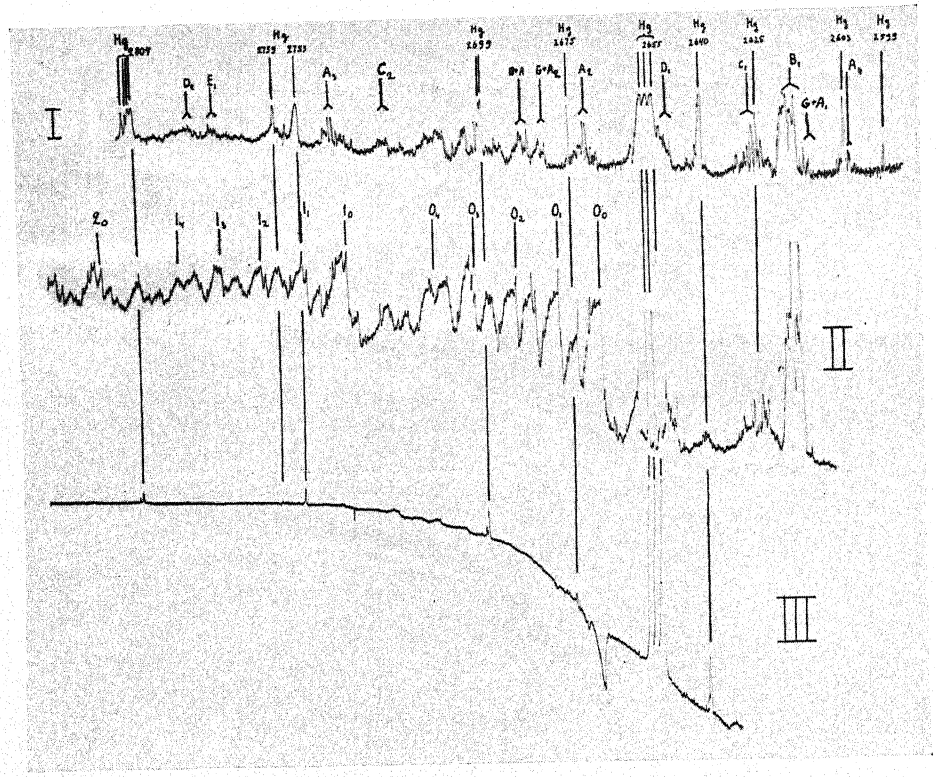


Fig. 2. Microphotometer records of fluorescence spectra. I. Benzene at low pressures. II. Benzene at high pressures. III. Toluene.

the figures 0, 1, 2 with subscripts. The entire spectrum on the plates obtained shows four such groups. They become weaker and less distinct towards the red.

Below 1 mm pressure the appearance of the emission spectrum gradually changes. At about 0.1 mm the band heads nearly disappear and the spectrum consists of numerous unresolved line groups, of which more than two hundred have been measured between 38,400 and 34,500 cm^{-1}. As the following will show, this spectrum represents the transition to the real resonance fluorescence. It does not show obvious regularities except some which are similar to the high pressure fluorescence and the recording here of our measurements

TABLE I. *Emission lines in resonance fluorescence.*

λ (air)	cm^{-1}	*I*	λ (air)	cm^{-1}	*I*
2588.67	38618.4	1	2742.29	36455.1	5
2600.31	444.0	0d	43.26	442.2	5
01.56	427.0	1	44.04	431.8	1dd
01.96	421.1	1	44.77	422.2	2d
03.15	403.5	0	56.13	272.1	3
12.00	273.4	0	58.02	247.2	0d
12.98	258.5	1	58.73	237.9	0d
15.23	226.1	10	67.44	123.8	0d
16.01	214.7	3d	68.99	103.6	0
16.49	207.5	3d	72.92	052.4	0d
17.25	196.6	10	73.67	042.7	0d
18.54	177.8	3d	77.02	35999.8	0
18.96	172.7	2d	77.71	990.3	0
23.76	101.9	1d	78.46	980.5	0
24.48	091.4	0d	79.26	970.2	1
26.29	065.2	3	81.61	939.8	0
27.46	048.2	2d	83.33	917.5	0d
28.13	038.5	0d	84.78	898.9	0d
29.86	013.5	0	85.60	888.3	0d
30.18	008.9	0	2813.52	532.2	0d
47.55	37759.5	1	14.83	515.7	0
49.11	737.3	1d	15.65	505.3	0
67.17	481.8	0	16.21	498.3	0d
67.62	475.5	0d	16.91	489.5	0
68.09	468.6	0d	18.39	470.8	2
70.10	440.7	3	19.58	455.9	2
70.77	431.3	3	20.42	455.8	0
81.29	284.4	1	21.35	433.6	0d
82.96	261.2	1d	22.16	423.4	0d
86.13	217.2	2d	28.99	337.9	0
87.67	195.9	1d	29.84	327.3	0d
88.25	187.9	0d	31.58	305.6	0d
93.57	114.4	0dd	32.51	294.0	1
95.21	091.9	1d	35.35	258.6	1
96.50	074.1	1d	36.13	249.0	0d
97.33	062.8	0d	36.97	238.5	0
2703.28	36981.0	2	37.86	227.5	0d
03.77	974.4	1d	39.08	212.3	0dd
04.26	967.7	1d	40.63	193.1	0dd
06.68	934.1	0	44.31	147.6	0
09.66	894.1	1d	89.17	34601.9	0d
10.27	885.8	0d	90.17	589.9	0d
11.41	870.3	1d	91.31	576.3	0d
14.13	833.3	0dd	97.16	507.4	0d
14.82	824.0	0d	98.70	488.1	1
21.11	738.8	0d	2900.13	471.1	1
21.93	727.8	1	12.76	321.7	0d
23.62	705.0	1d	21.01	224.7	0d
24.32	695.5	0d	21.84	215.0	0d
25.96	673.5	0d	22.62	205.9	0d
26.98	659.8	0d	24.08	188.8	0
27.67	650.5	0d	25.69	170.0	0d
28.37	641.1	0d	3001.80	33303.7	0
36.18	536.5	1	04.75	271.0	0d
38.53	505.2	1	06.83	248.0	0dd
39.62	490.6	0	08.20	232.8	0d
40.88	473.8	2	09.47	218.8	0d

will be omitted since not much significance can be attached to them at the present time.

Still further pressure decrease produces a considerable simplification of the spectrum through a gradual disappearance of the majority of lines and

the enhancement of the others. Table I gives the results of measurements on plates taken at 0.01 mm benzene vapor pressure. The accuracy of these wavelength determinations is rather low, an error of ± 1 cm^{-1} or even more being probable for most of the lines. This is due to the diffuseness of the lines and lack of contrast owing to a continuous background coming from the light source. Fig. 2, curve 1, gives the microphotometer record of the short wavelength part of this spectrum. It shows that the stronger emission lines form a system of doublets, several weaker lines being usually grouped around each of these. The whole resembles the well-known resonance fluorescence of iodine vapor discovered by Wood more than twenty years ago. Indeed, it can be interpreted on essentially the same basis, as representing transitions from a certain vibrational level attained on absorption of the 2536A line to different vibrational levels of the normal molecule. However, several modes of vibration being possible in benzene molecules, more than one progression of doublets is observed. As the following Table II shows, several vibrational frequencies can be identified with more or less certainty. This table presents in successive columns: (1) the assignment of the line group (2) the frequency separation of the center of the doublet from the exciting line (2536.6A) or, when the line group does not appear as a doublet the separation of its center of density; (3) the separation from the preceding line group of the same series; (4) the second frequency difference; (5) the doublet separation; (6) the intensity of the doublet lines. Table III compares the frequencies here obtained with some of those known from Raman spectra and from the infrared bands of benzene.[10] The correspondence is, on the whole, very good, since the 160 cm^{-1} frequency can be interpreted as the fundamental of the infrared band

TABLE II. *Vibrational frequencies in resonance fluorescence.*

Line group	Separation from the exciting line, cm^{-1}	$\Delta\nu$ cm^{-1}	$\Delta^2\nu$ cm^{-1}	Doublet separation cm^{-1}	Intensity
F_1	792.6	792.6			1
A_1	987.0	987.0		5.9	1
			+ 1.0		
A_2	1975.0	988.0		9.4	3
			− 0.6		
A_3	2962.4	987.4		12.9	5
			− 2.2		
A_4	3947.6	985.2		14.9	2
			− 1.4		
A_5	4931.4	983.8		17.0	1
B_1	1199.6	1199.6		29.5	10
C_1	1354.3	1354.3		17.0	3
			−14.0		
C_2	2694.6	1340.3		22.8	1
D_1	1662.6	1662.6		22.2	1
			−27.9		
D_2	3297.0	1634.7		20.2	0
E_1	3138.9	3138.9		?	3
			−92.3		
E_2 (?)	6185.2	3046.3		14.0	0
A^1+G	1145.0	158.0		14.9	2
A_2+G	2138.2	163.2		23.2	2

TABLE III. *Comparison of fluorescence, Raman and infrared frequencies.*

Fluorescence cm^{-1}	Raman lines cm^{-1}	Infrared bands cm^{-1}
160	—	—
—	—	310
—	—	442
—	—	515
—	605	—
793	—	—
—	849	—
988	991	—
1200	1178	1235
1354	—	1316
—	1583	—
1663	1605	—
—	2947	—
—	3047	3030
—	3060	—
3139	3164	—
—	3184	—

at 310 cm^{-1}, while the 791 cm^{-1} frequency is very doubtful anyway on account of the faintness of the single line observed there. It should be pointed out that in accordance with selection rules holding for electronic transitions, both Raman and infrared frequencies may appear in fluorescence. The numerical agreement of fluorescence data with the data from other sources is not as good as the probable errors of these measurements would seem to indicate. Part of this, at least, should be attributed to an error arising from the use here of the center of the doublets for the determination of the frequencies. Another reason why the data cannot be strictly compared is that liquid benzene is usually used for the infrared and Raman spectra, whereas the fluorescence was obtained with benzene vapor.

In addition to the line groups recorded in Table II, the plates show some diffuse groups which can be identified on the microphotometer record between the mercury lines 2753 and 2699A. Using some imagination one can assign these groups to additional frequencies of benzene or to combinations of those already described. This assignment is highly uncertain in view of the diffuse nature of the groups and it is omitted here. The possibility also exists that these groups are the last remnants of the high pressure fluorescence and will disappear on further lowering of benzene vapor pressure. Further work now being undertaken will probably settle this point.

The fine structure of the line groups observed in low pressure fluorescence can be, at least partially, understood from the point of view here developed. In the absence of any information to the contrary one might assume that the benzene molecule behaves as a symmetric top not only in the lower but also in the upper electronic levels. For this case it has been shown[11] that, if j is the quantum number of the total angular momentum, while k is that of the rotation around the axis of symmetry, the following rotational transitions

[10] K. W. F. Kohlrausch, Der Smekal-Raman Effekt, Springer, Berlin (1931).
[11] Dennison, Rev. Mod. Phys. **3**, 280 (1931).

take place depending on whether the bands are of the parallel or the perpendicular type:

parallel

$$k \to k \begin{cases} j \to j+1^* \\ j \to j \\ j \to j-1^* \end{cases} \qquad k \to k+1 \begin{cases} j \to j+1^* \\ j \to j; \\ j \to j-1 \end{cases}$$

perpendicular

$$k \to k-1 \begin{cases} j \to j+1 \\ j \to j \\ j \to j-1^* \end{cases}$$

For larger values of k the transitions marked by a star are the ones with the greatest *a priori* probability. Now, the 2536A mercury line happens to fall near the tail of a benzene band in the third band group of the absorption spectrum. This makes it probable that the molecules participating in the absorption process have a large value of k and therefore, irrespective of whether the bands are of the parallel or of the perpendicular type, one should expect in emission two strong and some weaker lines. The existence of the hyperfine structure in the 2536A line makes it probable that more than one rotational level of the upper electronic state is reached on absorption. This may account for the diffuseness of the emission lines. The feature which remain unexplained is the variation in the separation of the doublet components which is very regular in the long A progression of doublets and is quite beyond a possible experimental error. It increases with increasing vibrational quantum numbers, whereas it would be expected to decrease, if the explanation given above is right.

It throws considerable doubt on the correctness of the whole interpretation as given above. Professor G. H. Dieke pointed out to us in a personal discussion that the two components of each doublet may represent independent but degenerate vibrations and that the increase in the doublet separation is due to a gradual removal of the degeneracy in higher vibrational quantum levels.

The information presented on the preceding pages together with the earlier known facts allows some conclusions to be drawn concerning the high pressure fluorescence, or at least, that part of it which consists of the band groups 0, 1, 2, etc. Its independence of the exciting source suggests immediately that at higher pressures benzene molecules lose the vibrational part of their excitation energy in inelastic collisions prior to light emission. The transitions giving rise to fluorescence occur therefore from the lowest level of the electronic state or states. The latter is more probable because the 83 cm^{-1} separation, found in the high pressure band groups, does not appear in resonance fluorescence. It should therefore be attributed to the existence of two upper electronic levels, both of which are reached by molecules upon inelastic collisions. This interpretation of the ordinary fluorescence finds further support in the fact that the first absorption band group coincides with the first, "0," group of fluorescence. They differ only in that the intensity of the different bands within the group falls off more rapidly towards the red (that is, with increasing quantum number of the 160 cm^{-1} frequency) in absorption than in emission. This fact is readily understood if the 160 cm^{-1} frequency is at-

tributed to the normal electronic state, as suggested by Shapiro. A point of difference between the resonance and the high pressure fluorescence is that in the short wave-length part of the latter only two frequencies, 920 and 160 cm^{-1} make their appearance. This might be attributed to particular transition probabilities characterizing the lowest level of the excited electronic states. An analogy to this is found in observations made with the absorption spectrum. Transitions from the nonvibrating level of the normal electronic state show also only one, the 920 cm^{-1}, frequency of the excited state. This holds, at any rate, for the longer wave-length part of the absorption spectrum, where the total vibrational energy of the molecule is small.

The structure of the fluorescence spectrum at vapor pressures in the neighborhood of 0.1 mm indicates that vibrational energy is much more readily exchanged on collisions than is rotational energy. Thus, here the bands, with their characteristic heads, are as yet undeveloped, but groups of lines are present throughout the spectral region in which these bands are located at higher pressures. The persistence of fluorescence even at atmospheric pressure or in the liquid state shows further that the benzene molecules are relatively stable against the loss of electronic energy on collisions. This is undoubtedly related to the exceptional sharpness of the absorption bands of benzene in the liquid state.[12]

Recently Almasy[13] in a short notice suggested that a predissociation occurs in the final state of the fluorescence transitions. He brings forward this suggestion to account for continuous emission, observed by him, which extends from 2670A to longer wave-lengths when benzene vapor is excited by the 2536A mercury line. The experiments here recorded lead us to disagree with Almasy both in matter of fact and in the conclusion. The emission at low pressures has been found to be wholly discontinuous. The plates, it is true, show a continuum extending from about 2650 to 3200A with a maximum at 3000A. However, several tests, made under conditions identical with the fluorescence experiments in every respect except that benzene vapor was absent from the inner quartz tube, showed conclusively that the entire continuum is due to scattered light from the light source. Only at high pressures of benzene vapor can the long wave-length end of the spectrum be described as continuous. The interpretation of Almasy, when applied to this continuum, meets, however, grave difficulties. The continuum starts at about 2800 and ends at 3200A. Thus, the energy left in the molecules after emission of radiation is less than one electron volt, even granting that the continuum is due to direct transitions from the excited level reached on absorption of the 2536A line. If, however, the molecules lose first some energy on collisions, as suggested on the preceding pages, the energy remaining upon emission of radiation is still less and does not exceed 0.5 electron volts. Predissociation has by now been definitely interpreted as due to radiationless transitions to continuous levels, that is, to a breaking up of the molecule. The well-known sta-

[12] Arnold and Kistiakowsky, J. Am. Chem. Soc. **54**, 1713 (1932).

[13] Almasy, Naturwiss. **20**, 296 (1932).

bility of benzene, on the other hand, does not allow one to believe that a decomposition occurs with only some 15 cal. of vibrational or electronic energy in the molecule. The continuum may be interpreted without this difficulty, by considering that the absorption and emission bands are degraded to the red so that the moment of inertia of the excited molecule must be larger than that of the normal molecule. The moment of inertia in higher vibrational states has usually been found to be larger than that of the non-vibrating molecule. The result of this is that, as the transitions occur to higher and higher vibrational levels of the normal state of benzene, the moments of inertia of the initial and final states approach each other and the band heads become less prominent. The rotational structure of the bands being entirely unresolved, this will cause the appearance of an apparently continuous emission. Curve 2, Fig. 2, shows very clearly how the band heads gradually weaken towards the red.

Another cause may also contribute to the effect. As has been pointed out by Kassel,[14] the spacing of vibrational quantum states in polyatomic molecules decreases very rapidly with increasing total energy. If, in transitions to higher vibrational quantum levels, frequencies other than 980 and 160 cm^{-1} take part, this crowding of levels must contribute considerably to the continuous appearance of the long wave-length part of the fluorescence spectrum.

In extending the present investigation to molecules other than benzene, toluene has been already studied. The pressure range covered was 20 to 1 mm, the weakness of emission preventing further decrease of pressure. The fluorescence was found to be wholly continuous with the exception of some quite diffuse bands between 2750 and 2650A. Fig. 2, curve 3, shows a microphotometer record of a part of this spectrum. The continuum in the case of toluene is much more pronounced than with benzene. It would be necessary to assume that toluene becomes unstable even when possessing some 0.3 electron volts of energy in order to account for the continuum on the assumption of predissociation. The suggestion advanced here, on the other hand, readily accounts for these observations. The decreased symmetry and an increased number of atoms in toluene are favorable to a crowding of vibrational levels at lower total energies and thus agree with the appearance of the continuum at shorter wave-lengths.[15]

[14] Kassel, J. Am. Chem. Soc. **53**, 2143 (1931).

[15] A note giving the above results and arguments was sent in June to Die Naturwissenschaften but was not accepted by the editor of that publication.

The Ionization of Neon and Argon by Positive Alkali Ions of Energies from 650 to 2000 Volts

By J. CARLISLE MOUZON
California Institute of Technology, Pasadena, California

(Received July 14, 1932)

With an apparatus of new design the study of the ionization of neon and argon by positive alkali ions has been extended to accelerating potentials as high as 2000 volts. The results obtained are in good quantitative agreement with the previous work at the low potentials. In a number of cases the efficiency of ionization reaches a maximum at accelerating potentials less than 2000 volts.

THE problem of the ionization of gases by impact of positive ions at low velocities is one in which it is necessary for a large amount of experimental evidence to be gathered before the theorist is able to hazard an intelligent guess at the processes involved.

As is usually the case it is impossible to say when and by whom investigations have begun on a particular problem. So it is with this problem. However, the history of its development up to a few years ago is one of a series of experiments giving either absolutely negative results, or results completely masked by secondary effects. It was because of these past futile attempts to obtain any conclusive evidence that Professor R. A. Millikan suggested to A. L. Klein at the California Institute in 1922 that he take up very carefully first the study of the possible ionization produced when positive ions impinge upon a metal surface. This proved to be a step in the right direction since Klein[1] found for the first time, and this was subsequently checked by other investigators, that positive ions of relatively low energy are quite capable of ejecting electrons from metal surfaces. He found further that the effect began to set in at an energy of the order of 100 volts, and also that positive ions themselves may be reflected from surfaces. It was then obvious that an apparatus which would prove successful in detecting pure ionization in a gas must be so built that it would be able to make these surface effects negligible, or else measurable independently of the main gas phenomenon. Such an apparatus was first built by R. M. Sutton with the advice and assistance of Professor Millikan at this Institute. The design of this apparatus had been suggested by Professor Millikan as early as 1924. A detailed account of it and of the difficulties encountered was given in Sutton's Ph.D. thesis in 1929 and, in a condensed form, in the Physical Review.[2]

The results of Sutton will be summarized briefly thus: Neon and argon were bombarded by singly charged positive ions of potassium of energies up to 750 volts. The collecting potentials were so adjusted as to eliminate practically all secondary effects due to the ions and to enable him to collect any

[1] Klein, Phys. Rev. **26**, 800 (1925).
[2] Richard M. Sutton, Phys. Rev. **33**, 364 (1929).

electrons liberated from the gases. A variation of pressure from 0.005 to 0.1 mm gave a definite variation in the ionization. This fact alone was sufficient to prove very definitely that the electrons collected were due to ionization of the gas. This was the first conclusive evidence presented by anyone on this subject. Sutton found that argon was ionized more efficiently than neon when potassium was used as an ionizing agent. Ionization was not observed when the bombarding ion had a velocity of less than about 100 equivalent volts. However, since his galvanometers did not afford high enough sensitivity, he was unable to measure the insetting potential accurately or even to prove that a sharp insetting potential actually exists. It will be well to add that the technique he devised for the collection of the initial positive ions and the electrons arising from the bombarded gas is essentially that which has been used by all observers anywhere who have later taken up and pushed farther the work on the ionization of gases by positives of low energies.

The writer began work with Dr. Sutton in January of 1929. The research was carried on jointly with him until December, 1930. During this period some revisions were made in the apparatus, making the measurements more exact, and the study was carried on in the three noble gases; neon, argon, and helium with the five alkali ions; lithium, sodium, potassium, rubidium, and caesium. The results were published in the Physical Review[3] in 1930 and 1931. In December of 1930 the writer continued at the Institute the investigations in krypton and xenon with Dr. Otto Beeck with a much more sensitive apparatus. Dr. Beeck had already studied the ionization in neon and argon by the alkali ions using Sutton's method, but improving the accuracy and sensitivity by separating the alkali ions in a magnetic analyzer and by using sensitive electrometers instead of galvanometers. He published his results in Naturwissenschaften in the summer of 1930, summarizing his work with the statement that the efficiency of ionization in a noble gas is highest for that alkali ion nearest it in atomic number. The investigations in xenon and krypton showed that this statement is not strictly true, though it holds in most cases. The fact that potassium is equally efficient an ionizer of krypton as is rubidium and the fact that potassium is more efficient as an ionizer of xenon than is rubidium brings one to the conclusion that so simple a statement falls short of the observed phenomena. However, an interesting result is obtained if the probabilities of ionization are computed for the most efficient alkalis in their neighboring gases.

The probability of ionization is simply the chance that an electron will be liberated when the positive ion collides with a gas atom. It is obtained by dividing N, the number of electrons liberated per initial positive per cm path per mm pressure by the number of collisions the ion makes per centimeter. The probability, P, is then $P=NL$, where L is the kinetic theory mean free path at 1 mm pressure. The kinetic theory mean free path is not quite the correct value to use, but it is certainly of the right order and is as good as any other value we know, unless the cross-section values[4] are a trifle better.

[3] Sutton and Mouzon, Phys. Rev. **35**, 694 (1930); Sutton and Mouzon, Phys. Rev. **37**, 319 (1931).

[4] Ramsauer and Beeck, Ann. d. Physik **87**, 1 (1928).

Table I gives the values of the probability of ionization thus computed. These values are for an accelerating potential of 500 volts. Because of the general shape of the curves of the efficiency of ionization plotted against accelerating potential, these values will remain the same for potentials of more than about 200 volts. It is interesting that these probabilities come out

TABLE I.

	P
Na^+ in neon	0.025
K^+ in argon	0.026
Rb^+ in krypton	0.038
Cs^+ in xenon	0.030

almost equal. As a matter of fact, the mean free path used could account for a wider variation than is found. If one considers the ionization as due largely to the kinetic impact of two elastic bodies, as does Dr. Fritz Zwicky[5] of this Institute, it is not surprising that the probabilities of ionization for the alkalis in their neighboring noble gases are about the same.

The writer and Beeck also made a very careful study of the potential at which ionization sets in, using the five alkali ions in neon, argon, krypton, and xenon. The ionization in helium is so small that it cannot be studied with any degree of accuracy with this apparatus since the gas pressures used are low. A summary of these findings appeared in the Physical Review.[6] A more detailed account was given in two articles in the Annalen der Physik.[7]

Unsuccessful attempts to use positive alkali ions of energies greater than 500 volts were made by Sutton and the writer, and later by Beeck and the writer. The apparatus used in the former case was limited because of a gas discharge taking place between the filament and cathode[3] at the higher potentials. Measurements were actually made up to 750 volts. In the latter case a very large reflection of positive ions occurred at the higher potentials.

A new apparatus has been built which is more suitable for the work and which gives quite satisfactory results. A further difficulty was encountered with the present apparatus which was masked by the other effects in the earlier pieces of apparatus at velocities in excess of 750 volts. This was the problem of secondary emission from the metal parts. By applying a potential of about 9 volts it is possible to prevent the escape of electrons from a metal when the bombarding ion has an energy of less than 600 volts. However, for greater energy positive ions, some of the electrons ejected seem to have an energy of much more than 9 volts. With proper adjustments the secondary emission was finally reduced to such a low value that, by making corrections for it, quite good results were obtainable.

Fig. 1 is a cross section of the apparatus. The source of positive ions, F, is a platinum foil coated with Kunsman catalyst. (The filament holder is not

[5] Zwicky, Proc. Nat. Academy of Sc. **18**, 314 (1932).
[6] Beeck and Mouzon, Phys. Rev. **38**, 967 (1931).
[7] Beeck and Mouzon, Ann. d. Physik **11**, 737, 858 (1931).

indicated in the drawing.) Ions of the five alkalis were thus obtained. The most satisfactory method of coating the filament with the source material was found to be as follows: The catalyst was mixed with paraffin oil to facilitate spreading it on the surface of the foil. Successive thin coats were painted on the foil, the source being heated to a yellow heat in an atmosphere of hydrogen after each coat. The result was that the catalyst adhered very firmly to the foil and no difficulty was encountered with the catalyst falling off when it was mounted upside down in the filament holder. This would occur if the source were not reduced in steps as was indicated.

The ions are accelerated to a grid and pass through the magnetic analyzer through 1×6 mm slits, S_1 and S_2. The Armco iron pole pieces of the mass spectrometer are separated 5 mm by brass spacers. The copper plate, B, is supported on A by means of a glass tube which insulates the two. The positive

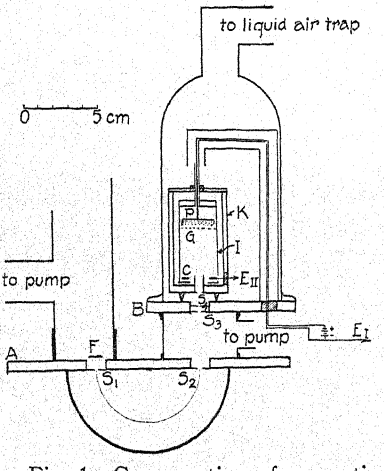


Fig. 1. Cross section of magnetic analyzer and ionization chamber.

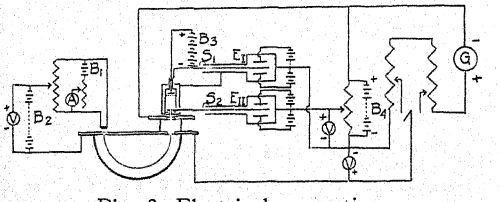


Fig. 2. Electrical connections.

ions enter the ion chamber through slits, S_3 and S_4. These slits are 1×6 mm and 0.5×6 mm, respectively. The channel shown prevents any of the initial positives reaching the electron collector, C. A small ring is shown projecting into this channel at its base. This is to prevent as many ions as possible from striking the walls of the channel from which secondary electrons might easily be ejected. The joints of glass to copper are made with picein wax.

A small bell jar sealed with wax to the ground plate, B, contains the ionization chamber and makes it easily accessible. The tube connected to the top of the bell jar leads directly to a liquid air trap which freezes out the vapors present.

The ionization chamber is surrounded by a soft iron cylinder K to shield it from the stray magnetic field. The whole rests on redminol feet, insulating it from the plate B. The collector for the initial positive ions is of a different design from that previously used, consisting of the collector P and the brass cylinder I. The major part of the beam is collected on P. Any alkali ions scattered by the gas are caught on the walls. The collector P is a brass box, 3 mm

deep, containing two 0.5 mm mesh screens inside and one 2 mm mesh screen at the opening. This cage effect is very successful in preventing the reflection of the initial positive beam which proved troublesome at the high energies in the previous apparatus.[8] The collection of all the positive ions entering the chamber, including those scattered by the gas, affords more accurate measurements than previously. However, the agreement of the results obtained with this apparatus with those obtained with the earlier pieces of apparatus indicates that the scattering is very small at the pressures used. The cage P is maintained at a potential of 18 volts above I by means of a small battery inside the shielded electrometer lead. For accelerating potentials in excess of 900 volts this is no longer sufficient to retard all of the secondary electrons. It is therefore necessary to make a correction for these ejected electrons.

The electron arising between the grid G and the upper end of the channel are collected on the plate C. Any other electrons arising from the bombardment of the metal walls are also collected there. It is true that the positive gas ions arising as products of ionization by the alkalis are measured with the initial positive ions, but the error introduced by this is very small since these are in general less than one percent of the value of the initial positive beam.

A diagram of the electrical connections is shown in Fig. 2. The filament is heated by means of the battery B_1. An initial acceleration of 54 volts is applied at the center of a large resistance across the filament by means of the battery B_2. A second acceleration is applied between plates A and B after the ions have passed through 180° in the magnetic field. This acceleration is variable as is shown, the potential being derived from the 2000 volt generator, G. A third acceleration of 48 volts from B_4 exists between the soft iron cylinder and the plate, B. This last acceleration is thus applied so that no electrons arising from the slits or from the gas streaming through the channel may enter the ionization chamber and be collected on C.

The cage P is maintained at 18 volts positive with respect to the cylinder I by means of the battery B_3 in the electrometer lead. The electrometer E_{I} measures the initial positive beam. The collector C for the electrons liberated from the gas is maintained at a potential positive with respect to the surrounding cylinder I by means of the battery B_4. This potential has to satisfy two conditions. It must be high enough so that all the electrons liberated between C and G are collected, but it must be less than the electron ionization potential of the gas. The collector C has to be large enough to make this possible. (This is the same restriction as existed in all of the previous work.) By plotting the charge collected on C against the collecting potential applied on C, for a given acceleration of the alkali, one can determine whether this condition is satisfied. 12 volts were found suitable for the work in argon and 15 volts for neon. The electron charge on C is measured by electrometer E_{II}. The two electrometers are of the string type. All leads to them were carefully insulated with amber, and carefully shielded. Switches S_1 and S_2 are electromagnetically operated *grounding* switches for the two instruments.

[8] Beeck, Ann. d. Physik **6**, 1001 (1930).

The gas is admitted to the ionization chamber from a reservoir through a fine capillary and is continuously pumped through, assuring purity. The pump leads are as indicated. The difference in pressure between the ionization chamber and the mass spectrometer is such that with the pressure as much as 10^{-2} mm in the chamber, a large number of positives are still undeviated from their path. Pressures are measured on a McLeod gauge at intervals during a run. The time of each reading of the electrometers is recorded and the pressure of the gas at that time may be obtained from a pressure-time graph. The change in pressure never amounts to more than 1.5×10^{-3} mm in ten minutes. The time of charging up of the electrometers is between 5 and 10 seconds, so that the change in pressure during that period is negligible. The pressure used were between 2×10^{-3} and 7×10^{-3}. The chance of multiple collisions is therefore small.

The ratio of the effective capacities of the two collecting systems with their leads and electrometers must be known in order to secure the true ratio of the charges collected. Obviously. there is an inductive effect of one system on the other, since the collector of the initial positive ions surrounds that of the electrons liberated from the gas. However, in this apparatus the inductive effect of the system of electrometer E_{II} on the system of E_I is very small. Therefore, the ratio of the capacities can be measured by simply putting a charge on E_I and sharing it with E_{II}, the deflections on E_I being measured before the charge is shared and immediately thereafter. The potential originally applied on E_I can be measured by a bridge, so that all of the data are obtainable to give the ratio of the capacities, C_1/C_2 by the formula: $C_I/C_{II} = V_1'/(V_1 - V_1')$ where V_1 and V_1' are the potentials as read on E_I before and after the charge is shared with E_{II}, respectively. This ratio was found to be 3.38.

The actual measurements are taken as follows: With E_I and E_{II} grounded the filament is turned on; S_1 and S_2 are then opened simultaneously. When the charge has reached a satisfactory value, the filament switch is opened and the deflection of E_I is read. S_1 is now closed, grounding E_I, and the deflection of E_{II} is read. This procedure is necessary since the relatively large positive charge on E_I induces a charge on E_{II}. E_I must, therefore, be grounded before the true electron charge on E_{II} can be measured. The whole process of taking one reading requires from 5 to 10 seconds only. However, at the high accelerating potentials the drift of electrometer, E_{II}, is sufficient in that length of time to require a correction. The results obtained speak for the validity of these methods employed in the measurements.

As was previously mentioned, a correction must be made for the secondary emission. Fig. 3 shows how this correction can be made. The value of the ratio of the total electron charge collected on C divided by the corresponding positive ion charge is plotted against the pressure. In Fig. 3, $N\times P$ represents this value multiplied by a constant. It is N, the efficiency of ionization (the number of electrons ejected from the gas per initial positive ion per cm path per mm pressure) that is finally desired, so that it is convenient to carry this multiplying constant. As is expected, if only single collisions occur, this ratio

is a linear function of the pressure. The intersection of the lines with the axis of zero pressure gives the portion of $N \times P$ due to secondary emission only.

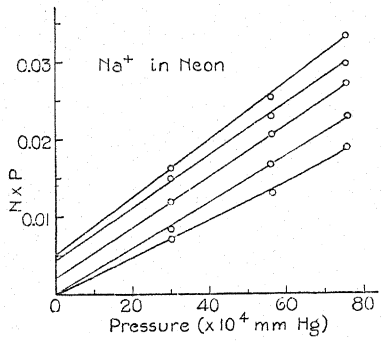


Fig. 3. Ratio of electron charge to positive ion charge as a function of pressure.

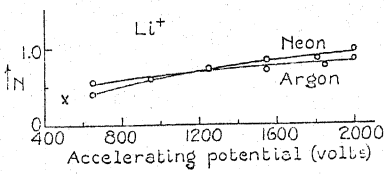


Fig. 4. Efficiency of ionization, N, of lithium in neon and argon as a function of accelerating potential.

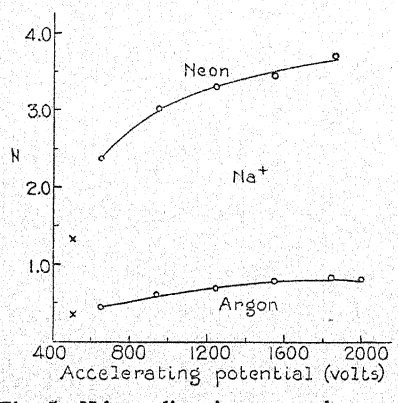


Fig. 5. N for sodium in neon and argon.

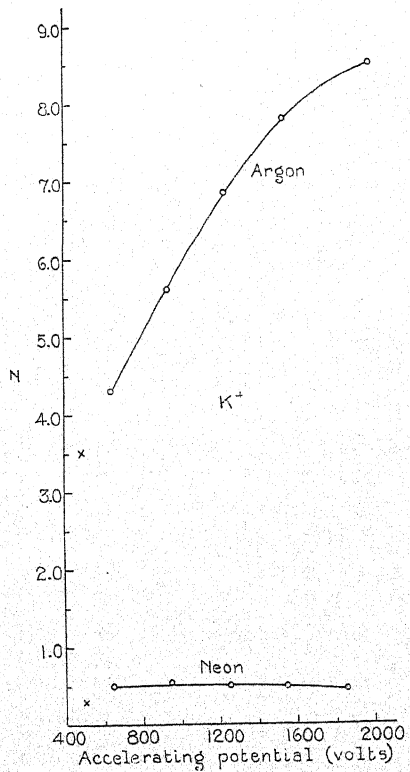


Fig. 6. N for potassium in neon and argon.

The results of the work in neon and argon are shown in Figs. 4, 5, 6, 7, and 8. The value of the efficiency of ionization, N, defined above is plotted against the accelerating potential. The crosses indicate the values obtained by Beeck[8]

at an accelerating potential of 500 volts. It is seen that in nearly all of the cases the agreement is excellent. Not only that, but also the slopes of the curves are such that, if extrapolated, the curves would strike the axis in good agreement with the values of the insetting potentials obtained by Beeck and the writer.[6] [7] That is particularly noteworthy when one considers that the apparatus used in the two cases is quite different. Too much accuracy cannot be claimed for the lower efficiencies, since the secondary emission was a considerable part of the charge measured. The fact that rubidium and caesium

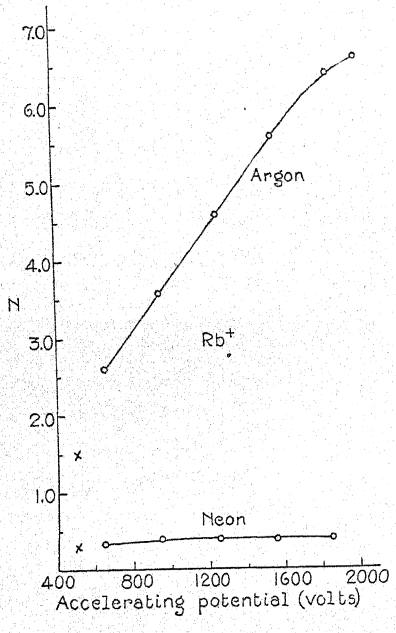


Fig. 7. N for rubidium in neon and argon.

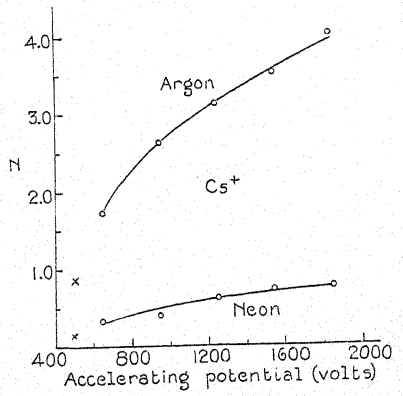


Fig. 8. N for caesium in neon and argon.

show relatively large efficiencies in argon again makes one wonder what role the electron configuration plays, since a simple *mass effect* cannot explain this. It is interesting to note that all of the curves show a tendency toward reaching maxima if they have not done so already at these potentials.

In conclusion, the writer wishes to express his appreciation for the interest of Dr. R. A. Millikan in this work and for the discussions with Dr. Otto Beeck concerning the whole problem.

The Photoelectric Properties of Alkali Metal Films as a Function of their Thickness

By JAMES J. BRADY
Physics Department, University of California

(Received May 11, 1932)

Previous workers have given very little consideration to the thickness of the alkali metal films under investigation. The purpose of the present work was to study the photoelectric properties of the films as a function of their thickness. A molecular beam was used to deposit a computed number of alkali metal atoms on a silver surface cooled with liquid air. In this way, films of various thicknesses were formed and their corresponding spectral response curves taken. The recorded thresholds were arbitrarily chosen as the points, where the currents became definitely measureable. For potassium, the maximum threshold, approximately 5800A, occurred at a film thickness of 3.0 molecular layers while the maximum total photoelectric emission occurred at 12.4 molecular layers, and the photoelectric properties remained constant after 19.0 molecular layers. The atomic spacing in the monomolecular layer is assumed to be the same as that in a solid mass of alkali metal. The threshold for the thick film was approximately 5500A. For rubidium, the maximum threshold, approximately 6200A, occurred at a film thickness of 1.5 molecular layers, while the maximum total photoelectric emission occurred at 5.0 molecular layers, and the photoelectric properties remained constant for film thicknesses beyond 12 molecular layers. The threshold for the thick film was approximately 5900A. For caesium, the maximum threshold, approximately 6600A, occurred at a film thickness of 1.5 molecular layers, while the maximum total photoelectric emission occurred at 5.0 molecular layers, and the photoelectric properties remained constant for film thicknesses beyond 10.0 molecular layers. The threshold for the thick film was approximately 6300A. Some anomalous effects are reported in the case of sodium. The maximum extension of the threshold was found to be much less than that reported by other investigators. A theory is advanced to account for the existence of a maximum in the excursion of the threshold.

PREVIOUS workers[1,2,3] have shown that large changes of the photoelectric properties of metal surfaces are produced by the deposition of thin alkali metal films but little has been done to study these effects quantitatively.

The present work was therefore undertaken for the purpose of studying the photoelectric effect as a function of a known number of deposited alkali metal atoms. One of the essential features of this work was the use of a molecular beam for controlling the amount of alkali metal deposited to form the film. The atoms were ejected from a pinhole opening in a reservoir containing the alkali metal, and allowed to condense on a metallic surface cooled with liquid air. The process was carried out in a very high vacuum. By using

[1] H. E. Ives, Astrophys. J. **60**, 209 (1924).
[2] Suhrmann and Theissing, Zeits. f. Physik **55**, 701 (1929).
[3] Ives and Olpin, Phys. Rev. **34**, 117 (1929).

this method, the chances for a uniform deposit were increased, and the calculation of the number of deposited atoms was possible.

Another feature of this work was the attempt to obtain a gas-free metallic surface on which to form the alkali metal film. This was done by evaporating the underlying metal under high vacuum conditions just before the alkali metal atoms were condensed on it.

The method proved successful in obtaining films of any desired thickness, which, although allowed to stand for several hours, showed no variation in photoeffect.

Apparatus and Experimental Procedure

A number of cells were constructed, with gradual modification of details, until the final form shown in Fig. 1 was adopted.

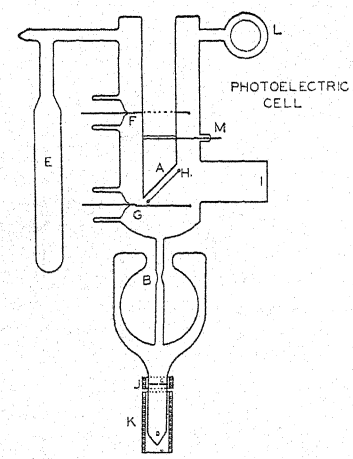


Fig. 1. Diagram of photoelectric cell.

The lower portion of the tube, *D*, acted as a reservoir for the alkali metal. It was separated from the rest of the tube by a thin glass partition with a pinhole (made by piercing the glass with a heated 30-mil tungsten wire which had been pointed on the end) in the center, *C*. That portion of the tube, *B*, just above this, was devoted principally to a container for liquid air which was used in defining the beam of alkali metal atoms. The constriction in the central tubing acted effectively as a defining slit for the beam, while the liquid air eliminated the possibility of reflection from the walls of the tubing. The condensation surface, *A*, was made from a glass tubing which was sealed off at one end and pressed against a slab of carbon while hot, so that the surface made an angle of 45° with the long axis of the tube. This formed a container into which liquid air could be placed. The purpose of this device was to insure the condensation of every alkali metal atom, and at the same time, to lower the pressure in the tube.

F and *G* were 15-mil tungsten filaments wrapped with No. 30 B and S gauge silver wire. By passing a current through these filaments, silver was

evaporated over the inside surface of the tube. This acted as a shield from electrostatic charges and as the underlying conducting surface for the deposit of the alkali metal atoms.

A grid, *H*, consisting of five 6-mil tungsten wires, spot-welded to 50-mil tungsten leads, served to pick up the photoelectrons. A guard ring was mounted inside of the tube through which the grid wire leads were brought out.

The tube, which was made of Pyrex glass, was exhausted to a high vacuum by means of a mercury diffusion pump working through a liquid air trap. A separate heater was used to bake out the charcoal in the side tube, *E*, which was raised to the softening point of glass while the rest of the tube was baked out at 450°C.

Due to the large amount of vapor and gas emitted from the heated charcoal, it was given a preliminary bake-out before the tube containing the alkali metal was connected. After the preliminary bake-out, air was allowed to pass into the cell through the liquid air trap, and the tube, containing the salt and calcium, was sealed on as quickly as possible. The cell was then reevacuated and baked out simultaneously with the charcoal trap for a period of 15 or 16 hours. The plate and grid of the ionization gauge were brought to a red heat by means of electrical bombardment, and remained in this state until no more gas was given off. This usually lasted for about an hour.

The inside of the tube was then given a coating of silver by passing a current through the filaments wound with silver wire. This process was performed very slowly (several hours), in order to outgas the silver. Contact was made to the silver coating by means of "cat whiskers" of tungsten wire, spot-welded to the tungsten leads. Four of these contacts were used to insure electrical connection. Silver wire, wrapped around the tube on which the alkali metal was deposited, and brought out to the tungsten lead, *M*, was also used for this purpose.

The alkali metal, which was vacuum distilled through several constrictions during the bake-out, was finally driven into the lower portion of the tube. The photocell was then sealed off from the vacuum system and tested.

In studying the photoelectric effect, a 6-volt, 110-watt, tungsten ribbon filament lamp was used as a source of light. By means of a lens this light was focused on the slit of a Van Cittert-type double monochromator. An achromatic lens was used to focus the dispersed light on the photocell. The photoelectric current was measured with a Compton quadrant electrometer having a sensitivity of 4000 mm per volt at one meter scale distance.

The temperature of the alkali metal was controlled by means of the heating coil, *K*. The pinhole was heated by another coil, *J*, and the temperature at this point was kept several degrees higher than the lower part of the tube, to prevent condensation at the small opening. Chromel-Alumel thermocouples were used to determine the temperatures. The hot junctions were held in contact with the glass by wrapping copper foil about them. The thermocouples were calibrated from the freezing point of water and the

boiling point of water, naphthalene, diphenylamine, and sulfur. The temperatures could be determined to 1°C.

After placing the tube in position in front of the monochromator, the containers A and B of the photocell, and the Dewar flask which was placed on the charcoal trap, were filled with liquid air. The ionization gauge was then connected so that the pressure in the cell could be determined. The plate current was measured by means of a galvanometer having a sensitivity of 3×10^{-9} amperes per mm deflection at a scale distance of one meter. With a grid current of 5 milliamperes, pressures producing currents as low as 1.5×10^{-9} ampere were obtained. The gauge indicated no change in the vacuum when heat was applied to the alkali metal reservoir.

After liquid air was placed in the containers A, B, and the Dewar flask, the cell was allowed to stand for several hours in order to give the vacuum time to improve. When the pressure in the tube had reached a value in the order of 10^{-8} mm of Hg, a current was passed through the heating coil, K, and the temperature brought up to a constant value. The usual procedure was to allow the temperature of the heater to reach its final value before placing it over the alkali metal reservoir. This plan was adopted in order to reduce the time taken for the equilibrium temperature to be reached. The heater was then left over the alkali reservoir for a definite period, and then removed. The temperature of the reservoir dropped immediately after the heater had been removed.

When there was a sufficient deposit to give a detectable photoeffect, the film was studied by means of a spot of nearly monochromatic light (about 20A), which was focused on the plate. The deposit of alkali metal was explored by examining the photocurrent as the light passed over different parts of the film. In this way, it was found that the deposit was quite uniform and sharply defined at the edges. The position of the light beam was varied by moving the achromatic lens, which was placed between the photocell and the monochromator. The film was then allowed to stand for several hours to test for any change in the photoelectric sensitivity. In the meantime, the proper containers were kept filled with liquid air. When the vacuum was in the neighborhood of 10^{-8} mm of Hg, and the alkali deposit had been made on a freshly evaporated surface of silver, there was found to be no variation in the photoeffect even after the tube had been left standing for several hours. A spectral distribution curve was taken for this particular surface, and the heater again applied to the lower part of the tube for a definite time. In this way any desired thickness of film could be investigated.

In order to begin a new set of measurements, the lower silver filament was heated and the silver evaporated over the surface until no photoeffect could be detected, even in the presence of a very strong light.

The distribution in energy throughout the spectral range was determined by placing a vacuum thermopile in front of the monochromator in the position usually occupied by the photocell. The thermopile galvanometer deflections were amplified by means of a photoelectric cell relay arrangement in order to determine the distribution in the blue part of the spectrum, where

the energy was low. The data obtained in this way were used in plotting the spectral response curves on an equal energy scale.

Calculation of Film Thickness

The formula used to determine the number of deposited alkali atoms was taken from an article by O. Stern.[4]

$$q = (5.83 \times 10^{-2}) pf/(MT)^{1/2}$$

where q represents the number of moles ejected in one second from the pinhole, C; M is the molecular weight of alkali metal; T the temperature, Kelvin, of the alkali metal reservoir; p the vapor pressure, in mm of Hg, of alkali, at temperature T; f the area of the pinhole in cm^2.

If J represents the number of moles striking the condensing surface in one second, then

$$J = q/\pi r^2,$$

where r is the distance in cm from the pinhole to the surface on which the deposit is formed.

The number of atoms striking the surface in one second, is given by the equation,

$$N = (6.06 \times 10^{23}) qJ.$$

It is inconvenient, in referring to the film thickness, to state the number of atoms deposited. Instead, a definition for a molecular layer will be given, and this expression used in reference to the thickness.

In a solid mass of metal, the number of atoms per cm^3 can be determined by dividing the density of the metal by the mass of a single atom. The cube root of this number gives the number of atoms along an edge, and the square of this quantity gives the number of atoms per cm^2. This will be used as a definition for a molecular layer. It is understood, however, that in forming a very thin film, the spacing may be quite different from that in a solid mass of the metal. A discussion of the number of atoms per cm^2 in monatomic layers has been given by Becker.[5]

The diameter of the pinhole was 0.75 mm and the distance from the pinhole to the condensation surface was 16.0 cm.

The vapor pressure of potassium was obtained by use of the empirical formula of Edmondson and Egerton[6] and for sodium, the formula given by Rodebush and de Vries[7] was used. The probable error as estimated by these experimenters is less than 5 percent.

The vapor pressures of rubidium and caesium were determined from the values of the constants given in the International Critical Tables.[8] The vapor pressures can be determined within 10 percent by means of these values.

[4] O. Stern, Zeits. f. Physik **39**, 754 (1926).
[5] J. A. Becker, Phys. Rev. **28**, 341 (1926).
[6] Edmondson and Egerton, Proc. Roy. Soc. **A113**, 526 (1928).
[7] Rodebush and de Vries, J. Amer. Chem. Soc. **45**, 2323 (1923).
[8] International Critical Tables III, 205.

However, this accuracy is uncertain inasmuch as there is a wide variation in values given by different experiments.[9,10] This has been pointed out by Rowe.[11]

The principal variable errors in the experiment were the measurement of the temperature of the alkali metal reservoir and the length of time it was heated. The error in the determination of the film thickness caused by the variation in temperature (after the reservoir had reached equilibrium temperature) was probably not more than 4 percent. The determination of the time of heating was made a little uncertain by the fact that it required a few minutes to reach the equilibrium temperature after the heater was applied to the reservoir. This error was not usually more than 10 percent. The total variable error then was probably less than 12 percent.

Constant errors may have been introduced in the calibration of the thermocouple and the measurement of the hole and distance between the hole and condensation surface. It is likely that the total constant error was less than 6 percent. The total error in the determination of the film thickness is probably less than 20 percent (this includes the possible error of 10 percent in vapor pressure).

Experimental Results

Potassium

Curves showing the photoelectric current as a function of the wave-length of the incident light are illustrated for the different film thicknesses in Fig. 2.

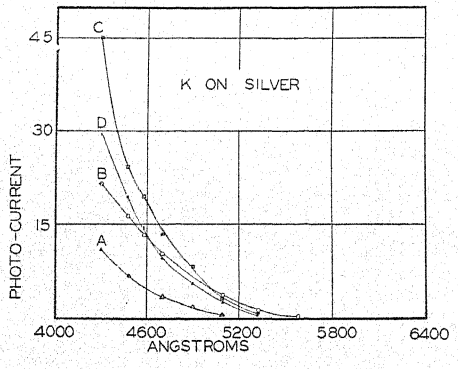


Fig. 2. Spectral response curves for different film thickness of potassium. *A*, 0.8 molecular layer; *B*, 3.0 molecular layers; *C*, 12.4 molecular layers; *D*, 19.2 molecular layers.

The ordinates represent photocurrent per unit light intensity in arbitrary units. The recorded thresholds were arbitrarily chosen as the points where the currents became definitely measurable.

A represents the spectral response curve for a film formed on a freshly coated silver surface, when the potassium reservoir was heated to a tempera-

[9] D. H. Scott, Phil. Mag. **47**, 32 (1924).
[10] T. J. Killian, Phys. Rev. **27**, 578 (1926).
[11] H. Rowe, Phil. Mag. **3**, 534 (1927).

ture of 150° for 15 minutes. The computed thickness in this case was 0.8 molecular layer. The long wave-length limit was in the neighborhood of 5100A and the shape of the spectral response curve was different from that for heavier deposits.

The next curve, *B*, was obtained after reheating the potassium reservoir to 150°C for 35 minutes, which brought the computed thickness up to 3.0 molecular layers. The threshold shifted to the neighborhood of 5800A and the shape of the spectral response curve changed.

The heating coil was then replaced over the reservoir and the temperature brought up to 170°C (vapor pressure $= 1.48 \times 10^{-3}$ mm). After it was allowed to remain at this temperature for 60 minutes, the data for curve *C* were taken. This film gave the maximum total emission, although the threshold did not extend as far toward the red as that of curve *B*. The computed thickness was 12.4 molecular layers.

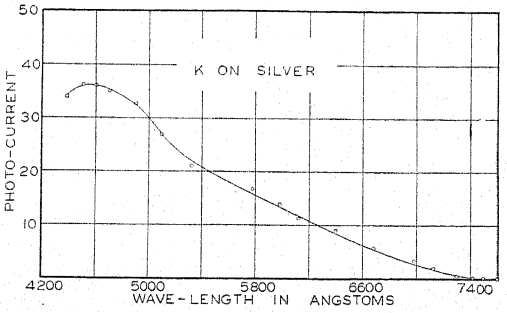


Fig. 3. Spectral response curve for contaminated potassium film.

Curve *D* was obtained from a film which was formed by reheating the potassium reservoir to 170° for 44 minutes. This film represented the thickness beyond which there was no further change in the photoelectric effect. The computed thickness was 19.2 molecular layers.

The curves were chosen from a set taken at various film thicknesses to illustrate the principal photoelectric changes which took place during the development of the film.

Separate experiments, in which different reservoir temperatures were used to secure the same film thickness, gave results which showed that the photoelectric effect was independent of the rate of deposition when varied as much as tenfold.

An attempt was made to study the films when the condensing surface was not cooled with liquid air, but the photoelectric effect did not remain constant after a deposit was made. There was a constant decrease in emission which indicated that changes were taking place on the surface.

The pressure in the photoelectric cell (measured with the ionization gauge) had to be in the neighborhood of 10^{-8} mm or less before consistent results could be obtained. In cases where the pressure was not this low, undesirable effects were noticed. One of these was the gradual decrease in emission just after the film was exposed to light. The original sensitivity could be

restored by allowing the cell to remain in the dark for several minutes. This fatiguing was found to be greater in the case of illumination by violet than for longer wave-lengths. Successive exposures to light and darkness produced no change in the effect.

In order to make a test of the effect of increasing the pressure in a tube from which reliable data had been obtained, the liquid air was removed from the charcoal after a thin film was deposited. Fig. 3 illustrates the results found in a typical case. The curve was taken four hours after the liquid air was removed. The shape of the spectral response curve as well as the position of the threshold was greatly changed by the increase in pressure in the cell. The results were not quantitatively reproducible in a case of this kind, but indicated that the change in the photoelectric effect was greater for films in the order of a monomolecular layer than for heavier deposits.

Sodium

Several tubes were constructed in which silver was used as the underlying surface for the study of sodium films. It was found, however, that in each case, the photoelectric emission began to decrease immediately after the heating coil was removed from the sodium reservoir. The pressure in the tube was measured each time and found to be in the neighborhood of 10^{-8} mm. The instability of photoelectric emission could not, then, be attributed to a poor vacuum.

A cell was next constructed with nickel as the underlying material, but here again there was a decrease in emission after the film was deposited.

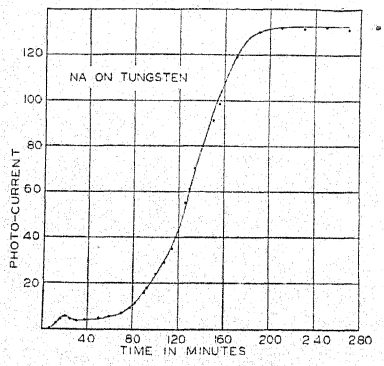


Fig. 4. *White light* curve for sodium. Rate of film formation, 1.1 molecular layers per minute.

Finally, a tube in which tungsten was used as the underlying material was constructed, and in this cell stable sodium films were formed. The emission from the thin films was found to be too small to be measured when the light from the monochromator was used, so a tungsten filament lamp, glowing at much less than its normal brilliancy, was used as a source. The *white light* curve, showing the emission as a function of film thickness, is illustrated in Fig. 4. In order to secure the data for this curve the sodium reservoir was heated to 270°C (vapor pressure $=7.64\times10^{-3}$ mm) and the

emission was recorded at intervals during the progress of the film development. The computed rate of film formation in this case was 1.09 molecular layers per minute.

A maximum appeared in the emission curve for a film thickness of 15 molecular layers. The emission was found to increase again for a computed film thickness of about 100 molecular layers. The magnitude of the emission in this case rose to a value about 25 times greater than the maximum for the very thin film. The film development, however, was not carried out far enough to determine definitely whether the emission remained constant or whether the large increase represented a second maximum.

This enormous increase in emission for deposits in the order of 100 molecular layers was not found in the other alkali films.

Rubidium

Fig. 5 shows the dependence of the photoelectric effect on the wavelength of the incident light for different film thicknesses. Curve *A* represents the spectral emission for a film formed by heating the rubidium reservoir to

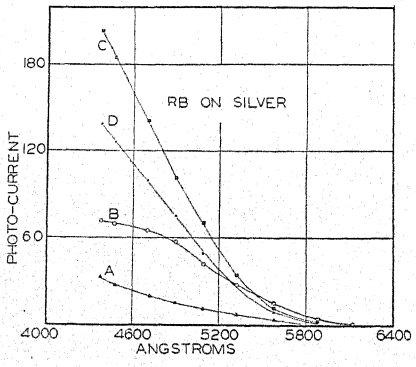


Fig. 5. Spectral response curves for different film thicknesses of rubidium. *A*, 0.6 molecular layer; *B*, 1.5 molecular layers; *C*, 5.0 molecular layers; *D*, 12 molecular layers.

110°C (vapor pressure $= 4.06 \times 10^{-4}$mm) for 11 minutes. The computed thickness was 0.4 molecular layer. The threshold was in the neighborhood of 5800A.

The rubidium reservoir was then reheated to 110°C for 30 minutes. This brought the computed thickness to 1.5 molecular layers. The threshold lies in the neighborhood of 6200A and was farther in the red than for any other thickness. The shape of the curve was quite different from that of the others and appeared to be nearing a maximum at 4000A.

The heating coil was again placed over the rubidium reservoir and the temperature raised to 130°C for 28 minutes. This brought the computed thickness to 5 molecular layers. This film gave the maximum photoelectric emission, but the threshold was not as far in the red as that for the preceding thickness.

The final curve, *D*, was obtained after reheating the reservoir to 130°C,

and the atoms were allowed to condense for 58 minutes. This brought the computed thickness to 12 molecular layers. The emission was less than that for the preceding film, and the threshold shifted farther toward the blue. Further increase in deposition produced no change in the photoeffect.

Caesium

The results for caesium are illustrated in Fig. 6. For this element the region near the threshold was investigated more carefully than for any of the other metals. This region of the curves was magnified as shown in the right hand corner of the figure. The data beyond 5800A were secured by opening the slits of the monochromator so that the light intensity was increased. In doing this, the wave-length band was broadened from 20 to 40A. The curves are seen to approach the wave-length axis asymtotically, and the existence of

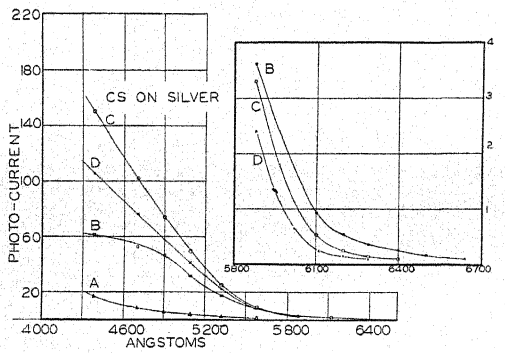


Fig. 6. Spectral response curves for different film thicknesses of caesium. *A*, 0.6 molecular layer; *B*, 1.5 molecular layers; *C*, 5.4 molecular layers; *D*, 10 molecular layers.

an optimum thickness for the maximum extension of the threshold is definitely established.

The results were very much the same as those for rubidium. Curve *A* was obtained after heating the caesium reservoir to 105°C (vapor pressure = 6.4×10^{-4} mm) for 12 minutes. This gave a computed thickness of 0.6 molecular layer. *B* represents data obtained after reheating the reservoir to 105° for 16 minutes. This brought the computed thickness to 1.5 molecular layers. This also represented the thickness for the maximum extension of the long wave-length limit.

As the deposition was increased, the emission increased, but the threshold receded toward the blue end of the spectrum. Curve *C* represents the thickness for maximum emission. In this case, the caesium reservoir was heated to 120°C (vapor pressure = 1.57×10^{-3} mm) for 33 minutes. This brought the computed thickness to 5.4 molecular layers.

Finally, the caesium reservoir was heated to 120°C for 43 minutes. This brought the thickness to 10.4 molecular layers. Curve *D* represents the spectral emission for this film.

Discussion of Results

According to Sommerfeld's theory,[12] a metal may be considered as a box of free electrons which are kept within the enclosure by a potential wall at the boundary. These electrons obey the Fermi-Dirac statistics so that at the absolute zero of temperature there is a definite upper limit for the energy that an electron may have. The work function of the metal is then defined as the energy necessary to remove an electron from this highest energy state (at 0°K) entirely away from the metal. It appears as $h\nu_0$ in Einstein's photoelectric equation,

$$h\nu = mv^2/2 + h\nu_0$$

where h is Planck's constant, ν the frequency of the incident light, and v the velocity of the ejected electron and ν_0 the threshold frequency. Thus, the determination of the threshold is a measurement of the work function of the surface.

The *grid* theory of activated surfaces may be used to advantage to account for the effect produced by the thin alkali films. This theory has been investigated by Becker[13] in his work on thermionic emission. It has also been discussed by Compton and Langmuir,[14] who refer to it as the *adion field theory*.

The fact that alkali ions are evaporated from heated filaments which have been previously coated with a deposit of alkali metal, indicates that the deposited atoms behave like ions on the surface. Then in the present experiment, as the atoms condense on the silver surface they produce an ionic layer which sets up an electric field which aids the electrons in their escape from the metal. For a first approximation, the field due to this ionic grid may be considered uniform and proportional to the number of ions in the layer.

The upper diagram in Fig. 7 represents the potential curve for silver. The horizontal dotted line represents the highest Fermi energy state. The vertical line AA' represents the boundary of the silver so that the portion of the curve to the left of this line is the potential of the interior of the silver. The light solid line (a trough) to the right of A illustrates the effect of a very small deposit of alkali atoms (perhaps 1/50 of a molecular layer). As more atoms are deposited on the silver the bottom of this trough becomes lower but no electrons will remain in the trough until it is lower than the highest Fermi energy state. A calculation[15] of the electric field near the surface due to the ions (for potassium on silver) shows that it requires only 0.2 of a monomolecular layer of ions to reduce the work function from that of the pure silver surface to that of a very thick film of alkali metal. This indicates that the atoms all become ions as soon as they are deposited, up to 0.2 molecular, after which they go on as atoms. On the potential curve this means that it

[12] A. Sommerfeld, Zeits. f. Physik **47**, 1 (1928).

[13] J. A. Becker, Bell Tech. Lab. Reprint B-412 (August 1929); Phys. Rev. **35**, 1431 (1930).

[14] Compton and Langmuir, Rev. Mod. Phys. **2**, 157 (1930).

[15] For method, see Hughes and DuBridge, *Photoelectric Phenomena*, page 86. (McGraw-Hill Book Co., 1932).

requires 0.2 molecular layer of ions to lower the trough to the highest Fermi energy level. For deposits less than this the electrons leave the trough and *spill over* into the silver. This theory is supported experimentally by the fact that the *threshold is shifted to within 85 percent of its thick-film value by a deposit of 0.2 of that required for the maximum excursion.**

This theory accounts very well for the extension of the threshold toward the red during the early stages of the deposit but does not account for the excursion of the threshold *beyond its value for the solid alkali*, nor for a *maximum in this excursion* for a thickness of a few molecular layers. However, Professor J. R. Oppenheimer has suggested the following possible explanation to the writer.

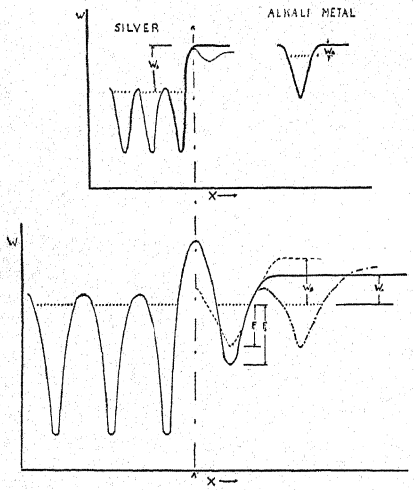


Fig. 7. Potential energy of an electron passing through silver and an alkali metal film; upper curve, before contact of metals. Lower, in contact.

The potential curve for an isolated monomolecular layer of alkali metal atoms is illustrated in the upper diagram of Fig. 7. This same curve is illustrated schematically as a dashed line in the lower diagram. It neglects the effect of the potential due to the silver. From this diagram it is seen that in this case (for potentials as drawn) the alkali metal potential trough *is narrowed* by the potential of the silver. If the wave mechanics is now applied to this *narrowed* trough to solve for the possible energy states in which electrons may exist, it is found that the states are distributed farther apart than in a normal trough. The distribution of energy states in a box of electrons depends upon the size of the box when its dimensions are in the order of a few atom diameters. F_2, in the figure, represents the total spread of energy values from the zero to the highest Fermi state. The work function, then, is W_A. The dashed line represents a normal potential trough (without the

* The threshold for outgased silver is about 2600A while the thick film threshold for potassium on silver is about 5500A. This is a threshold shift of 2900A. A 0.6 molecular layer gave a shift of 2500A which is 85 percent of the 2900A shift.

narrowing effect produced by the proximity of the silver) and the work function in this case would be W_B. The total spread in energy states would be F_1.

For these same potentials the dash-dot line represents the effect of adding a second layer of atoms.

The course of the potentials schematically drawn in Fig. 7 is a wholly reasonable one, and would account simply for the observed excursion of the threshold.

Lawrence and Linford[16] have shown that the work function of a surface may be changed by the application of strong electric fields. Their experiment also showed that for a composite surface of potassium on tungsten this change in work function has very little effect on the shape of the spectral response curve. In other words, the curves are shifted very nearly parallel to themselves along the frequency axis. It might be assumed, therefore, that the difference in shape of the curves for different thicknesses (in the present experiment) was due entirely to a difference in the source from which photoelectrons originate. For instance, one might assume that in the early stages of the film development the electrons came principally from the underlying material but as the deposit increased beyond that necessary to form a monomolecular layer, the photoelectrons originate principally in the alkali metal. As the electron density in the two metals differs considerably, one might assume that the spectral response curve for the very thin film would be quite different in shape from that obtained for a thicker one.

An attempt was made to test this assumption by means of Houston's modified form of Wentzel's theoretical expression for the complete spectral emission of photoelectrons. The equation is given in the paper by Lawrence and Linford.

For deposits of a monomolecular layer or less in thickness, the value of ϵ (the maximum energy of the Fermi distribution at 0°K) was calculated from the electron density in silver. For a thick film the value of ϵ was calculated by using the electron density in the alkali metal.

The experimental values for the threshold found for the monomolecular film and the thick film were used in Houston's expression, and two theoretical curves were plotted for photoelectric current against frequency of exiting light. The shapes of these curves were then compared with the two experimental curves (monomolecular layer and thick film). According to this theory the emission from silver should be greater than from the alkali, (using the reduced value for the work function), but experimentally the emission was found to increase for films greater than a monomolecular layer. This discrepancy between Houston's theory and the present results might possibly be ascribed to Houston's failure to correct adequately for the binding of the conduction electrons in silver.

Also, the experimental curves for rubidium and caesium for a thickness in the order of a monomolecular layer appear to approach a maximum near

[16] Lawrence and Linford, Phys. Rev. **36**, 482 (1930).

4000A and the calculated maximum (Houston's formula) is nearer 3000A and is slightly farther in the violet for silver than it is for the alkali metal.

Hughes and DuBridge[17] have shown that the theory gives a curve which is of approximately the correct shape near the threshold, but at higher frequencies departs widely from the form of the curve obtained experimentally for the alkali metals.

No conclusion can be drawn on this point until a more exact theoretical expression is obtained for the total spectral emission.[18]

In general the results of the present investigation show the same phenomena as that reported by previous workers. However, there are two important differences. One is the difference in film thickness between that found for the maximum total emission and that for the maximum extension of the threshold. The other difference deals with the magnitude of the maximum excursion of the threshold. Ives and Olpin[19] found shifts in the order of 1000A in going from the thickness of maximum threshold to the thick film. In the present work the shifts were in the order of 300A. This difference may be due to the fact that the underlying material in the present experiment was freshly evaporated while Ives and Olpin used a solid plate of metal. It is thought that the use of a freshly evaporated underlying surface minimized the possibility of occluded gas on the surface. This is based on the fact that larger shifts in the threshold were found when the silver surface was allowed to stand a day before depositing the alkali metal. The recorded shifts were obtained by depositing the alkali metal immediately after evaporating the silver.

In conclusion the author wishes to thank Professor E. O. Lawrence for proposing the problem and for his suggestions and constant interest throughout the course of the work.

[17] Hughes and DuBridge, *Photoelectric Phenomena*, page 228.

[18] Ives and Briggs in a recent paper (Phys. Rev. **40**, 802 (1932) have presented evidence that indicates that the photoelectrons originate partly in the underlying metal and partly in the alkali metal film, the relative proportions varying with the film thickness.

[19] Ives and Olpin, Phys. Rev. **34**, 117 (1930).

Optical Dissociation of Iodine and Enhancement of Predissociation by Collisions

By LOUIS A. TURNER
Palmer Physical Laboratory, Princeton University

(Received July 5, 1932)

Optical dissociation of iodine molecules is demonstrated by absorption by the atoms of light of wave-lengths 1830, 1783, 1642, 1618, 1583 and 1515A these being the lines in the region 2100 to 1514 which arise from transitions to the normal state of the iodine atom. This dissociation is produced in iodine-argon mixtures by light of wave-length >5100A, which produces only excited molecules immediately upon absorption so that the atoms presumably result from dissociation produced by collisions. Spectra of electrical excitation and of fluorescence in iodine-argon mixtures show that molecules of higher v' are more effectively quenched, this larger quenching setting in at about $v'=12$. This suggests that the effect is a sort of predissociation, enhanced by collisions. A possible theoretical interpretation of such an effect is discussed.

SOME years ago[1] it was found possible to detect the optical dissociation of iodine *molecules* by observing the absorption of light by the iodine *atoms* resulting from this dissociation. The ultraviolet light from a discharge in iodine was passed through an absorption cell containing iodine which could be illuminated by the visible light from a carbon arc, and then into a small quartz spectrograph. The 1830 atomic line was less intense for those exposures during which the cell was illuminated by the visible light, because of its absorption by the iodine atoms produced in the absorption cell. It was suggested at that time that this arrangement might be of use in various experiments as a means of detecting the presence of iodine atoms, for it seems to be the only method so far discovered that will differentiate between iodine molecules and iodine atoms. Subsequent work on the magnetic quenching[2] of the fluorescence of iodine led to a theory which implies that the magnetic field produces atoms by means of a predissociation. It seemed desirable to try to verify this theory by demonstrating the production of the atoms by the magnetic field, and so work was begun in the endeavor to improve the absorption method of detecting atoms in order to make it a more useful tool for such researches. The experiments show that the method is not of as wide usefulness as originally hoped but various results were obtained which seem to be of sufficient interest to warrant publication.

EXPERIMENTAL METHOD

The three principal improvements in method in these experiments as compared with the former are in the use of a vacuum fluorite spectrograph, of a discharge at low pressures as light source in order to give narrow unreversed

[1] Louis A. Turner, Phys. Rev. **31**, 983 (1928).
[2] Louis A. Turner, Zeits. f. Physik **65**, 464 (1930).

lines, and of argon in the absorption cell to slow down the diffusion of atoms to the wall. The iodine lines absorbable by atoms in the normal state lie for the most part in the Schumann region,[3] the one of longest wave-length being the line at 1830A. This latter line was the only one which could be observed with the old apparatus and then with difficulty, whereas several lines are usable with the new apparatus (see below). The vacuum spectrograph was one of the small ones described by Cario and Schmidt-Ott.[4] This method of the reversal of emission lines can be thought of as making it possible to do experiments of a sort ordinarily requiring high resolving power with spectroscopic instruments of low resolving power. The emission lines have automatically a distribution of energy in wave-length over the very narrow region of wave-length in which the absorption coefficient is large so that a large percentage of their energy is absorbable. A weakening of such lines can be observed

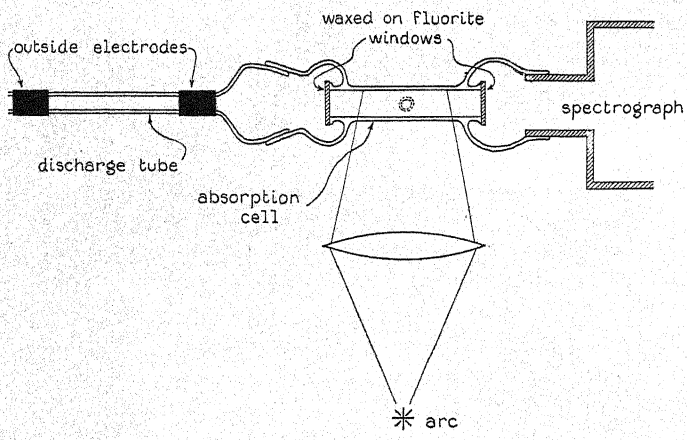


Fig. 1. Apparatus.

quite readily by a small spectrograph with which it would be impossible to detect the absorption as fine black lines crossing a continuous background. The failure of Sponer and Watson[5] to observe the phenomenon may possibly thus be accounted for. That the condition be fulfilled it is necessary that the source of the emission lines be one which will give narrow and unreversed lines. For them to be narrow the source should be at a low temperature to make the Doppler width as small as possible, and the pressure should be low, which also minimizes self-reversal by reabsorption in the source. Such a source was obtained by exciting iodine at a pressure of 0.03 mm in a straight tube of a diameter of 8 mm by means of a high-frequency field from a short wave oscillator applied to two metal foils wrapped around the outside of the tube. Argon at various pressures up to 55 mm was put into the absorption cell in order to cut down the rate of diffusion to the walls of any iodine atoms formed. Inasmuch as the recombination of atoms to form molecules presumably takes place principally at the walls, this addition of argon ought to in-

[3] Louis A. Turner, Phys. Rev. **27**, 397 (1926).
[4] G. Cario and H. D. Schmidt-Ott, Zeits. f. Physik **69**, 719 (1931).
[5] H. Sponer and W. W. Watson, Zeits. f. Physik **56**, 184 (1929).

crease the concentration of atoms for any given rate of formation by slowing down the rate at which they leave the region of their formation. It was found, however, that the argon introduces further complicating effects which will be discussed below.

The absorption cell was illuminated by the light from a carbon arc run with a current of 13 amperes. It was focussed as an astigmatic bundle along the axis of the absorption cell by use of a suitable nonspherical lens. A diagram of the apparatus is given in Fig. 1.

Results of Absorption Experiments

Fig. 2 is a reproduction of a plate which shows the absorption clearly for the 1830, 1783 and 1642 lines. (1642 is the left hand line of the 1642–1641–

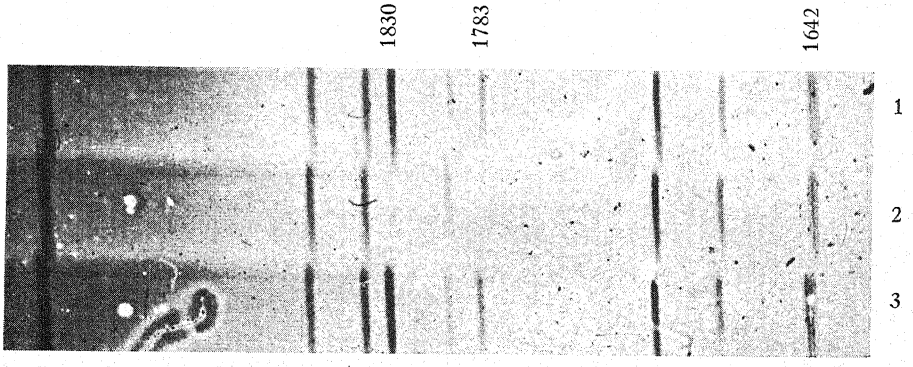


Fig. 2. Absorption by iodine atoms. Spectra 1 and 3, absorption cell not illuminated. Spectrum 2, absorption cell illuminated.

1639 group.) Others made with longer exposures are more suitable for showing the effect with lines of shorter wave-length. For this one the pressure of the iodine in the absorption cell was 0.2 mm and that of the argon 50 mm.

It has been pointed out previously[1] that the lines which arise from transitions to the normal state of iodine are known with practical certainty in spite of the fact that the spectrum has not yet been completely analyzed. Such lines appear as members of the shorter wave-length of doublets having the $\Delta\nu$ of the inverted ^2P term of the normal p^5 configuration (transitions from upper levels having J's of 1/2 and 3/2) or as single lines (transitions from upper levels having $J=5/2$). All other lines must be the long wave-length members of doublets (transitions to the $p^5\ ^2P_{1/2}$ level from upper levels having J's of 1/2 and 3/2) unless there be present unsuspected terms arising from other electronic configurations close to the $p^5\ ^2P$ term, which seems most improbable. In the region of the spectrum here investigated (2100–1514A) there are seven lines resulting from transitions to the normal $p^5\ ^2P_{3/2}$ level, of wave-lengths 1830, 1783, 1642, 1618, 1583, 1527, and 1515A. All of these, with the exception of 1527, have been observed to show the absorption. The result is, however, doubtful for 1583 as it is a relatively weak line appearing on only one plate and there showing but a very slight absorp-

tion. Three more lines than those given in the preliminary report of these experiments[6] have thus been found to show the absorption. No trace of it was noted with nine other lines in the region investigated, all of these being the members of longer wave-length of doublets.

According to the theory of optical dissociation[7] only light of wave-lengths falling in the region of the continuous absorption ($\lambda < 4995$A for iodine) should cause dissociation. This was tested by using filters to isolate different regions of the spectrum of the carbon arc. The absorption effect was obtained not only as expected when a filter was used transmitting light of wave-length less than 5100A (and some red light of $\lambda > 7600$ which is not strongly absorbed by I_2), but also, and indeed more strongly, when another filter which transmitted only light of wave-length greater than 5100A was used. The pressure of the iodine was 0.3 mm and that of the argon 53 mm in both experiments. With no argon present there was only slight absorption even with the full radiation, presumably because of the rapid diffusion of atoms to the walls where they recombine. This feebleness of the effect with iodine alone rather severely limits the range of usefulness of the method in the detection of iodine atoms and, in particular, makes it valueless in connection with experiments on the magnetic quenching.

The result of the experiment with light of wave-length greater than 5100A was a surprising one. Such light will upon absorption immediately produce excited molecules which, if isolated, reradiate the energy as fluorescence, as is well known. These excited molecules do, to be sure, contain an excess of energy over the energy of dissociation but the strength of the fluorescence indicates that few, if any, dissociate spontaneously rather than reradiate the absorbed energy. The absorption of the atomic lines with argon present indicates, therefore, either that these excited molecules dissociate upon collision with argon atoms or that the presence of the argon merely helps toward the building up of a concentration of iodine atoms resulting from a small percentage of spontaneous dissociation. If the latter be the case the argon should have little influence on the fluorescence. If the former be the true explanation then the argon should cause a considerable quenching of the fluorescence and the dependence of the magnitude of this effect upon the state of excitation of the molecule should be of interest.

Fluorescence Experiments

In view of these considerations experiments on fluorescence were undertaken. A tube was rigidly attached to a system so that argon could be admitted and pumped out without disturbing the optical arrangement. The source of the exciting light was a 400 watt tungsten lamp. The fluorescence light was photographed with an F3 Steinheil glass spectrograph. Exposures were made with argon at various pressures. Fig. 3 shows three such spectra on one plate chosen from several showing the same phenomenon. They were

[6] Louis A. Turner and E. W. Samson, Phys. Rev. **37**, 1023A (1931).

[7] J. Franck, Trans. Faraday Soc. **21**, part 3 (1925).

taken on the same plate with conditions as indicated, and also printed together. The final enlarged prints all made in just the same way were then cut in order to place the spectra side by side. It is of interest that the spectrum shows a banded structure in spite of the fact that continuous light was used for the excitation. This results from the fact that of the many possible $v' \rightarrow v''$ transitions only a few have a relatively large transition probability, in particular, the $v' \rightarrow 0$ transitions for $v' > 16$. (See below on the electrically excited spectra.) The width of the bands results from the distribution of the molecules among the various rotation states. That such long exposures are

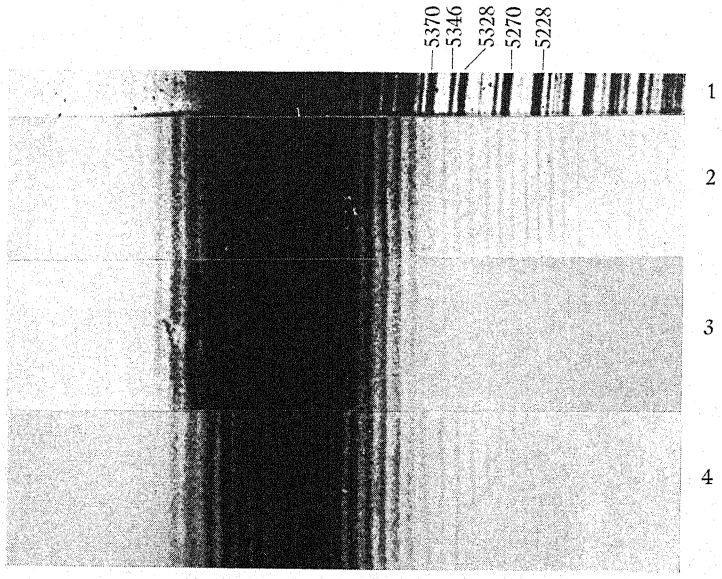


Fig. 3. Quenching by argon. (1) Fe arc; (2) iodine alone, 0.3 mm, 1 hr. 50 min; (3) iodine at 0.3 mm, argon at 11 mm, 4 hr., 45 min; (4) iodine alone, 0.3 mm, 1 hr. 20 min.

necessary with the argon present indicates that there is an extinction of excited molecules of all values of v'. There is further an obvious greater quenching of the fluorescence at shorter wave-lengths. Since all absorbed energy must either be re-emitted as fluorescence or remain in the gas it is plain that the large quenching of the fluorescence indicates that the argon does have the effect of causing the excited molecules to dissociate. It is particularly noteworthy, however, that the quenching is greater for those molecules having a higher v'. It appeared from visual inspection that this increase of quenching set in at $v' = 29$ as was stated in the preliminary report[8] of these experiments. Subsequent work on these plates with a microphotometer, following apparently contradictory results by Loomis and Fuller discussed below, has shown that this result is illusory, the weakening of the bands appearing to begin in the neighborhood of $\lambda = 5710$A in fair agreement with their observations.

[8] Louis A. Turner, Phys. Rev. **38**, 574 (1931).

Electrically Excited Spectra

The general results of these experiments with fluorescence have been confirmed by other work done by the electrical excitation of the band spectrum of iodine in the pure vapor and in mixtures of it with argon. The same high-frequency excitation as used for the absorption experiments was found to be suitable although the light was rather weak. The iodine was kept at a pressure of 0.3 mm and argon at a pressure of 5 mm was used. In order to have the bands at longer wave-lengths at the same strength in the spectrum of the mixture as they were in the spectra of the pure iodine, exposures twelve times as long were needed. The same general result as that of the fluorescence experiment was obtained. For two exposures where the blackening of the plate for the bands of longer wave-length was the same in both, the bands at shorter wave-length (higher values of v') were weaker in the exposure made with the mixture. Examination of the plates with a microphotometer showed that this effect apparently begins with the bands at about 5900A and not at shorter wave-lengths as originally judged by inspection. These exposures were taken with a Hilger El glass spectrograph so that the band heads are nicely resolved. It is of interest that the only heads appearing with any strength are those of the bands observed by Mecke[9] in absorption. In particular for $v'>16$, only the $v'\rightarrow 0$ of all possible $v'\rightarrow v''$ bands appear, thus emphasizing the fact of the much greater transition probability for the $v'\rightarrow 0$ transitions.

Discussion of Experiments

The fluorescence experiment is merely a refinement of one done many years ago by Franck and Wood.[10] They observed the quenching of the iodine fluorescence by various gases including argon and noticed a reddening of the fluorescence light which corresponds to the greater quenching of the light of shorter wave-lengths noted above. Professor Franck suggested that the quenching might be the result of dissociation and that the reddening[11] was the result of the loss of vibrational energy excited molecules by collisions of the second kind with atoms of the admixed gas. The recent work of Heil[12] demonstrates the occurrence of this process in various molecules including iodine. Without additional hypothesis, however, this explanation does not suffice to account for the setting-in of increased quenching at any particular value of v'. It was for this reason that the author suggested[8] that these experiments gave evidence for an enhancement of a predissociation process by collision. Since the increase of quenching now appears to be not nearly so sudden as it originally seemed, this hypothesis might be considered questionable were it not for the experiments of Loomis and Fuller[13] on the absorption of mixtures of iodine with various gases. They found that with increase of

[9] R. Mecke, Ann. d. Physik (4) **71**, 104 (1923).
[10] J. Franck and R. W. Wood, Phil. Mag. (6), **21**, 314 (1911).
[11] J. Franck, Ergebnisse der Exakten Naturwissenschaften **2**, 118 (1923).
[12] O. Heil, Zeits. f. Physik **74**, 18 (1932).
[13] F. W. Loomis and H. Q. Fuller, Phys. Rev. **39**, 180 (1932).

pressure of the admixed gas of various sorts, including argon, the absorption of light from a continuous background was relatively greater for wavelengths corresponding to $v' > 12$. They attributed this increased absorption to a relatively greater broadening of the absorption lines.[14] This broadening of the lines is what is observed in ordinary predissociation phenomena and corresponds to the shortening of the life of the molecule in the excited state. Loomis and Fuller independently arrived at the idea of predissociation caused by collision, their evidence being more convincing.

There remains the question as to why the collisions should produce predissociation. The author is not competent to develop a mathematical theory of the effect but would like to present for consideration an amplification of the suggestion previously made.[8] It has been pointed out[2,8] that there is a possibility of the occurrence of an ordinary natural predissociation in iodine vapor. The probability of it must be very small because the lines of the band spectrum of iodine are sharp. It would presumably have its probability increased by any influence which would tend to break down any of the selection rules. One of these is that J does not change, which is simply a quantum formulation of the law of the conservation of angular momentum, obviously applicable to a radiationless transfer in an isolated molecule. This principle should also be applicable to the more complicated system made up of an iodine molecule and an additional argon atom. The angular momentum of this system before collision can be conveniently thought of as being composed of the angular momentum of the iodine molecule about its own center of gravity plus that of the molecule and argon atom with respect to the center of gravity of the whole system. After collision and dissociation there will be three separate atoms and the total angular momentum will be the same. The part of it which can be thought of as associated with the motion of the two iodine atoms with respect to their mutual center of gravity need not, however, be the same as it was before the collision in order that the total angular momentum remain constant. The iodine molecule presumably loses its separate identity at the collision. This virtually amounts to a breaking down of the J selection rule of the predissociation which would tend to make the process a more probable one. A more detailed analysis might show that an initial probability for predissociation in the iodine molecule is not necessary, although it is difficult to see how an atom like one of argon in a $'S$ state could produce a change of the electronic states of the combined temporary triatomic molecule which would permit predissociation transitions otherwise impossible.

Since these fluorescence experiments with excitation by white light are very complicated in that excited molecules of all different vibration and

[14] The author has found in conversations that there is considerable confusion about this matter. If k_ν be the absorption coefficient at frequency ν for a single line the absorbed energy will be represented by $E = I_0 \int_0^\infty (1 - e^{-k_\nu l}) d\nu$. Even though $\int_0^\infty k_\nu d\nu$ remains constant upon adding a foreign gas E will not necessarily do so. A simple consideration shows that if there is greater absorption at the center of the line, the total energy absorbed will be increased with a broadening of the line even though $\int_0^\infty k_\nu d\nu$ remains constant.

rotation quantum numbers are produced it seemed advisable to proceed next to a study of the quenching by argon and other gases of the fluorescence excited by approximately monochromatic radiation. Such work has been in progress here during the past year but is not yet completed. Various complicating factors, the importance of which was not realized at the outset, have had to be taken into account. The transfer effect, i.e., the loss of vibrational energy upon collision is more probable than was at first realized, the reabsorption of the fluorescent light in the tube must be considered, the widening of the absorption lines changes the amount of energy absorbed from the beam of exciting light and this must be measured in order to make the measured apparent quenching be of significance,[15] the auto-quenching by other iodine molecules is also of sufficient magnitude to influence the results. Clean-cut, significant quantitative results concerning the effect of the added gas are thus difficult to get and it remains to be seen what the final degree of success in the experiments will be.

For his skill and perseverance my thanks are due to my former assistant, Dr. E. W. Samson, who did practically all of the experimental work here reported.

Note added in proof, August 13, 1932. A recent paper by V. Kondratiew and L. Polak (Zeits. f. Physik **76,** 386 (1932)) describes experiments showing the influence of added oxygen on the absorption spectrum of bromine vapor and NO_2. They also suggest the occurrence of predissociation produced by collision with bromine and show that the oxygen added to NO_2 increases the predissociation already present with NO_2 alone. The present author suggests that the effects observed with iodine and perhaps also with bromine may well be of this latter sort, the natural predissociation being, however, much less prominent.

[15] The importance of this consideration in such work has recently been emphasized by L. v. Hámos, Zeits. f. Physik **74,** 379 (1932).

Reflection of Thallium, Lead, and Antimony Atoms from Sodium Chloride Crystals

By J. M. B. KELLOGG
Department of Physics, State University of Iowa

(Received July 13, 1932)

The reflection of atomic beams of thallium, lead, and antimony from a freshly cleaved surface of a crystal of sodium chloride has been studied by means of a deposit method. The beams of thallium and lead are in part scattered at random and in part reflected so that the angle of reflection is equal to the angle of incidence. Antimony incident at a large grazing angle is reflected so that the reflected beam makes a larger angle with the normal than the incident beam. It is suggested that the direction of this deviation may be qualitatively accounted for on the basis of the ideas of Duane and of Williams on the interchange of momentum between the incident particle and the crystal.

INTRODUCTION

ALTHOUGH the experiments of Stern and his collaborators[1,2,3] on the reflection of hydrogen and helium from sodium and potassium chloride crystals, and of Johnson[4] on the reflection of atomic hydrogen from lithium fluoride show the existence of surface diffraction phenomena, the experiments on the reflection of atomic beams of the metallic elements are so far not susceptible of such explanation. The specular reflection of beams of cadmium, zinc, and tetra-atomic arsenic from sodium chloride has been reported,[5,6] and the existence of a directed beam of atomic mercury after reflection from certain of the alkali halide crystals has been verified in considerable detail.[7] However, mercury is scattered at random from a crystal of potassium iodide[7] and no evidence of a specular beam can be found for cadmium reflected from orthoclase or fluorite.[5] Furthermore, Ellett and Olson,[8] and Taylor[9] have reported random scattering of certain of the alkali metals from sodium chloride.

There is no obvious explanation of this difference in behavior of different metallic atoms scattered from the same crystals, or of the same atoms scattered from different crystals, and it therefore seemed desirable to extend the work to other metals. In particular it was desired to obtain data on the reflection of thallium, for it was thought possible that the difference in be-

[1] Knauer and Stern, Zeits. f. Physik **53**, 779 (1929).
[2] Estermann and Stern, Zeits. f. Physik **61**, 95 (1930).
[3] Estermann, Frisch, and Stern, Phys. Zeits. **32**, 670 (1931).
[4] Johnson, Phys. Rev. **37**, 847 (1931).
[5] Ellett, Olson and Zahl, Phys. Rev. **34**, 493 (1929).
[6] Zahl, Phys. Rev. **36**, 893 (1930).
[7] Zahl and Ellett, Phys. Rev. **38**, 977 (1931).
[8] Ellett and Olson, Phys. Rev. **31**, 643 (1928).
[9] Taylor, Phys. Rev. **35**, 375 (1930).

havior of the alkali metals and of zinc, cadmium, and mercury might be attributed to the difference in their magnetic moments. Thallium has the same magnetic moment as the alkali metals.

Apparatus

A condensation method of detection of the beam was used throughout. The atomic vapor emitted from an orifice in a small steel boiler was defined by a circular slit, and, after reflection from the crystal, collected on a liquid air cooled glass surface. In the earlier runs the boiler, or *gun*, was heated by currents induced in it by means of high-frequency current circulated in a surrounding water cooled coil. This coil was made as small as possible and introduced into the experimental tube itself in order to minimize the heating

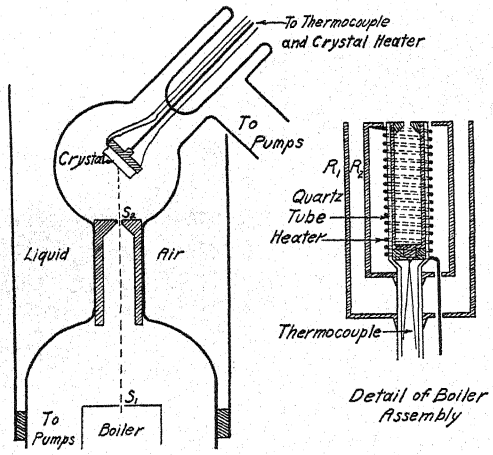


Fig. 1. Experimental arrangements.

effect on the metal of the beam defining slit S_2 and on the metal deposit formed above the gun during a run. However, this method proved to be rather unsatisfactory, for when the vapor pressure of the metal issuing from the boiler reached a value sufficiently large to permit detection of the beam, a discharge would start above the gun. This discharge rapidly worked down the coil and across the lead in wires. The pressure in the experimental tube during this time increased greatly.

Fig. 1 shows the final arrangement of the apparatus. The boiler, a steel cylinder 6 mm in diameter and 33 mm long, fitted into a quartz tube about which a heater of 20 mil tungsten wire was wound. The metal under investigation was inserted into the boiler from the top and a plug containing the boiler orifice forced in. When empty the boiler may be thrown away and a new one inserted. With two radiation shields, R_1 and R_2, Fig. 1, a boiler temperature of 1100°C could be reached with a heater input of 45 watts. Thermocouples attached to the top and bottom of a *dummy* boiler showed the top to be at a temperature only slightly lower than the bottom. This difference, about 3°C, was not sufficient to cause any condensation in the boiler orifice, or to change the vapor pressure by more than a small amount.

In all the runs the crystal was kept at 350°C. As usual, the upper limit for crystal temperature was set by the temperature at which distortion and disintegration of the crystal set in. The lower limit was set in this work by the tendency of the metals to condense on the crystal surface itself.

The dimensions of the apparatus used in the runs on thallium and antimony were as follows: boiler orifice S_1 to beam defining slit S_2, 10 cm; slit to crystal, 2 cm; crystal to collector, 2 cm. The aperture defining the beam was circular and 2 mm in diameter; the boiler orifice was also circular, and 1 mm in diameter. For lead, the beam-defining slit and the gun aperture were 1 mm, and 0.7 mm in diameter, respectively.

Although the angles of incidence and reflection of the beam were not determined with a precision greater than $\pm 2°$, the position of a specular spot could be ascertained quite accurately by sighting through the collecting surface at the image of the gun opening in the crystal. This position was then marked on the collector, and, after a run, compared with the position of the center of the deposit obtained.

RESULTS

1. Reflection of thallium from sodium chloride

Table I shows the results obtained, α_0 being the grazing angle of the incident beam and α the grazing angle of the reflected beam as measured to the center of the deposit formed by the condensed reflected atoms. T is the gun temperature in degrees C, P the vapor pressure of the metal in mm of Hg, L the length of the run in minutes, and D the diameter of the spot in cm.

TABLE I. *Thallium reflected from sodium chloride.*

T	P	L	α_0	α	D
800	1.7	25	50	50	1.5
800	1.7	30	44	44	1.7
750–800	0.9–1.7	60	46	46	3
860	4	10	25	25	1
890	5	20	23	23	1.5

Due to the rather large diameter of the spots it is not possible to conclude that the reflected beam was accurately specular, but there can be no doubt of the existence of a beam at or quite near the specular position. The size of the deposit could be reduced by shortening the length of run, but only at the expense of density of the deposit. In the second and fourth runs the spot had well-defined borders, but in the other runs the confines were marked only by a rapid shading. A background apparently formed by a cosine distribution was evident in all cases. Thallium oxidizes readily, and the deposit disappeared rapidly on exposure to air.[10]

2. Reflection of lead from sodium chloride

Lead is also scattered from sodium chloride with the angle of reflection equal to the angle of incidence. Table II gives the results of five runs. In all

[10] Gerlach, Ann. d. Physik **76**, 179 (1925).

runs but the first the deposit required development. This was done by the method of Estermann and Stern.[11] After the run the liquid air is removed from a trap, and the mercury vapor which enters the crystal chamber condenses preferentially on the slight deposit of lead already present on the glass, thus rendering the deposit more easily visible.

TABLE II. *Lead reflected from sodium chloride.*

T	P	L	α_0	α	D
1010	1.5	45	32	32	1.4
1000	1.2	20	45	45	
870	0.2	30	44	44	
800	0.05	30	45	45	1.5
750	0.002	180	45	45	1.8

Considerable difficulty was experienced in keeping the lead from condensing on the crystal face. In the first two runs this deposit was quite noticeable, while in the next, with the vapor pressure cut down to 1/6 its former value, the deposit on the crystal was barely visible. No explanation of the formation of a specular beam by reflection from a crystal coated with a metallic film can be offered here, unless it be that the formation of the specular deposit had started before the crystal became coated.

It is to be expected from the results of Chariton and Semenoff[12] that for a given crystal temperature there should exist a critical beam density below which reflection may be obtained without condensation on the crystal. This expectation was borne out by the results of the last two runs, for with the low vapor pressures used, a specular deposit was obtained, while no evidences of a deposit on the crystal appeared.

3. Reflection of antimony from sodium chloride

The results for antimony definitely show the existence of a directed rather than a specular beam. The details are given in Table III. In a consideration of the third and fourth runs it should be remembered that although the actual values of the angles α_0 and α were not known to within 2 or 3 degrees,

TABLE III. *Antimony reflected from sodium chloride.*

T	P	L	α_0	α	D
825–850	1–1.8	10	49	41	1
880	4	15	50	40	0.5
780	0.6	25	22	24	1
860	2.3	20	26	25	1.5

any displacement of the center of the deposit from the position which would be occupied by a strictly specular beam could be determined. On the other hand, the center of a deposit is not necessarily the region of maximum density of the deposit. Consequently no great weight can be attached to the slight

[11] Estermann and Stern, Zeits. f. physik. Chem. **106**, 399 (1923).
[12] Chariton and Semenoff, Zeits. f. Physik **25**, 287 (1924).

deviation of the beam from the specular in these runs. Any attempt to do so would be further complicated by the existence of the ever present background of randomly scattered atoms. If this background is intense enough to produce any shift in the apparent position of the deposit, it will be in a direction towards the normal. This is just the shift found to occur here.

However the shifts in the first two runs made at grazing angles of 49° and 50° are real. These deviations are of the order of 8 or 10 degrees and in a direction away from the normal.

Discussion

Zahl and Ellett[7] pointed out in their paper on the scattering of mercury by the alkali halides, that a deviation of the reflected beam from the specular path may be accounted for on the basis of the ideas advanced by Duane,[13] Compton,[14] and Williams.[15] It is assumed that momentum is transferred from an incident particle to the crystal in quanta and only in directions parallel to the principal axes of the crystal, and that an energy interchange takes place between the particle and the crystal. The mass of the crystal to be considered in applying the laws of conservation of momentum and energy is not the mass of the entire crystal, but only of that portion of it which scatters coherently, i.e., as a rigid body. Thus the larger the portion of the crystal scattering coherently, the less will the reflected beam deviate from the specular path. This is in accord with the experimental evidence of Zahl and Ellett. For as they point out, it is to be supposed that at higher crystal temperatures the increased thermal agitation would decrease the size of the part of the crystal which scatters coherently, and consequently increase the deviation of the path of the reflected beam from the specular, which was precisely the result obtained.

Furthermore, their results show that in every case in which a directed beam was observed, the direction of the reflected beam makes an angle with the normal smaller than would be made by a strictly specular beam. The present results for antimony show a directed beam making an angle with the normal larger than the specular. However, the corrected data on the reflected beams of mercury atoms were taken at rather small grazing angles of incidence (less than 22°), while the grazing angle of incidence for the antimony beam was 50°. This difference in the direction of deviation of the two atomic beams may be accounted for if it is further assumed that, given the same impulse, the portion of the crystal which scatters coherently is equally likely to absorb momentum in each of the three preferred directions. For these considerations require that a particle incident on the crystal almost normally should lose more momentum in the normal than in the tangential direction, and consequently experience a greater decrease in velocity in the normal than in the tangential direction. As a result the particle will be deflected from the specular position in a direction away from the normal. This is in agreement

[13] Duane, Proc. Nat. Acad. Sci. **9**, 158 (1923).
[14] Compton, Proc. Nat. Acad. Sci. **9**, 359 (1923).
[15] Williams, Proc. Camb. Phil. Soc. **24**, 343 (1928).

with the results obtained for antimony. On the other hand a particle incident at a small grazing angle should lose more momentum in the tangential than in the normal direction. Reasoning exactly similar to that above then leads to the conclusion that in this case the particle will be deflected toward the normal, which is in accord with the experiments on mercury.

In conclusion the writer wishes to acknowledge his indebtedness to Professor A. Ellett who proposed the problem, and to express his appreciation for the advice and many helpful suggestions advanced throughout the course of the work.

The Electrical Resistance and the Critical Point of Mercury

By FRANCIS BIRCH
Harvard University

(Received July 22, 1932)

Values are given for the relative resistance, the instantaneous pressure coefficient of resistance and the instantaneous temperature coefficient of resistance of liquid mercury in the region between 0° and 1200°C, and 1 and 4000 atmospheres. All of these quantities increase with rising temperature and decrease with rising pressure in this region. With the assumption that the resistance must be a continuous function of the temperature, for pressures higher than the critical pressure, the critical constants of mercury have been determined as 1460 ± 20°C and 1640 ± 50 kg/cm².

INTRODUCTION

THE resistivities at atmospheric pressure of a large number of liquid metals have been measured by various writers, including de la Rive,[1] Vincentini and Omodei,[2] Northrup,[3] Tsutsumi,[4] and Matsuyama.[5] The resistance of eight liquid metals, including the alkali metals, has been measured by Bridgman[6] at high pressures up to 100°C. It appeared of interest to observe the conductivity of a liquid metal over a larger proportion of its region of existence, combining high temperatures with high pressures. The metal chosen was mercury for the obvious reasons of accessibility of the liquid phase and unusual chemical purity. Still another reason was this: not only are the melting and boiling points of mercury at atmospheric pressure readily attainable, but there was cause to believe that its liquid—vapor critical point would also be within reach.

From general considerations, one would expect that above the critical pressure increase of temperature at constant pressure would be accompanied by a continuous change of resistivity; below the critical pressure, the phenomenon of boiling is possible with a discontinuous change of resistivity. This seems so certain that it may be accepted as a criterion for detecting the critical point, and its application leads to the values 1460°C and 1640 kg/cm² for the critical temperature and pressure.

DESCRIPTION OF APPARATUS

The pressure apparatus consisted of three steel cylinders and a pump; two of the cylinders contained moving pistons and were used to produce the desired pressure in the third or test cylinder. Details of the pressure tech-

[1] De la Rive, Arch. des Sci. Phys. (Geneva) **17**, 362 (1863).
[2] Vincentini and Omodei, Atti. Acc. Soc. Torino **25**, 90 (1889).
[3] Northrup, Jour. Frank. Inst. **177**, 1,287 (1914); **178**, 85 (1917).
[4] Tsutsumi, Sci. Rep (Tohoku) **7**, 93 (1918).
[5] Matsuyama, Sci. Rep. (Tohoku) **16**, 447 (1927).
[6] Bridgman, Proc. Am. Acad. **56**, 61 (1921).

nique may be found in the papers of P. W. Bridgman.[7] The pressure fluid in the test cylinder and the connecting system was nitrogen, the pump and its system using a mixture of glycerine and water. In the test cylinder was placed a small furnace made of concentric tubes of fused quartz, with helical windings of molybdenum wire. The mercury to be studied was placed in the innermost tube; next came a thermocouple, then a quartz tube for insulation, then the first heating coil, another quartz tube and finally another furnace winding. These tubes were all open at one end so that the pressure acted on both sides of the quartz walls. This furnace was assembled in a thin-walled steel tube, the spaces filled with zirconium oxide to act as a thermal insulator and to reduce convection in the nitrogen, and placed in the test cylinder. Electrical connections were made through a plug with six insulated conductors, the plug being held down by a large screw at the top of the cylinder.

The resistance of the mercury was measured in two ways, with a Carey-Foster bridge, and with a null-substitution potentiometer method. The results with these two methods, which involve different corrections, were in good agreement. When the bridge is employed, the resistance of the entire circuit is measured, including that of the mercury at the desired temperature, of some mercury at lower temperatures, of the leads, contacts and so on. In order to reduce the extraneous resistance to as small a fraction as possible, the mercury container was drawn down to a fine constriction for about 1 cm near its center; this constricted portion was placed in the hottest part of the furnace, and its resistance when filled with mercury at room temperature, was about ten times that of the rest of the circuit. As the temperature of the furnace increased, the resistance of the rest of the circuit increased, but not so fast as that of the constricted portion. Special runs gave a sufficiently accurate knowledge of this increase of lead resistance with furnace temperature to permit a correction, with a final uncertainty from this cause not exceeding one percent.

The use of the potentiometer demanded the construction of a four-terminal conductor. This was accomplished by passing fine quartz tubes inside the mercury container from the two ends, up to the constricted portion. The threads of mercury inside these fine tubes were thus insulated from the mercury cylinders between the fine tubes and the walls of the mercury container. The former served as potential leads, the latter as current leads. The resistance of the leads being eliminated by this method, the constricted portion of the container could be very short, with correspondingly decreased temperature difference over the important region.

Contact with the mercury must of course be made somewhere with solid wires, so that thermal electromotive forces are introduced if the contacts are at different temperatures. The contacts were therefore removed as far as possible from the furnace, by the use of mercury containers about 18 cm long with the contacts near the ends. The remaining thermal e.m.f. was eliminated when using the bridge by keeping the galvanometer circuit permanently closed and reading from a false zero on application of the bridge current.

[7] See for example, P. W. Bridgman, *The Physics of High Pressure*, Macmillan.

When using the potentiometer, it was necessary to take readings with the current reversed, adopting the mean value.

The furnace generally consisted of two concentric windings of 0.010 inch molybdenum wire, the inner one of about 5 feet of wire wound closely on a tube of one-quarter inch diameter, so that the length of the winding was 1.5 inches, the outer one wound on a tube fitting closely over the inner, of about 12 feet of wire forming a coil 2.5 or 3 inches long. With these two windings connected in parallel, a current of 5 amperes was sufficient to give temperatures of the order of 1200°C. This temperature existed in a small region which included the junction of the thermocouple and the constricted portion of the mercury container if this was made sufficiently short.

The chief difficulty in using a thermocouple in the interior of a high pressure cylinder is to bring the fine wires of the thermocouple to the exterior through the pressure packing, especially in the case of couples of platinum and its alloys. If this can be done, the cold junctions may be kept at 0°C and the only uncertainties are those arising (1) from the effect of pressure on the thermal e.m.f. and (2) from the effect of stress gradients combined with temperature gradients in those parts of the wires in the packing. The uncertainty from the first of the causes should not exceed 8° at 1200°C and 4000 atm.[8] for the couple employed, of platinum and platinum-10 percent rhodium. The second effect cannot be estimated but is certainly quite small.

Electrical connections between the inside and outside of the test cylinder were made by means of suitably insulated and packed steel conductors, situated in the plug at the top of the cylinder. A special device was employed for the thermocouple leads. Two of the steel conductors, which were about 3 inches long, were drilled with a 0.030 inch drill to within one-quarter inch of the ends which extended inside the cylinder; the holes were completed with a 0.013 inch drill. Wires of platinum and of platinum-10 percent rhodium, 0.010 inch in diameter, were passed one through each of these conductors and soldered at the inner ends, in the fine holes; for the rest of the length they were insulated from the steel by thin glass tubes. When the thermocouple on the inside was soldered to these leads the thermoelectric circuit was perturbed only by the contact over a small region of each wire with a mass of steel and solder, itself completely insulated from everything else. So long as the temperature was uniform over these contacts, no additional e.m.f. was introduced, and the steel pieces were sufficiently large, and far enough removed from the furnace so that this condition was very closely satisfied.

The electromotive force of the couple was measured with a Leeds and Northrup potentiometer and a Pye galvanometer, the combination being sensitive to 1 microvolt, corresponding with this couple to one-tenth degree. The pressure in the test cylinder was given by the change of resistance of a man-

[8] P. W. Bridgman, Proc. Am. Acad. 53, 346 (1918). These measurements extend only to 100°C, for platinum alone; the temperature coefficient of thermal e.m.f. seems to decrease, however, as the temperature rises. The assumptions are made that it remains constant up to 1200°, and that the coefficient of platinum-rhodium has the same sign.

ganin gauge coil, placed in a separate steel block connected by a pipe which passed through the water bath surrounding the test cylinder. The temperature of the gauge coil was independent of the temperature of the furnace; and the pressures may be considered exact to within 10 kg/cm².

Electrical Resistance

Tables I, II and III contain the smoothed results of a large number of independent runs, using different mercury containers, different methods of

Table I. *Relative resistance of liquid mercury.*

t°C	$p=0$	500	1000	2000	3000	4000 kg/cm²
0	1.00	0.985	0.97	0.94	0.91	0.89
100	1.10	1.08	1.06	1.02	0.99	0.97
200	1.21	1.18	1.16	1.12	1.08	1.04
300	1.35	1.32	1.28	1.23	1.18	1.13
400		1.46	1.42	1.36	1.30	1.24
500		1.65	1.59	1.51	1.43	1.36
600		1.89	1.80	1.69	1.60	1.51
700		2.19	2.06	1.91	1.79	1.67
800		2.61	2.40	2.18	2.02	1.86
900		3.11	2.83	2.51	2.30	2.11
1000		3.90	3.48	2.96	2.68	2.43
1100		4.95	4.38	3.56	3.11	2.82
1200				4.53	3.77	3.31
1300					4.65	4.04

Table II. *Instantaneous pressure coefficient of resistance.* $(1/\omega)(\partial\omega/\partial p)_T \cdot 10^5$.

t°C	$p=0$	500	1000	2000	3000	4000 kg/cm²
0	3	3	3	3	3	3
100	4	4	3	3	3	3
200	4	4	4	4	4	4
300		5	5	4	4	4
400		6	6	4	4	4
500		7	7	5	5	5
600		10	9	6	6	6
700		14	11	7	7	7
800		17	14	8	8	7
900		21	17	10	9	8
1000		26	20	12	10	9
1100		33	24	17	13	10
1200				24	15	11
1300					18	12

Table III. *Instantaneous temperature coefficient of resistance.* $(1/\omega)(\partial\omega/\partial T)_p \cdot 10^4$.

t°C	$p=0$	1000	2000	3000	4000 kg/cm²
0	9.5	9.0	8.5	7.5	7.5
100	10.5	10	9	8	7.5
200	13.5	12	10	9	8
300	14.5	13	12	10	9
400		15	13	12	11
500		18	16	15	13
600		24	19	17	15
700		30	23	20	17
800		38	28	24	21
900		53	37	31	26
1000		82	56	45	39

measuring the resistance and different furnaces and thermocouples. The runs were all made at approximately constant pressure, varying the temperature from room temperature to the maximum desired and retracing the curve on cooling. The values of resistance are all relative to the value for 1 atmosphere (zero gauge pressure) and 0°C. The change of dimensions of the quartz mercury container is neglected; such data as are available indicate that the correction due to thermal expansion and compressibility of the quartz would not exceed one-third of 1 percent at 4000 atmospheres, which is less than the other uncertainties. At 1100°C, the various runs agree to within 3 percent; at lower temperatures, the uncertainty is smaller, probably not exceeding one-half percent below 500°C.

Critical Point

A rather extensive literature has grown up concerning the critical constants of mercury, including experimental and theoretical attacks upon the problem. A bibliography which I hope is complete is given below.[9–24] Estimates of the critical constants by comparison of the vapor-pressure curve of mercury with that of argon were given by Happel[12] as 1100°C and 456 atm., by Ariés[18] as 1080°C and 420 atm.; using another method, van Laar[19] obtained 900°C and 179 atm. Observations up to 1430°C failed, however, to disclose the critical point. Bernhardt[24] traced the boiling curve of mercury to 1435°C and 2000 atm., concluding that the critical point lay at a still higher temperature and pressure. Since my measurements lead me to conclude that the critical constants are about 1460°C and 1640 atm., a brief comparison of my method with that of Bernhardt seems desirable.

The apparatus which I used for detecting the critical point was essentially the same as that already described for measuring the resistance, except that the mercury container was made still smaller, permitting a more efficient furnace assembly, and the external circuit connected in series with the mercury column consisted simply of a milliammeter, a resistance of about 150 ohms and a dry cell. As the temperature approaches the critical temperature, the rate of increase of electrical resistance with temperature becomes so rapid

[9] Cailletet, Colardeau et Rivière, C. R. **130,** 1585 (1900).
[10] Strutt, Phil. Mag. **4,** 596 (1904).
[11] Traube and Teichner, Ann. d. Physik **13,** 620 (1904).
[12] Happel, Ann. d. Physik **13,** 351 (1904).
[13] Koenigsberger, Chem. Ztg. **36,** 1321 (1912).
[14] Menzies and Smith, Amer. Chem. Soc. **32,** 1432 (1910).
[15] Menzies, Amer. Chem. Soc. **35,** 1085 (1913); **41,** 1783 (1919).
[16] Thorpe and Rucker, Journ. Chem. Soc. **35,** 1065 (1913).
[17] Bender, Phys. Zeits. **16,** 246 (1915); **19,** 410 (1918).
[18] Ariés, C. R. **166,** 334 (1918).
[19] Van Laar, Versl. K. Ak. van Wetensch. **25,** 1498 (1917).
[20] Rassow, Zeits. f. anorg. Chem. **114,** 117 (1920).
[21] Walden Zeits. f. anorg. Chem. **112,** 1087 (1920).
[22] Weber, Comm. Phys. Lab. Leiden, Supp. 43 to Nos. 145–156, p. 23 (1920).
[23] Meyer, Phys. Zeits. **22,** 76 (1921).
[24] Bernhardt, Phys. Zeits. **26,** 265 (1925).

that the use of a bridge for measuring the resistance is not practicable unless the temperature can be maintained constant to within a small fraction of a degree. This was not possible under the conditions of this experiment, so the following procedure was adopted. The pressure being approximately constant, and having any desired value, the mercury was heated slowly and the current through the milliammeter was observed. At low temperatures, this current was about 10 milliamperes, for the resistance of the mercury cold was a few hundredths of an ohm (there was no constriction in the mercury containers used for this purpose). If the pressure was low enough to permit boiling, then at a well-defined temperature, the current fell brusquely to the zero of the instrument, indicating a relative resistance of the vapor of not less than 10^6. In this way the boiling curve was traced, up to a certain pressure above which the character of the phenomenon became quite different. At 1640 atm., and at higher pressures, the fall of the current was no longer abrupt; as the temperature increased the current decreased, first slowly, then rapidly, but permitting readings of current and temperature to be taken up to temperatures well beyond the prolongation of the boiling curve, where the current was not yet zero, nor in fact less than abuot 1/10 m.a.

It may be objected that the small residual current at these high temperatures was due to conduction by the quartz container. I think that the resistivity of the quartz is not of the right order of magnitude. If we suppose it to be about 10^5 ohms/cm^3 at 1500°C, which does not seem too high, then the current from a 1.5 volt cell through a section 5 mm long of a tube with a 1 mm bore and 2 mm outside diameter, will be about 10^{-6} amperes. But the smallest current observed was about 10^{-4} amperes, so that conduction by the quartz does not explain even the residual current at the highest temperatures, and *a fortiori*, does not account for the larger currents observed at slightly lower temperatures. Furthermore, conduction by the quartz would not be expected to vary greatly with a change of pressure from 1500 to 1700 atm., whereas the nature of the phenomenon changes completely in this region.

Additional weight to the interpretation of this behavior as indicating the critical region is provided by comparison of the current-temperature curves at different pressures above 1600 atm. It would be expected, I think, that these curves would move toward higher temperatures and tend to flatten out as the pressure increased. This is in fact the case, at 2040 atm. the drop from 10 to 0.1 milliampere is spread over about 70°, whereas at 1750 atm. it takes place in about 40° and at 1640 atm. in 15°. At 2040 atm., the resistivity still increases about 100 times between 1520° and 1540°.

The last remark leads to an explanation of the effect observed by Bernhardt, who heated a thin cylinder of mercury by passing a low-voltage alternating current through the mercury itself, detecting boiling up to 2020 atm. by oscillations of the heating current and constancy of the temperature. But oscillations would also be observed under these circumstances if the resistance increased notably in any small temperature range, and this is what I have observed in the region above 1600 atm. The heating of the mercury in my

apparatus was independent of the resistance of the mercury, so that it was possible to reach temperatures which could not be obtained, without arcing or using a high-voltage source, by passing a current through the mercury itself. Bernhardt's temperatures for the boiling curve are also slightly different from mine, being generally lower by about 20–30°. A variety of causes may be responsible for this, in particular the fact that Bernhardt's thermocouple made connections with steel conductors on the inside of the pressure cylinder. The temperature of the junctions could only be estimated and the error on these estimates enters directly in the final temperature.

It is difficult to give the resistivity corresponding to any given current through the mercury, because the length of the mercury column at the maximum temperature is not known. Using a mercury container with a very short constricted section, and a potentiometer, a few fairly precise values were obtained for the higher pressures, which could be used to obtain approximate values in the critical region. These are tabulated in Table IV, along with some measurements of Northrup[25] on the resistance of the vapor at 1 atm. The resistances are given relative to the resistance of the liquid at 0°C and 1 atm.

TABLE IV. *Relative resistance of mercury, times* 10^{-6}.

t°C	1 atm.	1640	1750	1870	2700
900	250				
1000	125				
1100	75	———	In this region, see Table I.	———	
1200	35				
1300	19				
1400	7			0.00002	0.000009
1500	3	0.12	0.08	0.0006	0.000017
1600				0.06	

It will be remarked that whereas the resistance of the vapor at 1 atm. decreases with rising temperature, the resistance at pressures well above the critical pressure increases with rising temperature, as does that of the liquid. Somewhere in between must be a region of resistance independent of the temperature.

CONCLUDING REMARKS

The variation of resistance of liquid mercury with pressure and temperature does not follow any simple law, nor is the resistivity simply related to the specific volume, so far as can be judged from the volume data available. Above 100°C, the specific volume is known only along the boiling curve, from the work of Bender.[17] Along this curve, the resistivity of the liquid increases much faster than does its volume.

The critical constants, as determined by the continuous variation of resistance with temperature at constant pressure, are 1460 ± 20°C and 1640 ± 50 kg/cm^2. These values are consistent with the data of Bender for the density of mercury and with the critical temperature deduced by Meyer[23]

[25] Northrup, Jour. Frank. Inst. July, 85 (1914).

from the temperature variation of surface tension. In conjunction with the data of Bender, the critical density is found to be about 5.[22] The critical pressure is much higher than any predicted by comparison with ordinary gases, leading to a value of the ratio RT_c/p_cv_c equal to 2.18. This is lower than the corresponding ratio for any substance hitherto studied, van der Waals' equation giving 2.66, while for hydrogen it is 2.86 and for most substances greater than 3.

The Bearing of the Earth's Internal Magnetic Permeability upon the Self- and Mutual Inductance by Coils Wound on its Surface

By W. F. G. SWANN
Bartol Research Foundation of the Franklin Institute

(Received July 7, 1932)

The paper comprises the solution of the following problems: 1. The mutual induction of two parallel circular loops wound as small circles upon the earth in such a manner that their distance apart is equal to their radius. The mutual induction varies from 2.8 henries for a permeability unity to 11 henries for infinite permeability. 2. The self-induction of a circular loop wound as a small circle upon the earth and of radius equal to half that of the earth. The self-induction varies from 79.8 henries for unit permeability to 167 henries for infinite permeability. 3. A solution is given for the self-induction of a single circular coil situated parallel to and at a distance h above an infinite medium of permeability μ. Data are given, showing the magnitude of the effect of the permeability for different distances of the coil from the plane. 4. The mutual induction of the coils considered in problem (1), and the self-induction for the coil considered in problem (2), are calculated for a case where the permeability of the earth varies from unity at its surface to infinity at the center. A fairly general formula, applicable to different degrees of rapidity of variation is developed for this purpose. The content of this problem will be most readily ascertained by immediate reference to Table IV, which is self-explanatory.

SOME years ago, the writer[1] discussed in a preliminary form the possibility of obtaining information concerning the internal permeability of the earth from measurements of the self- or mutual inductance of cables. On returning to the matter recently, it appeared that the solution of some of the fundamental problems concerned with the matter were simpler than might at first sight be supposed, and such solutions are developed in the present paper. While a very casual inspection of the problem will reveal the orders of magnitude involved, these orders of magnitude may seem rather surprising to one who has not thought about the matter. Thus, to quote a few of the illustrations to be developed later, it may seen rather surprising that the self-inductance of a single circular loop of cable of cross-sectional radius one centimeter, wound around the earth in a small circle of radius half that of the earth, has a self-inductance of 80 henries, and that the self-inductance would be increased by a factor of about 2 if the earth were made of iron. It may seem startling to realize that two parallel circular loops wound on the earth at a distance apart equal to their radii have a mutual induction of 2.8 henries and that, if the earth were replaced by an iron sphere, it would be increased to 11 henries.

[1] "Status, Scope, and Problems of the Section of Terrestrial Magnetism and Electricity of the American Geophysical Union," *Bulletin of the National Research Council*, **41**, 60–68 (1924).

Part I of this paper is devoted to a statement of the problems solved, together with the solutions obtained. Part II contains numerical applications, illustrating the results obtained. Part III is devoted to the derivations of the formulae quoted in Part I.

Those interested only in the numerical results as suggestive of experimental possibilities in relation to measurements on the earth will find it advantageous to read only Part II.

It will be immediately obvious that many variations of the problem are soluble, and some of these would be of greater service in actual experimental measurements. However, the problems solved have been chosen to illustrate the general principles in their simplest form.

In collaboration with the Moore School of Electrical Engineering of the University of Pennsylvania, experiments are in preparation leading ultimately to application to the earth. As a preliminary procedure, spheres of different permeability and of permeability varying with the distance from the center are being constructed out of mixtures of iron and concrete. Upon these it will be possible to build model systems representative of actual cable and telephone distributions, and so investigate the experimental possibilities with a view to later application to the earth itself.

Part I. Problems Solved and Formulae Obtained

Problem 1: Deduction of mutual induction of two parallel circular loops of radii b_1 and b_2, respectively, wound on a sphere of radius a and of permeability μ

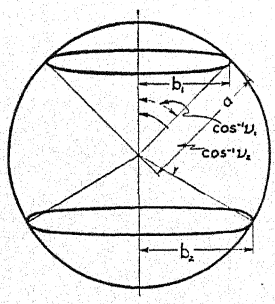


Fig. 1.

The cross section of the wire is negligible in its effect in this case unless the circuits are abnormally close together, and we find for the mutual induction M, in electromagnetic units,

$$M = 4\pi^2 \frac{b_1^2 b_2^2}{a^3} \sum_{n=1}^{\infty} \left[\frac{1}{n(n+1)} + \frac{\mu - 1}{n[n(\mu+1)+1]} \right] P_n'(\nu_1) P_n'(\nu_2) \qquad (1)$$

where ν_1 and ν_2 are the cosines of the half angles subtended by the two circles at the center of the sphere, both angles being, of course, measured from a common axis, (see Fig. 1).

Problem 2: Deduction of the formula for the self-induction of a circular loop of radius b wound with wire of cross-sectional radius ϵ upon a sphere of radius a and permeability μ

The self-induction L in electromagnetic units is

$$L = \frac{2\mu}{\mu+1} L_0 + 4\pi^2\mu\left(\frac{\mu-1}{\mu+1}\right)\frac{b^4}{a^3} \sum_1^\infty \frac{[P_n'(\nu)]^2}{n(n+1)[n(\mu+1)+1]} \tag{2}$$

where L_0 is the self-induction of the circle for the case $\mu=1$, and is given by

$$L_0 = 4\pi b\left[\left(1+\frac{\epsilon^2}{8b^2}\right)\log_e\frac{8b}{\epsilon} + \frac{\epsilon^2}{24b^2} - \frac{7}{4}\right] \tag{3}$$

where, moreover, ν is the cosine of the half angle subtended by the circular loop at the center of the sphere of radius a (see Fig. 1), so that ν is given by $(1-\nu^2)a^2=b^2$, and where $P_n'(\nu)=(d/d\nu)P_n(\nu)$, $P_n(\nu)$ being the Legendre polynomial of degree n.

Problem 3: A circular loop of radius b made of wire of cross-sectional radius ϵ is placed with its plane parallel to and at a distance h above an infinite plane which is the upper boundary of an infinite medium of permeability μ

The solution has been obtained for the self-induction of this coil as a function of its dimensions and of h and μ. It is found that the self-induction L is given by

$$L = L_0 + [(\mu-1)/(\mu+1)]M_{AA'} \tag{4}$$

where L_0 is the self-induction of the circular loop in the absence of the medium of permeability μ, i.e., for $\mu=1$, and is given by (3), and where $M_{AA'}$ is the mutual induction between the circular loop and its image, which is a coil similar to the original coil, symmetrically situated, parallel to it, and with its plane at a distance h below the bounding surface between the two media.

The expression for $M_{AA'}$, the mutual induction of the two coils, is, of course, well known and is given by $M_{AA'}=4\pi b\,[(2/k-k)K-2E/k]$, where K and E are complete elliptic integrals of the first and second kind to a modulus K, and where

$$k^2 = b^2/(b^2+h^2).$$

Problem 4: Deduction of the solution for problem 1 modified to the case where permeability μ is not constant, but is a function of the distance from the center of the sphere

The solution of the problem has been outlined for the case of a general functional dependence of μ upon r, and has been carried out in detail for the case where

$$\mu = (a/r)^m \text{ for } r < a,$$
$$\mu = 1 \text{ for } r > a.$$

Here m is a positive integer. This form contains as representative a wide generality of cases of increase of μ with different rapidities from unity at the

surface of the sphere to infinity at the center. The expression for the mutual induction for this case is

$$M = 4\pi^2 \frac{b_1^2 b_2^2}{a^3} \sum_1^\infty \left[\frac{1}{n(n+1)} + \frac{c_n - n}{n^2(n+1+c_n)} \right] P_n'(\nu_1) P_n'(\nu_2) \tag{5}$$

where $2c_n = m - 1 + (m^2 - 2m + 1 + 4n(n+1))^{1/2}$.

Problem 5: The solution for problem 2, modified to the case where the permeability μ is a function of the distance from the center of the sphere

The problem has been worked out for the variation of μ with r assumed in problem 4, and the self-induction for this case is given by

$$L = L_0 + \frac{4\pi^2 b^4}{a^3} \sum_{n=1}^\infty \frac{c_n - n}{n^2(n+1+c_n)} [P_n'(\nu)]^2 \tag{6}$$

where L_0 is the normal self-induction of the loop in the absence of the sphere.

Limiting cases for $\mu = \infty$. It is of interest to compare some of the results for the limiting case $\mu = \infty$ with those for $\mu = 1$. Thus, for the mutual induction of the two coils discussed in problem 1, we have

$$M_{\mu=\infty} = 4\pi^2 \frac{b_1^2 b_2^2}{a^3} \sum_1^\infty \left[\frac{1}{n^2+n} + \frac{1}{n^2} \right] P_n'(\nu_1) P_n'(\nu_2) \tag{7}$$

$$M_{\mu=1} = 4\pi^2 \frac{b_1^2 b_2^2}{a^3} \sum_1^\infty \left[\frac{1}{n^2+n} \right] P_n'(\nu_1) P_n'(\nu_2)$$

so that, clearly, the presence of the sphere of infinite permeability more than doubles the mutual induction.

For the self-induction of a single loop, we have, from problem 2,

$$L_{\mu=\infty} = 2L_0 + 4\pi^2 b^4/a^3 \sum_1^\infty \frac{[P_n'(\nu)]^2}{n^2(n+1)} \tag{8}$$
$$L_{\mu=1} = L_0.$$

Hence, the self-induction is more than doubled by the presence of the sphere of infinite permeability.

For the case of the circular loop, placed at a distance h above the surface of a medium of permeability μ (problem 3), we have

$$L_{\mu=\infty} = L_0 + M_{AA'} \tag{9}$$

where, as before, $M_{AA'}$ is the mutual induction between the coil and its image.

Part II. Numerical Illustrations

In Tables I to IV, which are self-explanatory, numerical examples corresponding to the foregoing formulae are given. They are calculated for the case of a sphere of radius equal to that of the earth in those problems where a sphere is involved.

Corresponding to Tables I, II, and IV, Fig. 2 is given, showing the results in a more vivid and graphical form.

TABLE I. *Mutual induction of two parallel circular loops wound on earth of permeability* μ.

Details of problem: radius of earth $=6.4\times10^8$ cm. Loops of equal radius, parallel to each other and separated by a distance equal to their radius. In other words, radius = separation $=5.7\times10^8$ cm.

μ:	1	2	4	9	∞
M (henries):	2.82	4.59	6.73	8.53	11.02

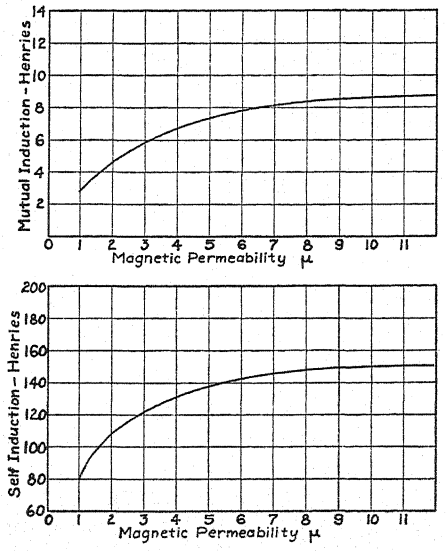


Fig. 2a. Corresponding to Table I. Mutual induction of two equal and parallel circular loops wound on an earth of permeability μ. Radius of the earth $=6.4\times10^8$ cm. Radius of the loops $=5.70\times10^8$ cm.

Fig. 2b. Corresponding to Table II. Self induction of a circular loop wound on an earth of permeability μ. Radius of the earth $=6.4\times10^8$ cm. Radius of the loop $=3.2\times10^8$ cm. Radius of the cross section of the wire = 1 cm.

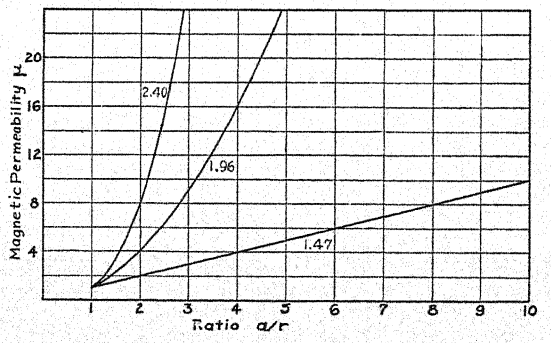


Fig. 2c. Corresponding to Table IV, but showing variation of μ with distance from the center of the earth necessary to produce various values shown for $(M/M_{\mu=1})$, the ratio of the mutual induction to that for the case when $\mu=1$ for the whole sphere. The coil dimensions correspond to those of the first curve shown above.

TABLE II. *Self-induction of circular loop wound on earth of permeability* μ.

Details of problem: radius of earth $=6.4\times10^8$ cm radius of loop $=3.2\times10^8$ cm, radius of cross section of wire $=1$ cm.

μ:	1	2	4	9	∞
L (henries):	79.8	107.9	131.1	149.0	167.4

TABLE III. *Alteration of self-induction of circular loop situated over and parallel to a plane below for which permeability is* μ.[2]

Details of problem: radius of circle $b=1000$ cm. The self-induction for the case $\mu=1$, for a case where the cross-sectional radius of the wire is 0.5 cm is $L_0=99.6$ microhenries.

h	h/b	Alteration in self-induction in microhenries			
		$\mu=2$	$\mu=4$	$\mu=9$	$\mu=\infty$
100	0.1	7.16	12.89	17.19	21.49
500	0.5	1.65	2.97	3.95	4.94
1000	1.0	0.47	0.85	1.14	1.42
5000	5.0	0.01	0.01	0.02	0.02

TABLE IV. *Mutual induction M of two parallel circular loops wound around the earth of radius a, for the case where* μ *varies with the distance r from the center according to the law* $\mu=(a/r)^m$ *also self-induction of a single loop. The dimensions of the coils are as in Tables I and II.*

m	Value of a/r for which $\mu=10$	Mutual inductance (henries)	Self-inductance (henries)
3	2.15	6.76	85.6
2	3.16	5.53	83.7
1	10.00	4.13	81.7
0	—	2.82[3]	79.8[3]

PART III. DEDUCTION OF THE FORMULAE

Definition of symbols, see Fig. 3

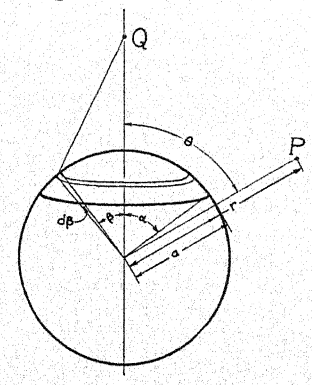


Fig. 3.

$a=$radius of sphere; $\alpha=$half angle subtended by circular wire at center of sphere; $\nu=\cos\alpha$; $\eta=1-\nu^2=$ratio of area of circular wire to area of great circle of the sphere; r, θ, polar coordinates for a point P in space; $x=\cos\theta$.

[2] The values of the alteration of self-induction for other values of b, but for the same values of h/b are to be obtained by multiplying the results here given by $b/1000$.

[3] This value corresponds, of course, to the case where the sphere has unit permeability throughout.

When two circular wires are involved, the quantities corresponding to α, ν, η, for the two wires are denoted by subscripts 1 and 2. β = half angle subtended at center of sphere by a circle drawn on the spherical cap bounded by the circle defined by α. $\lambda = \cos\beta$. I = current in circular wire; H = magnetic-field intensity; B = magnetic induction. We shall work throughout in c.g.s. electromagnetic units.

Problem 1. The mutual induction of two circular loops wound on the sphere

We shall first write down the expressions for the magnetic potential from which may be derived the field due to a current in a circular loop of wire of infinitesimal cross section when the permeability of the sphere is unity. The potential ω is that due to a shell bounded by the current and of moment per unit area equal to I. The shell may be taken to coincide with the portion of the surface of the sphere of radius a which is bounded by the current. The expression for ω is well known and is[4]

$$\omega = -2\pi I\left[1 - \nu + \eta\sum_{n=1}^{\infty}\left(\frac{1}{n}\right)\left(\frac{r}{a}\right)^n P_n'(\nu)P_n(x)\right] \text{ for } r < a \tag{10}$$

$$\omega = 2\pi I\eta\sum_{n=1}^{\infty}\left(\frac{1}{n+1}\right)\left(\frac{a}{r}\right)^{n+1} P_n'(\nu)P_n(x) \text{ for } r > a \tag{11}$$

where P_n refers to the Legendre polynomial of degree n, and $P_n'(\nu) = dP_n(\nu)/d\nu$.

We now turn to the problem of the field produced by the combined action of the current in the wire discussed above and the magnetizable sphere for which in general μ is not unity. The fundamental equation controlling the phenomena is

$$\text{div } B = 0, \tag{12}$$

which, in our case may be supplemented by

$$B = \mu H. \tag{13}$$

If we obtain a solution satisfying (12) and (13), we know that it is unique provided that it satisfies the following additional requirements.[5]

For the case of integration around a complete contour,

$$\left.\begin{aligned}\int (H\cdot ds) &= 4\pi I \text{ for case where contour encircles } I\\ &= 0 \text{ for case where contour does not encircle } I\end{aligned}\right\} \tag{14}$$

$$B_{ni} = B_{n0} \tag{15}$$

$$H_{Ti} = H_{T0} \tag{16}$$

$$B_{n\infty} = 0 \tag{17}$$

[4] See, for example, Maxwell's *Electricity and Magnetism*, Vol. **2**, third edition, p. 333.

[5] While matters relating to the boundary conditions are well known, the reader who wishes to examine the question rather fully may refer to a recent paper by the writer, "The Solution of Steady-State Problems in Dielectric, Magnetically Permeable and Conducting Media, with Special Reference to Mathematical Analogies between Magnetic Problems and Current-Flow Problems," Journal of The Franklin Institute, **213**, 155–170 (1932).

where B_{ni} and B_{n0} are the normal components of the magnetic induction just inside and just outside the sphere, respectively, H_{Ti} and H_{T0} are the corresponding tangential components, and $B_{n\infty}$ is the normal component of B over the infinite boundary.

Let us now write the resultant H in the form

$$H = h + H_s \tag{18}$$

where h is the magnetic field as calculated for the case $\mu = 1$, i.e., the field obtained from the potentials given by (10) and (11), with the usual convention as to continuity within the shell itself. Eq. (18) really constitutes the definition of H_s.

Since h provides for the whole of the line integral of H specified by (14), H_s has no line integral, and consequently is derivable from a potential. Also div H_s is zero since div H and div h are both zero. Thus, if Ω_s is the potential from which H_s may be derived, we have

$$\nabla^2\Omega_s = 0. \tag{19}$$

Hence Ω_s is expressible as a series of spherical harmonics of the type

$$\Omega_s = \sum_{n=0}^{\infty} k_n (r/a)^n P_n(x) \text{ for } r < a \tag{20}$$

and

$$\Omega_s = \sum_{n=0}^{\infty} g_n (a/r)^{n+1} P_n(x) \text{ for } r > a \tag{21}$$

provided, of course, that with this choice the boundary conditions can be satisfied. The quantities k_n and g_n are, of course, constants.

Now, outside the sphere $B = H$, so that (21) insures, in conjunction with the properties of h, that (17) is satisfied.

Since the tangential component of h is continuous across the surface of the sphere, (16) will be satisfied provided that Ω_s is continuous at the boundary, i.e., provided that

$$\sum_{n=0}^{\infty} k_n P_n(x) = \sum_{n=0}^{\infty} g_n P_n(x). \tag{22}$$

Having in mind (10) and (11), condition (15) requires that

$$\mu\left[\frac{2\pi I\eta}{a} \sum_{n=1}^{\infty} P_n'(\nu) P_n(x) - \sum_{n=0}^{\infty} \frac{nk_n}{a} P_n(x)\right] = \frac{2\pi I\eta}{a} \sum_{n=1}^{\infty} P_n'(\nu) P_n(x) + \sum_{n=0}^{\infty} \frac{(n+1)}{a} g_n P_n(x). \tag{23}$$

It is certainly possible to determine the k's and g's so as to satisfy (22) and (23). A sufficient condition to satisfy (22) is $k_n = g_n$. With this condition substituted, (23) gives as the necessary condition for its being satisfied

$$(2\pi I/a)\eta(\mu - 1)P_n'(\nu) = (k_n/a)[(\mu + 1)n + 1] \text{ for } n > 0$$

and $0 = k_0$ for $n = 0$.

Hence, $$k_n = g_n = \frac{2\pi I\eta(\mu - 1)}{[(\mu + 1)n + 1]} P_n'(\nu) \text{ for } n > 0.$$

$$k_0 = g_0 = 0 \text{ for } n = 0.$$

Hence, the potential Ω giving the complete field is

$$\Omega = -2\pi I\left[(1-\nu)+\eta\sum_{n=1}^{\infty}\left\{\frac{1}{n} - \frac{(\mu-1)}{[n(\mu+1)+1]}\right\}\left(\frac{r}{a}\right)^n P_n'(\nu)P_n(x)\right] \text{ for } r<a \quad (24)$$

$$\Omega = 2\pi I\eta \sum_{n=1}^{\infty}\left\{\frac{1}{n+1}+\frac{(\mu-1)}{[n(\mu+1)+1]}\right\}\left(\frac{a}{r}\right)^{n+1} P_n'(\nu)P_n(x) \text{ for } r > a. \quad (25)$$

The flux through a circular loop defined by ν_2, due to unit current in a circular loop defined by ν_1, is the desired mutual induction between the two coils. Thus

$$M = \int\int B_{n1}dS,$$

where B_{n1} is the normal component of B due to unit current in loop 1 at any point on a cap bounded by loop 2. The cap may be taken as a portion of the sphere of radius a, subtending the angle corresponding to ν_2. Thus, using the notation indicated above, and in Fig. 3, and writing Ω_1 for the potential due to loop 1,

$$\begin{aligned} M &= -2\pi a^2 \int_1^{\alpha_2} (\partial\Omega/\partial r)_{r=a} \sin\beta d\beta \\ &= 2\pi a^2 \int_1^{\nu_2} (\partial\Omega_1/\partial r)_{r=a} d\lambda. \end{aligned} \quad (26)$$

Thus, from (24) or (25)

$$M = 4\pi^2\eta_1 a \sum_{n=1}^{\infty}\left[1 + \frac{(n + 1)(\mu - 1)}{[n(\mu + 1) + 1]}\right] P_n'(\nu_1) \int_1^{\nu_2} P_n(\lambda)d\lambda.$$

Now, from the fundamental equation for $P_n(\lambda)$, we have,

$$n(n + 1)P_n(\lambda) + (d/d\lambda)[(1 - \lambda^2)dP_n(\lambda)/d\lambda] = 0.$$

Hence,

$$\begin{aligned} \int_1^{\nu_2} P_n(\lambda)d\lambda &= \frac{1}{n(n + 1)}[(1 - \lambda^2)P_n'(\lambda)]_1^2 \\ &= \frac{(1 - \nu_2^2)}{n(n + 1)} P_n'(\lambda). \end{aligned}$$

Hence, since $1-\nu_2^2=b_2^2/a^2$, and since $\eta_1=1-\nu_1^2=b_1^2/a^2$

$$M = 4\pi^2 \frac{b_1^2 b_2^2}{a^3} \sum_{n=1}^{\infty} \left[\frac{1}{n(n+1)} + \frac{\mu - 1}{n[n(\mu+1)+1]} \right] P_n'(\nu_1) P_n'(\nu_2), \quad (27)$$

which is the result quoted in Eq. (1).

Problem 2. The self-induction of a circular loop wound on the sphere

We cannot obtain the self-induction of a single loop by simply putting $\nu_1=\nu_2$ in (27); for, the series diverges for that case as indeed it must do since the self-induction of a loop made of wire of infinitesimal cross section is infinite. While the cross-sectional area of the wire is irrelevant for the problem of mutual induction if it is small, it plays a part which increases in importance with diminution of cross section in the case of the self-induction, on account of the rapid increase of magnetic field as we approach the axis of an infinitely thin wire. In the case of self-induction, we cannot neglect the cross section of the wire. The self-induction for a wire of finite cross section is defined as

$$L = (\sum N)/t$$

where the cross section is supposed divided into t filaments, each carrying a current $1/t$, and ΣN is the summation of the magnetic fluxes for the circuits corresponding to each of these filaments.

If L_{pq} refers to the mutual induction for a pair of filaments

$$L = \frac{1}{t^2} \sum_p \sum_q L_{pq}.$$

The total number of terms in the sum is, of course, t^2.

We shall consider two filaments of infinitesimal cross section within the wire, and lying on spheres of radii r_1 and r_2 concentric with the main sphere of radius a. The filaments shall subtend, at the center, half angles α_1 and α_2 whose cosines are ν_1 and ν_2, respectively. Following the line of procedure adopted above for the mutual induction of two circular loops, we find for the mutual induction of these two filamentary loops

$$\Delta M = -2\pi r_2 \int_1^{\alpha_1} \left(\frac{\partial \Omega_1}{\partial r} \right)_{r=r_2} \sin\beta d\beta,$$

where Ω_1 now refers to the potential as calculated for unit current from (25) with $\eta=\eta_1=1-\nu_1^2$, and with a replaced by r_1.

Proceeding exactly as before, but avoiding replacing r_2 by r_1 as we formerly replaced r by a, we obtain

$$\Delta M = 4\pi^2 \eta_1 \eta_2 r_2 \sum_{n=1}^{\infty} \left[\frac{1}{n(n+1)} + \frac{\mu - 1}{n[n(\mu+1)+1]} \right] \left(\frac{r_1}{r_2} \right)^{n+2} P_n'(\nu_1) P_n'(\nu_2).$$

In order to obtain the self-induction L of the wire, we must evaluate the quadruple summation of this quantity for all the pairs of filaments in the wire, each pair being characterized by its own particular values of r_1 and r_2,

and ν_1 and ν_2, with the understanding that $r_1<r_2$. We must then multiply by $1/t^2$.

$$L=\frac{1}{t^2}\sum_{\nu_1}\sum_{\nu_2}\sum_{r_1}\sum_{r_2}4\pi^2\eta_1\eta_2 r_2 \sum_{n=1}^{\infty}\left[\frac{1}{n(n+1)}+\frac{\mu-1}{n[n(\mu+1)+1]}\right]\left(\frac{r_1}{r_2}\right)^{n+2}P_n'(\nu_1)P_n'(\nu_2). \tag{28}$$

Now the series under the last summation is always convergent so long as $r_1<r_2$, or $\nu_1\neq\nu_2$. However, if r_1 is very nearly equal to r_2 and ν_1 is very nearly equal to ν_2, as is here the case, the series would be very slowly convergent and impracticable of actual use. We can evade the difficulty in this matter by the following artifice, however. We observe that if $\mu=1$, our expression for L must revert to the known expression L_0 given by (3) for a circular wire and calculable by other means. Thus,

$$L_0=\sum_{\nu_1}\sum_{\nu_2}\sum_{r_1}\sum_{r_2}\frac{4\pi^2}{t^2}\eta_1\eta_2 r_2\sum_{n=1}^{\infty}\left(\frac{1}{n(n+1)}\right)\left(\frac{r_1}{r_2}\right)^{n+2}P_n'(\nu_1)P_n'(\nu_2). \tag{29}$$

Again,

$$\frac{1}{n(n+1)}+\frac{\mu-1}{n[n(\mu+1)+1]}=\frac{1}{n(n+1)}\left[\frac{2\mu}{\mu+1}+\frac{(\mu-1)}{(\mu+1)}\left(\frac{\mu}{n(\mu+1)+1}\right)\right].$$

Thus, (28) may be written

$$L=\frac{4\pi^2}{t^2}\left(\frac{2\mu}{u+1}\right)\sum_{\nu_1}\sum_{\nu_2}\sum_{r_1}\sum_{r_2}\eta_1\eta_2 r_2\sum_{n=1}^{\infty}\left[\frac{1}{n(n+1)}\right]\left(\frac{r_1}{r_2}\right)^{n+2}P_n'(\nu_1)P_n'(\nu_2) \tag{30}$$

$$+\frac{4\pi^2}{t^2}\mu\left(\frac{\mu-1}{\mu+1}\right)\sum_{\nu_1}\sum_{\nu_2}\sum_{r_1}\sum_{r_2}r_2\sum_{n=1}^{\infty}\frac{\eta_1\eta_2}{n(n+1)[n(\mu+1)+]1}\left(\frac{r_1}{r_2}\right)^{n+2}P_n'(\nu_1)P_n'(\nu_2).$$

Comparing this with (29), we see that

$$L=\left(\frac{2\mu}{\mu+1}\right)L_0+\frac{4\pi^2\mu}{t^2}\left(\frac{\mu-1}{\mu+1}\right)\sum_{\nu_1}\sum_{\nu_2}\sum_{r_1}\sum_{r_2}r_2 \sum_{n=1}^{\infty}\frac{\eta_1\eta_2}{n(n+1)[n(\mu+1)+1]}\left(\frac{r_1}{r_2}\right)^{n+2}P_n'(\nu_1)P_n'(\nu_2). \tag{31}$$

Now, the series under the last summation in (31) does not depend for its convergence upon the condition $r_1<r_2$ or $\nu_1\neq\nu_2$. If, in fact, we put $r_1=r_2=a$ in (31), and if we also put $\nu_1=\nu_2=\nu$, the sum assumes the form

$$S=\sum_{n=1}^{\infty}\frac{1}{n(n+1)[n(\mu+1)+1]}[(1-\nu^2)P_n'(\nu)]^2. \tag{32}$$

Now, from the fundamental equation for $P_n(\nu)$

$$(1-\nu^2)P_n'(\nu)=-n(n+1)\int_1^{\nu}P_n(\nu)d\nu. \tag{33}$$

Now, the asymptotic expression for $P_n(\nu)$ is[6]

$$P_n(\nu) = [2/n\pi \sin \alpha]^{1/2} \sin [(n + \tfrac{1}{2})\alpha + \pi/2]$$

where $\nu = \cos \alpha$. Thus,

$$\int_1^{\nu} P_n(\nu)d\nu = -\left(\frac{2}{n\pi}\right)^{1/2} \int_0^{\alpha} \sin^{1/2} \alpha \sin \left[(n + \tfrac{1}{2})\alpha + \frac{\pi}{2}\right] d\alpha.$$

The integral on the right-hand side is certainly less than $\int_0^{\alpha} d\alpha$, and is thus certainly less than π. Hence,

$$\left[\int_1^{\nu} P_n(\nu)d\nu\right]^2 < \frac{2\pi}{n}.$$

Therefore, using (33), we see that the *remainder*, R_n, in S is certainly less than

$$2\pi \sum_{n=n}^{\infty} \frac{1}{n[n(\mu + 1) + 1]}.$$

If a_n is written for the general term of this sum, we readily prove that

$$\lim_{n=\infty} n\{\,|(a_n + 1)/a_n| - 1\} = -2.$$

Hence[7] the sum converges. We can thus write $r_1 = r_2 = a$, and $\nu_1 = \nu_2 = \nu$ in (31). Then, recalling that there are t^2 terms in the quadruple summation, we find, finally,

$$L = \left(\frac{2\mu}{\mu + 1}\right) L_0 + 4\pi^2\mu \left(\frac{\mu - 1}{\mu + 1}\right) \frac{b^4}{a^3} \sum_{n=1}^{\infty} \frac{[P_n'(\nu)]^2}{n(n + 1)[n(\mu + 1) + 1]} \qquad (34)$$

which is the result quoted in (2).

Problem 3. The self-induction of a circular loop of cross-sectional radius ϵ placed with its plane parallel to and at a distance h above an infinite plane which is the upper boundary of an infinite medium of permeability μ

Again, the fundamental equation controlling the phenomenon is (12). Eq. (13) is assumed, and the solutions of (12) are to be subjected to the condition (14), (15), (16) and (17).

Let us suppose that the loop carries a current I. Then, following the line of procedure in electrostatic problems, we can satisfy these conditions by calculating the field above the infinite plane as the field in empty space produced by the current I, together with that of an equal loop symmetrically situated below the plane, and carrying a current I_1, and the field below the plane can be calculated as the field in free space calculable from a current I_2 in a coil equal to and coincident with the position of the coil carrying the current I_1, provided that

[6] Hobson: *Spherical and Ellipsoidal Harmonics*, p. 299.

[7] Whittaker and Watson: *Modern Analysis*, third edition, p. 23.

$$I_1 = (\mu - 1)I/(\mu + 1) \tag{35}$$

$$I_2 = 2I/(\mu + 1). \tag{36}$$

For, conditions (14) and (17) are obviously satisfied by these requirements. Again, the tangential component of the field just outside the plane and due to each of the circuits I_1 and I_2 is radial to the axis of symmetry. Moreover, if its value is $If(r\cdot\theta)$ for the current I, it is $-I_1 f(r_1\theta_1)$ for the current I_1, where r,θ, are the polar coordinates of a point on the plane with respect to the center of the loop as origin, r_1 is the mirror image of r and θ_1 is the mirror image of θ. Furthermore, the tangential field due to I_2 just below the plane is radial to the axis of symmetry, and equal to $If(r\cdot\theta)$. Thus, since $r_1=r$, and $\theta_1=\theta$, condition (16) is satisfied if

$$I - I_1 = I_2. \tag{37}$$

Condition (15) leads in an analogous way to

$$I + I_1 = \mu I_2 \tag{38}$$

as the condition necessary for its validity. Eqs. (37) and (38) are satisfied if I_1 and I_2 have the values given by (35) and (36).

The increase of flux through the real circuit as a result of the iron is equal to the flux through it due to the image current I_2. Thus,

$$L = L_0 + [(\mu - 1)/(\mu + 1)]M_{AA'} \tag{39}$$

in agreement with Eq. (4).

General theory for the case where μ varies with the distance from the center of the sphere

As before, the fundamental equation controlling the phenomena is (12). Eq. (13) is to be assumed, and the solutions of (12) are to be subjected to the conditions (14), (15), (16), (17).

Now, however, (12) assumes the form

$$\text{div}\,(\mu H) = 0 \quad \text{where} \quad \mu = f(r). \tag{40}$$

Transferring to polar coordinates, and limiting ourselves to symmetry with regard to the polar coordinate ϕ, (40) becomes

$$\frac{1}{r^2}\left[\frac{\partial}{\partial r}(r^2\mu H_r)\right] + \frac{1}{r\sin\theta}\frac{\partial}{\partial\theta}[\mu H_\theta \sin\theta] = 0. \tag{41}$$

Proceeding as in problem 1, we again split the total field H into two parts, a part h calculable for the loop in free space, and a part H_s defined by (18). Then, as before, condition (14) is provided for by h. H_s must satisfy the conditions (15), (16), (17), and is derivable from a potential Ω_s. For $r>a$, where $\mu=1$, we may write

$$\Omega_s = \sum_{n=0}^{\infty} g_n (a/r)^{n+1} P_n(x) \text{ for } r > a \tag{42}$$

since $\nabla^2\Omega_s=0$ for $r>a$.

For $r<a$, however, we must use (41), and apply it to the total field, so that

$$\frac{1}{r^2}\frac{\partial}{\partial r}\left(r^2\mu\frac{\partial\Omega_s}{\partial r}\right)+\frac{1}{r^2\sin\theta}\frac{\partial}{\partial\theta}\left(\mu\sin\theta\frac{\partial\Omega_s}{\partial\theta}\right)=\operatorname{div}\mu h. \tag{43}$$

We then have $\Omega_s=\Omega_{s1}+\Omega_{s2}$, where Ω_{s1} is the solution of (43) with the right-hand side put equal to zero, and Ω_{s2} is the particular integral. Considering then the solution of

$$\frac{\partial}{\partial r}\left(r^2\mu\frac{\partial\Omega_{s1}}{\partial r}\right)+\frac{1}{\sin\theta}\frac{\partial}{\partial\theta}\left(\mu\sin\theta\frac{\partial\Omega_{s1}}{\partial\theta}\right)=0 \tag{44}$$

and following the usual procedure, we seek solutions of the equation of the form

$$\Omega_{s1}=R\Theta$$

where R is a function only of r and Θ is a function only of θ. Remembering that μ is a function only of r, we find

$$\frac{1}{\mu R}\frac{\partial}{\partial r}\left(r^2\mu\frac{\partial R}{\partial r}\right)+\frac{1}{\Theta\sin\theta}\frac{\partial}{\partial\theta}\left(\sin\theta\frac{\partial\Theta}{\partial\theta}\right)=0.$$

Since the first term is independent of θ and the second is independent of r, we may write one of them equal to $n(n+1)$ and the other equal to $-n(n+1)$, where n is a constant, which, again in accordance with usual procedure, we limit to an integer. Thus

$$\frac{d}{dr}\left(r^2\mu\frac{dR_n}{dr}\right)-n(n+1)\mu R_n=0 \tag{45}$$

$$\frac{d}{d\theta}\left(\sin\theta\frac{d\Theta_n}{d\theta}\right)+n(n+1)\Theta_n\sin\theta=0. \tag{46}$$

On putting $\cos\theta=x$ (44) becomes Legendre's equation $(d/dx)[(1-x^2)(d\Theta_n/dx)]+n(n+1)\Theta_n=0$ the solution of which is $\Theta=AP_n(x)+BQ_n(x)$. Eq. (45) cannot be solved until some assumption is made regarding μ. If we write

$$\mu=(a/r)^m \tag{47}$$

we shall have $\mu=1$ when $r=a$, $\mu=\infty$ when $r=0$. Hence, we represent a condition of affairs in which μ grows from unity at the surface of the sphere to infinity at the center, with different degrees of rapidity depending upon our choice of m. This form of function consequently provides a means of representing, qualitatively, with reasonable generality, the sort of conditions which may prevail within the earth. It is also to be remembered that insofar as the effect of a permeability equal to about 10 approximates in its results the effects of infinite permeability, the fact that our function (47) really gives $\mu=\infty$ when $r=0$ involves no illogical assumption as regards the calculation of the fields. The latter would be practically the same if μ, instead of following (47) strictly to the center of the sphere, departed from that law at $\mu=1000$, for example, and never attained a value greater than 2000.

Inserting the value (47) in (45), and putting $r/a=y$, we have

$$(d/dy)[y^{2-m}(dR_n/dy)] - n(n+1)y^{-m}R_n = 0$$
$$y^2d^2R_n/dy^2 + (2-m)ydR/dy - n(n+1)R_n = 0$$

This equation becomes solved by putting $R_n=y^{c_n}$ if

$$c_n(c_n-1) + (2-m)c_n - n(n+1) = 0$$
$$2c_n = -(1-m) \pm [(1-m)^2 + 4n(n+1)]^{1/2}.$$

Put

$$2c_{n1} = -(1-m) + [(1-m)^2 + 4n(n+1)]^{1/2}$$
$$2c_{n2} = -(1-m) - [(1-m)^2 + 4n(n+1)]^{1/2}.$$

Then $(r/a)^{c_{n1}}P_n(x)$, $(r/a)^{c_{n1}}Q_n(x)$, $(r/a)^{c_{n2}}P_n(x)$, $(r/a)^{c_{n2}}Q_n(x)$, are all solutions of (44) within the sphere.

Since m is greater than unity, c_{n1} is positive, and c_{n2} is negative. For the solution inside the sphere, we are concerned, consequently, only with c_{n1}. We may then write

$$\Omega_{s1} = \sum_{n=0}^{\infty} k_n(r/a)^{c_n}P_n(x) \quad r < a \tag{48}$$

where

$$c_n = (m-1)/2 + \tfrac{1}{2}[(m-1)^2 + 4n(n+1)]^{1/2}.$$

We must now turn to the particular integral (Ω_{s2}) of (43). The field h, for a point inside the sphere is obtainable from the potential ω given by (10), and since $\partial\mu/\partial\theta$ is zero

$$-\operatorname{div}\mu h = \frac{1}{r^2}\frac{\partial}{\partial r}\left(r^2\mu\frac{\partial\omega}{\partial r}\right) + \frac{1}{r^2\sin\theta}\frac{\partial}{\partial\theta}\left(\mu\sin\theta\frac{\partial\omega}{\partial\theta}\right)$$
$$= \frac{\mu}{r^2}\left\{\frac{\partial}{\partial r}\left(r^2\frac{\partial\omega}{\partial r}\right) + \frac{1}{\sin\theta}\frac{\partial}{\partial\theta}\left(\sin\theta\frac{\partial\omega}{\partial\theta}\right)\right\} + \frac{\partial\mu}{\partial r}\frac{\partial\omega}{\partial r}.$$

Since the field derivable from ω satisfies Laplace's equation, the term in curly brackets is zero, and we have $-\operatorname{div}\mu h = \partial\mu/\partial r\cdot\partial\omega/\partial r$. Inserting $\mu=(a/r)^m$, and the value of ω given by (10), we, consequently, have from (43),

$$\frac{\partial}{\partial r}\left(r^2\frac{\partial\Omega_s}{\partial r}\right) + \frac{\partial}{\sin\theta\,\partial\theta}\left(\sin\theta\frac{\partial\Omega_s}{\partial\theta}\right) + \frac{1}{\mu}\frac{\partial\mu}{\partial r}\left\{r^2\frac{\partial\Omega_s}{\partial r} + r^2\frac{\partial\omega}{\partial r}\right\}.$$

Since

$$\frac{1}{\mu}\frac{\partial\mu}{\partial r} = \frac{\partial}{\partial r}(\log\mu) = -\frac{m}{r}$$

$$\frac{\partial}{\partial r}\left(r^2\frac{\partial\Omega_s}{\partial r}\right) + \frac{1}{\sin\theta}\frac{\partial}{\partial\theta}\left(\sin\theta\frac{\partial\Omega_s}{\partial\theta}\right) = mr\left(\frac{\partial\Omega_s}{\partial r} + \frac{\partial\omega}{\partial r}\right) = 0.$$

Let us try, as a solution of this equation,

$$\Omega_s = \sum_1^\infty A_n (r/a)^\zeta P_n'(\nu) P_n(x).$$

Then

$$\sum \left\{ \zeta(\zeta+1)P_n(x) + \frac{d}{dx}\left[(1-x^2)\frac{dP_n(x)}{dx}\right] - m\zeta \right\} A_n P_n'(\nu) \left(\frac{r}{a}\right)^\zeta + 2\pi I m\eta \left(\frac{r}{a}\right)^n P_n'(\nu) P_n(x) = 0. \tag{49}$$

Using (33), we see that (49) is satisfied if $\zeta = n$, and A_n is such that

$$\{n(n+1) - n(n+1) - mn\} A_n + 2\pi I m\eta = 0.$$

$$A_n = 2\pi I\eta/n.$$

Hence, having in mind the particular integral (46) already found, we have

$$\Omega_s = k_0 \left(\frac{r}{a}\right)^{c_0} + \sum_{n=1}^\infty \left\{ k_n \left(\frac{r}{a}\right)^{c_n} + \frac{2\pi I}{n}\eta \left(\frac{r}{a}\right)^n P_n'(\nu) \right\} P_n(x) \text{ for } r < a. \tag{50}$$

For $r > a$, we have (42). The condition (17) is satisfied by (42). Condition (16) is provided for if Ω_s is continuous on the boundary, i.e., if

$$\left.\begin{aligned} g_0 &= k_0 \text{ for } n = 0 \\ g_n &= k_n + (2\pi I\eta/n) P_n'(\nu) \text{ for } n \neq 0. \end{aligned}\right\} \tag{51}$$

Since $\mu = 1$ at $r = a$, condition (15) is satisfied if

$$\left.\begin{aligned} -g_0 &= k_0 c_0 = (m-1)k_0 \\ -(n+1)g_n &= k_n c_n + 2\pi I\eta P_n'(\nu). \end{aligned}\right\} \tag{52}$$

Combining (51) and (52), we have $k_0 = g_0 = 0$

$$-(n+1)g_n = \left(g_n - \frac{2\pi I}{n}\eta P_n'(\nu)\right) c_n + 2\pi I\eta P_n'(\nu)$$

$$g_n = \frac{2\pi I\eta}{n(n+1)}(c_n - 1)P_n'(\nu)$$

$$g_n = \frac{2\pi I\eta(c_n - n)}{n(n+1+c_n)} P_n'(\nu).$$

Hence, for the value of Ω_s applicable to points outside the sphere, we have

$$\Omega_s = 2\pi I\eta \sum_{n=1}^\infty \frac{c_n - n}{n(n+1+c_n)} \left(\frac{a}{r}\right)^{n+1} P_n'(\nu) P_n(x) \text{ for } r > a.$$

The complete potential Ω from which the field for $r>a$ may be derived is obtained by adding ω as given by Eq. (11). Thus,

$$\Omega = 2\pi I\eta \sum_{n=1}^{\infty} \left\{\frac{1}{n+1} + \frac{c_n - n}{n(n+1+c_n)}\right\}\left(\frac{a}{r}\right)^{n+1} P_n'(\nu)P_n(x) \text{ for } r > a. \quad (53)$$

Problem 4. The mutual inductance of a pair of circular loops wound upon a sphere of variable permeability

Proceeding exactly as in the case of the derivative for constant μ, we have (26) for the mutual induction of two coils defined by α_1 and α_2.

We thus find

$$M = 4\pi^2\eta_1 a \sum_{n=1}^{\infty} \left[1 + \frac{(n+1)(c_n - n)}{n(n+1+c_n)}\right] P_n'(\nu_1) \int_1^{\nu_2} P_n(\lambda)d\lambda.$$

Again, proceeding in the same manner as before, for the evaluation of the integral, we find

$$M = 4\pi^2 \frac{b_1^2 b_2^2}{a^3} \sum_{n=1}^{\infty} \left[\frac{1}{n(n+1)} + \frac{c_n - n}{n^2(n+1+c_n)}\right] P_n'(\nu_1)P_n'(\nu_2) \quad (54)$$

where $2c_n = m - 1 + \{(m-1)^2 + 4n(n+1)\}^{1/2}$, which is the result quoted in Eq. (5).

Problem 5. The self-inductance of a circular loop wound upon a sphere of variable permeability

The passage from the case of a mutual induction to that of a self-induction is simpler in the present case than it was in the case of constant permeability; for, in the present problem $\mu = 1$ at the surface of the sphere, both inside and outside. As a consequence, the magnetization of the sphere does not contribute a field of infinite amount near the wire even in the case of a wire of infinitesimal cross section. Mathematically, this is shown by the fact that the part L_s of the self-induction contributed by the magnetization of the sphere, and given by putting $b_1 = b_2 = b$, and $\nu_1 = \nu_2 = \nu$, in (54), and omitting the term $1/n(n+1)$ is expressible in the form of a convergent series. Thus,

$$L_s = 4\pi^2 \frac{b^4}{a^3} \sum_{n=1}^{\infty} \frac{c_n - n}{n^2(n+1+c_n)} [P_n'(\nu)]^2. \quad (55)$$

Putting b^2/a^2 back to the forms $\eta^2 = 1 - \nu^2$

$$L_s = 4\pi^2 a \sum_{n=1}^{\infty} \frac{c_n - n}{n^2(n+1+c_n)} [(1-\nu^2)P_n'(\nu)]^2.$$

Proceeding now exactly as in the case of (32), we see that the *remainder* of

$$\sum_{n=1}^{\infty} \frac{c_n - n}{n^2(n+1+c_n)} [(1-\nu^2)P_n'(\nu)]^2$$

is less than

$$2\pi \sum_{n=n}^{\infty} \frac{(c_n - n)(n+1)}{n^2(n+1+c_n)}.$$

Now, when n is large, $c_n - n$ approximates to

$$\frac{m-1}{2} + n\left(1+\frac{1}{n}\right)^{1/2}\left(1+\frac{(m-1)^2}{8n(n+1)}\right) - n$$

i.e., to

$$\frac{m-1}{2} + n\left(1+\frac{1}{2n}+\frac{(m-1)^2}{8n(n+1)}\right) - n$$

i.e., to $m/2$, so that, if a_n is the general term of the sum, we have

$$\lim_{n=\infty} n\left\{\left|\frac{a_{n+1}}{a_n}\right| - 1\right\} = -2.$$

Hence, the sum converges.[7] We may thus incorporate L_s as given by (55) with the ordinary self-induction L_0 for the wire as calculated for free space, and we thus find for the complete self-induction

$$L = L_0 + 4\pi^2 \frac{b^4}{a^3} \sum_{n=1}^{\infty} \frac{c_n - n}{n^2(n+1+c_n)}[P_n'(\nu)]^2 \tag{56}$$

where $2c_n = m-1+[(m-1)^2+4n(n+1)]^{1/2}$, which is the result quoted in (6).

The Value of the Townsend Coefficient for Ionization by Collision at Large Plate Distances and Near Atmospheric Pressure

By FREDERICK H. SANDERS
University of California

(Received June 13, 1932)

The Townsend coefficient of ionization by collision was measured at a pressure of 380 mm in air at plate distances ranging from one to five cm for values of X/p (the ratio of the field strength to the pressure in mm) from 20 to 36.5. It was found that the simple Townsend relation, $i=i_0e^{\alpha d}$, is valid at the above pressure and over the above range of plate distances. The ratio α/p of the Townsend coefficient to the pressure in mm was determined as a function of X/p and the least-square reduction shows the function giving closest agreement with the observed data to be $\alpha/p=(2.67\pm0.26)\times10^{-8}\epsilon^{(0.350\pm0.002)X/p}$. From these results it is evident that ionization by collision exists at much lower values of X/p than those given by Paavola. The rise in the saturation photoelectric current at the lowest X/p was compared with the recent work of Bradbury on the nature of the saturation photoelectric current and compares in order of magnitude with values found by extrapolation of the latter's equations. This indicates that below $X/p=20$ the lack of saturation produces a fictitious value of α which renders measurements of α below $X/p=20$ of doubtful value. No abnormal increase in the current with plate distance was found even within two percent of sparking. This indicates that if ionization by positive ions does exist it must occur at fields closer to sparking than two percent.

INTRODUCTION

IN 1900 J. S. Townsend[1] investigated the increase of the photoelectric saturation current from an electrode as a function of the distance between plane parallel electrodes for high values of the electric field or, better, for high values of X/p, the ratio of the electric field strength to the pressure. It was found that the current increased with the plate distance d at constant field strength according to the equations:

$$i = i_0e^{\alpha d} \tag{1}$$

where i is the current at a distance d, i_0 the saturation photoelectric current at lower field strengths, and α a constant depending on X/p and the nature of the gas. A theoretical derivation of the experimental relation (1) was achieved by assuming that for a given X/p, α was the number of new ion pairs produced per centimeter of path in the gas by electron impacts. Townsend[2] evaluated α for various values of X/p and found α/p to be a function of X/p of a form closely analogous to that given by the equation:

$$\alpha/p = Ae^{-Bp/X} \tag{2}$$

where A and B are constants. This law he deduced theoretically, assuming the negative ions to make inelastic impacts with the gas molecules. Townsend[2]

[1] J. S. Townsend, Nature **62**, 340 (1900).
[2] J. S. Townsend, Phil. Mag. **2**, 598 (1903).

further found that the currents for very high values of X/p could not be expressed by Eq. (1) but that a more rapid increase in current took place. This he explained by assuming that in these high fields the positive ions also produced ions by collisons with the gas molecules. The equation deduced on the assumption that each positive ion in the assumed uniform field X/p produced β new pairs of ions per centimeter of path was:

$$i = i_0 \frac{(\alpha - \beta)e^{(\alpha-\beta)d}}{\alpha - \beta e^{(\alpha-\beta)d}} \tag{3}$$

where β/p was evaluated from the experiments and found to be a function of X/p. It is seen that i approaches infinity when $\alpha - \beta e^{(\alpha-\beta)d}$ approaches zero. This is the condition for spark breakdown proposed by Townsend.

All of Townsend's investigations were confined to *low pressures*, *small plate distances* and *high values of* X/p for the more common gases, due to the limited experimental facilities available at the time. The investigations of Franck[3] and countless others on the ionization and radiation potentials as well as Townsend's own work on the elasticity of electron impact made his theoretical deduction of Eq. (2) untenable as Compton[4] and others have pointed out, although it appeared to fit fairly well as an empirical equation. It was later pointed out by Holst and Oosterhuis,[5] by Rogowski, and by Loeb[6] that while the values of β/p could be expected to play a rôle in spark discharge at low pressures and high values of X/p (in the region of the minimum sparking potential) it was impossible to expect β/p to have finite values of a magnitude leading to the Townsend sparking mechanism at values of X/p of 39 which is the value of X/p for spark breakdown in air at atmospheric pressure. This led Loeb[6] and Rogowski[7] independently and contemporaneously to suggest that at higher pressures where the positive ions could not ionize by impact in the uniform fields assumed to exist between the electrodes before breakdown, the increase in the number of ions due to the ionization by electrons in the dark current preceding breakdown might produce distorted fields, due to space charges, of sufficient magnitude to give β/p finite values and to cause the Townsend mechanism to occur.

Acting on this suggestion several attempts were made to develop such theories mathematically, stimulated further by recent discoveries connected with the short time interval involved in spark breakdown. All these theories required a knowledge of the Townsend coefficient α in gases like air for values of X/p corresponding to that required for a spark in air at atmospheric pressure and lower. These were not available as Townsend's measurements in air extended only to $X/p = 40$ and were rather meager in this region, most of his measurements extending upwards from $X/p = 100$.

[3] Franck and Hertz, Verh. d. deut. phys. Ges. **15**, 373, 613 (1913). J. Franck, Zeits. f. Physik. **25**, 312 (1924).

[4] K. T. Compton, Phys. Rev. **7**, 489, 501, 509 (1916). Compton and Benade, Phys. Rev. **11**, 234 (1918).

[5] Holst and Oosterhuis, Phil. Mag. **46**, 1117 (1923).

[6] L. B. Loeb, Jour. Frank. Inst. **205**, 305 (1928).

[7] W. Rogowski, Archiv f. Elek. **16**, 761 (1926).

In order to supply the missing data it was thought worth while to study Townsend's coefficient α for electron ionization at pressures of the order of magnitude of an atmosphere and plate distances of the order of centimeters to correspond more nearly with the actual conditions involved in the study of spark discharge. The realization of the very elaborate equipment required for this investigation was in part made possible by a grant in aid from the National Research Council and the task was begun in the fall of 1929. When the work was well under way the results of M. Paavola[8] working on the same problem under Professor Rogowski in Aachen were published. Paavola had extended Townsend's measurements to atmospheric pressure and to plate distances between two and five millimeters. Inasmuch as the present work promised further results at lower values of X/p in view of the greater plate distances involved, the work was continued with the gratifying results reported in this paper.

Apparatus and Experimental Procedure

The experimental arrangement is shown in Fig. 1. The primary of the high tension transformer T was supplied by the 220-volt, 500-cycle a.c.

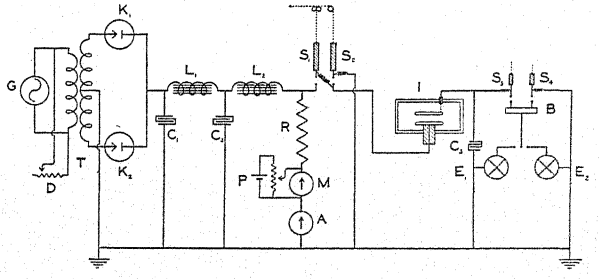


Fig. 1.

generator G which was operated by a 110-volt, 2-kilowatt d.c. motor. This motor was operated on the direct-current line, the voltage being held constant by means of a hot wire stabilizer.

The secondary of the transformer T was tapped at its center and connected to ground. The current was rectified by means of two General-Electric kenotrons of the KR-1 type. The filter system consisted of two condensers C_1 and C_2 of combined capacity 0.04 microfarads and two choke coils L_1, L_2, each of about 1000 henries inductance. As the maximum current drawn was 0.4 milliamperes the ripple was computed to be of the order of one one-hundredth of one percent or less which was considerably smaller than the possible errors in the voltage settings.

The voltage was measured by means of a bank R of 20 five-megohm resistors and the 2 milliammeters M and A. The instrument A was a Weston milliammeter checked at the factory in August 1931, but as a further precaution it was calibrated over the range from zero to 0.4 milliamperes with a Wolff standard potentiometer, a Weston standard cell and a 1000-ohm standard resistance. It was found to be accurate over this range to within 1/4 of

[8] Paavola, Archiv f. Elek. **22**, 443 (1929).

1 percent, no apparent consistent error existing. The resistors were also calibrated and found to be of an equal order of accuracy. The other milliammeter M which was of ten times the sensitivity of A was used merely as an amplifying device.

The switches S_1 and S_2 were used to connect the negative plate of the ionization chamber I either to the high potential or to ground. Both were fitted with platinum contacts and were mechanically connected together so that when one was opened the other was automatically closed. The upper plate of the ionization chamber I was connected permanently to the electrometer switch S_3 and to the sulphur-insulated, cylindrical condenser C_3. The switch S_4 was connected permanently to ground and was used either to remove the charge from the working electrometer or to protect the instrument whilst measurements were being taken. The measuring instruments were the two Dolazalek electrometers E_1 and E_2 which were capable of covering a range of voltages varying from 0.01 volt to 100 volts. The two electrometers and the condenser C_3 were enclosed in a grounded chamber and all external leads to the electrometer system were carefully shielded in brass tubing and insulated with sulphur.

The capacity of the condenser C_3 was measured very carefully on a capacity bridge and the capacity of the ionization chamber and electrometer system measured for a number of different plate distances. This made it possible to compute the absolute values of the current. It also made possible a small but necessary correction to the voltage due to the fact that the ionization chamber and condenser C_3 formed a pair of condensers in series, so that the actual drop in potential across the gas was slightly less than that registered by the voltage-measuring instruments. This correction amounted to about 1 percent at a plate distance of 1 cm and decreased to less than 1/4 of 1 percent at the larger plate distances.

The ionization chamber I is shown in detail in Fig. 2. The case consisted of a cylindrical brass casting 45 cm in height and 50 cm in diameter, the inner surfaces being all heavily plated with tin. The lid rested on a lead gasket which was coated with stop-cock grease to ensure a vacuum-tight fit. The upper plate 20 cm in diameter was supported by a brass tube T from which it was insulated by a block of amber A. This tube was connected at its upper end to an iron armature F by means of a ball-bearing race. This armature revolved on the long screw S_1 which was connected to the top of the cylindrical housing H and could be turned by means of the magnet M. The magnet also revolved on the screw S_2 of the same pitch as S_1 so that the armature and magnet were always at the same height. By this means the upper plate could be set at any desired distance from the lower one. The rods RR were merely guides which kept the upper plate accurately in position.

In order to have the two plates always accurately parallel the lower plate was supported on a porcelain insulator I_1 resting on the circular plate P. This plate was connected to the lid by three rods with threaded ends and adjusted until the two plates were parallel to within a few hundredths of a millimeter. The lower insulator I_2 was made of Pyrex tubing and filled with pump

oil. It was ground to fit the taper in the bottom of the chamber and waxed into place. Contact was effected between the two leads passing through the insulators by means of a mercury cup in the top of the lower insulator. The upper plate was connected to the electrometer system by means of a gold chain C and a lead running through the amber bushing B. The distance between the plates was read by the use of a cathetometer through the glass window G. The ultraviolet radiation entered through the quartz window Q and fell obliquely upon the lower plate.

The whole interior of the chamber was carefully cleaned and the plates polished with jewellers' rouge before closing it for a set of observations. It was then exhausted to a pressure of about 10^{-3} mm. Lower pressures than this

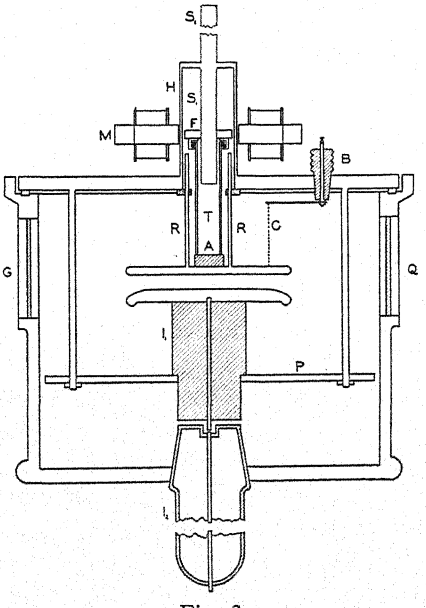


Fig. 2.

could not be attained on account of the vapor pressure of the mercury. The air was admitted slowly over a bank of drying tubes containing $CaCl_2$, KOH and P_2O_5. As a final precaution in ensuring perfectly dry air, the air was passed over a liquid air trap. The pressure could be regulated as desired. The original intention was to carry on the investigations at atmospheric pressure but on account of the high voltages required at the larger plate distances it was decided to use a pressure of 380 mm throughout the experiment. The actual pressure during the observations never varied more than 1/2 mm from 380 mm.

The source of ultraviolet radiation was a Heraeus quartz mercury arc lamp operating on 220 volts. This was placed at a horizontal distance of 50 cm from the center of the lower plate and at a height of 5 cm above it. The light was rendered parallel by a quartz lens placed at its own focal length from the lamp and was admitted through a variable aperture of rectangular cross section. The horizontal aperture was 3 cm and the maximum vertical aperture

6 mm, which rendered the area of plate illuminated a rectangle 3 cm by 6 cm. This area lay well within the area, 14 cm in diameter, over which the field was uniform as determined below. The field between the plates was investigated by means of a full-size cross-section model of the plates immersed in a bath of electrolyte. An induction coil, telephone head set and exploring electrodes were used to find the equipotentials and it was found that the field was sensibly uniform over an area 14 cm in diameter. Thus, with the spot of light carefully focussed on the center of the lower plate, electrons could only be emitted in the portion of the field which was known to be uniform. For this reason no guard ring was used.

In order to keep the current through the mercury arc constant a current stabilizer was placed in series with the lamp. Even with these precautions there were occasional fluctuations in the photoelectric current which probably account for the large probable errors in some of the results.

The method of measuring the currents was as follows: The voltage was set at the desired value. Switch S_1 (Fig. 1) would be open and S_2, S_3, and S_4 all closed so that both plates of the ionization chamber, the condenser C_3, and the working electrometer were all grounded. S_3 was then opened, thus isolating the upper plate and the condenser C_3. S_1 was then closed, S_2 opening automatically so that the lower plate was raised to the negative potential indicated by the milliammeters M and A. The ionization current was allowed to pass for a known time (usually 10 seconds), then S_1 was opened, S_2 again closing automatically and grounding the lower plate. S_4 was then opened and S_3 closed, thus connecting the upper plate of the ionization chamber and the condenser C to the electrometer which measured the potential to which the condenser had become charged. This procedure was repeated four times for each voltage setting with the lower plate illuminated and once with the ultraviolet radiation cut off to insure the absence of corona discharge. The usual variation in current of the four readings was about 5 percent. The chance of a consistent error due to variation in voltage, photoelectric current, or timing was small. One advantage of this method was that any charge produced by the so-called *capacity current* mentioned by Paavola[9] due to slight fluctuations in voltage was removed when the lower plate was grounded. Another was that the working electrometer was fully protected in case of breakdown of the gap.

In a preliminary series of measurements each run was taken at a constant plate distance, the current being measured as a function of the field. Observations were taken covering a range of plate distances varying from 1 to 3 cm at 2.5 mm intervals. This method had the advantage of giving values of the current for all possible fields from a few thousand volts up to breakdown. The disadvantage, however, lay in the fact that each run took seven hours to complete. During this time the photoelectric current was apt to vary greatly. Current-plate-distance curves were plotted from these data for values of X/p varying from 30 to 36.5.

Owing to the unsatisfactory nature of the preliminary results, resort was had to essentially the same method as that employed by Townsend in his

[9] M. Paavola, Archiv f. Elek. **22**, 450 (1929).

original researches. A certain value of X/p was chosen and the currents measured as a function of plate distance over a range varying from 1.00 or 1.25 cm to as high as the voltage limits or the breakdown potential would permit. As a great deal of time was taken up in changing the plate distances, during which intervals the ultraviolet illumination was cut off, the decay in the photoelectric current was now found to be negligible. However, as an additional precaution against any consistent change in i_0 which might influence the slopes of the curves, the plate distances were chosen entirely at random.

Experimental Results

The curves giving $\log_e i$ as a function of plate distance are shown in Fig. 3. The fact that these are all linear bears out the validity of the simple Town-

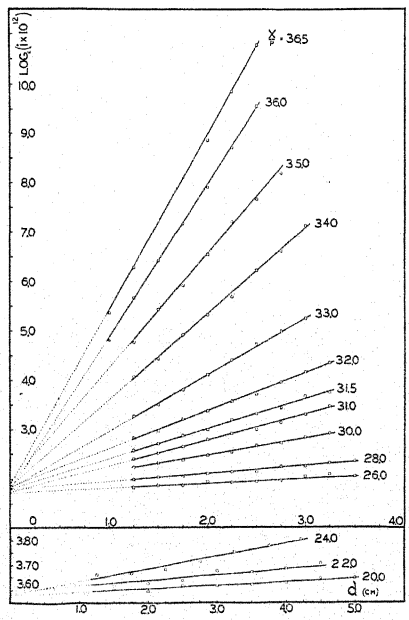


Fig. 3.

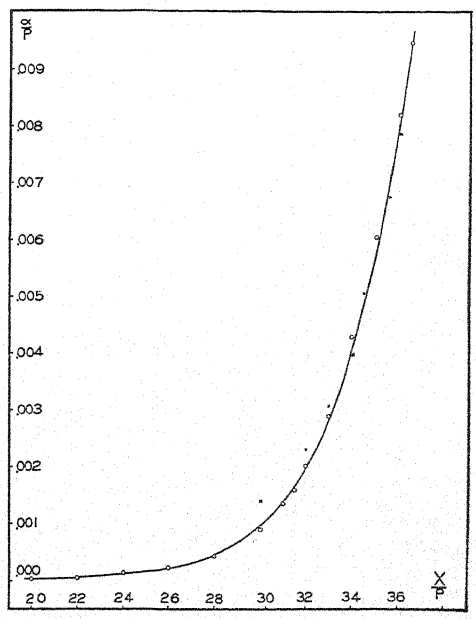


Fig. 4.

send Eq. (1). The value of the coefficient was obtainable directly from the slope of any one curve and the value of i_0 from the intercept with the axis of zero plate distance. These slopes and intercepts were first measured graphically but were later computed by the method of least squares. This eliminated entirely the personal bias which might occur in drawing the best straight line through any one set of points. For most of the curves the graphical and least-square solutions were found to check very closely. Below an X/p of 28 the points are rather more scattered. This is probably because the increase in current with plate distances is so small that variations due to other causes become evident. The probable errors here are accordingly quite large.

It will be noticed that the curves at X/p of 20, 22 and 24 have a larger value of i_0 than the remainder. This was necessary on account of the limitations of the measuring instruments. Although Townsend has shown that α is

independent of i_0 for plate distances below 1 cm it was thought advisable, in view of possible space-charge effects which might exist at these larger plate distances, to determine roughly whether or not the value of α was affected by a change in i_0. Several curves were taken at X/p of 33 and 34 with widely different values of i_0. No consistent change in the value of α was noted, which seems to justify the use of these larger currents.

In Fig. 4 the circles give the values of α/p as obtained by dividing the least-square solutions of the curves in Fig. 3 by the pressure, 380 mm. The crosses represent the values of α/p obtained graphically from the earlier set of readings taken at constant plate distances. It is seen that they check quite

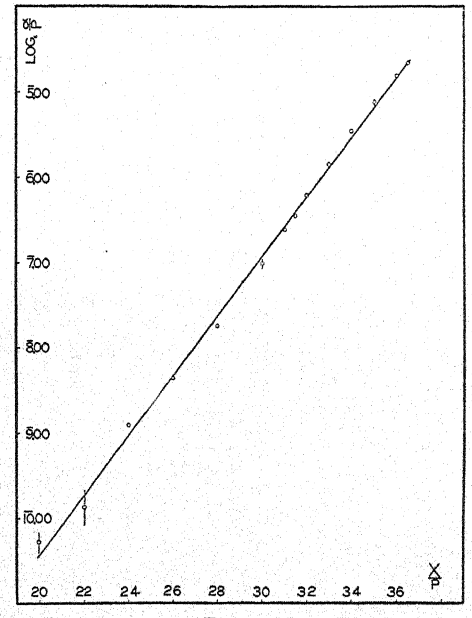


Fig. 5.

well above $X/p=32$. Below this value the values indicated by the crosses are considerably greater than those indicated by the circles, but as mentioned before, the data here were too erratic to have much meaning. The curve represents a pure exponential relation of the form

$$\alpha/p = Ae^{bX/p}. \tag{4}$$

It was obtained as follows: The natural logarithms of the values of α/p indicated by the circles in Fig. 4 were plotted against X/p. The result is shown in Fig. 5 where it is seen that the points appear to lie on a curve very nearly a straight line. A least-square solution was again applied and is represented by the straight line in the latter figure. Knowing the slope and intercept of this line it was a simple matter to obtain the constants in Eq. (4). The constant b is merely the slope of the straight line and A is obtained by taking the anti-$\log_\epsilon$ of the intercept. The idea of plotting $\log_\epsilon \alpha/p$ against X/p was inspired by the fact that a rough curve through the points shown in Fig. 4 had the appearance of a pure exponential.

The probable errors of some of the observed values of α/p are shown in Fig. 5 as short vertical straight lines through the points. The values of the slope a_{11} and intercept a_{01} of the straight line with their respective probable errors are: $a_{11}=0.3504\pm0.0032$; $a_{01}=\overline{18}.5615\pm0.0966$. This gives the values of the constants in Eq. (3) as: $b=0.350\pm0.003$; $A=2.67\times10^{-8}$.

The probable error in the case of A is not quite symmetrical on account of the fact that A is obtained by taking the antilog of the intercept a_{01}. The probable upper and lower limits to the value of A are respectively, 2.94×10^{-8} and 2.43×10^{-8}.

The interesting thing about this expression for α/p as a function of X/p is that α/p does not suddenly become zero at a definite value of X/p as found by Paavola but decreases in an asymptotic fashion with X/p. Whilst the values of α/p observed for X/p's around 20 are very small they are certainly not equal to zero.

Another phenomenon noted in these measurements which has a definite bearing on the above was the lack of any definite saturation current. This is in good agreement with the work recently carried on in this laboratory by Dr. N. E. Bradbury[10] on the nature of the photoelectric saturation current. Bradbury found that saturation of such currents cannot be obtained at field strengths below sparking. By extrapolation of Bradbury's equations to values of X/p in the neighborhood of 20 his results may be compared with the data obtained in these measurements. At $X/p=20$ Bradbury's results give for $(d/dX)(i/I_0)$ where X is the field strength, I_0 the saturation current in vacuum and i the measured photoelectric current at a field X, an approximate value of 1.0×10^{-5}. The writer's work gives about 2.0×10^{-5}. In view of the extrapolated nature of the first of these values, numerical correction of values of α cannot be made. The indication, however, is that at values of X/p below 20 the natural slope of the photoelectric current produces a fictitious value of α which merges smoothly with the real values existing above $X/p=20$.

The empirical expression found by Paavola to fit his observations is:

$$\alpha/p = 0.000156(X/p - 30.1)^2. \qquad (5)$$

This would indicate that ionization by collision ceases to exist at lower field strengths than those corresponding to $X/p=30.1$. As seen from the curves in Fig. 3, the slope of the curves below $X/p=30$ is quite small and would be very difficult to detect over the small range of plate distances (2.0−5.0 mm) used by Paavola.

The actual values of α/p obtained in this investigation are considerably greater than those obtained by the above investigator as shown by the following table which also contains a few of Townsend's lower values:

X/p	20.0	26.0	26.9	30.0	30.1	33.0	33.5	36.5	37.0	40.0	40.4	45.7	50.0
α/p Townsend										0.0190			0.0550
α/p Paavola			0		0		0.00205		0.00703		0.0160	0.0407	
α/p writer	0.0000343	0.000234		0.00090		0.00289		0.00946					

[10] N. E. Bradbury, Phys. Rev. **40**, 508 (1932).

The reason for this discrepancy is not apparent but it seems likely that with the greater resolving power of the apparatus used in this investigation the chances of error are somewhat less. The air used in the present work was carefully dried as previously described and kept at constant pressure. This was not entirely the case in Paavola's work. It is doubtful, however, whether this has any bearing on the above discrepancy.

As mentioned in the introduction, Townsend has suggested that the function $\alpha/p=f(X/p)$ takes the form:

$$\alpha/p = Ae^{-Bp/X}. \tag{2}$$

This is a theoretical expression based on a deduction as to the mechanism of ionization which is not applicable to the present problem in the light of modern knowledge of ionization processes.[11] Townsend himself limits it to values of X/p above 300. Whilst it is an exponential form, it is entirely different from the empirical expression (4) and obviously cannot fit the present data for any values of the constants.

The phenomenon noted by both Townsend[2] and Paavola[8] when the field is increased to within 3 percent of sparking, *viz.*, that the current increases with plate distance more rapidly than Eq. (1) would lead us to expect, was not observed in these measurements. At X/p of 36.5 and a plate distance of 2.5 cm the field was within less than 2 percent of sparking, yet there was no evidence of an abnormal increase in the current. Paavola noted this increase within 3 percent of sparking at plate distances of 4.5 and 5.0 mm. He also noted no current without ultraviolet excitation even on the verge of sparking. In the present investigation, currents were noted without excitation at a field slightly above X/p of 36.5. It may be that, at these greater plate distances, space charges build up and a corona discharge is produced preceding breakdown. The plates of the ionization chamber were carefully machined and polished so that there was very little chance of corona being produced by high fields at sharp points or edges.

With the care taken in these measurements it seems safe to assume that if such an increase in current actually exists as that ascribed to positive ion ionization it must occur at fields closer to the breakdown potential than 2 percent. This is completely in keeping with the values of β/p observed by Townsend,[2] who could not detect any measurable values of β/p at lower fields than those corresponding to X/p 100. It also agrees with recent information[12,13,14] as to the inability of positive ions to ionize by impact at lower fields. It thus appears that the important factor in the early period preceding spark breakdown is the ionization by electrons and the subsequent distortion of the field by space charges to values where ionization by positive ions can occur. This must take place at values of X/p within 2 percent of sparking.

[11] J. S. Townsend, Phil. Mag. **45**, 1071 (1923).
[12] J. J. Thomson, Phil. Mag. **48**, 1 (1924).
[13] L. B. Loeb, Science **66**, 627 (1927).
[14] R. M. Sutton, Phys. Rev. **34**, 547 (1929). O. Beeck, Phys. Rev. **38**, 967 (1931).

In conclusion the writer desires to express his gratitude to the National Research Council for the financial assistance which in part made these investigations possible and his sincerest thanks to Professor L. B. Loeb at whose suggestion the problem was undertaken and under whose direction it was carried out. In addition the writer wishes to acknowledge his indebtedness to the mechanical skill of Mr. Wm. R. Stamper, without whose assistance in overcoming the many instrumental difficulties due to the large dimensions involved, the work could not have been brought to a successful conclusion, and to Mr. W. E. Bowls for his assistance in taking readings.

LETTERS TO THE EDITOR

Prompt publication of brief reports of important discoveries in physics may be secured by addressing them to this department. Closing dates for this department are, for the first issue of the month, the twenty-eighth of the preceding month; for the second issue, the thirteenth of the month. The Board of Editors does not hold itself responsible for the opinions expressed by the correspondents.

Experimental Evidence for and Determination of the Predicted $^1\Delta$ Level of the Neutral Oxygen Molecule[1,2]

The ground level of the neutral oxygen molecule is a $^3\Sigma$ state. The next higher known level is a $^1\Sigma$ state which is observed in the atmospheric absorption bands ($^1\Sigma \leftarrow {}^3\Sigma$). The $^1\Sigma$ state is 1.62 volts above the $^3\Sigma$ state. According to theoretical considerations there should be another state, $^1\Delta$, between the $^3\Sigma$ and $^1\Sigma$ states which presumably lies about midway between them.[3]

Recently we have used the explosion method to determine the specific heats of the oxygen molecule up to temperatures of 2500° K by exploding mixtures of ozone and oxygen. After correcting for dissociation of the oxygen molecule into atoms[4] the values so obtained may be compared with values calculated from optical data,—i.e., the vibrational and rotational levels of the normal state of the molecule. The experimental values are always higher than the calculated values in the temperature range investigated, the difference becoming more pronounced with higher temperatures.

It would appear that this difference is due to some low-lying electronic level. Calculations show that it in no way can be accounted for by molecules being raised to the $^1\Sigma$ level, but that the level responsible must be still lower, or in all probability is the predicted $^1\Delta$ level. It is thus possible from our experimental data to place the position of this state relative to the $^3\Sigma$ state.

Before such a calculation can be made it is necessary to know what the *a priori* probabilities of the $^3\Sigma$ and $^1\Delta$ states are. The statistical weights of the vibrational and rotational levels belonging to the $^3\Sigma$ state follow from the fact that the resultant orbital momentum of the two outer electrons is zero, while their resultant spin vector is 1. The corresponding statistical weights for the $^1\Delta$ state follow from the fact that the resultant orbital momentum of the electrons is 1, while their resultant spin vector is zero. For both states the number of orientations of the molecule in space, $(2j+1)$, is equal. For $^3\Sigma$, the number of orientations of the resultant spin vector of the electrons, relative to the line joining the nuclei, is 3, and for $^1\Delta$ it is 1. In the $^1\Delta$ state there is λ-type doubling which doubles its weight. The resultant statistical weights are: for $^3\Sigma$, $3(2j+1)$; for $^1\Delta$, $2(2j+1)$ or a ratio of the weights of $^1\Delta/{}^3\Sigma$ of 2/3. The fraction of the molecules reaching the $^1\Delta$ state at any temperature T is then given by

$$N_{^1\Delta}/N_{^3\Sigma} = (2/3)e^{-E_{^1\Delta}/RT} \qquad (1)$$

where $E_{^1\Delta}$ is the energy of the $^1\Delta$ state. The energy difference H determined from the difference between the experimental molal specific heats and those calculated from the oxygen vibrational-rotational levels is given by

[1] Published by permission of the Director, U. S. Bureau of Mines. (Not subject to copyright.)

[2] Contribution from the Pittsburgh Experiment Station, U. S. Bureau of Mines at Pittsburgh, Pa., and the Cobb Chemical Laboratory of the University of Virginia.

[3] R. S. Mulliken, Phys. Rev. **32**, 213, 887 (1928). F. Hund, Zeits. f. Physik **51**, 759 (1928); **63**, 726 (1930). E. Hückel, Zeits. f. Physik **60**, 442 (1930).

[4] Details of this work will be published soon in the Journal of the American Chemical Society.

$$H = E_{^1\Delta}\ (2/3)e^{-E_{1\Delta}/RT} \qquad (2)$$

$E_{1\Delta}$ can be evaluated from (2). It turns out out to be 0.75 ± 0.05 volts. The new theoretical specific heat curve which includes the contribution from the above determined $^1\Delta$ level, fits the experimental values of specific heats very well over the whole temperature range investigated—i.e., 1400° to 2500°K.

BERNARD LEWIS
GUENTHER VON ELBE

Pittsburgh, Pa.,
July 22, 1932.

A Remark on Erikson's Measurements of the Ionization by γ-Rays at Various Pressures and Potentials

In the Physical Review of July 1, 1932, I. S. Bowen has published measurements on the ionization of air by γ-rays under pressures from 1 to 93 atmospheres applying collecting fields from 1.55 to 1009 volts per cm of a high degree of uniformity.

This author as well as others working in this field recently do not seem to have noticed the work of H. A. Erikson[1] who, as early as 1908, carried out measurements with air for pressures varying from 20 to 400 atmospheres and collecting fields up to 2500 volts over a distance of about 0.8 cm, hence 3100 volts per cm. He also investigated the influence of the temperature on the ionization at a pressure of 200 atmospheres and carried out measurements for carbon dioxyde. The purpose of the present note is to call attention to this beautiful paper of Erikson, which somehow seems to have been overlooked by most of the workers in this field.

H. ZANSTRA
J. CLAY

Natuurkundig Laboratorium der Universiteit,
Amsterdam,
July 25, 1932.

[1] H. A. Erikson, Phys. Rev. **27**, 473 (1908).

Dependence of the Ionization Produced by γ-Rays upon Pressure and Temperature

Broxon[1] has measured the variation of ion current with pressure alone, up to 170 atmospheres. Upon a beta-ray absorption hypothesis, he could explain the form of his i *vs.* p curve very well. However, Millikan and Bowen[2] and Compton, Bennett and Stearns[3] have independently offered an explanation of this curve, based on the idea that at high pressures, there is a lack of saturation. On the basis of their suggestion, Compton, Bennett and Stearns[4] have derived an equation relating ion current to density and temperature. This equation is

$$i = I\rho(1 + A^2\rho^2/T^2)^{-1/2}$$

where A is a constant for each gas, and from this, the temperature coefficient of ionization is found to be

$$\beta = di/idT = (A^2\rho^2/T^3)/(1 + A^2\rho^2/T^2)$$

In order to test this theory, the writer has performed experiments in which β was measured when the temperature range was from 8°C to 38°C, and others in which the ion current was measured when the temperature was varied from room temperature to about 160°C. Though the results obtained seem sufficiently definite to report at this time, it is hoped that several features can soon be investigated further.

A cylindrical steel chamber with inside dimensions of about 30 cm long and 6 cm diameter was surrounded by a brass cylinder to contain the water or glycerine bath. No gas leak was detected at any pressure over a period of a weak. Gas and electric heaters heated the bath evenly, and its temperature was read with a mercury in glass thermometer. The collecting rod was insulated with amber from a brass guard ring which in turn was insulated from the chamber with hard rubber. Protection for the insulators from the heat was provided. The electrical leak was found to be negligible at both low and high temperatures though it appeared to be slightly greater at high temperatures. The Lindemann electrometer was used usually at 80 divisions per

[1] J. W. Broxon, Phys. Rev. **37**, 1320 (1931).
[2] R. A. Millikan and I. S. Bowen, Nature **128**, 582 (1931).
[3] A. H. Compton, R. D. Bennett and J. C. Stearns, Phys. Rev. **38**, 1565 (1931).
[4] A. H. Compton, R. D. Bennett and J. C. Stearns, Phys. Rev. **39**, 873 (1932).

volt, together with a chamber voltage of 180 volts. At 40 atmospheres pressure, an increase of the chamber voltage from 90 to 135, caused an increase of 3 percent in the ion current, but with an increase from 135 to 180 volts, no detectable further increase was noted. The γ-ray source was placed in a fixed position during each run, and it was found that using different intensities led essentially to the same result. Commercial air at high pressures was introduced directly from the two large tanks to the chamber. Finally, one test was made for the difference in absorption of the bath at high and low temperatures, but no effect was observed.

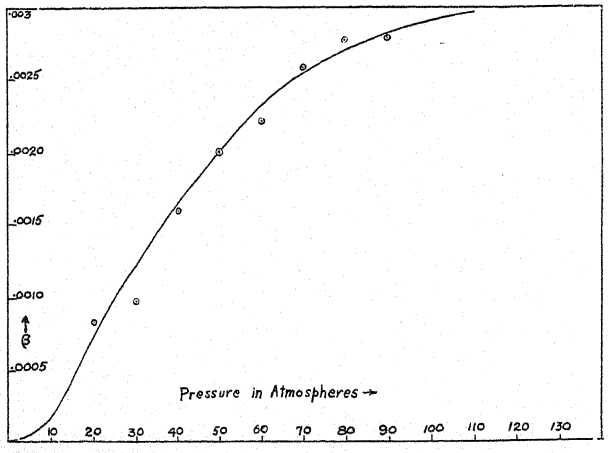


Fig. 1. Showing variation of the temperature coefficient of ionization with air pressure at 293°K.

Fig. 1 shows the values of β obtained at different pressures when the temperature range was nearly 8°C to 38°C in all cases. The solid line represents the theoretical value of β for air at 293°K. It was found necessary to wait almost half an hour after the bath reached a constant temperature before consistent current readings could be obtained, and the values at the lower pressures are, perhaps, less reliable than those at the higher pressures.

Fig. 2 shows the ion current as a function of the temperature between room temperature and about 160°C. Two or more runs were taken in each case, and the points for each run are marked alike. The solid curves are plotted from the first equation above, with ρ a constant for each case. The constant I was adjusted so that the theoretical curve would pass through the first experimental point in each case. The observed and predicted slopes agree well in the case of 60 atmospheres pressure, but they do not agree well in the cases of 20 or 40 atmospheres. Some work with 10 atmospheres indicated a greater increase of current with temperature than would be expected, also. Tests for electrical leakage and for the change of density of the bath with temperature, failed to reveal any cause for these discrepancies. Though the pressure gauge was not calibrated, it is improbable that an explanation could be found in faulty calibration since an error of about 10 atmospheres would be necessary to make agreement in the 20 atmosphere case. It was thought that

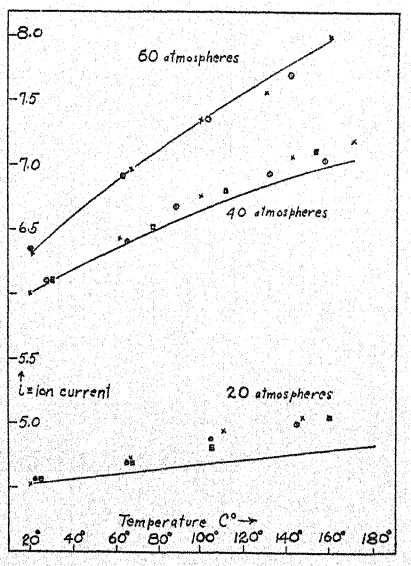


Fig. 2. Showing variation of ion current with temperature at different densities.

perhaps the constant A was not a constant for all pressures, and to test this $1/i^2$ was plotted against $1/T^2$ for various pressures and for runs in which the ionization per unit density, I, was the same. The slope of this curve is A^2/I^2, and should show up any variation in A. This relation was found to be a straight line for 60 and 40 atmospheres, but was distinctly curved for 20 and 10 atmospheres. Thus it may be that for low pressures and high temperatures, A is not strictly constant.

In regard to Broxon's[5] remark that the "variation of the ionization with temperature is greater at higher temperatures," these experiments distinctly disagree with that conclusion. Furthermore, these experiments definitely lead to the conclusion that the temperature effect is greater at high pressures than at low pressures. His observation that there is an "apparent slight dependence of the ionization upon time rate of change of temperature" has been observed in these experiments. However, if sufficient time is allowed for the gas in the chamber to come to equilibrium, consistent readings can be obtained.

The writer is indebted to Professor R. D. Bennett and Dr. L. A. Young for their suggestions in connection with this work.

NEWELL S. GINGRICH

Department of Physics,
Massachusetts Institute of Technology,
July 25, 1932.

[5] J. W. Broxon, Phys. Rev. **40**, 1022 (1932).

Progress of Cosmic-Ray Survey

We have recently extended our measurements previously reported[1] to include southeastern Australia, equatorial Pacific, Panama, and Peru. The results confirm our earlier conclusion, that the intensity of the cosmic rays at sea level becomes greater as we go farther from the equator. Comparison of the Australian data with those taken in New Zealand shows that for the same geographic latitude the rays in Australia are the stronger whereas for the same magnetic latitude (or magnetic dip) the intensity in the two regions is nearly the same. Our measurements to date of the cosmic rays at sea level may be expressed satisfactorily as a function only of the dip of the earth's magnetic field.

The results of these sea level measurements are shown in Table I. The quantities I_C and I_L are the intensities of the cosmic rays (reduced to sea level) and of the local radiation respectively, expressed in ions per cc per second in air at atmospheric pressure, as measured through 2.5 cm of copper and 5.0 cm of lead. The measurements 1 to 4 have previously been reported,[1] but are here corrected for a radiation of 0.14 ions from the walls of the ionization chamber itself, as determined by measurements in a deep tunnel in Peru. The absolute values of the ionization are somewhat uncertain, due to an uncertainty in the ionization by the standard radium capsule. The relative values should however be reliable.

Several series of measurements have been made in different localities to determine the rate at which intensity increases with altitude. The most significant of these were two series

[1] A. H. Compton, Phys. Rev. **41**, 111 (1932).

TABLE I. *Cosmic-ray intensity, reduced to sea level, at different localities.*

Location	Lat.	Long.	Mag. dip	I_C	I_L	Date
1. Honolulu	21°N	158°W	+39°	1.74 ions	0.12 ion	4/ 5/32
2. S.S.Aorangi	4°S	173°W	−10°	1.69	0.32	4/10/32
3. Dunedin	46°S	170°E	−70°	2.02	0.12	4/29/32
4. Wellington	41°S	175°E	−65°	1.97	0.15	5/ 2/32
5. Sydney	34°S	151°E	−64°	2.02	0.42	5/ 9/32
6. Brisbane	28°S	152°E	−57°	1.93	0.20	5/16/32
7. Auckland	37°S	175°E	−62°	1.92	0.10	5/28/32
8. SS. Mataroa	13°S	106°W	−10°	1.69	0.15	6/ 9/32
9. Panama	9°N	80°W	+33°	1.72	0.21	6/17/32
10. Lima	12°S	77°W	0°	1.69	0.20	6/30/32
11. Mollendo	17°S	72°W	−10°	1.70	0.09	7/23/32

done in Peru. In the first series the apparatus was installed in a special car, and measurements of from 12 to 24 hours made at each of five stations along the Central Railroad of Peru (Ferrocarril Central), at elevations of from 165 to 5150 meters. The second series included measurements on the top of El Misti (6280 m), Monte Blanco (5110 m), Arequipa (2520 m) and Mollendo (30 m), made on four successive days. The two series of measurements are in excellent agreement, and indicate an increasingly rapid increase of intensity with increasing altitude. At the highest point, barometer 376 mm, the cosmic-ray ionization was 9.50 ions per cc per second in air, through a shield of 2.5 cm copper and 5.0 cm lead. With only the copper shield, the ionization due to the cosmic rays would have been about 22.5 ions.

On the basis of Millikan and Bowen's and Kohlhorster's early balloon measurements, it has been inferred[2] that the ionization approaches a maximum at an altitude of not over 9000 meters, and then decreases. Millikan has indeed used this supposed fact as proof of the photon character of the cosmic rays. If a maximum exists in the neighborhood of 9000 meters, its approach should have become apparent in our work at 6280 meters. Our measurements show no suggestion of such a maximum, confirming Piccard's provisional estimate of 200 ions per cc per second at 16,000 meters rather than Millikan and Bowen's estimate of not more than 6 ions at the same altitude. Thus the intensity of the cosmic rays seems to increase continuously to as high altitudes as the measurements have as yet been made.

Further measurements of the diurnal variation of cosmic rays have also been made at a higher altitude (4930 m) than heretofore attempted. The result of 120 hours observations at Huaytapallacu, Peru, shows that the average intensity between 10 and 4 o'clock in the daytime is greater than between 10 and 4 at night by 1.6 ± 0.8 percent. Unfortunately, time did not permit a more extended series of observations; but as far as our data go, they support our results on Mt. Evans (3900 m)[3] as indicating a real difference between daytime and nighttime cosmic radiation, which is greater at the higher altitudes.

Steinke has noted[4] bursts of ionization, representing of the order of 10^6 ion pairs, occurring in his cosmic-ray ionization chamber at the rate of two or three per day. During the course of our measurements we have observed 8 or 9 ionization bursts of this type under such conditions that we have been able to check immediately the condition of the apparatus to see that the effect was not due to any instrumental defect. In these cases the sudden ionization current corresponded to the liberation of from 3 to 7×10^6 ion pairs in the individual bursts. Taking 30 electron-volts as necessary on the average to produce an ion pair in argon, this represents a sudden liberation within the chamber of from 0.9 to 2×10^8 electron-volts of energy. It would seem that these bursts of ionization are much more frequent at high than at low altitudes, for we have not noticed any when lower than 1300 meters, whereas on top of El Misti two were noted within half an hour of each other.

Steinke's suggestion of a high speed proton traversing the chamber could not account for more than 10 percent of the current observed in our chamber. It would seem rather that there must occur a shower of ionizing particles, as from a violently bursting nucleus, within the gas of the ionization chamber. The increasing frequency of these events at high altitudes suggests further that these nuclear disintegrations are excited by the less penetrating component of the cosmic rays.

It is a pleasure to acknowledge the cordial cooperation in this work of Professor Von Willer at Sydney, Professor Parnell at Brisbane, Professor Burbidge at Auckland, Captain Gaskell of the S.S. Mataroa, Mr. James Zetek and Dr. Robert Enders at Panama, and especially of Mr. Paul Ledig and Dr. J. C. Cairns of the Carnegie Magnetic Observatory at Huancayo, who gave most helpful assistance with the measurements in Peru. The work is being done by the help of a grant from the Carnegie Foundation.

ARTHUR H. COMPTON

University of Chicago,
at present, Panama,
August 1, 1932.

[2] Millikan, Nature, Oct. 24 (1931).

[3] Bennett, Stearns and Compton, Phys. Rev. **41**, 119 (1932).

[4] Steinke, Phys. Zeits. **31**, 1019 (1930); Zeits. f. Physik **72**, 115 (1932).

Diurnal Variation of Cosmic Rays and Terrestrial Magnetism

Quite recently A. H. Compton[1] and Bennett, Stearns and Compton[2] have secured data showing that the intensity of the softer components of the penetrating radiation increase with magnetic latitude and with the altitude of the sun above the horizon. They suggest that the variation with latitude results from the ionic nature of the ionizing ray. Indeed, this is just what one would conclude from the expansion chamber experiments which show tracks corresponding to ionic energies of 10^9 electron volts and these would be greatly deflected by the earth's magnetic field. It is the purpose of this note to point out that the diurnal variation of the cosmic-ray intensity is a necessary consequence of the newly demonstrated deflectibility of the ionizing particles by the earth's magnetic field.

The observed variation of cosmic-ray intensity with latitude shows that the intensity is quite sensitive to the magnitude and the direction of the earth's magnetic field. Thus since the earth's magnetism is subject to a large diurnal variation we should expect a reflected variation in the cosmic-ray intensity.

We have shown that diamagnetism in the ionized regions of the high atmosphere distorts the earth's magnetic field in much the same way as the solar magnetic field is distorted, except the distortion is much less and is confined pretty much to the sunlit side of the earth. This diurnal distortion decreases the magnetic field above 200 km by 0.1 percent or more in noonday regions so that the cosmic rays (or perhaps, more precisely, the secondary rays) are less deflected and produce locally more intense ionization at low levels. Qualitatively the observed diurnal variation is about what we would infer from the way that the ionization changes with latitude.

Thus it does not seem necessary to suppose that the sun is a weak source of penetrating radiation or that space in the direction of the sun has special properties.

Perhaps, we should point out finally that the asymmetry of the earth's magnetic field will introduce variations of the cosmic-ray intensity with longitude and with the time of year.

Ross Gunn
Naval Research Laboratory,
Washington, D. C.,
August 1, 1932.

[1] A. H. Compton, Phys. Rev. **41**, 111 (1932).

[2] Bennett, Stearns and Compton, Phys. Rev. **41**, 119 (1932).

The Spin of the Neutron

From some of the recent information reported about neutrons it seems possible to find out whether the neutron has a spin and if so what its value is. In order to do this it is necessary to make several assumptions about the structures of light nuclei: (1) They are built as far as possible out of alpha-particles. (2) The nuclear spin is determined from the spin of its component spins alone. (3) From the evidence that neutrons may be obtained from Li, it is assumed that at least one of the isotopes contains a neutron in its nucleus. (4) The possibilities considered for the spins of the various particles in the nucleus are proton 0, $\frac{1}{2}$; neutron 0, $\frac{1}{2}$, 1; electron 0, $\frac{1}{2}$; alpha-particle 0. The first assumption is one commonly made and is supported by studies on the artificial disintegration of the light elements. The second assumption seems reasonable for the light elements in view of what is known about their nuclear moments. (If orbital moments quantized to integer values are assumed for the nucleus, deductions about whether the nuclear moment should be integer or half integer are not disturbed but those utilizing the actual value are.)

The spin of the free proton is determined from hydrogen to be $\frac{1}{2}$ and that of the extranuclear electron is well known to be also $\frac{1}{2}$ but the possibility of both of these losing their spin in a nucleus should not be overlooked. The various possibilities given above will be divided into two groups for which the proton spin is considered to be 0 and $\frac{1}{2}$ respectively.

As nuclei on which to try these various possibilities the two isotopes of Li, and N^{14} are considered. Curie and Joliot[1] have recently discovered that the highly penetrating radiation emitted from lithium when it is bombarded with alpha-particles from polonium consists of neutrons. They are similar to the particles emitted by Be and B recently dis-

[1] Curie and Joliot, Nature **130**, 57 (1932).

cussed by Chadwick,[2] though having less energy. It thus seems probable that one of the two isotopes of lithium contains a neutron. Under the above assumptions we have the following possibilities for the structure of Li^6, Li^7 and N^{14}:

Li^6	(A)	$1\alpha+2p+1e$
	(B)	$1\alpha+1p+1n$
Li^7	(C)	$1\alpha+3p+2e$
	(D)	$1\alpha+2p+1n+1e$
	(E)	$1\alpha+1p+2n$
N^{14}	(F)	$3\alpha+2p+1e$
	(G)	$3\alpha+1p+1n$.

Let us first consider that the proton has zero spin when it is a part of a complex nucleus. Let us denote the spin of the proton, electron, and neutron by s_p, s_e, and s_n, respectively. The possible resultants may be presented in Table I.

The Li^7 nucleus is known to have a resultant moment of $1\frac{1}{2}$. This possibility appears only once in the table and to obtain it s_e must be $\frac{1}{2}$ and $s_n=1$. These same conditions however for Li^6, give a resultant of either $\frac{1}{2}$ or 1 and it is known that the resultant moment is 0. This contradiction means that the spin of the nuclear proton must not be 0.

Let us now consider that the proton has spin $\frac{1}{2}$ in the nucleus. The possible resultant spins for Li^6, Li^7, and N^{14}, may be presented in Table II.

Using the facts that the resultant nuclear spins of Li^6, Li^7, and N^{14} are 0, $1\frac{1}{2}$ and 1, respectively, one sees that if $s_n=0$ then s_e must be 0 and hence neither Li^6, Li^7, or N^{14} may contain a neutron. But since we consider the fact that neutrons are observed from lithium to indicate that they are present in the nucleus of either or both Li^6 and Li^7, this is not possible and the neutron must have a spin. If $s_n=1$ then s_e must be 0 and cases A, C, E, and G satisfy the requirements. If $s_n=\frac{1}{2}$, then s_e may be either 0 (all cases acceptable) or $\frac{1}{2}$ (B, C, E, and G acceptable).

Three possibilities remain:

I $s_p=\frac{1}{2}$, $s_n=\frac{1}{2}$, $s_e=0$
II $s_p=\frac{1}{2}$, $s_n=\frac{1}{2}$, $s_e=\frac{1}{2}$
III $s_p=\frac{1}{2}$, $s_n=1$, $s_e=0$.

If $s_n=\frac{1}{2}$ and $s_e=\frac{1}{2}$ then Li^6 must contain a neutron. If this neutron is the one which is dislodged by bombardment with alpha-particles then either with or without capture of the alpha-particle the products give isotopes which are not known and which in addition belong to a class of which an isotope has never been found to exist, namely with more than twice as many protons as electrons:

$$Li^6+He^4=n_1+B^9$$
$$Li^6+He^4=n_1+Li^5+He^4.$$

Of course there could be complete disintegration but it is doubtful whether this would furnish sufficient energy to eject the neutron. Also if $s_n=\frac{1}{2}$ and $s_e=\frac{1}{2}$, N^{14} must contain a neutron but there is no evidence for this though there is ample evidence that it disintegrates with the emission of a proton when bombarded with alpha-particles. Finally, if $s_e=\frac{1}{2}$ then it must be assumed that its magnetic moment is diminished to about 0.001th the value which it has for an extra-nuclear electron to account for the small size of hyperfine structure separations. This all seems improbable.

Consider the possibility $s_n=1$ and $s_e=0$. There are over fifteen isotopes of various ele-

TABLE I.

Nucleus	Case	Structure			$s_e=0$			$s_e=\frac{1}{2}$		
		p	n	e	$s_n=0$	$s_n=\frac{1}{2}$	$s_n=1$	$s_n=0$	$s_n=\frac{1}{2}$	$s_n=1$
Li^6	A	2	0	1	0	0	0	$\frac{1}{2}$	$\frac{1}{2}$	$\frac{1}{2}$
	B	1	1	0	0	$\frac{1}{2}$	1	0	$\frac{1}{2}$	1
Li^7	C	3	0	2	0	0	0	0, 1	0, 1	0, 1
	D	2	1	1	0	$\frac{1}{2}$	1	$\frac{1}{2}$	0, 1	$\frac{1}{2}$, $1\frac{1}{2}$
	E	1	2	0	0	0, 1	0, 2	0	0, 1	0, 2

[2] J. Chadwick, Proc. Roy. Soc. **A136**, 692 (1932).

TABLE II.

Nucleus	Case	Structure			$s_e=0$			$s_e=\frac{1}{2}$		
		p	n	e	$s_n=0$	$s_n=\frac{1}{2}$	$s_n=1$	$s_n=0$	$s_n=\frac{1}{2}$	$s_n=1$
Li^6	A	2	0	1	0, 1	0, 1	0, 1	$\frac{1}{2}, 1\frac{1}{2}$	$\frac{1}{2}, 1\frac{1}{2}$	$\frac{1}{2}, 1\frac{1}{2}$
	B	1	1	0	$\frac{1}{2}$	0, 1	$\frac{1}{2}, 1\frac{1}{2}$	$\frac{1}{2}$	0, 1	$\frac{1}{2}, 1\frac{1}{2}$
Li^7	C	3	0	2	$\frac{1}{2}, 1\frac{1}{2}$	$\frac{1}{2}, 1\frac{1}{2}$	$\frac{1}{2}, 1\frac{1}{2}$	$\frac{1}{2}, 1\frac{1}{2}, 2\frac{1}{2}$	$\frac{1}{2}, 1\frac{1}{2}, 2\frac{1}{2}$	$\frac{1}{2}, 1\frac{1}{2}, 2\frac{1}{2}$
	D	2	1	1	0, 1	$\frac{1}{2}, 1\frac{1}{2}$	0, 1, 2	$\frac{1}{2}, 1\frac{1}{2}$	0, 1, 2	$\frac{1}{2}, 1\frac{1}{2}, 2\frac{1}{2}$
	E	1	2	0	$\frac{1}{2}$	$\frac{1}{2}, 1\frac{1}{2}$	$\frac{1}{2}, 1\frac{1}{2}, 2\frac{1}{2}$	$\frac{1}{2}$	$\frac{1}{2}, 1\frac{1}{2}$	$\frac{1}{2}, 1\frac{1}{2}, 2\frac{1}{2}$
N^{14}	F	2	0	1	0, 1	0, 1	0, 1	$\frac{1}{2}, 1\frac{1}{2}$	$\frac{1}{2}, 1\frac{1}{2}$	$\frac{1}{2}, 1\frac{1}{2}$
	G	1	1	0	$\frac{1}{2}$	0, 1	$\frac{1}{2}, 1\frac{1}{2}$	$\frac{1}{2}$	0, 1	$\frac{1}{2}, 1\frac{1}{2}$

ments which have odd mass numbers and odd nuclear moments which are quite certain. If $s_n=1$, then neutrons can exist in the nuclei of any of these only in pairs, which seems to be a peculiar limitation.

The possibility $s_n=\frac{1}{2}$, $s_e=0$, meets with none of these objections as far as is known. In addition it is more satisfying than either of the other two possibilities if one thinks of the neutron as composed of a proton and an electron in some way, since II, which gives both electron and proton a spin of $\frac{1}{2}$ in the nucleus, would require one or the other to lose its spin in the neutron and III, which gives only the proton a spin, would require both to have spin in the neutron.

One may conclude that, under the assumptions mentioned at first, the neutron must have a spin and that the proton must have a spin of $\frac{1}{2}$ in the nucleus. Of the three possibilities which present themselves the case with $s_p=\frac{1}{2}$, $s_n=\frac{1}{2}$, and $s_e=0$ seems most probable.

R. F. BACHER[3]
E. U. CONDON

Massachusetts Institute of Technology,
August 4, 1932.

[3] National Research Fellow.

Electron Affinity of Hydrogen

From simple Bohr theory one calculates the electron affinity of the hydrogen atom to be 1.69 electron-volts which must be too large in the same way that the ionization potential of helium so calculated is 28.5 electron-volts as compared with the experimental value of 24.47 volts. Pauling[1] thought to improve the calculation of the electron affinity of hydrogen by determining the screening-constant for a two electron system from the Known ionization potential of helium. He however found hydride ion unstable (−0.08 volts). Lately the ionization potentials of Li^+ and Be^{++} have been determined spectroscopically by Edlin and Ericson[2] to be 75.28 and 153.15 electron-volts respectively. It is then possible to find the variation of screening constant (s) with atomic number (Z) and to interpolate S for hydride ion. The empirically determined *electron affinity of hydrogen is found to be* +0.66 *electron-volts.* Bartlett[3] assumes a linear relation between the square root of the ionization potential of He, Li^+, Be^{++} and their atomic numbers and finds by extrapolation +1.4 electron-volts. Hylleraas[4] calculates the electron affinity of hydrogen from wave mechanics to be +0.715 electron-volts.

Atom	S	Ioniz. potential
Bohr	0.2500	
H^-	(0.2780)	(0.66)
He	0.2961	24.47
Li^+	0.3020	75.28
Be^{++}	0.3047	153.15

GEORGE GLOCKLER
University of Minnesota,
August 5, 1932.

[1] L. Pauling, Phys. Rev. **29**, 285 (1927).

[2] B. Edlin and A. Ericson, Nature **124**, 688 (1929).

[3] J. H. Bartlett, Jr., Nature **125**, 459 (1930).

[4] E. A. Hylleraas, Zeits. f. Physik **65**, 209 (1930).

Equilibrium between Positive Ions and Neutral Atoms in Positive Rays of the Rare Gases

It has been shown by several experimenters that the particles in a positive ray beam may gain or lose electrons in passage through a gas at low pressure without appreciable change of velocity or direction. Rutherford[1] and Henderson[2] have found that in an α-ray beam an equilibrium is established between doubly charged and singly charged particles at high velocities but that at lower velocities the equilibrium shifts to one between singly charged and neutral particles with the fraction of neutral atoms increasing with decreasing velocity. Friedersdorff[3] found that the arc lines of argon do not show a Doppler shift in an end on spectrogram of the positive ray beam, at least, for accelerating voltages less than 30,000 volts; Romig[4] got the same result with neon. Miss McPherson,[5] using quite a different method of excitation, obtains agreement with this conclusion. It has been suggested that this indicates that at the voltages used (of the order of 20,000 volts) the moving particles are predominantly positive, as in high velocity α-rays, rarely becoming neutral and, therefore, emitting the shifted arc lines with inappreciable intensity. In order to check this suggestion directly, Rudnick's work[6] with helium has been extended to neon, argon, and krypton over the velocity range from 10,000 to 22,000 volts. Contrary to expectations, with neon the equilibrium was established with the beam approximately 87 percent neutral at 13,000 volts, this value changing to 85 percent at 22,000 volts. In argon the fraction of neutral atoms changed from 94 to 92 percent as the accelerating potential was increased from 10,000 to 22,000 volts. At all velocities in the range from 13,000 to 22,000 volts the krypton beam was approximately 95 percent neutral. Readings as low as 7000 and as high as 25,000 volts indicated no large changes in the neutral fraction. In agreement with Henderson's and Rudnick's work, the percentage of neutral atoms in the beam in the equilibrium condition decreased with increasing velocity in the case of neon and argon. The behavior of krypton was peculiar in this respect, the fraction of neutral atoms apparently increasing with increasing velocity, but the change was so small (about half of one percent) as to be uncertain.

It might be pointed out that in the present work the velocity of the ions was smaller than in Henderson's experiments so that at higher velocities it is quite possible that the beam might remain predominantly positive since the equilibrium shifted in that direction but the results obtained do appear to rule out the suggested explanation of the absence of arc lines in the Doppler effect observations since the same velocity range was investigated in the two cases.

Complete results, including measurements of the free paths of the positive ions and neutral atoms, will be published shortly.

HAROLD F. BATHO

Ryerson Physical Laboratory,
University of Chicago,
August 5, 1932.

[1] E. Rutherford, Phil. Mag. **47**, 277 (1924).

[2] G. H. Henderson, Proc. Roy. Soc. **A109**, 157 (1925).

[3] K. Friedersdorff, Ann. d. Physik **47**, 737 (1915).

[4] W. Romig, Phys. Rev. **38**, 1709 (1931).

[5] A. I. McPherson, Phys. Rev. **41**, 686 (1932).

[6] P. Rudnick, Phys. Rev. **38**, 1342 (1931).

Radiation from Moving Helium, Neon and Argon Ions

Dempster and Batho[1] report obtaining a beam of hydrogen ions of homogenous velocity; the ions were formed in a low-voltage arc, and were accelerated in passage through perforated electrodes maintained at a high-potential difference, of the order of 20,000 volts.

This method has been extended to study some of the rare gases. In the spectrum of such a beam of positive rays observed end on, some lines show the Doppler effect; that is, each such line is accompanied by an additional sharp line displaced toward the higher frequencies by an amount agreeing well with that expected from the velocity of a singly charged ion which had fallen through the applied field.

In argon, only the spark (blue) lines showed

[1] Dempster and Batho, Astrophysical Journal, January, 1932.

the Doppler effect, the displaced lines emitted by the moving ions being in intensity and sharpness comparable to the undisplaced lines excited in the gas at rest. The arc (red) lines were relatively weak, and showed no Doppler effect; the neutral particles in the beam were evidently not excited to emission by collisions. Experiments by Batho[2] indicate such a beam in argon to consist of at least 90 percent neutrals. The single sharp displaced Doppler line does not bear out the observation of earlier workers, who found in their diffuse displaced Doppler strip several maxima, apparently corresponding to ions with multiple charges, in some cases in the red spectrum as well as the blue.

In neon, the arc spectrum was not excited, the lines of the first spark spectrum were intense and showed the Doppler effect strongly. In the recent experiments of Romig[3] the manner of excitation was different; the arc lines appeared but with no Doppler effect. Batho finds such a beam of neon particles to consist of at least 85 percent neutrals.

In helium, lines of the arc spectrum and the spark line 4686 show a Doppler effect. Most of the displaced lines are relatively less intense than those of argon or neon, and vary more in intensity relative to the undisplaced line. The displaced and the undisplaced spark line 4686 are of approximately equal intensity. The spark line 4541 of the "Pickering" series is excited in the gas at rest, but as it shows no displaced line, is evidently not emitted by the moving helium particles in the beam.

It is of interest to give a preliminary restatement in terms of the atomic phenomena at a collision. At these velocities a collision involves the complete interpenetration of the electron systems. During the process electron transitions to other molecular states may occur so that when the two nuclei separate, they are accompanied by new electron arrangements. In neon, neutral atoms emerge from a collision always in an unexcited state, the neutrals left behind are also unexcited, while positive atoms emerge or are left in an excited state. With the velocity used the positive helium atom may emerge from a collision in the 4-quantum excited state but not in the 9-quantum excited state.

A. I. McPherson

Ryerson Physical Laboratory,
University of Chicago,
August 5, 1932.

[2] Batho, Phys. Rev. **41**, 686 (1932).
[3] Romig, Phys. Rev. **38**, 1709–1715 (1931).

Some Evidence Indicating a Removal of Positive Ions from Cold Surfaces by Electric Fields

It has been clearly demonstrated that the discharge produced between two plane or spherical electrodes in high vacua, when a sudden electrical potential is applied across them is started by the field electron current from the cold cathode.[1,2,3] The electric field necessary to produce a field current from the cathode of sufficient magnitude to start the discharge in a few microseconds, although found to be somewhat variable and to depend upon the metal and its previous treatment, is of the order of magnitude of a half million volts per cm. For some time, as an auxiliary to an investigation of the initiation of discharges in ion free gases,[4] the writer has been experimenting in high vacua with point and plane (as well as wire and cylinder) electrodes. It was hoped that by making the point (or wire) positive, to increase the applied potential for a given electrode spacing until electrons were pulled out of the plane or cylindrical cathode by the field in sufficient number to start the discharge. This was found, probably to be the case when the point (or wire) is of properly treated tungsten, for example, and free from impurities on its surface. However, when the point (or wire) is not free from impurities (especially the alkali metals) it is believed that this is no longer always true.

In the first experiments a tungsten point was placed opposite a polished nickel plane in a high vacuum. The plane was grounded through a variable non-inductive resistance, and positive electrical surge potentials were applied to the point for a time whose order of magnitude was 10^{-6} sec. (time constant of circuit was 1.5×10^{-6} sec.). This time was held

[1] R. W. Wood, Phys. Rev. [1] **5**, 1 (1897).
[2] Hull and Burger, Phys. Rev. **31**, 1121 (1928).
[3] L. B. Snoddy, Phys. Rev. **37**, 1678 (1931).
[4] Street and Beams, Phys. Rev. **38**, 416 (1931).

constant throughout all the experiments here described. This resistance (a portion of which was shunted by a neon tube) served to protect the point when the discharge was once initiated, yet was low enough to allow a small luminous spot to form on the point when the discharge occurred. The point was either measured or photographed after each discharge so that the form factor could always be obtained. If the point and plane were untreated, i.e., merely mounted in the tube and the air pumped out, it was found that the discharge would take place when the field at the point reached only from five to ten million volts per cm. However if the point and plane were baked out and several discharges allowed to take place the field at the anode necessary to produce discharge was increased many times and exceeded fifty million volts per cm for tunsten points. If then the point and plane were allowed to stand over night in 0.01 mm of air pressure with the solid CO_2 removed from the traps, the next morning, upon pumping, out, the positive field at the point necessary to produce discharge was usually lowered by a large amount. Caesium distilled into the tube also reduced the fields at the point necessary to produce discharges. A one mil tungsten wire was then mounted along the axis of a polished steel cylinder of 8 mm internal diameter. The wire was grounded and negative surge potentials were applied to the cylinder. The electrical connections were the same as in the case of the point and plane. The results were similar to those obtained with tungsten points. If the wire was heated almost to the melting point for a few seconds in the presence of commercial hydrogen at a pressure of about one cm, then allowed to cool and the hydrogen pumped out, the field at the surface of the wire necessary to produce discharge was definitely lowered. In the case of a one mil thoriated tungsten wire mounted along the axis of an 8 mm steel cylinder and treated to bring thorium to its surface the field necessary to produce discharges was lower than in the case of the treated pure tungsten wire first mentioned.

As the electrodes were in high vacua and the potential applied for only about 10^{-6} sec. the residual gas could not have been effective in starting the discharge. The discharge must then have been initiated by electrons pulled out of the plane (or cylinder), electrons, negative ions or positive ions pulled off the glass surface, or positive ions pulled off the surface of the point (or wire) by the electric field, or else a combination of these. In the case of the wire and cylinder, discharges occurred when the field at the surface of the cylinder (assuming the surface of the cylinder smooth) was less than twenty-five thousand volts per cm so that electrons pulled out of the cathode could not have started the discharge. Hence the discharges must have been initiated either by ions and electrons pulled off of the glass surface or positive ions pulled off of the surface of the anode by the electric field. Several attempts were made to separate these two effects but always without complete success. However, in some of the experiments the complete initiation of the discharge by ions and electrons coming from the glass surface was rendered unlikely by the arrangement of the electrode potentials by shielding and by the geometry of the glass tube. Therefore, it is believed that in these cases the discharge was started by the positive ions pulled off the surface of the positive point or wire by the field. This explanation is also supported by the fact that the magnitude of the fields necessary to start the discharge depended upon the previous treatment of the wire anode. It is believed by several investigators[5] that adsorbed alkali ions (Becker's "adions" for example) can exist on the surface of tungsten since the work function of tungsten is greater than the ionization potential of many of the alkalis. Also, it is thought that these adsorbed ions can exist on tungsten oxide. Hence the positive ions that are believed to be pulled off of the anode by the field in the above experiments are probably alkali ions. The experiments are being continued and it is hoped that a detailed paper can be published later.

J. W. BEAMS

University of Virginia,
August 6, 1932.

[5] Compton and Langmuir, Rev. Mod. Phys. 2, 124 (1930); Dushman, Rev. Mod. Phys. 2, 381 (1930).

The Reflecting and Resolving Power of Calcite for X-Rays

The writer has recently published the results of a research in which experimental values of the coefficient of reflection of calcite in a range from 0.2 to 2.3A, as obtained in the

$(1,-1)$ position of a double x-ray spectrometer are compared with calculated values from theories of diffraction by a perfect crystal.[1] In this issue of the Physical Review, Mr. L. G. Parratt[2] reports experiments performed in the author's laboratory which extend the wave-length range investigated to 5A. This extended range includes the K critical absorption wave-length of calcium at 3.06A. In order to compare the results of Mr. Parratt's work with the diffraction equation of Prins[3] a large extension of the laborious calculations of the author's paper was necessary, and certain approximations, sufficiently accurate in the shorter wave-length range, could not be retained. In particular, it has been found that the method which was used by the author in allowing for the polarization is not correct when applied to Prins' equation, although in accord with the earlier treatment of Darwin.[4] The purpose of this letter is to point out some of the modifications necessary in the author's previous treatment of the calculations.

Choice of an angular unit for the purpose of describing the diffraction pattern. In the author's previous work the angular unit chosen was the angular range over which, on Darwin's equations, 100 percent reflection would result. This unit is not merely a function of the wave-length, but changes with the polarization, also depending in size on the particular structure factor assumed. In view of these undesireable features, in Mr. Parratt's work the unit of angular deviation has been made $(\theta-\theta_0)$, where

$$\theta-\theta_0=\delta \sec\theta_0 \operatorname{cosec}\theta_0.$$

For a given crystal this is a function of wave-length only.

Calculation of the amplitude scattered from the unit cell. The quantity $D+iB$ which appears in Eq. (15) of the author's paper is fundamental to the calculation of the diffraction pattern and is proportional to the amplitude of the wave scattered from the unit cell of the crystal. In the previous paper an approximation (Eq. (17)) was made in the calculation of $D+iB$ which involved setting the fraction of the incident beam absorbed by an atom in the cell proportional to the fraction of the total number of electrons in the cell contained in the atom in question. Obviously this assumption is far from correct for wave-lengths shorter than the K limit of calcium, for in this region the K electrons of calcium absorb far more efficiently than do the other, more lightly bound, electrons in the unit cell. In the calculations in Mr. Parratt's paper no such approximation has been made, the absorption of each atom being calculated from tables of atomic absorption coefficients.

Another factor entering the computation of $D+iB$ is the ratio of the amplitude scattered by an atom of the unit cell at angle $2\theta_0$ to that scattered in the forward direction. In the author's paper, these values were obtained from a table of atomic structure factors published by Bragg and West.[5] In the newer calculations, these ratios were obtained from structure factor tables published by James and Brindley,[6] and Pauling and Sherman.[7] These newer atomic structure factors alone have the effect of making the quantity $D+iB$ about 6 percent greater for the same wave-length than obtained previously by the author.

The effect of polarization. The method which was adopted by the author to take account of polarization in Prins' equation is only strictly applicable to the limiting case of short wave-length and correspondingly small glancing angle in which Prins' equation and Darwin's are indistinguishable. (To the accuracy of the present experiments this occurs at about 0.7A.) For longer wave-lengths no such formula as Eq. (33) of the author's paper can be considered sufficiently accurate, and each polarized component of the incident beam must be completely worked out, as expressed in Eq. (11) of Mr. Parratt's paper. This considerably increases the labor of calculations but up to the present no method of shortening it has been devised. In the author's paper it was stated that the percent reflection (P_0) is independent of polarization. This is incorrect on Prins' calculations, but correct in Darwin's theory. This question of the polarization cal-

[1] S. K. Allison, Phys. Rev. **41**, 1 (1932).
[2] Parratt, Phys. Rev. 41, 561 (1932).
[3] Prins, Zeits. f. Physik **63**, 477 (1930).
[4] Darwin, Phil. Mag. **27**, 325 and 675 (1914).
[5] Bragg and West, Zeits. f. Krist. **69**, 118 (1928).
[6] James and Brindley, Phil. Mag. **12**, 81 (1931).
[7] Pauling and Sherman, Zeits. f. Krist. **81**, 1 (1932).

TABLE I.

	Calculated		Observed	
Cu $K\alpha_1$, 1.54A	Allison	Parratt	Allison	Parratt
Half width at half max. (w)	4.7″	4.9″	4.9″	5.0″
Percent reflection (P_0)	68%	69%	62%	60%
Coefficient of reflect. (R)	3.49×10^{-5}	3.82	3.46	3.80
Cr $K\alpha_1$, 2.28A				
Half width at half max. (w)	6.9″	7.5″	7.1″	7.4″
Percent reflection (P_0)	56%	58%	55%	51%
Coefficient of reflect. (R)	4.53×10^{-5}	4.84	4.68	4.79

culations is also discussed in reference 9 of Mr. Parratt's paper. The difference between the new and old calculations for two wave-lengths is expressed in Table I. The "observed" values of Allison were obtained on calcites III, those of Parratt on calcites II.

SAMUEL K. ALLISON
University of Chicago,
August 13, 1932.

The Variation of the Cosmic-Ray Intensity with Azimuth

We have measured the intensity of the cosmic rays at an angle of 30° with the vertical in the magnetic N, S, E, and W azimuths using three G. M. counters as a telescope. The point of observation was the roof of the Bartol Laboratory in Swarthmore, Pennsylvania, latitude 40° N. The apparatus was protected from the weather by a covering of $\frac{1}{2}$ mm thick sheet iron but was not otherwise influenced by absorbing material. The three counter tubes were arranged with their axes horizontal and perpendicular to the direction of observation. They were 12 cm long, 4 cm in diameter and were spaced at 10 cm between adjacent centers. The circuits were arranged for recording triple coincidences and a previous observation had shown that the number of accidental coincidences was less than 0.1 percent of the real ones at this separation. Our results up to the present time are given in Table I with the statistical probable errors indicated. The barometric pressure at the middle of each run is also included.

TABLE I.

Direction	Date	Duration of run, minutes	Barometer	Number of coincidences	Coincidences per minute
E	7–21	1040	759	939	0.90 ± 0.02
W	7–22	1380	756	1253	0.90 ± 0.02
N	7–23	1495	754	1445	0.97 ± 0.02
S	7–24	1370	760	1373	1.00 ± 0.02
E	7–25	1447	762	1207	0.83 ± 0.02
W	7–26	1418	760	1175	0.83 ± 0.02
N	7–27	1432	760	1244	0.87 ± 0.02

The results show that the intensity is about the same in the E and W azimuths but the cosmic rays are from 5 to 10 percent more intense in the magnetic meridian than perpendicular to it. There is possibly a greater intensity towards the S than towards the N. Unfortunately the data show a variation of the counting rate with time which is probably instrumental but we believe the variation with azimuth cannot be accounted for in this way. These measurements are preliminary to a more complete investigation which is now in progress.

We wish to acknowledge the cooperation of Dr. E. C. Stevenson.

THOMAS H. JOHNSON
J. C. STREET

The Bartol Research Foundation
of the Franklin Institute,
August 13, 1932.

BOOK REVIEW

Architectural Acoustics. VERN O. KNUDSEN. Pp. 617+viii, Figs. 272. John Wiley and Sons, Inc., New York. Price $6.50.

The last ten years have seen a marked increase of interest in the subject of acoustics in general. This has been evidenced by the appearance of a number of texts on sound, and of numerous papers dealing with problems in this field. Among these, the behavior and control of sound in buildings has claimed no small share of interest. The author of this book has been a tireless and fruitful worker in this field. Both from his own investigations and his active participation in the stimulation and organization of acoustical research, he is well qualified for the task of putting into comprehensive and permanent form the considerable volume of material that has recently become available.

This book is intended primarily as a reference work for architects, builders, and others interested in the design or construction of buildings. In order to facilitate its use as a text, a number of problems and exercises have been included in an apprendix. The treatment throughout is descriptive rather than analytical. Formal mathematical derivation of the fundamental equations is given however, and considerable space is devoted to the technique of acoustical measurements. The text is copiously illustrated.

The introductory chapters, comprising about one-fifth of the book, deal with the facts of physical and physiological acoustics. To the reader who comes to the subject with only an elementary knowledge of the physics of sound this portion of the book may prove somewhat disappointing. Both in choice and arrangement of material, the treatment may leave the uninitiated still hazy in his fundamental concepts of the mechanics of sound waves. Further, a considerable portion of the chapters devoted to the nature of hearing and speech and music might well have been more briefly covered in view of Fletcher's fuller earlier treatment of these subjects.

The second part of the book concerns itself with the theory and phenomena of sound in inclosed spaces and the transmission of sound by building structures. In the chapter on reverberation, the earlier treatment given by W. C. Sabine is supplemented by the recent work of Schuster, Waetzmann, Norris, and Eyring, as well as the author's own work on the effect of atmospheric absorption and of the shape of a room on the time of reverberation. Various methods for reverberation and absorption measurements are described, and the physical and acoustical properties of many commercial sound absorbents are given in detail. The chapters on sound insulation include a full account of methods of measurement of sound transmission by solid septa, data compiled from various sources on the sound insulating properties of materials and types of construction, and the principles of machine isolation.

The last section of the book is taken up with the application of the principles deduced in the preceding sections to practical problems in building design. Particularly interesting and valuable are the results of the author's own investigations of out of doors hearing conditions. These studies were made in the Hollywood Bowl, a natural amphitheater seating some 25,000 people, and in the Mohave desert under conditions of extreme quiet. Detailed suggestions are made for the acoustical treatment of homes, schools, small theaters, legitimate theaters, sound picture theaters, country churches, village churches, city churches, hospitals, oral English rooms, music rooms, lecture halls, auditoriums, gymnasiums, cafeterias, museums and libraries, office, bank and industrial buildings, concert halls, opera houses, dance halls, radio studios and sound recording rooms.

As is apparent, the thoroughness with which the details of the subject are covered will necessitate judicious selection of material in the use of the book for teaching purposes. As a compendium of present knowledge of the acoustics of buildings, it will be found an extremely useful book of reference for that large and growing group who have to deal with acoustical problems in the design and erection of buildings.

PAUL E. SABINE
Riverbank Laboratories, Geneva, Illinois

CURRENT LITERATURE OF PHYSICS

Extracts from the Tables of Contents of Some of our Contemporaries

PROCEEDINGS OF THE ROYAL SOCIETY

SERIES A, VOL. 137, No. A832 — AUGUST 2, 1932

Bakerian Lecture.—The Combustion of Hydrocarbons. By **W. A. Bone** 243
Velocity of Propagation of Light in Vacuo in a Transverse Magnetic Field. By **C. C. Farr and C. J. Banwell** 275
Growth of Waves on Water due to the Action of Wind. By **the late Sir Thomas Stanton, and D. Marshall and R. Houghton** 283
Argon and Amorphous Carbon, 15° to 710°C. By **M. W. Travers** 294
Intensities of Certain Nebular Lines and the Mean Lives of Atoms Emitting them. By **A. F. Stevenson** 298
Diffraction of Elastic Waves at the Boundaries of a Solid Layer. By **J. H. Jones** 325
Velocity of Corrosion from the Electrochemical Standpoint.—Part II. By **U. R. Evans and T. P. Hoar** 343
On the Absorption Spectrum of Sulphur Trioxide and the Heat of Dissociation of Oxygen. By **A. K. Dutt** 366
Polarization Measurements on Basic Beryllium Acetate and Beryllium Acetylacetonate. By **J. W. Smith and W. R. Angus** 372
Measurement of Pressures Developed in Explosion Waves. By **C. Campbell, W. B. Littler and C. Whitworth** 380
X-Ray Study of Phase Boundaries in Thermal Diagrams of Alloy Systems—Cu-Zn System. By **E. A. Owen and L. Pickup** 397
Study of the System Water-Phenol.—Part I. Densities. By **O. R. Howell** 418
Modified Method of Counting Particles. By **L. H. C. Tippett** 434
Collision of α-particles with Atomic Nuclei. By **H. S. W. Massey** 447
Surface Ionization of Potassium by Tungsten. By **P. B. Moon and M. L. E. Oliphant** .. 463

PHILOSOPHICAL MAGAZINE

VOL. 13, No. 88 — JUNE, 1932

On the Variation of the Resistance of Thermionic Valves at High Frequencies. By **S. K. Mitra and Bhabani Charan Sil** 1081
Damping of Pendulums Immersed in a Viscous Fluid. By **E. Tyler** 1099
Graphic Computation of Solar Altitude. By **A. F. Dufton** 1128
Entropy, Strain and the Pauli Exclusion Principle. By **W. S. Kimball and G. Berry** 1131
Operational Calculus.—Part II. The Valves of Certain Integrals and the Relationships between Various Polynomials and Series Obtained by Operational Methods. By **H. V. Lowry** 1144
Hume-Rothery Relationship between the Ionization Potentials of the Elements and their Atomic Number. By **H. Yagoda** 1163
Photoelectric Properties of Films of Beryllium, Aluminum, Magnesium and Thalium. By **H. de Laszlo** 1171
Discharges Maintained by Electrical Oscillations in Solenoids. By **G. D. Yarnold** 1179
Similitude and the Heatflow through a Granulated Material. By **O. A. Saunders** 1186
Note on the Electrocapillary Effect of Capillary-Active Organic Molecules. By **A. W. Davis** 1188
Dielectric Constant of Nitrogen up to 150 Atmospheres at 25°, 75° and 125°C. By **A. and C. Michels** 1192
On the Superconductivity of Alloys containing Gold and Silver. By **J. C. McLennan, J. F. Allen and J. O. Wilhelm** 1196

Second Series *September 15, 1932* *Vol. 41, No. 6*

THE
PHYSICAL REVIEW

The Faraday Effect with X-Rays

By DAROL K. FROMAN
Physics Laboratory, Macdonald College, McGill University

(Received July 19, 1932)

Voigt's theory for the rotation of the plane of polarization of light by a magnetic field is discussed and one of the equations used by W. Kartschagin and E. Tschetwerikowa who investigated the Faraday effect with x-rays transmitted through ferromagnetic materials, is shown to be inapplicable. The theory for the effect given by Drude is modified for the case of x-ray wave-lengths giving a rotation of $\chi = -2\pi\mu eIL/mc^2$ radians. μ is the refractive index, I is the intensity of magnetization, l the thickness of the material through wich the x-rays are transmitted. The other quantities have their usual meanings. Kartschagin and Tschetwerikowa found evidence suggesting a rotation in the case of x-rays. An experiment was performed which confirmed these suggestions and which checked the equation for χ given above well within the experimental error. The experimental error was large, but a rotation of the order of 10° was shown to occur for x-rays of wave-length 0.3A transmitted through 0.05 cm of iron in a field of 300 gauss.

INTRODUCTION

THE Faraday effect with x-rays has been studied by Kartschagin and Tschetwerikowa[1] using paraffin and iron in the magnetic field to produce a rotation of the plane of polarization. Their results were negative in the case of paraffin, but in the case of iron they say that their experimental results do not entirely justify the conclusion that a rotation exists but indicate a rotation of about 10°. They used iron of effective thickness about 0.01 cm in a magnetic field of 750 gauss. They compared their experimental results with Voigt's[2] theory which, under their experimental conditions, predicted a rotation of only 4′.

It is the purpose of this paper to discuss the applicability of Voigt's equation to paramagnetic materials; to modify the theory of Drude[3] for x-ray frequencies; to describe an experimental investigation on iron, indicating the differences between the method used and that of Kartschagin and Tschetwerikowa; and to compare the experimental results with the predictions of the two theories.

[1] W. Kartschagin and E. Tschetwerikowa, Zeits. f. Physik **39**, 886 (1926).

[2] W. Voigt, *Magneto- und Elektrooptik*, p. 130. Much of the fundamental work of this theory is due to H. Becquerel, C. R. **125**, 679 (1897).

[3] P. Drude, *The Theory of Optics*, Ch. VII.

Applicability of Voigt's Equation

On the basis of the electromagnetic theory Voigt deduces an equation for the rotation, χ, of the plane of polarization of light traversing a distance l of a material in the direction of an applied magnetic field of strength R_0, *viz:*

$$\chi = \lambda l R_0 e/mc^2 \cdot d\mu/d\lambda \tag{1}$$

where e, m, c and λ have their usual meanings and μ is the refractive index of the material. All quantities are in the C.G.S. system. This equation is not applicable to ferromagnetic materials since it is well known[4] that in this case χ is proportional to the intensity of magnetization and not to the magnetic field strength. Voigt himself points this out.[5] It does not suffice to substitute for R_0 the field produced by the magnetization alone, i.e., $4\pi I$ where I is the intensity of magnetization, since Eq. (1) is deduced on the assumption that the equations of motion of an electron in the medium under the action of the incident light and the applied magnetic field are:[6]

$$\begin{aligned} m\ddot{x} + h\dot{x} + kx - (eR_0/c)\cdot\dot{y} &= eX \\ m\ddot{y} + h\dot{y} + ky + (eR_0/c)\cdot\dot{x} &= eY \\ m\ddot{z} + h\dot{z} + kz &= eZ. \end{aligned} \tag{2}$$

In these equations the incident light travels in the direction of the magnetic field, h and k are the friction and elastic constants respectively and the other quantities have their usual meanings. Since eR_0/c cannot be replaced in these equations by $4\pi Ie/c$ it is not permissible to do so in Eq. (1).

As it is not known how to modify the magnetic force factors of Eqs. (2) for paramagnetic materials, the problem is attacked in a different way.

Modification of Drude's Theory for X-Rays

Drude assumes that a material contains rotating ions, electrons, whose magnetic moments may be alined, at least in paramagnetic materials, by the application of a magnetic field. The only effect of the electric field of a light wave is to displace the center of rotation of the electron if the natural frequency of the electron is far removed from that of the incident light. Thus the time rate of change of magnetic flux through a given area is composed of two parts, *viz:* the change which is produced directly by the magnetic vector of the light wave, and the change produced by the motion of the center of rotation of the electron due to the action of the light wave. Drude calculates these quantities and the corresponding current densities and substitutes directly in Maxwell's equations. On this basis he deduces the index of refraction and the rotation of the plane of polarization.

The index of refraction, μ, is given by:

$$\mu^2 = 1 + \sum_h \alpha_h n_h + \sum_k \beta_k n_k \tag{3}$$

[4] P. Drude, reference 3, p. 449.
[5] W. Voigt, reference 2, p. 20.
[6] W. Voigt, reference 2, p. 125.

where the subscripts h and k refer to nonconducting and conducting electrons respectively. n is the number of a particular type of electron per unit volume and α and β are functions of the properties of the medium and the period of the incident light. β is proportional to the square of the period and may be neglected in the case of x-rays since the frequency is very high. This approximation has been shown to be valid by experimental determinations of μ which agree within experimental error with Eq. (3), even for conductors, when β is put equal to zero. In this case h goes from 1 to the total number of different types of electrons present whether conducting or not.

Lorentz[7] also derives an expression for μ, namely:

$$\mu^2 = 1 + e^2/\pi m \cdot \sum_h n_h/(\nu_h^2 - \nu^2) \tag{4}$$

where e and m have their usual values, ν_h is the natural frequency of all of the n_h electrons and ν is the frequency of the incident light. Since the sums in Eqs. (3) and (4) are taken over the same range we can solve for α_h.

$$\alpha_h = e^2/\pi m(\nu_h^2 - \nu^2). \tag{5}$$

Drude also shows that the plane of polarization of plane-polarized light is rotated through an angle, χ, when a beam of light passes through a magnetized substance in a direction parallel to the magnetic field. χ is given by:

$$\chi = f\mu l/2c^2\tau^2 \tag{6}$$

where l is the thickness of the material traversed by the light, c is the velocity of light and $\tau = 2\pi\nu$. By convention χ is positive when the rotation is right-handed to an observer looking in the direction of the field. f is given by the equation

$$f = (1/c) \cdot \sum_h n_h'\alpha_h q_h/T_h + \sum_k n_k'\beta_k q_k/T_k. \tag{7}$$

Drude assumes that an electron of type h moves in an orbit of area q_h with a period T_h. n_h' is the effective number of electrons of this type per unit volume having their magnetic moments parallel to the external magnetic field. It is shown also that the number of lines of magnetic induction per unit area produced by these n_h' electrons is

$$M_h = 4\pi e q_h n_h'/cT_h. \tag{8}$$

The total flux per unit area is

$$4\pi I = \sum_h M_h \tag{9}$$

where I is the intensity of magnetization.

We may neglect the second sum in Eq. (7) as was done in Eq. (3) and combining Eqs. (7) and (8) we get

$$f = \sum_h \alpha_h M_h/4\pi e. \tag{10}$$

[7] H. A. Lorentz, *The Theory of Electrons*, 2nd Ed. p. 149.

It has been shown[8] that for x-rays we can neglect ν_h^2 compared to ν^2. Thus Eq. (4) becomes

$$\left.\begin{aligned} \mu^2 &= 1 - e^2n/\pi m\nu^2 \\ \text{or} \qquad \mu &= 1 - e^2n/2\pi m\nu^2 \end{aligned}\right\}. \tag{11}$$

This is the usual expression for μ.

Here $n = \Sigma_h n_h$ = the total number of electrons per unit volume and since μ differs only slightly from unity, the approximation in the second of Eqs. (11) is justified. Also Eq. (5) becomes

$$\alpha_h = -e^2/\pi m\nu^2. \tag{12}$$

Combining Eqs. (9), (10) and (12) we get

$$f = -\sum_h e^2M_h/4\pi^2 em\nu^2 = -eI/\pi m\nu^2. \tag{13}$$

Substituting from Eq. (13) in Eq. (6)

$$\begin{aligned} \chi &= -\mu eIl/2c^2\tau^2\pi m\nu^2 \\ &= -2\pi\mu eIl/mc^2. \end{aligned} \tag{14}$$

It can be seen from Eq. (11) that $\mu < 1$ and α_h is negative. Consequently it appears that the sign of χ has a real significance in this case. For example, iron shows a positive rotation for visible light and in this range $\mu > 1$. Thus the quantity corresponding to α_h is positive for this region and χ is calculated as positive. The minus sign here indicates then that the rotation will be negative. The direction of rotation cannot be predicted for ordinary light from the magnetic properties of the substance but if the direction is known in one case and the calculated χ is of opposite sign in a second case, it is expected that the direction of rotation will differ in the two cases.

The work of several experimenters[9] has shown that the planes of electronic orbits are not rotated in a magnetic field but it may be pointed out that the deduction of Eq. (14) is independent of the mode of magnetization and depends only on the assumption that magnetization is an electronic effect.

It is interesting to note that χ is independent of the wave-length, λ, of the x-rays except in so far as μ is a function of λ. Since μ is very nearly unity for a wide range of x-ray wave-lengths, it is to be expected that χ will be approximately constant for all x-rays.

[8] H. A. Lorentz, reference 7.

[9] M. de Broglie, Le Radium **10**, 186 (1913).
K. T. Compton and E. A. Trousdale, Phys. Rev. **5**, 315 (1915).
A. H. Compton and Oswald Rognley, Phys. Rev. **16**, 464 (1920).
T. D. Yensen, Phys. Rev. **31**, 714 (1928).
J. C. Stearns, Phys. Rev. **35**, 1 (1930).
J. C. Stearns, Phys. Rev. **35**, 292 (1930).

The Experimental Arrangement

The general radiation of effective wave-length about 0.3A from a gas-filled x-ray tube was used in these experiments. This white radiation was about 10 percent polarized thus giving a much greater effective intensity than could be obtained by scattering. The arrangement of apparatus is shown in Fig. 1. The x-rays passed through holes in the pole pieces of an electromagnet, in a direction parallel to the magnetic field, and fell upon a cylindrical carbon scattering block which served as analyzer. The radiation scattered by the carbon block at right angles to the primary beam was detected by a photographic film bent into the shape of a cylinder having the same axis as the carbon block. The diameter of the cylindrical film holder was about 4 cm and of the block about 0.5 cm. The total distance from target to analyzer was about 25 cm. The holes in the pole pieces were just large enough to ensure

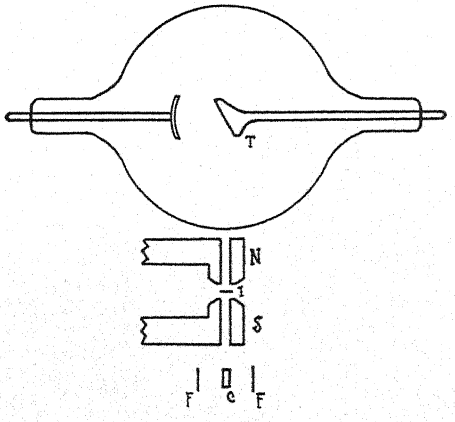


Fig. 1. Arrangement of apparatus. *T* is the target of the x-ray tube, *N* and *S* are the perforated magnetic pole pieces, *I* is the iron disk, *C* is the carbon analyzer and *F* is the photographic film.

uniform illumination over the scattering block. Any desired thickness of iron could be placed between the poles of the magnet.

The x-rays had a predominant polarization with the electric vector in the plane containing the stream of incident cathode rays at the target. The angle which this plane made with the straight line joining cathode and target depended upon the strength of the field produced by the magnet at the center of the x-ray tube. Thus a reversal of the magnetic field produced a rotation of the plane of predominant polarization even if there were no substance between the poles of the magnet. In order to eliminate this effect produced by the change in the direction of the cathode rays photographs were taken with different thicknesses of iron between the poles. The thickness of the iron was never changed enough to affect the magnetic field in the x-ray tube.

Photographs were taken with 0.05 cm and 0.075 cm of iron between the poles of the magnet with the field first in one direction and then in the other. A fixed lead stop between the scattering block and the film and just in front of the latter served to mark a constant angle with the axis of the x-ray tube

on the various films used. A microphotometer was used to measure the intensity on the film. As a continuously-recording microphotometer was not available the galvanometer deflections were read directly and the curves plotted. Fig. 2 shows two typical examples. These two curves represent the intensity arriving at the film after passing through 0.075 cm of iron in the magnetic field. Curve (1) was taken for the magnetic field in the direction of propagation of the x-rays and curve (2) with the field reversed. The angular displacement of one of these curves with respect to the other measures the combined effect of the magnetic field on the cathode rays and of any roation of the plane of polarization in transmission through the iron. The process was repeated using 0.05 cm of iron between the poles of the magnet. Since the effect on the cathode rays was the same as in the case for the thicker iron, any difference between the angular displacement of these curves and of those for 0.075 cm of iron measures the rotation of the plane of polarization produced by 0.025 cm of iron upon reversal of the magnetic field.

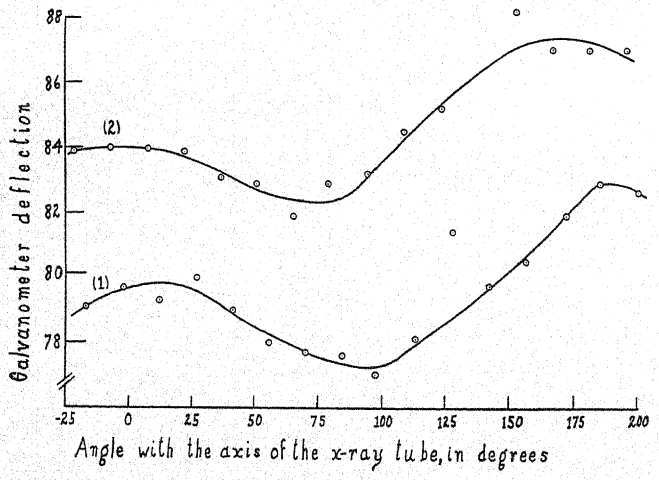


Fig. 2. Microphotometer curves.

Three sets of curves for each thickness of iron were obtained, the average displacements measured and the mean differences found.

The iron used was in the form of disks 0.025 cm thick and of diameter just greater than the holes in the pole pieces. On account of the difficulty of determining the magnetic properties of the iron and of estimating the demagnetizing effect of the free poles, a direct measurement of magnetization was made. As is well known[10] the force between two magnetic poles in contact is $2\pi I^2$ dynes per cm^2. The force required to separate one of the disks from the other two in the field was measured and the intensity of magnetization calculated. This was repeated with but two disks present. Mechanical difficulties rendered these results somewhat inaccurate but they are probably as precise as the measurement of angular displacements. The strength of the magnetic field producing magnetization was measured in order to test Voigt's equation.

[10] S. G. Starling, *Electricity and Magnetism*, p. 283.

If there is appreciable dispersion in the magnetic rotation the apparent percentage of polarization should be less with a magnetic field across the iron than without the field. That is, if the planes of polarization of different wave-lengths were rotated through different angles, the microphotometer curves would be flattened by the application of a field. No appreciable difference in the apparent percentage of polarization was obtained with the iron magnetized and not magnetized. Kartschagin and Tschetwerikowa did obtain a difference in this case but they were using the iron itself as the analyzing scatterer. They assumed that the effective thickness of iron traversed before scattering was equal to the thickness of iron which would absorb one-half of a primary beam of wave-length equal to the wave-length of maximum energy from their x-ray tube. Thus their primary rays travelled various distances in the direction of magnetization before analysis and a decrease in the apparent percentage of polarization is to be expected even if there is no dispersion.

TABLE I.

Trial	$\theta_1°(l=0.05$ cm)	$\theta_2°(l=0.075$ cm)	$\theta_2°-\theta_1°$ $=\chi_2°-\chi_1°$	$\chi_2°-\chi_1°$	$\chi_2°-\chi_1°$
1	−4.3	−14.4	from	from theory	from Voigt's
2	−4.3	−15.8	experiment	given in this	theory for
3	−5.8	−15.8		paper	nonferromagnetic materials
Average	−4.8	−15.3	−10.5	−14.0	-1.1×10^{-7}

In Table I θ_1 is the apparent rotation produced by a thickness of 0.05 cm of iron, and θ_2 by 0.075 cm, on reversal of the field. Both θ_1 and θ_2 include the effect of the field on the cathode rays. One might expect θ_1 to be much larger compared to θ_2. However the demagnetizing effect of the free poles is considerably reduced on increasing the thickness of the iron so that by Eq. (14) χ is increased by the increase of both l and I. The magnetic field was kept constant at 300 gauss. The intensity of magnetization measured 79 unit poles per cm^2 for 0.05 cm of iron and 97 unit poles per cm^2 for a thickness of 0.075 cm. $\theta_2-\theta_1$ is independent of any magnetic effect on the cathode rays. Values of χ were calculated for these two cases, χ_1 for 0.05 cm of iron and χ_2 for 0.075 cm of iron both from Voigt's theory (Eq. 1) and from Eq. (14). $\chi_2-\chi_1$ is given in Table I for comparison with $\theta_2-\theta_1$ as observed. $d\mu/d\lambda$ was calculated for Eq. (1) from Eq. (11). The minus sign indicates the direction of the rotation in the conventional manner.

CONCLUSIONS

The results given in the last three columns of Table I differentiate between the two theories in a striking and unmistakable way. Voigt's theory is certainly not applicable in this case. The comparatively large estimate of the rotation, 4′, made by Kartschagin and Tschetwerikowa in their case for Voigt's equation came about since their effective wave-length was near the K absorption level of iron. Thus their estimate of $d\mu/d\lambda$, based on the anomalous dispersion theory, was many times that given by Eq. (11). The effective fre-

quency used in the present experiments was certainly so much greater than any of the characteristic frequencies of iron that Eq. (11) contains no appreciable error.

It is very difficult to estimate the probable error in the experimental value of $\chi_2 - \chi_1$. After careful consideration of the various errors which may have entered due to the particular equipment used, and to the photographic method of measuring intensities, the author is forced to conclude that the results given here indicate only the correct order of magnitude of the effect. However it can be concluded with little doubt that the plane of polarization is rotated a few degrees under the conditions described. For these reasons no calculation of the Verdet constant has been made from the experimental results. It is greatly desired that accurate ionization-chamber measurements be made, using a much steadier source of x-rays than was available for this work, and it is hoped that such work, if not done elsewhere in the meantime, may be accomplished in this laboratory in the near future.

The author wishes to take this opportunity to thank Drs. W. and M. L. Rowles, and his wife, Ethel Froman, for their advice and assistance in the experimental part of this work.

New Measurements of the Ranges of Alpha-Particles from Polonium, Uranium I and Uranium II with the Wilson Chamber*

By F. N. D. KURIE†
Sloane Physics Laboratory Yale University

(Received July 5, 1932)

The Wilson cloud chamber method of range measurement described by the author in another paper has been applied to the α-particle ranges of polonium, uranium I, and uranium II. The polonium measurements were undertaken as a check on the method, but are in sufficiently good accord with previous results to stand alone. The range of polonium α-particles at 0°C and 760 mm is 3.690 ± 0.005 cm. The range of uranium I α-particles is 2.58 ± 0.015 cm and that of uranium II α-particles is 3.11 ± 0.01 cm. The polonium range is derived from 335 tracks while the uranium ranges are due to a total of 594 tracks. A method of separating the number-distance curves of the two uraniums is described which eliminates the uncertainty of finding the shorter range. The uranium data are in excellent agreement with the results of Laurence. This agreement is thought to be entirely fortuitous in so far as uranium I is concerned. The precision of Laurence's work is criticised.

INTRODUCTION

A PARALLEL beam of α-particles does not possess a sharp terminus, but the distances traversed by single particles before they can no longer be detected are governed by a probability law such that the number of particles stopping between x and $x+dx$ (the distance x being measured from the source) is given by the normal probability function $(1/\alpha\pi^{1/2})\exp(x-l)^2/\alpha^2$, where α is a parameter called in this case the straggling coefficient. The distribution is symmetrical about l, the most probable range. There are many reasons why it is more desirable to use this range in other discussions, but experimental difficulties, however, have made it hard to assign precise values to it so one usually measures the extrapolated number-distance range defined by the following considerations. The number N of α-particles which pass beyond a given distance x is readily obtainable by integrating the normal function and is $N=(1/2)\{1-\text{erf}\ (x-l)/a\}$. This curve exhibits a sharply descending linear portion which on extrapolation meets the distance axis at R (the extrapolated number-distance range), where R is given by $R=l+\pi^{\frac{1}{2}}\alpha/2$. This may be written independently of α for short range particles, by making use of the data relating α to R given by Briggs.[1] Thus,

$$R = l + 4.2R^{1/2}\{1 - 1.51/R\}^{1/2}(10)^{-2}.$$

Another type of range is given by ionization current measurements, the interpretation of which is more obscure than that of the ranges derived sta-

* Part of a dissertation presented for the degree of Doctor of Philosophy at Yale University.

† Sterling Fellow.

[1] G. H. Briggs, Proc. Roy. Soc. A118, 594 (1928).

tistically from measurements on single particles. The relation between the ionization range and the number-distance range has recently been derived by Lewis and Wynn-Williams[2] on the basis of the ionization curve of a single α-particle. They deduce that the extrapolated number-distance range exceeds the extrapolated ionization range by 0.006 cm.

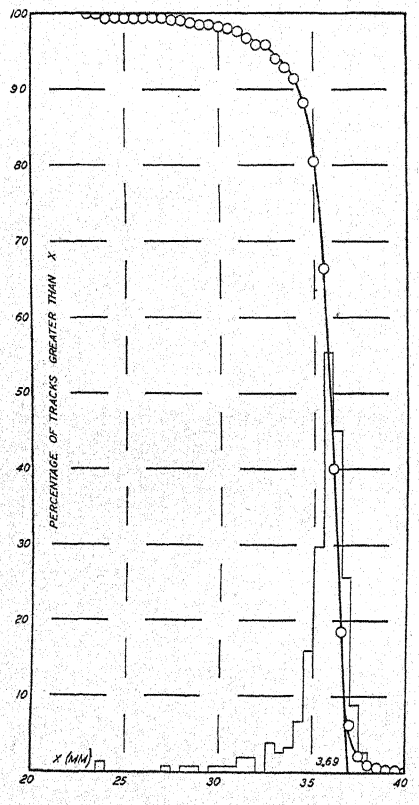


Fig. 1. Number-distance curve for polonium α-particles.

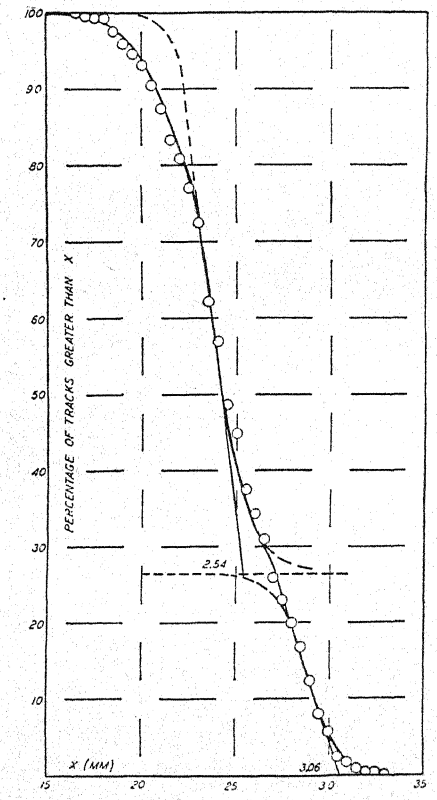


Fig. 2. Number-distance curve for uranium α-particles.

These remarks have been made with the view of helping to relieve some of the lack of uniformity in the interpretation given by different authors and texts to the phrase "the range of α-particles." In this paper the phrase will be taken to refer to the extrapolated number-distance range.

Polonium

The author has outlined in another paper[3] the procedure for obtaining the range of α-particles from weak sources. This briefly consists in taking two photographs of the tracks due to the α-particles in question formed in a large

[2] W. B. Lewis and C. E. Wynn-Williams, Proc. Roy. Soc. **A136**, 349 (1932).
[3] To be published in the Review of Scientific Instruments.

Wilson cloud chamber, and from them reconstructing a replica of the original track. This replica is measured and reduced to standard conditions (0°C, 760 mm). Because of the large size of the sources employed there are no slits or shutters; tracks are formed on ions of all ages. Those formed at constant density after an expansion are, however, much sharper than any others. That this sharpness can be used as a criterion for rejecting old tracks needs proof, and it was for that purpose that the range of polonium α-particles was examined.

The sources were prepared on silver wires, about 10 cm long and 0.001 inch in diameter, by deposition from a weakly acid (HCl) solution of polonium. It was found that with even the weakest of acid solutions there was a noticeable tarnish on the wire. It seemed likely that the only compound which might be formed would be silver chloride, which is soluble in ordinary hypo. A source deposited on a polished silver plate and showing the tarnish became perfectly clear on bathing it in hypo, without having lost any activity. A wire source after treatment with hypo gave a range 0.03 cm in excess of measurements before the treatment. The variation from source to source was never more than 0.01 cm, even with badly tarnished sources; after the hypo treatment was introduced the variation dropped below this value. All the sources used in the final measurements were bathed in hypo.

The results are shown in Fig. 1. The distribution curve of the ranges is shown in outline; it is drawn for $dx=0.05$ cm. The number-distance curve is plotted on a percentage scale, 100 percent corresponding to 335 tracks. Extrapolating the linear portion of this curve to the distance axis gives the range in the sense defined above, as $R_0=3.690\pm0.005$ cm at 0°C, 760 mm.

The limit of reliability is obtained by assigning to each column in the distribution histogram the error appropriate to the number of particles it contains. One gets thus two limiting histograms and so two limiting number-distance curves. The extreme extrapolated straight line portions of these meet the distance axis at R_0+p and R_0-p, where p is the limit of reliability.

This range corresponds to an extrapolated ionization range of 3.68 cm and to a mean range of 3.63 cm. The most reliable values of the polonium range are given in Table I. Those values marked with an asterisk were not measured directly but calculated by some relation of the form already mentioned.

TABLE I. *Range of polonium α-particles.*

Observer	Mean range	Extrapolated number-distance range	Extrapolated ionization range
Geiger[4]	—	—	3.72
I. Curie[5]	3.65	3.72	3.67
Harper and Salaman[6]	—	—	3.67
Lewis and Wynn-Williams[2]	3.61	—	3.65*
Kurie[7]	3.63*	3.69	3.68*

[4] H. Geiger, Zeits. f. Physik **8**, 45 (1921).
[5] I. Curie, Ann. de Physique **3**, 299 (1925).
[6] G. I. Harper and E. Salaman, Proc. Roy. Soc. **A127**, 175 (1930).
[7] This paper.

The results of the polonium measurements not only furnish a new value for the range of polonium α-particles but they show that the method of using the cloud chamber without slits or shutter for the α-particles does not hamper its precision.

URANIUM

The two uraniums present a particularly difficult problem, being so weak that thick sources must be used. This leads to a broadening of the straggling curve and nearly masks the fact that the radiation from uranium is complex. Indeed, all the work up to 1910 gave uranium a single group of α-particles with a range between 2.7 cm and 3.4 cm.

Recently a number of attempts have been made to measure these two ranges more exactly. This has become very important in view of the difference between the ionization measurements of Geiger and Nuttall,[8] which gave ranges of 2.53 cm and 2.91 cm for uranium I and uranium II respectively, and the pleochroic haloe measurements of Gudden[9] which gave ranges of 2.68 cm and 2.76 cm for the same bodies.

The most notable effort is that of Laurence[10] who measured the ranges in a Wilson cloud chamber getting 2.59 cm and 3.11 cm. His work received corroboration from Rutherford[11] who showed by the scintillation method that the range of uranium II is not less than 3.06 cm, and from Ziegert[12] who found the number of ions produced per α-particle to correspond roughly to ranges of 2.7 cm and 3.1 cm.

Laurence's work, while representing a pronounced advance both in the technique of the Wilson chamber and in our knowledge of the range of uranium α-particles, nevertheless seems unsatisfactory and unconvincing as a precision measurement. The present work was undertaken because it was believed possible to avoid most of the assumptions and corrections used by Laurence.

This author has mentioned elsewhere that it is quite essential for precision that a cloud chamber be operated periodically at regular intervals; that the length of the interval be chosen with due regard to the thermodynamics of the chamber; that the illuminating arc be screened from the chamber until the moment of the expansion; and that the camera be properly synchronized with the expansion to prevent turbulences altering the lengths of the tracks.

The reasons which Laurence gives to prove that 98 percent of the tracks he photographed are formed at constant density are quite erroneous. Tracks of all ages are present in the chamber, those formed at constant density, however, being much sharper. This criterion of selection has already been mentioned above.

The corrections which Laurence was obliged to apply for the obliquity

[8] H. Geiger and J. M. Nuttall, Phil. Mag. [6] **23**, 439 (1912).

[9] B. Gudden, Zeits. f. Physik **26**, 110 (1924).

[10] G. C. Laurence, Trans. Nova Scotian Inst. Science **17**, 103 (1927); Phil. Mag. [7] **5**, 1027 (1928).

[11] Sir Ernest Rutherford, Phil. Mag. [7] **4**, 580 (1927).

[12] H. Ziegert, Zeits. f. Physik **46**, 668 (1928).

of the tracks to the chamber floor and for the heating of the gas in the chamber are difficult to estimate and have been avoided in the present work.

When one considers two superimposed number-distance curves it is clear, as is found for uranium, that the range of the shorter group is got by extrapolating the linear portion of the upper curve to the flat maximum of the lower curve (no-particle line of the upper curve). Unfortunately in uranium this flat maximum does not show up in the experimental curve. Instead of attempting to find its position Laurence has merely extrapolated the gentle curve of the uranium II particles until it cut the extended straight part of the uranium I section, calling their intersection the range of uranium I. A method will be described later which accomplishes the separation of the two curves and allows the shorter range to be got without such uncertain extrapolation.

Laurence's work, then, does not appear to be entirely unsusceptible to improvement. All possible improvements have been used in the present measurements.

The sources were prepared from uranium oxide (U_3O_8) by the method of McCoy[13] on a backing of mica 0.01 cm long, 1 cm wide and 0.001 inch thick. Subliming from an arc did not yield satisfactory sources; their weight and ionization currents did not check. That impurities are unavoidable in this respect is substantiated by Laurence's report that he got one track in 80 expansions from a source rougly four times as heavy as the ones here used which gave 0.6 tracks per expansion. This is much greater than can be explained on the basis of the relative sizes of the two cloud chambers.

The final results are shown in Fig. 2 in the form of a number-distance curve plotted on a percentage scale, 100 percent corresponding to 594 tracks. The curve consists of two portions, one pertaining to uranium I and the other to uranium II. The range of α-particles from uranium II (uncorrected for absorption in the source) is 3.06 cm.

The same data are shown in Fig. 3 plotted on probability paper, where the curve has reduced to three straight lines. The conclusion at once suggests itself that the midpoint M of the short connecting line gives the fraction of uranium II tracks. This idea was tested by constructing several two-component number-distance curves, whose relative proportions were known, distorting these by adding an excess of short range particles and plotting them on probability paper. The excess of short range particles was known from the work of Mlle. Curie and from the observations of the author in connection with the polonium measurements to be in the neighborhood of 10–15 percent of the total. The fractions of the two curves as got from the midpoint of the short connecting line were in all cases within 1 percent of their known values. We thus find the uranium group to constitute 26.5 percent of the total number of α-particles.

With this known we can now find the true number-distance curves to which the data best conform by making separate plots for uranium I and

[13] H. N. McCoy, Phil. Mag. [6] **11**, 176 (1906).

uranium II on probability paper. These true curves are shown dotted in Fig. 2.

The small fraction of uranium II tracks is due to the solid angle available for complete tracks in the cloud chamber being smaller for the long range particles than for the short range particles. A very rough calculation from the dimensions of the chamber has borne this out quantitatively.

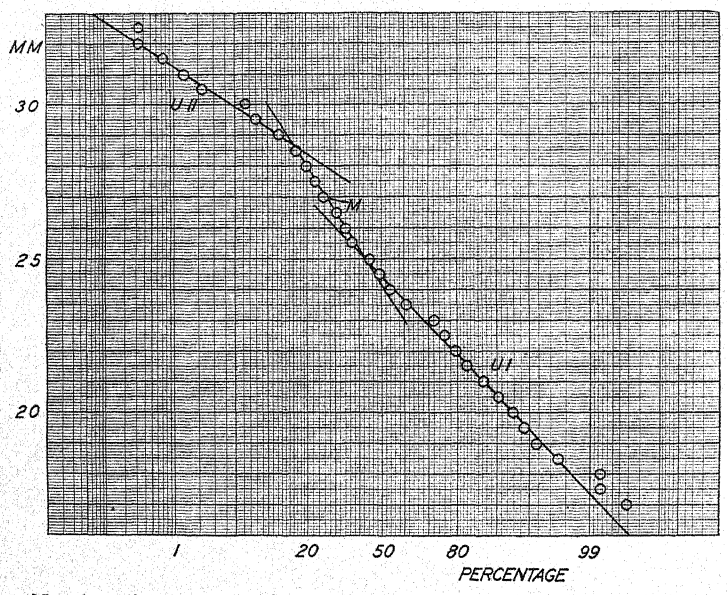


Fig. 3. Number-distance curve for uranium α-particles plotted on probability paper.

The correction for absorption in the source was calculated by Laurence in the paper discussed above. For sources of the thickness used in these measurements (of the order of 2 mg/cm^2) the correction is independent of the thickness and reduces to $\alpha\pi^{1/2}/2$, where α is the straggling coefficient. The straggling coefficients are 0.048 cm and 0.058 cm, respectively, for uranium I and uranium II, so that the corrections are 0.043 cm and 0.051 cm.

The final corrected ranges at 0°C and 760 mm are

$$R_{\mathrm{U\,I}} = 2.58 \pm 0.015 \text{ cm};$$

$$R_{\mathrm{U\,II}} = 3.11 \pm 0.01 \text{ cm}.$$

The limits of reliability have been calculated in the same manner as was done for polonium, but in addition the uranium I range is subject to an uncertainty due to the error in ascertaining the fractions of the two groups. This latter was estimated from the experiments with the fictitious curves to be 1 percent, corresponding to 0.006 cm in the range.

These results clearly agree with those of Laurence within the experimental error. This agreement is believed to be entirely fortuitous in so far as uranium I is concerned, for had the data been treated in the manner of Laurence a very much smaller value would have been obtained—nearer 2.50 cm than 2.59 cm.

The value of the half-life of uranium II as deduced from the range of its particles, assuming the Geiger-Nuttall law, is much smaller than that measured by Walling[14] and Collie.[15] When the range and Walling's value of λ is plotted on a Geiger-Nuttall graph of the uranium-radium series uranium II falls off the curve. The reason for this is not clear; the range seems to be sufficiently well established to lay the divergence to either a failure of the Geiger-Nuttall law or to inaccuracies in the experimental determinations of λ. The latter seems more probable since uranium I fits the slight curve (best form of the Geiger-Nuttall law) very well.

The author is greatly indebted to Professor Alois F. Kovarik, who suggested this problem, for the kind interest he showed and the friendly counsel he gave during the course of the experiments.

[14] E. Walling, Zeits. f. physik. Chem. **10**, 467 (1930).
[15] C. H. Collie, Proc. Roy. Soc. **A131**, 541 (1931).

The Relativistic Thomas-Fermi Atom

By M. S. VALLARTA AND N. ROSEN
Massachusetts Institute of Technology

(Received August 4, 1932)

The Thomas-Fermi equation determining the inner atomic potential and the charge distribution is generalized to take care of the relativistic change of mass with velocity. The relativistic equation is then solved numerically by means of a first order perturbation method and with the help of the differential analyzer. The solution is applied to the case of mercury and it is shown that while the atomic potential changes only slightly, the charge density is appreciably increased in the immediate vicinity of the nucleus and slightly decreased at larger distances.

THOMAS[1] and, independently, Fermi[2] have devised a valuable heuristic statistical method of finding the potential and the electron distribution around an atomic nucleus, in which the electrons are treated as if they formed an ideal gas obeying the Fermi-Dirac statistics. The charge density obtained in this manner, although admittedly not the actual one, is a sufficiently close approximation, at least for heavy atoms, that it can be successfully used in many problems, e.g., the calculation of x-ray scattering by heavy atoms and molecules.[3] It is a matter of some interest to investigate the modifications introduced in this atomic model by the relativistic variation of mass with velocity. While this correction may be expected to be negligible for most atoms, it becomes more appreciable as the atomic number increases because for very heavy atoms the electron velocities in the vicinity of the nucleus become high. For such atoms the electron density close to the nucleus may be appreciably changed by the relativity correction. In any case the latter is greatest just for those cases where the Thomas-Fermi distribution may be expected to be a good approximation to the actual one. Even for heavy atoms however, this correction is probably less important than the exchange correction. No satisfactory method of taking into account the exchange phenomenon has yet been devised and hence it will not be considered in the present paper.[4]

We proceed to derive the relativistic form of the Thomas-Fermi equation. Let V be the atomic potential and r the distance from the nucleus; then $V(r)$ satisfies the Poisson equation $\nabla^2 V = -4\pi\delta$ and the boundary conditions:

$$\lim_{r\to 0} V = Ze/r \quad \lim_{r\to\infty} V = 0 \tag{1}$$

[1] L. H. Thomas, Proc. Camb. Phil. Soc. **23**, 542 (1927).
[2] E. Fermi, Zeits. f. Physik **48**, 73 (1928).
[3] The literature in this connection is summarily reviewed by E. O. Wollan, Rev. Mod. Phys. **4**, 205 (1932).
[4] P. A. M. Dirac, Proc. Camb. Phil. Soc. **26**, 376 (1930).

where Z is the atomic number. The electron density δ in ordinary three dimensional space, taking into account spin and assuming that the electrons form a gas obeying the Fermi-Dirac statistics, is

$$-\delta = (2e/h^3)(4\pi p^3/3) \tag{2}$$

where e is the electron charge, h Planck's constant and p the momentum of the electrons having maximum energy. For a bound electron the energy E (sum of the kinetic and potential energies) is negative and its maximum value is zero. From the relativistic Hamiltonian

$$p^2 - (W+eV)^2/c^2 + m_0^2c^2 = 0 \tag{3}$$

where $W=E+m_0c^2$ is the total energy, m_0 the electron's rest mass and c the velocity of light in vacuum, we have, using the condition $E=O$ or $W=m_0c^2$ that

$$p^2 - e^2V^2/c^2 - 2m_0eV = 0. \tag{4}$$

Hence the electron density now becomes

$$-\delta = (2e/h^3)(4\pi/3)(2m_0eV + e^2V^2/c^2)^{3/2} \tag{5}$$

and from Poisson's equation

$$\nabla^2V = 4\pi(2e/h^3)(4\pi/3)\ (2m_0eV + e^2V^2/c^2)^{3/2} \tag{6}$$

which is the relativistic Thomas-Fermi equation.

To transform this equation into a simpler form we introduce so-called atomic units and the new variables $r=\alpha\rho$ and $V=\beta\phi$, where

$$\alpha = a_0/Z^{1/3} \qquad \beta = 9\pi^2eZ^{4/3}/128a_0 \tag{7}$$

and a_0 is the radius of the first Bohr circle. Eq. (6) now becomes

$$\frac{1}{\rho^2}\frac{d}{d\rho}\left(\rho^2\frac{d\phi}{d\rho}\right) = \phi^{3/2}(1+\lambda\phi)^{3/2} \tag{8}$$

where

$$\lambda = e\beta/2m_0c^2 = 1.841 \times 10^{-5}Z^{4/3}. \tag{9}$$

Eq. (8) can now be solved by a first order perturbation method as follows: let $\phi=\phi_0+\lambda\phi_1$, then keeping first order terms we have

$$\phi^{3/2}(1+\lambda\phi)^{3/2} \doteq \phi_0^{3/2} + (3/2)\lambda\phi_0^{1/2}\phi_1 + (3/2)\lambda\phi_0^{5/2}$$

and equating like powers of λ in (8) we obtain two equations:

$$\nabla^2\phi_0 = \phi_0^{3/2} \tag{10}$$

$$\nabla^2\phi_1 = (3/2)\phi_0^{1/2}(\phi_1+\phi_0^2) \tag{11}$$

of which the first is the ordinary Thomas-Fermi equation whose numerical solution is known,[5] and the second is the equation for the relativistic correction.

To solve Eq. (11) we place $\phi_1 = F/\rho$ and obtain

$$d^2F/d\rho^2 = (3/2)\phi_0^{1/2}F + (3/2)\rho\phi_0^{5/2}. \tag{12}$$

The numerical value of the coefficients in this equation is calculated from the data of Bush and Caldwell.[5] The boundary conditions for the function F are immediately derived from the boundary conditions for V; they are simply that F vanishes both at zero and infinity. For small values of $\rho(\rho<0.1)$ the solution of (12) can be expressed in a power series, using the results of Baker.[6] The series expansion is found to be:

$$\begin{aligned} F = &-6\rho^{1/2} + C\rho - 5B\rho^{3/2} - 2\rho^2 + (3B^2/4 + 2C/5)\rho^{5/2} - 2B\rho^3 \\ &- (11/35 + 3B^3/56 + 3BC/35)\rho^{7/2} + \cdots \end{aligned} \tag{13}$$

where B is the negative slope of the Thomas-Fermi function $(B=1.5886)$[5,6] and C is a constant chosen so as to satisfy the boundary conditions for F. The numerical value of this constant as determined from the solution of Eq. (12) to be described below is $C=11.92$.

TABLE I.

ρ	$-F$	$-\phi_1$	ρ	$-F$	$-\phi_1$
0	0	∞	0.600	0.784	1.307
0.010†	0.490	49.0	0.704	0.725	1.032
0.030†	0.726	24.2	0.809	0.670	0.828
0.060†	0.878	14.62	0.913	0.621	0.681
0.080†	0.934	11.68	1.000	0.582	0.582
0.100	0.960	9.65	1.500	0.411	0.274
0.121	0.981	8.11	2.001	0.301	0.1505
0.142	0.994	7.00	3.00	0.1748	0.0583
0.163	0.999	6.13	4.00	0.1106	0.0277
0.180	1.001	5.57	5.00	0.0741	0.01482
0.204	0.999	4.90	6.00	0.0519	0.00865
0.309	0.958	3.11	7.00	0.0370	0.00568
0.413	0.898	2.175	8.00	0.0267	0.00334
0.517	0.834	1.612	9.00	0.0188	0.00209
			10.00	0.0123	0.00123

† Calculated from series expansion (13).

The numerical integration of Eq. (12) can be conveniently carried out in the differential analyzer, a machine for the solution of differential equations developed at this Institute by V. Bush.[7] The result of this integration is given in Table I and Fig. 1.

[5] References 1 and 2, also V. Bush and S. H. Caldwell, Phys. Rev. **38**, 1898 (1931).

[6] E. B. Baker, Phys. Rev. **36**, 630 (1930).

[7] V. Bush, Jour. Franklin Inst. **212**, 447 (1931). The authors take advantage of the present opportunity to thank Professor Bush and his assistants, Messrs. S. H. Caldwell, A. J. McLennan, S. D. Caldwell, J. F. Cummings, B. V. Holmes, and R. S. Jameson for their friendly help with the integration of this differential equation.

For the electron density we now have, from (5)

$$-\delta = (8\pi e/3h^2)(2m_0e\beta)^{3/2}\phi^{3/2}(1+\lambda\phi)^{3/2} \tag{14}$$

whereas for the same quantity calculated according to the Thomas-Fermi theory one has

$$-\delta_0 = (8\pi e/3h^3)(2m_0e\beta)^{3/2}\phi_0{}^{3/2} \tag{15}$$

hence for the ratio of the relativistic to the nonrelativistic charge density one obtains

$$\delta/\delta_0 = \phi^{3/2}(1+\lambda\phi)^{3/2}/\phi_0{}^{3/2}. \tag{16}$$

This ratio is appreciably different from, and greater than, unity at small distances from the nucleus; at large distances the ratio is very close to, but smaller than, unity. The total charge is of course the same in both cases.

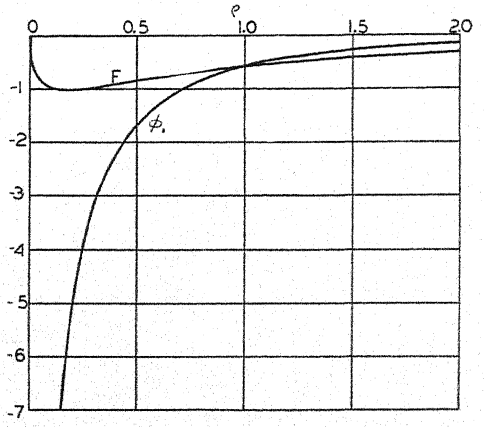


Fig. 1. Functions involved in relativity correction to Thomas-Fermi potential.

As an example let us take the case of mercury ($Z=80$). Here $\alpha=0.1225\text{Å}$ and $\lambda=0.00635$. The value of the ratio (16) for different values of the distance

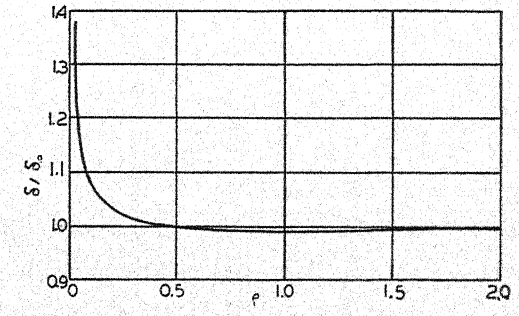


Fig. 2. Ratio of relativistic to nonrelativistic charge density for the mercury atom.

from the nucleus is given in Table II and plotted in Fig. 2. The relativistic and the nonrelativistic atomic potentials for mercury may be read off Table II. It is immediately seen that they are very nearly the same.

TABLE II.

ρ	r (X-units)	ϕ_0	ϕ	δ/δ_0
0.010	1.227	98.5	98.2	2.06
0.030	3.68	32.0	31.85	1.315
0.060	7.36	15.40	15.31	1.141
0.080	9.81	11.27	11.20	1.099
0.100	12.27	8.82	8.76	1.073
0.417	51.2	1.561	1.547	1.002
0.584	71.7	0.975	0.966	0.996
1.000	122.7	0.425	0.422	0.991
1.500	184.0	0.314	0.312	0.995
2.00	245.	0.244	0.243	0.996

The present investigation was suggested by Professor P. Debye to whom we wish to acknowledge our indebtedness.

The Wentzel-Brillouin-Kramers Method of Solving the Wave Equation

By J. L. DUNHAM
Harvard University

(Received May 11, 1932)

A more general treatment than has been available of the Wentzel-Brillouin-Kramers method of solving Schrödinger's equation for one degree of freedom is given. Wentzel's original energy-level condition is shown to be an asymptotic expression, good for large masses and large values of the quantum number. The connection between this method and that of Young is discussed. Finally the formulas are written in a form convenient for application to the calculation of energy levels from actual potential functions.

INTRODUCTION

THE Wentzel[1]-Brillouin[2]-Kramers[3] method of handling the wave equation (hereafter referred to as the W. B. K. method) is very well suited to the calculation of energy levels in heavy systems. This is evident from the fact that for such systems the Bohr theory levels fit the experimental facts rather well. Now these levels are the first approximation of the W. B. K. method, and hence we would expect it to give us rapidly converging results. Also such behavior is indicated by the correspondence principle, which predicts approximately classical properties for heavy systems as well as for high quantum numbers.

The usefulness of this method, however, has been limited by the fact that those treatments of it which have been rigorous have all been approximate, so that results of only a limited accuracy can be obtained. It is therefore the purpose of the present paper to extend the theory of the W. B. K. method to higher approximations, and to show that Wentzel's original generalization of the phase integral can be justified entirely. We shall also discuss the connection between this method and that of local momentum recently suggested by Young.[4]

Owing to the fact that Zwaan's[3] work on this subject is not very accessible we shall take up some of the points which he has discussed.

THE W. B. K. METHOD

The W. B. K. method of solving Schrödinger's equation is briefly as follows. Schrödinger's equation can usually be written

[1] G. Wentzel, Zeits. f. Physik **38**, 518 (1926).
[2] L. Brillouin, Comptes Rendus **183**, 24 (July 1926).
[3] H. A. Kramers, Zeits. f. Physik **39**, 828 (1926). See also A. Zwaan, Arch. Néerl. des Sciences **12**, 33 (1929), and L. A. Young and G. E. Uhlenbeck, Phys. Rev. **36**, 1154 (1930). For a good short account of Wentzel's presentation and some simple applications see Sommerfeld, Ergänzungsband, p. 158.
[4] L. A. Young, Phys. Rev. **38**, 1612 (1931) and **39**, 455 (1932).

$$d^2\psi/dx^2 + (8\pi^2 m/h^2)(E - V)\psi = 0. \tag{1}$$

Let

$$\psi = e^{(2\pi i/h)\int y dx}. \tag{2}$$

y is then determined by

$$(h/2\pi i)(dy/dx) = p^2 - y^2 \tag{3}$$

where $p_2 = 2m(E - V)$. We now expand y in a series;

$$y = y_0 + (h/2\pi i)y_1 + (h/2\pi i)^2 y_2 + \cdots. \tag{4}$$

Substituting this in Eq. (3) and equating the coefficients of different powers of h to zero separately, we find a set of equations to determine the y_n's. They are given by the recurrence formula

$$y'_{n-1} = -\sum_{m=0}^{n} y_{n-m} y_m, \qquad n = 0, 1, 2 \cdots \tag{5}$$

$$y_0 = \pm p, \tag{6}$$

from which we can obtain the y_n's by simple algebraic manipulation.

$$\begin{aligned} y_0 &= [2m(E - V)]^{1/2} \quad y_1 = V'/4(E - V) \\ y_2 &= -(1/32)(5V'^2 + 4V''(E - V))(2m)^{-1/2}(E - V)^{-5/2} \\ y_3 &= (1/128)(4V'''(E - V)^2 + 18V'V''(E - V) + 15V'^3)m^{-1}(E - V)^{-4} \\ &\cdots\cdots\cdots\cdots\cdots\cdots\cdots\cdots\cdots\cdots\cdots\cdots \end{aligned} \tag{7}$$

So, if we know V, we can at once calculate ψ by means of Eqs. (7), (4) and (2). Eq. (4) can now be written

$$\begin{aligned} 2\pi i y/h = \pm\, & iB^{-1/2}(E - V)^{1/2} + V'/4(E - V) \\ & \pm (iB^{1/2}/32)(5V'^2 + 4V''(E - V))(E - V)^{-5/2} + \cdots \end{aligned} \tag{8}$$

where $B = h^2/8\pi^2 m$.

It is well known that this expression gives good approximations to y, and hence to ψ, when $(E - V)$ is fairly large. Obviously the same will be true in regions where the potential curve approaches some finite value asymptotically so that all of its derivatives vanish. Furthermore, if B is very small, at least the first few terms appear to converge rapidly. In fact it is known[4a] that this expression is asymptotically convergent both as B becomes small and as $|x|$ becomes large (if $\pm\infty$ are the boundaries of the region). That is to say, as we let B approach zero, the difference between the sum of the first n terms

[4a] See Zwaan, reference 3.

[5] For a discussion of asymptotic series see: W. B. Ford, "Studies on Divergent Series," Macmillan 1916, p. 22 and Chap. III; E. Borel, "Leçons sur les Series Divergentes," Gauthier-Villars 1928, p. 21. Also for applications to differential equations. J. Horn, Math. Ann. **52**, 271 (1899); and "Gewohn. Diff. Gleich." 1927, p. 188; L. Schlesinger: "Gewohnliche Differentialgleichungen," Vieweg 1922, p. 248. A very clear discussion of this subject is given by G. G. Stokes: "Math. and Phys. Papers." Vol. IV, pp. 77–109 and 283–298.

of Eq. (8) and the true value of y will be a small quantity of the order of $B^{n/2}$ for all values of n. A similar relation is true if, instead of letting B become small, we let $|x|$ become large. Consequently we can use a finite number of terms of Eq. (8) and, if B is small or $|x|$ large, this will give us a good approximation to y in spite of the fact that the series actually diverges.[5]

We shall find it convenient here to distinguish between two possible definitions of y. So far it has been defined as the solution of Eq. (3), but it could also be defined by means of Eq. (8). Now Eq. (8) has singular points where $E=V$, and in the neighborhood of those points it does not behave even approximately like the solution of Eq. (3), for we shall see later that the latter has no singularities on the real axis. Thus the two definitions are really different. We shall hereafter call the solution of Eq. (3), $\bar{y}$, to distinguish it from the quantity defined by Eq. (8), which we shall call plain y. For values of x such that $E \neq V$ the two definitions approach each other asymptotically as B approaches zero.

It should be noticed that y has two branches due to the fact that y_0 is given by the square root of p. All of the even numbered y_n's involve square roots, and the sign of the root is to be taken as the same as that in y_0. All of the odd numbered y_n's are single valued.

The Energy Level Condition

We turn now to a derivation of the energy level condition. Kramers[3] and Zwaan[3] have found the energy level condition using only the first two terms of Eq. (8). Their methods differed in that Kramers used another expansion for ψ to supplement Eq. (8) at points where it has singularities (i.e., where $E=V$), whereas Zwaan avoided such points by going around them in the complex plane. Kramers also pointed out that the earlier and more general work of Wentzel[1] was not rigorous, though his own work verified Wentzel's energy level condition as far as it went. This criticism of Wentzel's proof is entirely justified as we shall see, but it is possible to show that Wentzel's result is correct and can be used to find higher approximations to the energy level formula in some cases. It is this more general proof which shall be given in this paper.

In carrying out this proof we use essentially Zwaan's method instead of Kramers', as it lends itself more readily to work with higher approximations. The proof given here, however, differs considerably in details from that of Zwaan.

We use the definition of an energy level as a value of E for which ψ can be (a) single valued, (b) real on the real axis, and (c) bounded on the real axis. We shall follow the usual procedure of starting with a function which is zero at one of the boundaries and carrying it to the other boundary to find what conditions must be satisfied if it is to be zero there also. It will simplify matters if we restrict ourselves to a potential function having only one minimum on the real axis and hence, as we shall deal only with the discrete spectrum, only two points for which $E=V$.

For convenience we divide the real axis into three regions: I, II, and III.

Region I is to the left of both points where $E=V$, (i.e., Q and R, see Fig. (1), II is the region between these two points, and III is the region to the right of them.

We shall designate the two branches of y by the symbols y_a and y_b (these subscripts are not to be confused with the number subscripts in Eq. (4)). y_a is defined as that branch of y whose first term is positive imaginary in region I. Furthermore, we shall suppose the cut in the x plane to be the real axis between Q and R, and we require that in no integral shall the path of integration cross this cut.

The general solution of Eq. (1) will be of the form

$$\psi = c_a e^{(2\pi i/h)\int^x y_a dx} + c_b e^{(2\pi i/h)\int^x y_b dx}. \tag{9}$$

Now in order that ψ be bounded for $x=-\infty$, c_a must be zero since $i\int^x y_a dx$ becomes infinite for large negative values of x.[6] Consequently in region I ψ will have the form

$$\psi_{\mathrm{I}} = c_b e^{(2\pi i/h)\int_P^x y_b dx}. \tag{10}$$

Here c_b is to be determined by normalization. The choice of P_1, the initial point of integration, is arbitrary, c_b assuming different values for different choices of P. For simplicity we shall consider P to be in region I, thus making c_b real.

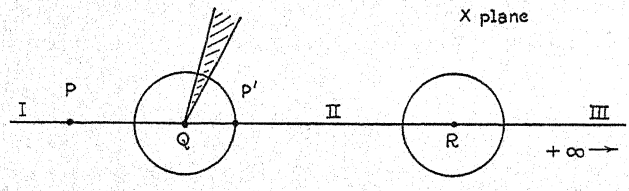


Fig. 1. Q and R are points where $E=V$. Region I is that part of the real axis to the left of Q, region II is between Q and R, and region III is to the right of R.

However, for ψ to have real values for points in region II, c_a *cannot* be equal to zero. Both terms will be needed there, because $\int ydx$ has complex values in region II and an expression of the form of Eq. (10) could not represent a real function. Consequently somewhere on the path from region I to region II (which we shall take so as to avoid the point Q at which $E=V$, and hence at which Eq. (8) has a singularity) it must be possible to change from an expression of the type of Eq. (10) to the more general form of Eq. (9). This sudden change in the coefficients of an asymptotic expression was first discussed by Stokes[5] and is a well-known phenomenon. It arises primarily from the fact that ψ has an essential singularity at infinity. If it did not it would not be necessary to resort to an asymptotic expression for its representation. Hence ψ may require different asymptotic representations for different paths to infinity.

[6] It will be noticed that the first term of Eq. (8) becomes the only important one near the boundaries of the region (here $-\infty$) since there either V becomes infinite or all its derivatives vanish. Also y is a pure imaginary in regions I and III, so that the exponents are real in these regions.

This change in the value of c_a can be looked at from the following point of view. For finite values of B and of x, Eq. (8) represents y only approximately. Hence Eq. (10) gives ψ in region I only to a certain degree of approximation, and similarly an expression of the form of Eq. (9) (with c_a suitably chosen) can represent ψ in region II only approximately. Now there must be some sector around Q (shown in Fig. 1 by the shaded area) where Eqs. (9) and (10) represent ψ with about the same accuracy. In this region it is immaterial which one we use, and we can consider the change in c_a as taking place there.

In order that ψ_{II} be real, c_a must be chosen as follows. Let

$$c_a = c_b e^{(2\pi i/h)\delta}. \tag{11}$$

Then

$$\delta = -\int_P^{P'} y_a dx - \left[\int_P^{P'} y_b dx\right]^* \tag{12}$$

where the asterisk denotes the complex conjugate. Then, since in region II, $y_a = -y_b{}^*$, we can write

$$\psi_{II} = c_b\left[e^{(2\pi i\int_P^x y_b dx)^*/h} + e^{2\pi i\int_P^x y_b dx/h}\right]. \tag{13}$$

By a study of the integrals involved in δ it is not difficult to show that the same value of ψ_{II} is obtained by going around Q in either sense. That is to say, ψ_{II} is also single valued.

We proceed with the continuation of ψ into region III. In going around the point R we find by the same type of argument that c_a must change back to zero if ψ is to be bounded in that region. In region III y_a is the negative imaginary branch of y, and $i\int^x y_a dx$ becomes infinite for infinite x. So in region III we can easily make ψ bounded but the following relation must be satisfied in order to make it real.

$$(2\pi i/h)\int_P^x y_b dx = \text{real number} + \pi n i, \tag{14}$$

where x is now in region III and n is an integer. This can also be written

$$\int_P^x y_b dx + \left(\int_P^x y_b dx\right)^* = nh. \tag{15}$$

Now in Eq. (14) the path of integration went, say, above the points Q and R. In that case the complex conjugate of the integral is equal to the negative of the integral taken in the same direction but on a path going below Q and R.[7] Eq. (15) therefore becomes

$$\oint y dx = nh, \tag{16}$$

[7] This can be verified by using the fact that for real functions the conjugate of a function is the function of the conjugate argument. In applying this rule to square roots a change of branches must also be taken into account.

the path of integration being taken around region II, but including no singularities of y which lie off the real axis. In this equation it makes only a trivial difference if we use y_a instead of y_b.

Eq. (16) is also the condition that ψ be single valued in the sense that the same value of ψ is found no matter what the path of integration for $\oint y dx$ as long as it does not cross the cut QR.

We have shown that Eq. (16) is a necessary condition that E be a characteristic value of Eq. (1). The argument can easily be reversed to show that Eq. (16) is also a sufficient condition.

Wentzel's[1] original generalization of the Bohr phase integral is therefore justified, though the proof that we have given is more complicated than the considerations which Wentzel gave. However as Kramers[3] pointed out, a proof such as the one given above is necessary, because it shows the nature of Eq. (16) as essentially an asymptotic expression for the energy levels rather than an exact condition. Occasionally the series for $\oint y dx$ breaks off after a finite number of terms, in which case Eq. (16) gives exact values, but this does not occur generally.

Due to its asymptotic character, the series in Eq. (16) diverges for actual, finite values of B, and it can therefore be used to find energy levels only to a limited degree of approximation. The quality of the approximation is, in general, better for systems which are nearly classical than for those showing large quantum effects. This is not surprising since the first term of the energy level equation gives the classical Bohr theory.

The way in which the quality of the approximation depends on the presence of quantum effects is well illustrated by the case of a potential function with a sharp kink in it. This kink will give rise to characteristic quantum diffraction effects which would not be present if the kink were smoothed over. Suck a kink often arises from the presence of a singularity in the potential function near the real axis. If, in carrying the integral of Eq. (14) around Q and R we are forced to go near such a singularity, there will be a considerable part of the path for which Eq. (8) does not give a good approximation, and so the energy level formula will be relatively inaccurate.

We shall turn now to the connection between the methods of the present paper and the original work of Wentzel. His proof of Eq. (16) was based in part on a relation derived from Eq. (2), namely that $2\pi i\bar{y} = h\psi'/\psi$. Since wave functions are known to have n nodes in the region II, and since ψ' is not zero at these nodes, he inferred that $\bar{y}$ would have n simple poles in this region and that therefore the integral of $\bar{y}$ around these poles would be exactly nh. This argument, however, is not permissible because the ψ of Eq. (2) is not the characteristic solution. This is obvious since it requires a linear combination of such ψ's to represent the wave function in region II. In fact we can prove that $\bar{y}$ has no poles at all in the classical region of oscillation. (See below.)

Young[4] has recently developed a way of solving Eq. (1) which is very similar to the W. B. K. method. He introduces a quantity P, called the local momentum, which, on the real axis, is the real part of our function $\bar{y}$. Letting

$$\bar{y} = u + iv \tag{17}$$

where u and v are real functions of x, Eq. (3) separates into the following for real values of x.

$$hv'/2\pi = p^2 - u^2 + v^2 \tag{18}$$

and

$$hu'/2\pi = 2uv. \tag{19}$$

P is given by $hP = 2\pi u$, and Young has found that P has neither zero's nor poles on the real axis. It follows, since v is the logarithmic derivative of P, that v has no poles on the real axis either. Therefore $\bar{y}$ has no poles on the real axis.

How then can Eq. (16) be true? The answer to this has been given by Kramers.[3] Eq. (16) applies to the case in which we have expanded $\bar{y}$ in the series Eq. (4). This series converges asymptotically as B approaches zero for all values of x except those for which $E = V$. Such points are singular points in the expansion, and allow the integral in Eq. (16) to take on values different from zero. It should be noted that Eq. (16) tends asymptotically to zero as $B \to 0$ so that in the limit it behaves as if y had no poles. In other words, Eq. (16) refers to y and not to $\bar{y}$.

By a very simple analysis Young has derived an energy level condition in the form of a phase integral involving P, and it would be convenient if we could derive Eq. (16) directly from it, thus avoiding the use of asymptotic series and the like. Unfortunately this cannot be done because, as we have seen, the singularities which appear in the expansion for y (Eq. (8)), but which $\bar{y}$ does not possess, are essential for the usefulness of Eq. (16). Another difficulty, also connected with the asymptotic character of Eq. (8), is that though our expansion of y is purely imaginary in regions I and III, $\bar{y}$ must have a real component in those regions. This follows from the fact that P is nowhere zero. We must therefore conclude that the two methods use essentially different ways of representing the wave functions, and that there is no simple way of showing the equivalence of the results.

It is, however, worth noting that the two methods are complementary in that each has its own peculiar usefulness. Young's method brings out the physical significance of the situation very clearly, but is of limited use for actual computation because of the complicated differential equation from which P must be calculated. On the other hand, though the derivation of the W. B. K. energy level formula is rather long, it enables one to find energy levels by means of a very simple integration.

Simplification of the Formula

Having discussed the nature of Wentzel's energy level condition it remains only to put it in a more useful form. Using Eq. (8) we find that Eq. (16) is a series of integrals whose form is given by Eqs. (7). We shall consider them one by one.

The term in y_l is the Bohr theory integral. It cannot be simplified until we know something more about V.

The term in y_1 gives us the half integer quantization. It has been discussed in all of the literature on the subject.

The term in y_2 adds something new. Integrating by parts we find:

$$(h/2\pi i)^2 \oint y_2 dx = (h/2\pi)^2 (2m)^{-1/2} \oint (5V'^2 + 4V''(E-V))(E-V)^{-5/2} dx \tag{20}$$
$$= -(h^2/128\pi^2)(2m)^{-1/2} \oint V'^2 (E-V)^{-5/2} dx.$$

The term in y_3 vanishes. This can be shown very easily because from Eq. (7)

$$y_3 = -d(y_2/2y_0)/dx, \tag{21}$$

and this integrates to zero around the closed cycle.

The term in y_4 can be reduced by integrating by parts. The result is:

$$(h/2\pi)^4 \oint y_4 dx = -h^4\pi^{-4}m^{-1}(2m)^{-1/2}2^{-16}\Big[49 \oint V'^4 (E-V)^{-1/2} dx \tag{22}$$
$$- 16 \oint V'V''(E-V)^{-7/2} dx\Big].$$

Collecting all of these expressions and neglecting y_5 and higher terms, we find for Eq. (16)

$$\oint (E-V)^{1/2} dx - (B/32) \oint V'^2 (E-V)^{-5/2} dx$$
$$- (B^2/2048) \oint [49V'^4 (E-V)^{-11/2} - 16V'V'''(E-V)^{-7/2}] dx \tag{23}$$
$$+ \cdots = (n + \tfrac{1}{2}) 2\pi B^{1/2}.$$

where $n = 0, 1, 2, 3 \cdots$. This is as far as Eq. (16) can be simplified without more knowledge of the function V.

I am indebted to Professor E. C. Kemble for suggestions and discussions of various points raised in this paper.

The Energy Levels of a Rotating Vibrator

By J. L. DUNHAM
Harvard University

(Received May 11, 1932)

The energy levels of a rotating vibrator are calculated in considerable detail by means of the Wentzel-Brillouin-Kramers method. The new terms determined are $\omega_e z$ and a set of correction terms which appear in the earlier members of the equation. These correction terms enter in such a way that ω_e is not exactly the coefficient of $(v+\frac{1}{2})$; B_e is not exactly the coefficient of $K(K+1)$, etc. However the differences are small and are detectable only in the case of light molecules. The correction terms are of the magnitude of B_e^2/ω_e^2. Formulas for the effect of the correction terms on isotope shifts are given, and for the calculation of the correction terms themselves. Also a method is given for obtaining actual potential functions from band spectrum data, based on Morse's potential function. Finally the numerical magnitude of the correction terms for several states of H_2 and for NaH is discussed.

INTRODUCTION

RECENT work on the measurement of isotope masses by means of band spectra[1,2,3] has led to the necessity of examining in more detail the theory of a rotating vibrator. The energy levels of this sytem were thoroughly investigated by Kratzer,[4] Born and Hückel,[5] Kemble[6] and Birge[7] on the basis of the Bohr theory, but no detailed quantum mechanical treatment of this system has been published. This seems to be at least partly because the potential function suggested by Morse[8] has energy levels which agree exactly with those predicted for it by the Bohr theory[9] (apart from the matter of half quantum numbers), and which fit the empirical energy levels remarkably well. Furthermore, the early work of Fues[10] indicated an almost complete agreement between the two theories for quite general potential functions, the difference between Fues' result and that of the Bohr theory being merely a constant term, spectroscopically undetectable. Calculation of the higher approximations, however, shows that this constant term is one of a set of terms which in general depend on the vibrational and rotational quantum numbers, adding small corrections to the familiar terms in the energy level formula. It happens that for Morse's potential function the corrections to the pure vibra-

[1] R. T. Birge, Phys. Rev. **37**, 841, 227, and 233 (1931).
[2] F. A. Jenkins, Phys. Rev. **39**, 549 (1932).
[3] Mecke and Wurm, Zeits. f. Physik **61**, 37 (1930).
[4] A. Kratzer: Zeits. f. Physik **3**, 289 (1920).
[5] M. Born and Hückel, Phys. Zeits. **24**, 1 (1923).
[6] E. C. Kemble, J. Opt. Soc. Am. **12**, 1 (1926).
[7] R. T. Birge, Nature **116**, 783 (1925) and Phys. Rev. **27**, 245 (1926). See also W. C. Pomeroy, Phys. Rev. **29**, 67 (1927).
[8] P. M. Morse, Phys. Rev. **34**, 57 (1929).
[9] P. M. Davidson and W. C. Price, Proc. Roy. Soc. **A130**, 105 (1931).
[10] E. Fues, Ann. d. Physik **80**, 367 (1926).

tion terms are exactly zero which leads us to expect they will be small in actual molecules. But the predictions of Morse's function for the corrections to the rotational terms are not zero, so we cannot expect these to be small.

The analysis shows that the coefficients of the various powers of $(v+\frac{1}{2})$ and $K(K+1)$ in the energy level formula are really a series in powers of the ratio B_e^2/ω_e^2. This ratio is, for most molecules, of the order of magnitude of 10^{-6} so that all of the terms beyond the first (given by the Bohr theory) are negligible. However, for hydrogen molecules and some of the hydrides this ratio is more nearly 10^{-3}, so that in these cases they cannot be neglected.

In this paper the energy levels of a rotating vibrator will be calculated in detail using a perfectly general type of potential function. To find the characteristic values of Schrödinger's equation we shall use the Wentzel-Brillouin-Kramers[11] method (hereafter called the W. B. K. method) because it solves our problem in a very simple fashion. The particular advantage of this method is that it uses the Bohr theory energy levels as its first approximation, correcting for higher quantum effects by its later approximations. Now according to the correspondence principle point of view, quantum effects become small not only for large quantum numbers, but also for large masses, and the nuclei of molecules have large masses compared to electronic masses. We would therefore expect the Bohr energy levels to be good approximations in this case. The W. B. K. method can make use of this fact by starting with the Bohr levels and calculating any further terms as small corrections. The details of the W. B. K. method necessary for application to this problem have been developed in the preceding paper and we shall apply them here to the solution of the rotating-vibrator, and then discuss applications to a few actual molecular states.

Calculation of the Energy Levels

Our first problem is to find the energy levels of a rotating vibrator. To do this we calculate the characteristic values of Schrödinger's equation for this system, which is:

$$\frac{d^2\psi}{d\xi^2}+\frac{8\pi^2 m r_e^2}{h^2}\left[E-V-\frac{h^2K(K+1)}{8\pi^2 r_e^2 m(1+\xi)^2}\right]\psi=0. \tag{1}$$

Here $\xi=(r-r_e)/r_e$, r_e being the equilibrium nuclear separation; m is the reduced nuclear mass; V the potential function with a minimum at r_e; and the last term in the bracket, which we shall call V_r, is due to the centrifugal force of rotation.

It would be convenient to use a potential function based on that of Morse, because this gives a very good approximation to actual energy levels. However, it is difficult to include the effect of rotation in Morse's potential function. In the end the simplest procedure is to use a power series expansion of

[11] G. Wentzel, Zeits. f. Physik **38**, 518 (1926); L. Brillouin, Comptes Rendus **183**, 24 (1926); H. A. Kramers, Zeits. f. Physik **39**, 828 (1926). For a good short account see A. Sommerfeld: Ergänzungsband, p. 158.

V around the point $\xi=0$, as V_r has a particularly simple expansion about this point. Having found the energy levels in terms of this sort of expansion, it is not difficult then to rewrite the formulas in terms of any simple expression for the potential function by expanding the latter in a power series about $\xi=0$ and equating coefficients. We shall therefore use

$$V = hca_0\xi^2(1 + a_1\xi + a_2\xi^2 + a_3\xi^3 + \cdots) \tag{2}$$

where $a_0=\omega_e^2/4B_e$; ω_e is the classical frequency of small oscillations expressed in cm^{-1} and $B_e=h/(8\pi^2mr_e^2c)$.

We shall first calculate the energy levels neglecting rotation (i.e., for the case $K=0$). The effect of rotation can then be found by rewriting the whole effective potential function in the form of Eq. (2) and comparing coefficients.

In the preceding paper I showed that the energy levels of a potential function with a single minimum could be found by evaluating a generalized phase integral (Eq. (23) of that paper). It will be convenient to express all quantities involving energy in this equation in terms of wave numbers. This involves replacing E by hcF and V by hcU. Eq. (23) then becomes

$$\oint (F-U)^{1/2}d\xi - (B_e/32)\oint U'^2(F-U)^{-5/2}d\xi + \cdots = 2\pi B_e^{1/2}(v+\tfrac{1}{2}). \tag{3}$$

The first integral on the left has been evaluated many times.[4,5,6] However, the method necessary to evaluate the second integral is also applicable to the first, and handles it in a particularly simple fashion, so we shall use it here.

The first step is to transform to the independent variable U. The integral becomes

$$\oint (F-U)^{1/2}d\xi = \oint (F-U)^{1/2}(U')^{-1}dU. \tag{4}$$

Here the integral is taken in the U plane twice around the two points $U=0$ and $U=F$ (the origin of energy being so chosen that $U=0$ for $\xi=0$). The cut in the ξ plane between the two turning points goes over into a cut in the U plane between the origin and the point $U=F$.

The integral can be evaluated if we know U' as a function of U, so we expand U'

$$U' = A_1U^{1/2} + A_2U + A_3U^{3/2} + A_4U^2 + \cdots, \tag{5}$$

from which we can calculate $(U')^{-1}$ in a series of the form

$$(U')^{-1} = A_1^{-1}U^{-1/2}[1 + B_1U^{1/2} + B_2U + B_3U^{3/2} + \cdots]. \tag{6}$$

We can therefore write the integral as:

$$\oint (F-U)^{1/2}d\xi = \oint iA_1^{-1}[1 - F/2U - F^2/8U^2 + \cdots][1 + B_1U^{1/2} + B_2U + \cdots]dU. \tag{7}$$

There is now a cut in the U plane extending from the point $U=0$ to ∞, introduced by the expansion Eq. (5). Consequently when the integration is performed all of the terms in $U^{n/2}$ for which n is odd will vanish because the integrand will have opposite signs on the two circuits around the point $U=0$. Of the remaining terms only those in U^{-1} will have a residue. The integration yields:

$$\oint (F-U)^{1/2}d\xi = (2\pi/A_1)[F + B_2F^2/4 + B_4F^3/8 + 5B_6F^4/64 + \cdots]. \quad (8)$$

The second integral in Eq. (3) can be evaluated similarly. As before we transform to U as independent variable. On substituting the expansion Eq. (5) for U' and expanding the denominator, we have

$$\oint U'(F-U)^{-5/2}dU = 4\pi[A_3 + 5A_5F/2 + 35A_7F^2/8 + 105A_9F^3/16 + \cdots]. \quad (9)$$

We have now evaluated the integrals of Eq. (3) in terms of the coefficients A_n of Eq. (5), and it remains to find these A_n's in terms of the a_n's of Eq. (2). If we expand $U^{n/2}$ and U' as power series in ξ and substitute all of these in Eq. (5), we can equate coefficients of like powers of ξ on both sides of the equation and obtain enough relations to determine the coefficients A_n.

The results of this procedure are:

$$\begin{aligned}
A_1 &= 2a_0^{1/2};\ A_2 = 2a_1;\ A_3 = a_0^{-1/2}(3a_2 - 7a_1^2/4)\\
A_4 &= a_0^{-1}(4a_3 - 6a_1a_2 + 5a_1^3/2)\\
A_5 &= a_0^{-3/2}(5a_4 - 19a_1a_3/2 - 17a_2^2/4 + 105a_1^2a_2/8 - 273a_1^4/64)\\
A_6 &= a_0^{-2}(6a_5 - 14a_1a_4 - 12a_2a_3 + 22a_1^2a_3 + 20a_1a_2^2 - 30a_1^3a_2 + 8a_1^5)\\
A_7 &= a_0^{-5/2}(7a_6 - 39a_1a_5/2 - 33a_2a_4/2 - 31a_3^2/4 + 279a_1^2a_4/8 + 75a_2^3/8\\
&\quad + 243a_1a_2a_3/4 - 825a_1^3a_3/16 - 2277a_1^2a_2^2/32 + 9009a_1^4a_2/128\\
&\quad - 8151a_1^6/512).\\
&\quad \cdots\cdots\cdots\cdots\cdots\cdots\cdots\cdots
\end{aligned} \quad (10)$$

We are now ready to go back to Eq. (3) and substitute the results we have obtained for the integrals. We shall at first express these in terms of the A_n's and B_n's for simplicity, using the a_n's only at the end.

Substituting Eqs. (8) and (9) in Eq. (3) we have

$$\begin{aligned}
&(2\pi/A_1)[F + B_2F^2/4 + B_4F^3/8 + 5B_6F^4/64 + \cdots]\\
&\quad - (2\pi B_e/16)[A_3 + 5A_5F/2 + 35A_7F^2/8 + \cdots] = 2\pi B_e^{1/2}(v+\tfrac{1}{2}).
\end{aligned} \quad (11)$$

By the inversion of this series we find F as a power series in $(v+\frac{1}{2})$. The result is:

$$\begin{aligned}
F &= B_eA_1A_3/16 + A_1B_e^{1/2}(v+\tfrac{1}{2}) + (B_e^{3/2}A_1^2/32)(5A_5 - B_2A_3)(v+\tfrac{1}{2})\\
&\quad - (B_eB_2A_1^2/4)(v+\tfrac{1}{2})^2 + (B_e^2A_1^3/128)(35A_7 - 15B_2A_5 + 3A_3B_2^2\\
&\quad - 3A_3B_4)(v+\tfrac{1}{2})^2 + (B_e^{3/2}A_1^3/8)(B_2^2 - B_4)(v+\tfrac{1}{2})^2\\
&\quad + (B_e^2A_1^4/64)(10B_2B_4 - 5B_2^3 - 5B_6)(v+\tfrac{1}{2})^4 + \cdots.
\end{aligned} \quad (12)$$

Substituting Eqs. (10) gives us the term value equation for an oscillator having Eq. (2) for a potential function up to and including terms in B_e^4/ω_e^4. (One term, not depending on $(v+\frac{1}{2})$, has been omitted.)

Before we carry out this substitution, however, it will be convenient to take account of rotation. In this case the effective potential function is $U+U_r=U_K$, which is of the form

$$U_K = a_0\xi^2(1 + a_1\xi + a_2\xi^2 + \cdots) + B_eK(K+1)(1 - 2\xi + 3\xi^2 - 4\xi^3 + \cdots). \quad (13)$$

We can introduce a new variable η such that $\xi=\eta+\epsilon$, ϵ being a constant, and choose ϵ so that the minimum of U_K falls at the point $\eta=0$. If we then express U_K as a power series in η of the same form as Eq. (2), and use the coefficients of this new series in Eq. (12) instead of the a_n's, we shall have the energy levels of a rotating vibrator.

The detail of determining these coefficients is rather tedious but quite straightforward, so we shall not reproduce it here. The energy level equation which one finds is most conveniently written in the following form

$$F_{vK} = \sum_{ij} Y_{ij}(v+\tfrac{1}{2})^i K^j(K+1)^j. \quad (14)$$

The first subscript under Y refers to the power of the vibrational quantum number, the second to that of the rotational quantum number.

The first fifteen Y_{ij}'s are found to be [12]

$$Y_{00} = (B_e/8)(3a_2 - 7a_1^2/4)$$

$$Y_{10} = \omega_e[1 + (B_e^2/4\omega_e^2)(25a_4 - 95a_1a_3/2 - 67a_2^2/4 + 459a_1^2a_2/8 - 1155a_1^4/64)]$$

$$Y_{20} = (B_e/2)[3(a_2 - 5a_1^2/4) + (B_e^2/2\omega_e^2)(245a_6 - 1365a_1a_5/2 - 885a_2a_4/2 - 1085a_3^2/4 + 8535a_1^2a_4/8 + 1707a_2^3/8 + 7335a_1a_2a_3/4 - 23865a_1^3a_3/16 - 62013a_1^2a_2^2/32 + 239985a_1^4a_2/128 - 209055a_1^6/512)]$$

$$Y_{30} = (B_e^2/2\omega_e)(10a_4 - 35a_1a_3 - 17a_2^2/2 + 225a_1^2a_2/4 - 705a_1^4/32)$$

$$Y_{40} = (5B_e^3/\omega_e^2)(7a_6/2 - 63a_1a_5/4 - 33a_2a_4/4 - 63a_3^2/8 + 543a_1^2a_4/16 + 75a_2^3/16 + 483a_1a_2a_3/8 - 1953a_1^3a_3/32 - 4989a_1^2a_2^2/64 + 23265a_1^4a_2/256 - 23151a_1^6/1024)$$

$$Y_{01} = B_e[1+(B_e^2/2\omega_e^2)(15+14a_1-9a_2+15a_3-23a_1a_2+21(a_1^2+a_1^3)/2)]$$

[12] Eq. (14) can be changed to a set of power series in $(K+1/2)^2$ instead of $K(K+1)$ by using the formulas

$$K^n(K+1)^n = [(K+\tfrac{1}{2})^2 - \tfrac{1}{4}]^n$$

This will affect only the second order terms (of the order of B_e^2/ω_e^2) in each of the Y's.

$$Y_{11} = (B_e^2/\omega_e)[6(1+a_1)+(B_e^2/\omega_e^2)(175+285a_1-335a_2/2+190a_3-225a_4/2 + 175a_5 + 2295a_1^2/8 - 459a_1a_2 + 1425a_1a_3/4 - 795a_1a_4/2 + 1005a_2^2/8 - 715a_2a_3/2 + 1155a_1^3/4 - 9639a_1^2a_2/16 + 5145a_1^2a_3/8 + 4677a_1a_2^2/8 - 14259a_1^3a_2/16 + 31185(a_1^4 + a_1^5)/128)] \quad (15)$$

$$Y_{21} = (6B_e^3/\omega_e^2)(5 + 10a_1 - 3a_2 + 5a_3 - 13a_1a_2 + 15(a_1^2 + a_1^3)/2)$$

$$Y_{31} = (20B_e^4/\omega_e^3)(7 + 21a_1 - 17a_2/2 + 14a_3 - 9a_4/2 + 7a_5 + 225a_1^2/8 - 45a_1a_2 + 105a_1a_3/4 - 51a_1a_4/2 + 51a_2^2/8 - 45a_2a_3/2 + 141a_1^3/4 - 945a_1^2a_2/16 + 435a_1^2a_3/8 + 411a_1a_2^2/8 - 1509a_1^3a_2/16 + 3807(a_1^4 + a_1^5)/128)$$

$$Y_{02} = -(4B_e^3/\omega_e^2)[1 + (B_e^2/2\omega_e^2)(163 + 199a_1 - 119a_2 + 90a_3 - 45a_4 - 207a_1a_2 + 205a_1a_3/2 - 333a_1^2a_2/2 + 693a_1^2/4 + 46a_2^2 + 126(a_1^3 + a_1^4/2))]$$

$$Y_{12} = -(12B_e^4/\omega_e^3)(19/2 + 9a_1 + 9a_1^2/2 - 4a_2)$$

$$Y_{22} = -(24B_e^5/\omega_e^4)(65 + 125a_1 - 61a_2 + 30a_3 - 15a_4 + 495a_1^2/4 - 117a_1a_2 + 26a_2^2 + 95a_1a_3/2 - 207a_1^2a_2/2 + 90(a_1^3 + a_1^4/2))$$

$$Y_{03} = 16B_e^5(3 + a_1)/\omega_e^4$$

$$Y_{13} = (12B_e^6/\omega_e^5)(233 + 279a_1 + 189a_1^2 + 63a_1^3 - 88a_1a_2 - 120a_2 + 80a_3/3)$$

$$Y_{04} = -(64B_e^7/\omega_e^6)(13 + 9a_1 - a_2 + 9a_1^2/4).$$

The new quantities are Y_{40}, Y_{13} and the second terms [13] in $Y_{10}Y_{20}Y_{01}Y_{11}Y_{02}$.

The connection between the Y's and the ordinary band spectrum constants is as follows:

$Y_{10} \sim \omega_e$	$Y_{20} \sim -\omega_e x$	$Y_{30} \sim \omega_e y$
$Y_{01} \sim B_e$	$Y_{11} \sim -\alpha_e$	$Y_{21} \sim \gamma_e$
$Y_{02} \sim D_e$	$Y_{12} \sim \beta_e$	$Y_{40} \sim \omega_e z$
$Y_{03} \sim F_e$	$Y_{04} \sim H_e$	

Throughout this paper the Y_{lj}'s will be used to denote the coefficients in Eq. (14), and the old coefficients will retain their mechanical significance. Thus B_e will be used only for $h/8\pi^2 I_e c$ and not for the coefficient of $K(K+1)$ in the energy level equation, etc.

Discussion of the Energy Level Formula

The most important point about Eq. (15) is that the Y's are not exactly equal to the coefficients given by the Bohr theory. For example, Y_{10}, which is the coefficient of $(v+\frac{1}{2})$, is not equal to ω_e, but differs from it by terms in B_e^2/ω_e^2. Similarly Y_{01} differs from B_e by small terms. In fact each of the Y's

[13] The second term in Y_{00} has been omitted because it is not important. It has the same form as Y_{40} or the second term in Y_{20}.

is a power series in B_e^2/ω_e^2. Now for many molecules this ratio is of the order of magnitude of 10^{-6} so that the first term of the power series is adequate for all practical purposes. But for some molecules, notably H_2, B_e^2/ω_e^2 is more nearly 10^{-3}, and higher terms in several of the Y's must be taken into consideration. This correction arises from the presence of the second term on the left hand side of Eq. (3), and one can see from the fact that m appears in the denominator of this term that the corrections will be small for heavy systems and large for light ones. It is for this reason that these terms will be most easily detectable in H_2.

Unfortunately the detection of the effect of these higher terms in actual spectra will be complicated by the fact that the nuclear potential function is defined only in so far as the nuclear and electronic wave functions are separable. This is ordinarily true to terms in B_e^2/ω_e^2, which means that this coupling will introduce terms of nearly the same size as the new terms which we have been discussing. In cases where the interaction is very large, such as l-uncoupling or when there are perturbations, the coupling effects will be much more important than the effects discussed here. This state of affairs can be detected by using the fact that for a simple rotator Y_{02} (D_e) is determined by the other Y's. The values of Y_{10} and Y_{11} determine all of the a_n's. Consequently Y_{02} can be found in terms of these Y's. If this theoretical value of Y_{02} does not agree with the observed value, the system is not a simple rotating vibrator, and we can expect that there is appreciable interaction. It is therefore important to find Y_{02} as accurately as possible from the data, as it is necessary to show that coupling effects are small before one can determine the size of the correction terms.

One of the chief uses of a detailed derivation of the energy level equation is to find how the terms depend on the nuclear mass. By definition we know that B_e is proportional to m^{-1} and that ω_e is proportional to $m^{-1/2}$, so we can find the mass dependence of the Y's if we assume that two isotopic molecules have identical potential functions.

The Bohr theory leads to the result suggested by Kemble[14] that

$$(Y_{lj}^i/Y_{lj}) = (m/m^i)^{(l+2j)/2} \tag{16}$$

the superscript i referring to one of the isotopes, but this equation takes account of only the first terms in the expressions for the Y's. The presence of the new correction terms will alter the mass dependence of the Y's, as they are now of the form

$$Y_{lj} = f_{lj}(B_e, \omega_e)\ [\alpha_{lj} - (B_e^2/\omega_e^2)\,\beta_{lj} + \cdots] \tag{17}$$

where $f_{lj}(B_e, \omega_e)$ contains that part of the first term in Y_{lj} which depends on m, whereas α_{lj} and β_{lj} do not depend on m. Since B_e^2/ω_e^2 is small, Eq. (16) now becomes

$$(Y_{lj}^i/Y_{lj}) = (m/m^i)^{l/2+j}[1 + (\beta_{lj}B_e^2/\alpha_{lj}\omega_e^2)((m - m^i)/m^i)] \tag{18}$$

[14] R. S. Mulliken, Phys. Rev. 25, 126 (1925).

This gives us a simple way of finding the correction to the isotope effect due to the presence of the new correction terms in the energy level formula.

We want to be able to find the coefficients β (in Eq. (17)) from the experimental data. This is simplified by the fact that these correction terms are small enough so that we can use a method of successive approximations. If we regard the Y's as being given experimentally, and if we neglect the correction terms, a set of approximate a_n's can be calculated from the Y_{l0}'s and the Y_{l1}'s. These a_n's can then be used to calculate the correction terms with sufficient accuracy for most purposes. Carrying out this procedure algebraically we find the following equations for the corrections which are designated by β_{lj}.

$$\begin{aligned}
\beta_{01} &= Y_{10}^2Y_{21}/4Y_{01}^3 + 16a_1Y_{20}/3Y_{01} - 8a_1 - 6a_1^2 + 4a_1^3 \\
\beta_{10} &= 5Y_{10}Y_{30}/4Y_{01}^2 + a_1Y_{10}^2Y_{21}/3Y_{01}^3 - 10a_1 - 20a_1^2 - 15a_1^3/2 \\
&\quad - 5a_1^4/2 + Y_{20}(4a_1 + 16a_1^2/3)/Y_{01} + Y_{20}^2/2Y_{01}^2 \\
\beta_{02} &= 73/2 + 37a_1 + 67a_1^2/2 + 33a_1^3 - 6a_1^4 - 9Y_{10}Y_{30}/2Y_{01}^2 \\
&\quad + Y_{10}^2Y_{21}(3 - 11a_1/6)/2Y_{01}^3 - Y_{20}(130/3 + 4a_1 + 74a_1^2/3)/2Y_{01} \\
&\quad + 31Y_{20}^2/9Y_{01}^2 \\
a_1 &= (Y_{11}Y_{10}/6Y_{01}^2) - 1
\end{aligned} \tag{19}$$

The other β's (β_{20}, β_{11}, and others not given in Eqs. (15)) are more complicated but can be calculated in the same fashion. Eqs. (19) are not as simple as the expressions for the corresponding β's in Eqs. (15). However to use Eqs. (19), it is not necessary to calculate all of the a_n's involved first.

In view of the importance of Morse's[8] potential function for vibrational analysis we shall discuss briefly its relation to the formulas which we have used.

The most striking property of Morse's potential function is the simplicity of the energy level equation to which it leads. It is interesting to see how this simplicity arises in the method we have used for calculating energy levels. Morse's potential function can be written

$$U = D(1 - e^{-a\xi})^2. \tag{20}$$

From this it is easy to show that

$$U' = 2a(DU)^{1/2} - 2aU. \tag{21}$$

Comparing with Eq. (5) we see that for this case

$$A_1 = 2aD^{1/2} \quad A_2 = -2a \tag{22}$$

and that all the other A's are zero. Now all of the Y_{l0}'s, except Y_{10} and Y_{20}, involve A_n's with $n \geqq 3$ so that they vanish, and the same is true of all of the terms beyond the first in Y_{10} and Y_{20}. A similar but no so far reaching simplification can be found in the case of Kratzer's potential function. This accounts in detail for the fact that the Bohr theory with half quantum numbers gives Morse's energy levels exactly.[9]

Because of its simplicity and because it represents actual molecular energy levels so well, it would be convenient to have a relatively simple potential function based on that of Morse. One could then determine a potential curve from band frequencies more easily than at present. The most satisfactory way to do this seems to be to write the potential function in the following form. (The a used here is equal to Morse's a multiplied by r_e.)

$$U = D[(1 - e^{-a\xi})^2 + P_4(1 - e^{-a\xi})^4 + P_5(1 - e^{-a\xi})^5 + \cdots]. \qquad (23)$$

This can be expanded about the point $\xi = 0$ in a power series and the a_n's so determined can be substituted in Eqs. (15) and then the P's determined in terms of the Y's. Morse determined a from the relation $a\ ^2B_e = -\omega_e x$. We shall use

$$a = 1 - (Y_{10}Y_{11}/6Y_{01}^2). \qquad (24)$$

Then the P_n's can be expressed as follows:

$$\begin{aligned} P_4 &= (2/3)[1 + Y_{20}/Y_{01}a^2] \\ P_5 &= [Y_{10}^2Y_{21}/6Y_{01}^3 - 5 + 10a - 23a^2/4 + 7a^3/6 - 3P_4a^2(a-1)]/5a^3 \qquad (25) \\ P_6 &= Y_{10}Y_{30}/5a^4Y_{01}^2 + P_4/5 - 17P_4^2/20 - P_5. \end{aligned}$$

Now since the first term in Eq. (23) is a very good representation of actual potential functions we would expect the P_n's to be quite small and Eq. (23) should converge rapidly.

In calculating Eqs. (25) the new correction terms were *not* used. For obtaining graphical potential functions they are not of enough importance. It should also be mentioned that although the P_n's make corrections to the heat of dissociation predicted by Morse's potential function, it is not to be supposed that these corrections are very reliable. It has been repeatedly shown that the extrapolation of energy levels to dissociation can be used only when most of the energy levels are actually known.

Discussion of Actual Data

We turn now to the calculation of the correction terms for some actual molecular states. These terms are most important in the case of the H_2 molecule. The upper states are known to show a good deal of l-uncoupling,[15] as can be seen easily from the difference between the observed and calculated values of $Y_{02}(D_e)$. The normal state of the molecule should be quite free from such coupling effects, but unfortunately the vibrational analysis has not been carried through with enough precision to be able to tell definitely whether or not this is the case.[16]

Nevertheless it is possible to see how large the correction terms will be for

[15] W. Weizel, Zeits. f. Physik **55**, 483 (1929) and **56**, 727 (1929); G. H. Dieke, Zeits. f. Physik **55**, 447 (1929).

[16] Birge and Jeppeson (Nature **125**, 463 (1930)) have found evidence for a "perturbation" of this lowest level, but there is not yet enough data on the constants of this state to determine the nature of the perturbation.

several states of this molecule, and they will give us some idea of what to expect.

For the normal state Hyman[17] has found the following values for the Y's

$$\begin{aligned} Y_{10} &= 4371 \qquad Y_{11} = 2.794 \\ Y_{01} &= 60.59 \qquad Y_{21} = 0.0105 \\ Y_{20} &= 113.5. \end{aligned} \tag{26}$$

From these β_{01} can be calculated and turns out to be

$$\beta_{01} = -1.37.$$

Also

$$B_e^2/\omega_e^2 = 1/5200.$$

So we conclude that Y_{01} differs from B_e by one part in 3790. In a careful analysis this would be detectable.

Similarly, using data from the analyses of Richardson and Davidson,[18] we find that for the $2^1\Sigma$ state

$$\begin{aligned} Y_{01} &= B_e(1 - 1/778) \\ Y_{10} &= \omega_e(1 - 1/9240) \\ Y_{02} &= D_e(1 - 1/213). \end{aligned} \tag{27}$$

Although in Y_{10} the correction is very small, it is obviously not negligible in either of the other two.

The behavior of the corrections for this state is of some interest as it seems to be typical. The correction to Y_{10} is very small. If Morse's potential function were correct it would be zero, and the fact that it is small shows that Morse's function is a good approximation. Now Morse's function is known to be a better fit for most molecules than for H_2,[9] so we would expect β_{10} to be even smaller for other molecules than it is here.

The correction to Y_{02} is quite large. This appears to be a typical behavior as can be seen from the fact that the value of β_{02} predicted by Morse's potential function varies between 10 and 500 for moderate values of a. This is considerably larger than the other β's we have been discussing.

In the $2^3\Sigma$ state[18] we find that the corrections are quite small. β_{02} is the largest, being equal to 5.2 so that

$$Y_{02} = D_e(1 - 1/1165).$$

The other two are negligible.

The corrections to Y_{20} and Y_{11} demand a knowledge of Y_{40} and of Y_{31}, but as these coefficients have not been determined for the states of H_2 it is not possible to find the corresponding corrections.

[17] H. H. Hyman, Phys. Rev. **36**, 187 (1930).
[18] O. W. Richardson and P. M. Davidson, Proc. Roy. Soc. **A125**, 23 (1929).

An interesting case arises in the alkali hydrides.[19] They are the only known bands for which Y_{20} is positive. We might therefore expect the correction terms to be abnormally large. Weizel[20] has tried to explain the strange behavior of these bands as due to l-uncoupling, but there also appears to be an abnormality in the pure vibration states, and it is therefore of interest to see how the corrections turn out in this case.

The best data available appear to be on NaH.[19] The value of B_e^2/ω_e^2 is 0.0000310 which is materially smaller than for the states of H_2. In this respect LiH would be the most suitable substance for finding large effects. The corrections are

$$\begin{aligned} Y_{01} &= B_e(1 - 1/2280) \\ Y_{10} &= \omega_e(1 - 1/3920) \\ Y_{02} &= D_e(1 - 1/886). \end{aligned} \tag{28}$$

In terms of β_{lj}'s one finds

$$\beta_{01} = -14.15 \qquad \beta_{10} = -8.23 \qquad \beta_{02} = -36.4.$$

These β's are, on the whole, larger than those for H_2 which indicates a slightly anomalous behavior of the potential function. The relatively small value of B_e^2/ω_e^2 prevents these large values of β from making large corrections to the Y's.

For molecules heavier than hydrides, the values of B_e^2/ω_e^2 are so small that unless the β's are abnormally large, the corrections will be undetectable.

A large part of this paper was prepared while I was a National Research Fellow at the University of Chicago. I wish to take this opportunity to express my appreciation of the grant of a Fellowship and of the generous way in which the facilities of the Ryerson Laboratory were placed at my disposal.

[19] LiH, G. Nakamura, Zeits. f. Physik **59**, 218 (1930); NaH, T. Hori, Zeits. f. Physik **62**, 352 (1930); KH, G. M. Almy and C. D. Hause, Phys. Rev. **39**, 178 (1932).

[20] W. Weizel, Zeits. f. Physik **60**, 599 (1930).

Rotational Analysis of Some CO_2 Emission Bands. Part I

By R. F. SCHMID
Ryerson Physical Laboratory, University of Chicago

By using the light of a hollow cathode discharge and that of a Back box with direct current, the red degraded CO_2 bands at λλ3247, 3254, 3370, 3377, 3503, 3511, 3534, 3545, 3674 and 3839A have been photographed in the third order of a 21 foot Rowland grating and analyzed. The bands are composed of *P* and *R* branches and on first inspection they show no alternately missing lines. The lines of the bands at λλ3254, 3377, 3511, 3534, and 3839A show staggering, while the lines of the other bands do not (in the limit of observational accuracy). The single structure of the bands indicates that the molecule is linear in both initial and final states. The distance between the carbon and an oxygen atom computed from the rotational constants is almost the same as computed from the CO and CO^+ bands. The above enumerated bands show no Zeeman effect of the observable lines. Other bands which are found to show more complicated structure and Zeeman effect will be the subject of further investigations.

EXPERIMENTAL

AS ALREADY reported,[1] the emission spectrum of CO_2 can be obtained in suitable intensity by pumping tank CO_2 quickly through a Back box, using a direct current discharge, the magnet pole-pieces serving as cathodes and a piece of tungsten between them as the anode. Besides the strong CO_2 bands, the plates show the entire, but weaker CO^+ spectrum, the third positive CO bands and rather strong angstrom bands. To suppress the CO and CO^+ bands the CO_2 pressure was kept about 4–6 cm Hg and the gas-streaming was made as fast as possible (the use of a *Hypervac* pump brought some success in that direction). The CO_2 consumption was about 5–6 kg per day exposure. In starting with low gas pressure and low current and gradually increasing both and by using magnetic field strengths over 12,000 gauss, the discharge could be kept on one of the magnet pole-pieces with a maximal current of 700–800 milliamperes. In this way the luminosity was enough to give strong third order pictures with the 21 foot grating in 50 hours exposure-time.

As already mentioned[1] some of the CO_2 bands show magnetic effects, and because the discharge in the Back box could not be concentrated on the one pole-piece front in suitable intensity without magnetic fields, it seemed necessary to find another source, which would give a strong CO_2 spectrum without any magnetic field. The steel hollow-cathode in the arrangement sketched in Fig. 1 was fastened in the center of a three liter bulb, the neck of which was cooled. A steel anode was placed 5 cm away from the cathode. This arrangement gave very satisfactory results in respect to CO_2 luminosity and relative weakness of CO and CO^+ bands. Of course, the spectrum contained some iron lines also, but no other metal could be used because of the high CO_2 pressure. Graphite, aluminum, tin, etc., burned away in a short time.

[1] R. F. Schmid, Phys. Rev. **39**, 589 (1932).

Some considerations (see below) showed it desirable to determine the effective emission temperature of the source used, which could be done by studying the rotational intensity distribution of certain well-known bands

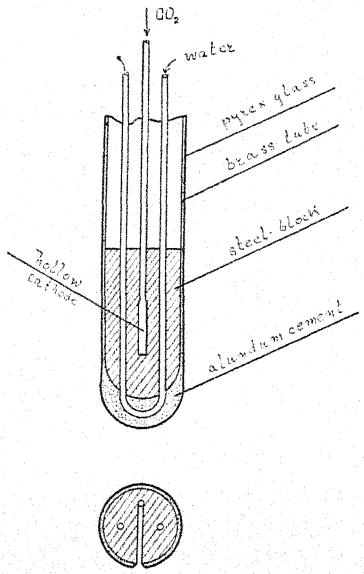


Fig. 1. Steel hollow cathode water-cooled and with direct gas-inlet in the hollow part itself.

present in the spectra. The λ 4835A, 0→1 angstrom band, having clear background and only a few overlappings, was especially suitable for that purpose and showed the maximal intensity in its P branch at $K''_{max}=15$ in the Q branch at $K''_{max}=14$ and in the R branch at $K''_{max}=13$. By using the formulas:[2]

$$P \text{ branch} \qquad kT = B'(K_{max}'' - 1)(2K_{max}'' - 1)$$

$$Q \text{ branch} \qquad kT = B'\tfrac{1}{2}(2K_{max}'' + 1)^2$$

$$R \text{ branch} \qquad kT = B'(K_{max}'' + 2)(2K_{max}'' + 3)$$

(where k is the Boltzmann factor and $B'=1.94$ cm^{-1}), it was found, in very good agreement for all the three branches: $kT=800$ cm^{-1}, that is $T=870$°C.

Besides that, having pictures on which (due to leaks) the λ3914A (0→0) and λ4278 (0→1) N_2^+ bands were also present, in which bands the maximum seemed to be between $K''_{max}=12$ for the stronger half R branch and $K''_{max}=13$ for the weaker odd numbered set, we have, by using the formula[3]

$$kT = B'(K_{max}'' + 1)(2K_{max}'' + 3)$$

with $B'=2.07$ cm^{-1} the value $kT=845$ cm^{-1} slightly higher than the above given one for CO, in agreement with what seems to be usual for ionized molecules.[4]

[2] F. London and H. Hönl, Zeits. f. Physik **33**, 803 (1925).
[3] R. S. Mulliken, Phys. Rev. **30**, 138 and 785 (1927).
[4] L. S. Ornstein, Zeits. f. Physik **49**, 315 (1928).

Results

The most recent report on the CO_2 emission spectrum—on the basis of low-dispersion photographs, however—was given by Smyth.[5] Comparing the pictures given by him in his Fig. 2, parts *a* and *b*, with the present plates, some differences were noticed, which are due probably to differences in methods of excitation.

(1) Smyth's electron beam discharge seems to be cooler than the present one, which gives better developed bands and is more suitable for rotational analysis purposes, while his pictures are more useful for a vibrational analysis.

(2) According to Smyth: . . . "from λ2900 to λ3500 the bands occur in five well-defined groups . . . from 3500 to 4000 is a terrific tangle." In the present pictures however, the bands from λ3500 to λ4000, as well as those from λ2900 to λ3500 fall into well-defined groups, four in number (at λλ3503, 3661, 3839 and 3905) in the former region.

(3) The electron beam method picture shows very strong bands at 3853, 3871 and 3961A. The present pictures show the two first mentioned bands much less intense and in the place of the third (about 3961A) they show practically nothing. Also the groups at 4108A and longer wave-lengths are weaker on the present plates.

Concerning the rotational fine structure, the present high-dispersion plates show that the strongest bands of the part of the spectrum which falls into groups, namely the bands λλ3247, 3254, 3370, 3377, 3503, 3511, 3534, 3545, 3674, and 3839A, all have the same simple structure, except that some show staggering and others do not (see below); they can be analyzed into P and R branches; Q branches could not be detected. The simple band structure indicates that the molecule is linear in both upper and lower energy states. The absence of a Q branch may be explained by assuming only such transitions, in which the orbital-angular momentum quantum number (in diatomic molecules Λ) does not change: $\Sigma\rightarrow\Sigma$, $\Pi\rightarrow\Pi$, etc. transitions.

Comparing pictures taken with and without magnetic fields, we find that the lines of the above-enumerated bands show no Zeeman effect. Other bands: λλ2880∼2900A and λ3661A, which differ from the above-mentioned bands in having more complicated structure also without fields, show up to the highest rotational states shiftings, broadenings, and in some places also splittings and polarizations in the magnetic field.

Calculations on the basis of the Zeeman effect energy level formula suitable for a diatomic molecule[6]

$$\Delta\nu = \Delta\nu_{\text{normal}} \cdot [M/K(K+1)]\Delta^2$$

with $M=-K, -(K-1) \ldots (K-1)\ K$ show that, assuming a $^1\Pi\rightarrow{}^1\Pi$ transition ($\Delta=1$), we would get for 30,000 gauss field strength for the line $P(5)$ an overall width of the patterns $\Delta\nu=0.16$ cm^{-1}, where, however, the intense components cover a width only of 0.06 cm^{-1}; for $P(9)$ we get an overall width

[5] H. D. Smyth, Phys. Rev. **38**, 2 000 (1931) and **39**, 380 (1932).
[6] J. S. Millis, Phys. Rev. **38**, 1148 (1931).

$\Delta\nu = 0.04$ cm^{-1}. In the case of a $^1\Delta \rightarrow {}^1\Delta$ transition ($\Lambda = 2$), we would get four times larger widths.

Now on the present plates the lines with the lowest rotational quantum number that can be observed are usually P lines from $P(7)$ or $P(9)$ up and R lines from $R(17)$ or $R(19)$ up. Only in two bands, λ3370 and λ3503A, where the overlappings with neighboring strong R lines are fewer, can we observe (without field) P lines from $P(3)$ or $P(4)$ up. The widths of the lines were found to be about 0.04 cm^{-1} and we may suppose that a broadening of the same magnitude in a magnetic field probably would be detected. However, the only observable effect of the magnetic field seems to be to cause a more

TABLE I. λ = *3503A*.

P		*R*		*P*		*R*		*P*	
M	ν(cm^{-1})	*M*	ν(cm^{-1})	*M*	ν(cm^{-1})	*M*	ν(cm^{-1})	*M*	ν(cm^{-1})
2	28,530.47?	18	28,534.92	23	28,498.12	39	28,511.12	44	28,438.77
3	29.58	19	34.37	24	96.02	40	9.24	45	35.30
4	28.54	20	33.84	25	93.78	41	7.56	46	31.71
5	27.55	21	33.00	26	91.50	42	5.44	47	28.11
6	26.39	22	32.49	27	89.10	43	3.54	48	24.37
7	25.22	23	31.78	28	86.65	44	1.53	49	20.51
8	23.99	24	30.94	29	84.10	45	499.37	50	16.82
9	22.72	25	30.05	30	81.50	46	97.14	51	13.05
10	21.40	26	29.09	31	78.83	47	94.85	52	08.78
11	19.96	27	28.07	32	76.12	48	92.57	53	05.06
12	18.52	28	26.96	33	73.31	49	90.18	54	01.27
13	17.03	29	25.87	34	70.56	50	87.88	55	396.88
14	15.43	30	24.67	35	67.59	51	85.35	56	92.73
15	13.77	31	23.43	36	64.65	52	82.69	57	88.39
16	12.01	32	22.09	37	61.66	53	80.18	58	84.15
17	10.28	33	20.73	38	58.72	54	77.47	59	79.79
18	08.42	34	19.32	39	55.43	55	74.80	60	74.86
19	06.47	35	17.81	40	52.14	56	72.03	61	70.80
20	04.71	36	16.24	41	48.90			62	66.29
21	02.49	37	14.64	42	45.64			63	61.65
22	00.41	38	12.87	43	42.29			64	56.87

TABLE II. λ = *3370A*.

P		*R*		*P*		*R*		*P*	
M	ν(cm^{-1})	*M*	ν(cm^{-1})	*M*	ν(cm^{-1})	*M*	ν(cm^{-1})	*M*	ν(cm^{-1})
3	29,656.18?	17	29,661.57	21	29,628.58	35	29,642.77	39	29,580.40
4	55.17	18	61.01	22	26.47	36	41.19	40	77.11
5	54.18	19	60.58	23	24.26	37	39.36	41	73.72
6	52.99	20	59.86	24	22.01	38	37.69	42	70.21
7	51.83	21	59.18	25	19.62	39	35.85	43	66.90
8	50.56	22	58.44	26	17.28	40	33.89	44	63.29
9	49.26	23	57.60	27	14.80	41	31.85	45	59.74
10	47.88	24	56.74	28	12.27	42	29.92	46	55.90
11	46.43	25	55.78	29	09.69	43	27.86		
12	44.95	26	54.80	30	07.08	44	25.61		
13	43.40	27	53.69	31	04.38	45	23.49		
14	41.78	28	52.50	32	01.50	46	21.11		
15	40.21	29	51.33	33	598.79	47	18.85		
16	38.32	30	50.06	34	95.90	48	16.30		
17	36.49	31	48.75	35	92.94	49	13.37		
18	34.61	32	47.34	36	89.82	50	11.34		
19	32.68	33	45.91	37	86.73	51	9.60		
20	30.69	34	44.41	38	83.45	52	7.11		

rapid decrease of intensity in the P branch in the direction of lower rotational quantum numbers. This may probably be attributed to an unresolved Zeeman splitting increasing in that direction. With field (25,400 gauss) the first observable P lines are about $P(8)$ or $P(9)$ in the above two bands. The widths of all the *observable* lines with field is the same (within observational accuracy) as without field.

TABLE III. $\lambda = 3247A$.

P		R	P		R	P	
M	$\nu(\text{cm}^{-1})$	M	M	$\nu(\text{cm}^{-1})$	M	M	$\nu(\text{cm}^{-1})$
	30,781.60	21	20	30,752.93	41	40	30,698.18
	80.59	22	21	50.76	42	41	94.74
	79.79	23	22	48.64	43	42	91.07
	78.83	24	23	46.36	44	43	87.64
	77.80	25	24	44.14	45	44	84.11
	76.67	26	25	41.72	46	45	80.37
	75.58	27	26	39.27	47	46	76.67
	74.39	28	27	36.73	48	47	72.61
	73.17	29	28	34.20	49	48	68.88
9	71.81	30	29	31.58	50	49	65.02
10	70.38	31	30	28.83	51	50	60.91
11	68.95	32	31	26.01	52	51	56.67
12	67.41	33	32	23.19	53	52	52.49
13	65.84	34	33	20.25	54	53	48.81
14	64.24	35	34	17.36	55	54	44.82
15	62.49	36	35	14.19	56	55	40.17
16	60.72	37	36	11.29	57	56	36.29
17	58.91	38	37	07.95	58	57	31.87
18	56.96	39	38	04.78	59	58	27.47
19	54.93	40	39	01.44			

TABLE IV. $\lambda = 3511A$.

	P		R		P		R
M	$\nu(\text{cm}^{-1})$	M	$\nu(\text{cm}^{-1})$	M	$\nu(\text{cm}^{-1})$	M	$\nu(\text{cm}^{-1})$
13	28,453.14	17	28,471.54	28	28,422.85	32	28,458.72
14	51.24	18	71.16	29	20.51	33	57.63
15	49.85	19	70.62	30	17.84	34	56.09
16	47.93	20	69.97	31	15.19	35	54.81
17	46.32	21	69.68	32	12.55	36	53.14
18	44.60	22	68.86	33	09.95	37	51.72
19	42.60	23	68.23	34	07.08	38	49.85
20	40.55	24	67.36	35	04.35	39	48.30
21	38.71	25	66.46	36	01.27	40	46.32
22	36.51	26	65.58	37	398.55	41	44.60
23	34.45	27	64.65	38	95.09	42	42.60
24	32.17	28	63.44	39	92.27		
25	30.01	29	62.35	40	89.08		
26	27.67	30	61.33	41	85.96		
27	25.62	31	60.12				

Considering these facts, we may conclude, that a $^1\Delta \rightarrow {}^1\Delta$ transition seems to be improbable, while the possibility of a $^1\Pi \rightarrow {}^1\Pi$ transition, and of course of a $^1\Sigma \rightarrow {}^1\Sigma$ transition (which should show no Zeeman effect) remain.

The bands beyond 3845A appear to be not much more complicated than the above-enumerated ten bands and also have no observable Zeeman effect, but there is so much overlapping that a third order picture does not permit their analysis into branches.

The present paper deals with the analysis of the ten bands enumerated above. Tables I to X contain the measurements of the bands. The accuracy

TABLE V. $\lambda = 3377A$.

P		R		P		R	
M	$\nu(cm^{-1})$	M	$\nu(cm^{-1})$	M	$\nu(cm^{-1})$	M	$\nu(cm^{-1})$
8	29,585.78	17	29,596.93	33	29,534.39	42	29,566.26
9	84.51	18	96.37	34	31.35	43	64.41
10	83.27	19	95.90	35	28.52	44	62.11
11	81.91	20	95.22	36	25.44	45	60.10
12	80.40	21	94.75	37	22.50	46	57.61
13	78.67	22	93.86	38	19.32	47	55.62
14	76.71	23	93.03	39	16.16	48	52.89
15	75.24	24	92.26	40	12.82	49	50.90
16	73.47	25	91.33	41	09.72	50	48.43
17	71.70	26	90.33	42	06.14	51	45.83
18	69.77	27	89.43	43	02.89	52	42.87
19	67.89	28	88.10	44	499.25	53	40.46
20	65.87	29	87.01	45	95.69	54	37.22
21	63.95	30	85.78	46	91.99	55	35.04
22	61.64	31	84.70	47	88.50	56	31.87
23	59.74	32	83.45	48	84.52	57	29.01
24	57.09	33	81.91	49	80.90	58	25.87
25	54.98	34	80.40	50	76.92	59	23.06
26	52.89	35	79.06	51	73.12	60	19.62
27	50.31	36	77.11	52	68.96		
28	47.74	37	75.70	53	64.97		
29	45.22	38	73.72	54	60.83		
30	42.43	39	72.09	55	56.78		
31	39.89	40	70.21	56	52.22		
32	37.09	41	68.38	57	48.19		

TABLE VI. $\lambda = 3254A$.

P		R		P		R	
M	$\nu(cm^{-1})$	M	$\nu(cm^{-1})$	M	$\nu(cm^{-1})$	M	$\nu(cm^{-1})$
6	30,708.77	17	30,717.36	29	30,665.02	40	30,689.08
7	07.59	18	16.75	30	62.28	41	87.12
8	06.41	19	16.17	31	59.69	42	84.76
9	04.78	20	15.63	32	56.67	43	82.97
10	03.68	21	14.93	33	53.96	44	80.37
11	02.15	22	14.19	34	50.86	45	78.36
12	00.60	23	13.31	35	48.10	46	75.78
13	699.20	24	12.26	36	44.82	47	73.63
14	97.51	25	11.29	37	41.64	48	70.95
15	95.91	26	10.17	38	38.39	49	68.13
16	93.88	27	09.27	39	35.33	50	65.57
17	92.14	28	07.95	40	31.87	51	63.37
18	90.19	29	06.84	41	28.61	52	60.28
19	88.36	30	05.38	42	24.82	53	57.82
20	86.07	31	04.25	43	21.47	54	54.61
21	84.11	32	02.64	44	18.08	55	51.96
22	82.01	33	01.44	45	14.31	56	48.81
23	79.86	34	699.62	46	10.30	57	45.82
24	77.44	35	98.18	47	06.90	58	42.56
25	75.13	36	96.30	48	02.72	59	39.74
26	72.61	37	94.70	49	598.99	60	36.29
27	70.26	38	92.68	50	94.84	61	33.40
28	67.60	39	91.07				

of the pure measurement is of the same order as that of the iron lines in that region serving as normals, i.e., a few thousandths of an angstrom unit or in

TABLE VII. $\lambda = 3534A$.

P		R		P		R	
M	$\nu(cm^{-1})$	M	$\nu(cm^{-1})$	M	$\nu(cm^{-1})$	M	$\nu(cm^{-1})$
9	28,275.43	17	28,288.23	25	28,247.12	33	28,273.99
10	73.99	18	87.75	26	44.69	34	72.76
11	72.76	19	87.13	27	42.41	35	71.34
12	71.34	20	86.62	28	39.69	36	69.47
13	69.79	21	86.00	29	37.45	37	68.37
14	68.37	22	85.45	30	34.64	38	66.28
15	66.74	23	84.80	31	32.39	39	64.88
16	64.88	24	84.00	32	29.68	40	62.86
17	63.27	25	83.12	33	27.19	41	61.18
18	61.18	26	82.13	34	23.99	42	59.02
19	59.55	27	81.21	35	21.49	43	57.43
20	57.43	28	80.12	36	18.28	44	54.97
21	55.65	29	79.06	37	15.54	45	53.43
22	53.43	30	77.79	38	12.28	46	50.71
23	51.49	31	76.74	39	09.42		
24	49.23	32	75.43	40	06.03		

TABLE VIII. $\lambda = 3545A$.

R		P		R		P	
$\nu(cm^{-1})$	M	M	$\nu(cm^{-1})$	M	M	$\nu(cm^{-1}$	
28,195.81	17	9	28,182.91	32	23	28,158.68	
95.33	18	10	81.67	33	24	56,53	
94.88	19	11	80.19	34	25	54.22	
94.24	20	12	78.69	35	26	51.87	
93.70	21	13	77.23	36	27	49.72	
92.87	22	14	75.67	37	28	47.10	
92.26	23	15	74.04	38	29	44.77	
91.43	24	16	72.28	39	30	42.09	
90.60	25	17	70.45	40	31	39.65	
89.75	26	18	68.83		32	36.84	
88.71	27	19	66.84		33	34.26	
87.65	28	20	64.84		34	31.38	
86.67	29	21	62.88		35	28.58	
85.53	30	22	60.81		36	25.62	
84.24	31						

TABLE IX. $\lambda = 3674A$.

R		P		R		P	
$\nu(cm^{-1})$	M	M	$\nu(cm^{-1})$	M	M	$\nu(cm^{-1})$	
27,205.77	18		27,195.54	31	20	27,175.44	
05.38	19		94.38	32	21	73.53	
04.82	20	9	93.24	33	22	71.57	
04.32	21	10	92.22	34	23	69.46	
03.69	22	11	91.48	35	24	67.36	
03.04	23	12	89.44	36	25	65.20	
02.28	24	13	88.00	37	26	62.76	
01.60	25	14	86.48	38	27	60.56	
00.64	26	15	83.94	39	28	58.16	
199.82	27	16	82.26	40	29	55.94	
98.83	28	17	80.76		30	53.66	
97.74	29	18	79.18		31	50.87	
96.71	30	19	77.17		32	48.15	

TABLE X. $\lambda = 3839A$.

P				*R*			
M	back	Δ	forth	*M*	back	Δ	forth
5			26,030.72	16	26,039.70		
		1.13				0.29	
6	26,029.59			17			26,039.41
		0.89				0.35	
7			028.70	18	039.06		
		1.27				0.46	
8	027.43			19			038.60
		1.22				0.39	
9			026.21	20	038.21		
		1.33				0.53	
10	024.88			21			037.68
		1.30				0.60	
11			023.58	22	037.08		
		1.44				0.57	
12	022.14			23			036.51
		1.46				0.71	
13			020.68	24	035.80		
		1.47				0.69	
14	019.21			25			035.11
		1.56				0.85	
15			017.65	26	034.26		
		1.63				0.77	
16	016.02			27			033.49
		1.66				1.01	
17			014.36	28	032.48		
		1.78				0.93	
18	012.58			29			031.55
		1.77				1.07	
19			010.81	30	030.48		
		1.88				1.02	
20	008.93			31			029.46
		1.88				1.24	
21			007.05	32	028.22		
		2.05				1.01	
22	005.00			33			027.21
		1.92				1.50	
23			003.08	34	025.71		
		2.14				1.09	
24	000.94			35			024.62
		2.07				1.58	
25			25,998.87	36	023.04		
		2.04				1.24	
26	25,996.83			37			021.80
		2.38				1.74	
27			994.45	38	020.06		
		2.36				1.23	
28	992.09			39			018.83
		2.25				1.79	
29			989.84	40	017.04		
		2.60				1.44	
30	987.24			41			015.60
		2.33				1.98	
31			984.91	42	013.62		
		2.75				1.49	
32	982.16			43			012.13
		2.33				2.11	
33			979.83	44	010.02		
		2.83				1.53	
34	977.00			45			008.49
		2.53				2.21	
35			974.47	46	006.18		
		2.97				1.62	

TABLE X. (Continued)
$\lambda = 3839A$

P				R			
M	back	Δ	forth	M	back	Δ	forth
36	25,971.50			47			26,004.56
		2.65				2.47	
37			25,968.85	48	26,002.09		
		3.15				1.72	
38	965.70			49			000.37
		2.67				2.54	
39			963.03	50	25,997.83		
		3.09				1.82	
40	959.94			51			25,996.01
		2.87				2.72	
41			957.07	52	993.29		
		3.22				1.85	
42	953.85			53			991.44
						2.90	
				54	988.54		
						1.97	
				55			986.57
						3.02	
				56	983.55		

wave numbers $\pm 0.03 \sim 0.04$ cm^{-1}. Unfortunately, however, the overlappings are very frequent in these bands and this—together with the extraordinary closeness of the lines—causes some errors which, especially in the combination differences, in the worst cases give deviations up to ± 0.5 cm^{-1} which, however, are not systematic.

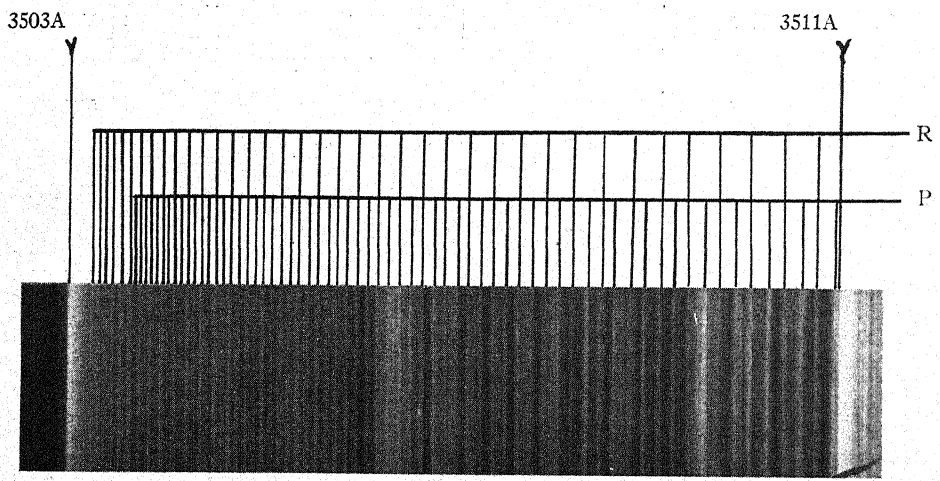


Fig. 2. Non-staggering CO_2 band at λ3503A.

Five of the measured bands, those at λλ3254, 3377, 3511, 3534 and 3839A show staggering, i.e., the lines of the branches are slightly displaced alternately toward lower and toward higher frequencies; the five others, in the limit of the observational accuracy do not. The staggering increases with the rotational quantum number. This phenomenon, together with the fact that

in the same or nearly the same place on the plates we have always P and R lines differing in rotational quantum number by 22–25 units, gives the impression that the P lines form a smooth series, while the R lines stagger back and forth between them. The measurements show, however, that the successive differences between adjacent P lines also alternate. To illustrate this fact, in Table X, for the band at λ3839A—which shows the staggering most prominently—these successive differences are listed in addition to the wave numbers. The rotational numbering of the lines listed in Table I–X should be taken as arbitrary. Some considerations (see below) show, however, that the true rotational numbering probably does not differ from that here given by more than a few units at most.

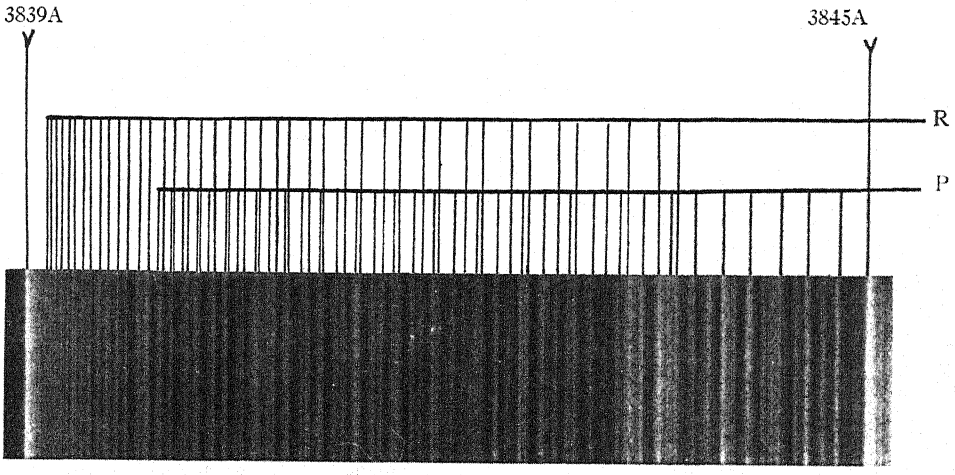


Fig. 3. Staggering CO_2 band at λ3839A.

A striking feature of the investigated bands may be mentioned now. This is: if we calculate differences between P and R lines, such as $R(M-2)-P(M)$ $R(M-1)-P(M)$, and so forth, we find that all the ten bands give almost the same sets of numbers. To illustrate this fact, in Table XI are listed the differences called $R(M)-P(M)$ for all bands. These differences are linear functions of M. At the bottom we find the values B, the constant coefficient (divided by four) of the in M linear sets. These, and B values calculated in other similar tables for several other difference sets, agree for all the ten bands within 0.004 cm^{-1}. This fact formed the common basis for the M numbering in all ten bands.

Since the time of their discovery, most of the CO_2 bands in the region here investigated have been believed to be members of v' progressions. The evidence for this opinion is that the wave numbers of the heads of most bands can be interpreted by the formula

$$\nu_{\text{head}} = \nu_a + 1136.85v' - 1.85v'^2 \qquad (1)$$

where v' is a vibrational quantum number. The different progressions have for ν_a different values (see Smyth[5] especially). The fact that the red degraded,

TABLE XI.

	Supposed $R(M)$–$P(M)$ combinations for all bands									
λ	3247	3254 stagg.	3370	3377 stagg.	3503	3511 stagg.	3534 stagg.	3545	3674	3839 stagg.
M										
15										
16										23.68
17		25.22	25.08	25.23		25.22	25.17	25.36		25.05
18		26.56	26.40	26.60	26.50	26.56	26.57	26.50	26.59	26.48
19		27.81	27.90	28.01	27.90	28.02	27.58	28.04	28.21	27.79
20		29.56	29.17	29.35	29.13	29.42	29.19	29.40	29.38	29.28
21	30.84	30.82	30.60	30.80	30.51	30.97	30.25	30.82	30.79	30.63
22	31.95	32.18	31.97	32.22	32.08	32.35	31.82	32.06	32.12	32.08
23	33.43	33.45	33.34	33.29	33.66	33.78	33.31	33.58	33.58	33.43
24	34.69	34.82	34.73	35.17	34.92	35.19	34.77	34.90	34.92	34.86
25	36.08	36.16	36.16	36.35	36.27	36.45	36.00	36.38	36.40	36.24
26	37.40	37.56	37.52	37.44	37.59	37.91	37.44	37.88	37.88	37.43
27	38.85	39.01	38.89	39.12	38.97	39.02	38.80	38.99	39.26	39.04
28	40.19	40.35	40.23	40.44	40.31	40.59	40.43	40.55	40.67	40.39
29	41.59	41.82	41.64	41.79	41.77	41.84	41.61	41.90	41.80	41.71
30	42.98	43.10	42.98	43.35	43.17	43.49	43.15	43.44	43.05	43.24
31	44.37	44.56	44.37	44.81	44.60	44.93	44.35	44.59	44.67	44.55
32	45.76	45.97	45.84	46.36	45.97	46.17	45.75	46.07	46.23	46.06
33	47.16	47.48	47.12	47.52	47.42	47.68	46.80	47.41		47.38
34	48.48	48.76	48.51	49.05	48.76	49.01	48.77	48.81		48.71
35	50.05	50.08	49.83	50.54	50.22	50.46	49.85	50.11		50.15
36	51.20	51.48	51.37	51.67	51.59	51.87	51.19	51.61		51.54
37	52.77	53.10	52.63	53.20	52.98	53.17	52.83			52.95
38	54.13	54.29	54.24	54.40	54.15	54.76	54.00			54.36
39	55.52	55.74	55.45	55.93	55.69	56.03	55.46			55.80
40	56.75	57.21	56.78	57.39	57.10	57.24	56.83			57.10
41	58.19	58.51	58.13	58.66	58.66	58.64				58.53
42	59.69	59.94	59.71	60.12	59.80					59.77
43	61.00	61.50	60.96	61.52	61.25					
44	62.25	62.59	62.32	62.86	62.76					
45	63.77	64.05	63.75	64.41	64.07					
46	65.05	65.48	65.21	65.62	65.43					
47	66.66	66.73		67.12	66.74					
48	67.85	68.23		68.37	68.20					
49	69.18	69.14		70.00	69.67					
50	70.67	70.73		71.51	71.06					
51		72.54		72.71						
52		73.65		73.91						
53		75.02		75.49						
54		76.43		76.39						
55		77.94		78.26						
56		79.53		79.65						
B	0.3467	0.3473	0.3464	0.3485	0.3482	0.3495	0.3468	0.3493	0.3497	0.3484

simple-structured CO_2 bands, and their lines themselves also, can be fitted in sets with almost the same constants, from the vibrational as well as from the rotational viewpoint, is one of the most prominent features of these bands, especially considering that a completely rigorous analysis has not yet been possible.

Among the ten bands here investigated there are three staggering and three non-staggering bands which form successive members of two v'progressions:

$\lambda\lambda$3503, 3370, 3247A . . . non-staggering

$\lambda\lambda$3511, 3377, 3254A . . . staggering.

To get the rotational numbering it therefore seemed suitable to look for identical sets of final state combination differences. The results of computations of this kind are given in Tables XII and XIII for the staggering and non-staggering sets, respectively.

In Table XII, best agreement is found in the set marked $R(M-2)-P(M)$. If we call this set $R(J-1)-P(J+1)$ and calculate the rotational constants as usual with the formula:

$$\Delta_2 T''(J) = R(J-1) - P(J+1) = 4B''(J+\tfrac{1}{2}) \qquad (2)$$

we get the surprising result, that the J values are (within limits of a few hundredths, which may be attributed to experimental error) half integers. The two neighboring sets $R(M-1)-P(M)$ and $R(M-3)-P(M)$, however, give whole numbers for J. It will be seen that the sets $R(M-1)-R(M+1)$ give almost as good agreements as $R(M-2)-R(M)$, while other sets give gradually increasing deviations which soon pass outside the range of possible experimental errors. Hence the correct combination set is probably not far different from $R(M-2)-P(M)$. If integral J values are assumed to be necessary, it is probably $R(M-1)-P(M)$. In any case, however, since the the calculated B'' values do not vary much from one set to another, the B'' value obtained from, say, $R(M-1)-P(M)$ is probably not far from correct. It also follows that the B' values are not very different from (slightly less than) the B'' values. For instance if $R(M-1)-P(M)$ gives $4B''(J+1/2)$, then $R(M+1)-P(M)=4B'(J+1/2)$. If we assume this we find that the B' values occur in succession as

$$B'_{3511} > B'_{3377} > B'_{3254}$$

in harmony with the vibrational numbering[5]

$$v'_{3511} < v'_{3377} < v'_{3254},$$

if we assume the formula well known for diatomic molecules:

$$B_v = B_0 - \alpha(v+\tfrac{1}{2})$$

with positive α, as is plausible for v' progressions with formula (1). The values for α seem to be very small, of the order of magnitude of 0.001 cm^{-1}. To this may be attributed the difficulty in deciding which combination sets are the correct ones. The alternate occurrence of whole and half J numbers for various possible combinations is marked in the right-hand corner of each combination in Tables XII and XIII.

Concerning Table XIII it should be mentioned that the data in the λ3247A band are in all probability not so accurate as those for the two others, because this band is composed of coincident P and R branches (at least for the eye), which among other things, results in a lower accuracy. Namely, the coinciding P and R lines have rotational quantum numbers differing by about 22 units, so that the coinciding components have not at all the same intensity and they contribute to the resulting line in unequal proportion and so a systematic shifting of the measured resulting line, i.e., of its center

TABLE XII. *Possible combinations in the staggering progressions.*

	$R(M-3)-P(M)$: *whole*			$R(M-2)-P(M)$: *half*			$R(M-1)-P(M)$: *whole*			$R(M)-P(M)$: *half*			$R(M+1)-P(M)$: *whole*		
M	3511	3377	3254	3511	3377	3254	3511	3377	3754	3511	3377	3254	3511	3377	3254
16													23.61	23.46	23.48
17													24.84	24.67	24.61
18										25.22	25.23	25.22	26.02	26.13	25.98
19							26.94	27.16	27.17	26.56	26.60	26.56	27.37	27.33	27.27
20	30.99	31.06	31.29	28.94	29.04	29.00	28.56	28.48	28.39	28.02	28.01	27.81	29.13	28.88	28.86
21	32.45	32.42	32.64	30.61	30.50	30.68	30.07	30.03	30.10	29.42	29.35	29.56	30.15	29.91	30.08
22	34.11	34.26	34.16	31.91	31.95	32.06	31.26	31.27	31.52	30.97	30.80	30.82	31.72	31.39	31.30
23	35.52	35.48	35.77	33.46	33.58	33.62	33.17	33.11	32.92	32.35	32.22	32.18	32.91	32.42	32.40
24	37.51	37.66	37.49	35.23	35.01	35.07	34.41	34.12	34.33	33.78	33.29	33.45	34.29	34.24	33.85
25	38.85	38.88	39.06	36.69	36.77	36.75	36.06	35.94	35.87	35.19	35.17	34.82	35.57	35.35	35.04
26	40.56	40.14	40.70	38.22	38.05	38.18	37.35	37.28	37.13	36.45	36.35	36.16	36.98	36.54	36.66
27	41.74	41.95	42.00	39.69	39.37	39.65	38.79	38.44	38.68	37.91	37.44	37.56	37.82	37.79	37.69
28	43.61	43.59	43.69	40.84	41.02	41.03	39.96	40.02	39.89	39.02	39.12	39.01	39.50	39.27	39.24
29	45.07	45.11	45.15	42.73	42.59	42.57	41.80	41.69	41.67	40.59	40.44	40.35	40.82	40.56	40.36
30	46.81	47.00	46.99	44.14	44.21	44.75	42.93	42.88	42.93	41.84	41.79	41.82	42.28	42.27	41.97
31	48.25	48.21	48.26	45.60	45.67	45.67	44.51	44.58	44.56	43.49	43.35	43.10	43.53	43.56	42.95
32	49.80	49.92	50.17	47.16	47.12	47.15	46.14	45.89	45.69	44.93	44.81	44.56	45.08	44.82	44.77
33	51.38	51.39	51.42	48.78	48.69	48.71	47.57	47.61	47.58	46.17	46.36	45.97	46.14	46.01	45.66
34	53.04	53.35	53.39	50.17	50.31	50.29	48.77	49.06	48.68	47.68	47.52	47.48	47.73	47.71	47.32
35	54.37	54.93	54.54	51.64	52.10	51.78	50.55	50.56	50.58	49.01	49.05	48.76	48.79	48.59	48.20
36	56.36	56.47	56.62	53.28	53.39	53.34	51.74	51.88	51.52	50.46	50.54	50.08	50.45	50.26	49.88
37	57.54	57.90	57.98	54.82	54.96	54.80	53.54	53.62	53.36	51.87	51.67	51.48	51.30	51.22	51.04
38	59.72	59.74	59.79	56.26	56.56	56.54	54.59	54.61	54.66	53.17	53.20	53.10	53.21	52.77	52.68
39	60.87	60.95	60.97	58.05	57.79	57.91	56.63	56.38	56.31	54.76	54.40	54.29	54.05	54.05	53.75
40	62.64	62.88	62.83	59.45	59.54	59.41	57.58	57.56	57.35	56.03	55.93	55.74	55.52	55.56	55.25
41	63.89	64.00	64.07	60.77	60.90	60.81	59.22	59.27	59.20	57.24	57.39	57.21	56.64	56.54	56.15
42		65.95	66.25	62.44	62.37	62.46	60.36	60.49	60.47	58.64	58.66	58.51		58.27	58.15
43		67.32	67.61		64.07	64.26		62.24	62.30		60.12	59.94		59.22	58.90
44		69.13	69.04		65.49	65.65		63.37	63.29		61.52	61.50		60.85	60.28
45		70.57	70.45		67.01	66.68		65.16	64.89		62.86	62.29		61.92	61.47
46		72.42	72.67		68.72	68.66		66.42	66.06		64.41	64.05		63.63	63.33
47		73.61	73.47		70.12	70.07		68.11	68.06		65.62	65.48		64.39	64.05
48		75.58	75.64		71.60	71.46		69.11	68.88		67.12	66.73		66.38	65.41
49		76.71	76.79		73.09	73.06		71.10	70.91		68.37	68.23		67.53	66.58
50		78.70	78.79		74.72	74.64		71.99	71.96		70.00	69.14		68.91	68.53
51		79.77	80.12		75.97	76.11		73.98	73.29		71.51	70.73		69.75	69.45
52		81.94	81.50		77.78	77.30		74.31	74.74		72.71	72.54		71.50	71.19
53		83.46	82.77		79.47	78.94		76.87	76.74		73.91	73.65		72.25	71.81
54		85.00	85.19		80.86	80.57		77.90	77.48		75.49	75.02		74.21	73.78
55		86.09	86.26		82.04	82.10		79.63	79.64		76.39	76.43		75.09	74.79
56		88.24	88.54		83.68	83.80		80.44	80.59		78.26	77.94		76.79	76.54
57		89.03			85.00	85.33		82.82	82.68		79.65	79.53		77.68	
					86.85			83.68			80.82				
B even	0.3942	0.3974	0.3986	0.3801	0.3800	0.3799	0.3768	0.3764	0.3758	0.3498	0.3485	0.3472	0.3464	0.3449	0.3431
B odd	0.3927	0.3960	0.3958	0.3798	0.3802	0.3800	0.3749	0.3742	0.3733	0.3493	0.3486	0.3474	0.3443	0.3430	0.3410
average difference		−0.11	−0.06		−0.02	−0.01		+0.02	+0.08		+0.08	+0.19		+0.16	+0.22
possible combinations		Δ_2T''			Δ_2T''			Δ_2T'			Δ_1T'			Δ_2T'	
									Δ_2T''						

Note to this table. The explanation of B_{even} and B_{odd} is given in the text together with the explanation of the same signs in Table XIV.

TABLE VIII. *Possible combinations in the non-staggering progression.*

M	$R(M-3)-P(M)$: whole 3503	3370	3247	$R(M-2)-P(M)$: half 3503	3370	3247	$R(M-1)-P(M)$: whole 3503	3370	3247	$R(M)-P(M)$: half 3503	3370	3247	$R(M+1)-P(M)$: whole 3503	3370	3247
16														23.25	
17											25.08		24.64	24.52	
18								26.96		26.50	26.40		25.95	25.97	
19					28.89		28.45	28.33		27.90	27.90		27.37	27.18	
20		30.88		30.21	30.32		29.66	29.89		29.13	29.17		28.29	28.49	28.67
21	32.43	32.43		31.88	32.00		31.35	31.28		30.51	30.60	30.84	30.00	29.86	29.83
22	33.96	34.11		33.43	33.39		32.59	32.71	32.96	32.08	31.97	31.95	31.37	31.13	31.15
23	35.72	35.60		34.88	34.92	35.24	34.37	34.18	34.23	33.66	33.34	33.43	32.82	32.48	32.47
24	36.98	37.17	37.46	36.47	36.43	36.45	35.76	35.59	35.65	34.92	34.73	34.69	34.03	33.77	33.66
25	38.71	38.82	38.87	38.00	37.98	38.07	37.16	37.12	37.11	36.27	36.16	36.08	35.31	35.18	34.95
26	40.28	40.32	40.52	39.44	39.46	39.56	38.55	38.50	38.53	37.59	37.52	37.40	36.57	36.41	36.31
27	41.84	41.94	42.10	40.95	40.98	41.07	39.99	40.00	39.94	38.97	38.89	38.85	37.86	37.70	37.66
28	43.40	43.51	43.60	42.44	42.53	42.47	41.42	41.42	41.38	40.31	40.23	40.19	39.22	39.06	38.97
29	44.99	45.11	45.09	43.97	44.00	44.00	42.86	42.81	42.81	41.77	41.64	41.59	40.57	40.37	40.23
30	46.57	46.61	46.75	45.46	45.42	45.56	44.37	44.25	44.34	43.17	42.98	42.98	41.93	41.67	41.55
31	48.13	48.12	48.38	47.04	46.95	47.16	45.84	45.68	45.80	44.60	44.37	44.37	43.26	42.96	42.94
32	49.75	49.83	49.98	48.55	48.56	48.62	47.31	47.25	47.19	45.97	45.84	45.76	44.61	44.41	44.22
33	51.36	51.27	51.56	50.12	49.96	50.13	48.78	48.55	48.70	47.42	47.12	47.16	46.01	45.62	45.59
34	52.87	52.85	53.02	51.53	51.44	51.59	50.17	50.01	50.05	48.76	48.51	48.48	47.25	46.87	46.88
35	54.50	54.40	54.76	53.14	52.97	53.22	51.73	51.47	51.65	50.22	49.83	50.05	48.65	48.25	48.30
36	56.08	56.09	56.12	54.67	54.59	54.55	53.16	52.95	52.95	51.59	51.37	51.20	49.99	49.54	49.43
37	57.66	57.68	57.89	56.15	56.04	56.29	54.58	54.46	54.54	52.98	52.63	52.77	51.21	50.96	50.96
38	59.09	59.32	59.46	57.52	57.74	57.71	55.92	55.91	55.94	54.15	54.24	54.13	52.40	52.40	52.18
39	60.81	60.79	61.05	59.21	58.96	59.28	57.44	57.29	57.47	55.69	55.45	55.52	53.81	53.49	53.49
40	62.50	62.25	62.54	60.73	60.58	60.73	58.98	58.74	58.78	57.10	56.78	56.75	55.42	54.74	54.75
41	63.97	63.97	64.17	62.22	62.13	62.22	60.34	60.17	60.19	58.66	58.13	58.19	56.54	56.20	56.02
42	65.48	65.64	65.89	63.60	63.68	63.86	61.92	61.64	61.86	59.80	59.71	59.69	57.90	57.65	57.57
43	66.95	66.99	67.29	65.27	64.95	65.29	63.15	63.02	63.12	61.25	60.96	61.00	59.24	58.71	58.72
44	68.79	68.56	68.82	66.67	66.63	66.65	64.77	64.57	64.53	62.76	62.32	62.25	60.60	60.20	60.03
45	70.14	70.18	70.39	68.24	68.12	68.27	66.23	65.87	66.99	64.07	63.75	63.77	61.84	61.37	61.35
46	71.83	71.96	71.97	69.82	69.71	69.69	67.66	67.59	67.47	65.43	65.21	65.05	63.14	62.95	62.60
47	73.42		73.75	71.26		71.53	69.03		69.11	66.74		66.66	64.46		64.12
48	75.00		75.26	72.77		72.84	70.48		70.39	68.20		67.85	65.81		65.32
49	76.63		76.70	74.34		74.25	72.06		71.71	69.67		69.18	67.37		66.56
50	78.03		78.36	75.75		7 .82	73.36		73.29	71.06		70.67	68.53		67.92
B	0.391	0.391	0.393	0.379	0.379	0.380	0.362	0.360	0.362	0.348	0.346	0.346	0.332	0.328	0.328

average difference −0.03 (between 3503 and 3370 columns)

average difference −0.19 (between 3370 and 3247 columns)

average difference +0.04 (between 3503 and 3370 columns)

average difference −0.12 (between 3370 and 3247 columns)

average difference +0.12 (between 3503 and 3370 columns)

average difference −0.07 (between 3370 and 3247 columns)

average difference +0.19 (between 3503 and 3370 columns)

average difference −0.003 (between 3370 and 3247 columns)

average difference +0.26 (between 3503 and 3370 columns)

average difference +0.06 (between 3370 and 3247 columns)

possible combinations

$\Delta_1 T'''$ $\Delta_1 T'$

$\Delta_2 T'''$ $\Delta_2 T'$

$\Delta_1 T''$ $\Delta_3 T'$

of gravity, may occur. Hence, less weight should be given to agreements involving the combination sets of this band.

In this table we may say that the supposed common final state may be interpreted by one of the left-hand columns. Anyway, we find that the numbering calculated on the basis of formula (2) does not differ from our arbitrary numbering by more than one or two (or by a half or one and a half) units .This is true for both progressions, and in view of Table XI, probably for all the bands. The B values for both initial and final states then probably lie within the interval of: $0.395 \sim 0.345$ cm^{-1}.

On the basis of these values, assuming the rotational axis perpendicular to the line through the three atoms of CO_2 and going through the carbon atom and assuming the effective mass for that axis:

$$\mu = 2M_{\text{oxygen}} = 53.12 \cdot 10^{-24}\text{g},$$

we can roughly calculate the distance between the carbon and one of oxygen atoms. We get in this way: r equal to about $1.25 \sim 1.15 \cdot 10^{-8}$ cm, that is, almost the same as, or slightly larger than, in the CO and CO^+ molecules.

In making the above computations concerning the numbering and rotational constants we have not mentioned the theoretical requirement that, because of the symmetry of the CO_2 molecule and the zero nuclear spin of the oxygen atoms, alternate rotational levels and band lines should be missing. As for the staggering bands, a very simple assumption (see below) may explain both staggering and missing lines. But considering only the non-staggering bands, the question might arise whether these bands could not be explained by supposing that they have alternately missing lines, so that the rotational constants would really have values roughly half as large and the rotational quantum numbers of the lines, values roughly twice as large as stated above. In making this assumption, we would encounter difficulties not only in the fact that in this case the nuclear separations would become improbably large, but also in interpreting the rotational intensity distribution of the bands. It was shown before that the intensity distribution of the angstrom bands present in the spectrum gives a value for $kT = 800$ cm^{-1} and assuming the formula

$$kT = B'(K_{\max}'' + 1)(2K_{\max}'' + 3)$$

for the R branches of the CO_2 bands, we would get with supposed B' values about $0.360 \sim 0.350$ (middle and left-hand columns in Table XIII) a value for $K''_{\max}$ about $31 \sim 32$; with B values half as large we get $K''_{\max}$ about $43 \sim 45$. The $R(43)$ or $R(45)$ line would of course be identical with our former lines $R(21) \sim R(23)$. Now the intensity distribution of the bands at λ3503A and λ3370A on several plates was registered with a Moll microphotometer and the curves show, although distorted by the close lying lines and some overlappings also, their maxima undoubtedly within the interval of $M = 30$ to 33. This confirms the assumption that alternate lines are not missing in the bands without staggering.

In surveying all the combinations given in Tables XII and XIII it seemed

of interest to determine whether the two progressions have or have not an exactly common level. Every conceivable kind of combination between the lines of the different bands in the different progressions was tried, but every set obtained showed—to be sure small but systematic deviations from the others.

A simple explanation of the staggering together with the theoretical requirement of missing levels can be given as follows: In analogy to diatomic molecules, we assume that the rotational levels of CO_2 form a set (in the first approximation) with the well-known formula

$$T(J) = BJ(J+1) \text{ or } T(K) = BK(K+1)$$

and in further analogy with diatomic molecules, we assume a splitting of the levels, something like the Λ-type doubling. Now, due to the zero nuclear spins

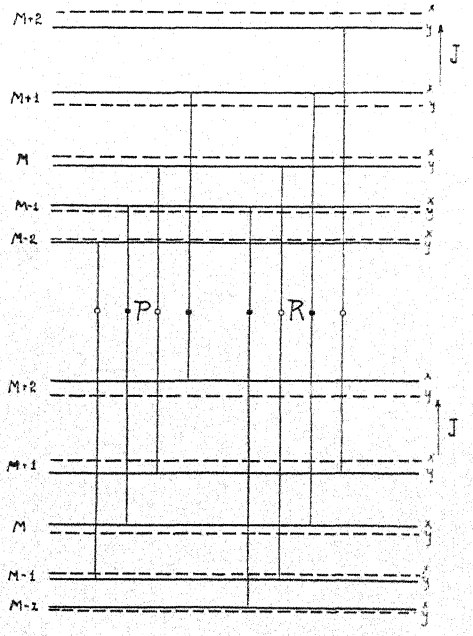


Fig. 4. Possible energy diagram and explanation of the staggering in some CO_2 bands. The rotational levels have doublings in analogy to the Λ-type doublings of a diatomic molecule. Because of the zero nuclear spin of the oxygen atoms, every second level is missing (broken lines). P and R branches appear to be divided into two alternating sets marked with full and empty circles. To get term-differences, we have to combine full circle R lines with full circle P lines and empty circle R lines with empty circle P lines.

of the oxygen atoms, every other level, alternately the upper and lower one of the sublevels of a Λ-like doublet, as in He_2, should be missing. The energy-level diagram could be drawn then somewhat as in Fig. 4 (where the Λ-like doublings are greatly exaggerated).[7] The P and R lines would then appear to be divided into the two sets, marked with full and empty circles (transitions

[7] See Figs. 17 and 32 for structure of bands like this given by R. S. Mulliken, Rev. Mod. Phys. 3, 89 (1931).

only between x sublevels and transitions only between y sublevels). To get the x level combinations, we have to combine full circle P and R lines, to get y level combinations, we have to combine empty circle lines. But the question which half of the P and of the R branches represent the empty and which the full circle lines, and therefore which set of P lines should be combined with which set of R lines, remains at first unanswered.

The magnitude of the staggering is different in the different bands. In the band at λ3839A it is the largest, in the progresssion λλ3511, 3377 and 3254A it is less and in the band λ3534 it is only just observable. This suggests that perhaps the non-staggering bands have staggering also, only its magnitude is less than enough to become observable.

The λ3839A band shows the most striking staggering, so it may serve as an example for the following considerations. In Table X the lines of the bands are fitted in two columns, marked "forth" and "back," where the "forth" means a deviation in the direction of higher frequencies, that is, since the band is red-degraded, toward the head, and "back" in the opposite direction. The arbitrary numbering was chosen in such a way that even numbers belong to "back" staggered, odd numbers to "forth" staggered lines in both branches. (This was done also in the other staggering bands, and this served as a second basis, besides that explained by discussing Table XI (see above), for the common M numbering in the different bands.)

Table XIV contains a number of possible combinations in the λ3839 band; combinations in which the M value of the P line is even or odd are listed respectively in the left and right subcolumns of each combination set. Before each combination value is given the value J which is calculated, assuming the formula

$$combination\ (R - P) = 4B(J + \tfrac{1}{2})$$

and the average constant differences in each column of two adjacent combination values are listed as "$8B$" at the bottom of the table. The approximate nature of the J values obtained is given at the top of each column under "whole" or "half." (In the bands without staggering, similar tables give almost exactly integers and half integers: cf., data in Tables XII, XIII.) Below these their deviations from the nearest whole and half numbers are also listed. The sum of the deviations for the two halves of each combination set seems to be zero in the "whole" sets. The deviations themselves seem to be two or three times as large in the "whole" combinations as in the "half" ones. The difference $8B_{even} - 8B_{odd}$ seems to be about four times as large in the "whole" sets as in the "half" sets, and also differs in sign.

The quantity $8B_{even} - 8B_{odd}$ in the other staggering bands also was found to be positive in the "whole" sets in all cases and negative in the "half" sets in most cases. Its magnitude (an approximate measure of the staggering) seems to be about $+0.016$ cm^{-1} in the "whole" sets. The calculated J values are equal to whole and half numbers within the lower observational accuracy—due to frequent overlappings in these bands, and do not permit a real calculation of their deviations from the next whole or half number.

TABLE XIV. *Possible combinations in λ3839A, strongly staggering band.*

	$R(M-2)-P(M)$: half				$R(M-1)-P(M)$: whole				$R(M)-P(M)$: half				$R(M+1)-P(M)$: whole				$R(M+2)-P(M)$: half				
	J	$R-P$	J	$R-P$	J	$R-P$	J	$R-P$	J	$R-P$	J	$R-P$	J	$R-P$	J	$R-P$	J	$R-P$	J	$R-P$	
	0.53		0.43		0.84		0.16		0.54		0.43		0.82		0.17		0.55		0.43		Average of the decimal part of apparent J.
	−0.03		+0.07		+0.16		−0.16		−0.04		+0.07		+0.18		−0.17		−0.05		+0.07		Deviation of apparent J from integers on half integers.
M																					
14																	15.54	20.49			
15															16.14	22.05			16.46	21.76	
16									16.53	23.68			16.85	23.39			17.54	23.04			
17							17.10	25.34			17.44	25.05			18.14	24.70			18.39	24.24	
18	17.52	27.12			17.87	26.83			18.54	26.48			18.80	26.02			19.57	25.63			
19			18.45	28.60			19.12	28.25			19.41	27.79			20.18	27.40			20.44	26.87	
20	19.52	30.13			19.81	29.67			20.55	29.28			20.83	28.75			21.54	28.15			
21			20.40	31.55			21.14	31.16			21.44	30.63	..		22.16	30.03			22.46	29.46	
22	21.57	33.21			21.87	32.68			22.57	32.08			22.88	31.51			23.61	30.80			
23			22.42	34.60			23.11	34.00			23.45	33.43			24.19	32.72			24.46	32.03	
24	23.52	36.14			23.85	35.57			24.57	34.86			24.85	34.17			25.59	33.32			
25			24.44	37.64			25.14	36.93			25.46	36.24			26.21	35.39			26.48	34.62	
26	25.40	38.97			25.71	38.28			26.41	37.43			26.70	36.66			27.41	35.65			
27			26.44	40.66			27.14	39.81			27.46	39.04			28.20	38.03			28.41	37.10	
28	27.53	42.17			27.84	41.40			28.54	40.39			28.78	39.46			29.56	38.39			
29			28.42	43.65			29.61	42.64			29.38	41.71			30.17	40.64			30.38	39.62	
30	29.57	45.24			29.83	44.31			30.59	43.24			30.82	42.22			31.58	40.98			
31			30.40	46.64			31.14	45.57			31.41	44.55			32.18	43.31			32.46	42.30	
32	31.61	48.32			31.88	47.30			32.62	46.06			32.92	45.05			33.60	43.55			
33			32.38	49.63			33.10	48.39			33.44	47.38			34.12	45.88			34.40	44.79	
34	33.54	51.22			33.87	50.21			34.52	48.71			34.83	47.62			35.54	46.04			
35			34.44	52.74			35.08	51.24			35.42	50.15			36.15	48.57			36.38	47.33	
36	35.53	54.21			35.86	53.12			36.56	51.54			36.82	50.30			37.52	48.56			
37			36.45	55.77			37.13	54.19			37.43	52.95			38.14	51.21			38.45	49.98	
38	37.61	57.34			37.90	56.10			38.59	54.36			38.92	53.13			39.69	51.34			
39			38.44	58.77			39.10	57.03			39.47	55.80			40.26	54.01			40.47	52.57	
40	39.45	60.12			39.81	58.89			40.56	57.10			40.79	55.66			41.53	53.68			
41			40.42	61.76			41.14	59.97			41.43	58.53			42.17	56.55			42.41	55.06	
42	41.49	63.19			41.77	61.75			42.48	59.77			42.74	58.28			43.48	56.17			
$8B$	3.0094		3.0186		2.9215		2.8802		2.7815		2.7921		2.6958		2.6504		2.5546		2.5665		
$8B_{even}-8B_{odd}$	−0.0092				+0.0413				−0.0106				+0.0454				−0.0119				

The levels of Λ-type doubling in a diatomic molecule can be interpreted by the formula[8]

$$\phi_i(J) = \kappa_i + \epsilon_i J + \delta_i J(J+1) + \cdots$$

where i refers to either x or y sublevels. We may try to use this formula for the present case.

Combining two sublevels differing by two units in J, but of the same kind (that is, two x, or two y levels) we get

$$\phi_i(J+1) + \phi_i(J-1) = 2\epsilon_i + 4\delta_i(J+\tfrac{1}{2}).$$

The difference between B_{even} and B_{odd} should then represent the difference between δ_x and δ_y, while the deviations of the apparent J's from whole numbers correspond to ϵ_x and ϵ_y, of which according to the observational data one is positive, the other negative. Both the "whole" and the "half" combinations in the band at λ3839A show effective B and J values which are consistent with this scheme, and there seems to be no way of deciding between them on this basis, nor of deciding which of the "whole" or of the "half" combinations is most likely to be correct, except roughly by assuming the intensity distribution to be analogous to that in the bands which belong to progressions.

In a separate paper Professor R. S. Mulliken expects to discuss some further points in connections with the theoretical interpretation of the CO_2 bands.

The writer wishes to express his thankfulness to Professor Robert S. Mulliken for his unceasing advice in analyzing the bands and to Professor George S. Monk for his kind assistance in experimental troubles, especially for the excellent temperature control of the grating-room.

[8] R. S. Mulliken, Rev. Mod. Phys. 3, 89 (1931).

Electronic Structures of Polyatomic Molecules and Valence. II. Quantum Theory of the Double Bond

By ROBERT S. MULLIKEN
Ryerson Physical Laboratory, University of Chicago

(Received August 4, 1932)

The electronic structure of CH_2 in its probable normal and first excited states is described in terms of molecular orbitals. The formation of C_2H_4 from two (excited) CH_2 radicals is discussed, and it is shown, with the help of the Slater-Pauling overlapping criterion, to be theoretically obvious, in agreement with experiment, that for the normal state of C_2H_4 the energy is surely considerably lower if the two CH_2 are arranged symmetrically in one plane than if their planes make an angle of 90° (Figs. 1, 2). Similar statements apply to the derivatives of C_2H_4. The C=N and N=N double bonds can be treated similarly. The C=C and O=O double bonds are compared. The $(BH_3)=(BH_3)$ bond in B_2H_6 probably resembles the O=O more than the C=C bond. For certain predicted excited states of C_2H_4 and its derivatives, which are probably the upper states of ultraviolet absorption bands of these compounds, it is shown that the energy should be higher for the plane form than for the perp. form (one CR′R″ plane rotated through 90°). Hence the plane form should tend to go over spontaneously by rotation into the perp. form (90°) and on to the other plane form (180°) after absorption of suitable ultraviolet light. In this way the observed transformations of *cis* into *trans* isomers or vice versa by ultraviolet light may be explained.

INTRODUCTION

SEVERAL attempts have been made to explain quantum-mechanically the well-known double bond of organic chemistry.[1] Hückel formulated the double bond, e.g., in C_2H_4, as consisting of two electron-pairs $[\sigma]^2[\pi]^2$, where $[\sigma]$ has approximate rotational symmetry around the C-C axis, $[\pi]$ an angular distribution approximately proportional to $\sin\phi$ ($\phi=0$ in the common plane of all the nuclei). The stability of the double bond toward rotation is connected with properties of the $[\pi]_{\sin\phi}$ orbital, but Hückel's discussion of this stability is unsatisfactory.

Slater[2] and Pauling[3] give a different explanation using their tetrahedral atomic orbitals (s, p hybrids), as follows: Each CH_2 has two such orbitals which have formed electron-pair bonds with H atoms, and two which are unpaired. In C_2H_4, the two unpaired CH_2 orbitals form two electron-pairs which determine a plane perpendicular to that in which all the atoms lie, and cause this arrangement to be stable toward rotation.

Although the Slater-Pauling method generally gives a good approximation and a valid explanation of valence angles, the approximation appears to

[1] Cf. R. S. Mulliken, Phys. Rev. **41**, 49 and especially 55–61 (1932) for a summary and references.

[2] J. C. Slater, Phys. Rev. **37**, 481 (1931).

[3] L. Pauling, Jour. Am. Chem. Soc. **53**, 1367 (1931).

be relatively crude in the case of C_2H_4 and of double bonds in general, essentially because of the assumption of s-p hybridization. As will now be shown, it seems possible by means of a different approximation, resembling Hückel's but going farther, to obtain a more detailed correspondence with existing empirical, especially chemical, knowledge of the behavior of double-bonded molecules.

Electronic Structure of CH_2

It is useful to consider the formation of C_2H_4 from 2 CH_2 for two cases: (a) all the atoms lie in one plane ("plane C_2H_4"); (b) the planes of the two CH_2 make an angle of 90° ("perpendicular C_2H_4"). For this purpose, it is convenient to describe the molecular electronic structures in terms of molecular orbitals[1] of CH_2 and of C_2H_4. The possible types of molecular orbitals and their symmetry properties depend on the symmetry of the nuclear arrangement. They can be conveniently determined by group theory methods, or in simple cases by inspection. The exact meanings of the term symbols used here for electronic states, e.g., $^1\Gamma_1$, will be explained in a later detailed paper; it should be noted that the meaning of a given symbol may differ according to the nuclear arrangement.

That CH_2 should be triangular, with an angle of perhaps about 110° between the two C-H directions, can be seen most easily by using the Pauling-Slater methods, assuming either pure p valence (predicted angle somewhat over 90°) or tetrahedral bonds (predicted angle slightly larger than the tetrahedral angle), or an intermediate condition. In the following, a z axis will be chosen bisecting the apex angle of CH_2, an x axis perpendicular to the CH_2 plane. [In forming p bonds, Slater and Pauling would use y' and z' axes making angles of 45° with the y and z axes used here.] The probable normal state and the probable lowest excited state of CH_2 can then be described in terms of molecular orbitals as:

$$1s^2[s]^2[y]^2[z]^2,\ ^1\Gamma_1;\ 1s^2[s]^2[y]^2[z][x],\ ^3\Gamma_3. \qquad (1)$$

The symbols $[s]$, $[x]$, $[y]$, $[z]$ stand for orbitals which may be approximately built up as linear combinations respectively of $2s$, $2p_x$, $2p_y$, $2p_z$ of carbon[2,3] and $1s$ of hydrogen; $[s]$ consists mostly of $2s$, some $1s$, and a little $2p_z$; $[x]$ of $2p_x$ only; $[y]$ of $2p_y$ and $1s$; $[z]$ of $2p_z$, some $1s$, and a little $2s$. The C-H binding is taken care of by the $[y]$, $[s]$, and $[z]$ orbitals, especially by the $[y]$.

Formation of C_2H_4 from CH_2

The Slater-Pauling criterion of maximum overlapping, which can be applied to formation of pairs of molecular orbitals as well as to formation of electron-pair bonds,[1] can now be used to show that the most stable form of C_2H_4 should be a plane configuration built out of two CH_2 radicals each in the state . . . $[z][x]$, $^3\Gamma_3$ in such a way that the z axes of the two radicals coincide and form what may be called the z axis of C_2H_4. [Although best thought of as built out of two $^3\Gamma_3$, normal C_2H_4 should dissociate adiabatically into two $^1\Gamma_1$ unexcited CH_2 radicals.] With this arrangement, the two $[z]$

orbitals of the two CH_2 overlap strongly to form Hückel's $[\sigma]$ bond, the two $[x]$ orbitals somewhat less strongly to form his $[\pi]$ bond. The resulting (C-C)-bonding orbitals of C_2H_4 are approximately *const.* $\{[z]_A+[z]_B\}$ and *const.* $\{[x]_A+[x]_B\}$, or more briefly, $[z+z]$ and $[x+x]$, where A and B refer to the two CH_2 radicals. The (C-H) bonding orbitals $[s]$ and $[y]$ of the two CH_2 radicals are not very much disturbed by the formation of C_2H_4, and take little part in the (C-C)-bonding, so that one may describe C_2H_4 in its normal state approximately as:

$$1s^21s^2[s]^2[s]^2[y]^2[y]^2[z+z]^2[x+x]^2,\ {}^1\Gamma_{1g}. \tag{2}$$

The $[z]$ orbitals, in forming $[z+z]$, withdraw largely from their previous (C-H)-bonding function, their share being taken over by the $[s]$ orbitals; in the process, there is probably a somewhat increased hybridization of $[s]$ and $[z]$ which facilitates the alterations in their bonding roles: for $\alpha[s]+\beta[z]$ and $\beta[s]-\alpha[z]$ are respectively better adapted to C-H and to (C-C)-bonding than are pure $[s]$ and $[z]$.

The interaction between $[y]_A^2$ and $[y]_B^2$, likewise that between $[s]_A^2$ and $[s]_B^2$, should be a repulsive one. Instead of $[y]^2[y]^2$ one *might* write $[y+y]^2[y-y]^2$, where $[y+y]$, which means *const.* $\{[y]_A+[y]_B\}$, is (C-C)-bonding, while $[y-y]$ is (C-C)-antibonding. Probably, however, the (C-C)-nonbonding formulation $[y]^2[y]^2$ represents a better approximation here. The difference between the C=C double bond in C_2H_4 and the O=O double bond in O_2 lies chiefly in this last fact. This can be seen on comparing (2) with the following formulations (3) and (4), and noting that $(\pi+\pi)$ and $(\pi-\pi)$ of O_2 (usually called $\pi 2p$ and $\pi^* 2p$) are two-foldly degenerate orbitals, respectively of the types $\{(x+x)$ and $(y+y)\}$ and $\{(x-x)$ and $(y-y)\}$,—or $\{(x+x)\pm i(y+y)\}$, and $\{(x-x)+i(y-y)\}$,—where x and y stand for $2p_x$ and $2p_y$ of the O atom.

$$C_2H_4\text{: } 1s^21s^2[s]^2[s]^2[y+y]^2[y-y]^2[z+z]^2[x+x]^2,\ {}^1\Gamma_{1g} \tag{3}$$

$$O_2\text{: } 1s^21s^2s^2s^2(z+z)^2(\pi+\pi)^4(\pi-\pi)^2,\ {}^3\Sigma^-_g. \tag{4}$$

Here $[y+y]^2[x+x]^2$ of C_2H_4 corresponds to $(\pi+\pi)^4$ of O_2, $[y-y]^2$ to $(\pi-\pi)^2$; but because of the degeneracy involved in $(\pi-\pi)$, which means that $(y-y)$ and $(x-x)$ of O_2 have equal energy unlike $[y-y]$ and $[x-x]$ of C_2H_4, the lowest state of O_2 is a paramagnetic triplet state with one electron in $(x-x)$, one in $(y-y)$, while that of C_2H_4 is a diamagnetic singlet state.

Besides the ${}^1\Gamma_{1g}$ normal state of C_2H_4, the union of two CH_2 each in the state . . . $[z][x]$, ${}^3\Gamma_3$ should give an unstable quintet state and an excited, possibly also unstable (cf. Fig. 1), triplet state of C_2H_4. This and a corresponding singlet state should probably be the lowest excited triplet and singlet state of C_2H_4. They are (cf. (2)):

$$1s^21s^2[s]^2[s]^2[y]^2[y]^2[z+z]^2[x+x][x-x],\ {}^3\Gamma_{4u},\ {}^1\Gamma_{4u}. \tag{5}$$

These states should have a very considerably larger equilibrium C-C distance than the normal state. Absorption of suitable ultraviolet frequencies by normal C_2H_4 should take it readily to the ${}^1\Gamma_{4u}$ state, since it can be shown that

the transition is in agreement with selection rules appropriate to the case; absorption bands leading to the $^3\Gamma_{4u}$ state should be very weak because of the change in multiplicity. If Fig. 1 is correct, the absorption to the $^3\Gamma_{4u}$ state should consist mostly of a weak continuum causing dissociation into two CH_2.

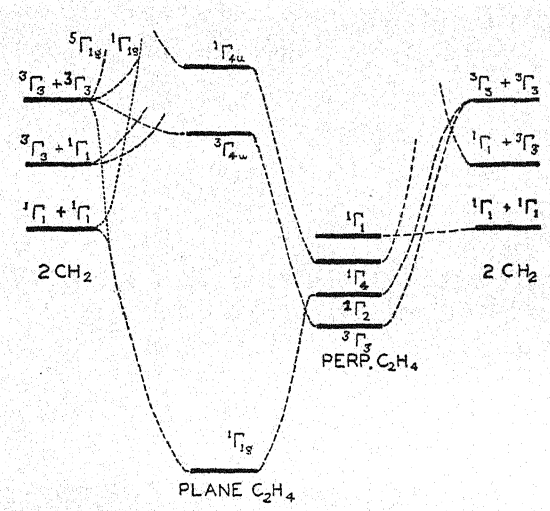


Fig. 1. Probable lowest energy levels of plane C_2H_4 and of perp. C_2H_4 (plane of one CH_2 at 90° to that of the other) and of 2 CH_2, and their adiabatic correlations as given by group theory. (The correlations with 2 CH_2 should not be considered absolutely certain, since the theory has not been carefully checked.) The spacings of the levels are of no more than qualitative significance, and the correct order of some of them may even be the reverse of that shown. It is not impossible that the energy of the $^3\Gamma_{4u}$ state of plane C_2H_4 may be higher than that of 2 $CH_2(^3\Gamma_3)$ so that the state is an unstable repulsive one. The state $^1\Gamma_{4u}$, however, is almost certainly stable. It should be noted that while C_2H_4 in its normal state may be thought of (dotted lines in the figure) as derived from, or to a considerable degree as consisting of, two excited CH_2 radicals both in the state $\cdots [z][x]$, $^3\Gamma_3$ (cf. (2) in the text), normal plane C_2H_4 would probably dissociate adiabatically into two unexcited $^1\Gamma_1$ CH_2 radicals (dashes in the figure). Various states of 2 CH_2 with only slightly higher energy than those shown could be added to the diagram, e.g., $^1\Gamma_1+{}^1\Gamma_3$, $^1\Gamma_3+{}^3\Gamma_3$, and $^1\Gamma_3+{}^1\Gamma_3$, but are not important for our purposes. The equilibrium separation of the two C atoms (r_e) is smallest for the normal state of plane C_2H_4, intermediate in value for the states of perp. C_2H_4, and relatively large for the Γ_{4u} excited states of plane C_2H_4. Diagrams similar to Fig. 1 would apply to *derivatives* of C_2H_4, e.g. $R'R''C=CR''R'''$, although the group theory designations of the electronic states would be different; also, there would be *two* plane forms (*cis* and *trans*) with slightly different energy levels. Further, the dissociation product correlations would be rather different, and some predissociation of the state corresponding to $^1\Gamma_{4u}$ of C_2H_4 seems likely. Perhaps this explains the more structureless character[8] reported for the absorption bands of C_2H_4 derivatives than for C_2H_4 itself.

It is instructive to consider what would be expected if two CH_2 each in the state $\ldots [z][x]$, $^3\Gamma_3$ were brought together with their planes at right angles. The orbitals $[z]$ would overlap nearly as strongly as before and their electrons would give a strong bond $[z+z]^2$, but the two $[x]$ orbitals would overlap very little, and give practically zero energy of bonding, as one sees clearly on examining carefully the appropriate interaction integrals, which

can conveniently be set up according to the methods of Slater.[4] Hence instead of getting a singlet state $[x+x]^2$ and a triplet state $[x+x][x-x]$ of widely different energy (cf. (2) and (5)), the singlet and triplet should be nearly equal in energy, and both probably fairly stable. There must of course also be an unstable quintet. Examination of the integrals indicates that the triplet state should be slightly below the singlet, but this is not certain. It will be noticed that with perp. C_2H_4 (the two CH_2 planes perpendicular), the x axis of one CH_2 is parallel to the y axis of the other, and vice versa. As can be shown conveniently by group theory, this leads to a degeneracy somewhat resembling the π degeneracy in O_2. One may write for perp. C_2H_4:

$$1s^2 1s^2 [s]^2 [s]^2 [\pi]_y^4 [z+z]^2 [\pi]_x^2,\ {}^3\Gamma_3,\ {}^1\Gamma_2,\ {}^1\Gamma_4,\ {}^1\Gamma_1. \tag{6}$$

It can be shown that the incomplete group $[\pi]_x^2$ yields four electron states ${}^3\Gamma_3$, ${}^1\Gamma_2$, ${}^1\Gamma_4$, ${}^1\Gamma_1$, of which ${}^3\Gamma_3$ and ${}^1\Gamma_2$ are the triplet and singlet state obtained by bringing together two CH_2 . . . $[z][x]$, ${}^3\Gamma_3$, with their planes at right angles. The states ${}^1\Gamma_4$ and ${}^1\Gamma_1$ probably lie a volt or so above the two lowest states ${}^3\Gamma_3$ and ${}^1\Gamma_2$ of perp. C_2H_4; their structure is as if derived from CH_2^+ plus CH_2^-.[5]

For the ${}^3\Gamma_3$ and ${}^1\Gamma_2$ (but not for the ${}^1\Gamma_4$ and ${}^1\Gamma_1$) one might write instead of (6):

$$1s^2 1s^2 [s]^2 [s]^2 [y]^2 [y]^2 [z+z]^2 [x][x],\ {}^3\Gamma_3,\ {}^1\Gamma_2. \tag{7}$$

This gives expression to the fact that the $[\pi]_y$ and $[\pi]_x$ orbitals of perp. C_2H_4 in (6), in the case of ${}^3\Gamma_3$ and ${}^1\Gamma_2$, really describe essentially the same state of affairs as if one had the original $[y]$ and $[x]$ orbitals of CH_2 unshared, only the $[z]$ orbitals of CH_2 forming a bond.[6]

Comparing plane C_2H_4 with perp. C_2H_4, it can be shown by group theory that (unless possibly other excited states of unexpectedly low energy intervene), the normal state ${}^1\Gamma_{1g}$ of plane C_2H_4 must go over, on rotation of the CH_2 planes, into the low state ${}^1\Gamma_2$ of perp. C_2H_4, and the two excited states ${}^3\Gamma_{4u}$ and ${}^1\Gamma_{4u}$ of plane C_2H_4 into the low states ${}^3\Gamma_3$ and ${}^1\Gamma_4$ of perp. C_2H_4. It is now of interest to consider the relative positions of the various energy levels

[4] J. C. Slater, Phys. Rev. **38**, 1109 (1931).

[5] The preceding results may appear less unfamiliar if it is remarked that ${}^3\Gamma_3$ of the present $[\pi]_x^2$ corresponds to ${}^3\Sigma_g^-$ of π^2 of a diatomic molecule, ${}^1\Gamma_2$ and ${}^1\Gamma_4$ correspond to ${}^1\Delta_g$ of π^2, and ${}^1\Gamma_1$ corresponds to ${}^1\Sigma_g^+$ of π^2. In fact if the H nuclei in perp. C_2H_4 could be united with the C nuclei to form O_2, the four above-mentioned states of $\cdots [\pi]_y^4 [\pi]_x^2$ of perp. C_2H_4 would go over into the three states of $\cdots \pi^4 \pi^{*2}$ of O_2, i.e., of $\cdots (\pi+\pi)^4 (\pi-\pi)^2$ of (4).

[6] In (6), $[\pi]_y^4$ is a degenerate group formed from $[y]_A^2$ and $[y]_B^2$, where the designation $[y]$ is based on a separate choice of axes for the two CH_2 radicals A and B. If a choice of x and y axes consistent for the *whole* perp. C_2H_4 *molecule* were used, one would have to speak of, say, $[y]_A^2$ and $[x]_B^2$ instead of $[y]_A^2$ and $[y]_B^2$. It is this peculiarity which causes these two types to belong to a single degenerate type, here called $[\pi]_y$, of perp. C_2H_4, regardless of whether or not they interact appreciably. Similarly the orbitals which, when expressed in terms of the x, y axes of the separate CH_2's, are called $[x]_A$ and $[x]_B$ of 2 CH_2, become $[x]_A$ and $[y]_B$ in terms of x and y axes consistent for the whole molecule. In C_2H_4 both, somewhat modified by the interaction of the two CH_2 of course, then belong to the degenerate type here called $[\pi]_x$.

of plane and perp. C_2H_4. Roughly, the energy differences depend only on that part of the energy of formation of C_2H_4 which is furnished by the interaction of the two $[x]$ electrons of the two CH_2. In perp. C_2H_4 this is approximately 0 volts ($^1\Gamma_4$ is perhaps about 1 volt higher). In plane C_2H_4 in its normal state it is the energy of the $[x+x]^2$ bond, say about -2.5 volts. In excited C_2H_4 with $[x+x][x-x]$ we may expect the anti-bonding action of $[x-x]$ to exceed considerably[7] the bonding action of $[x+x]$, giving a net result of say perhaps $+3$ volts. These estimates are plotted in Fig. 1, which shows qualitatively how we may expect the energies of the various states to change on going from plane C_2H_4 to perp. C_2H_4, also the probable correlations of the various states with those of CH_2+CH_2.

Other Double-Bonded Compounds

From Fig. 1 it will be seen that the normal state of plane C_2H_4 should be stable with respect to a relative rotation of the planes of the two CH_2's, but that the excited states $^3\Gamma_{4u}$ and $^1\Gamma_{4u}$ shown in Fig. 1 might be expected to rotate spontaneously into the corresponding states $^3\Gamma_3$ and $^1\Gamma_4$ of perp. C_2H_4. By applying methods similar to the above to ethylene derivatives, such as for example $R_1R_2C=CR_1R_3$, it is easily shown that they should show qualitatively the same behavior as $H_2C=CH_2$ itself, and should have energy level diagrams similar to Fig. 1. Experimentally, their lowest excited energy levels are apparently nearer the normal level than in C_2H_4, since the ultraviolet absorption bands of the derivatives begin at longer wave-lengths than those of C_2H_4 itself, the shift increasing with the complexity of the molecule.[8]

Application of the quantum theory to C=N and N=N double bonds along the lines used for the C=C bond indicate that they also have the structure $[z+z]^2[x+x]^2$ characteristic of the C=C bond (cf. (2)). But the bond in B_2H_6 is probably more like that in O_2, giving a paramagnetic normal state, and has probably almost no stability toward a relative rotation of the two BH_2 groups. Details will be given in later papers.

It is well known that derivates of ethylene, e.g., $R_1R_2C=CR_1R_3$, exist in two forms called *cis* and *trans*, where in the *cis* form the two R_1's are on the

[7] The difference between $[x+x]^2$, $^1\Gamma_{1g}$ and $\cdots[x+x][x-x]$, $^1\Gamma_{4u}$ of plane C_2H_4 is analogous to that between $\cdots(\pi+\pi)^4(\pi-\pi)^2$, $^3\Sigma^-_g$ and $(\pi+\pi)^3(\pi-\pi)^3$, $^3\Sigma^-_u$ of O_2, unless possibly the electron configuration assigned in the latter case is wrong. In this O_2 case the energy difference is 6.1 volts from $v=0$ of the $^3\Sigma_g^-$ to $v=0$ of the $^3\Sigma_u^-$. Another example of the dominant effect of antibonding electrons is the case of H_2, where the energy of $(1s_A+1s_B)^2$, $^1\Sigma^+_g$ is -4.4 volts compared with H+H, while for the same internuclear distance the energy of $(1s_A+1s_B)(1s_A-1s_B)$, $^3\Sigma^+_u$ is about $+5$ volts.

[8] Cf. J. Stark and collaborators, Jahrbuch der Rad. und Elek. **10**, 10–188 (1913); and data in Int. Crit. Tables, Vol. 5. It seems likely that the "first band" of Stark corresponds in each case to a transition to the state analogous to the $^1\Gamma_{4u}$ of C_2H_4. (In the case of C_2H_4 itself, Stark's "second band" near $\lambda 2000$ is probably really the "first band.") The transition to the state analogous to $^3\Gamma_{4u}$ of C_2H_4 is perhaps represented by weak absorption at longer wave-lengths, not carefully investigated by Stark. It is perhaps best not to venture an interpretation of Stark's second band at shorter wave-lengths, except to suggest that *possibly* it may belong to the same transition as the first band,—but more probably not. In regard to the structures of the "first bands," cf. remark at end of the Fig. 1 caption.

same side of the z axis (C-C axis), in the *trans* form on opposite sides.[9] Usually both forms are stable at low temperatures, but the higher-energy form (usually *cis*) can usually be transformed into the lower-energy form (*trans*) by heating. The "energy of activation" for this process is evidently the energy difference between the normal state of the plane form ($^1\Gamma_{1g}$ for C_2H_4 in Fig. 1) and the lowest state of the perp. form ($^3\Gamma_3$ of perp. C_2H_4 in Fig. 1). Experimentally, there is evidence that this energy of activation is lower in the ethylene derivatives than is indicated by Fig. 1 for ethylene itself.[9]

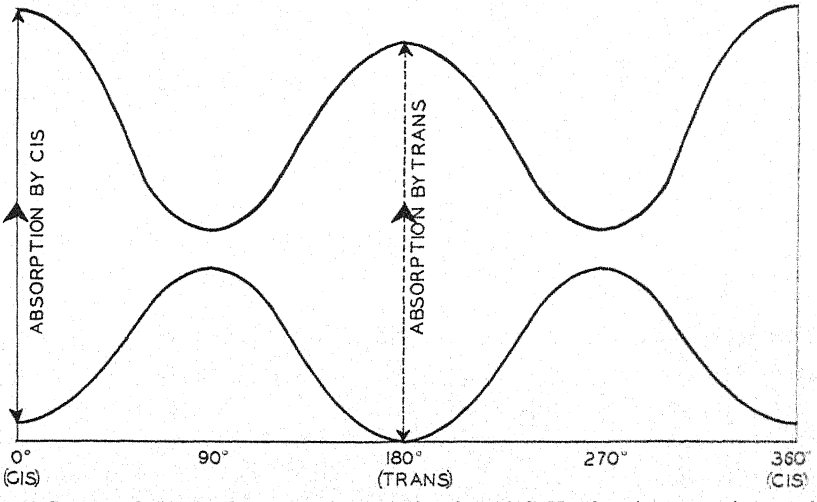


Fig. 2. Curves of electronic energy for a derivative of C_2H_4, for the normal state (lower curve) and (upper curve) for an excited state analogous to $^1\Gamma_{4u}$ of C_2H_4 in Fig. 1. The curves are of no more than qualitative significance. The *cis* form would probably usually correspond to 0°, the *trans* form to 180°, in a figure of the type of Fig. 2. The process of absorption of ultraviolet light by either form is indicated by vertical arrows. After such absorption, the molecule performs rotational vibrations about, or rotations through, the energy maxima at 0° and 180°. If light is emitted, or the energy is lost in a collision, when the angle of rotation away from the original angular position exceeds 90°, the molecule has been transformed from *cis* into *trans*, or vice versa.

Interpretation of Photochemical Experiments

Experimentally it is well known that the absorption of ultraviolet light can convert *cis* into *trans* forms and vice versa.[10] Probably the absorption carries the molecule to the singlet level analogous to $^1\Gamma_{4u}$ of C_2H_4 (Fig. 1), where it is unstable with respect to rotation into the perp. form.[11] [Olson[12] has pre-

[9] Cf. E. Hückel, Zeits. f. Physik **60**, 423 (1930) for a review of the experimental evidence on the behavior and nature of double-bonded compounds. This includes definite evidence for a plane arrangement of the six atoms nearest to the double bond.

[10] R. Stoermer and collaborators. Ann. d. Chemie **342**, 1 (1905); Chem. Ber. **42**, 4865 (1909); **44**, 637 (1911) and later articles.[9]

[11] Most absorbed frequencies would give rise to strong vibrations as well as to relative rotation of the CH_2 groups, but this has no necessary primary effect on the *cis-trans* transformation discussed here, except for absorbed frequencies causing direct dissociation or predissociation of $R_1R_2C_2R_1R_3$ into CR_1R_2 and CR_1R_3. Experimentally, the ultraviolet frequencies which cause the *cis-trans* change usually do not produce much decomposition.

[12] A. R. Olson, Faraday Soc. Trans. **27**, 69 (1931).

viously discussed the possible transformation of the *cis* into the *trans* isomer or vice versa by relative rotations of the CR′R″ groups as a result of ultraviolet absorption, but did not consider the simple mechanism which the present theory indicates.] The momentum of the rotation should, however, carry the molecule past the perp. form (90° rotation) into the form (*trans* or *cis*, as the case may be) opposite to that (*cis* or *trans*) in which it started (180° rotation): cf. Fig. 2. If the molecule is undisturbed, many rotations or rotational vibrations should take place, until eventually the energy is lost by a collision or by radiation, or sometimes perhaps by predissociation. For any individual molecule which has absorbed suitable light, the chances should then be nearly equal of returning to the original form or of ending in the isomeric form. Experiments of Warburg,[13] however, on the isomeric acids fumaric (*trans* form, higher energy) and maleic (*cis* form) of formula $(H \cdot C \cdot COOH)_2$ show only from 3 to 12 percent conversion of either isomer into the other per light quantum absorbed. Quite possibly this discrepancy can be attributed to disturbing factors, e.g., perhaps interference by collisions before completion of a single rotation or rotational vibration, since the experiments were made in water solution.

Prolonged exposure of ethylene derivatives to ultraviolet light tends to set up a photochemical equilibrium. Apparently this equilibrium is usually such that the lower-energy isomer is changed rather completely into the higher-energy isomer.[10] In the case of maleic and fumaric acid, equilibrium exists when there is about 75 percent of maleic acid;[13] the equilibrium ratio, however, apparently depends on the absorbed wave-lengths. Such results can be readily understood in terms of the present theory. They depend somewhat on the relative heights of the *cis* and *trans* maxima of the excited-state curve in Fig. 2, but probably more, or more directly at least, on differences in the absorption coefficients of the two isomers, which cause one to be transformed more rapidly than the other.

In conclusion, it may be remarked that the correctness of the preceding interpretation of the excited levels of ethylene and its derivatives, and of the effect of ultraviolet light on them, has not been proved. For the interpretation depends in part on estimates of the relative positions of energy levels which may conceivably be wrong to a sufficient extent to upset it. The interpretation should, however, be capable of experimental testing, and might also be the subject of theoretical calculations.

[13] E. Warburg, Sitzungsber. der Preuss. Akad. der Wiss., No. 50, p. 964 (1919).

Production of Infrared Spectra with Electric Fields

By E. U. CONDON
Palmer Physical Laboratory, Princeton University

(Received July 26, 1932)

A substance in a strong electric field acquires a new infrared spectrum owing to changes in the selection rules. The spectrum is governed by matrix components of the molecular polarizability and hence has the same intensity rules as the Raman effect.

IT IS well known from experience and from the theory of the Stark effect in atomic spectra that electric fields break down selection rules which apply to the atom when not in an electric field. It is natural therefore to suppose such effects might occur in molecular spectra with the consequence that nonpolar molecules like H_2 which have no infrared absorption would become absorbing when placed in a strong electric field. This question is given consideration in the following paper.

For a molecule the matter can be simply considered in terms of two properties: the molecular polarizability and the electric moment. The former is a tensor α_{ij} whose components have fixed values relative to a coordinate system fixed in the molecule. These values are functions of the coordinates fixing the nuclear configuration of the molecule. The electric moment is a vector M_i whose components are likewise most naturally taken in a coordinate fixed in the molecule and which are also functions of the nuclear coordinates of the molecule. The ordinary infrared spectrum of the molecule is determined by the matrix components of the electric moment M_σ referred to axes fixed in space. Suppose *1*, *2*, *3* are the unit vectors along which the axes $i=1, 2, 3$ are taken and that the orientation of these relative to an $(i\ j\ k)$ system fixed in space is specified by Eulerian angles θ, ϕ, ψ, then, if M_σ specifies a component of M in the new system

$$M_\sigma = a_{\sigma i} M_i \tag{1}$$

(using summation convention on double indices). Since the $a_{\sigma i}$ are functions of Euler's angles and the M_i are functions of the internal nuclear coordinates these electric moment components are functions of the vibration and rotation coordinates of the nuclear motion.

To find the infrared spectrum we have to calculate the matrix of the M_σ relative to the stationary states of the motion in the usual way. Letting j, m, λ be the quantum numbers of the rotational motion and writing n shortly for the ensemble of the vibrational motion's quantum numbers we have, for the eigenfunction of the molecule's nuclear state,

$$\psi(n, j, m, \lambda) = F_{\theta\phi\psi}(j, m, \lambda) G_q(n, j, m, \lambda) \tag{2}$$

where F and G are functions of the coordinates indicated as subscripts. F will be the rotator eigenfunctions of the unsymmetrical top in general but may be in special cases the simpler ones for the symmetrical top or even, for straight-line molecules, for the simple rotator. We neglect complicated cases of coupling of rotation and vibration motions. Because of the form of (1) and (2) the matrix components become

$$(n, j, m, \lambda \mid M_\sigma \mid n'j'm'\lambda') = \int \overline{F}(jm\lambda) a_{\sigma i} F(j'm'\lambda') \cdot \int \overline{G}(njm\lambda) M_i G(n'j'm'\lambda') \quad (3)$$

The first factor is simply the matrix components of the direction cosines which transform from the rotating to the fixed coordinate system and so can be calculated once and for all for the various simple cases, like the simple rotator and the symmetrical top. The probabilities for transitions by emission or absorption of light are given in the usual way by the squared absolute magnitudes of the matrix components in (3). This is the ordinary infrared spectrum.

Now let us consider the behavior of a molecule with regard to radiation when it is in a constant electric field of components, E_σ. It now has an induced electric moment which we call P_σ to distinguish from M_σ, the permanent electric moment. We shall have

$$P_\sigma = \alpha_{\sigma\tau} E_\tau \quad (4)$$

where $\alpha_{\sigma\tau}$ represents the components of α in the fixed coordinate system. By the tensor transformation law we have

$$\alpha_{\sigma\tau} = a_{\sigma i} a_{\tau j} \alpha_{ij}. \quad (5)$$

The new radiative transitions which the molecule may undergo while in the electric field are given by the matrix components of P_σ just as those in the absence of the field are given by the matrix of M_σ. Of course the ordinary infrared spectrum due to M_σ will be present perhaps with very small shifts due to a small Stark effect shift of the levels. The levels in the field are altered by the amount appropriate to the energy of an induced dipole in the field, i.e., by $-\frac{1}{2} P_\sigma E_\sigma$. The level with quantum numbers (n, j, m, λ) is therefore altered by the appropriate diagonal matrix element of this quantity, $(njm\lambda \mid -\frac{1}{2} P_\sigma E_\sigma \mid njm\lambda)$. We are not as much interested in such small shifts as we are in the new transition possibilities.

The matrix components of P_σ are evidently

$$(njm\lambda \mid P_\sigma \mid n'j'm'\lambda') = \int \overline{F}(jm\lambda) a_{\sigma i} a_{\tau j} F(j'm'\lambda') \cdot \int \overline{G}(njm\lambda) \alpha_{ij} G(n'j'm'\lambda') \cdot E_\tau \quad (6)$$

The important point is that the selection rules for radiation associated with P_σ will be quite different from those for that due to M_σ for they depend on quite different characteristics of the molecule. As far as rotation is concerned however we can see immediately what the selection rules are for this induced

spectrum in terms of those for the ordinary spectrum, because of the form of the part of (6) that depends on the $a_{\sigma i}$. By the rules of matrix multiplication,

$$(jm\lambda \mid a_{\sigma i}a_{\tau i} \mid j'm'j') = (jm\lambda \mid a_{\sigma i} \mid j''m''\lambda'')(j''m''\lambda'' \mid a_{\tau j} \mid j'm'\lambda'),$$

which expresses the rotational factors of the new spectrum's matrix components in terms of those of the usual spectrum.

So far as rotation levels are concerned the transitions of $(jm\lambda) \rightarrow (j'm'\lambda')$ occurring in the induced spectrum will be those which are related by the property of each combining in the ordinary way with some third state (j'', m'', λ''). For the simple rotator this leads to the rule $\Delta j = \pm 2, 0$ in view of the $\Delta j = \pm 1$ of the usual spectrum. This is the selection rule of the Raman effect.

This last remark has a more deep-lying significance than an accidental coincidence, for on looking back over the work we see that the ideas involved are exactly those of Placzek's theory of the Raman effect. He calculates[1] the matrix components of the electric polarizability to get at the intensities and selection rules of the Raman effect. There the induced moment is due to the electric vector of the light wave, here it is due to the steady applied electric field. The induced spectrum we are describing is therefore what might be called the limit of the Raman effect as the frequency of the exciting light tends to zero. It has the same selection rules as the Raman effect.

When the Raman effect was first discovered it was assumed that it would be simply the usual infrared spectrum moved up into the visible part of the spectrum by combination with the frequency of the scattered light. This erroneous view was soon corrected by the facts and by a closer examination of the consequences of the Kramers-Heisenberg theory. This paper however points out how we can do the converse of the original view, namely put the Raman spectrum down into the infrared simply by letting the exciting light frequency tend to zero, it thus becoming an electrostatic field.

The connection with the Raman effect seems also to give a possibility of estimating the possibility of obtaining the induced spectrum in the laboratory. The integrated absorption coefficient over line width $\int \alpha d\nu$ is connected with the number of molecules in unit volume in the lowest state N_1 and the spontaneous transition probability A_{21} by the relation[2]

$$\int \alpha d\nu = N_1(c^2/8\pi\nu)A_{21}.$$

Using the relation of A_{21} to electric moment matrix components we have

$$\int \alpha d\nu = N_1(8\pi^3/3h^2)(h\nu/c) \mid P \mid^2$$

[1] Placzek, Zeits. f. Physik **70**, 84 (1931). Actually Placzek omits consideration of the rotational motion of the molecule. The writer worked out the above formulation including rotation last spring and would have calculated it through in detail but for the fact that W. V. Houston reported this problem at the Pullman meeting of the American Physical Society. His calculations are to be published soon according to what I have learned from his associate Mr. C. M. Lewis who is also a visitor at Massachusetts Institute of Technology this summer.

[2] Tolman, Phys. Rev. **23**, 693 (1924).

where P is written shortly for the matrix component in question. It is known that easily observable absorption is obtained say in HCl with $P \sim 10^{-19}$ and $N_1 \sim 10^{19}$ that is with a product of the order $N_1 P^2 \sim 10^{19}$. The polarizability of molecules is of the order 10^{-24} cm^3 and so if we use a liquid or a solid to make $N_1 \sim 10^{22}$ cm^{-3} and a field of 30,000 volts,cm $= 10^2$ e.s.u., we can obtain a product $N_1 P^2 \sim 10^{-22}$ which is still but 10^{-3} of that in HCl. Nevertheless, by use of long tube lengths it might be possible to observe the induced absorption.

One could use a long absorption cell with long condenser plates, applying the field with a high-potential transformer. The alternations of the potential would make no difference since their only effect would be to impress the alternation frequency on the spectrum which would be negligible in spectroscopic units.

The Impacts of Fast Electrons and Magnetic Neutrons

By J. F. CARLSON AND J. R. OPPENHEIMER
University of California, Berkeley, California

(Received July 18, 1932)

In this paper we consider the behavior of electrons with energy very large compared to their proper energy in their passage through matter, and further treat the impacts suffered by a certain type of hypothetical elementary neutral particle whose existence was tentatively suggested by Pauli. In the introduction we outline the problem and the methods to be employed, and give a summary of the formulae which embody our results. In Section I we develop the method suggested by Møller for the relativistic treatment of impacts; in (a) we apply it to the impacts of two free electrons; in (b) we show how it is to be applied to those impacts of a fast electron in which little energy is transferred to the secondary; in (c) we develop the theory of the magnetic neutron, and apply Møller's method to the treatment of its impacts. In II we give the detailed calculation of the energy transfers from a fast electron to the electrons of the matter through which it is passing, and compute the range and ionizing power of the primary electron. In III we apply the theory of the neutron to compute the number and nature of its impacts.

INTRODUCTION

RECENT experiments on the cosmic rays and on the penetrating radiation produced in the artificial disintegration of beryllium have raised again the question of the behavior of particles of very high energy in their passage through matter. Both these radiations have been shown to be extremely penetrating; and cloud chamber photographs have shown that both are accompanied by electrons of velocity very close to that of light; in the case of the cosmic rays the presence of electrons of energy over 10^9 volts has been established. The range of such particles, the number and nature of the secondary particles produced in their passage through matter can be computed theoretically. It has seemed to us desirable for a better understanding of the nature and properties of these radiations to have a more complete theoretical answer to these questions than is available. We shall, in this paper, be concerned with the behavior of two types of particle; chiefly we wish to study the electron of high energy; energy large, that is, compared with the proper energy mc^2. But we shall also study the impacts of a certain type of neutron, a hypothetical elementary neutral particle carrying a magnetic moment. This particle necessarily has a spin and presumably satisfies the exclusion principle; its existence was tentatively proposed by Pauli,[1] on the ground that by its introduction certain difficulties in the theory of nuclei could be resolved, and on the further ground that such a particle could be described by a wave function which satisfies all the requirements of quantum mechanics and rela-

[1] Professor Pauli presented the considerations which led him to the introduction and definition of the magnetic neutron at a seminar on theoretical physics in Ann Arbor in the summer of 1931.

tivity. These requirements, for instance, show that an elementary particle can have a magnetic but not an electric dipole moment; they do not suffice to fix the magnitude of the moment nor of the mass of the particle. Pauli supposed that such neutrons might form a third element in the building of nuclei, in addition to the electrons and protons; in this way one could understand the anomalous spin and statistics of certain nuclei, and the apparent failure of the conservation of energy in beta-particle disintegration. Pauli accordingly supposed that the mass of the neutron was not much greater than that of the electron, and that its magnetic moment was small compared to the Bohr magneton. One may, however, assume that the neutron has a mass very close to that of the proton, and that such neutrons are substituted for pairs of electrons and protons in certain nuclei, instead of being added to them; such neutrons would help explain the anomalous spin and statistics of nuclei, although they would throw no light on the beta-ray disintegrations. The experimental evidence on the penetrating beryllium radiation suggests that neutrons of nearly protonic mass do exist; and since our calculations may be carried through without specifying the mass or magnetic moment of the neutron, we shall consider the most general particle which satisfies the wave equation proposed by Pauli. It is important to observe that there may very well be other types of neutral particles, which are not elementary, and to which our calculations do not apply; and for clarity we shall call the particle which satisfies Pauli's wave equation a magnetic neutron. Certain of our results, such as the relatively great penetration of the particle, relatively rare impacts, and large mean energy loss per impact, characterize the behavior of any neutral particle.

The collisions and range of beta-particles have been often studied theoretically; and even the case in which the primary velocity of the beta-particle is very close to that of light has been studied by Bohr[2] in his classical theory of range. But Bohr used a classical model for the atom and the beta-particle, and a classical method for treating their interaction; and Bohr's treatment of the close impacts involving large energy losses is even classically not free from ambiguity. A very complete quantum theoretical calculation has been made by Bethe[3] for the case that the electron has a velocity not comparable with that of light; and our first problem in this paper is to make this calculation relativistically, so that it may be applied to electrons of energy very large compared to their proper energy.

At first sight the semi-classical method used by Gaunt[4] would appear appropriate for our purpose. Gaunt's method is semi-classical in that, in the quantum mechanical expression for the probability of excitation (ionization) of an atom, the matrix component of the interaction energy between primary and atomic electrons is in part replaced by a Fourier component, replaced, that is, by the matrix component for the transition of the atomic electron of the Fourier component of the potential of the primary electron. For transi-

[2] N. Bohr, Phil. Mag. **30**, 58 (1915).
[3] H. Bethe, Ann. d. Physik **6**, 325 (1930).
[4] J. A. Gaunt, Proc. Cam. Phil. Soc. **23**, 732 (1928).

tions in which the primary electron has a small change of momentum, small energy loss and small deflection, this method constitutes a valid application of the correspondence principle. And this method is readily extended to high velocity primaries, since we have now only to take, in place of the electrostatic potential, the Fourier component of the retarded four-vector potentials of the primary as a perturbation which induces transitions of the atomic electrons. The method is, however, not very elegant, even for the computation of the probability of small energy losses, because it gives an incorrect and very large probability of transitions involving small energy losses but large deflections, transitions to the study of which it may not legitimately be applied. We shall, therefore, not use this method; but in §II we shall give an outline of it, because it gives an illuminating insight into our formulae, and makes clear in a simple way the reason for the increase in ionization power with increasing energy of the primary. Quite recently Møller[5] has given a beautiful method of treating the relativistic impact of two electrons. This method is based upon a refinement of the correspondence principle; it neglects higher powers of the interaction energy between the electrons, and the effect of radiative forces; but within these limits it is strict and unambiguous, and enables one to take account, not only of the relativistic variation of mass with the velocity of the electrons, but of the retardation of the forces between them, of the spin forces, of interchange and the exclusion principle. The method is applicable not only to the impacts between two free electrons, but to the impacts of a free and an atomic electron in which small energies are transferred; it is further applicable to the impact of a neutron with an electron or proton; and it is this method which we shall use. In doing this we may take advantage of the fact that for energy losses very large compared to the ionization energy of the atomic electron we may treat both electrons as free; whereas for small energy losses we may neglect relativistic effects for the atomic electron, and, as it turns out, interchange. For extranuclear electrons there is a region of energy loss large compared to the binding energy and small compared to the proper energy where the two calculations merge and agree. For the neutron the probability of small energy losses is small, and the binding of an atomic electron can be largely neglected.

In §I then we shall give an outline of Møller's method, and its application to the three calculations; intimate collisions with an electron, collisions with a bound electron involving small energy loss, and collisions of a neutron. We shall have to discuss here the limitations imposed upon the method by the neglect of higher powers of the interaction energy and of radiative forces. These points cannot be fully settled without an adequate quantum electrodynamics, since they involve questions whose classical analogue is the theory of the structure of the electron. But we shall see that our method gives an upper limit to the range and a lower limit to the ionizing power; and we shall see further that the neglect we have made is small of the order of the fine structure constant. We shall have to carry the details of the calculation of the

[5] C. Møller, Zeits. f. Physik **70**, 786 (1931). Further L. Rosenfeld, ibid. **73**, 253 (1931).

impact of two free electrons rather further than was done by Møller, and shall obtain a formula for the differential probability of a given energy loss, a formula which may be applied to the impact of an electron with an atomic electron for all energy losses large compared to the binding energy.

In §II we shall treat impacts involving small energy losses, and compute the range and the number of primary ions for a beta-particle. In §III we shall carry through the calculations of the impacts of a magnetic neutron, and apply them for a few typical values of the constants characterizing the particle.

We shall give here a summary of certain of our results. Let the energy of the primary electron be

$$E = \epsilon mc^2 \tag{I}$$

and the binding energy of the second electron be I, and the energy lost by the primary be E'. We have to consider only collisions in which

$$E' \leqq \tfrac{1}{2}[(\epsilon - 1)mc^2 - I] \tag{II}$$

since one particle has always at least half the initial energy (see 1.32). The following formulae hold for large ϵ.

1.

The differential cross section for an energy loss $E' \gg I$ is

$$\sigma dE' = \frac{2\pi e^4}{mc^2}\,\frac{dE'}{E'^2}\cdot\frac{E^4 + E'^4 + (E - E')^4}{2E^2(E - E')^2}\,. \tag{III}$$

The angle γ between the trajectories of the two electrons after such an impact is given by

$$\gamma^2 = (2mc^2/E')(1 - E'/E)\,.$$

2.

If the cross section for ionization of the atomic electron by a primary electron of velocity v be

$$\sigma_{\text{ion}} = k_1(2\pi e^4/mv^2I)\ln mv^2/k_2I \tag{IVa}$$

then the cross section for ionization by the fast electron of energy ϵmc^2 is

$$\sigma_{\text{ion}} = k_1(2\pi e^4/mc^2I)\{\ln (mc^2/k_2I) + 2\ln\epsilon\}\,. \tag{IVb}$$

When the atomic electron was initially bound in the normal state of a hydrogen-like atom,

$$k_1 = 0.29;\ k_2 = 0.024. \tag{IVc}$$

3.

If the mean energy loss to the atomic electron for a primary of velocity v is

$$\delta E = (4\pi e^4/mv^2)\ln mv^2/k_3I \tag{Va}$$

then for a primary of large energy

$$\delta E = (4\pi e^4/mc^2)\{\ln mc^2/k_3I + (3/2)\ln\epsilon + 0.22\}\,. \tag{Vb}$$

For an electron in the normal state of a hydrogen-like atom

$$k_3 = 1.1. \tag{Vc}$$

4.

When a magnetic neutron hits a charged particle, the mean energy loss per impact is of the same order as the maximum energy loss permitted by the conservation laws. If the mass of the neutron be M, its magnetic moment μ, its velocity small compared to that of light and its energy E, and if the charge and mass of the secondary be respectively e, and $m = \lambda M$, then the mean energy loss of the neutron is

$$\delta E = (7\pi^3 e^2 \mu^2 / 6h^2 c^2) E \tag{VIa}$$

for $\lambda = 1$

and

$$\delta E = (2\pi^3 e^2 \mu^2 / h^2 c^2) \lambda E \tag{VIb}$$

for $\lambda \ll 1$. Further details and other cases of impacts of the magnetic neutron are treated in §III.

NOTE: After the completion of this work, a very interesting paper[6] of Heisenberg has come to hand. Heisenberg is concerned with the problem of the nature of cosmic rays; and he derives theoretical formulae for the range of high speed particles with which to compare the experimental findings. Heisenberg's formula for the range of a fast electron differs only very slightly from that which we have found (Vb); we do not believe that the application of our formulae would lead to sensibly different conclusions. Note added in proof: An outline of a derivation of a formula for the energy loss of a fast electron, by a method also based on Møller's and altogether similar to that used by us in II, has been given in a recent paper of Bethe (Zeits. f. Physik, **76**, 283 (1932)).

I. RELATIVISTIC THEORY OF IMPACTS

The method which Møller proposed for the relativistic treatment of impacts is a generalization of two familiar elementary methods; the nonrelativistic collision theory of the quantum mechanics, and the theory of the transitions induced in a quantum mechanical system by a known electromagnetic field. According to the nonrelativistic quantum mechanics, we can write down the interaction energy V of the two particles which are colliding as a function of the coordinates (and in some cases momenta) of the particles; for two electrons this energy is just the electrostatic interaction energy. We can further specify the stationary states of the non-interacting particles by certain quantum numbers r, ρ, e.g., the components of momenta of the two particles. In the matrix scheme in which these quantum numbers are diagonal there will be a matrix $V_{rs}^{\rho\sigma}$ which corresponds to the interaction energy. Then with neglect of higher powers of the interaction energy, and with suitable normalization, the transition probability for a transition in which the one particle changes its state from $s \to r$ and the other from $\sigma \to \rho$ will be given by

$$P_{rs}^{\rho\sigma} = (4\pi^2/h) \left| V_{rs}^{\rho\sigma} \right|^2 \delta(E_r + E_\rho - E_s - E_\sigma). \tag{1.1}$$

[6] W. Heisenberg, Ann. d. Physik [5,] **13**, 430 (1932).

(The energy of a particle in state r is written E_r; and $\delta(x)$ is the delta function.) Further, when we know the wave functions for the particles in their non-interacting stationary states

$$\begin{aligned} \psi_s &= u_s e^{(-2\pi i/h)\cdot E_s t} \\ \psi_\sigma &= u_\sigma e^{(-2\pi i/h)\cdot E_\sigma t} \end{aligned} \tag{1.2}$$

we can compute the matrix $V_{rs}{}^{\rho\sigma}$:

$$V_{rs}{}^{\rho\sigma} = \int\int d\boldsymbol{r}d\boldsymbol{r}'\bar{u}\bar{u}_\rho' V u_s u_\sigma'. \tag{1.3}$$

(Integral over configuration space $\boldsymbol{r}$, $\boldsymbol{r}'$ of two particles.) Now when we are dealing with particles whose velocity is close to that of light, we must of course use relativisitic wave functions to characterize their stationary states; there is no difficulty in doing this. For the electron we must use solutions of Dirac's wave equation; for the neutron we may use solutions of the wave equation given by Pauli. But the function V no longer exists, since one cannot, when the retardation of the forces is taken into account, express the interaction energy as a function of the coordinates and momenta alone. What then, in the relativistic theory, should replace the matrix element $V_{rs}{}^{\rho\sigma}$?

We can answer this question if we consider first the perturbation induced in a quantum mechanical system by a given electromagnetic field. Let the four-vector potential of the field be $\phi_\mu(x, y, z, t)$; $\mu = 1 \cdots 4$, and the charge and current density vector of the system be

$$J^\mu = \psi j^\mu \psi. \tag{1.4}$$

Then

$$V = -1/c\phi_\mu j^\mu \tag{1.5}$$

is the operator representing the interaction energy of field and system. We resolve this operator in a Fourier integral

$$V = \int V_\nu e^{-2\pi i\nu t} d\nu;\ V_\nu = (-1/cj^\mu)\int e^{2\pi i\nu t}\phi_\mu dt. \tag{1.6}$$

To V_ν there now corresponds a matrix in the scheme of the stationary states without field

$$V_\nu{}^{\rho\sigma} = \int u_\rho V_\nu \mu_\sigma d\boldsymbol{r}. \tag{1.7}$$

Here, again neglecting higher powers of the interaction energy, we find for the transition probability

$$4\pi^2/h \left| V_\nu{}^{\rho\sigma} \right|^2 \delta(E_\rho - E_\sigma - h\nu). \tag{1.8}$$

Now when the field ϕ_μ is produced by a particle of known trajectory, a trajectory uninfluenced by the reaction of the system upon it, we express the potentials in terms of the retarded charge and current density J'^μ of this particle:

$$\phi^{\mu}(\boldsymbol{r}, t) = (1/c) \int d\boldsymbol{r}' \frac{[J'^{\mu}]}{r} t - r/c;\ r = \left| \boldsymbol{r} - \boldsymbol{r}' \right| . \tag{1.9}$$

Then

$$V_{\nu} = (-1/c^2) \int d\boldsymbol{r}' \left[j_{\mu} \int J'^{\mu} e^{2\pi i \nu t} dt \right] (e^2/r) e^{\pi i \nu r/c} \tag{1.10}$$

and the transition probability $\sigma \rightarrow \rho$ is given by

$$(4\pi^2/h) \left| V_{\nu}^{\rho\sigma} \right|^2 \delta(E_{\rho} - E_{\sigma} - h_{\nu})$$

with

$$V_{\nu}^{\rho\sigma} = (-1/c^2) \int\int d\boldsymbol{r} d\boldsymbol{r}' \tilde{u}_{\rho} \left[j_{\mu} \int J'^{\mu} e^{2\pi i \nu t} dt \right] \frac{e^{2\pi i \nu r/c}}{r} u_{\sigma} . \tag{1.11}$$

This at once suggests that, when the trajectory of the particle is influenced by the reaction of the system, so that the state of the particle also changes as a result of the interaction, we replace the Fourier component of the retarded potentials of the particle by the matrix component corresponding to the transition in question. Thus if again

$$J'^{\mu} = \tilde{\psi} j'^{\mu} \psi$$
$$\psi_r = u_r e^{(-2\pi i/h) E_r t}$$

are the wave functions for the stationary states of the particle, we have to replace $\int J'^{\mu} e^{2\mu i \nu t} dt$ by $\tilde{u}_r j'^{\mu} u_s$ with $E_s - E_r = h\nu$.
This gives

$$\begin{aligned} P_{rs}^{\rho\sigma} &= (4\pi^2/h) \left| V_{rs}^{\rho\sigma} \right|^2 \delta(E_r + E_{\rho} - E_s - E_{\sigma}) \\ V_{rs}^{\rho\sigma} &= (-1/c^2) \int\int d\boldsymbol{r} d\boldsymbol{r}' \tilde{u}_r \tilde{u}_{\rho}' j_{\mu} j'^{\mu} e^{(2\pi i/hc)(E_s - E_r) r} u_s u_{\sigma}'/r . \end{aligned} \tag{1.12}$$

This reduces to (1.3) when retardation may be neglected and the velocity of the particles is small compared to that of light; it reduces to (1.11) when the reaction of the system on the particle may be neglected.

This is the formula proposed by Møller.[5] Although the derivation of the formula distinguishes between the system and the particle, the result which we obtain for $V_{rs}^{\rho\sigma}$ when we reverse the roles of the two

$$(-1/c^2) \int\int d\boldsymbol{r} d\boldsymbol{r}' \tilde{u}_{\rho} \tilde{u}_r' j^{\mu} j_{\mu}' e^{2\pi i/hc (E_{\sigma} - E_{\rho}) r} u_s' u_{\sigma}/r .$$

gives the same transition probability, and the same matrix to represent the interaction energy.

We are thus led to consider the interaction energy represented by the matrix (1.12), $V_{rs}^{\rho\sigma}$. One might at first suppose that by the use of this expression for the energy, and the higher approximations of the method of variation of constants by which the transition probabilities may be computed, one

could obtain a strict expression for these transition probabilities. This is not so, however, because in the derivation of (1.12) the reaction of each particle to its own field had been neglected; this reaction should be taken into account in any strict theory, and its omission makes the higher approximations —involving higher powers of the charge or moment of the particles, invalid. Thus (1.12) gives no account of collisions between the particles in which radiation is emitted; but we know that such transitions will in fact occur. Their relative frequency, frequency relative to the transitions in which no radiation is emitted, is known to be of the order

$$\alpha(\bar{v}/c)^2 \tag{1.13}$$

where α is the fine structure constant, and $\bar{v}$ the mean velocity of the charges. This probability can thus be neglected when one of the particles moves with a velocity small compared to light; even when this is not so, radiative processes are presumably relatively rare because of the smallness of α. We shall see that in our theory of the impact of a high velocity electron upon matter the impacts in which very little energy is lost are the only ones of importance. But in these impacts the secondary electron has very low velocities, so that we know that radiative processes cannot be important in these impacts. For this reason the results we obtain with neglect of radiative forces furnish a lower limit to the ionizing power and energy loss of the fast electron. On the other hand the formulae derived from (1.12) for impacts in which large energies are transferred may be seriously in error; this error is at least of the order α.

When the two colliding particles are electrons, (1.12) must be modified to take account of interchange and the exclusion principle. When the interaction energy matrix corresponds to an operator in configuration space, it is known that this may be done by writing for the interaction energy

$$\tfrac{1}{2}\sum_{r,s\ \rho,\sigma} V_{rs}{}^{\rho\sigma} a_\rho{}^+ a_r{}^+ a_s a_\sigma \tag{1.14}$$

and by treating the a's as dynamical variables which satisfy

$$\begin{aligned} a_\rho{}^+ a_\sigma + a_\sigma a_\rho{}^+ &= \delta_{\rho\sigma}; & a_\rho a_\sigma + a_\sigma a_\rho &= 0 \\ & & a_\rho{}^+ a_\sigma{}^+ + a_\sigma{}^+ a_\rho{}^+ &= 0. \end{aligned} \tag{1.15}$$

The order of the a's has been so chosen that the interaction of each particle with its own field has been eliminated. Now although $V_{rs}{}^{\rho\sigma}$ corresponds to no operator in configuration space, and there is no wave equation in the configuration space of the two particles with which to compare our results, we still take (1.14) to represent the interaction energy. Since each $a_r{}^+$ corresponds to a transition in which a particle enters the state r, and each a_r to one in which a particle leaves the state r, there are now four terms in this sum which give rise to a transition in which the two particles go from the states s and σ to r and ρ. Because of the symmetry of $V_{rs}{}^{\rho\sigma}$, these four terms are equal in pairs; for the transition probability we find, in place of (1.12)

$$P_{rs}{}^{\rho\sigma} = (4\pi^2/h)\left| V_{rs}{}^{\rho\sigma} - V_{r\sigma}{}^{\rho s}\right|^2 \delta(E_r + E_s - E_\rho - E_\sigma). \tag{1.16}$$

In dealing with the impacts of a fast electron on an atom, it is easy to see that when the energy transferred to the atomic electron is small the interchange terms in (1.16) are negligible; for such impacts we may use (1.12) in place of (1.16).

We have now to apply these formulae to the three cases: (a) Impacts of two free electrons. (b) Impacts of a fast electron with an atomic electron, in which little energy is given to the secondary. (c) Impacts of a neutron with an electron or proton.

(a) High velocity impacts of free electrons

To apply (1.16) to the impacts of two free electrons we have to write down explicitly the wave functions for the stationary states of the free electrons and the expressions for the matrix components of the charge and current vector. The states of each electron we may specify by giving the components of momentum

$$\boldsymbol{p}^{(1)} = (p_x^{(1)}, p_y^{(1)}, p_z^{(1)}); \ \boldsymbol{p}^{(2)} = (p_x^{(2)}, p_y^{(2)}, p_z^{(2)})$$

and the component of spin $\sigma^{(1)}$, $\sigma^{(2)}$ of each electron in the z direction. (We exclude states of negative energy; and to the approximation here considered this causes no ambiguity.) For each of the electrons we take the wave functions to be solutions of the equations

$$[(h/2\pi i)(\partial/\partial t) + (hc/2\pi i)(\alpha \ \mathrm{grad}) - \alpha_0 mc^2]\psi = 0 \tag{1.17}$$

in which for each electron we take the α's in the familiar form

$$\alpha_x = \begin{pmatrix} 0 & 0 & 0 & 1 \\ 0 & 0 & 1 & 0 \\ 0 & 1 & 0 & 0 \\ 1 & 0 & 0 & 0 \end{pmatrix}; \quad \alpha_y = \begin{pmatrix} 0 & 0 & 0 & -i \\ 0 & 0 & i & 0 \\ 0 & -i & 0 & 0 \\ i & 0 & 0 & 0 \end{pmatrix};$$
$$\alpha_z = \begin{pmatrix} 0 & 0 & 1 & 0 \\ 0 & 0 & 0 & -1 \\ 1 & 0 & 0 & 0 \\ 0 & -1 & 0 & 0 \end{pmatrix}; \quad \alpha_0 = \begin{pmatrix} 1 & 0 & 0 & 0 \\ 0 & 1 & 0 & 0 \\ 0 & 0 & -1 & 0 \\ 0 & 0 & 0 & -1 \end{pmatrix}. \tag{1.18}$$

The solutions of these equations we write in the form

$$\psi_{p\sigma}{}^{i} = a_{p\sigma}{}^{i} e^{(2\pi i/h)[(\boldsymbol{p}\cdot\boldsymbol{r})-Et]} \tag{1.19}$$

with

$$E = c(m^2c^2 + p^2)^{1/2}$$

and with the $a_{p\sigma}{}^{i}$ functions of $(\boldsymbol{p}, \sigma)$. For an electron initially at rest we take for the a^i:

$$\begin{array}{cc} \sigma = +1 & \sigma = -1 \\ a_1 = a_2 = a_4 = 0; \ a_3 = 1; & a_1 = a_2 = a_3 = 0; \ a_4 = 1. \end{array} \tag{1.20}$$

These states will be characterized by an index (0). Thus

$$p^{(0)} = 0,\ E^{(0)} = mc^2;\ \sigma^{(0)} = \pm 1;\ \text{etc.}$$

This wave function represents a uniform electron density of one electron per unit volume. For an electron moving in the z direction we take

$$\begin{aligned} &\sigma = +1 && \sigma = -1 \\ &a_2 = a_4 = 0 && a_1 = a_3 = 0 \\ &a_1 = -Np_z/g && a_2 = Np_z/g \\ &a_3 = N && a_4 = N \end{aligned} \tag{1.21}$$

where

$$g = mc + E/c$$

and

$$N^2 = 2g\,(E^2 - m^2c^4)^{1/2}.$$

These states will be characterized by a superscript (i). This wave function is normalized to represent a stream of unit flux, so that the transition probabilities computed from it will give directly the cross section for scattering.

We may without loss of generality suppose that after impact both electrons are moving in the xz plane, since, as we shall see, momentum is conserved in the impact. For such an electron we take

$$\begin{aligned} &\sigma = +1 && \sigma = -1 \\ &a_1 = -Np_z/g && a_1 = -Np_x/g \\ &a_2 = -Np_x/g && a_2 = Np_z/g \\ &a_3 = N && a_3 = 0 \\ &a_4 = 0 && a_4 = N \end{aligned} \tag{1.22}$$

where

$$g = mc + E/c$$

and

$$N^2 = -gc/2Eh^3.$$

These states will be characterized by superscripts (1) and (2). This wave function is normalized to $dp_x\,dp_y\,dp_z = dp$. We shall need the Jacobian

$$J^{(1)} = \partial(p_x^{(1)}, p_y^{(1)}, p_z^{(1)})/\partial(E^{(1)} + E^{(2)}, \vartheta^{(1)}, \phi^{(1)})$$

where, by the conservation of momentum,

$$E^{(2)}(p^{(2)}) = E^{(2)}(p^{(i)} - p^{(1)}). \tag{1.23}$$

We find

$$j^{(1)} = \frac{2mp^{(1)}E^{(1)}E^{(2)} \sin \vartheta^{(1)}}{mc^2(1 + \cos^2 \vartheta^{(1)}) + E \sin^2 \vartheta^{(1)}}$$

Note: There is at this point in Møller's paper an error, in that Møller uses in place of j^1

$$j^{(1)} = \partial(p_x^{(1)}, p_y^{(1)}, p_z^{(1)})/\sigma(E^{(1)}, \vartheta^{(1)}, \phi^{(1)}).$$

Now $J^1 \neq J^{(1)}$, because by the conservation laws $E^{(2)}$ depends on $p^{(1)}$. It is $J^{(1)}$ that we must use to take out the $\delta(E^{(0)}+E^{(i)})-(E^{(1)}+E^{(2)})$ in (1.16). We are indebted to Dr. Heisenberg for tellung us that Møller had found an error at this point in his paper.

Further the charge density is given by

$$e\sum_{j=1}^{4}\tilde{\psi}^j\psi^j \tag{1.24}$$

and the current density by

$$ec\sum_{j,k}\tilde{\psi}^j\alpha jk\psi^k. \tag{1.25}$$

If we put these expressions in (1.16), we find for the transition probability from the intial states [(1.20) and (1.21)] of the two electrons to states

$$p^{(1)}, \sigma^{(1)}, p^{(2)}\sigma^{(2)}$$

such that

$$E^{(1)} + E^{(2)} = E^{(0)} + E^{(i)}$$

the expression

$$4h^3e^4J^{(1)}\left|A\right|^2\left|\int dre^{2\pi i/h([p^{(i)}-p^{(1)}-p^{(2)}]\cdot r)}\right|^2 dp^{(2)}d\vartheta^{(1)}d\phi^{(1)} \tag{1.26}$$

$$A = \frac{A_{1,i}{}^0A_{2,0}{}^0 - (A_{1,i}\cdot A_{2,0})}{\left|p^{(i)}-p^{(1)}\right|^2 - (1/c^2)(E^{(i)}-E^{(1)}\left|{}^2\right.} - \frac{A_{1,0}{}^0A_{2,i}{}^0 - (A_{1,0}\cdot A_{2,i})}{\left|p^{(i)}-p^{(2)}\right|^2 - (1/c^2)(E^{(i)}-E^{(2)})^2}. \tag{1.27}$$

Here

$$A_{1,0}{}^0 = \sum_{j=1}^{4}\tilde{a}^j(p^{(1)},\sigma^{(1)})a^j(p^{(0)},\sigma^{(0)}).$$

$$A_{1,0} = \sum_{j,k=1}^{4}\tilde{a}^j(p^{(1)},\sigma^{(1)})\alpha jka^k(p^{(0)},\sigma^{(0)}).$$

Now

$$Q = \lim_{V\to\infty}\left|\int_V dre^{(2\pi i/h)([p^{(i)}-p^{(1)}-p^{(2)}]\cdot r)}\right|^2 \to V\delta(p^{(i)}-p^{(1)}-p^{(2)}). \tag{1.28}$$

Thus momentum as well as energy are conserved, and we may set

$$p^{(2)} = p^{(i)} - p^{(1)}. \tag{1.29}$$

Further if we divide (1.27) by V we get the cross section for impact with a single electron at rest. In (1.27) we have to consider all the possible orientations of spin of the two electrons in initial and final states: to take one fourth the sum of (1.27) over the sixteen combinations of values of $\sigma^{(i)}$, $\sigma^{(0)}$, $\sigma^{(1)}$, $\sigma^{(2)}$. The resulting cross section can be expressed as a function of ϵ and ϑ, the angle of deflection of one of the electrons; it is independent of the azimuth of deflection of this electron; and all the components of momentum are determined by the conservation laws when ϑ and ϕ are given for one electron. Before carrying out this reduction we may make a few observations on the geometry of the impact.

According to the conservation laws, if the two electrons after impact have direction of motion making the angles ϑ_1, ϑ_2 with the z axis,

$$p^{(1)} \sin \vartheta_1 = p^{(2)} \sin \vartheta_2. \tag{1.30}$$

Further, the energy of a particle coming off at an angle ϑ is

$$E' = mc^2 \frac{2\epsilon - (\epsilon - 1)\beta^2}{2 + (\epsilon - 1)\beta^2}; \quad \begin{matrix} \alpha = \cos\vartheta; \\ \beta = \sin\vartheta; \end{matrix} \tag{1.31}$$

and the absolute value of its momentum is $mc[2\alpha(\epsilon^2-1)^{1/2}]/[2+(\epsilon-1)\beta^2]$. Thus the particle with the smaller energy always comes off at a larger angle; when the energy is shared equally the two particles come off at the same angle ϑ_m such that

$$\sin^2 \vartheta_m = 2/(\epsilon + 3). \tag{1.32}$$

In general the angle γ between the particles is

$$tg\gamma = [2 + (\epsilon - 1)\beta^2]/[(\epsilon - 1)\alpha\beta] \tag{1.33}$$

which reduces to

$$\gamma^2 = (2mc^2/E')(1 - E'/E) \tag{1.34}$$

for large ϵ. [Here E' is the smaller of the two energies $E^{(1)}$, $E^{(2)}$.] In no impact do both electrons come off at an angle larger than ϑ_m; and since (0. 7) gives the probability that an electron come off at an angle ϑ, and the other at the corresponding angle determined by (1.30), we have only to consider impacts in which $\vartheta \leqq \vartheta_m$; impacts in which $\vartheta > \vartheta_m$ will be the same impacts as those for which $\vartheta < \vartheta_m$, but in which the angle ϑ refers to the slower and not the faster of the two electrons.

We should note that by (1.34) the angle between the electrons grows smaller as the both the primary energy and the energy transferred grow large compared to the proper energy. This point is of some importance in connection with the interpretation of cloud chamber experiments, since it leads us to expect that very high energy secondary electrons produced by elastic impact with high energy primaries will come off nearly parallel to the direction of the primary.

We shall let then ϑ be the angle which the faster of the two secondary electrons, for which we use (1), makes with the primary direction. Further we

shall write $\alpha=\cos\vartheta$, $\beta=\sin\vartheta$, $q=(\epsilon-1)\beta^2$. Then the conservation laws give us the relations

$$
\begin{aligned}
p_x^{(1)} &= -\,p_x^{(2)} = [(\epsilon^2-1)^{1/2}2\alpha\beta/(2+q)]mc\\
p_z^{(i)} &= (\epsilon^2-1)^{1/2}mc\\
p_z^{(1)} &= [2\alpha^2(\epsilon^2-1)^{1/2}/(2+q)]mc\\
p_z^{(2)} &= [(\epsilon^2-1)^{1/2}(\epsilon+1)\beta^2/(2+q)]mc\\
|\boldsymbol{p}^{(i)}-\boldsymbol{p}^{(1)}|^2-(1/c^2)(E^{(i)}-E^{(2)})^2 &= [2(\epsilon^2-1)\beta^2/(2+q)]m^2c^2\\
|\boldsymbol{p}^{(i)}-\boldsymbol{p}^{(2)}|^2-(1/c^2)(E^{(i)}-E^{(2)})^2 &= [4(\epsilon-1)\alpha^2/(2+q)]m^2c^2\\
g^{(0)} &= 2mc \qquad g^{(2)} = [(4+(\epsilon+3)q)/(2+q)]mc\\
g^{(i)} &= (\epsilon+1)mc \qquad p^{(1)} = [2\alpha(\epsilon^2-1)^{1/2}/(2+q)]mc \qquad (1.35)\\
g^{(1)} &= [2(\epsilon+1)/(2+q)]mc \qquad E^{(1)} = [(2\epsilon-q)/(2+q)]mc^2.
\end{aligned}
$$

Thus we get for the differential cross section,

$$
\sigma d\alpha = \frac{\pi e^4}{m^2c^4}\cdot\frac{(\epsilon+1)^2\alpha}{2(\epsilon-1)^2}\cdot\frac{4+(\epsilon+3)q}{(2+q)^2}\cdot d\alpha \sum_{\sigma^{(0)},\sigma^{(1)},\sigma^{i},\sigma^{(2)}}^{\pm}\left|\frac{L(\sigma)}{(\epsilon+1)\beta^2}-\frac{M(\sigma)}{2\alpha^2}\right|^2 \qquad (1.36)
$$

Here each of the $L(\sigma)$, $M(\sigma)$ refers to a different one of the sixteen possible orientations of electron spin; $L(\sigma)$ is the direct term, $M(\sigma)$ the interchange term. The L and M can be tabulated as a function of ϵ and ϑ. We write

$$
y=(\epsilon-1)/(\epsilon+1);\quad S^{-1}=4+(\epsilon-1)(\epsilon+3)\beta^2;
$$

$\sigma^{(0)}$	$\sigma^{(i)}$	$\sigma^{(1)}$	$\sigma^{(2)}$	$L(\sigma)$	$M(\sigma)$
$+$ $-$	$+$ $-$	$+$ $-$	$+$ $-$	$1+y\alpha^2-(1+\alpha^2)(\epsilon^2-1)\beta^2S$	$1-y\alpha^2+(\epsilon^2-1)\beta^4S$
$-$ $+$	$+$ $-$	$-$ $+$	$+$ $-$	$1+y\alpha^2+(\epsilon-1)[4\alpha^2\beta^2$ $-(1+\alpha^2)(\epsilon+1)\beta^2]S$	$-2y\alpha^2[1+3\alpha^2+\epsilon\beta^2]S$
$-$ $+$	$+$ $-$	$+$ $-$	$+$ $-$	$\mp 2\alpha\beta(\epsilon-1)(2+q)S$	$\pm 2\alpha\beta y[2(\epsilon+2)\alpha^2+(\epsilon+1)^2\beta^2)S$
$+$ $-$	$+$ $-$	$+$ $-$	$-$ $+$	$\pm 2\alpha\beta(\epsilon-1)(1+\alpha^2)S$	$\mp 2\alpha\beta qS$
$-$ $+$	$-$ $+$	$+$ $-$	$-$ $+$	$\mp 4\alpha^3\beta yS$	$\pm 2\alpha\beta y[2\alpha^2+(\epsilon+1)\beta^2]S$
$+$ $-$	$-$ $+$	$+$ $-$	$+$ $-$	$\mp 4y\alpha\beta(1+\epsilon\beta^2)S$	$\pm 2y\alpha\beta[4\alpha^2+(\epsilon+1^2)\beta^2]S$
$+$ $-$	$+$ $-$	$-$ $+$	$-$ $+$	$2\alpha^2qS$	$2\alpha^2qS$
$-$ $+$	$+$ $-$	$-$ $+$	$+$ $-$	$-2q(1+\epsilon\beta^2)S$	$1-y\alpha^2+q[4\alpha^2+(\epsilon+1)\beta^2]S$

(1.37)

For large ϵ the last six contribute nothing to the cross section; the first four are important for energy losses not large compared to the proper energy; the next four are important for all energy losses comparable with the proper

energy; the next two are important only for energy losses comparable with the primary energy. From (1.35) the energy transferred is

$$E' = mc^2(\epsilon + 1)q/2 + q. \tag{1.38}$$

We must consider only impacts for which

$$\theta \leqq \theta_m, \; E' \leqq \tfrac{1}{2}(\epsilon - 1)\cdot mc^2. \tag{1.39}$$

For these the differential cross section is given by

$$\sigma dE' = \frac{2\pi e^4}{mc^2}\frac{dE'}{E'^2}\cdot\frac{E^4 + E'^4 + (E - E')^4}{2E^2(E - E')^2}\cdot \tag{1.40}$$

This concludes our study of the impacts in which large energies are transferred. Certain further calculation by this method, primarily for the case of smaller ϵ, were given[5] by Møller; and there, too, the connection between certain results of this calculation with earlier attempts at the calculation of impacts were given. One point we may mention here: when ϵ is not large, we may use Rutherford's formula to give us the differential cross section for energy loss,—or rather the nonrelativistic quantum mechanically extension of Rutherford's formula which takes account of interchange and the exclusion principle. This gives, for $E' \ll E$,

$$\sigma dE' \cong 2\pi e^4 dE'/EE'^2. \tag{1.41}$$

This agrees with our result for energy losses small compared to the proper energy; but for larger energy transfers it gives too large a cross section. When higher powers of the interaction energy are not neglected, terms of the order of the fine structure constant must be added to (1.40). In the case of the nonrelativistic calculation (1.41) these are only of importance when E' is of the same order as E; and presumably, although not certainly, these terms will not be of importance for large ϵ except in this case $E' \sim E$.

(b) Small energy transfers to bound electrons

We have now to consider the case that a primary electron of very large energy gives to a secondary which was originally bound in an atom an energy not comparable to its proper energy. The states for the primary electron are still given by (1.21) and (1.22); but certain simplifications are introduced even here by the fact that the energy of the primary changes very little. For practically all such impacts involve a very small deflection for the primary; and in their treatment it is legitimate to neglect quantities which are small when the primary momentum changes by a relatively very small amount. With this understanding we see that only the matrix components of the charge and current of the primary in which the spin of the primary does not change are important, and that these are independent of the original orientation of the primary spin, which we may thus take parallel to z. (Case $\sigma = +1$). Further the components of current, and thus of vector potential, in the xy plane, are negligible. We have to consider only the scalar potential and the z component of the vector potential of the primary.

There are two further simplifications. In the first place interchange is negligible (interchange terms are important in general only when the energy transferred in of the order of the primary energy); we may thus use (1.12) in place of (1.16). In the second place the secondary electron never gets a velocity comparable with that of light, so that for it we may use nonrelativistic wave functions and expressions for charge and current density; and we may neglect the spin of this electron. On the other hand we may not use wave functions which neglect the binding of the atomic electron, and must replace for it (1.19) and (1.21). Let the initial energy and wave function of the electron be

$$E^{(0)} = -I;\ \psi_0 = e^{(2\pi i/h)It}u_0. \tag{1.42}$$

After the impact the atomic electron may be excited or ionized. Let the corresponding energies and wave functions be

$$\begin{aligned} E_{nl};\ \psi_{nl} &= e^{(-2\pi i/h)E_{nl}t}u_{nl}; \\ E,\ \psi_{El} &= e^{(-2\pi i/h)Et}u_{El}; \end{aligned} \tag{1.43}$$

where l stands for the two other quantum numbers in addition to the energy, necessary in the most general case to specify the state of the electron. Further let the continuous wave functions for energies above the ionizing potential be normalized in the energy scale.

The expressions for the charge and current density are then simply

$$\begin{aligned} \rho &= e\tilde{\psi}\psi \\ J &= (e/2m)\left[(h/2\pi i)(\tilde{\psi}\ \mathrm{grad}\ \psi - \psi\ \mathrm{grad}\ \tilde{\psi})\right. \\ &\quad \left. - (2e/c)\tilde{\psi}A\psi\right] \sim (eh/2\pi im)\tilde{\psi}\ \mathrm{grad}\ \psi. \end{aligned} \tag{1.44}$$

The terms in the vector potential A are of higher order in the interaction energy and may be dropped.

If as before we let the primary electron be deflected in the plane, and call the angles of deflection again ϑ, ϕ, we get from (1.12) for the probability of excitation to a state n, l:

$$\sigma_{nl} = \frac{4\pi^2e^4}{h^4c}\int\int d\vartheta d\phi J^{(1)} \left| V_{p^{(1)}nl} \right|^2 \qquad r = |\boldsymbol{r}_1 - \boldsymbol{r}_2|$$

$$\begin{aligned} V_{p^{(1)}nl} = \int\int d\boldsymbol{r}_1 d\boldsymbol{r}_2 \bar{u}_{nl}(r_2)\ \exp\{2\pi i/h[([\boldsymbol{p}^{(i)} - \boldsymbol{p}^{(1)}]\cdot\boldsymbol{r}_1) \\ - (1/c)(E^{(i)} - E^{(1)})r\}[1 - h/2\pi imc(\partial/\partial z_2)/r]u_0(r_2) \end{aligned} \tag{1.45}$$

and for the probability of ionization to a state of energy in the range dE

$$\sigma_E dE = \frac{4\pi^2e^4}{h^4c}dE\int\int d\vartheta d\phi J^{(1)}\sum_a \left| V_{p^{(1)}El} \right|^2.$$

To get the total probability of excitation or ionization these expressions must be summed over n, l; to get the energy loss per impact they must be multiplied by

$$E' = E_{nl} + I,\quad E' = E + I \tag{1.47}$$

and summed over l, summed and integrated over n and E. In the next section we shall evaluate these expressions as far as possible when we leave the atomic wave functions arbitrary; and we shall evaluate them in detail for the case that the wave functions are those of a hydrogen like atom. From them we shall find, for the differential cross section for an energy loss E' large compared to the ionizing energy I,

$$\sigma dE' = 2\pi e^4 dE'/mc^2 E'^2$$

in agreement with (1.40); but for smaller energy losses we shall obtain results which differ very markedly from those given by (1.40).

(c) **Theory of magnetic neutron**

For the impacts of a neutron with a free electron we have again to use (1.12). Here the wave function for the electron before impact is given by (1.29); that after impact by (1.22); and the charge and current density of the electron by (1.24–5). We have only to find the matrix components of the charge and current density of the neutron.

The wave equation proposed by Pauli[1] for the magnetic neutron is simply related to the Dirac equation for the electron. In the absence of a field this latter may be written

$$[\gamma^\mu p_\mu - imc]\phi = 0; p_4 = (-h/2\pi i)(\partial/\partial t); p_0 = (h/2\pi i)(\partial/\partial x_l); \quad l = 1, 2, 3 \tag{1.48}$$

where the γ^μ satisfy

$$\gamma^\mu\gamma^\nu + \gamma^\nu\gamma^\mu = 2\delta_{\mu\nu}. \tag{1.49}$$

In the absence of a field this equation is to hold for the magnetic neutron, except that the neutron's mass M must be substituted for that of the electron. In the presence of a field new terms are to be added to the wave equation:

$$[\gamma^\mu p_\mu - iMc + P]\phi = 0; P = k\sigma^{\mu\nu}F_{\mu\nu}. \tag{1.50}$$

Here $F_{\mu\nu}$ is the field tensor,

$$\sigma^{\mu\nu} = \gamma^\mu\gamma^\nu - \gamma^\nu\gamma^\mu$$

and κ is a constant which is related to the magnetic moment μ of the neutron:

$$\kappa = \mu/4c. \tag{1.51}$$

These terms are not altogether arbitrary. Thus $\sigma^{\mu\nu}$ must be an antisymmetric tensor; it may not involve the coordinates nor powers of the momenta higher than the first. Thus (1.50) turns out to be the only hermitian not identically vanishing possibility which involves the field strengths linearly. The fact that κ is real is required by the hermiticity of the term; otherwise one could not interpret the wave function of a particle which was conserved. The sign of the term is arbitrary, and determines whether the magnetic moment of the neutron is parallel or antiparallel to its spin.

From (1.50) one may deduce two conservations laws. One asserts that the divergence of the four vector

$$s^\mu = \phi^+\gamma^\mu\phi \tag{1.52}$$

vanishes, and gives the conservation law for the neutron density. The other

$$\partial J^\mu/\partial x^\mu = 0; J^\mu = (-\mu/2)(\partial/\partial)x^\nu(\phi^+\sigma^{\mu\nu}\phi) \tag{1.53}$$

gives, as we shall show, the conservation of the charge and current vector. The two four vectors-particle density and flux, charge and current density, do not, as in the case of the electron, differ merely by a constant factor.

The first justification for calling μ the magnetic moment of the neutron we obtain if we reduce (1.50) for the case of velocities small compared to that of light. We find then that the neutron is described by a two-component wave function which satisfies

$$[(h/2\pi i)(\partial/\partial t) - h^2/8\pi^2 M\Delta + \mu(\boldsymbol{H}\cdot\sigma)]\phi = 0. \tag{1.54}$$

Here the σ's are the Pauli spin matrices

$$\sigma_x = \begin{pmatrix} 0 & 1 \\ 1 & 0 \end{pmatrix}; \quad \sigma_y = \begin{pmatrix} 0 & -i \\ i & 0 \end{pmatrix}; \quad \sigma_z = \begin{pmatrix} 1 & 0 \\ 0 & -1 \end{pmatrix} \tag{1.55}$$

and $\boldsymbol{H}$ the magnetic field. This is just what we should expect for the wave equation of a neutral particle carrying a spin and a magnetic moment μ.

A further justification for calling μ the magnetic moment of the neutron we can obtain by showing that

$$J^\mu = (-\mu/2)(\partial/\partial x^\nu)(\phi^+\sigma^{\mu\nu}\phi) \tag{1.56}$$

does correspond to the charge and current vector. For if we calculate the potentials and field strengths of a wave packet moving with low velocity by using (1.53) for the charge and current vector, we get just the field we should expect for the neutron of magnetic moment. Here as in the case of the electron the components of momentum do not completely specify the state; we need also to specify the orientation of the spin; and by doing this we determine the orientation of the field-producing magnetic moment.

We can verify that (1.53) is right in the following way. The wave equation (1.50) and its adjoint equation may be obtained by variation of ϕ^+ and ϕ in the Lagrangian.

$$L = \int dV\phi^+[\gamma^\mu p_\mu - iMc + \kappa\sigma^{\mu\nu}F_{\mu\nu}]\phi. \tag{1.57}$$

If we add to (1.54) the Lagrangian of the empty electromagnetic field,

$$(1/16\pi)\int dVF^{\mu\nu}F_{\mu\nu} \tag{1.58}$$

and in this vary, precisely as in the familiar case of the electron, the potentials, we get in place of Maxwell's equations for the empty field

$$\partial F^{\mu\nu}/\partial x^\nu = 4\pi J^\mu \tag{1.59}$$

with J^μ given by (1.53). Thus, as far as the field produced by the neutron is concerned, J^μ given by (1.53) acts like the charge and current density. It is a four vector, and its divergence vanishes.

It is convenient to rewrite the Eqs. (1.50) in the form corresponding to (1.17). Thus for the free neutron (no field), we get

$$[(h/2\pi i)(\partial/\partial t) + (hc/2\pi i)(\mathfrak{a}\cdot\mathrm{grad}) - \alpha_0 Mc^2]\psi = 0 \tag{1.60}$$

where the α's are given by (1.18), if we take

$$\gamma^4 = \alpha_0;\ \gamma^l = i\alpha_0\alpha_l;\ \phi = i\alpha_0\psi. \tag{1.61}$$

The density current four vector then becomes

$$\tilde{\psi}\psi,\ c\tilde{\psi}\alpha\psi. \tag{1.62}$$

The neutron density is, as it must be, essentially non-negative. The terms corresponding to P in (1.50) then become

$$-i\alpha_0\kappa\sigma^{\mu\nu}F_{\mu\nu} \tag{1.63}$$

and the charge and current vector is given by

$$J^\mu = -\mu\partial/\partial x^\nu(\tilde{\psi}\tau^{\mu\nu}\psi). \tag{1.64}$$

Here the four row matrices $\psi^{\mu\nu}$ are given in terms of the Pauli spin matrices (1.55) by

$$\begin{aligned} \tau^{\mu\mu} &= 0 \\ \tau^{l4} &= -\tau^{4l} = \begin{pmatrix} 0 & is_l \\ -is_l & 0 \end{pmatrix} \\ \tau^{kl} &= -\tau^{lk} = \begin{pmatrix} -s_m & 0 \\ 0 & s_m \end{pmatrix}. \end{aligned} \tag{1.65}$$

Here (k, l, m) are a cyclic permutation of (1, 2, 3). This expression must be used in (1.12) to compute cross sections for impacts. For the states of the free neutron we may again use the wave functions (1.20) and (1.21). In place of (1.27) we find

$$16\pi^2 he^2\mu^2 J^{(1)} \left| B \right|^2 Q d\boldsymbol{p}^{(2)} a\vartheta^{(1)} d\phi^{(1)} \tag{1.66}$$

where Q is given by (1.28) and where now

$$B = \frac{A_{2,0}{}^0 T_{1,i}{}^4 + (A_{2,0}\boldsymbol{T}_{1,i})}{\left| \boldsymbol{p}^{(i)} - \boldsymbol{p}^{(1)} \right|^2 - 1/c^2(E^{(i)} - E^{(0)})^2}. \tag{1.67}$$

Here the A's are given by (1.27) and the T's are defined

$$\begin{aligned} T_{1,i}{}^\mu &= \sum_{j,k} a^\tau(p^{(1)}, \sigma^{(1)}) T_{jk}{}^{\mu\nu} a^k(p^{(1)}\sigma^{(1)}) \Delta p_{1,i}{}^\nu \\ \Delta\boldsymbol{p}_{1,i} &= \boldsymbol{p}^{(1)} - \boldsymbol{p}^{(1)}; \\ \Delta p_{1,i}{}^4 &= -(1/c)(E^{(i)} - E^{(1)}). \end{aligned} \tag{1.68}$$

As before $Q \rightarrow V\delta(\boldsymbol{p}^{(i)} - \boldsymbol{p}^{(1)} - \boldsymbol{p}^{(2)})$.

We can write the cross section for a particular set of spin orientations

$$16\pi^2 he^2\mu^2 J^{(1)} \left| B(\sigma) \right|^2 d\vartheta^{(1)} d\phi^{(1)}. \tag{1.69}$$

As before we must take, to find the differential cross section, one fourth the sum of these expressions over all sixteen orientations of initial and final spins:

$$\sigma d\vartheta d\phi = 4\pi^2 h e^2 \mu^2 J^{(1)} \sum^{\pm}_{\sigma^{(i)},\sigma^{(1)}\ \sigma^{(0)},\sigma^{(2)}} \left| B(\sigma) \right|^2 d\delta d\phi. \tag{1.70}$$

The quantities T occurring here may be tabulated in terms of the initial and and final momenta and energy of the neutron. If for brevity we write

$$\begin{aligned} &p_z^{(i)} = r; \quad p_z^{(1)} = r'; \quad p_x^{(1)} = p'; \\ &g^{(i)} = g; \quad g^{(1)} = g'; \qquad \Delta r = r - r'; \ \Delta g = g - g'; \end{aligned} \tag{1.71}$$

then we find for the T's the following values:

$\sigma^{(i)}$	$\sigma^{(1)}$	T_z	T_y
$+$	$+$	$i\Delta r(rp'/gg')+i\Delta g p'/g'$	$\mp p'(1-rr'/gg')\pm\Delta r p'/gg'\pm\Delta g p'/g$
$-$	$-$		
$+$	$-$	$\pm\Delta r(rp'/gg'\pm i\Delta g((r/g)+r'/g')$	$(\pm rp'^2/gg')+\Delta r(1+rr'/gg')$ $+\Delta g((r/g)+r'/g')$
$-$	$+$		
$\sigma^{(i)}$	$\sigma^{(1)}$	T_z	T^4
$+$	$+$	$(-ip'^2 r/gg')-i\Delta g((r/g)-r'/g')$	$(-ip'^2/g')+i\Delta r((r/g)-r'/g')$
$-$	$-$		
$+$	$-$	$\pm ip'(1+rr'/gg')\pm i\Delta g p'/g'$	$\pm ip'(r/g)+r'/g')\mp i\Delta r p'/g'$
$-$	$+$		

(1.72)

It is not possible, without knowing the mass of the neutron, to reduce these expressions further. We shall, therefore, postpone until §III the discussion of these formulae. There, too, we shall make such elementary investigations of the effect of the binding of the electron as are necessary to our purpose.

Before proceeding to the further application of this method of Møller, we wish again to emphasize the approximate character of the method. We have throughout neglected two things: the reaction of the particles to their own field, and all radiative processes; and higher order terms in the interaction of the two particles. In the case of the electron, both these neglects mean the omission of terms of the order of the fine structure constant, terms which are genuinely small unless both particles involved are moving with velocities comparable to light. Just what effect these terms could have on the things in which we are most interested—range and ionizing power of the primary, energy distribution of the secondaries—we shall discuss when we have our results before us. But the formula (1.40), which is derived with neglect of these terms, is subject to grave doubt, since we have no assurance that terms of the form $e\alpha$ will not appear, and no physical assurance that in the intimate collision of two electrons this approximate method can be legitimately employed. It seems at present by far the soundest method available, and perhaps experiment can show in what measure it is inadequate. The further study of impacts involving neutrons, a study which should not neglect

higher powers of the interaction energy, presents even in the nonrelativistic case serious analytic complications; and we have not thought it advisable to attempt these without some more certain information about the characteristic constants, in particular the moment, of this hypothetical particle.

II. Ionizing Power and Range of Fast Electrons

We must now consider in detail the small energy losses suffered by a fast electron in its impacts with an atom. Just as in the nonrelativistic theory, if we neglect the binding of the atomic electron we find an infinite probability for small energy losses; and just as in the nonrelativistic treatment the proper consideration of the binding gives us a finite probability of energy loss and a finite range.

Before using our formula (1.46) to study these impacts we may outline briefly the semiclassical method of treating this same problem. This method, it will be remembered, is valid only for such impacts as involve small energy loss and small deflection of the primary; in this method we treat the primary particle classically, neglect the reaction of the atom upon it, and use the field calculated for this undeflected trajectory as a perturbation causing transition of the atomic electron. If we choose our coordinates so that the particle passes along the z-axis, and goes through the origin at $t=0$, then the field of the particle is given by the potentials

$$\begin{aligned} &A_x = A_y = 0;\ A_z = (ev\epsilon/c)\left[x^2 + y^2 + \epsilon^2(z - vt)^2\right]^{-1/2}; \\ &\phi = e\epsilon\left[x^2 + y^2 + \epsilon^2(z - vt)^2\right]^{-1/2}; \end{aligned} \tag{2.1}$$

where v is the velocity of the particle and

$$1/\epsilon = (1 - v^2/c^2)^{1/2}.$$

The probability of a transition of the atomic electron in which its energy changes by E' is determined by the Fourier component of this field of frequency $\nu' = E'/h$. We therefore analyze the potentials by a Fourier integral:

$$\begin{aligned} A_z &= (4e/c)\int_0^\infty K_0(2\pi\nu p/\epsilon v)\cos 2\pi\nu(t - z/v)d\nu \\ \phi &= (4e/v)\int_0^\infty K_0(2\pi\nu p/\epsilon v)\cos 2\pi\nu(t - z/v)d\nu \end{aligned} \tag{2.2}$$

where K_0 is the Hankel function:

$$K_0(\xi) = \int_0^\infty \frac{\cos\lambda d\lambda}{(\lambda^2 + \xi^2)^{1/2}};\ \text{and}\ p = (x^2 + y^2)^{1/2}.$$

The perturbation energy for the atomic electron is given by

$$V = e\phi - (1/c)A_z j_z \tag{2.3}$$

where j is the current operator which, to a sufficient approximation, is given by (1.44): $j_z = (he/2\pi mi)\partial/\partial z$. Thus the transition probability for an atomic

transition $n \rightarrow n'$ in which the energy of the atom changes by $E' = E_{n'} - E_n = h\nu'$ is just

$$P_{nn'} = (4\pi^2/h^2) \left| \int \bar{u}_{n'} (2e^2/v) K_0(2\pi\nu' p/\epsilon v) e^{2\pi i \nu' z/v} [1 - (hv/2\pi imc^2)\partial/\partial z] u_n d\boldsymbol{r} \right|^2 \quad (2.4)$$

where the u's are the wave amplitudes for the atomic electron. The nonrelativistic expression is[5]

$$P_{nn'} = \frac{4\pi^2}{h^2} \left| \int \bar{u}_{n'} \frac{2e^2}{v} K_0\left(\frac{2\pi\nu' p}{v}\right) e^{2\pi i \nu' z/v} u_n d\boldsymbol{r} \right|^2. \quad (2.5)$$

Now for distant collisions, to which alone this method may be legitimately applied, we may expand the potentials about the position of the nucleus of the atom, which we take to be on the y axis at a distance from the track, and consider only the first two terms of the expansion, i.e., the dipole moment of the atom. If we let the y-component of the displacement of the electron from the center of the atom be ζ then we find

$$P_{nn'}(p) = (16\pi^2 e^4/h^2 v^2) \left| \zeta_{nn'} \right|^2 [K'(2\pi\nu' p/v\epsilon)]^2 \quad (2.6)$$

where $K'(\xi) = \partial K_0(\xi)/\partial\xi$ and $\zeta_{nn'} = \int \bar{u}_{n'} \zeta u_n d\boldsymbol{r}$. The nonrelativistic formula is[5]

$$P_{nn'}(p) = (16\pi^2 e^4/h^2 v^2) \left| \zeta_{nn'} \right|^2 [K'(2\pi\nu' p/v)]^2. \quad (2.7)$$

Thus in this calculation the effect of retardation is to introduce p/ϵ in place of p in the argument of K'. Since K' is a rapidly decreasing function

$$\begin{aligned} K'(\xi) &\sim 1/\xi \text{ for } \xi \rightarrow 0, \\ K'(\xi) &\sim -(\pi/2\xi)^{1/2} e^{-\xi} \text{ for } (\xi) \rightarrow \infty, \end{aligned} \quad (2.8)$$

this means that for a given transition and a given position of the atom the probability of a given energy loss is increased by considering retardation; energy losses occur at greater and greater distances from the track as the velocity of the primary approaches more and more closely that of light. We are, therefore, led to expect a greater number of low velocity secondaries than we should find from an extrapolation of the nonrelativistic formula; and this is just what we shall find. It is an immediate consequence of the flattening out of the field of the electron in the equatorial plane.

As the position of the atom approaches the track, $p \rightarrow 0$, and the total number of transitions becomes infinite. For these intimate collisions the expansion of the potentials about p and the assumption that the track is undeflected are both illegitimate. There are a number of ways in which, for small energy losses, we might try to modify the calculation of these close impacts, in such a way that the integral over p converges and gives a finite result. Perhaps the simplest is to stop the integration at a point $\bar{p}$ where, according to (2.6), the probability of inelastic impact is unity. This point turns out to be, for a hydrogen-like electron, of the order of the Compton wave-length divided by the effective nuclear charge z:

$$\bar{p} = 1.4h/2\pi mcz \sim h/2\pi mcz. \quad (2.9)$$

This procedure gives for the mean energy loss due to small energy transfer, small compared to the proper energy,

$$\delta E = (4\pi e^4/mc^2) \ln (mc^2\epsilon/W) \tag{2.10}$$

where W is of the order of the ionizing potential I, and for a hydrogen like atom is $W=3.0\ I$. This result is in remarkable agreement with that which we shall obtain by our strict calculations with the help of (1.46); and it is of some interest to inquire into the ground for this. The answer is very simple. We shall see that in our strict calculations (2.6) is right for distant impacts, impacts, that is, in which the deflection of the primary is negligible. For angles of deflection ϑ which are much smaller than

$$\bar{\vartheta} = (2mI)^{1/2}/mc\epsilon \tag{2.11}$$

we get just this result (2.6), if we connect ϑ and the parameter p by the dynamical relation $p\vartheta \sim e^2/mc^2\epsilon$. For larger ϑ i.e., smaller p, the transition probability for transitions involving small energy loss decreases rapidly, instead of becoming infinite as it does by (2.6). Thus it is approximately right to break off the integral over p at a point

$$\bar{p} \sim (e^2/mc^2\epsilon\bar{\vartheta}) \sim (h/2\pi mcz)$$

and this is what, in these preliminary calculations, we have done.

We must now turn to the strict calculation. We shall here be dealing only with small energy losses, and since our expressions converge very rapidly as the angle of deflection ϑ increases, we have only to evaluate them for small ϑ. As before, we shall assume throughout that ϵ is a large number, and neglect higher powers of $1/\epsilon$. We need to know the change of momentum of the primary in terms of the energy lost E' and the angle of deflection ϑ. Thus, with these approximations,

$$\begin{gathered} p_z^{(i)} - p_z^{(1)} = E'/c;\ p_x^{(1)} = E\vartheta/c; \\ \left| \boldsymbol{p}^{(i)} - \boldsymbol{p}^{(1)} \right|^2 = (1/c^2)(E'^2 + E^2\vartheta^2). \end{gathered} \tag{2.12}$$

Further

$$\left| \boldsymbol{p}^{(i)} - \boldsymbol{p}^{(1)} \right|^2 - (1/c^2)(E^i - E^{(1)})^2 \backsimeq (1/c^2)((E'^2/\epsilon^2) + E^2\delta^2) \tag{2.13}$$

and

$$J^{(1)} = \frac{\partial(p_x^{(1)}, p_y^{(1)}, p_z^{(1)})}{\partial(E, \vartheta, \phi)} = \frac{p^{(1)}E^{(1)}}{c^2} \sin\vartheta \sim m^2\epsilon^2 c \sin\vartheta. \tag{2.14}$$

We start with the formulae (1.45), (1.46):

$$\begin{aligned} V_{p^{(1)}nl} = \int d\boldsymbol{r}_1 d\boldsymbol{r}_2 \bar{u}_{nl}(r_2) \exp\{(2\pi i/h)[([\boldsymbol{p}^{(i)} - \boldsymbol{p}^{(1)}]\cdot \boldsymbol{r}_1) \\ - 1/c(E^{(i)} - E^{(1)})r]\}[(1 - (h/2\pi imc)\partial/\partial z)u_0(r_2)]/r. \end{aligned}$$

In all cases the matrix integral may be written as the product of two integrals if we replace throughout

$$r_1 = r_2 + r_{12}.$$

Thus

$$V_{p^{(1)}nl} = \rho_{12}(p^{(1)})\rho_2(n, l, p^{(1)}) \tag{2.15}$$

where

$$\rho_{12}(p^{(1)}) = \int (dr/r) \exp\{(2\pi i/h)[([p^{(i)} - p^{(1)}]\cdot r) - (1/c)(E^{(i)} - E^{(1)})r]\} \tag{2.16}$$

and

$$\rho_2(n, l, p^{(1)}) = \int d\tau \tilde{u}_{nl} \exp\left\{\frac{2\pi i}{h}([p^{(i)} - p^{(1)}]\cdot r)\right\}[1 - (h/2\pi imc)\partial/\partial z]u_0. \tag{2.17}$$

The former integral may be evaluated at once, and gives just, by (2.14)

$$\rho_{12}(p^{(1)}) = (h^2c^2/\pi)1/((E'^2/\epsilon^2) + E^2\vartheta^2). \tag{2.18}$$

The second integral may be considerably simplified, for it may be replaced by

$$\rho_2 = \int d\tau \tilde{u}_{nl} e^{-i\gamma x} u_0; \text{ with } \gamma = 2\pi mc\epsilon \sin\vartheta/h. \tag{2.19}$$

We may see this in the following way. We may expand

$$\exp\{(2\pi i/h)([p^{(i)} - p^{(1)}]\cdot r)\}$$

in powers of ϑ:

$$e^{(2\pi i/hc)\cdot E'z}\left\{1 - \frac{2\pi i}{hc} E\vartheta_x - \frac{2\pi^2}{h^2c^2} E^2\vartheta^2 \cdots\right\}. \tag{2.20}$$

In all terms but the first the factor

$$e^{(2\pi i/hc)E'z}[1 - (h/2\pi imc)(\partial/\partial z)] \tag{2.21}$$

gives a correction of the order, by (2.12), E'/mc^2 which is small of the order $(v/c)^2$ for the atomic electron, and negligible. If we neglect (2.21) in the first term the integral vanishes; and we have to show that here, too, this neglect is justified. But now the integral

$$\int d\tau \tilde{u}_{nl} e^{(2\pi i/hc)E'z}[1 - (h/2\pi imc)\partial/\partial z]u_0 \tag{2.22}$$

is just the matrix component of a perturbation produced by a field of potential

$$A_x = A_y = 0;\ A_z = -e^{(2\pi i/hc)E'(z-ct)};\ \phi = e^{(2\pi i/h)E'(z-ct)}. \tag{2.23}$$

These potentials may be derived for the scalar

$$\Lambda = -h/2\pi i e^{(2\pi i/hc)E'(z-ct)} \tag{2.24}$$

by differentiation $A = \text{grad}\,\Lambda;\ \phi = -\partial\Lambda/\partial t$. They thus correspond to no field;

and the corresponding matrix element vanishes. (This may be verified by direct calculation as far as the dipole moment of the atom is concerned.)

The transition probability is thus given by

$$\sigma_{nl} = (e^4h^2c^2/\pi)\int d\gamma^2 \left| \rho_2(n, l, \gamma)\right|^2 [1/(\gamma^2+\eta^2)^2] \tag{2.25}$$

with $\eta = 2\pi E'/hc\epsilon$ and $\rho_2(n,l,\gamma) = \int d\boldsymbol{r}\, \bar{u}_{n\epsilon} e^{-i\gamma x} u_0$. This expression may, of course, be evaluated when we know the u's. We shall not need this evaluation to calculate the energy loss of the primary; but we do need it to compute the probability of ionization; and it is instructive to have the explicit expressions. We shall consider the very simplest case of an electron bound in the normal state of a hydrogen-like atom, with an effective nuclear charge z; we shall calculate σ for transitions to the continuum. We need to introduce the length

$$1/b = h^2/4\pi^2 mze^2 \tag{2.26}$$

and the quantum number

$$n = 1/bk = 2\pi e^2 z/hv;\ k = 2\pi mv/h;\ v = (2E/m)^{1/2} = [(2/m)(E' - I)]^{1/2}; \tag{2.27}$$

which measures the energy of the secondary electron. If we now use parabolic coordinates with the pole along the x axis, and use the well-known wave functions for the hydrogen-like atom in such coordinates, we can evaluate not only ρ_2, but the sum (integral) of $|\rho_2|^2$ over all states l of the same energy. We thus find

$$\sum_l \left| \rho_2(n, l, \gamma)\right|^2 = \frac{z^{10}\pi^2 m b^6}{h^2} \frac{\exp\left[-2ntg^{-1}2kb/(b^2+\gamma^2-k^2)\right]}{1-e^{-2\pi n}} \frac{\gamma^2[\gamma^2 + (b^2 + k^2/3]}{\{[b^2+(\gamma-k)^2][b^2+(\gamma+k)^2]\}^3}. \tag{2.28}$$

For very small energy losses

$$E' \sim I \tag{2.29}$$

the integrand $G(\gamma)$ of the expression for the transition probability decreases with increasing γ, and becomes very large for $\gamma \to 0$. For small γ $G(\gamma) \sim \gamma^2/(\gamma^2+\eta^2)^2$ whereas for larger $\gamma \gg b$; $G(\gamma) \sim \gamma^{-12}$. Thus the transition probability begins to fall off more rapidly with increasing angle of deflection when the angle grows of the order

$$\bar{\vartheta} = hb/2\pi mc\epsilon. \tag{2.30}$$

This is the result quoted before (2.11) in connection with the semi-classical calculation. In this earlier calculation we neglected higher powers of γ higher moments of the atomic electron—and thus replaced $e^{-i\gamma x}$ by $1 - i\gamma x$. And this reduced expression becomes wrong when $\gamma \sim b, \vartheta \sim \bar{\vartheta}$.

For energy losses large compared to the ionizing potential the value of G for $\gamma \to 0$ grows very small, and the integral over γ comes entirely from the

region $\gamma^2 \sim k^2$; with neglect of higher powers of I/E' the integral may then be evaluated, and gives just

$$\sigma dE' = 2\pi e^4 dE'/mc^2 E'^2. \tag{1.40a}$$

This agrees with our result (1.40) for the energy loss to a free electron for $E' \ll mc^2$.

We may use (2.28) to compute the cross section for ionization. For (1.40) gives a negligible contribution for high energy losses, and we do not need here to supplement it with the result (1.40). We so find, carrying out approximately the quadratures over γ and E for the cross section for ionization

$$\sigma_{\text{ion}} = 0.29(2\pi e^4/mc^2 I) \ln (mc^2\epsilon^2/0.024I). \tag{2.31}$$

The nonrelativistic result is, for this case of a hydrogen like[3] atom

$$\sigma_{\text{ion}} = 0.29(2\pi e^4/mv^2 I) \ln (mv^2/0.024I) \tag{2.32}$$

where v is the velocity of the primary. The two differ by $(1.2\pi e^4/mc^2)\ln\epsilon$ for $v \to c$. The constant 1.2 is here computed only for the simple atom which we have considered; it depends upon the f-values for the atomic electron, and no universal closed formula can be given for it. We may get a somewhat more general result by comparing our formula with the nonrelativistic one. For (2.25) differs from the corresponding nonrelativistic formula in three points: (1) In the nonrelativistic formula c is to be replaced throughout by v. (2) In the nonrelativistic formula the quantity η in the denominator of (2.25) is to be replaced by $\eta' = 2\pi E'/hv$. (3) The upper limits of integration for γ and E' are greater in our formula. This third difference is not essential in computing the probability of ionization, since high energy loss impacts contribute relatively little to this probability. Now the nonrelativistic formula may always be written[3]

$$\sigma_{\text{ion}} = k_1(2\pi e^4/mv^2) \ln (mv^2/k_2 I). \tag{2.33}$$

By (1) this becomes

$$k_1(2\pi e^4/mc^2 I) \ln (mc^2/k_2 I), \tag{2.34}$$

and (2) may be taken into account in the following way. For the range $0 \leqq \gamma \leqq \eta'$, γ/b is small, and we may write

$$\int d\boldsymbol{r} \bar{u}_{nl} e^{-i\boldsymbol{\gamma}\boldsymbol{r}} u_0 \sim -i\gamma x_{nl,0},\ x_{nl,0} = \int \bar{u}_{nl} x u_0 d\boldsymbol{r}.$$

Thus the term to be added to the nonrelativistic cross section is

$$\frac{16\pi^3 e^4}{h^2 c^2} \int_\theta^\infty dE \sum_l |x_{El,0}|^2 \ln \frac{\eta'^2}{\eta^2}. \tag{2.35}$$

But the nonrelativistic cross section (2.34) itself may with $v = c$ be written

$$\frac{16\pi^3 e^4}{h^2 c^2} \int_0^\infty dE \sum_l |x_{El,0}|^2 \cdot \ln \frac{mc^2}{k^2 I}$$

i.e., $k_1=(8\pi^2mI/h^2)\cdot\int_0^\infty dE\sum_l|x_{El0}|^2$. Thus our result is

$$\sigma_{\text{ion}} = k_1(2\pi e^4/mc^2I)\ln mc^2\epsilon^2/k_2I. \tag{2.36}$$

This shows that the number of ions produced by a fast electron increases as its velocity approaches that of light. The ionizing power passes through a minimum for $\epsilon\sim3$; the increase is very slow; if we use the value of k_2 given by (2.31) for a hydrogen-like atom; and if for air we take I to be about fifty volts, then the number of ions is double the minimum value for electrons of $\epsilon\sim10^3$, or energy of the order of 10^9 volts.

To compute the mean energy loss, and thus the range, of the fast electron, we might again use the hydrogen-like atomic model, and supplement (2.28) with the corresponding expression for the probability of excitation. But here, too, it is simpler to compare our expression (2.25) with the corresponding non-relativistic one. It is simpler still to use the sum theorem of Bethe[3]

$$(8\pi^2m/h^2\gamma^2)\sum_{nl}(E_n-E_0)\left|\int d\boldsymbol{r}\bar{u}_{nl}e^{-i\gamma x}u_0\right|^2=1 \tag{2.37}$$

directly. If we apply this directly, we get for the mean energy loss

$$\delta E'=\frac{2\pi e^4}{mc^2}\int_0\frac{d\gamma^2}{\gamma^2+\tilde{\eta}^2} \tag{2.38}$$

where $\tilde{\eta}=(2\pi/hc\epsilon)W$, and $W=k_3I$ is an appropriately chosen mean value of the energy transferred per impact; and where the integration over γ is to be taken up to the maximum value permitted by the conservation laws. We have here, however, to consider that the method used in the derivation of(2.25) is not applicable for large energy losses and large values of γ, since it leads to (1.40a) in place of the correct (1.40). It is easy to correct for this, because of the fact that when

$$E'\gg I \tag{2.39}$$

we may use the calculations of §I for free electrons. Since when (2.39) is satisfied the conservation laws are fulfilled, we know that in the range $I\ll E'\ll mc^2$ we may set

$$E'=h^2\gamma^2/8\pi^2m. \tag{2.40}$$

Thus if we integrate (2.38) up to a γ value corresponding to an energy loss $\overline{E}$:

$$I\ll\overline{E}\ll mc^2;\ \bar{\gamma}^2=8\pi^2m\overline{E}/h^2 \tag{2.41}$$

we get

$$\delta E'=(2\pi e^4/mc^2)\ln 8\pi^2m\overline{E}/h^2\tilde{\eta}^2. \tag{2.42}$$

And we may add to this the mean energy loss given by (1.40) for impacts involving an energy transfer $E'\geqq\overline{E}\gg I$. This gives for large ϵ

$$\delta E''=\int_{\overline{E}}^{E_m}E'dE'\frac{E^4+(E-E')^4+E'^4}{2E^2(E-E')^2E'^2}\sim\frac{2\pi e^4}{mc^2}\left[\ln\frac{mc^2}{\overline{E}}+\ln\epsilon+9/8-2\ln2\right] \tag{2.43}$$

Thus for the total energy loss

$$\delta E = \delta E' + \delta E'' = \frac{2\pi e^4}{mc^2}\left[2 \ln \frac{mc^2}{W} + 3 \ln \epsilon + 0.43\right] \tag{2.44}$$

which is our result for the mean energy loss.

The direct calculation with the model of a hydrogen-like atom gives (2.44) with the constant

$$k_3 = 1\Big| \cdot \Big|1; W = 1.1I. \tag{2.45}$$

This result gives just *half* the energy loss we should expect from Bohr's classical formula;[2] it gives twice the range. When ϵ is large we get for the range R of the particle in a gas containing N electrons per cc

$$R^{-1} = (4\pi e^4 N/m^2c^4\epsilon)\left[\ln mc^2/W + (3/2) \ln \epsilon\right] \tag{2.46}$$

where now W is a properly taken average energy of the order of the mean ionization potential. As ϵ grows large compared with mc^2/W this approaches

$$R^{-1} \rightarrow (6\pi e^4 N)/(m^2c^4) \ln \epsilon/\epsilon. \tag{2.47}$$

Note: We get an upper limit for the range if we set

$$\partial E'' = 0,$$

since this means that no large energy losses occur, and since we know that the neglects of our theory (radiative forces) can have no sensible effect upon the small energy losses. With $\delta E^{11} = 0$ we get asymptotically

$$R^{-1} \rightarrow 4\pi e^4 N/m^2c^4 \ln \epsilon/\epsilon,$$

which is four times the distance traveled according to the Klein-Nishina formula, by a gamma-ray before its first Compton encounter. This range (2.47) is just one-sixth the distance which (according to the Klein-Nishina formula) a quantum of energy (ϵmc^2) travels, on the average, before its first Compton encounter. Thus even for the greatest energies a gamma-ray is, according to theoretical results at present available, more penetrating than an electron of the same energy. It should be remarked that in the application of these formulae nuclear electrons may not, presumably, be neglected; they should be included in counting the total number (N) of electrons per cc. But unless ϵ is very large, the contribution of these electrons to the stopping power will be smaller than that of the extranuclear electrons, since the binding energy of the former must be of the order of a few million volts. It seems at present impossible to extend our calculations to the case of electrons bound in nuclei, because of our ignorance of the nature of that binding. But insofar as wave mechanics is applicable to such particles, (2.46) should give a reliable estimate of their effect on a fast electron.

III. Impacts of the Magnetic Neutron

We want now to study in a little more detail the expression which we have derived for the impact of a magnetic neutron with a free electron. The cross section for such encounters is given in (1.67) and the somewhat complicated quantities occurring in this expression are given in (1.69). We shall consider first and chiefly the case that the neutron has a velocity small compared with that of light; in this case it will be unable to give the electron a very high velocity, and we may greatly simplify (1.67) by neglecting higher powers of v/c for both particles. The complicated summation of the square of the numerators of (1.67) then reduces to

$$N = 2\left| T_{++}{}^{4}\right|^{2} + 2\left| T_{+-}{}^{4}\right|^{2} \tag{3.1}$$

and we find from (1.72)

$$N = (1/2M^2c^2)\{p'^4 + p'^2(4r^2 - 8r\Delta r + 2(\Delta r)^2] + (\Delta r)^4\}. \tag{3.2}$$

Further the denomination of (1.67) becomes

$$\left|\boldsymbol{p}^{(i)} - \boldsymbol{p}^{(1)}\right|^{2} = (\Delta r)^2 + p'^2. \tag{3.3}$$

If we introduce for the ratio of the mass m of the secondary to that of the neutron

$$\lambda = m/M \tag{3.4}$$

and the further abbreviations

$$\alpha = \cos\vartheta,\ \beta = \sin\vartheta,\ g = [\alpha + (\lambda^2 - \beta^2)^{1/2}]/(1 + \lambda), \tag{3.5}$$

we find

$$\sigma d\alpha = \frac{2\pi^3e^2\mu^2}{h^2c^2} g d\alpha \frac{\{g^4\beta^4 + g^2\beta^2[4 - 8(1 - g\alpha) + 2(1 - g\alpha)^2] + (1 - g\alpha)^4\}}{(1 - 2g\alpha + g^2)^2}. \tag{3.6}$$

The energy transferred is

$$E' = (E/\lambda)(1 - 2g\alpha + g^2). \tag{3.7}$$

Several points are at once clear. Since for $\alpha\to1$, $g\to1$ the cross section behaves for small angles like

$$\sigma d\alpha \sim d\alpha/(1 - \alpha) \sim d\beta^2/\beta^2 \tag{3.8}$$

whereas in the case of the Coulomb field it behaved like

$$d\alpha/(1\alpha)^2 \sim d\beta^2/\beta^4. \tag{3.9}$$

The mean energy transferred may be computed without considering the binding of the secondary, since $\delta E = \int \sigma E' d\alpha$ converges. Further, the cross section is independent of the velocity or energy of the neutron, and the mean energy loss is directly proportional to the initial energy; finally the cross section is proportional to the square of the magnetic moment of the neutron.

We shall reduce (3.6) for the case that the neutron has a mass equal to that of the secondary, $\lambda = 1$, or much smaller, $\lambda \gg 1$ or much larger $\lambda \ll 1$.

$\lambda = 1$. Here $g = \alpha$,

$$\sigma d\alpha = \frac{2\pi^3 e^2 \mu^2 \alpha}{h^2 c^2 \beta^4} \{\alpha^4\beta^4 + 2\alpha^2\beta^2(2 - 4\beta^2 - \beta^4) + \beta^8\}. \tag{3.10}$$

The quadrature over the angle of deflection gives for the energy loss

$$\delta E = \int \sigma E' d\alpha = (7/96)\sigma_0 E \tag{3.11}$$

where $\sigma_0 = 16\pi^3 e^2 \mu^2 / h^2 c^2$. This cross section σ_0 may be written

$$\sigma_0 = \pi e^4 n^2 / m^2 c^4, \text{ with } n = \mu/\mu_B;\ \mu = eh/4\pi mc \cdot n \tag{3.12}$$

where n is the magnetic moment of the neutron measured in Bohr magnetons. This quantity n is presumably quite small, so that σ_0 is very small indeed. The expression for the total number of impacts

$$\sigma = \int \sigma d\alpha \tag{3.13}$$

does not converge in the small angles. The preponderance of small energy losses is not nearly so marked here as for the impacts of an electron; and it is easy to show, by repeating the familiar nonrelativistic calculations for the impact of a particle with a bound electron, that the total number of impacts in which an energy of the order of a few times the binding energy or less in transferred is finite and independent of the primary energy and corresponds to a cross section of the order of σ_0. The total cross section thus turns out to be

$$\sigma = \int \sigma d\alpha \sim \sigma_0 \{\tfrac{1}{4} \ln (E/W) - 7/16\} \tag{3.14}$$

where W is of the order of the ionizing energy. The mean energy transferred per impact is thus

$$\delta E/\sigma \sim (E/24) \ln E/W. \tag{3.15}$$

Such a magnetic neutron, quite apart from the great infrequency of its impacts, a factor $In^2/4mc^2$ smaller cross section than an electron—will never produce ion tracks in a cloud chamber, since it tends to lose an appreciable fraction of its energy, and suffer an appreciable deflection at every impact.

$\lambda \gg 1$. For this case we find

$$\sigma \sim (\sigma_0/4) \ln 2E/\lambda W \tag{3.16}$$

$$\delta E = (19/96)\sigma_0 E/\lambda \tag{3.17}$$

and for $\lambda \ll 1$:

$$\sigma = (\sigma_0/4) \ln E\lambda/W \tag{3.18}$$

$$\delta E = \sigma_0 E\lambda/8. \tag{3.19}$$

In both these cases impacts are relatively rare; in both, the mean energy loss is necessarily smaller than for equal masses; only for a heavy neutron are impacts without large deflection possible. If such a neutron as this had a large magnetic moment, large compared to the Bohr magneton, it could produce recognizable cloud chamber tracks; but values of n large enough to give this seem *a priori* extremely improbable.

The formulae we have given apply equally—especially to the impacts of a magnetic neutron with a proton or nucleus. They do not account very well for the phenomena observed in the penetrating radiation from Be bombarded with alpha-particles. In the first place, such a magnetic neutron would have more impacts with highly charged nuclei than with protons, whereas the observations show that this is not so; in the second place the number of impacts would depend so little on the energy of the neutron, so that it would be hard to account for the observed inhomogeneous absorption of the radiation. Finally the distance between impacts would be enormous; with $n=10^{-3}$ and $\lambda=1$, a neutron of 5.10^6 volts would travel$\sim$100 km before ejecting a visible proton from paraffin.

One might suppose that in the general case of velocities not small compared to that of light, different and more satisfactory results might be obtained. We have investigated this case only for $\lambda=1$, in which case the conservation laws give simple algebraic relations between angle of deflection and final momenta and energy. For this case the total cross section increases with ϵ, where again $E=\epsilon Mc^2$ is the initial energy of the neutron, and is of the order.

$$\sigma_0\epsilon^2. \tag{3.20}$$

In this case $\epsilon\gg1$, the preponderance of small deflections and relatively small energy losses is still less marked than in the case of low velocity magnetic neutrons. When

$$\epsilon > \ln E/W$$

the electron tends to lose a large part of its energy in each encounter it makes. Such a neutron could not produce cloud chamber tracks; and since it is certain on energetic grounds that the radiation from beryllium does not consist of such neutrons, we have not thought it desirable to give further details in the evaluation of (1.67).

We believe that these computations show that there is no experimental evidence for the existence of a particle like the magnetic neutron.

Photoelectric and Thermionic Emission from Composite Surfaces

By WAYNE B. NOTTINGHAM*
Massachusetts Institute of Technology

(Received August 6, 1932)

Classical methods when applied to photoelectric and thermionic emission from composite surfaces often lead to inconsistent results. A study of the thermionic emission, with a new thyratron circuit for heating tungsten and thoriated tungsten filaments, reveals that many points can be explained if we take into consideration the complex form of the potential barrier produced by an atom layer of electropositive metal when deposited on an "electronegative" base. From an experimental knowledge of the transmission coefficient of the barrier as a function of electron energy and the use of the Wentzel approximation for the transmission coefficient $D(v)=\exp-(4\pi/h)\int_{x_1}^{x_2}(2mH)^{1/2}dx$), it is possible to calculate the shape of the barrier which turns out to be practically parabolic and about 4.3×10^{-8} cm in width one electron-volt below the top of the hill. Since the width and perhaps the height of the barrier seem to depend upon the temperature, it becomes clear that the Richardson-Dushman equation $I=AT^2\exp(-b_0/T)$ is applicable only as an empirical representation of the data obtained with composite surfaces as emitters. This surface model explains very naturally the fact that the electrons emitted from a composite have an apparently Maxwellian distribution of velocities corresponding to a temperature fifty percent higher than that of the filament as reported by Koller and Rothe. It also gives a qualitative explanation of the observed dependence of the photoelectric long wave-length limit on the applied potential for thin films of sodium on nickel using very low fields.

INTRODUCTION

A COMPOSITE surface may be formed by depositing a thin layer of "electropositive" metal on a more "electronegative" one. Many investigators have found such surfaces to be more active thermionic and photoelectric emitters of electrons than either of the metallic constituents when taken in bulk. The thermionic current from a composite surface has been observed to depend on the temperature according to the Richardson equation $I=AT^2\exp(-e\phi_0/kT)$ but differences between values of the work function ϕ_0 for different surfaces are not in satisfactory agreement with measurements of the contact difference in potential.[1]

The thermionic current varies with the accelerating field according to the Schottky mirror image theory[2] only for high fields.[3] At low fields the current falls much more rapidly than might be expected. Electrons emitted from a

* Fellow at the Bartol Research Foundation, Swarthmore, Pennsylvania, while carrying on the experimental work reported in this paper.

[1] I. Langmuir and K. H. Kingdon, Phys. Rev. **34**, 129 (1929).

[2] K. T. Compton and I. Langmuir, Rev. Mod. Phys. **2**, 123 (1930). See part B (5) for complete discussion.

[3] J. Becker and D. Mueller, Phys. Rev. **31**, 431 (1928); N. B. Reynolds, Phys. Rev. **35**, 158 (1930).

clean tungsten surface have been found to have a Maxwellian distribution of velocities[4] with a temperature equal to that of the filament but according to the results of Koller[5] and Rothe,[6] the apparent temperature of the electrons emitted from a composite surface is at least fifty percent higher than that of the emitting surface.

The above difficulties serve to illustrate the nature of some of the broader aspects of the problem at hand. We see that the observed results follow more or less according to the theories which have been well able to describe the thermionic emission from clean surfaces, but in almost every case there is a definite difference between observation and theory which is much larger than the experimental error. It is the object of the first part of this paper to describe as concisely as possible a series of experiments on the thermionic emission from thoriated filaments and the photoelectric emission from films of sodium deposited on nickel. In the latter part of this paper an attempt will be made to coordinate these new, and many of the old, results into a theory.

The experimental work upon which this paper depends was carried on at the Bartol Research Foundation with the liberal support of the Franklin Institute of Philadelphia between January, 1929, and August, 1931.

The Experimental Problem

From his studies of *photoelectric emission*, Dr. Ives[7] reported that as a thin film of sodium is deposited on a platinum surface, "the long wave limit of the emission first moves toward the red as the film increases in thickness and then, after the maximum of the photoelectric sensitiveness is passed, moves back toward the violet." Later, Ives and Olpin[8] reported that in the cases of lithium, sodium, potassium, rubidium and caesium this maximum "excursion" of the long wave limit was "found to coincide with the first line of the principal series, i.e., the resonance potential." Stimulated by these researches an attempt was made to investigate the energy distribution of the emitted electrons and test the linearity of photoelectric response of these surfaces to light of a wave-length very near that of the threshold. What was thought to be a nonlinearity in the response[9] and reported as such was later found[10] to be due to a nonlinearity in the amplifier system used to measure the extremely small currents. These studies also yielded results which were interpreted as a departure from Einstein's photoelectric equation.[11] The experimental data, which are now being published in detail for the first time, can apparently be explained on the wave-mechanical theory of electron transmission through a potential barrier.

[4] L. H. Germer, Phys. Rev. **25**, 795 (1925).
[5] L. R. Koller, Phys. Rev. **25**, 671 (1925).
[6] H. Rothe, Zeits. f. Physik **37**, 414 (1926).
[7] H. E. Ives, Astrophys. J. **60**, 209 (1924).
[8] Ives and Olpin, Phys. Rev. **33**, 281 (1929); **34**, 117 (1929).
[9] W. B. Nottingham, Phys. Rev. **33**, 633 (1929).
[10] W. B. Nottingham, Phys. Rev. **35**, 669 (1930).
[11] W. B. Nottingham, Phys. Rev. **33**, 1081 (1929).

In the field of *thermionic emission*, Reynolds[12] reported work which might be considered as an extension of that of Becker and Mueller[13] on the variation of the thermionic emission from a thoriated tungsten filament as a function of the electric field. The fact that the results reported by Reynolds could be interpreted qualitatively with the same "surface models" as those used in the interpretation of the photoelectric[14] emission data made it clear that a thorough investigation of the problem of the thermionic emission from a thoriated tungsten wire using small retarding and accelerating potentials on the collector, might greatly extend our understanding of the general problem of composite surface emitters. Two important difficulties of the experiment not satisfactorily disposed of by Reynolds were (1) the lack of uniformity of potential difference between the filament and the collector due to the filament heating current and (2) the adequate insulation of the collector. Preliminary work done by the author before these difficulties were overcome verified the general experimental results of Reynolds, but suggested new explanations.

With the help of wave mechanics, it is now possible to explain many of the observed facts of electron emission from composite surfaces by considering the transmission *through* the potential barrier produced by an atom layer of an electropositive element when deposited on a more electronegative base. These points will be discussed in detail later in this paper. Since practically all of the experimental work being reported in this paper was done before an application of the present theory[15] was made, it will not be difficult to discover points in the argument which can be disposed of by additional experiments. Although there are a number of such investigations under way already, it has been thought worth while to report in detail on the results obtained to date, partly to help other workers in the field and partly to invite criticism of the experiments and theories presented here.

Electric Circuits

a. Filament heating circuit

In order to heat the filament and yet have no drop in potential over it during measurement an intermittent heating system like that used so successfully by Germer[16] was employed. Instead of using a 500 cycle generator and tungar rectifiers as done by Germer, a thyratron "inverter" circuit was developed at the suggestion of Dr. A. W. Hull and patterned essentially after his circuit.[17] This is shown in Fig. 1.

With thyratron T_1 conducting 0.25 ampere the plate P_1 is only about 12 volts positive with respect to the filament and there is a difference in potential of 250 volts across the condenser C. When the oscillator voltage carries

[12] N. B. Reynolds, Phys. Rev. **35**, 158 (1930).
[13] J. Becker and D. Mueller, Phys. Rev. **31**, 431 (1928).
[14] W. B. Nottingham, Phys. Rev. **35**, 669 (1930).
[15] W. B. Nottingham, Phys. Rev. **38**, 1918 (1931).
[16] L. H. Germer, Phys. Rev. **25**, 795 (1925).
[17] A. W. Hull, Gen. Elec. Rev. **32**, 390 (1929).

the grid G_2 of thyratron T_2 *positive*, this tube suddenly becomes conducting and the quick drop of potential at P_2 causes that of P_1 to become very negative with respect to F_1. If the de-ionization time is shorter than the time required for the condenser C to charge up through the 1000 ohm resistance, then thyratron T_1 will remain nonconducting until the next half cycle of the oscillator at which time G_1 is made positive and the cycle of operation as described above is repeated. It is easy to see that the wave form of the current through T_1 will be qualitatively that of Fig. 2.

The part of the cycle during which the filament is heated is shown cross-hatched. The sharp peaks showing reverse current for an extremely short

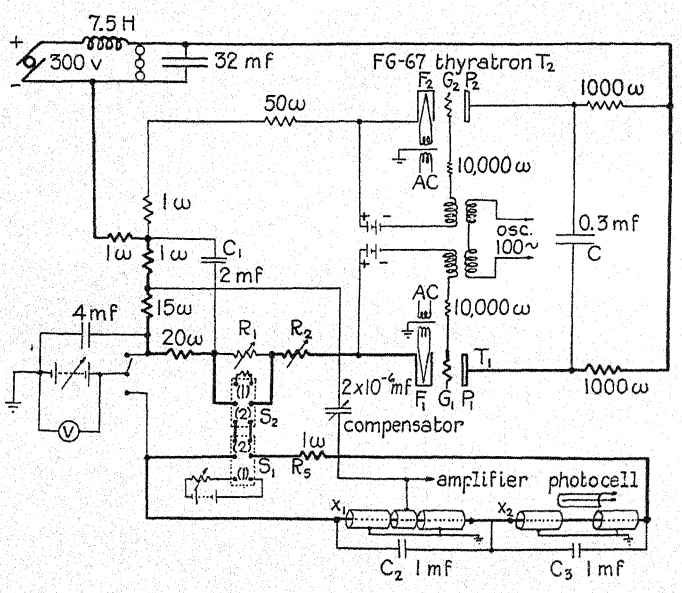


Fig. 1. Thyratron[18] inverter circuit for heating filament with pulsating current.

time were assumed to be there on indirect evidence only. The condensers C_1, C_2 and C_3 were introduced to eliminate the effect due to this reverse current. Now that a cathode-ray oscillograph which can follow such rapid

[18] Since the thyratron has not yet come into common use in physical research, it will perhaps be desirable to describe very briefly its operating characteristics.

The thyratron is a gas filled (mercury vapor) three-electrode tube containing a cathode, anode and grid. With positive potentials of a few hundred volts on the plate, a few volts negative grid potential prevents the electron current flow from cathode to anode. At a certain critical value of grid bias enough current flows, however, to start ionization in the gas. Within a few microseconds an arc is fully developed with the current limited only by the external circuit under normal conditions. After the formation of the arc the grid has no control over the flow of current. Thus in a circuit with a d.c. plate supply, provision must be made for stopping the flow of current through the thyratron after it has once been started by effectively cutting off the plate supply. It is for this reason that we have the plates of the two thyratrons of Fig. 1 connected together by the 0.3 mf condenser.

For detailed discussion see: A. W. Hull, reference 17; W. B. Nottingham, J. Frank. Inst. **211**, 271 (1931); W. B. Nottingham, J. Frank. Inst. **211**, 751 (1931).

changes in potential is available, the exact nature of this objectionable reverse peak is to be investigated.

The power was supplied by a 300 volt d. c. generator driven by a three-quarter hp, three phase synchronous motor. With the generator brushes in good condition the output voltage was steady to within about 0.1 percent for a considerable period of time.

An inductance and condenser were used as shown to eliminate the commutator ripple.

b. Adjustment of filament temperature

The Langmuir and Jones[19] temperature scale for pure tungsten was used. Approximate values of the temperature were calculated from measurements of the current flowing and the diameter of the filament. With this approximate temperature, the end loss correction was calculated[20] and the final temperature was determined from the Langmuir-Jones table for $V'(A')^{1/3}$ which involves measurement of the filament length, voltage drop, and current.

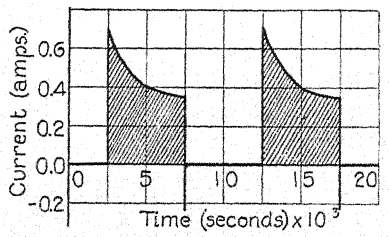


Fig. 2. Wave form of current through thyratron T_1.

The current was determined by measuring the drop in potential over a standardized one ohm resistance R_s using a Leeds and Northrup type K potentiometer. The voltage drop over the filament was accurately measured using a type K potentiometer with ten times the usual current flowing through the coils and slide wire. With this method, it was possible to measure accurately d.c. voltages as high as 16.1 volts. By throwing the switch S_1 to position (1) the filament under test X_1 and the auxiliary filament X_2 were heated by d.c. These two filaments were of approximately equal length and from the same stock. Under this condition the temperature of the test filament could be determined and the light emitted from the auxiliary filament accurately measured by a null method. With switches S_1 and S_2 both in position (2) filaments X_1 and X_2 could be heated with pulsating current. By adjusting R_1 and R_2 the temperature of X_2 was brought very accurately to that previously determined by observing the photoelectric current produced by the light emitted from X_2. It was then assumed that the temperature of the test filament was the same as that determined from the d.c. measurements. The frequency of the pulsating current was varied from 100 to 500 cycles per second with no change in the thermionic current observed. Prac-

[19] I. Langmuir and H. A. Jones, Gen. Elec. Rev. 30, 310, 354, 408 (1927).
[20] Langmuir, McLane and Blodgett, Phys. Rev. 35, 478 (1930).

tically all measurements were therefore carried out with the oscillator set to deliver 100 cycles.

c. Amplifier circuit for photoelectric current

The photoelectric current produced by the light from the auxiliary filament X_2 was measured with the circuit shown in Fig. 3.

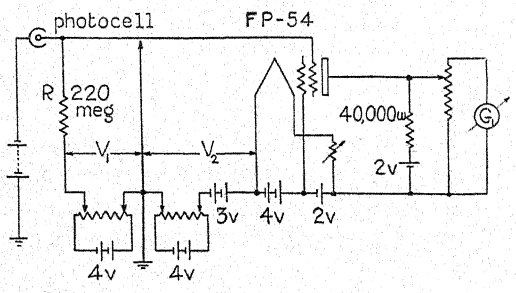


Fig. 3. Amplifier circuit for photoelectric current.

The underlying theory of the operation of this type of circuit has been discussed elsewhere.[21] The low voltage batteries used were 150 amp.-hr. storage batteries and were carefully maintained. Under these conditions the single tube amplifier circuit has been found to be more steady than the two tube circuit and much easier to maintain. With no light on the photoelectric cell and V_1 zero, potential V_2 was adjusted to make the current through the galvanometer G_1 zero.

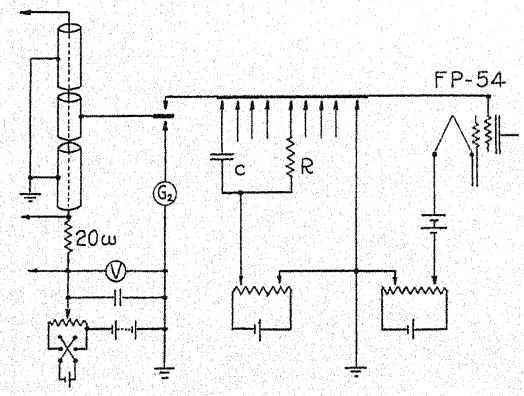


Fig. 4. Grid circuit of vacuum tube amplifier used to measure thermionic current.

When the filaments X_1 and X_2 were heated by direct current, the light from the auxiliary filament X_2 falling on the cell caused a current to flow through R. The potential V_1 was then adjusted to bring the galvanometer to zero. The pulsating current was adjusted to maintain the light emitted from X_2 constant as indicated by the galvanometer.

[21] W. B. Nottingham, J. Frank. Inst. **209**, 287 (1930); L. A. DuBridge, Phys. Rev. **37**, 392 (1931).

d. Amplifier circuit for thermionic current

The circuit for measuring the thermionic current was very similar to that of Fig. 3, except that a 25,00-b type R galvanometer was used in place of a 2500-e instrument. Instead of a standard FP-54 vacuum tube, an early model of the same general design having a higher mutual conductance was used with a resulting maximum sensitivity of about 10.5 cm per millivolt applied to the grid. Certain special features incorporated in the grid circuit are shown in Fig. 4.

Condensers or resistances were used in the grid circuit to give a means of varying the sensitivity. The capacities of a specially selected set of fixed condensers ranged from 0.002 mf to 8.0 mf and the values of resistance ranged from 5000 megohms to zero. With the capacities it was possible to use the rate of deflection method of measurement for the current range of 10^{-13} to 5×10^{-8} amp after which the galvanometer G_2 could be used directly.

Experimental Tubes

a. Construction and preparation

The filaments, kindly furnished by the Research Laboratory of the General Electric Company, were of types known as "T," "E," and "C" wire. "T" and "E" were thoriated tungsten, the latter being free from carbon and the "C" wire was pure tungsten. The wire diameter was approximately 1.6 mils and the length of the filaments were about 10.8 cm. The collector was 1 cm in diameter and about 2.5 cm long. Cylinders of the same diameter and about 4 cm long were used to make the field uniform near the ends of the collector and also receive the emission from the cool ends of the filament.

The collector was supported on long "beads" held by "sealed-in" tungsten connections maintained at the collector potential. A special lead was brought out for the collector to give high insulation from the other leads coming through the press. All the metal parts were made of "baked out" nickel or tungsten. A rather elaborate outgassing schedule was carried out with oven baking at temperatures up to 400°C and heating of the collectors with the induction furnace as well as extensive heating of the filament.

b. Activation of the filament

Langmuir and Rogers[22] found that tungsten wire containing about one percent of thorium oxide could be made, by a proper heat treatment, a much more efficient emitter of electrons than pure tungsten at filament temperatures of less than 2000°K. The details of this process are given in full by Langmuir[23] and also by Dushman.[24] At a filament temperature of 2700°K to 2900°K some of the thorium oxide decomposes leaving a small amount of thorium between the tungsten crystals and near enough to the surface so that the thorium can diffuse, at the activation temperature, to the surface and form a layer of thorium atoms. The filament temperature must be 1800°K

[22] I. Langmuir and W. Rogers, Phys. Rev. 4, 544 (1914).
[23] I. Langmuir, Phys. Rev. 22, 357 (1923).
[24] S. Dushman, Rev. Mod. Phys. 2, 381 (1930).

or greater for this "activation" to take place at a reasonably rapid rate. After a long time of activation the equilibrium surface condition is governed by the rate of diffusion and the rate of evaporation.

Fig. 5 shows a typical set of curves[25] representing the first activation carried out in steps at $T_a = 1920°K$.

The accumulated time is plotted along the abscissa while the thermionic current observed at a test temperature of $T_t = 1230°K$ and a collector potential of +20.0 volts is plotted as the ordinate. The maximum found after 90 minutes' acitvation is undoubtedly related to the maxima found by Becker[26] in his studies of the thermionic emission from a caesium covered tungsten filament. In Becker's work the surface coverage corresponding to the maximum emission was thought to correspond to a monatomic layer of caesium

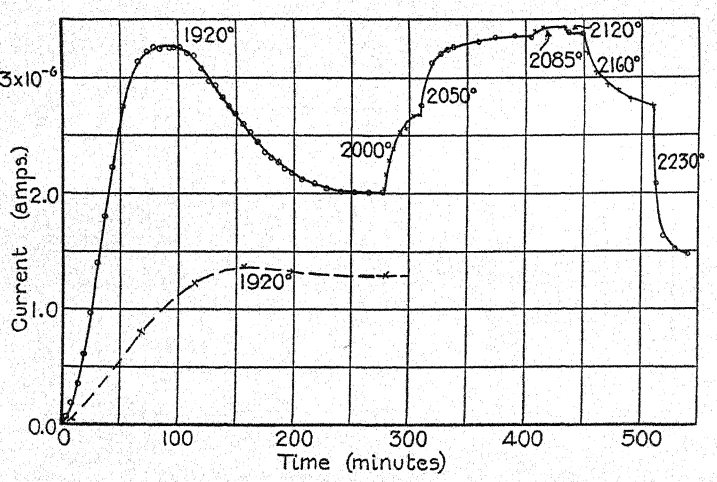


Fig. 5. Activation of a thoriated filament with test temperature 1230°K (T wire). Solid curves applied accelerating potential 20 volts; dashed curve potential 2.0 volts.

atoms on the tungsten and by analogy it is thought that the maximum in Fig. 5 corresponds to a monatomic layer of thorium atoms on tungsten. With $T_a = 1920°K$ the equilibrium condition was practically reached after 280 minutes of activation. By raising the activation temperature to 2000°K this equilibrium was disturbed immediately and a sharp *rise* in the curve was observed. At about 2100°K the *equilibrium* condition corresponds very closely to that of the maximum observed at 90 minutes. Activation at still higher temperatures, leaves the surface only partly covered. At low fields the maximum practically disappears. The significance of this observation will be discussed later.

The main features of the activation curve shown in Fig. 5 are thus easily understood. There are, however, many details concerning the activation process which may be of importance in the explanation of results obtained with more complicated composite surfaces. For example, after a filament has been

[25] W. B. Nottingham, Phys. Rev. **35**, 1128 (1930).
[26] J. A. Becker, Phys. Rev. **28**, 341 (1926).

fully activated, the emission has been observed to *increase* two to six fold in the cource of time even though the filament is maintained at liquid air temperature between observations. This effect is undoubtedly brought about by the adsorption of some gas. A detailed examination of this effect is being undertaken.

Measurement of Thermionic Current

a. Velocity distributions

The experimental difficulties associated with the measurement of the thermionic emission from composite surfaces have long been recognized. For example, work function measurements involving a change in temperature of

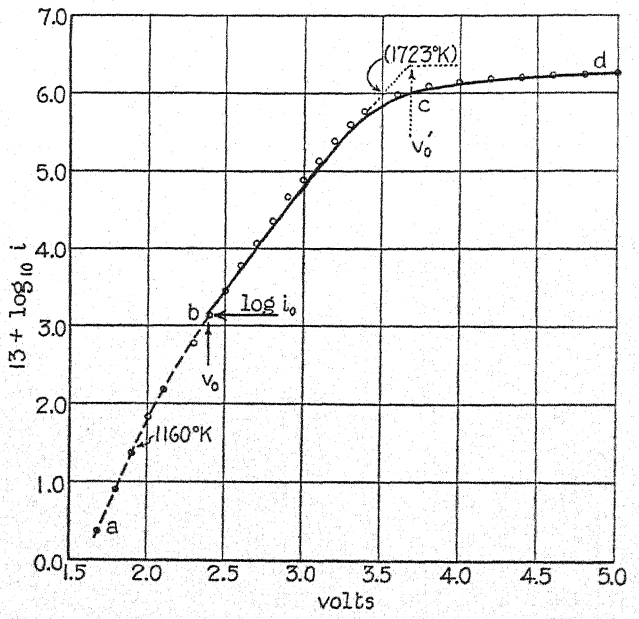


Fig. 6. Thermionic current from a fully activated filament at 1160°K (pulsating filament current used). Range *ab* calculated by Schottky equation. Range *bcd* identical to that observed with tungsten filament at 1723°K.

the emitter are often invalidated because the surface conditions may change with the temperature. Some of these changes are slow enough to be observed; others may be rapid and escape observation. Surface conditions also change with an alteration in the current drawn from the filament and may thus be subject to variation with applied field and temperature. Changes at the surface of the collector as indicated by a shift in contact potential have also been observed.[27] In order to minimize these difficulties a definite procedure of measurement was adopted. Before beginning a set of measurements, maxima of accelerating potential (usually less than 10 volts) and temperature (about 1200°K) were decided upon. During the run these standard conditions were maintained except during the time required for each reading, i.e., after

[27] W. B. Nottingham, Phys. Rev. **39**, 183 (1932).

making a reading standard conditions were reproduced before taking the next. In Fig. 6 a typical curve is given showing the thermionic current received by the collector as a function of the applied potential difference between the collector and the filament.

The points enclosed in circles are the observed points. The curves drawn through the points are of theoretical significance. The dashed curve from *a* to *b* is the theoretical curve, computed from the classical equation developed by Schottky,[28] for the current received against a retarding potential by a cylindrical collector from a filament of small diameter supported along the axis of the cylinder, with the distribution of velocities assumed to be Maxwellian and the temperature that of the filament. Over the part of the range covered, there is a very close agreement between the observed points and the theoretical curve.

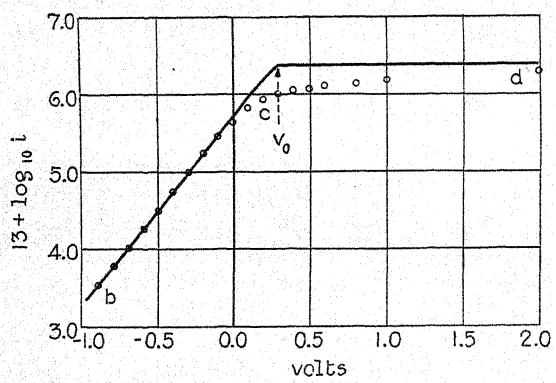


Fig. 7. Thermionic current from a pure tungsten filament at 1723°K. (Pulsating filament current used.)

There is, however, no sign of saturation at the point *b* as one would expect from classical theory and on the basis of Germer's experience with pure tungsten filaments. It is only natural to suggest that the observed results are distorted by space charge effects which would invalidate a calculation using the Schottky theory. In order to test this point measurements were made on a filament of "*E*" wire in the *completely deactivated* state and also on a pure tungsten "*C*" wire. These filaments were heated to such a temperature that the saturation current was exactly equal to that observed on the activated filament with about 6 volts applied potential. The results of one of these tests are shown in Fig. 7.

In the case of the clean tungsten filament, the Schottky curve and the observed points agree almost perfectly up to within about 0.2 volt of the theoretical saturation point. At lower temperatures the agreement is even closer. These results are in very close agreement with those of Germer which showed that space charge effects could be neglected in the case of pure tungsten filaments up to about 1830°K. Since space charge phenomena are controlled

[28] Walter Schottky, Ann. d. Physik **44**, 1011 (1914). Germer's table in Phys. Rev. **25**, 795 (1925) was used for all of these computations.

primarily by the current density and the electric field near the surface of the filament, the fact that the space charge can be neglected in the case of the pure tungsten indicates that it can also be neglected in the case of an activated thoriated filament for temperatures less than 1200°K.

A comparison was made between the observed curves for clean tungsten at 1723°K and thoriated tungsten at 1160°K and it was found that the curves were almost identical over the range *b c d* of Figs 6 and 7. The range *bc* in the case of pure tungsten indicates that the velocity distribution of the electrons is Maxwellian with a temperature of 1723°K. *But the similar range bc for the thoriated filament is also characteristic of* 1723°K, *although the temperature of the filament was only* 1160°K. This is a fundamentally important result, and it will be shown that the new theories of transmission through potential barriers can give just this result, i.e., given a potential barrier of the required dimensions, the distribution of electron velocities of those electrons which are transmitted through the barrier can be described as Maxwellian with a temperature 45 to 50 percent *higher* than that of the filament.

Measurements of the velocity distribution of the electrons from thoriated filaments operated at 987°K, 1045°K and 1103°K showed the same agreement between observed points and the Schottky curve for the range of applied potential negative to that designated as "v_0," while over the range of potential positive to "v_0" the distribution was quite accurately the same as that of a pure tungsten filament operated at temperature high enough to give the same saturation current at about 6 volts applied potential. With the filament in a particular state of activation all of the values of "v_0" for the various temperatures were the same within about ± 0.1 volt and the ratio of these temperatures was extraordinarily constant, as indicated by Table I.

TABLE I.

Thoriated fil. temp.	Case 1		Case 2	
	Tungsten	Ratio	Tungsten	Ratio
987	1458	1.48	1490	1.51
1045	1540	1.47	1570	1.50
1103	1620	1.47	1650	1.50
1160	1685	1.45	1723	1.48

It will be noticed that these results check well with the estimations made by Koller[5] and Rothe[6] that the electron temperature as indicated by the apparent velocity distribution is 50 percent higher than that of the filament, although their work applied to the oxide-coated filament. The theory to be proposed here would presumably be approximately applicable also to this more complicated type of surface.

These experiments have therefore suggested the existence of two groups of emitted electrons, the one with higher speeds classically characteristic of the filament temperature and the other (comprising nearly 99.9 percent of the saturation emission) being apparently characteristic of a 50 percent higher temperature. The discovery of the former group is due to the experimental extension of the velocity distribution curve through a larger range of

values than is usually done. The latter group, which has heretofore been treated classically is, on the present theory, a group which could not escape classically but is allowed to escape by wave mechanics according to a probability factor which depends jointly on the "potential barrier" created by the adsorbed electropositive layer and on the applied potential.

b. Work-function measurements

Really accurate determinations of the thermionic constants ϕ_0 and A of the Richardson equation $I=A\ T^2 \exp -e\phi_0/kT$, are exceptionally difficult when the range of permissible temperature variation is small. Data which were obtained show definitely that both of the constants depend very decidedly on the exact state of the surface. No two activation and filament aging curves have been observed which are exactly alike and therefore no two values of ϕ_0 and A are the same although attempts have been made to control activation conditions accurately. Studies now under way will no doubt throw new light on this question.

With an applied accelerating potential of 6.0 volts, the observed values of ϕ_0 ranged from 2.38 to 2.83 electron-volts while the value of A ranged from 0.56 to 10.2 amp. per cm^2 per deg.^{2}.

One of the best determinations gave $\phi_0=2.64$ and $A=3.2$ which compare very satisfactorily with those of Dushman and Ewald[29] of $\phi_0=2.63$ and $A=3.0$. Measurements with applied potentials of 2.0 and 2.4 volts, corresponding to values of v_0 as defined above for various conditions of activation, gave ϕ_0 between 3.1 and 3.5 electron-volts and A between 10 and 60 amp. per cm^2 per deg.^{2}.

The results reported[30] for solid thorium are $\phi_0=3.35$ v with $A=60$. This suggests that the effective work function of a composite surface measured at a very low potential such as v_0 changes from that of the base metal to that of the surface metal as the film thickness increases to that of a single layer or greater. Thus we have a qualitative explanation of the fact that the activation curve of Fig. 5 taken at a very low field shows no maximum. The analogous result has been found photoelectrically.

Photoelectric Experiments

Although considerable work was done on the problem, photoelectric emission from composite surfaces, very little of it is of permanent value since the problem must be reinvestigated in the light of the recent theories of photoelectric effect such as that of Fowler.[31] The results reported here are therefore preliminary and show simply some of the more easily observed facts.

A sketch of one of the experimental tubes is shown in Fig. 8.

[29] S. Dushman and J. W. Ewald, Phys. Rev. **29**, 857 (1927).

[30] Dushman, Rev. Mod. Phys. **3**, 394 (1931). (Calculation based on data of C. Zwikker, Proc. Amst. Acad. Sci. **29**, 792 (1926). W. Espe gives $\phi_0=3.39$ v and $A=70$ in Zeits. f. tech. Physik **10**, 489 (1929).

[31] R. H. Fowler, Phys. Rev. **38**, 45 (1931).

The collector c_1, c_2, c_3 was made in three parts and the circuit arranged so that only the current collected on c_2 was measured. The emitter was a nickel cylinder 8 mm in diameter and about 6 cm long mounted on a movable support. By means of the iron weight sealed into a glass envelope, this electrode could be moved to positions I, II or III. During the baking and exhaust it

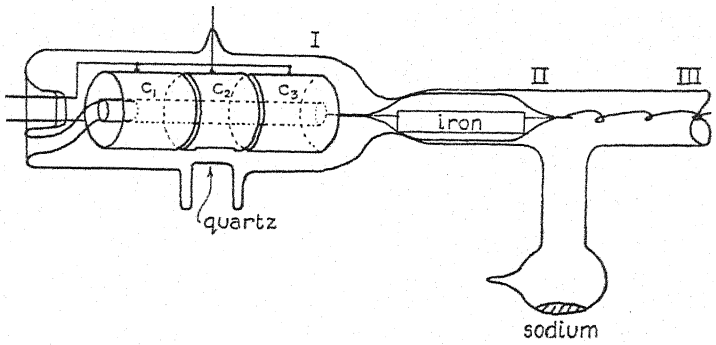


Fig 8. Tube for study of photoelectric emission from a thin film of sodium on nickel.

was in position III. In position II sodium could be deposited on the surface by evaporation from the side tube. While in position I, the electrode was supported concentric with the collecting cylinders by a glass tube sealed in the end as shown. A slit in collector c_2 permitted the light to fall on the emitter after having entered the tube through the quartz window.

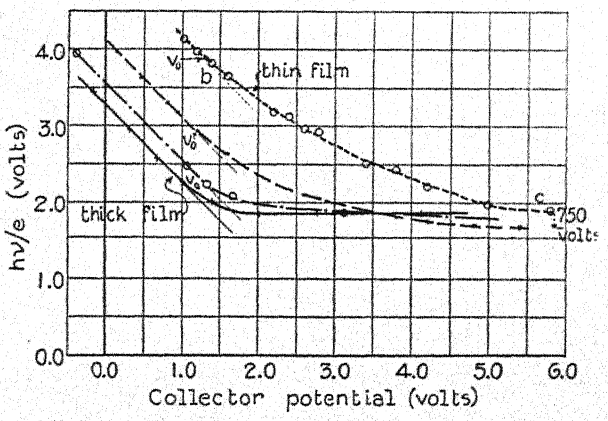


Fig. 9. Minimum-frequency limit as a function of applied potential.

The primary object of the study was to observe the dependence of the effective photoelectric long wave limit on film thickness and applied potential. The range of applied potential varied from a few volts retarding to about 700 volts accelerating. The most interesting results were obtained at low potentials and are shown in Fig. 9.

Over the range of applied potentials greater than 3 volts, the current was measured as a function of the wave-length holding the potential constant. The curve covering a range of current from 10^{-13} to 10^{-14} amp. was then extra-

polated into the axis to give the long wave limit. Over the range of small positive and negative potentials, the current was measured as a function of applied potential while the light frequency was constant. The extrapolation of these curves thus gave additional points for the limiting frequency at which an emission of the order of 10^{-14} amp. would take place under the particular conditions of illumination and applied potential. This limiting frequency expressed in equivalent electron volts is plotted as the ordinate while the applied potential is shown on the abscissa.

According to this method of plotting, points at the left of each curve which fall on straight lines with a slope of (-1) correspond to the range of applied potential over which the Einstein photoelectric equation is applicable. The fact that the points do not break away from this line and quickly approach a nearly horizontal line at some definite value of applied potential is a characteristic phenomenon of composite surfaces. The experimental facts of particular interest are (1) the frequency ν_0 at which the departure from the Einstein line takes place decreases progressively as the thickness of the film increases, presumably starting at that for nickel and finally reaching that for solid sodium; (2) with an accelerating potential of five volts or more the minimum-frequency "limit" undoubtedly decreases as the film thickness increases going through a "maximum excursion" and then returning to that of sodium in bulk. This fact was demonstrated by Ives[8] some years ago but it is interesting to note that the extent of this "excursion" is considerably greater than that of the resonance lines of sodium.

Analysis of Data According to Classical Methods

a. Theory*

If we assume that the curves of Fig. 9 give us a measure of the *effective* photoelectric work function ϕ_e as a function of the applied potential, we can deduce the "force-distance" curve against which the electrons must be working. In the absence of an applied field we have for the work of escape:

$$e\phi_0 = e\int_0^\infty F(s)ds \tag{1}$$

where $F(s)$ is the electric intensity against which the electron is working and s is distance measured from the surface of the metal. If we have an applied field the force against which an electron works in order to escape is increased or decreased. The decrease in work which the electron must do in order to escape with the help of an accelerating field is

$$\Delta\phi_e = \int_0^{s_c} V\phi(s)ds + \int_{s_c}^\infty F(s)ds. \tag{2}$$

Here s_c is the critical distance which the electron must go in order to escape V is the difference in potential between the electrodes and $\phi(s)$ depends on

* The theory presented here has undoubtedly been worked out by others. A less general discussion is given by Hughes and DuBridge, *Photoelectric Phenomena* p. 210.

the geometry of the electrodes. The critical distance is of course given by the condition

$$V\phi(s_c) = F(s_c). \tag{3}$$

If we make a small variation in V we obtain

$$\Delta\phi_c + (d(\Delta\phi_c)/dV)\delta V = \int_0^{s_c+(ds_c/dV)\delta V} (V+\delta V)\phi(s)ds + \int_{s_c+(ds_c/dV)\delta V}^{\infty} F(s)ds. \tag{4}$$

After subtracting Eq. (2) from Eq. (4) it follows that

$$d(\phi_c)/dV = \int_0^{s_c} \phi(s)ds \tag{5}$$

since $d(\Delta\phi_c)/dV = d(\phi_c)/dV$.

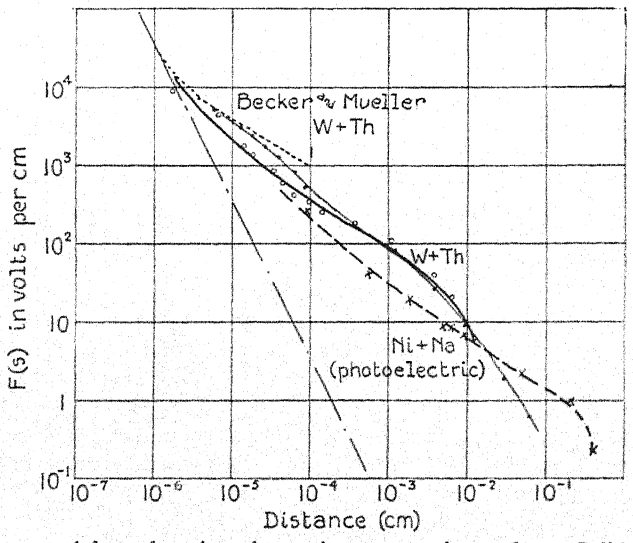


Fig. 10. Computed force functions for various composite surfaces. Solid lines thoriated tungsten; dotted line Becker-Mueller data thoriated tungsten; dashed line sodium on nickel observed photoelectrically. Dot-dash line given by mirror image theory.

The left-hand side of Eq. (5) comes from the slope of such curves as those of Fig. 9. If $\phi(s)$ can be integrated s_1 can be determined as a function of V and using Eq. (3), $F(s)$ can be deduced. For infinite cylinders we obtain

$$s_c = r\left[(R/r)^{d\phi_e/dV} - 1\right] \tag{6}$$

where R = radius of outer and r = radius of inner cylinder.

Thermionic data can also be analyzed in this way if we assume that all current changes with applied potential are due to an alteration in the work function. Differentiating the Richardson equation we obtain

$$d(\log i)/dV = -(e/kt)(d\phi_e/dV). \tag{7}$$

In this way $d\phi_e/dV$ as a function of V can be obtained from observed data and Eqs. (6) and (3) can be used to determine the "force function" $F(s)$.

b. Experimental test of classical method

The results of the experimental test of this method of analysis are best illustrated by the curves of Fig. 10.

It is interesting to note that the general trend of the curves is remarkably uniform. It is not difficult to show that data taken at different temperatures, such as that summarized in Table I above, will give the same force function if the temperature ratios of columns three and five are constant.

There are at least two serious objections to this method of analysis which are (1) forces as great as 5.0 to 10.0 volts per cm at distances as great as 10^{-2} cm from the surface are certainly impossible, and (2) determinations of the thermionic constant A made with applied potentials between 2.6 and 6.0 volts have not been found to be constant as is required if the entire change in thermionic current with field is the result of a change in the effective work function.

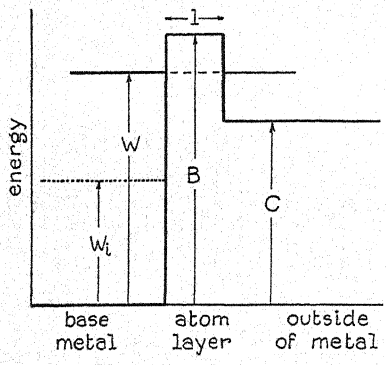


Fig. 11. Hypothetical potential barrier of Fowler and Nordheim. W_i is the highest electron energy assuming a Fermi-Dirac distribution in the base metal at 0°K. Electrons with energy $B > W > C$ must pass *through* a barrier of width l in order to escape.

Transmission through Potential Barrier Explains Results at Low Fields

a. Theory and application to thermionic data

Although the theories of Fowler[32] and Nordheim[33] and the approximate solution to the wave equation used by Wentzel[34] and others have been known for some years, no applications of these results to the voltage-current thermionic curves were made until last year.[15] It is clear that a hypothetical potential barrier of the Fowler-Nordheim type, shown in Fig. 11, will give results qualitatively like those shown in Fig. 6.

Upon heating, the electrons in a metal acquire energies greater than W_i. Those with energy greater than B can escape and the probability of escape upon approach to the boundary should be independent of the energy. The distribution of velocities of these electrons will of course follow the classical

[32] R. H. Fowler, Proc. Roy. Soc. A122, 36 (1929).
[33] L. Nordheim, Phys. Zeits. 30, 177 (1929). Further bibliography here.
[34] Wentzel, Zeits. f. Physik 38, 518 (1926).

laws and therefore be practically Maxwellian as is indicated by the observed curve *ab* of Fig. 6. For electrons of energy $W<B$ the probability transmission is distinctly less than that for $W>B$ and is furthermore a function of the energy W. Since the transmission coefficient decreases as W decreases the group of electrons with energy $B>W>C$ received by a collector will certainly not have a Maxwellian distribution at the temperature of the filament and if they have anything like a Maxwellian distribution at all it will certainly correspond to a temperature considerably higher than that of the filament since the transmission coefficient decreases with decreasing W thus favoring the high velocity electrons.

With a barrier of this type in mind, we see that the electron emission received with the collector at the potential v_0 (Fig. 6) corresponds to all of the electrons with energies greater than B.

From the fact that the velocity distribution of these electrons is Maxwellian at the temperature of the filament, we can calculate the number of electrons with energy greater than W which approach the barrier from within the metal and can therefore calculate the transmission coefficient as a function of W which must be obtained in order to produce the observed current-voltage curve. This was done using the Nordheim equation. For this B and C of Fig. 11 were held constant and three values of I were determined for three arbitrary values of W. The smooth curve drawn through the points looked very much like a parabola and the width at 1.0 electron-volt below the top of the "hill" was 4.5×10^{-8} cm. This result suggested that the barrier might be assumed to be parabolic and the Wentzel equation used.

The current-voltage characteristic of Fig. 6 can be idealized as shown in Fig. 12. The line *abb'* is given by the equation

$$\log_\epsilon i = \log_\epsilon i_0 + (e/kT_1)(v - v_0)/300 \tag{8}$$

while the line *c'c* is given by

$$\log_\epsilon i = \log_\epsilon i_2 + (e/kT_2)(v - v_0)/300. \tag{9}$$

We know that the complete curve must be given by

$$i = i_0 \frac{e}{300kT_1}\int_{-\infty}^{v} \epsilon^{e(v-v_0)/300kT_1} D(v)\,dv \tag{10}$$

where $D(v)$ is the transmission coefficient. Our experiments show that we may take

$$D(v) = 1 \text{ for } (v - v_0) < 0 \tag{11}$$

and

$$D(v) = \epsilon^{e(v-v_0)(1/T_2-1/T_1)/300k} \text{ for } v - v_0 > 0, \tag{12}$$

for then Eq. (10) reduces to

$$i = i_0\epsilon^{e(v-v_0)/300kT_1} \text{ for } (v - v_0) < 0 \tag{13}$$

and

$$i = i_0[1 + T_2/T_1(\epsilon^{e(v-v_0)/300kT_2} - 1)] \text{ for } v - v_0 > 0. \tag{14}$$

For values of $(v-v_0)>0.3$ volt, this equation reduces to Eq. (9) with $i_2=i_0T_2/T_1$. The complete curve given by Eqs. (13) and (14) is shown by the solid line of Fig. 12.

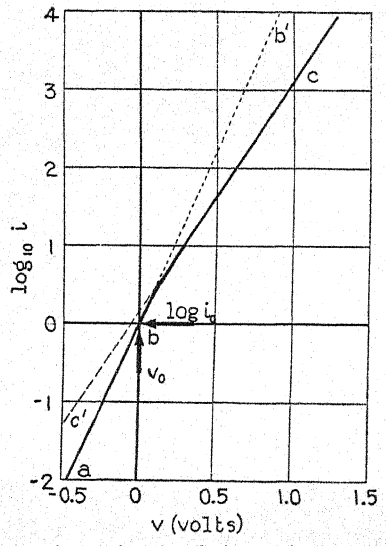


Fig. 12. Idealized current-voltage characteristic; equivalent to observed curve Fig. 6.

The Wentzel approximation gives the transmission coefficient for a barrier like that of Fig. 13 as

$$D(v) = \epsilon^{-(4\pi/h)\int_{x_1}^{x_2}(2mH)^{1/2}dx}. \tag{15}$$

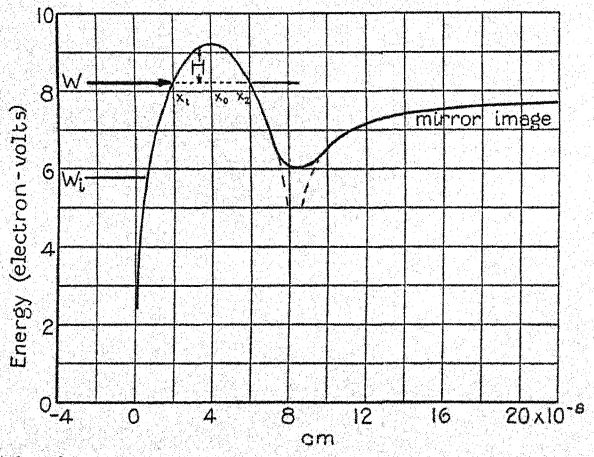


Fig. 13. Potential barrier calculated from observed data on thoriated filament $T=1160°K$.

Let us assume that the potential curve is a parabola above the line at W and is given by

$$H = [e(v - v_0)/300] - C^2(x - x_0)^2 \tag{16}$$

where C is a constant and x_0 is the value of x at the maximum. Remembering that $H=0$ at x_1 and x_2 Eq. (15) reduces for this case to

$$D(v) = e^{[-2\pi^2(v-v_0)e(2m)^{1/2}/300hC]}. \tag{17}$$

Equating the empirical Eq. (12) and the theoretical Eq. (17) we can solve for C to get

$$C = [2\pi^2 k(2m)^{1/2}/h]T_1T_2/(T_2 - T_1) \tag{18}$$

$$= 17.54 \times 10^{-8}T_1T_2/(T_2 - T_1). \tag{19}$$

The width of the barrier at any point is thus given as a function of v by

$$(x_2 - x_1) = 1.438 \times 10^{-4}[(T_2 - T_1)/T_1T_2](v - v_0)^{1/2}. \tag{20}$$

Putting in $T_1=1160$ and $T_2=1723$ we obtain $(x_2-x_1)=4.05\times10^{-8}$ cm with $(v-v_0)=1.0$ volt which is a reasonably good check on the result obtained using the Nordheim formula which gave 4.5×10^{-8} for the same data.

Using Eq. (20) we can calculate the appropriate barrier widths at one volt under the hill to fit the data summarized by Table I. The results are given in Table II.

TABLE II.

T_1	Barrier width $(v-v_0)=1$ volt Case I.	Case II.
987	4.77×10^{-8} cm	4.92×10^{-8} cm
1045	4.39	4.6
1103	4.15	4.33
1160	3.87	4.05

According to these data the effective width of the barrier seems to be *decreasing* with *increasing* temperature. This may be due to the inaccuracy of determining the appropriate value of T_2 although it is possibly a real effect since the transmission coefficient is probably determined more by the minimum distance of approach of the thorium atom to the tungsten surface rather than by its average position. If this result is true, it is evident that the use of the equation $I=AT^2\exp(-b_0/T)$ to determine the thermionic work function for composite surfaces cannot be of much theoretical significance since the observed current must depend on some "effective" work function which must be a complicated time average and also a function of the temperature. The area over which the emission actually takes place would also be decreased with the result that the surface area of the filament could not be used as is usually done to calculate a value of A.

This method of analysis thus provides a possible explanation for that part of the current-voltage characteristic which has been most troublesome for the classical theory, namely, that of the low voltage range. It also shows how the apparent velocity distribution of the electrons can very well be described as Maxwellian with a temperature 50 percent higher than that of the emitting surface as first pointed out by Koller.[5]

b. Application to photoelectric data

It is evident that a surface model similar to that of Fig. 13 is in qualitative agreement with the results shown by Fig. 9 in which we have the observed minimum-frequency limit shown as a function of the applied field. We see that if the collector potential is adjusted to turn back all electrons transmitted through the barrier, as the potential is varied, then the measured results can be expected to follow the Einstein equation and we will obtain a linear relation between potential and the minimum-frequency limit. Since the minimum-frequency limit as measured depends on the reception of a current of about 10^{-14} amp. at the collector over the range of small positive potentials, the apparent minimum-frequency limit will decrease less rapidly than before, thus accounting for the range *bc* of the curve shown in Fig. 9. With moderate accelerating fields the minimum-frequency limit is set primarily by the height of the plateau (Fig. 13) above the highest occupied energy level in the metal W_i. It is at once clear that photoelectric and thermionic studies should be carried out on the same filament under well controlled conditions for results so obtained are complimentary in many respects and would almost certainly give us the necessary information out of which a detailed picture of composite surface phenomena could be constructed.

It is with the greatest pleasure that I acknowledge my obligation to the members of the staff at the Franklin Institute, the Bartol Research Foundation and the director, Dr. W. F. G. Swann. To Dr. Karl T. Compton, I am greatly indebted for his continued interest and his many helpful suggestions.

A Relation between the Electric and Diamagnetic Susceptibilities of Monatomic Gases

By J. P. VINTI
Massachusetts Institute of Technology

(Received August 6, 1932)

A relation is derived by quantum-mechanical perturbation theory, using a center of gravity argument and the Kuhn-Reiche sum rule, between the polarizability and diamagnetic susceptibility of monatomic gases. On comparison with a similar paper by Kirkwood, who uses a variational method, a criterion is derived for the validity of a perturbed wave function of the form $\psi_0(1+\lambda v)$, where ψ_0 is the unperturbed wave function of the normal state and v the perturbing potential energy of a uniform electric field. It is also pointed out that inclusion of an electronic interaction term σ neglected by Kirkwood removes a difficulty appearing in his paper.

ACCORDING to dispersion theory,[1] if a uniform electric field vibrating sinusoidally with frequency ν is applied to an N-electron atom in the ground state 0, the polarizability (induced electric moment per unit field) is given by the equation:

$$\alpha = \frac{2e^2}{h} \sum_{n \neq 0} \frac{\nu_{n0} |z_{0n}|^2}{\nu_{n0}^2 - \nu^2}$$

where the direction of the electric field is taken as the z-axis, $z = \sum_{\mu=1}^{N} z_\mu$ (where z_μ refers to the μth electron),

$$\nu_{n0} = (W_n - W_0)/h, \quad z_{0n} = \int \bar{\psi}_0 z \psi_n d\tau,$$

(matrix elements referred to unperturbed wave functions), and the summation is extended over all the excited states n, continous included. For a static field ($\nu = 0$), this becomes:

$$\alpha = 2e^2 \sum_{n \neq 0} \frac{|z_{0n}|^2}{W_n - W_0}. \tag{1}$$

Let us denote this summation by $\sum'$, and abbreviate $W_n - W_0$ to W_{n0}. In order to evaluate this sum, it is necessary to find a suitable center of gravity of the term system W_{n0}. We may define the proper average $\bar{W}_{n0}$ by the equation

$$\bar{W}_{n0} \sum' = \sum_{n \neq 0} |z_{0n}|^2,$$

but by the rule for a matrix product,

$$\sum_{n \neq 0} |z_{0n}|^2 = (z^2)_{00} - |z_{00}|^2.$$

[1] J. H. Van Vleck, *Theory of Electric and Magnetic Susceptibilities*, p. 362, Eq. (31) (Oxford 1932).

Thus

$$\tilde{W}_{n0}\sum{}' = (z^2)_{00} - |z_{00}|^2.$$

We may define another average W_{n0}^* by the equation

$$W_{n0}^* \sum_{n\neq 0} |z_{0n}|^2 = \sum_n W_{n0}|z_{0n}|^2,$$

which by the Kuhn-Reiche sum rule equals $(h^2/8\pi^2 m)N$. Since ez_{00} denotes the electric moment averaged with respect to the wave function of the normal state unperturbed by the electric field, it must vanish, since experimentally no atoms have permanent dipole moments. One can also show[2] this by writing z_{00} as $\int|\psi_0|^2 z d\tau$ and applying the transformation $z_\mu' = -z_\mu$, whereupon $\psi_0(z) = \pm\psi_0(z')$, from which $z_{00} = -z_{00}$ and therefore vanishes. Thus

$$\sum_{n\neq 0}|z_{0n}|^2 = \sum_n |z_{0n}|^2 = (z^2)_{00},$$

so that

$$W_{n0}^* = (h^2/8\pi^2 n)N/(z^2)_{00}.$$

If we now take as an approximation $\tilde{W}_{n0} = W_{n0}^*$, we find:

$$\sum{}' = (8\pi^2 m/h^2)[(z^2)_{00}]^2/N. \tag{2}$$

Now

$$(z^2)_{00} = \sum_i \sum_j (z_i z_j)_{00} = \sum_{i=1}^N (z_i^2)_{00} + \sum_{i\neq j}\sum (z_i z_j)_{00}$$

and

$$(z_i^2)_{00} = (x_i^2)_{00} = (y_i^2)_{00},$$

since these are averages with respect to the unperturbed wave function, in which the z direction is not favored; thus

$$(z_i^2)_{00} = \tfrac{1}{3}(x_i^2 + y_i^2 + z_i^2)_{00} = \tfrac{1}{3}(r_i^2)_{00}.$$

Similarly

$$(z_i z_j)_{00} = \tfrac{1}{3}(\vec{R}_i\cdot\vec{R}_j)_{00},$$

so that

$$(z^2)_{00} = \tfrac{1}{3}\sum_i (r_i^2)_{00} + \tfrac{1}{3}\sum_{i\neq j}\sum (\vec{R}_i\cdot\vec{R}_j)_{00}. \tag{3}$$

Let us denote

$$\sum_{i\neq j}\sum (\vec{R}_i\cdot\vec{R}_j)_{00}$$

by σ, and recall that for a monatomic gas, the molal diamagnetic susceptibility[3] is given by

$$\chi = -\frac{e^2 L}{6mc^2}\sum_{i=1}^N (r_i^2)_{00}, \tag{4}$$

[2] J. H. Van Vleck, reference 1, p. 202.
[3] J. H. Van Vleck, reference 1, p. 206, Eq. (2).

where L is Avogadro's number. Then, using Eqs. (1), (2), (3), and (4),

$$\alpha = \frac{16\pi^2 e^2 m}{9h^2 N}\left(\frac{6mc^2}{e^2 L}|\chi| + \sigma\right)^2. \tag{5}$$

We have here an approximate relation between the polarizability and the diamagnetic susceptibility of a monatomic gas, which can be tested only for the inert gases, since almost all others have strong paramagnetic susceptibilities which greatly outweigh the diamagnetic part. Since electrons repel each other, the average angle between two of the radius vectors R_i and R_j in an atom is expected to be greater than $\pi/2$, thus making σ a negative number. Actual calculation for helium using a wave function due to Hylleraas which gives the energy correct to one part in 3000, gave for σ the value $-0.146\ a_0^2$, so that σ is small compared to $(6mc^2/e^2L)|\chi| = \sum_i (r_i^2)_{00} = +2.34\ a_0^2$ for helium. For neon σ was calculated by means of Slater's theory of complex spectra, using hydrogenic radial functions (with screening) for $1s$, $2s$, $2p$, giving a value of the order $-1.5\ a_0^2$; this is also small compared to $\sum_i (r_i^2)_{00} = 8.31\ a_0^2$ for neon.

We can rewrite (5) in the form:

$$|\chi| = (e^2 a_0^{1/2}/4mc^2)(N\alpha)^{1/2} - (e^2 L/6mc^2)\sigma. \tag{6}$$

We can now test this equation by calculating $|\chi|$ from the observed polarizability, and comparing with the observed $|\chi|$. We get the Table I.

TABLE I. *In this table K is the volume susceptibility reduced to 20°C and 1 atmos. $= K_{20} = (\rho_{20}/M)\chi$, where ρ is the density and M the atomic weight.*

	N	$10^{24}\alpha$ (obs.)	$10^6\lvert K\rvert$ (calc.)	$10^6\lvert K\rvert$ (obs.)
He	2	0.205	0.000088	0.000078
A	10	0.390	0.00031	0.00028

The law (6), with σ placed equal to zero, has been derived by Kirkwood,[4] using a method quite different formally from ours, so that it is of interest to show the equivalence of his assumptions to ours. Letting ψ_0 be the wave function of the normal state and $v = -eF\sum_1^N z_\mu$ the perturbing potential energy due to a uniform electric field of strength F, he writes an approximate wave function for the perturbed atom in the form $\psi_0(1+\lambda v)$, where λ is a parameter which he determines by minimizing the energy $\int \bar{\psi} H \psi d\tau$. Using the fact that v_{00} vanishes, the energy turns out after variation to be W_0 plus a second order term $-(\frac{1}{2})\alpha F^2$, where $\alpha = (8\pi^2 m/h^2)[(z^2)_{00}]^2/N$. He thus gets a formula for the polarizability which checks with ours except for the fact that he arbitrarily neglects [5]σ. If one makes use of the theorem that such a variational method applied to the lowest state of an atom must always give an

[4] J. G. Kirkwood, Phys. Zeits. 33, 57 (1932).

[5] Kirkwood does not take his z-axis parallel to the field, but one can verify that on doing so, his method does lead directly to our Eq. (5). He places $\sigma = 0$ by writing $\Theta_x = \sum_{i=1}^N (x_i^2)_{00}$ instead of $\Theta_x = \sum_i \sum_k (x_j x_k)_{00}$.

energy higher than the true energy, one sees that the calculated $|K|$ should be larger than the true $|K|$ in all cases. Kirkwood finds $|K|$ (calc.) for neon and argon less than $|K|$ (obs.), contrary to expectation; this is to be explained by his neglect of the interaction term σ.

Now the perturbed wave function which leads to the formula (1) for polarizability is that deducible from first-order perturbation theory:

$$\psi = \psi_0 + \sum_{j\neq 0}(v_{j0}/W_{0j})\psi_j. \tag{7}$$

If we make the assumption that

$$\sum_{j\neq 0}(v_{j0}/W_{0j})\psi_j = \lambda_a v\psi_0 \tag{8}$$

(where λ_a is the adjusted value of λ), our wave function checks with Kirkwood's and will thus give the same second order energy and the same polarizability. Eq. (8), however, on multiplication by $\bar{\psi}_0 v$ and integration over the electron coördinates leads (using Kirkwood's $\lambda_a = -(8\pi^2 m/h^2)(v^2)_{00}/(e^2F^2N)$), to

$$\sum_{j\neq 0}\frac{v_{j0}v_{0j}}{W_{0j}} = \lambda_a(v^2)_{00} = -\frac{8\pi^2 m[(v^2)_{00}]^2}{h^2e^2F^2N}.$$

Using $v = -eFz$, this becomes

$$\sum_{j\neq 0}|z_{0j}|^2/W_{j0} = (8\pi^2 m/h^2N)[(z^2)_{00}]^2,$$

or, using the Kuhn-Reiche sum rule,

$$\sum_{j\neq 0}\frac{|z_{0j}|^2}{W_{j0}} = \frac{[(z^2)_{00}]^2}{\sum_j W_{j0}|z_{0j}|^2}. \tag{9}$$

This, however, is just the assumption $\tilde{W}_{n0} = W_{n0}{}^*$ of our method. Thus the assumption (8) that leads to Kirkwood's treatment also leads to our assumption as to averages. Eq. (9) can be written:

$$\frac{\sum_{j\neq 0}|z_{0j}|^2/W_{j0}}{\sum_j|z_{0j}|^2} = \frac{\sum_j|z_{0j}|^2}{\sum_j W_{j0}|z_{0j}|^2}. \tag{10}$$

That is, the average (formed with respect to the squared matrix elements) of the reciprocal of W_{j0} must equal the reciprocal of the average of W_{j0}, in order that $\psi = \psi_0(1+\lambda v)$. The accuracy of fulfilment of this relation thus constitutes a criterion for the accuracy of a perturbed wave function of the form $\psi_0(1+\lambda v)$. Eq. (10) is seen to work well when $|z_{01}|^2 \gg |z_{02}|^2$ etc., with the $|z_{0j}|^2$ falling off rapidly. It is thus expected to work well in the case of the alkali vapors, since the first absorption line is very strong compared to the succeeding ones; unfortunately, however, these vapors are paramagnetic, so

that comparison with experiment is impossible. For the alkaline earth vapors (ground state $^1S_0$), there is no paramagnetism, but also no susceptibility measurements. Since they have no permanent magnetic moment, however, the Zeeman effect would be a measure of the magnetic polarizability. One should thus be able to use the law (6) to predict qualitatively second order Zeeman effect of the normal state from refractive index data or vice versa.

The author takes this opportunity to acknowledge his gratitude to Professors J. C. Slater and P. M. Morse, who have read the manuscript and taken a helpful interest in the paper.

Variation of the Principal Magnetic Susceptibilities of Certain Paramagnetic Crystals with Temperature

By B. W. BARTLETT
Bowdoin College and Columbia University

(Received July 19, 1932)

Curie and Weiss Constants for the Principal Susceptibilities of Certain Crystals. The Curie and Weiss constants, respectively C_m and Δ of the equation $\chi_m = C_m/(T+\Delta)$, over the temperature range 60° to −45°C have been determined for 5 crystals of the isomorphic monoclinic double sulphate series [M $R_2(SO_4)_2$ $6H_2O$] containing cobalt, nickel, or copper, and for cobalt sulphate heptahydrate. The measurements were made by Rabi's method of determining the principal magnetic susceptibilities of crystals, which was found applicable over this temperature range. The use of ethyl alcohol as a solvent for the auxiliary paramagnetic salt permitted the extension of the method to temperatures below the freezing point of water solutions, such as those used by Rabi, for crystals of volume susceptibilities less than 35×10^{-6}. The lower limit of the applicability of the method depends only on the availability of low freezing point solutions of sufficient susceptibility. In general the Curie constants for the principal susceptibilities of any given crystal were very nearly the same. The Weiss constant showed considerable variation, both between the different principal magnetic axes of the same crystal, and from one crystal to another. Both the Curie and Weiss constants decreased progressively as the metal ion was changed from cobalt to nickel to copper. The effect of change in the alkali ion from NH_4 to potassium was less pronounced, although there was a slight tendency for the Curie constant to increase and for the Weiss constant to become more positive. The accuracy claimed for the measurements is 1 percent. In general there was a small continuous change in the orientation of the principal magnetic axes in the plane of symmetry of the crystal with respect to the crystallographic axes as the temperature was varied.

INTRODUCTION

A NUMBER of investigators have made measurements by various methods of the principal magnetic susceptibilities of crystals. An interesting set of crystals is the isomorphic monoclinic double sulphate hexahydrate series, upon which very complete crystallographic and optical data have been obtained by Tutton.[1] The principal susceptibilities of several members of this series have been measured by Fincke[2] and by Jackson.[3] There is considerable disagreement between the results of these two investigators for the same members of the series. Using a quite different method, Rabi[4] has determined the principal susceptibilities of a large number of crystals of this series. His method has two intrinsic advantages over those of the other investigators;

[1] A. E. H. Tutton, Proc. Roy. Soc. London **A88**, 361 (1913); Phil. Trans. Roy. Soc. **A216**, 1 (1916).

[2] W. Fincke, Ann. d. Physik [4] **31**, 149 (1910).

[3] L. C. Jackson and H. Kamerhigh Onnes, Phil. Trans. Roy. Soc. **A224**, 1 (1923); Proc. Roy. Soc. **A104**, 671 (1923); L. C. Jackson, Phil. Trans. Roy. Soc. **A226**, 107 (1927).

[4] I. I. Rabi, Phys. Rev. [2] **29**, 174 (1927).

it requires no accurate knowledge of the fields and field gradients involved, and it permits a direct measurement of the orientation of the principal axes of susceptibility with respect to the crystallographic axes.

The present paper is concerned primarily with the effects of temperature upon the principal susceptibilities. It also serves, however, as a further check on the values already obtained at room temperatures. A comparison of existing results with those obtained during this research will be given later.

Jackson[3] has made measurements on two crystals of the double sulphate series over a considerable range of temperatures. Due to the disagreement between his values and those of Fincke and Rabi at room temperatures it was considered desirable to repeat these measurements over as wide a range as possible by Rabi's method, in addition to measurements on members of this series not previously investigated over a range of temperatures. The need for accurate data of this kind has been enhanced by recent advances in the quantum theory of susceptibilities.[5,6]

METHOD

In Rabi's method[4] of measuring the principal susceptibilities of crystals the crystal is suspended from a torsion head by a glass fibre so as to lie in the inhomogeneous part of the field of a Weiss magnet, in the position shown in Fig. 1. In this position it rests in a solution, the susceptibility of which may be varied at will by the addition of a strongly paramagnetic salt. In general the direction of the field and that of the resulting intensity of magnetization in the crystal will not coincide. In this case displacement of the crystal will result, no matter what the susceptibility of the solution, when the field is applied. If, however, the crystal is so oriented that either its axis of maximum or minimum susceptibility in the XY plane is parallel to the field, the directions of field and resulting intensity in the plane coincide. In this case if the susceptibility of the solution is the same as that of the crystal in the direction of the field, the resultant force on the crystal is zero and it suffers no displacement. For mathematical demonstration of this statement and those which follow the reader is referred to Rabi's paper. It should be noted that the foregoing statement applies to the axes of maximum and minimum susceptibility in the XY plane, these being 90° apart.

In the special case where the direction of one of the principal axes of susceptibility is known, the crystal may be suspended parallel to this direction, and then the other two principal axes will automatically lie in the XY plane. This is the case with monoclinic crystals, in which one principal axis coincides with the symmetry axis of the crystal. In this case the three principal susceptibilities and the orientation of the axes may be determined very simply and directly. The crystal is suspended parallel to its symmetry axis, the torsion head turned and the susceptibility of the solution varied until no displacement of the crystal occurs when the field is applied. The value of one of the

[5] J. H. Van Vleck, *Theory of Electric and Magnetic Susceptibilities*, Oxford University Press, New York, 1932.

[6] O. M. Jordahl, W. G. Penney, and R. Schlapp, Phys. Rev. [2] **40**, 637 (1932).

principal susceptibilities in the plane of symmetry is then directly equal to that of the solution, which may be measured very simply by the well-known Gouy method.[7] The crystal is then rotated through 90° and the susceptibility of the solution again varied until no displacement takes place, determining the other principal susceptibility in the symmetry plane. The crystal is next suspended perpendicular to the symmetry axis, rotated until this axis is parallel to the field, and the susceptibility of the solution is then varied as before until there is no displacement. The susceptibility of the solution is then equal to that of the third principal axis. In practise, displacement of the crystal along the X and Y axes of the magnet (Fig. 1) is observed independently. Motion along the Y axis is governed by the susceptibility of the solution, and along the X axis largely by the angular orientation of the crystal about the axis of suspension. The procedure is therefore simply to turn the

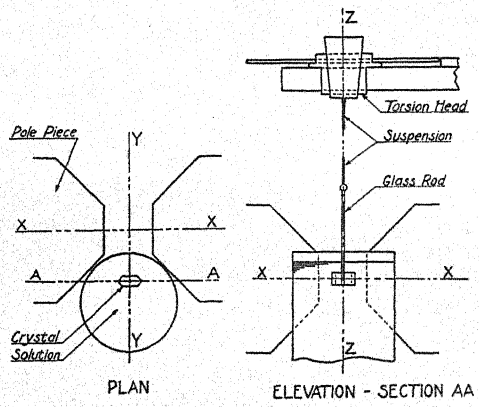


Fig. 1. Method of suspension of crystal.

crystal until there is no motion along the X axis when the field is applied, and then to vary the susceptibility of the solution until displacement in the Y direction is eliminated.

The angle which the maximum axis of principal susceptibility in the plane of symmetry of the crystal makes with one of the crystallographic axes, say the c axis, may be obtained directly as follows. The orientation of the c axis of the crystal is first determined with respect to the X axis of the magnet by reflecting a beam of light back on itself from a known face of the crystal along the Y axis of the magnet. The angle through which the crystal must be turned to obtain a balance with the solution with either its maximum or minimum principal axis parallel to X is then read from the torsion head. Since the angle which the c axis makes with X is determined from this reading and its previous orientation, the angle between the c axis and the principal axis is also given. It is assumed throughout that the glass fibre is stiff enough not to allow the crystal to twist with respect to the torsion head.

The sensitivity of the measurement of the orientation of the principal axes is high. Displacement of the crystal in the X direction for any given field

[7] E. C. Stoner, *Stoner, Magnetism and Atomic Structure*, E. P. Dutton, New York, p. 40 (1916).

strength is a function of the difference between maximum and minimum susceptibility in the XY plane. It is greater when the axis of minimum principal susceptibility is being balanced, and in the case of crystals for which the difference in principal susceptibilities is 10 percent or more it is considerable even if the crystal is away from balance by only one degree. Observation is simplified by the fact that the displacement along the X axis changes direction as the crystal is rotated from one side of the equilibrium position to the other.

This method of determining principal susceptibilities is independent of the shape of the crystal, provided it is not too large. It does not, therefore, require the grinding of crystal sections of definite shape and orientation with respect to the crystallographic axes. This discussion has been limited to the application of the method to monoclinic crystals. It is, however, perfectly general, although in the most general case a greater number of observations and somewhat more complicated calculations are required.

Experimental Procedure

The experimental procedure followed in this research was essentially the same as that described in Rabi's paper. Certain minor modifications were made necessary to permit measurements to be made satisfactorily over the temperature range. Two magnets were used, one for the comparison of the crystals with the solution, and one for the determination of the susceptibilities of the solutions by the Gouy method. While this arrangement facilitates the measurements under any conditions, it is essential with hot and cold solutions that the two measurements be made as nearly simultaneously as possible to prevent change in the solution, either by evaporation, condensation, or precipitation.

The crystals were suspended from a torsion head graduated in degrees by glass suspensions about 30 cm long and 5 mils in diameter. It was found that Rabi's method of attaching the crystals to the suspension with molten shellac was impracticable at the higher temperatures, as the shellac softened and the crystals dropped off. The same thing occurred at all temperatures when alcohol was used as a solvent, as might be expected. After considerable experimentation with other adhesives, it was finally found necessary to drill a properly oriented hole through each crystal, and suspend it upon a slightly tapered glass rod inserted through the hole and attached in turn to the suspension. The diameter of the hole thus drilled was in general less than 10 mils and the rods used had a maximum diameter of about this value. The holes were drilled by hand with a jeweler's drill, and after a little practise it was found easily possible to orient them within one or two degrees of the desired direction.

Motion of the crystals was observed by means of two microscopes focussed on the rods just as they came out of the solution. Both microscopes had scales in their eyepieces, and in particular that used for observing motion in the Y direction had sufficient magnification to detect displacement of 0.002 cm, which was less than the random motion of the crystals due to convection

currents in the solution. The solution was contained in a Dewar flask inserted in the angle of the pole pieces so as to permit the crystal to be suspended in a reasonably strong gradient. Temperatures were measured to half a degree by means of a standard thermometer graduated in tenths. This was sufficiently accurate for the balance of crystal and solution, the critical temperature measurement being that made when the solution was being measured by the Gouy method.

To ensure constancy of temperature during the measurement of the susceptibility of the solution the magnet used for this purpose had a jacketed brass tube inserted between its pole pieces. The jacket was connected to a coil run through a three gallon bath, and constant temperature was maintained by pumping water or alcohol through the system. For temperatures above the room the bath was water heated by an immersion heater, and for low temperatures it was alcohol or alcohol and water cooled with solid carbon

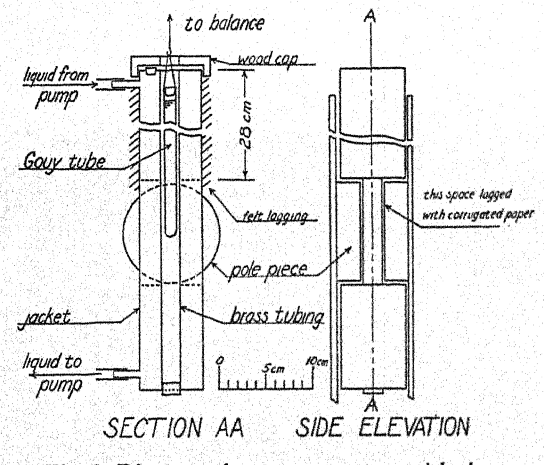


Fig. 2. Diagram of temperature control jacket.

dioxide. Fig. 2 shows diagrammatically the arrangement of the jacket. The whole investigation was carried on in a double walled constant temperature room to ensure constancy of temperature of the magnet throughout.

The Gouy tubes used were of Pyrex glass, approximately 30 cm long and 1 cm in diameter. They were suspended from a chainomatic balance, sensitivity 0.05 mg, located well out of the field, which had no detectable influence upon the balance or suspension. The Gouy tubes were calibrated with distilled water, -0.720×10^{-6} being taken as standard for the susceptibility of water.[8]

Temperatures of the solutions were measured by the insertion of a thermocouple into the tube containing the solution at the time of measurement. Constancy of temperature during the measurement was checked by means of another couple inserted through the walls of the jacket into the inside of the brass tube in which the Gouy tube was suspended. As there was a slight

[8] Int. Crit. Tables, Vol. VI, p. 356.

gradient in the Gouy tube, care was taken to measure the temperature at the point where the field gradient was a maximum.

For measurements at room temperatures and above water solutions were used, saturated with respect to the material of the crystal. Susceptibilities were varied by the use of manganous chloride, the amount of this salt in the solution being varied as necessary to balance the crystal. The maximum temperatures at which measurements could be made by this method were limited in general by the disturbance of the solution due to convection currents, although in the case of cobalt sulphate heptahydrate change in the chemical state set the limit. Obviously the lower limit to the method is the freezing point of the solution. In general with water solutions freezing started, or at least the solution became too thick for precise observations, in the neighborhood of $-25°$C. Accordingly search was made for satisfactory solvents of lower freezing point. Experimentation with alcohols, acetone, and other organic liquids of low freezing point resulted in the choice of ethyl alcohol as solvent and anhydrous manganous chloride as solute. This combination gave the largest volume susceptibility of those tried, about 35×10^{-6}, a value sufficiently high for all the crystals except those containing cobalt. For the latter the lower limit was therefore the freezing point of the water solutions. The use of the alcohol solution extended the range to $-45°$C for the copper and nickel crystals. Below $-50°$C the alcohol solutions became so viscous as to prevent further measurements.[9]

Crystals

The crystals measured were Co $(NH_4)_2(SO_4)_26H_2O$, Co $K_2(SO_4)_26H_2O$, Co SO_4 $7H_2O$, Ni $(NH_4)_2(SO_4)_26H_2O$, Cu $(NH_4)_2(SO_4)_26H_2O$, Cu $K_2(SO_4)_2$ $6H_2O$. Of these the hexahydrates are of the isomorphous monoclinic series so thoroughly investigated crystallographically by Tutton.[1] The two containing cobalt have been investigated magnetically by Jackson[3] over a considerable range of temperatures. Cobalt sulphate heptahydrate is also monoclinic, and has been investigated crystallographically by Marignac,[10] and magnetically by Fincke[2] at room temperatures. The mean susceptibilities of all these salts, in powdered form, except those containing copper have been measured over a wide range of temperatures by Jackson.[3]

Some of the crystals were grown by slow cooling and some by evaporation. Only materials of tested purity were used, and all the crystals selected for measurement had been recrystallized at least twice for further purification. Further check on the purity of the specimens was provided by using at least 6 different crystals for each set of measurements and rejecting any which varied by more than two percent from the mean value. It was found that

[9] Work is in progress at Columbia University on the susceptibilities of these and other crystals at liquid air temperatures. Paramagnetic and diamagnetic liquids offer no difficulties at these temperatures, since liquid oxygen is paramagnetic and liquid nitrogen is diamagnetic, and they are miscible in all proportions. For measurements at intermediate temperatures special liquids would have to be found.

[10] C. de Marignac, Mem. Soc. Phys. Genève **14**, 245 (1858); C. F. Rammelsberg, Hdb. d. Kr-Phys. Chem. **1**, 419 (1881).

great care was required in selecting crystals without flaws or cloudiness if consistent results were to be obtained. In this connection it is suggested that some of the disagreement in published results may have come from the use of imperfect crystals. The writer found that some crystals which were perfect in outward appearance gave out small amounts of saturated liquid when pierced by the drill, indicating imperfect crystallization within the core of the crystal. In general the crystals used were about 0.5 cm on an edge.

It was found necessary to wash the crystals very carefully after each measurement to prevent any manganous chloride drying out of the solution onto the crystal. If this was not done errors of five percent or more were introduced into the results. As a check on the care with which this was done each set of crystals was measured again at room temperature at the completion of the temperature run.

In addition to the measurements on the individual crystals a check on the general consistency of the results was obtained by making a run on powdered crystals by the Gouy method. The accuracy of such measurements was limited by the uniformity with which the powders could be packed into the tube. Also the measurement of temperature was not so accurate as with the solutions, as the temperature of the powder could not be read directly, but had to be determined from dummy tubes held at the same jacket temperatures for the same lengths of time. These measurements however serve as a check against any gross errors in the individual measurements.

Accuracy

The absolute accuracy of the method of the present investigation is definitely limited by the accuracy of the standard value for the susceptibility of water, which is probably about 0.5 percent. In the present work the sensitivity of the null balance of crystal against solution was of the order of 0.1 percent except in the case of the crystals containing copper, for which it was about $\frac{1}{4}$ percent. The sensitivity of the gravitational balance was 0.1 percent or better. The measurement of temperature had a precision of 0.2°, and allowing for temperature gradient in the tube was probably accurate to better than 0.5°. The couples used were calibrated against standard thermometers and against the freezing point of mercury. The field of the Gouy method magnet was checked for constancy by a meter with a precision of 0.1 percent. The magnet itself was in a constant temperature room, and its temperature did not vary by more than one or two degrees throughout the investigation. Heating of the magnet by the current used was highly improbable, as the currents were well below the capacity of the magnet, and were on only for comparatively short time intervals. Further check on this fact is afforded by the fact that the currents were remarkably constant, indicating no heating of the coils.

The insertion of the glass rod through the crystal introduces a systematic error approximately equal to the ratio of the volume of the rod in the solution to the volume of the crystal. From the geometrical dimensions involved this error was in all cases well under 0.5 percent.

Probably the most serious source of error, aside from impurities and irregularities in the crystals themselves, was that which might arise from change in the solution between the balancing of the crystal and the measurement of the susceptibility of the solution. To get the solution from the Dewar flask into the Gouy tube in general required from one to two minutes. To prevent precipitation from the solution the temperature of the bath and the

TABLE I. *Principal susceptibilities.* Axes 1 and 2 refer respectively to the maximum and minimum principal susceptibilities in the plane of symmetry of the crystal, axis 3 to the principal susceptibility perpendicular to this plane. Temperatures are given in degrees centigrade. K is the volume susceptibility, x the mass susceptibility, and x_m' the molecular susceptibility corrected for diamagnetism.

Crystal	T	$K\times10^6$ 1	2	3	$x\times10^6$ 1	2	3	$x_m'\times10^6$ 1	2	3
$Co(NH_4)_2(SO_4)_2$-$6H_2O$	55.0	50.4	38.1	44.8	26.5	20.0	23.6	10660	8080	9500
	20.0	58.3	41.5	50.5	30.7	21.8	26.6	12300	8790	10690
	3.0			53.5			28.2			11320
	−3.5	64.1	44.4		33.7	23.4		13480	9430	
	−11.0			56.4			29.7			11900
	−20.0	69.3	46.8	58.9	36.4	24.6	31.0	14570	9900	12440
$CoK_2(SO_4)_26H_2O$	55.0	52.2	41.1	44.0	23.5	18.6	19.8	10460	8330	8840
	20.0	58.6	44.9	48.6	26.4	20.2	21.9	11720	9010	9750
	0.0	63.5	47.7		28.6	21.5		12690	9580	
	−5.0			51.7			23.3			10360
	−20.0	67.8	50.2	54.6	30.5	22.6	24.6	13500	10060	10930
$CoSO_47H_2O$	45.0			59.5			30.5			8700
	40.0	67.3	55.9		34.5	28.6		9830	8170	
	21.0	71.8	59.4	63.9	36.8	30.4	32.8	10470	8680	9350
	0.0	76.4	63.0	67.9	39.2	32.3	34.8	11150	9210	9910
	−15.0			71.6			36.7			10440
	−20.0	81.7	67.2		41.9	34.5		11920	9830	
$Ni(NH_4)_2(SO_4)_2$-$6H_2O$	51.0	18.75	18.23	18.47	9.74	9.47	9.59	4030	3920	3970
	21.0	20.62	20.12	20.02	10.72	10.48	10.40	4420	4320	4290
	−15.0	23.11	22.57	22.46	12.03	11.75	11.66	4930	4820	4790
	−42.0	25.65	25.20	25.28	13.37	13.10	13.15	5460	5350	5370
$Cu(NH_4)_2(SO_4)_2$-$6H_2O$	53.0	6.35	5.17	6.13	3.30	2.69	3.18	1500	1257	1452
	19.0	7.27	5.81	7.02	3.78	3.02	3.65	1692	1388	1640
	−5.0	7.97		7.65	4.14		3.97	1837		1768
	−9.0		6.49			3.37			1528	
	−45.0	9.55	7.53	9.26	4.96	3.91	4.81	2163	1743	2103
$CuK_2(SO_4)_26H_2O$	55.0	6.62	5.24	6.26	2.96	2.34	2.80	1490	1215	1420
	22.0	7.47	5.90	7.10	3.34	2.64	3.18	1658	1349	1587
	−15.0	8.51	6.78		3.81	3.04		1865	1523	
	−45.0	9.71	7.72	9.16	4.35	3.46	4.10	2105	1710	1998

Note: It may be wise to emphasize here that the actual experimental results obtained by the method of this paper are the volume susceptibilities.

solution had to be very closely the same. By working rapidly results could be checked to about $\frac{1}{4}$ percent at any temperature, although the precision of the check was better the closer the temperature of the solution was to that of the room. While in the Gouy tube the solutions were enclosed with a stopper to prevent evaporation or condensation. In calibrating the Gouy tubes correction for the susceptibility of air was necessary. From the foregoing, the

agreement of the writer with the results of Rabi, and the general consistency of the results, it appears reasonable that the values of susceptibility given in this paper are accurate to 1 percent, and that their relative accuracy is somewhat greater, probably of the order of 0.5 percent.

The measurements of the angle between the maximum axis of principal susceptibility and the crystallographic c axis are probably accurate to $1°_4$ and consistent to $\frac{1}{2}°$, except in the case of the nickel crystal, for which the sensitivity of angle measurement was very low with the fields available, about 2°.

RESULTS

Table I gives the results of the measurements of the principal susceptibilities of the various crystals, including volume susceptibilities, mass susceptibilities, and molecular susceptibilities corrected for diamagnetism. Each value is the average of several individual crystals, in most cases six. The average deviation in no case exceeded 1 percent, and in all except a very few cases was less than $\frac{1}{2}$ percent. Table II gives the angle, θ, which the maximum axis of principal susceptibility in the symmetry plane makes with the c crystallographic axis. Fig. 3 shows the symmetry plane of the double sulphates, and Fig. 4 that of cobalt sulphate heptahydrate. Table III gives the Curie and Weiss constants for the crystals. Figs. 5, 6, and 7 show curves of the reciprocal of the molecular susceptibilities corrected for diamagnetism plotted against absolute temperature.

TABLE II. *Orientation of principal susceptibilities.* The numbers in this table are the values in degrees of the angle, θ, which the maximum axis of principal susceptibility in the plane of symmetry makes with the c crystallographic axis. θ is measured positive in the direction of the acute angle between the c and a crystallographic axes.

Crystal	Temperature in degrees centigrade									
	55	50	45	40	30	20	0	−10	−20	−45
$Co(NH_4)_2(SO_4)_26H_2O$	$-43\frac{1}{2}$					$-43\frac{1}{2}$			$-43\frac{1}{2}$	
$CoK_2(SO_4)_26H_2O$	−14					−13	$-12\frac{1}{2}$		$-11\frac{1}{2}$	
$CoSO_47H_2O$			*$-56\frac{1}{2}$			$-55\frac{1}{2}$	$-54\frac{1}{2}$		$-53\frac{1}{2}$	
$Ni(NH_4)_2(SO_4)_26H_2O$		−13				−17			−21	−23
$Cu(NH_4)_2(SO_4)_26H_2O$		−87	−84	−83	−81	−79		−76		$-72\frac{1}{2}$
$CuK_2(SO_4)_26H_2O$	$-101\frac{3}{4}$					$-102\frac{1}{2}$			−104	−105

* Above this point a large and variable change in angle indicated a change in the state of the crystal. This change was accompanied by a corresponding change in susceptibilities, and a distinct change in the appearance of the crystal, probably due to dehydration.

TABLE III. *Curie and Weiss constants.* In the following table the Δ's and the C_m's are those of the Weiss formula $x_m' = C_m/(T+\Delta)$, in which x_m' is the molecular susceptibility corrected for diamagnetism and T is the temperature in degrees Kelvin.

Crystal	Δ_1	Δ_2	Δ_3	C_{m1}	C_{m2}	C_{m3}
$Co(NH_4)_2(SO_4)_26H_2O$	−50	81	−10	2.9	3.3	3.0
$CoK_2(SO_4)_26H_2O$	5	88	67	3.5	3.5	3.4
$CoSO_47H_2O$	23	44	45	3.3	2.9	3.2
$Ni(NH_4)_2(SO_4)_26H_2O$	30	25	25	1.42	1.36	1.36
$Cu(NH_4)_2(SO_4)_26H_2O$	−9	24	−2	0.475	0.44	0.47
$CuK_2(SO_4)_26H_2O$	14	20	18	0.51	0.425	0.49

Correction for diamagnetism included that for water of crystallization, the alkali molecule, and the sulphate ion of the metal molecule, and totalled 180×10^{-6} for the double sulphates and 100×10^{-6} for cobalt sulphate hepta-

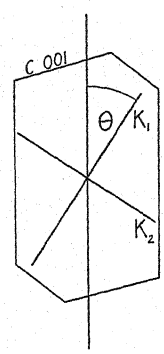


Fig. 3. Plane of symmetry of double sulphate crystals.

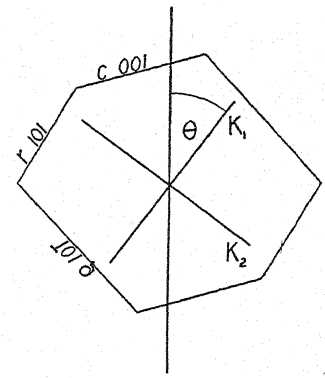


Fig. 4. Plane of symmetry of cobalt sulphate heptahydrate.

hydrate. The values used were those given in the International Critical Tables, vol. IV, page 365. In the case of crystals containing cobalt and nickel the diamagnetic correction is small compared with the total susceptibilities. In

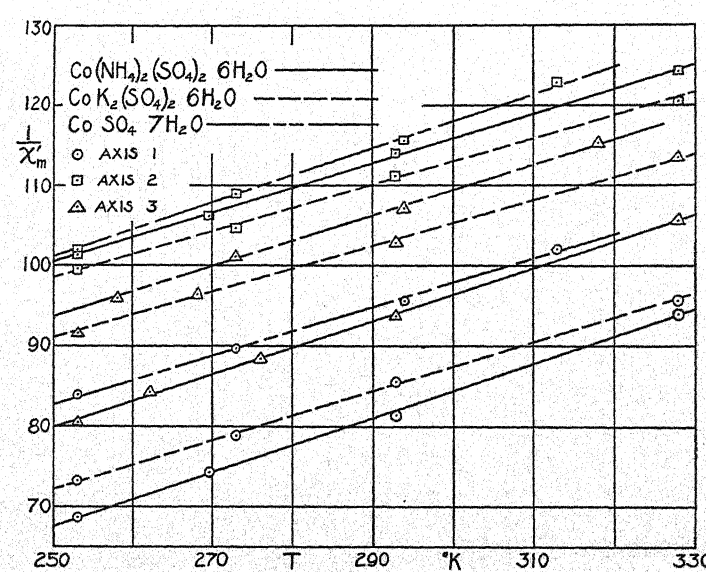


Fig. 5. Curves of $1/x_m'$ against temperature for crystals containing cobalt.

the case of the copper crystals, however, it becomes considerable, 15 percent in the extreme. This undoubtedly introduces some uncertainty into the values of the Curie and Weiss constants for these crystals, as the accuracy of the diamagnetic correction may be held in question. There is no certainty

that the linking of the components in the complex molecule does not alter the commonly accepted values of the ionic susceptibilities, and there is further no inherent reason that the diamagnetic correction is the same along

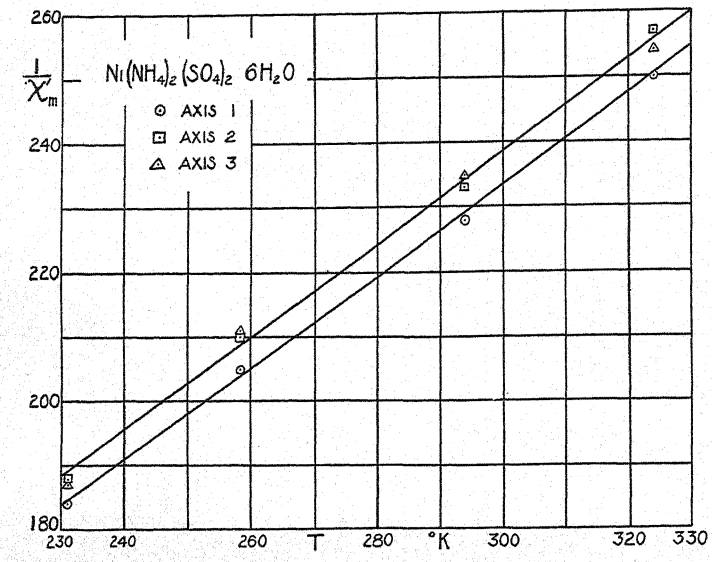


Fig. 6. Curves of $1/x_m'$ against temperature for nickel ammonium sulphate.

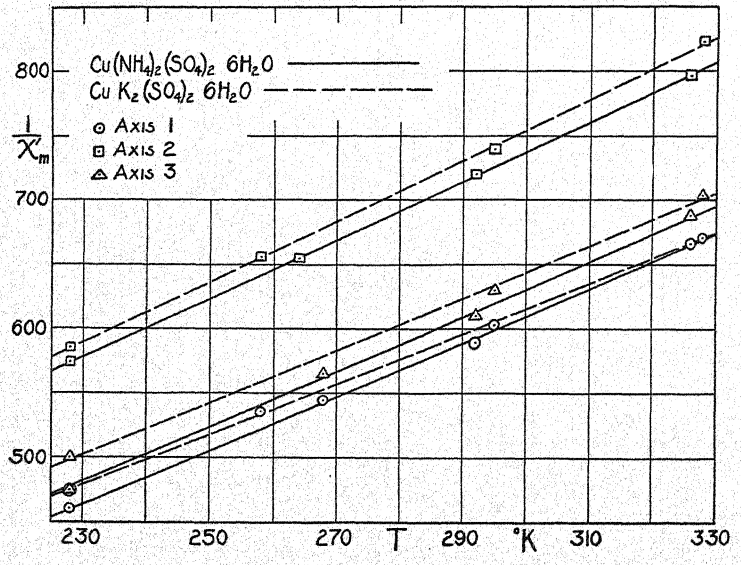


Fig. 7. Curves of $1/x_m'$ against temperature for crystals containing copper.

each axis, as has been assumed in making the correction for want of data on the subject.

The results of Table I have not been corrected for the volume expansion of the crystals with temperature. This will introduce some error into the

mass and molecular susceptibilities given in the table. Values for the coefficient of volume expansion of these crystals are not available, at least to the knowledge of the writer. Coefficients of volume expansion for crystals such as $MgSO_47H_2O$ and $CuSO_45H_2O$ as given in the International Critical Tables, vol. III, page 44, are, however, all less than 10^{-4} per °C. In the extreme case this would entail a correction of about 1 percent in the mass susceptibilities. The effect of this correction would be to increase the Curie constants slightly, and to make the Weiss constants all slightly more positive. Table IIIA gives values of these constants corrected for an assumed coefficient of volume expansion of 10^{-4} per °C. Additional evidence that this correction is small is furnished by the measurements on the powdered crystals. In this case mass susceptibilities are measured directly, so that if the effect is appreciable it should show up when the mass susceptibilities of the powders are compared

TABLE IIIA. *Curie and Weiss constants corrected for volume expansion.* The values in this table are the Curie and Weiss constants obtained after the mass susceptibilities were corrected for volume expansion, the coefficient of volume expansion being assumed as 10^{-4} per degree centigrade for all the crystals.

Crystal	Δ	Δ_2	Δ_3	C_{m1}	C_{m2}	C_{m3}
$Co(NH_4)_2(SO_4)_26H_2O$	−44	93	0	3.05	3.4	3.1
$CoK_2(SO_4)_26H_2O$	15	100	78	3.6	3.6	3.5
$CoSO_47H_2O$	31	55	56	3.4	3.0	3.3
$Ni(NH_4)_2(SO_4)_26H_2O$	40	35	35	1.47	1.40	1.40
$Cu(NH_4)_2(SO_4)_26H_2O$	−1	33	6	0.49	0.465	0.485
$CuK_2(SO_4)_26H_2O$	23	30	27	0.525	0.435	0.505

TABLE IV. *Susceptibilities of powdered crystals.* In this table x is the mass susceptibility, and x_m' the molecular susceptibility corrected for diamagnetism. C_m and Δ are the Curie and Weiss constants, respectively. Temperatures are in degrees centigrade.

Crystal Powder	T	$x\times10^6$	$x_m'\times10^6$
$Co(NH_4)_2(SO_4)_26H_2O$	56	23.2	9340
$C_m=3.2$	22	25.9	10400
$\Delta=14$	−7	28.8	11560
$CoK_2(SO_4)_26H_2O$	55	21.3	9490
$C_m=3.45$	19	23.8	10580
$\Delta=37$	−38	28.5	12600
$CoSO_47H_2O$	45	30.7	9030
$C_m=3.4$	19	34.3	9780
$\Delta=60$	−20	38.3	10880
$Ni(NH_4)_2(SO_4)_26H_2O$	52	9.60	3960
$C_m=1.38$	20	10.55	4350
$\Delta=27$	−40	13.08	5340
$Cu(NH_4)_2(SO_4)_26H_2O$	56	3.00	1380
$C_m=0.47$	20	3.42	1550
$\Delta=15$	−39	4.25	1890
$CuK_2(SO_4)_26H_2O$	56	2.68	1363
$C_m=0.46$	20	3.06	1538
$\Delta=13$	−40	3.86	1888

with the average mass susceptibilities of the crystals. In general there is no appreciable consistent difference of the sort which might be expected if the correction for volume expansion were of importance.

In Table IV are given the results of the measurements on the powdered crystals. These were not originally intended as precision measurements, and as has already been pointed out under the heading *Crystals*, they are probably somewhat less accurate than the results of Table I. The agreement between the powder measurements and the averages for the crystals is in general so good, however, as to warrant their inclusion as a check on the latter.

Discussion

Comparison of the results obtained at room temperatures by Fincke, Jackson, Rabi, and the writer is given in Table V. The agreement between the two latter is in general within the experimental error, except for the crystals containing copper, where there is a consistent difference of from 2 to 4

Table V. *Comparison of results.* This table contains a comparison of the results of different investigators at room temperatures reduced to the common temperature 27°C. The K's are the principal volume susceptibilities, and θ is the angle between K_1 and the c crystallographic axis.

Investigator	$K_1\times10^6$	$K_2\times10^6$	$K_3\times10^6$	θ
		$Co(NH_4)_2(SO_4)_26H_2O$		
Bartlett	56.8	40.6	49.3	−43
Fincke*	55.9	43.6	45.5	−27
Jackson	48.0	40.4	46.9	−31
Rabi	56.2	40.7	48.9	−44**
		$CoK_2(SO_4)_26H_2O$		
Bartlett	57.3	43.9	47.6	−13
Fincke*	66.6	49.6	77.2	−21
Jackson	61.1	49.6	53.6	−20
Rabi	57.6	44.6	48.6	−13**
		$CoSO_47H_2O$		
Bartlet	70.4	58.2	62.6	−55
Fincke*	70.9	64.0	68.5	−40
		$Ni(NH_4)_2(SO_4)_26H_2O$		
Bartlett	20.2	19.7	19.7	−17
Fincke*	19.6	15.8	18.0	−16
Rabi	20.2	19.9	20.0	−17**
		$Cu(NH_4)_2(SO_4)_26H_2O$		
Bartlett	7.08	5.65	6.83	−79
Rabi	6.80	5.40	6.62	−74
		$CuK_2(SO_4)_26H_2O$		
Bartlett	7.14	5.80	6.98	−102
Rabi	7.52	5.62	6.83	−99

* Fincke does not state the temperature at which his measurements were made.

** There is a misprint in the published values of θ in Rabi's paper. The values given for cobalt ammonium and cobalt potassium sulphate should be interchanged, as should those for nickel ammonium and nickel potassium.

percent. This difference may be partially explained by an indeterminate temperature correction, as Rabi's measurements were not primarily concerned with temperature, which accordingly was not determined with care. There remains a discrepancy in the value of K_1 for copper potassium sulphate which is not consistent with the other differences. Comparing the values of the copper group with those of the nickel and cobalt groups in Rabi's paper, it appears that the value given in this paper is more consistent than that given by Rabi. In general Fincke's and Jackson's results do not agree nearly so closely, either with each other or with Rabi.

Comparison of the Curie and Weiss constants found for the cobalt double sulphates by Jackson and by the writer shows qualitative agreement for the Weiss constants, and reasonably good quantitative agreement for the Curie constants, considering the accuracy of the determinations. For the Curie constants this is of the order of 3 percent, and for the Weiss constants not better than 5°. Jackson's value for the maximum principal susceptibility of cobalt ammonium sulphate is inconsistent with the relative values bound by the other three investigators of this salt. Agreement between the average values of the constants in this paper and those found by Jackson for the cobalt and nickel double sulphates in powdered form is qualitatively good. In the case of the curves in this paper for nickel ammonium sulphate, the writer has drawn them as straight lines. An equally good case might be made for drawing them with a slight downward curvature at the lower end. Further data at still lower temperatures are needed to indicate which is nearer the truth.

The effect of changing the alkali ion from ammonium to potassium seems to be to increase slightly the Curie constants, and to make the Weiss constants more positive. There appear to be definite, though small, differences in the Curie constants for different axes of the same crystal in some cases. A recent note by Jordahl, Penney, and Schlapp[6] states that this may be expected from theoretical considerations.

Thus far most of the work done on this problem has been done over a comparatively small range of temperatures near room temperature, or at very low temperatures. The first type is open to the objection that the range of temperature is scarcely sufficient to give high accuracy to the determination of the constants, while the second has the difficulty that at low temperatures the variation from the Weiss law makes computation of the constants somewhat uncertain. Thus in certain of Jackson's work no values of susceptibilities are available between room temperature and about 75°K, at which point deviation from the Weiss law is already taking place. A complete run upon a typical crystal like cobalt ammonium sulphate from room temperature or above down to the lowest temperatures obtainable, with points at frequent temperature intervals, seems needed as an adequate test of theory.

Any theoretical discussion of the magnetic behavior of these crystals must recognize that in the case of the copper group the diamagnetic correction is particularly important, a small uncertainty having a considerable effect on the constants. It is quite probable from results on diamagnetic crystals[4,11]

[11] W. Voigt and S. Kinoshita, Ann. d. Physik [4] 24, 492 (1907).

that this correction should be different in different directions. At present it is practically impossible to obtain from susceptibility measurements an accurate knowledge of what the paramagnetic susceptibilities of this group really are. The thermal expansion is in all likelihood different along different axes, and consequently the force field acting on the paramagnetic ion will be changed in both magnitude and direction. That this may be the case is shown by the particular example of copper ammonium sulphate, where the ellipsoid of induction is rotated almost 15 degrees with respect to the crystallographic axes over a temperature range of 95 degrees. This type of datum may serve to give insight into the nature of these force fields and their dependence on temperature. An investigation of triclinic crystals, where there are no necessary fixed relations between crystal axes and ellipsoid of induction, might yield results of interest.

In conclusion the writer wishes to express his appreciation of the interest and advice of Professor I. I. Rabi, who suggested this problem to him, and his thanks to Professor N. C. Little for placing at his disposal the magnet used for measuring the susceptibilities of the solutions.

Supersonic Dispersion and Absorption in CO_2

By W. H. PIELEMEIER
Pennsylvania State College

(Received August 8, 1932)

Since supersonic velocity determinations in air near a crystal oscillator usually yield values in excess of the accepted value, $V_0 = 331.6$ m/sec., a similar effect with CO_2 was suspected. The velocity and the absorption coefficient were measured at frequencies beginning in the dispersion region, theoretically and experimentally investigated by Kneser, and extending beyond it to 2.09 megacycles. The author's velocity values are slightly less than Kneser's experimental values but they fit his theoretically determined dispersion curve equally well. At the lowest frequency tested (303 kilocycles) the absorption coefficient was found to exceed, by the greatest amount, its value computed from Lebedew's formula. This frequency is near the middle of the dispersion region where maximum absorption is expected. According to Pierce the absorption becomes excessive also when this frequency is approached from lower values. The results are presented in tabular and in graphical form. A sharp absorption maximum appears at 217 k.c.

IF THE satellite spacing is used to compute the velocity of high-frequency sound in air as outlined in a previous article[1] the value $V_0 = 331.6$ m/sec. is obtained. If, however, the major peak spacing for short resonance columns is used the value of V_0 is usually about 0.5 percent higher than this, the excess being due, apparently, to the much greater intensity. A similar effect was suspected in the case of CO_2. It was, therefore, considered desirable to check the velocity measurements of H. O. Kneser[2] and to extend the region which he investigated, if possible. It was also considered desirable to search the dispersion region determined theoretically[3] and experimentally by Kneser for excessive absorption.

The general method of investigation is the same as that used previously by the author[1] and by many other investigators. Some of the latest experimental investigations were reported by Barnes,[4] Hershberger,[5] Hopwood,[6] Richards[7] and Randall.[8]

APPARATUS

The apparatus is the same as that used in the previous investigation[1] with the addition of another thermometer mounted beside the sound path and a

[1] W. H. Pielemeier, Phys. Rev. **38**, 1236 (1931).
[2] H. O. Kneser, Ann. d. Physik [5] **11**, 777 (1931).
[3] H. O. Kneser, Ann. d. Physik [5] **11**, 761 (1931).
[4] G. F. Barnes, J. Acous. Soc. Am. **3**, 579 (1932).
[5] W. D. Hershberger, J. Acous. Soc. Am. **3**, 263 (1931); also, Physics **2**, 269 (1932).
[6] F. L. Hopwood, Nature **128**, 748 (1931).
[7] W. T. Richards, Proc. Nat. Acad. Sci. **17**, 611 (1931); also, G. B. Kistiakowsky and W. T. Richards, Jour. Am. Chem. Soc. **52**, 4661 (1930).
[8] C. R. Randall, Bureau of Standards Jour. of Research **8**, 79 (1932).

radiometer or pressure vane which could be interchanged with the moveable reflector. An orsat apparatus was used to analyze the gas after a run was completed.

Results

The results are presented in Table I and in Figs. 1 and 2. The ratio, $V^2(CO^2)/V^2(A)$, is plotted against $\log \nu$ in Fig. 1. In this figure $V(CO_2)$ represents the velocity of sound in CO_2 reduced to 0°C, the relative humidity ranging from 24 to 30 percent and the purity of the CO_2 ranging from 91 to 95 percent. $V(A)$ represents the velocity in argon reduced to 0°C ($V(A)=307.8$ m/sec.). This method of plotting is used in order to make a direct comparison with Kneser's[2] dispersion curve. The values of A, the absorption constant, are plotted against $\log \nu$ in Fig. 2. These values were computed from pressure vane deflections and also from the height of the peaks which were used for the velocity determinations.

Table I.

Frequency, in kilocycles	$V(CO_2)$ in meters per sec.	Percent CO_2	Relative humidity, H, in percent	$V^2(CO_2)/V^2(A)$ in percent	c	$A=c\lambda^2 \times 10^{-3}$
303.8	262.5 to 265.1*	91 to 95	27 to 31	72.7 to 74.2	1.6	14.
409.6	264.3	94	—	73.7	1.7	8.1
645.8	265.1 to 267.0	91	24 to 30	74.2 to 75.3	1.7	3.2
1159.1	268.1 to 268.6	92 to 95	25 to 26	75.5 75.7	1.8	1.1
1224.	268.6 to 268.7	90	30	75.8 75.9	2.2	1.1
1403.	269.6 to 269.9	91 to 92	25 to 26	76.0 76.2	1.7	0.67
2089.	268.2	94	24	75.6	2.7	0.49

* The value from each of five runs was 263.6 (94 to 95 percent CO_2).

Discussion of Results

With a resonance column of cross section small in comparison with the wave-length the wave fronts in the component trains rapidly lose their flatness and their intensity decreases much more rapidly than it would on account of mere absorption. If the cross section is kept constant and the frequency is increased this effect *diminishes* but the actual absorption *increases* in general. (Neglecting absorption *bands*, the coefficient of absorption should be porportional to the square of the frequency.) If the deviation from flatness is not prevented nor taken into account in absorption measurements an apparent or false absorption minimum might be found. With velocity depending on intensity such a minimum would be accompanied by an apparent dispersion. In consideration of these statements the measurements of Pierce,[9] Barnes,[4] and Kneser[2] on the velocity of high-frequency sound in CO_2 were viewed with a possible doubt and the upper range covered by Kneser was remeasured and extended to $\nu=2089$ k.c. The coefficient of absorption was also measured over this range. Sound beams of greater cross section were

[9] G. W. Pierce, Proc. Amer. Acad. **60**, 271 (1925).

used. The original intention was to use the satellites for the velocity determinations but they were so weak with CO_2 that this plan was rejected. Even with the lowest frequency ($\nu = 303.8$ k.c.) the satellites could be definitely located for only a few wave-lengths from the crystal surface. This fact and the constant space rate at which the logarithm of the peak height decreases

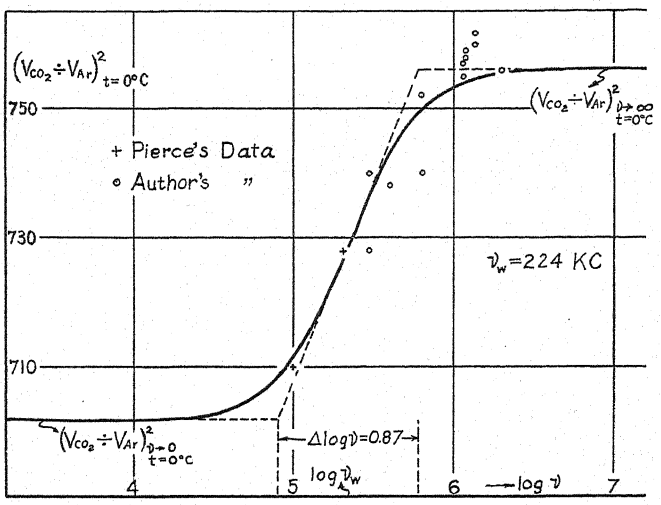


Fig. 1. Kneser's dispersion curve (ordinates $\times 10^{-3}$).

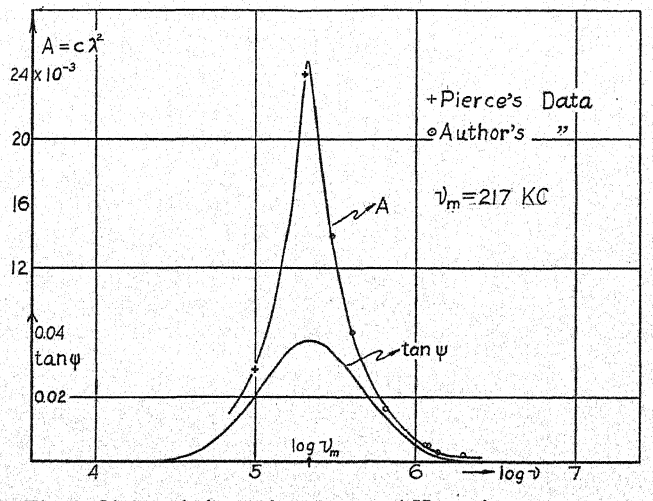


Fig. 2. Observed absorption curve and Kneser's tan ψ curve.

after the first few peaks, are good evidence that there is but one effective return trip of the emitted waves in CO_2.

Since the satellites observed with air at mirror positions such as to give resonance for low intensity (minimum velocity) waves could not be used with CO_2, the velocity values are probably slightly greater than the *limiting* velocity at the given frequency. The presence of some air (5 to 9 percent)

also has the effect of increasing the velocity. Probably the apparent drop in velocity between 1.4 and 2.09 megacycles is merely an approach to the limiting velocity for low intensity waves. (The intensity decreases through this range.)

A dispersion approximately as located by Kneser is quite evident in spite of the uncertainties listed above. Kneser's[2] observed maximum dispersion occurs at approximately 224 k.c. Pierce's[9] velocity curve ends near this point (205.6 k.c.). It is in good agreement with Kneser's[2] curve. The author's data agree reasonably well with the remainder of Kneser's curve (see Fig. 1).

A number of different symbols for the absorption coefficient are used in the publications on sound absorption. Lebedew and Neklapajew[10] use A/λ^2, Abello[11] uses k for one percent CO_2 and therefore 100 k for the pure gas, Herzfeld and Rice[12] use $4\pi k_2$ which they also express in terms of other constants including n^2 and τ, n being the frequency and τ a time measuring the rate of exchange between external and internal degrees of freedom. In Table I the symbol c is used for the absorption coefficient. ($I=I_0e^{-cx}$). We may then write

$$100k = 4\pi k_2 = n^2a = a/V^2 = c. \qquad (1)$$

From Eq. (1) $$a = A/\lambda^2n^2 = A/V^2.$$

If there were no internal degrees of freedom nor dissociation of the molecules or if the internal energy were at all times in equilibrium with the external energy A and a would have constant values for all frequencies. This, however, is not the case with CO_2. As may be seen from Table I, the greatest value of A observed by the author occurs with the lowest frequency (303.8 k.c.). Even this is above Kneser's[2] observed value for ν_w, the frequency for maximum dispersion, which is approximately 224 k.c. If that value of β is selected which yields 224 k.c. it is found to be 0.95 $(10)^{-6}$ and not 0.95 $(10)^{-5}$ sec. as he records it. This may be seen from Kneser's equation,

$$\nu_w = 224\,\text{k.c.} = 2.24(10)^5 = \frac{1}{2\pi}\,\frac{1}{\beta}\,\frac{C}{Ca} = \frac{1}{2\pi}\,\frac{1}{\beta}\,\frac{3.349}{2.5}.$$

Thus ν_m, the frequency for maximum value of ψ, has for its value 217 k.c. ψ represents the phase lag of the density behind the pressure. A *maximum* value of A is also expected at 217 k.c. Evidently A is approaching this maximum at the lower end of the observed frequency range. If the value of c at 303.8 k.c. is used to compute τ from the equation[12]

$$c = 4\pi k_2 = n^2a = n^2[3.16(10)^{-13} + 1.16(10)^{-4}\tau] \qquad (2)$$

we obtain $\tau=0.9\ (10)^{-7}$ sec.

This is not in agreement with Kneser's[2] *Abklingungszeit der inneren Energie* nor with β', the life of the vibration quanta; *Lebensdauer der Schwingungs-*

[10] N. Neklapajew, Ann. d. Physik **35**, 175 (1911).
[11] T. P. Abello, Phys. Rev. **31**, 1083 (1928).
[12] K. F. Herzfeld and F. O. Rice, Phys. Rev. **31**, 691 (1928).

quanten. $\beta' = (10 \pm 2)(10)^{-7}$ sec. The difference may be due to the values of c and n used in Eq. (2). With Abello's[11] exterpolated value for 100 k, τ becomes 0.66 $(10)^{-7}$ sec. This is for $n = 612$ k.c. which is farther above the peak frequency. Pierce[9] states that 4 mm of CO_2 at 205.6 k.c. are more than equivalent to 204 mm of air. Accordingly τ is 3 $(10)^{-7}$ sec. and $A = 24$ $(10)^{-3}$. If τ is computed from the first 2 mm of Pierce's[9] curve the result is 8 $(10)^{-7}$ sec. This frequency is just below that for the absorption peak. Probably τ for 217 k. c. would agree better with $\beta' = 10$ $(10)^{-7}$ sec. Peirce's[9] data for 100 k.c. gives 5.7 $(10)^{-3}$ as the value of A. This is definitely on the low-frequency side of the absorption maximum.

Small but very definite variations in the values of A for a given frequency were obtained by the author. These are probably due to the differences in the temperature and the humidity for the separate runs. This problem is being investigated and will be reported by H. H. Rogers.

Simultaneous measurements on velocity and absorption in other gases by a new method of detection[13] are being investigated by H. L. Yeagley and H. L. Saxton.

Hershberger[5] states two possible reasons for the multiple peaks which he observed. One is a frequency shift as the mirror approaches a resonance position. The other is the complexity in the motion of the crystal itself. The latter might well be the cause of those observed by the author. It is thought, however, that this complexity is *caused* by the slight deviation from simultaneity in arrival of the multiply reflected components of the stationary waves. Only the components of lowest intensity and minimum velocity arrive *together* if the length of the resonance column is adjusted for this minimum velocity.

[13] In a recent article by Grossmann (Ann. d. Physik [5] **13**, 681 (1932)) a somewhat similar method is outlined. Grossmann's ν_m is lower and his maximum value of A is much greater than the author's corresponding values. The value of τ computed from Grossmann's maximum A is much in excess of $10(10)^{-7}$ sec. Possibly his method of correcting for diffraction is not sufficient to prevent an apparent additional absorption at the lower frequencies. If so, it would explain the above deviations. Further measurements near the peak frequency and below it are being made.

LETTERS TO THE EDITOR

Prompt publication of brief reports of important discoveries in physics may be secured by addressing them to this department. Closing dates for this department are, for the first issue of the month, the twenty-eighth of the preceding month; for the second issue, the thirteenth of the month. The Board of Editors does not hold itself responsible for the opinions expressed by the correspondents.

The Angular Distribution of Elastically Scattered Electrons in Mercury Vapour

In a recent paper[1] in the Physical Review Tate and Palmer have reported results of an investigation of the angular scattering of electrons in mercury vapour, which confirm in general the results obtained by the writer about two years ago.[2] However, in the particular case of the scattering of 80-volt electrons between 5° and 60°, Tate and Palmer obtain a curve which does not fall off so steeply as the curve I obtained first in 1929 for 82-volt electrons.[3]

Tate and Palmer suggest in explanation of this disagreement that I "collected not only electrons scattered elastically but also a large number of inelastically scattered electrons" owing to the fact that I used an accelerating potential between the Faraday cylinder and its shield to prevent secondary electron emission from the Faraday cylinder.

This must surely be a mistake, for reference to my paper will show that, in the apparatus I used in 1929 to obtain the curve reproduced by Tate and Palmer, I had no means of applying such an accelerating potential. A retarding potential only was applied in the collecting system to prevent the collection of inelastically scattered electrons.

It is true that I obtained an almost identically similar curve with my new apparatus in which an accelerating potential was applied to prevent secondary emission, but the very fact that the curve was almost identical shows that no error was introduced by using this accelerating potential.

The reason why an accelerating potential may lead to the collection of inelastically scattered electrons is that part of the retarding potential may be rendered ineffective in stopping electrons which have lost energy, owing to penetration of the accelerating field into the retarding field. The extent of this penetration will obviously depend upon the size of the opening in the diaphragm separating the two fields, and the fraction of the retarding field neutralized by the accelerating field will depend upon the ratio of the size of this opening to the distance between the slits across which the retarding potential is placed. In my new apparatus this ratio is 2/5, whereas in the apparatus used by Tate and Palmer the ratio is about 5/3, i.e., the width of the slit is *greater* than the distance over which the retarding field extends. It is not surprising therefore that serious distortion of the retarding field was produced by the accelerating field in their apparatus, while in my apparatus the effect of the accelerating field was very small. There is thus no justification for the statement made by Tate and Palmer that "as Arnot's slit system is similar in dimensions to ours it would seem that his measurements are subject to this error."

A very slight interpenetration of the fields was observed in my work, but the small reduction in the retarding field so caused was always corrected by increasing the retarding field until only the elastically scattered electrons were received. This was effected by the following procedure. At each energy of the primary electron beam a velocity distribution curve of the scattered electrons was taken. From an examination of this curve the retarding potential could then be set so as to exclude all inelastically scattered electrons from the Faraday cylinder. In an investigation of this nature one naturally takes such precautions as these.

F. L. ARNOT

The University
St. Andrews
August 9, 1932.

[1] J. T. Tate and R. R. Palmer, Phys. Rev. **40**, 731 (1932).

[2] F. L. Arnot, Proc. Roy. Soc. **A130**, 655 (1931); **A133**, 615 (1931).

[3] F. L. Arnot, Proc. Roy. Soc. **A125**, 660 (1929).

Lower Limit for the Ground State of the Helium Atom

In a recent paper[1] I have derived an expression for a lower limit of the lowest energy level of a Schrödinger equation. In order to show how practical this expression was, it was evaluated for the case of helium with a hydrogen-like function. This turned out to involve an integral which I was not then able to evaluate, and what was thought to be a safe approximation of $(7/16)a^2$ was given. Through Mr. E. B. Wilson, Jr., however, I have obtained the exact value, which is $(2/3)a^2$. The result is that the lower limit is pushed so far down (9.4 *Rh*, experimental value 5.809 *Rh*) that this simple example is of no value. This does not vitiate the expression theoretically inasmuch as it approaches the true value from the bottom as rapidly as the upper limit does from the top, but practically its usefulness is strongly impaired since more exact functions, such as those given by Hylleraas,[2] are required in order to get a reasonably close lower limit; and for these functions the computations are much more involved. So far, the computations have been carried out only for the worst function of a group given by Hylleraas.

[1] D. H. Weinstein, Phys. Rev. **40**, 797 (1932).

[2] E. A. Hylleraas, Zeits. f. Physik **54**, 347 (1929).

I have found an expression for a lower limit which is an improvement over the one originally given. We have in the same notation as before,

$$I_2 - I_1^2 = \sum_{n=0}^{\infty} (w_n - I_1)^2 a_n^2$$
$$= (w_0 - I_1)^2 + \sum_{n=1}^{\infty} (w_n - w_0)(w_n + w_0 - 2I_1)a_n^2 .$$

If now $I_1 \leqq (w_1+w_0)/2$, Eq. (1a) will contain positive terms only. Hence, $I_2 - I_1^2 \geqq (w_0 - I_1)^2$. Now since $I_1 \geqq w_0$, $I_1 - (I_2 - I_1^2)^{1/2} \leqq w_0$. This new lower limit is virtually an absolute lower limit since the restriction (2) is nearly always satisfied, and a theoretical discussion of it can be easily made.

It is also worth noting that $I_2 \geqq I_1^2$ in general, as is obvious from Eq. (1).

If we use a hydrogen-like function we get $I_1 - (I_2 - I_1^2)^{1/2} = -7.6$ *Rh*, while the upper limit is -5.5 *Rh*. If we use the Hylleraas function $\xi = (1 + c_1 t^2)\exp(c_2 s)$ we obtain -6.8 *Rh* for the lower limit and -5.75 *Rh* for the upper limit. It is seen that, as expected, improving the function also improves the lower limit, which, however, does not approach the experimental value so rapidly as the upper limit.

D. H. WEINSTEIN
California Institute of Technology,
August 16, 1932.

BOOK REVIEW

Elektrolyte. HANS FALKENHAGEN. Pp. 346+xvi, Figs. 104. S. Hirzel, Leipzig. Price 23. RM.

This is a comprehensive monograph on various aspects of the electrolyte problem from the point of view of the Debye-Hückel theory. The author has made valuable contributions to the subject of electrolytic conductance and is well qualified to present this subject. Purely thermodynamic properties are treated in extenso as well as important related subjects, such as the dielectric constants and viscosities of electrolytes.

The mathematical treatment naturally follows closely the notation and methods developed by the German school, but significant variations and advances introduced by others receive recognition. Both the expert and the investigator who approaches the subject for the first time will find the book a valuable source of information.

VICTOR K. LA MER
Columbia University

AUTHOR INDEX TO VOLUME 41

References with (A) are to abstracts of papers presented at meetings of the Physical Society and references with (L) are to Letters to the Editor.

Abbott, Frank R. (see Henderson, Jos. E.)—261(A)

Abramson, Harold A. and Hans Mueller. Surface charge of large particles in liquids—386(A)

Adams, W. S. and Theodore Dunham, Jr. Absorption bands in the infrared spectrum of Venus—264(A)

Allison, Samuel K. Reflecting and resolving power of calcite for x-rays—1; 688(L)

Almy, John E. Book reviews—259

Anderson, Carl D. Energies of cosmic-ray particles —405

Appleyard, E. T. S. Electronic structure of the a-X band system of N_2—254(L)

Arnot, F. L. Angular distribution of elastically scattered electrons in mercury vapour—838

Bacher, R. F. and E. U. Condon. Spin of the neutron —683(L)

Bainbridge, K. T. Isotopic weight and packing fraction of H^2—115(L)—396(A)

Banta, H. E. Some thermo- and galvanomagnetic properties of a bismuth crystal—239

Barker, E. F. Constants of the N_2O molecule—369(L)

——— (see Martin, P. E.)—291

Bartlett, B. W. Variation of the principal magnetic susceptibilities of certain paramagnetic crystals with temperature—818

Bartlett, James H., Jr. Structure of atomic nuclei—370(L)

Barton, Vola P. and Geo. A. Lindsay. Fine structure in the x-ray K absorption edge of calcium in compounds—391(A)

Batho, Harold F. Equilibrium between positive ions and neutral atoms in positive rays of the rare gases—686(L)

Bayley, P. L. (see Thorne, A. M.)—376(L)

Bayliss, Noel S. (see Gibson, G. E.)—388(A)

Beals, C. S. On the temperatures of Wolf-Rayet stars and novae—264(A)

Beams, J. W. Some evidence indicating a removal of positive ions from cold surfaces by electric fields—687(L)

——— **and John W. Flowers.** Initiation of electrical discharges in effectively ion free gases—394(A)

Bearden, J. A. Status of x-ray wave-lengths—399(A)

Beck, F. J. and L. W. McKeehan. Monocrystal Barkhausen effects in rotating fields—385(A)

Bennett, R. D., J. C. Stearns, and A. H. Compton. Diurnal variation of cosmic rays—119

Benz, Carl A. (see Poulter, Thos. C.)—366

Berkey, Donald K. Yield of fluorescent x-rays from the K shells of various elements—390(A)

Birch, Francis. Electrical resistance and the critical point of mercury—641

Bitter, Francis. Magnetism and plasticity—401(A)

——— Experiments on the nature of ferromagnetism—507

Bleakney, Walker. Search for isotopes of hydrogen and helium—32

Bond, W. N. Probable values of e, h, e/m and α.—Reply to R. T. Birge—368(L)

Bowen, I. S. Ionization of air by γ-rays as a function of pressure and collecting field—24

Bozorth, Richard M. and Joy F. Dillinger. Barkhausen effect. III. Nature of change of magnetization in elementary domains—345

Bradbury, Norris E. Photoelectric currents in gases between parallel plates as a function of the potential difference—262(A)

Brady, James J. Photoelectric properties of alkali metal films as a function of their thickness—613

Bramley, A. (see Swann, W. F. G.)—393(A)

Brasefield, Charles J. Ionization of helium, neon and argon under impact of their own positive ions—394(A)

Breit, G. (see Rosenthal, Jenny E.)—459

Brown, R. R. H. and J. J. Muir. Vapor pressure of sulphur at 50°C—111(L)

Bruce, C. W. Kerr electro-optical effect in carbon dioxide—394(A)

Buckley, Francis (see Poulter, Thos. C.)—364

Campbell, J. W. Book review—118

Carlson, J. F. and J. R. Oppenheimer. Impacts of fast electrons and magnetic neutrons—763

Clay, J. (see Zanstra, H.)—679(L)

Cole, Kenneth S. Theory of surface conductance at an electrolyte-solid interface—387(A)

——— Electric phase angle of cell membranes—387(A)

Compton, Arthur H. Variation of the cosmic rays with latitude—111(L)
——— Progress of cosmic-ray survey—681(L)
——— (see Bennett, R. D.)—119
——— **and John J. Hopfield.** Use of argon in the ionization method of measuring cosmic rays—539(L)
Condon, E. U. Production of infrared spectra with electric fields—759
——— (see Bacher, R. F.)—683(L)
Cooksey, D. and M. C. Henderson. Threshold counting voltage of the Geiger-Müller tube and some related phenomena—392(A)
Cork, J. M. Further experiments on x-ray reflections from quartz crystals oscillating piezoelectrically—391(A)
——— (see Witmer, R. B.)—391(A)
Coven, Allen W. Scattering of x-rays from solids—422
Cram, W. and J. G. Winans. Observations on the fluorescence spectra of cadmium vapor—388(A)
Cunningham, W. Peyton. Zeeman effect in the $^2\Pi^2\Sigma$ CaH bands—389(A)
Curtis, H. J. Dielectric constant of liquid sulphur—386(A)
Curtiss, L. F. Rôle of gas adsorption in counting chambers—379(L)

Dahlstrom, R. K. (see Henderson, Jos. E.)—261(A)
Davis, H. M. (see Glockler, Geo.)—370(L)
Del Rosario, C. Very soft x-ray spectra of heavy elements—136
Dennison, David M. Vibrational levels of linear symmetrical triatomic molecules—304
——— **and G. E. Uhlenbeck.** Two-minima problem and the ammonia molecule—313
De Vore, H. B. (see Workman, E. J.)—262(A)
Dillinger, Joy F. (see Bozorth, Richard M.)—345
Du Mond, J. W. M. X-ray evidence for high electron momenta in atoms and in solid bodies—398(A)
Duncan, J. A. Absorption spectrum of sulfur dioxide—388(A)
Dunham, J. L. Wentzel-Brillouin-Kramers method of solving the wave equation—713
——— Energy levels of a rotating vibrator—721
Dunham, Theodore, Jr. (see Adams, W. S.)—264(A)

Eckart, Carl. Book review—382
Elbe, Guenther von. (see Lewis, Bernard)—678(L)
Epstein, Paul S. On the specific heats of ferromagnetic materials—262(A)
——— On ferromagnetism and related problems of the theory of electrons—91
Evjen, H. M. On the effect of a secondary structure upon the interference of x-rays—265

Flowers, John W. (see Beams, J. W.)—394(A)
Ford, O. Rex. Survey of the *K*-satellites—577
Foster, Ronald M. Mutual impedance of grounded wires above the surface of the earth—536
Froman, Darol K. Faraday effect with x-rays—693

Giacomini, Amedeo. Production of ultra-short electromagnetic waves—113(L)
Gibbs, R. C. (see Kruger, P. Gerald)—322
Gibson, G. E. and Noel S. Bayliss. Continuous absorption spectrum of chlorine—388(A)
Gingrich, Newell S. Dependence of the ionization produced by γ-rays upon pressure and temperature—679(L)
Glockler, George. Electron affinity of hydrogen—685(L)
——— **and H. M. Davis.** Raman effect of methyl acetylene—370(L)
Gray, J. A. Spectrum of scattered radiation—397(A)
Green, J. B. and R. A. Loring. Zeeman effect of Pb III—389(A)
Grew, K. E. Variation with temperature of the thermoelectric power of nickel and some copper-nickel alloys—356
Gropper, L. (see Uhlenbeck, G. E.)—79
Gunn, Ross. Diurnal variation of cosmic rays and terrestrial magnetism—683(L)

Hanawalt, J. D. Fine structure in x-ray absorption spectra—399(A)
Hardy, J. D. and G. B. B. M. Sutherland. Isotope separations in the infrared absorption spectrum of HCl and the possible existence of a chlorine isotope of Mass 39—471
Harrington, E. L. New type of vacuum or circulating pump—395(A)
Hartig, Henry E. Book review—380
Havens, Glenn G. Magnetic susceptibility of nitrogen dioxide—337
Henderson, Jos. E., R. K. Dahlstrom and Frank R. Abbott. Energy distribution of electrons in field current emission—261(A)
Henderson, M. C. Gamma-ray spectrometer—392(A)
——— (see Cooksey, D.)—392(A)
Higley, Elizabeth A. and Carolyn C. Thorsen. Mobilities of gaseous ions in mixtures of hydrogen and nitromethane and hydrogen and methyl cyanide—263(A)
Hill, E. L. Book review—117
Holmes, F. T. Raman effect in crystalline NH_4Cl—389(A)
Hopfield, John J. (see Compton, Arthur H.)—539(L)
Houston, William V. Theory of the Raman rotation spectra—263(A)

Hoyt, Archer. Errata: Shape of an x-ray line—110
Hubbard, J. C. Acoustic resonator interferometer: II. Ultrasonic velocity and absorption in gases—523
Hughes, A. L. and J. H. McMillen. Elastic and inelastic electron scattering in hydrogen—39
——— **J. H. McMillen and G. M. Webb.** Elastic electron scattering in helium—154

Jauncey, G. E. M. and P. S. Williams. Diffuse scattering of x-rays from sodium fluoride—127
Joffe, Joseph. Alternation of intensities in the sodium bands—388(A)
Johnson, Thomas H. Interpretation of cosmic-ray phenomena—393(A); 545
——— **and J. C. Street.** Variation of the cosmic-ray intensity with azimuth—690(L)

Kaplan, Joseph. Predissociation in nitrogen—114(L)
Kellogg, J. M. B. Reflection of thallium, lead and antimony atoms from sodium chloride crystals—635
Kelly, M. J. (see Prescott, C. H., Jr.)—395(A)
Kenty, Carl. Escape of imprisoned resonance radiation from a gas—390(A)
Kistiakowsky, G. B. and M. Nelles. Resonance fluorescence of benzene—595
Korff, S. A. Frequency of resonance radiation—538(L)
Kruger, P. Gerald and R. C. Wagner. Note on the hyperfine structure of beryllium lines—373(L)
——— **R. C. Gibbs and R. C. Williams.** Nuclear moment of barium as determined from the hyperfine structure of the Ba II lines—322
Kuhn, H. and O. Oldenberg. Evidence of space quantization of atoms upon impact—72
Kunz, Jakob. Distribution of electrons in the photoeffect by Roentgen rays, classically treated—263(A)
Kurie, F. N. D. New measurements of the ranges of alpha-particles from polonium, uranium I and uranium II with the Wilson chamber—392(A); 701
La Mer, Victor. Book review—840
Langer, R. M. Theorem on spectroscopic stability—390(A)
——— Book review—258
Lewis, Bernard and Guenther von Elbe. Experimental evidence for and determination of the predicted $^1\Delta$ level of the neutral oxygen molecule—678(L)
Lewis, Charlton M. Rotational Raman effect of gases—389(A)
Linder, Ernest G. Mass-spectrograph study of the ionization and dissociation by electron impact of benzene and carbon bisulfide—149
Lindsay, Geo. A. (see Barton, Vola P.)—391(A)
Loeb, Leonard B. Mobilities of sodium ions in helium measured in short time intervals—261(A)
Loring, R. A. (see Green, J. B.)—389(A)
Luyten, W. J. Book reviews—380; 381

March, H. W. Book review—259
Martin, Emmet V. Band spectrum of sulphur monoxide—167
Martin, P. E. and E. F. Barker. Infrared absorption spectrum of carbon dioxide—291
McKeehan, L. W. (see Beck, F. J.)—385(A)
McMillen, J. H. (see Hughes, A. L.)—39; 154
McPherson, A. I. Radiation from moving helium, neon and argon ions—686(L)
Meserve, Wilbur E. Some photovoltaic properties of $Cu:Cu_2O\,|\,Pb(NO_3)_2$ solution $|\,Cu:Cu_2O$ photocells—396(A)
Miller, Henry J. Study of getter action of phosphorous—394(A)
Mimno, Harry R. and P. H. Wang. New devices for recording Kennelly-Heaviside layer reflections—395(A)
Mouzon, J. Carlisle. Ionization of neon and argon by positive alkali ions of energies from 650 to 2000 volts—605
Mueller, Hans (see Abramson, Harold A.)—386(A)
Muir, J. J. (see Brown, R. R. H.)—111(L)
Muller, R. H. and A. Spector. Becquerel effect as a special case of the barrier-layer photoelectric cell—371(L)
Mulliken, Robert S. Electronic structures of polyatomic molecules and valence. II. General considerations—49
——— Electronic structures of polyatomic molecules and valence. III. Quantum theory of the double bond—751
Murphy, George M. and Harold C. Urey. On the relative abundances of the nitrogen and oxygen isotopes—141

Nathansen, J. B. Newton's rings in transparent metallic films—373(L)
Nelles, M. (see Kistiakowsky, G. B.)—595
Nottingham, Wayne B. Photoelectric and thermionic emission from composite surfaces—793

O'Brien, Brian and Vernon L. Parks. Photographic reciprocity and intermittency defects near the long wave-length limit of plate sensitivity—387(A)
Oldenberg, O. (see Kuhn, H.)—72
Olpin, A. R. Book review—116
Oppenheimer, J. R. (see Carlson, J. F.)—763

Parker, Allan E. Analysis of the (0,0) $^2\Pi \rightarrow {}^2\Sigma$ CN band at 9168A—274

Parks, Vernon L. (see O'Brien, Brian)—387(A)
Parratt, Lyman G. X-ray diffraction from calcite for wave-lengths 1.5 to 5A—561
——— Design of a double-crystal x-ray vacuum spectrometer—553
Pearce, J. A. Absolute magnitudes of the 05 to B2 stars determined from the interstellar lines—264(A)
Penney, William G. and Robert Schlapp. Influence of crystalline fields on the susceptibilities of salts of paramagnetic ions. I. The rare earths, especially Pr and Nd—194
Pielemeier, W. H. Supersonic dispersion and absorption in CO_2—833
Plesset, Milton S. Dirac electron in simple fields—278
Potapenko, G. Investigations in the field of the ultra-short electromagnetic waves. IV. On the dependence of the ultra-short electromagnetic waves upon the heating current and upon the amplitude of the oscillations—216
Poulter, Thos. C., Carter Ritchey and Carl A. Benz. Effect of pressure on the index of refraction of paraffin oil and glycerine—366
——— **and Francis Buckley.** Diamond windows for withstanding very high pressures—364
Prescott, C. H., Jr. and M. J. Kelly. Caesium-oxygen-silver photoelectric cell—395(A)

Rao, S. Ramachandra. Total secondary electron emission from metal faces—374(L)
Rashevsky, N. Some remarks on the physical constants of cells in connection with their size and shape—387(A)
Rayton, W. M. (see Wilkins, T. B.)—396(A)
Richardson, R. S. Investigation of the hydrocarbon bands in the solar spectrum—264(A)
Ritchey, Carter (See Poulter, Thos. C.)—366
Robertson, H. P. Book reviews—543
Rogers, Henry H. Relation of relative humidity to the absorption of supersonic waves in various mixtures of CO_2—369(L)
Rojansky, V. Book review—380
Rosen, N. (see Vallarta, M. S.)—708
Rosenthal, Jenny E. and G. Breit. Isotope shift in hyperfine structure—459
Roth, Herman. Elimination of one boundary condition for a sphere in radiative equilibrium by a layer in adiabatic equilibrium—327
Ruedy, J. E. Series and term values in the arc spectrum of tellurium—588

Sabine, Paul E. Book review—691
Sanders, Frederick H. Determination of the coefficient of ionization by collision using large plate distances and higher pressures—263(A)
——— Value of the Townsend coefficient for ionization by collision at large plate distances and near atmospheric pressure—667
Sanford, R. F. Further details ascribable to bands of the carbon isotope C_{13} in stars of spectral classes R and N—264(A)
Schlapp, Robert. (see Penney, William G.)—194
Schmid, R. F. Rotational analysis of some CO_2 emission bands—732
Serber, Robert. Theory of the Faraday effect in molecules—489
Silverman, S. Absorption spectrum of benzene in the region of 6.75μ—486
Sixtus, K. J. (see Tonks, Lewi)—539(L)
Slater, J. C. Note on molecular structure—255(L)
Smallwood, Hugh M. Infrared dispersion of carbon dioxide—164
Smith, P. T. Book review—382
Soroos, Adolf. Thermoelectric power of single crystal bismuth near the melting point—516
Spector, A. (see Muller, R. H.)—371(L)
Spencer, Roy C. Additional theory of plane gratings for x-rays—392(A)
Stearns, J. C. (see Bennett, R. D.)—119
Street, J. C. (see Johnson, Thomas H.)—690(L)
Sutherland, G. B. B. M. (see Hardy, J. D.)—471
Swann, W. F. G. Electrons as cosmic rays—540(L)
——— Bearing of the earth's internal magnetic permeability upon the self- and mutual inductance by coils wound on its surface—649
——— **and A. Bramley.** Generalization of wave mechanics suggested by higher order terms in the classical electrodynamic equation of motion, and its influence on β-particles ionization for velocities approaching that of light—393(A)

Thorne, A. M. and P. L. Bayley. Raman spectra of two liquid phases of nitrobenzene—376(L)
Thorsen, Carolyn C. (See Higley, Elizabeth A.)—263(A)
Tonks, Lewi and K. J. Sixtus. Strain and magnetic orientation—539(L)
Turner, Louis A. Optical dissociation of iodine and enhancement of predissociation by collisions—627

Uhlenbeck, G. E. and L. Gropper. Equation of state of a non-ideal Einstein-Bose or Fermi-Dirac gas—79
——— (see Dennison, David M.)—313
Urey, Harold C. (see Murphy, George M.)—141

Valasek, Joseph. Book review—381
Vallarta, M. S. and N. Rosen. Relativistic Thomas-Fermi atom—708
Vance, Bruce B. Spectra of Na II, III, and IV in the extreme ultraviolet—480

Van Vleck, J. H. Theory of the variations in paramagnetic anisotropy among different salts of the iron group—208; 385(A)
——— (see Whitelaw, N. G.)—389(A)
——— Book reviews—117; 381; 543
Vinti, J. P. Relation between the electric and diamagnetic susceptibilities of monatomic gases—813
——— Sum rules for atomic transition probabilities—432

Wagner, R. C. (see Kruger, P. Gerald)—373(L)
Walther, H. (see Wegel, R. L.)—402(A)
Wang, P. H. (see Mimno, Harry R.)—395(A)
Waterman, A. T. Form of potential barrier at the surfaces of conductors—395(A)
Watson, William W. New band system of barium hydride in the infrared—377(L)
——— Zeeman effect and perturbations in the CO angstrom and N_2^+ bands—378(L)
Webb, G. M. (see Hughes, A. L.)—154
Wegel, R. L. and H. Walther. Internal dissipational resistance to distortion in solids and its correlation with other physical properties—402(A)
Weinstein, D. H. Lower limit for the ground state of the helium atom—839(L)
Wheeler, Mary A. Magnetic susceptibilities of alpha- and beta-manganese—331
Whitelaw, N. G. and J. H. Van Vleck. Theory of quantum defect due to polarization, with application to multiplet anomalies in Al II—389(A)
Wilkins, T. B. and W. M. Rayton. Isotopes of uranium—396(A)
Williams, J. W. Dielectric constant and particle weight—386(A)
Williams, P. S. (see Jauncey, G. E. M.)—127
Williams, Robley C. Deposition of chromium on glass—255(L)
——— (see Kruger, P. Gerald)—322
Williams, S. R. Mechanical hardness influenced by magnetism—386(A)
———Does nickel show a positive elongation in the Joule magnetostrictive effect?—251
Winans, J. Gibson. Origin of the mercury bands at 2480A—388(A)
——— (see Cram, W.)—388(A)
Witmer, R. B. and J. M. Cork. X-ray wave-lengths by ruled grating—391(A)
Wolfe, Hugh C. Multiplet splitting and intensities of intercombination lines—Part I—443
Woo, Y. H. Scattering of x-rays by gases and crystals—21
Wood, Lawrence A. Hall effect with audiofrequency currents—231
Workman, E. J. Secondary effects in the ionization by hard gamma-rays—264(A)
——— **and H. B. De Vore.** Electroscope of high charge sensitivity—262(A)
Wulf, Oliver R. Theory of the ozone of the lower atmosphere and its relation to the general problem of atmospheric ozone—375(L)

Zanstra, H. and J. Clay. Remark on Erikson's measurements of the ionization by γ-rays at various pressures and potentials—679(L)
Zwicky, F. On the problem of the solid state—400(A)

ANALYTIC SUBJECT INDEX TO VOLUME 41

References marked (A) are to abstracts of papers presented at meetings of the Physical Society, those marked with (L) are to Letters to the Editor.

Acoustics

Humidity and absorption supersonic waves, H. H. Rogers—369(L)

Supersonic dispersion and absorption in CO_2, W. H. Pielemeier—833

Ultrasonic velocity and absorption, J. C. Hubbard —523

Affinity

Electron affinity of H, G. Glockler—685(L)

Alpha-particles (see also **Radioactivity**)

Ranges from Po, Ur I and Ur II, F. N. D. Kurie—701; 392(A)

Astrophysics

Sphere in radiative equilibrium, H. Roth—327

Atomic and molecular beams

Equilibrium between ions and neutral atoms, H. F. Batho—686(L)

Radiation from He, N and A, A. I. McPherson —686(L)

Reflection of Tl, Pb and Sb from NaCl crystals, J. M. B. Kellogg—635

Atomic structure (see also **Energy states of atoms; Spectra**)

Ground state of He, D. H. Weinstein—839(L)

High electron momenta in atoms, J. W. M. Du Mond—398(A)

Relativistic Thomas-Fermi atom, M. S. Vallarta, N. Rosen—708

Atmosphere

Theory of the ozone of the lower atmosphere and its relation to the general problem of atmospheric ozone, O. R. Wulf—375(L)

Atmospheric electricity (see also **Geophysics**)

Recording Kennelly-Heaviside layer reflections, H. R. Mimno, P. H. Wang—395(A)

Barkhausen effect (see **Magnetic properties**)

Biophysics

Electric phase angle of cell membranes, K. S. Cole —387(A)

Size and shape of cells, N. Rashevsky—387(A)

Book reviews

Bateman, H. Partial Differential Equations of Mathematical Physics—543

Brinkman, H. C. Zur Quantenmechanik der Multipolstrahlung—382

ten Bruggencate, P. Ergebnisse der Exacten Naturwissenschaften—380

Darwin, C. G. New Conceptions of Matter—259

Falkenhagen, Hans. Elektrolyte—840

Gans, Richard. Vector Analysis, with Applications to Physics—380

Gorter, C. J. Paramagnetische Eigenschaften von Salzen—117

Hanle, W. and K. Larché. Die Lichtausbeute bei Stossanregung—382

Hopf, Ludwig. Die Relativitätstheorie—543

Hughes, A. L. and L. A. DuBridge. Photoelectric Phenomena—116

International Research Council and the International Union of Pure and Applied Chemistry. Annual Tables of Constants and Numerical Data, Chemical, Physical, Biological and Technological—258

Jeffreys, Harold. Cartesian Tensors—117

Knudsen, Vern O. Architectural Acoustics—691

v. Laue, M. Die dynamische Theorie der Roentgenstrahlinterferenzen in neuer Form—381

Pease, F. G. Interferometer Methods in Astronomy—381

Pirani, N. Graphische Darstellung in Wissenschaft und Technik—380

Pohl, R. W. Einführung in die Mechanik und Akustik—118

Stuart, H. A. Kerr-Effekt, Lichtzerstreuung und Molekülbau—381

Tietjens, O. Hydro- und Aeromechanik nach Vorlesungen von L. Prandtl, Bd. II—259

Waerden, B. L. van der. Die gruppentheoretische Methode in der Quantenmechanik—543

Wiersma, E. E. Eenige Onderzoekingen over Paramagnetisme—117

Colloids

Dielectric constant, J. W. Williams—386(A)

Conductivity, electrical (see **Electrical conductivity; Discharge of electricity in gases**)

Constants, physical

Status of x-ray wave-lengths, J. A. Bearden—399(A)

Values of e, h, e/m and α, W. N. Bond—368(L)

Cosmic radiation

Absorption coefficients, interpretation of phenomena, T. H. Johnson—545; 393(A)

β-particle ionization for velocities approaching that of light, W. F. G. Swann, A. Bramley—393(A)

Dependence of ionization on pressure and temperature, N. S. Gingrich—679(L)

Diurnal variation, R. D. Bennett, J. C. Stearns, A. H. Compton—119

Diurnal variation and terrestrial magnetism, R. Gunn—683(L)

Electrons as cosmic rays, W. F. G. Swann—540(L)

Energies of particles; photographs, C. D. Anderson—405

γ-ray ionization at high pressure, H. Zanstra, J. Clay—679(L)

Impacts of fast electrons and neutrons, J. F. Carlson, J. R. Oppenheimer—763

Ionization as a function of pressure and collecting field, I. S. Bowen—24

Use of A for measuring rays, A. H. Compton, J. J. Hopfield—539(L)

Variation with azimuth, T. H. Johnson, J. C. Street—690(L)

Variation with latitude and altitude, A. H. Compton—111(L); 681(L)

Crystals and crystal structure

Reflection of x-ray from calcite; mosaic structure, S. K. Allison—1; 688(L)

Seconday structure and the interference of x-rays, H. M. Evjen—265

Secondary structures. Solid state, F. Zwicky—400(A)

Thermo- and galvanomagnetic properties of Bi, H. E. Banta—239

Thermoelectric power of near melting point. Crystals in liquid state, A. Soroos—516

X-ray diffraction from calcite, L. G. Parratt—561; S. K. Allison—688(L)

Dielectric constants

Of liquid S, H. J. Curtis—386(A)

And particle weight, J. W. Williams—386(A)

Dielectrics and dielectric properties

Electric and diamagnetic susceptibilities of monatomic gases, J. P. Vinti—813

Diffraction of molecules (see **Atomic and molecular beams**)

Discharge of electricity in gases

Townsend coefficient for ionization by collision, F. H. Sanders—667; 263(A)

Discharge of electricity in high vacua (see also **Thermionic emission; High voltage tubes and machines**)

Energy distribution, J. E. Henderson, R. K. Dahlstrom, F. R. Abbott—261(A)

Initiation of discharge, J. W. Beams, J. W. Flowers—394(A)

Positive ions from cold surfaces by electric fields, J. W. Beams—687(L)

Dissociation

Of benzene and carbon bisulfide, E. G. Linder—149

Of I_2 by light, L. A. Turner—627

Efficiency of ionization

By positive ions, J. C. Mouzon—605

Elasticity

Internal resistance; correlation with other physical properties, R. L. Wegel, H. Walther—402(A)

Magnetic hardening of metals, S. R. Williams—386(A)

Magnetism and plasticity, F. Bitter—401(A)

Strain and magnetic orientation, L. Tonks, K. J. Sixtus—539(L)

Electrical conductivity and resistance

Of Hg and its critical point, F. Birch—641

Electrical circuits

Inductance of coils wound on the earth, W. F. G. Swann—649

Mutual impedance of grounded wires, R. M. Foster—536

Electrolytes

Conductance at an electrolyte-solid interface, K. S. Cole—387(A)

Electromagnetic theory

Inductance of coils wound on the earth, W. F. G. Swann—649

Mutual impedance of grounded wires, R. M. Foster—536

Electromagnetic waves

Ultra-short waves, G. Potapenko—216

Electrons, scattering of
Angular distribution in Hg, F. L. Arnot—838(L)
In He; elastic, A. L. Hughes, J. H. McMillen, G. M. Webb—154
In H; elastic and inelastic, A. L. Hughes, J. H. McMillen—39

Electrons, secondary
Number from metal surfaces, S. R. Rao—374(L)

Electrons, thermionic (see **Thermionic emission**)

Electron tubes (see **Discharge of electricity in high vacua; Vacuum tubes**)

Electro-optical effects (see also **Photoelectric effect and properties**)
Kerr effect in CO_2, C. W. Bruce—394(A)

Energy states of atoms (see also **Atomic structure; Spectra, atomic**)
Ground state of He, D. H. Weinstein—839(L)

Errata
Shape of an x-ray line, A. Hoyt—110

Faraday effect (see also **Magneto-optical effects**)
Faraday effect with x-rays, D. K. Froman—693

Field currents (see also **Discharge of electricity in high vacua**)
Energy distribution, J. E. Henderson, R. K. Dahlstrom, F. R. Abbott—261(A)
Positive ions from cold surfaces by electric fields, J. W. Beams—687(L)

Fluorescence
Of benzene, G. B. Kistiakowsky, M. Nelles—595
Of Cd, W. Cram, J. G. Winans—388(A)
Space quantization of atoms upon impact, H. Kuhn, O. Oldenberg—72

Galvanomagnetic effects
In Bi crystal, H. E. Banta—239

Geophysics
Permeability of the earth, W. F. G. Swann—649

Getters
Getter action of P, H. J. Miller—394(A)

Hall effect
In Te with audiofrequency currents, L. A. Wood —231

High voltage tubes and machines
Removal of positive ions from cold surfaces by electric fields, J. W. Beams—687(L)

Hyperfine structure
Of Ba II lines, P. G. Kruger, R. C. Gibbs, R. C. Williams—322
Of Be, P. G. Kruger, R. C. Wagner—373(L)
Isotope shift, J. E. Rosenthal, G. Breit—459

Instruments (see **Methods and instruments**)

Intensities in spectra (see also **Spectra, etc.**)
And multiplet splitting, H. C. Wolfe—443

Interference phenomena
Newton's rings in metallic films, J. B. Nathanson —373(L)

Ionization by positive ions (see also **Ionization potentials**)
Of C_6H_6 and CS_2, E. G. Linder—149
β-particle ionization for velocities approaching that of light, W. F. G. Swann, A. Bramley—393(A)
Ionization of He, Ne and A under impact of their own positive ions, C. J. Brasefield—394(A)
Ne and A by alkali ions, J. C. Mouzon—605

Ionization by radiation (see also **Photo-ionization**)
Dependence of the ionization produced by γ-rays upon pressure and temperature, N. S. Gingrich —679(L)
Use of A in the ionization method of measuring cosmic rays, A. H. Compton, J. J. Hopfield——539(L)

Ionization potentials
Of C_6H_6 and CS_2, E. G. Linder—149
Of He, Ne and A by atoms and positive ions, C. J. Brasefield—394(A)

Ions, in gases
Townsend coefficient for ionization by collision, F. H. Sanders—263(A)

Ions, mobility (see also **Ions, in gases**)
In H_2 with nitromethane and methyl cyanide, E. A. Higley, C. C. Thorsen—263(A)
Of Na ions in He, L. B. Loeb—261(A)
Photoelectric currents in gases, N. E. Bradbury —262(A)

Isotopes
Existence of Cl^{39}; separations in the infrared absorption spectrum of HCl, J. D. Hardy, G. B. B. M. Sutherland—471
Of H and He, W. Bleakney—32
Relative abundances in N and O, G. M. Murphy, H. C. Urey—141

Isotopes continued
Theory of rotation spectra, W. V. Houston—263(A)
Of U, T. B. Wilkins, W. M. Rayton—396(A)
Weight of H^2, K. T. Bainbridge—115(L); 396(A)

Kerr effect (see **Electro-optical effects**)

Liquids
Surface charge of large particles, H. A. Abramson, Hans Mueller—386(A)

Magnetic properties
Barkhausen effects in rotating fields, F. J. Beck, L. W. McKeehan—385(A)
Of Bi crystal, thermo- and galvanomagnetic properties, H. E. Banta—239
Electric and diamagnetic susceptibilities of monatomic gases, J. P. Vinti—813
Ferromagnetism and theory of electrons, P. S. Epstein—91
Mechanical hardness influenced by magnetism, S. R. Williams—386(A)
Paramagnetic anisotropy in salts of the iron group, J. H. Van Vleck—208; 385(A)
Patterns showing irregularities of magnetization, F. Bitter—507
And plasticity, F. Bitter—401(A)
Specific heats of ferromagnetic materials, P. S. Epstein—262(A)
Strain and magnetic orientation, L. Tonks, K. J. Sixtus—539(L)
Susceptibilities of α- and β-Mn, M. A. Wheeler—331
Susceptibilities of salts of paramagnetic ions, W. G. Penney, R. Schlapp—194
Susceptibility of NO_2, G. G. Havens—337
And thermoelectric power of Ni and Cu-Ni alloys, K. E. Grew—356
Transverse Barkhausen effect. Domain theory, R. M. Bozorth, J. F. Dillinger—345
Variation of susceptibilities of crystals with temperature, B. W. Bartlett—818

Magneto-optical effects
Faraday effect in molecules, R. Serber—489
Faraday effect with x-rays, D. K. Froman— 693

Magnetostriction
Does nickel show a positive elongation, S. R. Williams—251

Mechanics, quantum—general
Dirac electron in simple fields, M. S. Plesset—278
Electric and diamagnetic susceptibilities of monatomic gases, J. P. Vinti—813
Equation of state of Einstein-Bose or Fermi-Dirac gas, G. E. Uhlenbeck, L. Gropper—79
Ferromagnetism and theory of electrons, P. S. Epstein—91
Impacts of fast electrons and neutrons, J. F. Carlson, J. R. Oppenheimer—763
Space quantization of atoms upon impact, H. Kuhn, O. Oldenberg—72
Transition probabilities, J. P. Vinti—432
Wentzel-Brillouin-Kramers method of solving wave equations, J. L. Dunham—713

Mechanics, quantum—molecular structure and spectra
Energy levels of rotating vibrator, J. L. Dunham—721
Two-minima problem, D. M. Dennison, G. E. Uhlenbeck—313

Mechanics, statistical
Equation of state Einstein-Bose or Fermi-Dirac gas, G. E. Uhlenbeck, L. Gropper—79

Methods and instruments
Cs-O-Ag photoelectric cell, C. H. Prescott, Jr., M. J. Kelly—395(A)
Deposition of Cr on glass, R. C. Williams—255(L)
Diamond windows for high pressures, T. C. Poulter, F. Buckley—364
Double-crystal x-ray vacuum spectrometer, L. G. Parratt—553
Electroscope of high-charge sensitivity, E. J. Workman, H. B. De Vore—262(A)
γ-ray spectrometer, M. C. Henderson—392(A)
Gas adsorption in counting chambers, L. F. Curtiss—379(L)
Getter action of P, H. J. Miller—394(A)
Recording Kennelly-Heaviside layer reflections, H. R. Mimno, P. H. Wang—395(A)
Refractometer for high pressures, T. C. Poulter, C. Ritchey, C. A. Benz—366
Threshold voltage of the Geiger-Müller tube, D. Cooksey, M. C. Henderson—392(A)
Vacuum or circulating pump, E. L. Harrington—396(A)

Mobility of ions (see **Ions, mobility**)

Molecular structure and constants (see also **Spectra, molecular; Raman spectra**)
Ammonia molecule; two-minima problem, D. M. Dennison, G. E. Uhlenbeck—313
$^1\Delta$ of O_2, B. Lewis, G. von Elbe—678(L)
Electron affinity of H, G. Glockler—685(L)

Molecular structure and constants continued
Of N_2O, E. F. Barker—369(L)
Of polyatomic molecules and valence, R. S. Mulliken—49; 751; J. C. Slater—255(L)
Vibrational levels of triatomic molecules, (CO_2), D. M. Dennison—304

Nuclear Spin (see also **Hyperfine structure**)
Of neutron, R. F. Bacher, E. U. Condon—683(L)

Nucleus
Moment of Ba from hfs, P. G. Kruger, R. C. Gibbs, R. C. Williams—322
Moment of Be, P. G. Kruger, R. C. Wagner—373(L)
Structure, J. H. Bartlett, Jr.—370(L)

Neutrons
In atomic nuclei, J. H. Bartlett, Jr.—370(L)
Magnetic neutrons, J. F. Carlson, J. R. Oppenheimer—763
Spin, R. F. Bacher, E. U. Condon—683(L)

Optical constants and properties (see also **Electro-optical effects**)
Effect of pressure on index of refraction, T. C. Poulter, C. Ritchey, C. A. Benz—366
Infrared dispersion of CO_2, H. M. Smallwood—164

Optical instruments (see also **Methods and instruments**)
Deposition of Cr on glass, R. C. Williams—255(L)

Oscillators (see also **Electrical circuits**)
Ultra-short electromagnetic waves, A. Giacomini—113(L)
Ultra-short electromagnetic waves, G. Potapenko—216

Packing fraction
Of H^2, K. T. Bainbridge—396(A)

Photoelectric effect and properties
Of alkali metal films as a function of thickness, J. J. Brady—613
Barrier-layer photoelectric cell and Becquerel effect, R. H. Muller, A. Spector—371(L)
Cs-O-Ag cell, C. H. Prescott, Jr., M. J. Kelly—395(A)
Cu:Cu_2O $Pb(NO_3)_2$ solution Cu:Cu_2O photocells, W. E. Meserve—396(A)
Distribution of electrons classically treated, J. Kunz—263(A)
Photoelectric currents in gases, N. E. Bradbury—262(A)
Properties of composite surfaces, W. B. Nottingham—793

Photography
Reciprocity and intermittency defects, B. O'Brian, V. L. Parks—387(A)

Photo-ionization (see also **cosmic radiation**)
Of A in cosmic-ray apparatus, A. H. Compton, J. J. Hopfield—539(L)
Of air by γ-rays, dependence on pressure and collecting field, I. S. Bowen—24
γ-ray ionization at high pressures, H. Zanstra, J. Clay—679(L)
By hard γ-rays, E. J. Workman—264(A)
Produced by γ-rays, pressure and temperature changes, N. S. Gingrich—679(L)

Photometry
Reciprocity and intermittency defects for long wave-length, B. O'Brian, V. L. Parks—387(A)

Piezoelectric effect
And x-ray reflection, J. M. Cork—391(A)

Potential barriers
Form at the surfaces of conductors, A. T. Waterman—395(A)

Predissociation
Of I_2 enhanced by collisions, L. A. Turner—627
In N, J. Kaplan—114(L)
In SO, E. V. Martin—167

Radiation
Sphere in radiative equilibrium, H. Roth—327

Radioactivity
Isotopes of U, T. B. Wilkins, W. M. Rayton—396(A)
Ranges of α-particles, F. N. D. Kurie—701; 392(A)

Raman spectra
In crystalline NH_4Cl, F. T. Holmes—389(A)
Of liquid phases of nitrobenzene, A. M. Thorne, P. L. Bayley—376(L)
Of methyl acetylene, G. Glockler, H. M. Davis—370(L)
Rotational effect of gases, C. M. Lewis—389(A)

Relativity
Applied to Thomas-Fermi atom, M. S. Vallarta, N. Rosen—708
Dirac electron in simple fields, M. S. Plesset—278

Resistance, electrical (see **Electrical conductivity and resistance**)

Resonance radiation
Escape from a gas, C. Kenty—390(A)
Frequency of resonance and exciting radiation, S. A. Korff—538(L)

Specific heat
a-X band of N_2, E. T. S. Appleyard—254(L)
Of Ba H, W. W. Watson—377(L)
Of ferromagnetic materials, P. S. Epstein—262(A)

Spectra, absorption
Of benzene. New H_2O lines, S. Silverman—486
Continuous of Cl, G. E. Gibson, N. S. Bayliss—388(A)
Infrared of CO_2, P. E. Martin, E. F. Barker—291
Isotope separations in spectrum of HCl, J. D. Hardy, G. B. B. M. Sutherland—471
Of N_2O, E. F. Barker—369(L)
Production of infrared with electric fields, E. U. Condon—759
Of O_4, O. R. Wulf—375(L)
Of SO_2, J. A. Duncan—388(A)

Spectra, atomic
Isotope shift in hfs, J. E. Rosenthal, G. Breit—459
Of Na II, III and IV in extreme ultraviolet, B. B. Vance—480
Ground state of He, D. H. Weinstein—839(L)
Quantum defect due to polarization, N. G. Whitelaw, J. H. Van Vleck—389(A)
Radiation from moving He, Ne and A atoms, A. I. McPherson—686(L)
Of Te I, J. E. Ruedy—588
Transition probabilities, J. P. Vinti—432

Spectra, general
Multiplet splitting and intensities, H. C. Wolfe—443
Production of infrared with electric fields, E. U. Condon—759
Spectroscopic stability, R. M. Langer—390(A)

Spectra, molecular (see also **Molecular structure and constants**)
CN band at 9168A, A. E. Parker—274
CO_2 emission bands rotational analysis, R. F. Schmid—732
Electronic structures of polyatomic molecules, R. S. Mulliken—49; J. C. Slater—255(L)
Energy levels of rotating vibrator, J. L. Dunham—721
Origin of Hg bands at 2480A, J. G. Winans—388(A)
Polyatomic molecules; double bonds, R. S. Mulliken—751
Of SO rotational and vibrational structure, E. V. Martin—167
Vibrational levels of triatomic molecules, (CO_2), D. M. Dennison—304

Spectra, Raman (see **Raman spectra**)

Statistical mechanics (see **Mechanics, statistical**)

Supersonics (see also **Acoustics**)
Relation of relative humidity to the absorption of supersonic waves in various mixtures of CO_2, H. H. Rogers—369(L)
Supersonic dispersion and absorption in CO_2, W. H. Pielemeier—833

Susceptibility, magnetic (see **Magnetic properties**)

Thermionic emission of electrons, emitting surfaces
And photoelectric emission from composite surfaces, W. B. Nottingham—793

Thermoelectric effects
Of Ni and Cu-Ni alloys, variation with temperature, K. E. Grew—356

Vacuum tubes
Ultra-short electromagnetic waves, G. Potapenko—216

Valence
Quantum theory of the double bond, R. S. Mulliken—751
Structures of polyatomic molecules, R. S. Mulliken—49; J. C. Slater—255(L)

Vapor pressure
Of S, R. R. H. Brown, J. J. Muir—111(L)

Viscosity
Dielectric constant variation with frequency, J. W. Williams—386(A)
Internal resistance; correlation with other physical properties, R. L. Wegel, H. Walther—402(A)

Wave mechanics (see **Mechanics, quantum, etc.**)

X-rays, absorption
Fine structure, J. D. Hanawalt—399(A)
Fine structure in Ca K edge, V. P. Barton, G. A. Lindsay—391(A)

X-rays, diffraction scattering, reflection and refraction

From calcite for wave-lengths 1.5 to 5A, L. G. Parratt—561; S. K. Allison—688(L)
From crystals oscillating piezoelectrically, J. M. Cork—391(A)
Diffuse scattering from NaF, G. E. M. Jauncey, P. S. Williams—127
Formula for scattering, Y. H. Woo—21
Reflecting and resolving power of calcite, S. K. Allison—1; 688(L)
Scattering from solids, A. W. Coven—422
Spectrum of scattered radiation, J. A. Gray—397(A)
Width of modified line, J. W. M. Du Mond—398(A)

X-rays, emission

Errata, shape of an x-ray line, A. Hoyt—110
Soft x-rays of heavy elements, C. Del Rosario—136
Survey of *K*-satellites, O. R. Ford—571
Yield of fluorescent x-rays, D. K. Berkey—390(A)

X-rays, polarization

Faraday effect with x-rays, D. K. Froman—693

X-ray spectra and spectroscopy, wave-length measurements

Additional theory of plane gratings, R. C. Spencer—392(A)
Crystal secondary structure and the interference of x-rays, H. M. Evjen—265
By ruled gratings, R. B. Witmer, J. M. Cork—391(A)
Status of wave-length measurements, J. A. Bearden—399(A)

X-ray tubes, apparatus

Double-crystal x-ray vacuum spectrometer, L. G. Parratt—553

Zeeman effect

In Ca *H* bands, W. P. Cunningham—389(A)
Of Pb III, J. B. Green, R. A. Loring—389(A)
And perturbations in CO and N_2^+, W. W. Watson—378(L)